# ONLINE DIAGNOSIS OF FLOW MALDISTRIBUTION IN PACKED BED REACTORS

**By**

**Tsitsi Maparanyanga, B. Eng (Hons), MSc.Eng**

A thesis submitted in the Discipline of Chemical Engineering
University of KwaZulu-Natal

In fulfilment of the requirements for the degree of
Doctor of Philosophy in Engineering, Chemical Engineering

November 2023

Supervisor: Professor David Lokhat

As the candidate's supervisor, I agree to the submission of this thesis:

[redacted]

Professor David Lokhat

## DECLARATION 1 - PLAGIARISM

I, TSITSI MAPARANYANGA, declare that:

The research reported in this thesis, except where otherwise indicated, is my original research.

This thesis has not been submitted for any degree or examination at any other university.

This thesis does not contain other persons' data, pictures, graphs or other information, unless specifically acknowledged as being sourced from other persons.

This thesis does not contain other persons' writing, unless specifically acknowledged as being sourced from other researchers. Where other written sources have been quoted, then:
Their words have been re-written but the general information attributed to them has been referenced
Where their exact words have been used, then their writing has been placed in italics and inside quotation marks, and referenced.

This thesis does not contain text, graphics or tables copied and pasted from the Internet, unless specifically acknowledged, and the source being detailed in the thesis and in the References sections.

Signed

……

## Acknowledgements

I am so grateful to Professor David Lokhat, my supervisor, for constantly guiding me through my research and greatly enriching my knowledge in reactor technology. I really appreciate his support.

I extend my thanks to Mr Trevor Madwe, the Chemical Engineering laboratory technician for assisting with practical support and sourcing of the needed experimental materials.

Finally, I would like to thank my family for believing in me. Overall thanks be to God, for had it not been for the Lord who was on my side I would not have sailed through.

# Table of Contents

## List of Figures

## List of Tables

## Abstract

Massive adiabatic fixed bed reactors are common in the process industries for conversion of raw materials into valuable products. The unit usually consists of a vessel filled with catalyst particles through which the process gas flows. In general, the operation of this unit is akin to the ideal plug flow reactor, i.e. there are no radial gradients of concentration or temperature. During the normal operation of the unit, the catalyst particles can undergo attrition and dusting, resulting in regions of the bed that have different void fractions. These differences in bed voidage can result in non-uniform flow through the packed bed. When the process gas finds a path of least resistance it can flow through this path with little contact with the catalyst. This is referred to as channelling. Channelling leads to low conversion of reactants to product as there will be little contact with the catalyst.

The maldistribution of flow through packed bed reactors can be determined by taking the unit offline and carrying out a residence time distribution test, for example a pulse of tracer is injected into the vessel inlet and the concentration of the tracer is measured at the exit. Although valuable information can be obtained from these measurements, it cannot be performed in most cases whilst the unit is online.

Experimental work was done to determine if there is an appreciable difference in the pressure fluctuations of pressure vessels during correct and incorrect flow through packed beds and to assess if the effect of pressure fluctuations can be used to develop a method for diagnosing flow maldistribution in packed bed reactors online. Correct and incorrect flow through packed beds were achieved by using uniform and non-uniform packing arrangements, to induce non-uniform flow during the operation of the packed bed reactor. To develop a model for analysing flow maldistribution in packed bed reactors online, experiments were done using a small and large vessel. Rachsig rings were used as packing material in the laboratory packed bed reactor. The pressure fluctuations were converted to an analysable form using the Fast Fourier Transform, resulting in dominant frequency for the oscillations. The dominant frequency data could not give a distinguishable difference in the pressure fluctuations data.

Experimental work done using various packings showed a significant difference in the measured amplitude as packing arrangement changes. Large(uniform) packing arrangement was seen to minimize pressure loss through the packed bed. The large packing also had the largest magnitude of pressure fluctuations. There was an inflection point in the amplitude vs flowrate data. The amplitude of pressure fluctuation first increased with an increase in gas flowrate up to a flowrate of 2 $dm^3$/minute. From 2 $dm^3$/minute to 2.33 $dm^3$/minute there was an inflection point and the amplitude dropped. There was a further decrease in amplitude with a further increase in gas flowrate. The non-uniform packing had the highest amplitude below 2.33 $dm^3$/minute but, after 2.33 $dm^3$/minute the uniform packing had the largest amplitude followed by the large and small packing at the side while the large and small packing

at the centre configuration had the least amplitude at high flowrates. This can be used online to check for particle breakage and the resulting maldistribution in flow in packed bed reactors.

A model was developed to analyse pressure fluctuations in packed bed reactors. The model was developed using equations, found from literature, for non-ideal flow in packed beds. MATLAB software was used to solve and analyse the model. The pressure fluctuations obtained from experimental work agreed with the simulated data. The uniform packing had the highest amplitude while the non-uniform (large and small at the centre) had the least amplitude. The model was in agreement with experimental data, as it was seen that the amplitude of pressure fluctuations can be used for diagnosing flow maldistribution in packed bed reactors.

# 1. Chapter 1: Introduction

## 1.1 Background

A packed bed reactor is a fixed column or cylinder filled with particles which can vary in shape or size. It is a porous medium in which the flow of a Newtonian fluid follows Darcy's law at low Reynold numbers (Koekemoer & Luckos, 2015). At high Reynold numbers, the Ergun equation is applicable as it contains both the viscous and inertial terms whereas the Darcy's law contains only the viscous term. A packed bed reactor is basically a tubular reactor loaded with solid catalyst particles (Fogler, 2006). The fluid which is passed over the packed bed and between the particles, causes numerous flow, chemical and thermal effects. Packed beds can use spherical, cylindrical, or other exotic shaped particles. Compared to other packing arrangements, Raschig rings have lighter weight, higher area per unit volume, higher porosity and lower pressure drop. (El-Shazly, et al., 2002). These help homogenize the flow, support catalytic reactions and to control reaction conditions such as pressure, velocity and temperature (Zeiser, et al., 2002). Packed beds have high specific surface area therefore they are ideally suited for heterogeneous catalytic reactions. Packed bed reactors are popular due to their effectiveness in terms of performance and their low capital and operating costs (Nemec & Levec, 2005). Both gas and liquid phase reactants can be used in packed bed reactors. Peregine Phillips was the first to patent a commercial packed bed reactor in 1831 (Rase, 1990). He patented a process for making Sulfur trioxide by passing Sulfur dioxide over a hot bed of platinum sponge. Since then, many fixed bed designs have been developed.

The performance of a packed bed is measured by its conversion, selectivity and pressure drop across the bed. The packed bed performance is affected by any factor that affects the conversion, selectivity of the packed bed or the pressure drop across the bed.

Particle or catalyst attrition usually occurs due to particle movement in circulating fluidized bed reactors (Effendi, et al., 2002). Catalyst material loss due to attrition should not be miscalculated. It is important to assess particle attrition to reduce fines productions, decrease bed loss, reduce down-stream residues or erosion and to maintain material activity (Ghods, et al., 2019). Attrition produces fines that cause increased pressure drop and localized bypassing (Rase, 1990).

Particle breakage is also possible in fixed beds as solid catalysts can undergo thermal stress during operation of the fixed bed reactor. When particle breakage occurs in fixed bed reactors, the fine material produced will also cause increased pressure drop as well as local bypassing in the bed.

Modal analysis studies the dynamic properties of a system in the frequency domain. Frequency domain is the analysis of mathematical functions or signals with respect to frequency, not time. It is used to describe the dynamic properties of structures in terms of the modal properties; modal mass, modal shape, damping factor and natural frequency. Modal analysis can be done mathematically or experimentally. Mathematical modal analysis uncouples equations allowing each equation to be solved separately. When it is not possible to find exact solutions, numerical approximations such as boundary-element and finite element methods are used (Rossing, 2014). Experimental modal analysis measures a variable in time domain, then the variations in the variable are mapped into frequency domain. The Fast Fourier Transform is one of the algorithms used to convert signals from time domain to frequency domain.

The operation of the packed bed unit is generally like that of an ideal plug flow reactor, that is there are no radial gradients of concentration or temperature (Sun, et al., 2000). It is usually assumed that the velocity profile in packed bed reactors is uniform, but it has been known that, even in uniformly packed beds, uniform flow does not occur because of the tendency for preferential flow near the walls. Non-uniform flow in packed beds may occur due to spatially non-uniform resistance to flow for example non-uniform porosity and laterally distributed temperature (Choudhary, et al., 1976). The catalyst in the packed bed can undergo attrition which will result in some regions in the bed having different void fractions and porosity. When the process gas finds a path of least resistance it can flow through this path with little contact with the catalyst. This is referred to as channelling.

In unstructured fixed beds, the void fraction in areas close to the tube wall will approach unity therefore flow through the packed bed is characterized by a channelling effect at the wall (Bey & Eigenberger, 1997). Channelling is a common cause of poor performance in fixed bed processing for example, in conversion in catalytic reactors (Oliveros & Smith, 1982).

At times scaled-up packed-bed reactors achieve lower yields than expected. This may be caused by changes in catalyst activity or gross flow maldistribution. Large packed beds are more susceptible to hot spot formation. These hot spots can cause sintering of catalyst particles which in turn reduce their activity (Stanek & Szekely, 1972). To differentiate between catalyst activity and flow maldistribution, tools for diagnosing flow maldistribution are needed. Tracers are mostly used to detect flow maldistribution. In this method, a tracer (detectable fluid with similar properties as flowing fluid) is injected into the entrance stream of the reactor (Hanratty & Dudukovic, 1990). The change in concentration of the tracer with time will be measured at the exit of the reactor.

During normal operation of the reactor unit the outlet pressure may experience very slight fluctuations due to the resistance to flow offered by the randomly packed bed. These fluctuations may be oscillatory and consistent. These pressure fluctuations can be converted to an analysable form using the Fast Fourier Transform, resulting in a dominant frequency for the oscillations. The pressure fluctuations may

change based on the flow characteristics of the bed and this may be used to diagnose flow maldistribution whilst the reactor is online.

## 1.2 Problem statement

The maldistribution of flow through packed bed reactors can be determined by taking the unit offline and carrying out a residence time distribution test, for example a pulse of tracer is injected into the vessel inlet and the concentration of the tracer is measured at the exit. Although valuable information can be obtained from these measurements, it cannot be performed in most cases whilst the unit is online. This means there could be a delay in detecting flow maldistribution in the reactor and there may be a compromise in the production targets as the vessel would be taken offline several times. A method is therefore required that allows of the diagnosing the maldistribution of flow while the unit is online.

## 1.3 Aim and Objectives

### Aim

The overall aim of this research project is the development of a simple and easily integrated real-time monitoring tool for the diagnosis of flow maldistribution in large-scale packed bed reactors, which is based on pressure measurements on the unit.

### Objectives

To carry out a comprehensive literature review on flow maldistribution in packed bed reactors.
To determine if appreciable exit pressure fluctuations exist during normal operation of a large, packed bed reactor.
To determine if exit pressure fluctuations can be used to establish dominant frequencies for correct and incorrect flow through packed beds.
To establish a relationship between pressure fluctuations and maldistribution of flow in packed bed reactors while the unit is online.

## 1.4 Dissertation Overview

This thesis contains six chapters and seven appendices.

Chapter 1is a general introduction to the overall research work including the rationale for the study, problem statement and the aim and objectives of the study.

Chapter 2 contains a general literature review of the maldistribution that occurs in packed bed reactors. Methods which have been used in literature to diagnose maldistribution will be detailed as well as their shortcomings. General reactions governing processes in packed bed reactors are also given.

Chapter 3 covers the equipment and materials used for the experiments. A detailed methodological approach used for the experiments is also outlined.

Chapter 4 describes the model development. Different model arrangements are given, and pressure drop correlations are developed using equations from literature. The pressure drop correlations are also formulated at different packing configurations.

Chapter 5 presents all the results from the experimental work including optimization of experimental conditions. The model results are also presented in the same chapter. The chapter also discusses both the model and experimental results and interprets the findings and challenges encountered.

Chapter 6 gives the concluding remarks for this work, as well as recommendations for improving the research.

The information on calculation procedures, raw experimental data as well as MATLAB software codes are contained in the appendices.

# 2. Chapter 2: Literature Review

This chapter will discuss the packed bed reactor as a unit operation, consider its various configurations and the factors that affect its performance. The chapter will also discuss the hydrodynamic concepts, and the factors that affect flow through packed beds. The modelling of this flow will thereafter be considered along with the interrelated heat and mass transfer processes in chemical reactors. The final part of the review will consider the use of modal analysis to treat pressure and vibration data that could be correlated against the flow conditions in packed beds.

## 2.1 Packed bed reactors

A packed bed is a hollow tube, vessel or pipe filled with packing material (Sachdev, et al., 2012). The packing material can be arranged in a random or structured way. Packed beds can also contain catalyst particles. Packed beds find use in improving the contact between two different phases of material in a reaction. Reactants flowing through a packed bed can be in gas or liquid form. A plug flow reaction is approximated in packed bed reactors. Plug flow reaction is characterised by an orderly flow throughout the reactor with no element of fluid overtaking or mixing with any other element ahead or behind. In a plug flow reaction, all fluid elements have the same residence time in the reactor (Levenspiel, 1999). Packed bed reactors fall under two main classifications that describe their energy exchange: adiabatic and non-adiabatic (Worstell, 2014). The adiabatic packed bed is often chosen when an acceptable conversion and selectivity to the desired product is possible. The adiabatic packed bed is simpler and cheaper than the non-adiabatic design (Rase, 1990).

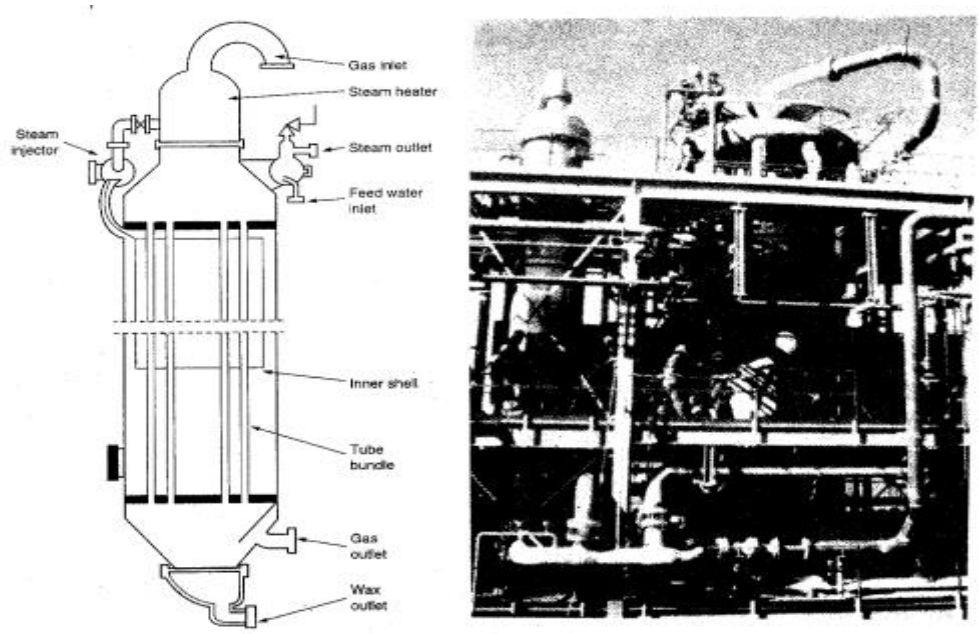


*Figure 2-1: Packed bed reactor (Schematic and photograph courtesy of Sasol/Sastech PT Limited) (Fogler, 2006)*

Figure 2-1 shows a schematic diagram and photography of a packed bed reactor.

### 2.1.1 Types of packed bed reactors

Packed beds can be further divided into 3 classes, according to the flow rate of gas or liquid in the reactor or movement of the packed bed,

Fixed beds: For fixed beds, the gas of liquid flowrate is kept low enough so that the bed remains stationary of fixed during operation of the reactor. Fixed beds can be solid-gas systems or solid-liquid systems. The solid-gas system can be used in blast furnace operations (Foutch & Johannes, 2003) while the solid-liquid system find use in water filtration and leaching (Perry, et al., 1997). Fixed beds have immobile catalyst particles as shown in Figure 2.2.

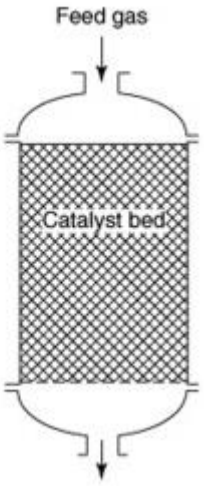


*Figure 2-2: Fixed bed reactor*

Moving beds: The gas or liquid flow rates in moving bed reactors in high enough to cause the packed bed to move during operation of the reactor. These are used in fluidized catalytic cracking processes and circulating fluidized bed combustion (Perry, et al., 1997). Figure 2.3 shows a typical moving bed reactor.

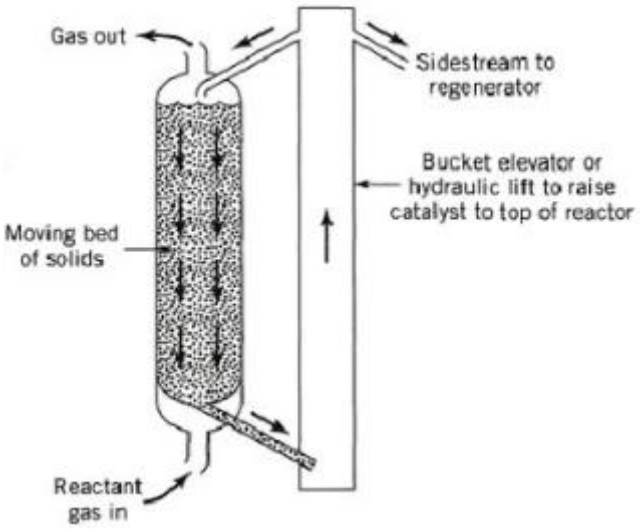


*Figure 2-3: Moving bed reactor (Levenspiel, 1999)*

Solid-liquid-gas system: this system find use as absorbers and scrubbers (Liu, et al., 2016). This system has solid, liquid and gas in the same vessel as shown in Figure 2.4.


*Figure 2-4: Solid-liquid gas system*

Table 2-1 shows some of the areas in which fixed bed catalytic processes find use. A huge number of packed bed reactors are used in the petroleum refinery industry making use of natural gas as the feed.

*Table 2-1: Examples of fixed bed processes (Jakobsen, 2008)*

| Basic Chemical Industry | Petrochemical Industry | Petroleum Refining |
|---|---|---|
| Primary steam reforming | Ethylene oxide | Catalytic reforming |
| Secondary steam reforming | Ethylene dichloride | Isomerization |
| Carbon monoxide conversion | Vinylacetate | Polymerization |
| Carbon monoxide methanation | Butadiene | (Hydro)desulfurization |
| Ammonia synthesis | Maleic anhydride | Hydrocracking |
| Sulfuric acid synthesis | Phthalic anhydride | |
| Methanol synthesis | Cyclohexane | |
| Oxo synthesis | Styrene | |
| | Hydrodealkylation | |

### 2.1.2 Packed bed reactor configurations

The packed bed reactor can be down flow where the gas flow can be from the top of the bed. The reactant moves down and comes out at the bottom of the bed reactor as a mixture consisting of product and unreacted reactant. The reactor can also be up flow where the reactant enters the reactor from the bottom, and flows upward. The product and unreacted reactant leaves the reactor from the top. There are five different fixed bed reactor configurations as follows.

Single adiabatic bed

In the single adiabatic bed reactor (Figure 2-5), inert ceramic balls or pellets can be used to support the catalyst bed and prevent catalyst movement by high velocity gas at the inlet. Inert packing prevents scale from collecting in the bed. A single inlet baffle is usually adequate for beds with length to diameter ratios greater than or equal to 10 (Rase, 1990). Spherical shells are used for large diameter short bed, when flow rates are large and pressure drop must be minimized. Concentric cone distributors are used along with exit collector screens to ensure good distribution. The single adiabatic beds are used for moderately exothermic or endothermic, temperatures below 70 $^{o}$C and Pressures below 30000 kPa $H_2$ (Durango-Giraldo, et al., 2022; Mitsudome, et al., 2017), non-equilibrium limited for example in mild hydrogenation.

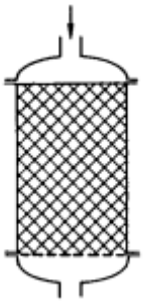

*Figure 2-5: Single adiabatic bed*

Radial-flow reactor

A radial-flow reactor (Figure 2-6) has the catalyst held in a toroidal basket held in a cylindrical shell or pipe. Flow in the radial-flow reactors is into the basket and out of the center pipe. The perforated distributor in the center pipe is usually designed for sufficient pressure drop to ensure good distribution along the entire length. The radial-flow reactors find use where low pressure drop is essential and useful where change in moles is large for example in the manufacture of styrene from ethylbenzene (Rase, 1990).

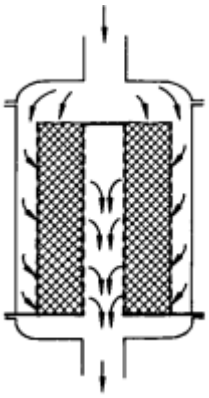

*Figure 2-6: Radial-flow reactor (Rase, 1990)*

Adiabatic beds in series

Equilibrium-limited exothermic reactions and rapid endothermic reactions require multiple beds with, respectively, intermediate cooling or heating. This can be accomplished by using multiple beds in a single shell using external or direct-contact heat exchange. Single separate reactors can also be used in series with intermediate exchange. The adiabatic beds in series are used in high conversion, equilibrium limited reactions such as sulfur dioxide oxidation, catalytic reforming, ammonia synthesis and hydrocracking (Rase, 1990). A series of adiabatic beds with inter-stage quench are shown in Figure 2-7.

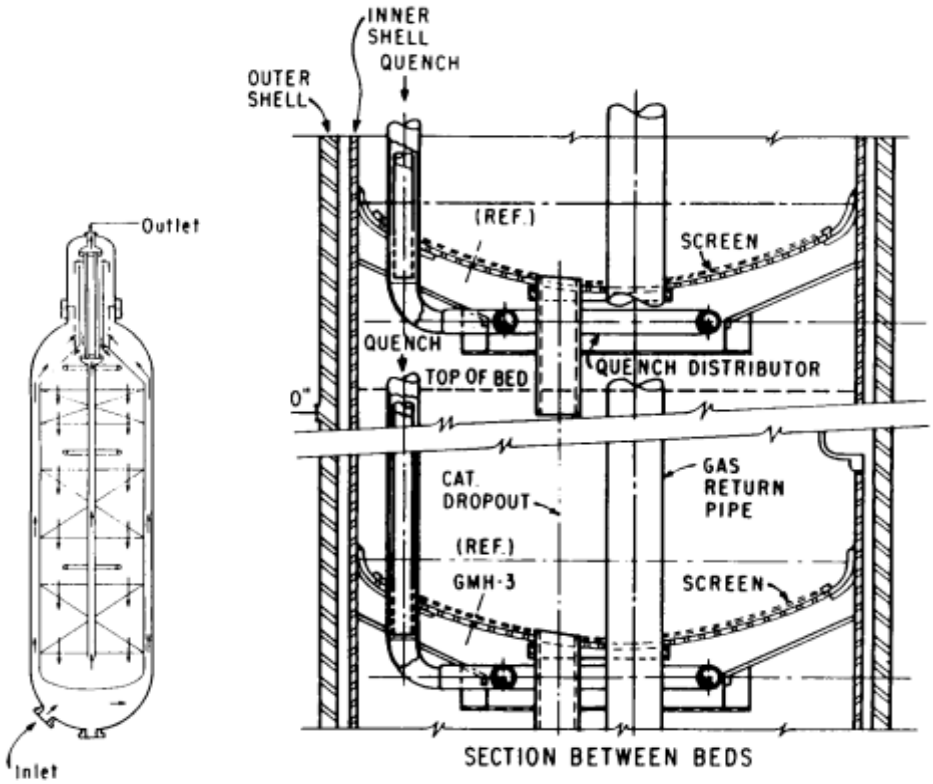


*Figure 2-7: Series of Adiabatic beds with inter-stage quench (Rase, 1990)*

Multitubular non-adiabatic reactor

These are used in extremely endothermic or exothermic reactions that require strict control of temperature to ensure high selectivity (Rase, 1990). They find applications in hydrogenation processes, formaldehyde by methanol oxidation, ethylene oxidation to ethylene oxide and phthalic anhydride production. Figure 2-8 shows a multitubular non-adiabatic reactor.

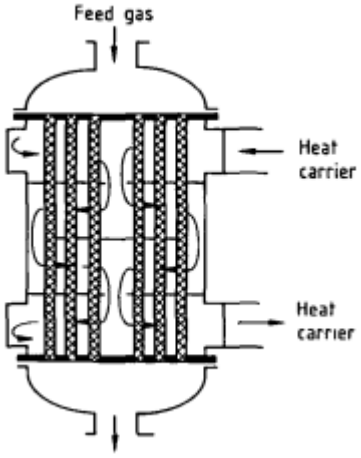


*Figure 2-8: Multitubular nonadiabatic reactor (Eigenberger, 1992)*

Direct-fired non-adiabatic reactor

The direct-fired non-adiabatic reactor (Figure 2-9) find use in high-temperature, fast endothermic reactions that require high fluxes obtainable by a radiant heat source. It is mainly used in steam reforming (Rase, 1990).

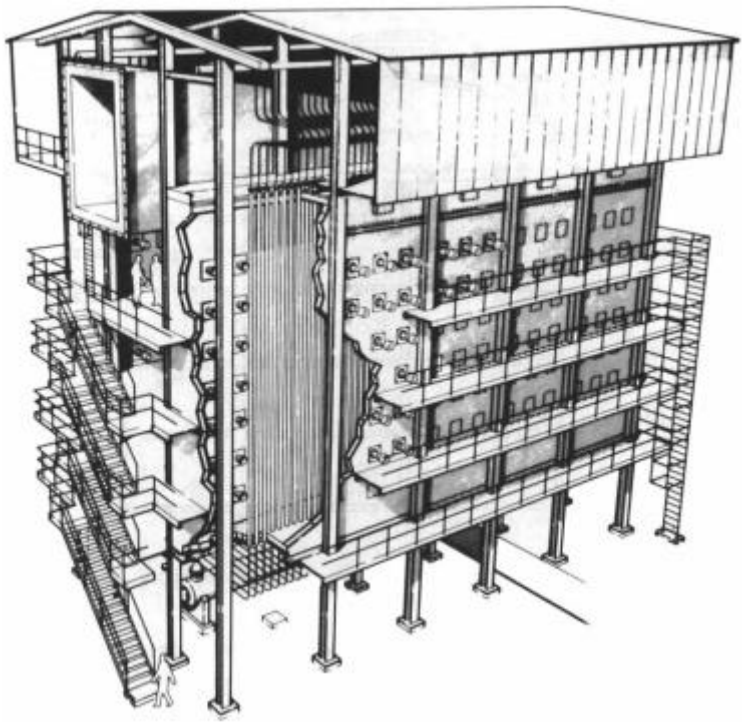

*Figure 2-9: Direct-fired nonadiabatic reactor (Rase, 1990)*

Packed bed reactors find application in numerous areas, include water treatment, petrochemical and bulk chemical processes, biochemical processes and environmental remediation systems (Ahmadi & Sefidvash, 2018). Processes in which the packed bed reactor can be applicable are, Waste water treatment, Air purification process, Gas absorption processes, Distillation processes and catalytic conversion processes.

## Factors affecting performance of packed beds

Packed bed performance is measured by its conversion, selectivity and pressure drop across the bed. Any factor that affects the conversion, selectivity of the packed bed or the pressure drop across the bed also affects the packed bed performance.

Packing geometry

The type of packing arrangement can affect the flow as well as pressure across the bed. There are two types of packing arrangements, regular and random packing. Random packing arrangement, although being inexpensive, are undesirable because of their small surface and poor fluid-flow characteristics (Sai Kumar, et al., 2007). Random packing arrangement has a larger specific surface and larger gas-pressure drop in the smaller sizes. The packed bed reactor's performance can be very sensitive to small

variations in the gas flow rate (Stanek & Szekely, 1972). Random packing costs less per unit volume in the larger sizes. Regular packing arrangements offer low pressure drop but are more costly than random packing (Treybal, 1981).

Packed bed porosity

Benenati & Brosilow (1962) concluded that, for distances more than five particle diameters from the wall, the packed bed porosity is uniform. This means uniform porosity can be achieved if the diameter of the reactor is less than or equal to five times the particle diameter. However, this is insignificant in commercial reactors as they have high reactor to particle diameter ratios that is when,

$$D > 5d \qquad \text{(Eqn 2-1)}$$

where, $D$ is reactor diameter and $d$ is particle diameter.

Density of the reacting fluid

The density of reacting fluid decreases in the direction of gravity, resulting in an increase in buoyancy force at the bottom of the reactor. This results in the uniform flow becoming maldistributed and co-existing regions of fast and slow flow being formed (Nguye & Balakotaiah, 1994). In their study, Nguye & Balakotaiah (1994) showed that regions where the reactant flows slowly will have higher temperatures due to increased local residence time which may result in the ignited catalysts forming hot spots. Flow maldistribution can therefore be reduced by increasing the fluid velocity however, this reduces the contact time and hence low conversion.

Volumetric flow rate of the fluid

Abdulmohsin & Al-Dahhan (2017) studied the effect of gas flow on pressure drop. They measured the pressure drop along a packed pebble bed using the differential pressure transducer and plotted the pressure drop against gas velocity at different tube to particle diameter ratios. They found that pressure drop decreased with an increase in particle size. This is because larger particles have higher voidage than smaller ones and hence lower pressure drop. They also found that the pressure drop increased with superficial gas velocity.

Particle Reynolds number

Reynolds number is given by,

$$Re = \frac{\rho_f u_f d_p}{\mu_f} \qquad \text{(Eqn. 2-2)}$$

where, $\rho_f$ is the fluid density, $u_f$ is the fluid velocity, $d_p$ is the particle diameter and $\mu_f$ is the dynamic viscosity of the fluid. The Reynolds number defines the flow regime, distinguishing streamline ($Re<10$), transitional ($10 \leq Re \leq 300$) and turbulent flow ($Re>300$) (Eisfeld & Schnitzlein, 2001).

The dimensionless pressure drop (Ψ),

$$\Psi = \frac{\Delta P}{\rho_f u_f^2} \frac{d_p}{L} \quad \text{(Eqn 2-3)}$$

is found to be proportional to 1/Re in streamline flow and becomes independent of the Reynolds number at Re≃$6\times10^4$ (Carman, 1937). Contrary to the flow in tubes, the dependence of the dimensionless pressure drop on Reynolds number changes slowly with an increase in Reynolds number, which inducts a smooth transition from lamina to turbulent flow (Eisfeld & Schnitzlein, 2001).

Particle diameter and Particle Size Diameter (PSD) width

The particle diameter of non-spherical particles is defined as the diameter of a sphere having the same volume as the particle. Particle size diameter width is defined as the difference between the diameters of the largest and smallest particles in the packed bed reactor (Koekemoer & Luckos, 2015). Particles with smaller particle diameter have lower bed permeability. As the particle size decreases, the surface area of the particle per unit volume of the bed increases leading to a more stable packing and increased pressure drop per unit of bed length (Koekemoer & Luckos, 2015).

Beds with wider PSD widths have low voidage because the smaller particles fill in the spaces between larger particles thus reducing total bed voidage and increasing the density of the bed. A decrease in voidage causes an increase in pressure drop.

A packed bed consists of particles which influence the flow properties of the bed. The particles can be uniformly sized or can be irregular. The diameter of non-spherical particle represents an equivalent sphere of the same volume, expressed as,

$$d_p = \frac{6(1-\varepsilon)}{a_p} \quad \text{(Eqn 2-4)}$$

Where, $a_p$ is the specific surface area

The arrangement in which particles are ordered within the bed influences the easy with which a fluid can pass through the media. For irregular shape or size particles the packing regime will always be random.

For simple cubic arrangement (spheres packed directly on top of one another), the packing density is;

$$\rho = \frac{\pi}{6} = 0.52 \quad \text{(Eqn 2-5)}$$

For face centered cubic arrangement (sphere layers arranged so that spheres on the second layer sit within the hollows formed by the first layer), packing density is;

$$\rho = \frac{\pi}{3\sqrt{2}} \quad \text{(Eqn 2-6)}$$

Pressure drop is a function of bed height, porosity, particle diameter, bed distribution, fluid viscosity, density and velocity.

## 2.2 Flow through packed beds

The flow through packed beds is complex and is affected by several factors as discussed in earlier sections of the review. The flow can be visualized through two methods; the pipe flow analogy and the discrete particle model. They both predict the pressure drop through packed beds of spherical and near spherical particles but are inappropriate for packed beds with packing material which greatly differ from the spheres (Yang, 2003). The pressure drop through packed beds can be caused by friction due to the resistance at the surface of a particle. Pressure drop also occurs when the flow expands or contracts through the spaces between the particles.

The pipe flow analogy is the most popular approach. It estimates the flow through the packed bed using the flow through a bundle of straight capillaries of the same size. When the porosity of the bed is uniform throughout and less than 0.6, the flow in packed beds can be modelled using an analogy with the flow in pipes. Frictional losses, which have a linear dependency on flow velocity, and inertia, which have a quadratic dependence on flow velocity, can both contribute to pressure drop in packed beds (Nemec & Levec, 2005). The discrete particle model is based on the assumption that the packed beds consist of a collection of discrete particles each of which has a boundary layer through the packed bed.

Fluid flow through packed beds with variable resistance is of practical importance in chemical engineering. The flow resistance is not uniform because the region that is close to the wall has a higher porosity compared to the greater part of the bed resulting in preferential flow. Differences in flow resistance can also arise from the non-uniform packing or from segregation of different sized particles during loading of the packed bed vessel (Szekely & Poveromo, 1975).

Operation of large packed bed reactors becomes complex due to the occurrences of flow maldistribution and hot spot formation. Hotspots can cause sintering of catalyst particles and induce decrease on their activity, whereas flow maldistribution can cause unwanted side reactions due to non-uniform temperature distribution and varying residence times of the reactant. Stanek & Szekely (1972) proposed the non-uniform porosity of the catalyst as giving rise to flow maldistribution.

### 2.2.1 Factors affecting flow through packed beds

Bed to particle diameter ratios

Large diameter packed beds are highly susceptible to gas and liquid maldistribution. It is a general opinion that gases are distributed uniformly within the packing, provided a good initial condition is ensured (Olujic, et al., 1991). It has been seen from experimental work that gas flow maldistribution is a function of the pressure drop in the packed bed, kinetic energy of inlet gas and to a lesser extent, the distance between the inlet and the bottom of the packed bed (Olujic, et al., 1991). If the depth or length of the column is several times larger than its diameter, the gas or fluid will become uniformly distributed

across the column. Shallow packed beds suffer gas maldistribution (Gio, et al., 2019). Shallow packed beds are referred to those whose length or depth is less than their diameter. They are mainly used to reduce gas pressure drop. Packed beds with low aspect ratios (ratio of vessel diameter to particle diameter less than 15) are often used in extremely exothermic processes such as ethylene production and extremely endothermic processes (ie.,steam reforming), where heat can be quickly removed from or added to the packed beds (Yang, et al., 2015). In most cases, there is a higher voidage near the wall of the bed, which gives rise to the wall effect. The concept of the wall effect is reduced by increasing the diameter of the packed bed.

Particle shape

The voidage of a packed bed depends on particle sphericity, particle size, surface roughness, method of packing and the ratio of vessel diameter to particle diameter (Lucks & Bunt, 2011). For a bed with particles of the same size, the voidage increases with decreasing sphericity as shown by the equation (Koekemoer & Luckos, 2015) expressed as,

$$\varepsilon = 1.0 - 0.8648\emptyset + 0.2745\emptyset^2 \qquad \text{(Eqn 2-7)}$$

where, $\varepsilon$ is the voidage and $\emptyset$ is the sphericity.

Equation 2-7 is valid for beds with voidage in the range 0.4 to 1.

Rougher particles have higher voidage than smoother particles. Irregular shaped particles with rough edges would deviate from the regular shaped particles in terms of the resultant voidage.

### 2.2.2 Attrition and particle breakage in packed beds

Solid circulation can lead to particle or catalyst attrition especially in circulating fluidized bed reactors (Effendi, et al., 2002). Particle breakage is also possible in fixed beds as solid catalysts can go under thermal stress during operation of the fixed bed reactor. The loss of catalyst material due to attrition or thermal stress should not be underestimated. It is important to assess particle attrition to reduce fines production, to decrease bed loss, to reduce down-stream residues or erosion and to maintain material activity (Ghods, et al., 2019). Attrition produces fines that cause increased pressure drop and localized bypassing (Rase, 1990).

### 2.2.3 Flow maldistribution, channelling, and bypassing

In irregular packed beds, the void fraction in areas close to the tube wall will approach unity therefore flow through the packed bed is characterized by a channelling effect at the wall (Bey & Eigenberger, 1997). Poor performance in fixed bed processing is commonly caused by channelling (Oliveros & Smith, 1982). Figure 2-10 shows an array of particles showing gas channelling in a packed bed. Poor conversions are generally obtained because of the preferential flows (Fogler, 2006).

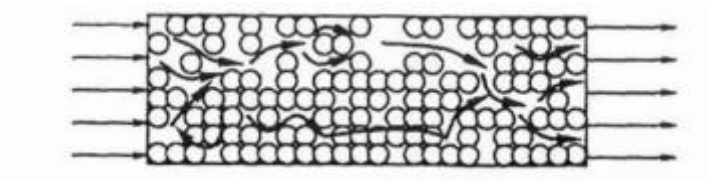

*Figure 2-10: Channelling in a Packed bed (Fogler, 2006)*

Atmakidis & Kenig (2009) studied the influence of confining walls on the pressure drop in different packed bed configurations using computational fluid dynamics. They compared experimental data to several correlations. From their study, they realized that the correlation by de Klerk (de Klerk, 2003), Equation 2-8, accurately describes the differences in porosity close to the confining wall while far from the wall, it yields higher bed porosities than from experiments.

$$\varepsilon(r) = \begin{cases} 2.14z^2 - 2.5z + 1, & z \leq 0.637 \\ \varepsilon_{inf} + 0.29\exp(-0.6z)\left[Cos\left(2.3\pi(z-0.16)\right)\right] + 0.15, & z > 0.637 \end{cases} \quad \text{( Eqn.2-8)}$$

where, $r$ is the radial position, $z$ is the distance from wall, $\varepsilon$ is radial porosity, $\varepsilon_{inf}$ is bed porosity of infinite in diameter packed beds.

Atmakidis & Kenig (2009) noticed that channelling in uniformly packed beds was available through the whole bed resulting in a lower pressure drop than that of an irregular packed bed with the same average void fraction. Carman's correlation (Carman, 1937), Equation 2-8, accurately predicts the pressure drop for small particle Reynolds number but yields underestimated values for higher Reynolds numbers because it does not consider the inertia forces.

$$\Psi = \frac{6^{3-n}k}{Re_p^{2-n}} \frac{(1-\bar{\varepsilon})^{3-n}}{\bar{\varepsilon}^3} \quad \text{(Eqn 2-9)}$$

where, n=1, k=5, $\bar{\varepsilon}$ is average porosity, $Re_p$ is particle Reynolds number

For irregular packing, channelling is not as structured as in the regular geometry. Atmakidis & Kenig (2009) observed that for irregular packing, there was more channelling near the wall than in the inner regions of the packing. This is due to the high local void fraction close to the wall. High velocities were noticed near the confining wall where there was a high void fraction. For irregular packing, their simulation results agreed with the correlations that consider the wall influence.

From comparing their measurements with predictions, (Eisfeld & Schnitzlein, 2001) concluded that the Reichelt's approach of correcting the Ergun equation for the wall is the most promising correlation for pressure drop measurement.

$$\Psi = \frac{K_1 A_w^2}{Re} \frac{(1-\varepsilon)^2}{\varepsilon^3} + \frac{A_w}{B_w} \frac{(1-\varepsilon)}{\varepsilon} \quad \text{(Eqn 2-10)}$$

The wall correction terms are expressed as,

$$A_w = 1 + \frac{2}{3\left(\frac{D}{d_p}\right)(1-\varepsilon)} \quad \text{(Eqn 2-11)}$$

$$B_w = \left[k_1 \left(\frac{d_p}{D}\right)^2 + k_2\right]^2 \quad \text{(Eqn 2-12)}$$

Where, $k_1$ and $k_2$ are coefficients of wall correction term, $K_1$ is the coefficient of pressure drop correlation, D is tube diameter and $\varepsilon$ is the voidage.

With the aid of computational fluid dynamics (CFD), Atmakidis & Kenig (2012) studied the influence of mass transfer in different irregular packed bed configurations. They imitated two methods that were used to determine mass transfer coefficients in literature. They determined the mass transfer coefficient in packed beds by the evaporation of water or hydrocarbons. In this approach, particles which have a constant drying rate and are capable of adsorbing large quantities of water and hydrocarbons are placed into the water or hydrocarbon after which dry air is passed through the impregnated particles. The concentration of water in the inlet and outlet of the packed bed are noted as well as weight of the particles before introducing air and at the end of the measurement. Another system used is the sublimation of naphthalene in air. These methods are only appropriate to use when the fluid medium is a gas. When the fluid medium is a liquid, researchers use systems that involve dissolving solids such as dissolution of benzoic acid in water. Atmakidis & Kenig (2012) used the dissolution of benzoic acid and the sublimation of naphthalene particles in air to determine the mass transfer coefficient. They observed low concentrations of naphthalene and benzoic acid near the confining walls due to channelling. The saturation concentration is reached in areas where the local void fraction is low and at particle contact points because of the low local velocities.

Atmakidis & Kenig (2015) also carried out simulations to determine the residence time distribution (RTD) in irregular packed beds. They injected a non-diffusive tracer into the computational domain using a Dirac function and followed and calculated the concentration of the tracer until it exited the computational domain. They estimated the dispersion coefficient using the numerically calculated tracer concentration at the outlet of the computational domain. In the second method, they used post processing where they solved an additional steady state equation to estimate the local residence time. They found that at low Reynolds numbers, the flow inside the packed bed deviates from the ideal plug flow.

### 2.2.4 Non-ideal flow in packed beds

An ideal fixed bed has perfect mixing, and the bed can be viewed as having perfectly mixed voids. However, in irregularly packed beds, close to the tube wall, the void fraction approaches unity leading to channelling (Inglezakis, 2010). The skin friction tends to reduce to a low value close to the wall (Schwartz & Smith, 1953).

The use of tracers to diagnose flow maldistribution is the most used method (Hanratty & Dudukovic, 1990; Hanratty & Dudukovic, 1992). This is done by injecting the slug of tracer into the reactor entrance stream and then measuring the tracer concentration in the reactor effluent versus time. To measure maldistribution of gas flow, there need to be a tracer that does not diffuse into the catalyst or get absorbed.

The three factors that make up the flow pattern in vessels are the state of aggregation of the flowing material, the residence time distribution, and earliness and lateness of mixing of the material in the vessel (Levenspiel, 1999).

Residence time distribution; recycling of fluid, channelling of fluid, or creation of stagnant regions in the vessel cause deviation from the two ideal flow patterns (mixed flow and plug flow).
State of aggregation of the flowing material; materials exhibit different states of aggregation when they flow, micro fluids, and macro fluids, depending on their nature. Single phase systems lie between the extremes of macro and micro fluids.
Earliness of mixing; for a single flowing stream, the fluid elements mix either early or late as they flow through a vessel (Levenspiel, 1999). Earliness of mixing affects the overall behavior of a system with two entering reaction streams more than it does for a single flowing fluid.

**Channelling of fluid**

In packed beds, the region of greatest void space is the region near the wall of the bed since the packing material cannot fit tightly with the plane wall as it does with itself. Naturally the fluid moves toward the region of greatest void space during its flow. Channelling causes more fluid to be delivered to some areas than others, resulting in poor mass transfer. This leads to poor mixing of reactants and therefore poor conversion of reactants to products. Figure 2-11 shows channelling in process equipment.

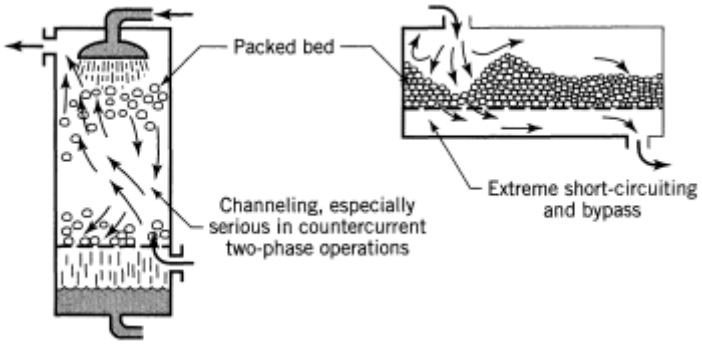


*Figure 2-11: Fluid Channelling in process equipment (Levenspiel, 1999)*

**Stagnant regions**

Stagnant regions within the bed are dead zones which reduce the effective volume of the reactor, resulting in lower residence time and conversion of reactants. Formation of stagnant regions in process equipment is shown in Figure 2-12.

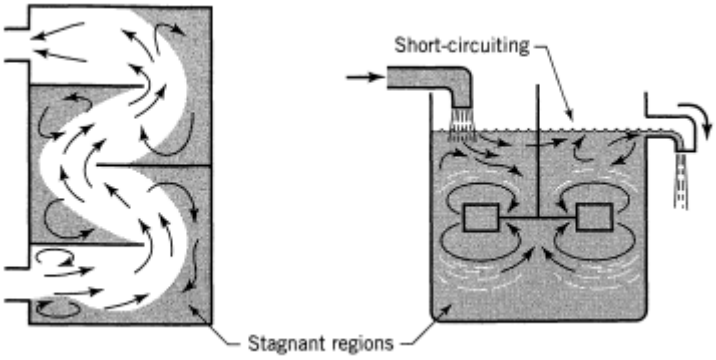


*Figure 2-12: Stagnant regions in process equipment (Levenspiel, 1999)*

**Macrofluid and Microfluid**

A microfluid is a fluid with freely moving, colliding and mixing molecules. Examples of microfluids are gases and thin liquid. A macrofluid is a fluid in which aggregates or globules, each containing large number of molecules of a given age, do not mix with other globules. Examples of macrofluids are non-coalesing droplets and very viscous liquids. The two extremes of aggregation of fluid are shown in Figure 2-13.

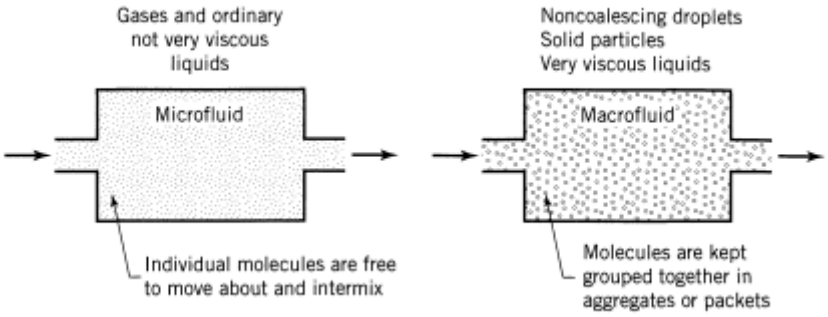


*Figure 2-13: Two extremes of aggregation of fluid (Levenspiel, 1999)*

For macrofluids, each aggregate of macrofluids acts as a separate batch reactor and reacts accordingly. This results in the fluid elements having different compositions. The reaction time for each of these batch reactors equals the time spend by aggregates in the reaction environment. For microfluids, a uniform conversion can be achieved as particles are free to move and collide.

**Earliness of mixing**

In early mixing, the fluids are well mixed at the entry and have more time for reaction, which results in high conversion. Conversely for late mixing, there is no mixing of the fluids at the entry and they only mix well towards the exit, thus, no enough time for reaction and lower conversion achieved. Figure 2-14 shows examples of early and late mixing of fluids. Late mixing favors reaction with the order of reaction less than one (Levenspiel, 1999). This is because the reactant starts at high concentration and react away quickly. On the other hand, early mixing favors reaction with the order of reaction greater than one. This is because the fluid drops instantly to low concentration. Since the rate of reaction drops faster than drop in concentration, it results in lower conversion.

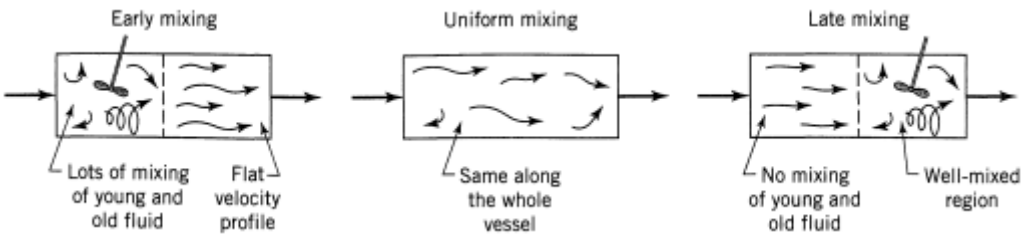


*Figure 2-14: Examples of early and late mixing of fluids (Levenspiel, 1999)*

### 2.2.5 Pressure fluctuations in packed beds

A lot of studies have been conducted on analysis of pressure fluctuations in packed beds (Falkowski, 2003; Trnka, et al., 2000; Alghamdi, et al., 2019; Punˇcochárˇ & Drahoš, 2005). Most of these studies focus on the fluidised-bed reactor. No information was found in literature on the study of pressure fluctuations in fixed bed reactors.

## 2.3 Modelling of flow through packed beds

### 2.3.1 Momentum, heat and mass balances

The momentum, energy and mass balances for the fixed bed reactor presented in this section have been extracted from literature (Eigenberger, 1992; Choudhary, et al., 1976) because they have been well established and have not been originated from first principles.

The momentum balance can be used to determine the pressure drop across the bed, an important operational parameter.

**Momentum Balance**

Ergun (Ergun, 1952) suggested the following relationship, applicable to solid particles travelling through the gas flow at Reynolds numbers lower than 1000.

$$\frac{\Delta P}{L} = 150\frac{(1-\varepsilon)^2}{\varepsilon^3}\frac{\mu U_m}{d_p^2} + 1.75\frac{1-\varepsilon}{\varepsilon^3}\frac{GU_m}{d_p} \quad \text{(Eqn 2-13)}$$

where, $\varepsilon$ is the fractional void volume, $d_p$ is the diameter of solid particles, $U_m$ is superficial fluid velocity measured at average pressure, $\mu$ is absolute viscosity of fluid and $G$ is mass flowrate of fluid ($G = \rho U$).

For higher ranges of Reynold's number, $\frac{Re}{1-\varepsilon} < 10^5$, the KTA method established by Kerntechnischer Ausschuss (KTA) in 1981 (KTA, 1981), can be used to predict pressure drop:

$$\frac{\Delta P}{L} = \varphi\frac{1-\varepsilon}{\varepsilon^3}\frac{1}{d_p}\frac{1}{2\rho}\left(\frac{\dot{m}}{A}\right)^2 \quad \text{(Eqn 2-14)}$$

where $\varphi$ is the coefficient of loss of pressure through friction,

$$\varphi = \frac{320}{\left(\frac{Re}{1-\varepsilon}\right)} + \frac{6}{\left(\frac{Re}{1-\varepsilon}\right)^{0.1}} \quad \text{(Eqn 2-15)}$$

$\dot{m}$ is mass flowrate of the gas in the bed and $A$ is the vessel cross sectional area.

Substituting for $\varphi$ in equation 2-14 and $U_m$ for $\frac{\dot{m}}{A}$:

$$\frac{\Delta P}{L} = 160\frac{(1-\varepsilon)^2}{\varepsilon^3}\frac{1}{d_p}\rho U_m^2 + \frac{3}{Re^{0.1}}\frac{(1-\varepsilon)^{1.1}}{\varepsilon^3}\frac{1}{d_p}\rho U_m^2 \quad \text{(Eqn 2-16)}$$

The vectorial form of the Ergun equation is given by Choudhary, et al., (1976) as:

$$\underline{\nabla} P = \underline{V}(f_1 + f_2 V) = 0 \quad \text{(Eqn 2-17)}$$

$$f_1 = \frac{150\mu(1-\varepsilon)^2}{(\emptyset d_p)^2\varepsilon^3} \quad \text{(Eqn 2-18)}$$

$$f_2 = \frac{1.75\rho(1-\varepsilon)}{(\emptyset d_p)\varepsilon^3} \quad \text{(Eqn 2-19)}$$

where, $\emptyset$ is shape factor

$$V_x\frac{\partial V_x}{\partial x} + V_y\frac{\partial V_x}{\partial y} = \frac{-1}{\rho}\frac{\partial P}{\partial x} - \frac{f_1 V_x}{\rho} - \frac{f_2 V_x V}{\rho} \quad \text{(Eqn 2-20)}$$

$$V_x\frac{\partial V_y}{\partial x} + V_y\frac{\partial V_y}{\partial y} = \frac{-1}{\rho}\frac{\partial P}{\partial y} - \frac{f_1 V_y}{\rho} - \frac{f_2 V_y V}{\rho} \quad \text{(Eqn 2-21)}$$

$$V = \left(V_x^2 + V_y^2\right)^{0.5} \quad \text{(Eqn 2-22)}$$

For an incompressible fluid, the x and y components of the differential version of the Ergun equation are written as (Stanek & Szekely, 1972);

$$\frac{\partial P}{\partial y} = \frac{A\mu G_y}{\rho} + \frac{BG_y}{\rho} \quad \text{(Eqn 2-23)}$$

$$\frac{\partial P}{\partial x} = \frac{A\mu G_x}{\rho} + \frac{BG_x}{\rho} \quad \text{(Eqn 2-24)}$$

$$A = \frac{150(1-\varepsilon)^2}{\varepsilon^3(\emptyset d_p)^2} \quad \text{(Eqn 2-25)}$$

$$B = \frac{1.75(1-\varepsilon)}{\varepsilon^3 \emptyset d_p} \quad \text{(Eqn 2-26)}$$

where G is gas mass velocity ($kgm^{-2}s^{-1}$)

$$shape\ factor = \frac{surface\ area\ of\ sphere\ of\ equal\ volume\ to\ the\ particle}{surface\ area\ of\ particle} \quad \text{(Eqn 2-27)}$$

In their simulation, Bai, et al., 2009, found that for packed beds with spherical particles, the packing porosity is given by;

$$\varepsilon = 1 - \frac{2Nd^3}{3D^2H} \quad \text{(Eqn 2-28)}$$

For packed beds with cylindrical particles, the packing porosity is given by;

$$\varepsilon = 1 - \frac{Nd^2h}{D^2H} \quad \text{(Eqn 2-29)}$$

where, $h$ is height of cylindrical particles, $H$ is height of packed bed, $D$ is inner tube diameter and $d$ is particle diameter.

Stanek & Szekely (1972) did experiments to see the effect of non-uniform porosity in causing flow maldistribution in isothermal packed beds. In their experimental study they showed that the presence of regions of different void fractions can appreciably modify the flow pattern in packed beds.

**Mass Balance in Packed beds**

The reaction for a packed bed reactor is based on the mass of the solid catalyst rather than the volume of the reactor. For heterogeneous systems,

$$-r_A = \frac{mol\ A\ reacted}{s.g\ catalyst} \quad \text{(Eqn 2-30)}$$

The mass of the catalyst is used as it governs the overall rate of product formation. The general mole balance is given by:

$$In - Out + Generation = Accumulation \quad \text{(Eqn 2-31)}$$

For a packed bed reactor;

$$F_{A/W} - F_{A/(W+\Delta W)} + r_A \Delta W = 0 \quad \text{(Eqn 2-32)}$$

Dividing by $\Delta W$ and taking limit as $\Delta W \rightarrow 0$;

$$\frac{dF_A}{dW} = r_A \quad \text{(Eqn. 2-33)}$$

When the pressure drop and catalyst decay are neglected,

$$W = \int_{F_{Ao}}^{F_A} \frac{dF_A}{r_A} = \int_{F_A}^{F_{Ao}} \frac{dF_A}{-r_A} \quad \text{(Eqn. 2-34)}$$

where, W is the catalyst weight necessary to reduce the entering molar flow rate of A, $F_{Ao}$ to a flow rate $F_A$.

$$F_A = F_{Ao} - F_{Ao}X \quad \text{(Eqn 2-35)}$$

where, X is the conversion of reactant A

Differentiating both sides yields,

$$dF_A = -F_{Ao}dX \quad \text{(Eqn 2-36)}$$

Substituting equation 2-36 into equation 2-33,

$$F_{Ao}\frac{dX}{dW} = -r_A \quad \text{(Eqn 2-37)}$$

$$W = F_{Ao}\int_0^X \frac{dX}{-r_A} \quad \text{(Eqn 2-38)}$$

The concentration of reactants and products is insignificantly affected by even large changes in the total pressure. Hence, the effect of pressure drop on the rate of reaction can be ignored for the liquid-phase chemical reactors. Because the concentration of the reactants in gas phase reactions is proportionate to the total pressure, it is crucial to account for the pressure drop. In many instances, accurate accounting of the pressure drop on the reaction system determines whether the reactor operates successfully or not.

**Navier-Stokes Equations**

The Navier-Stokes equations form a set of nonlinear second-order partial differential equations. They are governing equations of Newtonian fluids. The Navier-Stokes equations can be broken down into three fundamental principles; the conservation of mass, conservation of energy and the conservation of momentum that is the first law of thermodynamics (Baker, 2011). For an incompressible laminar flow, the Navier-Stokes equations are expressed in the differential Eulerian form,

$$\nabla v = 0 \quad \text{(Eqn 2-39)}$$

$$\rho\left(\frac{\partial v}{\partial t}+v.\nabla v\right)=-\nabla P+\mu\nabla^2 v+f \quad \text{(Eqn 2-40)}$$

$$\frac{\partial \rho U_i}{\partial t}+\frac{\partial(\rho U_i U_j)}{\partial x_j}=\frac{\partial P}{\partial x_i}+\frac{\partial\left[\mu\left(\frac{\partial U_i}{\partial x_i}+\frac{\partial U_j}{\partial x_i}\right)\right]}{\partial x_j} \quad \text{(Eqn 2-41)}$$

where, $\frac{\partial v}{\partial t}$ is unsteady acceleration , $v.\nabla v$ is the convective or advective term and $-\nabla P$ is the pressure gradient.

If the flow velocity in air is less than 100 m/s and $-\nabla P < 5\%$, the flow is deemed incompressible (Cengel & Cimbala, 2018).

**Heat balance in packed beds**

According to Stanek & Szekely (1973), in the absence of heat generation, the conservation of thermal energy can be written as;

$$G_y\left(\frac{\partial T_g}{\partial y}\right)+G_x\left(\frac{L}{D}\right)\left(\frac{\partial T_g}{\partial x}\right)=\left[\frac{6hL(1-\varepsilon)}{C_{pg}G_o d_p}\right]\left(T_s-T_g\right)-\varepsilon\left(\frac{\rho_g}{\rho_{og}}\right)\left(\frac{\partial T_g}{\partial t}\right) \quad \text{(Eqn 2-42)}$$

$$\frac{\partial T_s}{\partial t}=\left[\frac{6h\rho_g L}{G_o d_p \rho_s C_{ps}}\right]\left(T_g-T_s\right) \quad \text{(Eqn 2-43)}$$

where, the following can normalise of $t$, $T_g$, $T_s$, $T$, $T'$, $t$ and $t'$,

$t=\frac{\grave{t}G_o}{\rho_{og}L}$ dimensionless time

$T_g=\frac{(\grave{T}_g-T_s)}{(T_i-T_o)}$ dimensionless gas temperature

$T_s=\frac{(\grave{T}_s-T_o)}{(T_i-T_o)}$ dimensionless solid temperature

$T$, $T'$ = dimensionless and dimensiona1 temperature, respectively

$t$, $t'$ = dimensionless and dimensiona1 temperature, respectively

### 2.3.2 Numerical methods for solving the balances

Porosity and its distribution over the cross section of the bed is essential for the bed efficiency and mass transfer in the chemical processes considered. Numerical analysis has full control over the process as it has unrestricted access to the structure parameters. It is more difficult to generate numerically a dense random structure than generating a structured packing which has a strictly defined position and orientation of a given element (Marek, 2013).

There are two different numerical approaches that describe the hydrodynamic and transport properties of packed beds (Atmakidis & Kenig, 2009);

The Ergun pressure drop correlation in conjunction with modified Navier-Stokes equations are used to account for the fluid-solid interaction. In this approach, packed beds are treated as pseudo-homogeneous media.

The actual packed bed geometry is considered when simulating the packed bed, which produces a detailed description of the fluid flowing within the gap between the particles and eliminates the need for extra empirical correlation in the porosity distribution.

Different numerical methods, including Finite-element method, Finite-volume method and the Lattice-Boltzmann method (Jurtz, et al., 2019) can be used to solve the momentum, heat and mass balances. Brief description of these methods is presented here.

Finite-element method- this method is rarely used to simulate fixed bed reactors. Some investigators (Motlagh & Hashemabadi, 2008; Lloyd & Boehm, 1994; Dalman, et al., 1986) used the finite-element method for simulating the fluid dynamics and heat transfer of very small packed beds. Although the finite element method is mainly used for computational solid and structural mechanics, it has also found application in fluid dynamics. It is one of the numerical methods widely used owing to its flexibility. The finite element method divides the domain of the problem into subdomains. Each subdomain will be represented by a set of element equations to the original problem. All sets of element equations will then be combined into a global system.

Finite-volume method solves the governing equations by the dividing a domain into a finite number of sub-volumes. The total integral of the flux over each sub-volume will then be approximated (Baker, 2011). Nowadays, the Finite-volume method is being used for most of the numerical work done in fixed bed reactors (Jurtz, et al., 2019). This is because of its applicability on unstructured meshes. One of the beneficial characteristics of the Finite-volume method is its noninvasive boundary conditions, as the variables are stored in the cell centers and the boundary condition acts on the surface.

Lattice-Boltzmann method -When compared to finite-volume method and finite-volume method as a method for solving systems of partial differential equations, the Lattice-Boltzmann method's drawback is that it might not be able to solve simulations involving conjugated heat transfer because doing so would require either a more intricate discretization of the velocity space or the incorporation of a separate temperature distribution function, both of which would increase computational effort and potentially promote instabilities (Jurtz, et al., 2019). The Lattice-Boltzmann method considers the behavior of a collection of particles as a unit. This approach assumes that continuous mechanical phenomena are the result of statistical averaged effects on a molecular level. Only a representative number of particles are taken and allowed to move on a discrete lattice as taking all the elements and interactions would cause an immense numerical effort. A sequential collision step allows for the exchange of momentum and energy, followed by the motion of the particles along the lattice, called streaming.

Some approaches use Discrete Element Method (DEM) simulations for bed generation (Marek, 2013).

### 2.3.3 Computational fluid dynamics

Computational modelling is the use of computers to study complex systems using mathematics, physics and computer science. Computational fluid dynamics is a computational modelling approach used to numerically solve physical phenomena involving fluid flows and heat transfer (Yan & Tu, 2023). To provide insight in flow patterns, computational fluid dynamics (CFD) is used to simulate packed beds (Jafari, et al., 2008). This saves times and money. CFD technique can be useful for obtain shorter product-process development cycles, to optimize existing processes, to optimize energy requirements and efficiently design new products and processes. Modelling and simulation are essential tools in the design of packed bed reactors, and as the performance requirements of these reactor are growing, it is required that the proposed model be able to define not only spatial distribution of involved fluids but also velocity profiles within the reactor (Jafari, et al., 2008). According to Marek (2017), computational fluid dynamics and computational methods modelling can be divided into two groups,

Based on averaged equations, without accounting for the microscopic details of the bed structure.
Directly treating the complex structure of the bed.

## 2.4 Pressure fluctuations and vibration induced by flow in packed beds

Vibration of pipes or pipe sections due to internal flow has been common in industrial plants and pipelines (Udoetok, 2018). Sources of vibrations in piping systems and vessels could be any or a combination of the following:

Pumps
Fans
Valves
Pressure fluctuations
Weak foundation and support systems
Internal fluid flow

Flow induced vibration is induced by flow velocity (PI Process Instrumentation, 2020). Pipes and process vessels have tendencies of vibrating at their natural frequencies. Each natural frequency has a definite and unique shape, called mode shape, which the replica dynamic deformation will assume when vibrating at the frequency. These modes and natural frequencies depend on the distribution of mass and stiffness through the piping system. The distribution is influenced by the wall thickness, fluid density, location of lumped masses, piping or vessel diameter, material properties and piping support. The relationship between the frequency and pattern of the applied excitation and the natural frequency of the pipe determines how the pipe responds to the applied excitation. When it is excited by a dynamic excitation which has a frequency that matches with one of its natural frequencies, a piping system undergoes great displacements and stresses. This phenomenon is known as resonance, and it can cause

high vibration (PI Process Instrumentation, 2020). Since the flow inside pipes is like the flow inside process vessels, maldistribution inside process vessels can therefore be checked by monitoring the vibrations of the process vessels.

The natural frequency shift refers to a change in the resonant frequency of a system or structure due to various factors such as alterations in its physical properties (mass, stiffness and damping), environmental conditions, or external influences. The natural frequency is inversely proportional to the mass on the system (Blevins, 2016). Adjustments in mass on a system or operating conditions can alter the natural frequency. The fundamental natural frequency of a pipe carrying a flowing fluid decrease as the flowrate increases. It would be possible to device a technique to measure the flow based on the natural frequency shift. The sensitivity of the technique for relatively low flow rates is poor. For higher flowrates, the natural frequency is significantly higher (Evan, et al., 2004).

Vibration helps the transition from random close packing (packing density approximately 0.60) to random close packing (packing density approximately 0.64) (An, et al., 2009).

According to Evan et al (2004), the flow rates in the pipe could be linearly related to the transverse vibrations into it,

$$\frac{\partial^2 r}{\partial t^2} = -\frac{g}{A\gamma} EI \frac{\partial^4 r}{\partial x^4} = -\frac{g}{A\gamma} \acute{p}(x) \qquad \text{(Eqn 2-44)}$$

where,$x$ is the length along axial direction, $r$ = radial length, $g$= gravity, $A$ is cross sectional area of the beam, $EI$ is flexural rigidity and $\gamma$ is the specific weight of the beam.

Several studies have shown that pressure fluctuations in packed beds are linked to a change in the bed parameters and these fluctuations can be used to diagnose the performance of the packed bed reactor. Most of these studies were carried on fluidised bed reactors (Schouten & van den Bleek, 1998) (Trnka, et al., 2000) (Falkowski, 2003) (Xiang, et al., 2017).

## 2.5 Modal analysis of pressure fluctuations in vessels

Modal analysis is used to describe the dynamic properties of a structure in terms of the modal properties; damping factor, natural frequency, modal shape and modal mass. Modal analysis can be done mathematically or experimentally. Mathematical modal analysis tries to uncouple equations so that each equation can be solved separately. Numerical approximations such as boundary-element and finite element methods are used when exact solutions are not possible (Rossing, 2014).

### 2.5.1 Mathematical transformations

Pressure is mainly used to characterize fluid dynamics in packed beds because it is easy to measure, even under harsh industrial conditions. Pressure measuring equipment are also relatively cheap and virtually non-intrusive (Van Ommen, et al., 2011).

Time series signals can be analyzed in three different ways (Xu, et al., 2004):

Statistical analysis or state space methods

Frequency analysis or frequency domain methods

Chaotic analysis or time domain methods

The Fast Fourier Transform (FFT) is used to analyze fluctuations in pressure signals in the frequency domain. Power spectral density analysis involves the investigation of the changes in the power spectra because of the changes in the dynamic behavior of the system, which is used to provide a quantitative description of the fluidization regimes in a column. The FFT is a mathematical tool that is used to determine the power spectral density analyses by converting a signal which is a function of time into a signal which is a function of frequency (Gyan, et al., 2014).

As can be seen in Figures 2-15 and 2-16 below, waveforms plotted in Microsoft Excel generally show the magnitude (Y axis) versus time (X axis). When the period of the waveform is known, the frequency can be calculated. The frequency spectrum (Figure 2-16) enables you to view a waveform according to its frequency content.

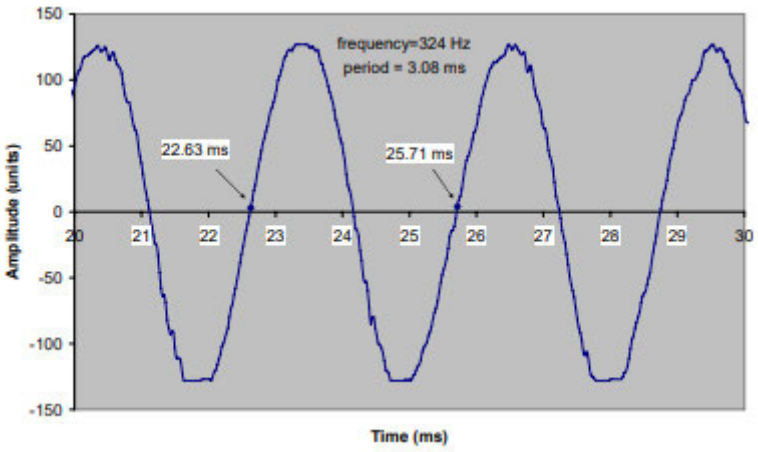


*Figure 2-15: Data in time domain (Klingenberg, 2005)*

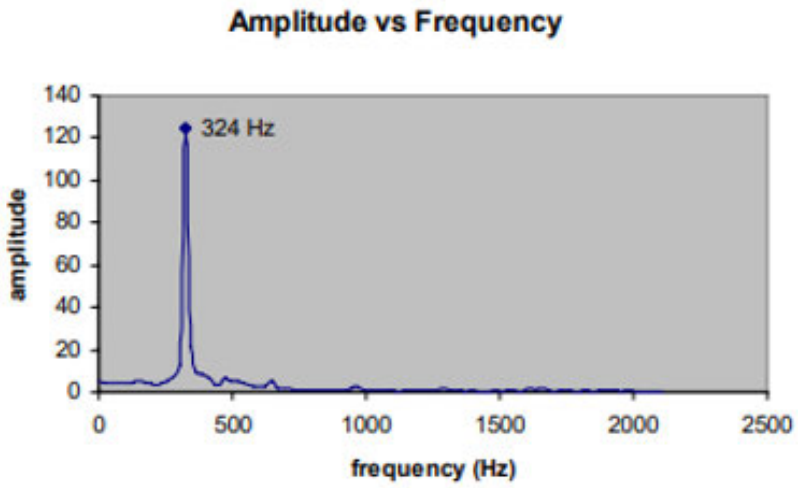


*Figure 2-16: Data in frequency domain (Klingenberg, 2005)*

Literature has only reported diagnosing of flow maldistribution while the unit is offline for example using tracers (Hanratty & Dudukovic, 1990). There is no reported method for online diagnosis of flow maldistribution in packed beds. Although modal analysis of pressure fluctuations has been analysed before, it has been used for characterising flow in fluidised bed reactors (Trnka, et al., 2000) (Schouten & van den Bleek, 1998) and no information is recorded to characterise flow in fixed bed reactors using the same method. It is necessary to investigate if pressure fluctuations can also be used to characterise the flow regime in fixed bed reactors.

# 3. CHAPTER 3: EXPERIMENTAL EQUIPMENT AND METHODS

This chapter gives the detailed experimental procedures done on two different sized vessels as well as the equipment used, the equipment setup as well as the parameters that were being measured. The chapter is divided into two sections. The first section describes the experiments performed using the small vessel while the second section describes the experimental work on the larger vessel.

## 3.1. Small Vessel Experiments

### 3.1.1 Experimental Equipment

The equipment used consisted of a hollow metal tube of height 48.3 cm and 10 cm diameter, which was obtained by welding together two smaller pieces of tubing. Other equipment included a large rotameter, black plastic tubing (6 mm diameter, 1 mm thickness) to connect the airline to the vessel, plugs to seal the extra holes on the vessel, tee-pieces to connect multiple tubes to the top and bottom of the vessel, and a stand to mount the equipment to. Two different rotameters were used. The first rotameter had maximum rotameter flowrate given as 272 $dm^3$/minute and calibrated at 85kPa and 20˚C. The second rotameter had maximum rotameter flowrate given as 50 $dm^3$/minute and calibrated at 100kPa and 20˚C. The experimental setup can be seen in Figure 3-2. The type of packing used in this experiment were large glass Raschig rings of 11 mm length by 15 mm outer diameter, and small packing of 7 mm length by 7 mm outer diameter.

This piping and instrumentation diagram (Figure 3-1) of the packed bed system was drawn with the use of Microsoft Visio™ software.

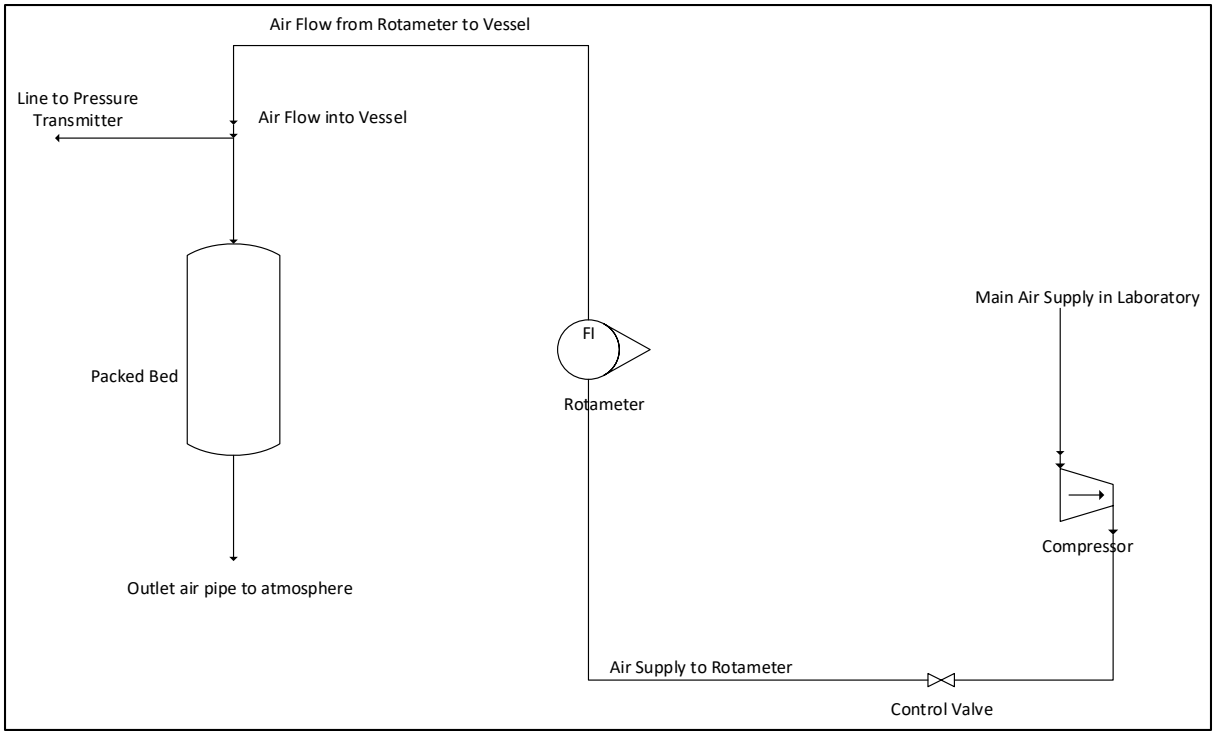


*Figure 3-1:Schematic representation of experimental equipment setup*

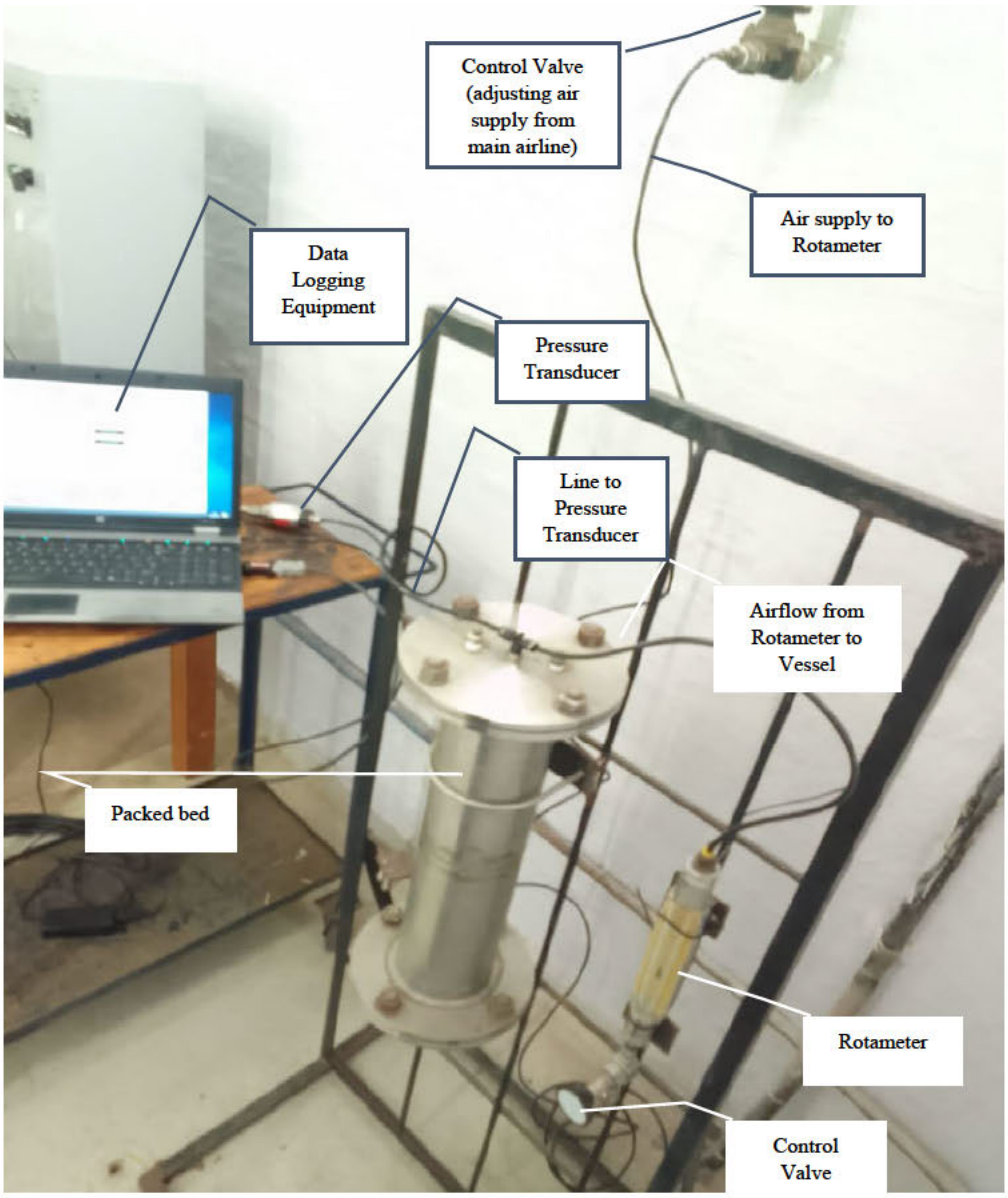


*Figure 3-2:Experimental equipment setup*

### 3.1.1 Experimental Conditions

The experiments were performed using different gas flow rates, with pressure measurements taken at the top of the vessel. The flow rates used were based on a percentage of the maximum allowable flow rate on the rotameter. The conversion of the percentages to actual flowrates is shown in Appendix G. All experiments were carried out at room temperature (~25-27 ˚C). The pressure-time data was recorded using the WIKA™ software on a laptop, by connecting a WIKA model D-10-P pressure transmitter to the side of the vessel on which the pressure was required and the other end to the computer. The pressure transmitter had a range of 0 to 2000kPa.

### 3.1.2. Experimental Setup

Three control runs with an empty vessel were first carried out. A distance of 2.5 cm was left between the air distributor and the top of the packing, to allow the air to evenly distribute before flowing through the packing.

The procedure for the normal packing (Raschig rings of 11 mm length by 15 mm outer diameter) consisted of passing compressed air through the packed tube of large rings at the specified flow rate. A stabilisation time (~10 minutes) was allowed before starting the software to measure the pressure-time data for each run (~20 minutes). The procedure was repeated at various flow rates.

For the mixed packing arrangement, a 4 cm diameter by 48 cm length PVC pipe of 2 mm thickness was inserted into the vessel and the pipe was filled with the smaller glass Raschig rings packing (7 mm length by 7 mm outer diameter), while the rest of the tube was filled with the large packing. After carefully removing the PVC pipe, two regions with different void fractions were created in the packed bed. Experiments were carried out using uniform and mixed packing arrangements, to investigate if there could be any difference in pressure and if any fluctuations could occur.

The following steps were taken;

1) a. For uniform packing, the large size Raschig rings were filled to the desired height in the vessel. This height was measured at 4 positions along the inner shell of the column. Figure 3-4 shows the uniform packing arrangement.

b. For non-uniform packing, the bed was configured by putting a vertical pipe into the bed then filling the pipe with a given size of Raschig rings. The rest of the bed was filled with Raschig rings of a different size from those loaded in the pipe. The pipe was removed carefully to prevent breakage. Figures 3-5—3-10, show the non-uniform packing arrangement.

2) The flanges were assembled, and the vessel was sealed. The compressed air feed was fitted directly into the inlet port of the vessel.

3) The compressed air rotameter was opened to a predetermined flowrate of 30 $dm^3$/minute. The vessel was checked for air leaks before data acquisition.

4) Compressed air was opened to a fixed rotameter flowrate and a 10-minute stabilisation time was allowed before starting to take pressure-time readings

5) Pressure-time readings were taken for 20 minutes

Table 3-1 shows the physical characteristics of the Raschig rings.

*Table 3-1: Borosilicate glass Raschig rings dimensions*

| | **Large** | **Small** |
|---|---|---|
| **Internal Diameter mm** | 13 | 5 |
| **Outer Diameter mm** | 15 | 7 |
| **Length mm** | 15 | 7 |
| **Wall Thickness mm** | 1 | 1 |
| **Density g/cm$^3$** | 2.23 | 2.23 |

### 3.1.3 Experimental Configuration

As previously mentioned, two sizes for the Raschig rings were used as the packing material. These were arranged such that any given portion of the packed bed contained only uniformly sized packing material. To provide a severe test for flow maldistribution, a wide range of packed bed configurations were examined. Figure 3-3(a)-(d) represents the various packed bed configuration; the hatched zone denotes the region that was packed with larger particles having diameter, length and thickness as 15 mm, 15 mm and 1 mm respectively while the solid zone corresponds to regions packed with smaller Raschig rings of 7mm×7mm×1mm. The solid zones show the region offering a higher resistance to flow. Figures 3-4 to 3-10 show how different the packing configurations were achieved in the packed bed.

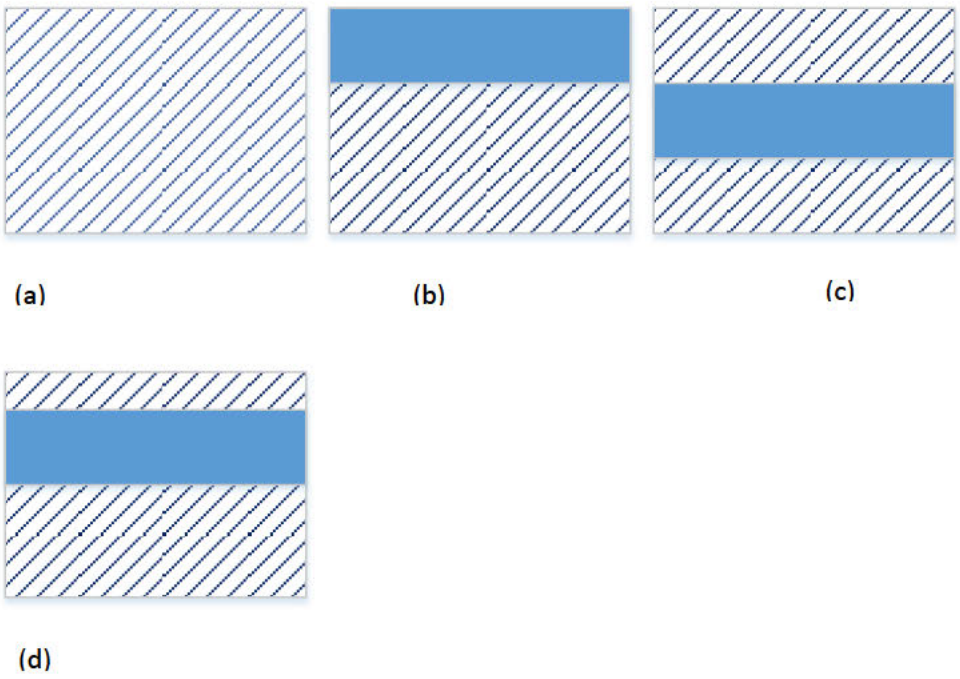


*Figure 3-3: Various packed bed configurations; hatched zone represents the large particle packing, while solid filled zones represent the small particle packing*

*Figure 3-4: Uniform Packing Arrangement*

*Figure 3-5: Non-Uniform Packing Arrangement (Small packing at the side)- Loading Process*

*Figure 3-6: Non-Uniform Packing Arrangement (Small packing at the side)- During Experiments*

*Figure 3-7: Non-Uniform Packing Arrangement (Small packing at the center)- Loading Process*

*Figure 3-8: Non-Uniform Packing Arrangement (Small packing at the center)- During Experiments*

*Figure 3-9: Non-Uniform Packing Arrangement (Small packing at middle (midway between center and side))- Loading Process*

*Figure 3-10: Non-Uniform Packing Arrangement (Small packing at middle (midway between center and side))- During Experiments*

## 3.2. Large Vessel Experiments

### 3.2.1 Experimental Equipment

The equipment that was used, consisted of a steel pipe of 4 m length and 0.41 m diameter. Other equipment included the following,

A large rotameter (ranging from 1.67 $dm^3$/minute to 16.67 $dm^3$/minute )
Black plastic tubing (6 mm diameter, 1 mm thickness) to connect the airline to the vessel
Plugs to seal the extra holes on the vessel, tee-pieces to connect multiple tubes to the top and bottom of the vessel, and a stand to hold the equipment.

The maximum flowrate of rotameter was 16.67 $dm^3$/minute and was calibrated at 700kPa and 25˚C. The experimental setup was the same as can be seen in Figure 3-1. The type of packing used in this experiment were large PVC rings of 50 mm length by 50 mm outer diameter, and small packing of 20 mm length by 20 mm outer diameter. Figures 3-11－3-14 show the experimental setup in four pictures. Figure 3-11 shows the large vessel and the port used to empty the vessel. Figure 3-12 shows the gas outlet from the vessel. Figure 3-13 the air supply connections. Figure 3-14 shows the data logging equipment as well as the pressure transducer.


*Figure 3-11:Experimental equipment setup*


*Figure 3-12: Experimental equipment setup*

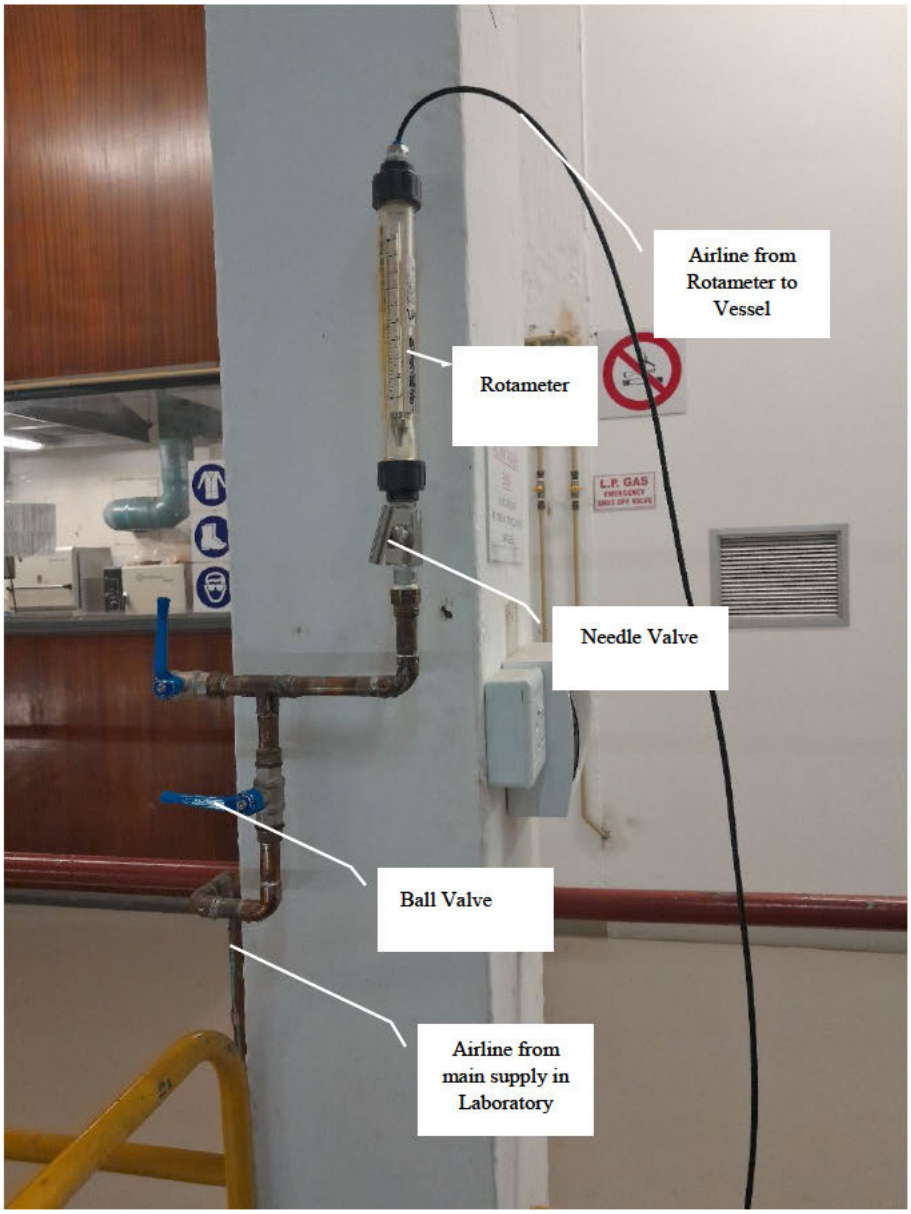


*Figure 3-13: Experimental equipment setup*

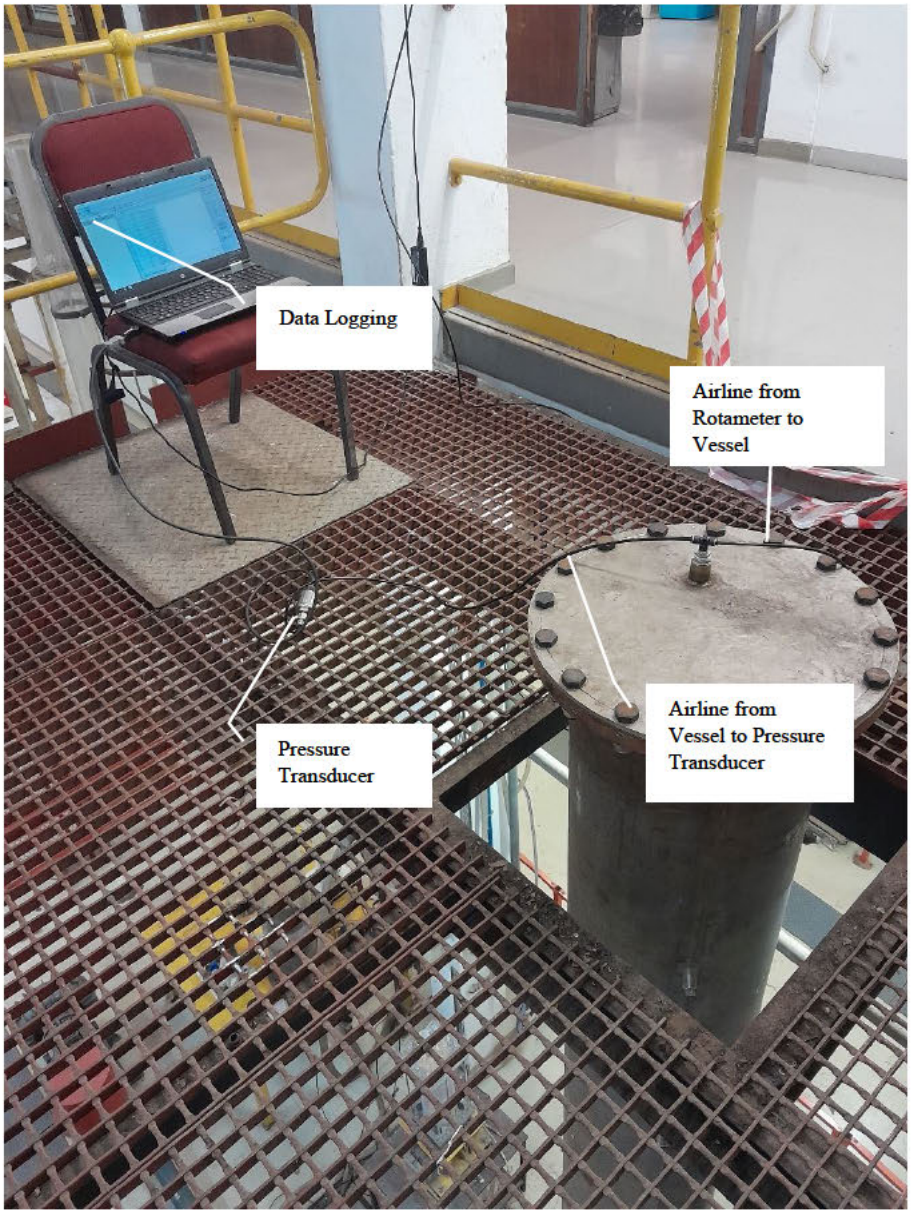


*Figure 3-14: Experimental equipment setup*

### 3.2.2 Experimental Conditions

The experiments were performed at five different flow rates (1.67 $dm^3$/minute, 2 $dm^3$/minute, 2.33 $dm^3$/minute, 2.67 $dm^3$/minute and 2.83 $dm^3$/minute), with pressure measurements obtained at the top of the vessel. The flow rates used were based on a percentage of the maximum allowable flow rate of 16.67 $dm^3$/minute by the rotameter. The conversion of the percentages to actual flowrates is shown in Appendix G. All experiments were carried out at room temperature (~25-27 ˚C). The pressure-time data was recorded using the WIKA™ software on a computer, by connecting a WIKA model D-10-P pressure transmitter to the vessel and computer as shown in Figure 3-14. The pressure transmitter has a range of 0 to 2000 kPa.

### 3.2.3. Experimental Procedure

Initially, eight control runs with the vessel emptied were carried out at each rotameter flowrate. Two sets of experiments were conducted, with a fully packed vessel and with the vessel packed to 75% full. A fully packed vessel meant leaving a 30cm distance between the air distributor and the top of the packing, to allow the air to evenly distribute before flowing through the packing.

The procedure for the normal packing (PVC rings of 50 mm length by 50 mm outer diameter) consisted of passing compressed air through the packed tube of large rings at the specified flow rate. A stabilisation time (~10 minutes) was allowed before starting the software to measure the pressure-time data for each run (~20 minutes). The procedure applicable to the top of the vessel, was repeated corresponding to a range of flow rates.

In case of the mixed packing arrangement with 75% of full vessel, a 0.19 m diameter by 3 m length PVC pipe of 10 mm thickness was inserted into the vessel. The pipe was filled with the smaller PVC rings packing (20 mm length by 20 mm outer diameter), while the rest of the tube was filled with the large packing. After carefully removing the PVC pipe, two regions with different void fractions were created in the packed bed. Experiments were carried out using uniform and mixed packing arrangements, to investigate if there could be any difference in pressure and if any fluctuations could occur. For the 100% packing, a 0.19 m diameter by 4 m length pipe was used to load the smaller PVC rings.

The following steps were taken;

1) a. For uniform packing, the large size PVC rings were filled to the desired height in the vessel. This height was measured at 4 positions along the inner shell of the column. Figure 3-2(a), shows the uniform packing arrangement.

b. For non-uniform packing, the bed was configured by putting a vertical pipe into the bed then filling the pipe with a given size of PVC rings. The rest of the bed was filled with PVC rings of a different size from those loaded in the pipe. The pipe was removed carefully to prevent breakage. Figures 3-2(b) and 3-2(c), show the non-uniform packing arrangement.

2) The flanges were assembled, and the vessel was sealed. The compressed air was fed directly through the inlet port into the vessel.

3) The compressed air rotameter was operated to a predetermined flowrate. The vessel was checked for air leaks before data acquisition.

4) When the compressed air was allowed to go through a fixed rotameter, a 10-minute time was waited for stabilisation of flowrate before starting to note pressure-time readings.

5) Pressure-time readings were taken for 20 minutes

Table 3-2 below shows the physical characteristics of the packing material used in the large vessel.

*Table 3-2: PVC rings dimensions*

| | Large | Small |
|---|---|---|
| **Internal Diameter mm** | 42.28 | 16.64 |
| **Outer Diameter mm** | 50 | 20 |
| **Length mm** | 50 | 20 |
| **Wall Thickness mm** | 3.86 | 1.68 |

### 3.2.3 Experimental Configuration

As previously mentioned, two sizes for the PVC rings were used as the packing material. These were arranged such that any given portion of the packed bed contained only uniformly sized packing material. To provide a severe test for flow maldistribution, a wide range of packed bed configurations were examined. Figure 3-3(a)-(c) represents the various packed bed configuration; the solid zone denotes the region that was packed with smaller particles having outer diameter, length and thickness corresponding to 20 mm, 20 mm and 1.68 mm respectively while the hatched zone corresponds to regions packed with larger PVC rings of by 50 mm by 50 mm by 3.86 mm. Figures 3-15 to 3-18 shows the packing arrangements as well as how the packing arrangements were achieved.

*Figure 3-15: Uniform Packing Arrangement*

*Figure 3-16: Non-Uniform Packing Arrangement (Small packing at the side)- During Vessel Loading*

*Figure 3-17: Non-Uniform Packing Arrangement (Small packing at the side)- During Experiments*

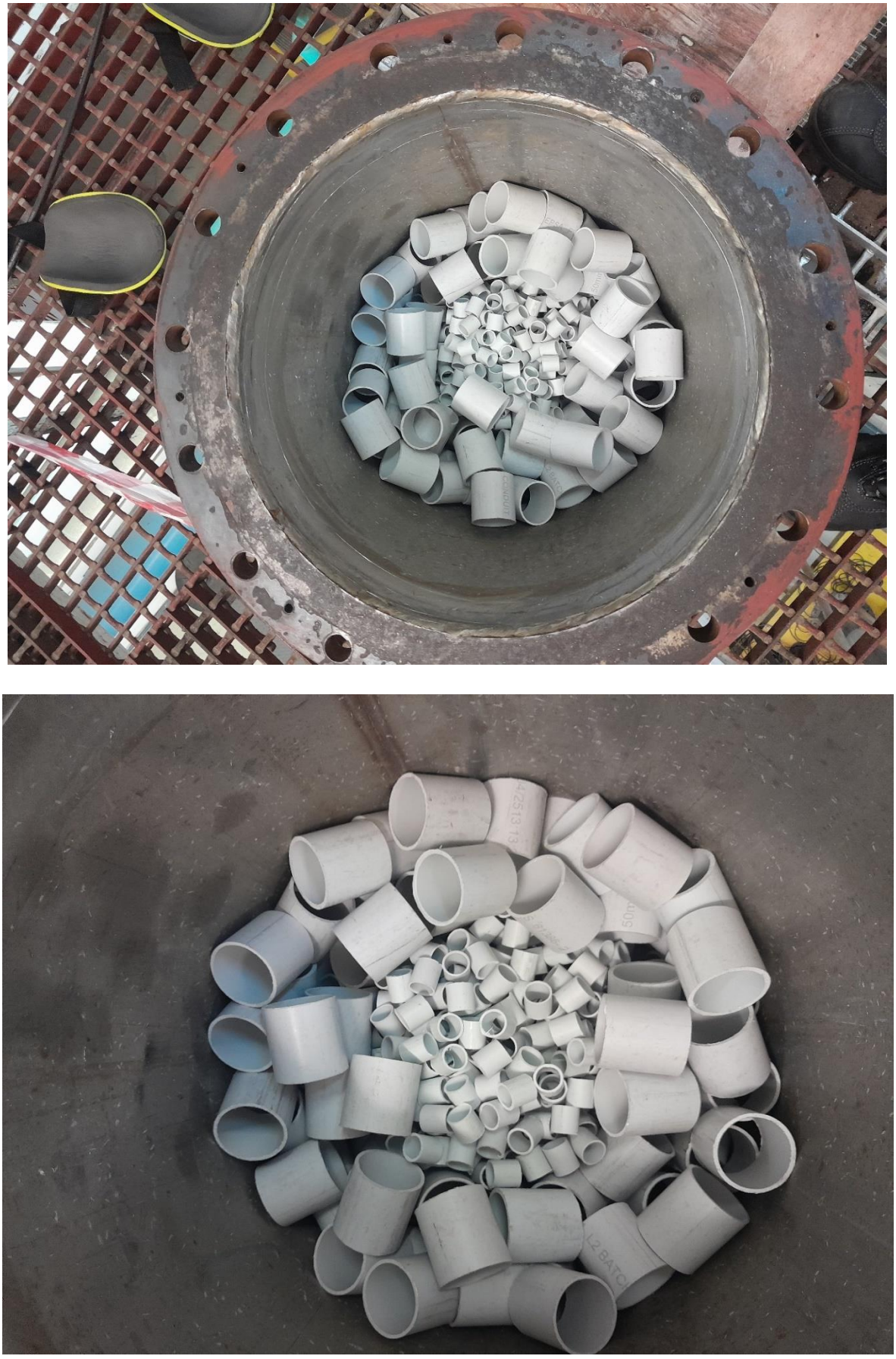

*Figure 3-18: Non-Uniform Packing Arrangement (Small packing at the center)*

The pressure data was first normalized, and the normalized data was smoothed using MATLAB's Savitky-Golay filter. Figure 3-19 below shows how the comparison between the normalized and smoothed data for a uniformly packed vessel at 54.40 $dm^3$/minute rotameter flowrate.

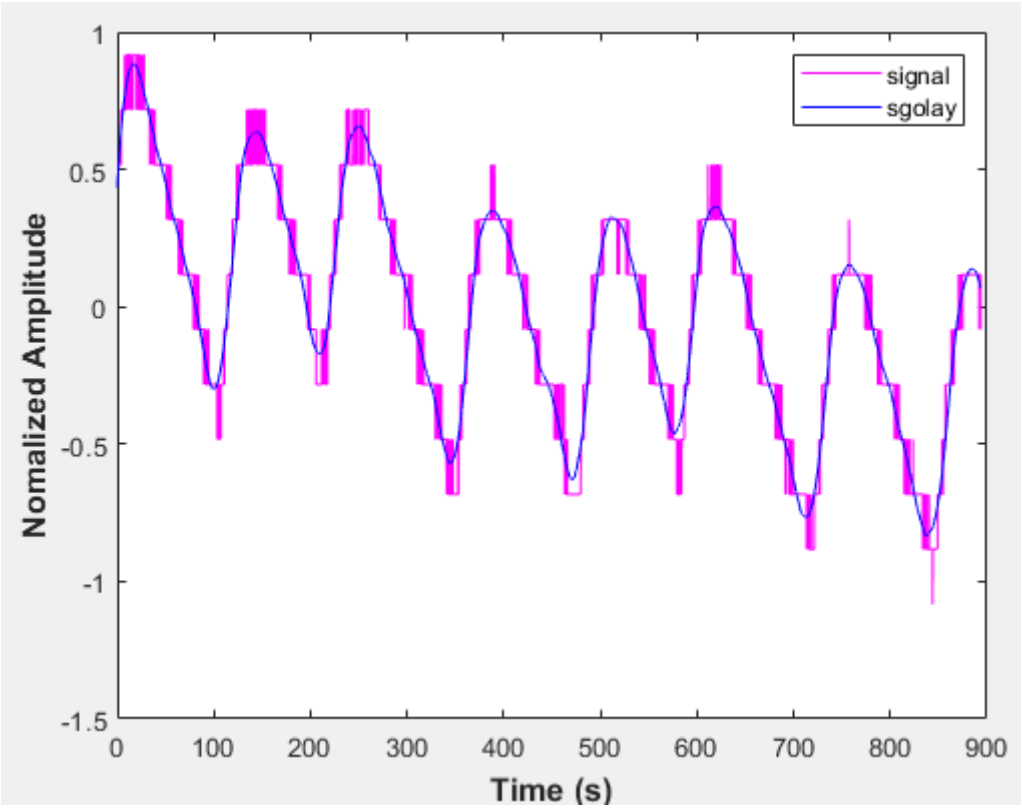


*Figure 3-19: Comparison of raw data and smoothed signal data*

Form Figure 3-19 the purple curve is the raw normalized data curve while the blue line is the curve after applying MATLAB's Savitky-Golay filter on the raw data.

Several models of non-ideal reactors have been outlined in literature (Fogler, 2006). These models can be used to approximate pressure drop as well as pressure fluctuations when there is flow maldistribution in packed beds. Different combinations of ideal reactors can be used to model the different packing arrangements that can be found in fixed beds.

# 4. CHAPTER 4: MODEL DEVELOPMENT

This chapter develops models for the packed bead reactor using different models for idea and non-ideal reactors provided from literature (Fogler, 2006; Levenspiel, 1999). Three different models were developed based on the packing arrangement in the vessel. The sections below discuss the different models in detail.

## 4.1 MODEL ARRANGEMENT 1- Uniform Packing

Model arrangement 1, shown in Figure 4-1, illustrates the case where the vessel is uniformly packed. Several cases with different conditions were analyzed, where X is input pressure and Y is output pressure.

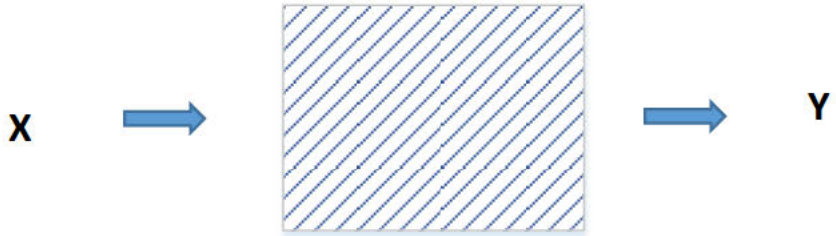


*Figure 4-1: Uniform Packed Bed*

**Case 1: Constant Gas Velocity**

Assuming that the gas velocity is constant, the change in pressure between the inlet and outlet pressure is given as,

$$P_{in} - P_{out} = \Delta P \qquad \text{(Eqn 4-1)}$$

$$P_{out}(t) = P_{in}(t) - \Delta P \qquad \text{(Eqn 4-2)}$$

where, $P_{in}$ is the inlet pressure (Pa), $P_{out}$ is the pressure at the outlet (Pa) and $\Delta P$ is the change in pressure (Pa)

### 4.1.1 Gas Pressure drop as a constant fraction of inlet pressure

When the pressure drop is a constant fraction of the inlet pressure,

$$\Delta P = b(P_{in}(t)) \qquad \text{(Eqn 4-3)}$$

Where b is the fraction of inlet pressure.

Therefore, equation 4-1 becomes:

$$P_{in} - P_{out} = b(P_{in}(t))$$

$$P_{out} = P_{in} - b\big(P_{in}(t)\big) = P_{in}(1 - b)$$

Leading to the ratio between output and input pressure,

$$\frac{P_{out}}{P_{in}} = (1 - b) \quad \text{(Eqn 4-4)}$$

Because the inlet pressure varies with time, substituting for equation 4-3 into equation 4-2;

$$P_{out}(t) = P_{in}(t) - b(P_{in}(t)) \quad \text{(Eqn 4-5)}$$

$$P_{out}(t) = P_{in}(t)\lfloor(1 - b)\rfloor$$

Gas inlet pressure is a sine function as it originates of compression.

$$P_{in}(t) = ASin(wt) \quad \text{(Eqn 4-6)}$$

Upon re-arranging Equation 4-6 and applying a Laplace Transforms (As shown in Appendix G, Equations G-2–G11), the pressure is given by,

$$P(t) = \frac{(b-1)\big(ACos(wt)\big)}{w} - \frac{A(b-1)}{w} \quad \text{(Eqn 4-7)}$$

### 4.1.2 Gas pressure drop as a non-constant fraction of inlet pressure

When the pressure drop is not a constant fraction of the inlet pressure, change in pressure is affected by diameter and porosity of the catalyst in the packed bed reactor.

Where, the relation between the gas leaving the vessel with respect to time is expressed as,

$$P_{out}(t) = P_{in}(t) - \Delta P$$

$$P_{out}(t) = ASin(wt) - \Delta P \quad \text{(Eqn 4-8)}$$

Whereas the pressure drop in a packed bed is given by the Ergun equation (Ergun, 1952);

$$\frac{\Delta P}{L} = 150\frac{(1-\varepsilon)^2}{\varepsilon^3}\frac{\mu.u}{d_p^2} + 1.75\frac{(1-\varepsilon)}{\varepsilon^3}\frac{\rho u^2}{d_p} \quad \text{(Eqn 4-9)}$$

where, $L$ is the length of the packed bed (m), $\varepsilon$ is the porosity of the catalyst, $\mu$ is the dynamic viscosity of the fluid (Pa. s), $u$ is superficial fluid velocity measured at average pressure (m/s), $d_p$ is the diameter of the catalyst (m) and $\rho$ is the density of the fluid (kg/m$^3$).

Taking a Laplace Transform on equation 4-8 as shown in Appendix G (Equations G-12—G-17), the pressure is given by,

$$P(t) = \frac{A}{w} - \frac{Acos(wt)}{w} - \Delta Pt \qquad \text{(Eqn 4-10)}$$

**Case 2:** Change in gas velocity with change in inlet pressure.

Change in gas velocity as a result of change in inlet pressure, can be related owing to the Ideal gas law, expressed as,

$$P_{in}\dot{V} = \dot{n}RT \qquad \text{(Eqn 4-11)}$$

where, $\dot{V}$ is the volumetric flowrate of the fluid (m$^3$/s), $\dot{n}$ is the molar flowrate of the fluid (mol/s), $R$ is the ideal gas constant (J/$^o$C Mole) and $T$ is the temperature ($^o$C)

Re-arranging Equation 4-11,

$$\dot{V} = \frac{\dot{n}RT}{P_{in}} \qquad \text{(Eqn 4-12)}$$

$$u = \frac{\dot{V}}{A_x} \qquad \text{(Eqn 4-13)}$$

Where $A_x$ is the cross-sectional area of the reactor. With substitution of $\dot{V}$ from Equation 4-12 into Equation 4-13, the following results,

$$u = \frac{\dot{n}RT}{P_{in} \times A_x} \qquad \text{(Eqn 4-14)}$$

So, the RHS of equation 4-2:

$$P_{out}(t) = P_{in}(t) - \Delta P$$

becomes

$$P_{out}(t) = f[P_{in}(t)] \quad \text{(Eqn 4-15)}$$

Pressure drop across a packed bed is given by,

$$\frac{\Delta P}{L} = 150\frac{(1-\varepsilon)^2}{\varepsilon^3}\frac{\mu.u}{d_p^2} + 1.75\frac{(1-\varepsilon)}{\varepsilon^3}\frac{\rho u^2}{d_p} \quad \text{(Eqn 4-16)}$$

Substituting for $u$ in equation 4-16 yields,

$$\frac{\Delta P}{L} = 150\frac{(1-\varepsilon)^2}{\varepsilon^3 d_p^2}\mu\left(\frac{\dot{n}RT}{P_{in}A_x}\right) + 1.75\frac{(1-\varepsilon)}{\varepsilon^3 d_p}\rho\left(\frac{\dot{n}RT}{P_{in}A_x}\right)^2 \quad \text{(Eqn 4-17)}$$

Which can be simplified as,

$$\frac{\Delta P}{L} = \frac{B}{P_{in}} + \frac{C}{{P_{in}}^2} \quad \text{(Eqn 4-18)}$$

Where,

$$B = 150\frac{(1-\varepsilon)^2}{\varepsilon^3 d_p^2}\mu\left(\frac{\dot{n}RT}{A_x}\right)$$

$$C = 1.75\frac{(1-\varepsilon)}{\varepsilon^3 d_p}\rho\left(\frac{\dot{n}RT}{A_x}\right)^2$$

Substituting for $\Delta P$ in equation 4-2 yields,

$$P_{out}(t) = P_{in}(t) - \frac{B}{P_{in}} - \frac{C}{{P_{in}}^2} \quad \text{(Eqn 4-19)}$$

Where $P_{in}(t) = ASin(wt)$

## 4.2 MODEL ARRANGEMENT 2- NON-UNIFORM PACKING (with small packing at the side of the vessel)

Figure 4-2 shows the model arrangement 2 where small diameter catalyst is along the side of the vessel while the other portion of the bed is packed with large diameter catalyst. This packing arrangement resembled catalyst breakage at the wall of the vessel. This type of model arrangement was schematically represented in Figure 4-3 as 2 different packed beds in parallel.


*Figure 4-2: Non-Uniform Packed Bed (small packing at the wall side)*

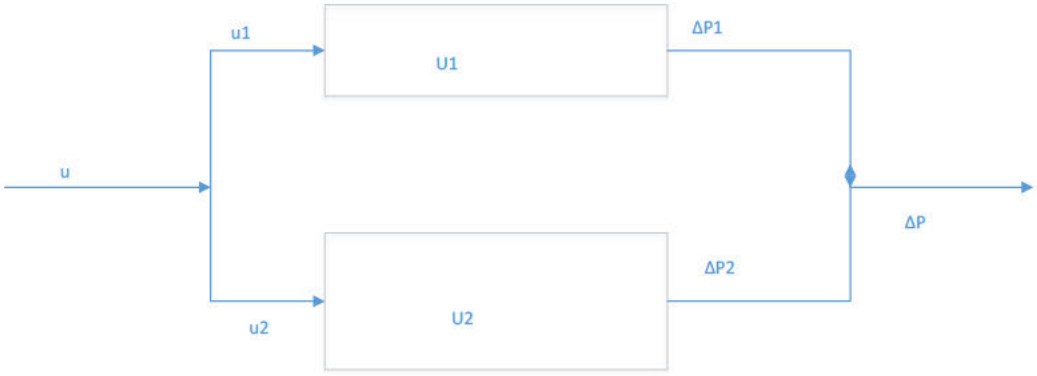


*Figure 4-3: Non-Uniform Packed bed (Packed bed reactors in parallel)*

For plug flow reactors,

$$\frac{V_1}{F_1} = \frac{V_2}{F_2} \qquad \text{(Eqn 4-20)}$$

Upon re-arranging Equation 4-20,

$$\frac{V_1}{V_2} = \frac{F_1}{F_2} \qquad \text{(Eqn 4-21)}$$

For conservation of momentum, the pressure drop across the two different routes is the same. This means,

$$\Delta P1 = \Delta P2 \qquad \text{(Eqn 4-22)}$$

From equation 4-14,

$$u = \frac{\dot{V}}{A_x} = \frac{\dot{n}RT}{P_{in} \times A_x}$$

For same length of packed beds, using Equation 4-9,

$$\Delta P1 = 150\frac{(1-\varepsilon_1)^2}{{\varepsilon_1}^3}\frac{\mu . u_1}{{d_{p_1}}^2} + 1.75\frac{(1-\varepsilon_1)}{{\varepsilon_1}^3}\frac{\rho {u_1}^2}{d_{p_1}}$$

$$\Delta P2 = 150\frac{(1-\varepsilon_2)^2}{{\varepsilon_2}^3}\frac{\mu.u_2}{{d_{p_2}}^2} + 1.75\frac{(1-\varepsilon_2)}{{\varepsilon_2}^3}\frac{\rho {u_2}^2}{d_{p_2}}$$

where, $\varepsilon_1$ is the porosity of small catalyst , $u_1$ is the superficial velocity in stream 1, $d_{p1}$ is the diameter of small catalyst , $\varepsilon_2$ is the porosity of large catalyst , $u_2$ is the superficial velocity in stream 2 and $d_{p2}$ is the diameter of large catalyst.

**Case 1: Constant gas velocity**

When the gas velocity remains constant with change in pressure, from Equations 4-1 and 4-3

$$P_{in} - P_{out} = b(P_{in}(t))$$

$$P_{out} = P_{in} - b\big(P_{in}(t)\big) = P_{in}(1-b)$$

Let x be the fraction of the feed into stream 1.

Pressure into stream 1 will be $xP_{in}$

Output pressure in stream 1 will be

$$P_{out1}(t) = x[P_{in}(t) - b(P_{in}(t))] \qquad \text{(Eqn 4-23)}$$

$$P_{out1}(t) = xP_{in}(t)\lfloor(1-b)\rfloor$$

Inlet pressure is a sine function.

$P_{in}(t) = ASin(wt)$

Substituting for $P_{in}(t)$ in Equation 4-23

$$P_{out1}(t) = x(ASin(wt))\lfloor(1-b)\rfloor \qquad \text{(Eqn 4-24)}$$

Taking a Laplace on equation 4-24 and applying the Ergun equation for pressure drop across a packed bed reactor (Workings shown in Appendix G) gives,

$$P(t) = \frac{A}{w} - \frac{Acos(wt)}{w} - \Delta Pt \qquad \text{(Eqn 4-25)}$$

Where

$$\Delta P = L\left[150\frac{(1-\varepsilon_1)^2}{\varepsilon_1^3}\frac{\mu.u_1}{d_{p1}^2} + 1.75\frac{(1-\varepsilon_1)}{\varepsilon_1^3}\frac{\rho {u_1}^2}{d_{p1}}\right] = L\left[150\frac{(1-\varepsilon_2)^2}{\varepsilon_2^3}\frac{\mu.u_2}{d_{p2}^2} + 1.75\frac{(1-\varepsilon_2)}{\varepsilon_2^3}\frac{\rho {u_2}^2}{d_{p2}}\right]$$

Appendix G also shows how the equations were simplified by substituting for the porosities, velocities and diameter of packing material.

**Case 2: Change in gas velocity with change in inlet pressure**

From Equation 4-14, when the gas velocity changes with inlet pressure,

$$u = \frac{\dot{n}RT}{P_{in} \times A_x}$$

Equation 4-16 shows that,

$$\frac{\Delta P}{L} = 150\frac{(1-\varepsilon)^2}{\varepsilon^3}\frac{\mu.u}{d_p^2} + 1.75\frac{(1-\varepsilon)}{\varepsilon^3}\frac{\rho u^2}{d_p}$$

Substituting for u in equation 4-16, the pressure drop in stream 1 becomes

$$\frac{\Delta P_1}{L_1} = 150\frac{(1-\varepsilon_1)^2}{{\varepsilon_1}^3}\frac{\mu}{d_{p1}^2}.\left(\frac{x.\dot{n}RT}{P_{in}A_{x1}}\right) + 1.75\frac{(1-\varepsilon_1)}{{\varepsilon_1}^3}\frac{\rho_1}{d_{p1}}.\left(\frac{x.\dot{n}RT}{P_{in}A_{x1}}\right)^2$$

Pressure drop in stream 2,

$$\frac{\Delta P_2}{L_2} = 150\frac{(1-\varepsilon_2)^2}{{\varepsilon_2}^3}\frac{\mu}{d_{p2}^2}.\left(\frac{(1-x).\dot{n}RT}{P_{in}A_{x2}}\right) + 1.75\frac{(1-\varepsilon_2)}{{\varepsilon_2}^3}\frac{\rho_2}{d_{p2}}.\left(\frac{(1-x).\dot{n}RT}{P_{in}A_{x2}}\right)^2$$

For conservation of momentum, the change in pressure is the same in both streams

$\Delta P_1 = \Delta P_2$

$$\frac{\Delta P}{L} = \frac{D}{P_{in}} + \frac{E}{{P_{in}}^2} = \frac{F}{P_{in}} + \frac{G}{{P_{in}}^2} \qquad \text{(Eqn 4-26)}$$

Where

$$D = 150\frac{(1-\varepsilon_1)^2}{{\varepsilon_1}^3 d_{p1}^2}\mu\left(\frac{x\dot{n}RT}{A_{x1}}\right)$$

$$E = 1.75\frac{(1-\varepsilon_1)}{{\varepsilon_1}^3 d_{p1}}\rho\left(\frac{x\dot{n}RT}{A_{x1}}\right)^2$$

$$F = 150\frac{(1-\varepsilon_2)^2}{{\varepsilon_2}^3 d_{p2}^2}\mu\left(\frac{(1-x)\dot{n}RT}{A_{x1}}\right)$$

$$G = 1.75\frac{(1-\varepsilon_2)}{{\varepsilon_2}^3 d_{p2}}\rho\left(\frac{(1-x)\dot{n}RT}{A_{x2}}\right)^2$$

### 4.3 MODEL ARRANGEMENT 3- MIXED PACKING (small catalyst at the centre of vessel)

Figure 4-4 shows the packed bed vessel with small catalyst at the centre of the vessel. This resembles catalyst breakage in the centre of the vessel. This was modelled as a network of three packed bed reactors in parallel as showed in Figure 4-5.


*Figure 4-4: Non-uniform Packing (Small packing at the center of vessel)*

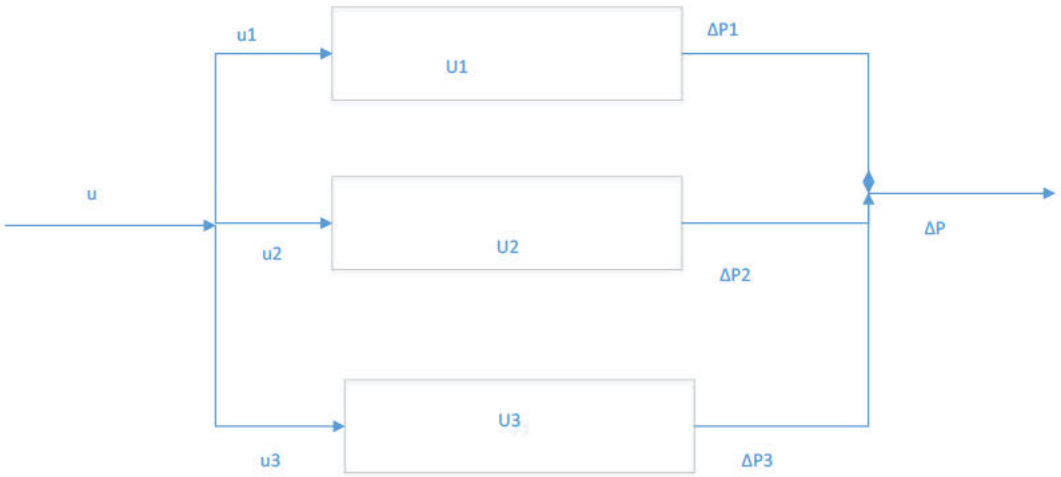


*Figure 4-5: Non-Uniform Packed bed (Packed bed reactors in parallel)*

**Case 1: Constant gas velocity**

Pressure drop in stream 1

$$\Delta P1 = L\left[150\frac{(1-\varepsilon_1)^2}{\varepsilon_1^3}\frac{\mu.u_1}{d_{p1}^2} + 1.75\frac{(1-\varepsilon_1)}{\varepsilon_1^3}\frac{\rho{u_1}^2}{d_{p1}}\right]$$

Pressure drop in stream 2

$$\Delta P2 = L\left[150\frac{(1-\varepsilon_2)^2}{\varepsilon_2^3}\frac{\mu.u_2}{d_{p2}^2} + 1.75\frac{(1-\varepsilon_2)}{\varepsilon_2^3}\frac{\rho {u_2}^2}{d_{p2}}\right]$$

Pressure drop in stream 3

$$\Delta P3 = L\left[150\frac{(1-\varepsilon_3)^2}{\varepsilon_3^3}\frac{\mu.u_1}{d_{p3}^2} + 1.75\frac{(1-\varepsilon_3)}{\varepsilon_3^3}\frac{\rho {u_2}^2}{d_{p3}}\right]$$

where, $\varepsilon_3$ is the porosity of large catalyst, $u_3$ is the superficial velocity in stream 3, $d_{p3}$ is the diameter of large catalyst

For conservation of momentum, $\Delta P1 = \Delta P2 = \Delta P3 = \Delta P$

$$P(t) = \quad \frac{A}{w} - \frac{Acos(wt)}{w} - \Delta Pt$$

Where

$$\Delta P = L\left[150\frac{(1-\varepsilon_1)^2}{\varepsilon_1^3}\frac{\mu.u_1}{d_{p1}^2} + 1.75\frac{(1-\varepsilon_1)}{\varepsilon_1^3}\frac{\rho {u_1}^2}{d_{p1}}\right] = L\left[150\frac{(1-\varepsilon_2)^2}{\varepsilon_2^3}\frac{\mu.u_2}{d_{p2}^2} + 1.75\frac{(1-\varepsilon_2)}{\varepsilon_2^3}\frac{\rho {u_2}^2}{d_{p2}}\right] = L\left[150\frac{(1-\varepsilon_3)^2}{\varepsilon_3^3}\frac{\mu.u_1}{d_{p3}^2} + 1.75\frac{(1-\varepsilon_3)}{\varepsilon_3^3}\frac{\rho {u_2}^2}{d_{p3}}\right] \quad \text{(Eqn 4-27)}$$

Calculations for the large vessel and small vessels are given in Appendix G.

**Case 2: Velocity changing with time**

When the gas velocity changes with inlet pressure, the pressure drop in stream 1 becomes

$$\frac{\Delta P_1}{L_1} = 150\frac{(1-\varepsilon_1)^2}{{\varepsilon_1}^3}\frac{\mu}{d_{p1}^2}.\left(\frac{x\dot{n}RT}{P_{in}A_{x1}}\right) + 1.75\frac{(1-\varepsilon_1)}{{\varepsilon_1}^3}\frac{\rho_1}{d_{p1}}.\left(\frac{x\dot{n}RT}{P_{in}A_{x1}}\right)^2$$

Where is the fraction of feed into stream 1 which is equal to fraction of feed in stream 3 since these streams flow in regions with catalyst of the same diameter.

Pressure drop in stream 2,

$$\frac{\Delta P_2}{L_2} = 150\frac{(1-\varepsilon_2)^2}{{\varepsilon_2}^3}\frac{\mu}{d_{p2}^2}.\left(\frac{(1-x)\dot{n}RT}{P_{in}A_{x2}}\right) + 1.75\frac{(1-\varepsilon_2)}{{\varepsilon_2}^3}\frac{\rho_2}{d_{p2}}.\left(\frac{(1-x)\dot{n}RT}{P_{in}A_{x2}}\right)^2$$

Pressure drop in stream 2,

$$\frac{\Delta P_3}{L_3} = 150\frac{(1-\varepsilon_3)^2}{{\varepsilon_3}^3}\frac{\mu}{d_{p3}^2}.\left(\frac{(x\dot{n}RT}{P_{in}A_{x2}}\right) + 1.75\frac{(1-\varepsilon_3)}{{\varepsilon_3}^3}\frac{\rho_2}{d_{p2}}.\left(\frac{(x\dot{n}RT}{P_{in}A_{x3}}\right)^2$$

For conservation of momentum, the change in pressure is the same in the 3 streams

$\Delta P_1$=$\Delta P_2 = \Delta P_3$

$$\frac{\Delta P}{L} = \frac{A}{P_{in}} + \frac{B}{P_{in}{}^2} = \frac{C}{P_{in}} + \frac{D}{P_{in}{}^2} = \frac{E}{P_{in}} + \frac{F}{P_{in}{}^2} \qquad \text{(Eqn 4-28)}$$

Where

$$A = E = 150\frac{(1-\varepsilon_1)^2}{\varepsilon_1{}^3 d_{p1}^2}\mu\left(\frac{x\dot{n}RT}{A_{x1}}\right)$$

$$B = F = 1.75\frac{(1-\varepsilon_1)}{\varepsilon_1{}^3 d_{p1}}\rho\left(\frac{x\dot{n}RT}{A_{x1}}\right)^2$$

$$C = 150\frac{(1-\varepsilon_2)^2}{\varepsilon_2{}^3 d_{p2}^2}\mu\left(\frac{(1-x)\dot{n}RT}{A_{x1}}\right)$$

$$D = 1.75\frac{(1-\varepsilon_2)}{\varepsilon_2{}^3 d_{p2}}\rho\left(\frac{(1-x)\dot{n}RT}{A_{x2}}\right)^2$$

# 5. CHAPTER 5: RESULTS AND ANALYSIS

This chapter discusses the results from the model as well as the experiments. Various experiments were conducted at different reactor configurations as well as varying gas flowrate. Two vessels of different sizes were used as packed bed reactors; a bigger vessel being employed in an attempt to get a clear trend of results as the results from the smaller vessel were not very clear. These were filled with packing material of different diameters at different packing arrangements to simulate catalyst breakage in packed bed reactors. This section will first discuss the results from the small vessel then those from the large vessel. The end of the chapter will discuss the results obtained from the model.

## 5.1 Small Vessel Results

Three batches of experiments were done. Various modifications were being made with each experiment to ensure a more accurate results could be produced. In the first and second batch experiments, the compressed air was coming from a subdivision of the laboratory's main compressed air line but on the third batch of experiments, the main line from the laboratory was being used as it supplies a more constant flow of compressed air. In first batch of experiments, there was no regulating valve between the compressed air outlet and the rotameter. The regulating valve was there in the second and third batch of experiments. The third batch experiment was therefore more controlled to give the most accurate set of results. A control experiment was carried out using bottled air instead of air from the compressor to verify the source of sinusoidal characteristic of the curves. The control experiment showed that the sinusoidal characteristic was emanating from the compressor.

Different packing material and packing arrangements were done to try to replicate particle breakage and non-uniformity in packed beds which could influence the flow pattern in the process vessels. Three types of mixed packing arrangements were used namely side, centre and middle. Side mixed packing refers to the smaller packing being placed on the left-hand side of the column while the rest of it was filled with large packing. Centre mixed packing refers to the smaller packing being placed at the centre of the column while the rest of it was filled with large packing. Middle mixed packing refers to the smaller packing being placed halfway between the side and centre of the column while the rest of it was filled with large packing. The maximum rotameter flowrate was given as 272 $dm^3$/minute which was calibrated at 85kPa and 20˚C.

After smoothing the normalised data using MATLAB's Savitky-Golay filter, the average amplitude and frequency for each curve was calculated. An example is shown below for a gas flowrate of 54.40 $dm^3$/minute for a uniformly packed vessel for the first batch of experiments.

Figure 5-1 shows the smoothed curve

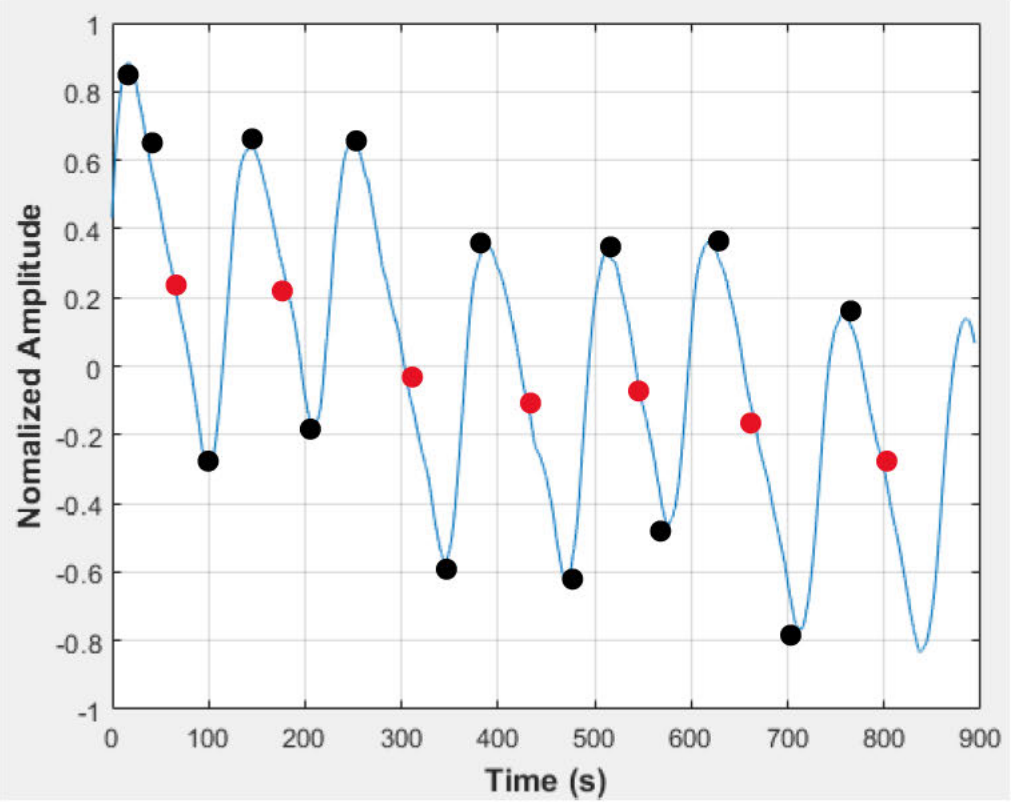


*Figure 5-1: Normalized Amplitude of Pressure Fluctuations for Uniformly Packed Vessel at 54.40 $dm^3$/minute Rotameter Flowrate*

**Calculating the average frequency**

The frequency for each cycle was calculated first the average of the frequencies from all the cycles.

Frequency for first cycle from 50 to 180 seconds (marked by the distance between the first and second red dots on the curve) $= \frac{1}{(180-50)} = \frac{1}{130} = 0.00769$

Likewise, the frequency for the next cycle was calculated from third to fourth red dot (180 to 300 seconds). Frequency $= \frac{1}{(300-180)} = \frac{1}{120} = 0.00833$

In the same way the frequencies for the third to sixth cycles were 0.00714, 0.01, 0.01 and 0,00714 respectively.

The average of the six frequencies was **0.00838**

**Calculating the average amplitude**

The amplitude for each cycle was calculated first the average of the amplitudes from all the cycles computed as shown below,

Amplitude in first cycle is given by the half of the height between the crest and trough of the wave.

The amplitude for the first cycle is half the height between the first and second black dot,

$$= \frac{0.3 + 0.9}{2} = 0.6$$

Likewise, amplitude for second cycle is height between third and fourth black dot,

$$= \frac{0.625 + 0.175}{2} = 0.4$$

Amplitudes for third to seventh cycles were 0.6, 0.45, 0.35, 0.6 ad 0.5

The average of the seven amplitudes was **0.50**

The calculated average frequencies and amplitudes for the first batch of experiments are summarised in Tables 5-1 and 5-2 respectively. Figures 5-1 and 5-2 show the amplitudes and frequencies on bar graphs.

*Table 5-1:First Batch Experimental Results- Frequency (mHz) data at Various Flowrates*

| **Flowrate ($dm^3$/minute)** | **48.96** | **54.40** | **65.28** |
|---|---|---|---|
| Empty Vessel | 9.54 | 8.53 | 9.46 |
| Large Packing | 8.19 | 8.39 | 9.24 |
| Large and small Packing (center) | 10.80 | 8.35 | 9.77 |
| Large and small packing (middle) | 10.52 | 12.33 | 13.76 |
| Large and small packing (side) | 7.81 | 8.46 | 9.45 |

*Table 5-2: First Batch Experimental Results- Amplitude data at Various Flowrates*

| **Flowrate ($dm^3$/minute)** | **48.96** | **54.40** | **65.28** |
|---|---|---|---|
| Empty Vessel | 0.51 | 0.63 | 0.75 |
| Large Packing | 0.28 | 0.50 | 0.65 |
| Large and small Packing (center) | 0.44 | 0.60 | 0.70 |
| Large and small packing (middle) | 0.45 | 0.73 | 0.33 |
| Large and small packing (side) | 0.58 | 0.75 | 0.52 |

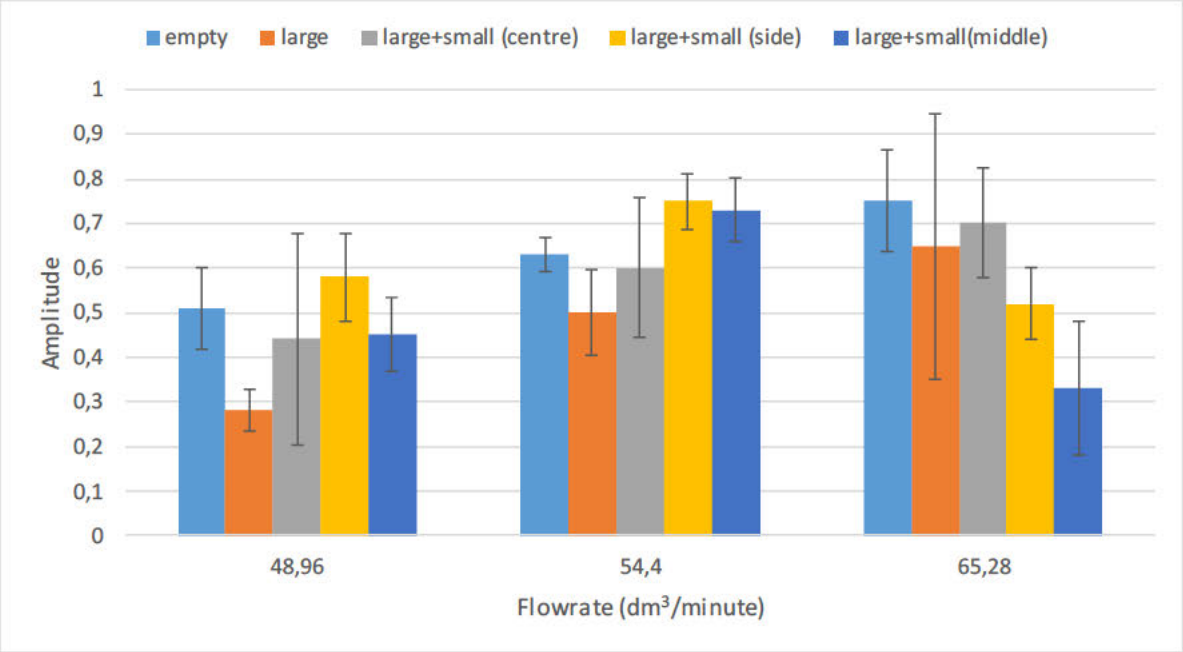


*Figure 5-2: Amplitudes of Pressure Fluctuations vs Flowrate- First Batch Experimental Data*

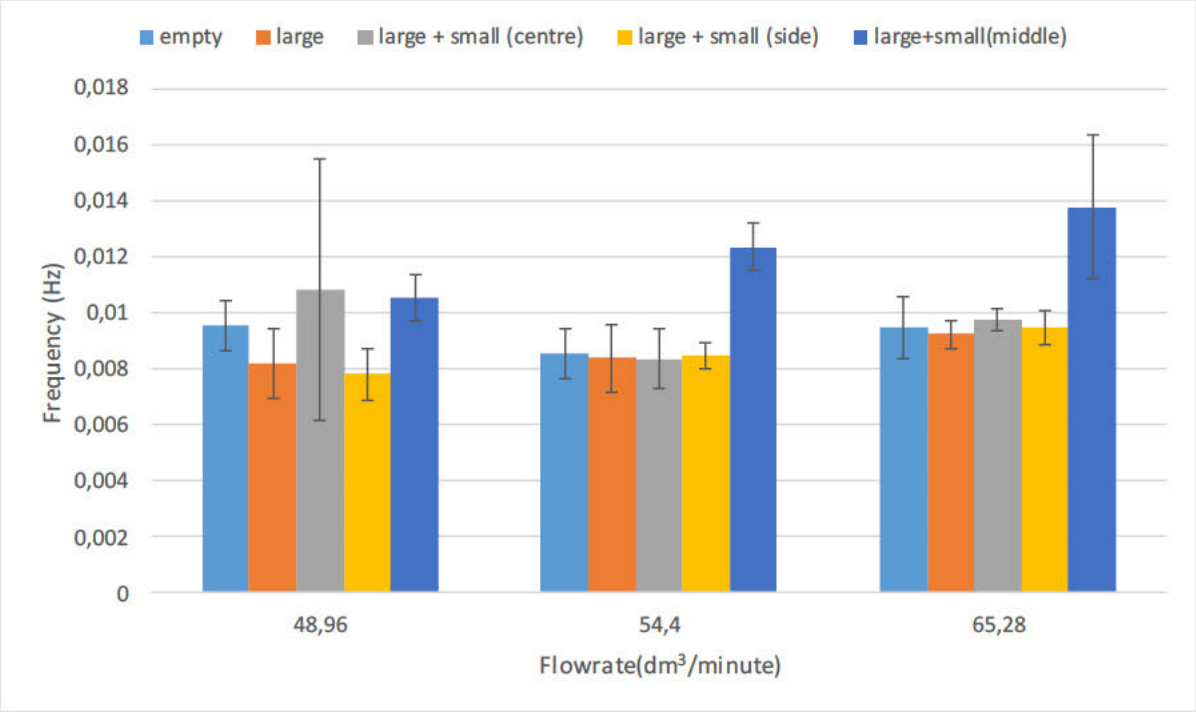


*Figure 5-3: Frequency vs Flowrate- First Batch Experimental Data*

Figure 5-2 show the changes in amplitudes of pressure fluctuations with increase in gas flowrate for the first batch of experiments. The amplitude increases with increase in flowrate for the empty tube, large (uniform) packing and large and small at the centre packing configurations. For the large and small at the middle and side packing configurations, the amplitude first increased with an increase in flowrate then decreased after the flowrate of 54.4 $dm^3$/minute.

Figure 5-3 shows the change in frequency with change in gas flowrate. From Figure 5-3, a noticeable change was seen on the large and small packing at the middle packing configuration where the frequency increased with an increase in gas flowrate. The frequency did not change significantly with the other packing configurations as the gas flowrate increased.

Although there was a strong spread of the data, there are statistically significant differences in the frequency and amplitude of the pressure drop response, based on the different packing arrangements (see Tables 5-1 and 5-2 as well as Figures 5-2 and 5-3).

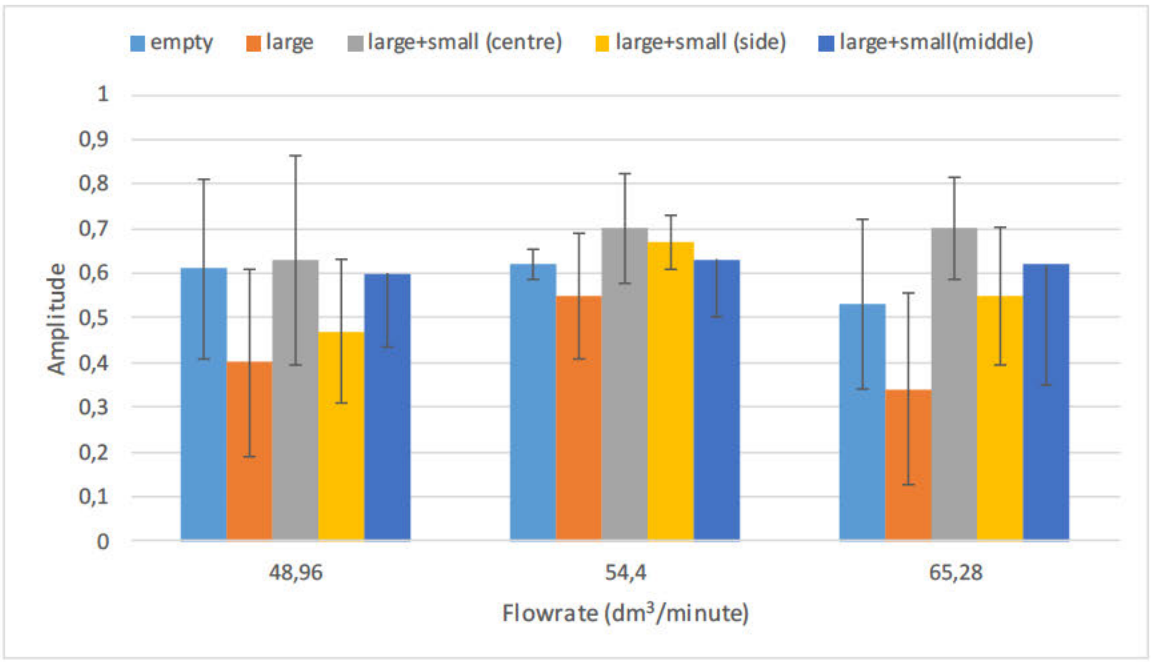


*Figure 5-4: Amplitudes of Pressure Fluctuations vs Flowrate- Second Batch Experimental Data*

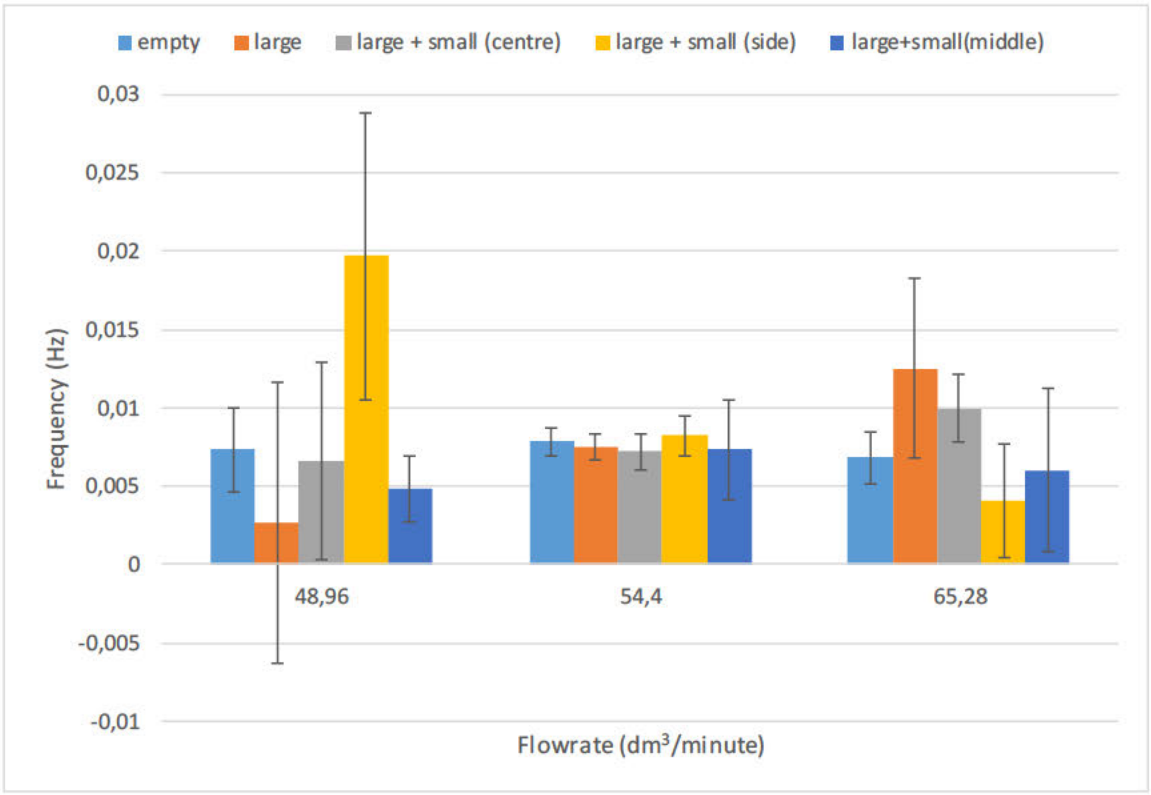


*Figure 5-5: Frequency vs Flowrate- Second Batch Experimental Data*

Figure 5-4 shows the how the amplitude of pressure fluctuations changed with increase in gas flowrate. Although there was no clear trend in how the amplitude changes with frequency, the uniform (large) packing arrangement showed the lowest amplitudes compared to the other packing arrangements. The mixed packing (large and small at the centre) had the highest amplitudes. There is a great uncertainty in the data as there is much overlapping in the error bars. Figure 5-5 shows how the frequency changed with change in gas flowrate. There was an increase in frequency with an increase in gas flowrate for the uniform packing arrangement. The mixed packing (large and small packing at the side) showed a decrease in frequency with an increase in gas flowrate. There was also a great uncertainty in the frequency versus flowrate data as there was much overlapping in the error bars.

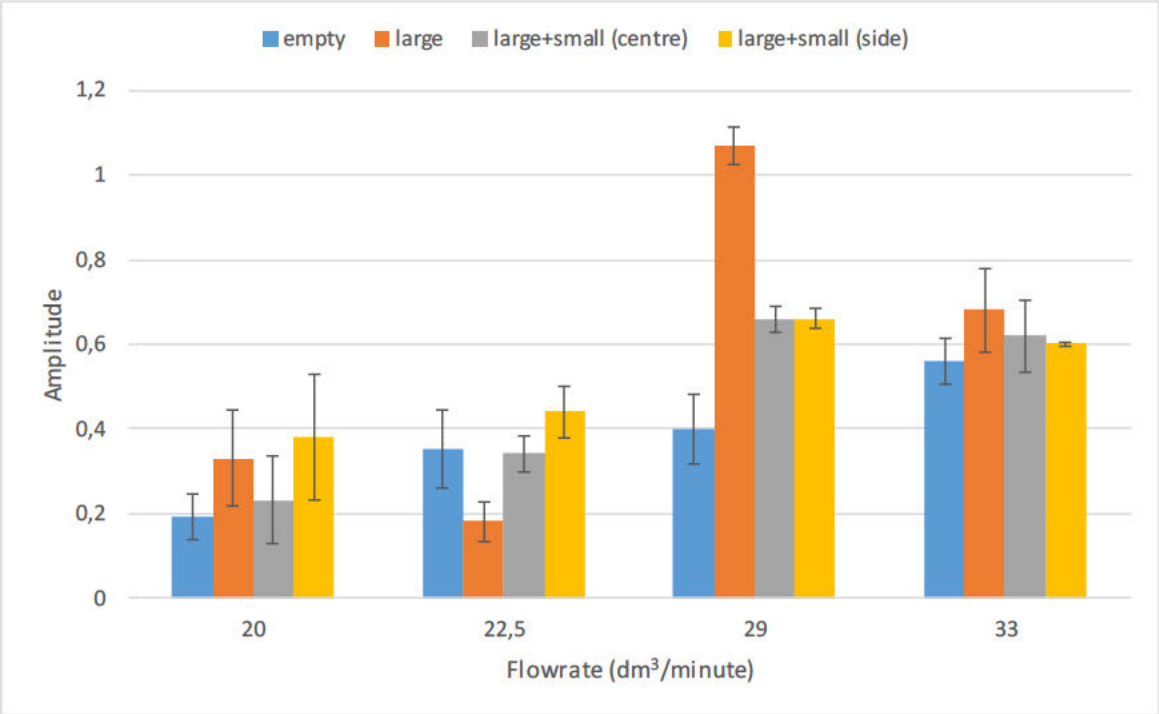


*Figure 5-6: Amplitudes of Pressure Fluctuations vs Flowrate- Third Batch Experimental Data*

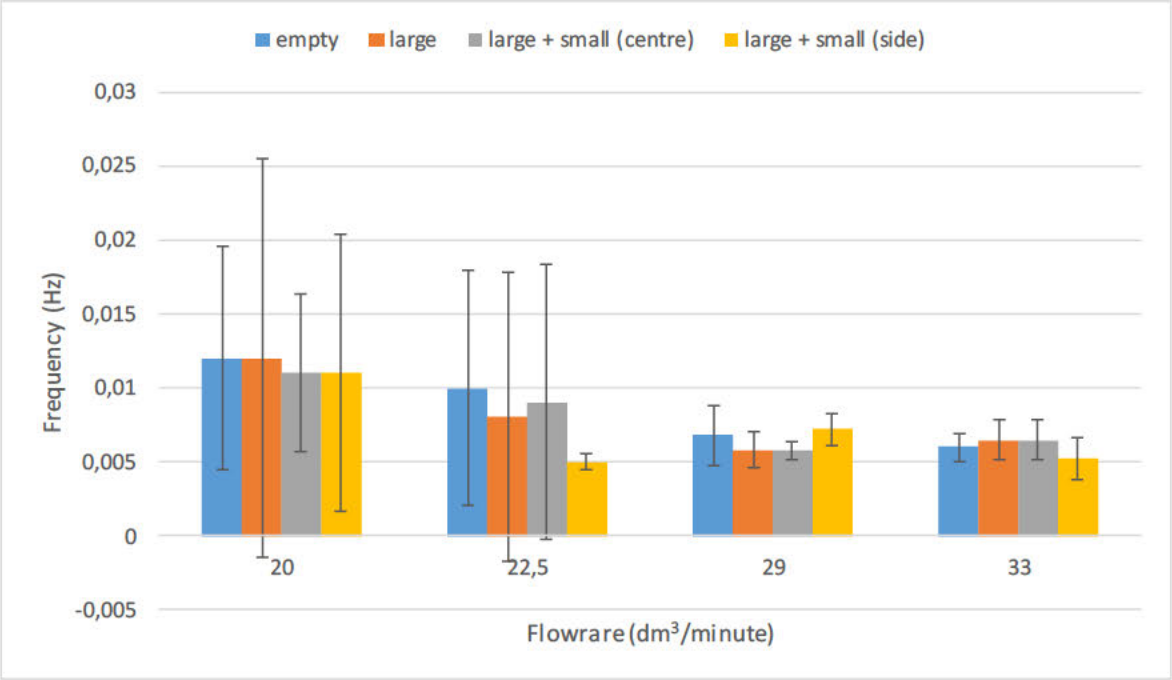


*Figure 5-7: Frequency vs Flowrate- Third Batch Experimental Data*

Figure 5-6 shows how the amplitude of pressure fluctuations changed with an increase in gas flowrate while Figure 5-7 shows how the frequency responses to a change in gas flowrate. Third batch experiments showed a clearer trend in the frequency data. The value of the highest frequency is decreasing as the flow rate increases. The frequency appears to decrease with increasing flowrate, which could indicate some kind of saturation in the response (increasing turbulence overcoming the flow distribution effects). The other important observation here is that the variability in response is much greater at lower flowrates which could indicate that there is a very complex flow pattern that is very sensitive to inlet conditions.

Figure 5-6 also shows a clearer trend in the amplitude data compared to figures 5-2 and 5-4. Initially the amplitude increases with an increase in flowrate from 20 $dm^3$/minute to 29 $dm^3$/minute. After 29 $dm^3$/minute, the amplitude decreases with further increase in compressed air flow rate.

There is a significant difference in the measured amplitude and frequency as packing changes. There is a high probability that in a small system, there was not enough resolution in the data to form a clear trend. A bigger reactor should be used as it may produce a clearer trend.

## Results- Large reactor

Two batches of experiments were done. The first batch had the vessel packed to 3m height (leaving 1m height allowance for air distribution. while the second batch of experiments had the vessel packed to 3.7m height, leaving a 0.3 m height for allowance of compressed air distribution. Compressed air from the main line from the laboratory was being used as it supplies a more constant flow of compressed air. There was a regulating valve and needle valve between the compressed air outlet and the rotameter.

Different packing material and packing arrangements were done to try to replicate particle breakage and non-uniformity in packed beds which could influence the flow pattern in the process vessels. PVC rings of different diameters were used as the packing material,50 mm by 50 mm rings and 20 mm by 20 mm. Two types of mixed packing arrangements were used namely side and centre. Side mixed packing refers to the smaller packing being placed on the left-hand side of the column while the rest of it was filled with large packing. Centre mixed packing refers to the smaller packing being placed at the centre of the column while the rest of it was filled with large packing. The maximum rotameter flowrate was given as 16.67 $dm^3$/minute which was calibrated at 700kPa and 25˚C.

The flowrate was varied from 1.67 $dm^3$/minute to 2.83 $dm^3$/minute for each packing arrangement. Up to eight repeat experiments were done keeping each flowrate and packing configuration constant.

The results are summarised in the Figures 5-8 to 5-11 below.

## Three quarter full vessel

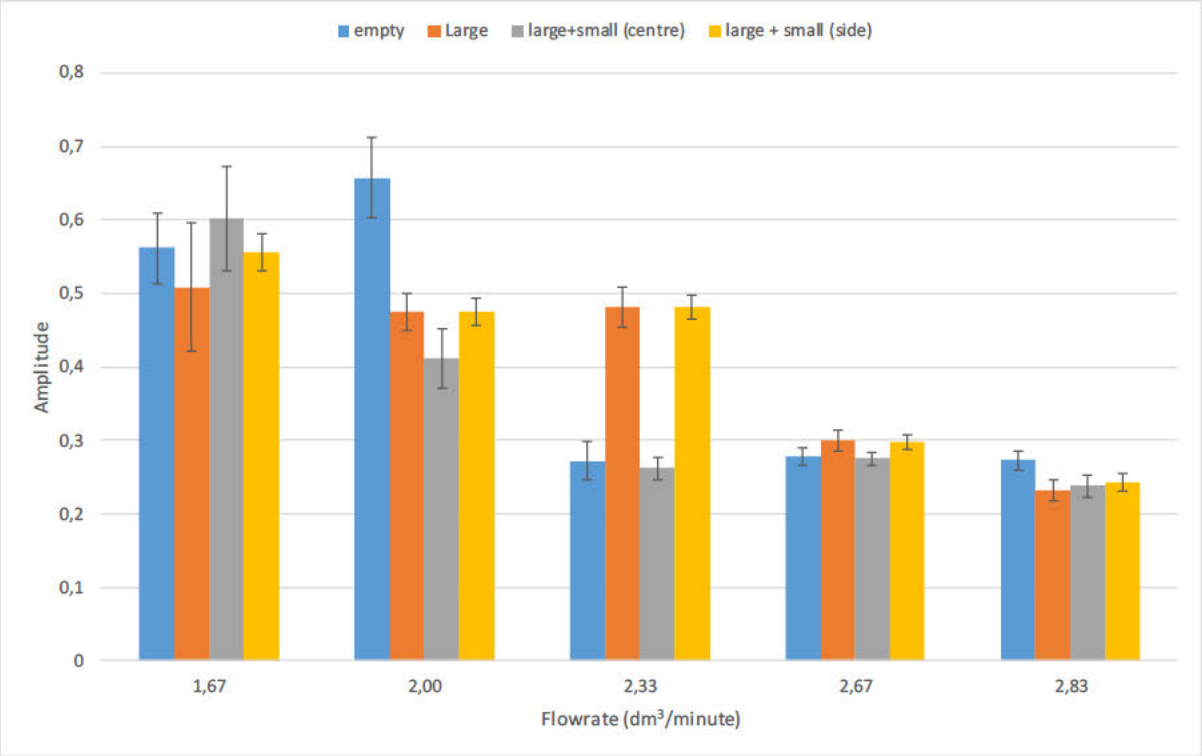


*Figure 5-8: Average amplitudes of Pressure Fluctuations at different packing arrangements for 75% full vessel*

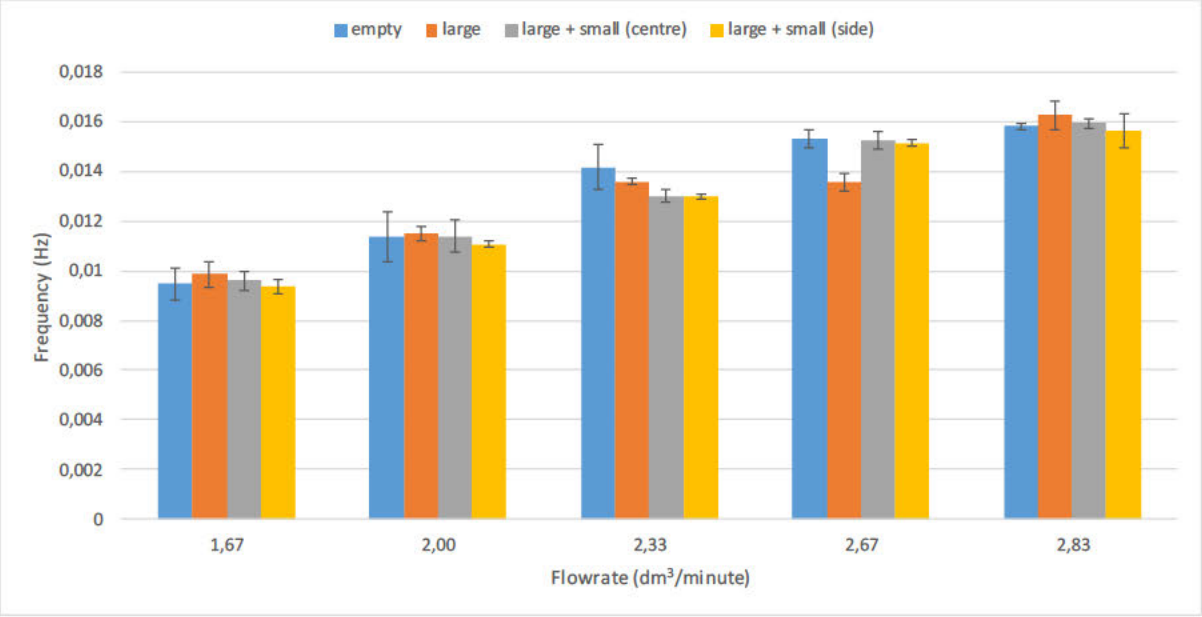


*Figure 5-9: Average frequencies of Pressure Fluctuations at different packing arrangements for 75% full vessel*

Figure 5-8 shows the average how amplitudes of pressure fluctuations changed with an increase in gas flowrate for a 75% full vessel at different packing arrangements. From the plot, there is a higher

amplitude at low gas flowrate. As the flowrate increase there is a decrease in the amplitude of pressure fluctuations.

At 1.67 $dm^3$/minute, the large and small at the centre configuration had the highest amplitude of pressure fluctuations. As the gas flowrate increase above 1.67 $dm^3$/minute, the large and small at the centre packing configuration has the least amplitude of pressure fluctuations. From the flowrate of 2 $dm^3$/minute, the large packing shows to have the highest amplitude among the different packing configurations. The large(uniform) packing had an amplitude slightly higher than that of large and small at the side packing arrangement.

Figure 5-9 shows how the frequency of pressure fluctuations respond to an increase in gas flowrate. The frequency increases uniformly with increase in gas flowrate across the packing arrangements. There is a slightly higher frequency for large packing than for the large with small at the centre and large with small at the side packing arrangements.

**Full vessel Results**

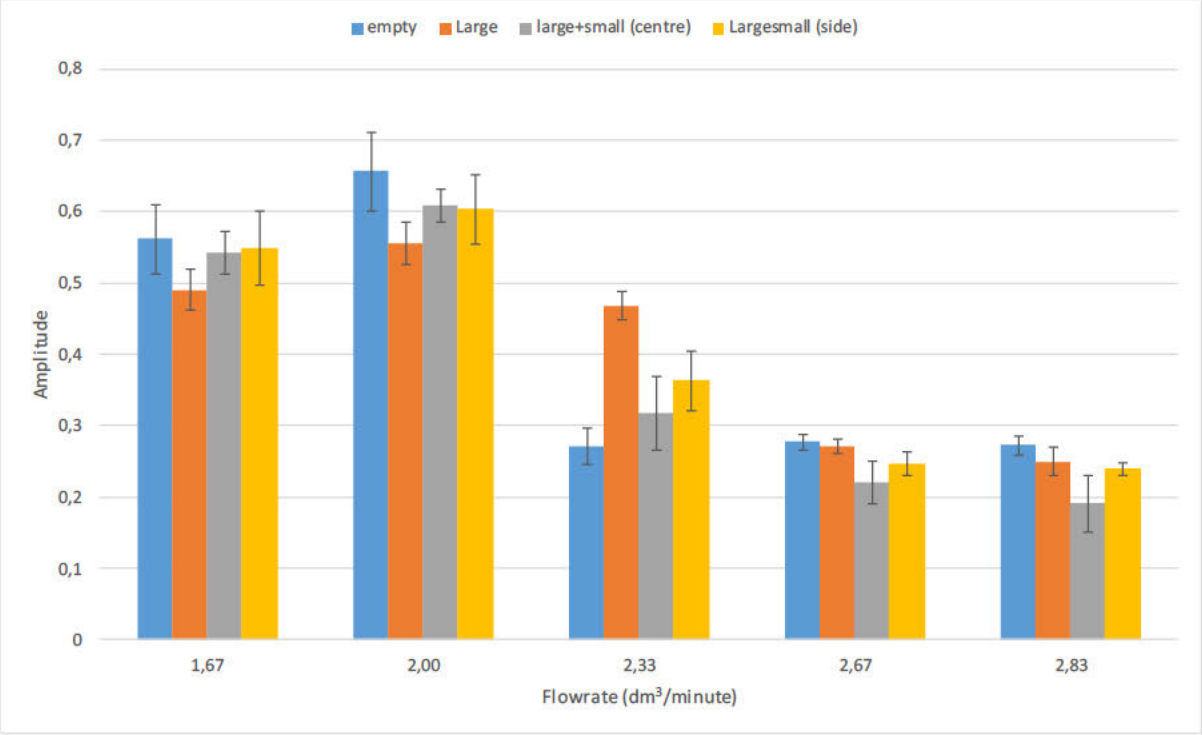


*Figure 5-10: Average amplitudes of Pressure Fluctuations at different packing arrangements for a full vessel*

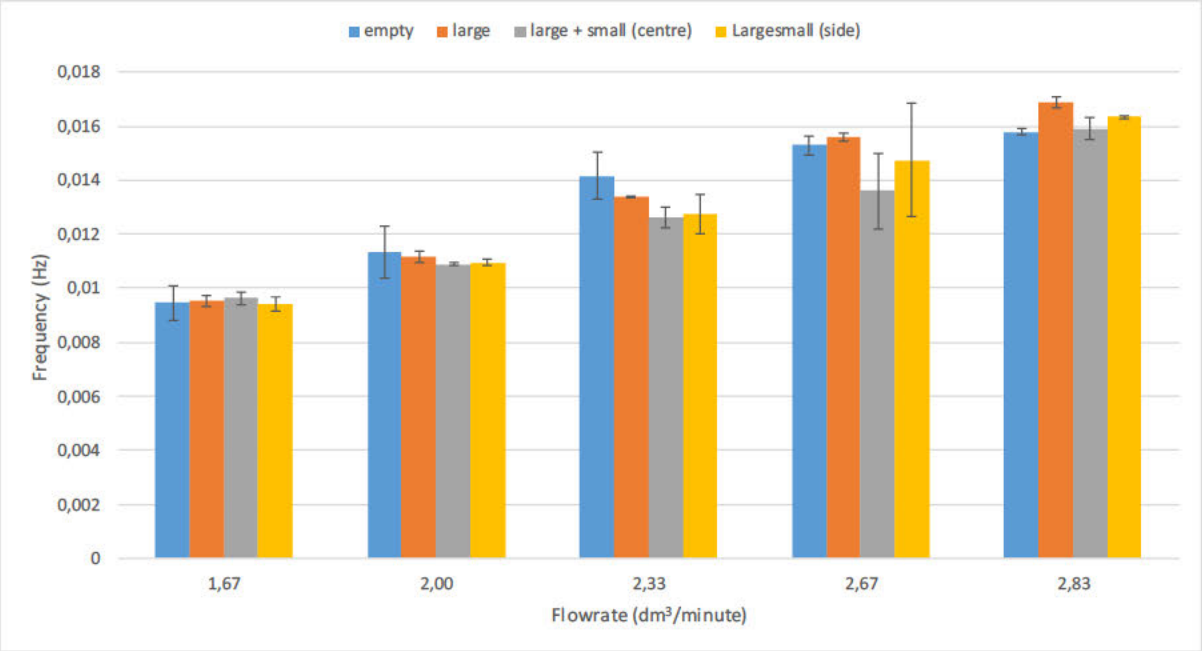


*Figure 5-11: Average frequencies of Pressure Fluctuations at different packing arrangements for a full vessel*

Figures 5-10 and 5-11, above show the changes in amplitude and frequencies of pressure fluctuations with an increase in gas flowrate at different packing configurations when the vessel is fully packed. The full vessel data shows a clearer trend in the results. There is an inflection point between 2 $dm^3$/minute and 2.33 $dm^3$/minute in Figure 5-10. The amplitude of pressure fluctuations decreases with a further increase in flowrate after 2 $dm^3$/minute. At lower flowrates, the amplitude of pressure fluctuations is higher.

This agrees with what Yang et al (2002) found in their experimental work when the mean amplitude initially increased then slightly decreased with increasing gas velocity. Simulation work by Das et al (2017) also confirmed that at high Reynold's number, the flow becomes unsteady, and, in these cases, the amplitude of pressure fluctuations remains small. It is the high solid fraction that suppresses these fluctuations. The decrease in amplitude at a higher flowrate in full packing compared to 75% full vessel was probably since air had to travel a longer distance through the packing in the full vessel than in the 75% full vessel.

The large packing had the highest amplitude of pressure fluctuations. The pressure fluctuations increase with increase in particle diameter (Linsong, et al., 2018).

Figure 5-11 shows that at low flowrate the difference in frequency is quite negligible. The difference increases as flowrate increases. For the full vessel, the frequency is marginally smaller for non-uniform compared to uniform packing.

Figure 5-10 shows that between 1.67 $dm^3$/minute and 2 $dm^3$/minute, the uniform(large) packing arrangement has small amplitude which increases as flowrate increases above 2.33 $dm^3$/minute. This change in amplitude can be used to diagnose some change in packing arrangement and maldistribution of flow in packed bed reactors. Industrial reactors are operated at high flowrates and there is turbulence. Therefore, the results obtained at high flowrates better approximate what would happen in industrial reactors.

**Dominant frequency data**

As shown in the Appendices A-F, there was no correlation in the dominant frequency data in both small and large vessels. Dominant frequency identifies the frequency associated with the greatest amplitude or power in a signal. As shown in Appendices A-F, the signals obtained from the pressure vs time data had low frequency oscillations thereby giving a low dominant frequency. The dominant frequency was very small and close to zero for all the vessels, packing arrangements and rotameter flowrates.

**Model Results**

MATLAB software was used to simulate the model equations for the various packing arrangements. Various flowrates were used during the simulation work, to serve as a benchmark against the experimental work conducted earlier.

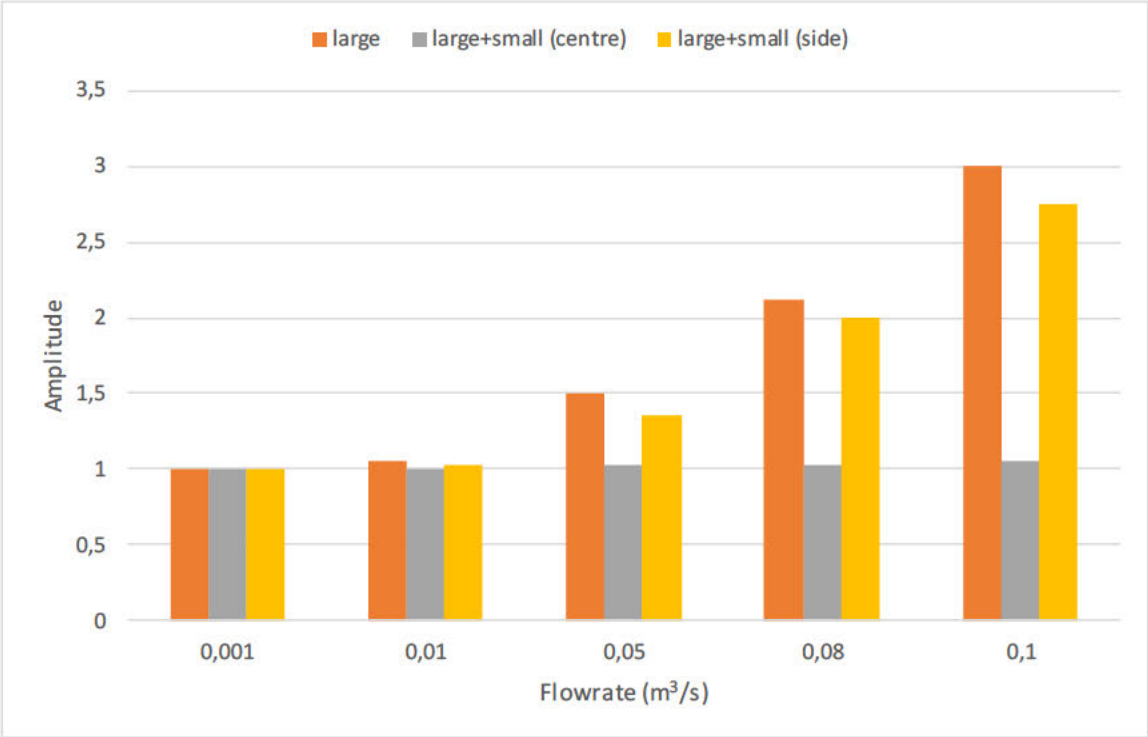


*Figure 5-12: Average amplitudes at different packing arrangements for a small vessel*

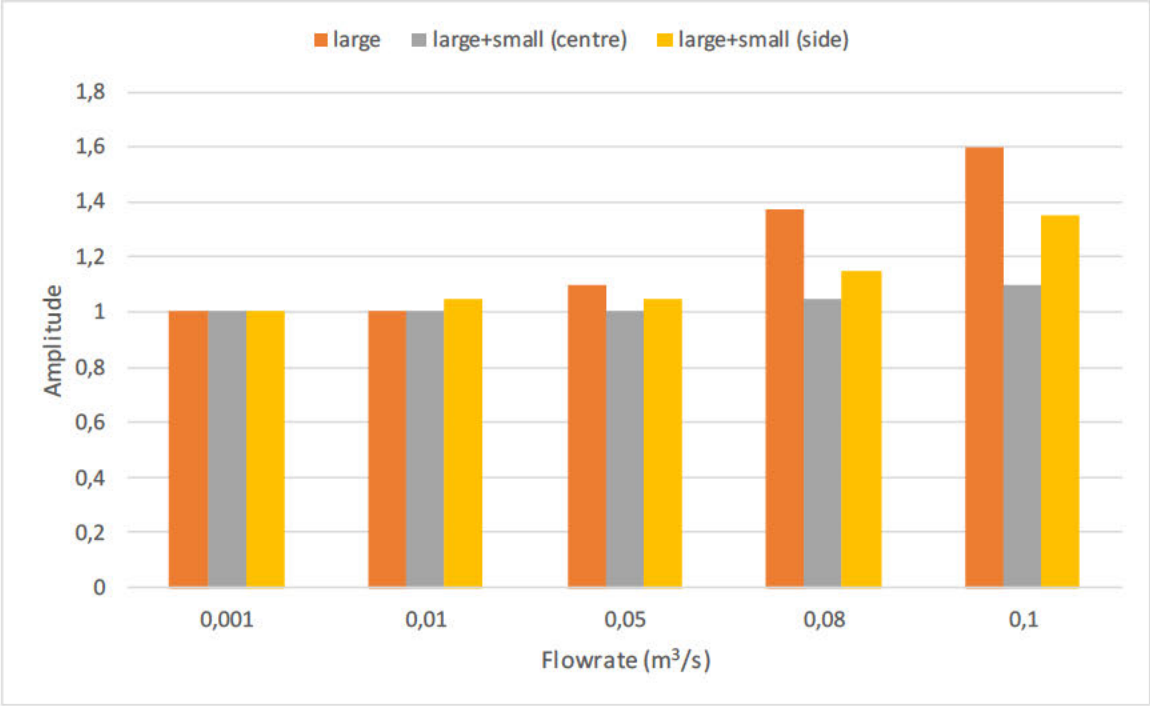


*Figure 5-13: Average amplitudes at different packing arrangements for a large vessel*

Figure 5-12 shows the model results using small vessel size and packing sizes while Figure 5-13 shows the model results using the large vessel size and packing sizes. Almost the same trends were obtained for the large and small vessel modelling. Figures 5-12 and 5-13 show a negligible difference in amplitude at low flowrates. As the flowrate increases, the amplitude of pressure fluctuations also increases. This agrees with what was seen in the experimental work at low flowrates. At flowrates below 2 $dm^3$/minute, Figures 5-8 and 5-10 show an increase in amplitude of pressure fluctuations with an in increase in gas flowrate.

There is a very small change in amplitude with increase in gas flowrate for the large and small at the centre packing in both Figures 5-12 and 5-13.

## 5.4 Experimental results versus Model results

At low gas flow rates, the model agrees well with the experimental results. At low gas flow rates, the amplitude of pressure fluctuations increases with an increase in gas flow rate. At high flow rates the model results do not agree with the experimental results. The model shows a continual increase in amplitude of pressure fluctuations with increase in gas flow rate while the experimental data shows an inflation point where the amplitude of pressure fluctuations begins to drop.

# 6. CHAPTER 6: CONCLUSIONS AND RECOMMENDATIONS

It has been found from experimental work and the model work that the amplitude of pressure fluctuations in a fixed bed reactor can be used to diagnose flow maldistribution that may be due to non-uniform packing arrangement. The amplitude of pressure fluctuations increased with an increase in gas flowrate up to an inflection point after which there was a decrease in the amplitude. The pressure fluctuations increase with an increase in particle diameter in agreement with what Linsong et al (2018) found in their simulations. The inflection point did not appear in the model results as the model showed a continuous increase in amplitude of pressure fluctuations with an increase in flowrate. There may be radial flows of gas within the bed that also affects attenuation of the pressure fluctuations.

The uniform packing arrangement had the highest amplitude at high flowrates. At low flowrates, the non-uniform packing arrangement had the highest amplitudes of pressure fluctuations. This could be because at low flowrates, the smaller particles are immobile (Tang, et al., 2019) and as flowrate increases the large particles in uniform packing arrangement become mobile and produce more pressure fluctuations than the non-uniform (mixed) packing arrangements.

The non-uniform packing arrangement with small packing at the side had an average amplitude 10.7% higher than the uniform packing arrangement, while the non-uniform packing arrangement with small packing at the centre had an amplitude 15% higher than the uniform packing. The amplitude difference between the non-uniform packing arrangement (large and small at the centre) and the uniform packing arrangement increased with the gas flowrate, reaching a difference of 38.9% at 2.33 $dm^3$/minute. The magnitude of variations in amplitudes of pressure fluctuations decreased after a gas flowrate of 2.33 $dm^3$/minute. The non-uniform packing arrangement (small packing at the centre) had the largest deviation from uniform packing arrangement.

In their experimental study on pressure drop in horizontally and vertically stratified structure, Li et al (2020), used a vertically stratified bed where the small particles were vertically packed to the left of the vessel while large diameter particles were packed vertically to the right side of the vessel. When the fluid was flowing through the small diameter particles section some of it moved to the area of less resistance to flow (the larger diameter particle section) leading to a reduction in pressure drop. They found that the pressure drop in the vertically stratified beds was less than the pressure drop of a bed packed uniformly with larger diameter particles but higher than for a bed packed uniformly with smaller diameter particles.

There was no clear trend in the dominant frequency data for both small and large vessels. All dominant frequency curves did not exhibit a sharp distinguishable peak. All dominant frequencies found were close to zero.

It is recommended that another separate project should be initiated to determine if flow induced vibrations could be used to diagnose flow maldistribution in packed beds. The case where velocity changes with change in inlet pressure (Equations 4-19, 4-26 and 4-28) should be investigated from a simulation perspective.

# References


Abdulmohsin, R. & Al-Dahhan, M., 2017. Pressure Drop and Fluid Flow Characteristics in a Packed Pebble Bed Reactor. *Nuclear Energy,* 198(1), pp. 17-25.

Ahmadi, S. & Sefidvash, F., 2018. Study of Pressure Drop in Fixed Bed Reactor Using a Computational Fluid Dynamics (CFD) Code. *ChemEngineering,* 2(14), pp. 1-26.

Alghamdi, Y. A. et al., 2019. Systematic Study of Pressure Fluctuation in the Riser of a Dual Inter-Connected Circulating Fluidized Bed: Using Single and Binary Particle Species. *Processes,* 7(890), pp. 1-25.

An, X. et al., 2009. Experimental study of the packing of mono-sized spheres subjected to one-dimensional vibration. *Powder Technology,* Volume 196, pp. 50-55.

Atmakidis, T. & Kenig, E., 2009. CFD-based analysis of the wall effect on the pressure drop in packed beds with moderate tube/particle diameter ratios in the laminar flow regime. *Chemical Engineering Journal,* Volume 153, pp. 404-410.

Atmakidis, T. & Kenig, E., 2012. Numerical analysis of mass transfer in packed-bed reactors with irregular particle arrangements. *Chemical ENgineering Science,* Volume 81, pp. 77-83.

Atmakidis, T. & Kenig, E., 2015. Numerical Analysis of Residence Time Distribution in Packed Bed Reactors with Irregular Particle Arrangements. *Chemical Product and Process Modeling,* 10(1), pp. 17-26.

Bai, H., Theuerkauf, J. & Gillis, P., 2009. A Coupled DEM and CFD Simulation of Flow Field and Pressure Drop in Fixed Bed Reactor with Randomly Packed Catalyst Particles. *Industrial & Engineering Chemistry Research,* 48(8), pp. 4060-4074.

Baker, M., 2011. *CFD simulation of flow through packed beds using the finite volume technique.* United Kingdom: University of Exeter.

Benenati, R. F. & Brosilow, C. B., 1962. Void fracton distributio in beds of spheres. *AIChE,* 8(7), p. 359.

Bey, O. & Eigenberger, G., 1997. Fluid flow through catalyst filled tubes. *Chemical Engineering Science,* 52(8), pp. 1365-1376.

Blevins, R. D., 2016. *Formulas for Dynamics, Acoustics and Vibration.* United Kingdom: John Wiley & Sons Ltd.

Carman, P., 1937. Fluid flow through granular beds. *Transactions of the Institution of Chemical Engineers,* Volume 15, pp. 150-166.

Cengel, Y. A. & Cimbala, J. M., 2018. *Fluid Mechanics Fundamentals and Applications.* 4th ed. New York: McGraw Hill.

Choudhary, M., Propster, M. & Szekely, J., 1976. On the importance of the inertial terms in the modelling of flow maldstribution in packed beds. *AIChE Journal,* 22(3), pp. 600-602.

Choudhary, M., Szekely, J. & Weller, S., 1976. The Effect of Flow Maldistribution on Conversion in a Catalytic Packed-Bed Reactor: Part 1. Analysis. *AIChE Journal,* 22(6), pp. 1021-1026.

Corrosionpedia, 2018. *Process Vessel.* [Online]
Available at: https://www.corrosionpedia.com/definition/1769/process-vessel
[Accessed 24 February 2021].

Dalman, M., Merkin, J. & McGreavy, C., 1986. Fuid Flow and Heat Transfer Past Two Spheres in a Cylindical Tube. *Computers & Fluids,* 14(3), pp. 267-281.

Das, S., Deen, N. G. & Kuipers, J., 2017. A DNS study of flow and heat transfer through slender fixed-bed reactors. *Chemical Engineering Science,* Volume 160, pp. 1-19.

de Klerk, A., 2003. Voidage variation in packed beds at small column to particle diameter ratios. *AIChE Journal,* Volume 49, pp. 20222-2029.

Durango-Giraldo, G., Zapata-Hernandez, C., Santa, J. & Buitrago-Sierra, R., 2022. Palm oil as a biolubricant: Literature review of processing parameters and tribological performance. *Journal of Industrial and Engineering Chemistry,* Volume 107, pp. 31-44.

Effendi, A. et al., 2002. Steam reforming of a clean model biogas over Ni/Al2O3 in fluidized- and fixed-bed reactors. *Catlysis Today,* Volume 77, pp. 181-189.

Eigenberger, G., 1992. *Fixed-Bed Reactors.* Stuttgart: VCH Pubh,hers..

Eisfeld, B. & Schnitzlein, K., 2001. The infuence of confining walls on the pressure drop in packed beds. *Chemical Engineering Science,* Volume 56, pp. 4321-4329.

El-Shazly, A., Nosier, S., El-Abd, M. & Sedahmed, G., 2002. Solid-Liquid Mass Transfer at an Oscillating Packed Bed of Raschig Rings. *Ind.Eng.Chem.Res,* Volume 41, pp. 5516-5522.

Ergun, S., 1952. Fluid Flow Through Packed Columns. *Chemical Engineering Progress,* Volume 48, pp. 89-94.

Evan, R., Blotter, J. & Stephens, A., 2004. Flow rate measurements using flow-induced pipe vibration. *Journal of Fluids Engineering,* Volume 126, pp. 280-285.

Falkowski, T. D., 2003. *The analysis and modeling of pressure fluctuations in a fluidized bed.* Iowa, United States of America: Iowa State University.

Fogler, H., 2006. *Elements of Chemical Reaction Engineering.* 4th ed. Mexico: Prentice Hall Professional Technical Reference.

Foutch, G. L. & Johannes, A. H., 2003. Reactors in Process Engineering. *Encyclopedia of Physical Science and Technology,* pp. 23-43.

Friedrich-Alexander-Universität Erlangen-Nürnberg, 2023. *Deep Conversion in Packed Bed Reactors.* [Online]
Available at: https://www.dip.fau.de/home/the-project/deep-conversion-in-packed-bed-reactors/
[Accessed 23 October 2023].

Ghods, N., Golshan, S., Zarghami, R. & Sotudeh-Gharebagh, R., 2019. CFD-DEM modelling of particles attrition in jet-in-fluidized beds. *Chemical Engineering Research and Design,* Volume 148, pp. 336-348.

Gio, Z. et al., 2019. Mean porosity variations in packed bed of monosized spheres with small tube-to-particle diameter ratios. *Powder Technology,,* Volume 354, pp. 842-853.

Gyan, R., Ntunka, M. & Carsky, M., 2014. Time-Series Analysis of Pressure Fluctuations in Gas-Solid Fluidized Beds. *South African Journal of Chemical Engineering,* 19(3), pp. 9-21.

Hanratty, P. & Dudukovic, M., 1990. Detection of Flow Maldistribution in Packed-Beds via Tracers. *AIChE Journal,* 36(1), pp. 127-131.

Hanratty, P. & Dudukovic, M., 1990. Detection of Flow Maldistribution in Packed-Beds via Tracers. *AIChE Journal,* 36(1), pp. 127-131.

Hanratty, P. & Dudukovic, M., 1992. Detection of Flow Maldistribution in Trickle-bed Reactors Via tracers. *Chemical Engineering Science,* 47(12), pp. 3003-3014.

Inglezakis, V., 2010. Non-Ideal Flow in Liquid-Solid Fixed Beds of Irreguar-Shaped particles: A Critical Review. *International Journal of Chemical Reactor Engineering,* Volume 8, pp. 1-15.

Jafari, A., Zamankhan, P., Mousavi, S. & Pietarinen, K., 2008. Modelling and CFD simulation of flow behavior and dispersivity through randomly packed beds. *Chemical Engineering Journal,* Volume 144, pp. 476-482.

Jakobsen, H., 2008. *Chemical Reactor Modelling Multiphase Reaction Flows.* Norway: Springer.

Jurtz, N., Kraume, M. & Wehinger, G., 2019. Advances in fixed-bed reactor modeling using particle-resolved computational fluid dynamics (CFD). *Reviews in Chemical Engineering,* 35(2), pp. 139-190.

Klingenberg, L., 2005. *Frequency Domain Using Excel.* Califonia: San Francisco State University School of Engineering.

Koekemoer, A. & Luckos, A., 2015. Effect of material type and particle size distribution on pressure drop in packed beds of large particles: Extending the Ergun equation. *Fuel,* Volume 158, pp. 232-238.

KTA, 1981. *Reactor Core Design of High-Temperature Gas-Cooled Reactor. Part 3: Loss of Pressure through Friction in Pebble Bed Cores. Safety Standards.* [Online]
Available at: https://www.kta-gs.de/e/standards/3100/3102_3_engl_1981_03.pdf
[Accessed 16 June 2021].

Levenspiel, O., 1999. *Chemical Reaction Engineering.* 3rd ed. New York: John Wiley & Sons.

Levenspiel, O., 1999. *Chemical Reaction Engineering.* 3rd ed. New York: John Wiley & Sons.

Li, L., Xie, W., Zhang, Z. & Zhang, S., 2020. Pressure drop in packed beds with horizontally or vertically stratified structure. *Nuclear Engineering and Technology,* Volume 52, pp. 2491-2498.

Linsong, J. et al., 2018. Pore-scale simulation of flow and turbulence characteristics in three-dimensional randomly packed beds. *Ptec,* pp. 1-50.

Liu, D. et al., 2016. Conceptual design of a packed bed for the removal of SO2 in Oxy-fuel combustion prior to compression. *International Journal of Greenhouse Gas Control,* Volume 53, pp. 65-78.

Lloyd, B. & Boehm, R., 1994. FLOW AND HEAT TRANSFER AROUND A LINEAR ARRAY OF SPHERES Numerical Heat Transfer, Part A: Applications. *An International Journal of Computation and Methodology,* 26(2), pp. 237-252.

Lucks, A. & Bunt, J., 2011. Pressure-drop predictions in a fixed-bed coal gasifier. *Fuel,* 90(3), pp. 917-921.

Marek, M., 2013. Numerical generation of a fixed bed structure. *Chemical and Process Engineering,* 34(3), pp. 347-359.

Marek, M., 2017. Numerical simulation of a gas flow in a real geometry of random packed bed of. *Chemical Engineering Science,* Volume 161, pp. 382-393.

Mitsudome, T. et al., 2017. Mild Hydrogenation of Amides to Amines over a Platinum-Vanadium Bimetallic Catalyst. *Angewandte Chemie International Edition,* 56(32), pp. Mitsudome, T., Miyagawa, K., Maeno, Z., Mizugaki, T., Jitsukawa, K., Yamasaki, J., … Kaneda, K. (2017). Mild Hydrogenation of 9381–9385.

Motlagh, A. A. & Hashemabadi, S., 2008. 3D CFD simulation and experimental validation of particle-to-fluid heat transfer in a randomly packed bed of cylindrical particles. *International Communications in Heat and Mass Transfer,* Volume 35, p. 1183–1189.

Navarro-Brull, F. J. & Gómez, R., 2017. Modeling Pore-scale Two-phase Flow: on How to Avoid Gas Channeling Phenomena in Micropacked-Bed Reactors via Catalyst Wettability Modification. *Industrial & Engineering Chemistry Research,* pp. 1-37.

Nemec, D. & Levec, J., 2005. Flow through packed bed reactors: 1. Single-phase flow. *Chemical Engineering Science,* 60(24), pp. 6947-6957.

Nguye, D. & Balakotaiah, V., 1994. Flow malsdirtibution and hot apots in downflow packed bed reactors. *Chemical Engineering Science,* 49(24B), pp. 5489-5505.

Oakley, D., 2014. *TYPES OF PRESSURE VESSELS AND DESIGN CONSIDERATION FOR ENSURING SAFETY.* [Online]
Available at: https://www.oakleysteel.co.uk/types-of-pressure-vessels
[Accessed 24 February 2021].

Oliveros, G. & Smith, J., 1982. Dynamic STudies of Dispersion and Channeling in Fixed Beds. *AIChE Journal,* 28(5), pp. 751-759.

Olujic, Z., Stoter, F. & de Graauw, J., 1991. Gas distribution in large-diameter packed columns. *Gas Separation & Purification,* 5(2), pp. 59-66.

Perry, R. H., Green, D. W. & Maloney, J. O., 1997. *Perry's Chemical Engineers' Handbook.* 7th ed. New York: McGraw-Hill.

PI Process Instrumentation, 2020. *Flow-induced vibration in piping systems.* [Online]
Available at: https://www.piprocessinstrumentation.com/piping-tubing-

hosing/article/21141872/flowinduced-vibration-in-piping-systems
[Accessed 29 April 2022].

Punˇcochárˇ, M. & Drahoš, J., 2005. Origin of pressure fluctuations in fluidized beds. *Chemical Engineering Science ,* Volume 60, p. 1193 – 1197.

Rase, H., 1990. *Fixed-Bead Reactor Design and DIagnostics, Gas-Phase Reactions.* Boston: Butterworth.

Rossing, T., 2014. *Springer Handbook of Acoustics.* 2nd ed. New York: Springer.

Sachdev, S., Pareek, S., Mahadevan, B. & Deshpande, A., 2012. *Modeling and Simulation of Single Phase Fluid FLow and Heat Transfer in Packed Beds.* Bangalore, COMSOL.

Sai Kumar, T., Patle, M. & Sujith, R., 2007. Characteristics of acoustic standing waves in packed-bed columns. *AIChE,* 53(2), pp. 297-304.

Schouten, C. J. & van den Bleek, M. C., 1998. Monitoring the Quality of Fluidization Using the Short-Term Predictability of Pressure Fluctuations. *AIChE,* 44(1), pp. 48-60.

Schwartz, C. & Smith, J., 1953. Flow Distribution in Packed Beds. *Industrial and Engineering Chemistry,* 45(6), pp. 1209-1218.

Stanek, V. & Szekely, J., 1972. The Effect of Non-Uniform Porosity in Causing Flow Maldistributions in Isothermal Packed Beds. *The Canadian Journal of Chemical Engineering,* Volume 50, pp. 9-14.

Stanek, V. & Szekely, J., 1973. Flow Maldistribution in Two Dimensional Packed Beds Part II: The Behaviour on Non-Isothermal Systems. *The Canadian Journal of Chemical Engineering,* Volume 51, pp. 22-30.

Sun, C. et al., 2000. Modelling and Simulation of Flow Maldistribution in Random Packed Bed Columns with Gas-Liquid Countercurrent Flow. *Trans IChemE,* 78(Part A), pp. 378-388.

Szekely, J. & Poveromo, J., 1975. Flow Maldistribution in Packed Beds: A Comparison of Measurements with Predictions. *AIChE,* 21(4), pp. 769-775.

Tang, Z., Gao, P., Sun, Y. & Han, Y., 2019. Experimental study on fluidization characteristics of different-sized particles in a U-type reduction chamber. *Advanced Powder Technology,* Volume 30, pp. 2430-2439.

Treybal, R., 1981. *Mass-Transfer Operations.* 3rd ed. Singapore: McGraw-Hill International Editions.

Trnka, O., Vesely, V. & Hartman, M., 2000. Identification of the State of a Fluidized Bed by Pressure Fluctuations. *AIChE,* 46(3), pp. 509-514.

Udoetok, E., 2018. Internal Fluid Flow Induced Vibration of Pipes. *Journal of Mechanical Design and Vibration,* 6(1), pp. 1-8.

Van Ommen, J. et al., 2011. Time-series analysis of pressure fluctuations in gas-solid fluidized beds- A review. *Interntational Journal of Multiphase Flow,* Volume 37, pp. 403-428.

Worstell, J., 2014. *Adiabatic Fixed-Bed Reactors Practical Guides in Chemical Engineering.* Oxford: Butterworth-Heinemann.

Xiang, J., Li, Q., Tan, Z. & Zhang, Y., 2017. Characterization of the flow in a gas-solid bubbling fluidized bed by pressure fluctuation. *Chemical ENgineering Science,* Volume 174, pp. 93-103.

Xu, J. et al., 2004. Statistical and frequency analysis of pressure fluctuations in spouted beds. *Powder Technology,* Volume 140, pp. 141-154.

Yang, D. H., Lee, D. H. & Han, G. Y., 2002. Pressure Fluctuation Characteristics of Polyethylene Particles. *Korean J. Chem. Eng,* 19(6), pp. 1112-1116.

Yang, J., Bu, S. D. Q., Wu, J. & Wang, Q., 2015. Experimental study of flow transitions in random packed beds with low tube to particle diameter ratios. *Experimental Thermal and Fluid Science,* Volume 66, pp. 117-126.

Yang, W., 2003. *Handbook of Fluidization and Fluid-Particle Systems.* 1st ed. Pennysylvania, USA: CRC Press.

Yan, Y. & Tu, J., 2023. *Bioaerosol Characterisation, Transportation and Transmission:Fundamental, Modelling and Application.* Singapore: Springer-TUP.

Zeiser, T. et al., 2002. Analysis of the flow field and pressure drop in fixed-bed reactors with the help of lattice Boltzmann simulations. *The Royal Society,* Volume 360, pp. 507-520.

## APPENDIX A: Small vessel experiments- First Batch

### Introduction

This section shows the graphs for the experiments done on the small vessel. Figures A-1 to A-30 show amplitudes and frequency curves for the first batch of experiments. Tables A-1 and A-2 show the summary from the amplitude and frequency data obtained from the first batch of experiments.

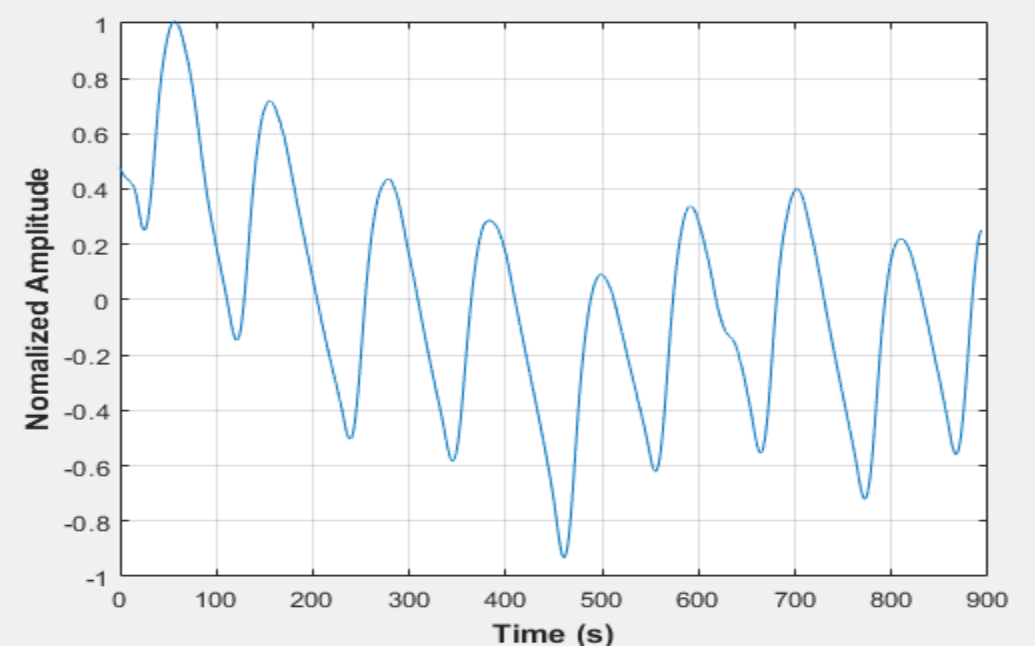


*Figure A-1: Pressure fluctuations in an empty vessel at 48.96 dm$^3$/minute gas flow rate*

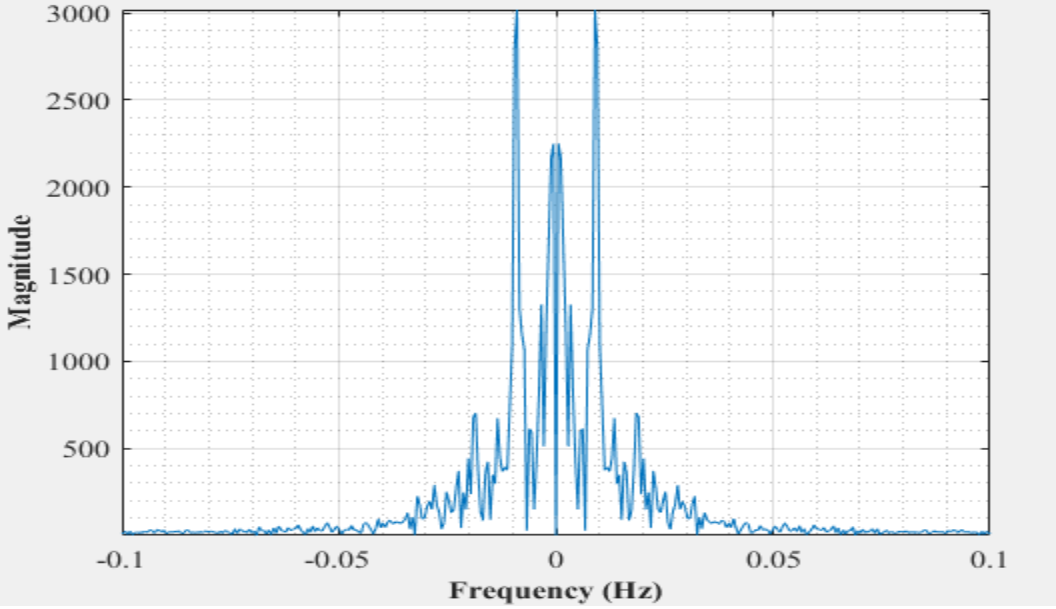


*Figure A-2: Dominant Frequency for an empty vessel at 48.96 dm$^3$/minute gas flow rate*

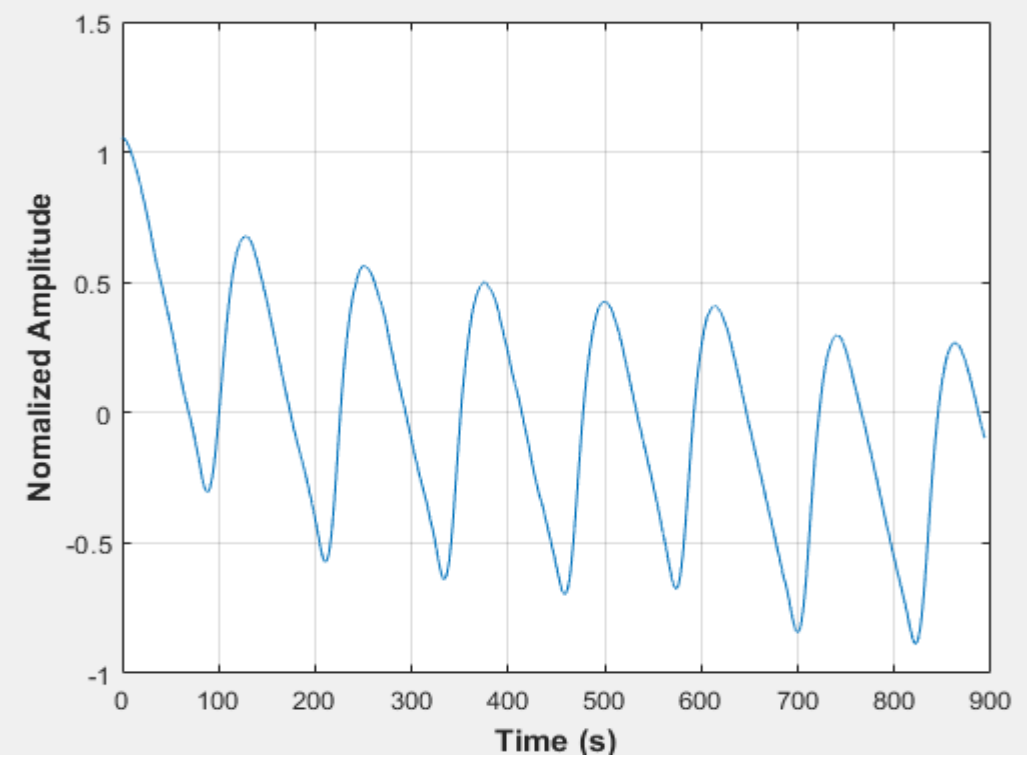


*Figure A-3: Pressure fluctuations in an empty vessel at 54.40 dm$^3$/minute gas flow rate*

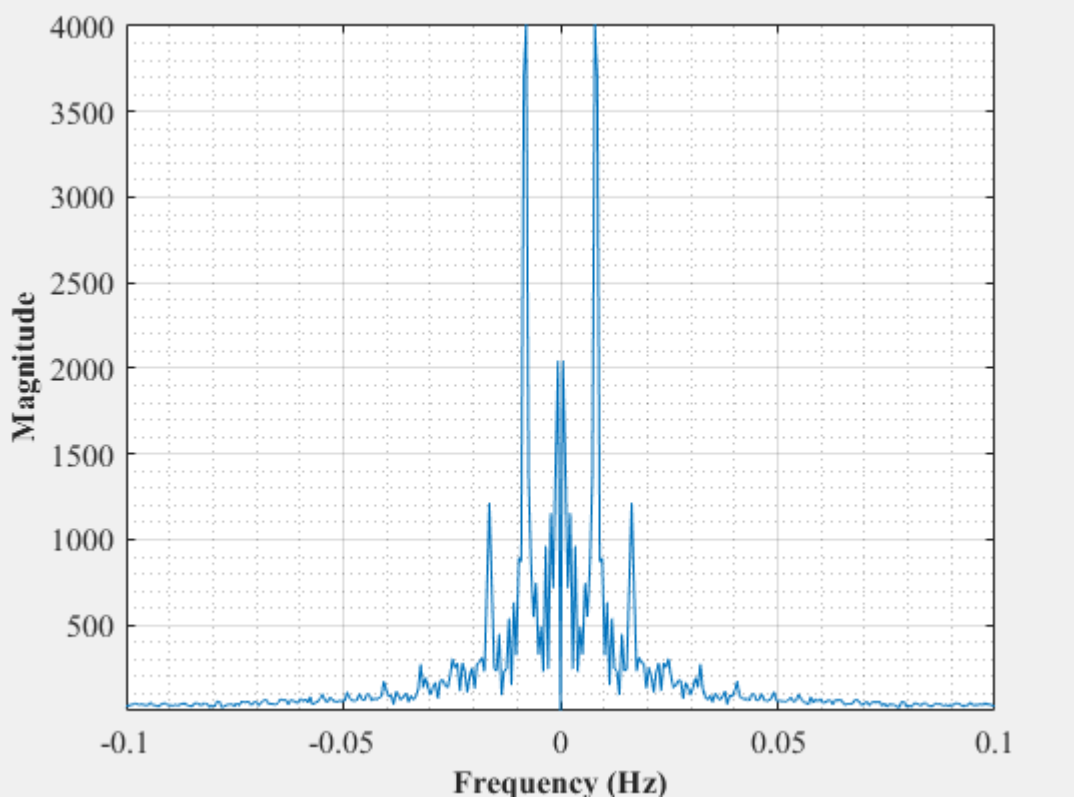


*Figure A-4: Dominant Frequency for an empty vessel at 54.40 dm$^3$/minute gas flow rate*

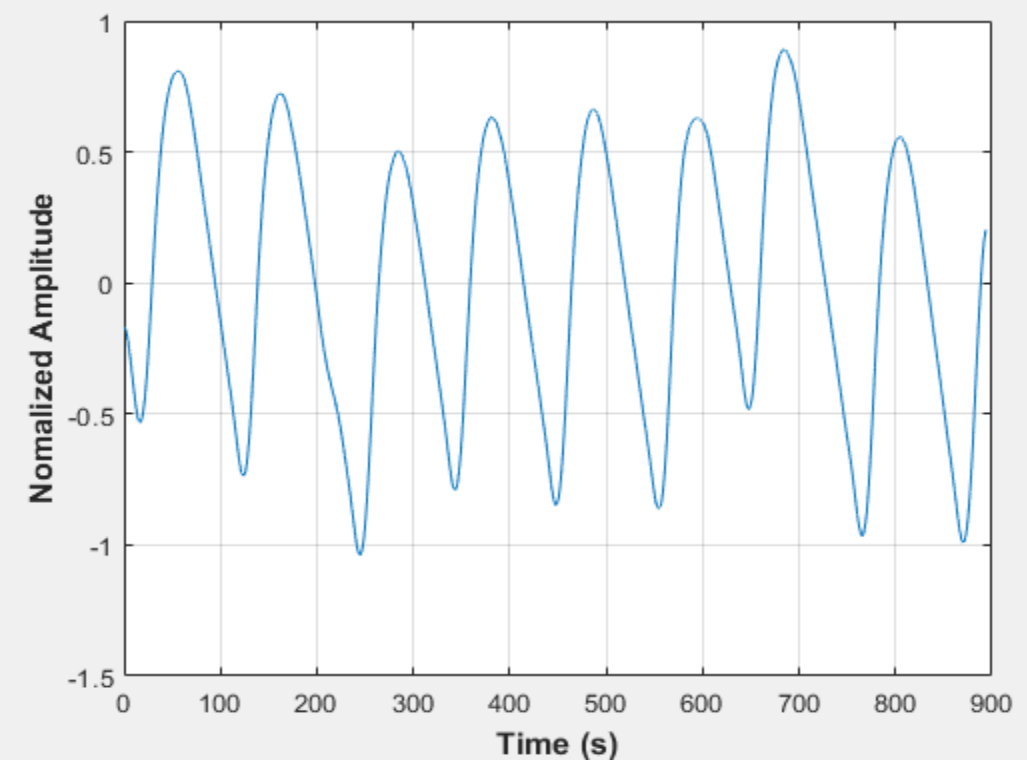


*Figure A-5: Pressure fluctuations in an empty vessel at 65.28 dm$^3$/minute gas flow rate*

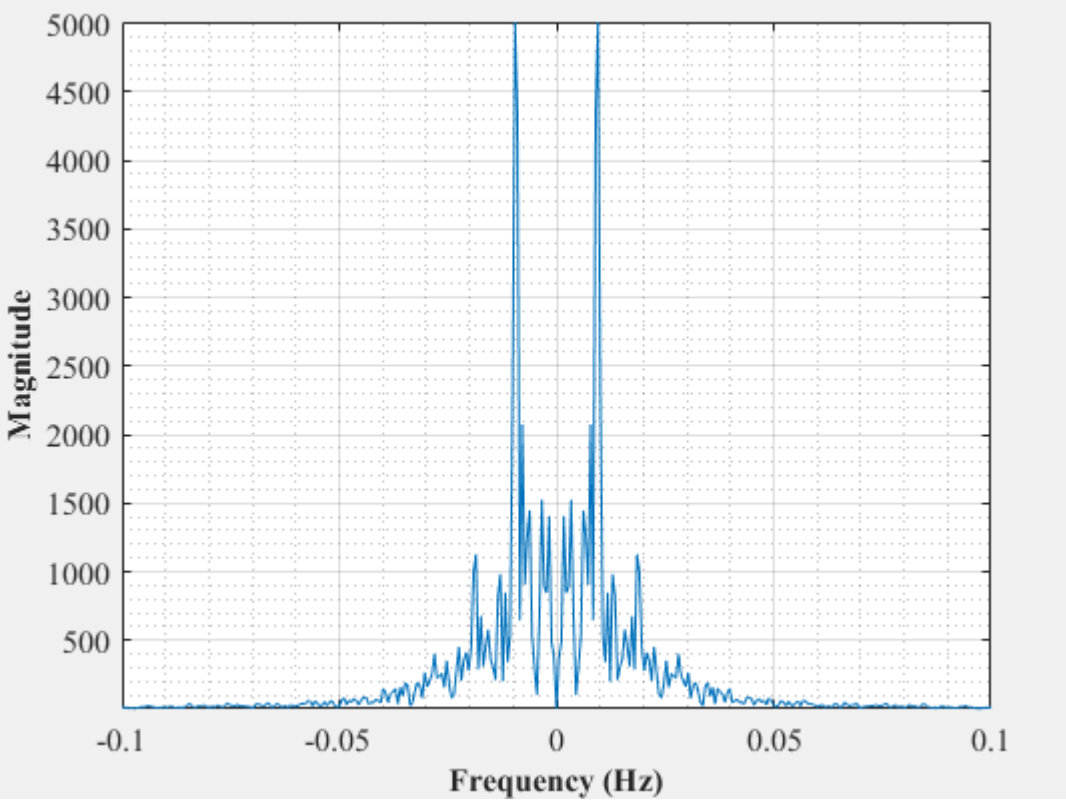


*Figure A-6: Dominant Frequency for an empty vessel at 65.28 dm$^3$/minute gas flow rate*

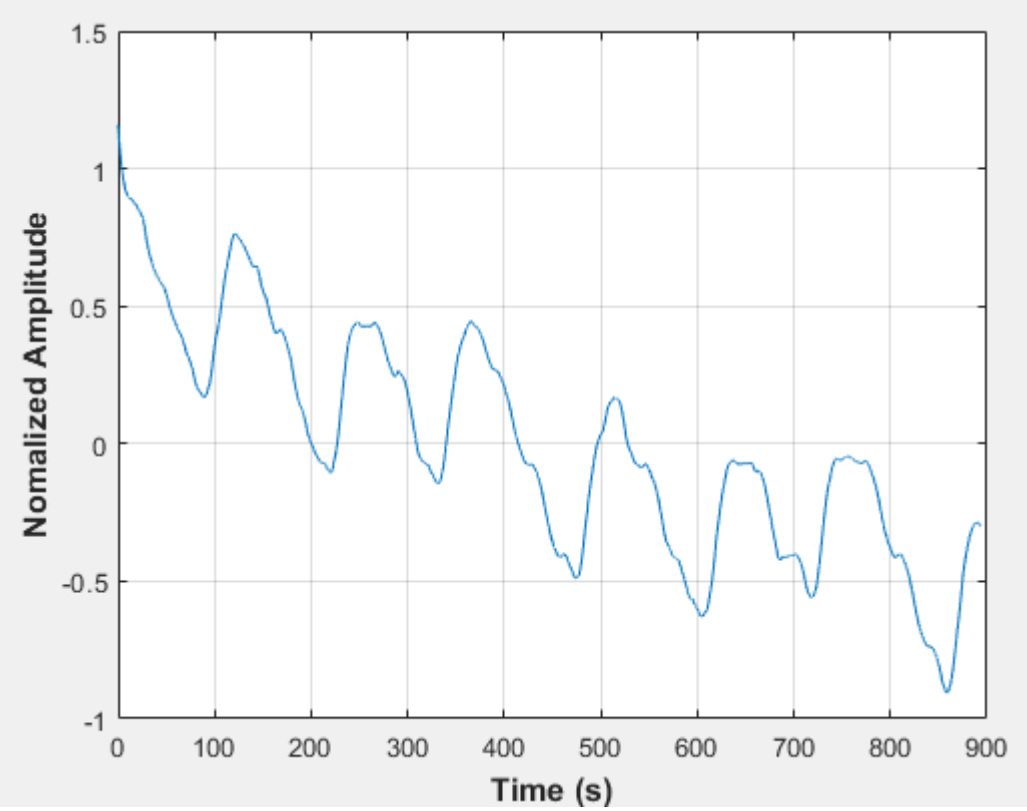


*Figure A-7: Pressure fluctuations in a uniformly packed vessel at 48.96 $dm^3$/minute gas flow rate*

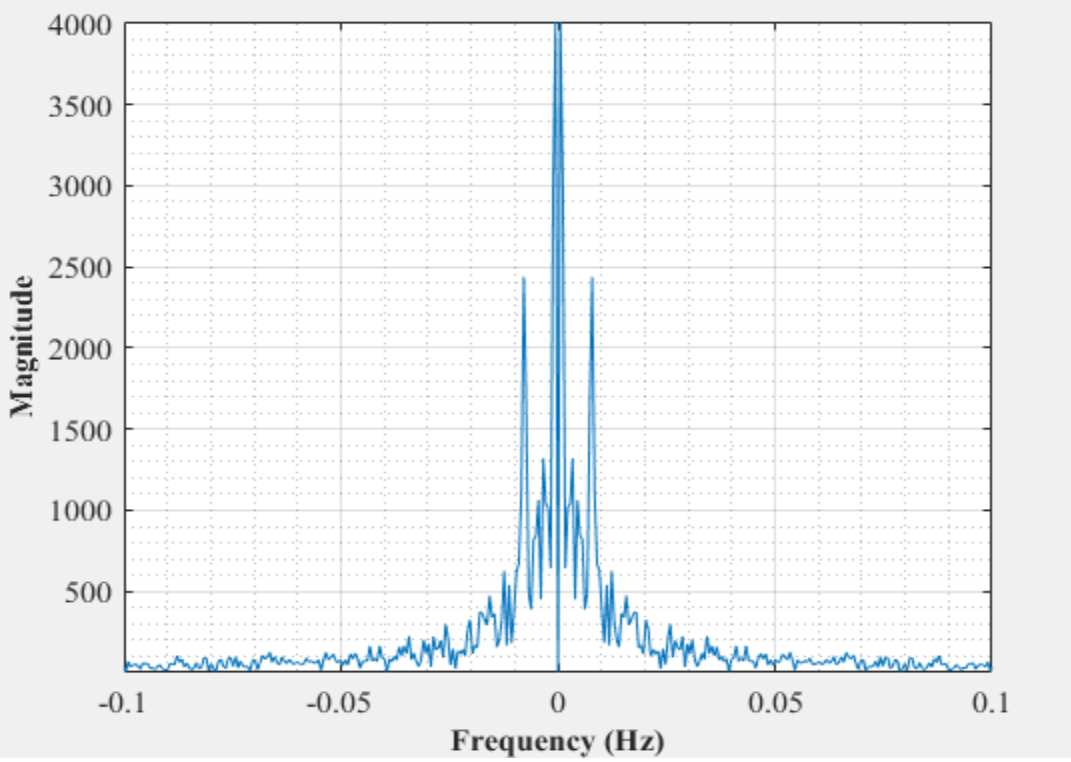


*Figure A-8: Dominant Frequency for a uniformly packed vessel at 48.96 $dm^3$/minute gas flow rate*

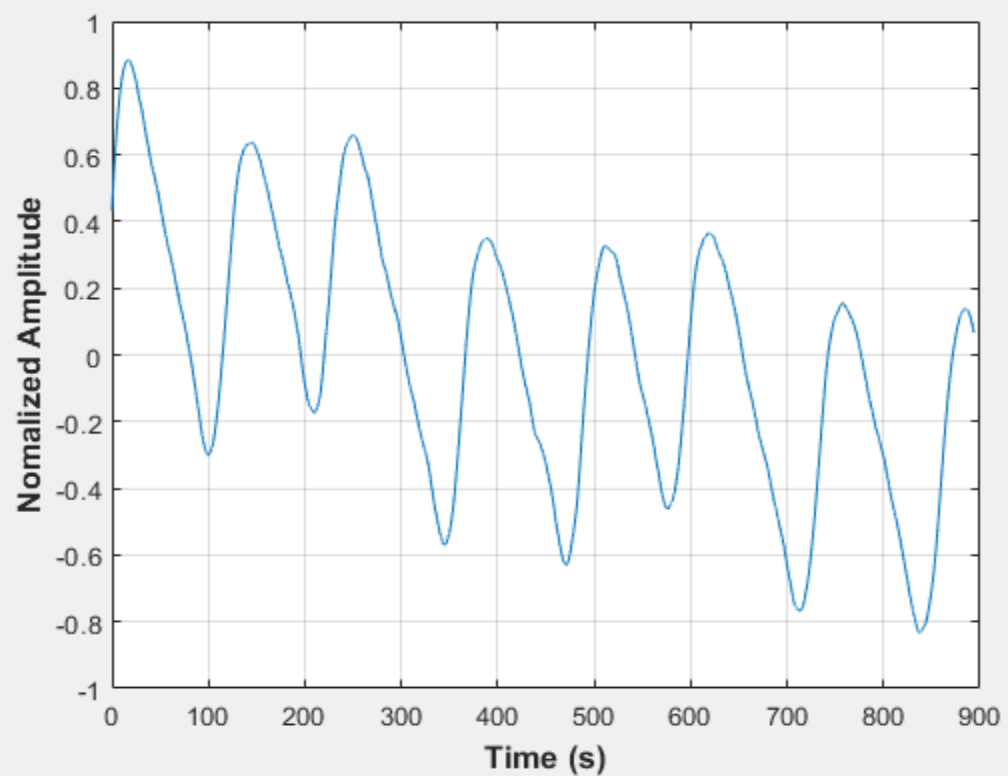


*Figure A-9: Pressure fluctuations in a uniformly packed vessel at 54.40 $dm^3$/minute gas flow rate*

*rate*

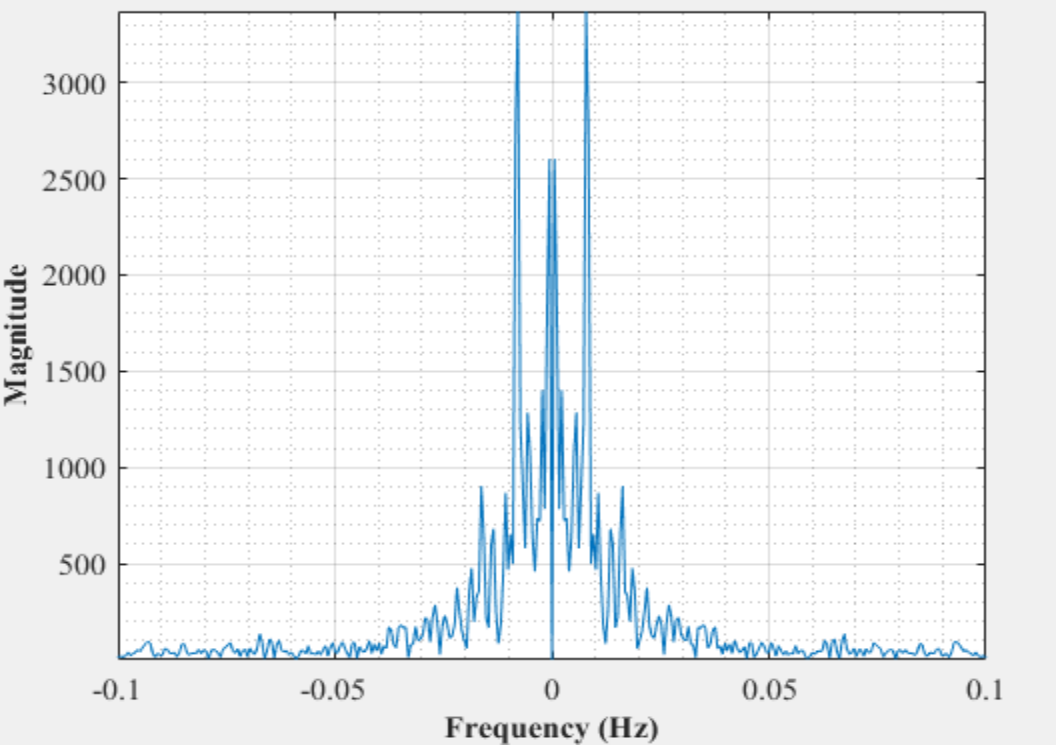


*Figure A-10: Dominant Frequency for a uniformly packed vessel at 54.40 $dm^3$/minute gas flow rate*

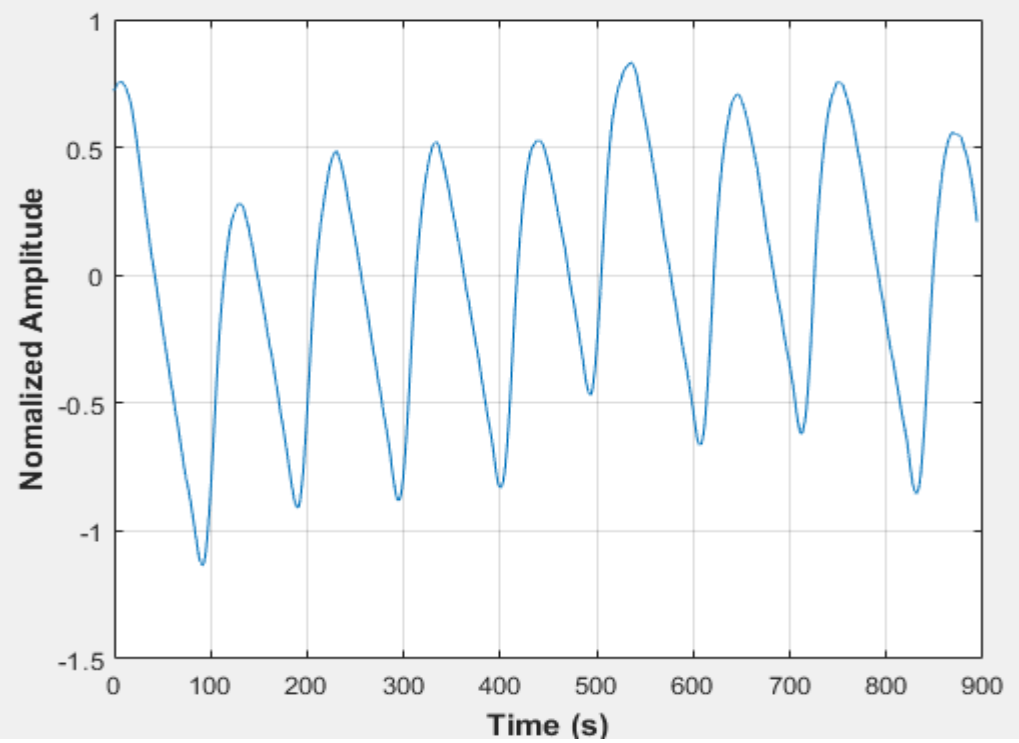


*Figure A-11: Pressure fluctuations in a uniformly packed vessel at 65.28 $dm^3$/minute gas flow rate*

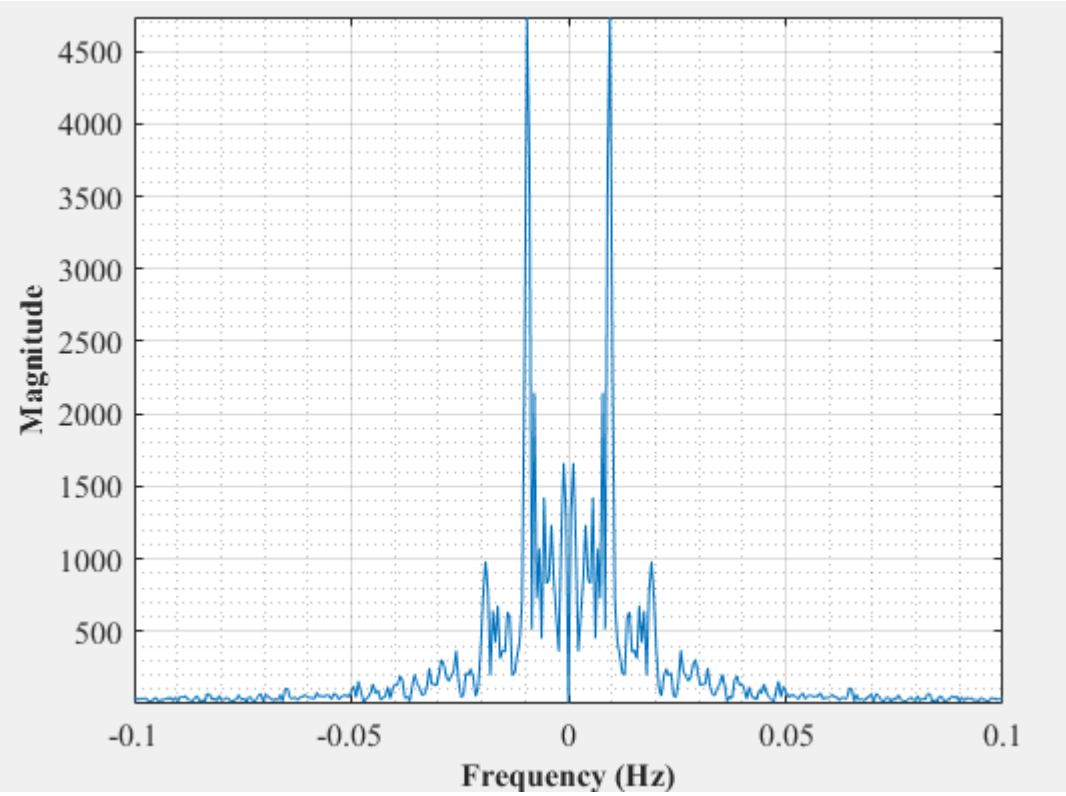


*Figure A-12: Dominant Frequency for a uniformly packed vessel at 65.28 $dm^3$/minute gas flow rate*

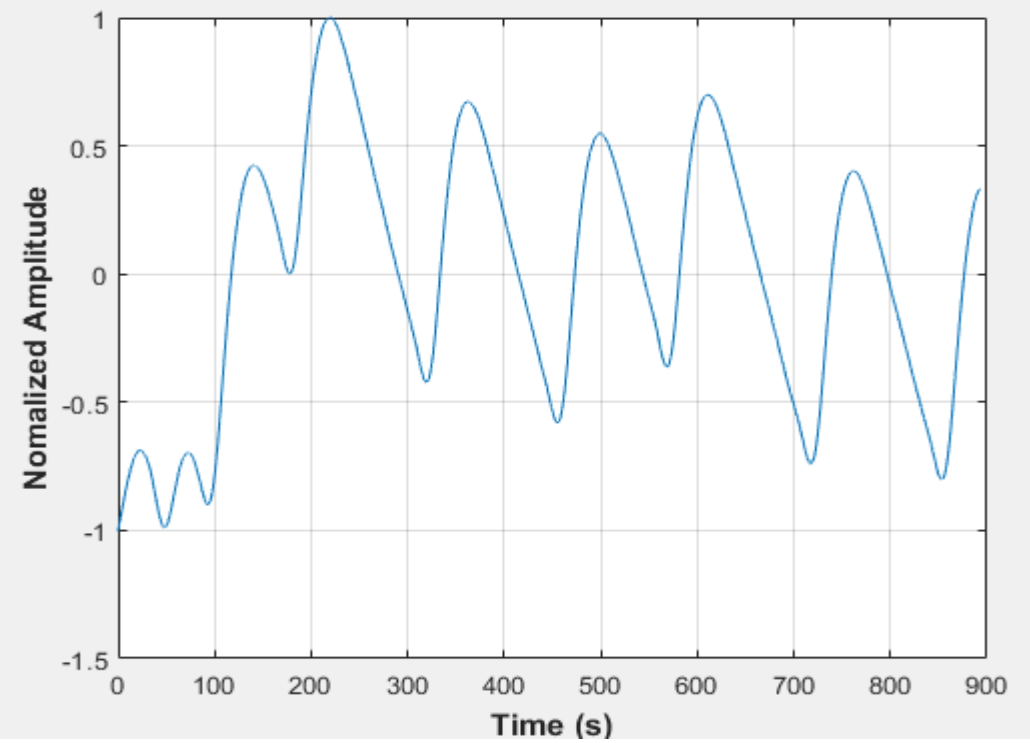


*Figure A-13: Pressure fluctuations in a non-uniformly packed vessel (large and small at the center) at 48.96 $dm^3$/minute gas flow rate*

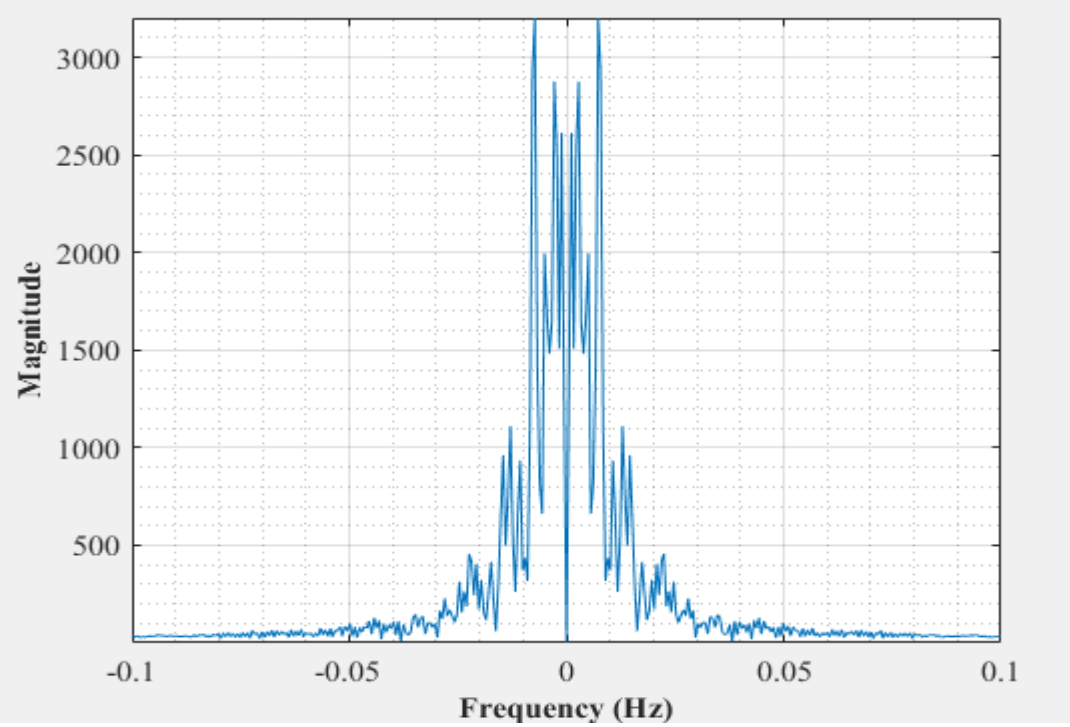


*Figure A-14: Dominant Frequency for a non-uniformly packed vessel (large and small at the center) at 48.96 $dm^3$/minute gas flow rate*

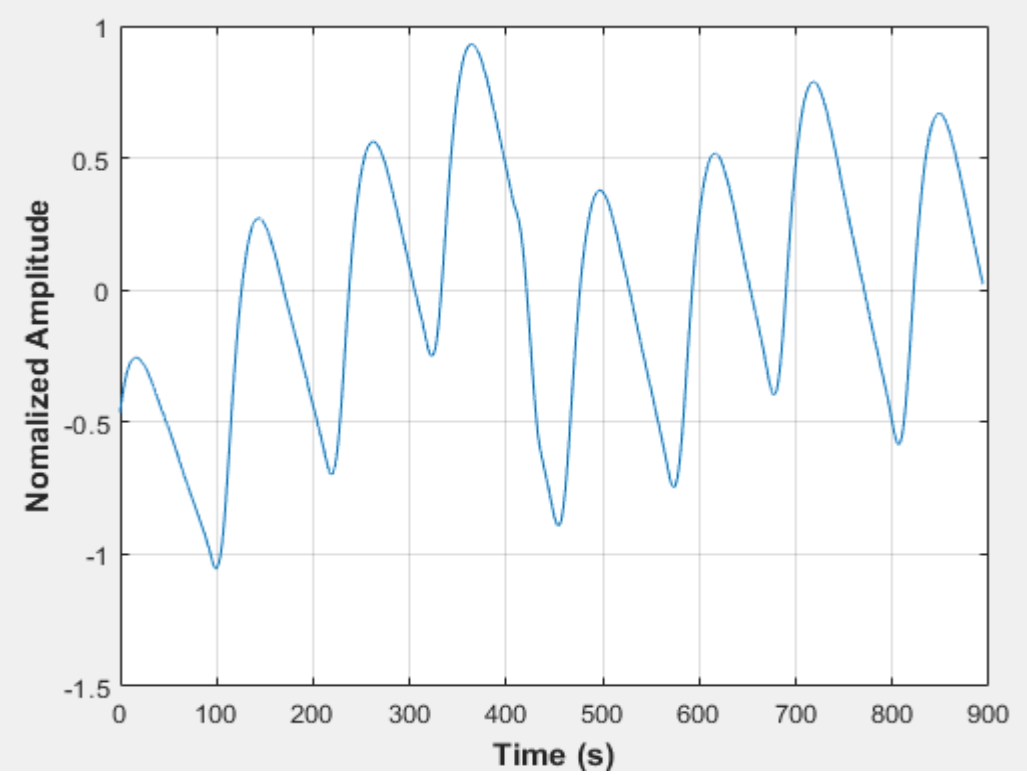


*Figure A-15: Pressure fluctuations in a non-uniformly packed vessel (large and small at the center) at 54.40 dm$^3$/minute gas flow rate*

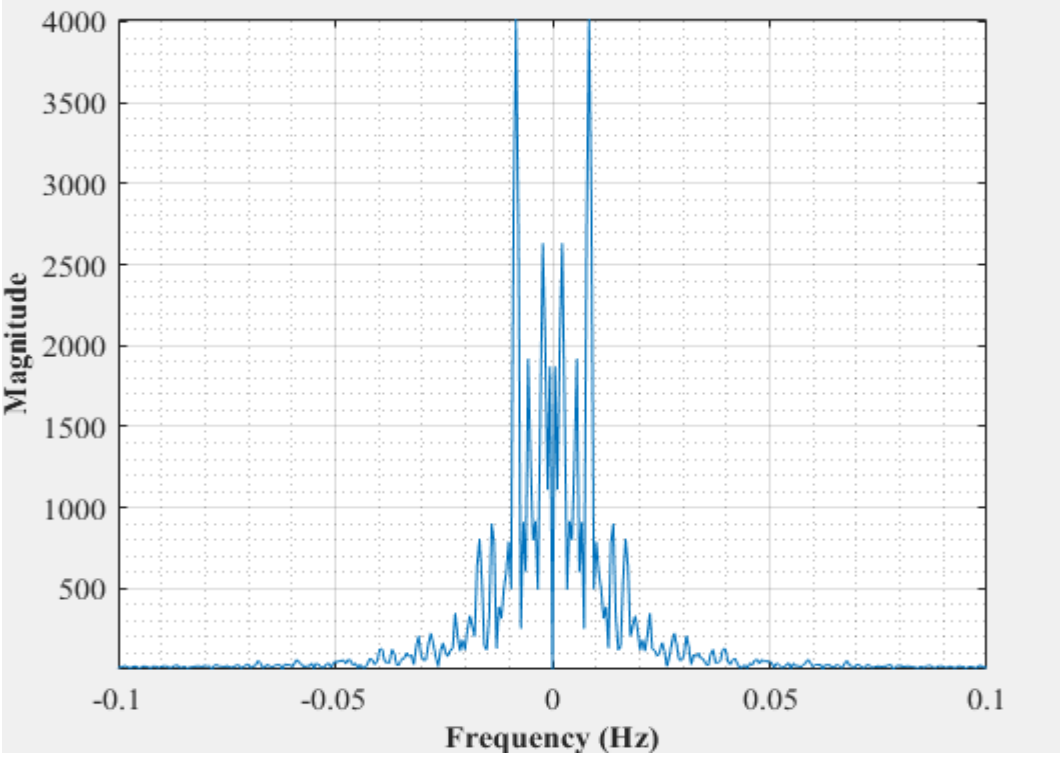


*Figure A-16: Dominant Frequency for a non-uniformly packed vessel (large and small at the center) at 54.40 dm$^3$/minute gas flow rate*

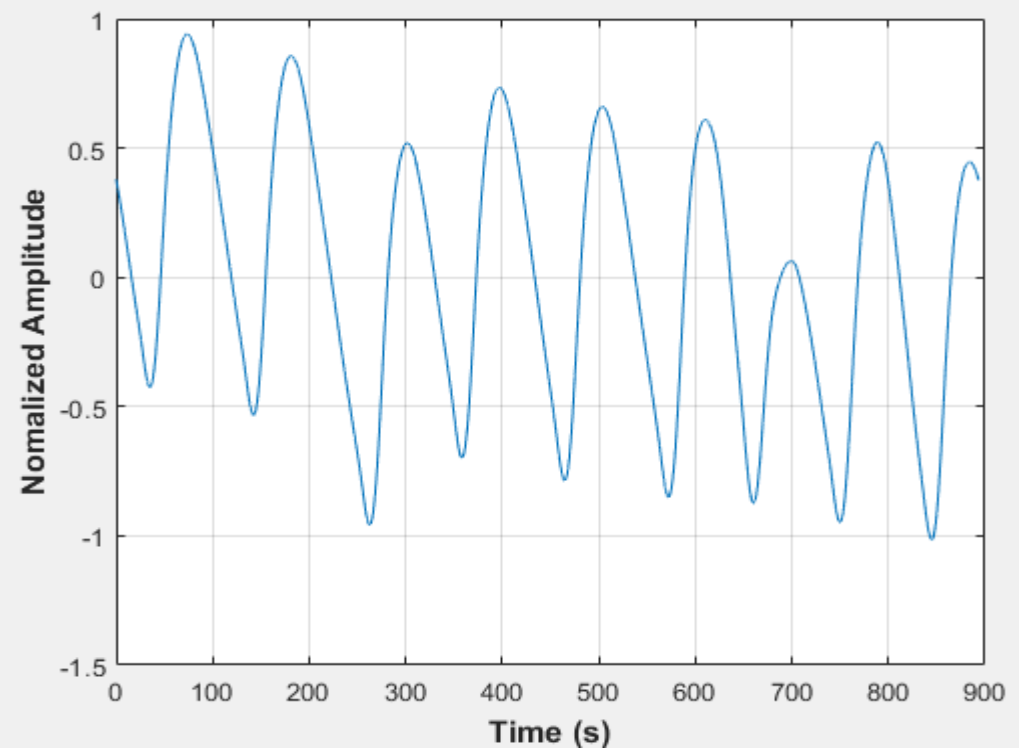


*Figure A17-: Pressure fluctuations in a non-uniformly packed vessel (large and small at the center) at 65.28 dm$^3$/minute gas flow rate*

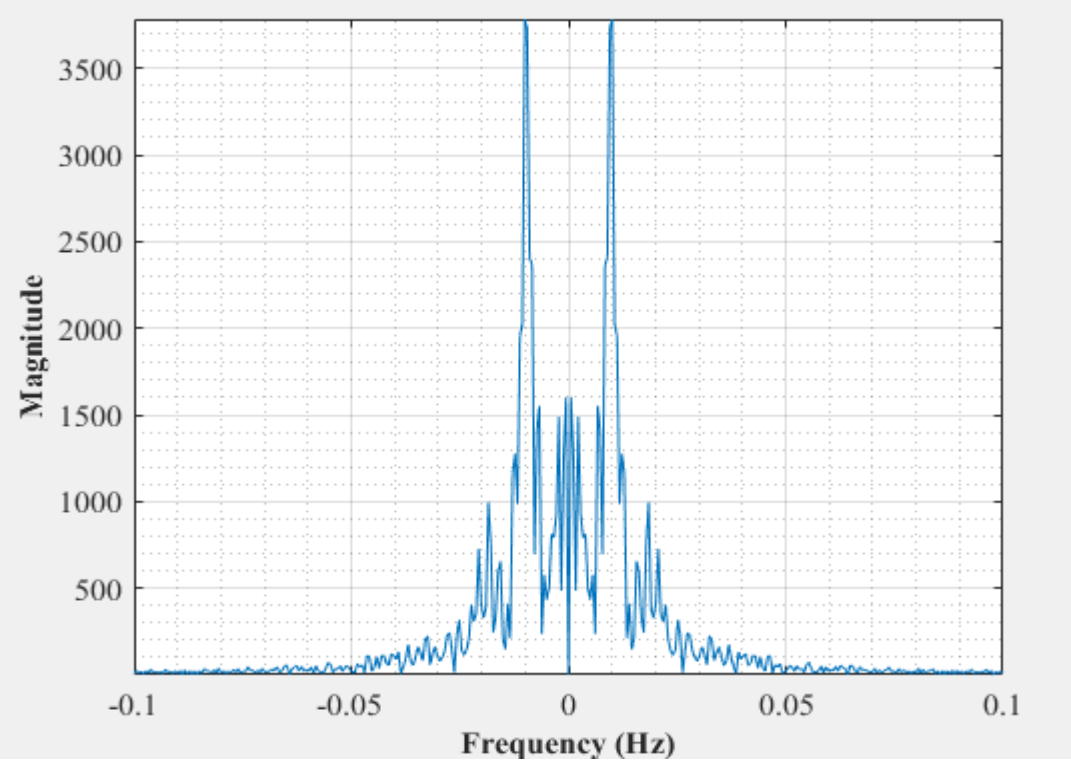


*Figure A-18: Dominant Frequency for a non-uniformly packed vessel (large and small at the center) at 65.28 dm$^3$/minute gas flow rate*

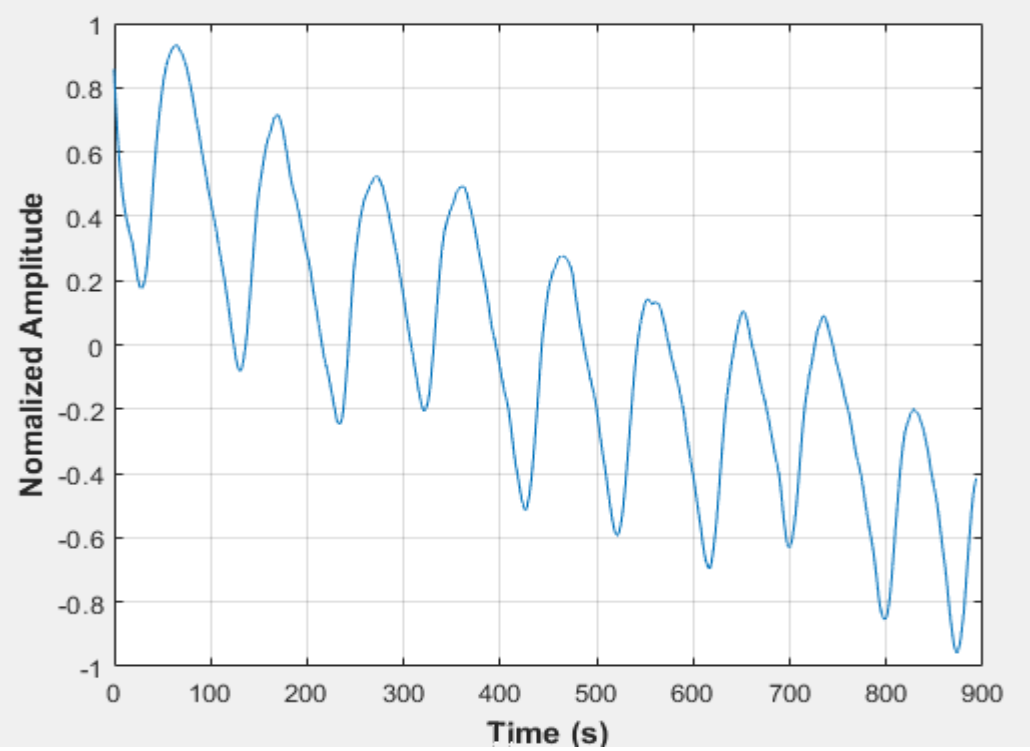


*Figure A-19: Pressure fluctuations in a non-uniformly packed vessel (large and small at the middle) at 48.96 $dm^3$/minute gas flow rate*

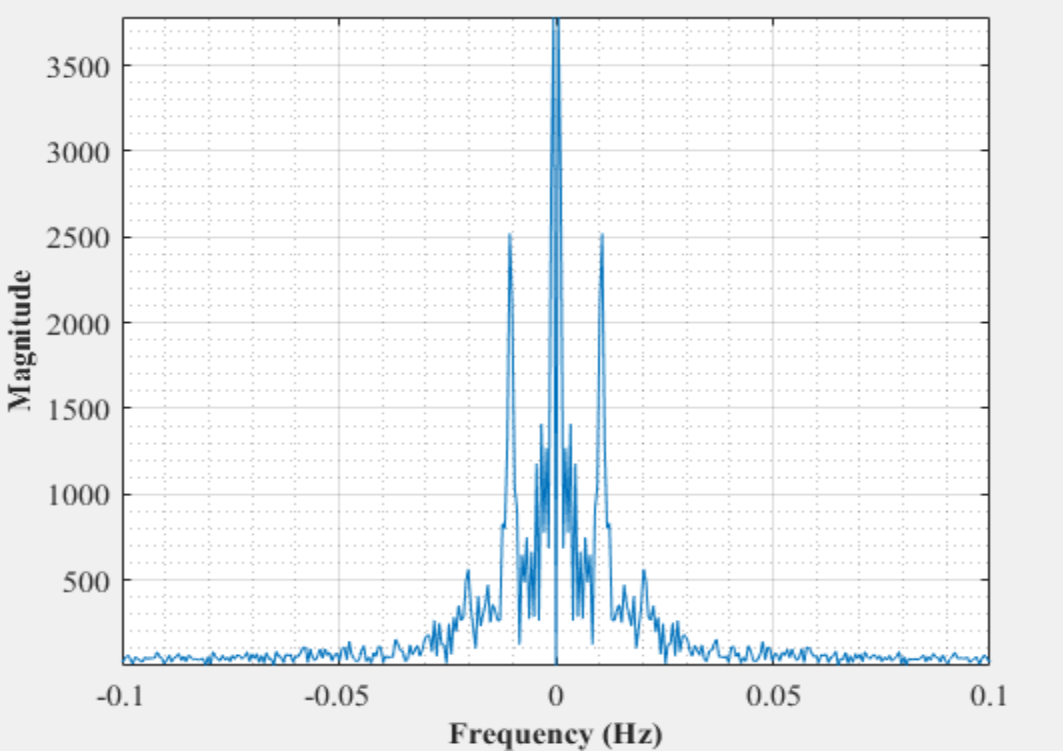


*Figure A-20: Dominant Frequency for a non-uniformly packed vessel (large and small at the middle) at 48.96 $dm^3$/minute gas flow rate*

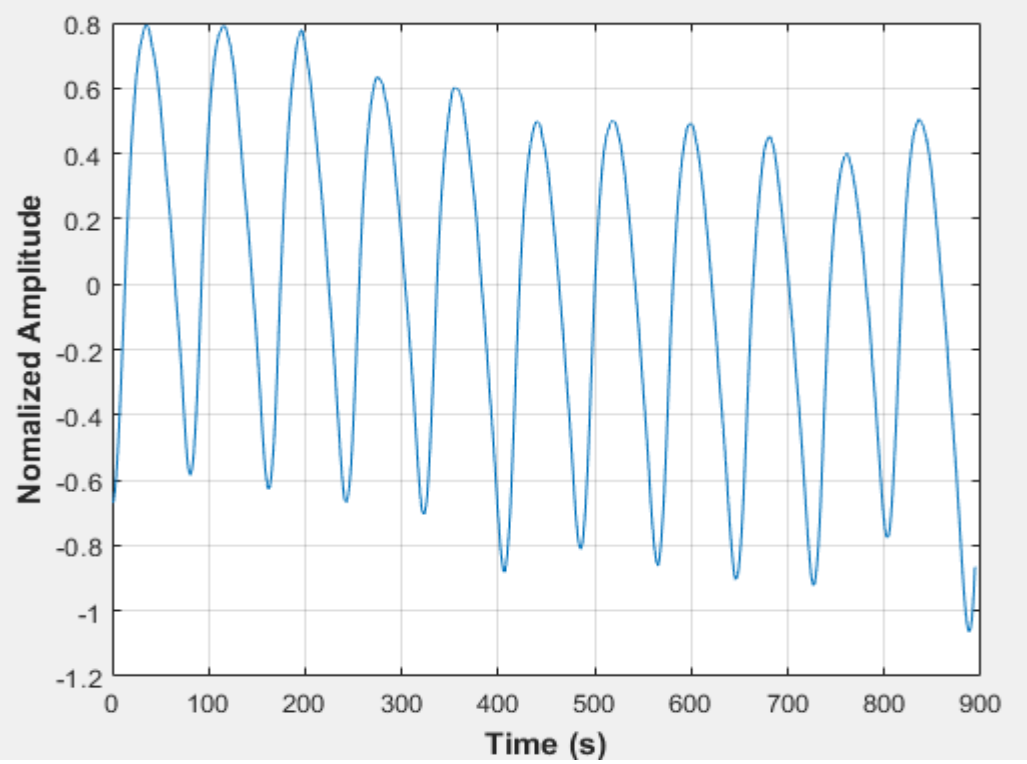


*Figure A-21: Pressure fluctuations in a non-uniformly packed vessel (large and small at the middle) at 54.40 dm$^3$/minute gas flow rate*

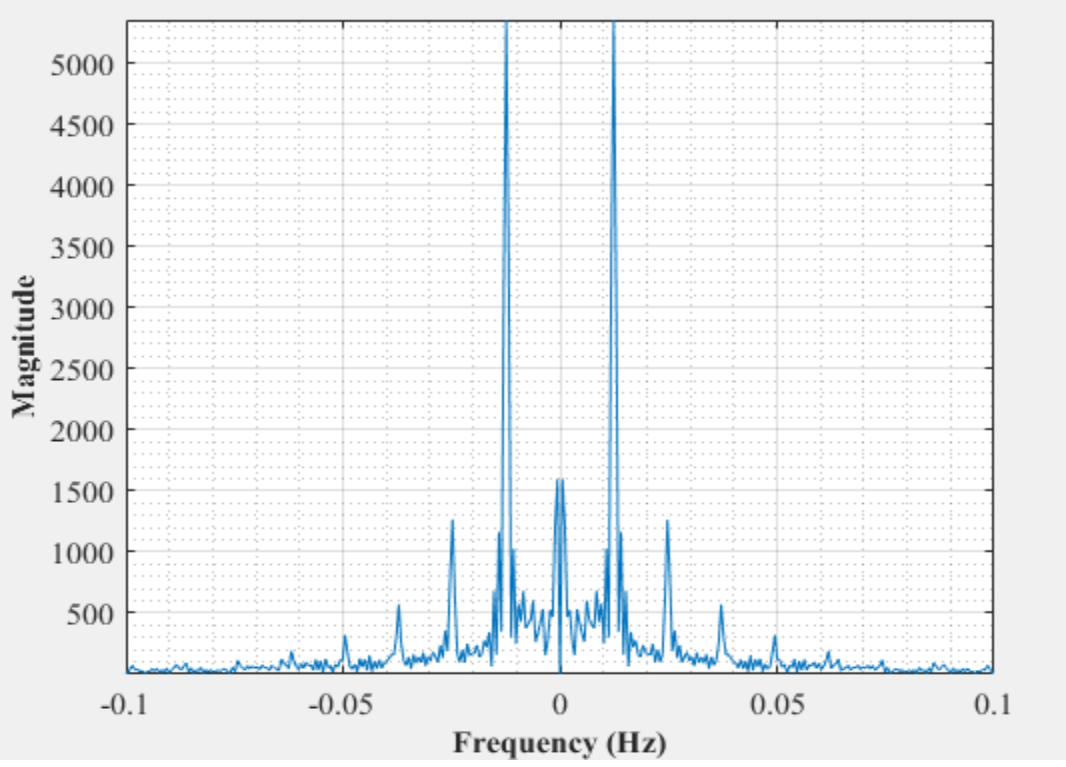


*Figure A-22: Dominant Frequency for a non-uniformly packed vessel (large and small at the middle) at 54.40 dm$^3$/minute gas flow rate*

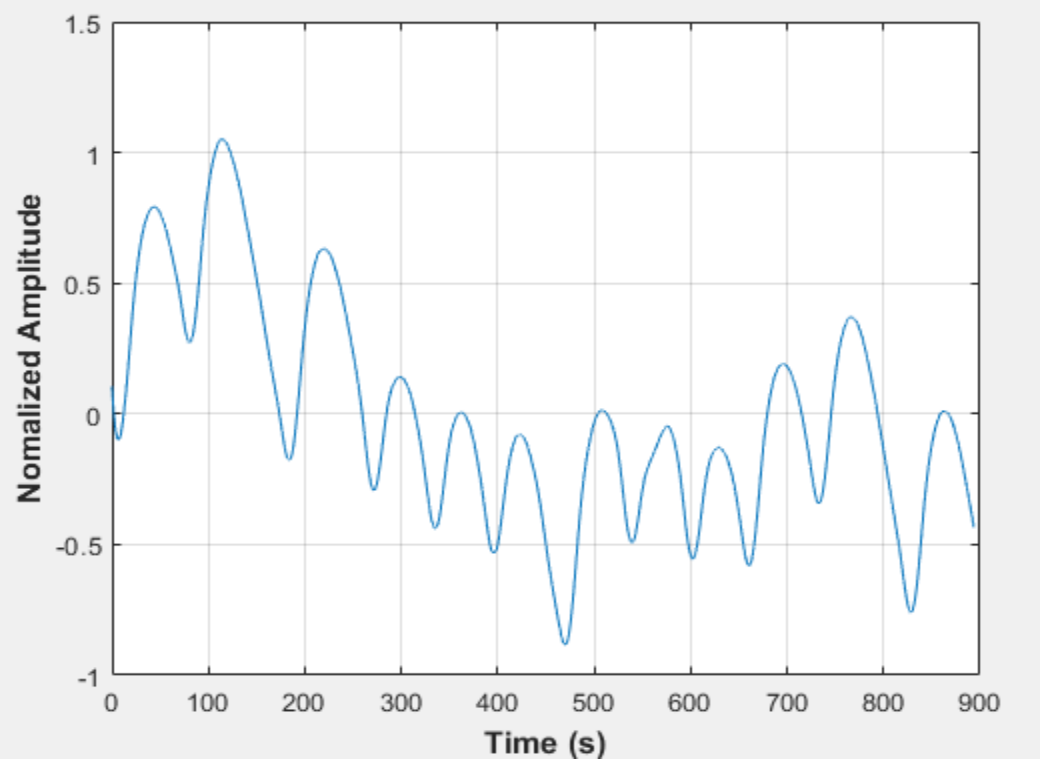


*Figure A-23: Pressure fluctuations in a non-uniformly packed vessel (large and small at the middle) at 65.28 $dm^3$/minute gas flow rate*

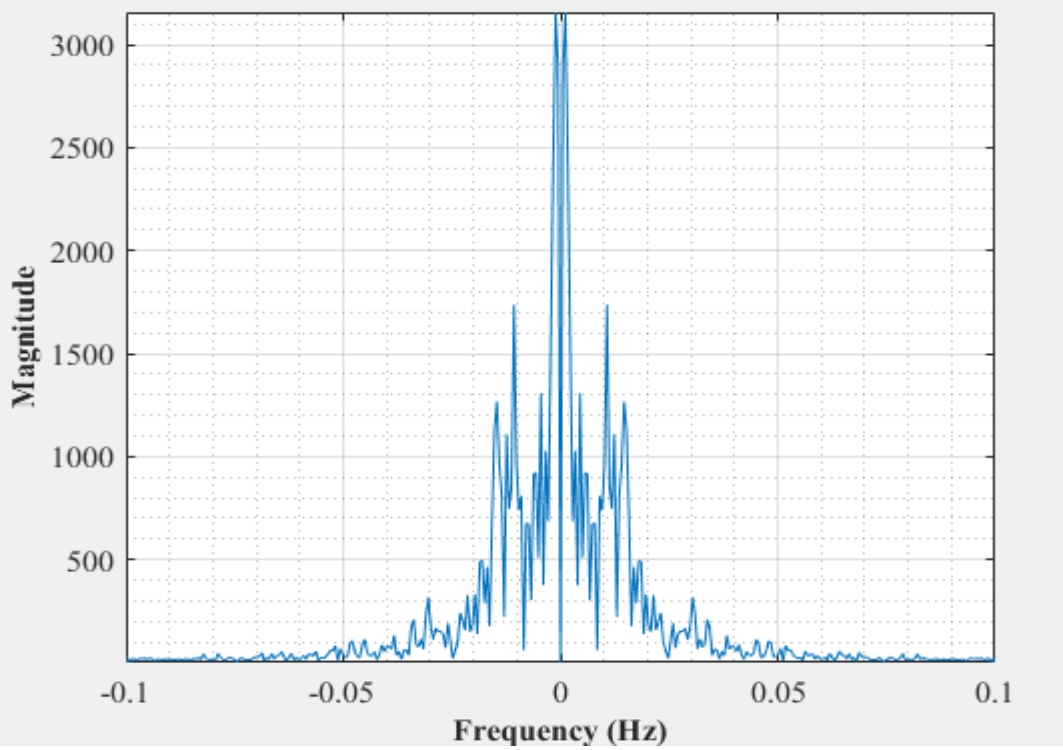


*Figure A-24: Dominant Frequency for a non-uniformly packed vessel (large and small at the middle) at 65.28 $dm^3$/minute gas flow rate*

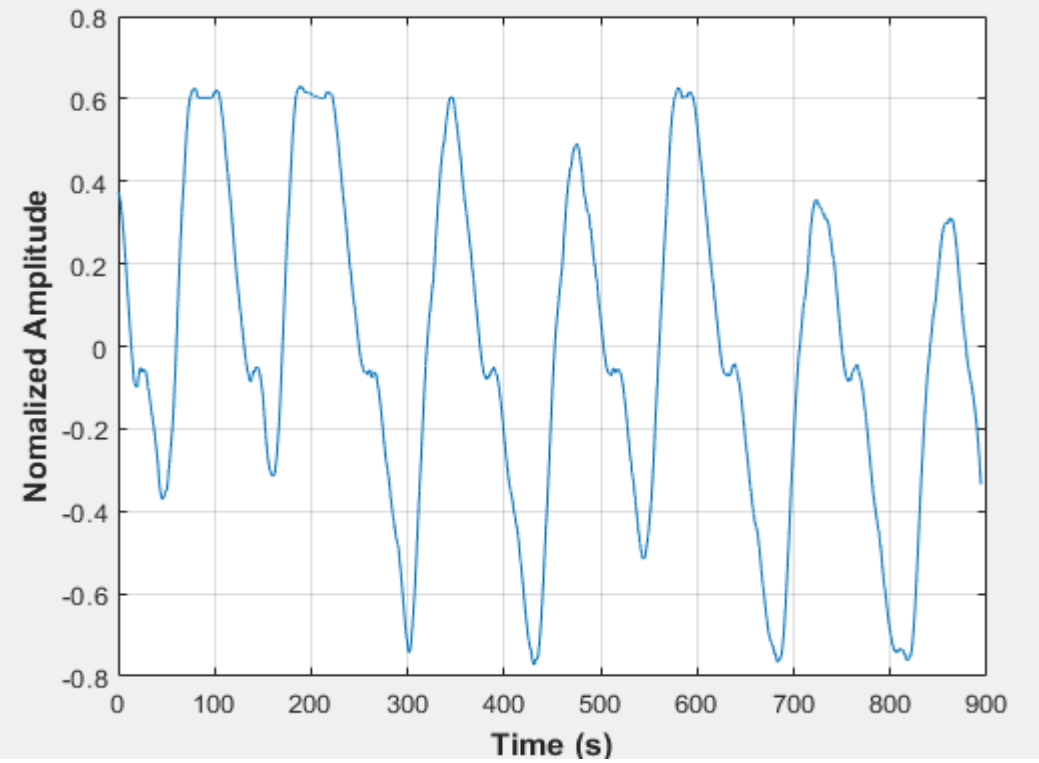


*Figure A-25: Pressure fluctuations in a non-uniformly packed vessel (large and small at the side) at 48.96 dm$^3$/minute gas flow rate*

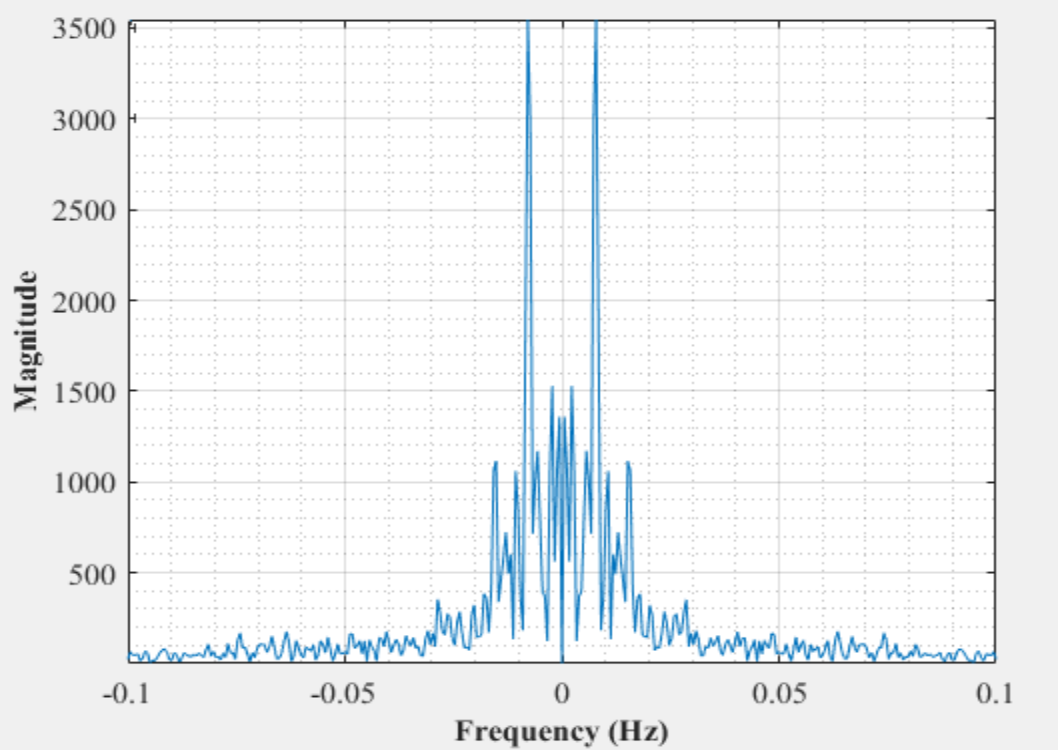


*Figure A-26: Dominant Frequency for a non-uniformly packed vessel (large and small at the side) at 48.96 dm$^3$/minute gas flow rate*

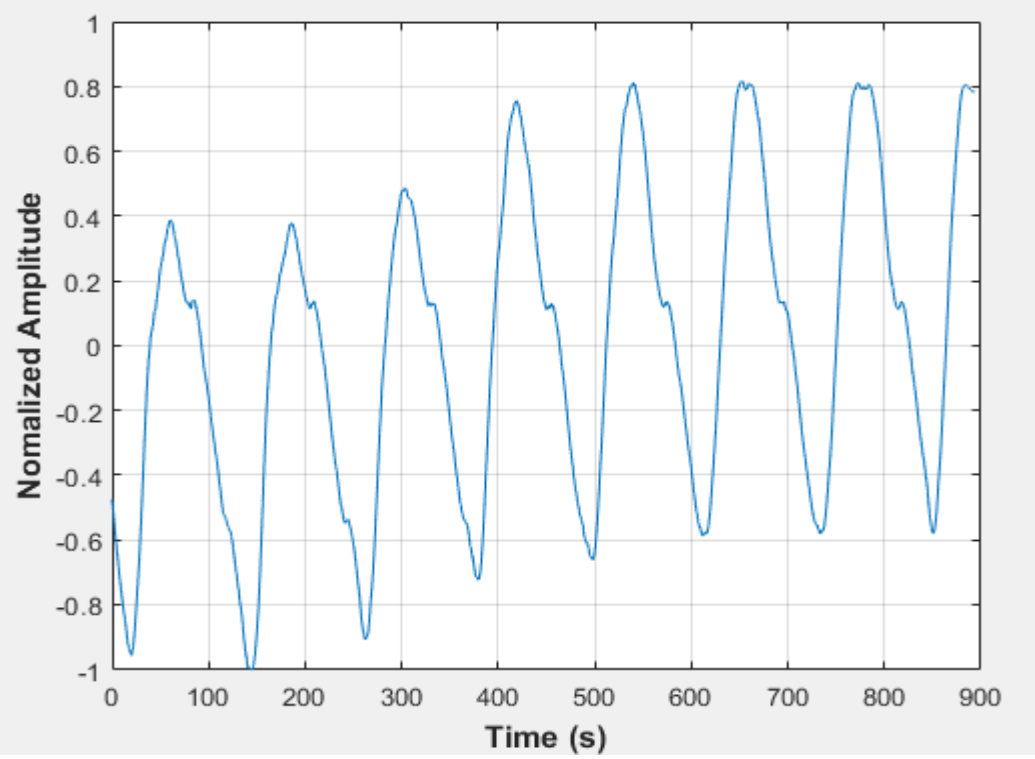


*Figure A-27: Pressure fluctuations in a non-uniformly packed vessel (large and small at the side) at 54.40 dm$^3$/minute gas flow rate*

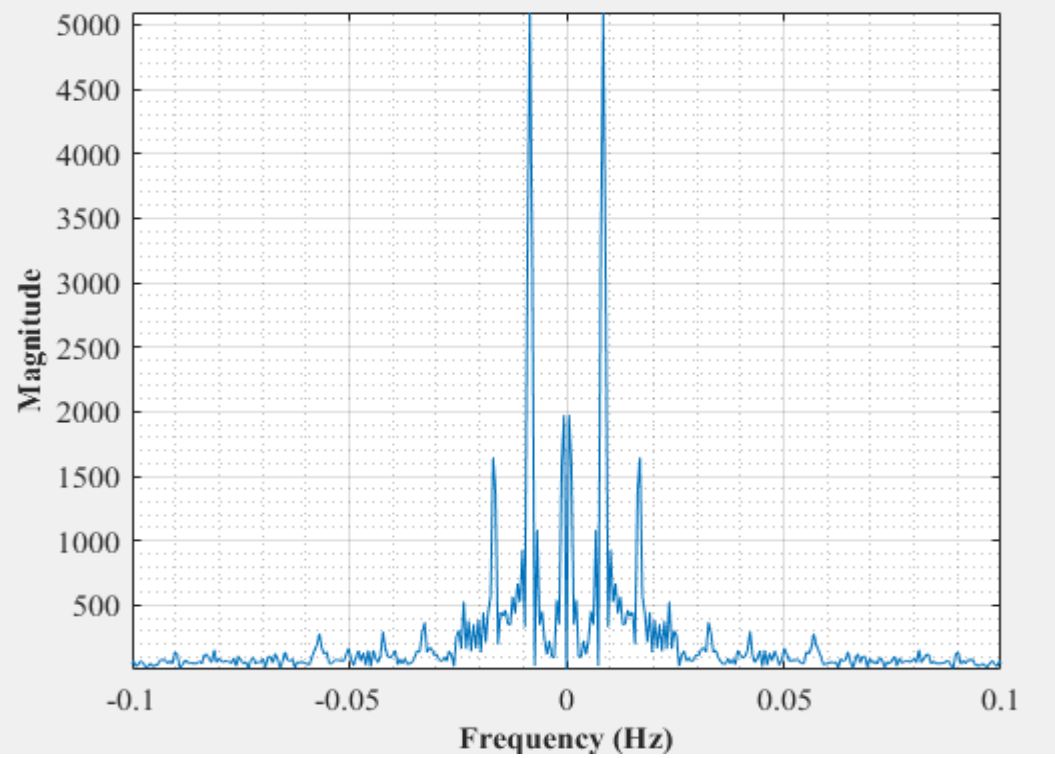


*Figure A-28: Dominant Frequency for a non-uniformly packed vessel (large and small at the side) at 54.40 dm$^3$/minute gas flow rate*

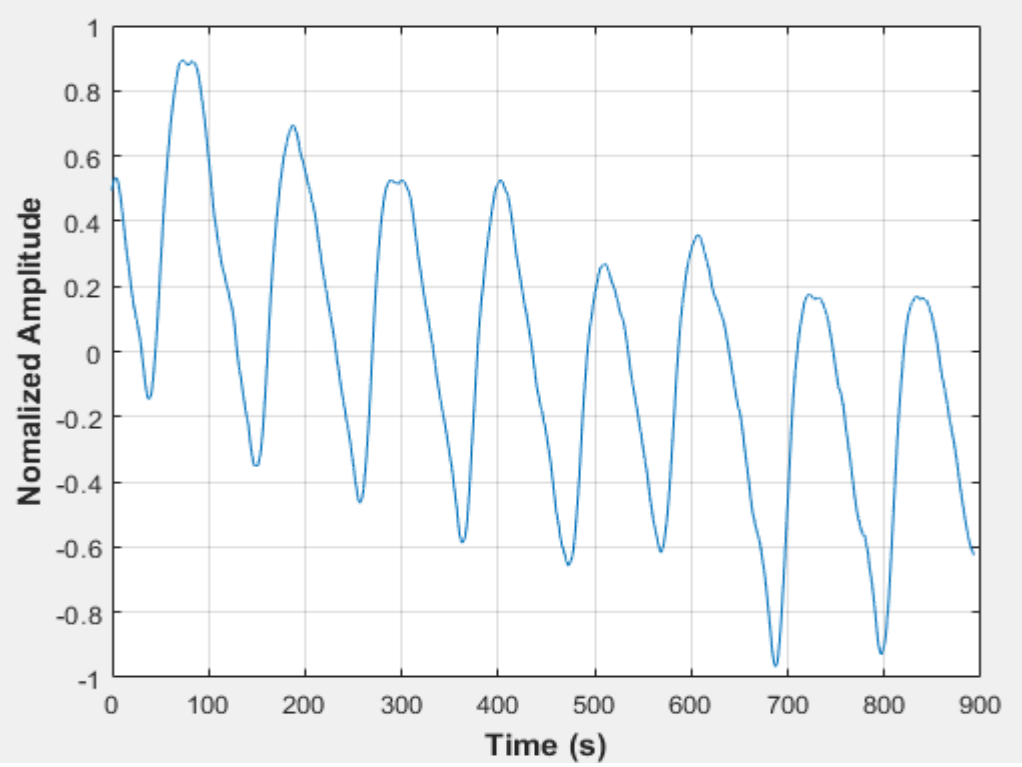


*Figure A-29: Pressure fluctuations in a non-uniformly packed vessel (large and small at the side) at 65.28 dm$^3$/minute rotameter flow*

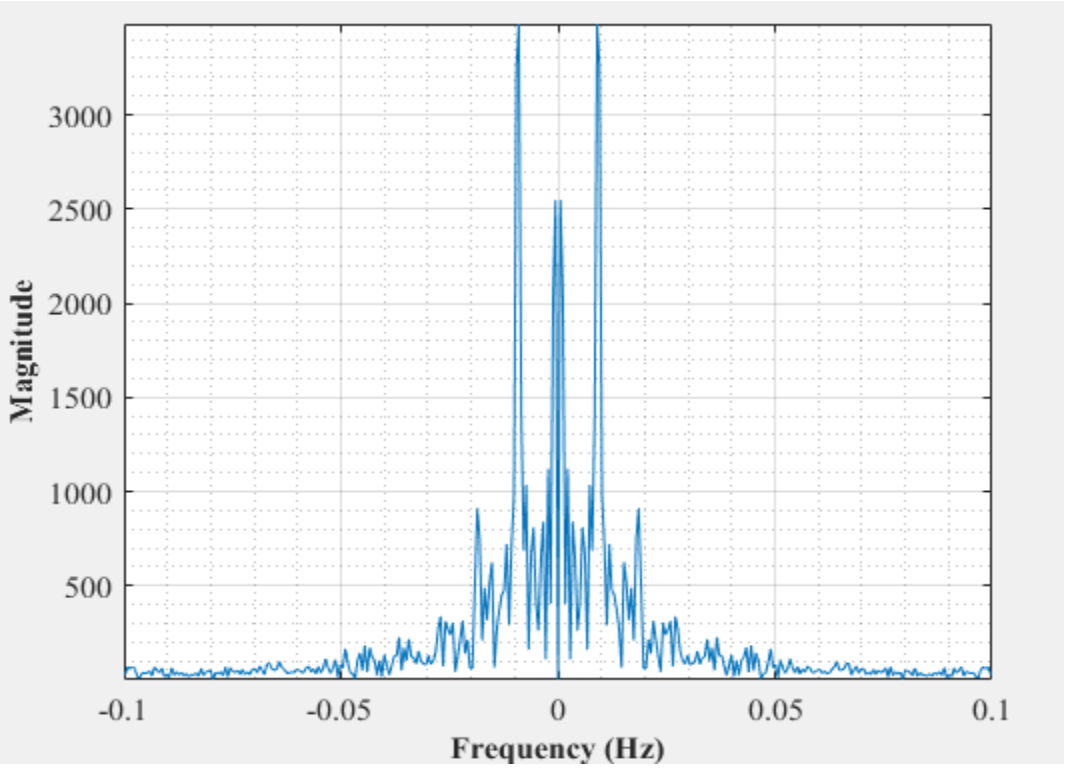


*Figure A-30: Dominant Frequency for a non-uniformly packed vessel (large and small at the side) at 65.28 dm$^3$/minute gas flow rate*

*Table A-0-1: First Batch Experimental Results- Frequency (mHz) data at Various Flowrates*

| **Flowrate ($dm^3$/minute)** | **48.96** | **54.40** | **65.28** |
|---|---|---|---|
| Empty Vessel | 9.54 | 8.53 | 9.46 |
| Large Packing | 8.19 | 8.39 | 9.24 |
| Large and small Packing (center) | 10.80 | 8.35 | 9.77 |
| Large and small packing (middle) | 10.52 | 12.33 | 13.76 |
| Large and small packing (side) | 7.81 | 8.46 | 9.45 |

*Table A-0-2: First Batch Experimental Results- Amplitude data at Various Flowrates*

| Flowrate ($dm^3$/minute) | 48.96 | 54.40 | 65.28 |
|---|---|---|---|
| Empty Vessel | 0.51 | 0.63 | 0.75 |
| Large Packing | 0.28 | 0.50 | 0.65 |
| Large and small Packing (center) | 0.44 | 0.60 | 0.70 |
| Large and small packing (middle) | 0.45 | 0.73 | 0.33 |
| Large and small packing (side) | 0.58 | 0.75 | 0.52 |

## APPENDIX B: Small vessel experiments- Second Batch

This section shows the graphs for the experiments done on the small vessel. Figures B1-B60 show the amplitude and frequency curves for the second batch of experiments. Tables B-1 and B-2 show the summary from the amplitude and frequency data from the second batch of experiments

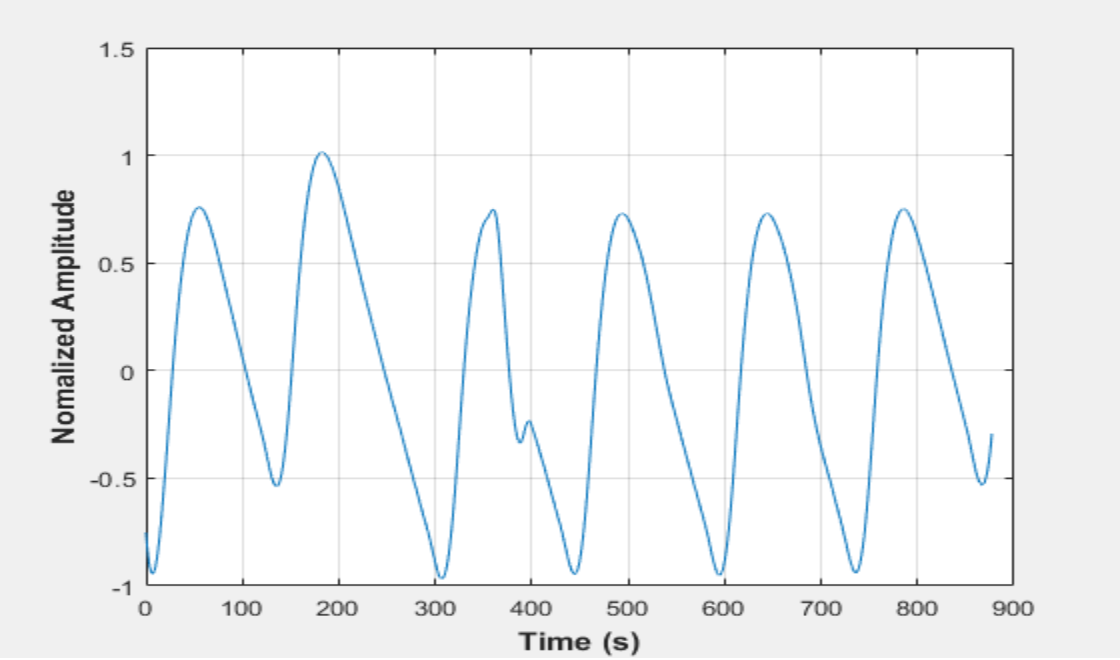


*Figure B-1: Pressure fluctuations in an empty vessel at 48.96 $dm^3$/minute gas flow rate*

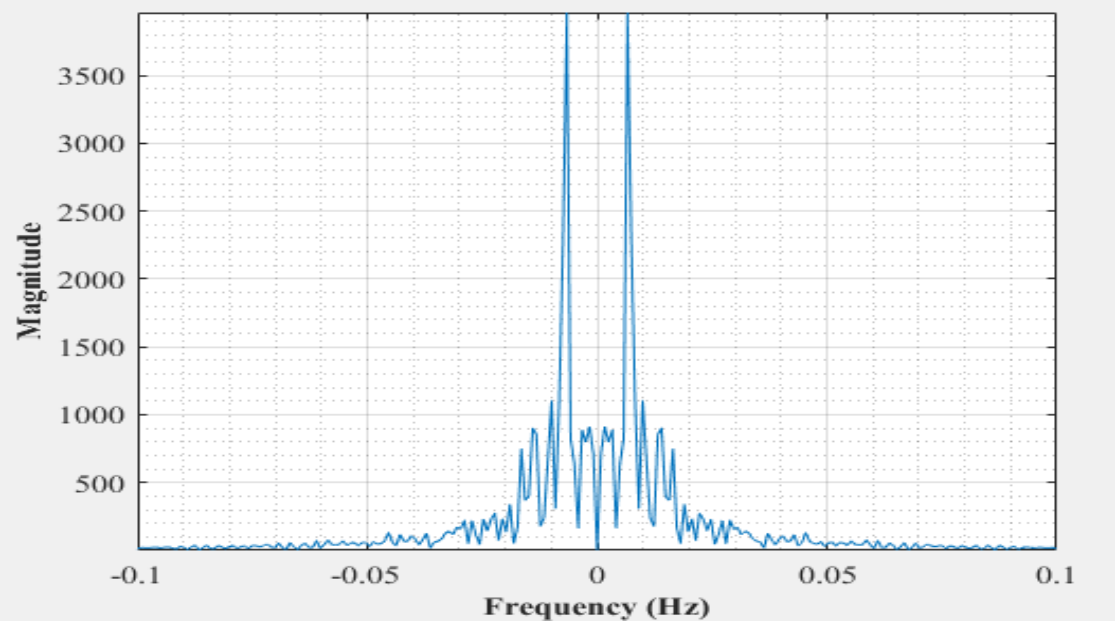


*Figure B-2: Dominant frequency for an empty vessel at 48.96 $dm^3$/minute rotameter flowrate*

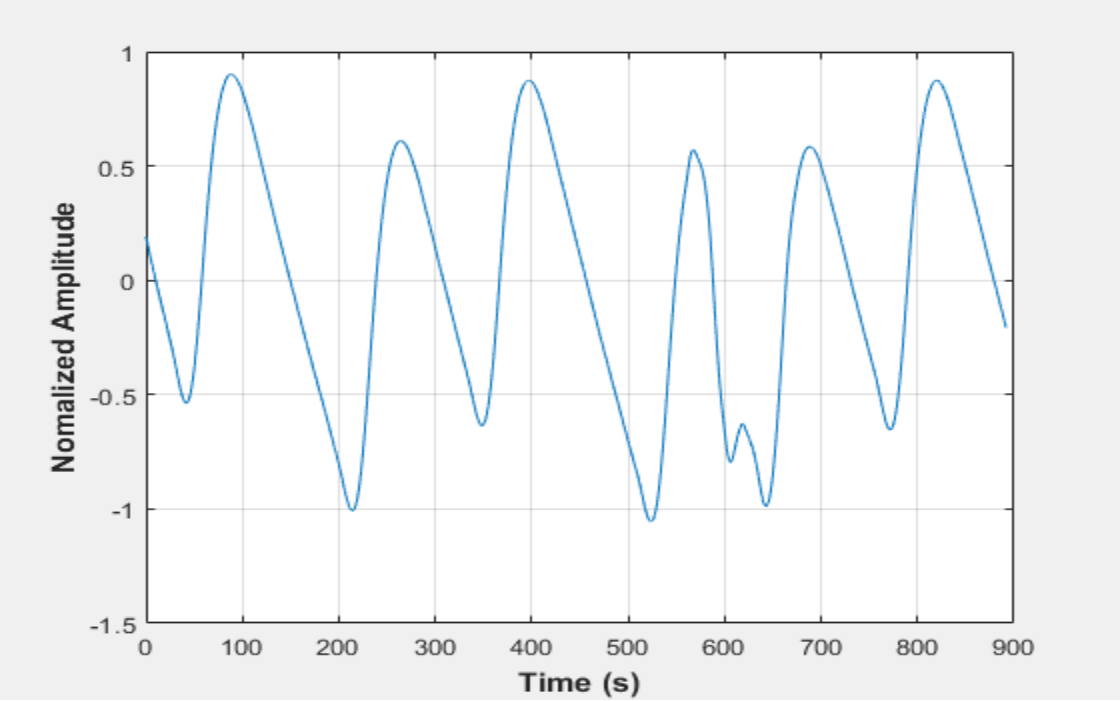


*Figure B-3: Pressure fluctuations in an empty vessel at 48.96 dm$^3$/minute gas flow rate- repeat test*

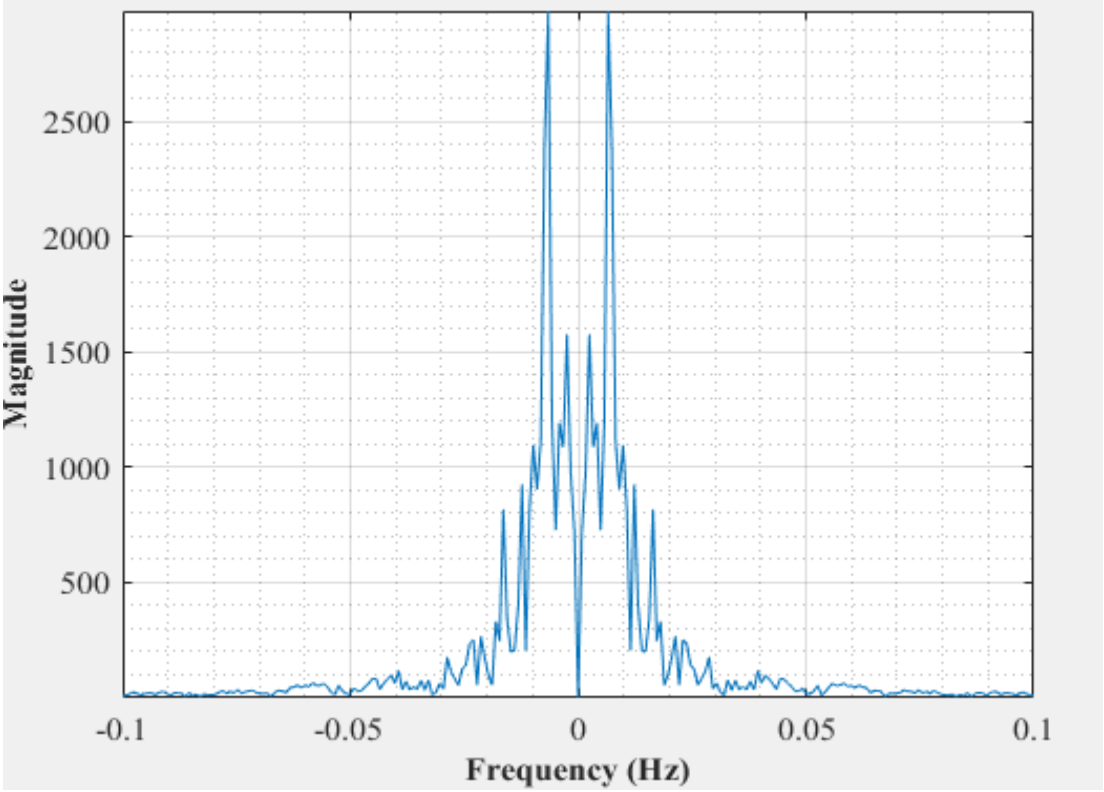


*Figure B-4: Dominant frequency for an empty vessel at 48.96 dm$^3$/minute rotameter flowrate- repeat test*

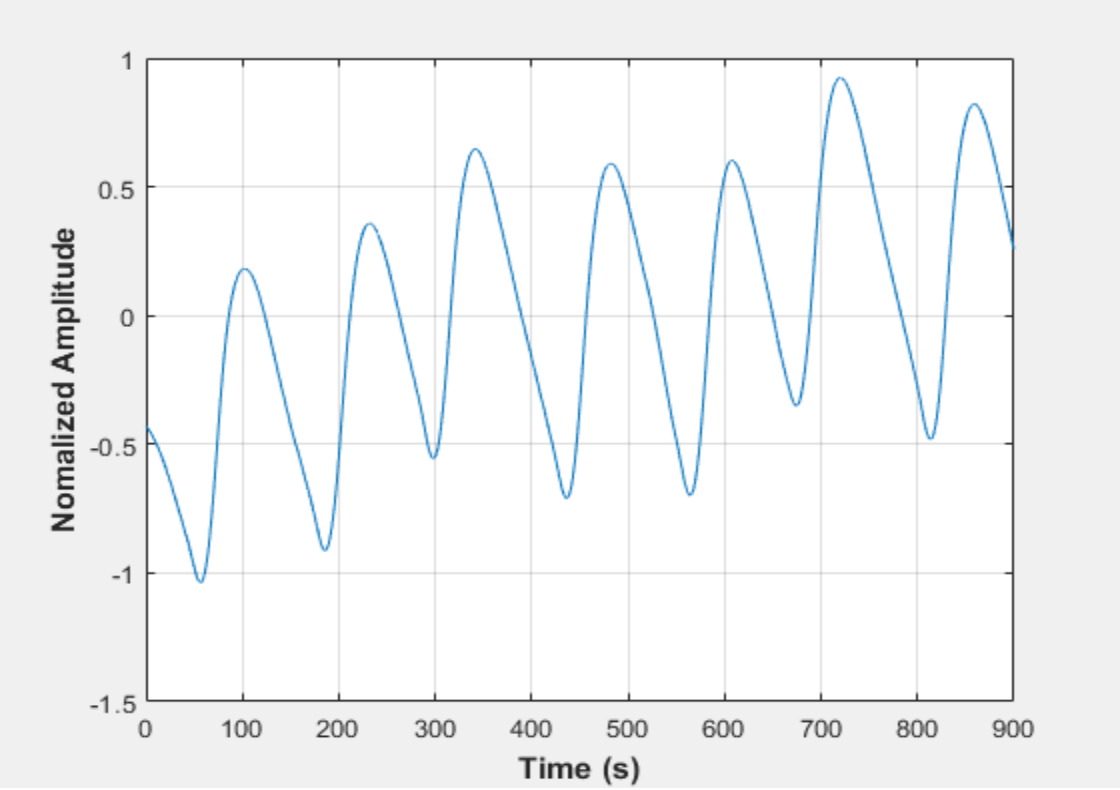


*Figure B-5: Pressure fluctuations in an empty vessel at 54.4 l/min gas flow rate*

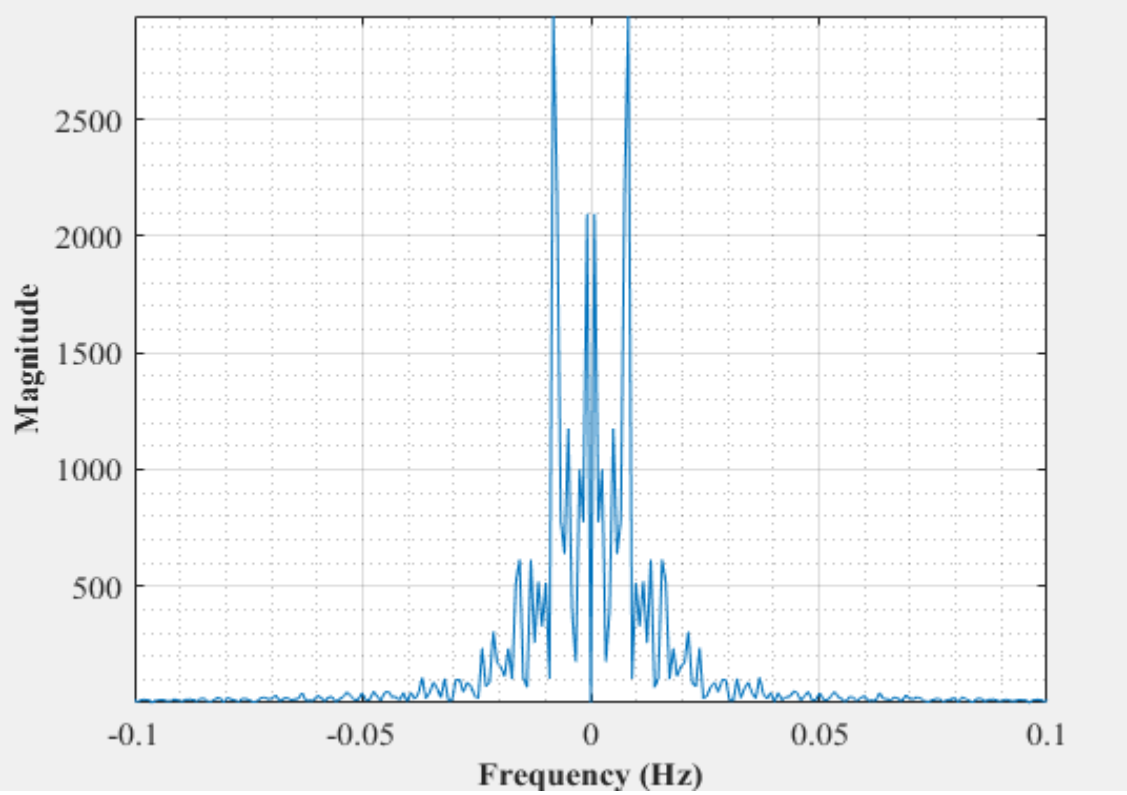


*Figure B-6: Dominant frequency for an empty vessel at 54.4 dm$^3$/minute rotameter flowrate*

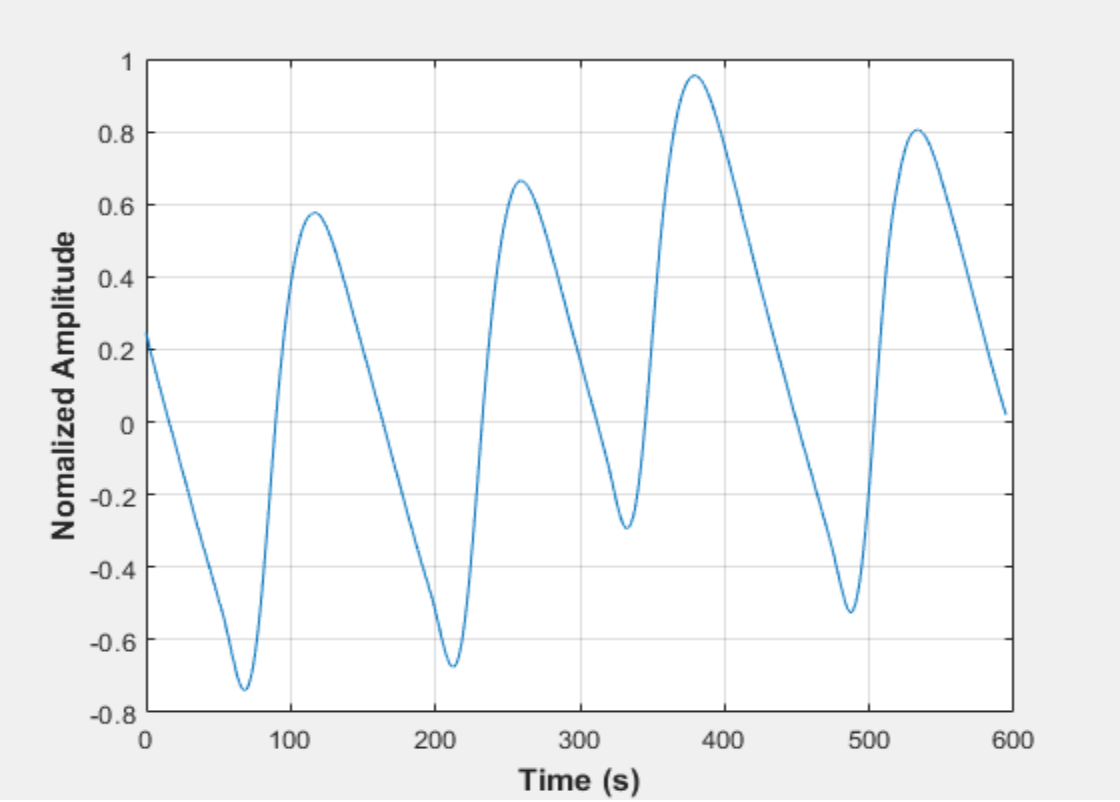


*Figure B-7: Pressure fluctuations in an empty vessel at 54.4 dm$^3$/minute gas flow rate-repeat test*

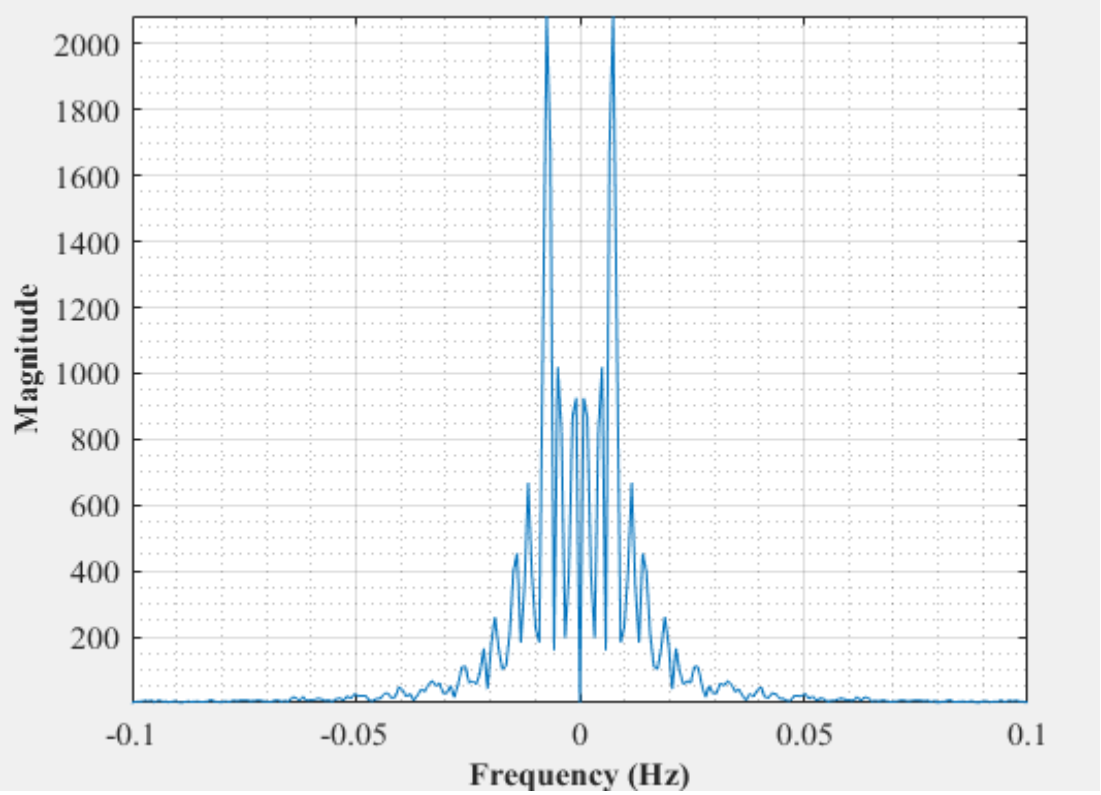


*Figure B-8: Dominant frequency for an empty vessel at 54.4 dm$^3$/minute rotameter flowrate-repeat test*

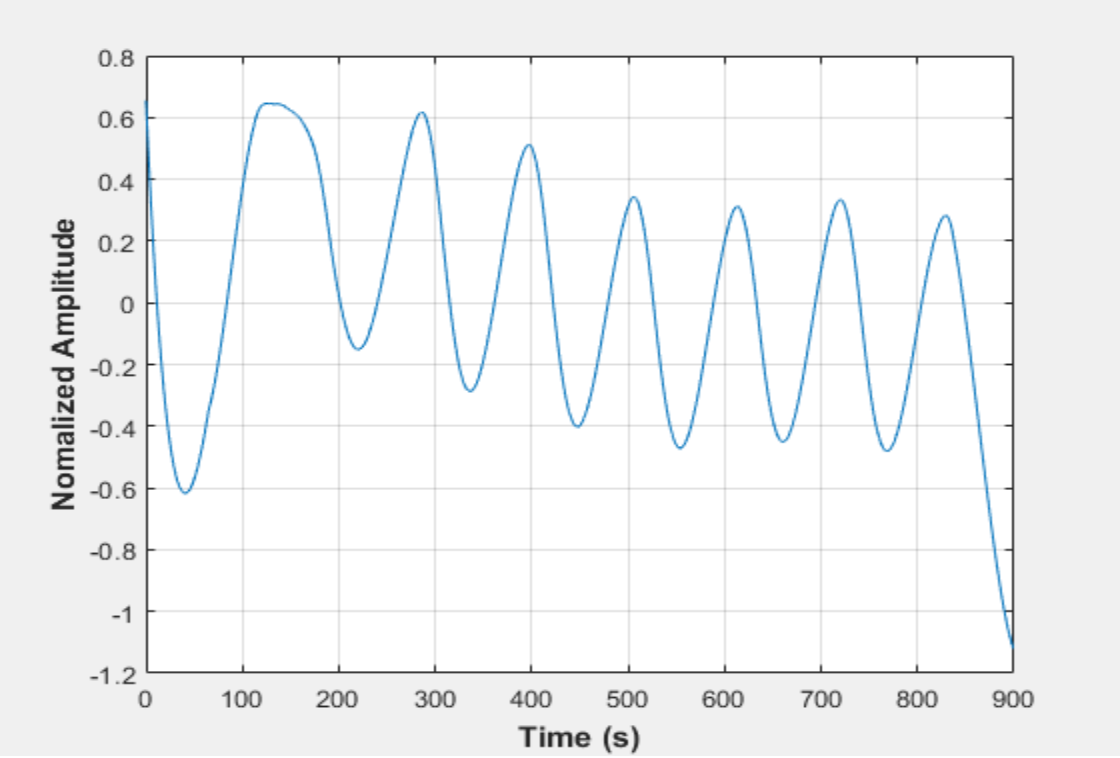


*Figure B-9: Pressure fluctuations in an empty vessel at 65.24 dm$^3$/minute gas flow rate*

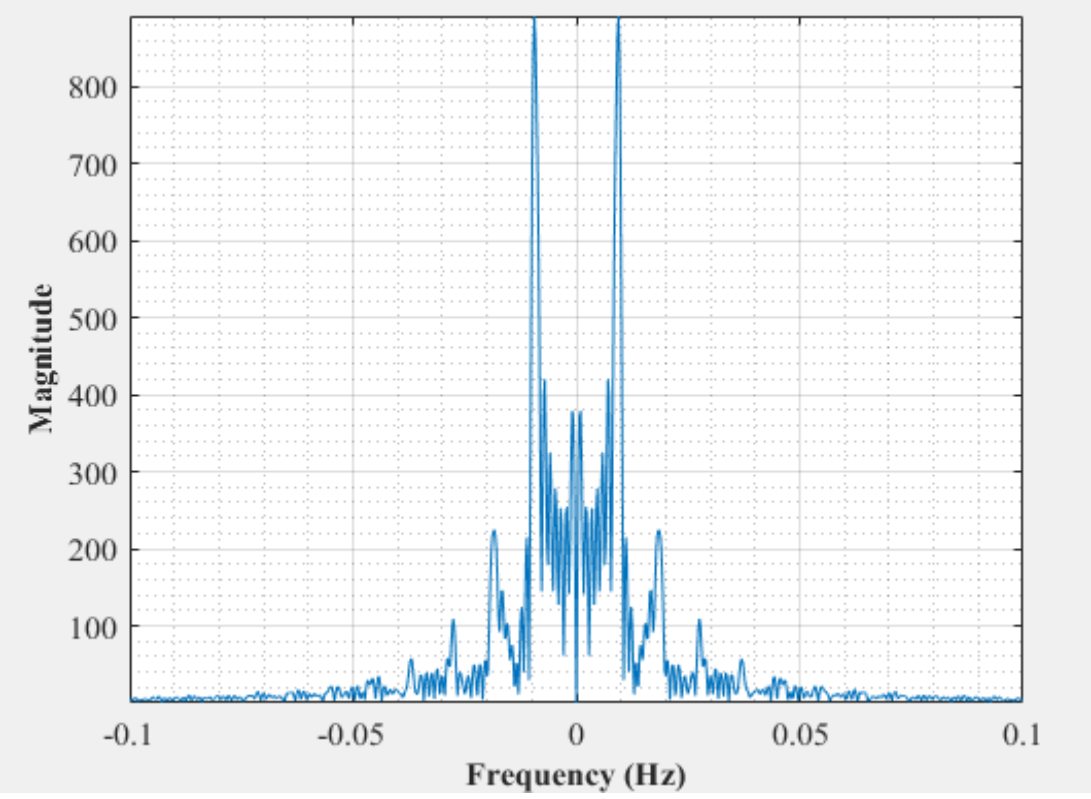


*Figure B-10: Dominant frequency for an empty vessel at 65.24 dm$^3$/minute rotameter flowrate*

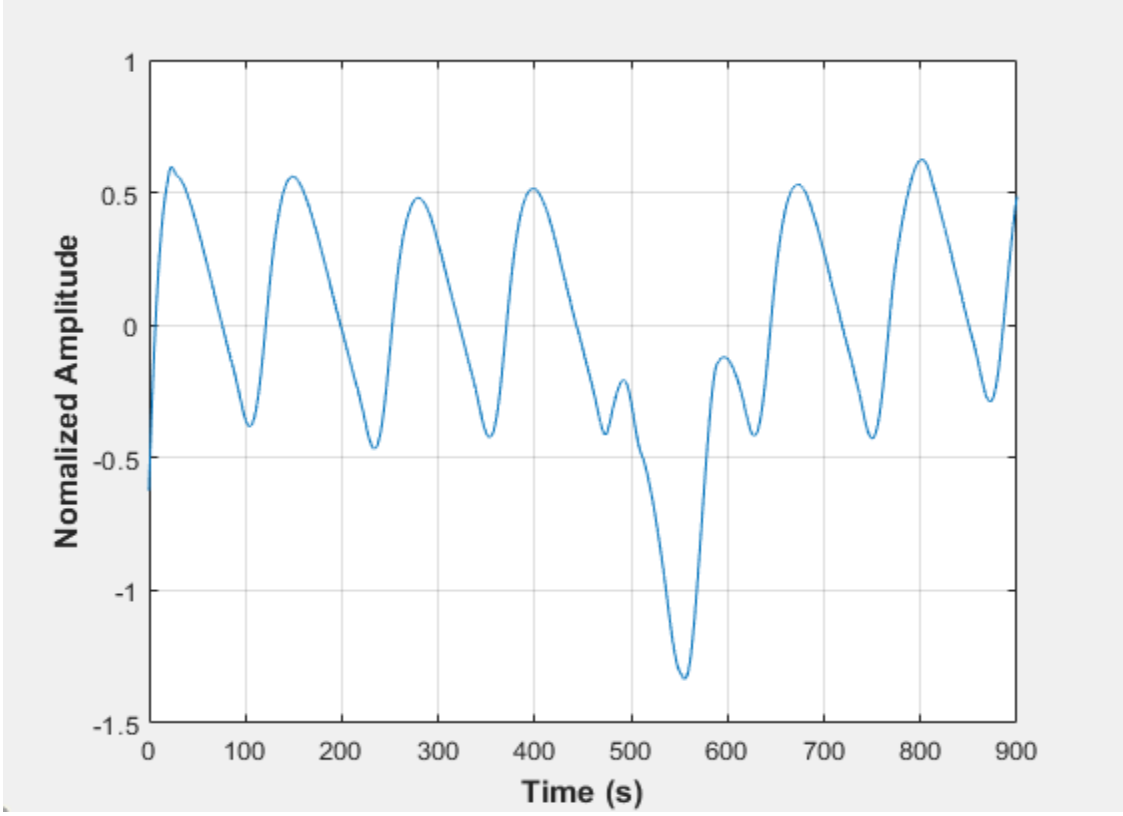


*Figure B-110-1: Pressure fluctuations in an empty vessel at 65.24 dm$^3$/minute gas flow rate-repeat test*

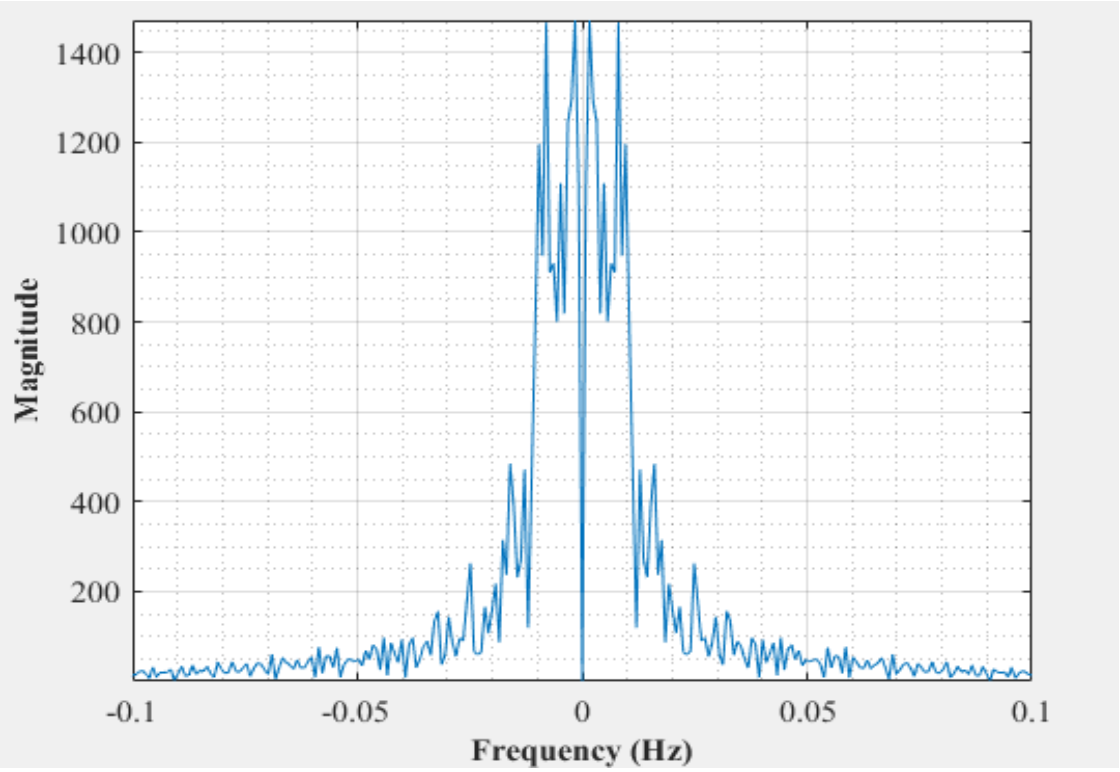


*Figure B-12: Dominant frequency for an empty vessel at 65.24 dm$^3$/minute rotameter flowrate-repeat test*

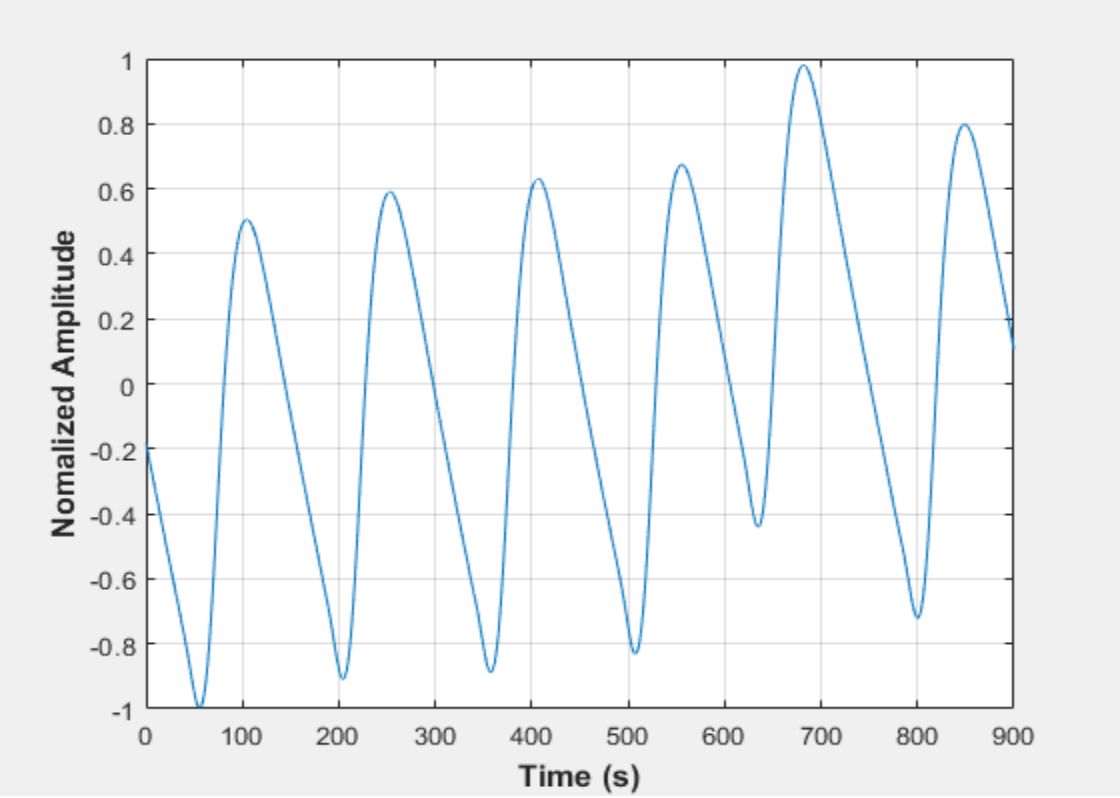


*Figure B-13: Pressure fluctuations in a uniformly packed vessel at 48.96 $dm^3$/minute gas flow rate*

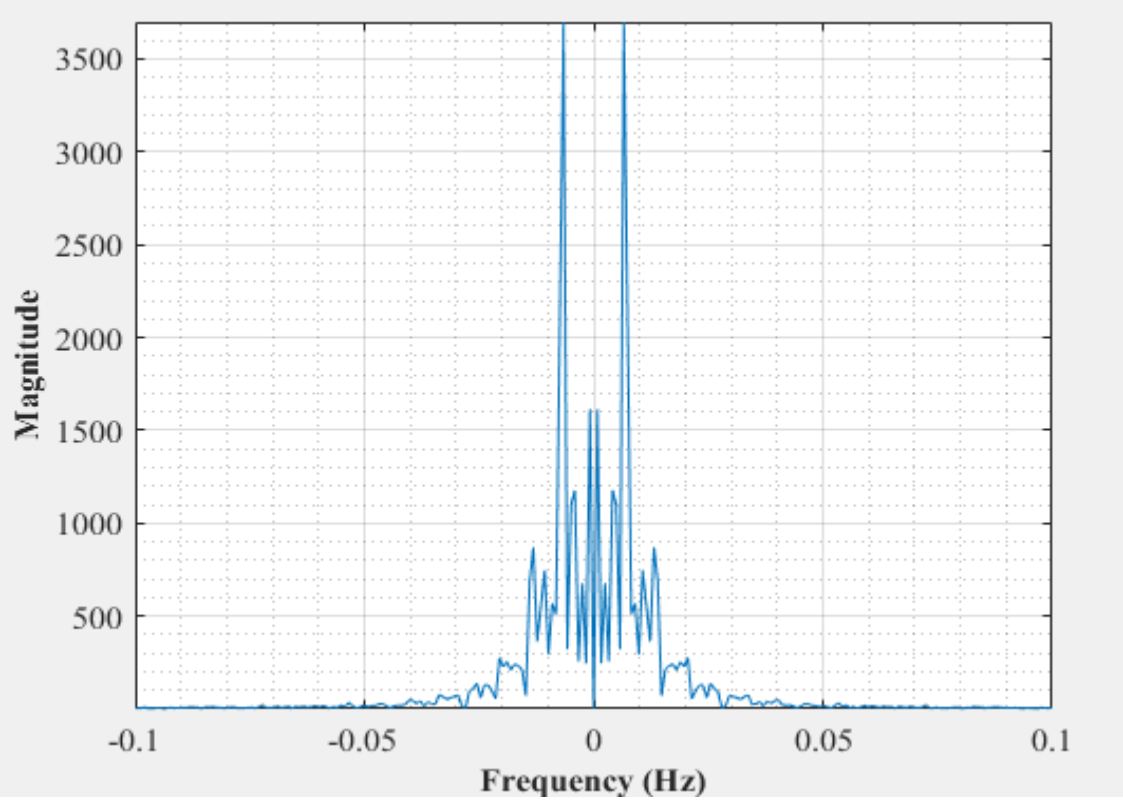


*Figure B-14: Dominant frequency for a uniformly packed vessel at 48.96 $dm^3$/minute rotameter flowrate*

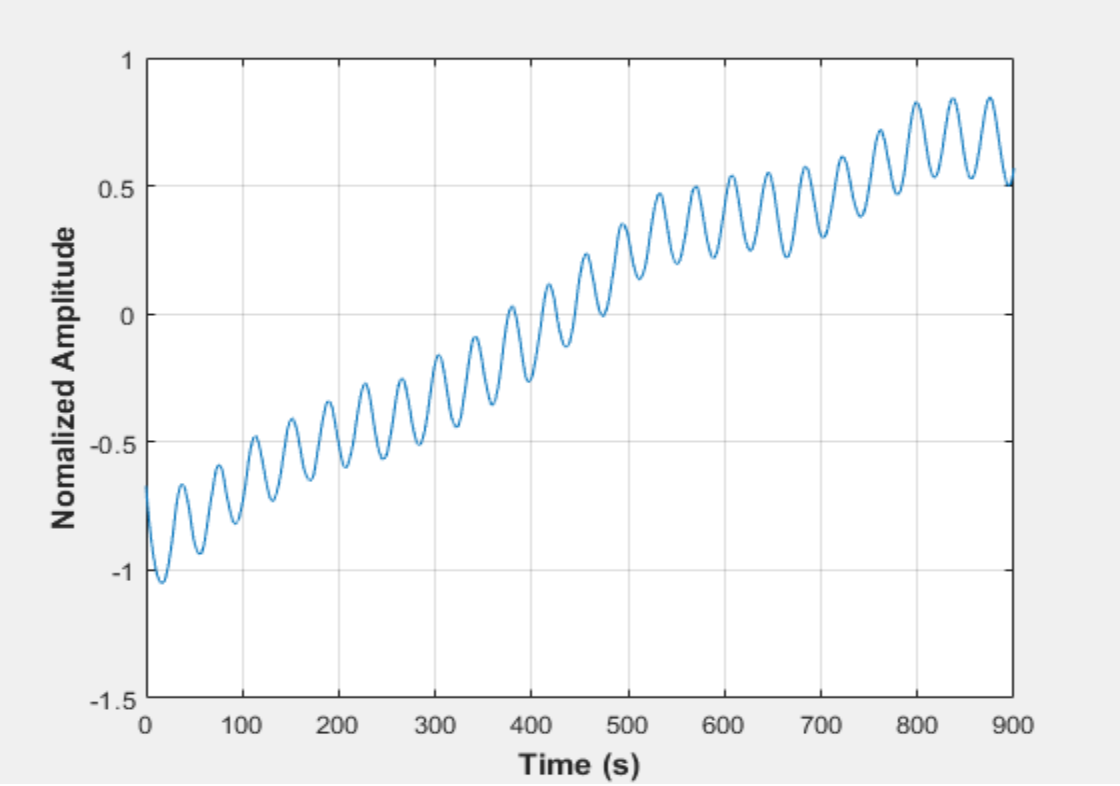


*Figure B-15: Pressure fluctuations in a uniformly packed vessel at 48.96 dm$^3$/minute gas flow rate- repeat test*

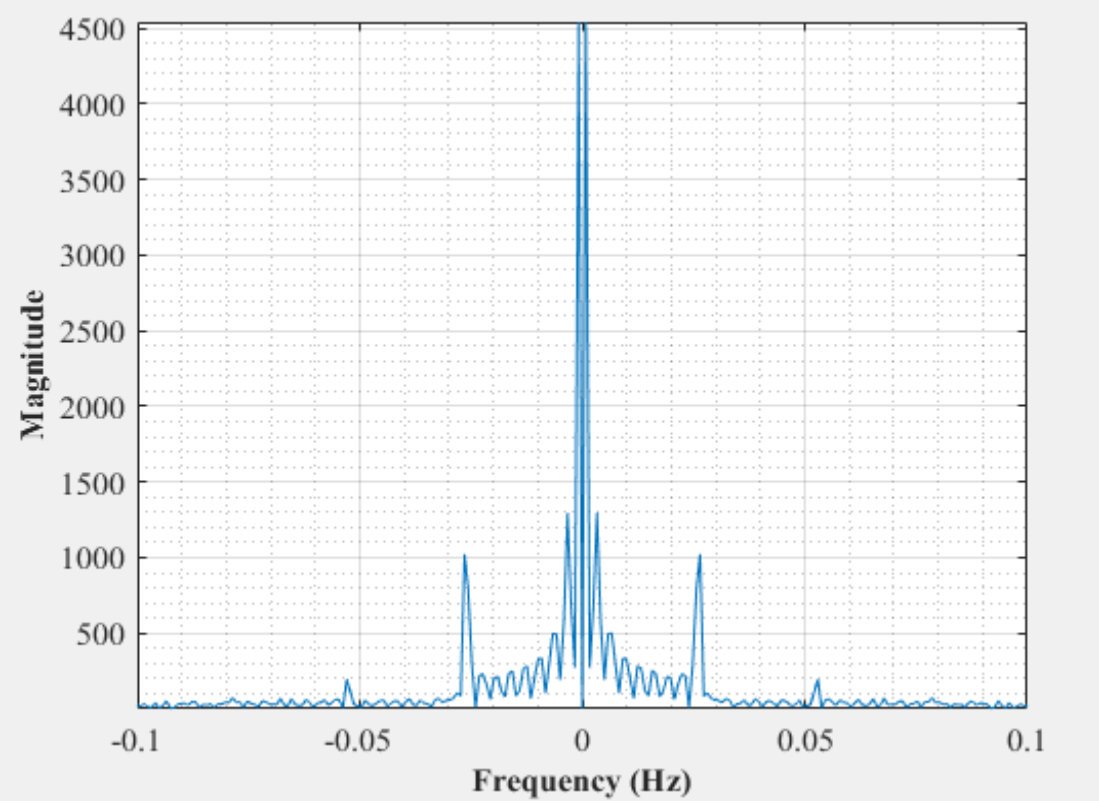


*Figure B-16: Dominant frequency for a uniformly packed vessel at 48.96 dm$^3$/minute rotameter flowrate- repeat test*

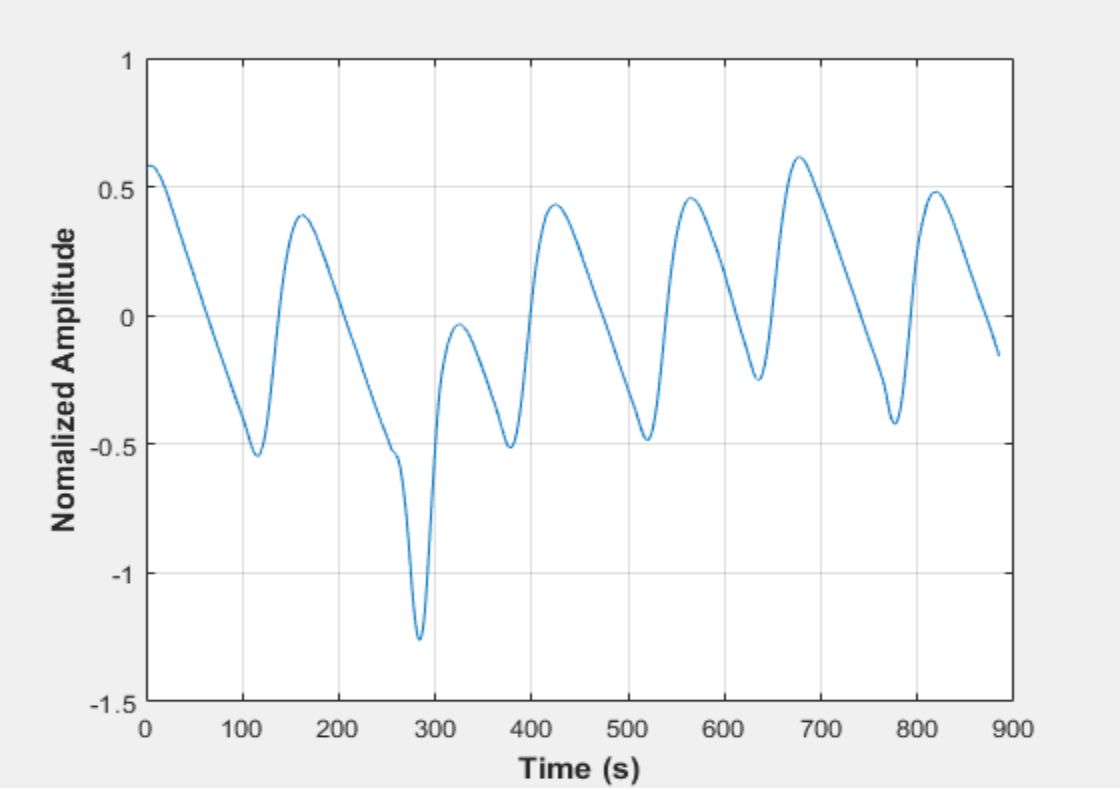


*Figure B-17: Pressure fluctuations in a uniformly packed vessel at 54.4 $dm^3$/minute gas flow rate*

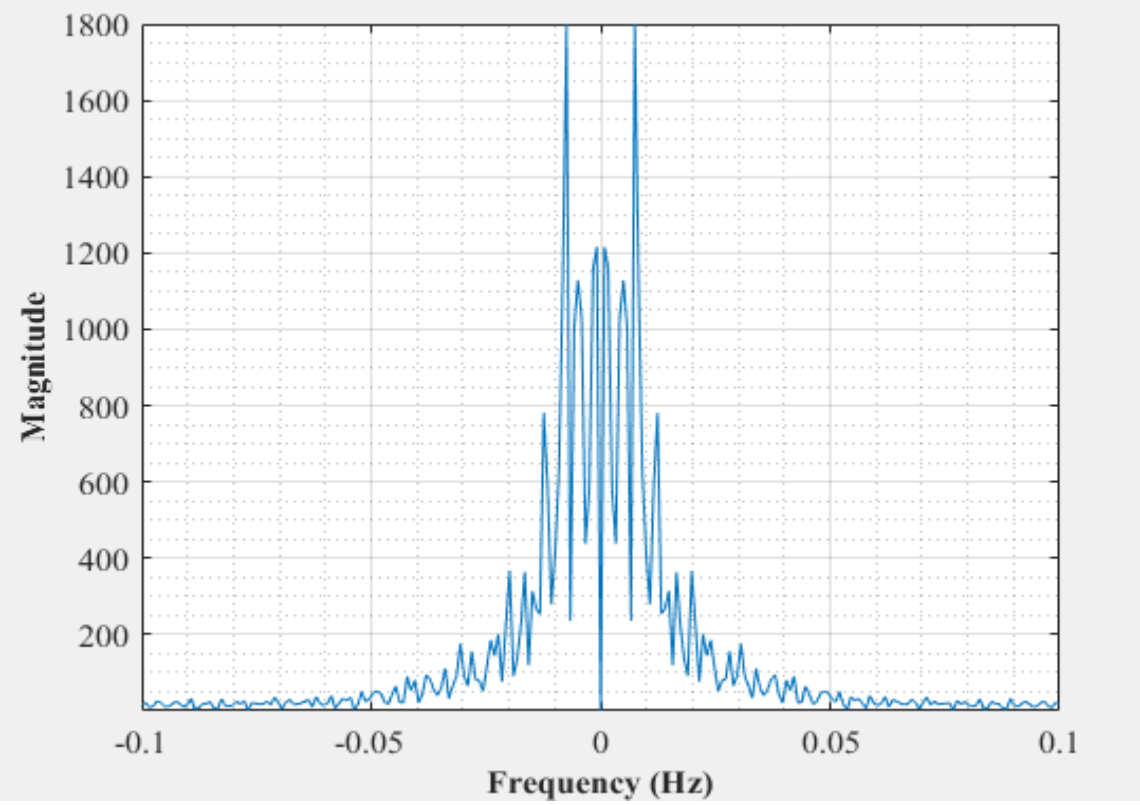


*Figure B-18: Dominant frequency for a uniformly packed vessel at $dm^3$/minute rotameter flowrate*

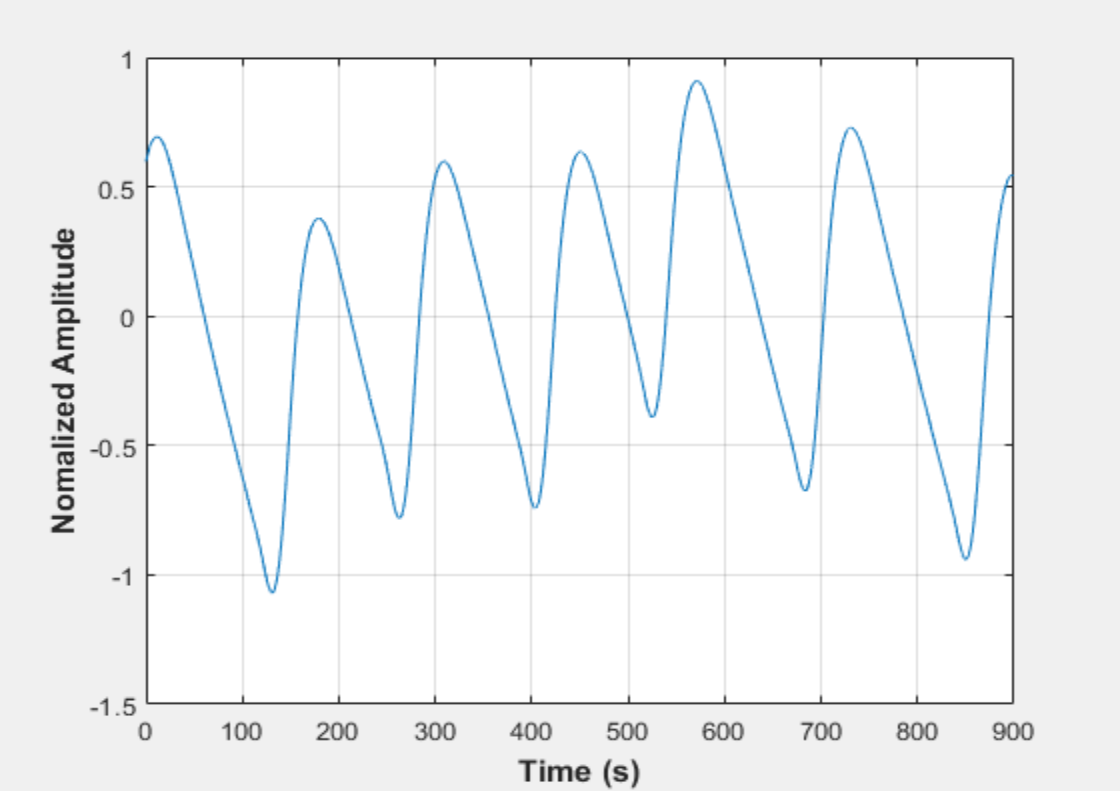


*Figure B-19: Pressure fluctuations in a uniformly packed vessel at 54.4 dm$^3$/minute gas flow rate- repeat test*

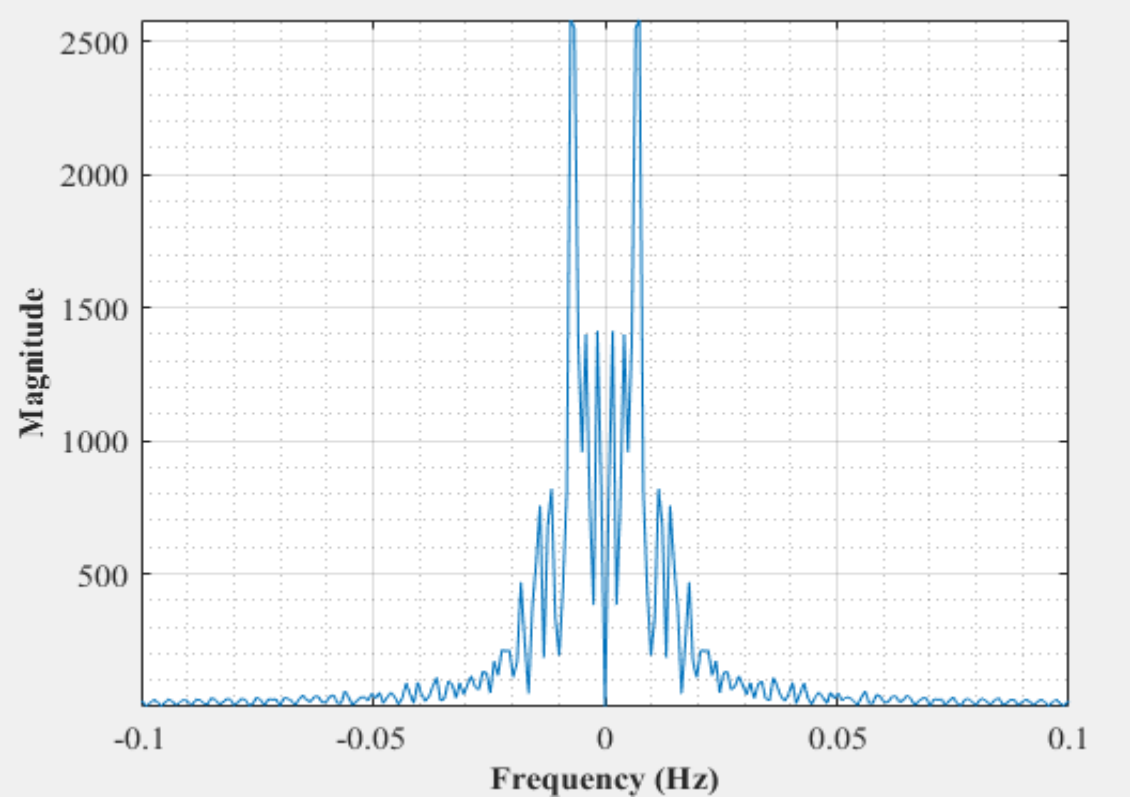


*Figure B-20: Dominant frequency for a uniformly packed vessel at 54.4 dm$^3$/minute rotameter flowrate- repeat test*

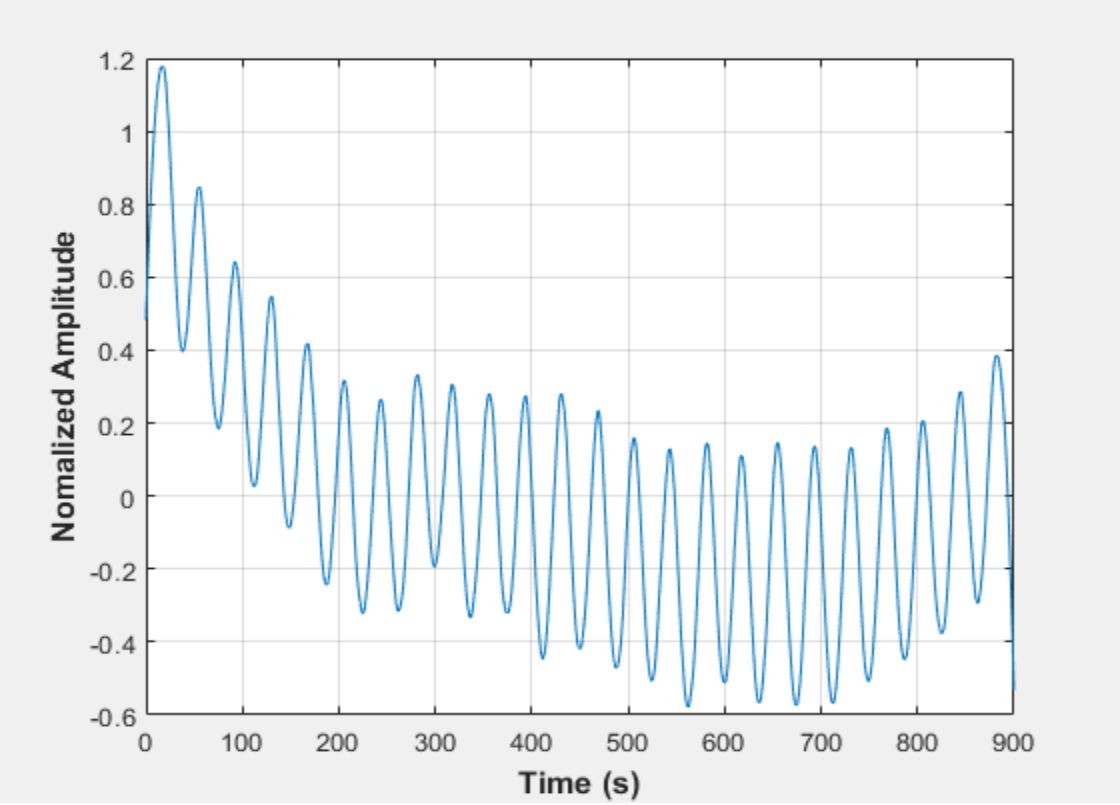


*Figure B-210-2:Pressure fluctuations in a uniformly packed vessel at 65.24 dm$^3$/minute gas flow rate*

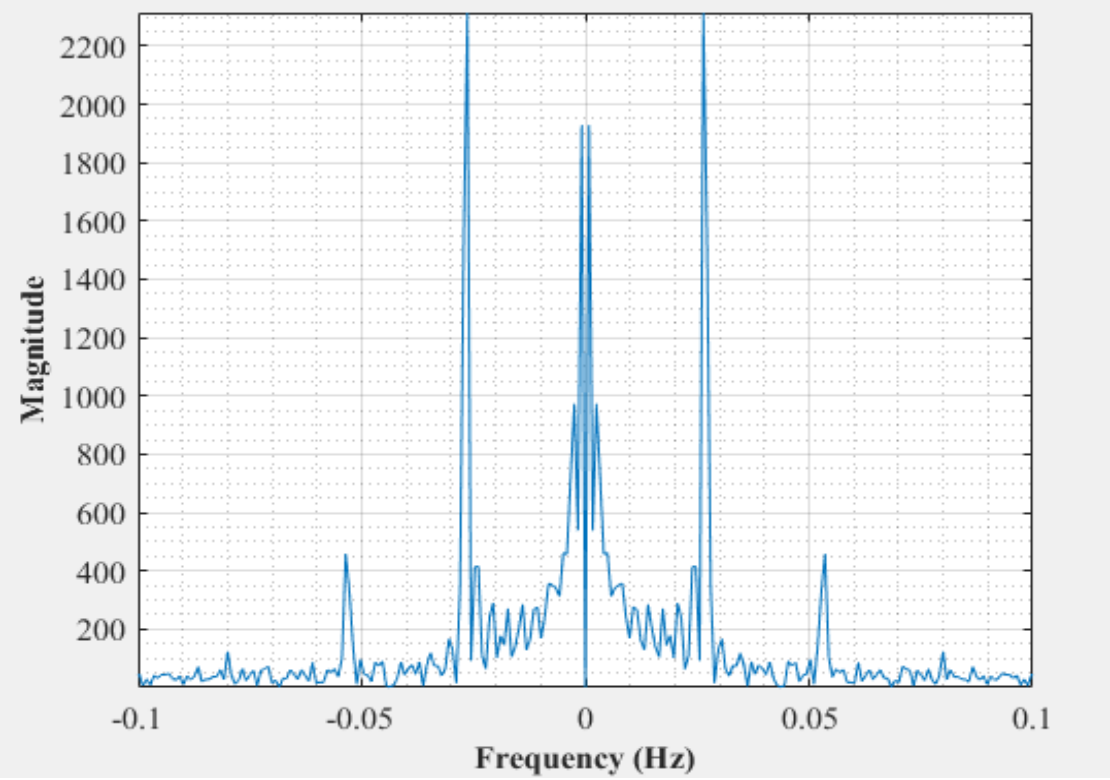


*Figure B-22: Dominant frequency for a uniformly packed vessel at 65.24 dm$^3$/minute rotameter flowrate*

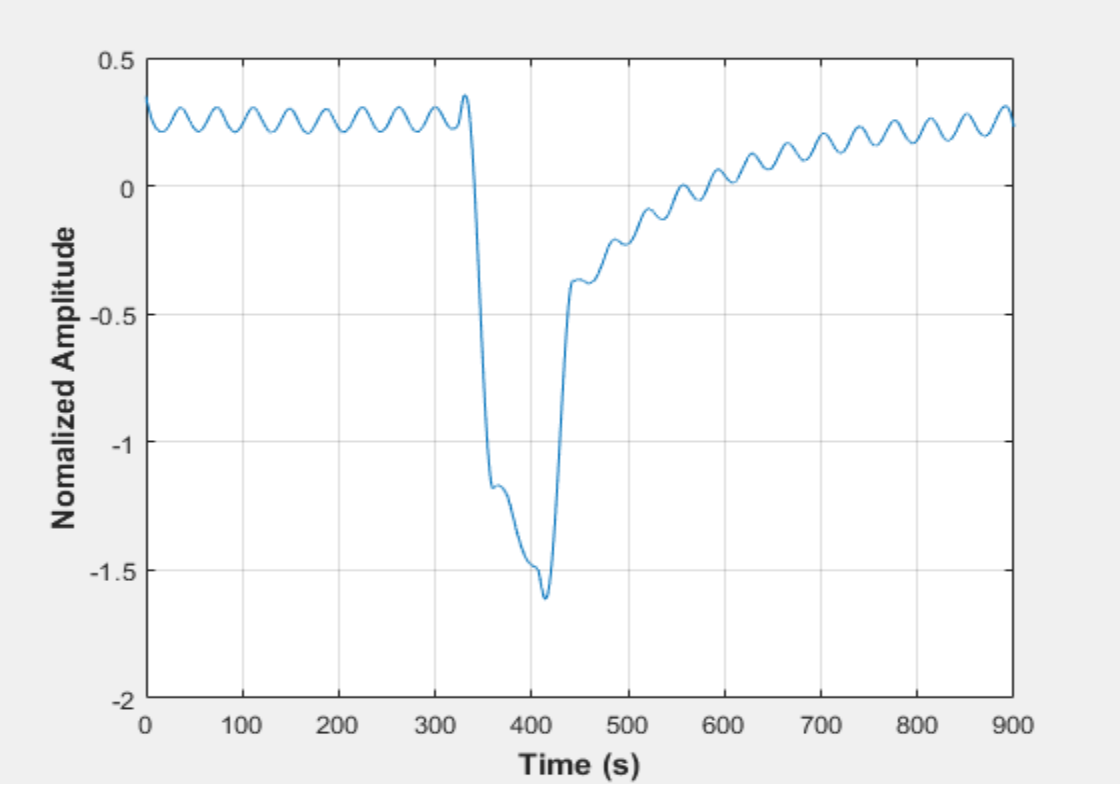


*Figure B-230-3:Pressure fluctuations in a uniformly packed vessel at 65.24 dm$^3$/minute gas flow rate-repeat test*

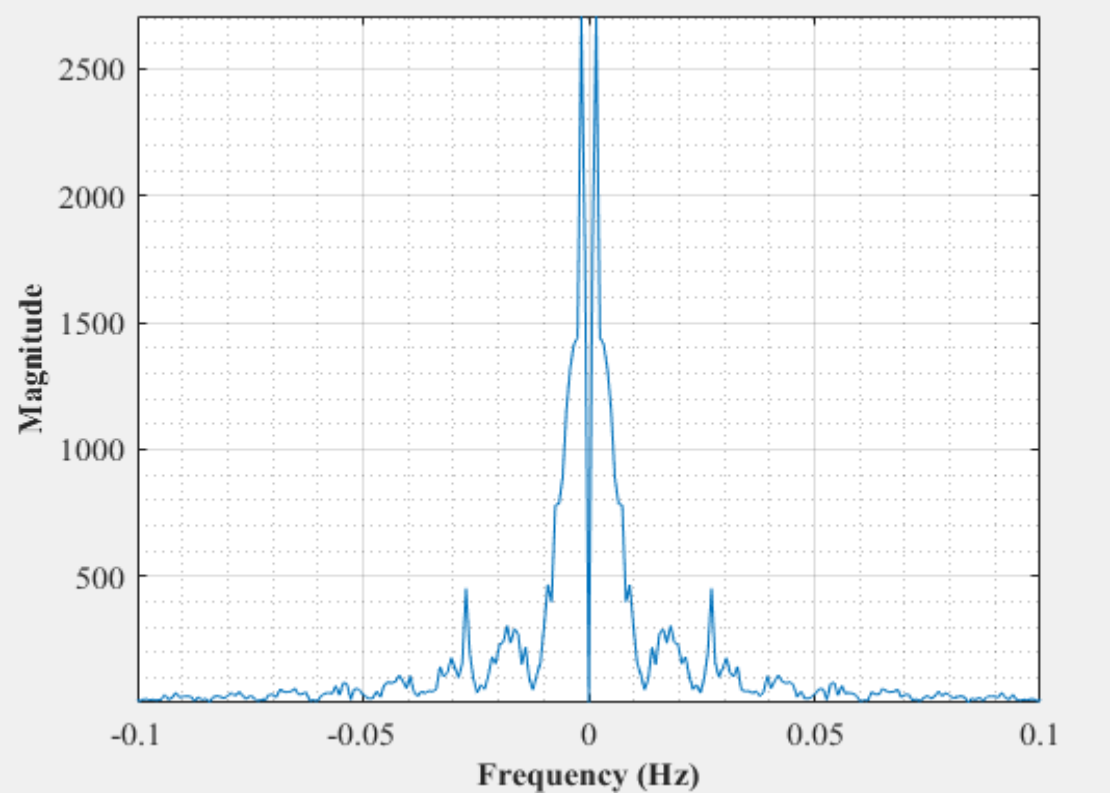


*Figure B-24: Dominant frequency for a uniformly packed vessel at 65.24 dm$^3$/minute rotameter flowrate-repeat test*

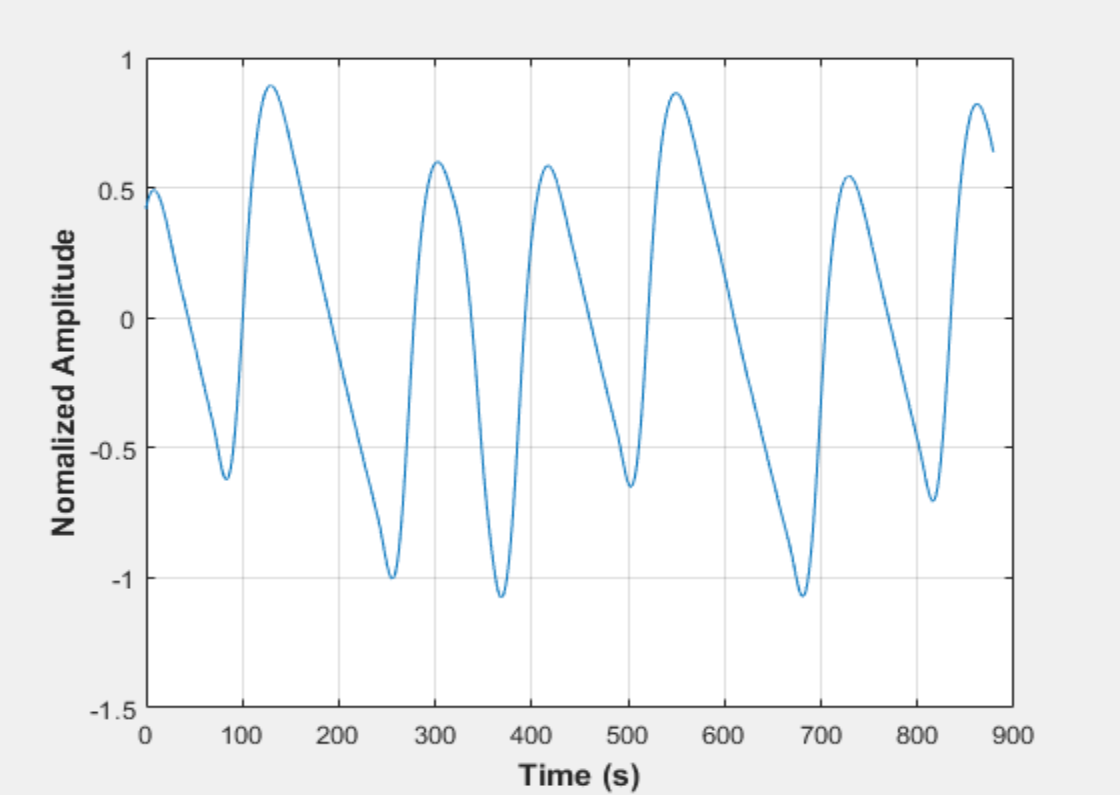


*Figure B-25: Pressure fluctuations in a non-uniformly packed vessel (large and small at the middle) at 48.96 dm$^3$/minute gas flow rate*

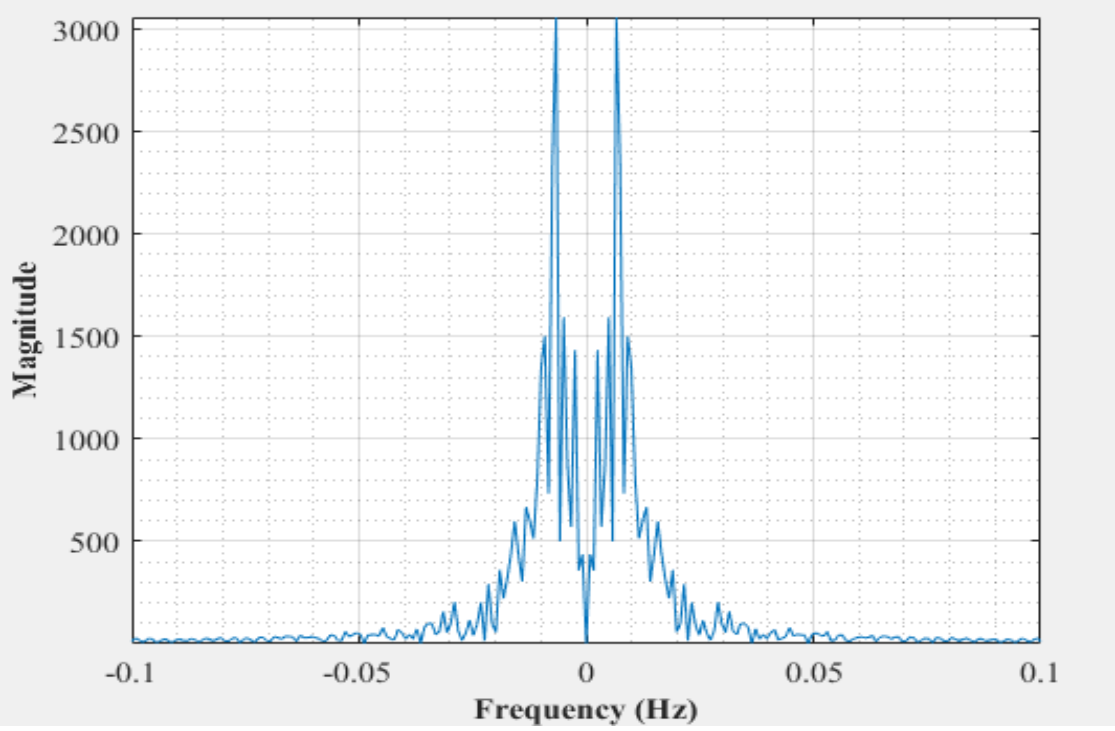


*Figure B-26: Dominant frequency for a non-uniformly packed vessel (large and small at the middle) at 48.96 dm$^3$/minute rotameter flowrate*

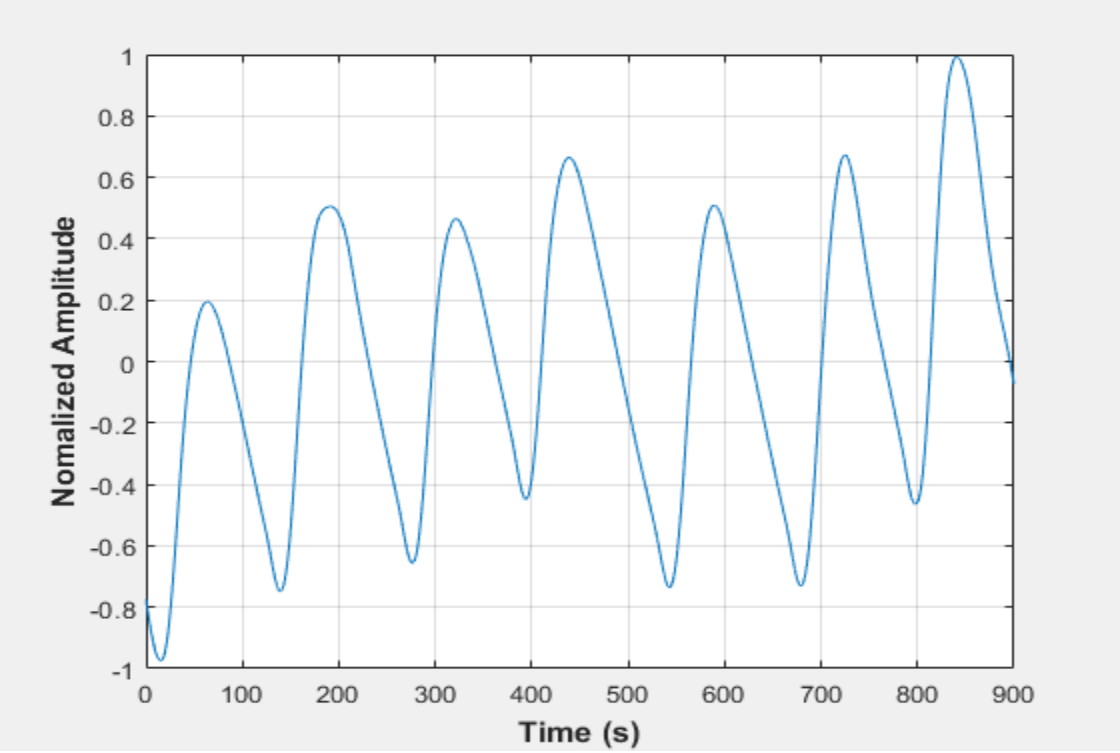


*Figure B-27: Pressure fluctuations in a non-uniformly packed vessel (large and small at the middle) at 48.96 dm$^3$/minute gas flow rate-repeat test*

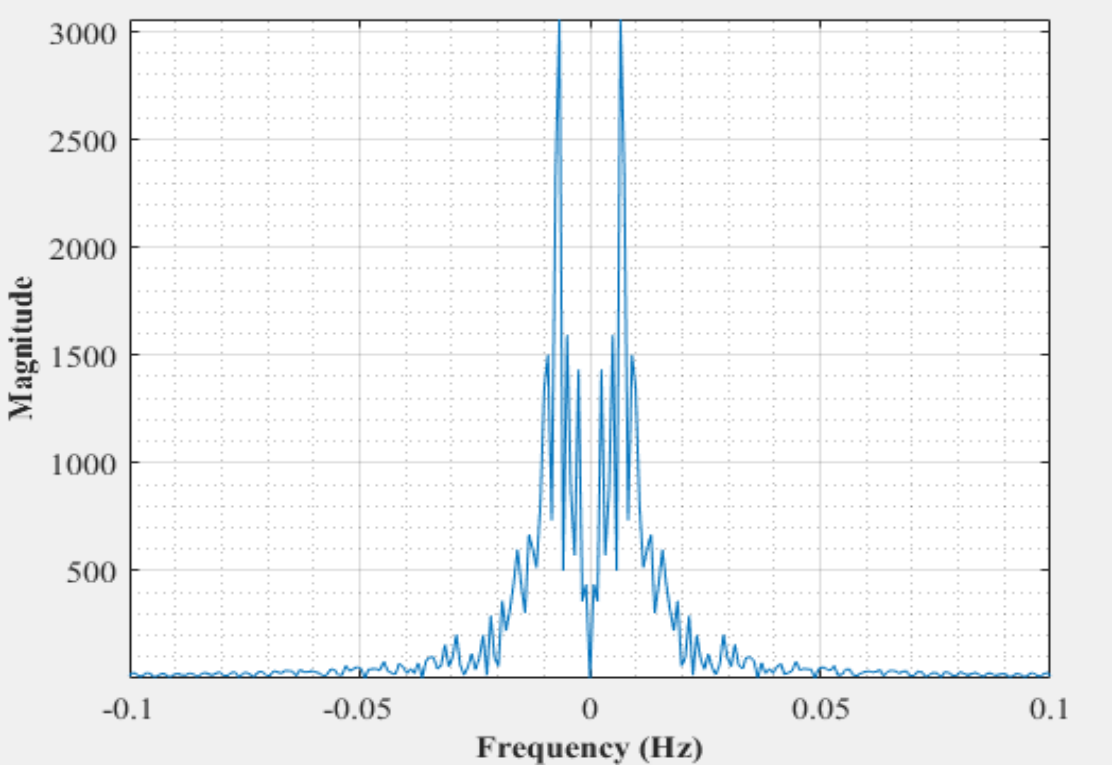


*Figure B-28: Dominant frequency for a non-uniformly packed vessel (large and small at the middle) at 48.96 dm$^3$/minute rotameter flowrate- repeat test*

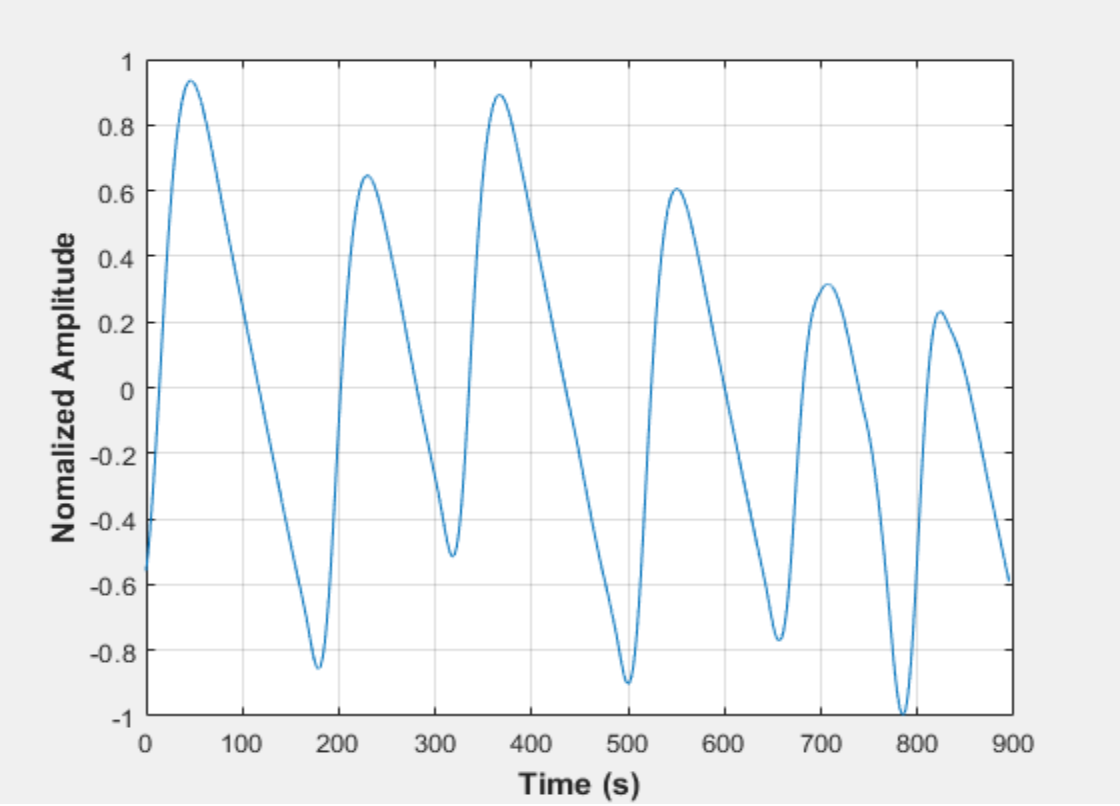


*Figure B-29: Pressure fluctuations in a non-uniformly packed vessel (large and small at the middle) at 54.4 dm$^3$/minute gas flow rate*

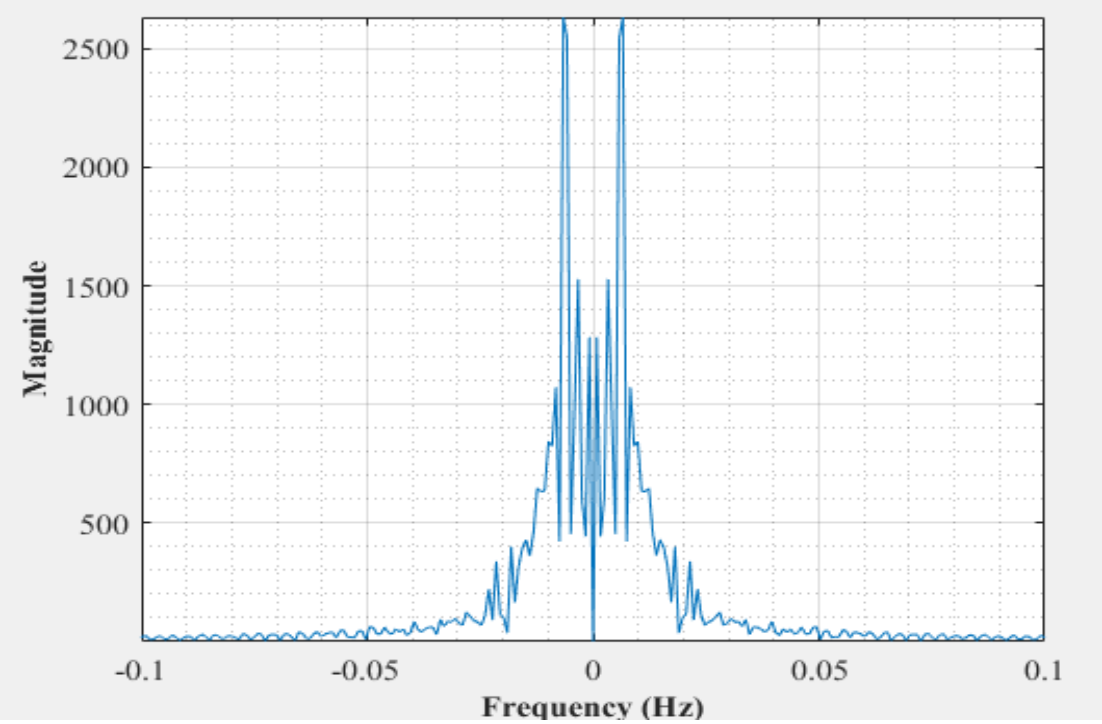


*Figure B-30: Dominant frequency for a non-uniformly packed vessel (large and small at the middle) at 54.4 dm$^3$/minute rotameter flowrate*

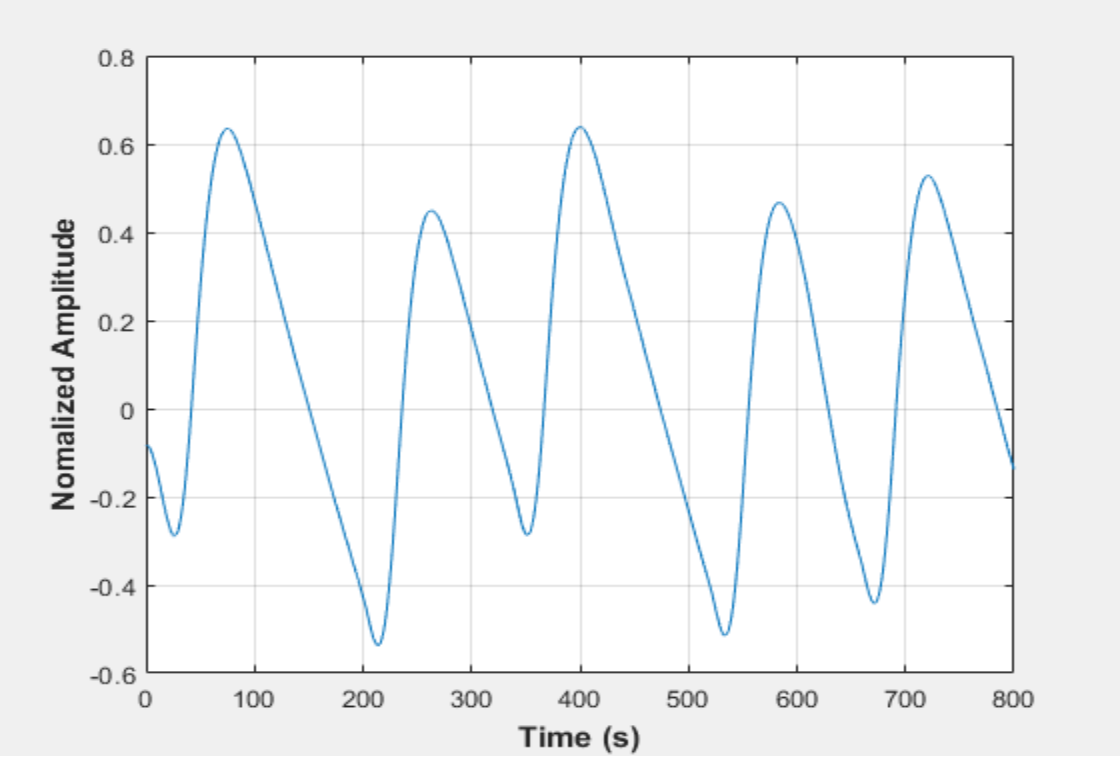


*Figure B-31: Pressure fluctuations in a non-uniformly packed vessel (large and small at the middle) at 54.4 dm$^3$/minute gas flow rate-repeat test*

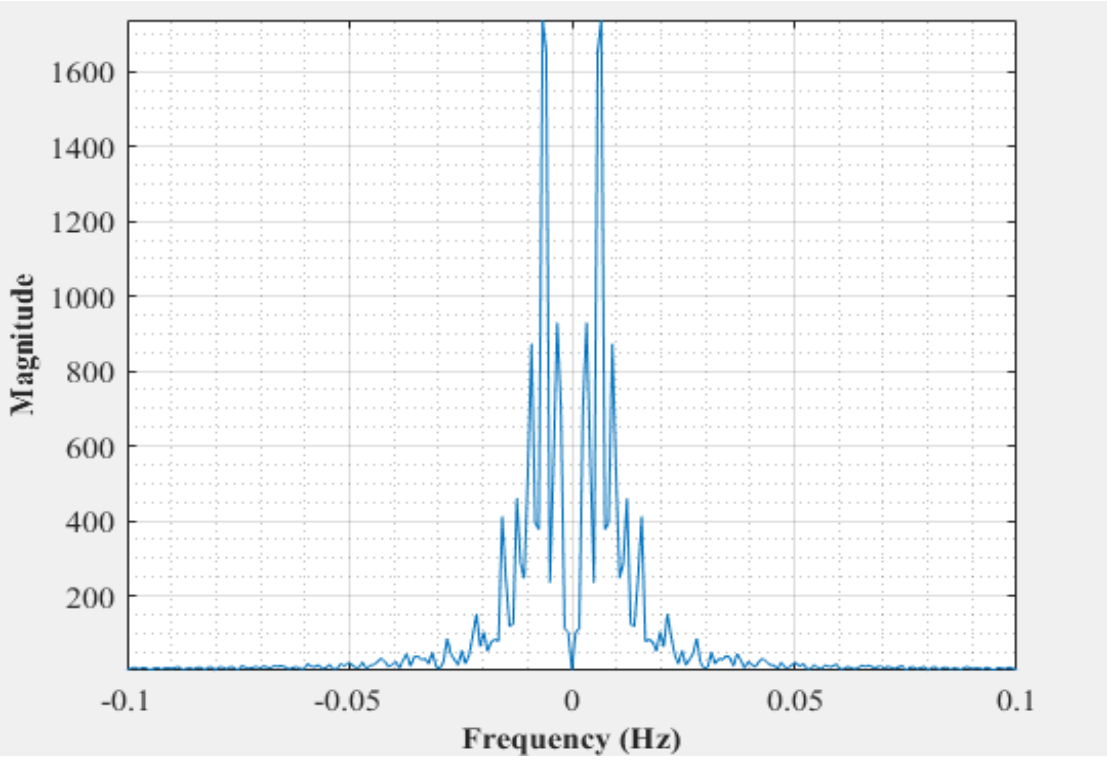


*Figure B-32: Dominant frequency for a non-uniformly packed vessel (large and small at the middle) at 54.4 dm$^3$/minute rotameter flowrate- repeat test*

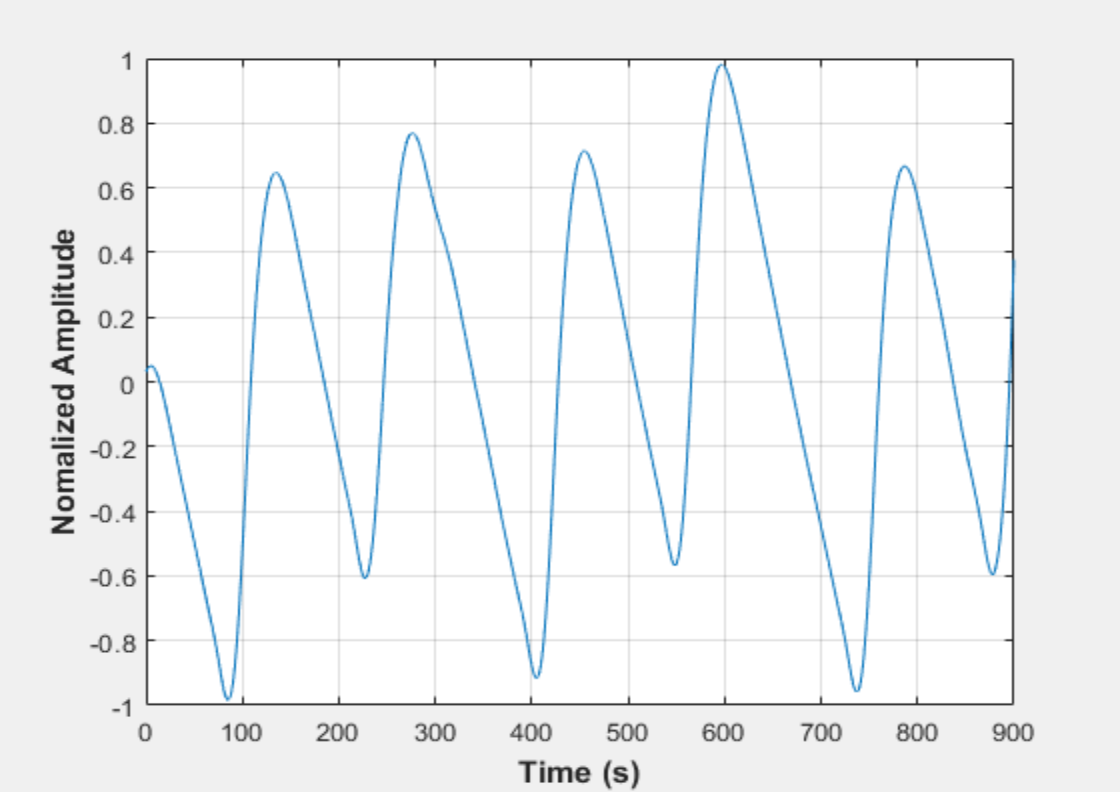


*Figure B-33: Pressure fluctuations in a non-uniformly packed vessel (large and small at the middle) at 65.24 dm$^3$/minute gas flow rate*

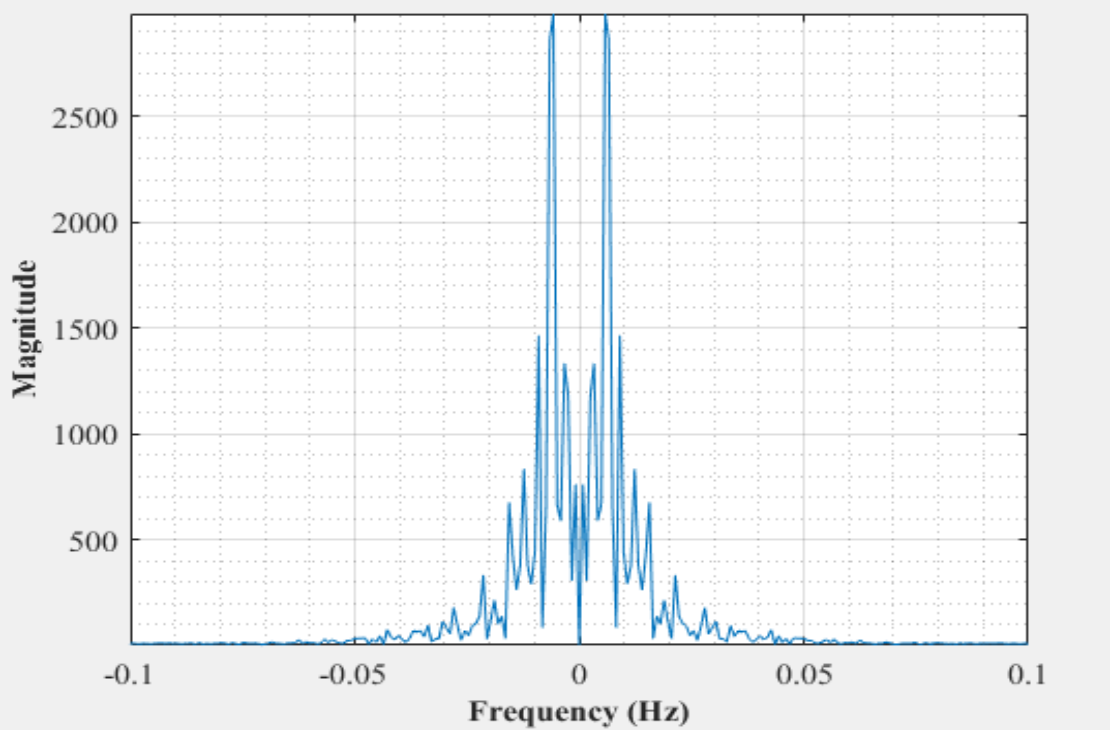


*Figure B-34: Dominant frequency for a non-uniformly packed vessel (large and small at the middle) at 65.24 dm$^3$/minute rotameter flowrate*

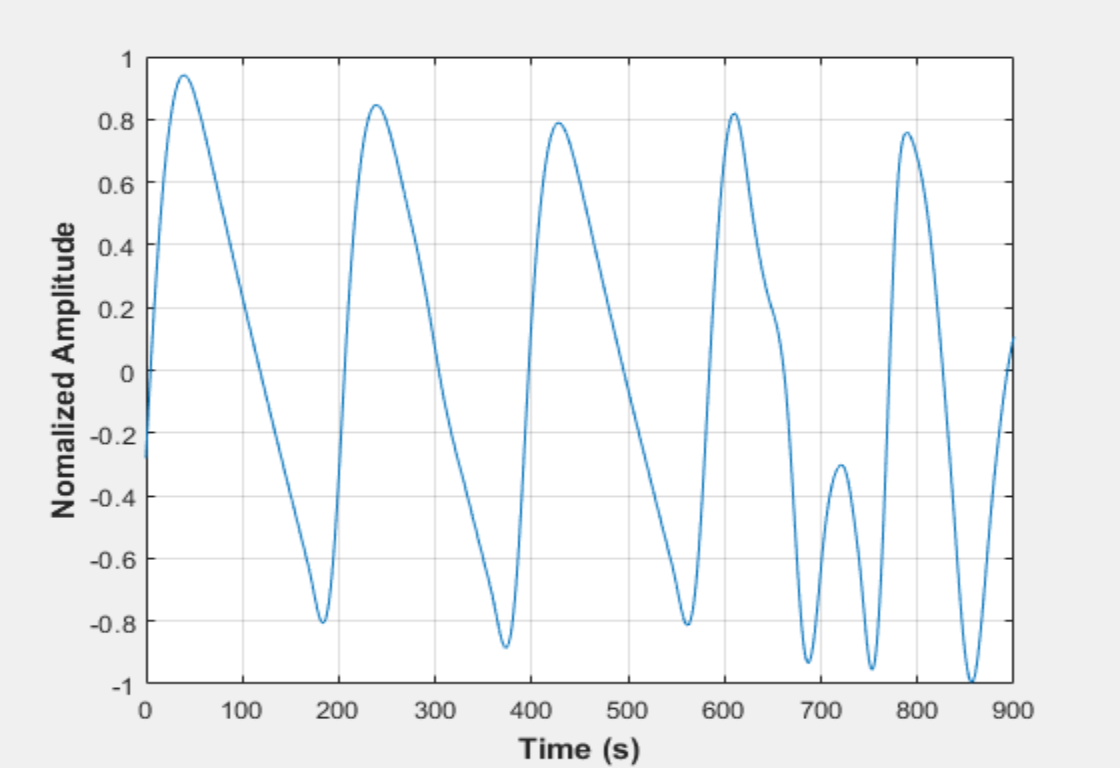


*Figure B-35: Pressure fluctuations in a non-uniformly packed vessel (large and small at the middle) at 65.24 dm$^3$/minute gas flow rate-repeat test*

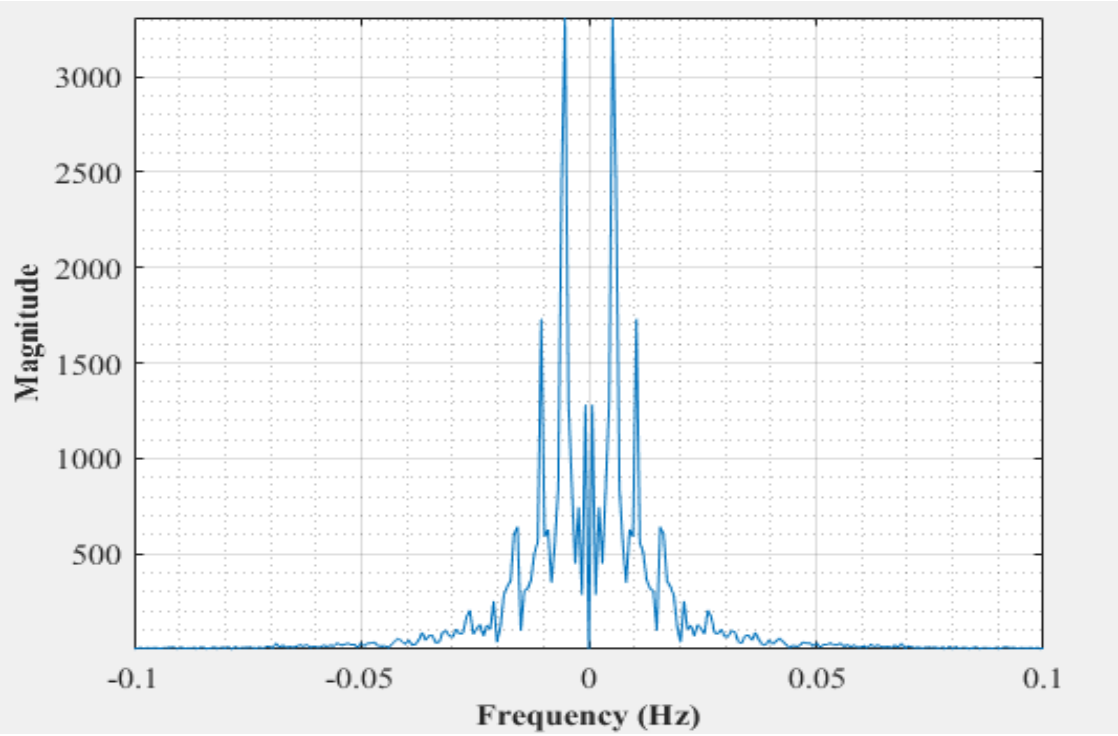


*Figure B-36: Dominant frequency for a non-uniformly packed vessel (large and small at the middle) at 65.24 dm$^3$/minute rotameter flowrate-repeat test*

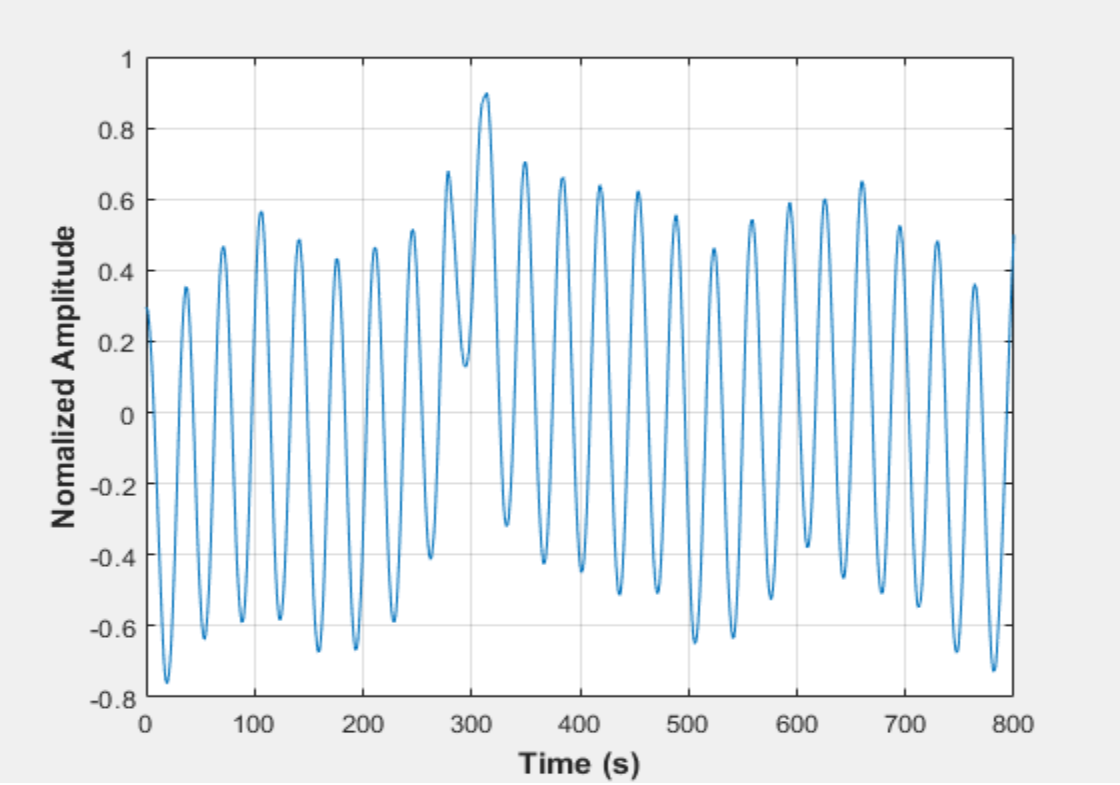


*Figure B-37: Pressure fluctuations in a non-uniformly packed vessel (large and small at the side) at 48.96 dm$^3$/minute gas flow rate*

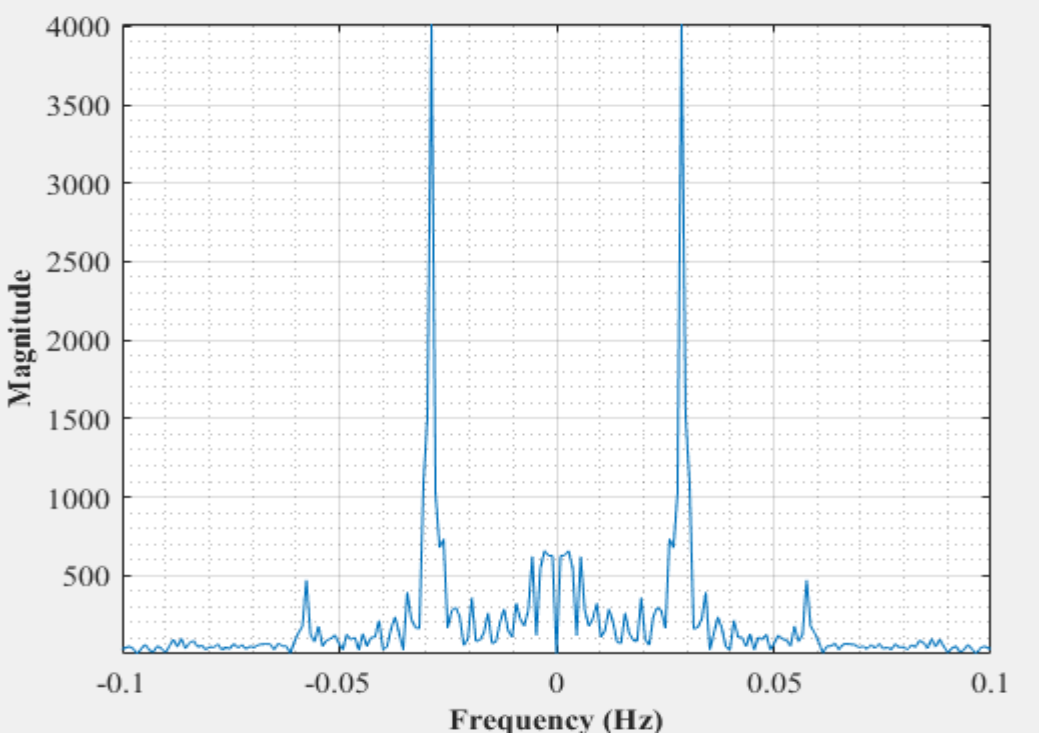


*Figure B-38: Dominant frequency for a non-uniformly packed vessel (large and small at the side) at 48.96 dm$^3$/minute rotameter flowrate*

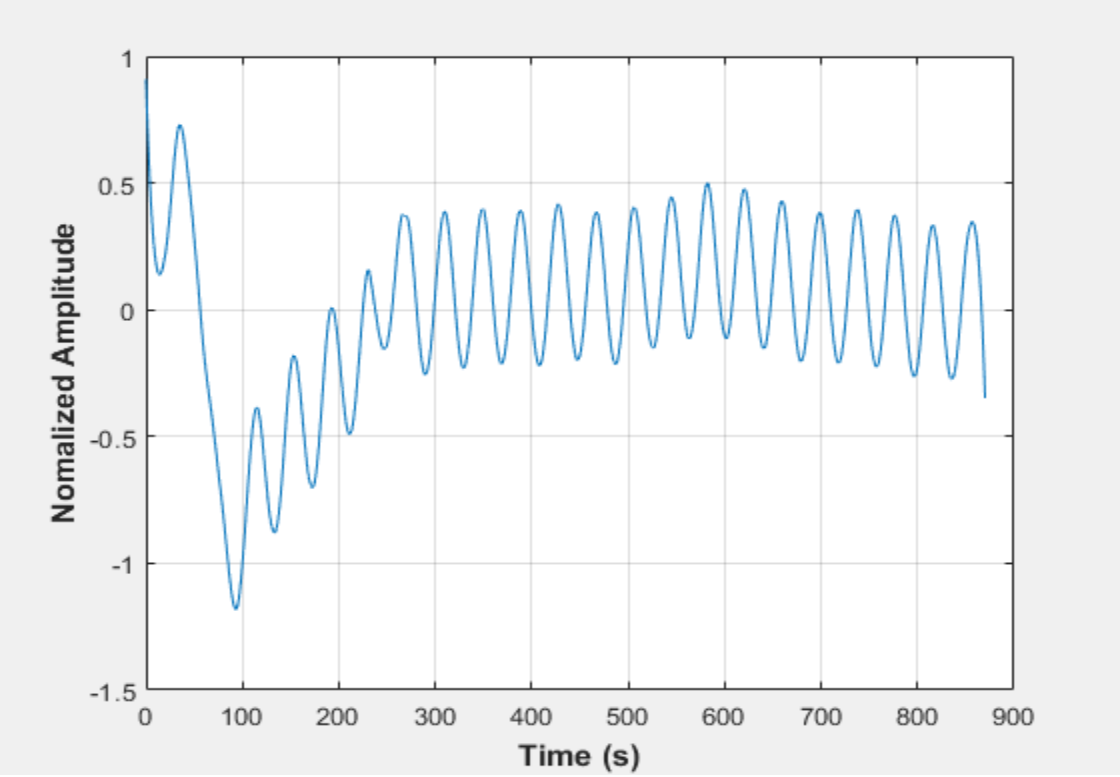


*Figure B-39: Pressure fluctuations in a non-uniformly packed vessel (large and small at the side) at 48.96 dm³/minute gas flow rate-repeat test*

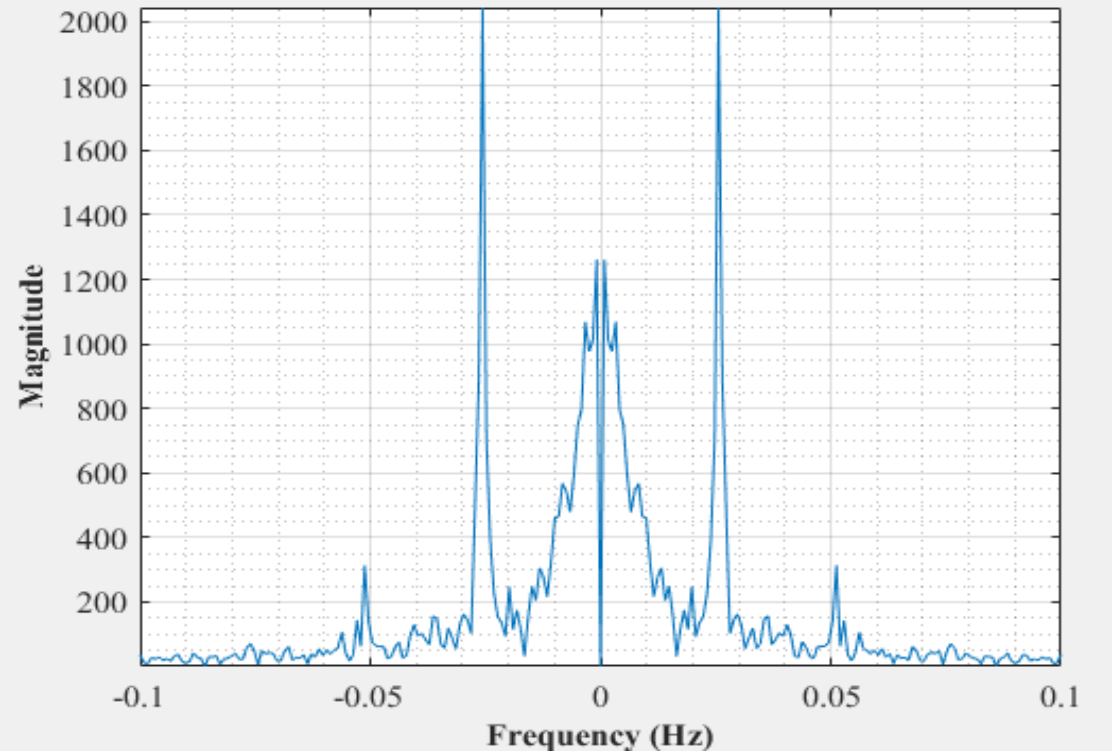


*Figure B-40: Dominant frequency for a non-uniformly packed vessel (large and small at the side) at dm³/minute rotameter flowrate-repeat test*

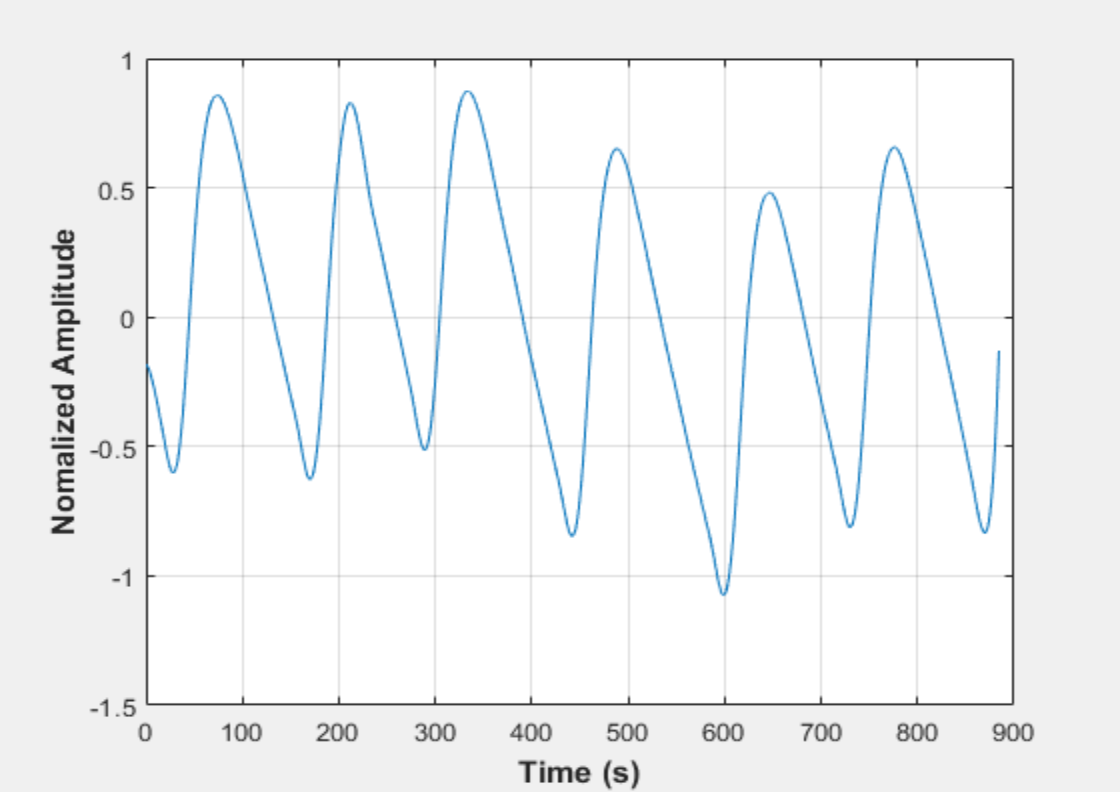


*Figure B-410-4:Pressure fluctuations in a non-uniformly packed vessel (large and small at the side) at 54.4 dm$^3$/minute gas flow rate*

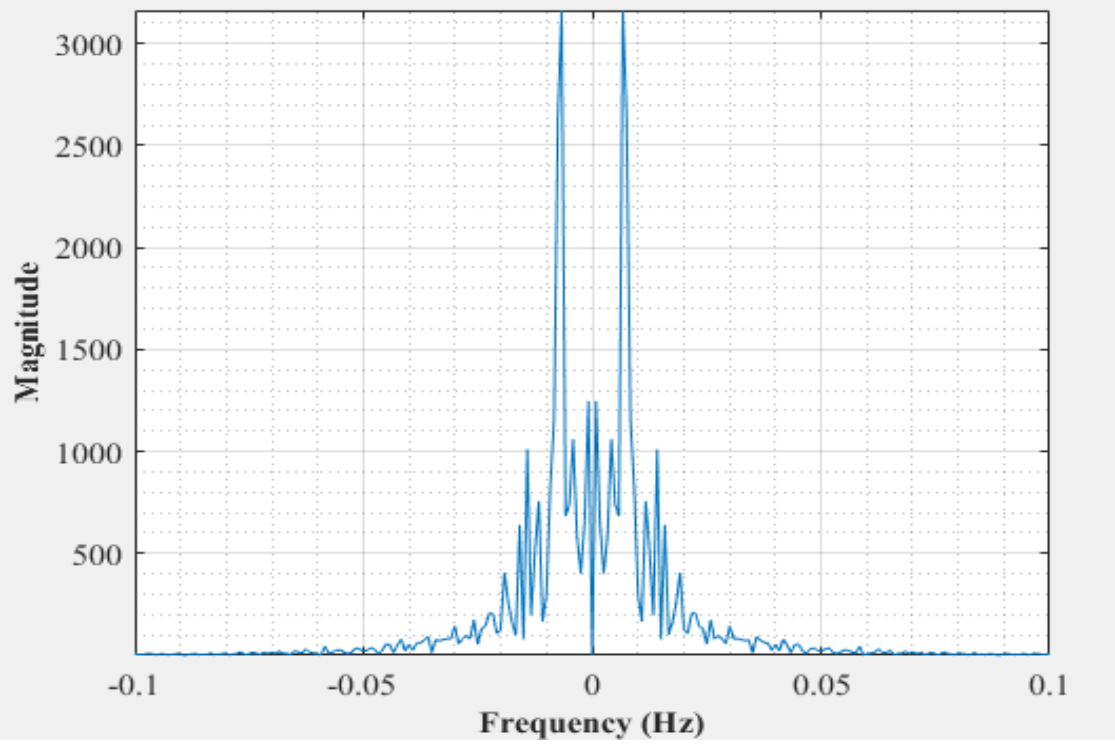


*Figure B-42: Dominant frequency for a non-uniformly packed vessel (large and small at the side) at 54.4 dm$^3$/minute rotameter flowrate*

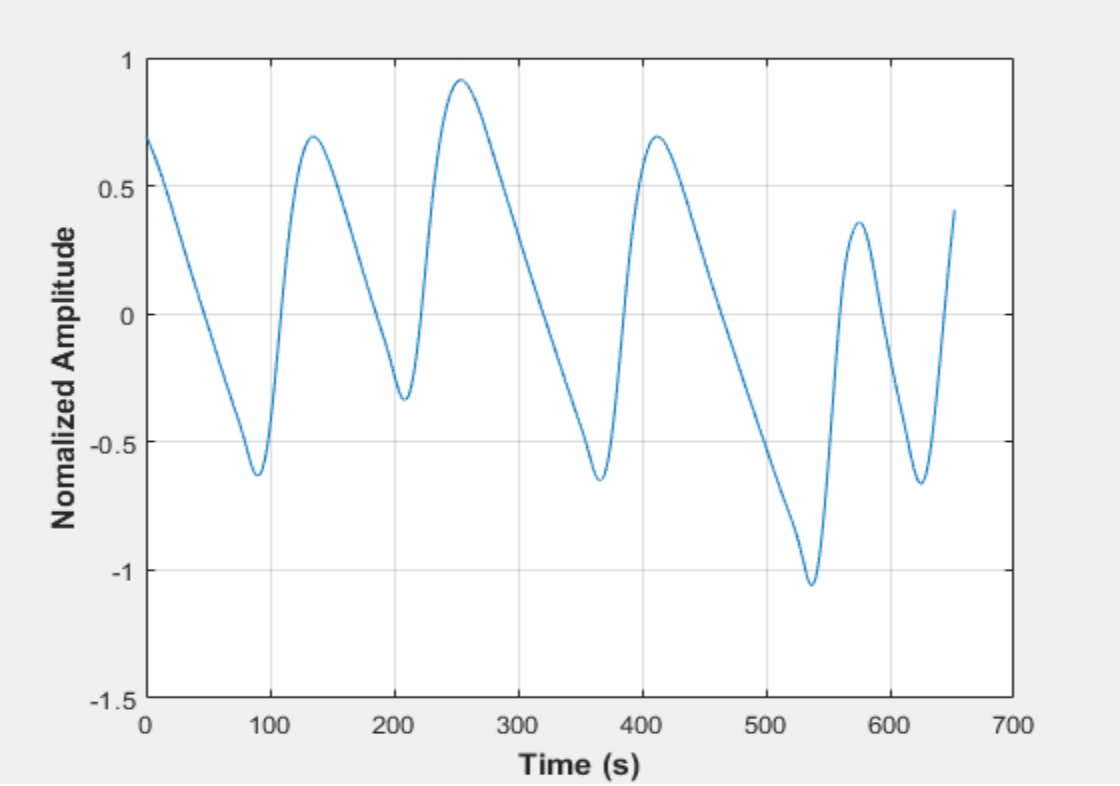


*Figure B-430-5:Pressure fluctuations in a non-uniformly packed vessel (large and small at the side) at 54.4 dm$^3$/minute gas flow rate- test*

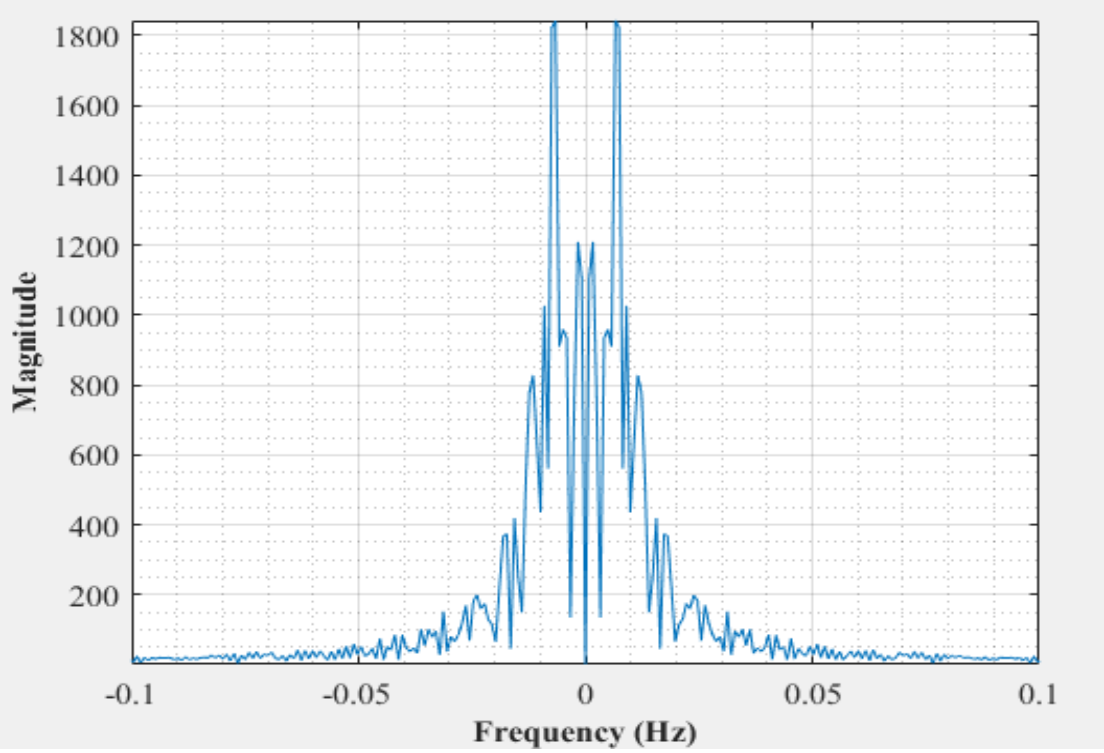


*Figure B-44: Dominant frequency for a non-uniformly packed vessel (large and small at the side) at 54.4 dm$^3$/minute rotameter flowrate-repeat test*

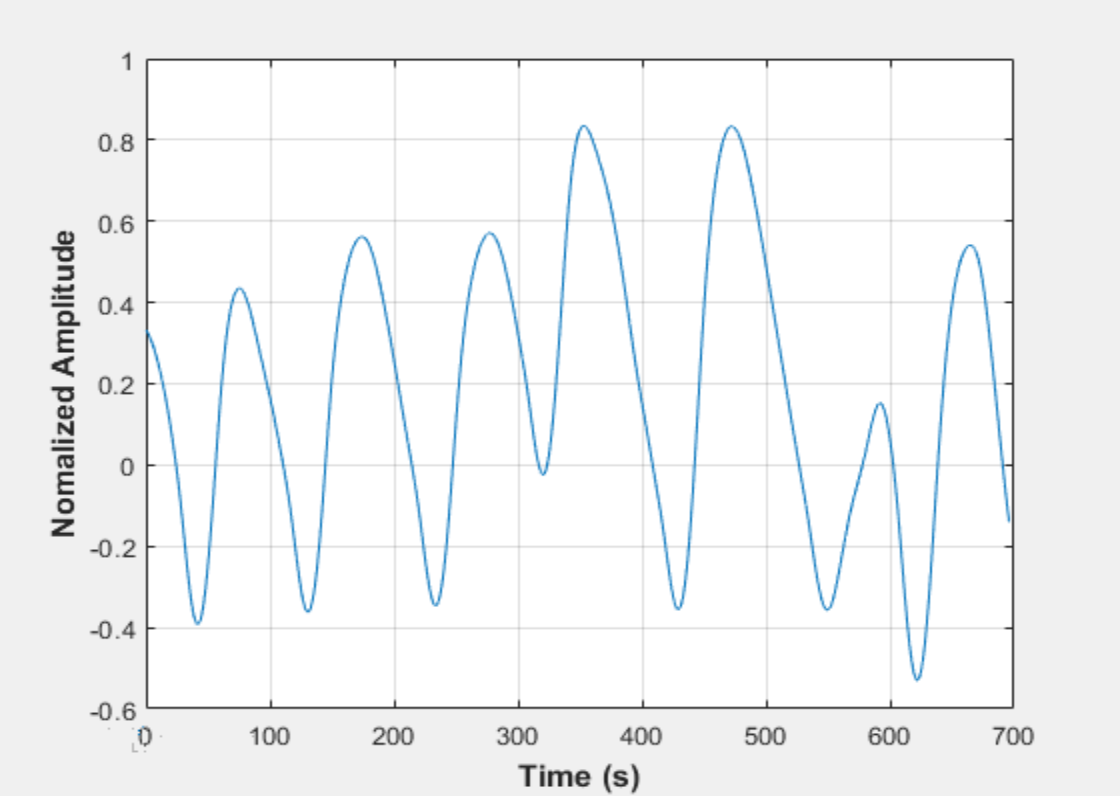


*Figure B-45: Pressure fluctuations in a non-uniformly packed vessel (large and small at the side) at 65.24 dm$^3$/minute gas flow rate*

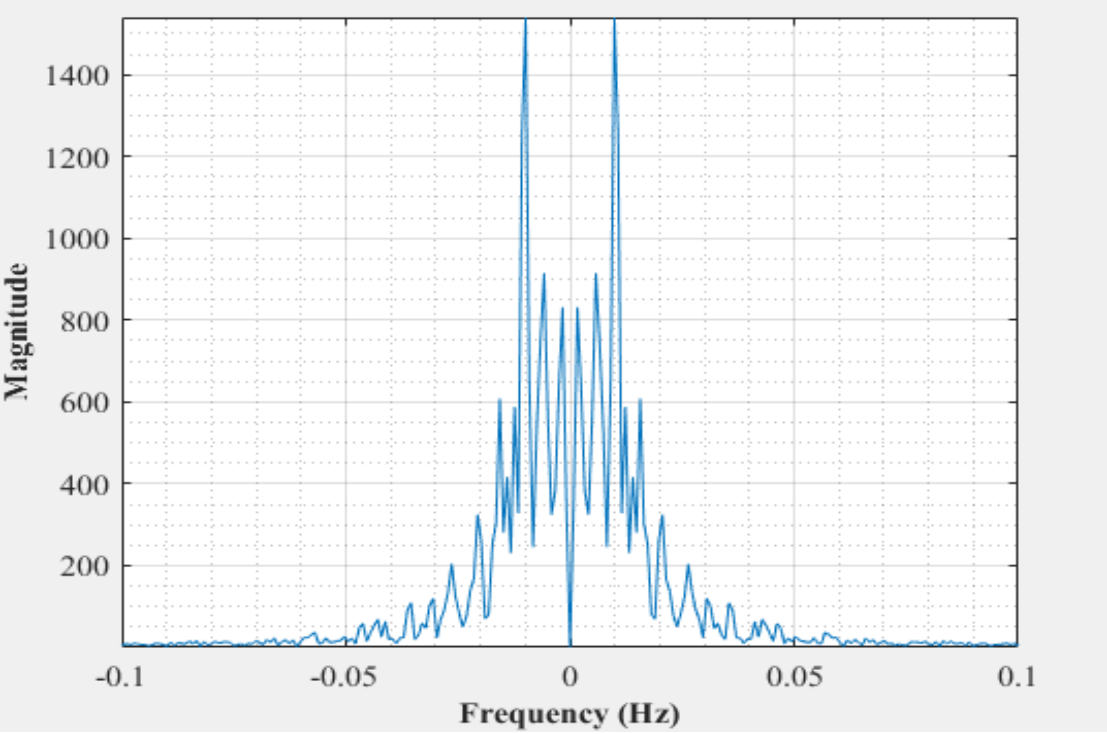


*Figure B-46: Dominant frequency for a non-uniformly packed vessel (large and small at the side) at 65.24 dm$^3$/minute rotameter flowrate*

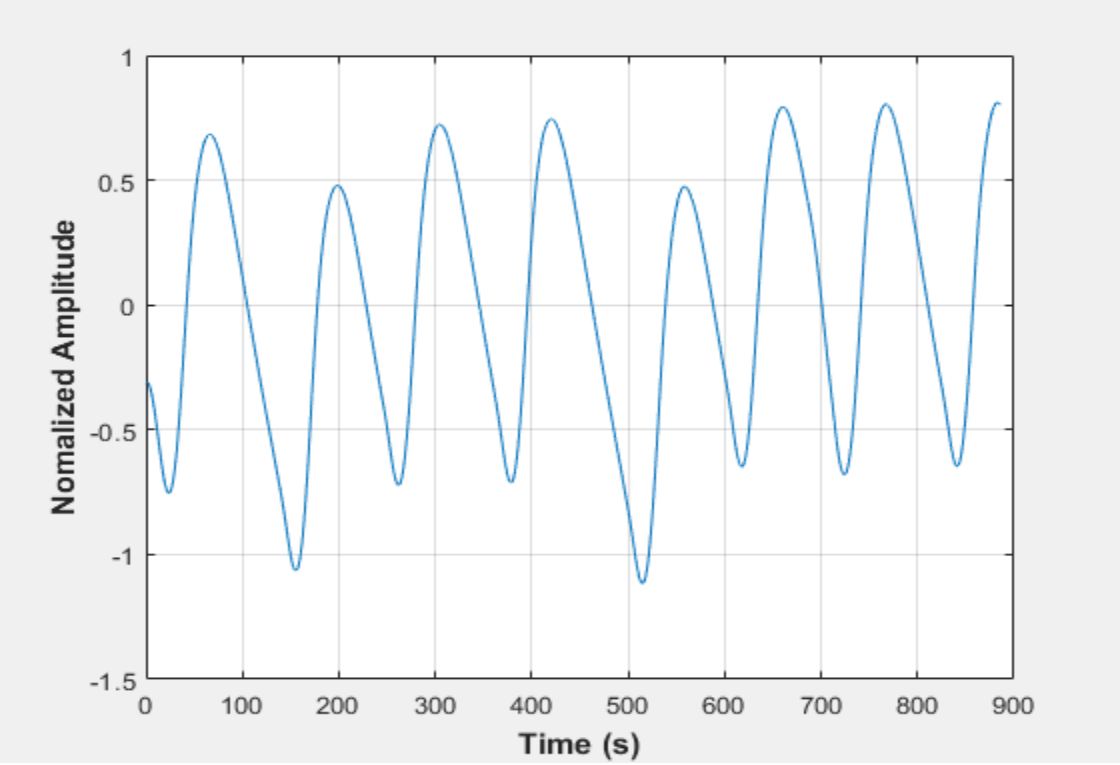


*Figure B-47: Pressure fluctuations in a non-uniformly packed vessel (large and small at the side) at 65.24 dm$^3$/minute gas flow rate- repeat test*

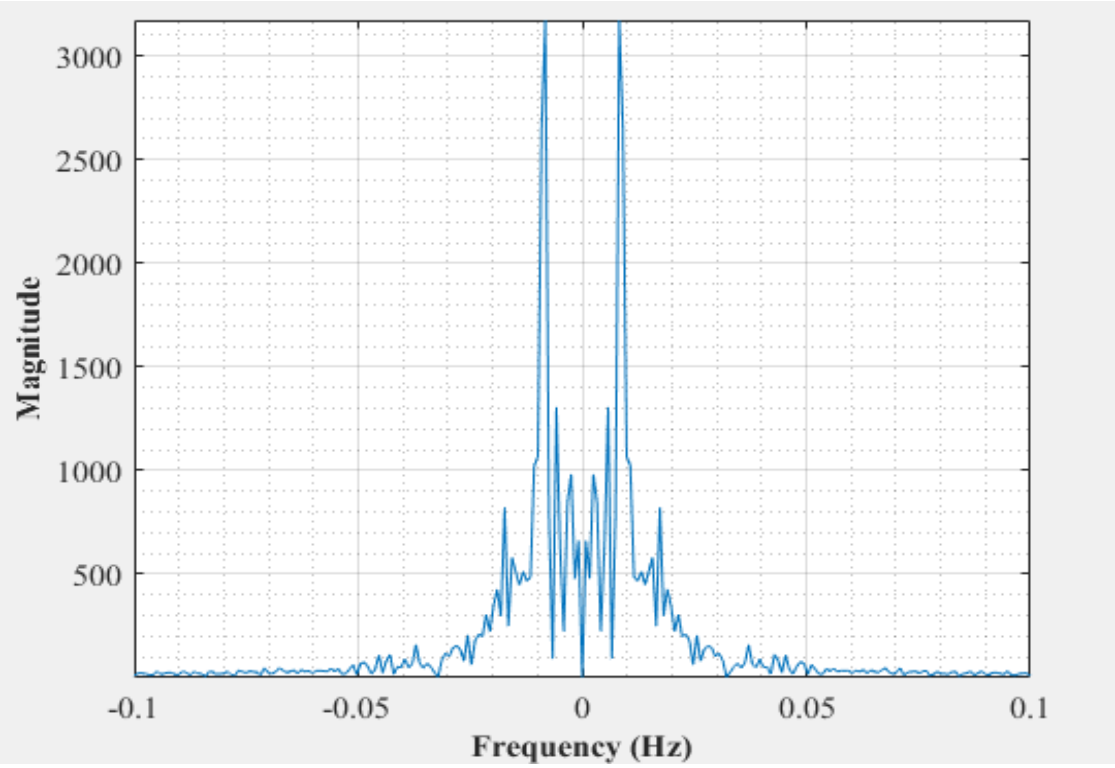


*Figure B-48: Dominant frequency for a non-uniformly packed vessel (large and small at the side) at 65.24 dm$^3$/minute rotameter flowrate- repeat test*

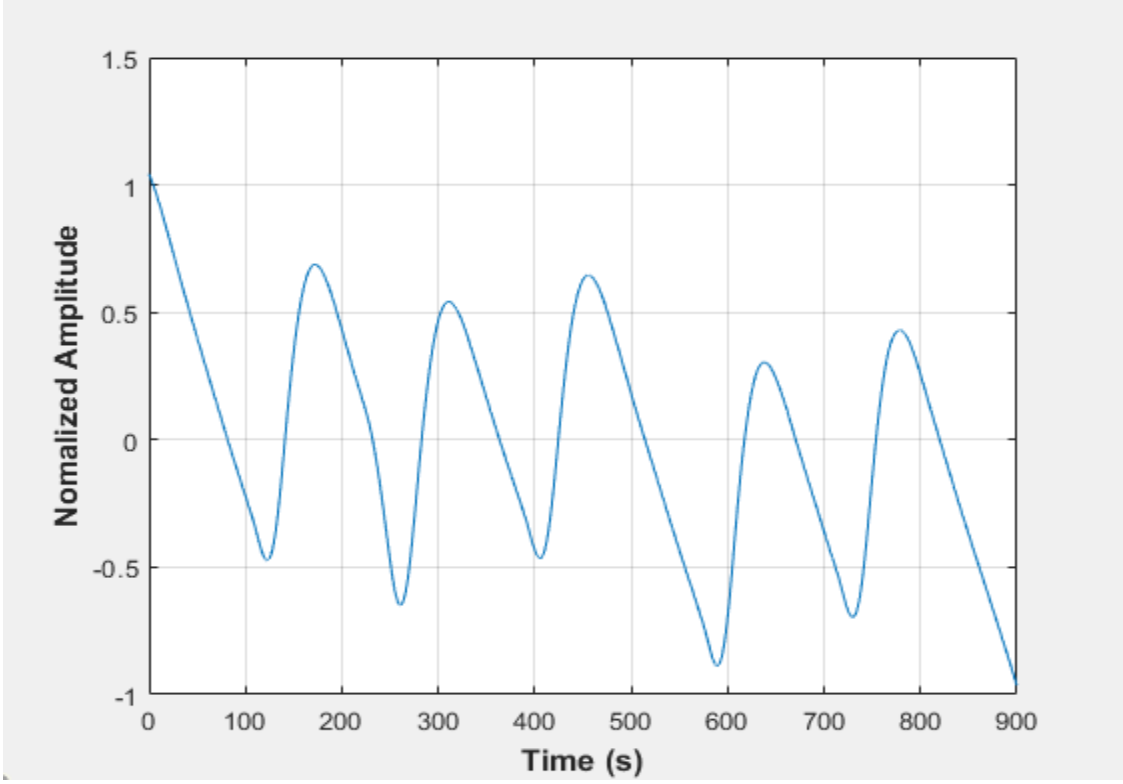


*Figure B-49: Pressure fluctuations in a non-uniformly packed vessel (large and small at the center) at 48.96 dm$^3$/minute gas flow rate*

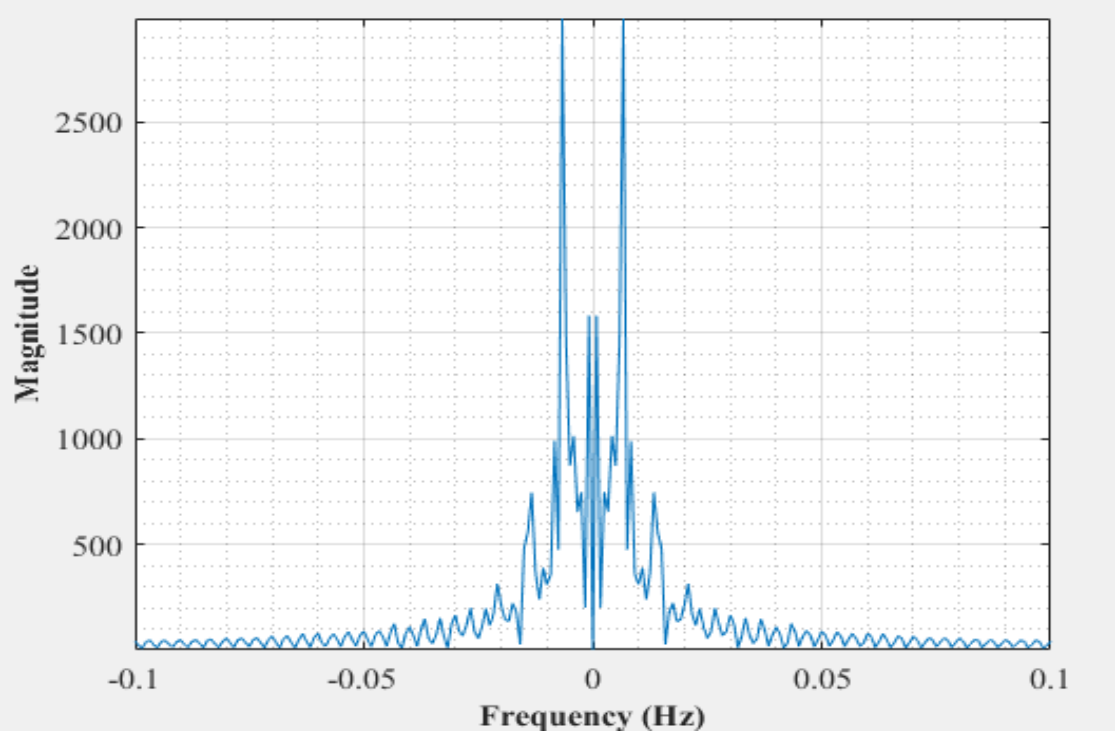


*Figure B-50: Dominant frequency for a non-uniformly packed vessel (large and small at the center) at 48.96 dm$^3$/minute rotameter flowrate*

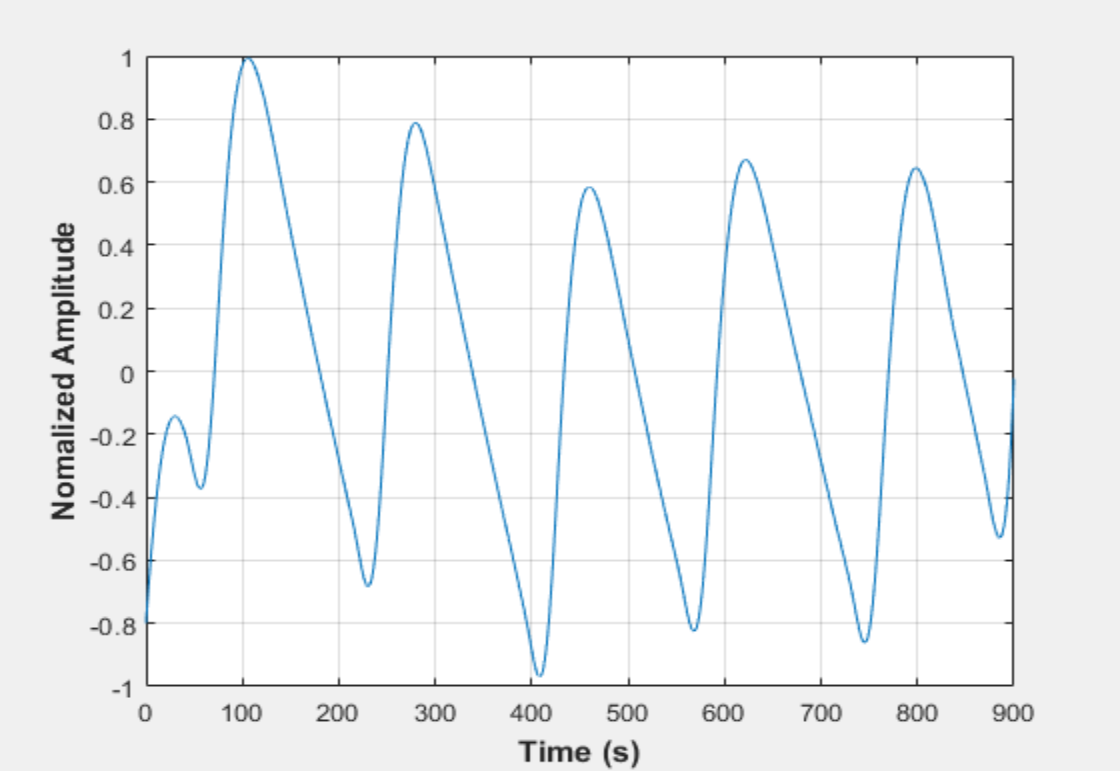


*Figure B-51: Pressure fluctuations in a non-uniformly packed vessel (large and small at the center) at 48.96 dm$^3$/minute gas flow rate-repeat test*

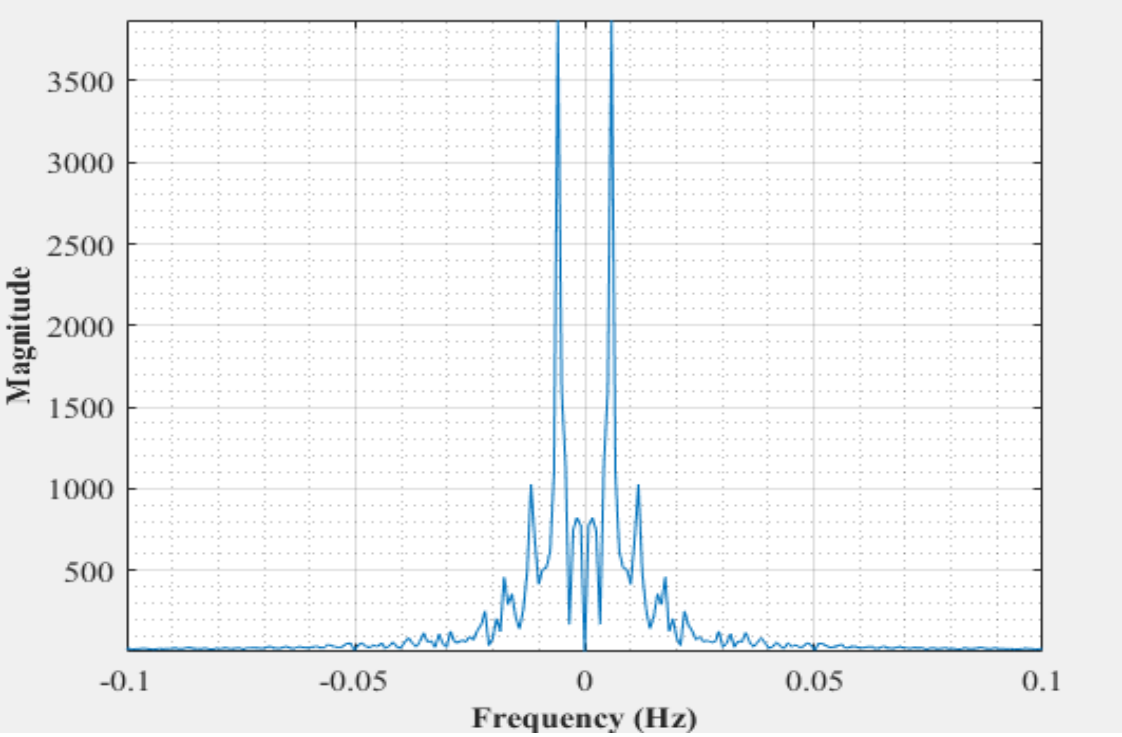


*Figure B-52: Dominant frequency for a non-uniformly packed vessel (large and small at the center) at 48.96 dm$^3$/minute rotameter flowrate- repeat test*

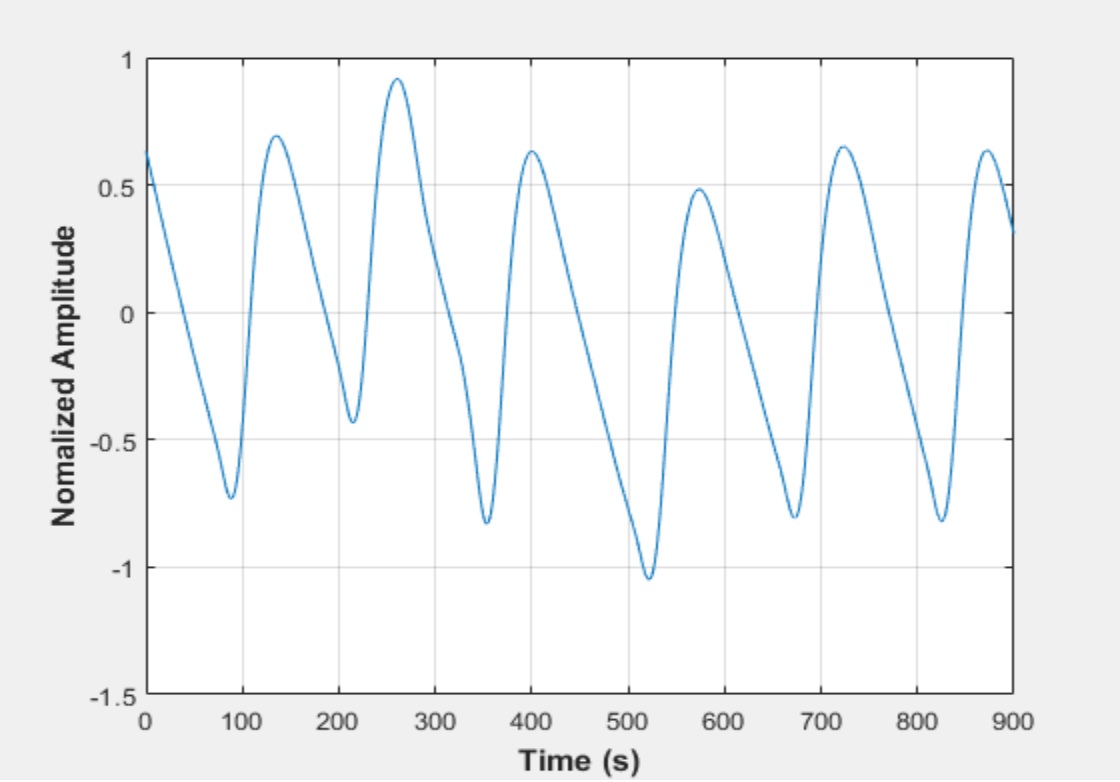


*Figure B-53:Pressure fluctuations in a non-uniformly packed vessel (large and small at the center) at 54.4 dm$^3$/minute gas flow rate*

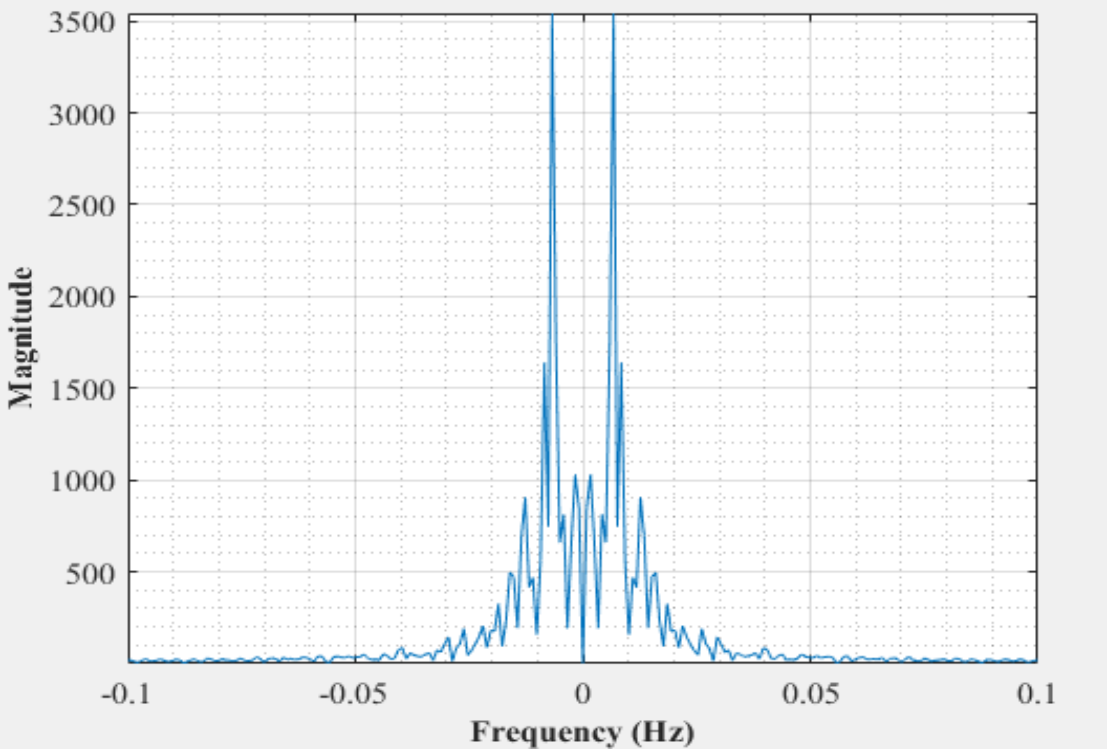


*Figure B-54: Dominant frequency for a non-uniformly packed vessel (large and small at the center) at 54.4 dm$^3$/minute rotameter flowrate*

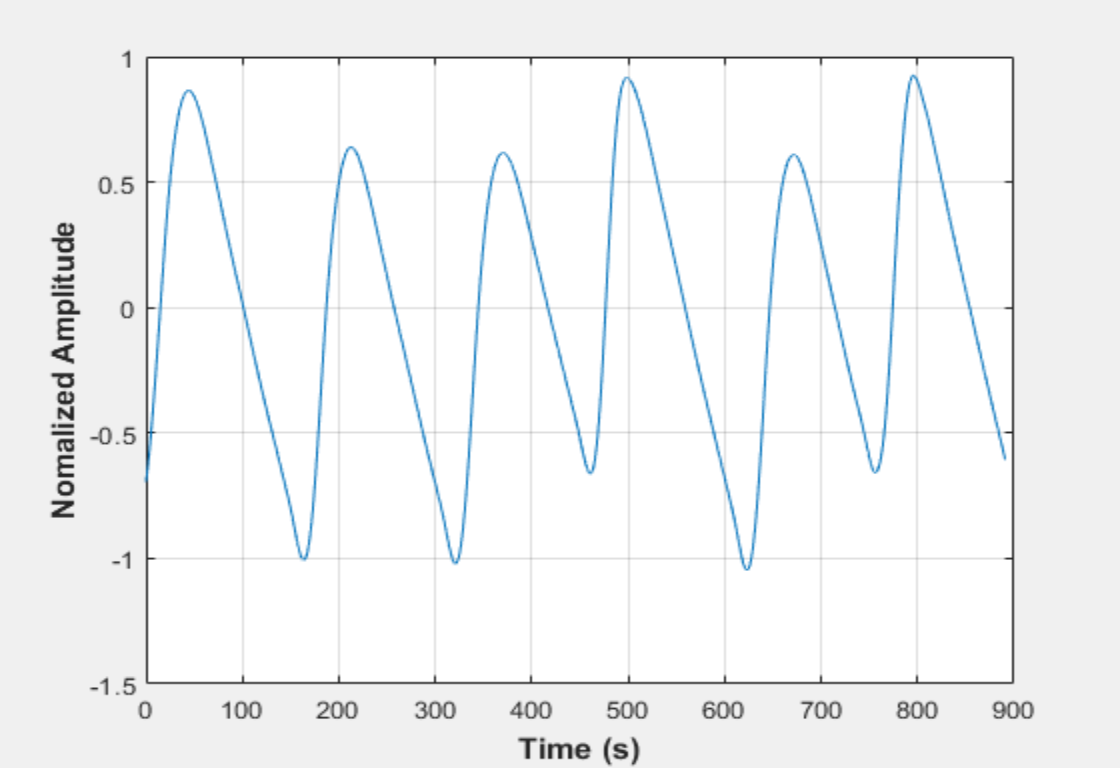


*Figure B-550-6:Pressure fluctuations in a non-uniformly packed vessel (large and small at the center) at 54.4 dm$^3$/minute gas flow rate- test*

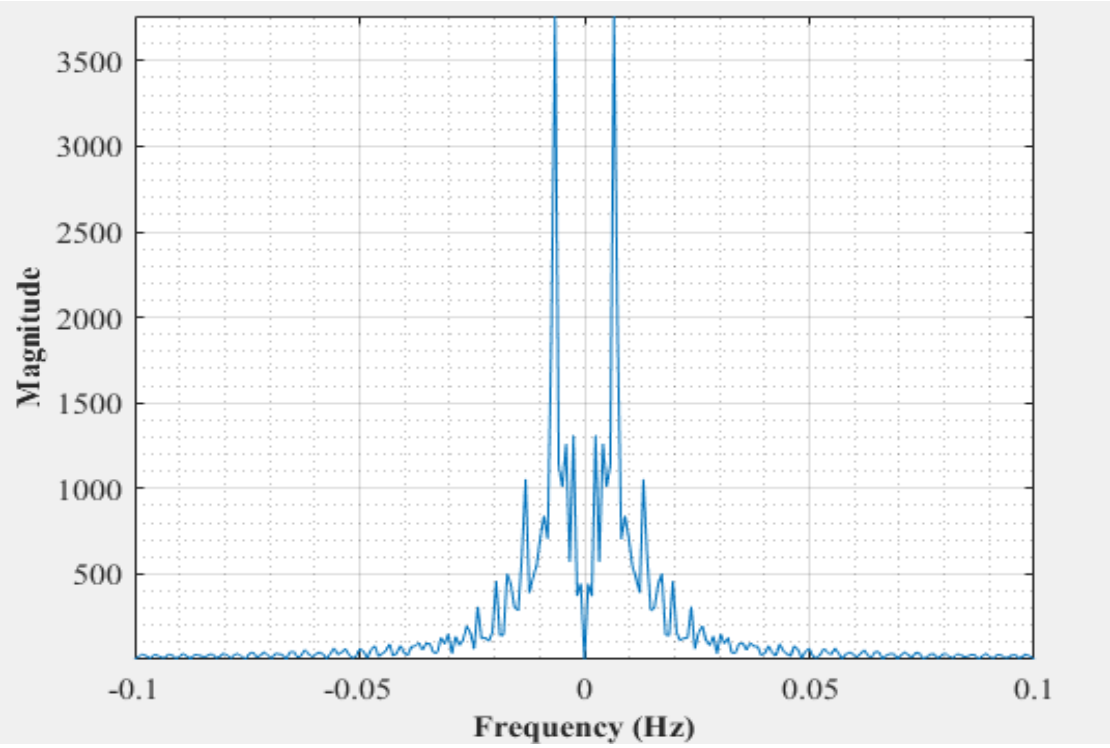


*Figure B-56: Dominant frequency for a non-uniformly packed vessel (large and small at the center) at 54.4 dm$^3$/minute rotameter flowrate- repeat test*

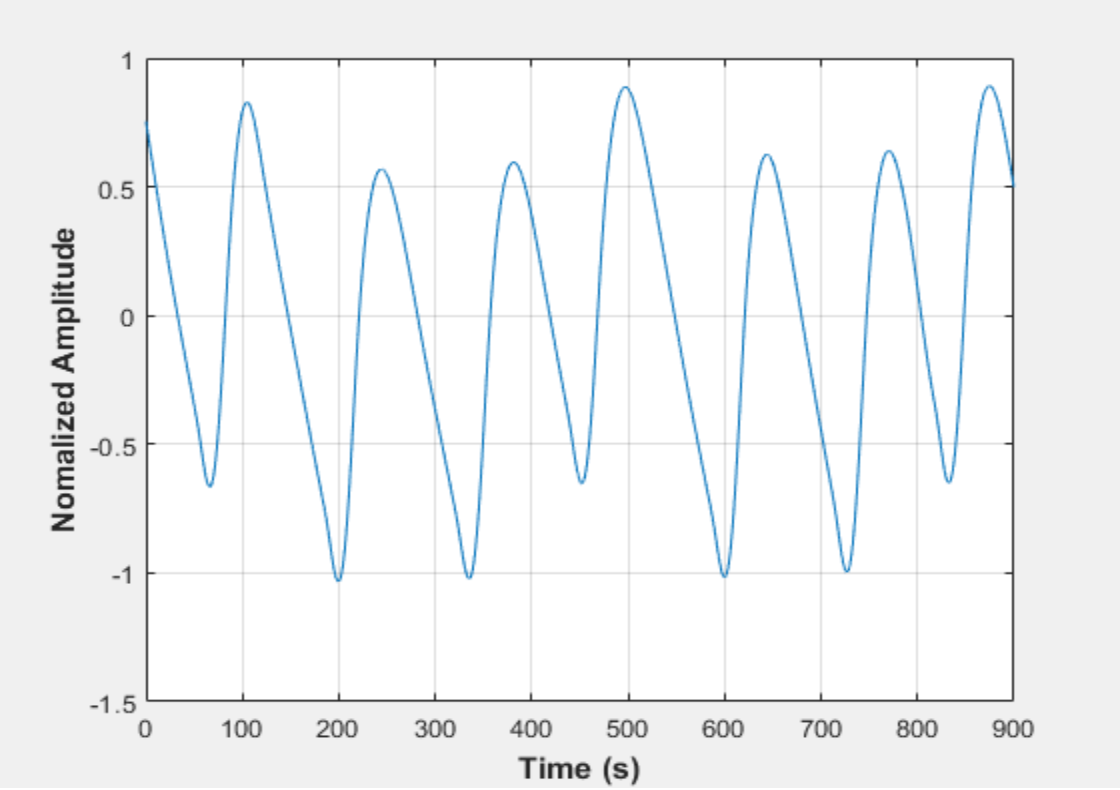


*Figure B-57: Pressure fluctuations in a non-uniformly packed vessel (large and small at the center) at 65.24 dm$^3$/minute gas flow rate*

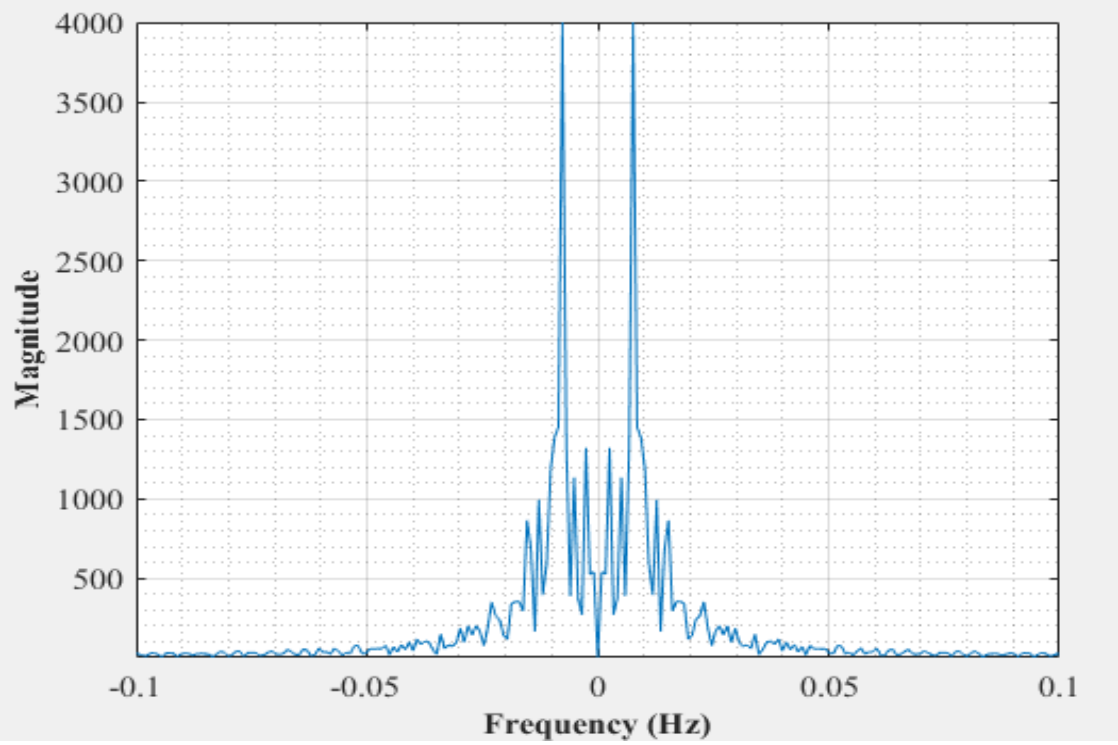


*Figure B-58: Dominant frequency for a non-uniformly packed vessel (large and small at the center) at 65.24 dm$^3$/minute rotameter flowrate*

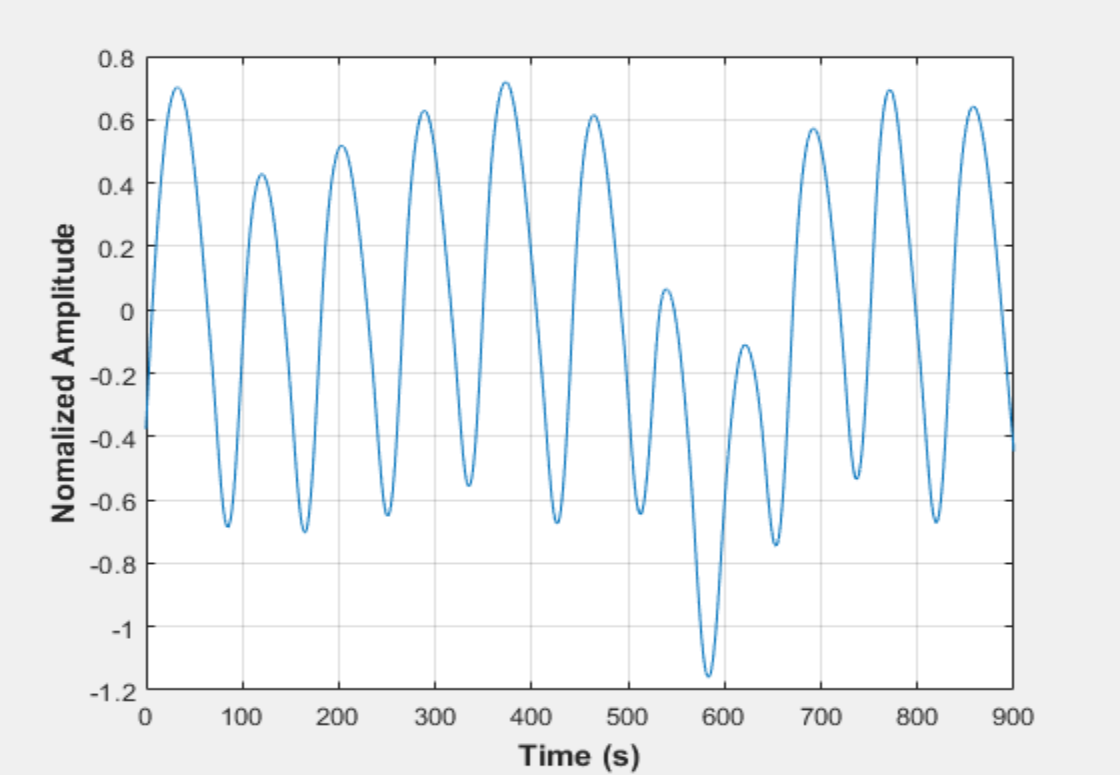


*Figure B-59: Pressure fluctuations in a non-uniformly packed vessel (large and small at the center) at 65.24 dm$^3$/minute gas flow rate- repeat test*

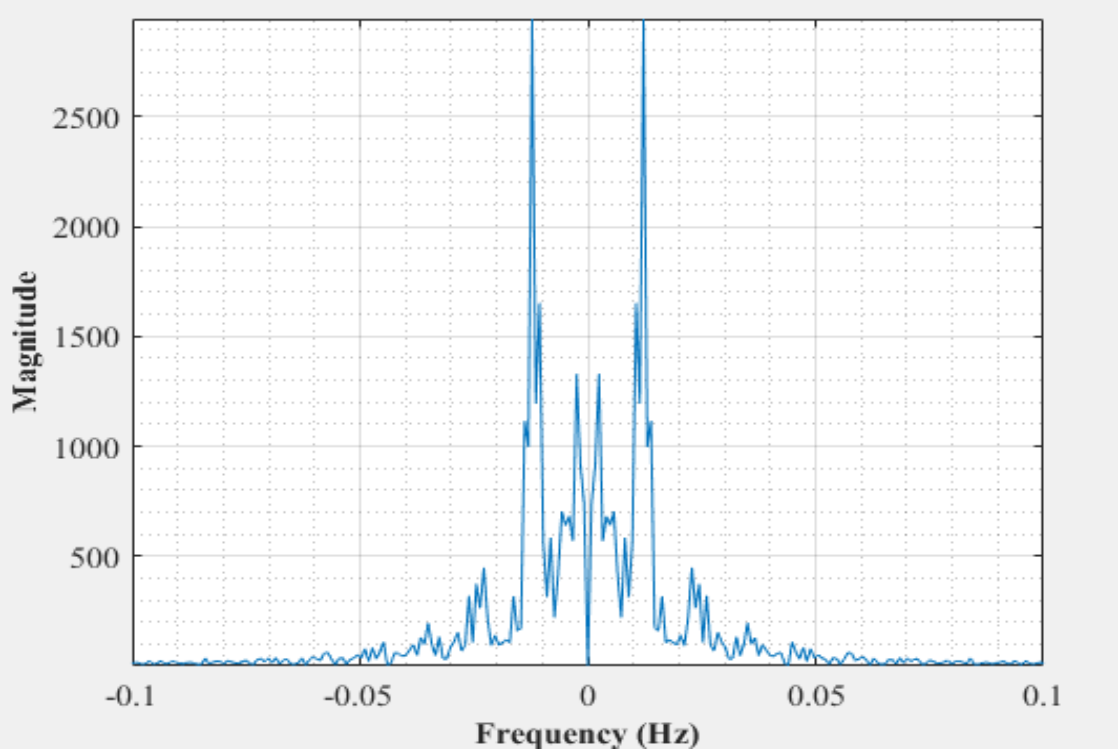


*Figure B-60: Dominant frequency for a non-uniformly packed vessel (large and small at the center) at 65.24 dm$^3$/minute rotameter flowrate- repeat test*

*Table B-1: Second Batch Experimental Results- Frequency (mHz) Data at Various Flowrates*

| **Rotameter flowrate ($dm^3$/minute)** | **48,96** | | | | **54,40** | | | | **65,28** | | | |
|---|---|---|---|---|---|---|---|---|---|---|---|---|
| | **Test 1** | **Test 2** | **Test 3** | **Average** | **Test 1** | **Test 2** | **Test 3** | **Average** | **Test 1** | **Test 2** | **Test 3** | **Average** |
| Empty vessel | 8,97 | 6,43 | 6,62 | 7,34 | 7,91 | 8,22 | 7,38 | 7,83 | 9,55 | 9,42 | 1,61 | 6,86 |
| Large packing | 0,56 | 6,60 | 0,83 | 2,66 | 7,86 | 7,31 | 7,42 | 7,53 | 9,56 | 26,38 | 1,65 | 12,53 |
| Large and small packing (middle) | 0,56 | 6,52 | 7,42 | 4,83 | 12,38 | 6,56 | 5,72 | 8,22 | 1,13 | 5,76 | 5,23 | 4,04 |
| Large and small packing (side) | 7,87 | 25,59 | 25,62 | 19,69 | 8,45 | 6,57 | 7,02 | 7,35 | 9,01 | 0,82 | 8,20 | 6,01 |
| Large and small packing (center) | 7,29 | 6,67 | 5,86 | 6,61 | 8,40 | 6,75 | 6,55 | 7,23 | 10,06 | 7,66 | 12,23 | 9,98 |

*Table B-2: Second Batch Experimental Results- Amplitude Data at Various Flowrates*

| **Rotameter flowrate ($dm^3$/minute)** | **48,96** | | | | **54,40** | | | | **65,28** | | | |
|---|---|---|---|---|---|---|---|---|---|---|---|---|
| | **Test 1** | **Test 2** | **Test 3** | **Average** | **Test 1** | **Test 2** | **Test 3** | **Average** | **Test 1** | **Test 2** | **Test 3** | **Average** |
| Empty vessel | 0,51 | 0,68 | 0,65 | 0,61 | 0,63 | 0,61 | 0,63 | 0,62 | 0,75 | 0,41 | 0,43 | 0,53 |
| Large packing | 0,28 | 0,74 | 0,18 | 0,40 | 0,50 | 0,45 | 0,69 | 0,55 | 0,65 | 0,32 | 0,05 | 0,34 |
| Large and small packing (middle) | 0,45 | 0,74 | 0,60 | 0,60 | 0,67 | 0,76 | 0,47 | 0,63 | 0,33 | 0,77 | 0,77 | 0,62 |
| Large and small packing (side) | 0,58 | 0,53 | 0,30 | 0,47 | 0,64 | 0,72 | 0,64 | 0,67 | 0,52 | 0,42 | 0,70 | 0,55 |
| Large and small packing (centre) | 0,44 | 0,56 | 0,63 | 0,54 | 0,60 | 0,71 | 0,78 | 0,70 | 0,70 | 0,76 | 0,65 | 0,70 |

## APPENDIX C: Small vessel experiments- Third Batch

This section shows graphs for the experiments carried out on the small vessel. Figures C1-C116 show the amplitude and frequency curves for the second batch of experiments. Tables C-1 and C-2 show the summary from the amplitude and frequency curves from the third batch of experimental data.

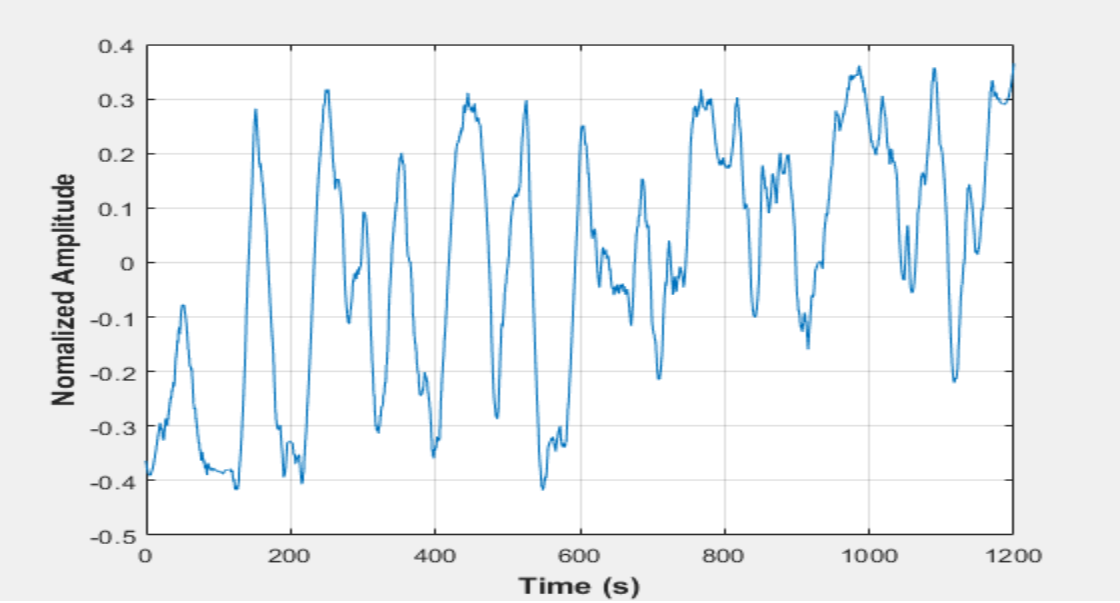


*Figure C-1: Pressure fluctuations in an empty vessel at 20 dm$^3$/minute gas flow rate- Test 1*

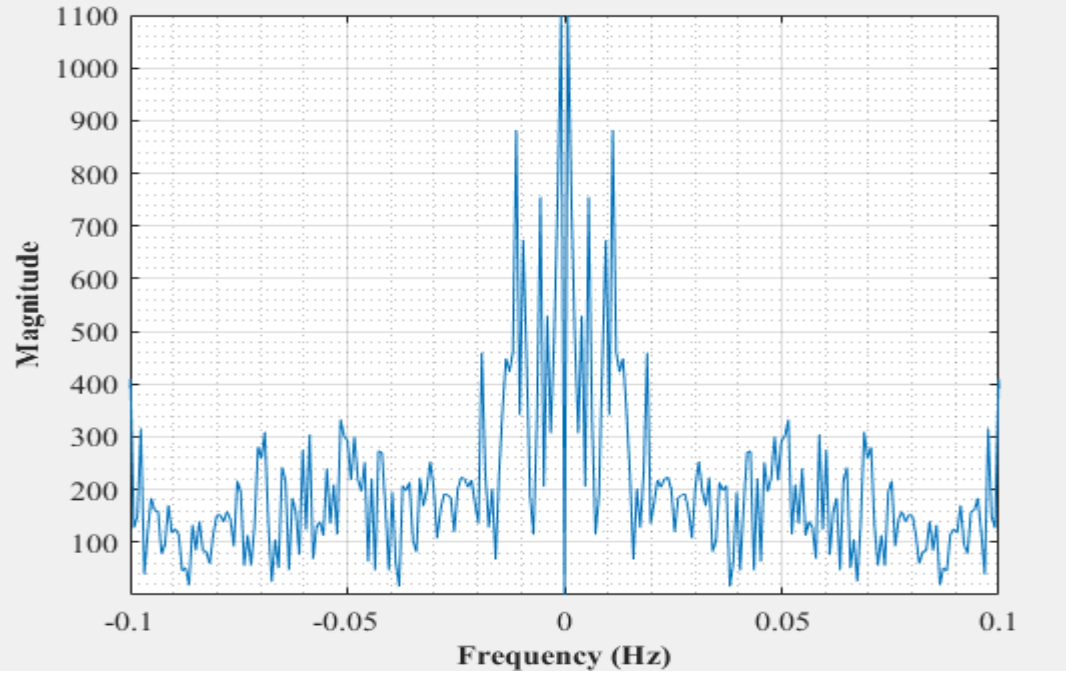


*Figure C-2: Dominant Frequency for an empty vessel at 20 dm$^3$/minute gas flow rate- Test 1*

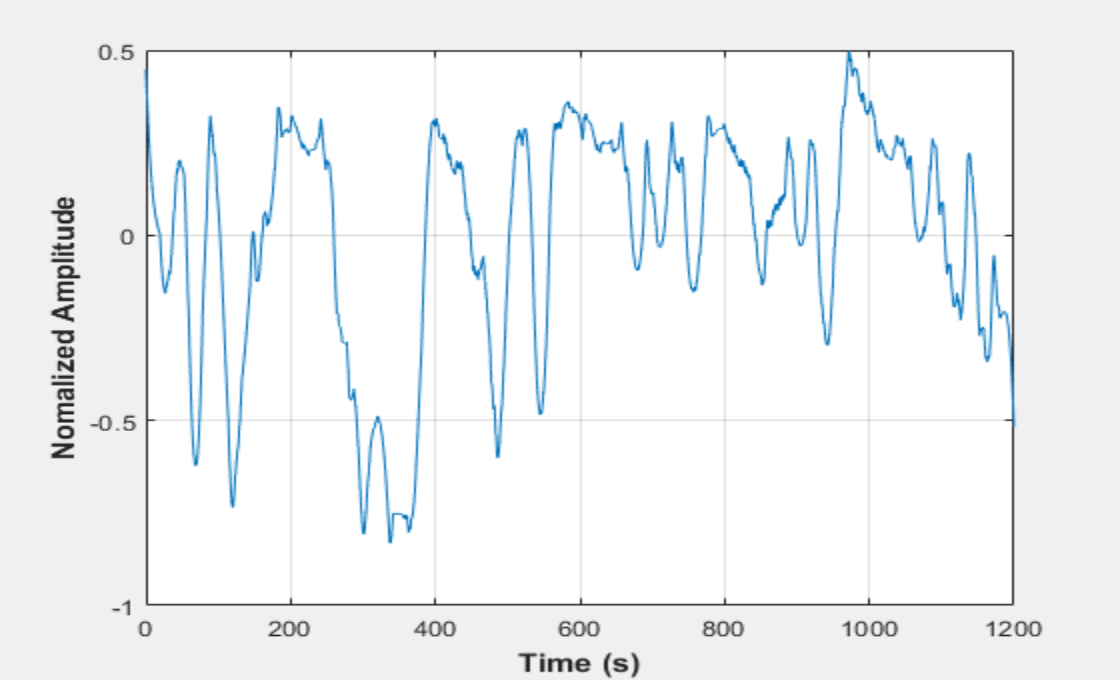


*Figure C-3: Pressure fluctuations in an empty vessel at 20 dm$^3$/minute gas flow rate- Test 2*

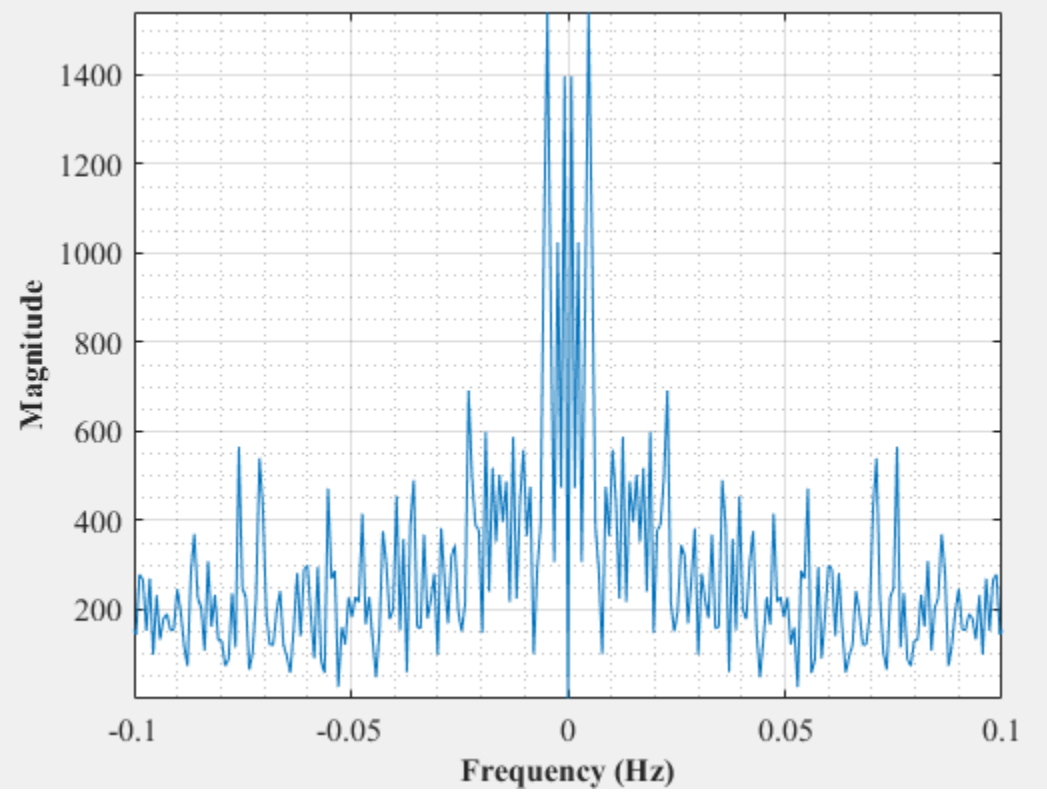


*Figure C-4: Dominant Frequency for an empty vessel at 20 dm$^3$/minute gas flow rate- Test 2*

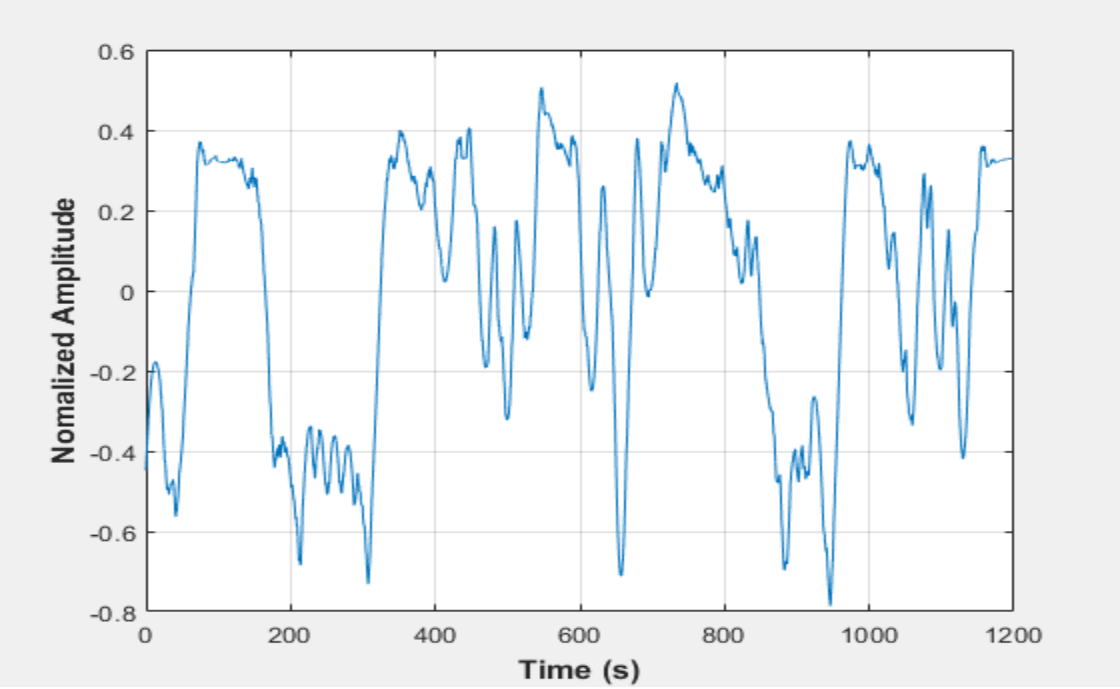


*Figure C-5: Pressure fluctuations in an empty vessel at 20 dm$^3$/minute gas flow rate- Test 3*

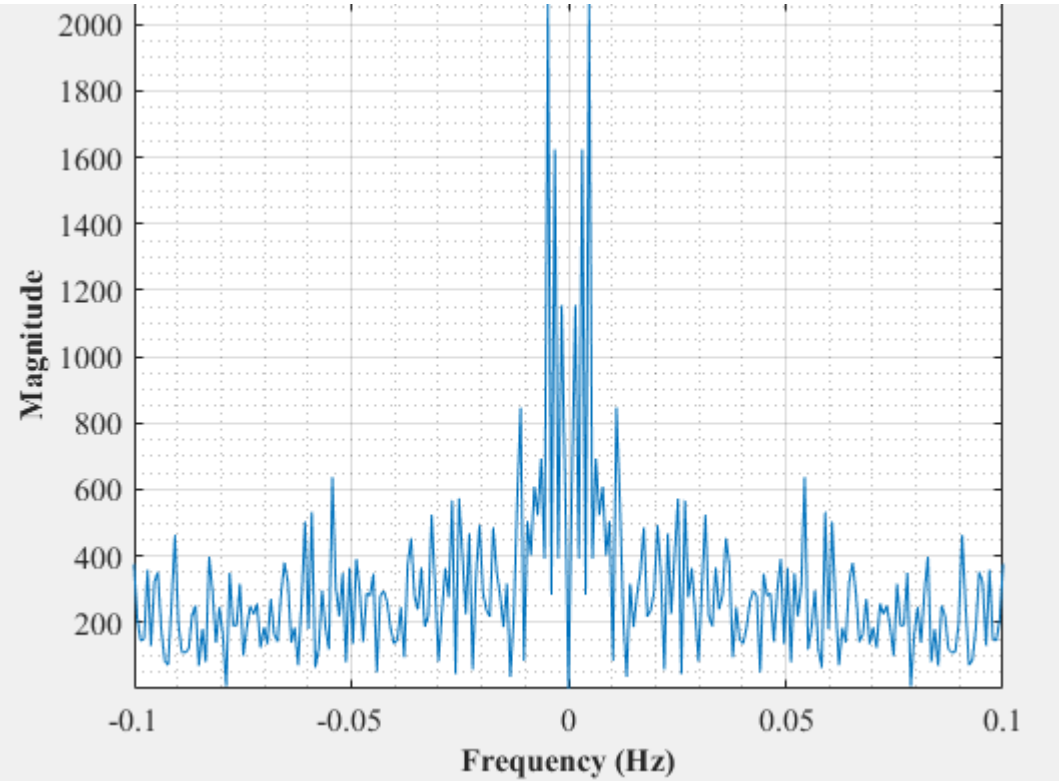


*Figure C-6: Dominant Frequency for an empty vessel at 20 dm$^3$/minute gas flow rate- Test 3*

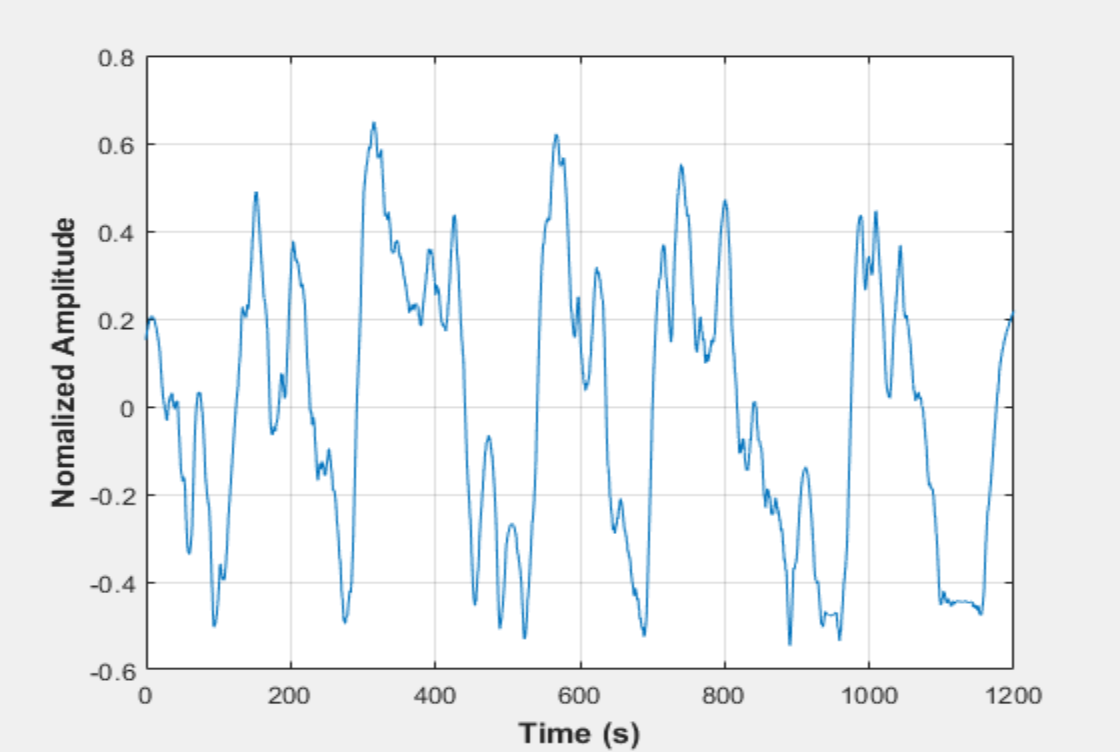


*Figure C-7: Pressure fluctuations in an empty vessel at 22.5 $dm^3$/minute gas flow rate- Test 1*

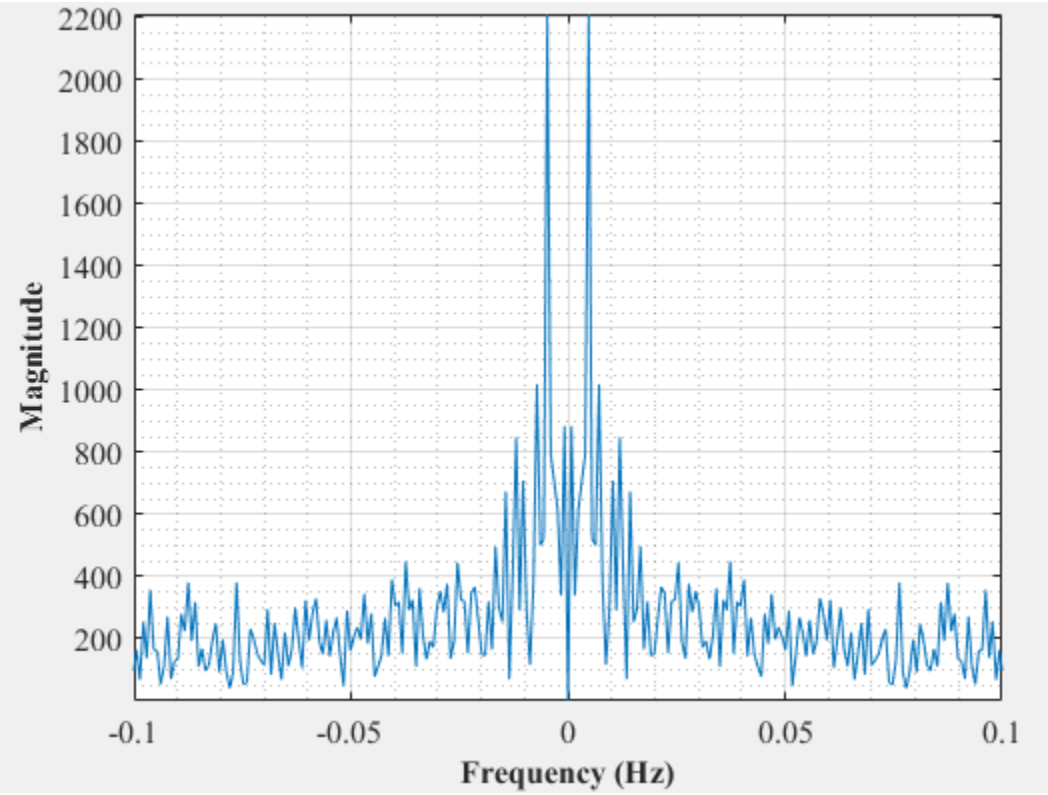


*Figure C-8: Dominant Frequency for an empty vessel at 22.5 $dm^3$/minute gas flow rate- Test 1*

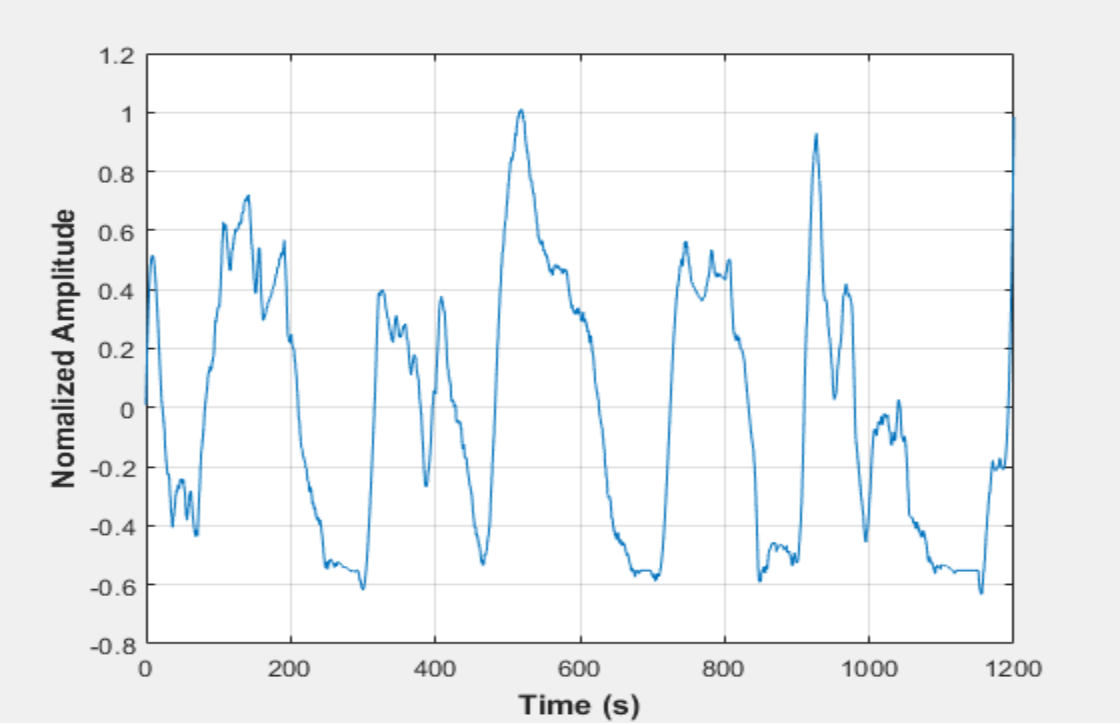


*Figure C-9: Pressure fluctuations in an empty vessel at 22.5 $dm^3$/minute gas flow rate- Test 2*

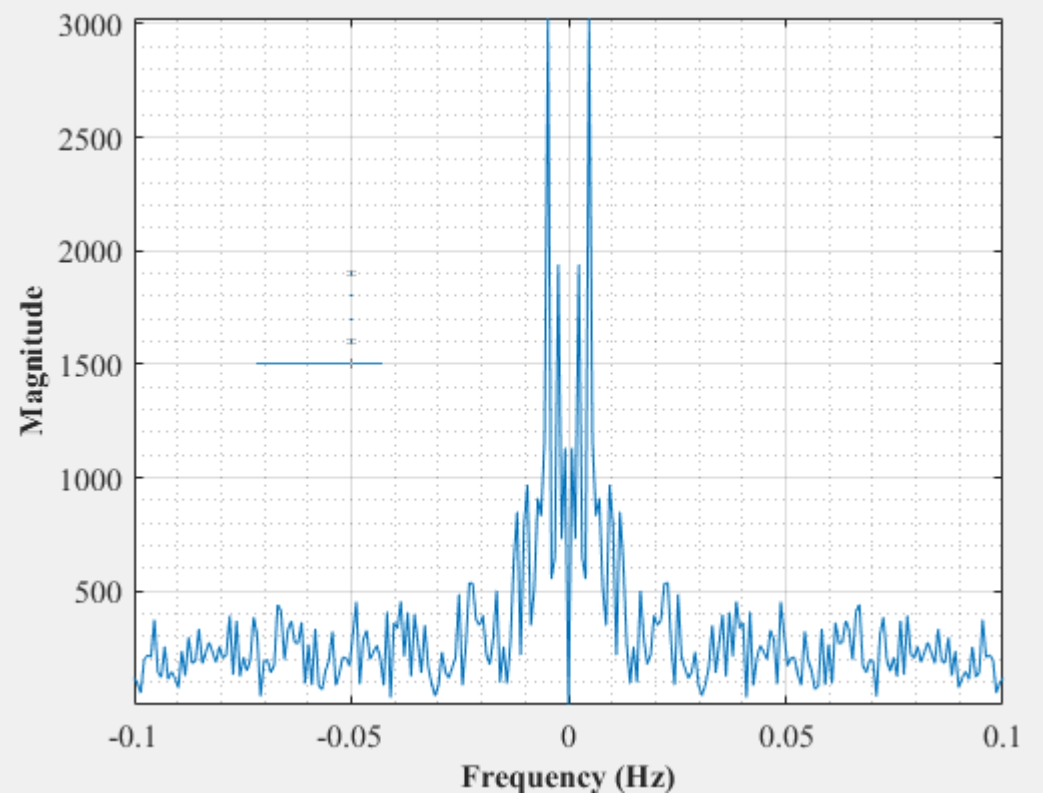


*Figure C-10: Dominant Frequency for an empty vessel at 22.5 $dm^3$/minute gas flow rate- Test 2*

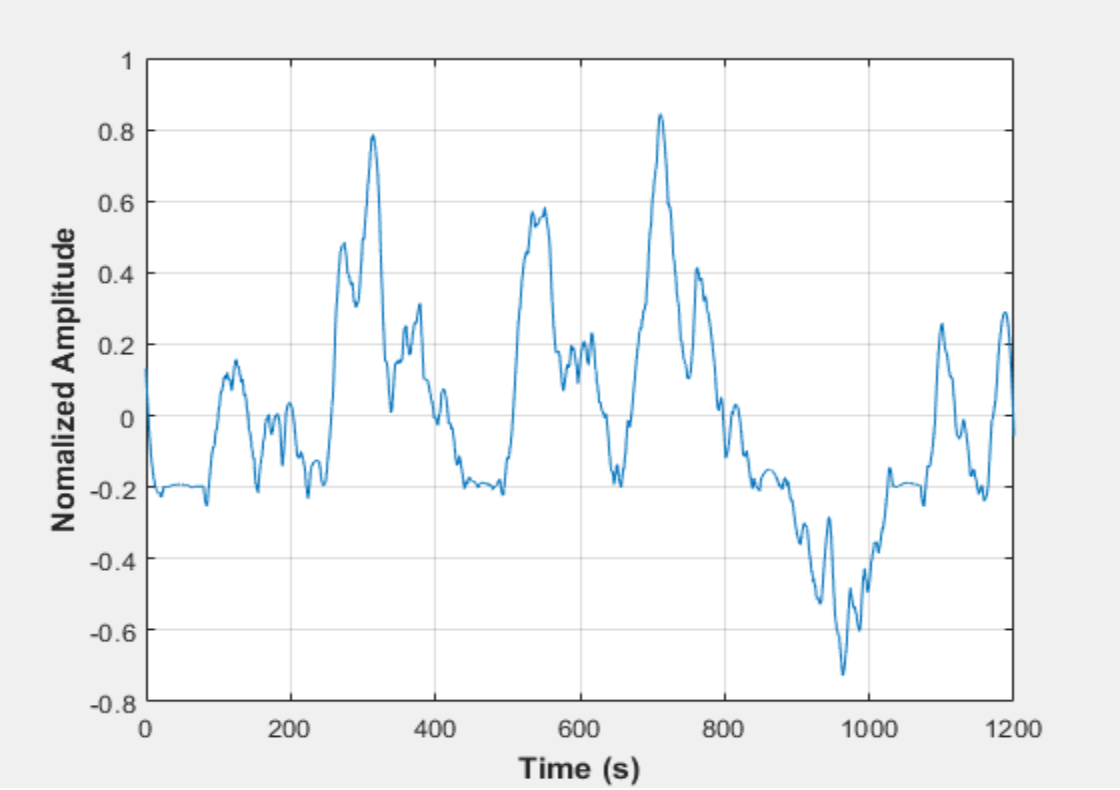


*Figure C-11: Pressure fluctuations in an empty vessel at 22.5 dm$^3$/minute gas flow rate- Test 3*

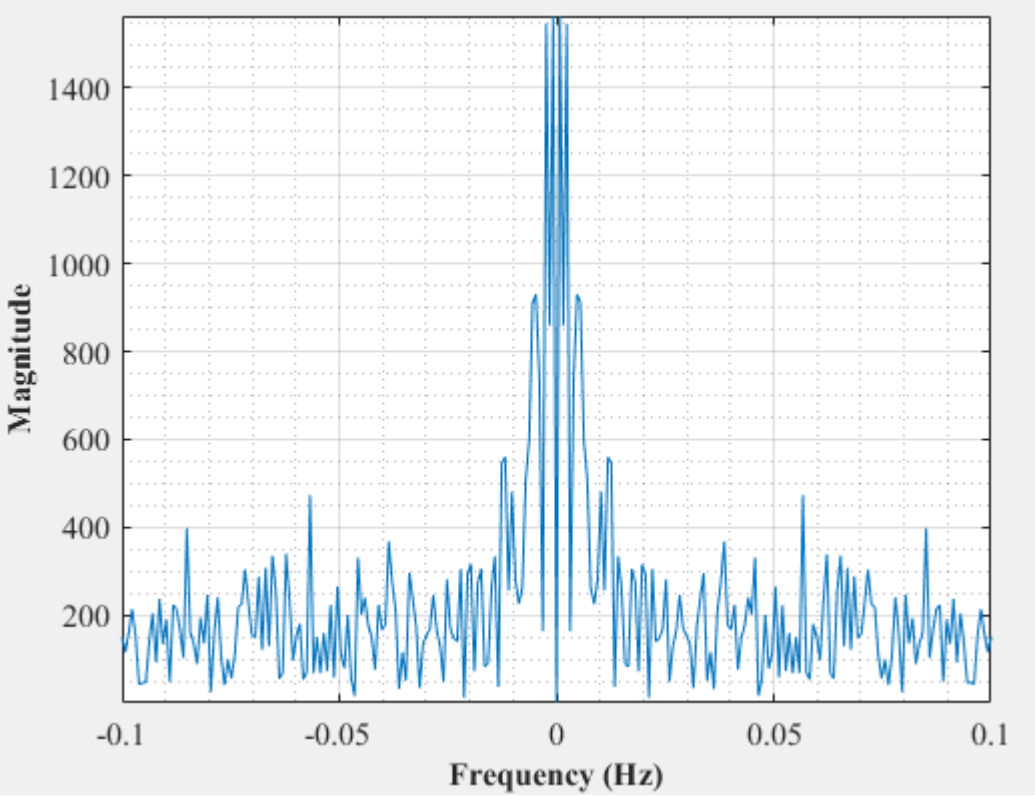


*Figure C-12: Dominant Frequency for an empty vessel at 22.5 dm$^3$/minute gas flow rate- Test 3*

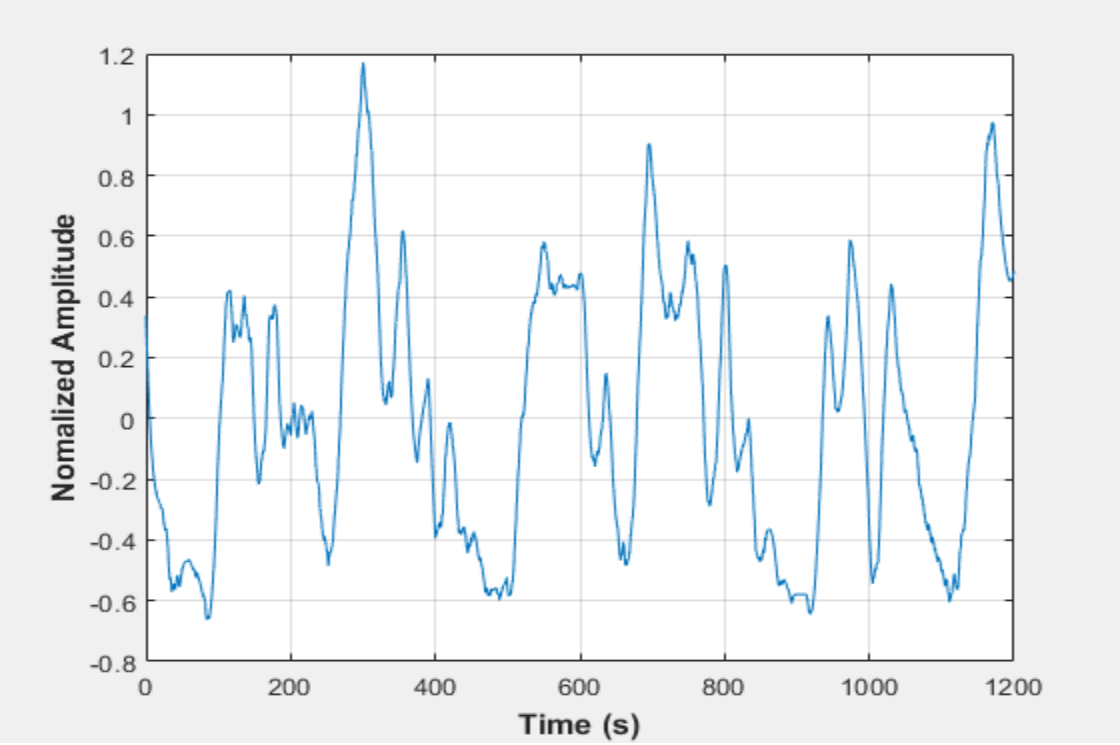


*Figure C-13: Pressure fluctuations in an empty vessel at 22.5 dm$^3$/minute gas flow rate- Test 4*

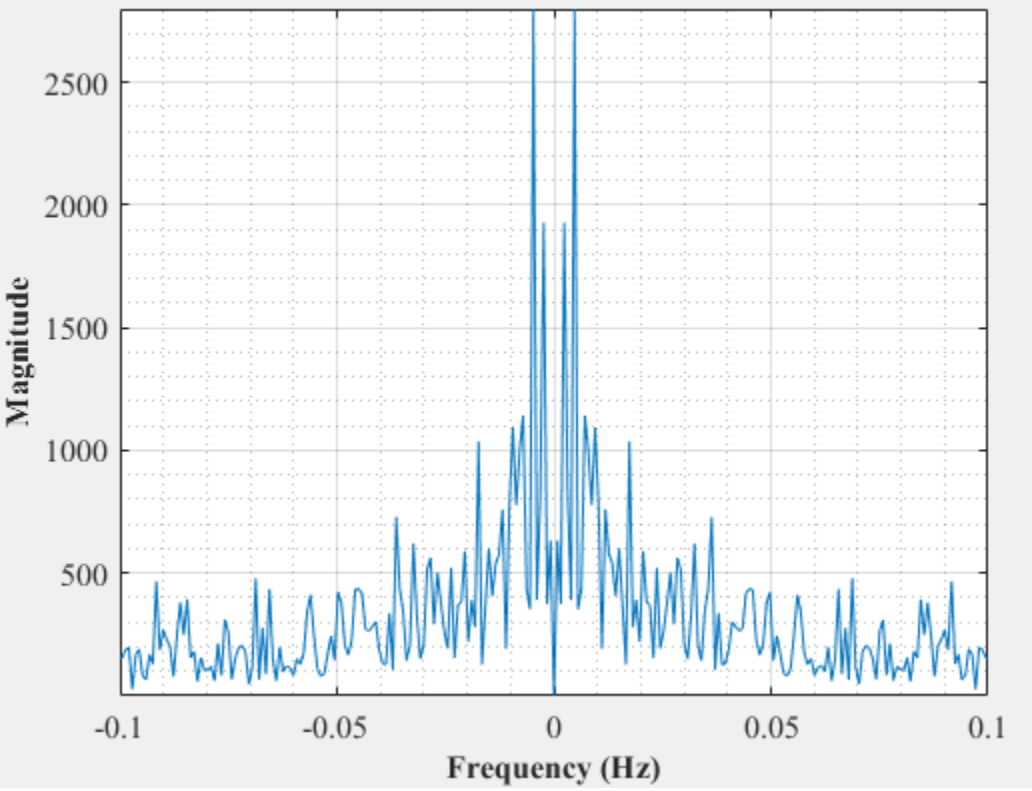


*Figure C-14: Dominant Frequency for an empty vessel at 22.5 dm$^3$/minute gas flow rate- Test 4*

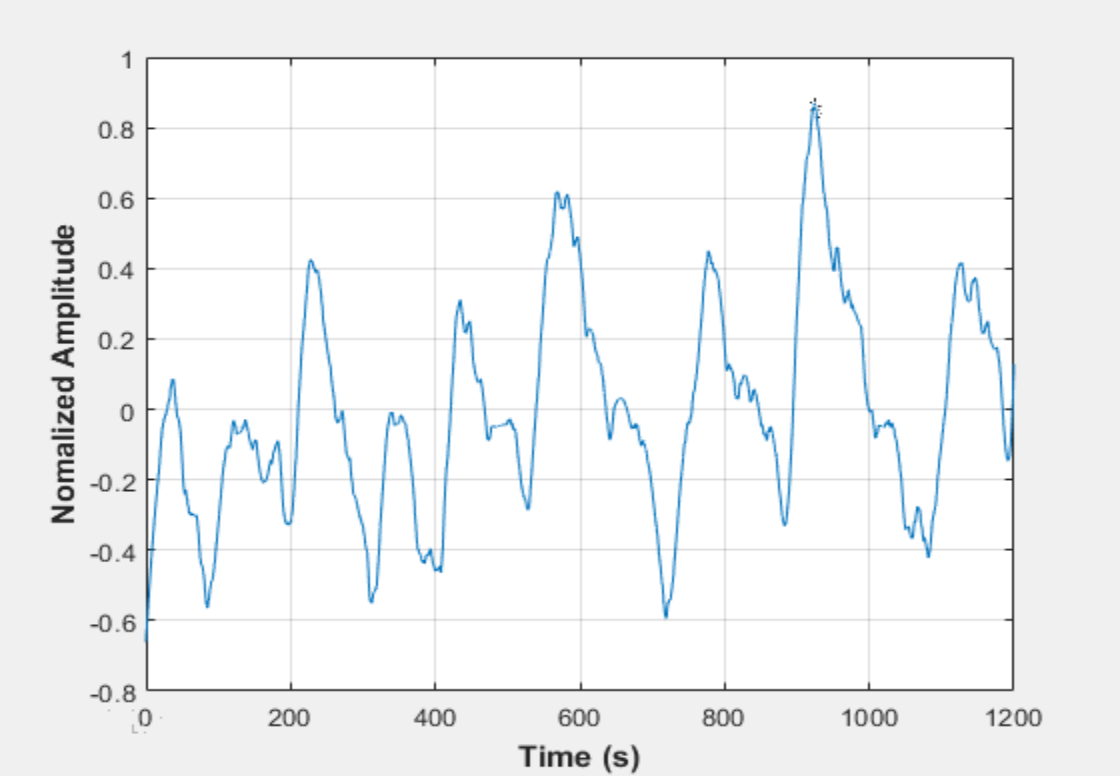


*Figure C-15: Pressure fluctuations in an empty vessel at 29 dm$^3$/minute gas flow rate- Test 1*

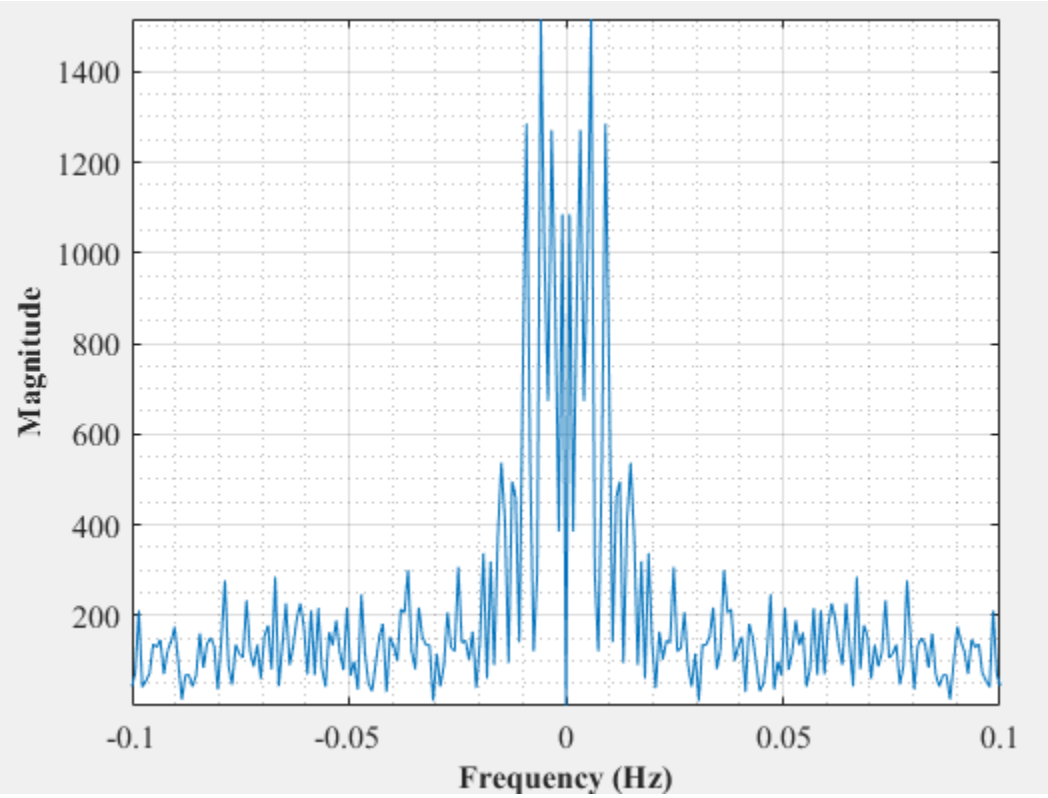


*Figure C-16: Dominant Frequency for an empty vessel at 29 dm$^3$/minute gas flow rate- Test 1*

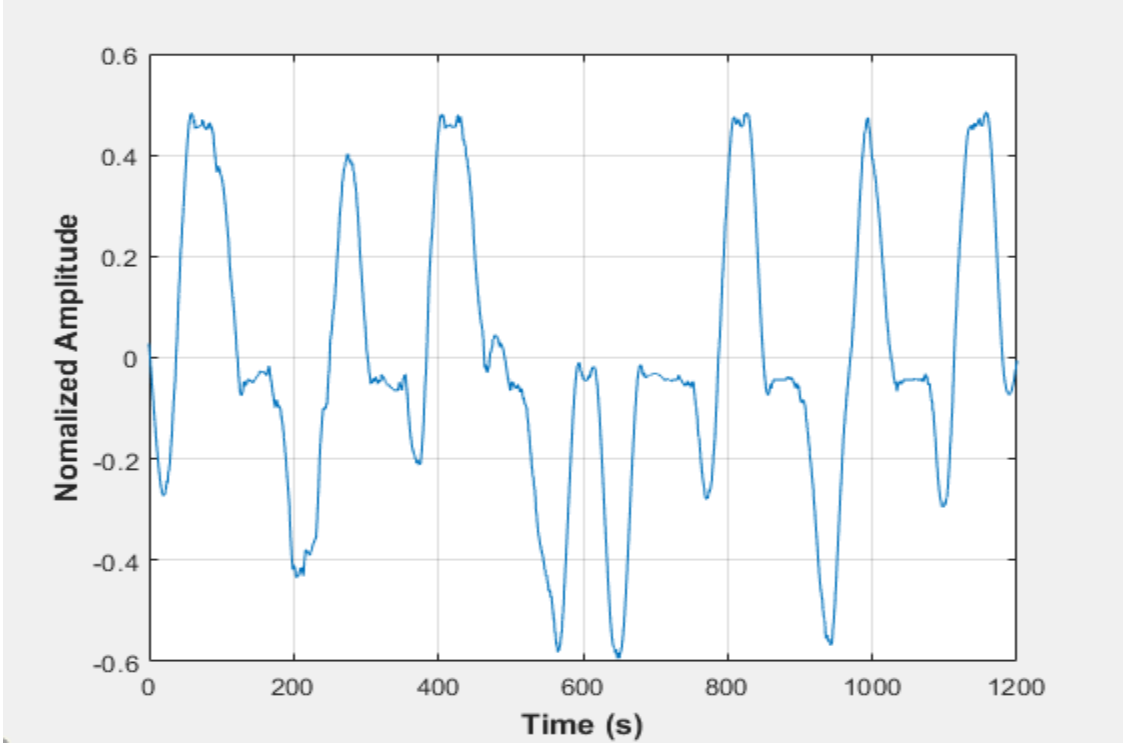


*Figure C-17: Pressure fluctuations in an empty vessel at 29 dm$^3$/minute gas flow rate- Test 2*

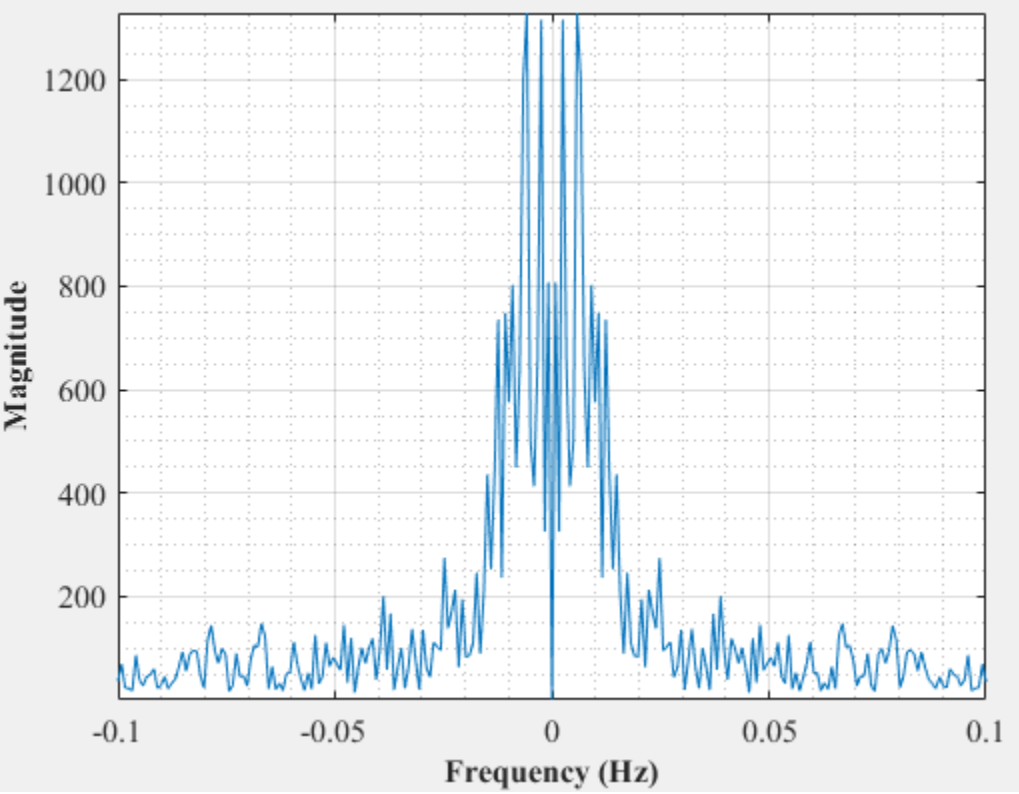


*Figure C-18: Pressure fluctuations in an empty vessel at 29 dm$^3$/minute gas flow rate- Test 2*

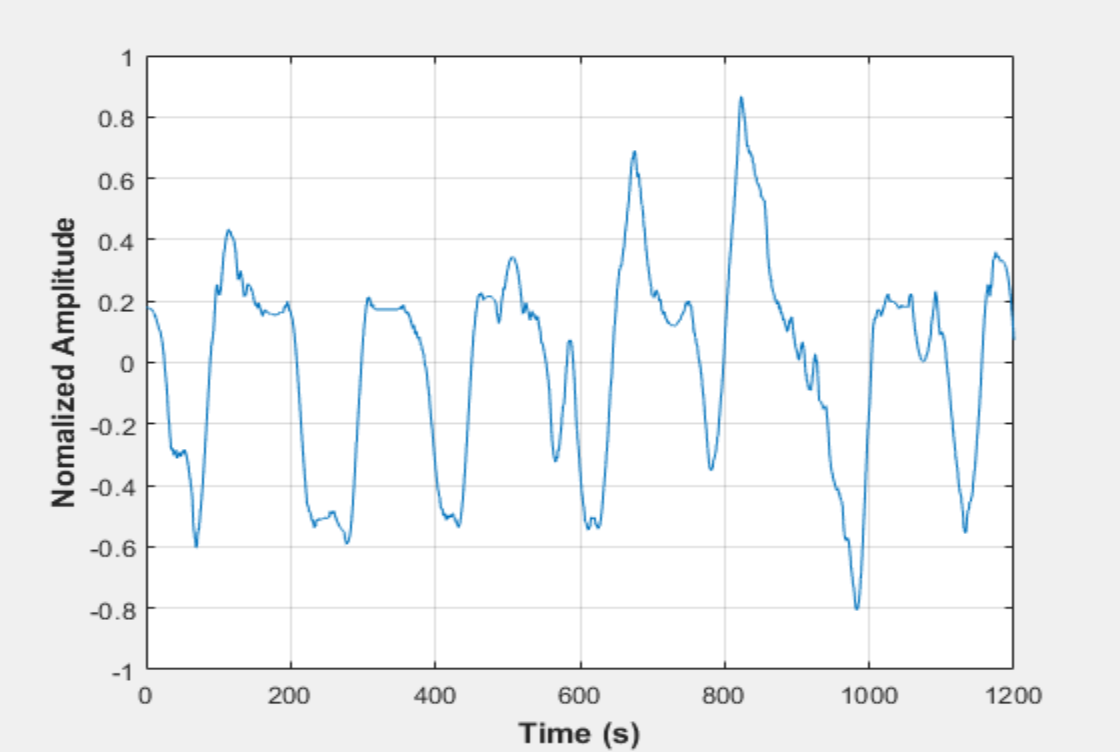


*Figure C-19: Pressure fluctuations in an empty vessel at 29 dm$^3$/minute gas flow rate- Test 3*

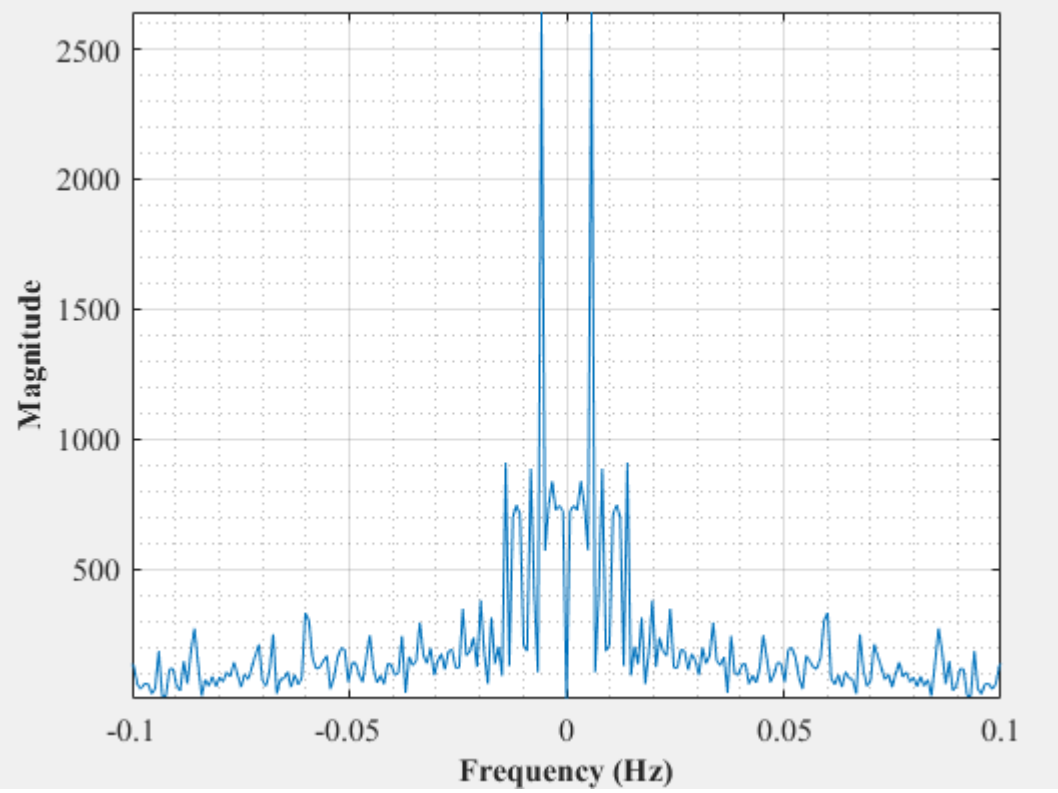


*Figure C-20: Dominant Frequency for an empty vessel at 29 dm$^3$/minute gas flow rate- Test 3*

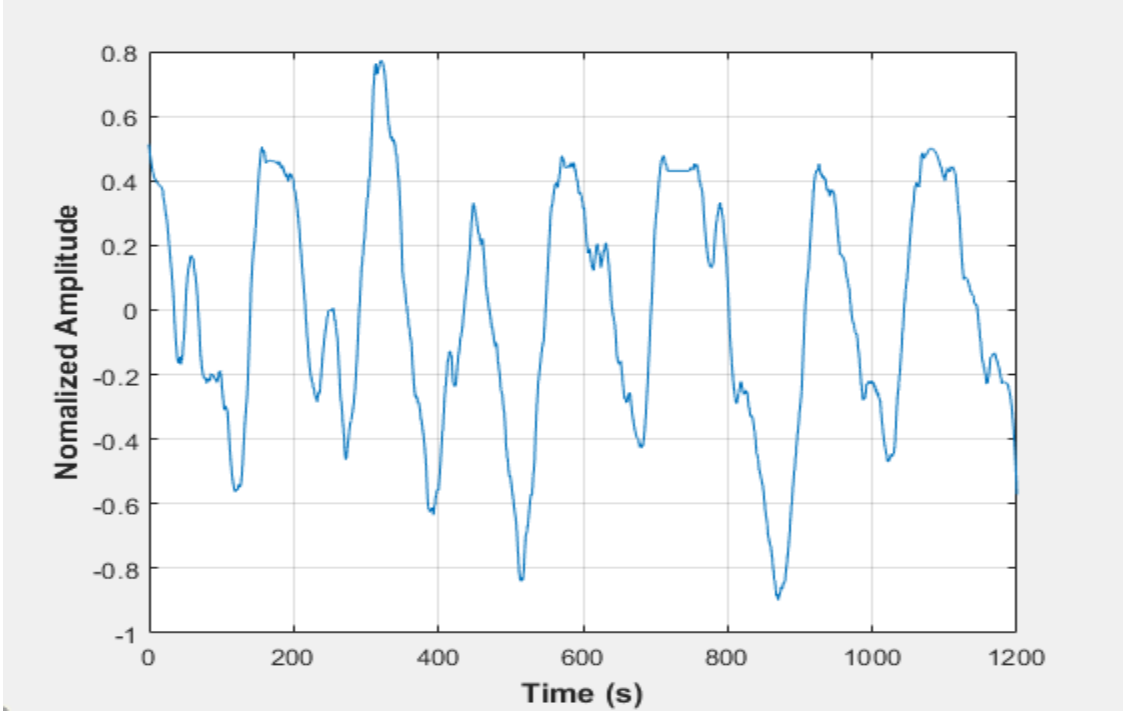


*Figure C-21: Pressure fluctuations in an empty vessel at 29 dm$^3$/minute gas flow rate- Test 4*

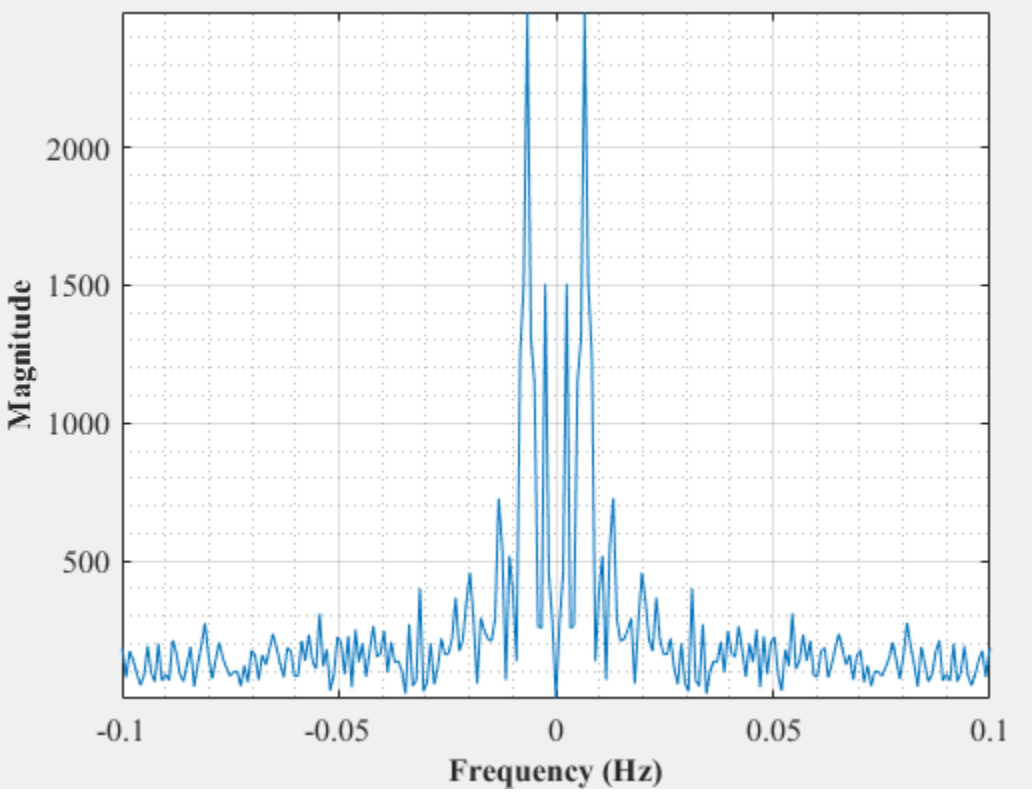


*Figure C-22: Dominant Frequency for an empty vessel at 29 dm$^3$/minute gas flow rate- Test 4*

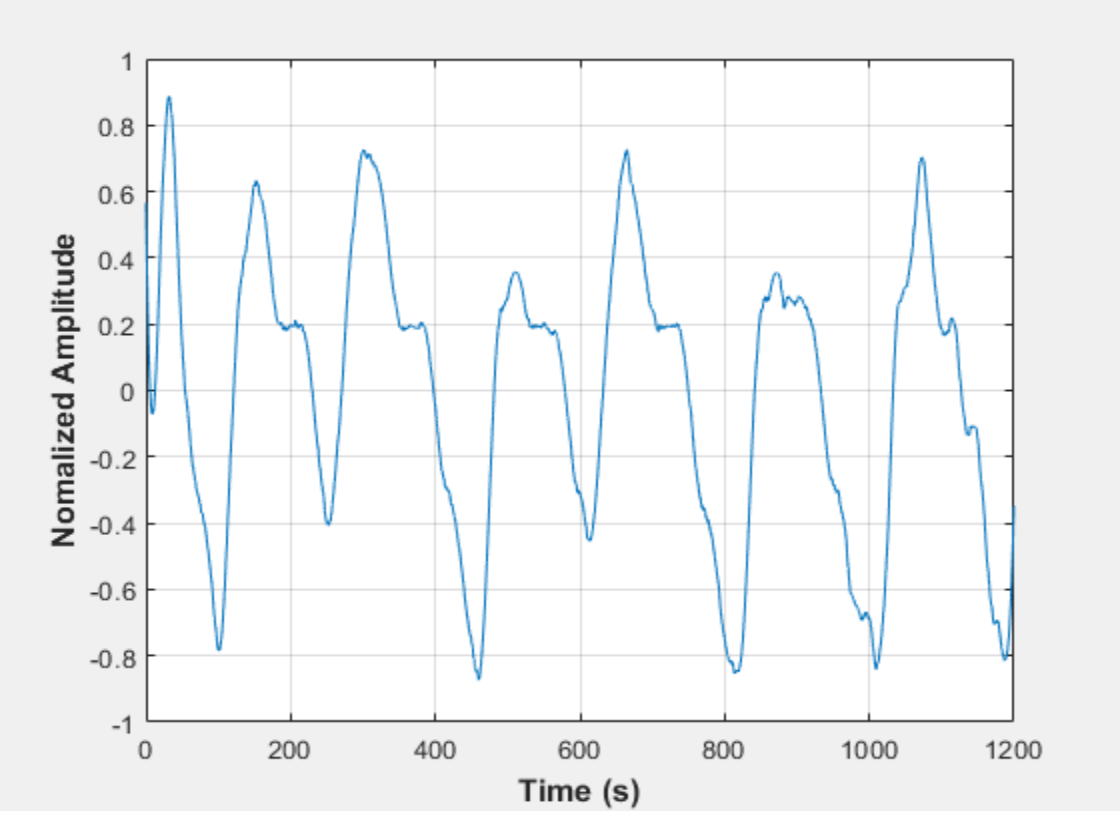


*Figure C-23: Pressure fluctuations in an empty vessel at 33 dm$^3$/minute gas flow rate- Test 1*

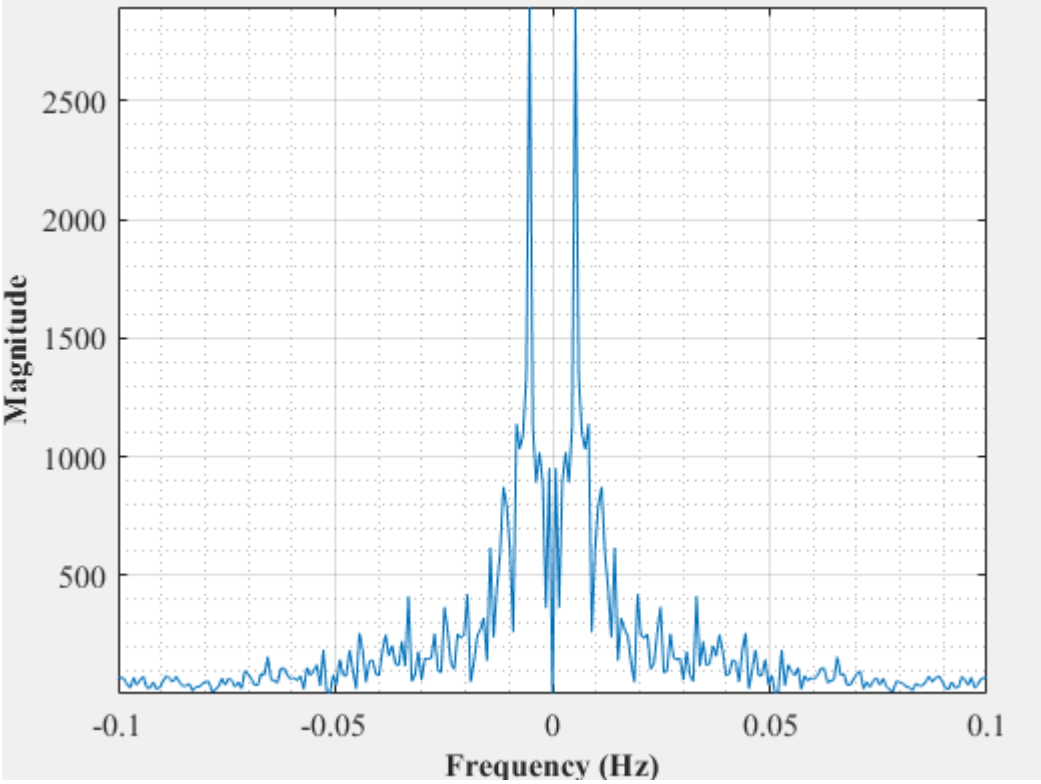


*Figure C-24: Dominant Frequency for an empty vessel at 33 dm$^3$/minute gas flow rate- Test 1*

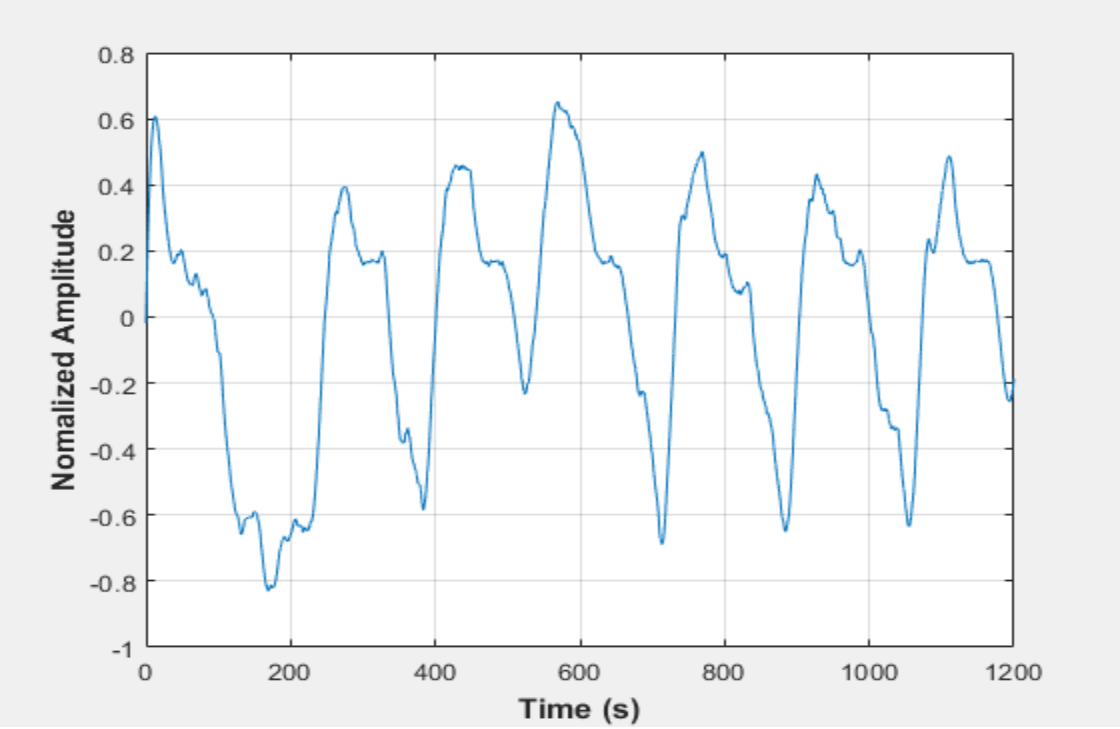


*Figure C-25: Pressure fluctuations in an empty vessel at 33 dm$^3$/minute gas flow rate- Test 2*

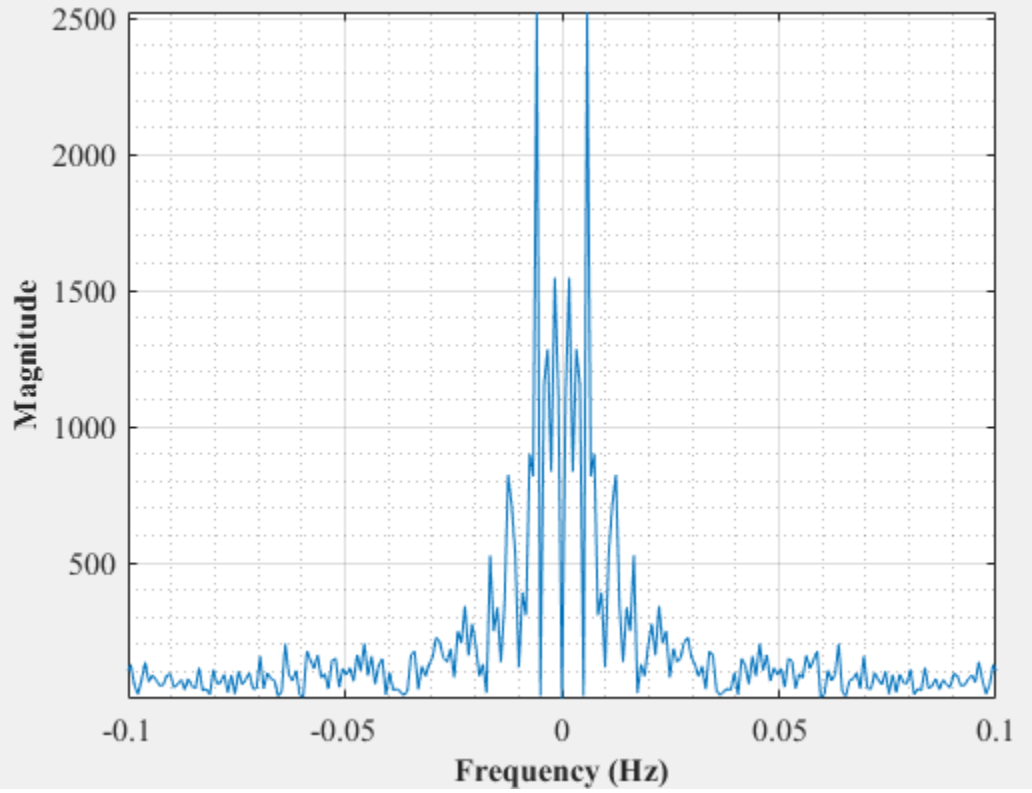


*Figure C-26: Dominant Frequency for an empty vessel at 33 dm$^3$/minute gas flow rate- Test 2*

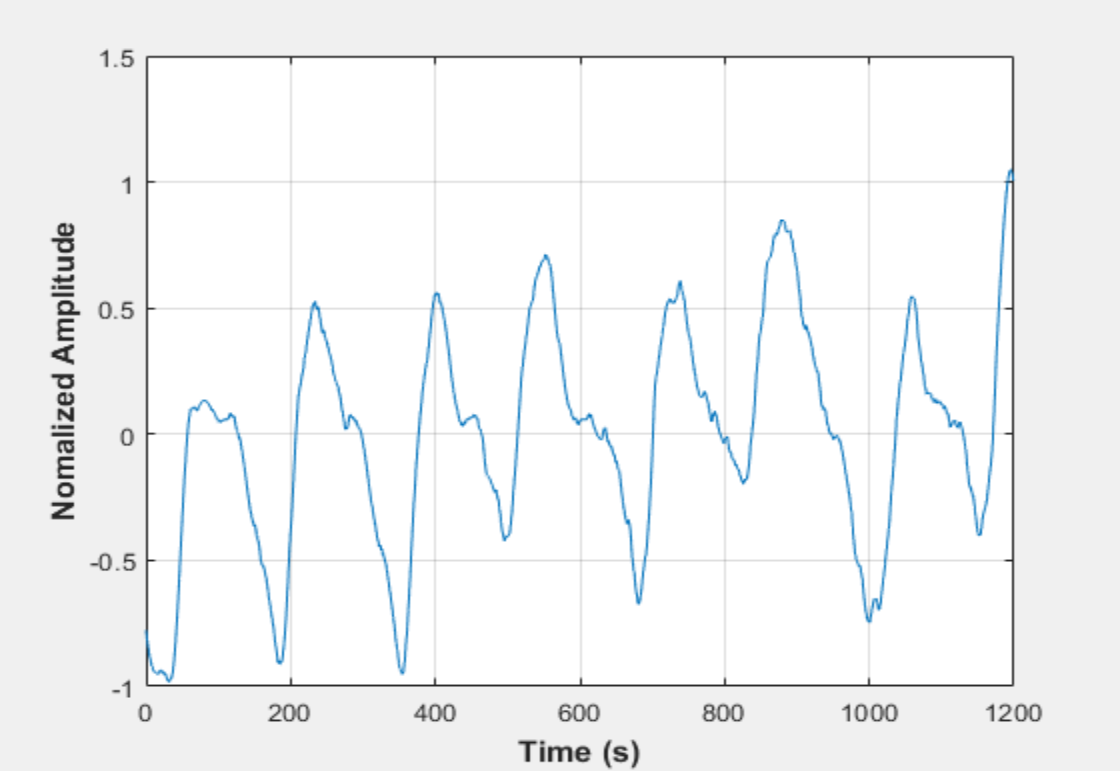


*Figure C-27: Pressure fluctuations in an empty vessel at 33 dm$^3$/minute gas flow rate- Test 3*

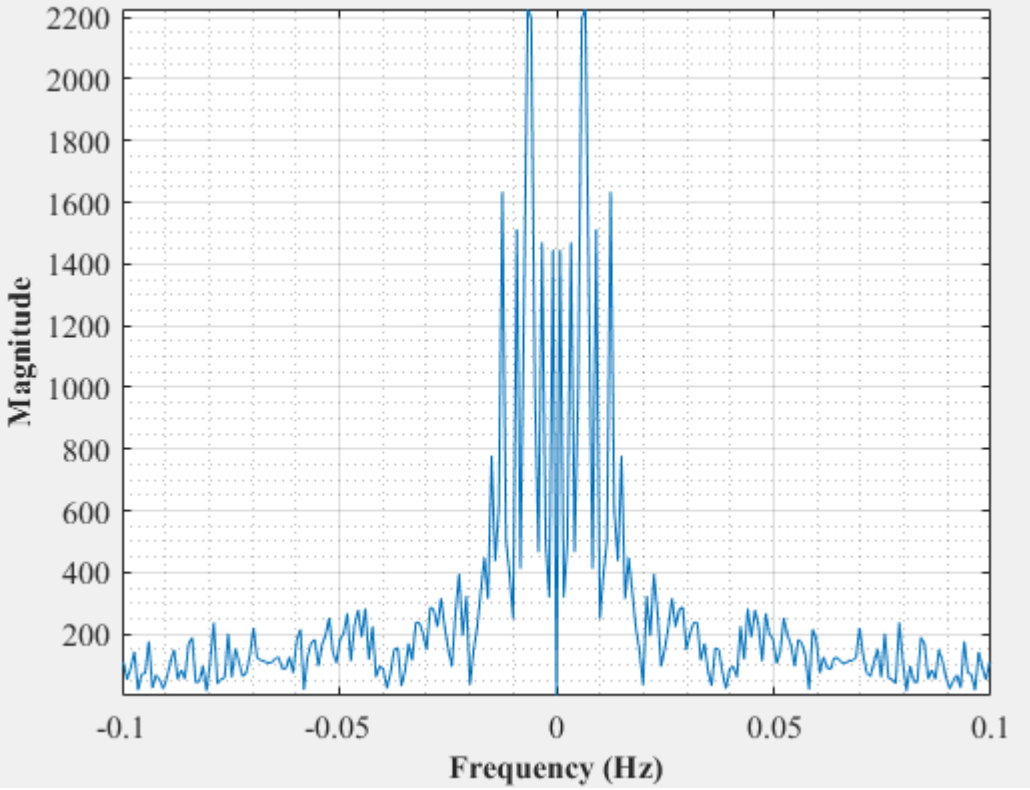


*Figure C-28: Dominant Frequency for an empty vessel at 33 dm$^3$/minute gas flow rate- Test 3*

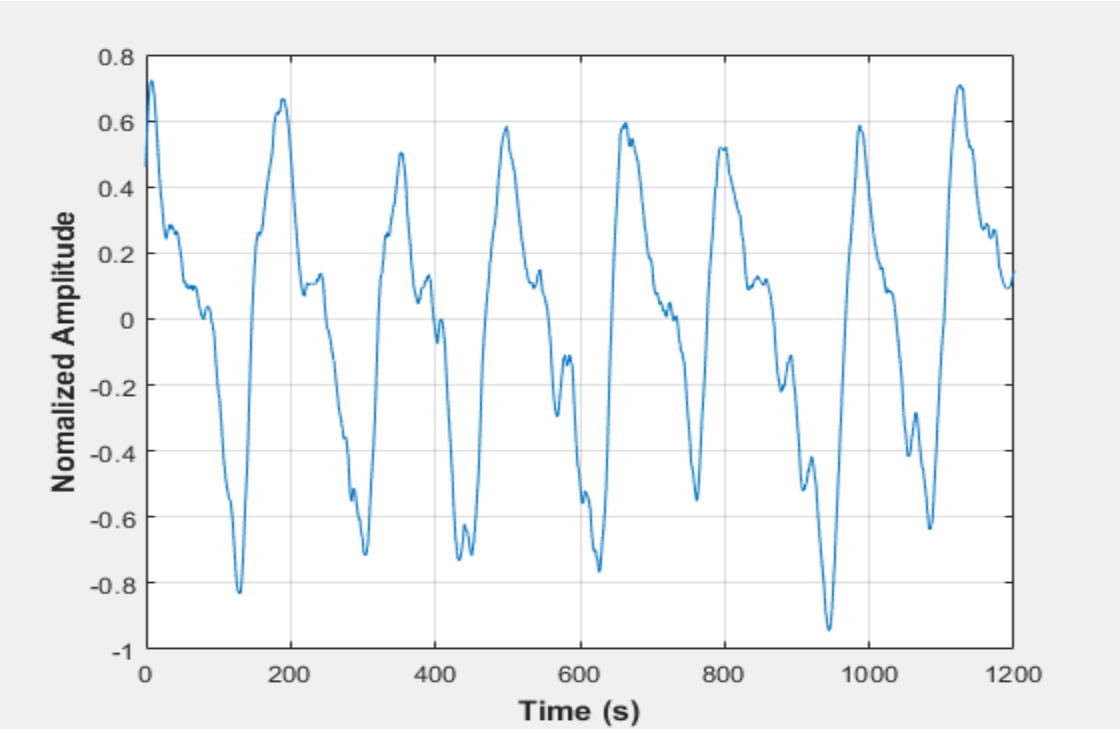


*Figure C-29: Pressure fluctuations in an empty vessel at 33 dm$^3$/minute gas flow rate- Test 4*

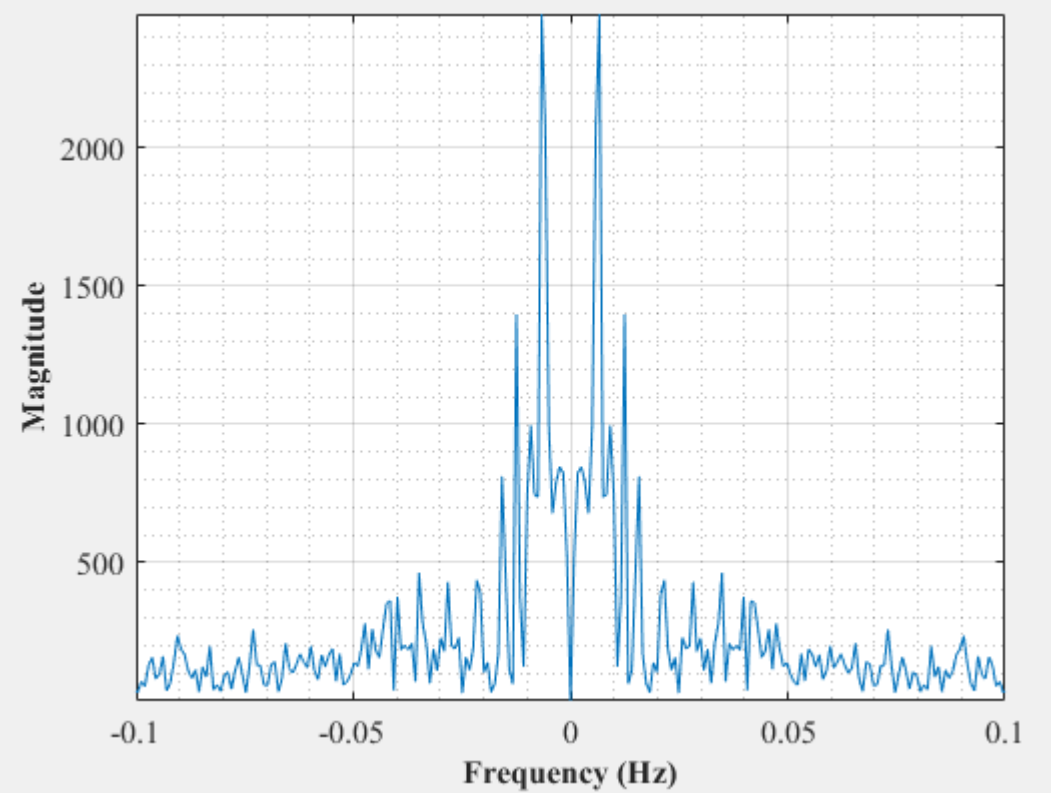


*Figure C-30: Dominant Frequency for an empty vessel at 33 dm$^3$/minute gas flow rate- Test 4*

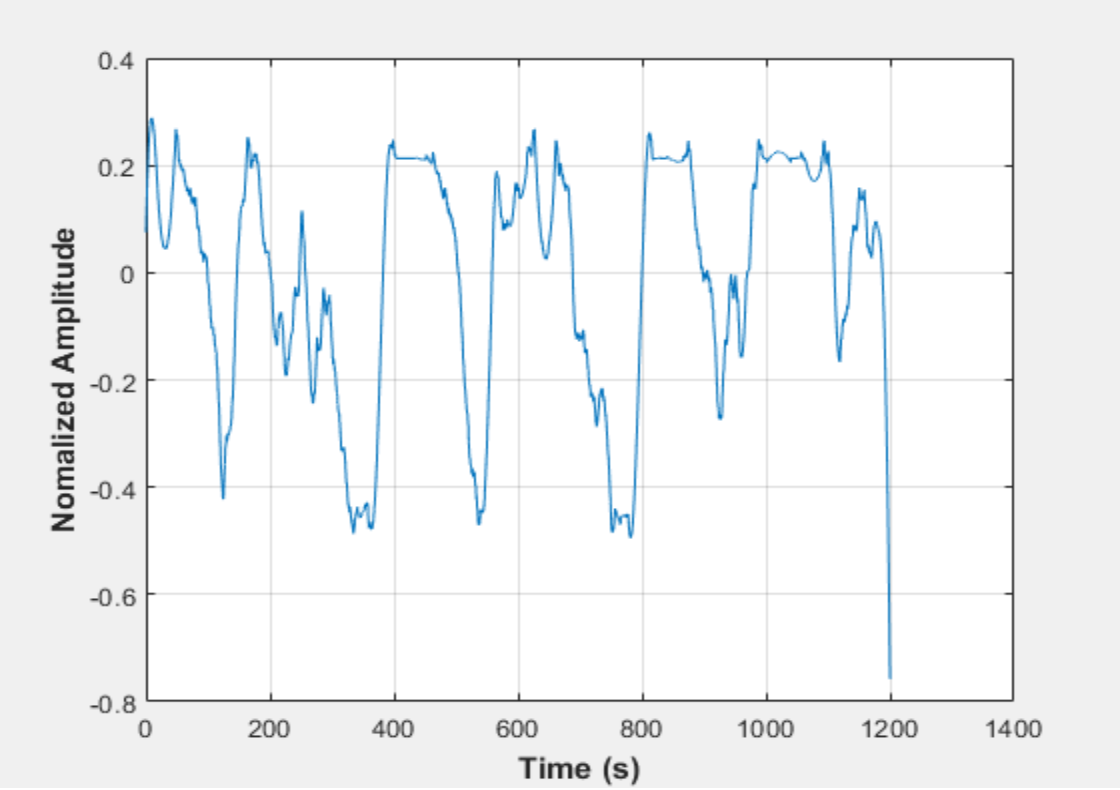


*Figure C-31: Pressure fluctuations in a uniformly packed vessel at 20 dm$^3$/minute gas flow rate- Test 1*

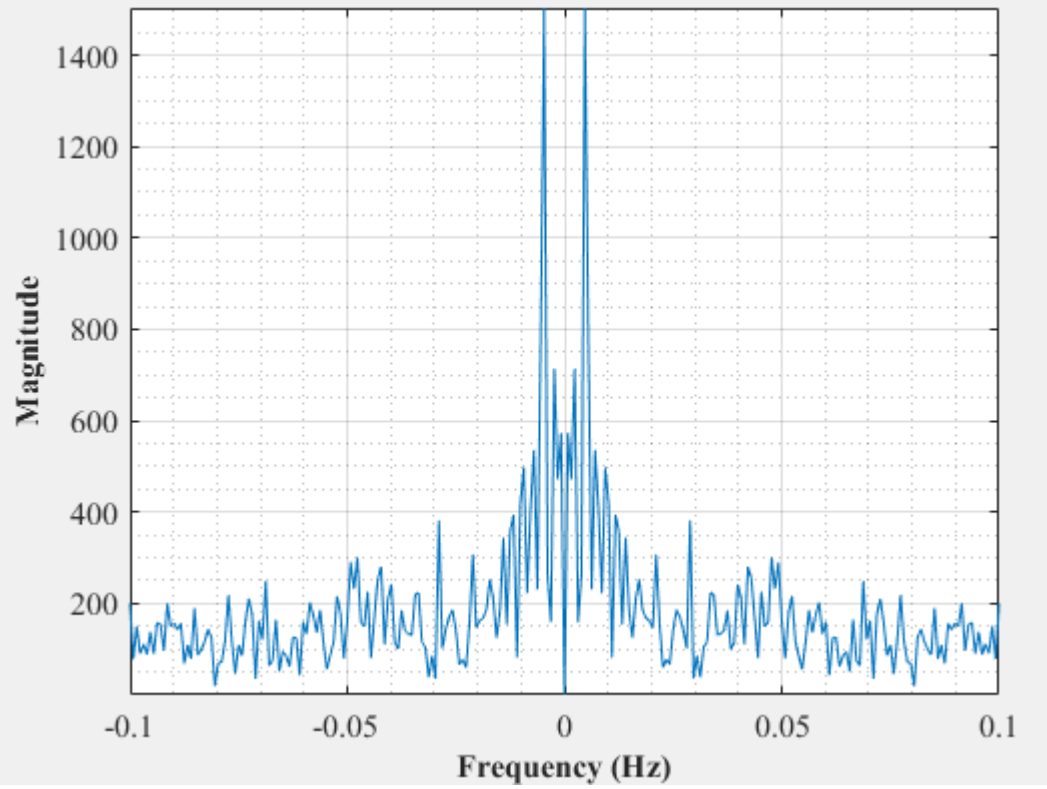


*Figure C-32: Dominant Frequency for a uniformly packed vessel at 20 dm$^3$/minute gas flow rate-Test 1*

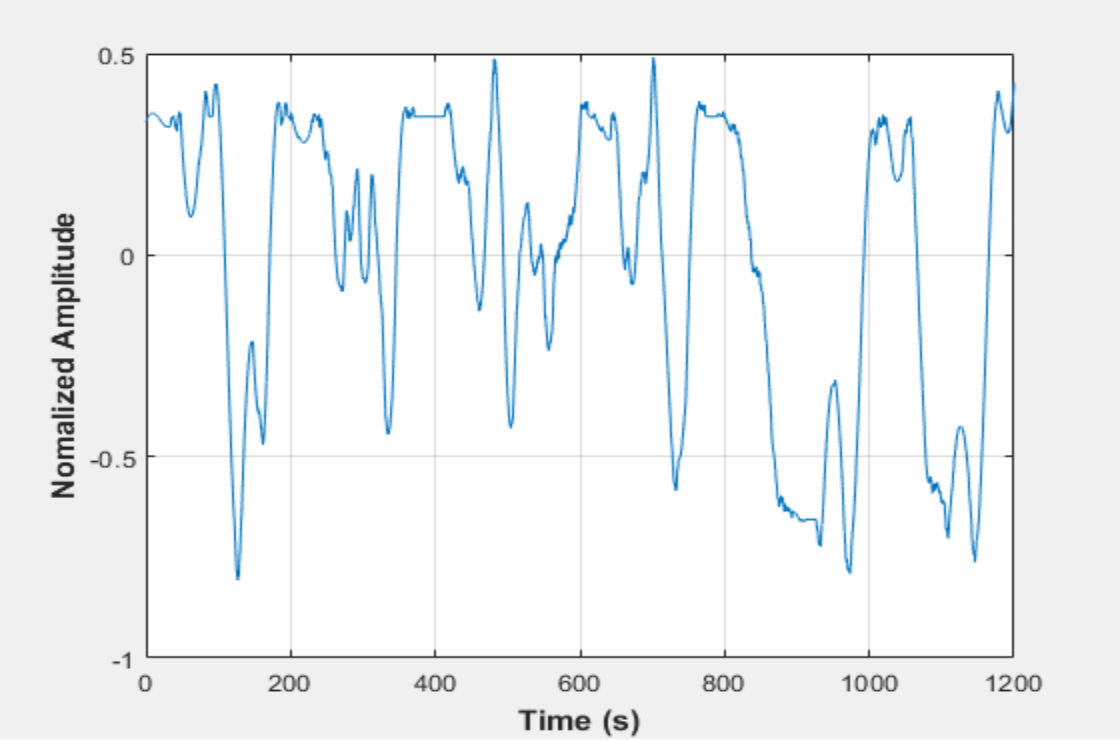


*Figure C-33: Pressure fluctuations in a uniformly packed vessel at 20 dm$^3$/minute gas flow rate- Test 2*

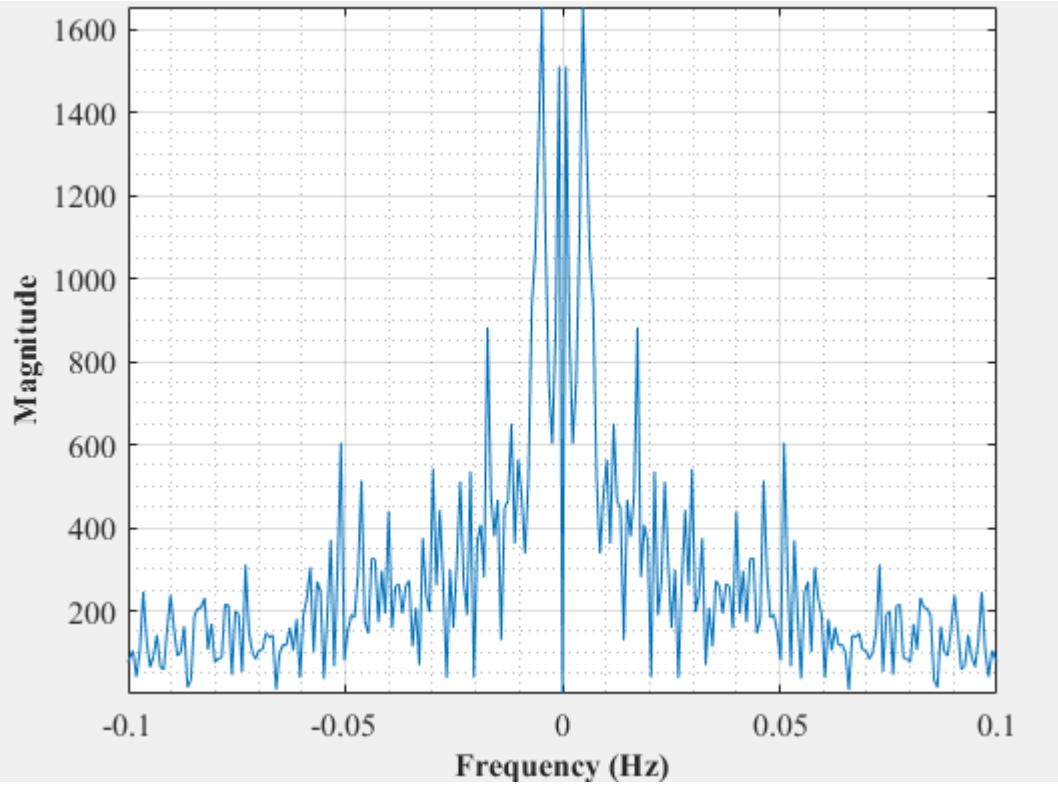


*Figure C-34: Dominant Frequency for a uniformly packed vessel at 20 dm$^3$/minute gas flow rate-Test 2*

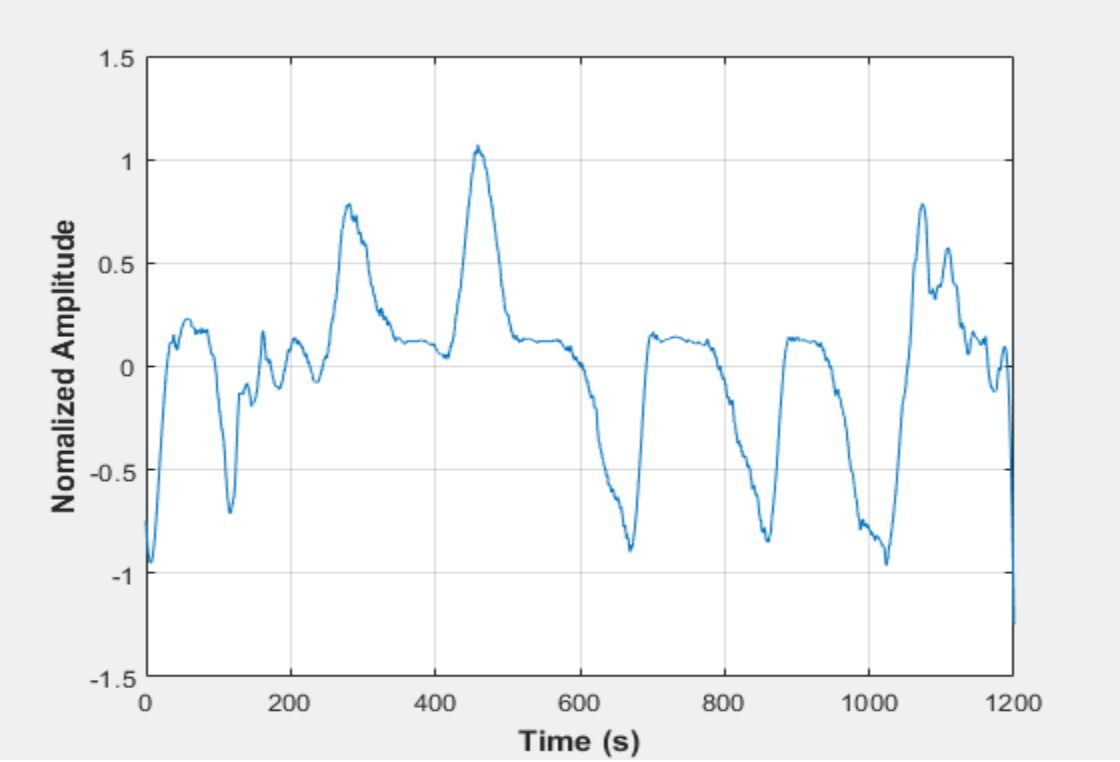


*Figure C-35: Pressure fluctuations in a uniformly packed vessel at 20 dm$^3$/minute gas flow rate- Test 3*

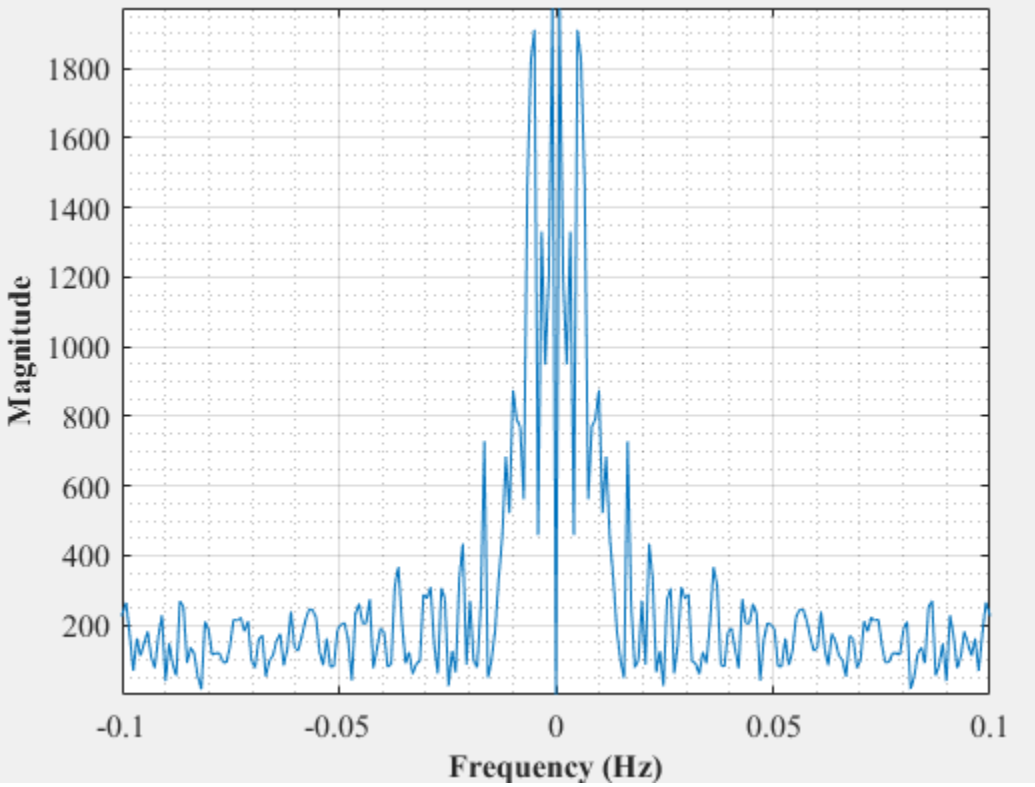


*Figure C-36: Dominant Frequency for a uniformly packed vessel at 20 dm$^3$/minute gas flow rate-Test 3*

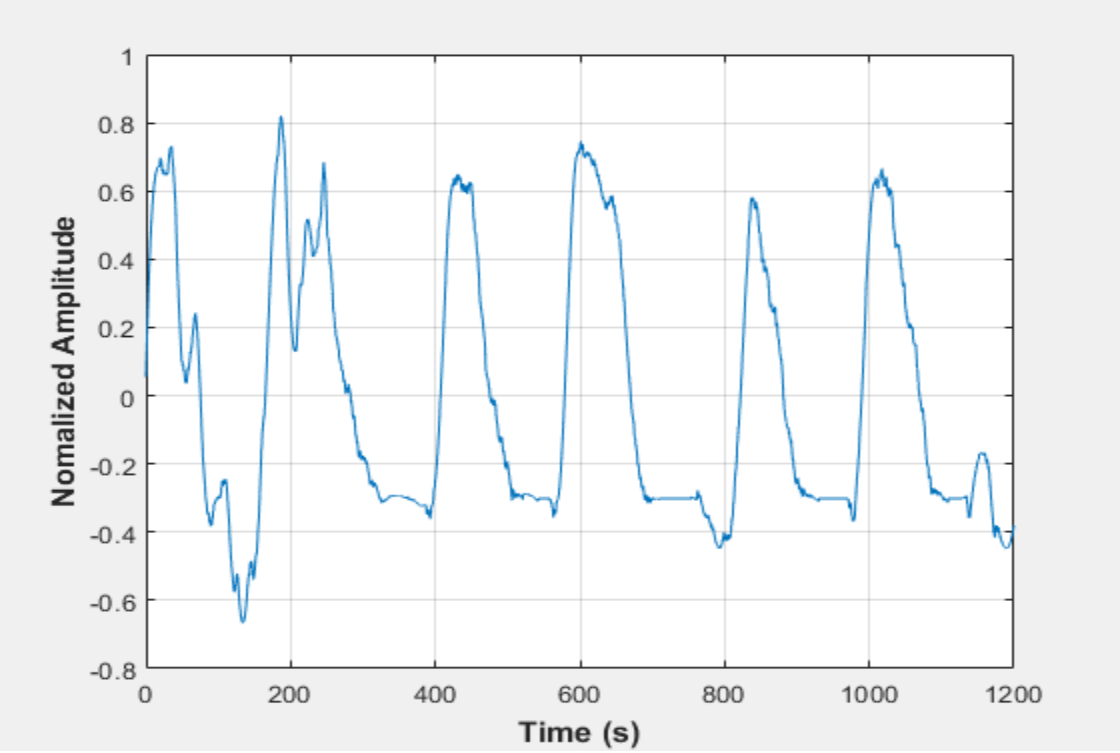


*Figure C-37: Pressure fluctuations in a uniformly packed vessel at 20 dm$^3$/minute gas flow rate- Test 4*

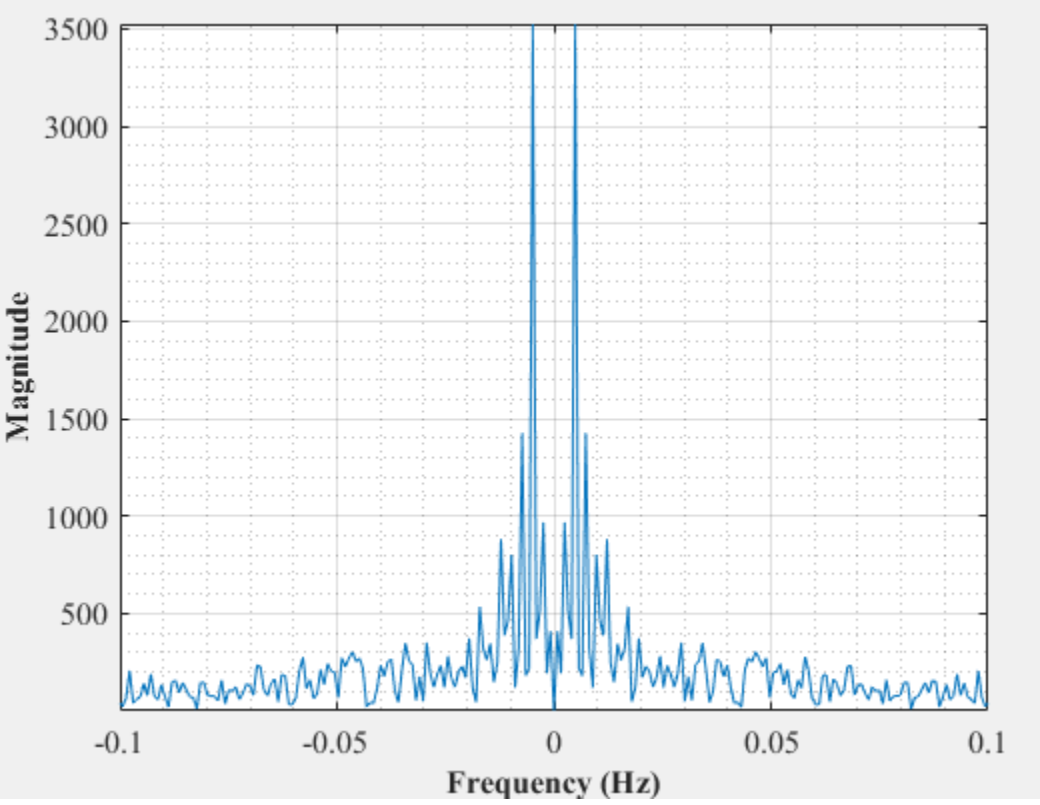


*Figure C-38: Dominant Frequency for a uniformly packed vessel at 20 dm$^3$/minute gas flow rate-Test 4*

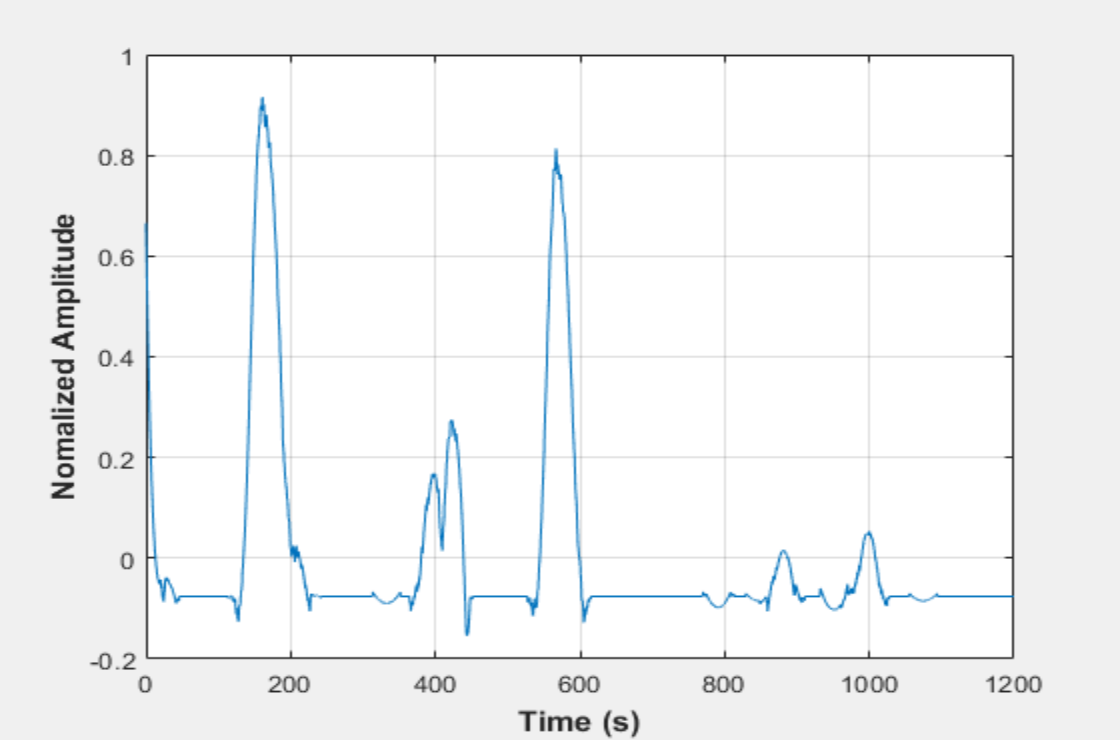


*Figure C-39: Pressure fluctuations in a uniformly packed vessel at 22.5 $dm^3$/minute gas flow rate- Test 1*

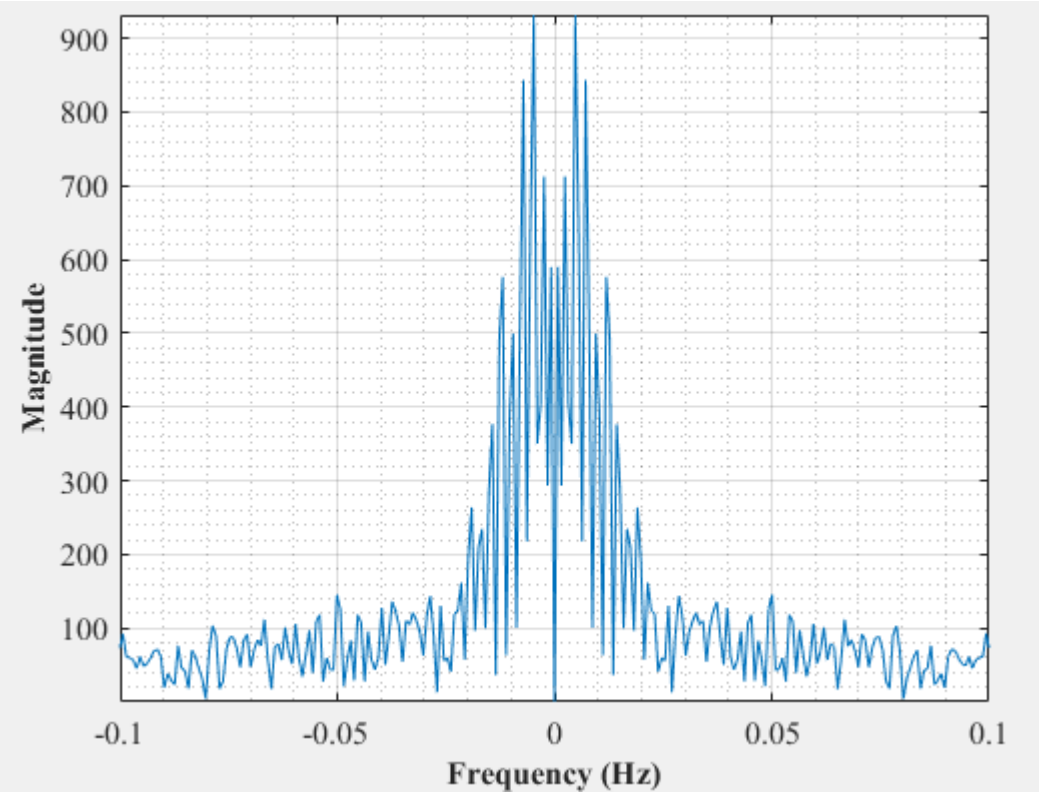


*Figure C-40: Dominant Frequency for a uniformly packed vessel at 22.5 $dm^3$/minute gas flow rate-Test 1*

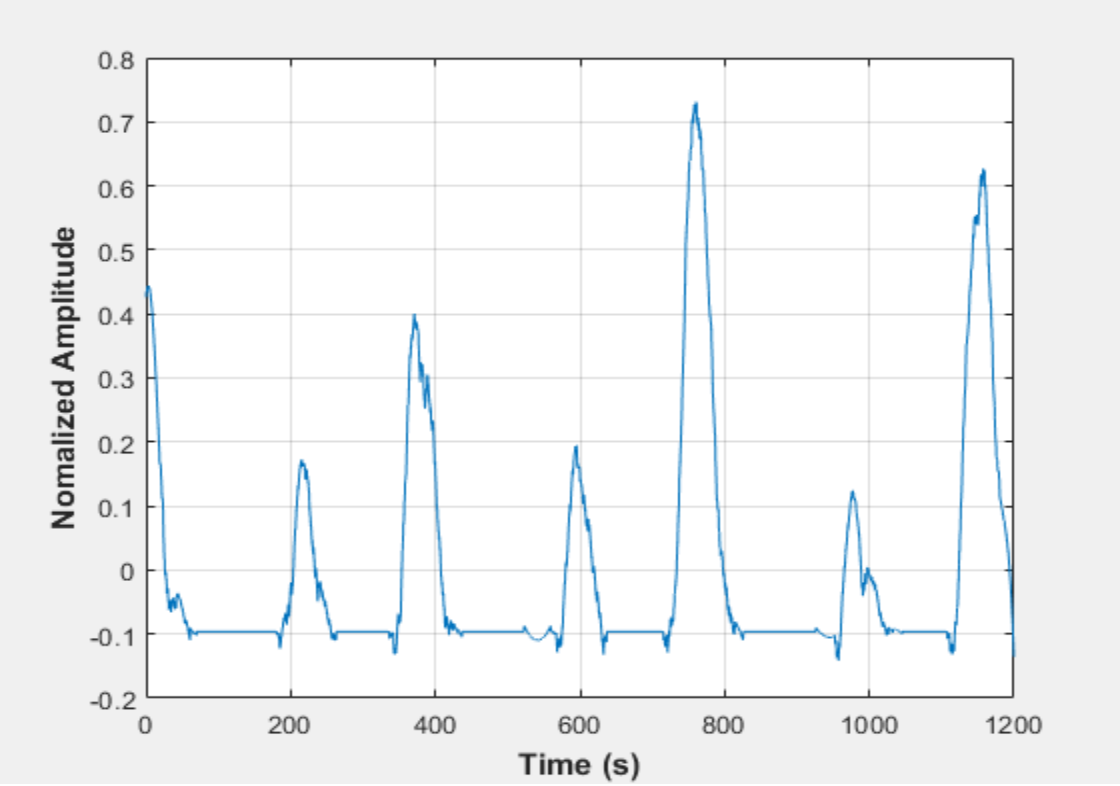


*Figure C-41: Pressure fluctuations in a uniformly packed vessel at 22.5 $dm^3$/minute gas flow rate- Test 2*

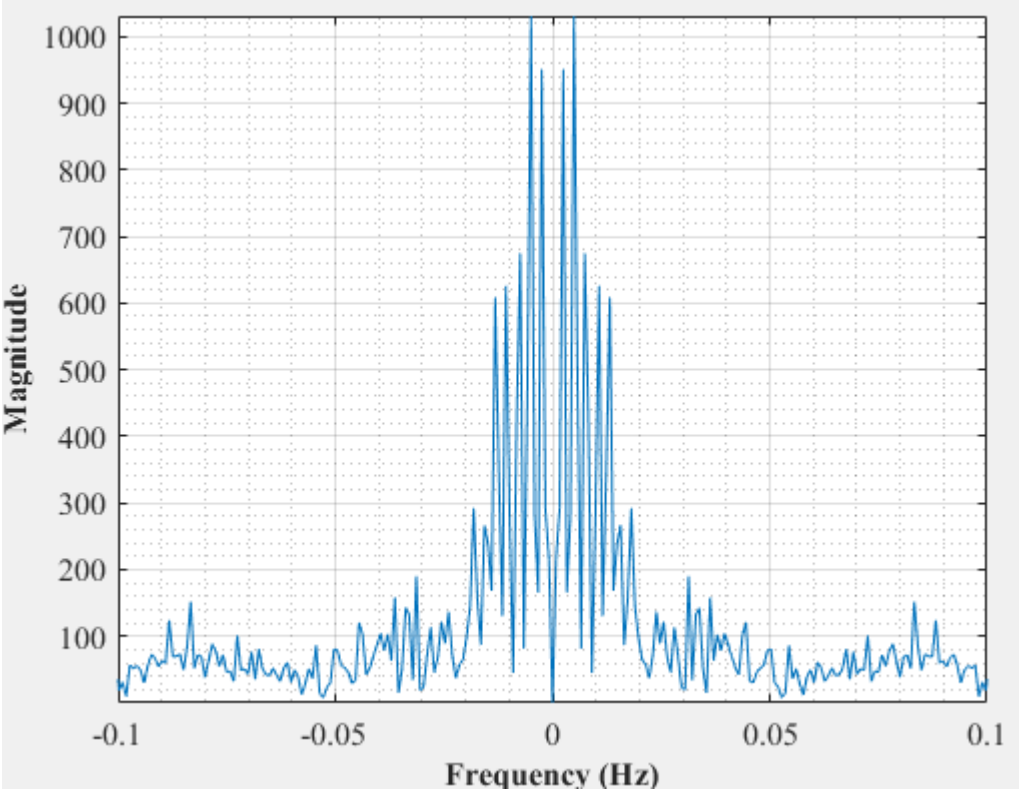


*Figure C-42: Dominant Frequency for a uniformly packed vessel at 22.5 $dm^3$/minute gas flow rate-Test 2*

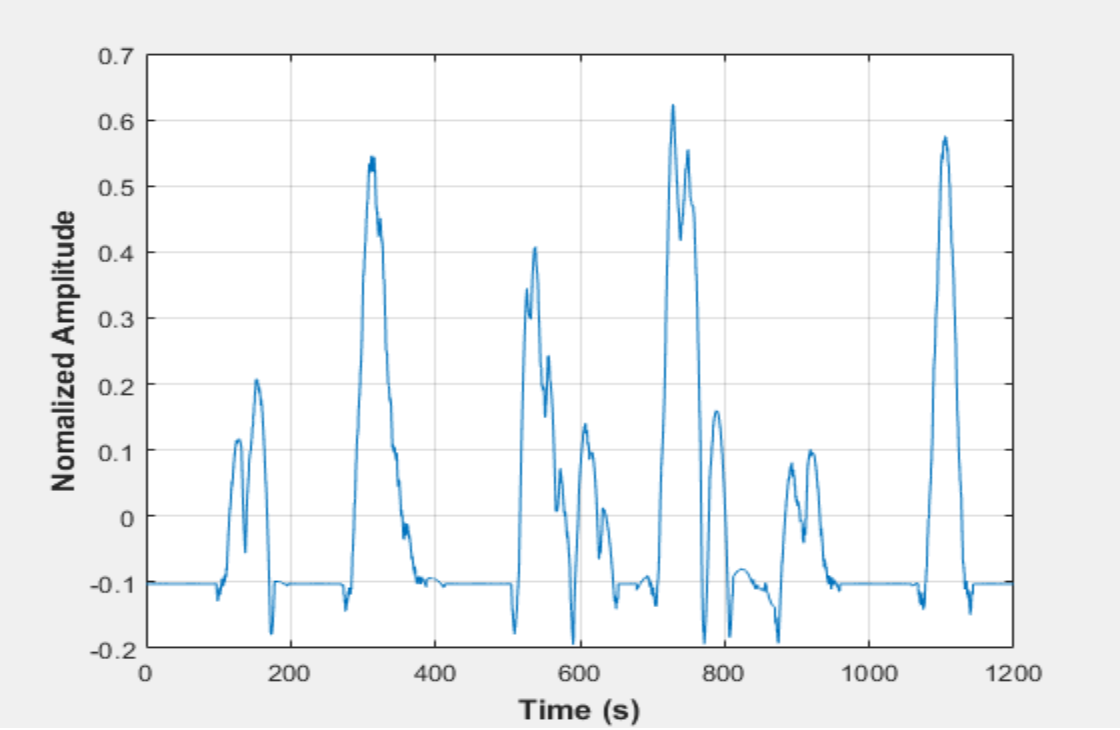


*Figure C-43: Pressure fluctuations in a uniformly packed vessel at 22.5 dm$^3$/minute gas flow rate- Test 3*

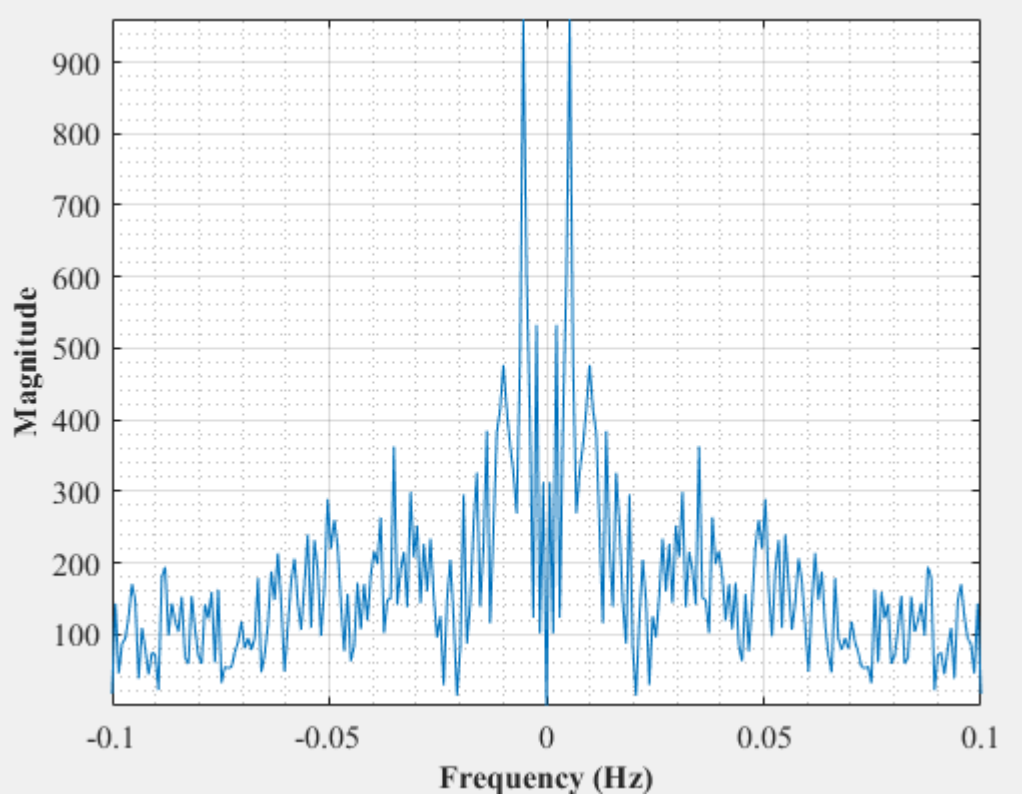


*Figure C-44: Dominant Frequency for a uniformly packed vessel at 22.5 dm$^3$/minute gas flow rate-Test 3*

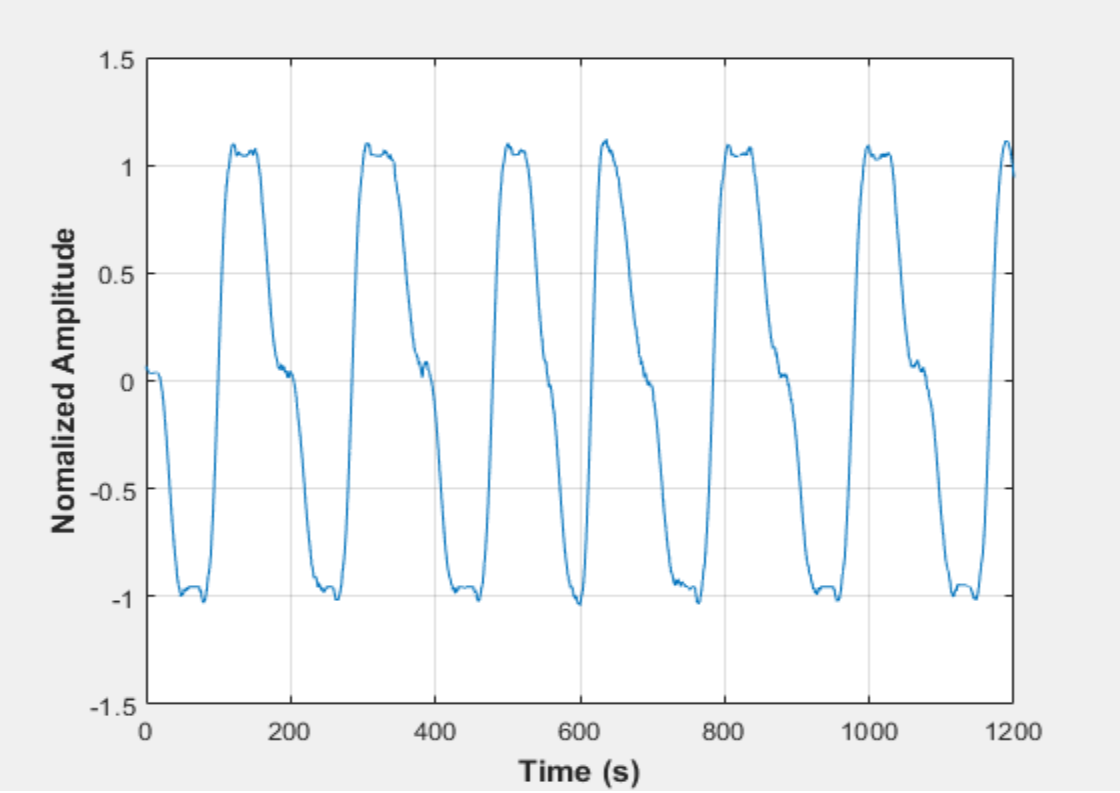


*Figure C-45: Pressure fluctuations in a uniformly packed vessel at 29 dm$^3$/minute gas flow rate- Test 1*

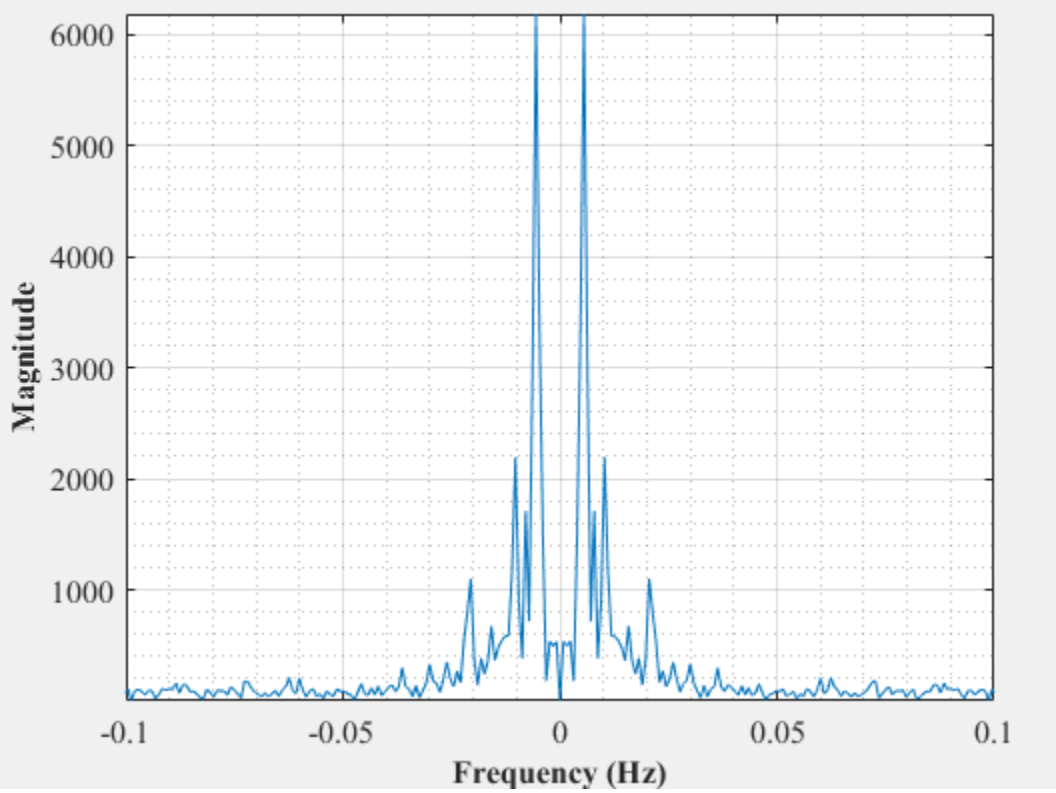


*Figure C-46: Dominant Frequency for a uniformly packed vessel at 29 dm$^3$/minute gas flow rate-Test 1*

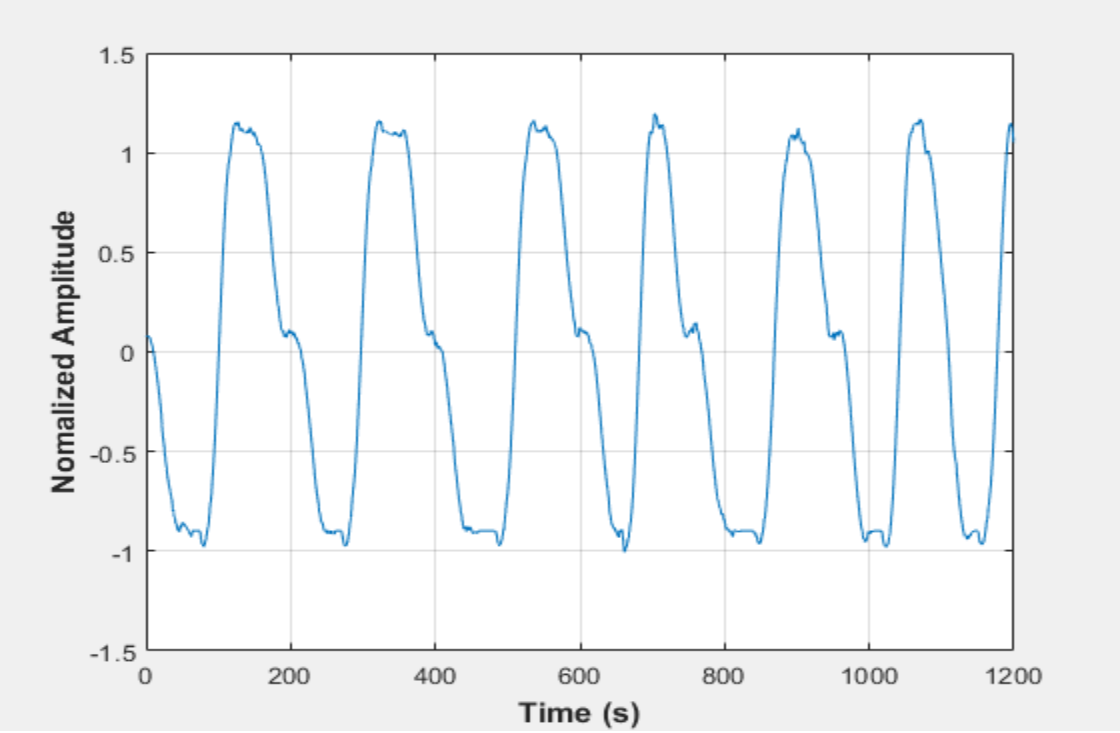


*Figure C-47: Pressure fluctuations in a uniformly packed vessel at 29 dm$^3$/minute gas flow rate- Test 2*

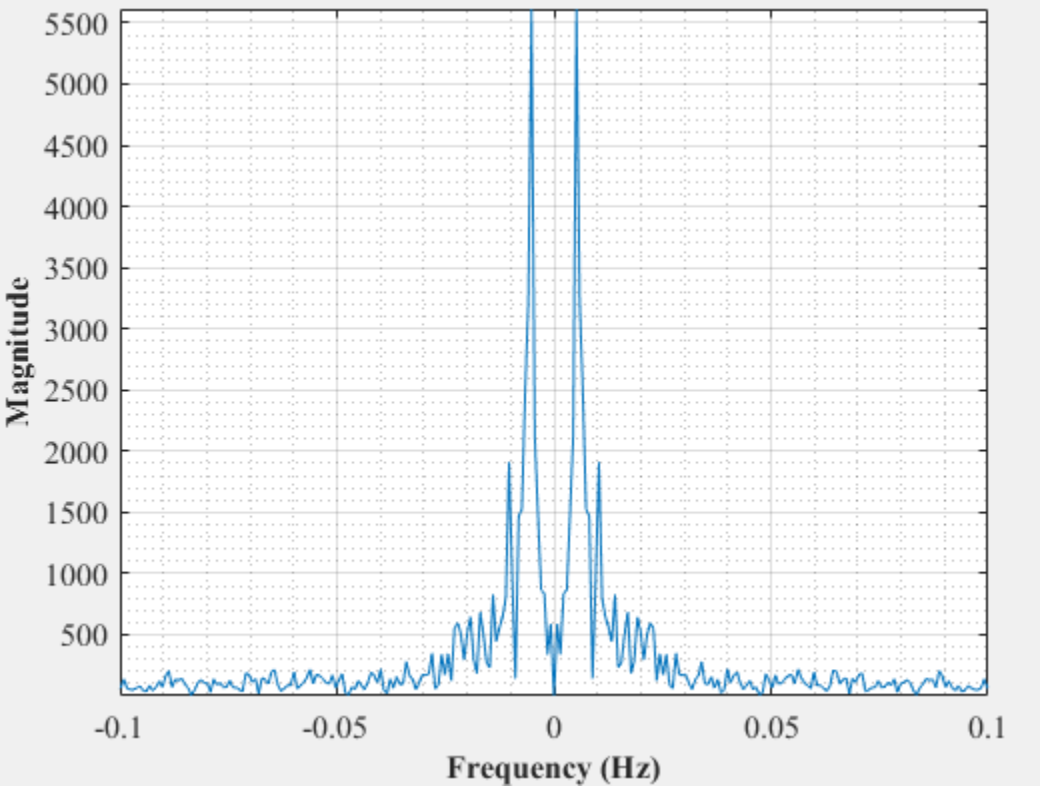


*Figure C-48: Dominant Frequency for a uniformly packed vessel at 29 dm$^3$/minute gas flow rate-Test 2*

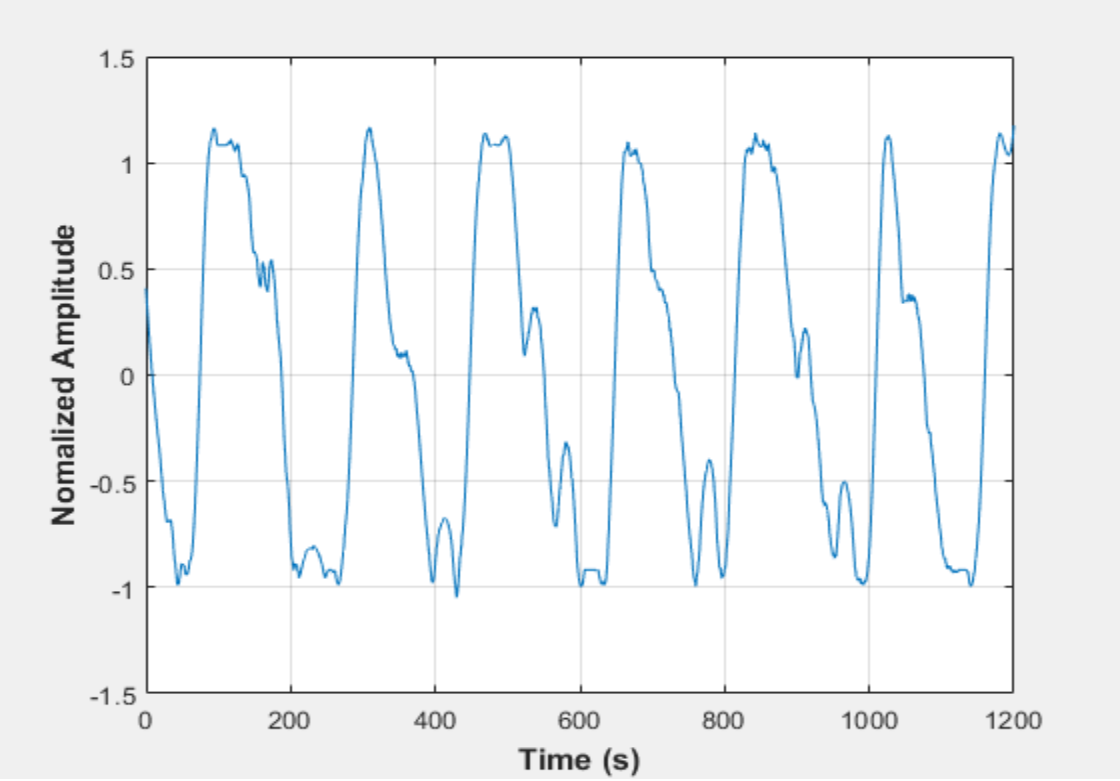


*Figure C-49: Pressure fluctuations in a uniformly packed vessel at 29 $dm^3$/minute gas flow rate- Test 3*

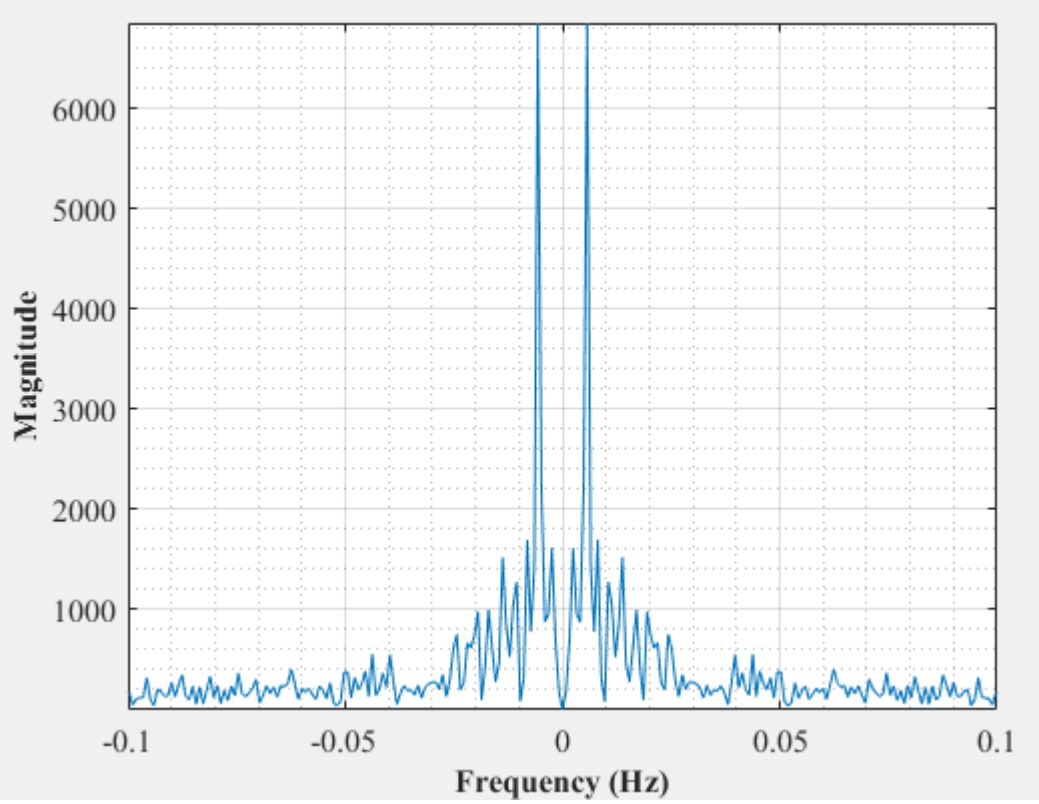


*Figure C-50: Dominant Frequency for a uniformly packed vessel at 29 $dm^3$/minute gas flow rate-Test 3*

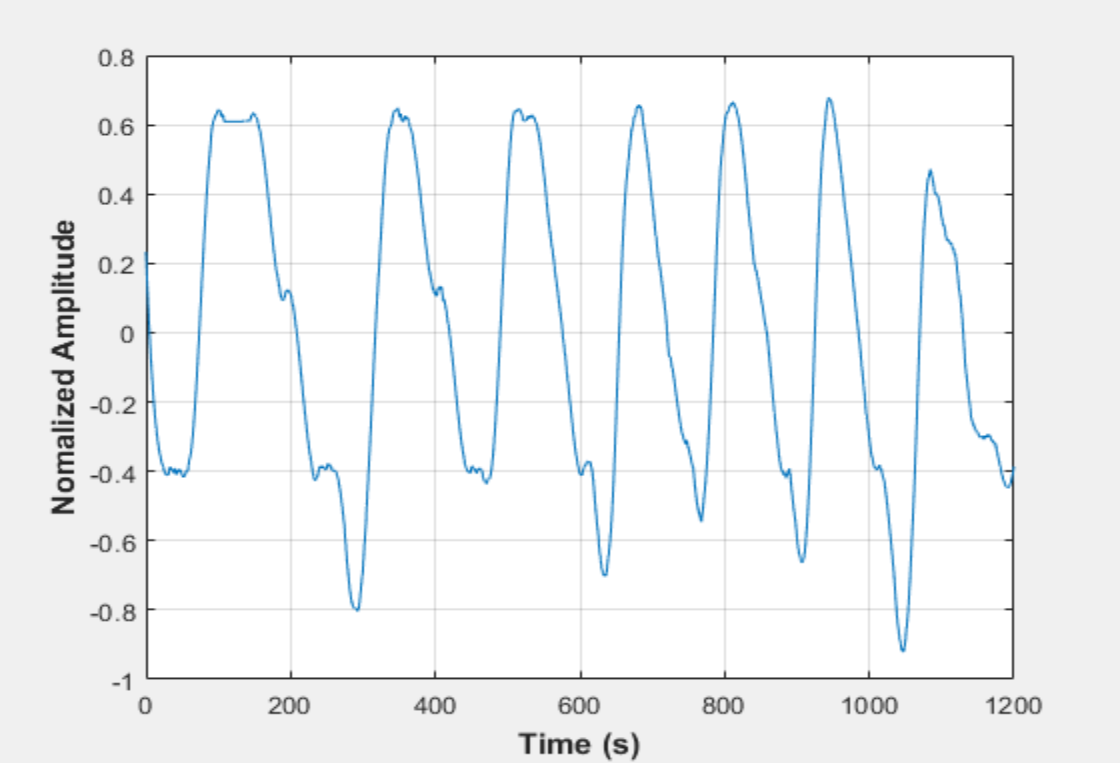


*Figure C-51: Pressure fluctuations in a uniformly packed vessel at 33 dm$^3$/minute gas flow rate- Test 1*

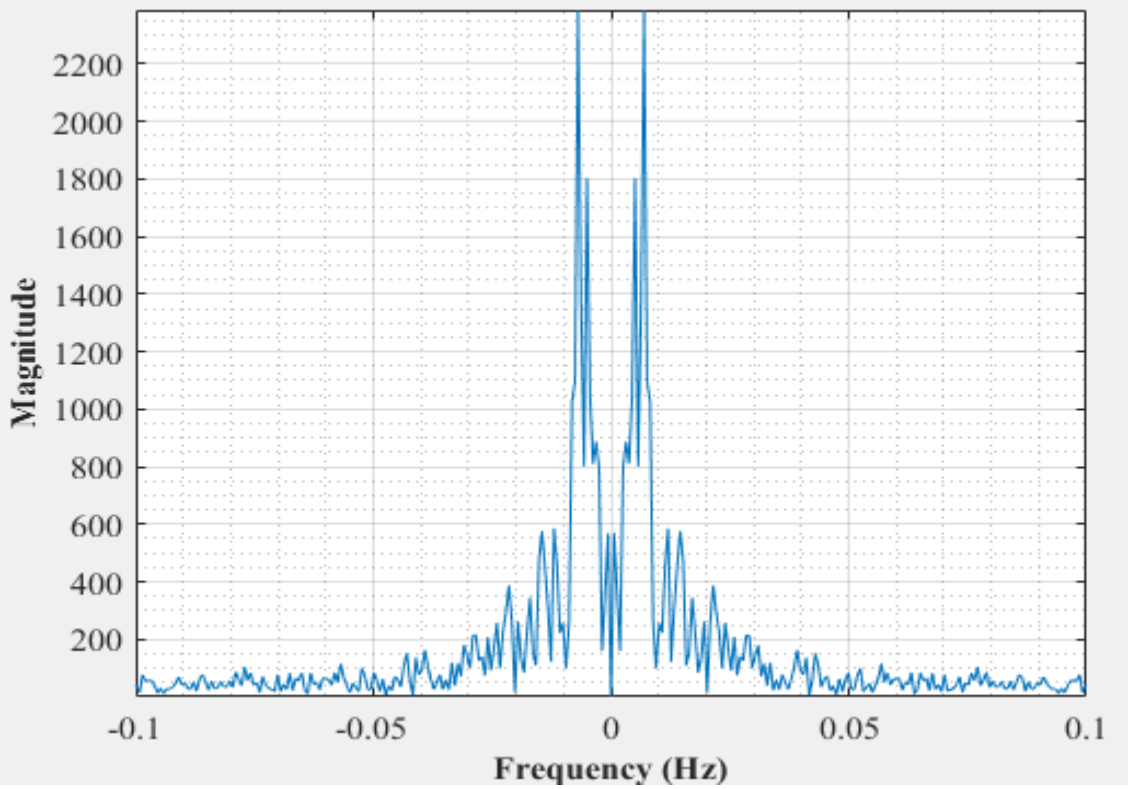


*Figure C-52: Dominant Frequency for a uniformly packed vessel at 33 dm$^3$/minute gas flow rate-Test 1*

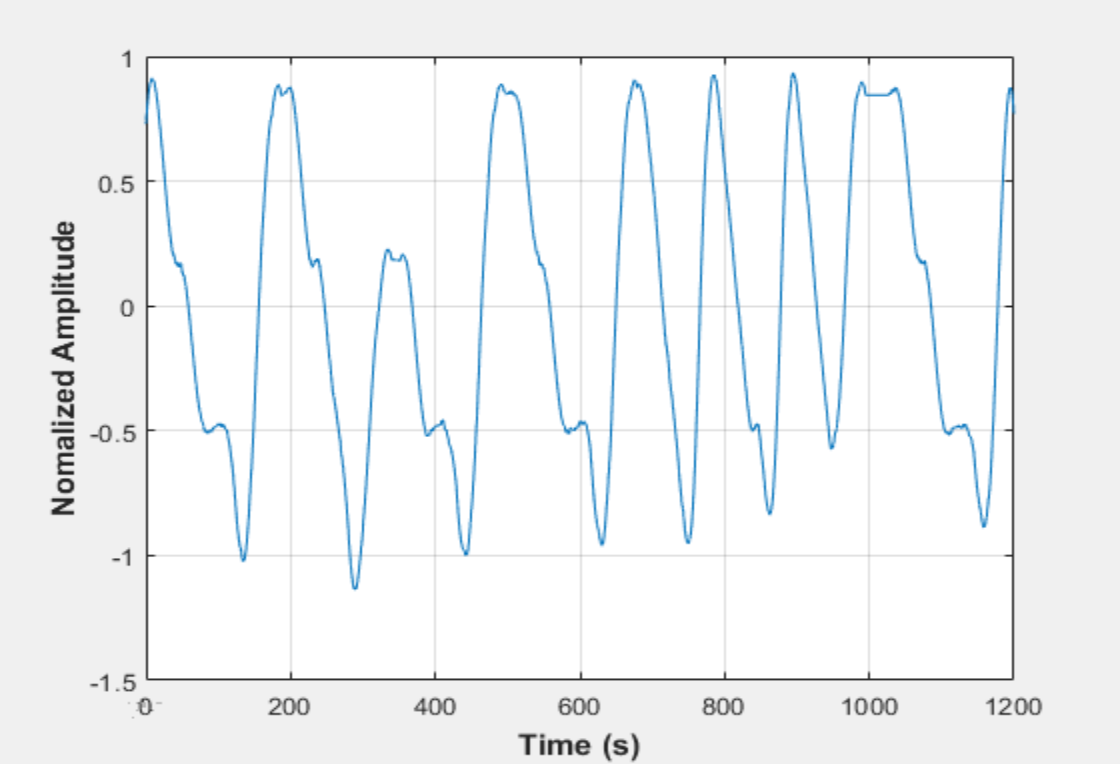


*Figure C-53: Pressure fluctuations in a uniformly packed vessel at 33 dm$^3$/minute gas flow rate- Test 2*

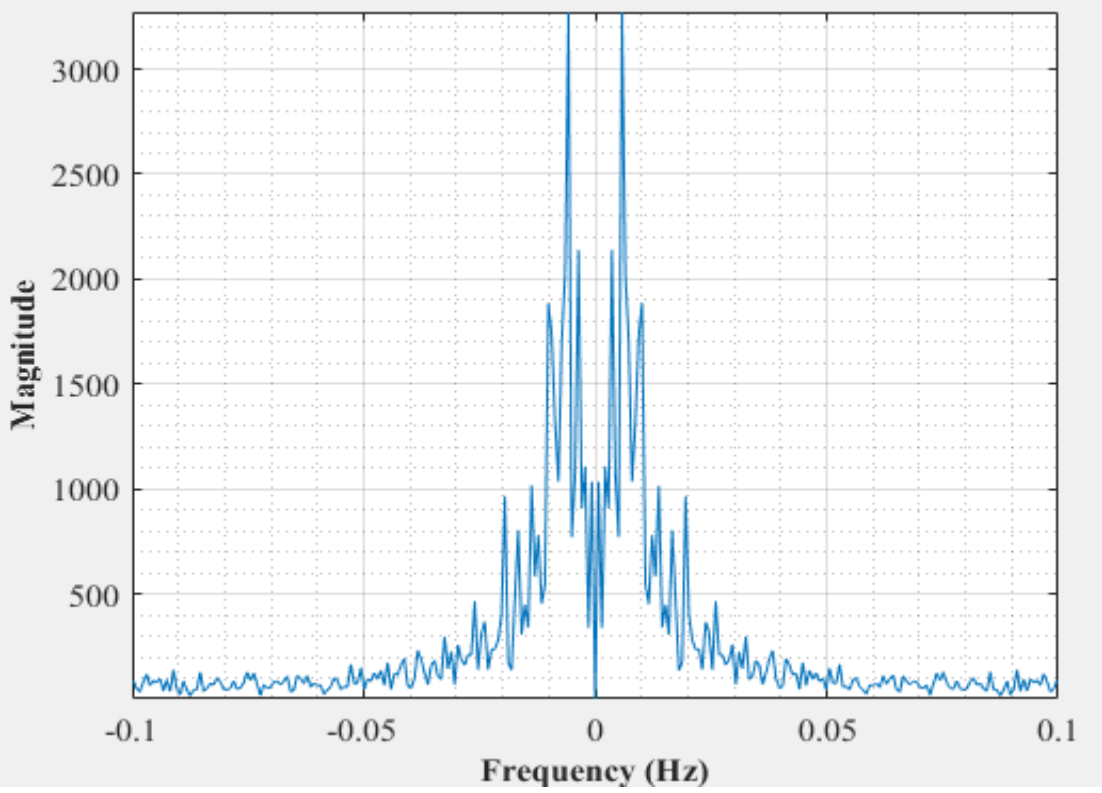


*Figure C-54: Dominant Frequency for a uniformly packed vessel at 33 dm$^3$/minute gas flow rate-Test 2*

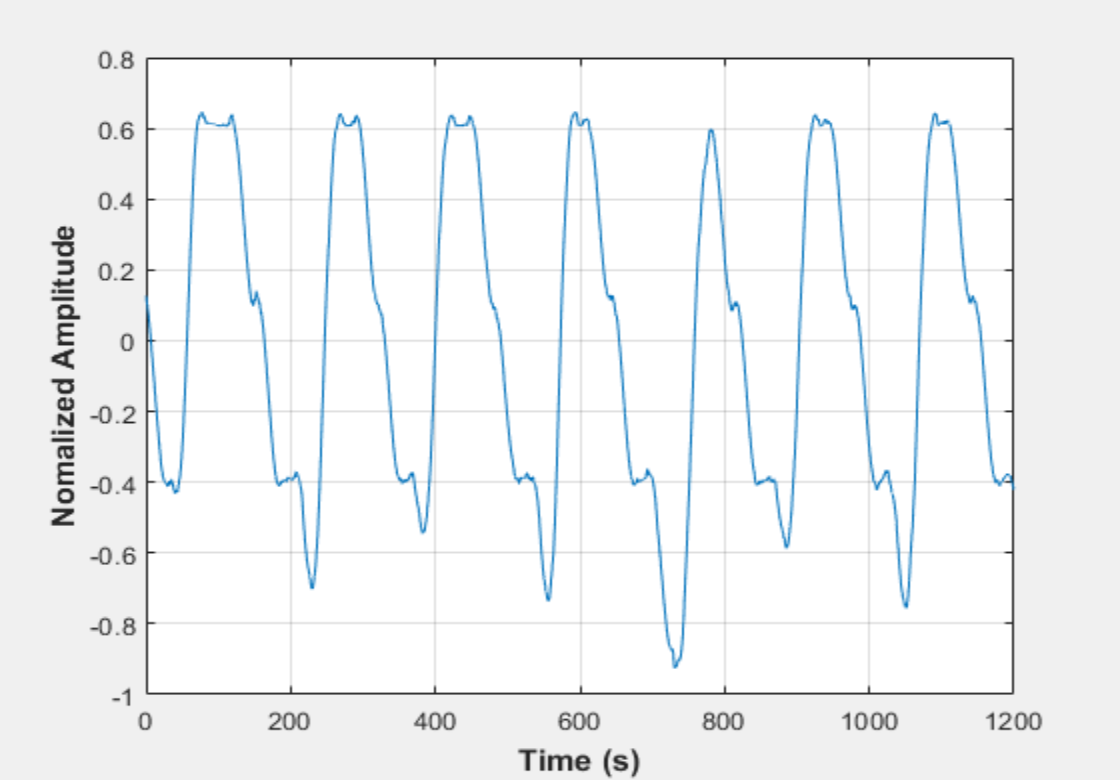


*Figure C-55: Pressure fluctuations in a uniformly packed vessel at 33 dm$^3$/minute gas flow rate- Test 3*

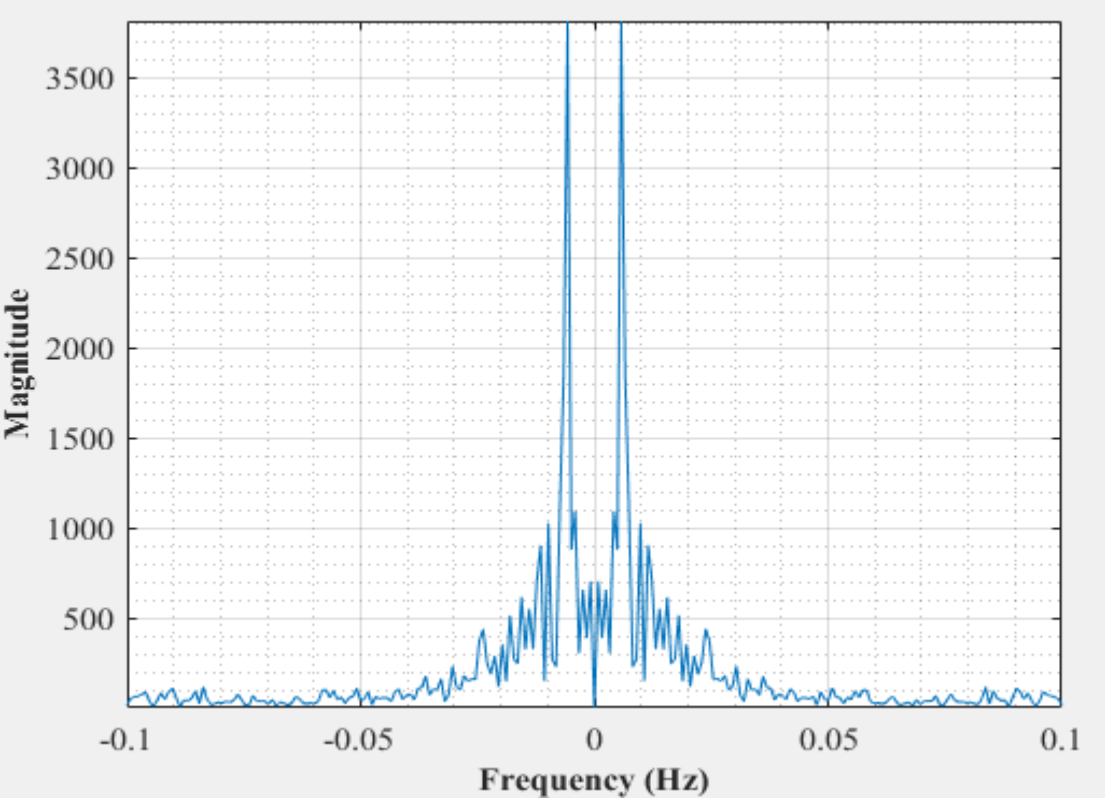


*Figure C-56: Dominant Frequency for a uniformly packed vessel at 33 dm$^3$/minute gas flow rate-Test 3*

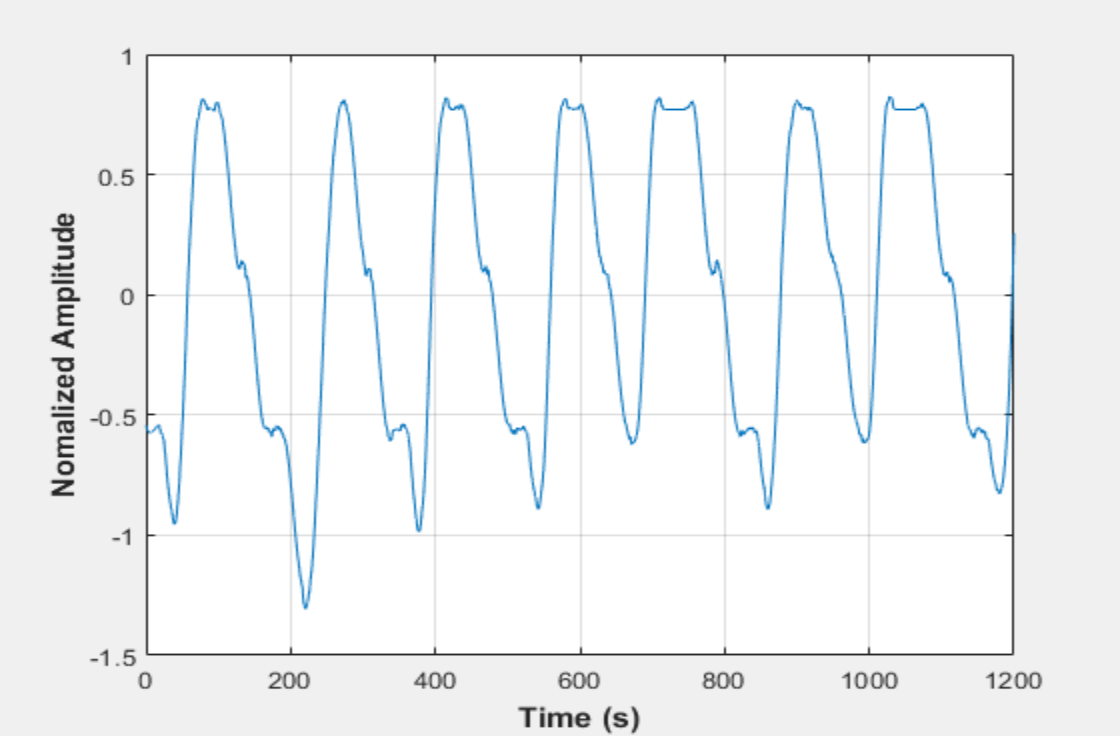


*Figure C-57: Pressure fluctuations in a uniformly packed vessel at 33 dm$^3$/minute gas flow rate- Test 4*

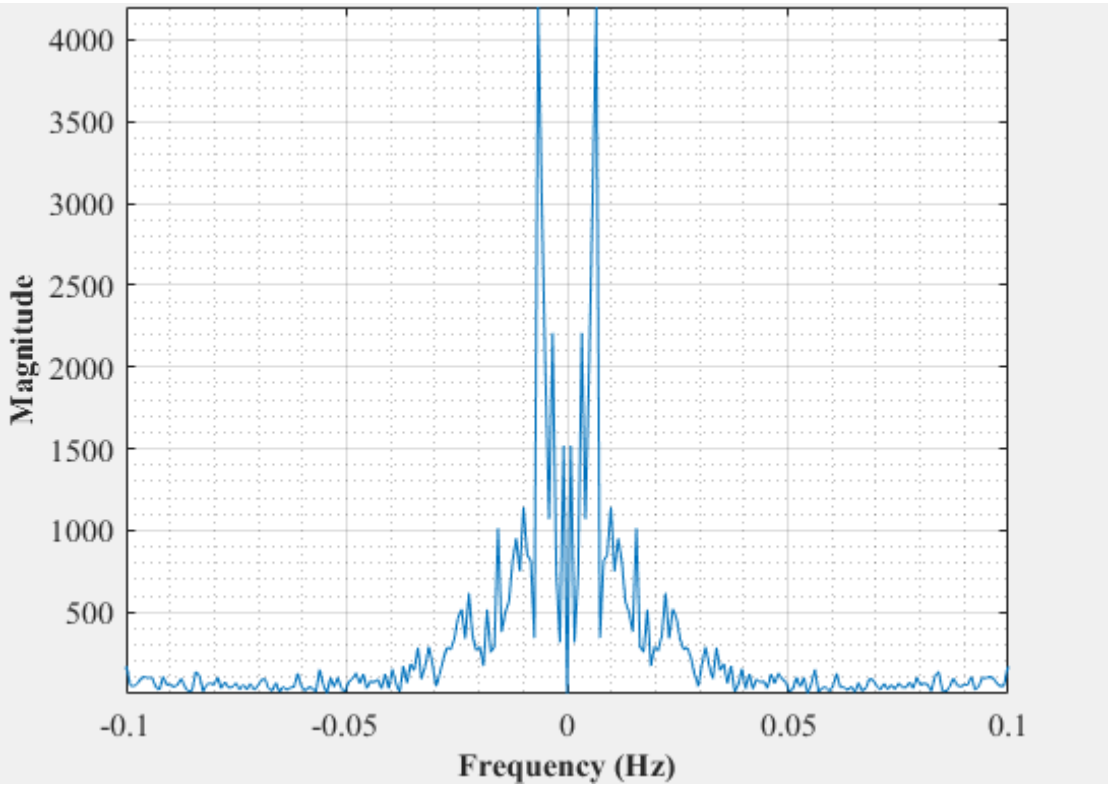


*Figure C-58: Dominant Frequency for a uniformly packed vessel at 33 dm$^3$/minute gas flow rate-Test 4*

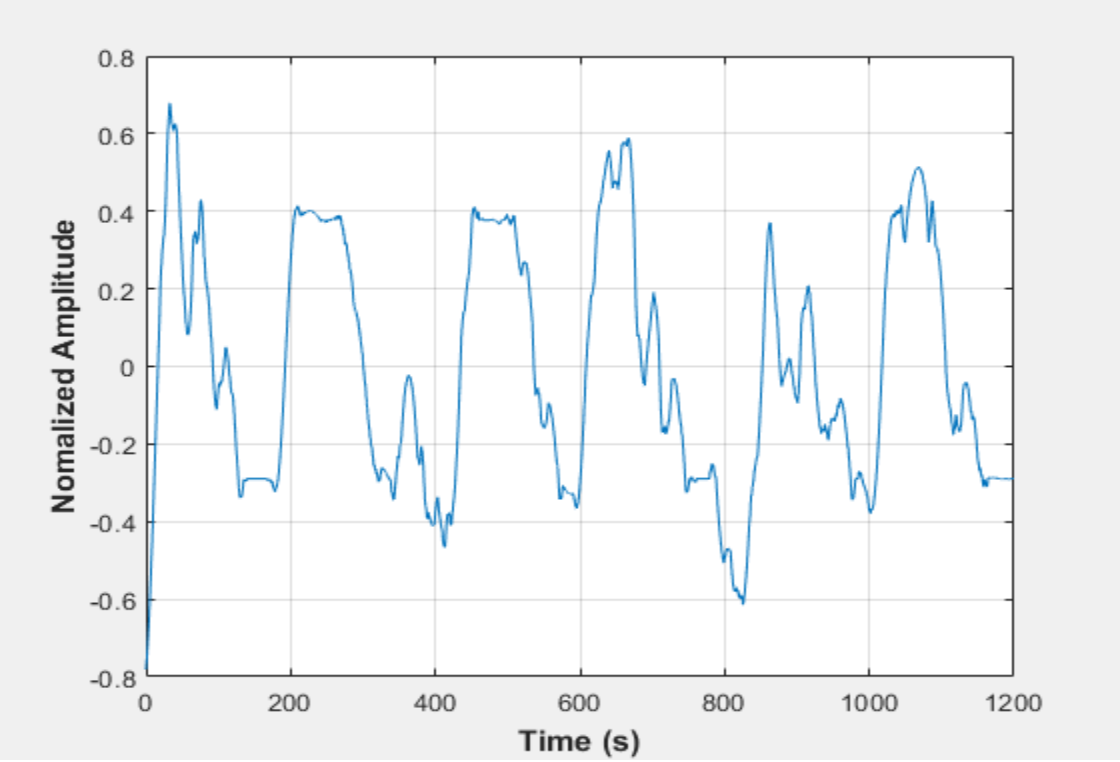


*Figure C-59: Pressure fluctuations in a non-uniformly packed vessel (large and small at the center) at 20 dm$^3$/minute gas flow rate- Test 1*

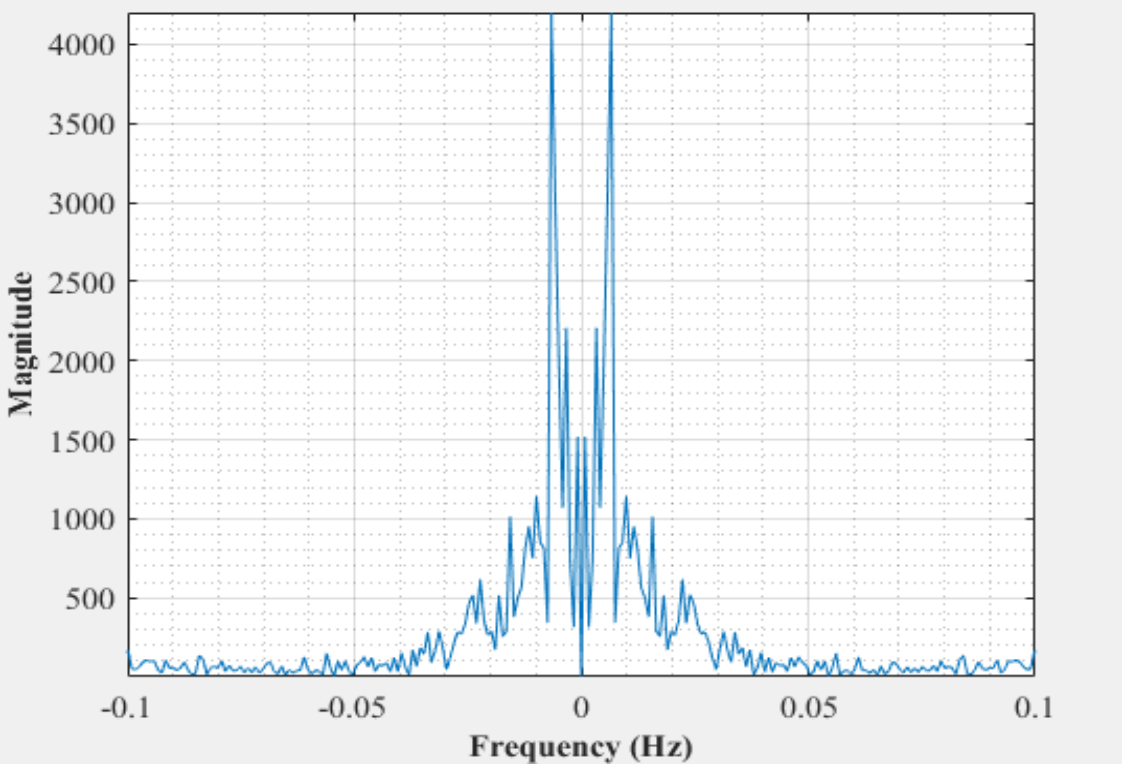


*Figure C-60: Dominant Frequency for a non-uniformly packed vessel (large and small at the center) at 20 dm$^3$/minute gas flow rate- Test 1*

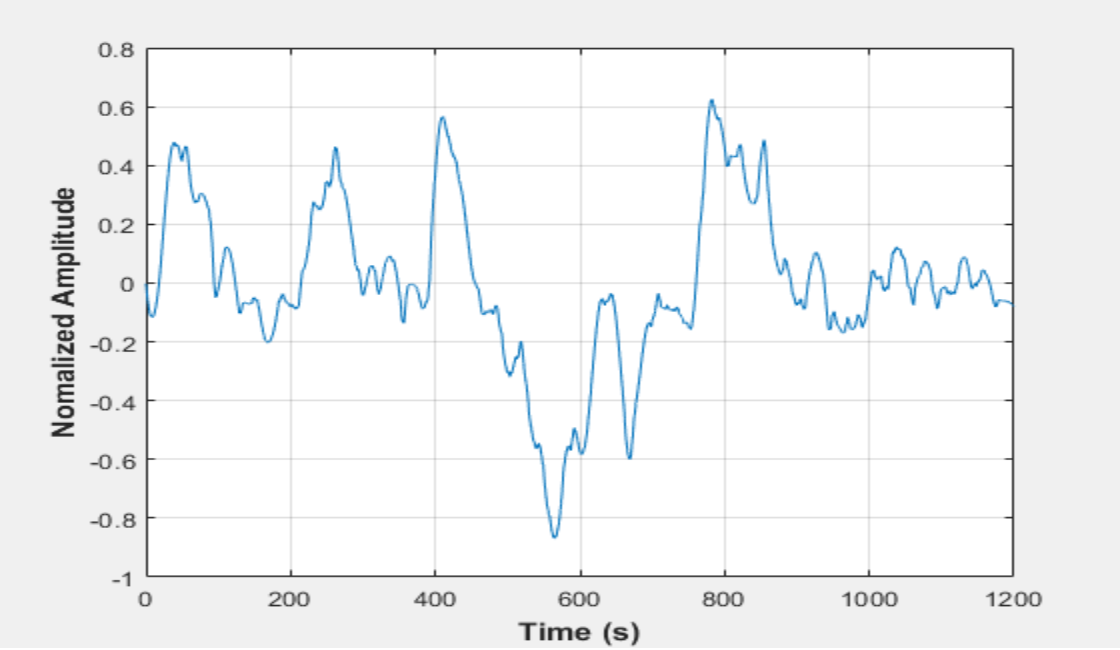


*Figure C-61: Pressure fluctuations in a non-uniformly packed vessel (large and small at the center) at 20 dm$^3$/minute gas flow rate- Test 2*

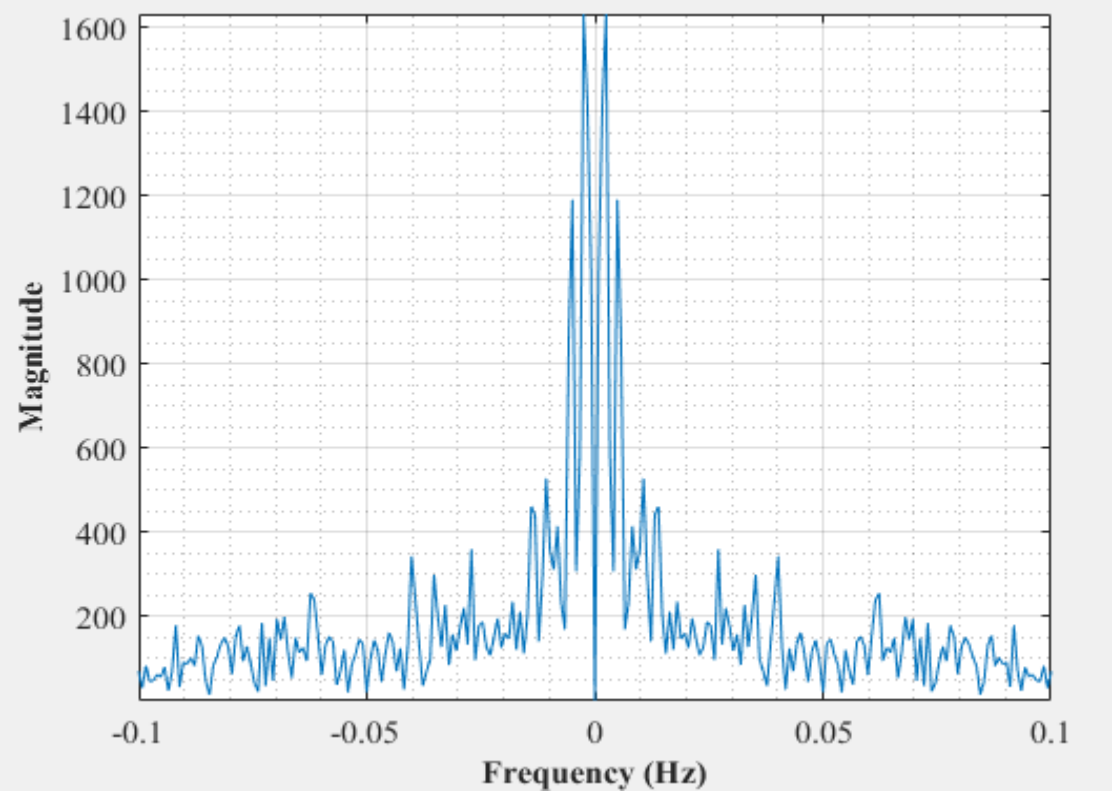


*Figure C-62: Dominant Frequency for a non-uniformly packed vessel (large and small at the center) at 20 dm$^3$/minute gas flow rate- Test 2*

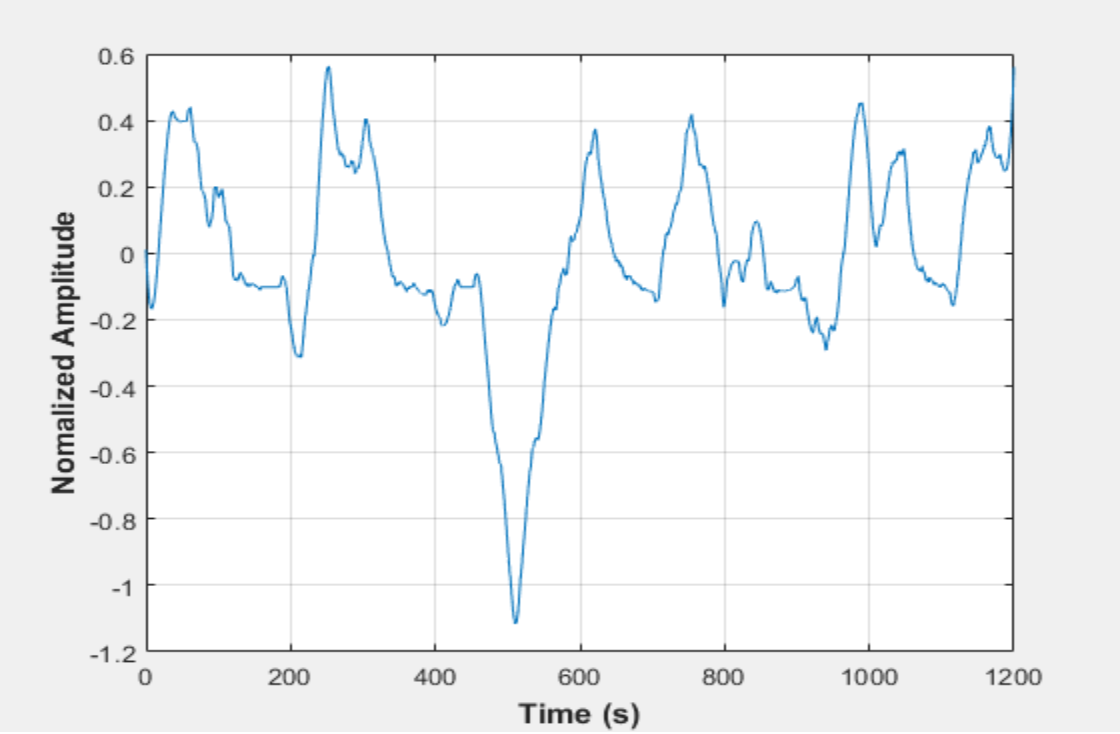


*Figure C-63: Pressure fluctuations in a non-uniformly packed vessel (large and small at the center) at 20 dm$^3$/minute gas flow rate- Test 3*

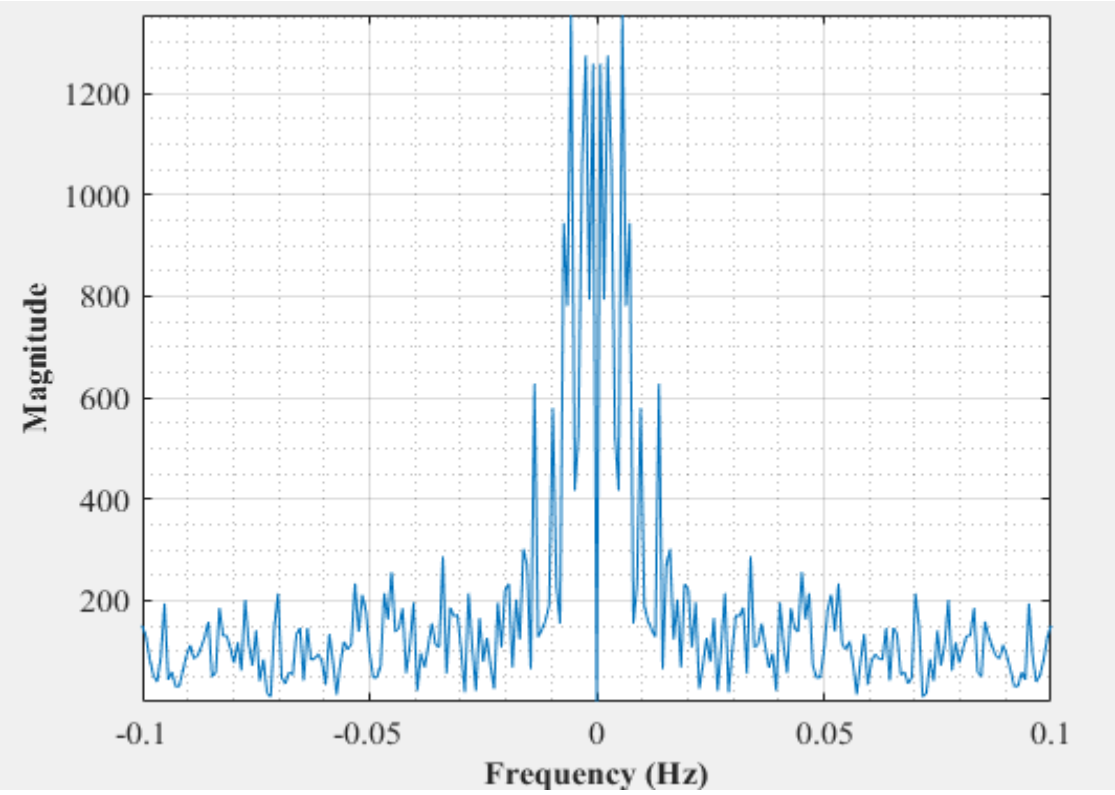


*Figure C-64: Dominant Frequency for a non-uniformly packed vessel (large and small at the center) at 20 dm$^3$/minute gas flow rate- Test 3*

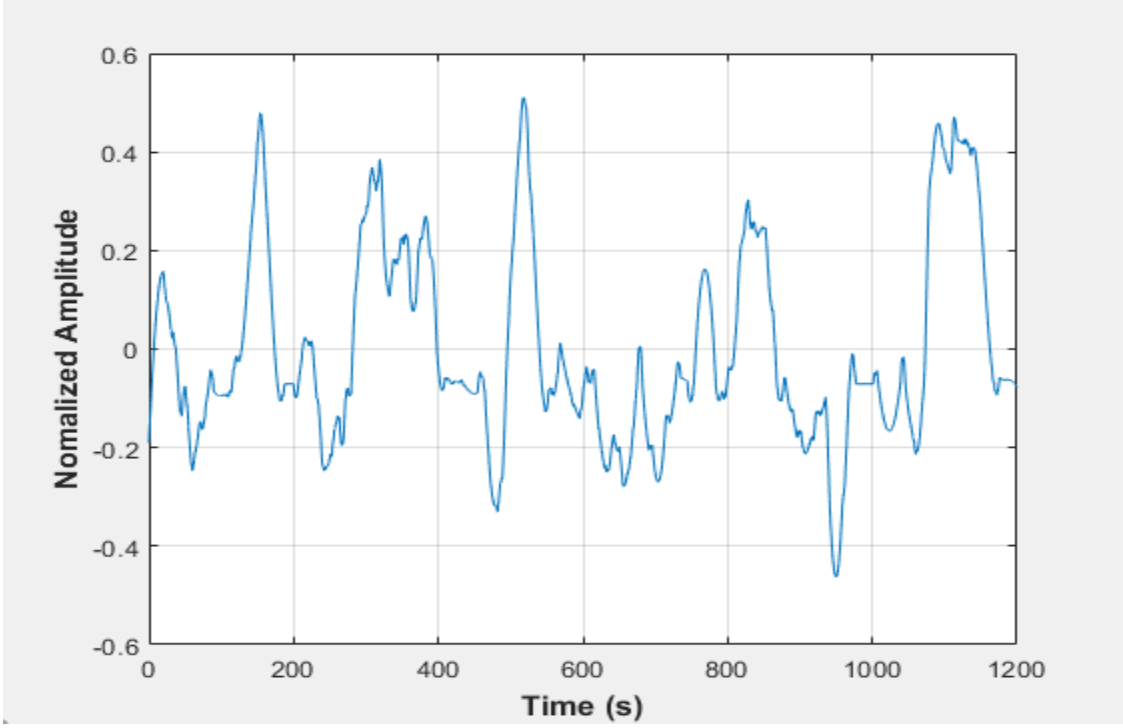


*Figure C-65: Pressure fluctuations in a non-uniformly packed vessel (large and small at the center) at 20 dm$^3$/minute gas flow rate- Test 4*

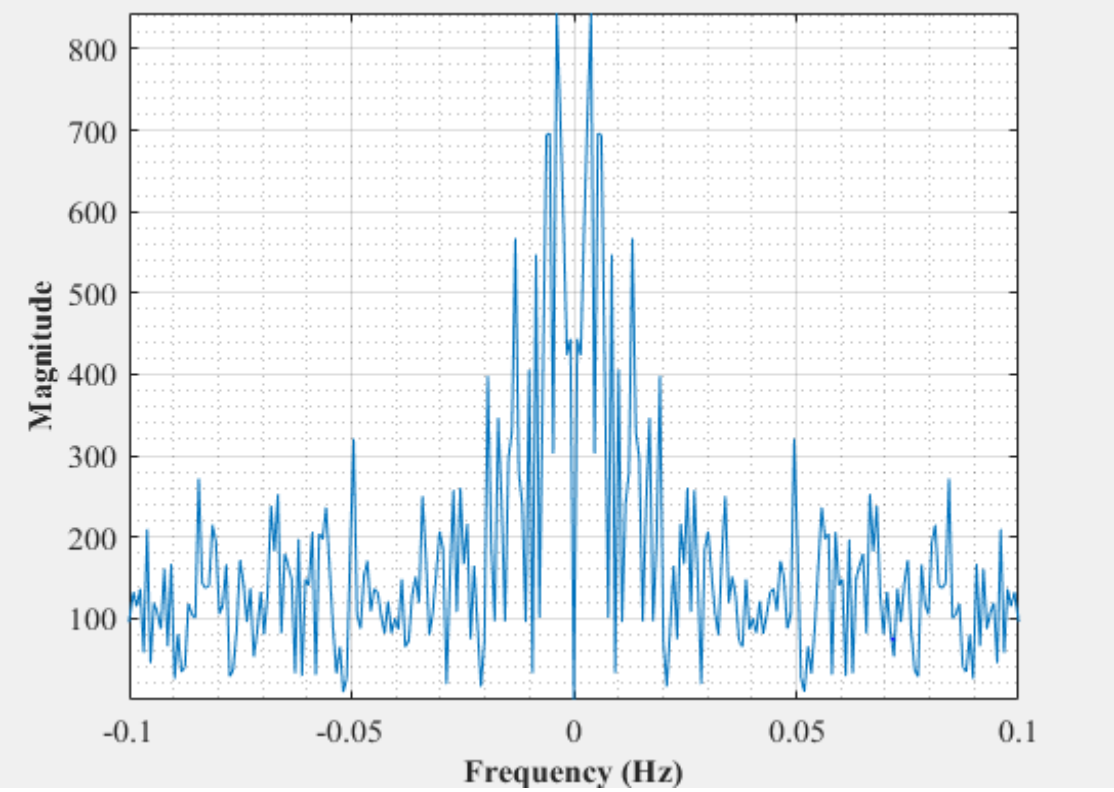


*Figure C-66: Dominant Frequency for a non-uniformly packed vessel (large and small at the center) at 20 dm$^3$/minute gas flow rate- Test 4*

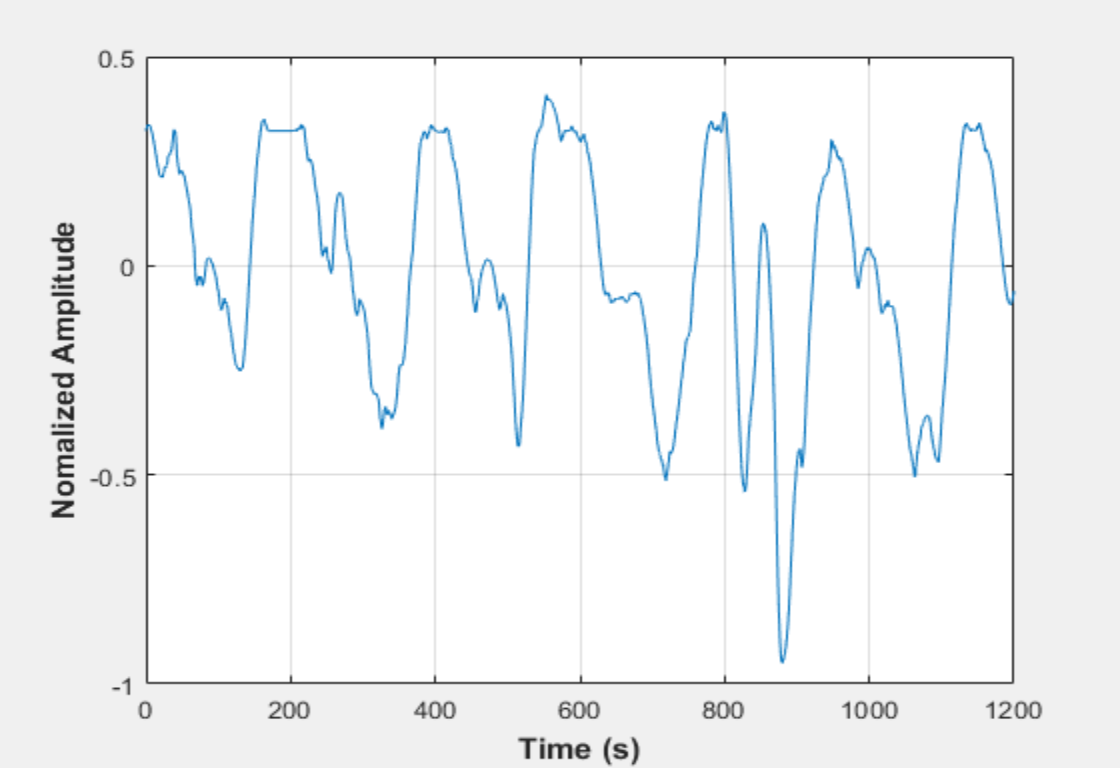


*Figure C-67: Pressure fluctuations in a non-uniformly packed vessel (large and small at the center) at 22.5 $dm^3$/minute gas flow rate- Test 1*

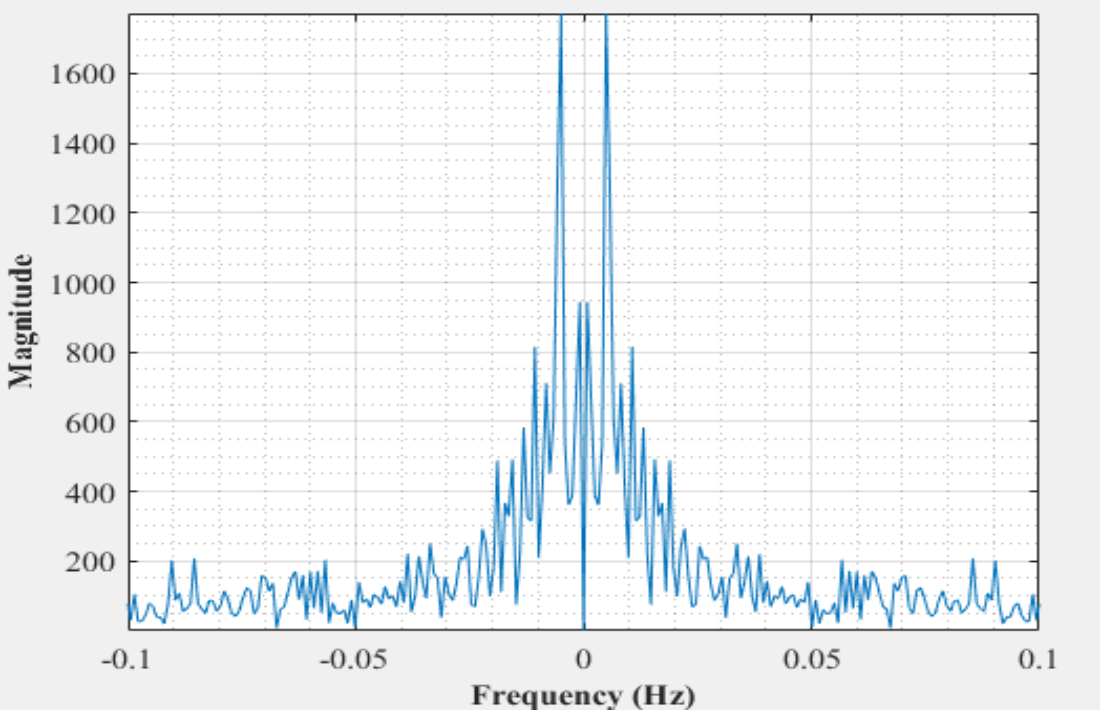


*Figure C-68: Dominant Frequency for a non-uniformly packed vessel (large and small at the center) at 22.5 $dm^3$/minute gas flow rate- Test 1*

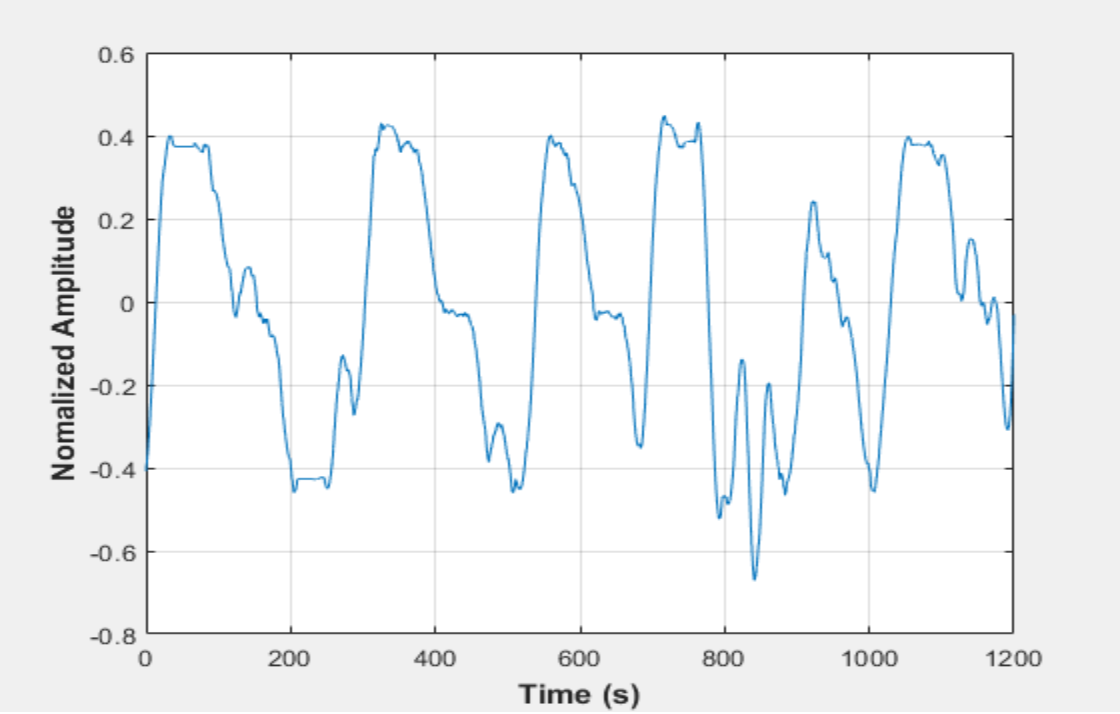


*Figure C-69: Pressure fluctuations in a non-uniformly packed vessel (large and small at the center) at 22.5 $dm^3$/minute gas flow rate- Test 2*

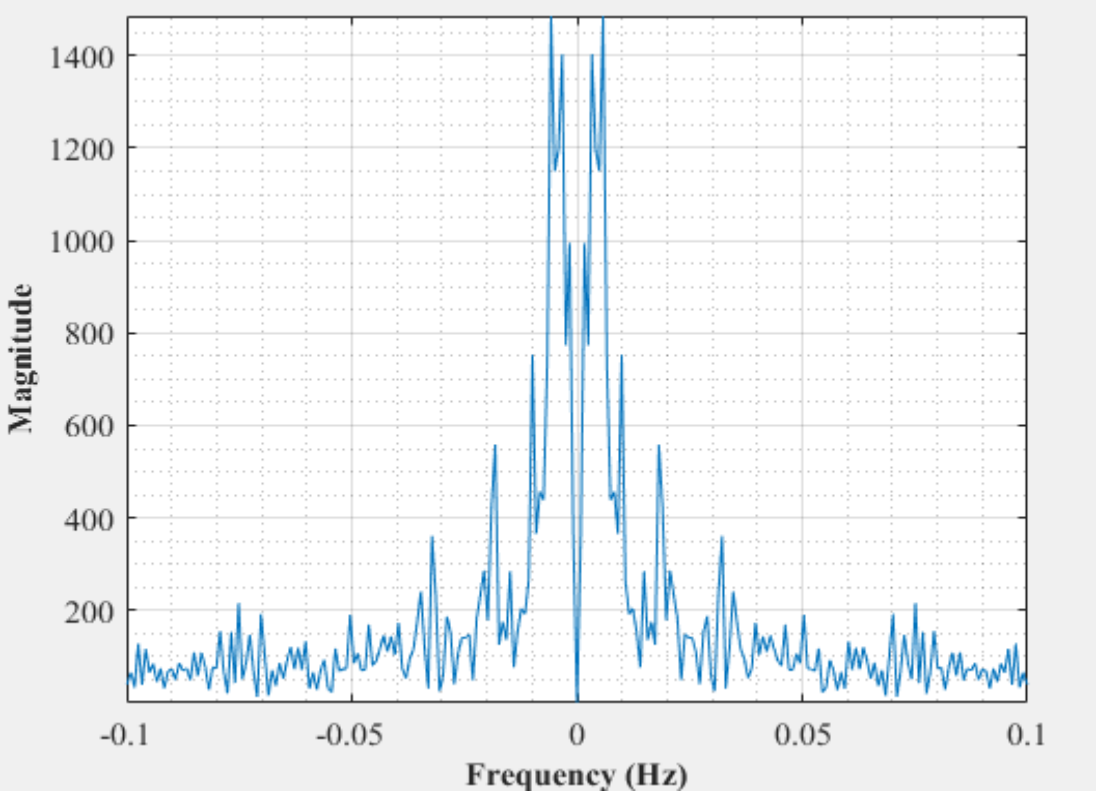


*Figure C-70: Dominant Frequency for a non-uniformly packed vessel (large and small at the center) at 22.5 $dm^3$/minute gas flow rate- Test 2*

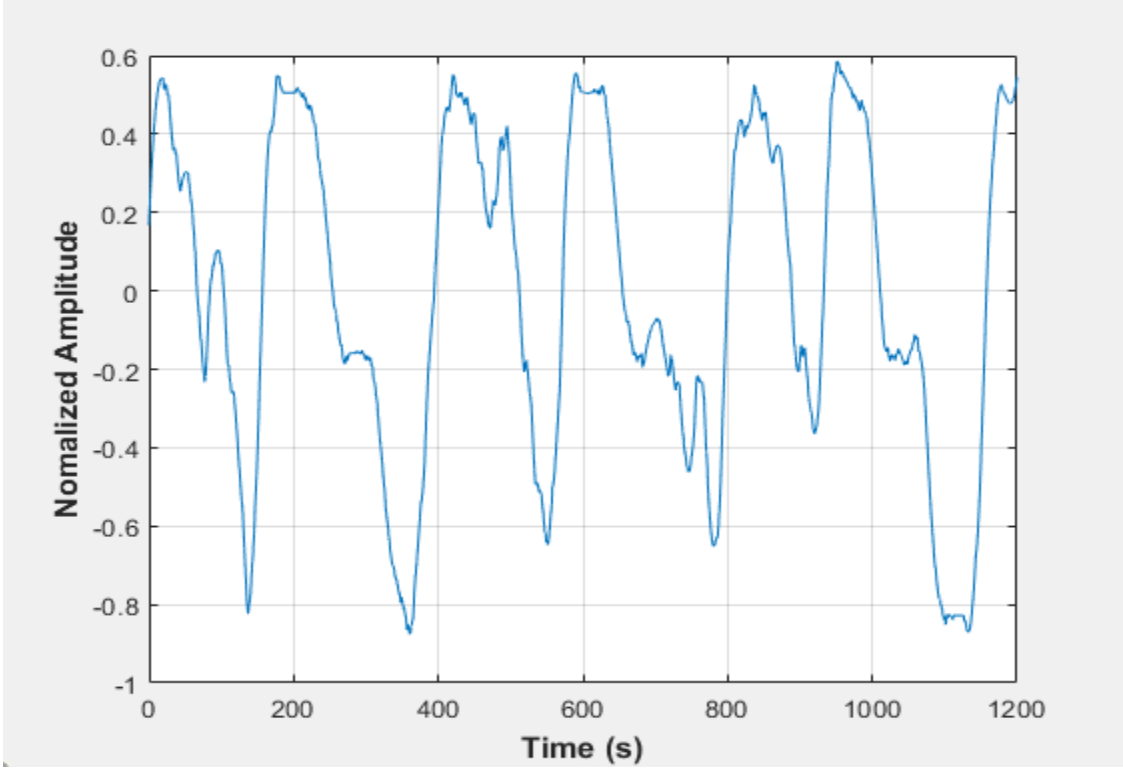


*Figure C-71: Pressure fluctuations in a non-uniformly packed vessel (large and small at the center) at 22.5 $dm^3$/minute gas flow rate- Test 3*

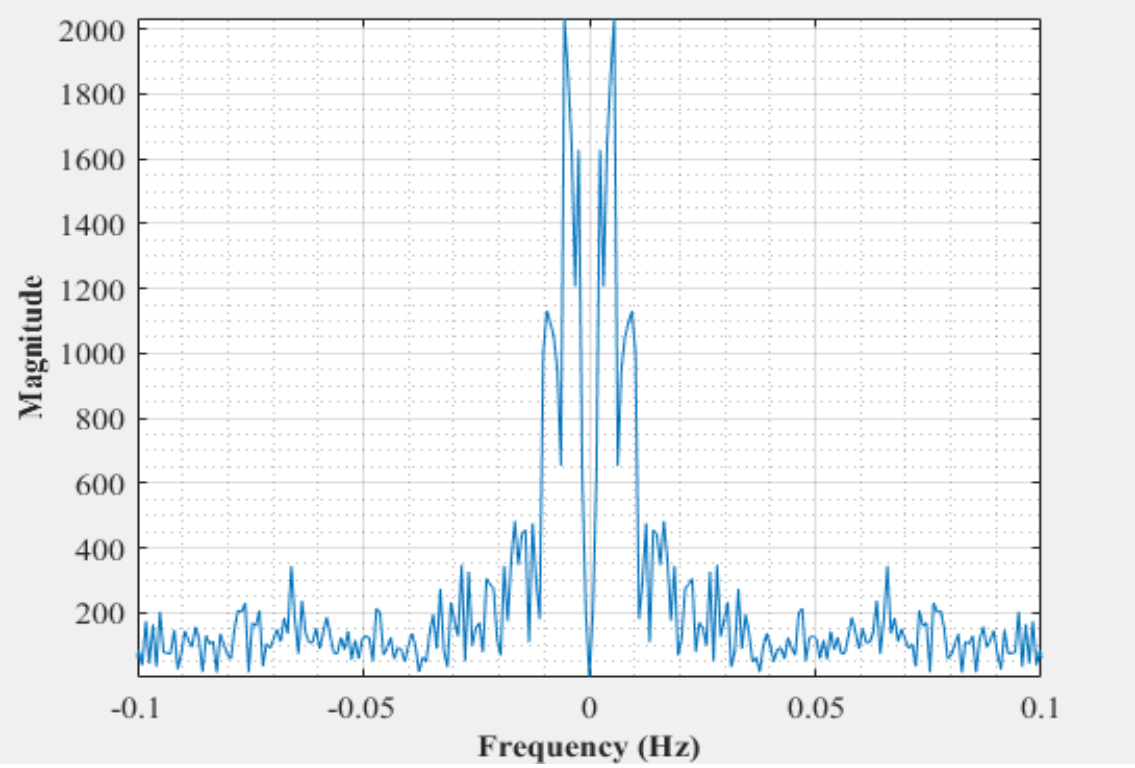


*Figure C-72: Dominant Frequency for a non-uniformly packed vessel (large and small at the center) at 22.5 $dm^3$/minute gas flow rate- Test 3*

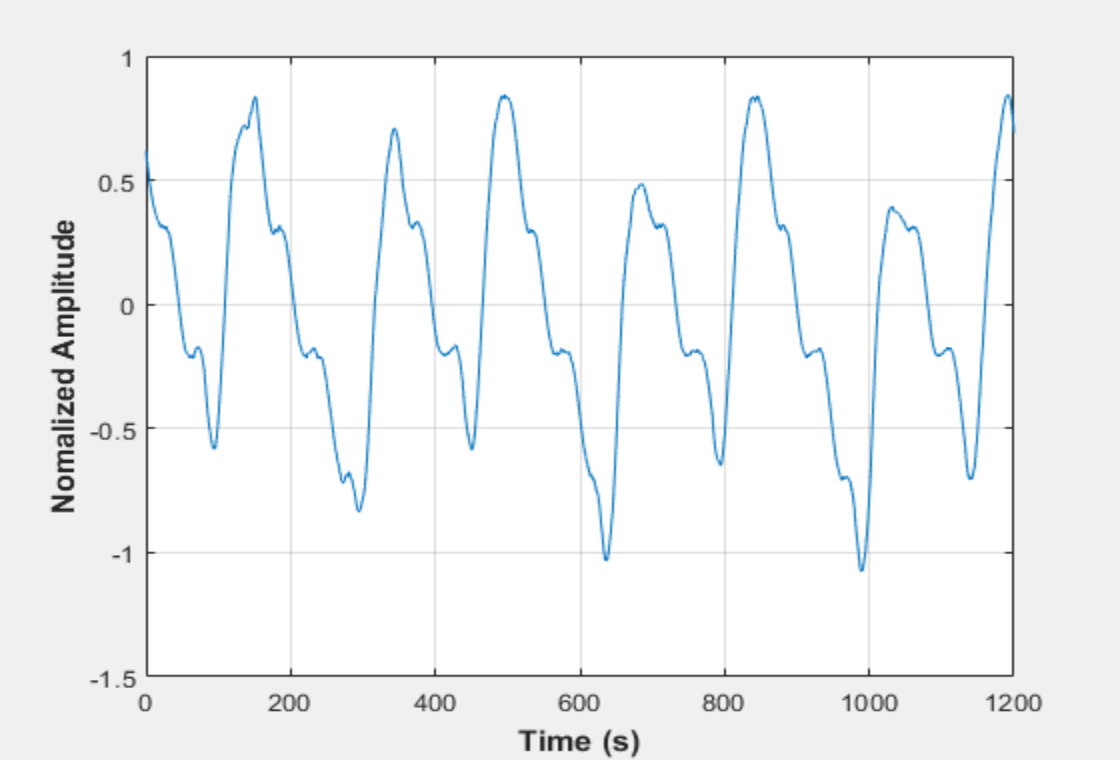


*Figure C-73: Pressure fluctuations in a non-uniformly packed vessel (large and small at the center) at 29 dm$^3$/minute gas flow rate- Test 1*

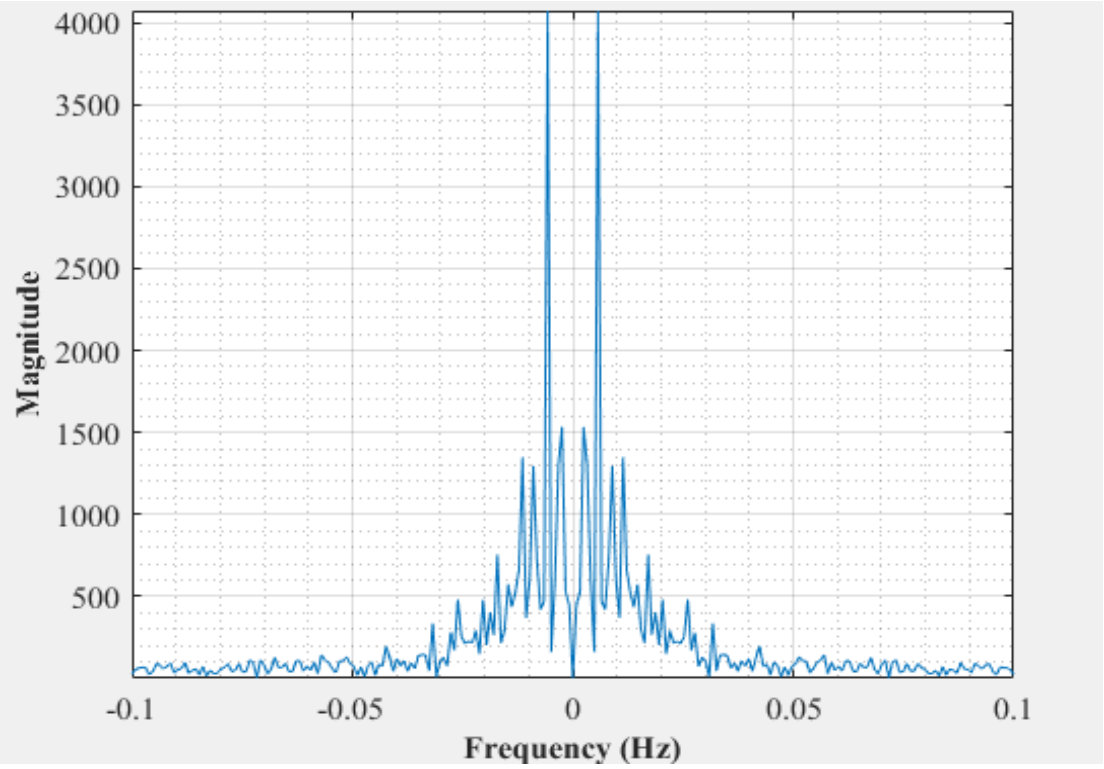


*Figure C-74: Dominant Frequency for a non-uniformly packed vessel (large and small at the center) at 29 dm$^3$/minute gas flow rate- Test 1*

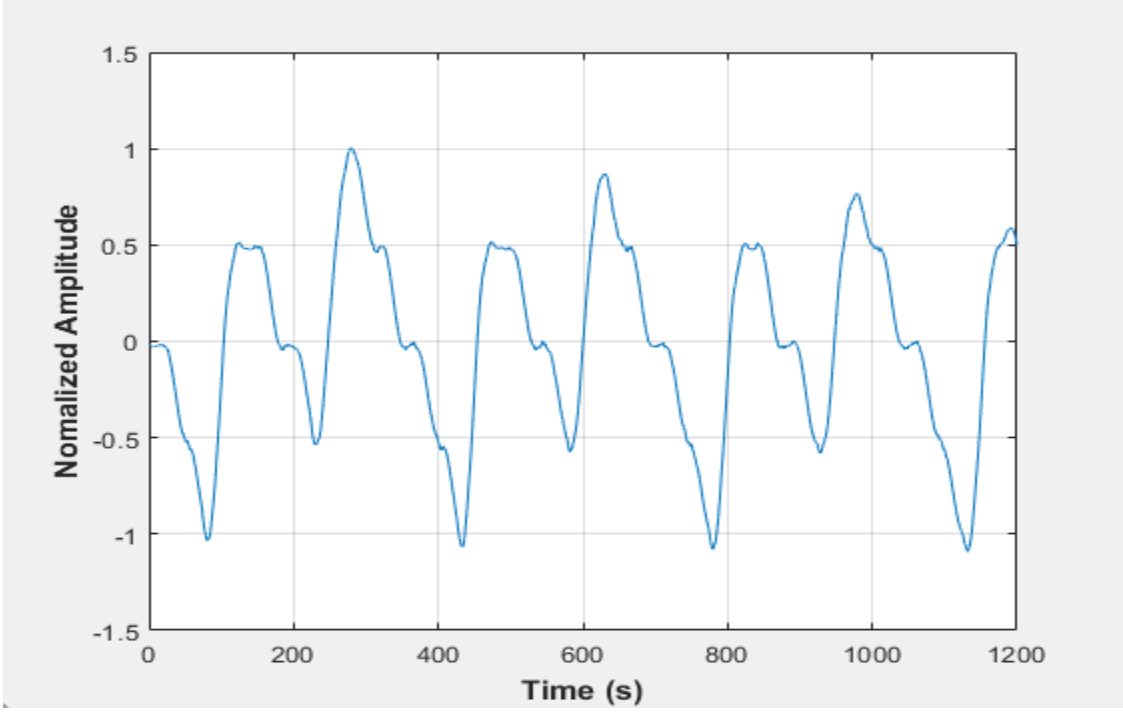


*Figure C-75: Pressure fluctuations in a non-uniformly packed vessel (large and small at the center) at 29 dm$^3$/minute gas flow rate- Test 2*

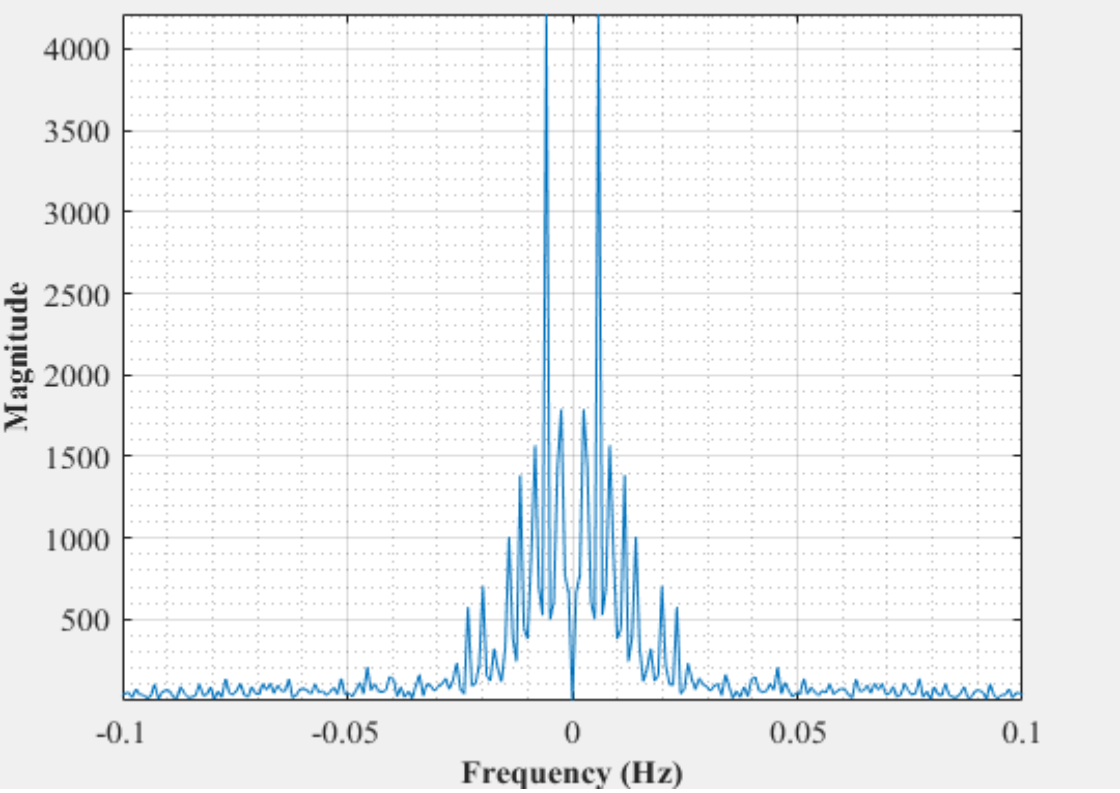


*Figure C-76: Dominant Frequency for a non-uniformly packed vessel (large and small at the center) at 29 dm$^3$/minute gas flow rate- Test 2*

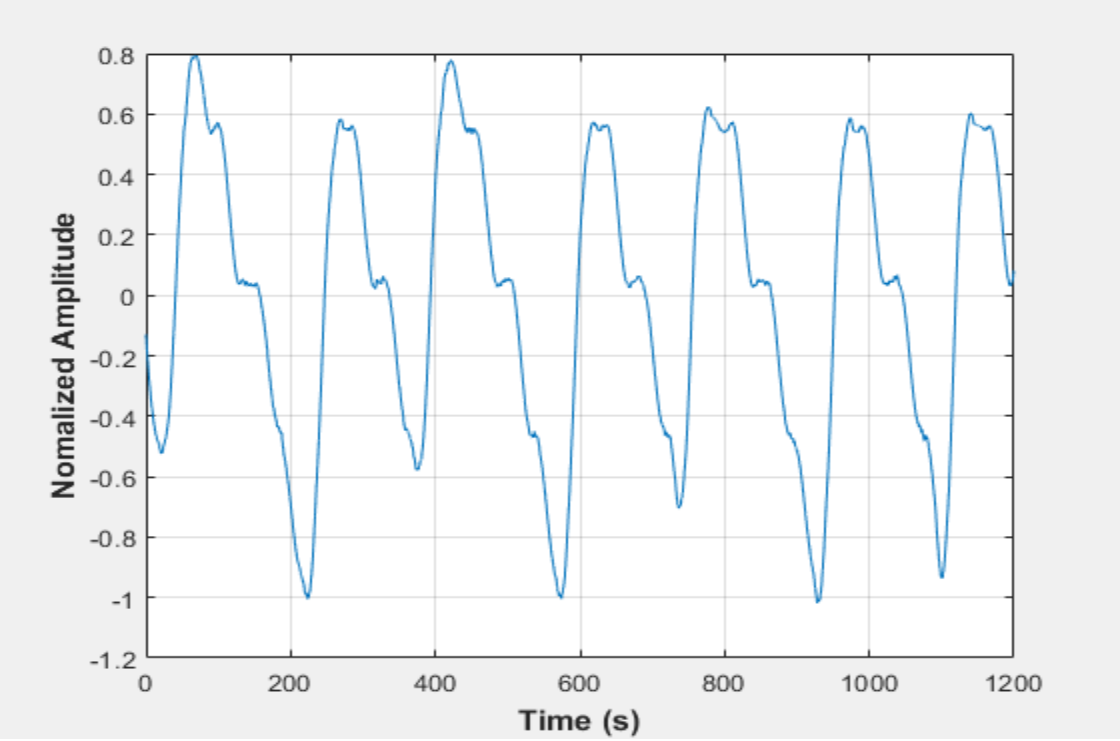


*Figure C-77: Pressure fluctuations in a non-uniformly packed vessel (large and small at the center) at 29 dm$^3$/minute gas flow rate- Test 3*

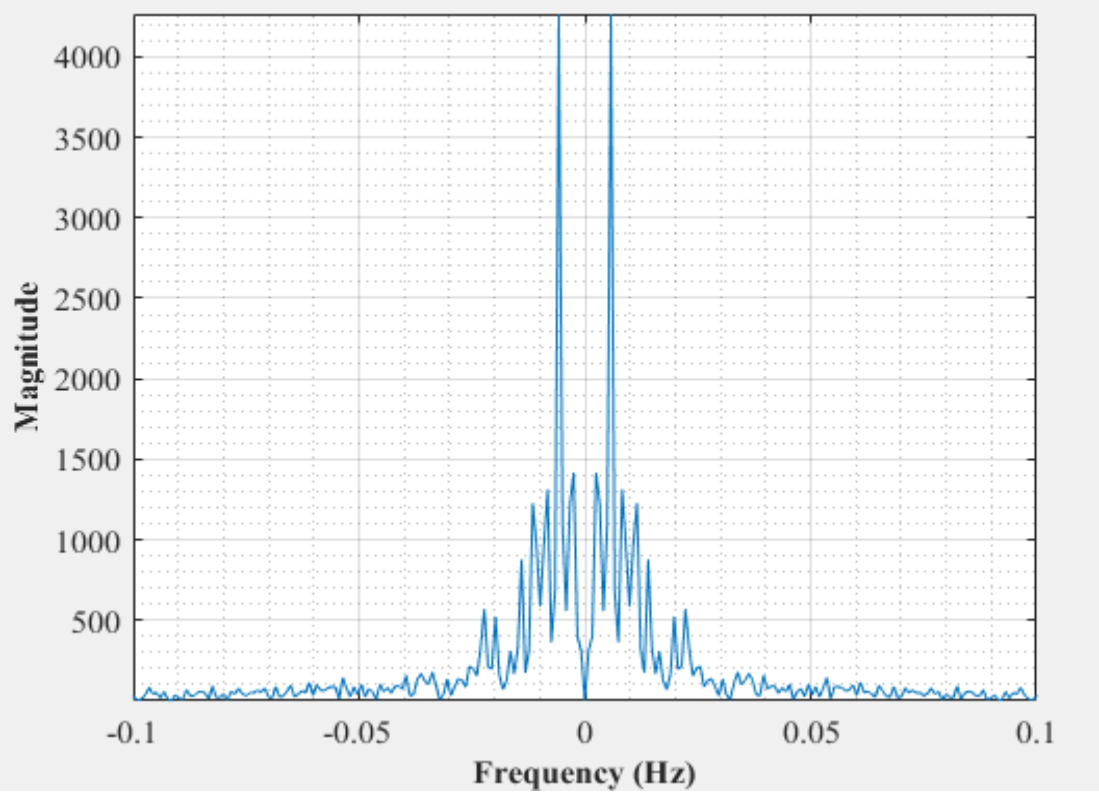


*Figure C-78: Dominant Frequency for a non-uniformly packed vessel (large and small at the center) at 29 dm$^3$/minute gas flow rate- Test 3*

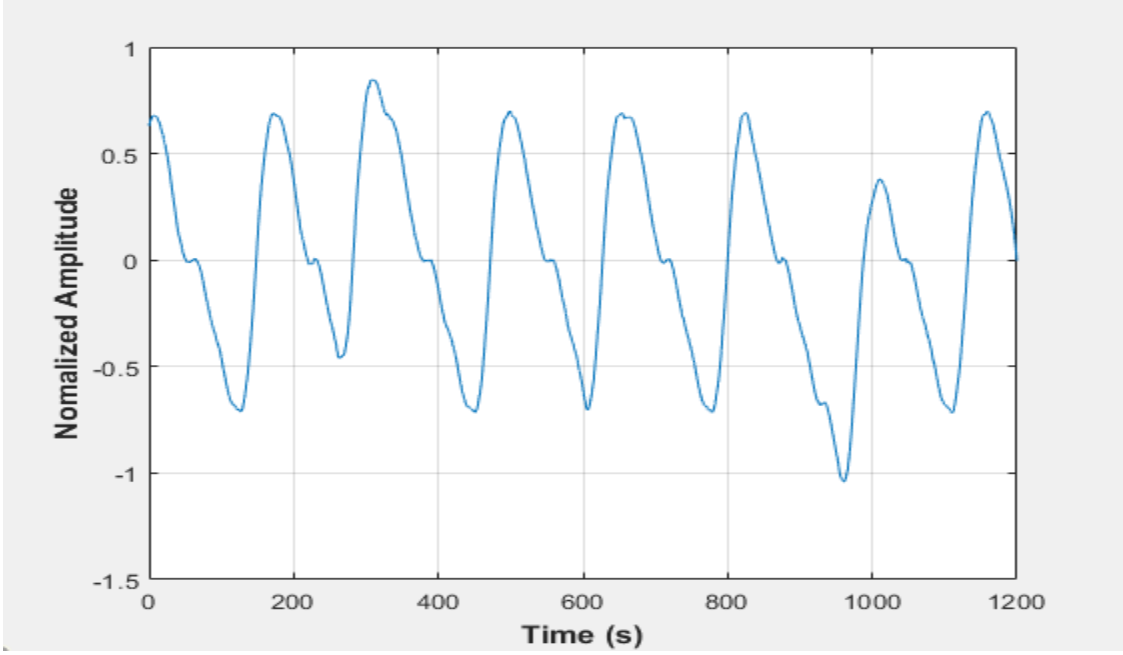


*Figure C-79: Pressure fluctuations in a non-uniformly packed vessel (large and small at the center) at 33 dm$^3$/minute gas flow rate- Test 1*

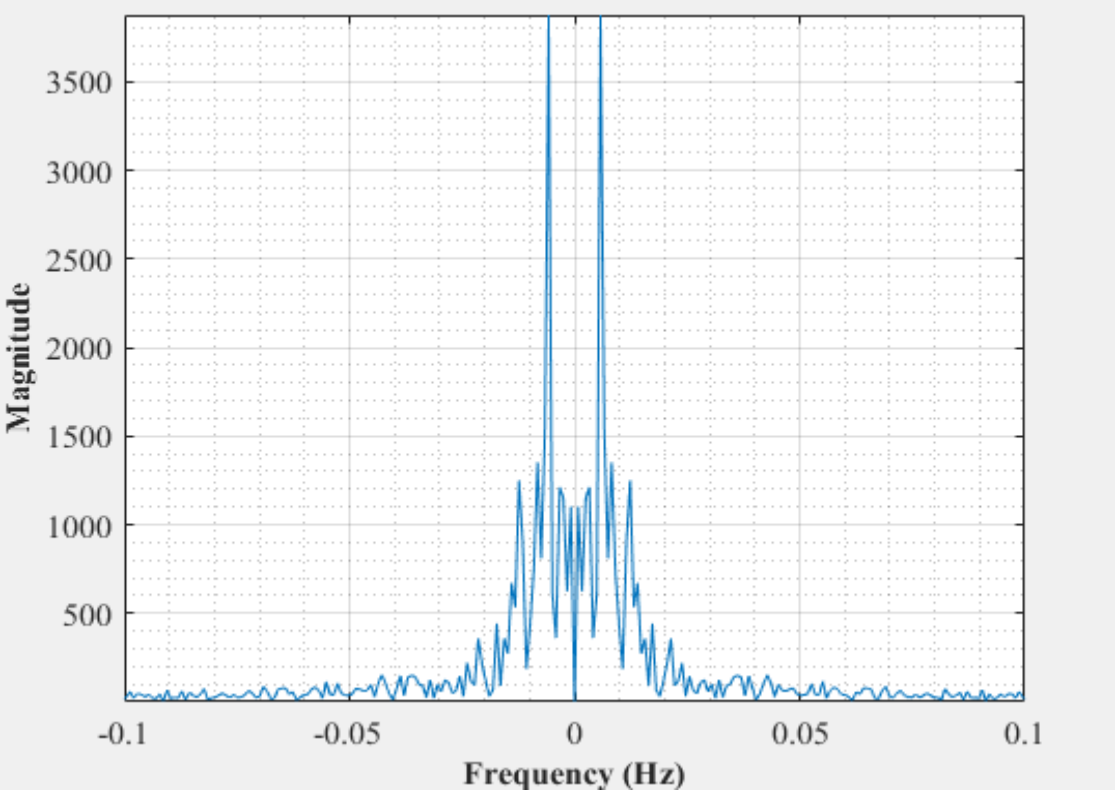


*Figure C-80: Dominant Frequency for a non-uniformly packed vessel (large and small at the center) at 33 dm$^3$/minute gas flow rate- Test 1*

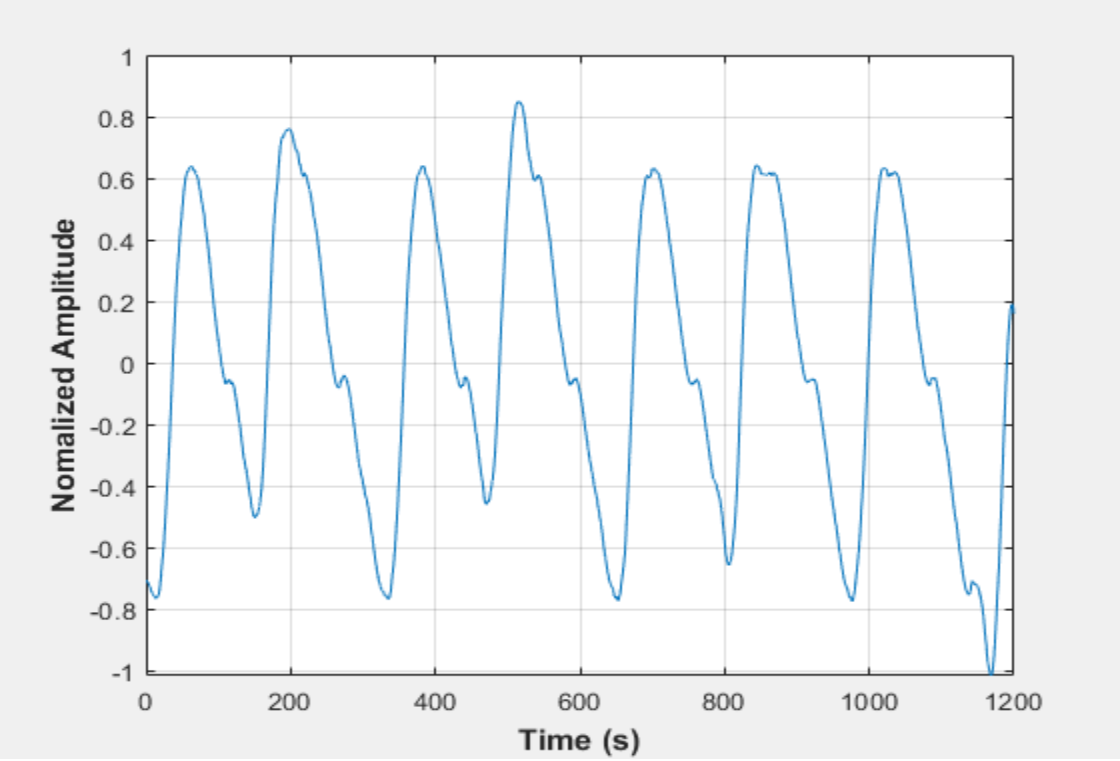


*Figure C-81: Pressure fluctuations in a non-uniformly packed vessel (large and small at the center) at 33 dm$^3$/minute gas flow rate- Test 2*

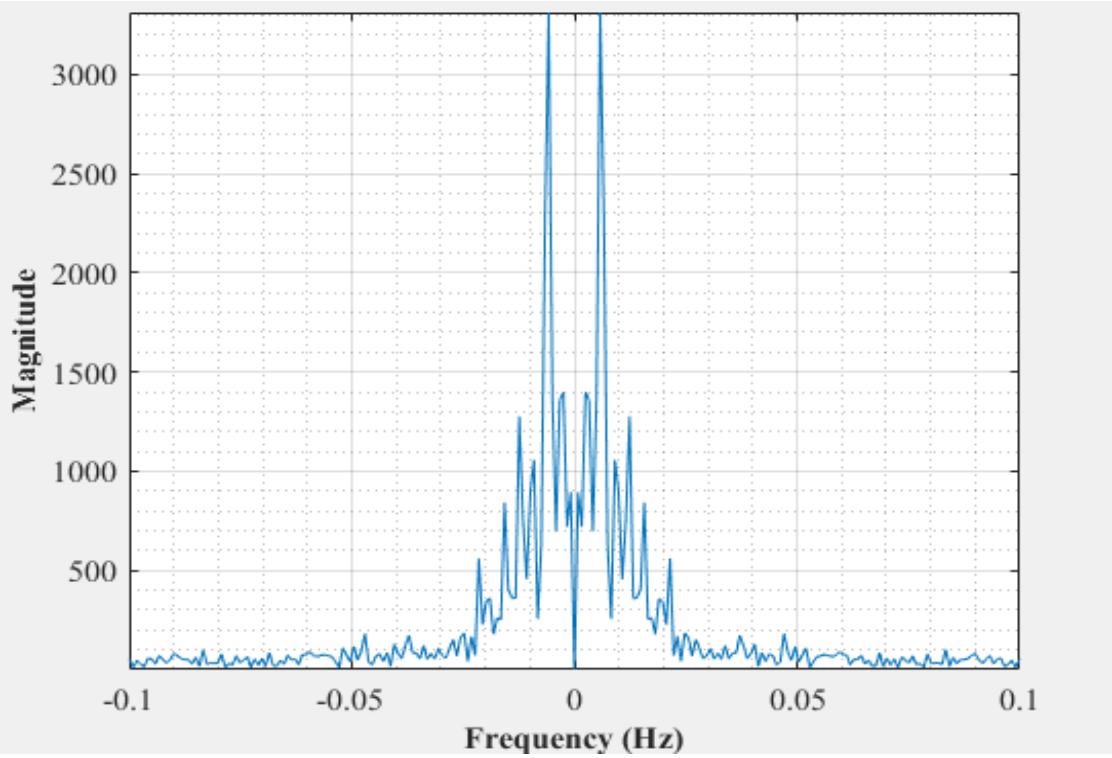


*Figure C-82: Dominant Frequency for a non-uniformly packed vessel (large and small at the center) at 33 dm$^3$/minute gas flow rate- Test 2*

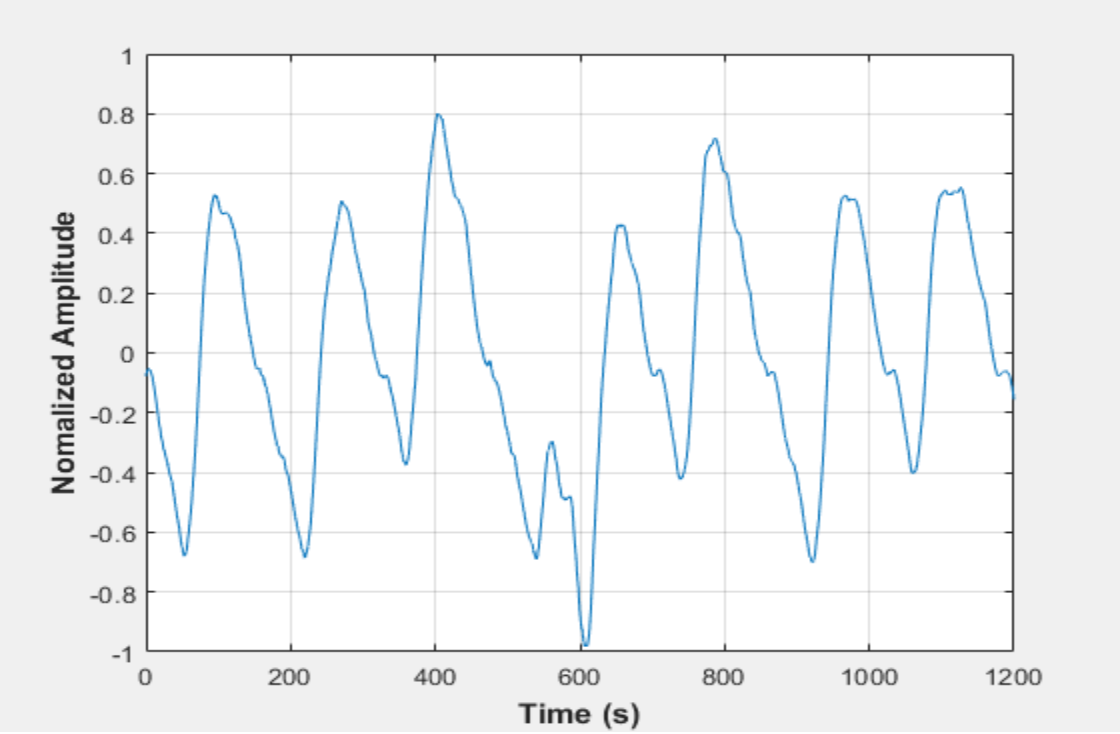


*Figure C-83: Pressure fluctuations in a non-uniformly packed vessel (large and small at the center) at 33 dm$^3$/minute gas flow rate- Test 3*

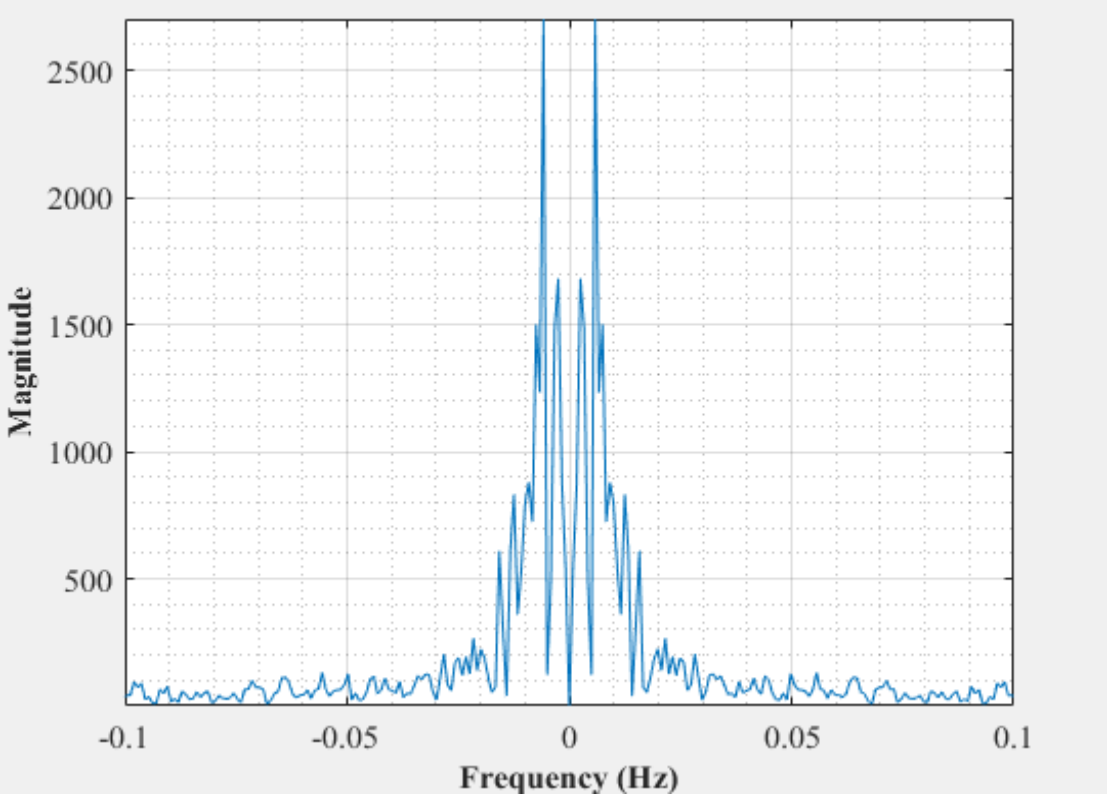


*Figure C-84: Dominant Frequency for a non-uniformly packed vessel (large and small at the center) at 33 dm$^3$/minute gas flow rate- Test 3*

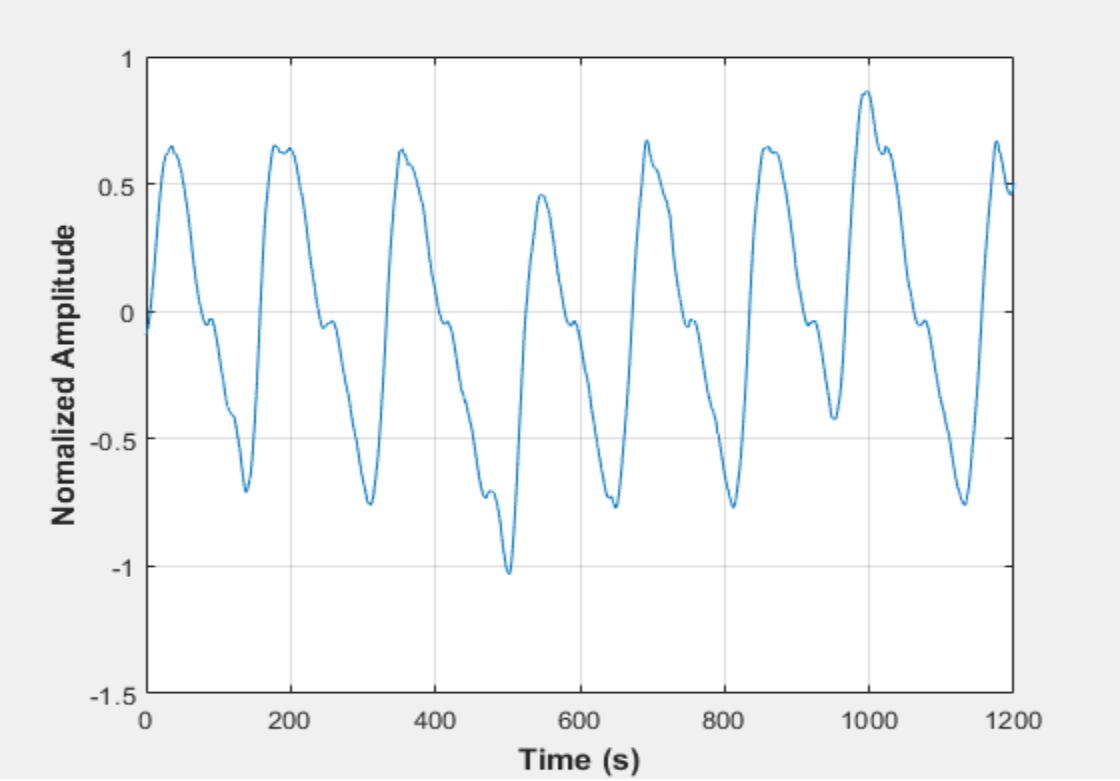


*Figure C-85: Pressure fluctuations in a non-uniformly packed vessel (large and small at the center) at 33 dm$^3$/minute gas flow rate- Test 4*

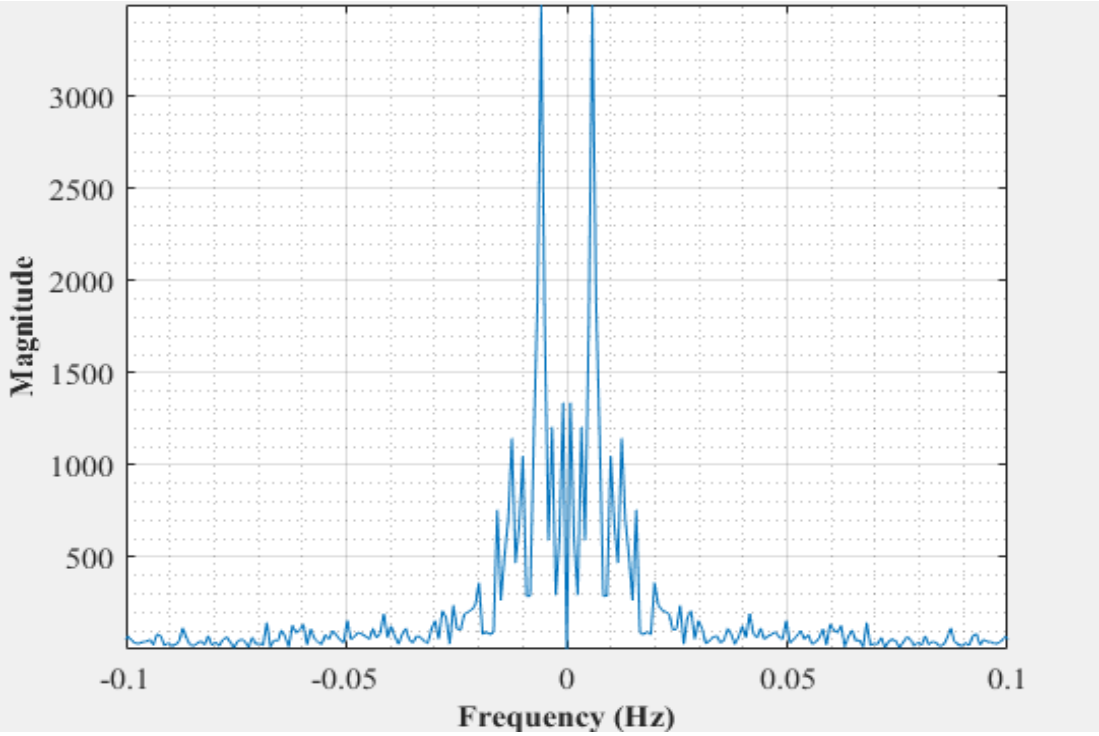


*Figure C-86: Dominant Frequency for a non-uniformly packed vessel (large and small at the center) at 33 dm$^3$/minute gas flow rate- Test 4*

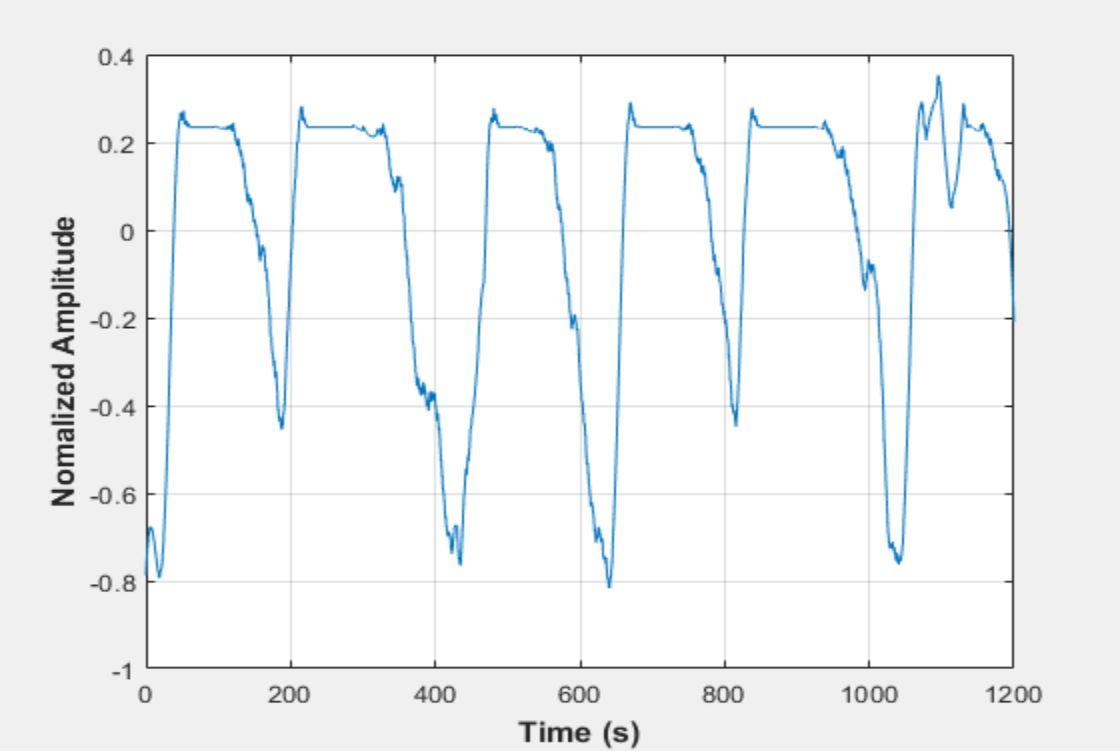


*Figure C-87: Pressure fluctuations in a non-uniformly packed vessel (large and small at the side) at 20 $dm^3$/minute gas flow rate- Test 1*

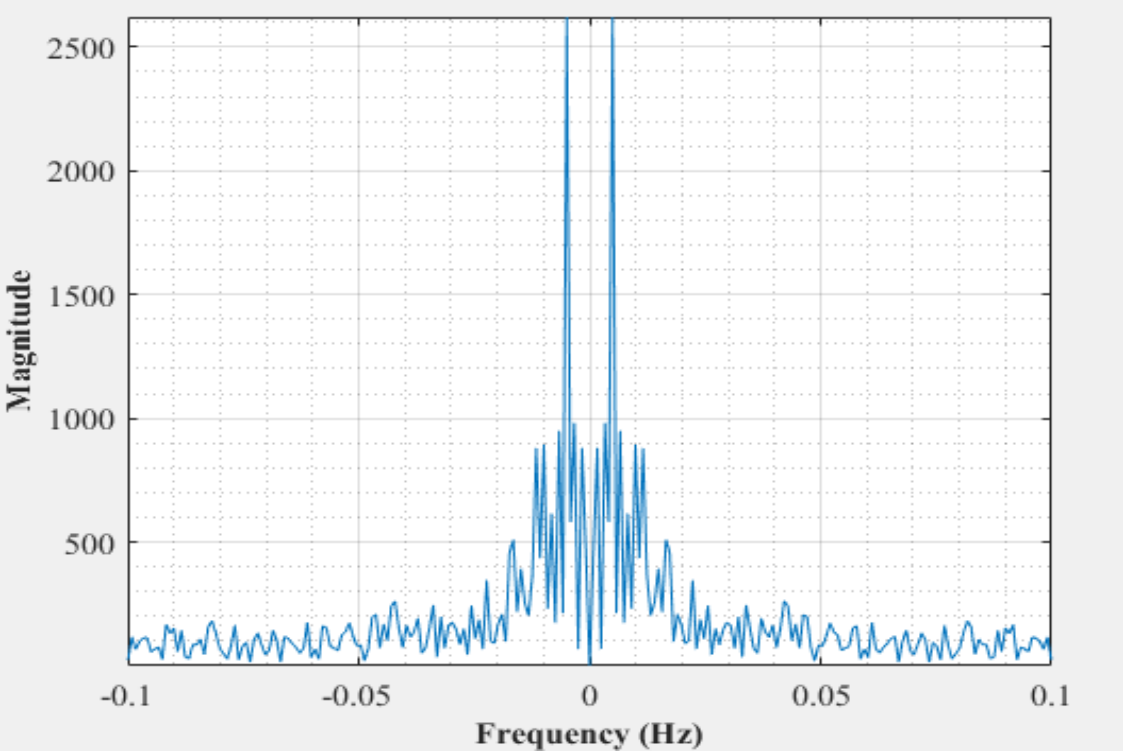


*Figure C-88: Dominant Frequency for a non-uniformly packed vessel (large and small at the side) at $dm^3$/minute gas flow rate- Test 1*

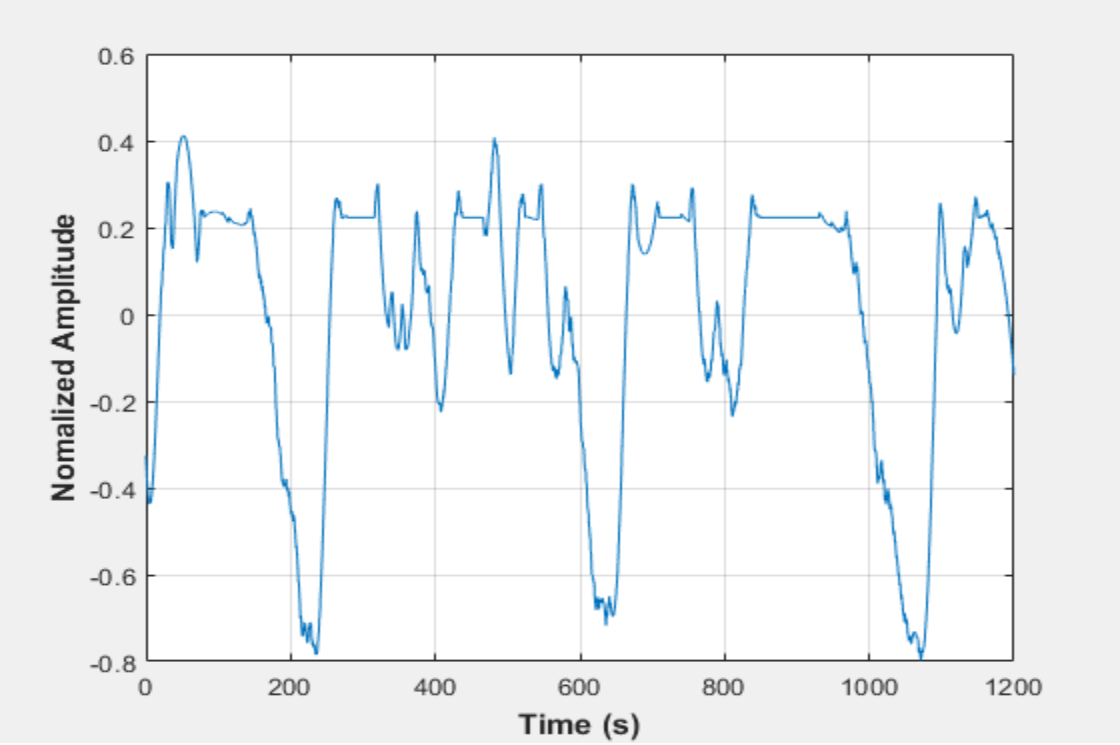


*Figure C-89: Pressure fluctuations in a non-uniformly packed vessel (large and small at the side) at 20 dm$^3$/minute gas flow rate- Test 2*

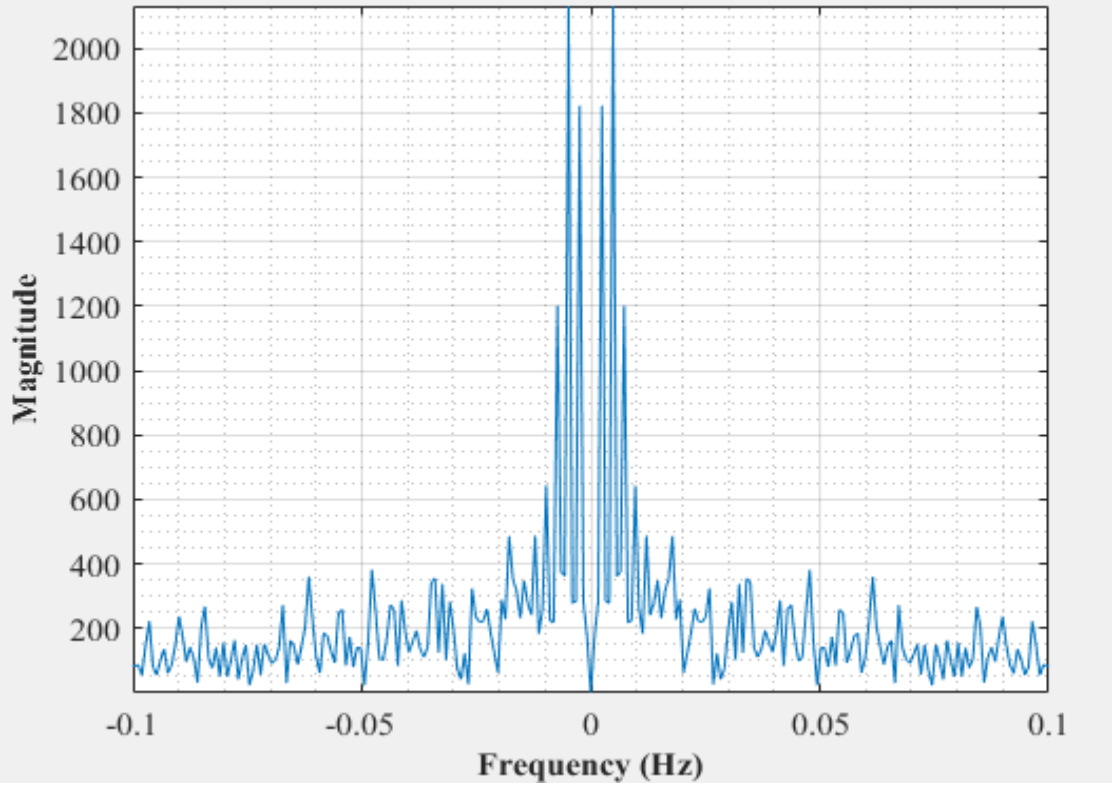


*Figure C-90: Dominant Frequency for a non-uniformly packed vessel (large and small at the side) at 20 dm$^3$/minute gas flow rate- Test 2*

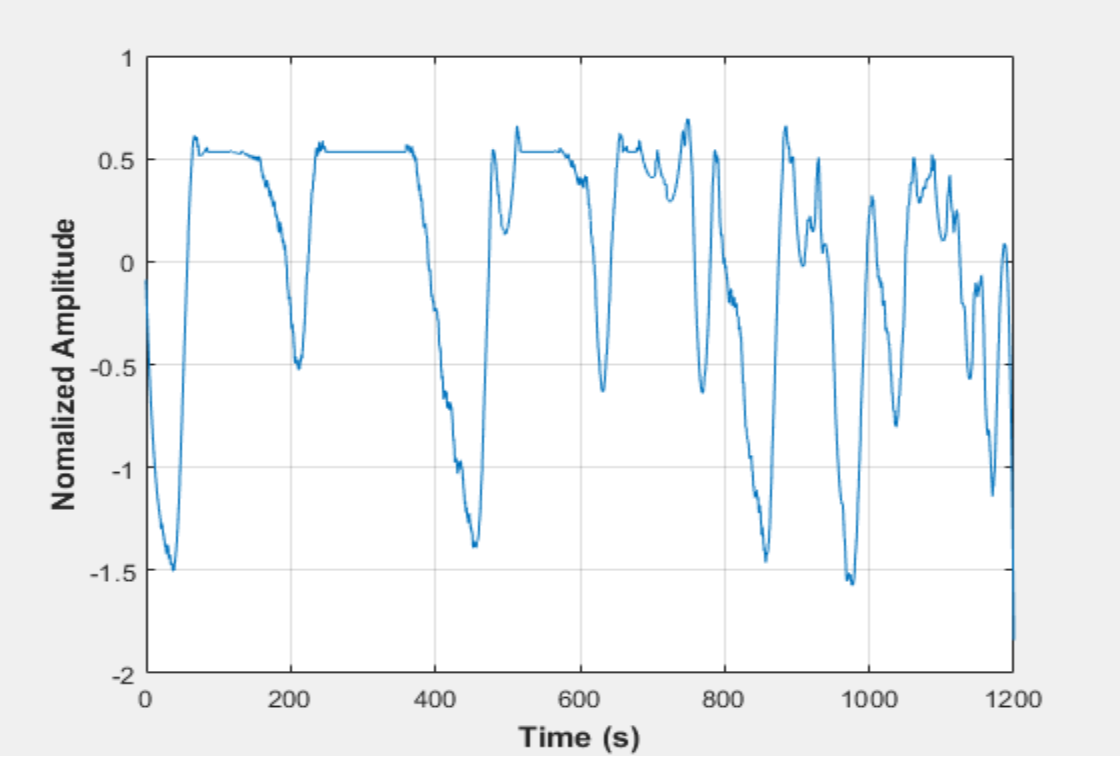


*Figure C-91: Pressure fluctuations in a non-uniformly packed vessel (large and small at the side) at 20 dm$^3$/minute gas flow rate- Test 3*

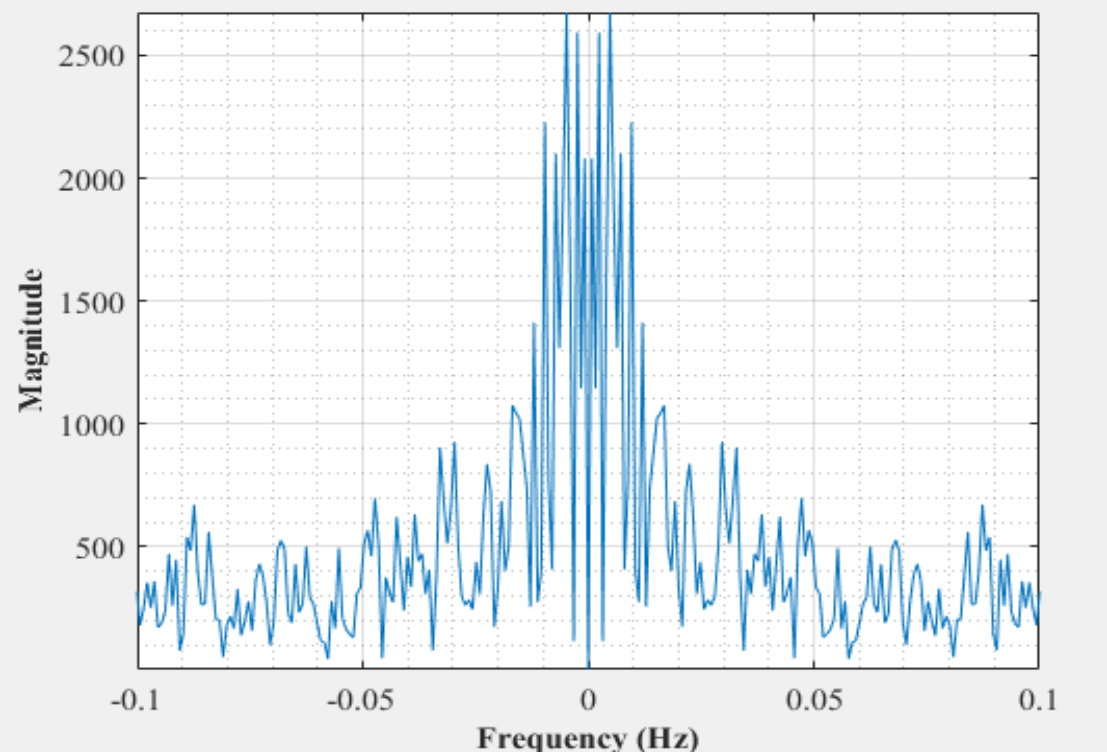


*Figure C-92: Dominant Frequency for a non-uniformly packed vessel (large and small at the side) at 20 dm$^3$/minute gas flow rate- Test 3*

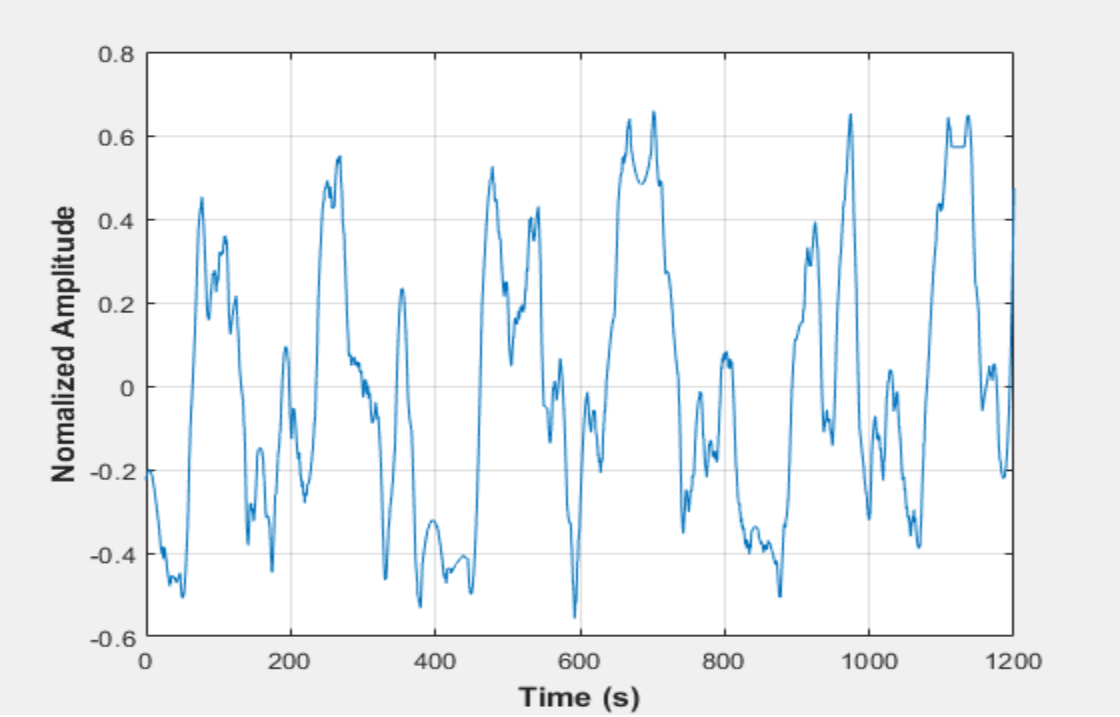


*Figure C-93: Pressure fluctuations in a non-uniformly packed vessel (large and small at the side) at 20 dm$^3$/minute gas flow rate- Test 4*

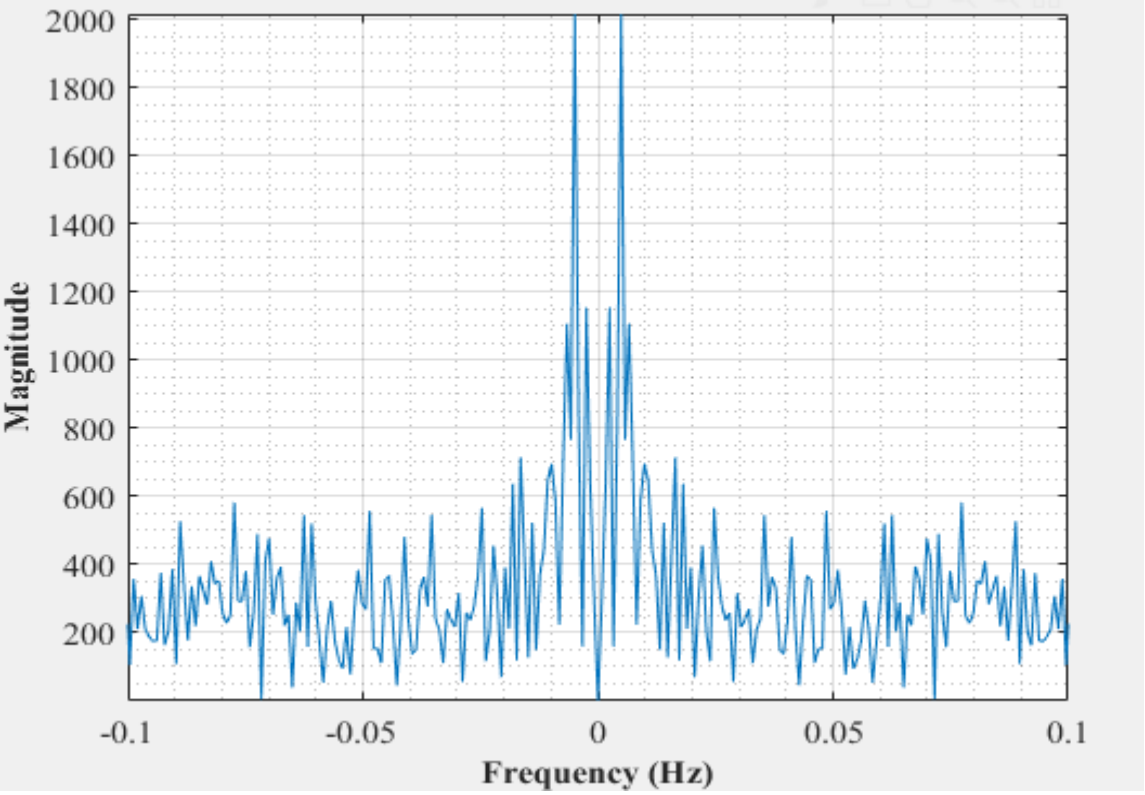


*Figure C-94: Dominant Frequency for a non-uniformly packed vessel (large and small at the side) at 20 dm$^3$/minute gas flow rate- Test 4*

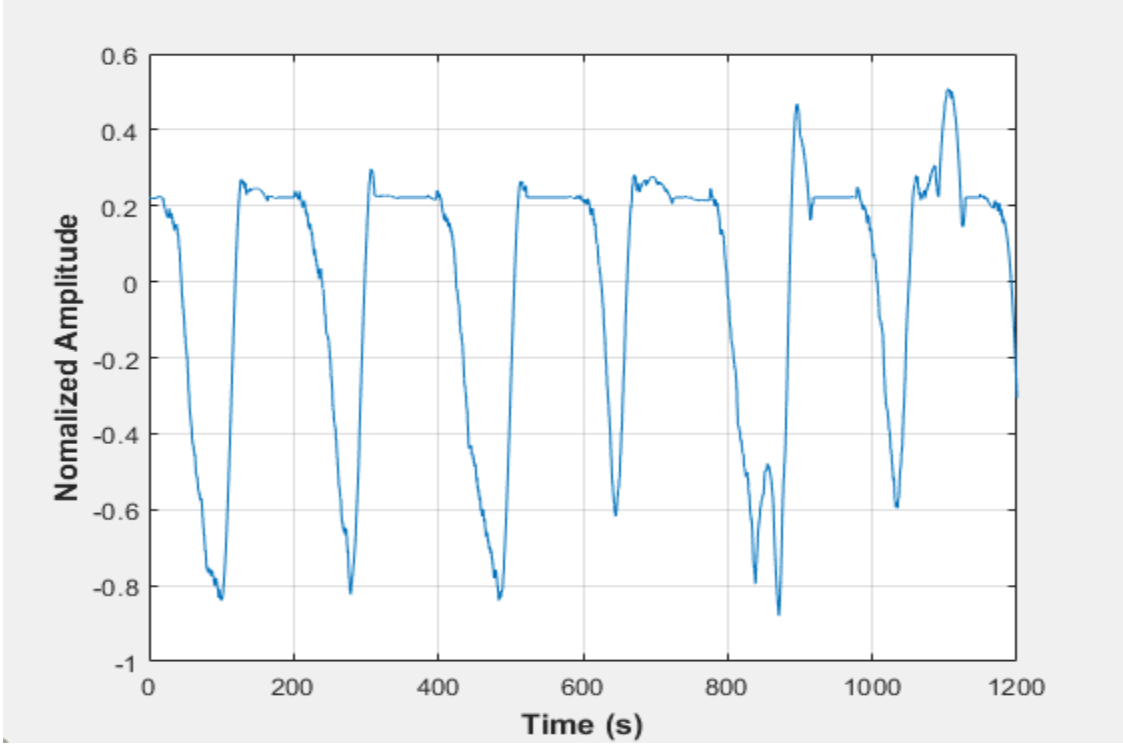


*Figure C-95: Pressure fluctuations in a non-uniformly packed vessel (large and small at the side) at 22.5 dm$^3$/minute gas flow rate- Test 1*

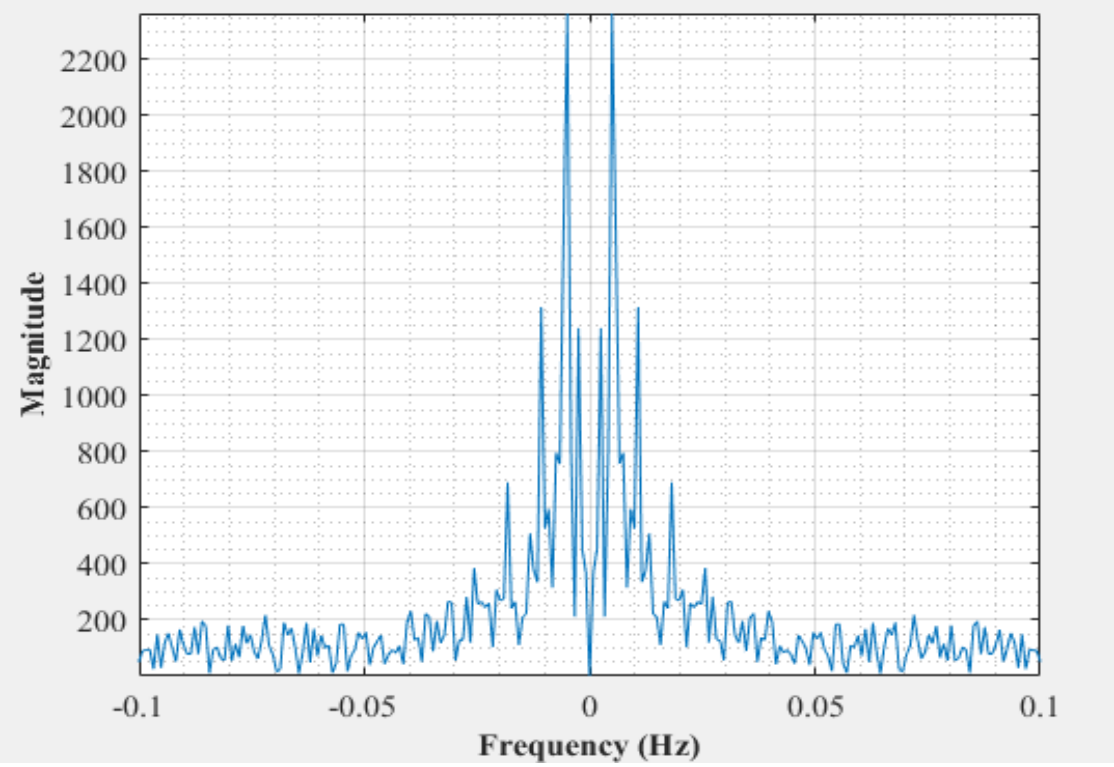


*Figure C-96: Dominant Frequency for a non-uniformly packed vessel (large and small at the side) at 22.5 dm$^3$/minute gas flow rate- Test 1*

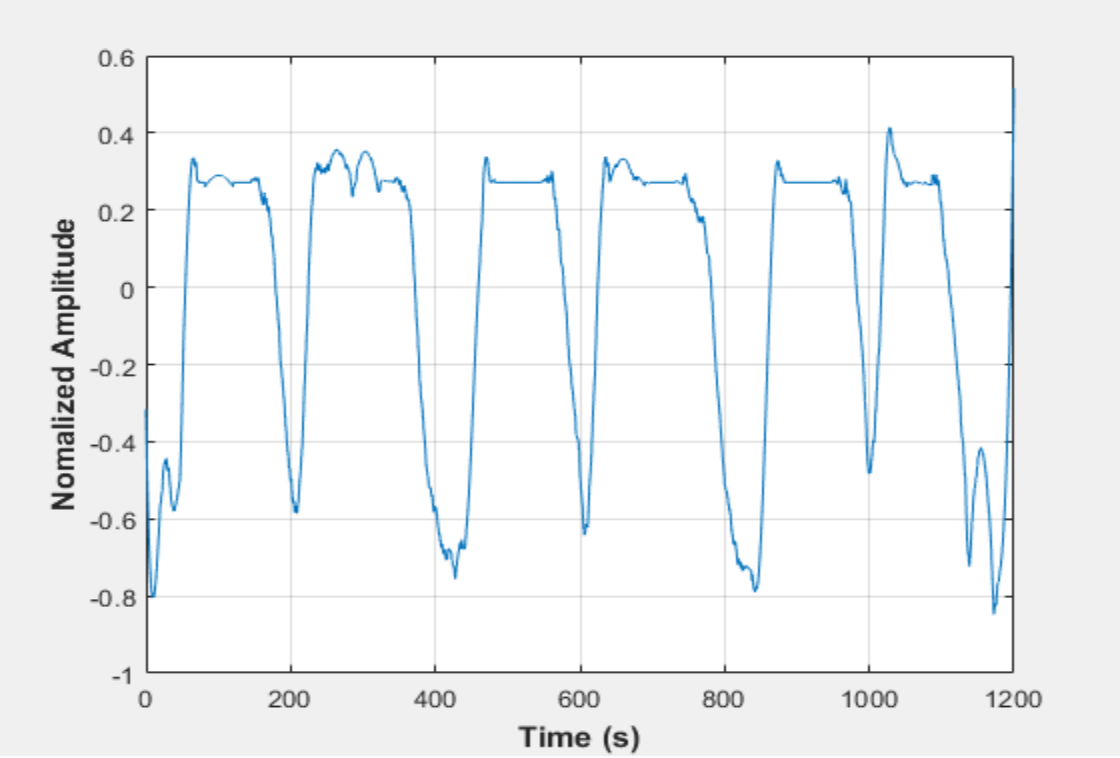


*Figure C-97: Pressure fluctuations in a non-uniformly packed vessel (large and small at the side) at 22.5 $dm^3$/minute gas flow rate- Test 2*

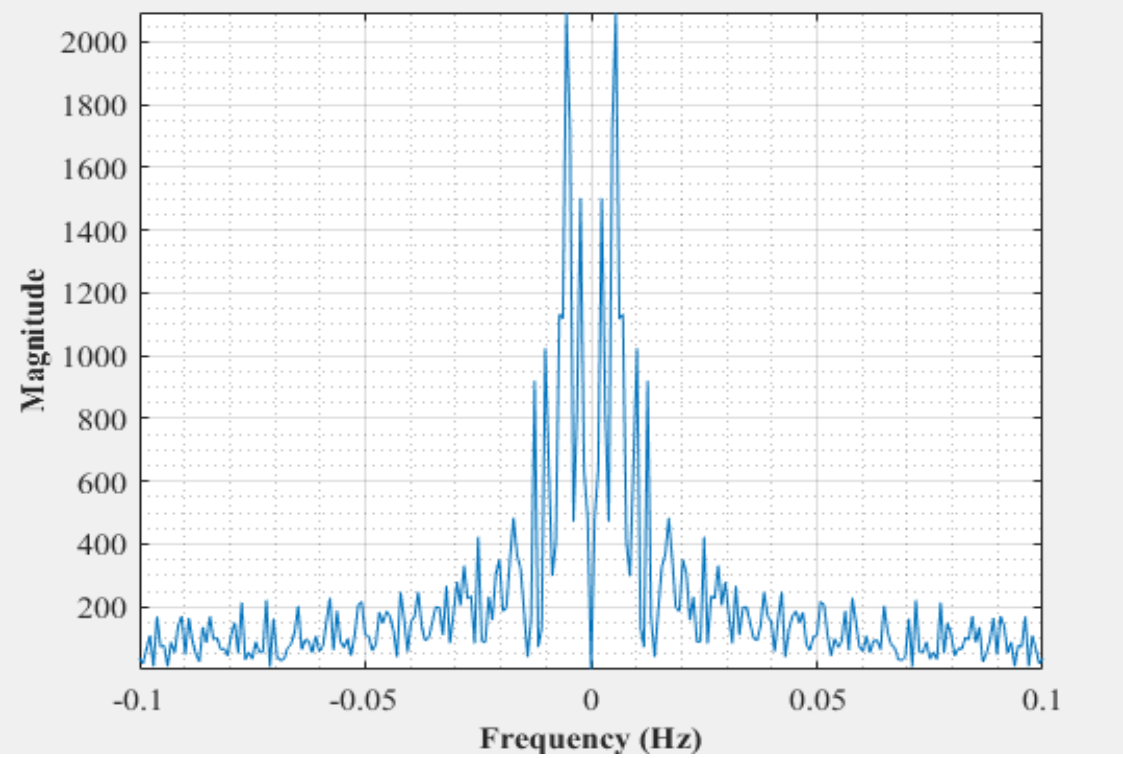


*Figure C-98: Dominant Frequency for a non-uniformly packed vessel (large and small at the side) at 22.5 $dm^3$/minute gas flow rate- Test 2*

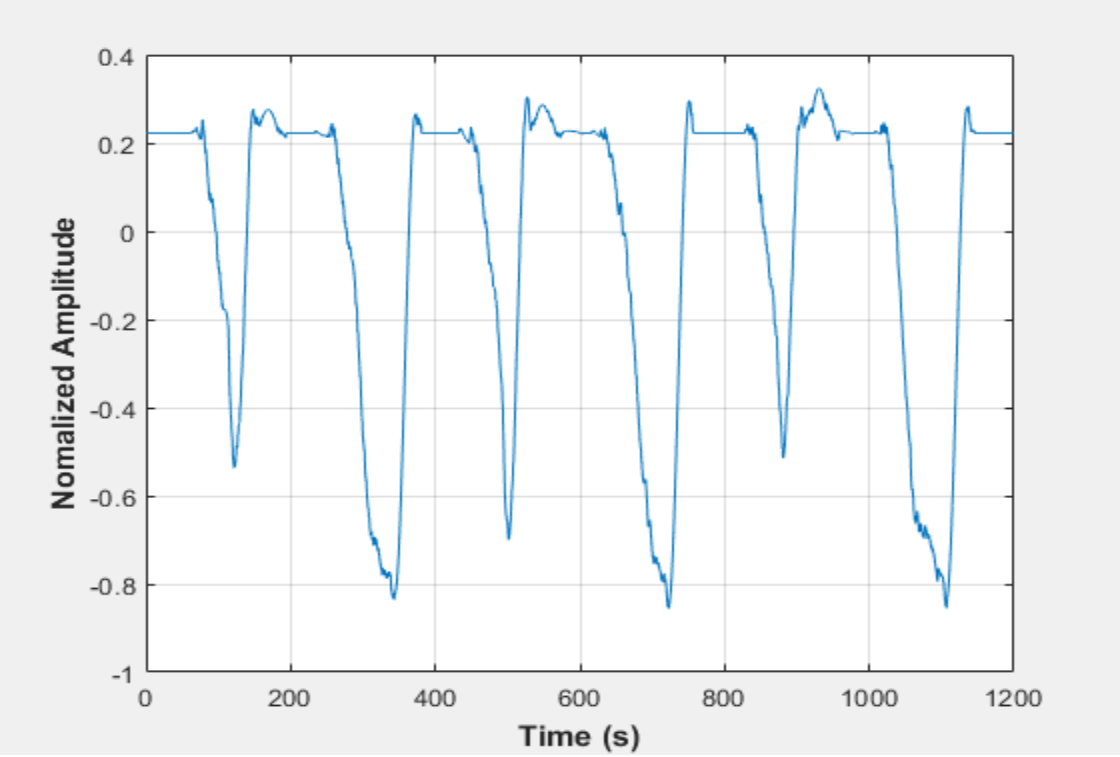


*Figure C-99: Pressure fluctuations in a non-uniformly packed vessel (large and small at the side) at 22.5 dm$^3$/minute gas flow rate- Test 3*

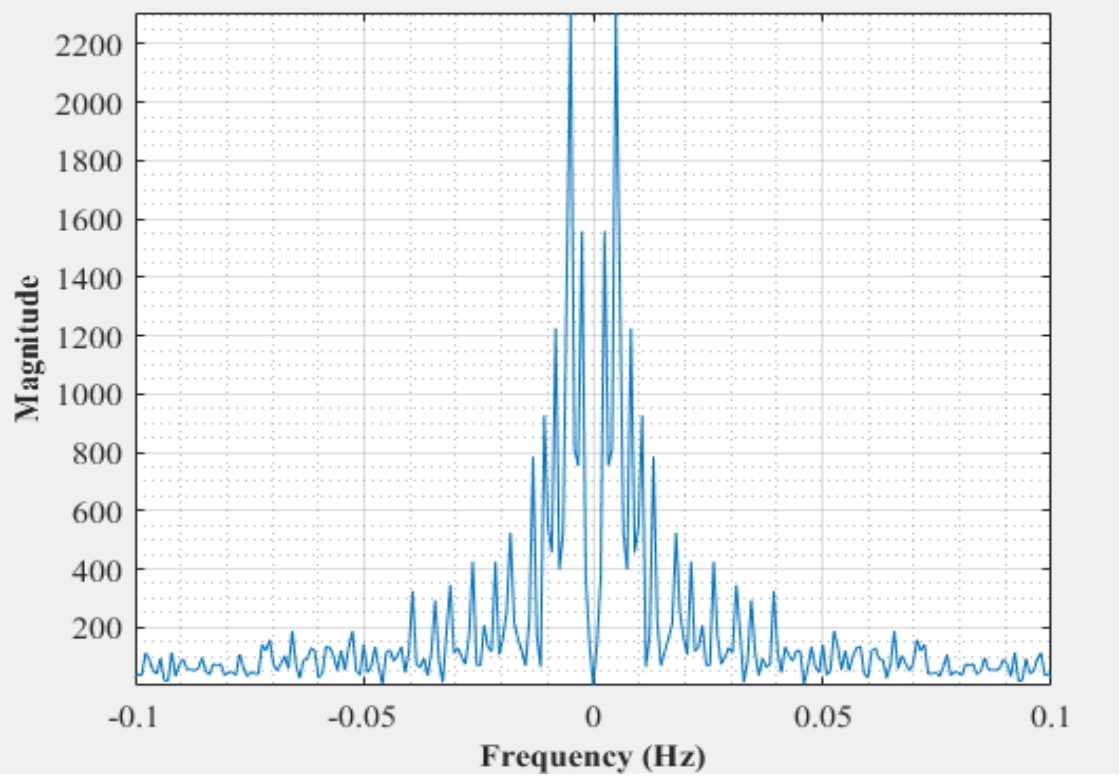


*Figure C-100: Dominant Frequency for a non-uniformly packed vessel (large and small at the side) at 22.5 dm$^3$/minute gas flow rate- Test 3*

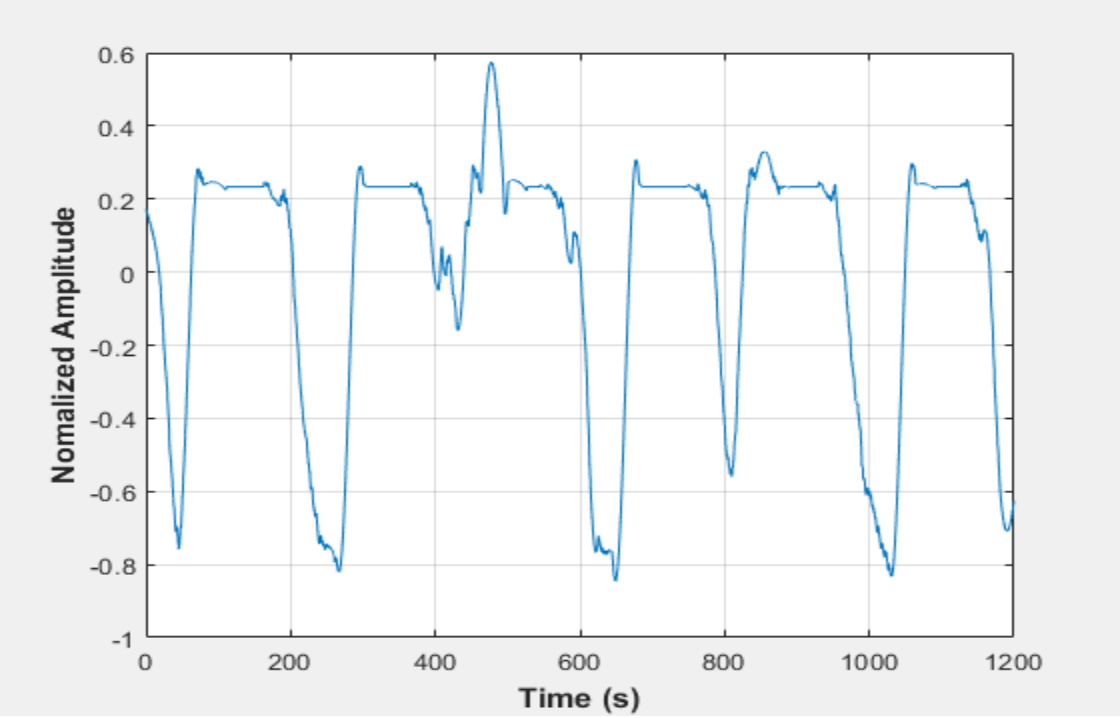


*Figure C-101: Pressure fluctuations in a non-uniformly packed vessel (large and small at the side) at 22.5 dm$^3$/minute gas flow rate- Test 4*

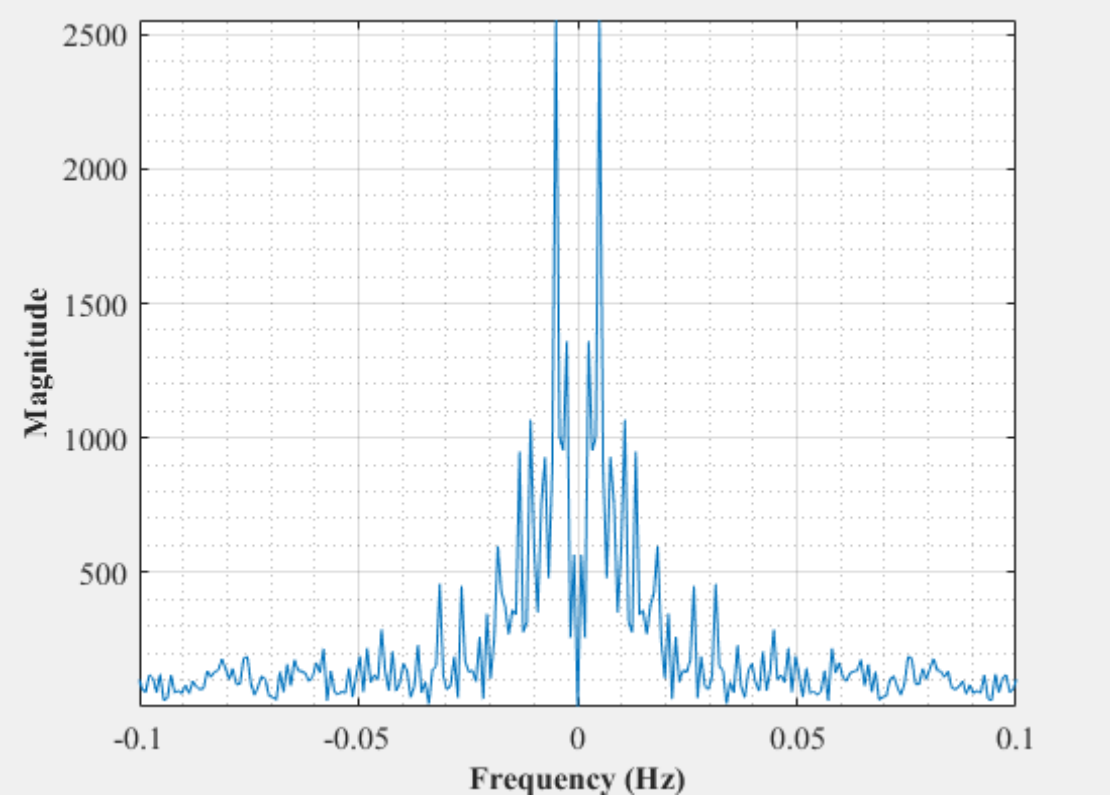


*Figure C-102: Dominant Frequency for a non-uniformly packed vessel (large and small at the side) at 22.5 dm$^3$/minute gas flow rate- Test 4*

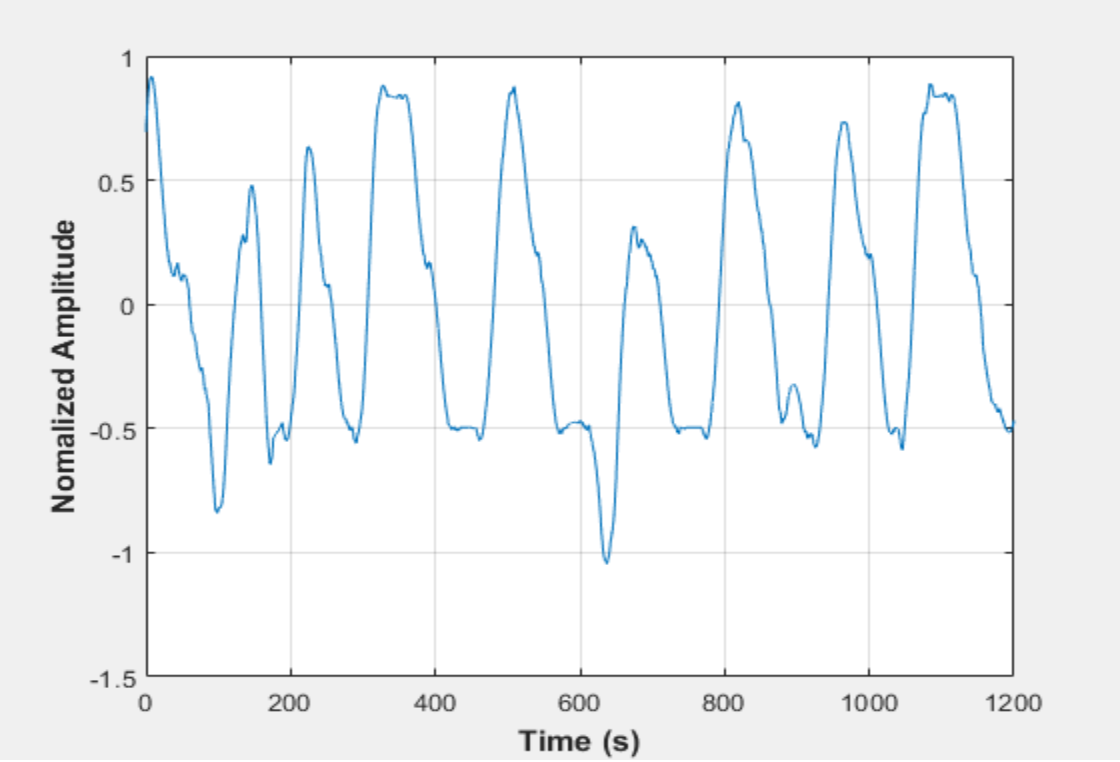


*Figure C-103: Pressure fluctuations in a non-uniformly packed vessel (large and small at the side) at 29 dm$^3$/minute gas flow rate- Test 1*

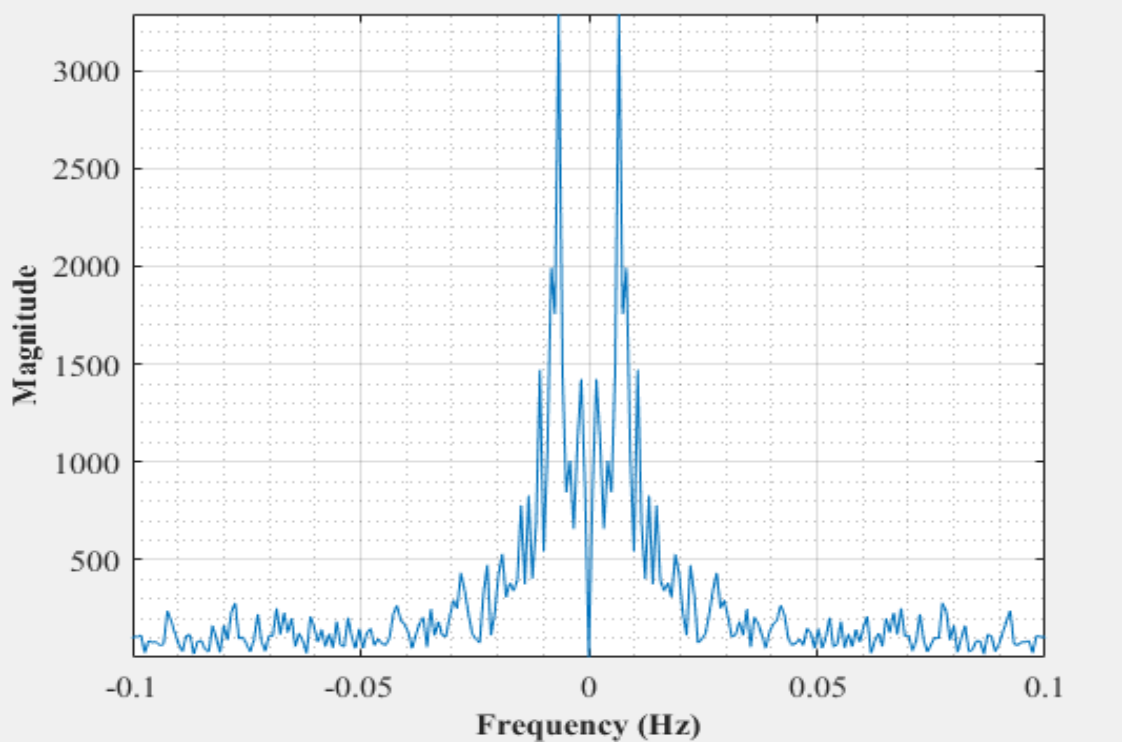


*Figure C-104: Dominant Frequency for a non-uniformly packed vessel (large and small at the side) at 29 dm$^3$/minute gas flow rate- Test 1*

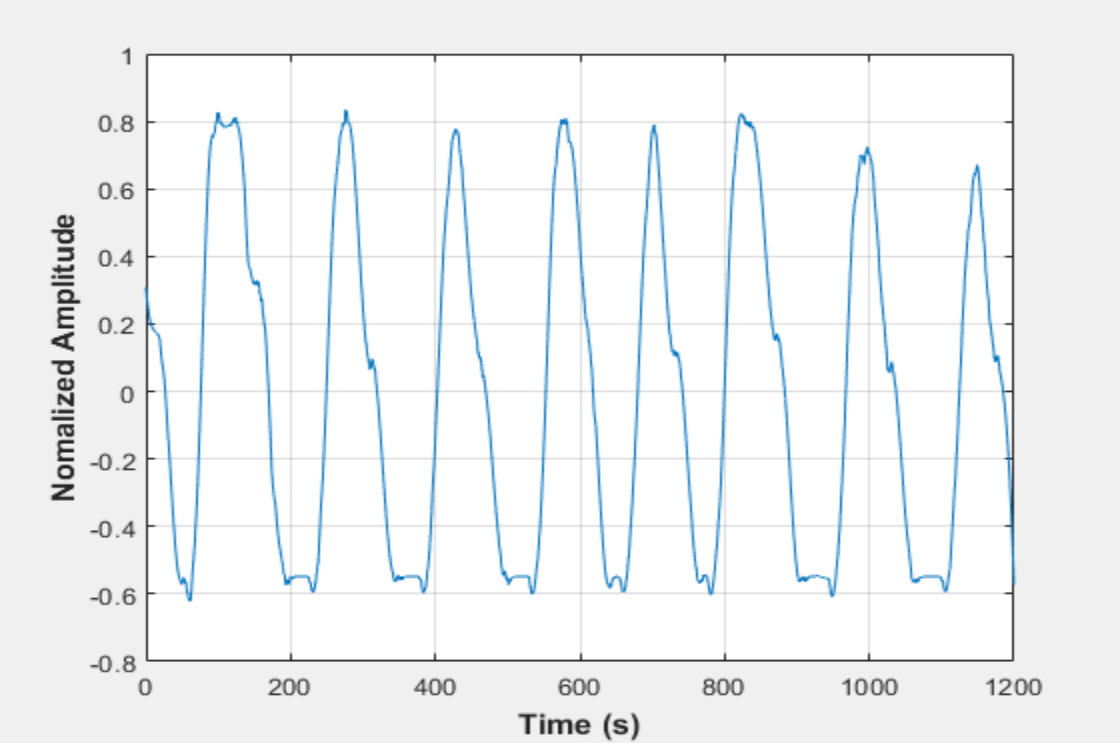


*Figure C-105: Pressure fluctuations in a non-uniformly packed vessel (large and small at the side) at 29 dm$^3$/minute gas flow rate- Test 2*

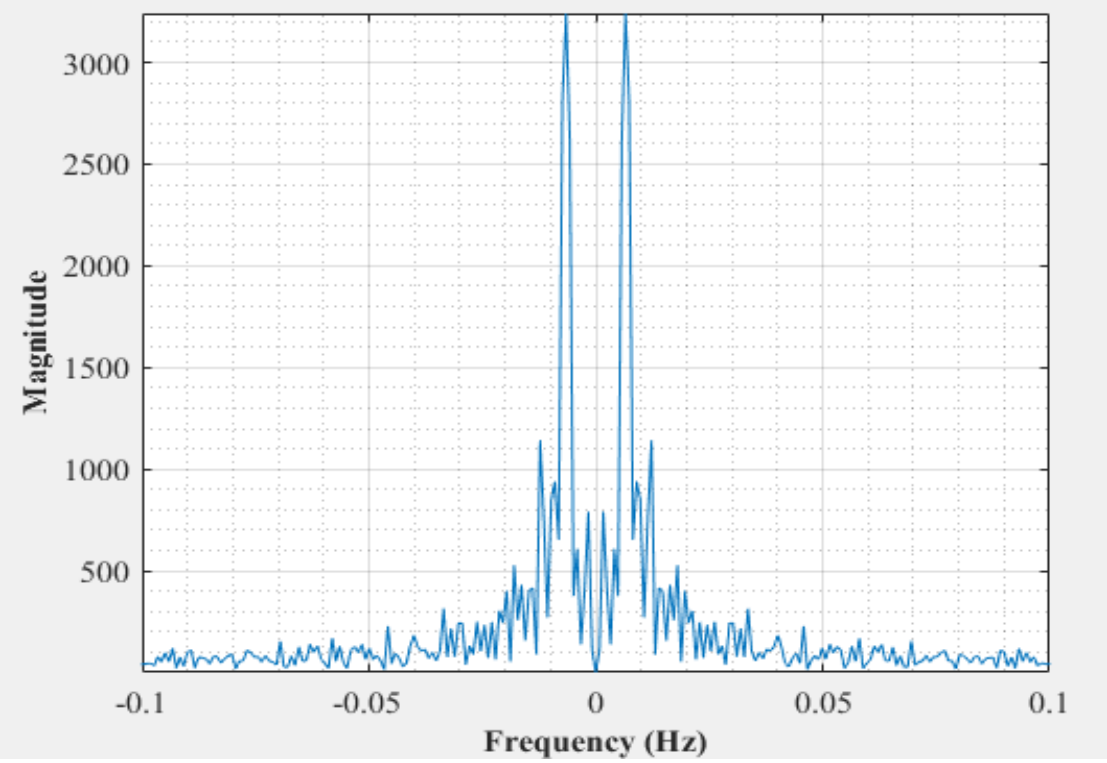


*Figure C-106: Dominant Frequency for a non-uniformly packed vessel (large and small at the side) at 29 dm$^3$/minute gas flow rate- Test 2*

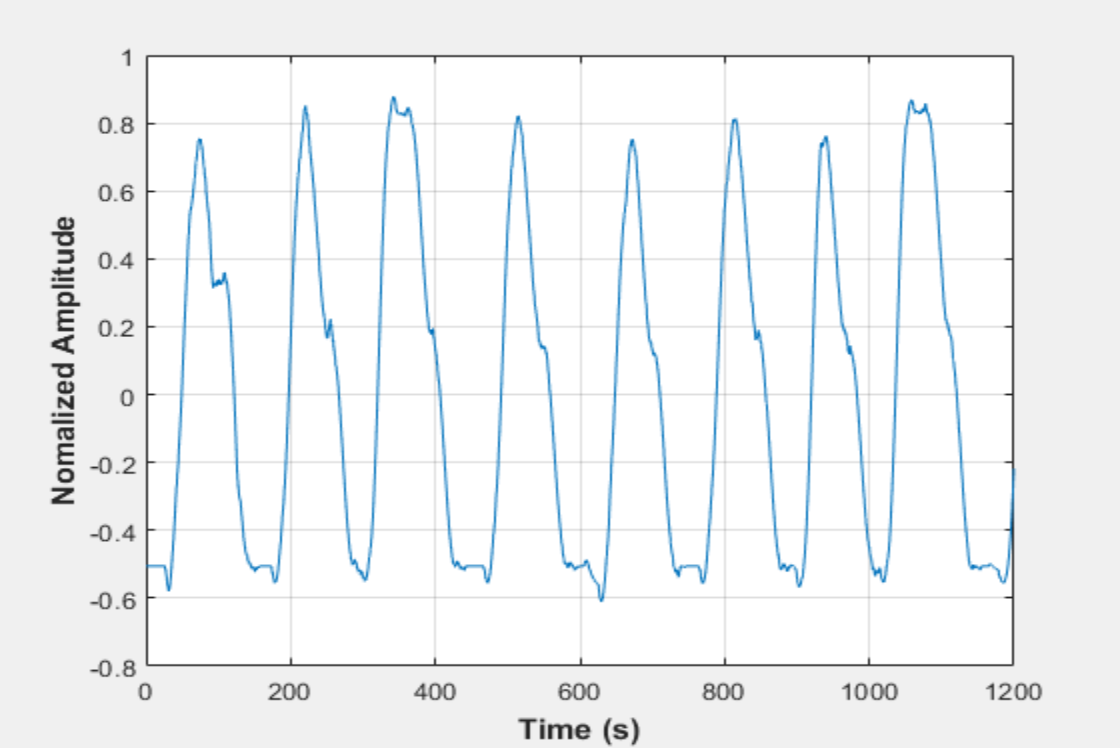


*Figure C-107: Pressure fluctuations in a non-uniformly packed vessel (large and small at the side) at 29 dm$^3$/minute gas flow rate- Test 3*

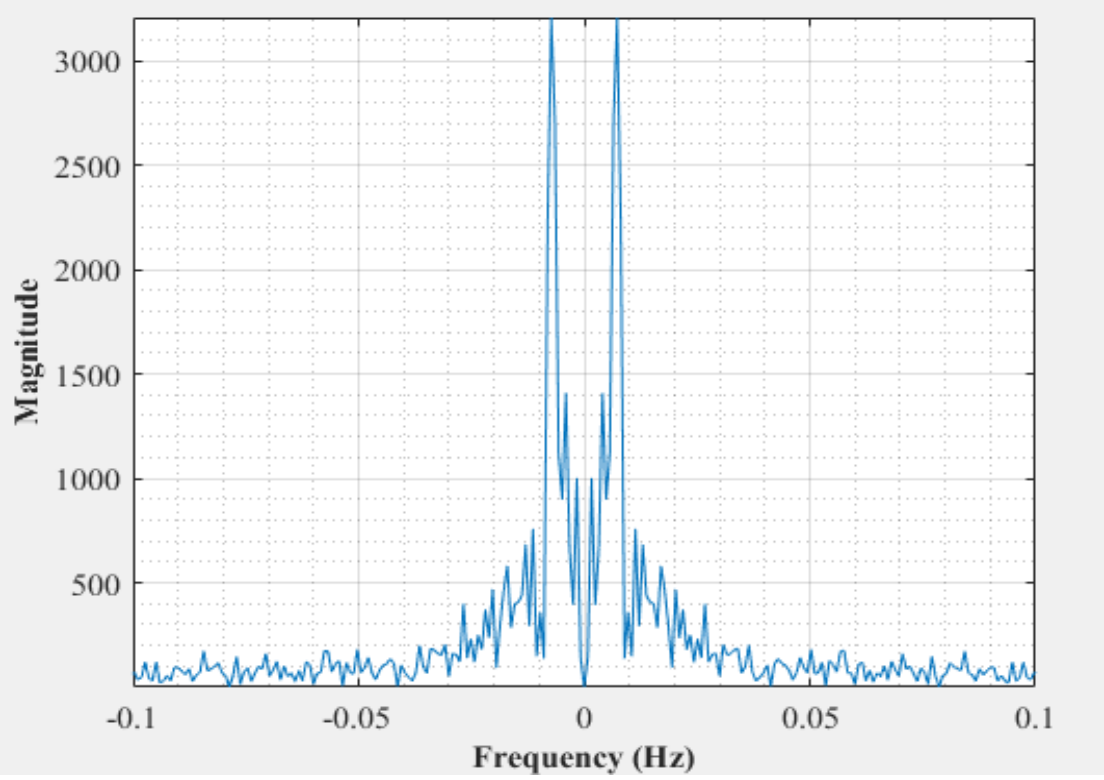


*Figure C-108: Dominant Frequency for a non-uniformly packed vessel (large and small at the side) at 29 dm$^3$/minute gas flow rate- Test 3*

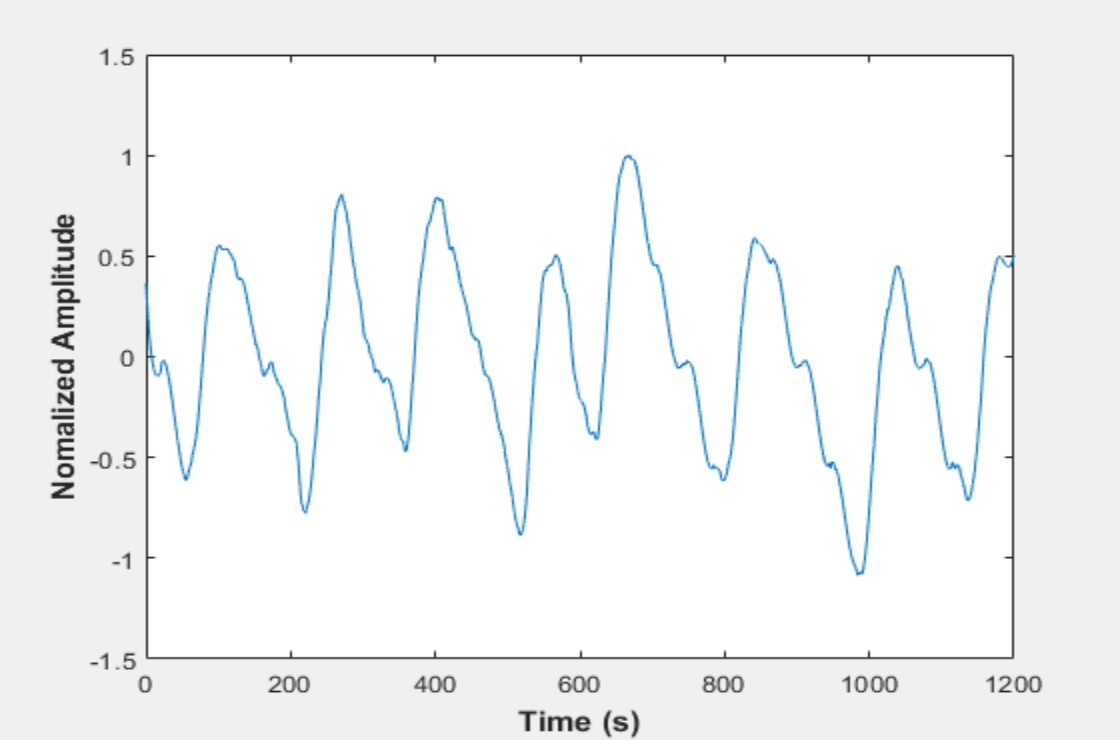


*Figure C-109: Pressure fluctuations in a non-uniformly packed vessel (large and small at the side) at 33 dm$^3$/minute gas flow rate- Test 1*

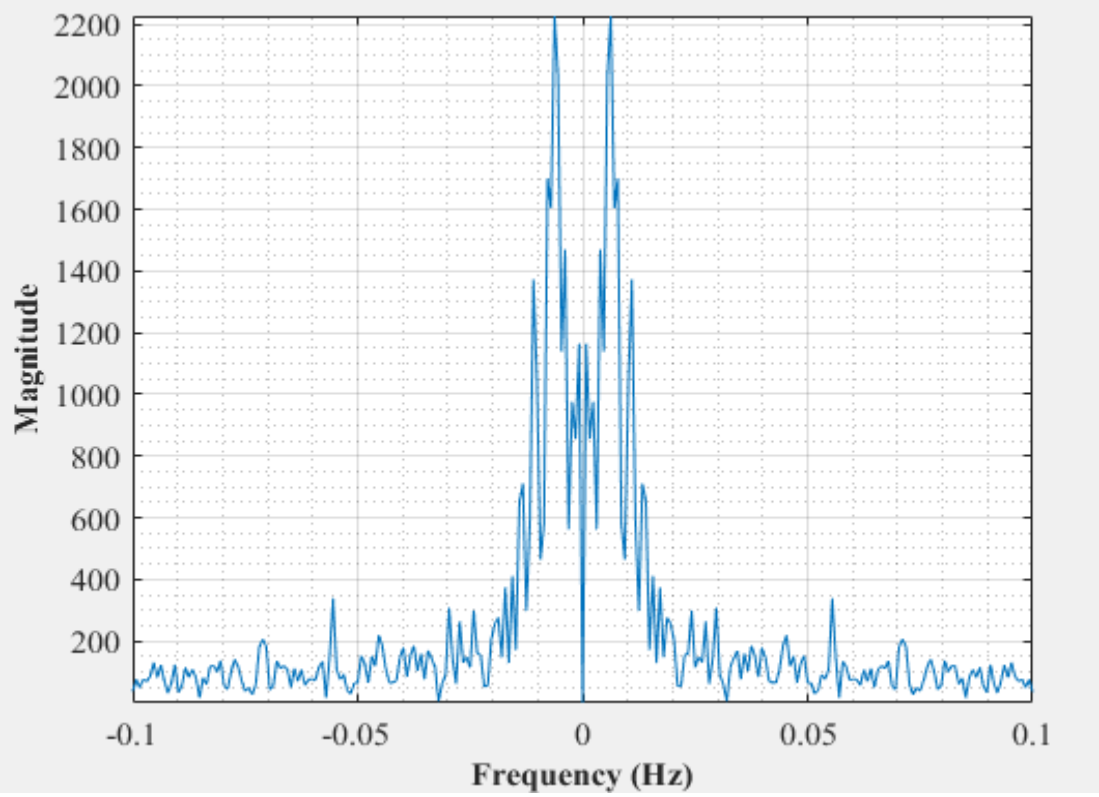


*Figure C-110: Dominant Frequency for a non-uniformly packed vessel (large and small at the side) at 33 dm$^3$/minute gas flow rate- Test 1*

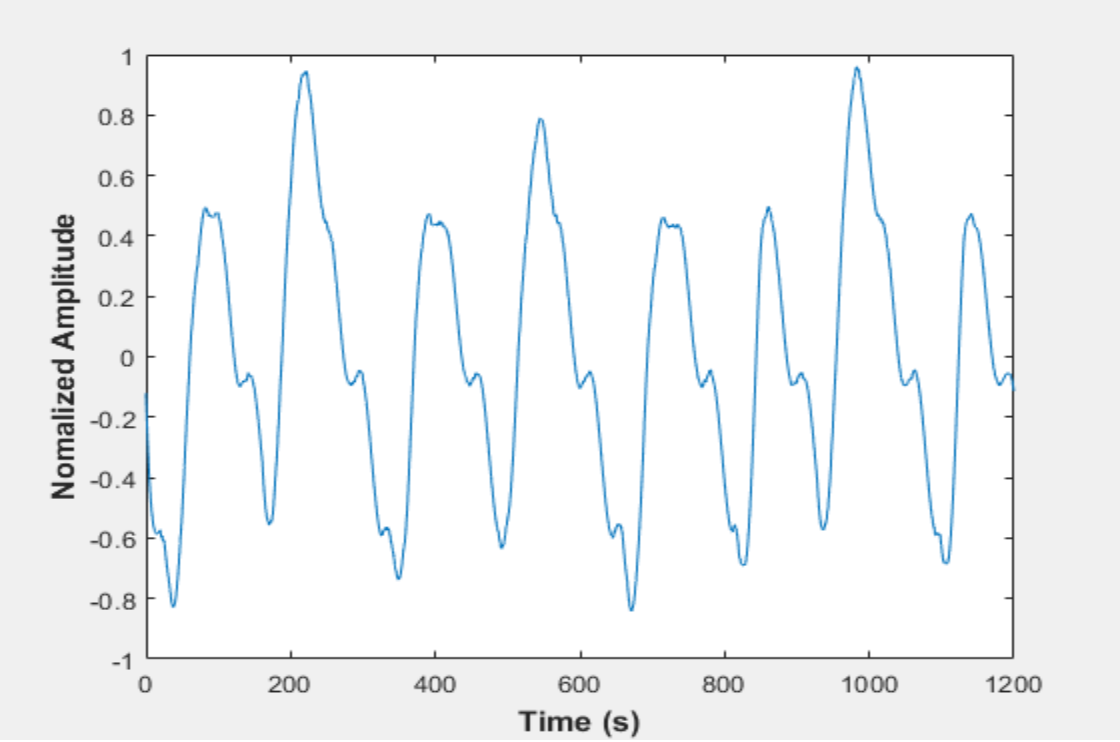


*Figure C-111: Pressure fluctuations in a non-uniformly packed vessel (large and small at the side) at 33 dm$^3$/minute gas flow rate- Test 2*

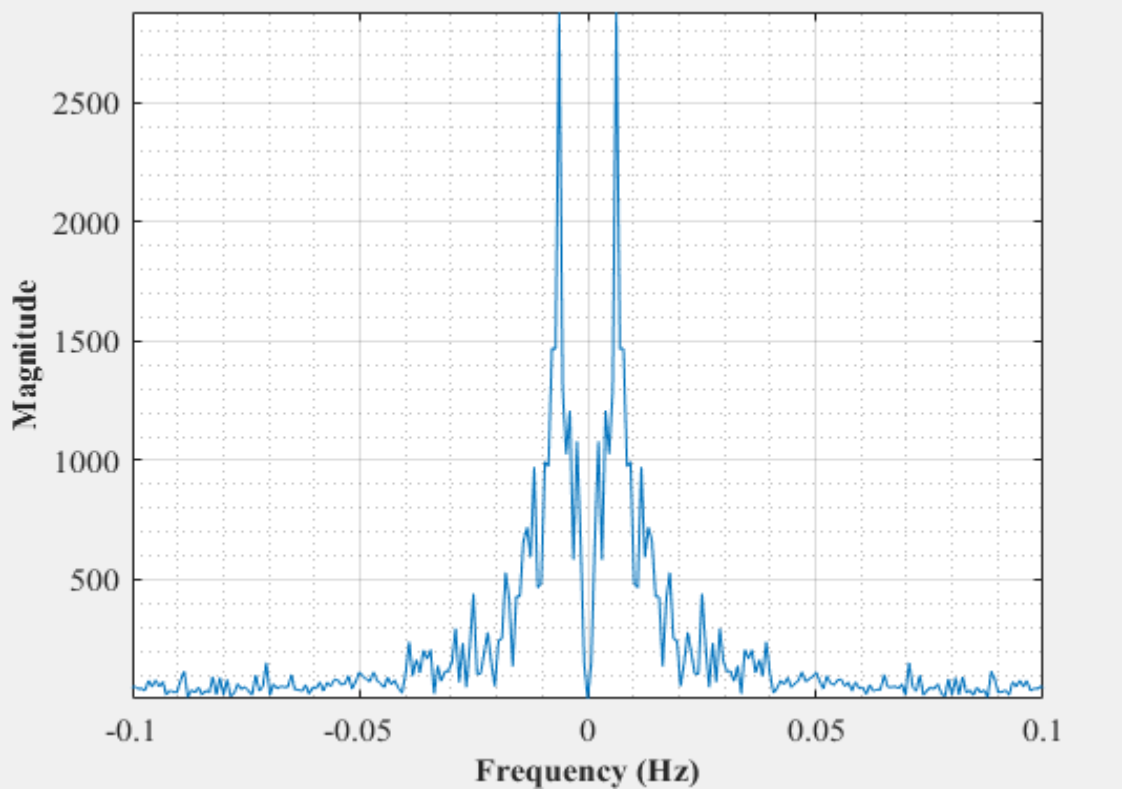


*Figure C-112: Dominant Frequency for a non-uniformly packed vessel (large and small at the side) at 33 dm$^3$/minute gas flow rate- Test 2*

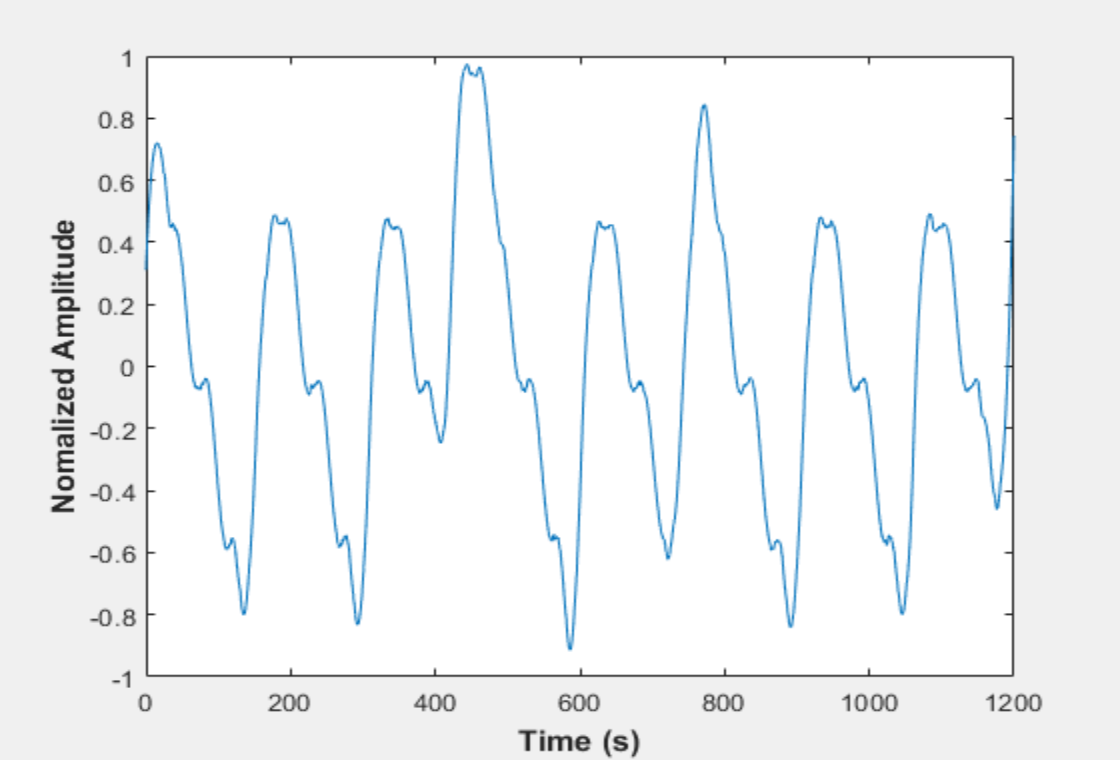


*Figure C-113: Pressure fluctuations in a non-uniformly packed vessel (large and small at the side) at 33 dm$^3$/minute gas flow rate- Test 3*

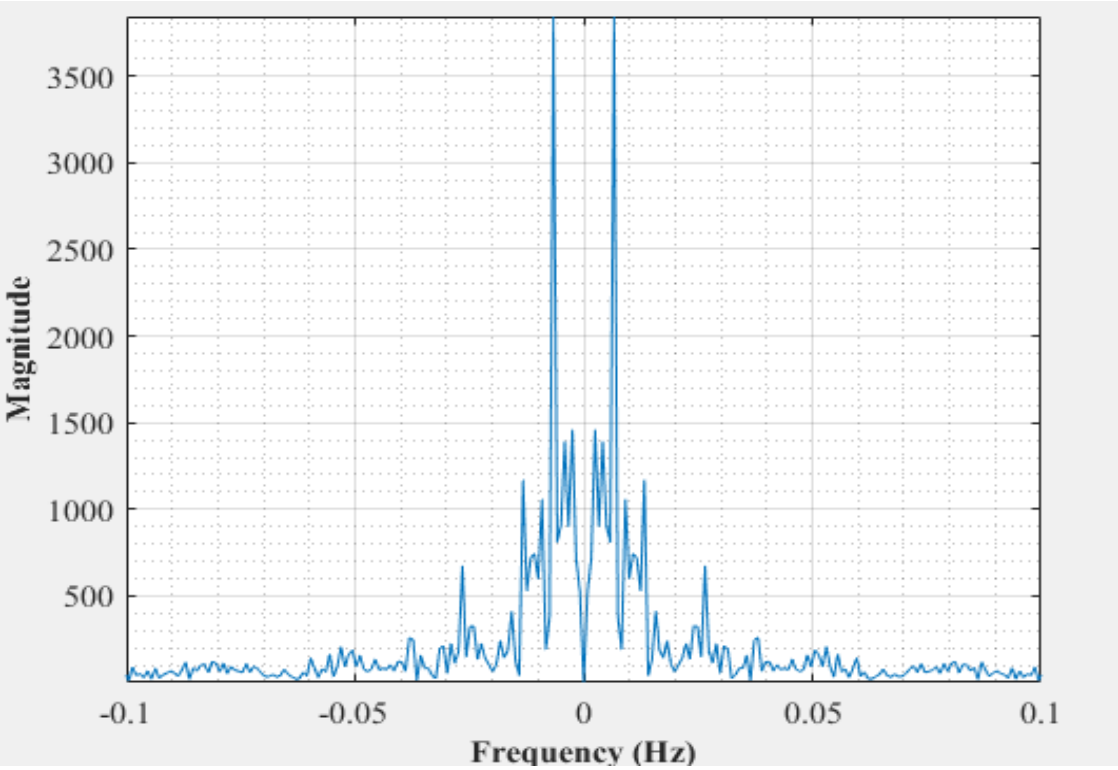


*Figure C-114: Dominant Frequency for a non-uniformly packed vessel (large and small at the side) at 33 dm$^3$/minute gas flow rate- Test 3*

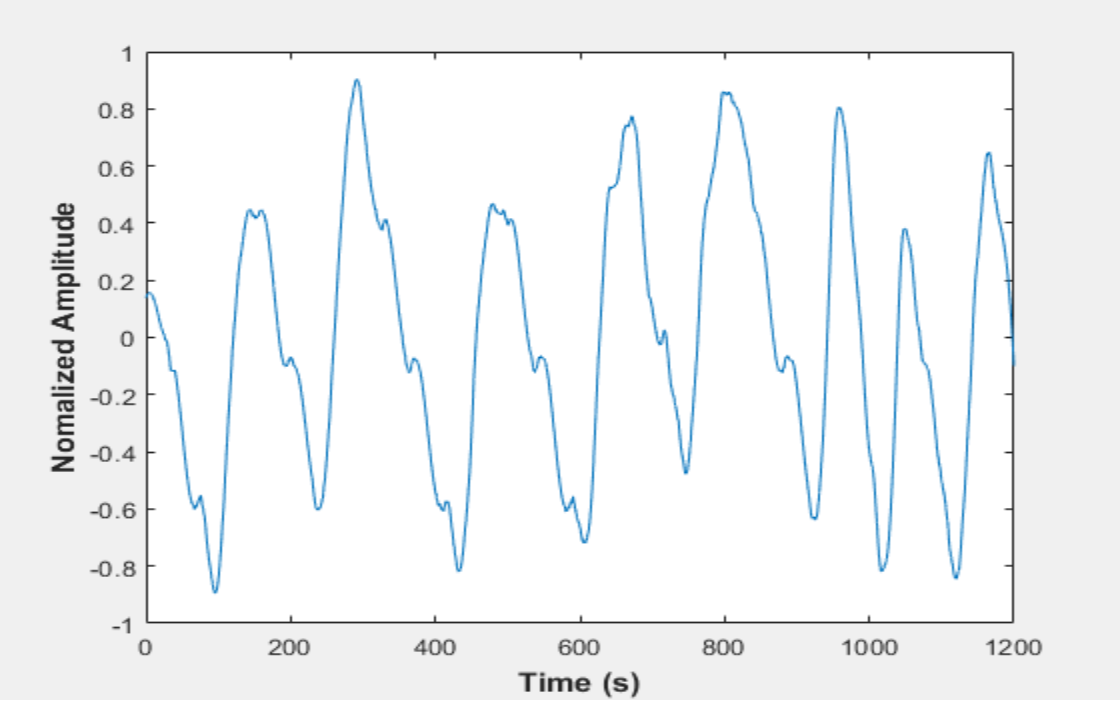


*Figure C-115: Pressure fluctuations in a non-uniformly packed vessel (large and small at the side) at 33 dm$^3$/minute gas flow rate- Test 4*

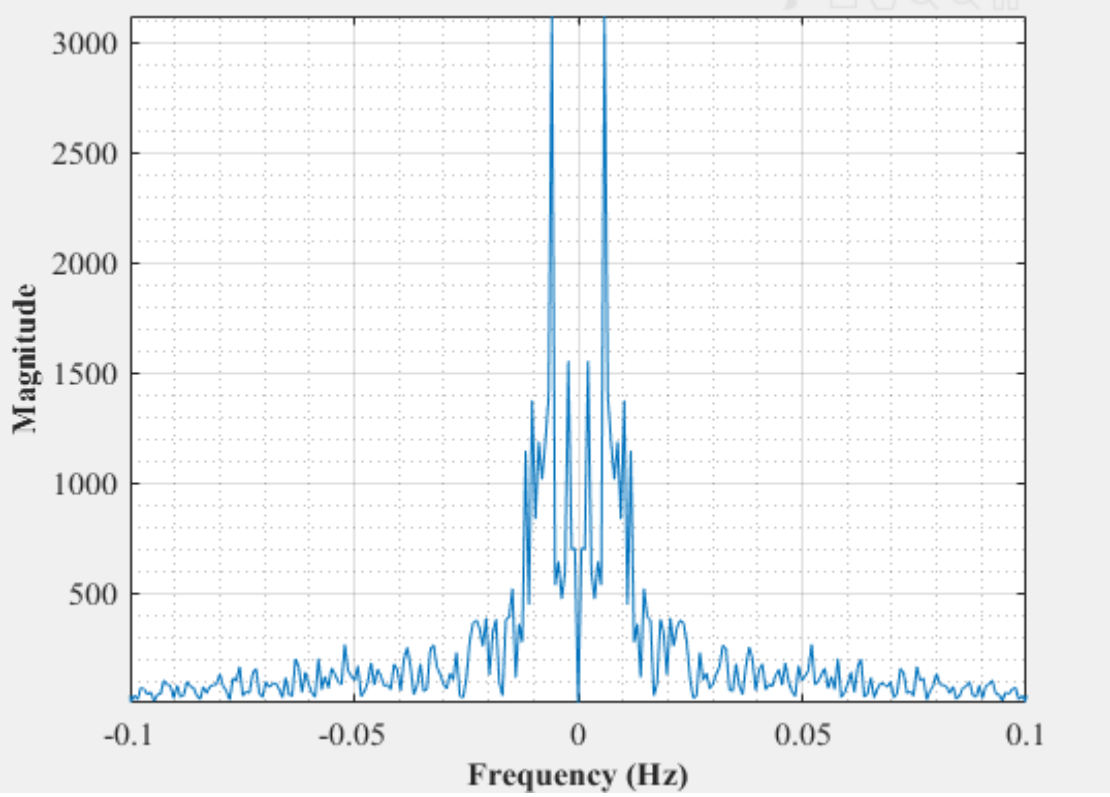


*Figure C-116: Dominant Frequency for a non-uniformly packed vessel (large and small at the side) at 33 dm$^3$/minute gas flow rate- Test 4*

*Table C-1: Third Batch Experimental Results- Frequency (mHz) Data at Various Flowrates*

| Rotameter Flowrate ($dm^3$/minute) | 20,0 | | | | | 22,5 | | | | | 29,0 | | | | | 33,0 | | | | |
|---|---|---|---|---|---|---|---|---|---|---|---|---|---|---|---|---|---|---|---|---|
| | Test 1 | Test 2 | Test 3 | Test 4 | Average | Test 1 | Test 2 | Test 3 | Test 4 | Average | Test 1 | Test 2 | Test 3 | Test 4 | Average | Test 1 | Test 2 | Test 3 | Test 4 | Average |
| Empty | 11,00 | 13,00 | 14,00 | | 12,67 | 10,02 | 7,26 | 8,51 | 13,02 | 9,70 | 7,59 | 7,07 | 5,51 | 7,17 | 6,83 | 5,56 | 5,56 | 6,43 | 6,64 | 6,05 |
| Large Packing | 6,50 | 21,00 | 14,00 | 7,00 | 12,13 | 5,42 | 5,42 | 15,29 | | 8,71 | 5,54 | 5,60 | 5,46 | | 5,53 | 6,27 | 7,44 | 5,88 | 6,49 | 6,52 |
| Large + small (centre) | 6,50 | 9,90 | 12,00 | 14,00 | 10,60 | 7,00 | 13,36 | 11,64 | | 10,67 | 5,84 | 6,02 | 5,72 | | 5,86 | 5,90 | 6,45 | 7,32 | 6,22 | 6,47 |
| Large +small (side) | 6,20 | 15,00 | 8,30 | 14,00 | 10,88 | 5,09 | 5,42 | 5,22 | 5,33 | 5,26 | 7,66 | 6,88 | 7,17 | | 7,24 | 6,54 | 6,63 | 0,64 | 7,14 | 5,24 |

*Table C-2: Third Batch Experimental Results- Amplitude Data at Various Flowrates*

| Rotameter Flowrate ($dm^3$/minute) | 20,0 | | | | | 22,5 | | | | | 29,0 | | | | | 33,0 | | | | |
|---|---|---|---|---|---|---|---|---|---|---|---|---|---|---|---|---|---|---|---|---|
| | Test 1 | Test 2 | Test 3 | Test 4 | Average | Test 1 | Test 2 | Test 3 | Test 4 | Average | Test 1 | Test 2 | Test 3 | Test 4 | Average | Test 1 | Test 2 | Test 3 | Test 4 | Average |
| Empty | 0,19 | 0,14 | 0,25 | | 0,19 | 0,32 | 0,44 | 0,23 | 0,41 | 0,35 | 0,33 | 0,33 | 0,45 | 0,50 | 0,40 | 0,59 | 0,48 | 0,57 | 0,59 | 0,56 |
| Large Packing | 0,23 | 0,24 | 0,43 | 0,43 | 0,33 | 0,20 | 0,21 | 0,13 | | 0,18 | 1,10 | 1,10 | 1,02 | | 1,07 | 0,59 | 0,76 | 0,62 | 0,78 | 0,68 |
| Large + small (centre) | 0,37 | 0,21 | 0,22 | 0,12 | 0,23 | 0,35 | 0,30 | 0,39 | | 0,34 | 0,65 | 0,64 | 0,70 | | 0,66 | 0,66 | 0,66 | 0,49 | 0,65 | 0,62 |
| Large +small (side) | 0,44 | 0,24 | 0,56 | 0,28 | 0,38 | 0,50 | 0,47 | 0,45 | 0,36 | 0,44 | 0,64 | 0,69 | 0,66 | | 0,66 | 0,60 | 0,60 | 0,61 | 0,60 | 0,60 |

## APPENDIX D: Large vessel experiments- 75 % Full

### Introduction

This section shows the graphs for the experiments done on the large vessel while it was 75 % full of packing material as well as when it was empty. Figures D-1 to D-210 show amplitudes and frequency curves for the first batch of experiments. Tables D-1 and D-2 show the summary from the amplitude and frequency data obtained from the experiments.

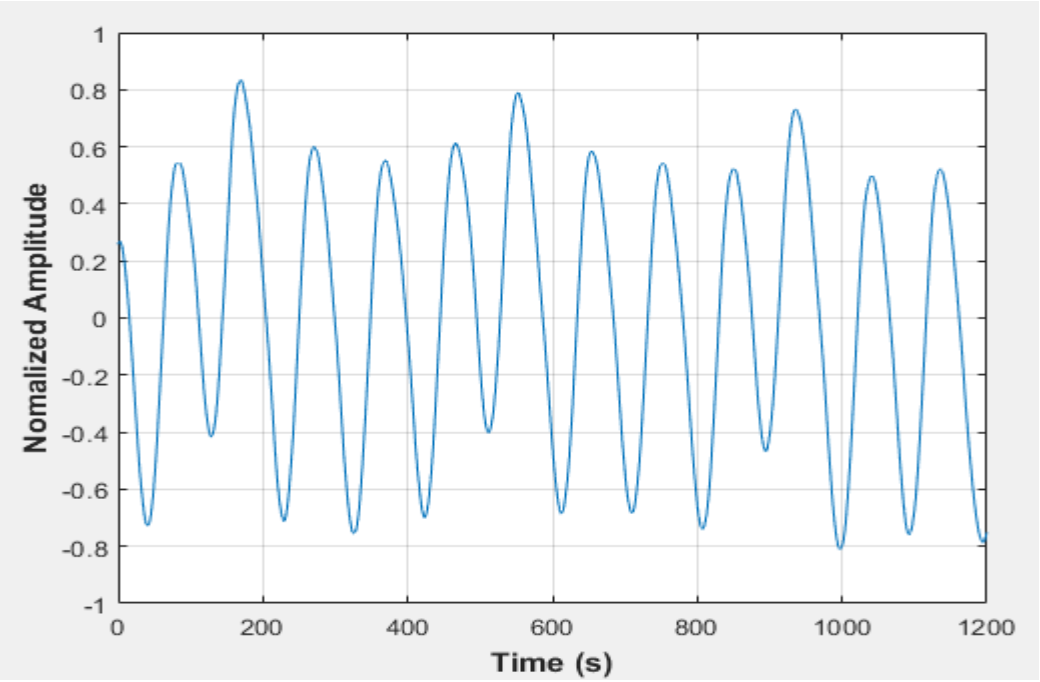


*Figure D-1: Pressure fluctuations in an empty vessel at 1.67 dm$^3$/minute rotameter flow rate- Test 1*

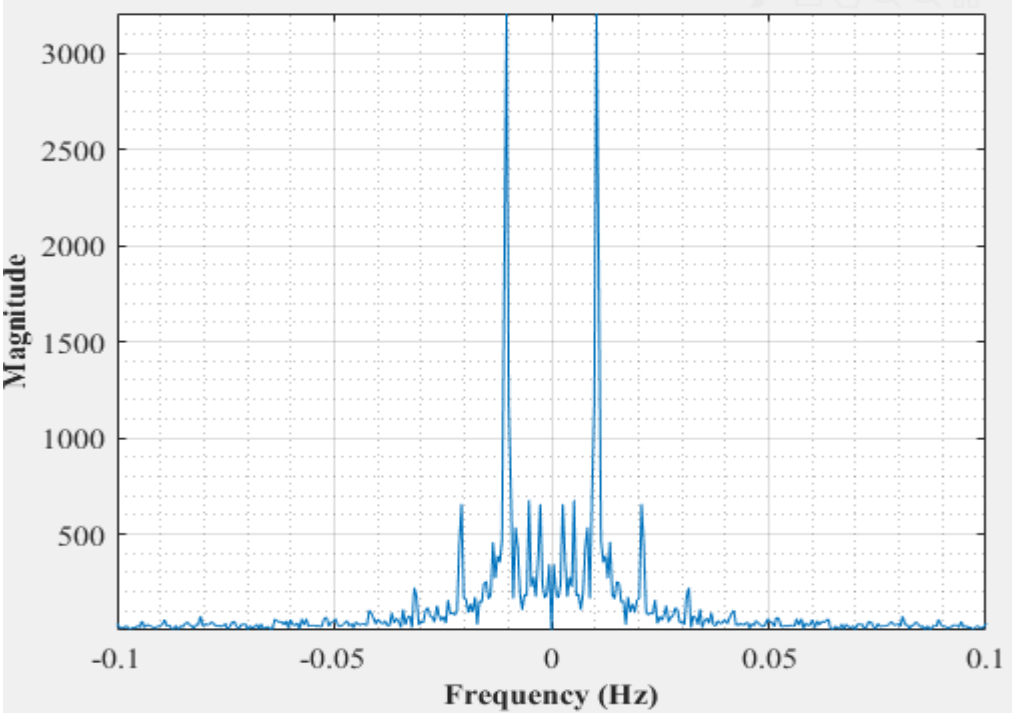


*Figure D-2: Dominant Frequency for an empty vessel at 1.67 dm$^3$/minute rotameter flow rate- Test 1*

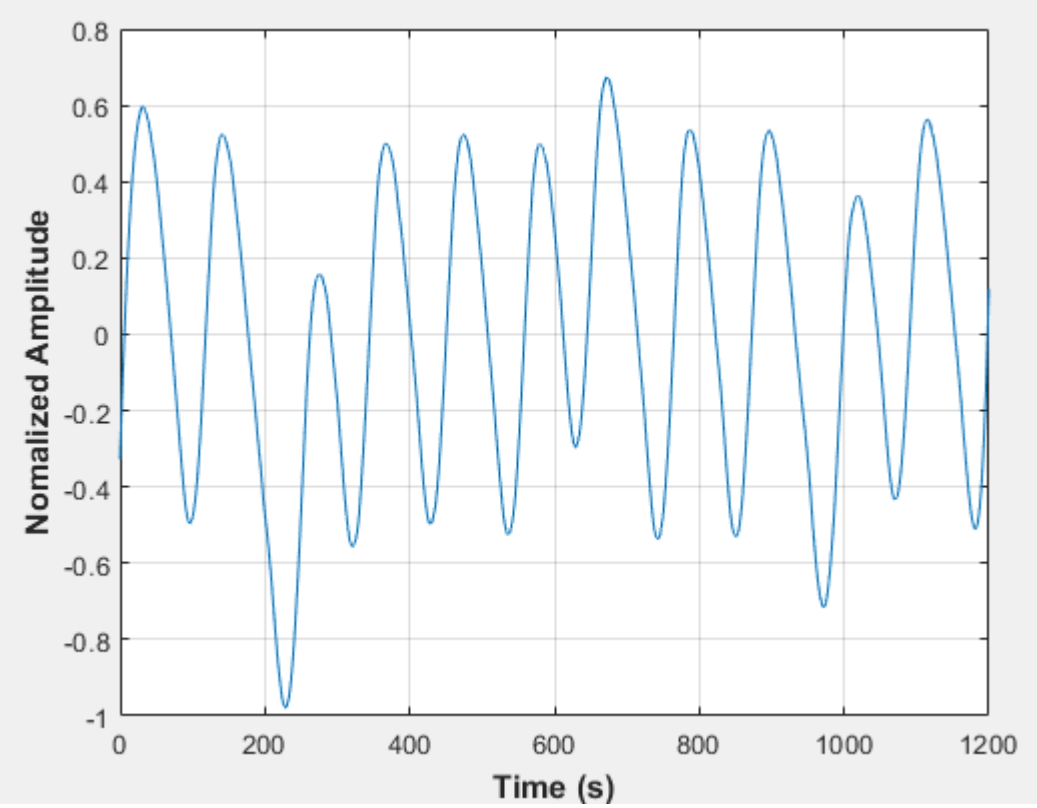


*Figure D-3: Pressure fluctuations in an empty vessel at 1.67 dm$^3$/minute rotameter flow rate- Test 2*

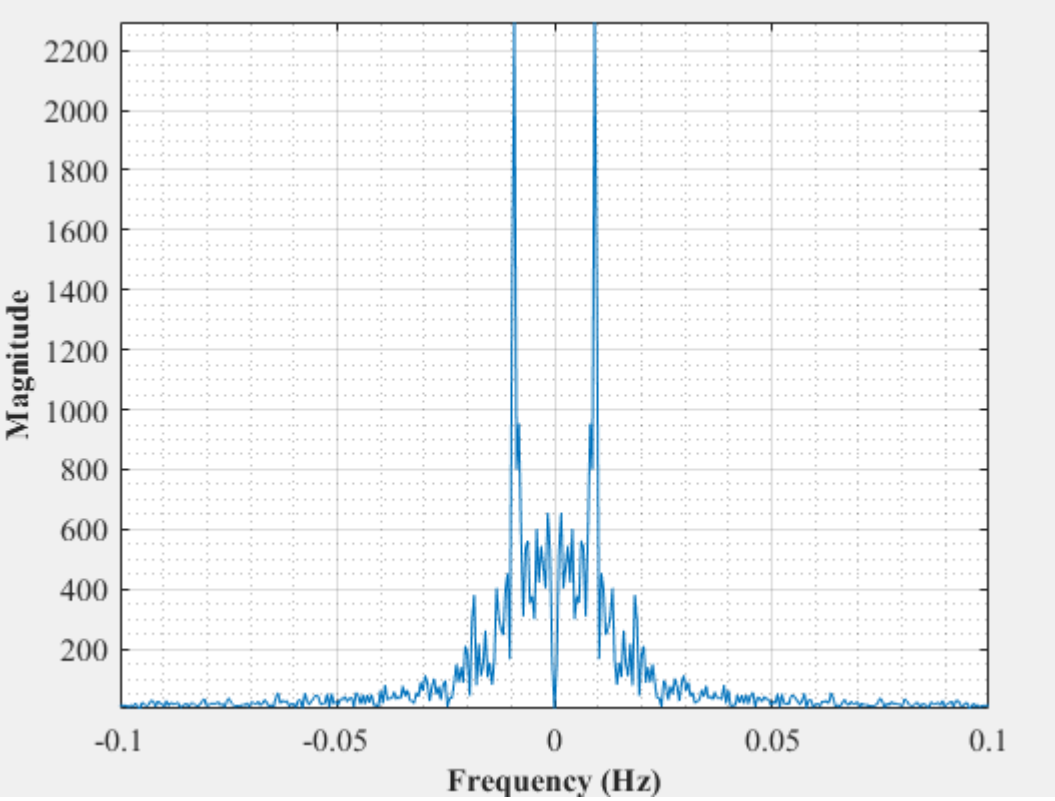


*Figure D-4: Dominant Frequency for an empty vessel at 1.67 dm$^3$/minute rotameter flow rate- Test 2*

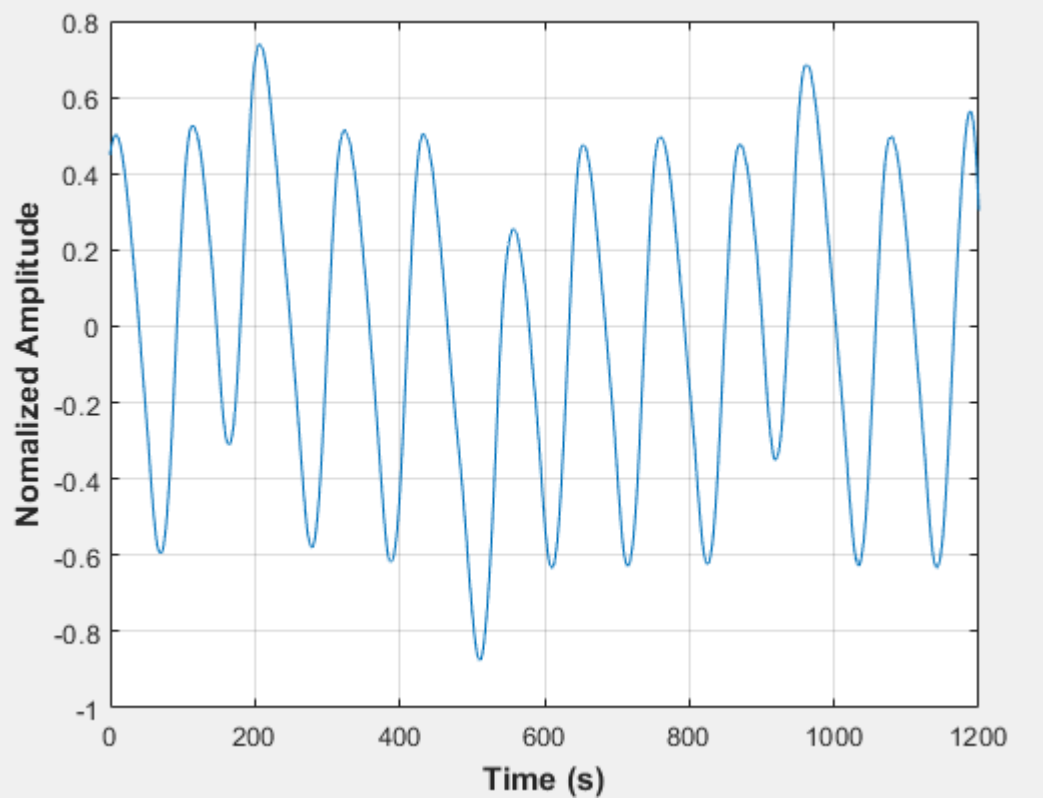


*Figure D-5: Pressure fluctuations in an empty vessel at 1.67 dm$^3$/minute rotameter flow rate- Test 3*

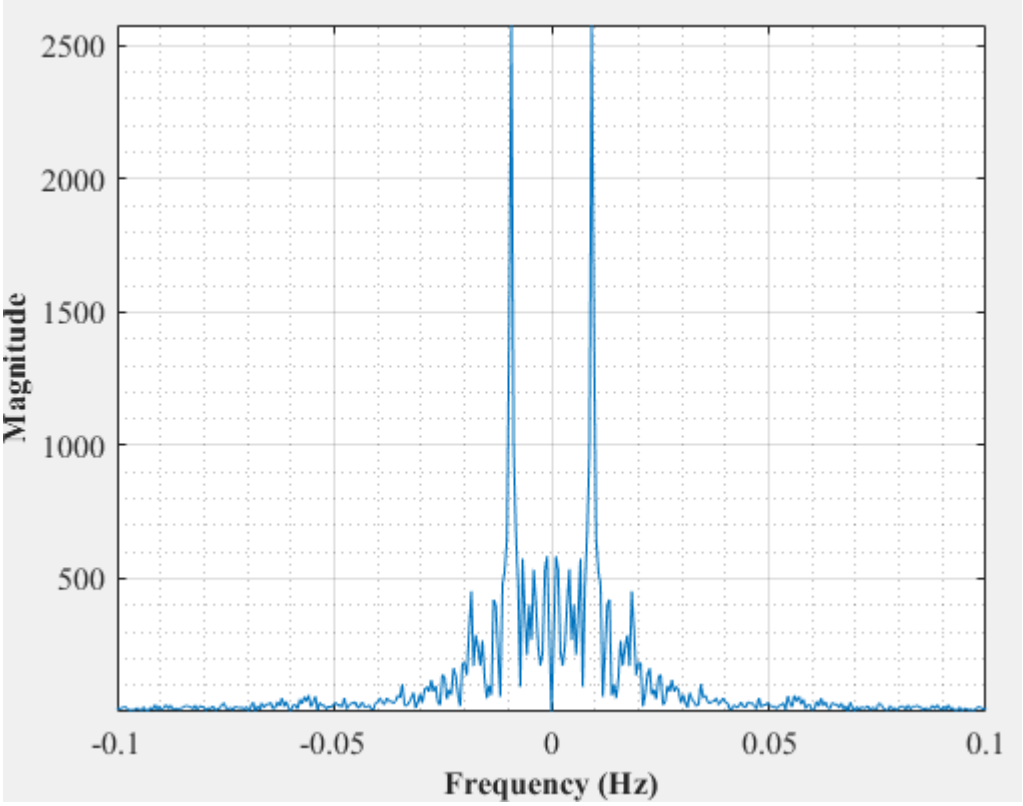


*Figure D-6: Dominant Frequency for an empty vessel at 1.67 dm$^3$/minute rotameter flow rate- Test 3*

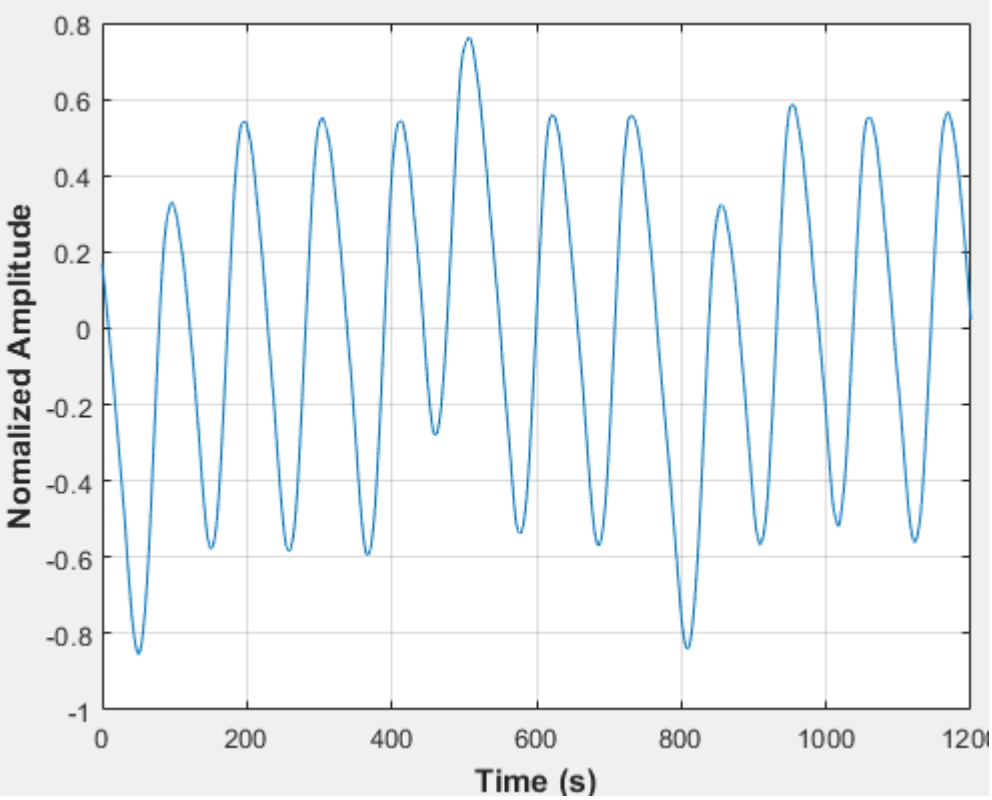


*Figure D-7: Pressure fluctuations in an empty vessel at 1.67 dm$^3$/minute rotameter flow rate- Test 4*

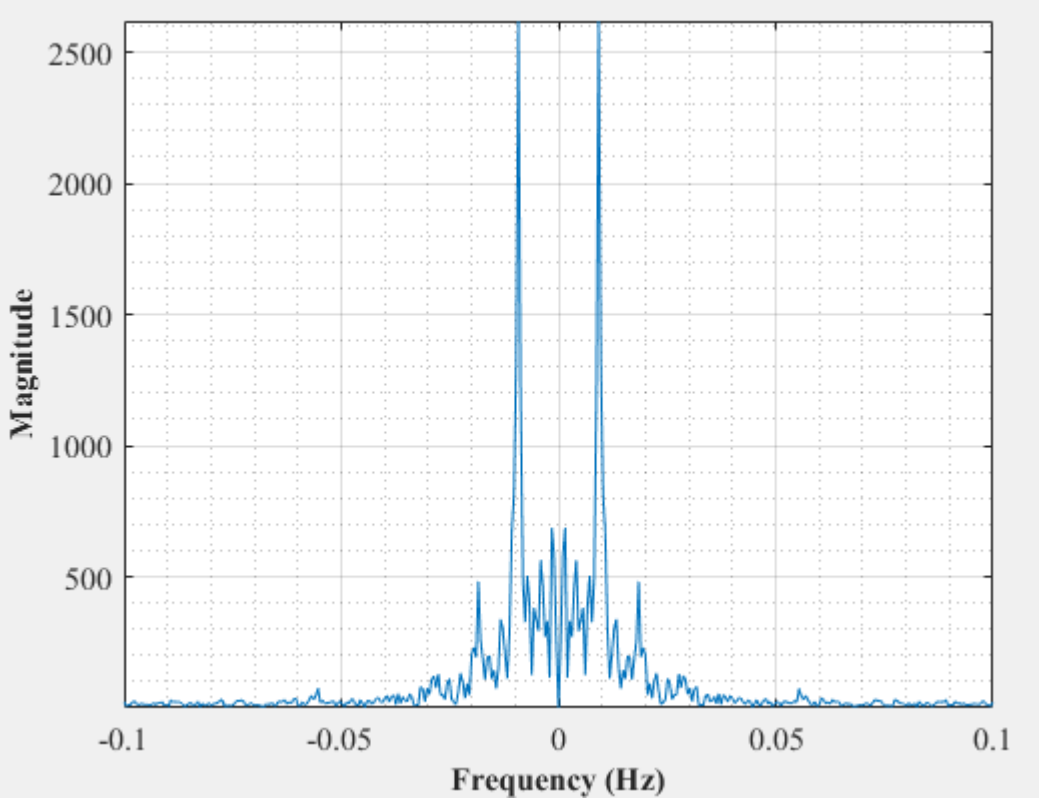


*Figure D-8: Dominant Frequency for an empty vessel at 100l/hour rotameter flow rate- Test 4*

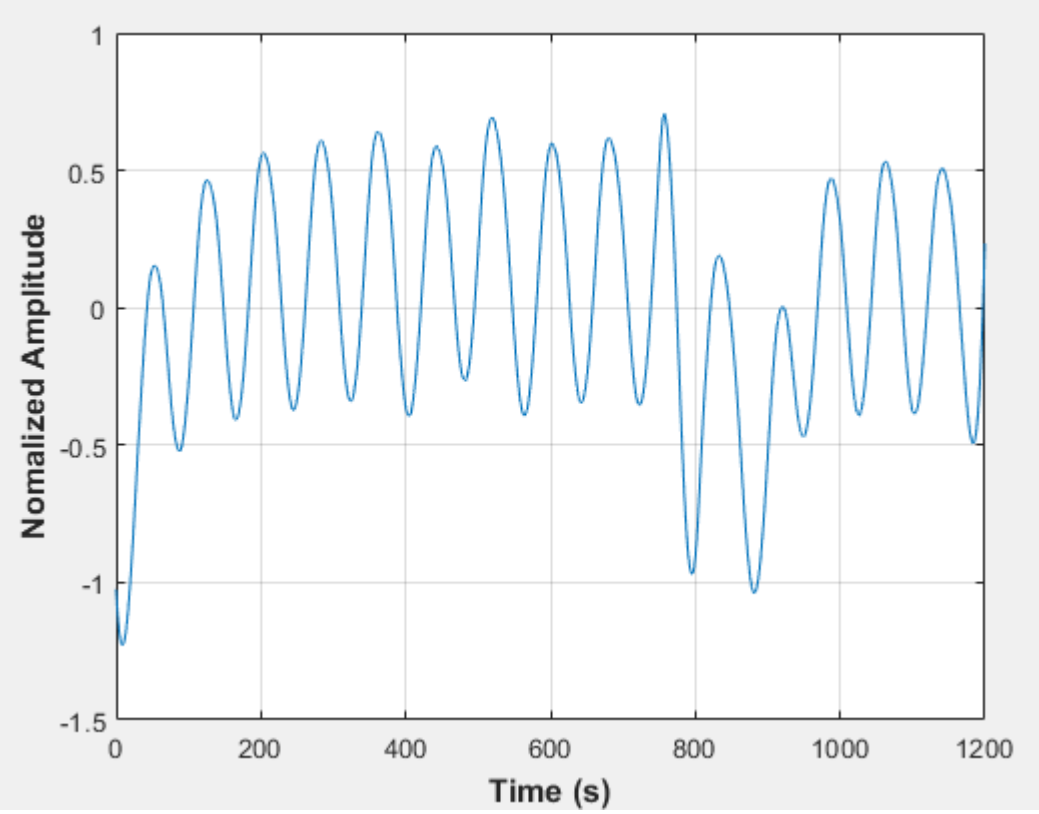


*Figure D-9: Pressure fluctuations in an empty vessel at 2 dm$^3$/minute rotameter flow rate- Test 1*

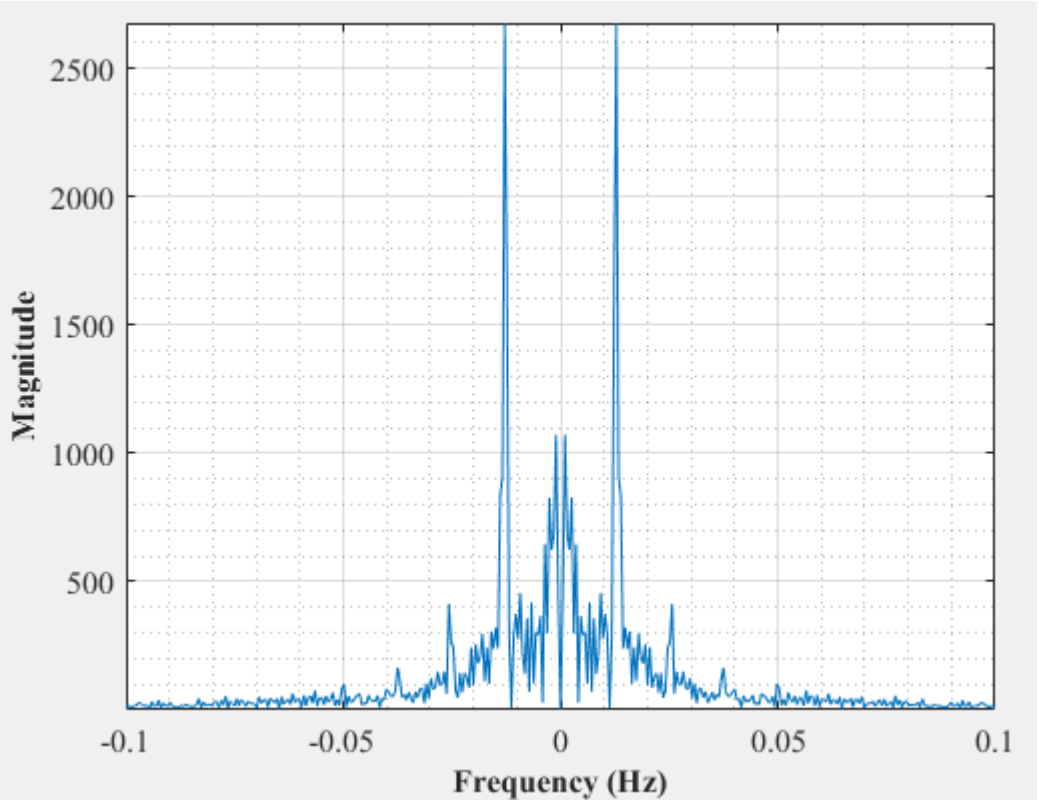


*Figure D-10: Dominant Frequency for an empty vessel at 2 dm$^3$/minute rotameter flow rate- Test 1*

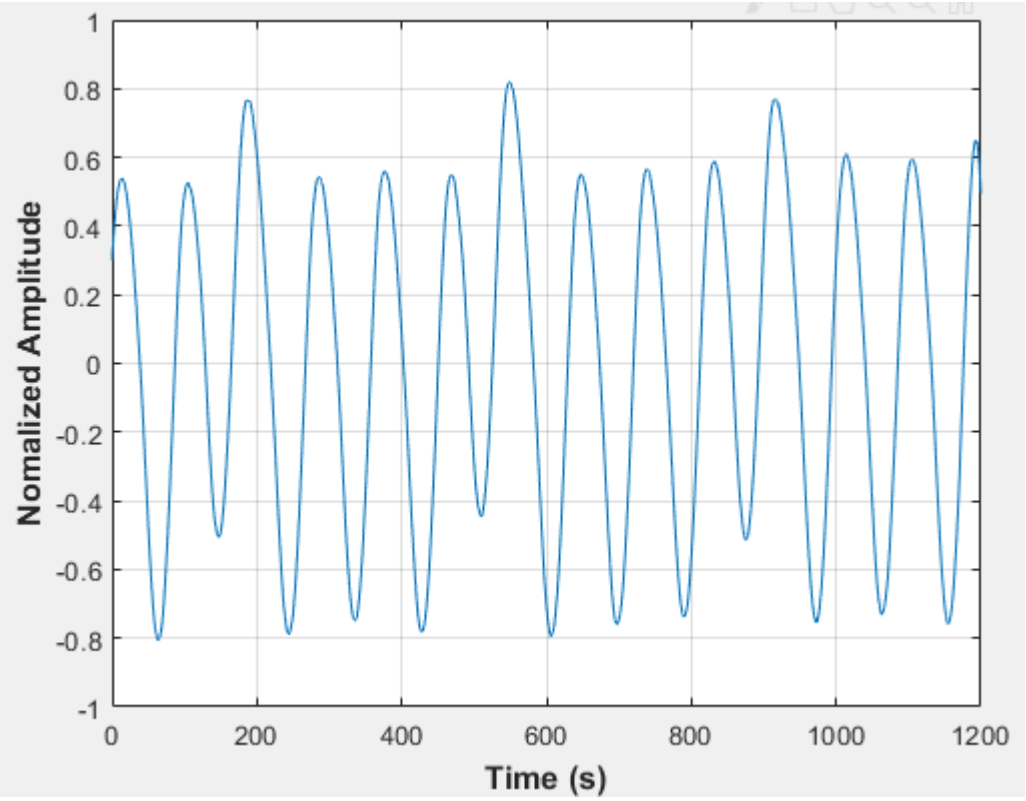


*Figure D-11: Pressure fluctuations in an empty vessel at 2 dm$^3$/minute rotameter flow rate- Test 2*

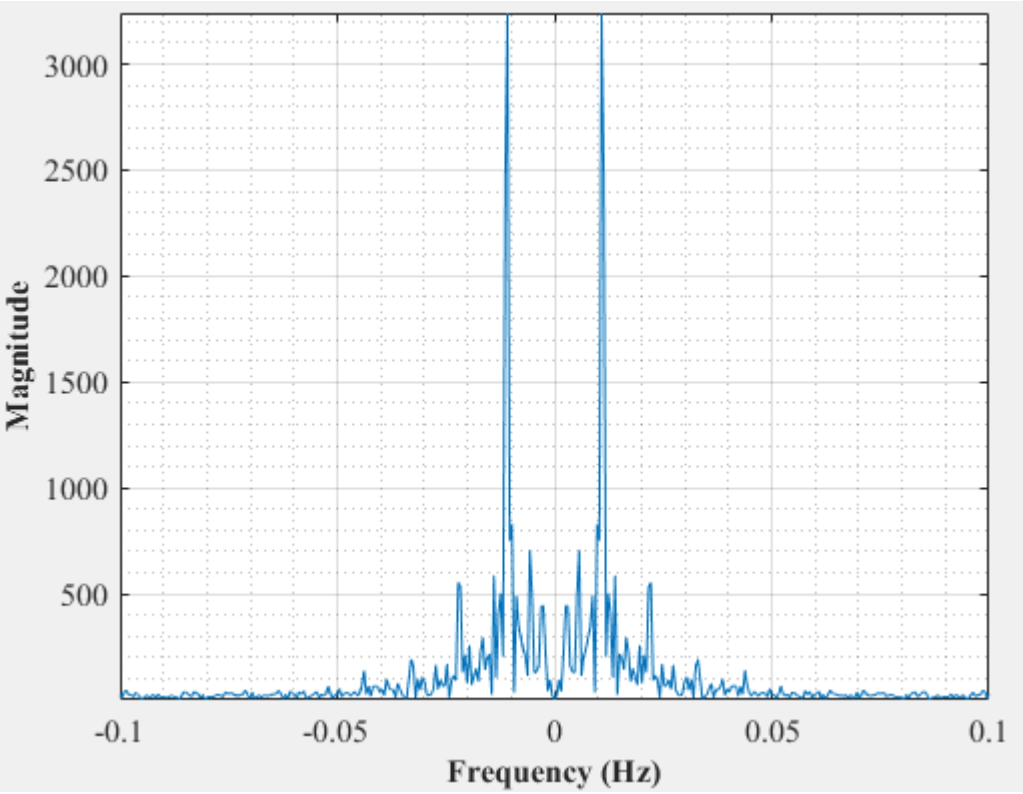


*Figure D-12: Dominant Frequency for an empty vessel at 2 dm$^3$/minute rotameter flow rate- Test 2*

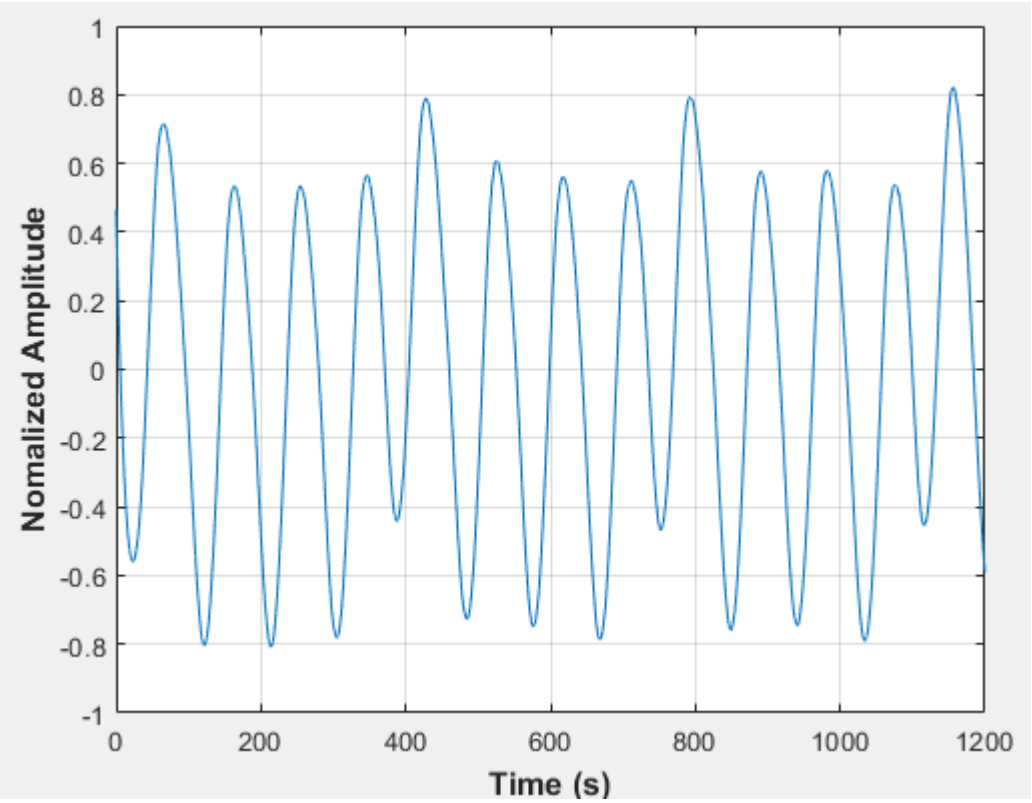


*Figure D-13: Pressure fluctuations in an empty vessel at 2 dm$^3$/minute rotameter flow rate- Test 3*

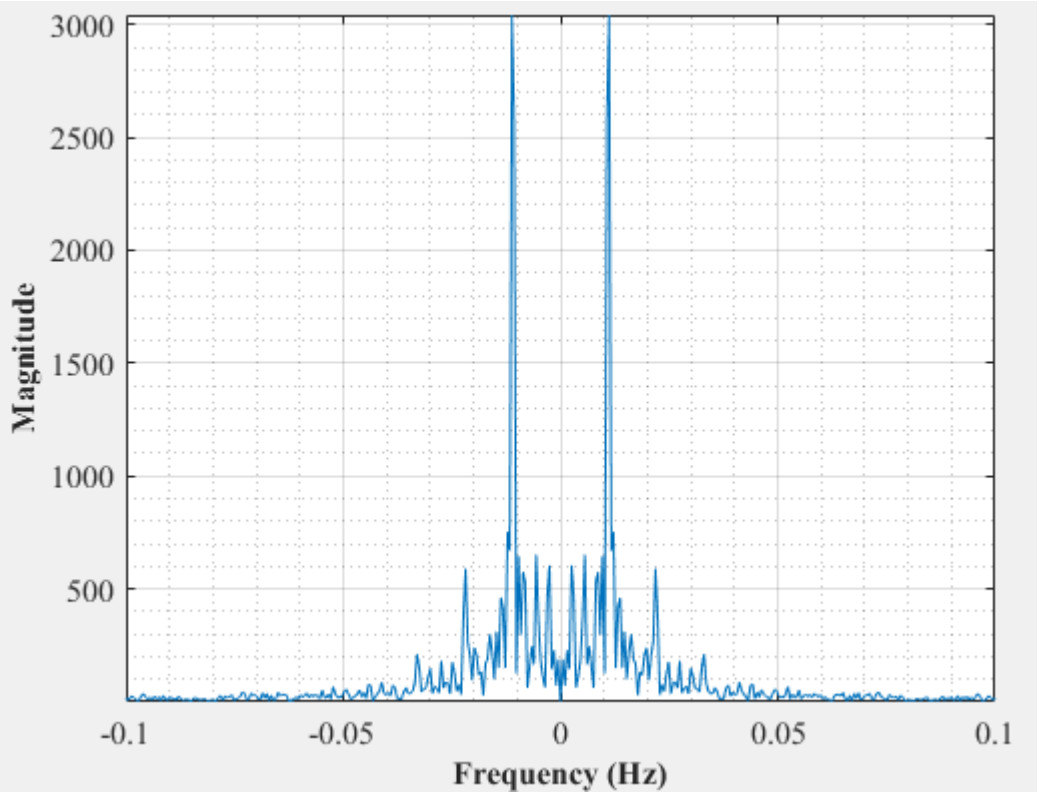


*Figure D-14: Dominant Frequency for an empty vessel at 2 dm$^3$/minute rotameter flow rate- Test 3*

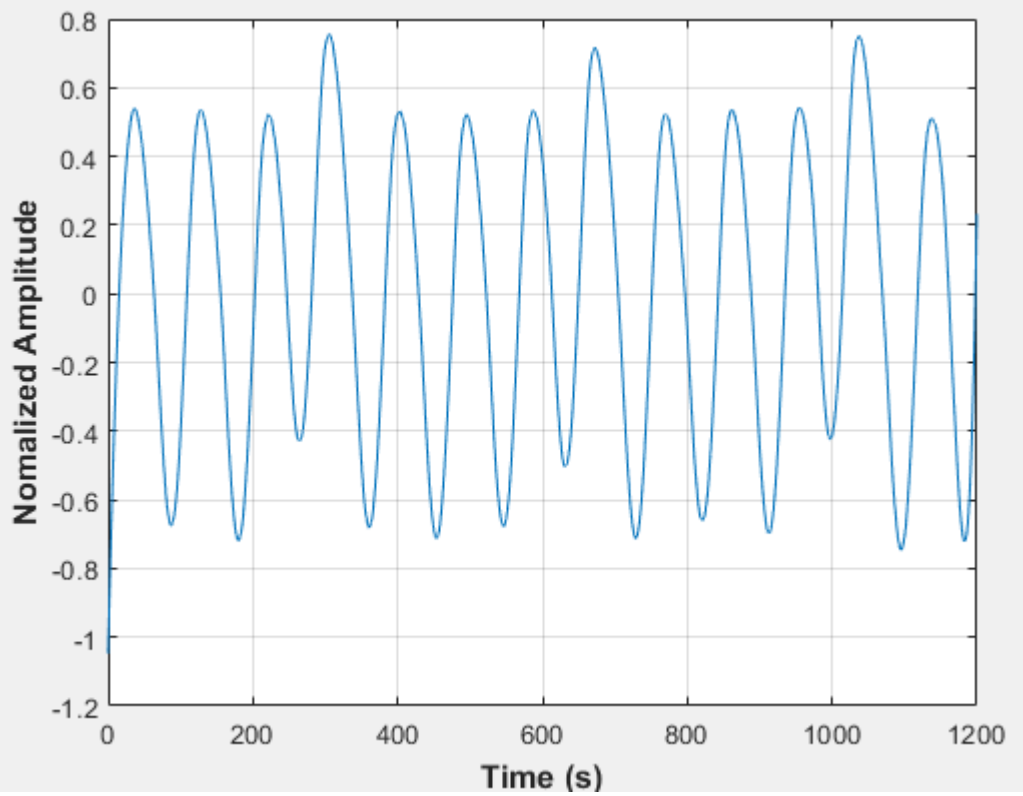


*Figure D-15: Pressure fluctuations in an empty vessel at 2 dm$^3$/minute rotameter flow rate- Test 4*

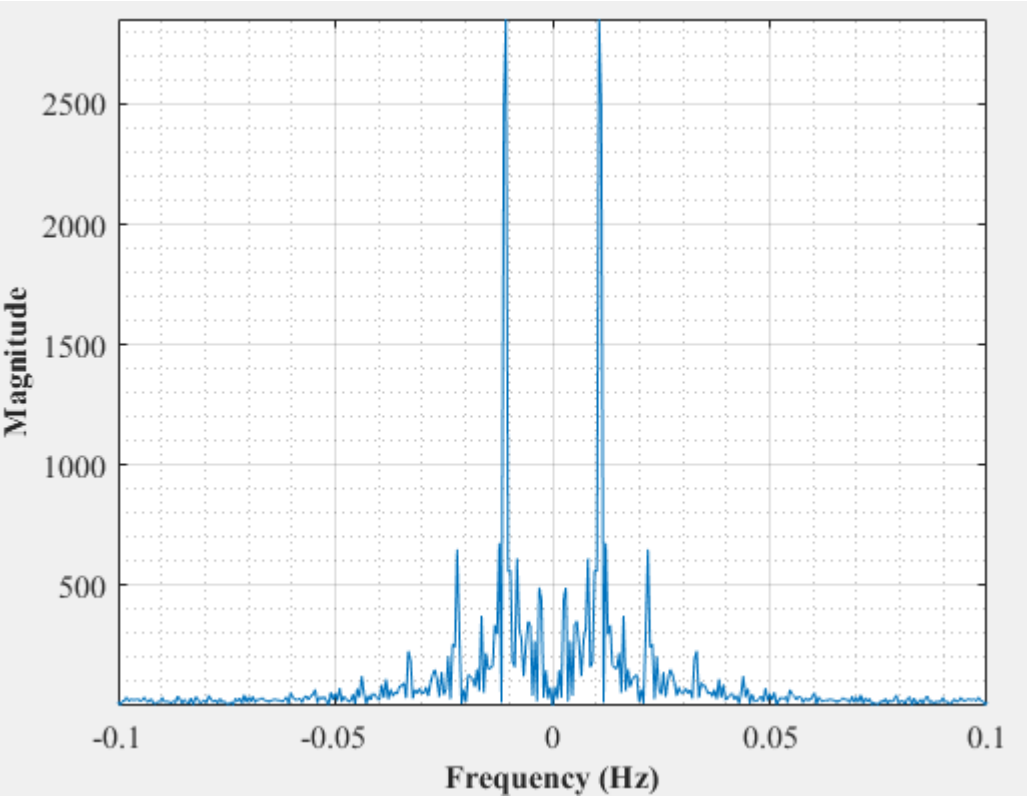


*Figure D-16: Dominant Frequency for an empty vessel at 2 dm$^3$/minute rotameter flow rate- Test 4*

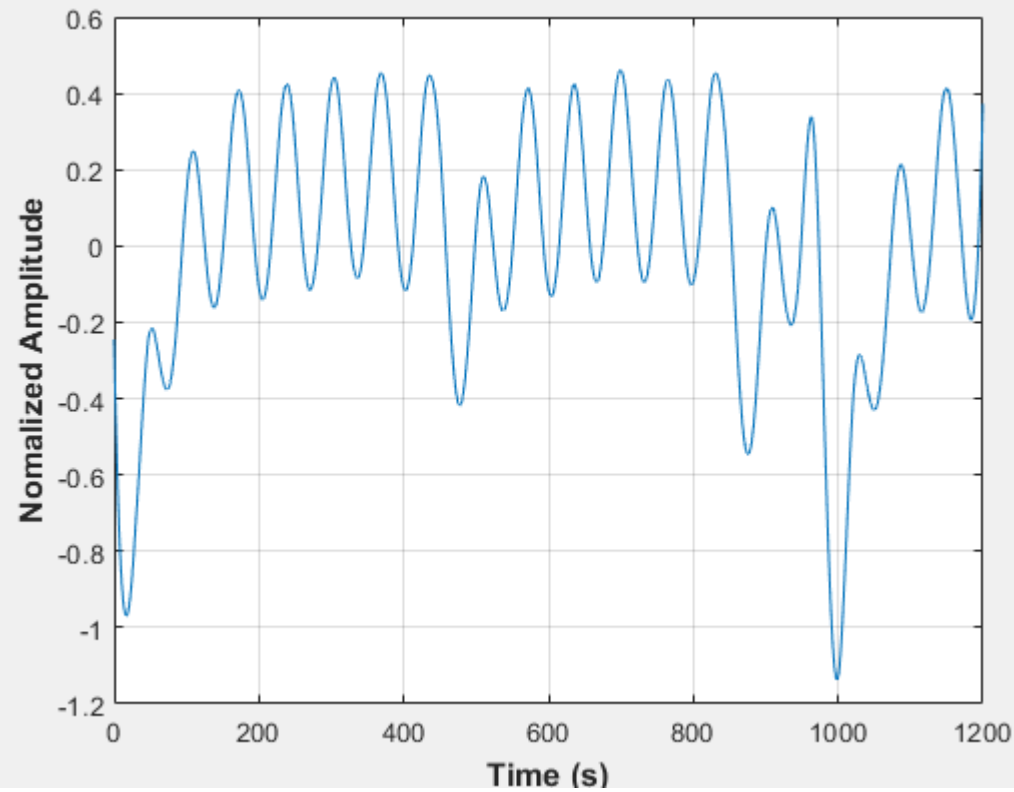


*Figure D-17: Pressure fluctuations in an empty vessel at 2.33 dm$^3$/minute rotameter flow rate- Test 1*

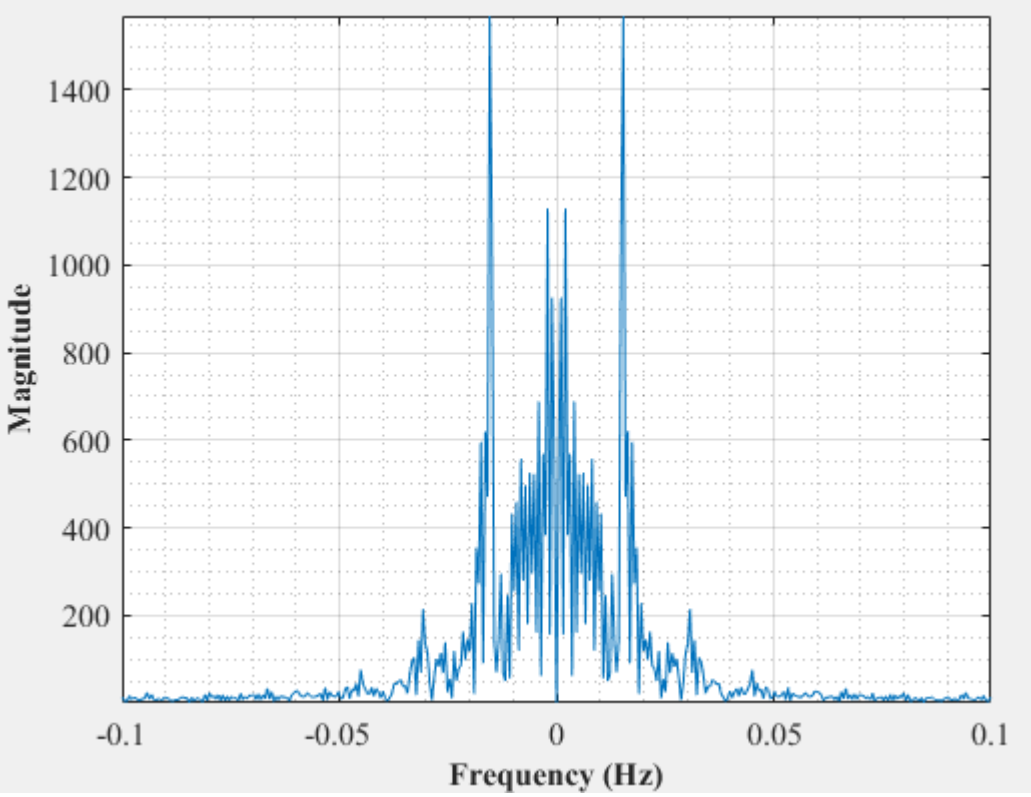


*Figure D-18: Dominant Frequency for an empty vessel at 2.33 dm$^3$/minute rotameter flow rate- Test 1*

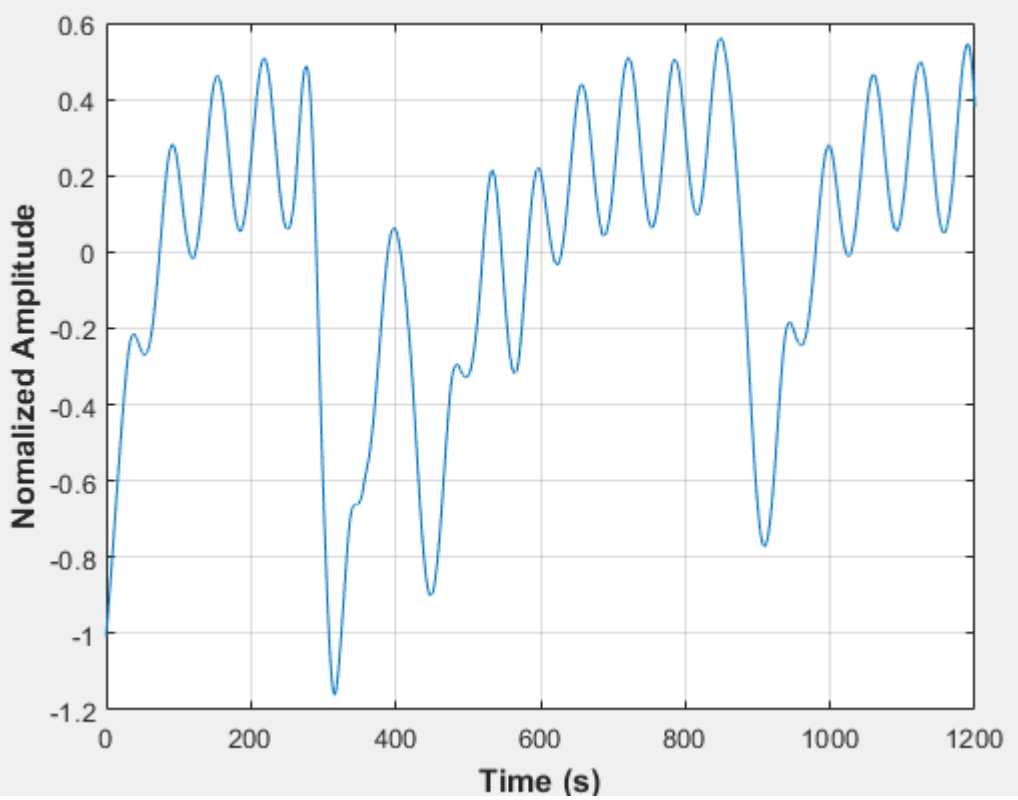


*Figure D-19: Pressure fluctuations in an empty vessel at 2.33 dm$^3$/minute rotameter flow rate- Test 2*

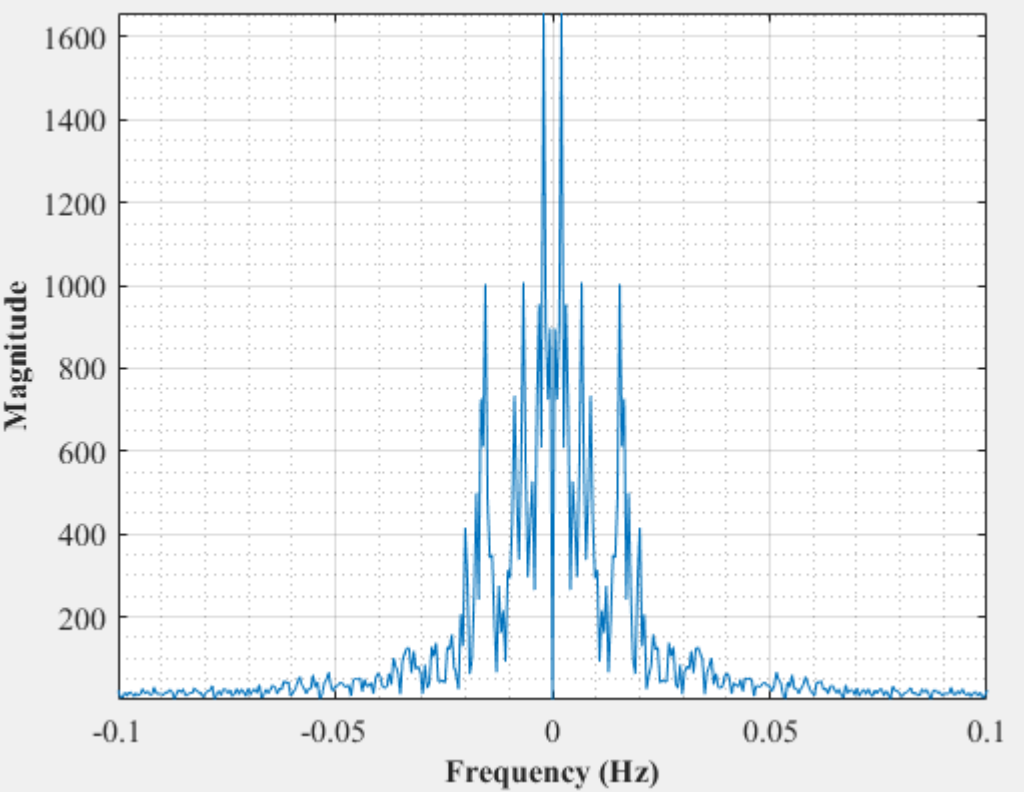


*Figure D-20: Dominant Frequency for an empty vessel at 2.33 dm$^3$/minute rotameter flow rate- Test 2*

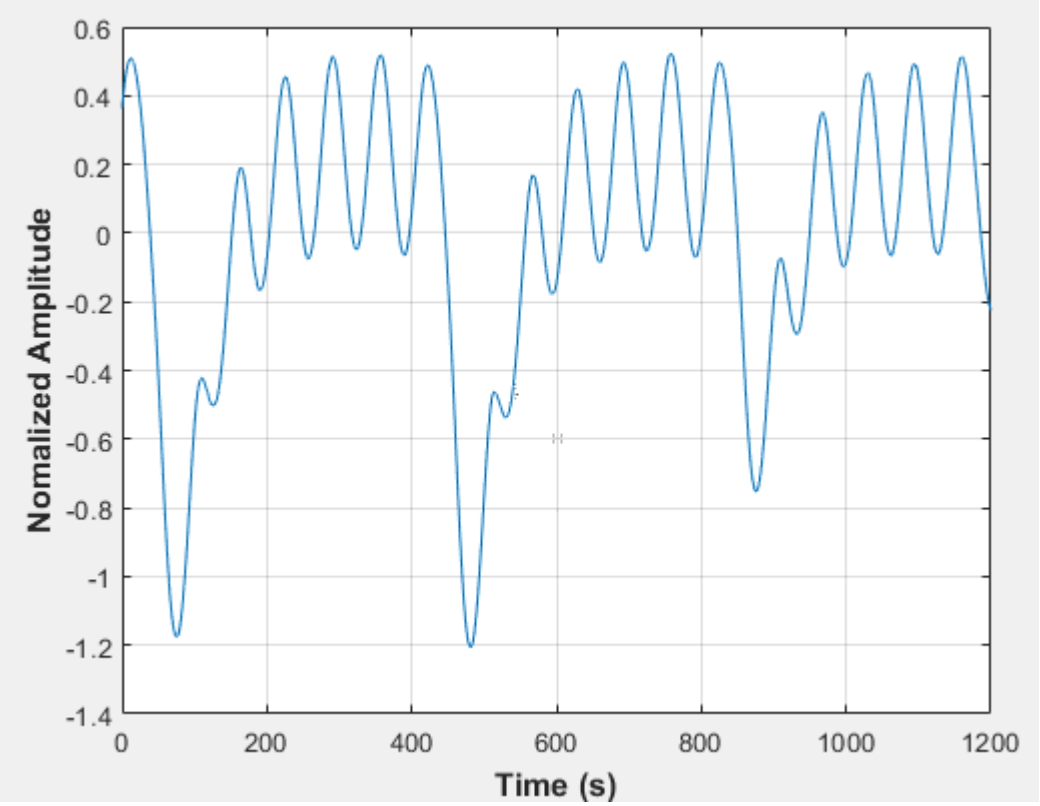


*Figure D-21: Pressure fluctuations in an empty vessel at 2.33 dm$^3$/minute rotameter flow rate- Test 3*

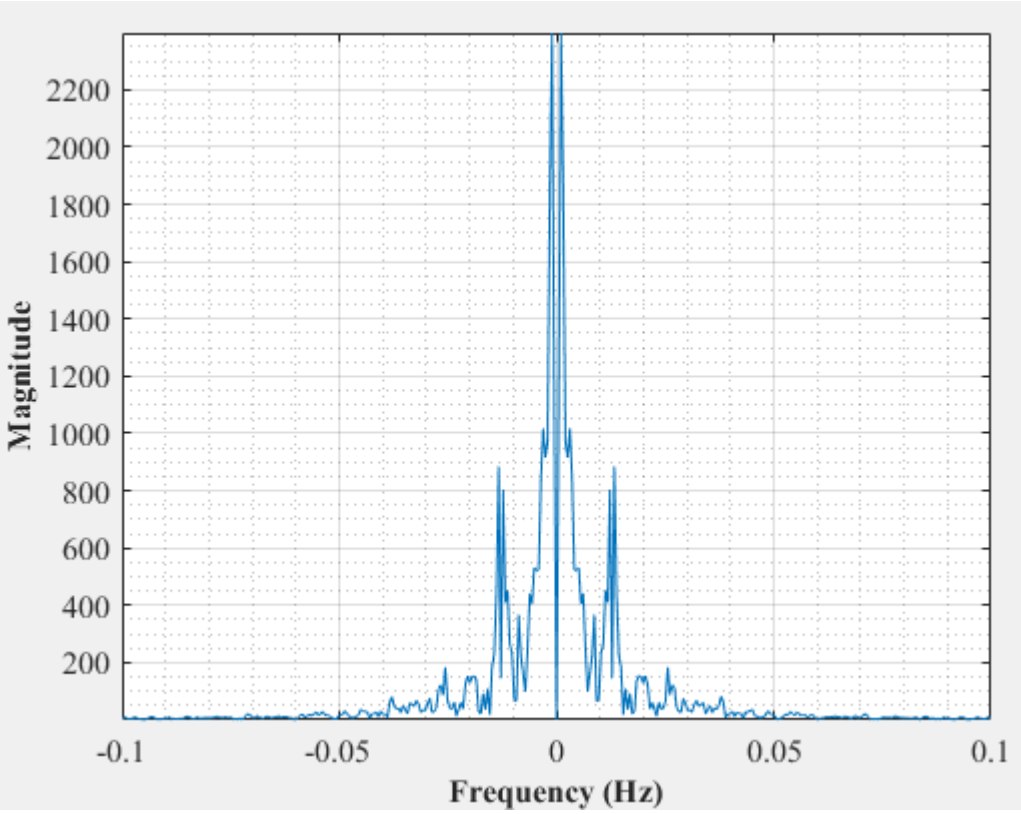


*Figure D-22: Dominant Frequency for an empty vessel at 2.33 dm$^3$/minute rotameter flow rate- Test 3*

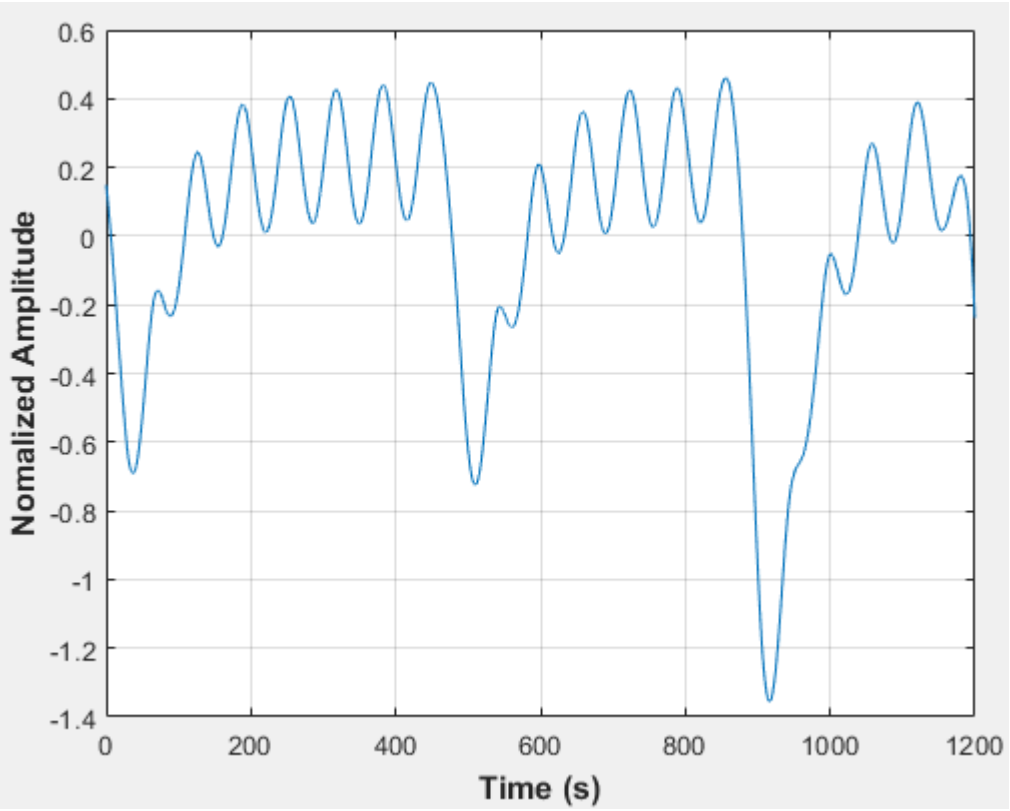


*Figure D-23: Pressure fluctuations in an empty vessel at 2.33 dm$^3$/minute rotameter flow rate- Test 4*

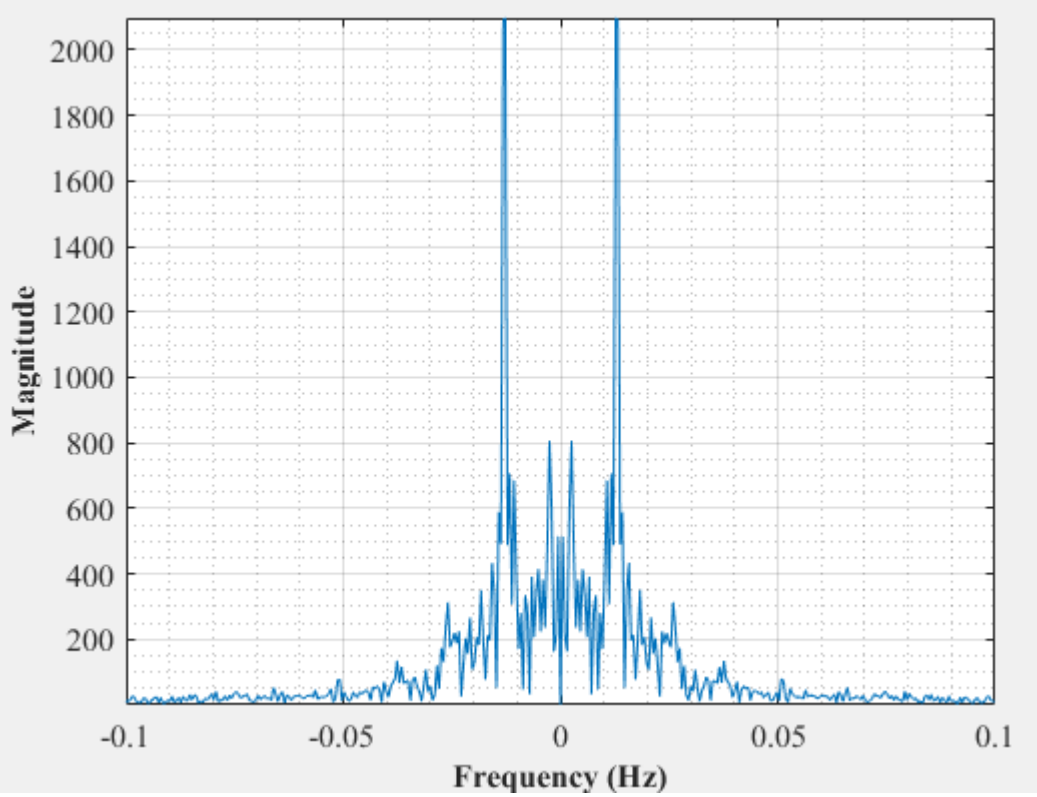


*Figure D-24: Dominant Frequency for an empty vessel at 2.33 dm$^3$/minute rotameter flow rate- Test 4*

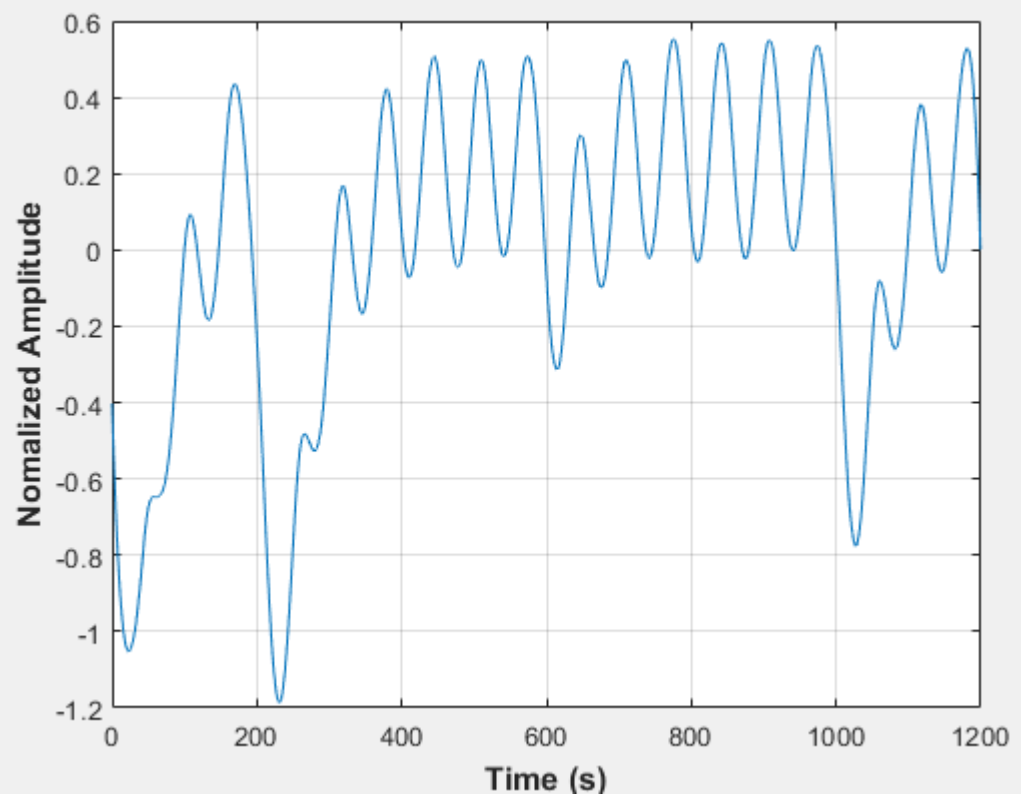


*Figure D-25: Pressure fluctuations in an empty vessel at 2.33 dm$^3$/minute flow rate- Test 5*

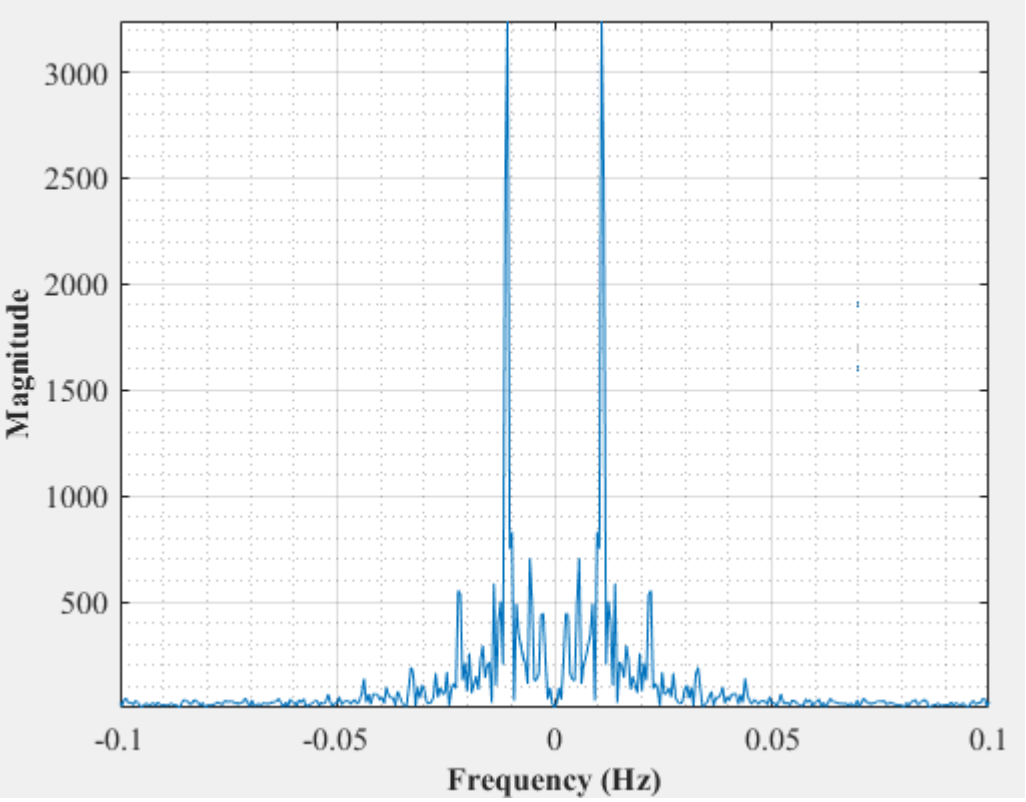


*Figure D-26: Dominant Frequency for an empty vessel at 2.33 dm$^3$/minute rotameter flow rate- Test 5*

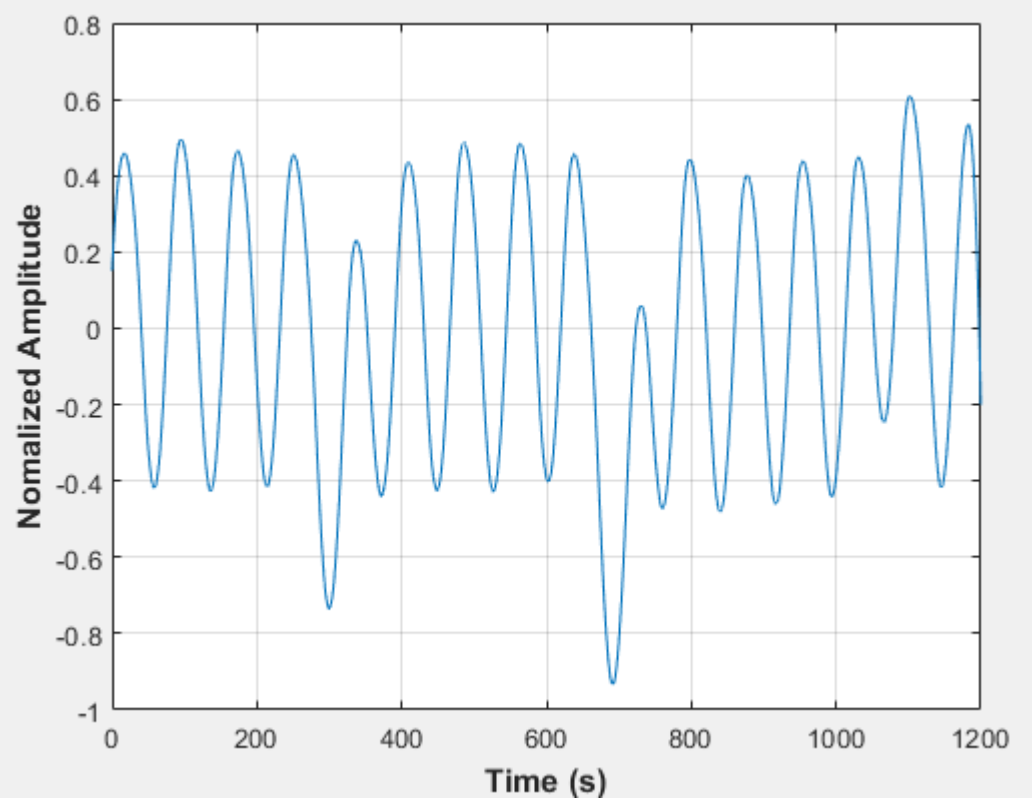


*Figure D-27: Pressure fluctuations in an empty vessel at 2.33 dm$^3$/minute rotameter flow rate- Test 6*

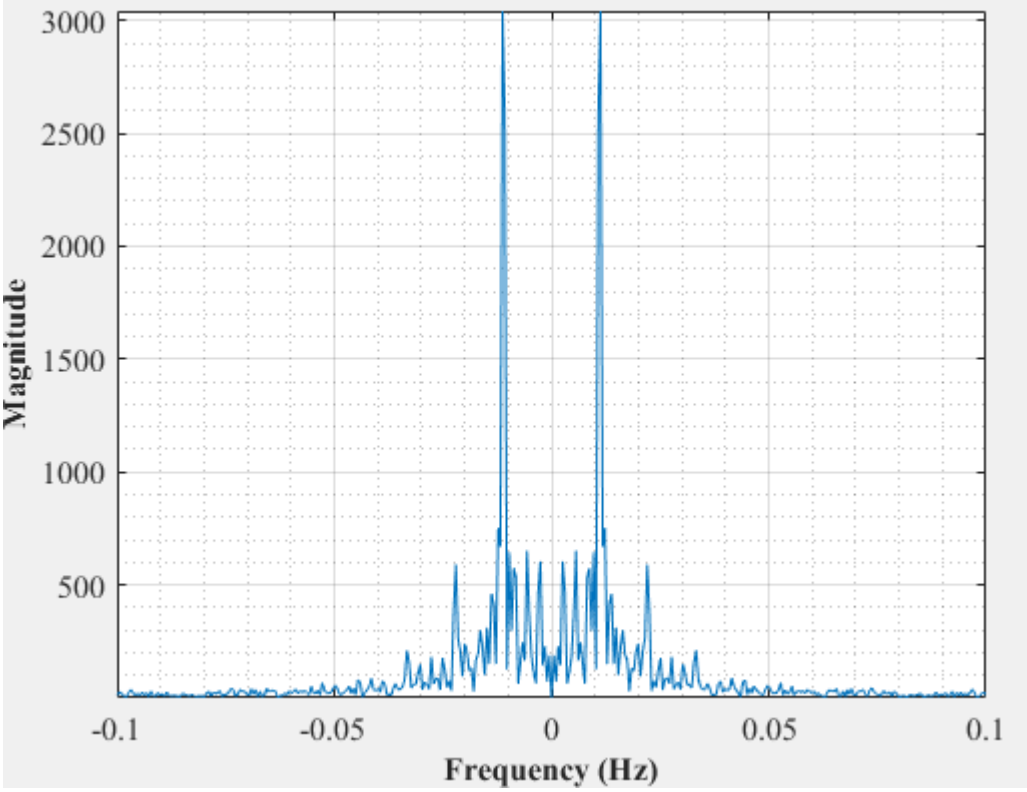


*Figure D-28: Dominant Frequency for an empty vessel at 2.33 dm$^3$/minute rotameter flow rate- Test 6*

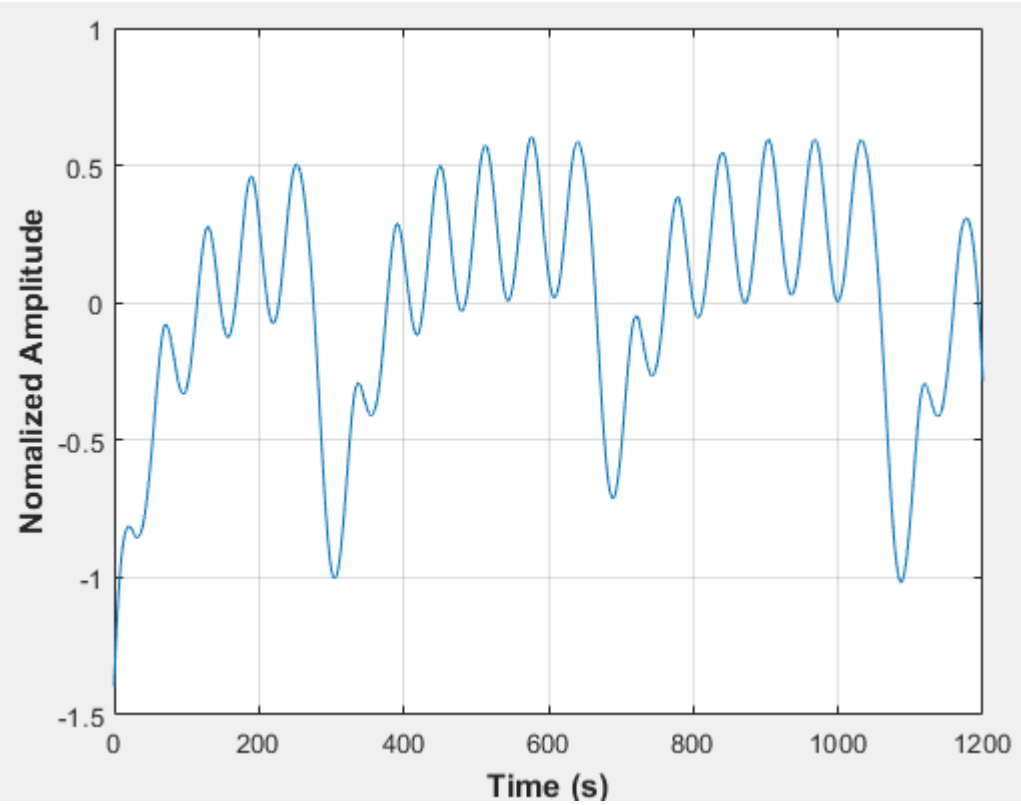


*Figure D-29: Pressure fluctuations in an empty vessel at 2.67 dm$^3$/minute rotameter flow rate- Test 1*

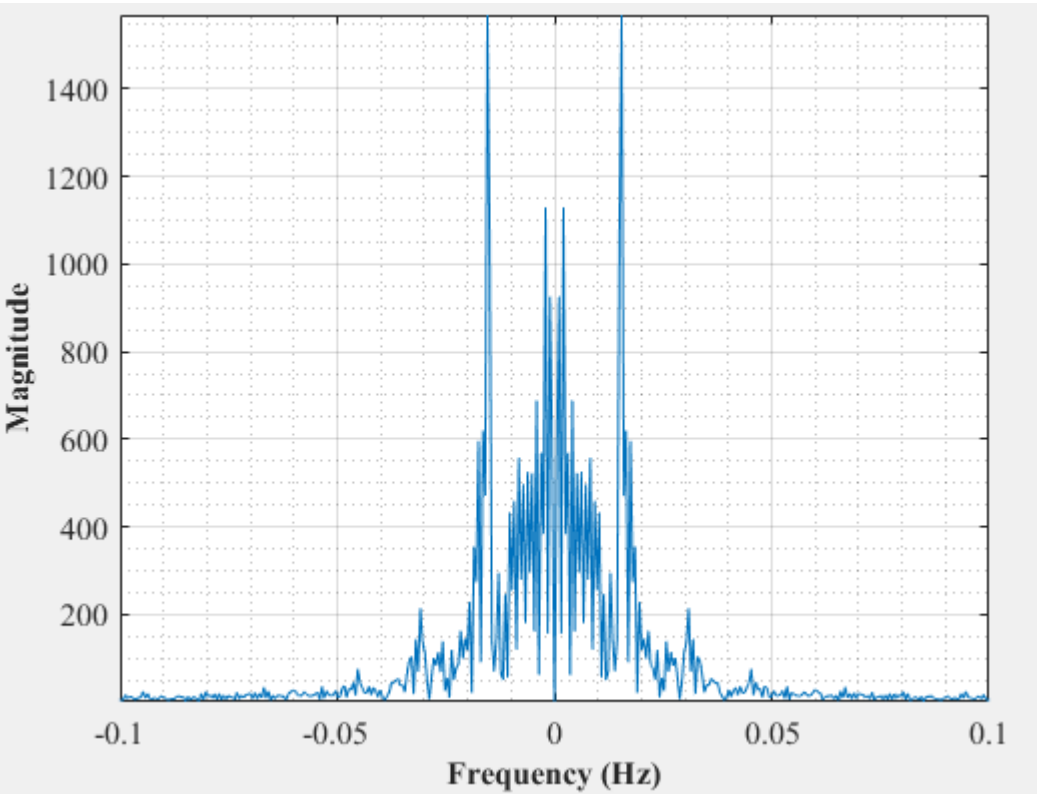


*Figure D-30: Dominant Frequency for an empty vessel at 2.67 dm$^3$/minute rotameter flow rate- Test 1*

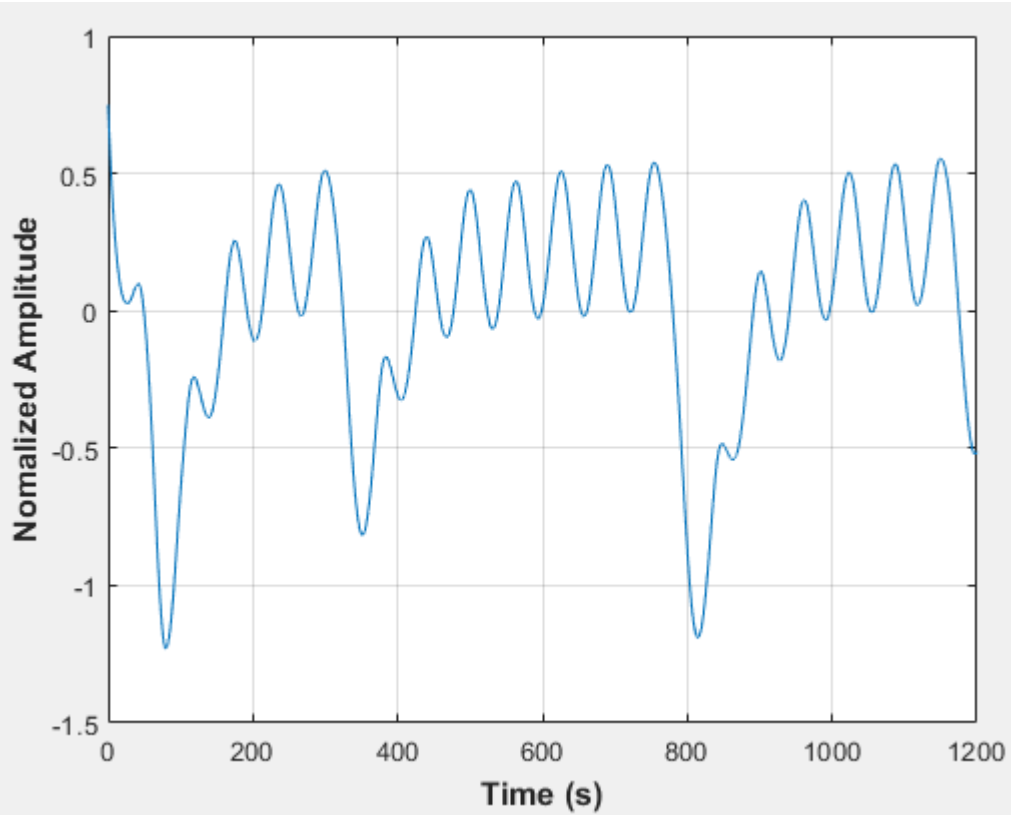


*Figure D-31: Pressure fluctuations in an empty vessel at 2.67 dm$^3$/minute rotameter flow rate- Test 2*

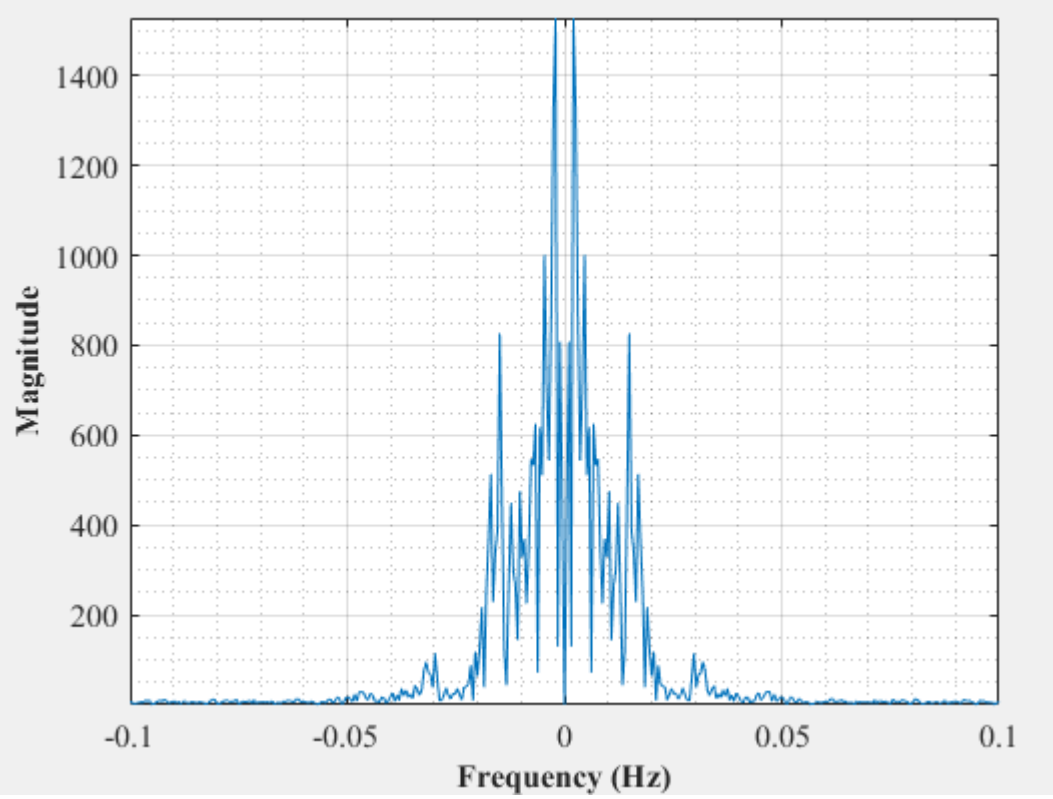


*Figure D-32: Dominant Frequency for an empty vessel at 2.67 dm$^3$/minute rotameter flow rate- Test 2*

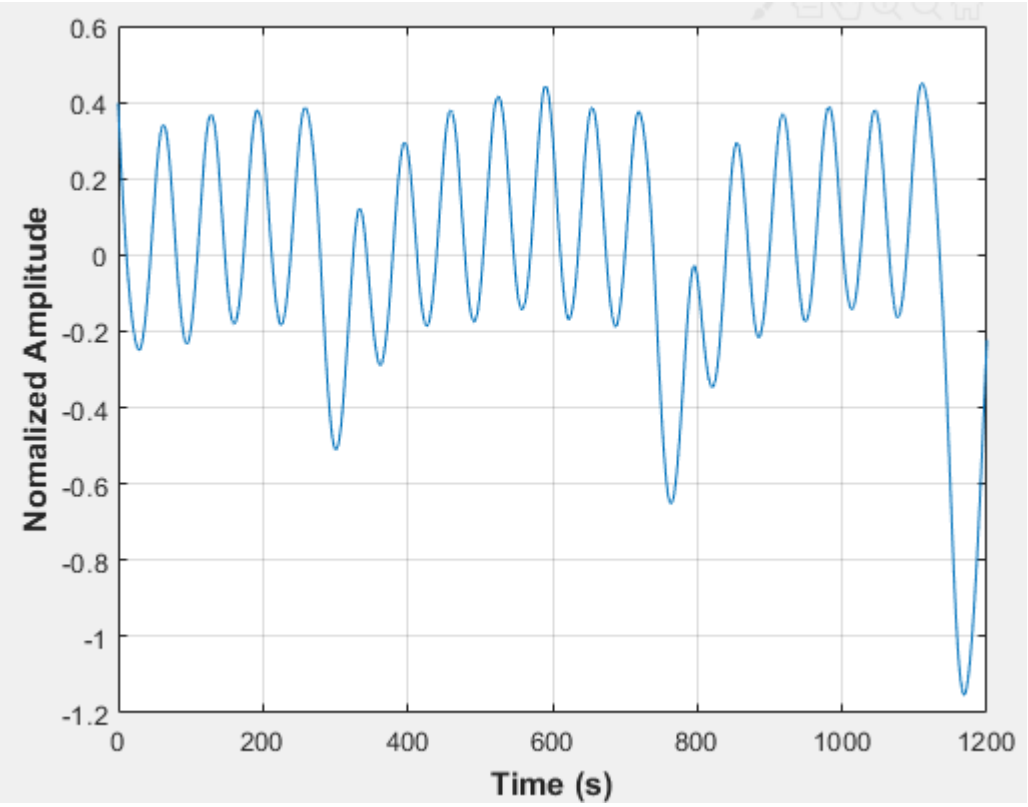


*Figure D-33: Pressure fluctuations in an empty vessel at 2.67 dm$^3$/minute rotameter flow rate- Test 3*

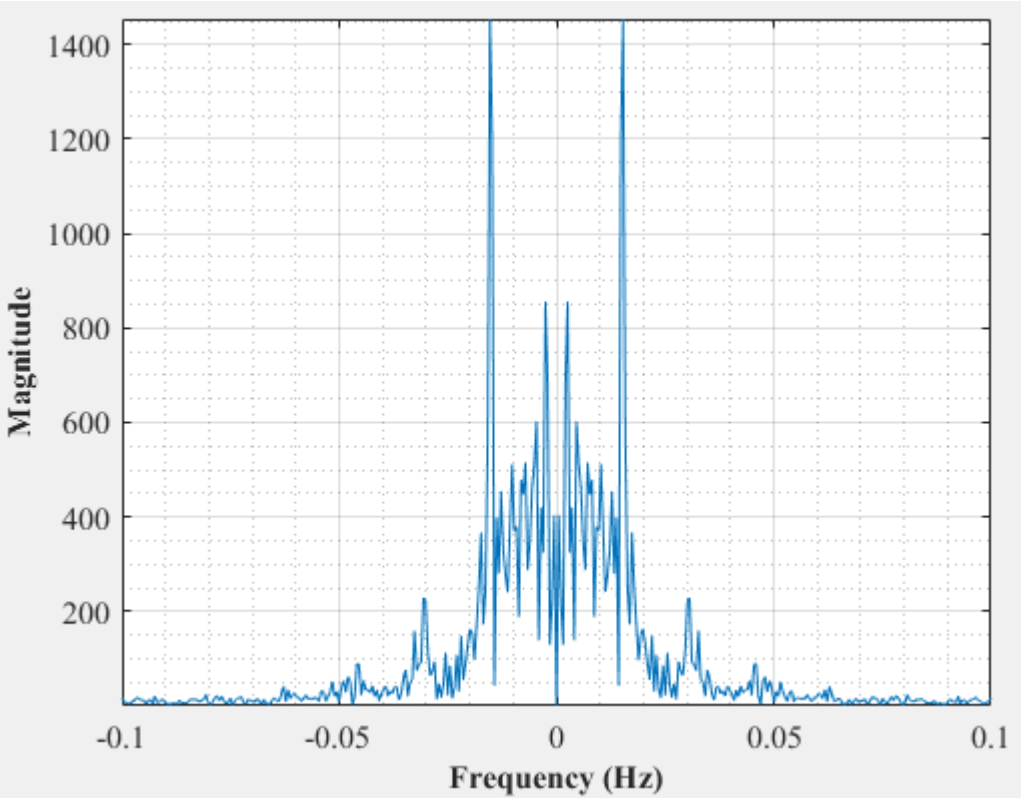


*Figure D-34: Dominant Frequency for an empty vessel at 2.67 dm$^3$/minute rotameter flow rate- Test 3*

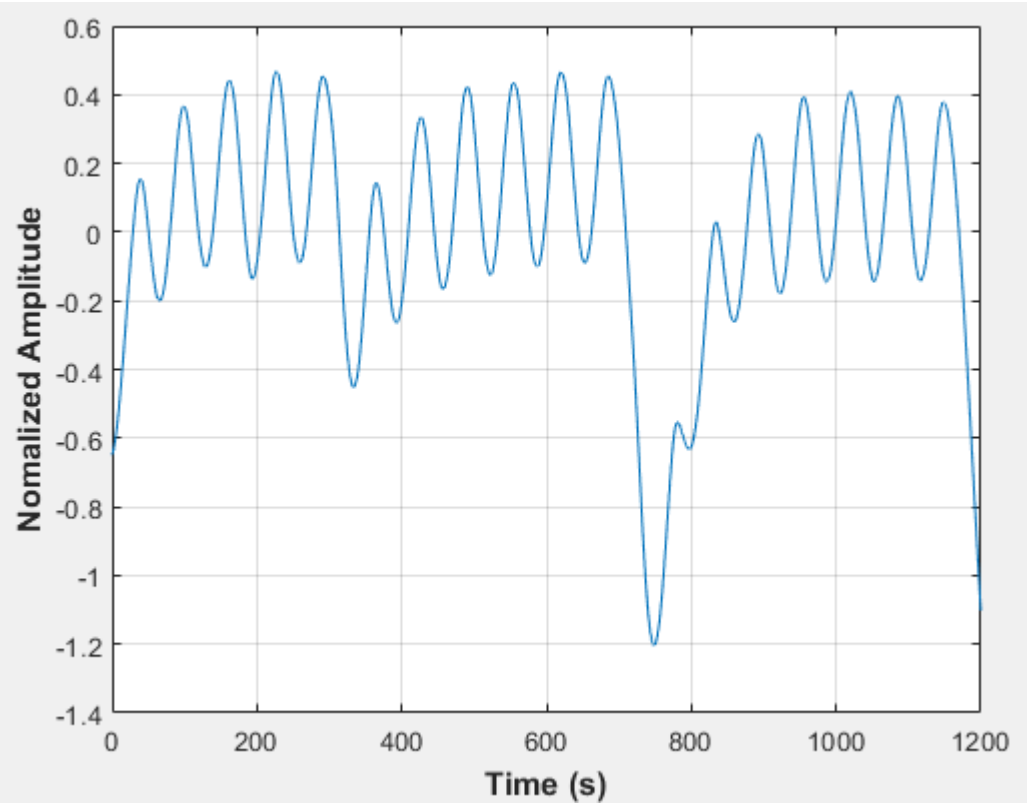


*Figure D-35: Pressure fluctuations in an empty vessel at 2.67 dm$^3$/minute rotameter flow rate- Test 4*

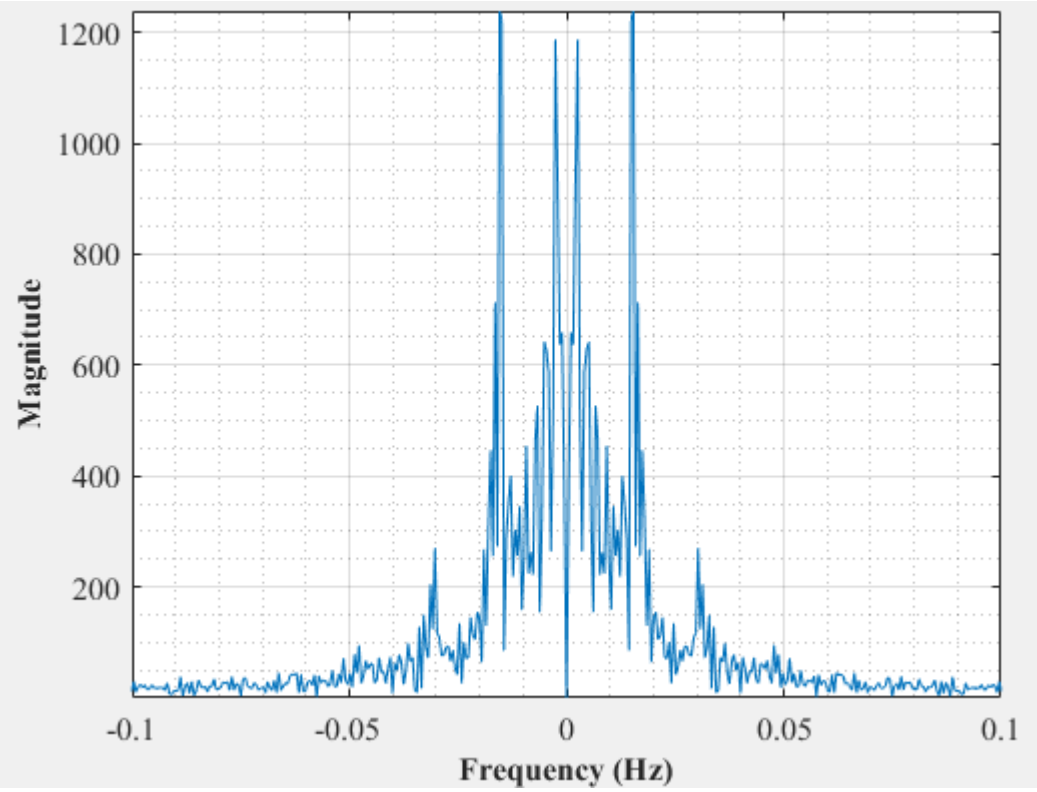


*Figure D-36: Dominant Frequency for an empty vessel at 2.67 dm$^3$/minute rotameter flow rate- Test 4*

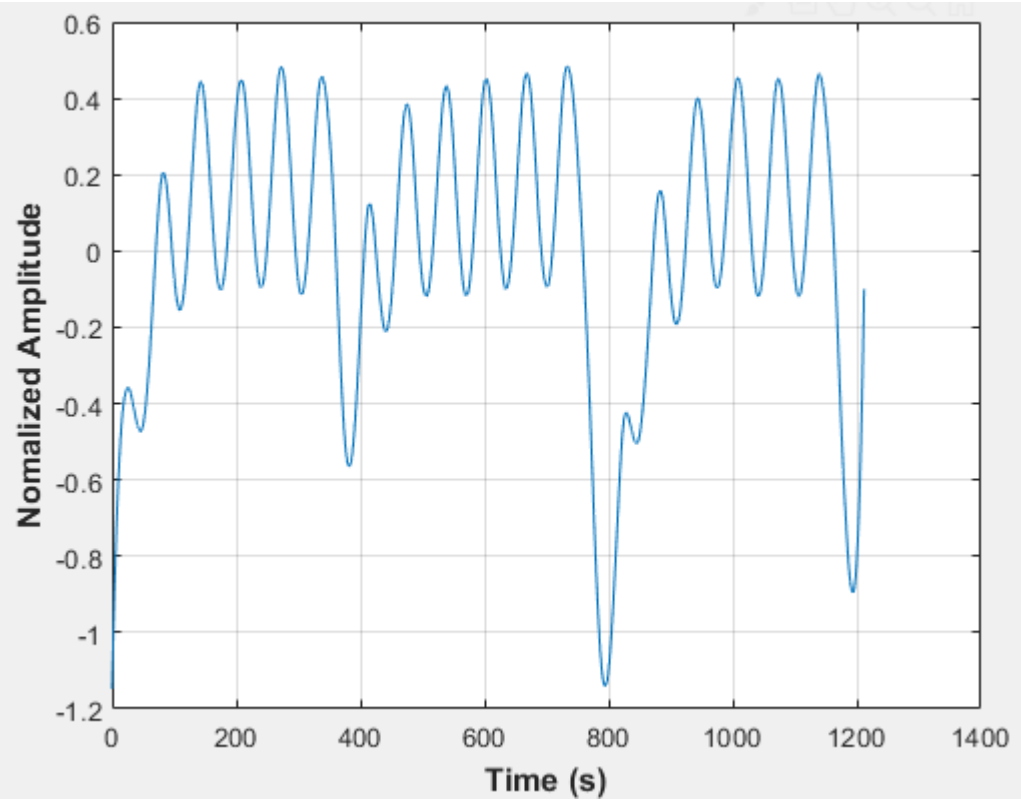


*Figure D-37: Pressure fluctuations in an empty vessel at 2.67 dm$^3$/minute rotameter flow rate- Test 5*

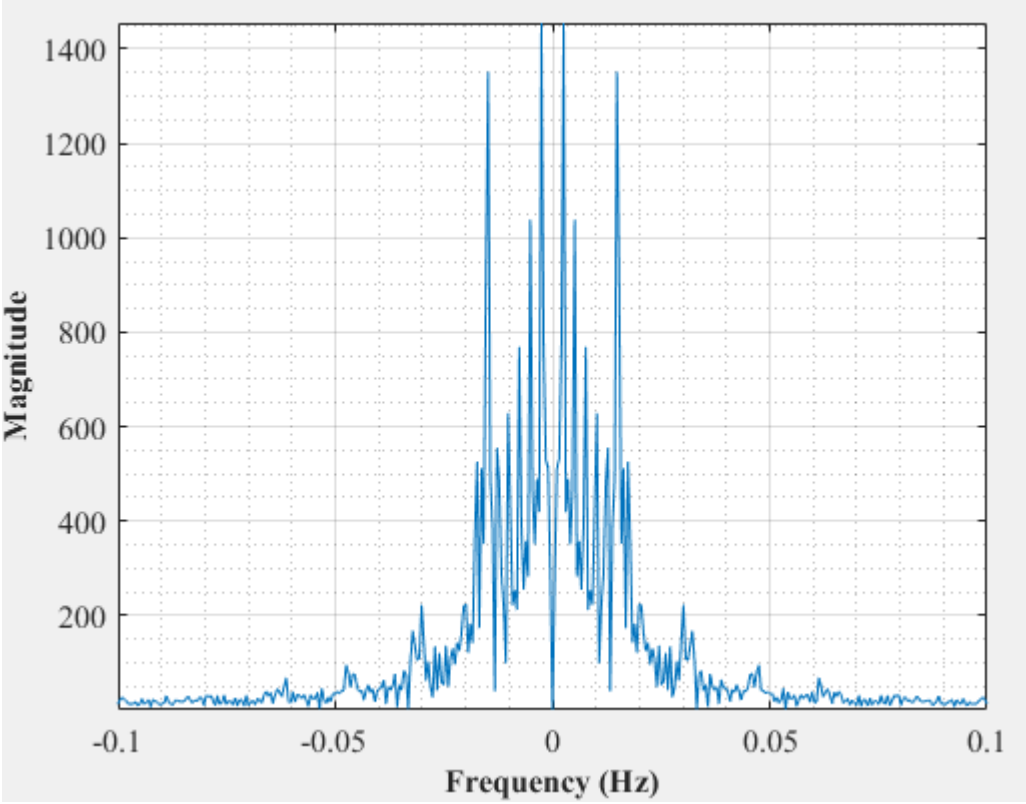


*Figure D-38: Dominant Frequency for an empty vessel at 2.67 dm$^3$/minute rotameter flow rate- Test 6*

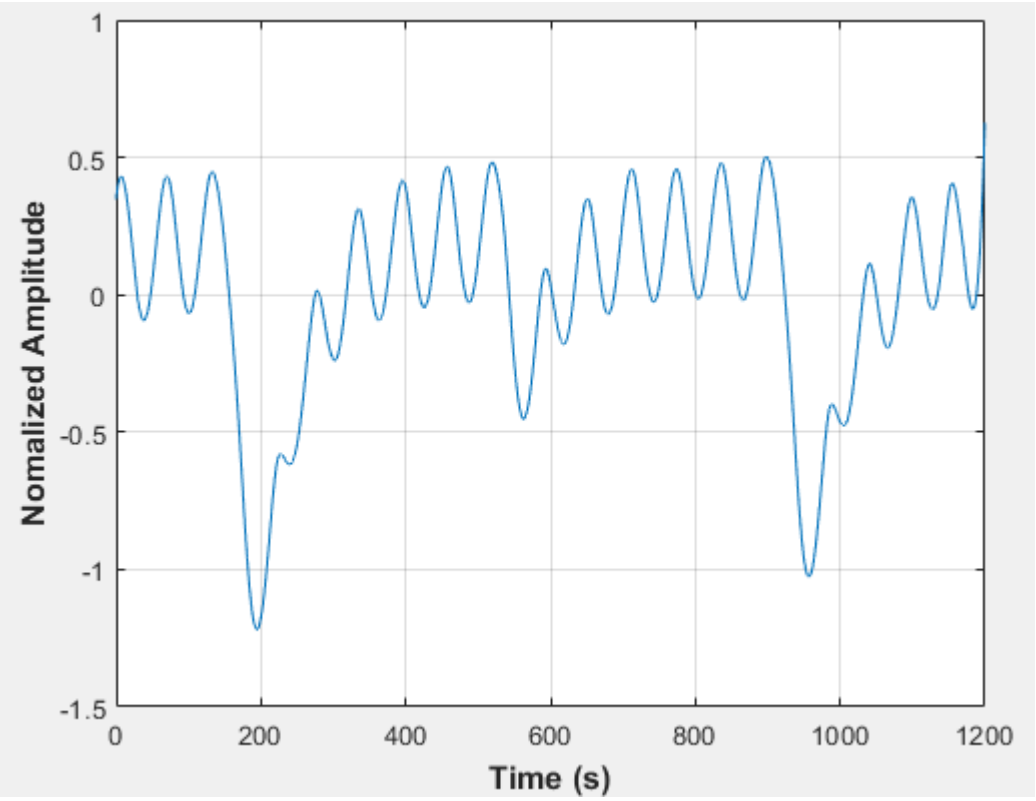


*Figure D-39: Pressure fluctuations in an empty vessel at 2.83 dm$^3$/minute rotameter flow rate- Test 1*

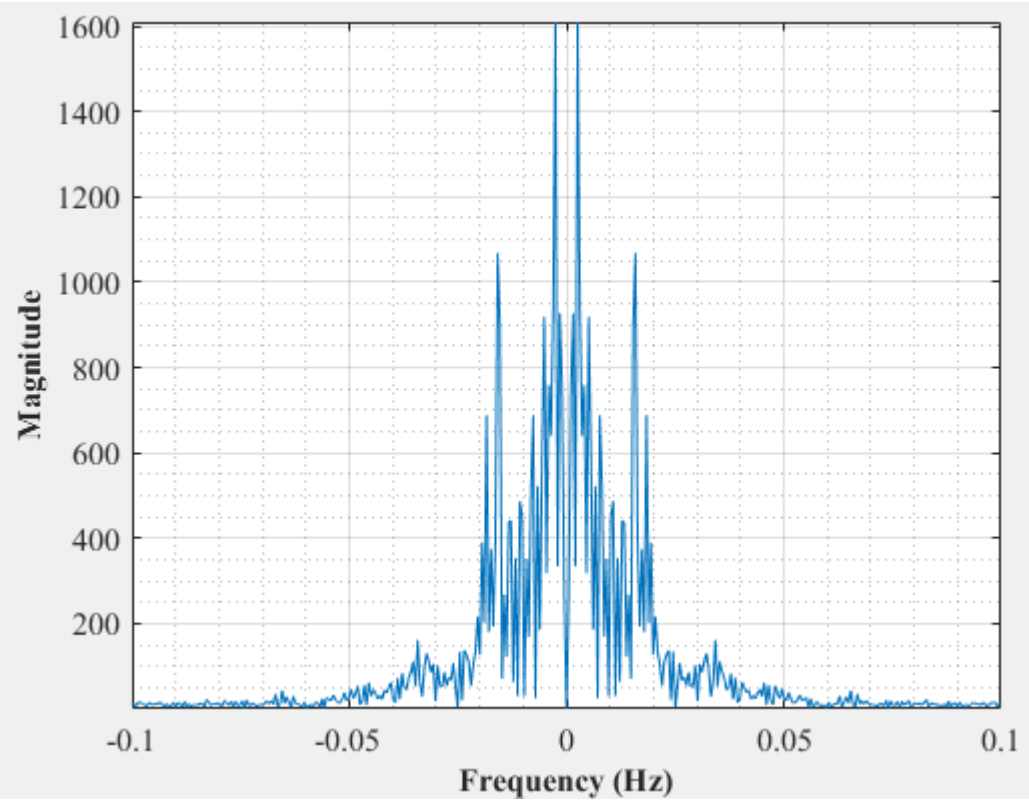


*Figure D-40: Dominant Frequency for an empty vessel at 2.83 dm$^3$/minute rotameter flow rate- Test 1*

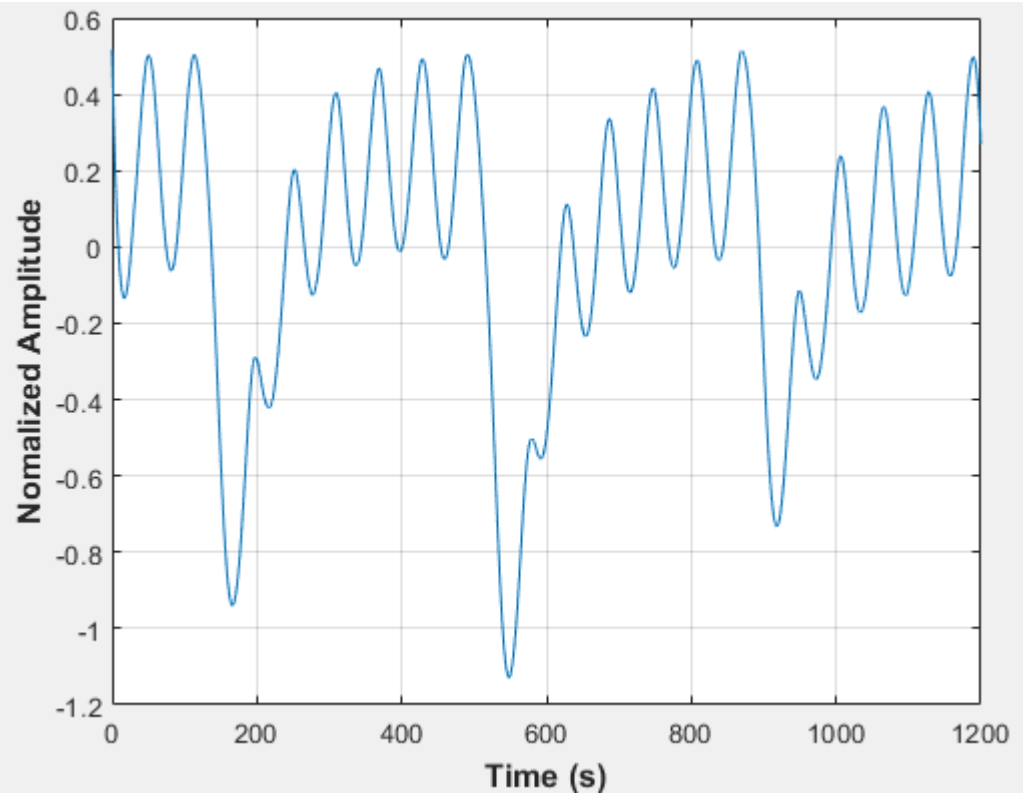


*Figure D-41: Pressure fluctuations in an empty vessel at 2.83 dm$^3$/minute rotameter flow rate- Test 2*

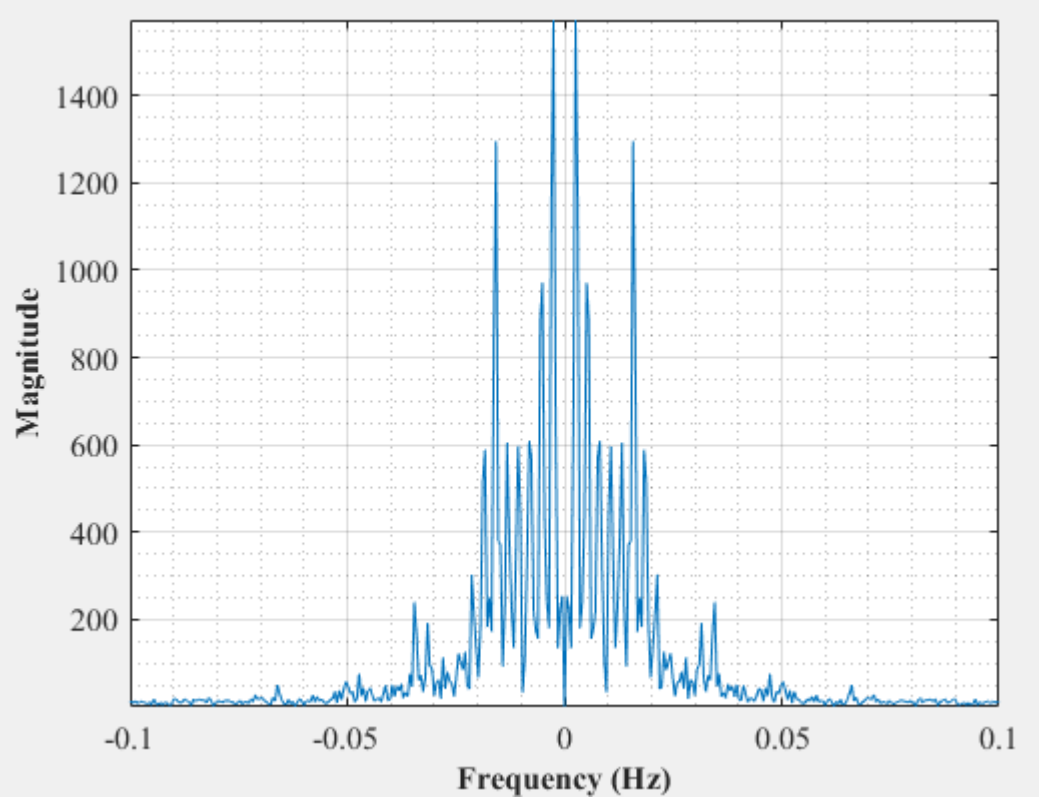


*Figure D-42: Dominant Frequency for an empty vessel at 2.83 dm$^3$/minute rotameter flow rate- Test 2*

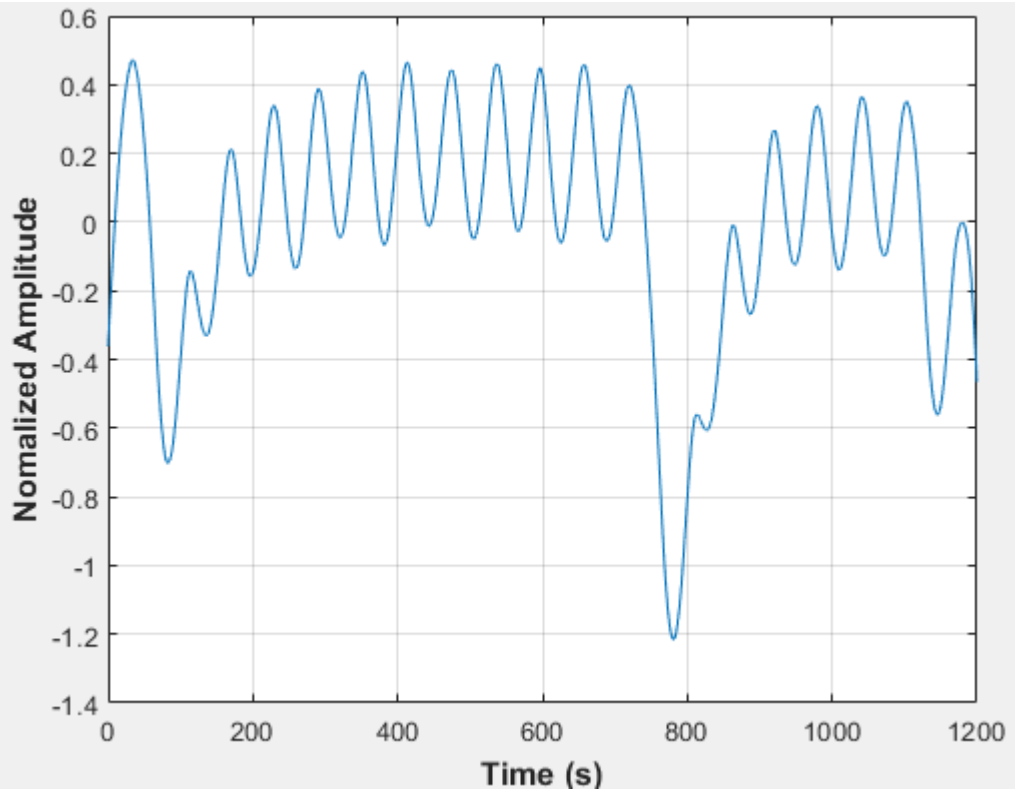


*Figure D-43: Pressure fluctuations in an empty vessel at 2.83 dm$^3$/minute rotameter flow rate- Test 3*

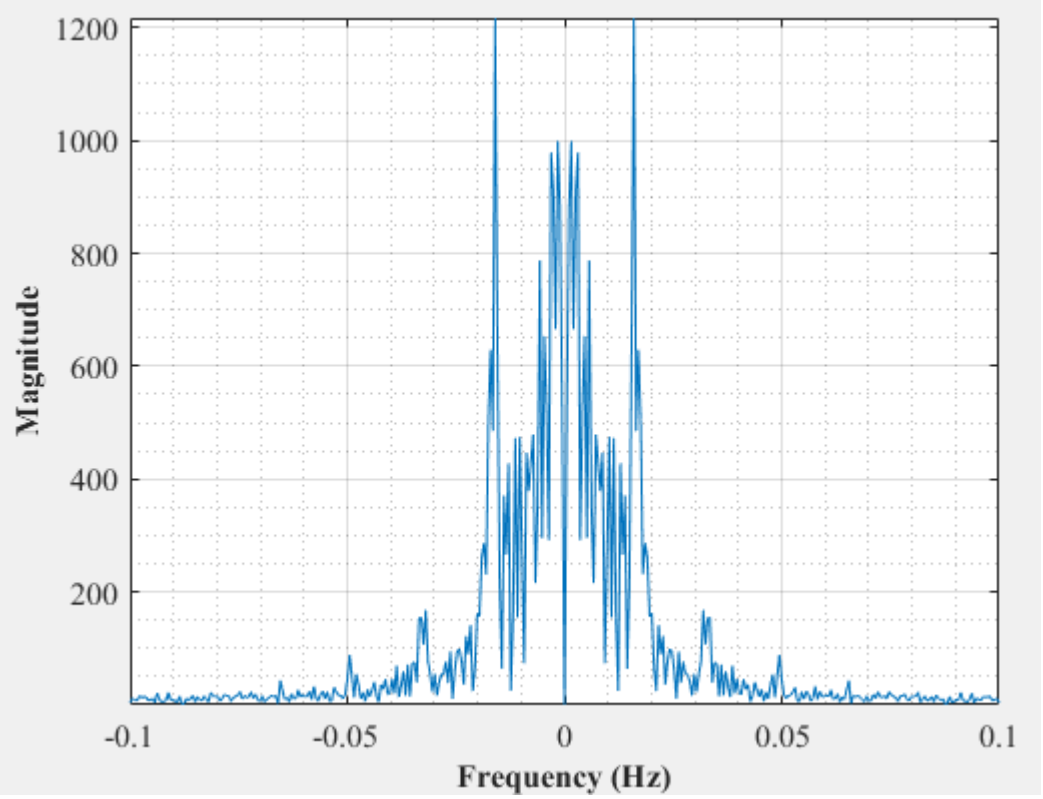


*Figure D-44: Dominant Frequency for an empty vessel at 2.83 dm$^3$/minute rotameter flow rate- Test 3*

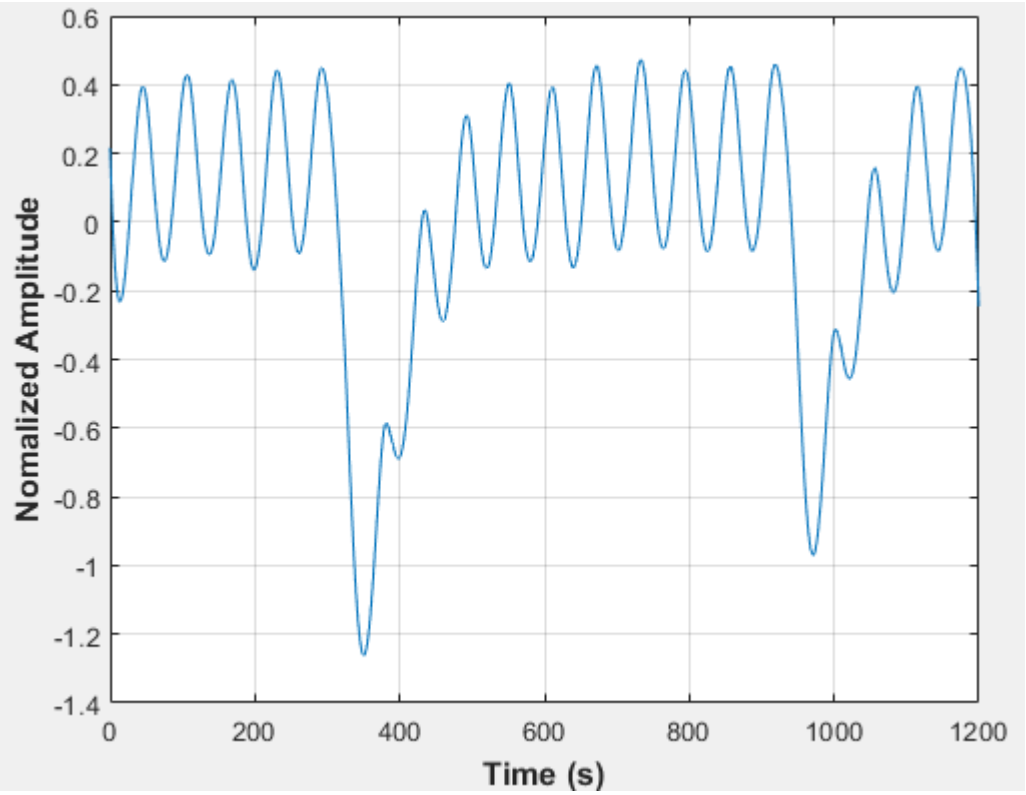


*Figure D-45: Pressure fluctuations in an empty vessel at 2.83 dm$^3$/minute rotameter flow rate- Test 4*

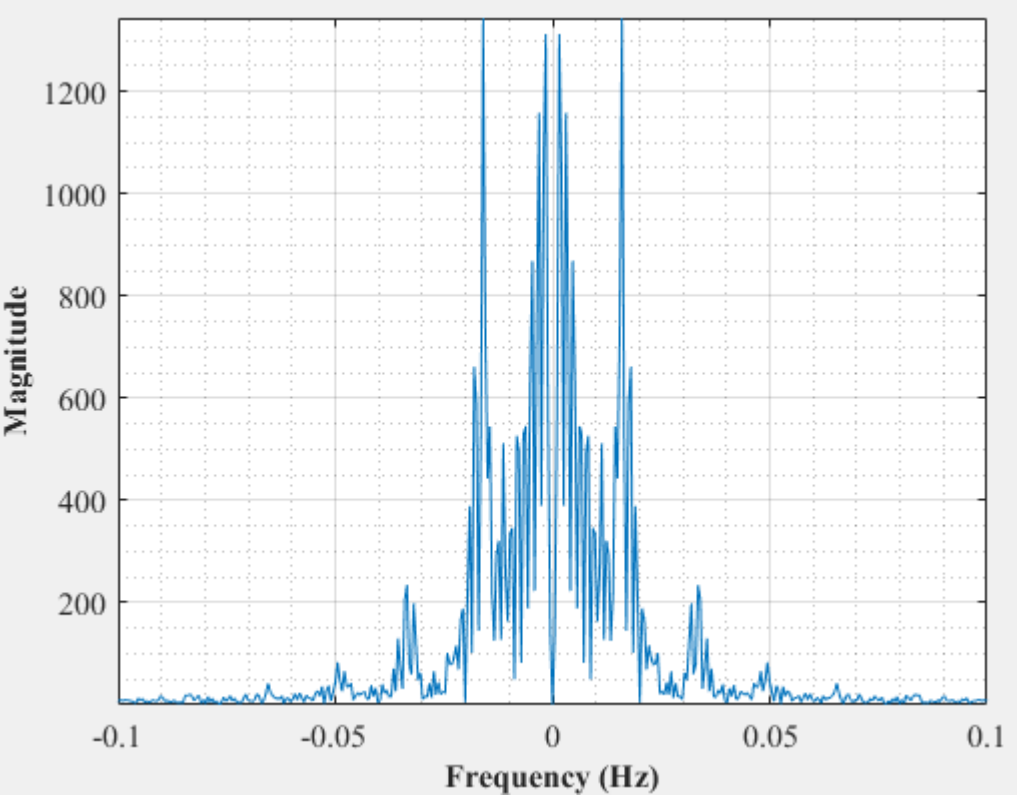


*Figure D-46: Dominant Frequency for an empty vessel at 2.83 dm$^3$/minute rotameter flow rate- Test 4*

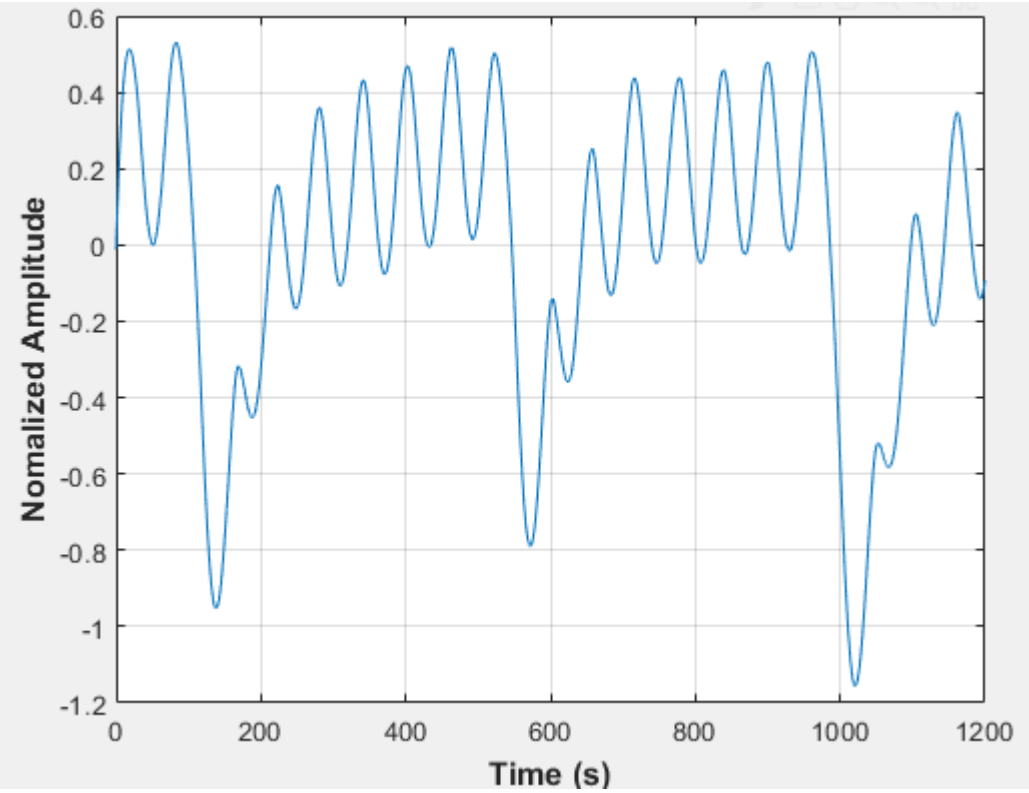


*Figure D-47: Pressure fluctuations in an empty vessel at 2.83 dm$^3$/minute rotameter flow rate- Test 5*

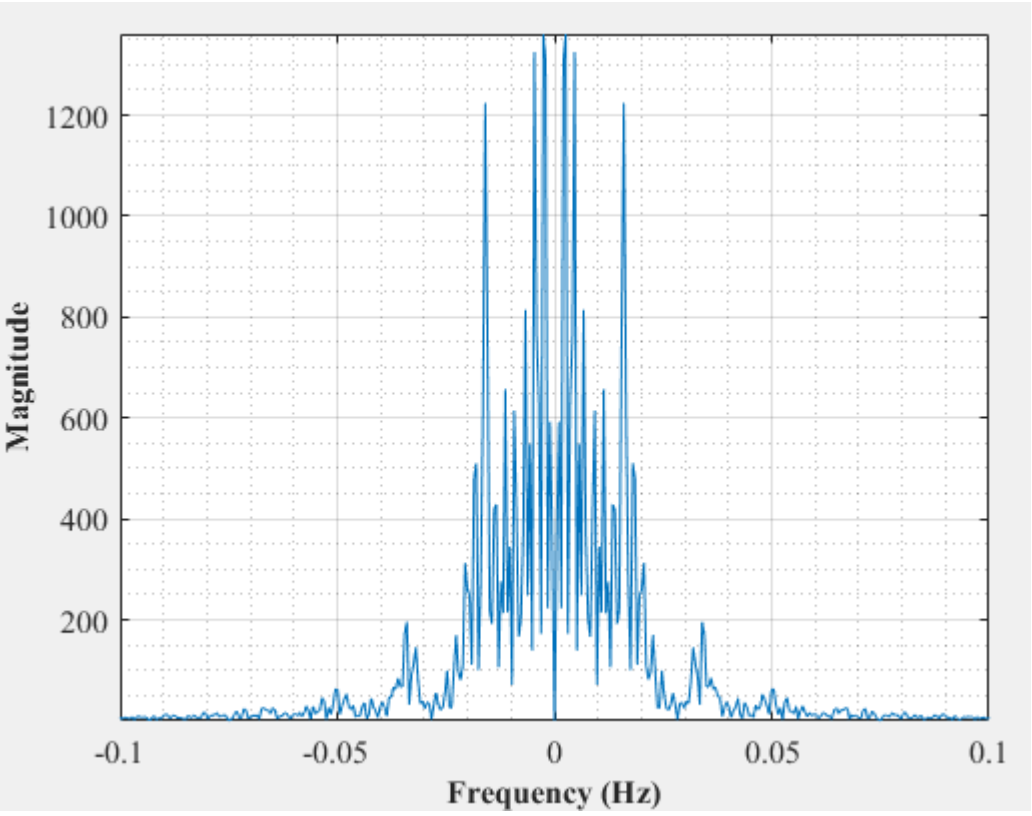


*Figure D-48: Dominant Frequency for an empty vessel at 2.83 dm$^3$/minute rotameter flow rate- Test 5*

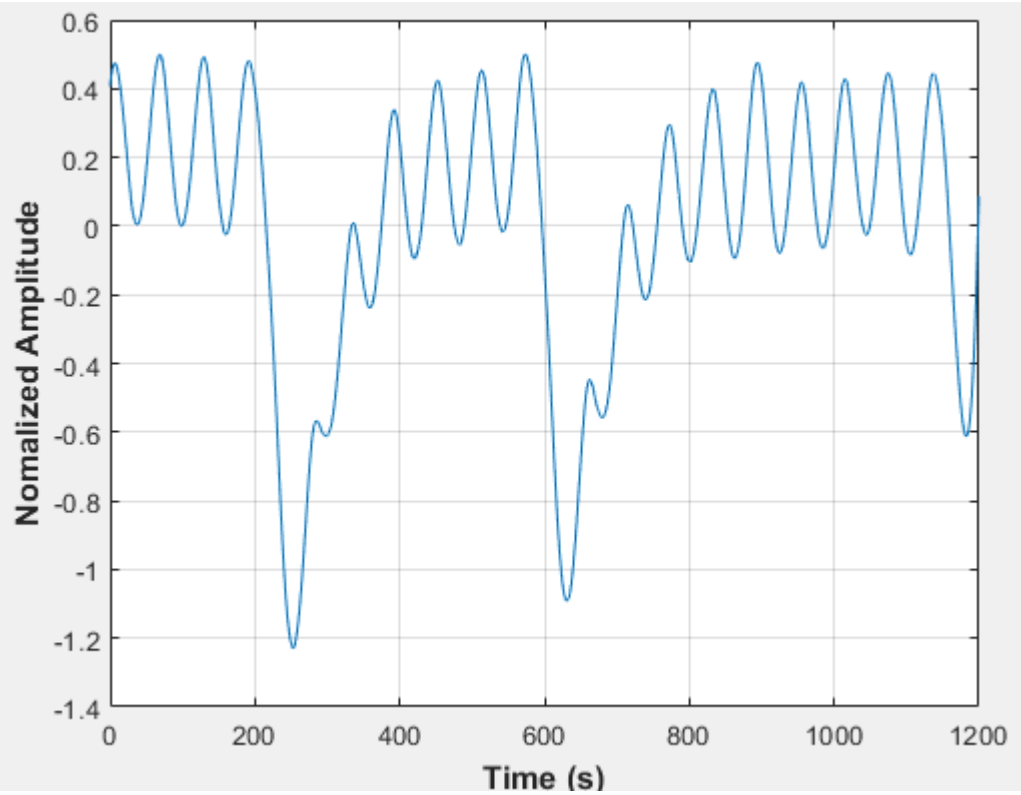


*Figure D-49: Pressure fluctuations in an empty vessel at 2.83 $dm^3$/minute rotameter flow rate- Test 6*

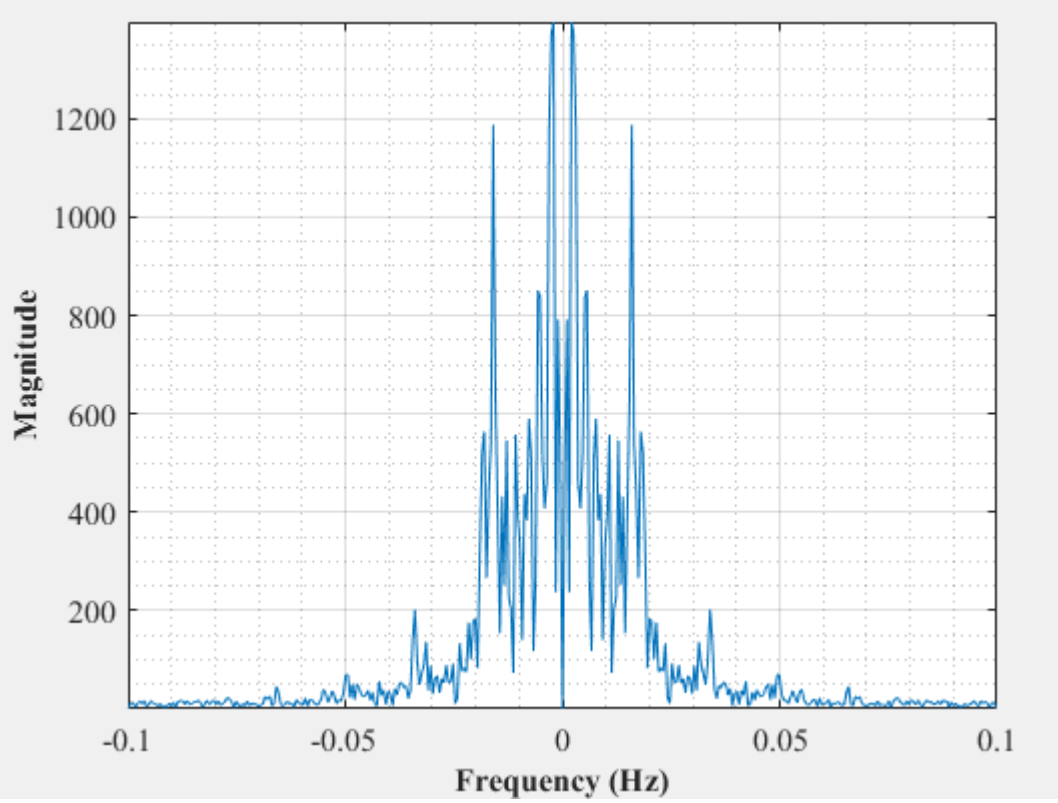


*Figure D-50: Dominant Frequency for an empty vessel at 2.83 $dm^3$/minute rotameter flow rate- Test 6*

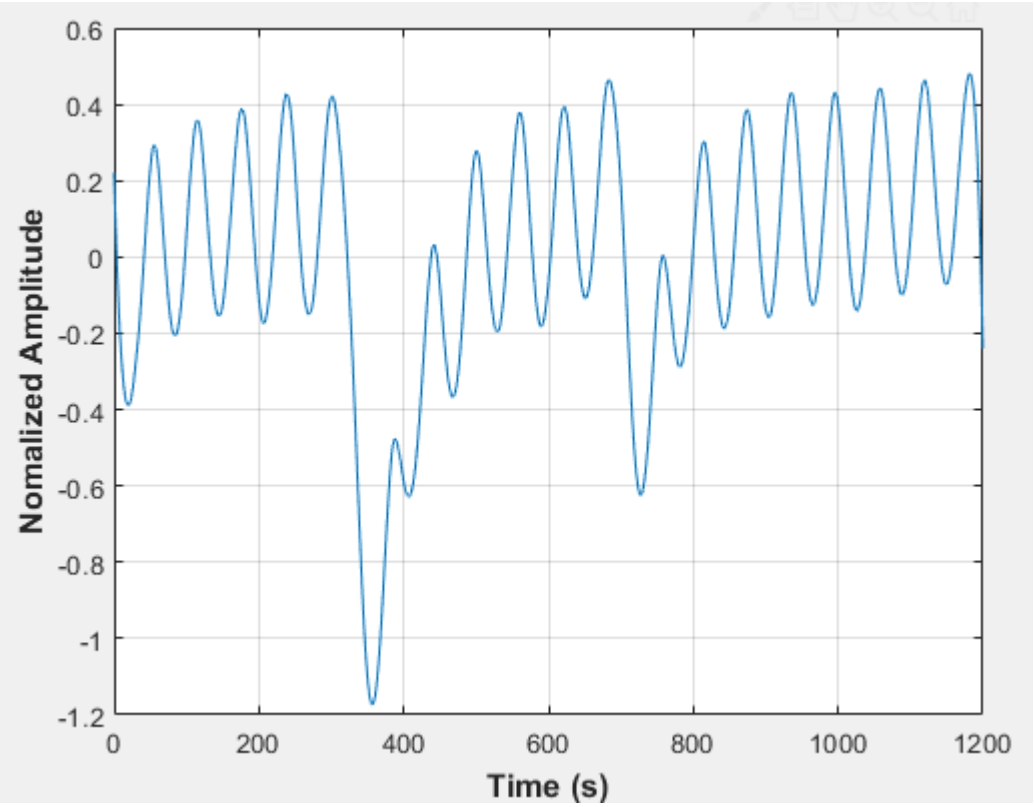


*Figure D-51: Pressure fluctuations in an empty vessel at 2.83 dm$^3$/minute rotameter flow rate- Test 7*

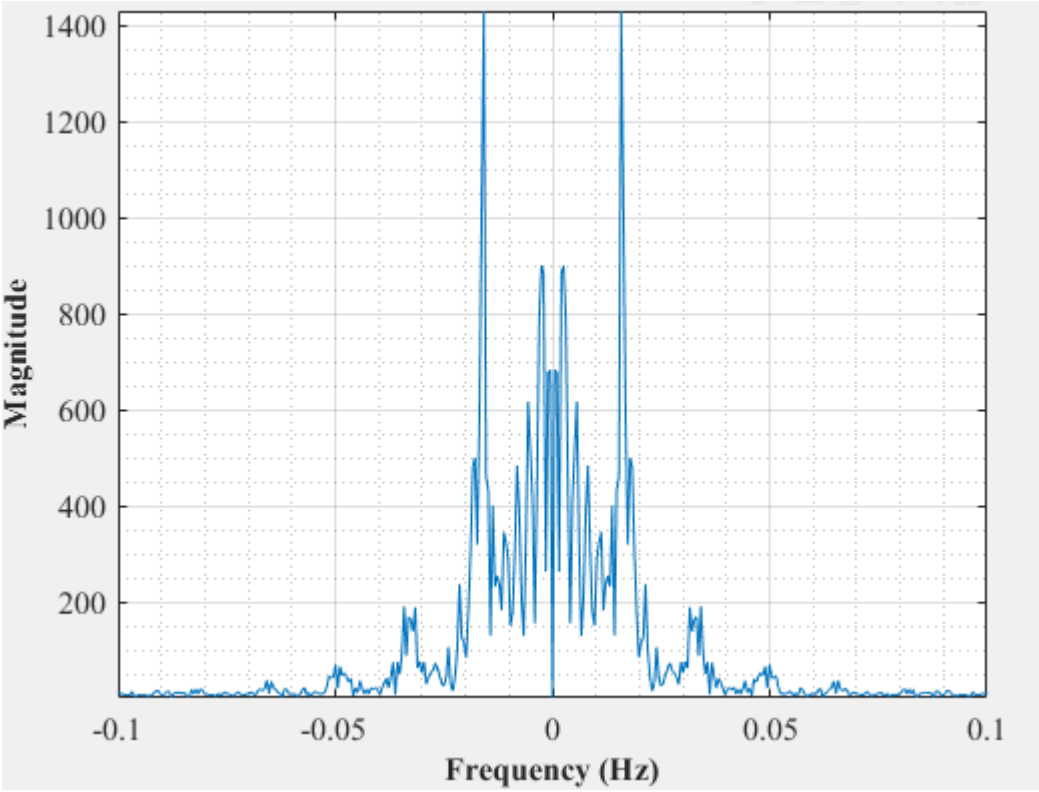


*Figure D-52: Dominant Frequency for an empty vessel at 2.83 dm$^3$/minute rotameter flow rate- Test 7*

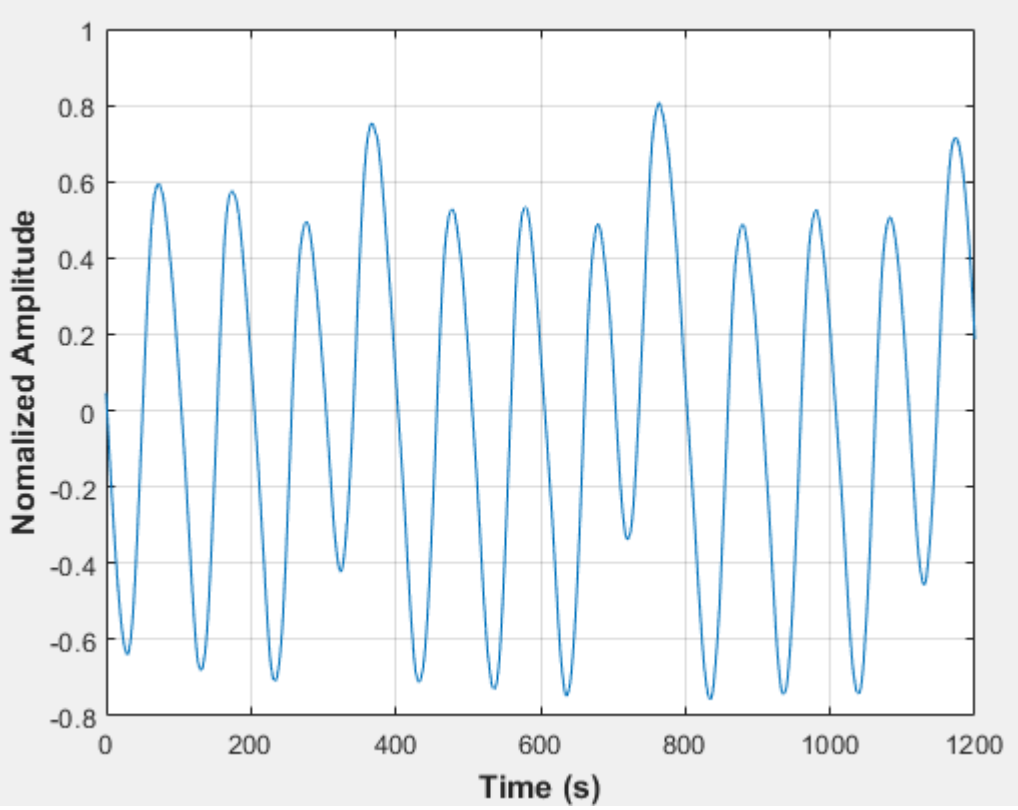


*Figure D-53: Pressure fluctuations in a uniformly packed vessel at 1.67 dm$^3$/minute rotameter flow rate- Test 1*

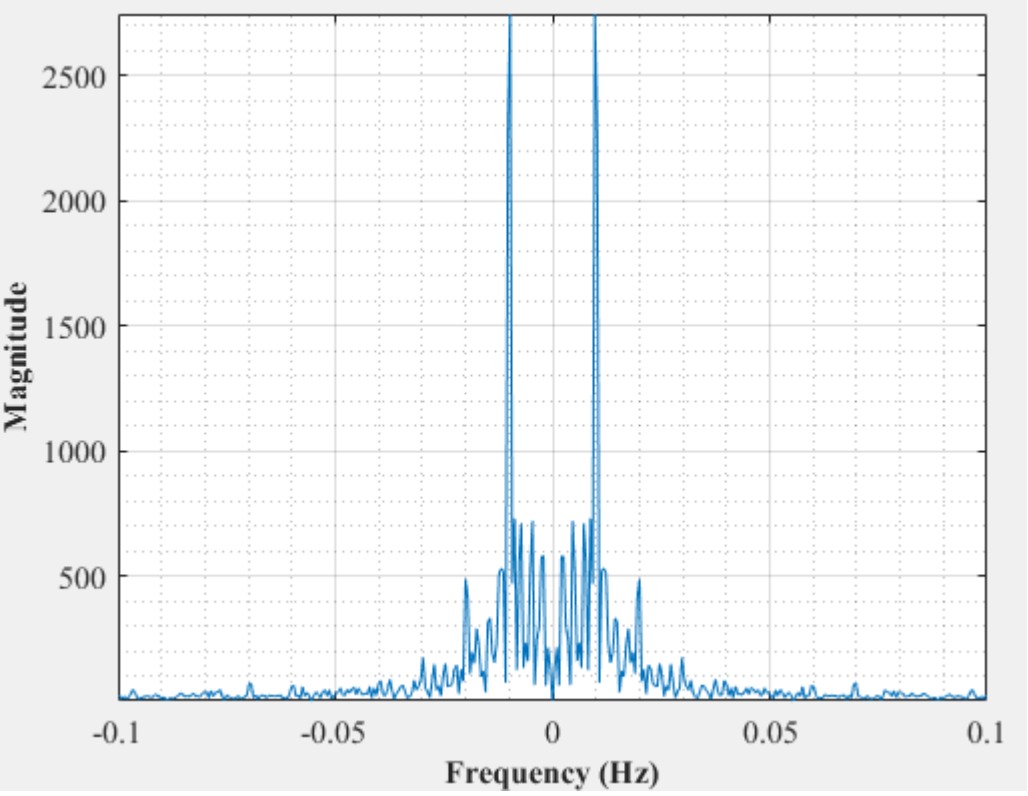


*Figure D-54: Dominant Frequency for a uniformly packed vessel at 1.67 dm$^3$/minute rotameter flow rate- test 1*

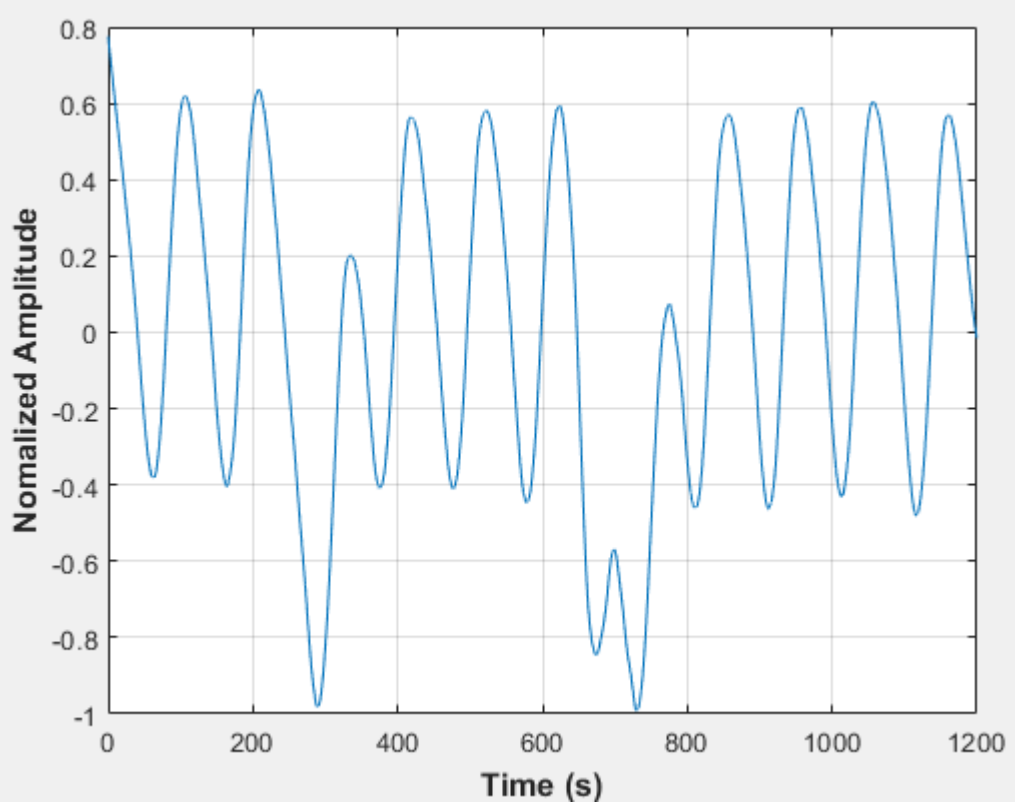


*Figure D-55: Pressure fluctuations in a uniformly packed vessel at 1.67 dm$^3$/minute rotameter flow rate- Test 2*

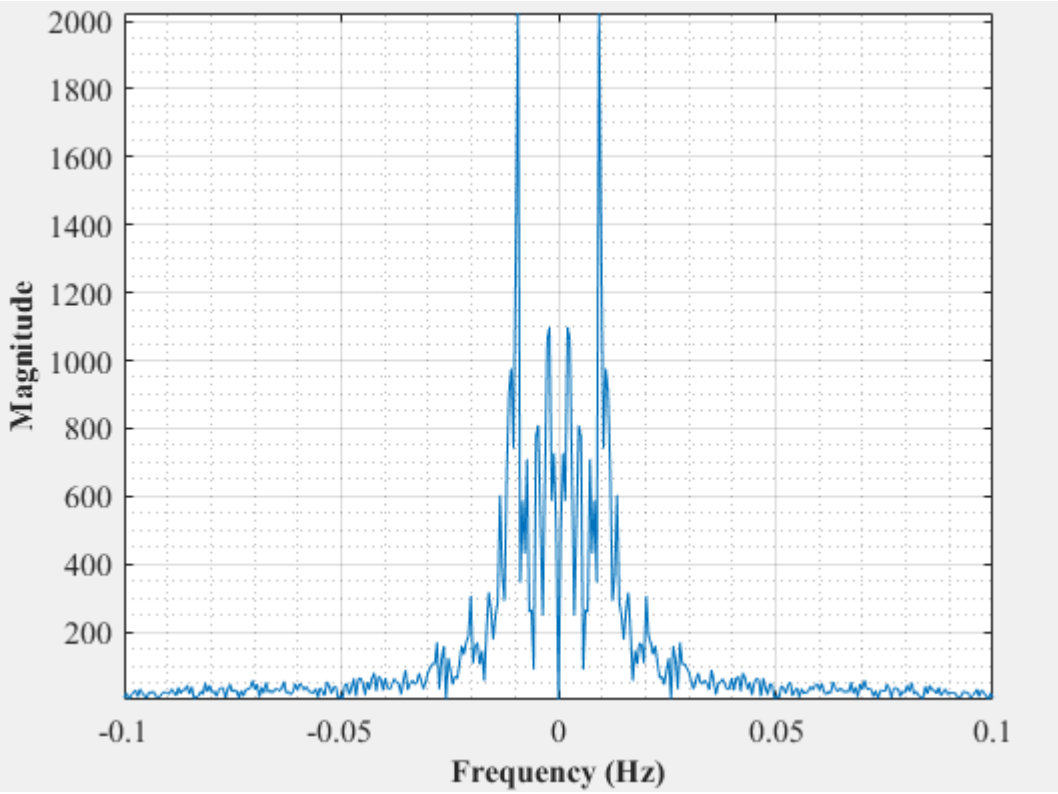


*Figure D-56: Dominant Frequency for a uniformly packed vessel at 1.67 dm$^3$/minute rotameter flow rate- test 2*

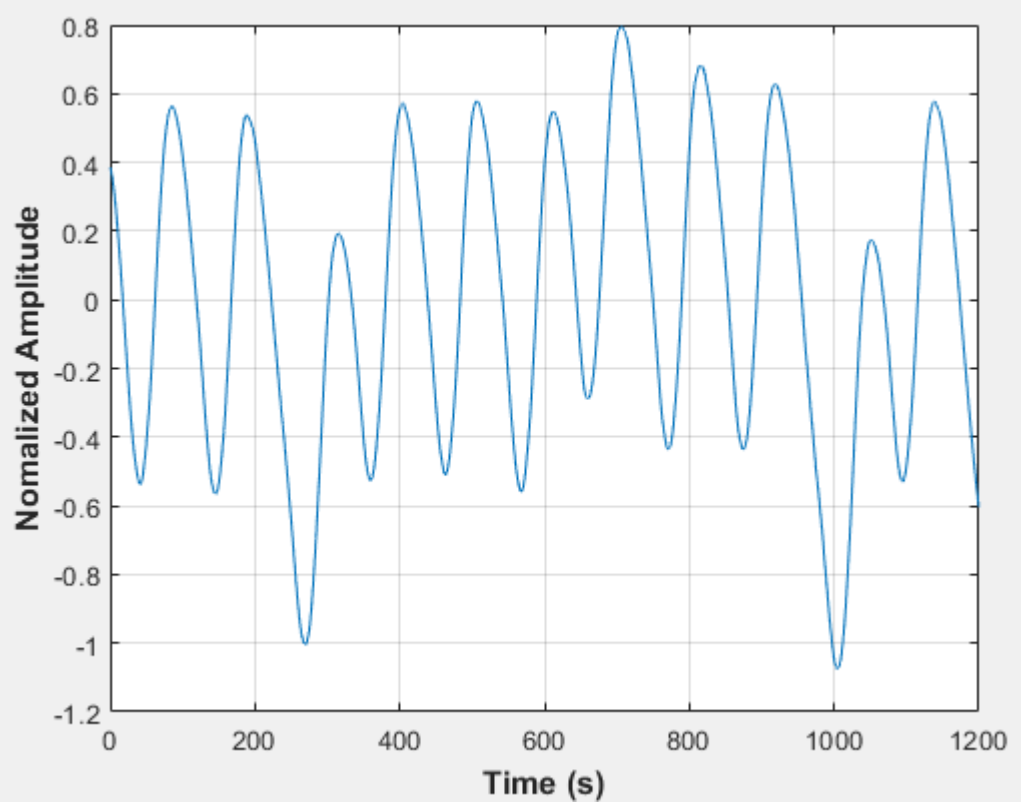


*Figure D-57: Pressure fluctuations in a uniformly packed vessel at 1.67 dm$^3$/minute rotameter flow rate- Test 3*

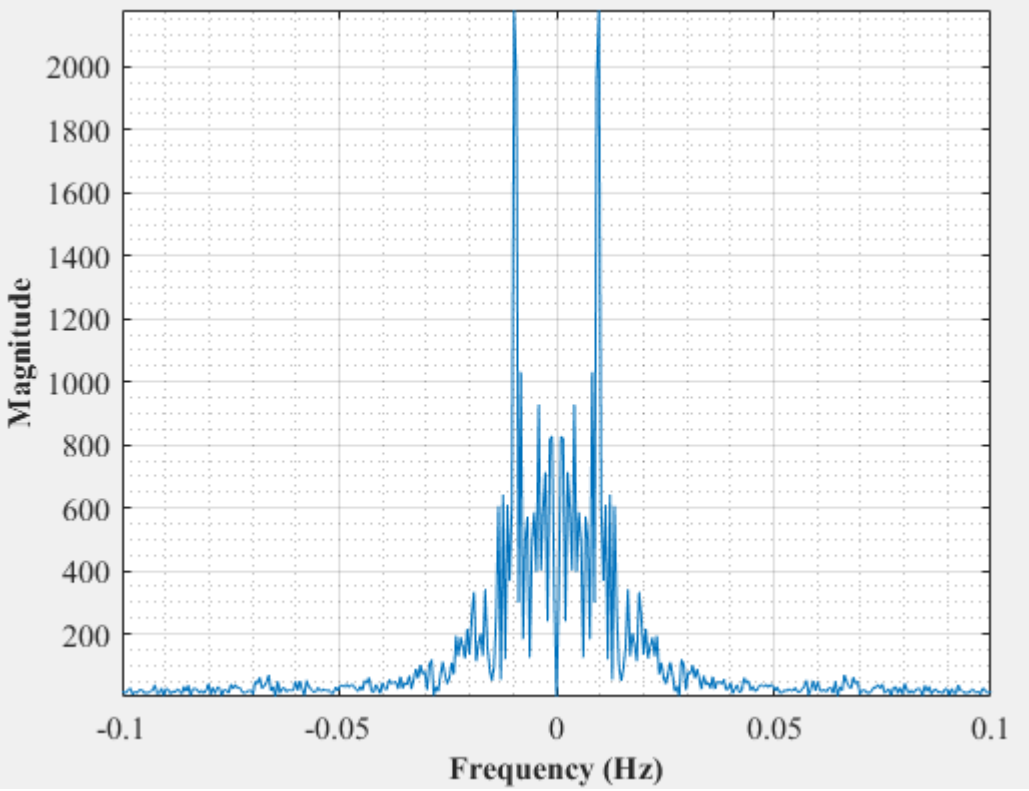


*Figure D-58: Dominant Frequency for a uniformly packed vessel at 1.67 dm$^3$/minute rotameter flow rate- test 3*

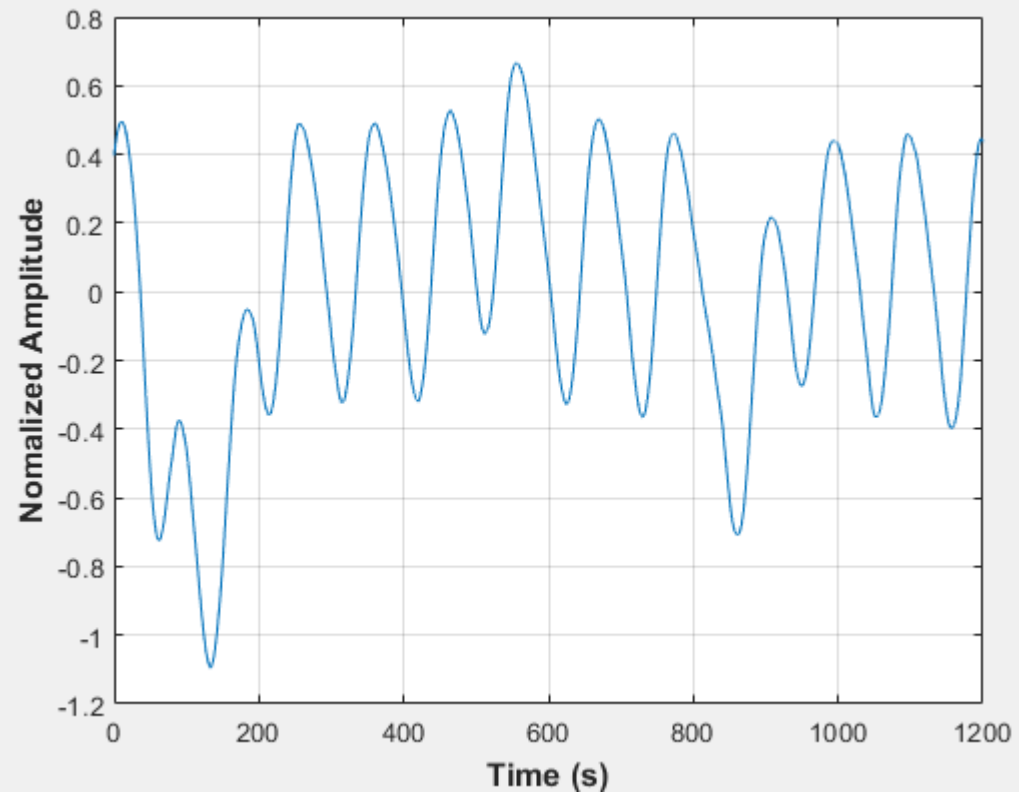


*Figure D-59: Pressure fluctuations in a uniformly packed vessel at 1.67 dm$^3$/minute rotameter flow rate- Test 4*

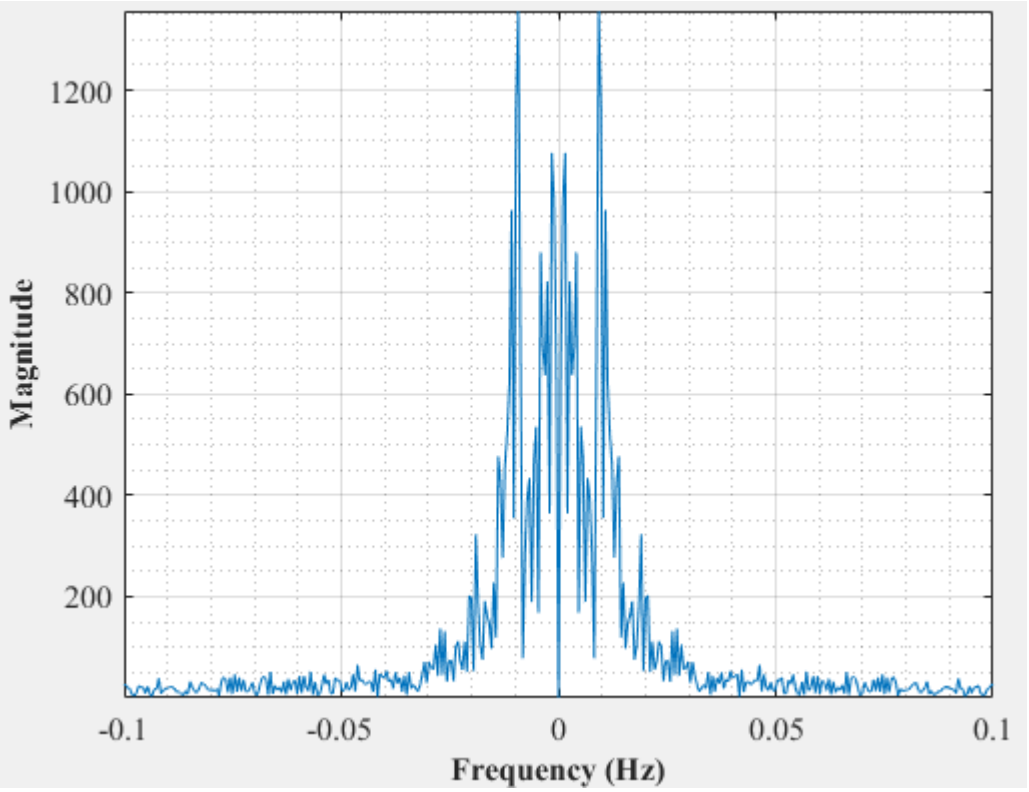


*Figure D-60: Dominant Frequency for a uniformly packed vessel at 1.67 dm$^3$/minute rotameter flow rate- test 4*

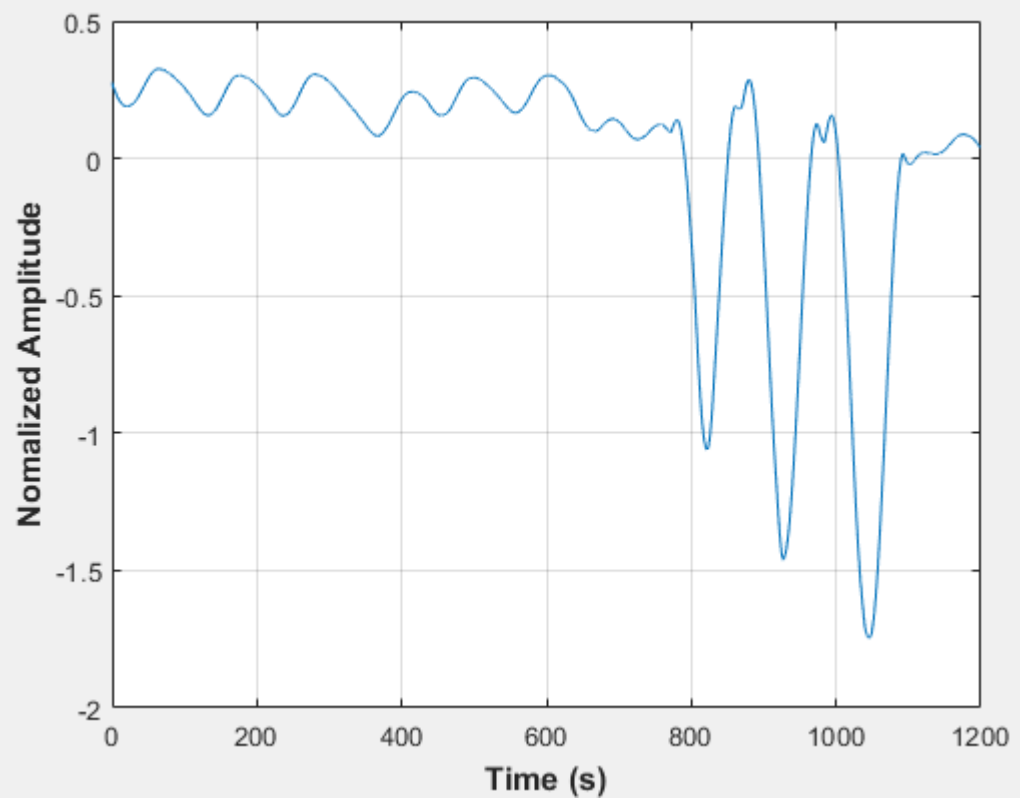


*Figure D-61: Pressure fluctuations in a uniformly packed vessel at 1.67 dm$^3$/minute rotameter flow rate- Test 5*

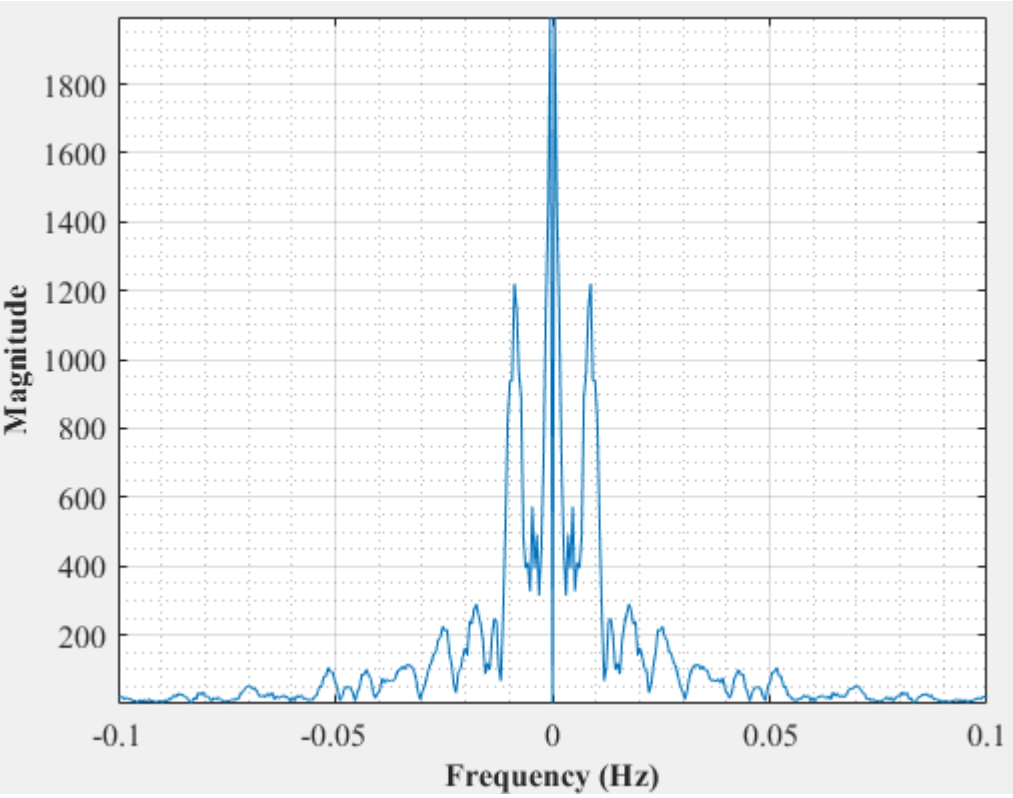


*Figure D-62: Dominant Frequency for a uniformly packed vessel at 1.67 dm$^3$/minute rotameter flow rate- test 5*

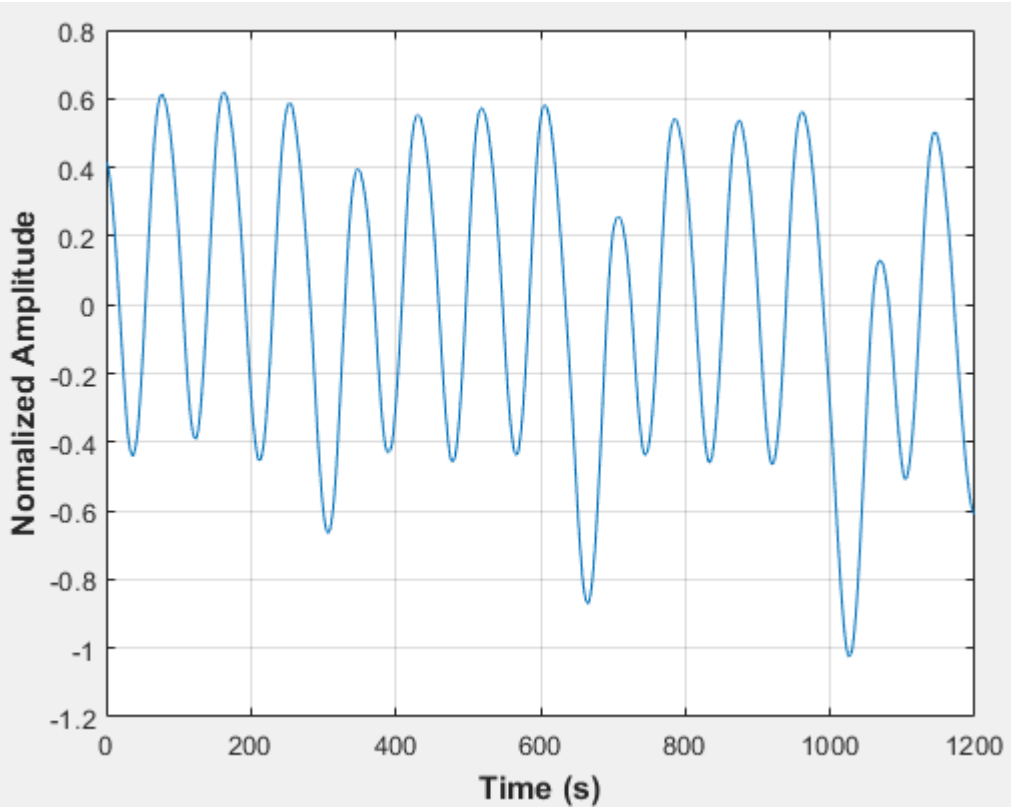


*Figure D-63: Pressure fluctuations in a uniformly packed vessel at 2 dm$^3$/minute rotameter flow rate- Test 1*

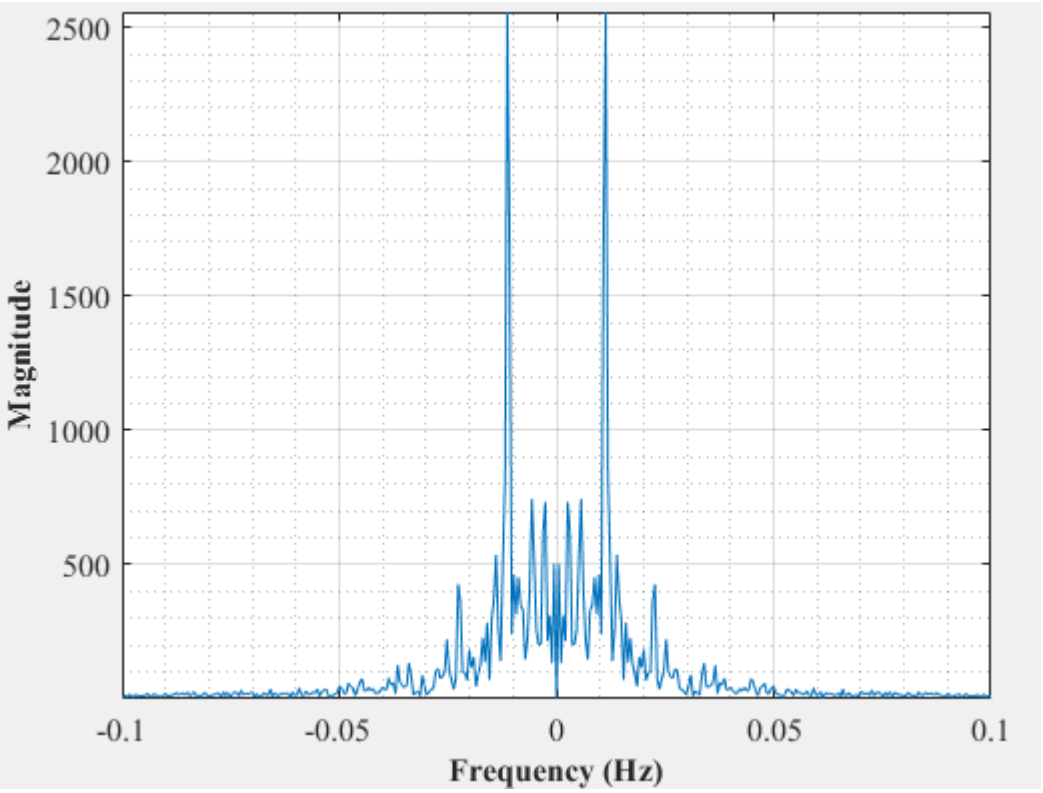


*Figure D-64: Dominant Frequency for a uniformly packed vessel at 2 dm$^3$/minute rotameter flow rate- Test 1*

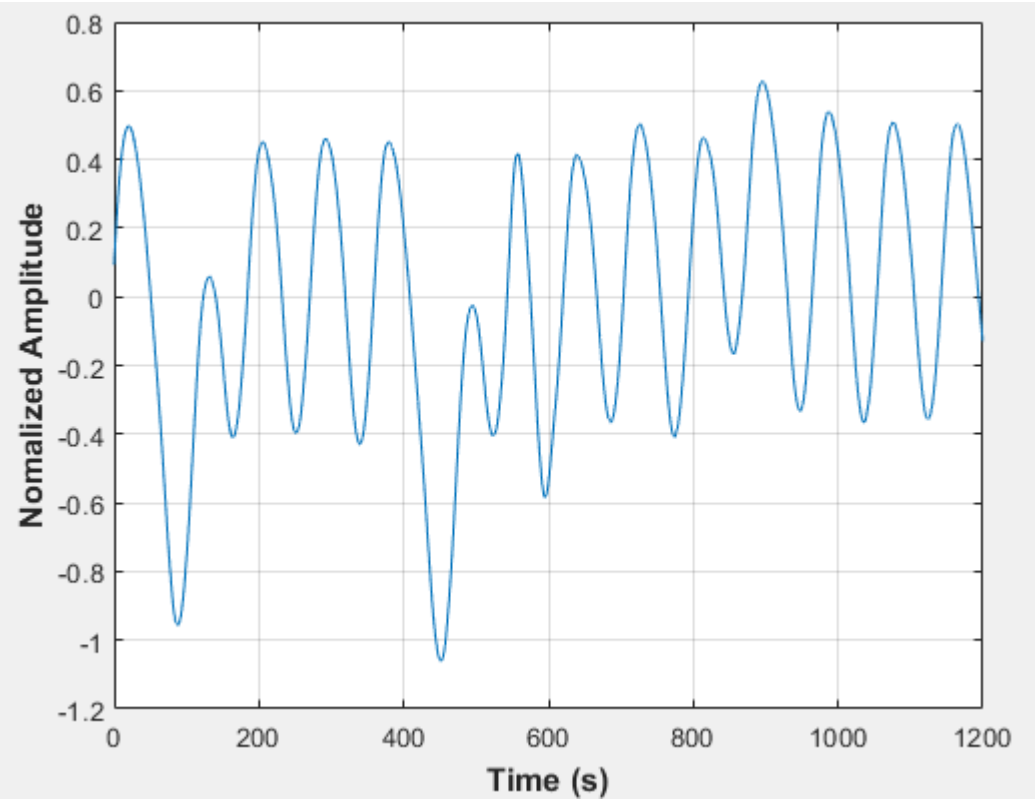


*Figure D-65: Pressure fluctuations in a uniformly packed vessel at 2 dm$^3$/minute rotameter flow rate- Test 2*

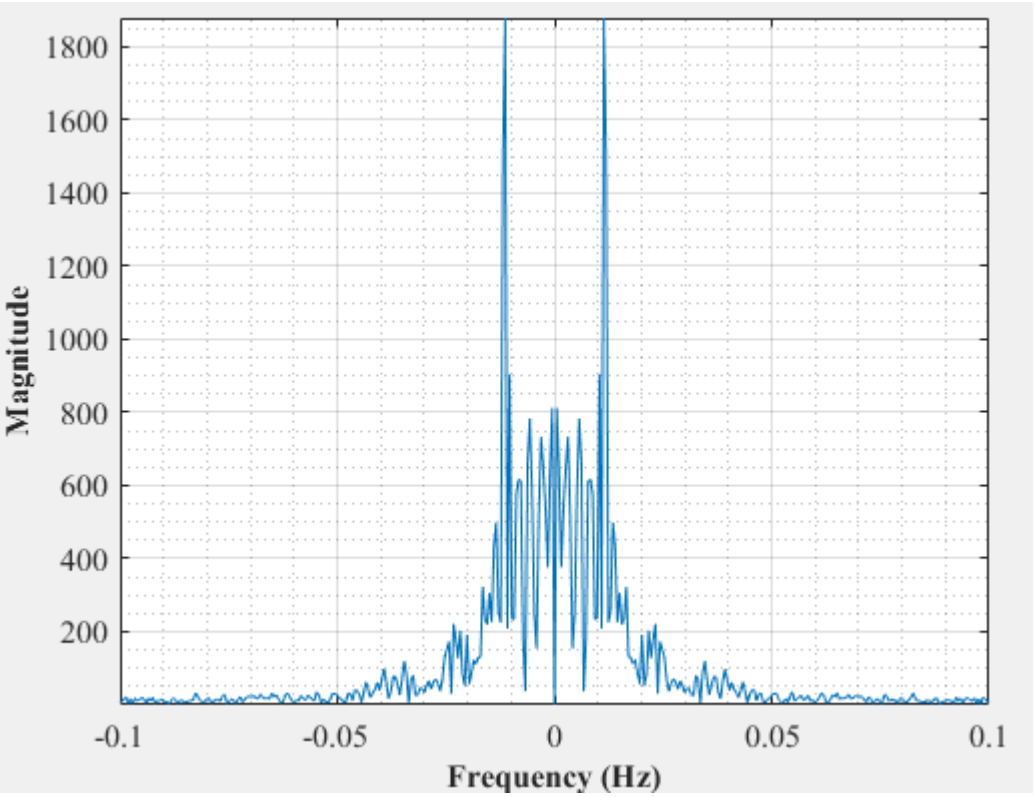


*Figure D-66: Dominant Frequency for a uniformly packed vessel at 2 dm$^3$/minute rotameter flow rate- Test 2*

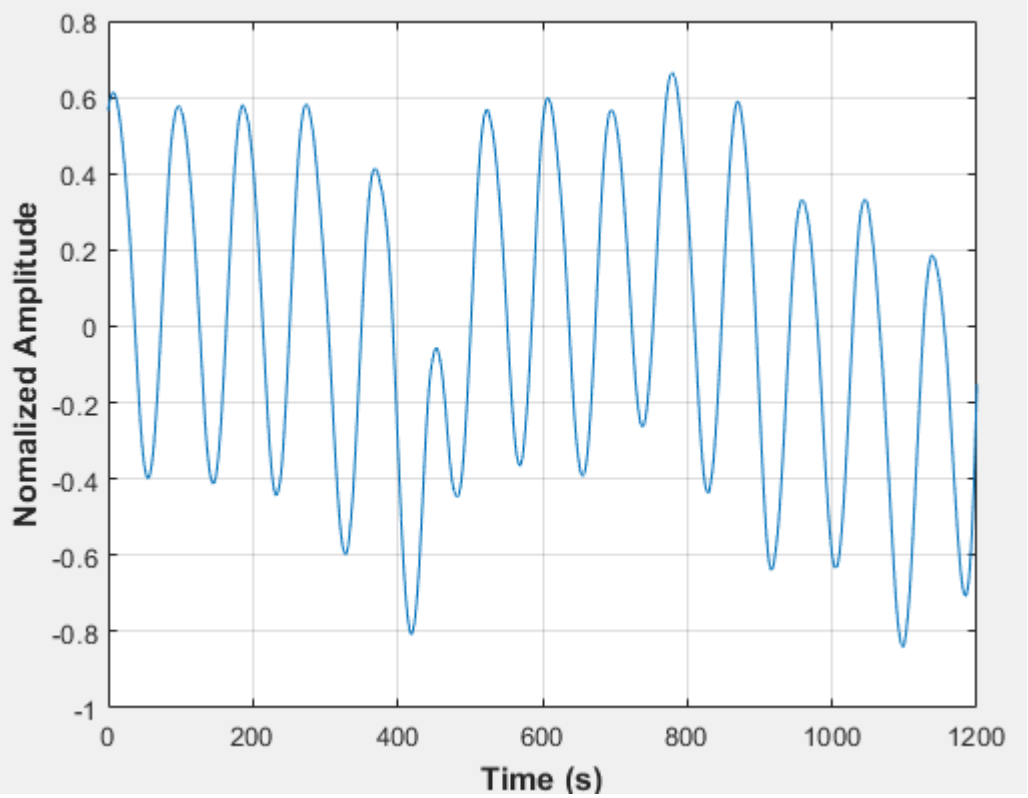


*Figure D-67: Pressure fluctuations in a uniformly packed vessel at 2 $dm^3$/minute rotameter flow rate- Test 3*

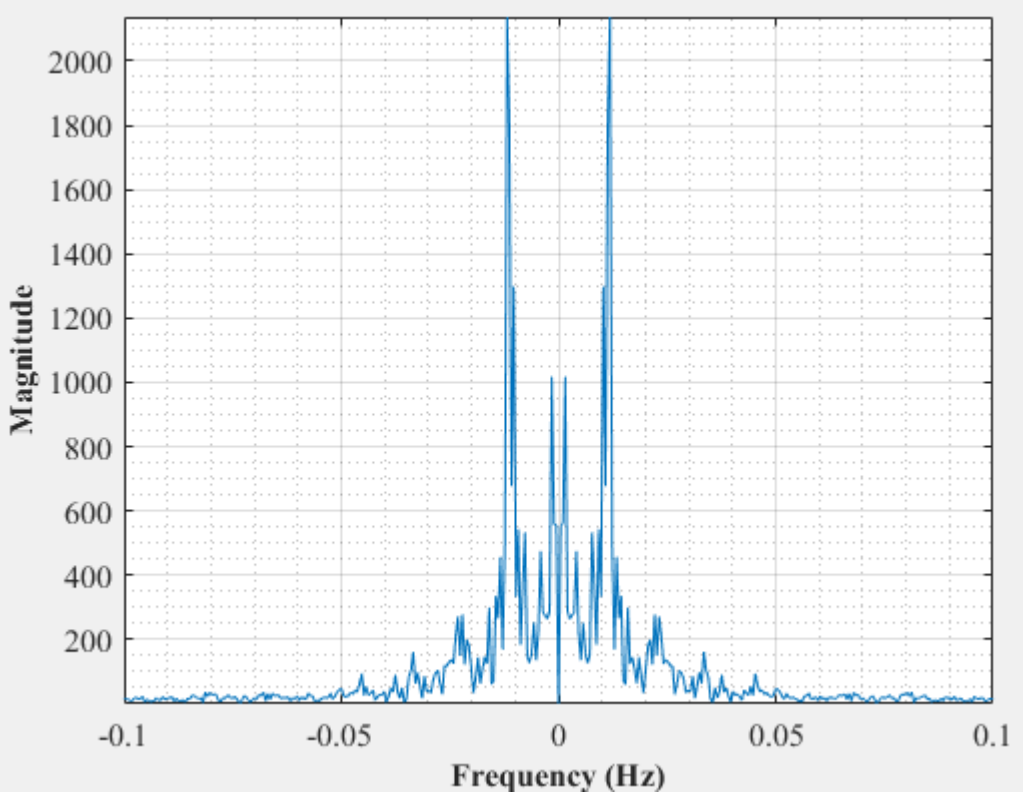


*Figure D-68: Dominant Frequency for a uniformly packed vessel at 2 $dm^3$/minute rotameter flow rate- Test 3*

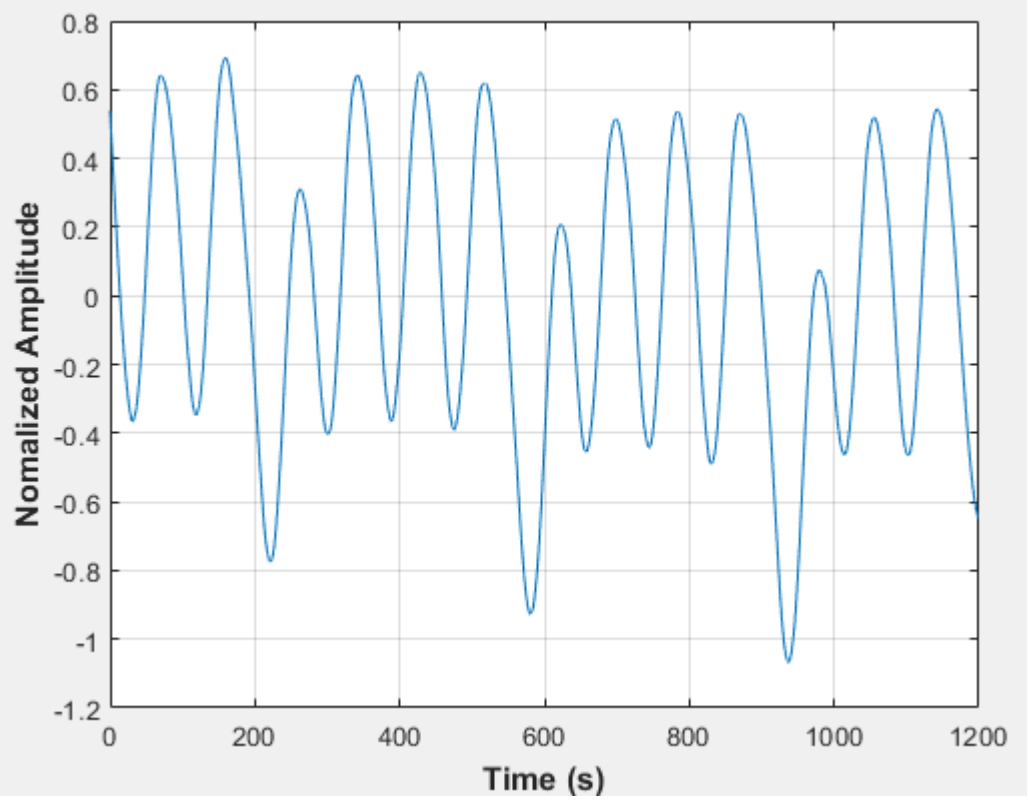


*Figure D-69: Pressure fluctuations in a uniformly packed vessel at 2 $dm^3$/minute rotameter flow rate- Test 4*

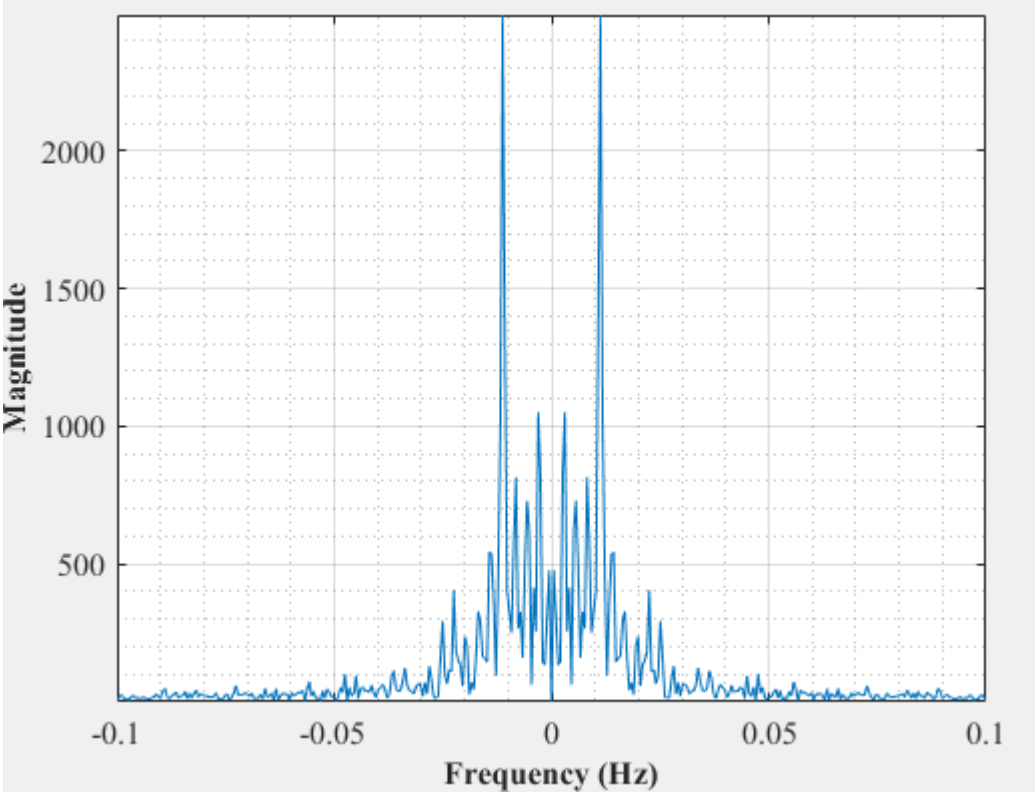


*Figure D-70: Dominant Frequency for a uniformly packed vessel at 2 $dm^3$/minute rotameter flow rate- Test 4*

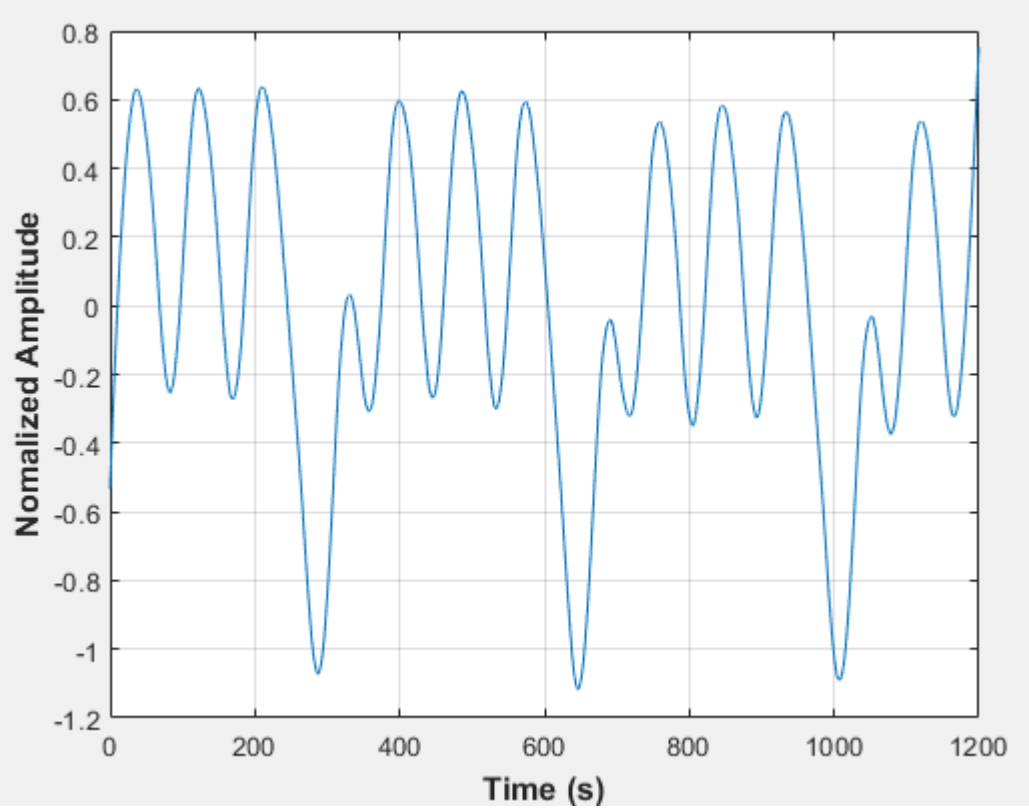


*Figure D-71: Pressure fluctuations in a uniformly packed vessel at 2 dm$^3$/minute rotameter flow rate- Test 5*

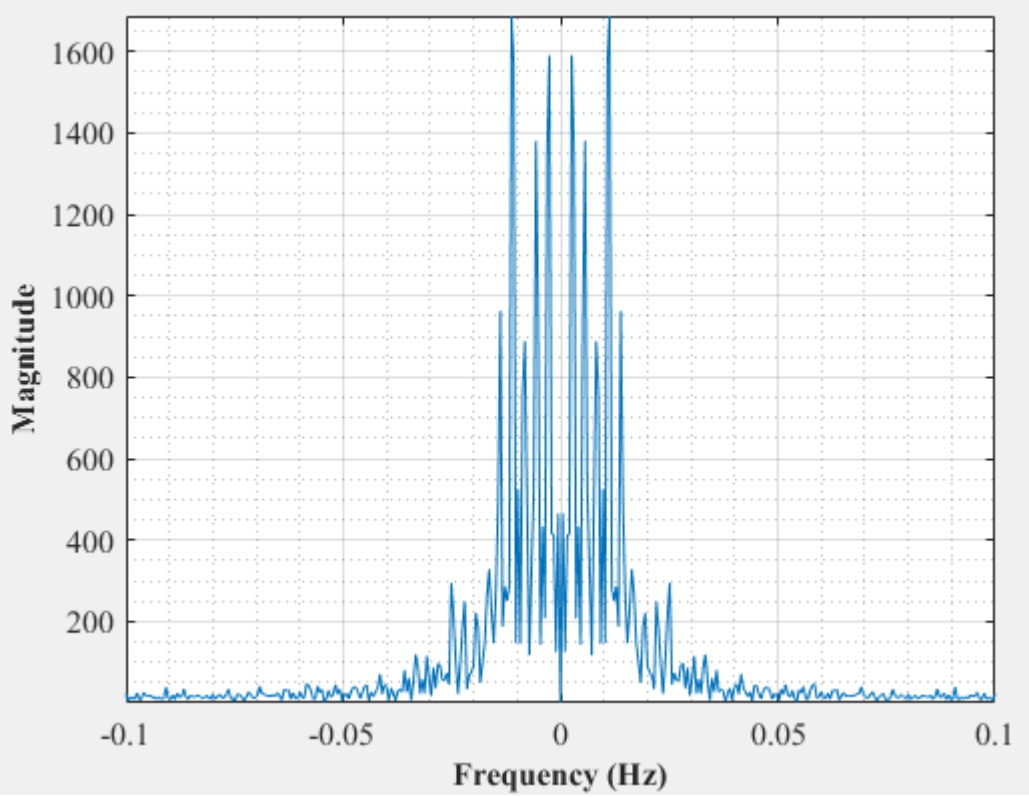


*Figure D-72: Dominant Frequency for a uniformly packed vessel at 2 dm$^3$/minute rotameter flow rate- Test 5*

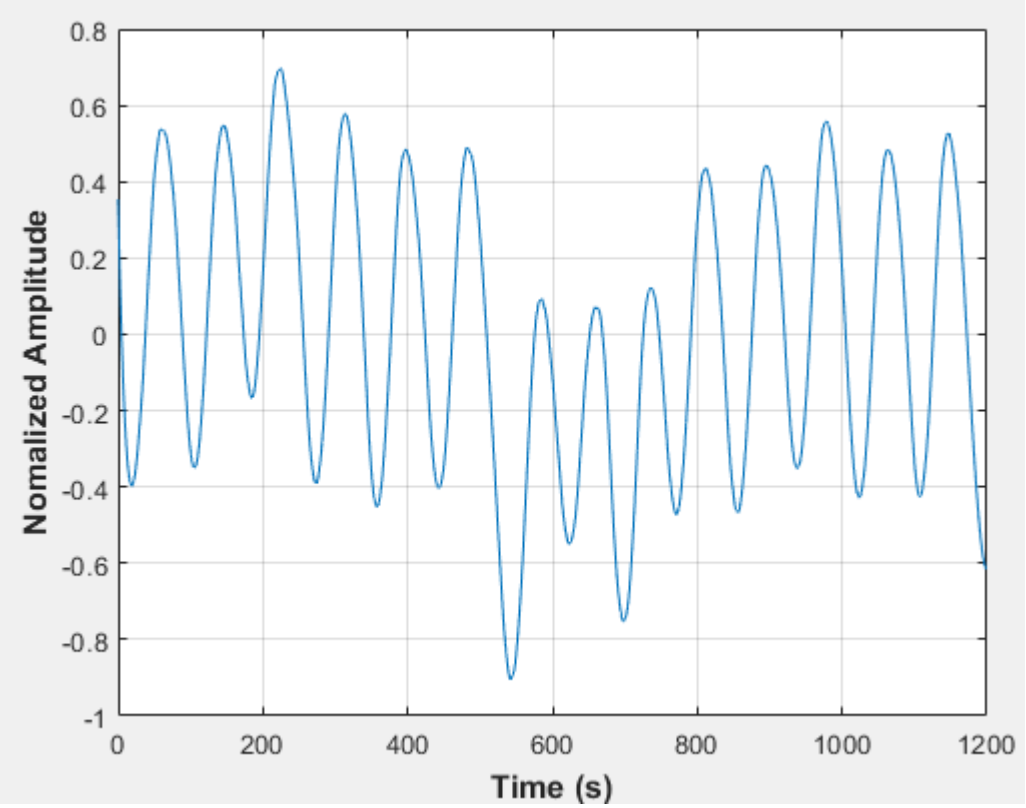


*Figure D-73: Pressure fluctuations in a uniformly packed vessel at 2 dm$^3$/minute rotameter flow rate- Test 6*

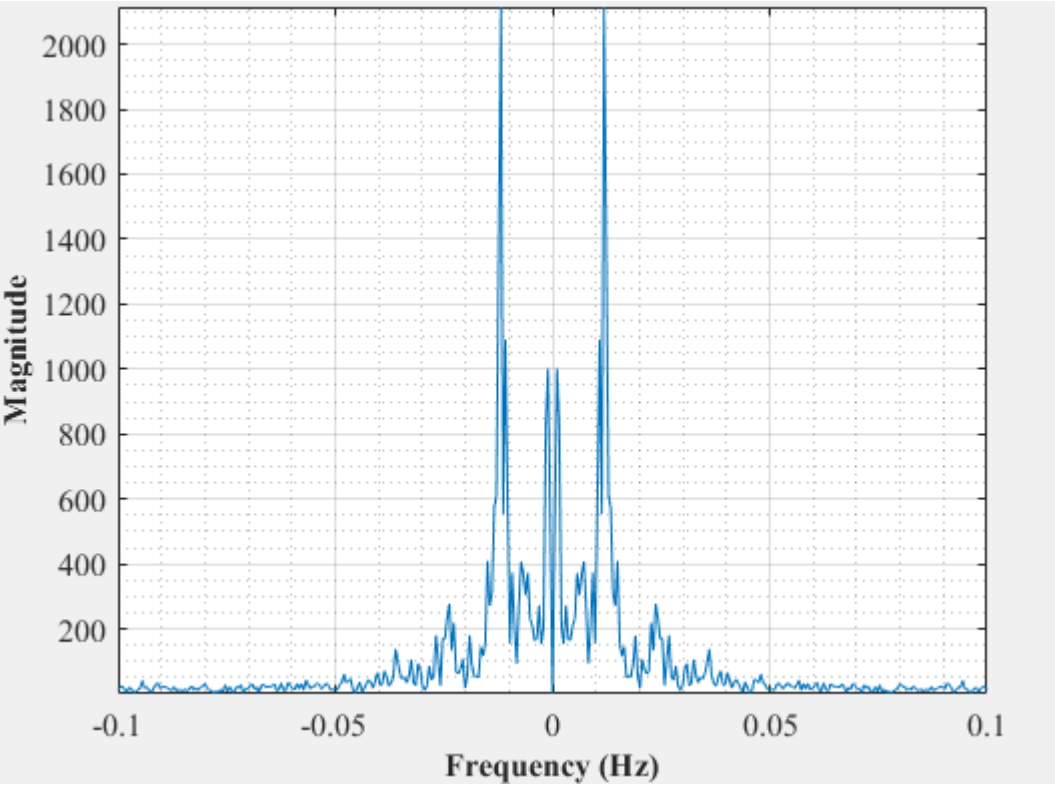


*Figure D-74: Dominant Frequency for a uniformly packed vessel at 2 dm$^3$/minute rotameter flow rate- Test 6*

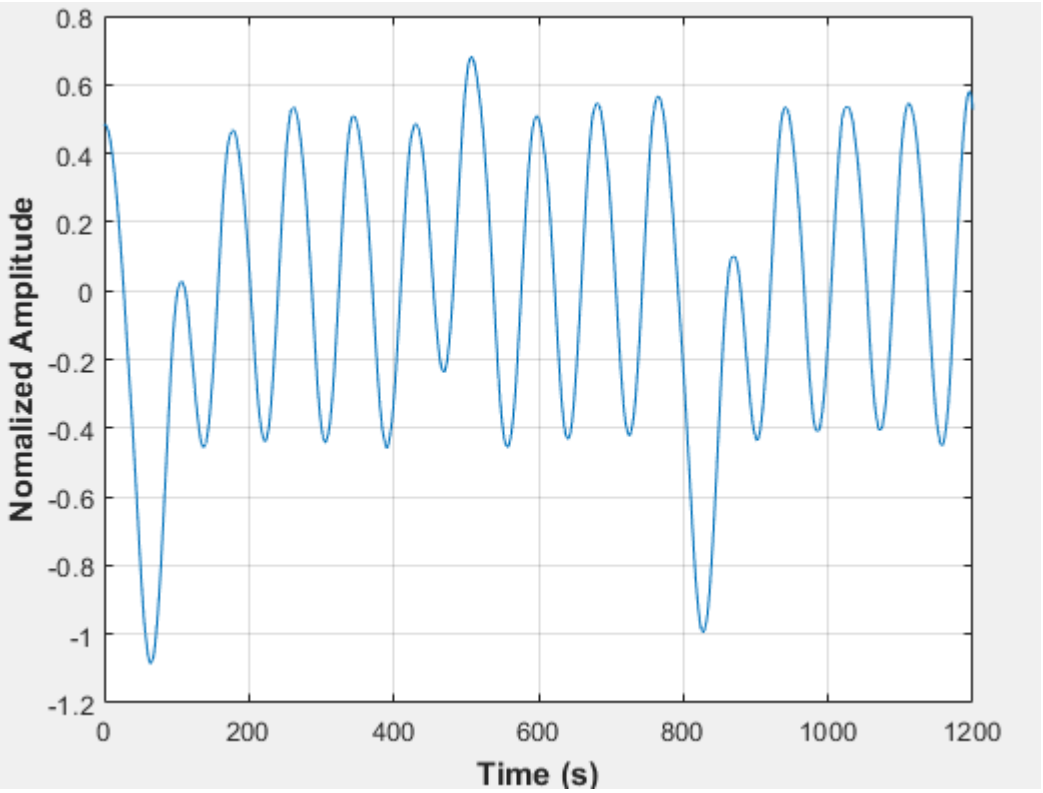


*Figure D-75: Pressure fluctuations in a uniformly packed vessel at 2 dm$^3$/minute rotameter flow rate- Test 7*

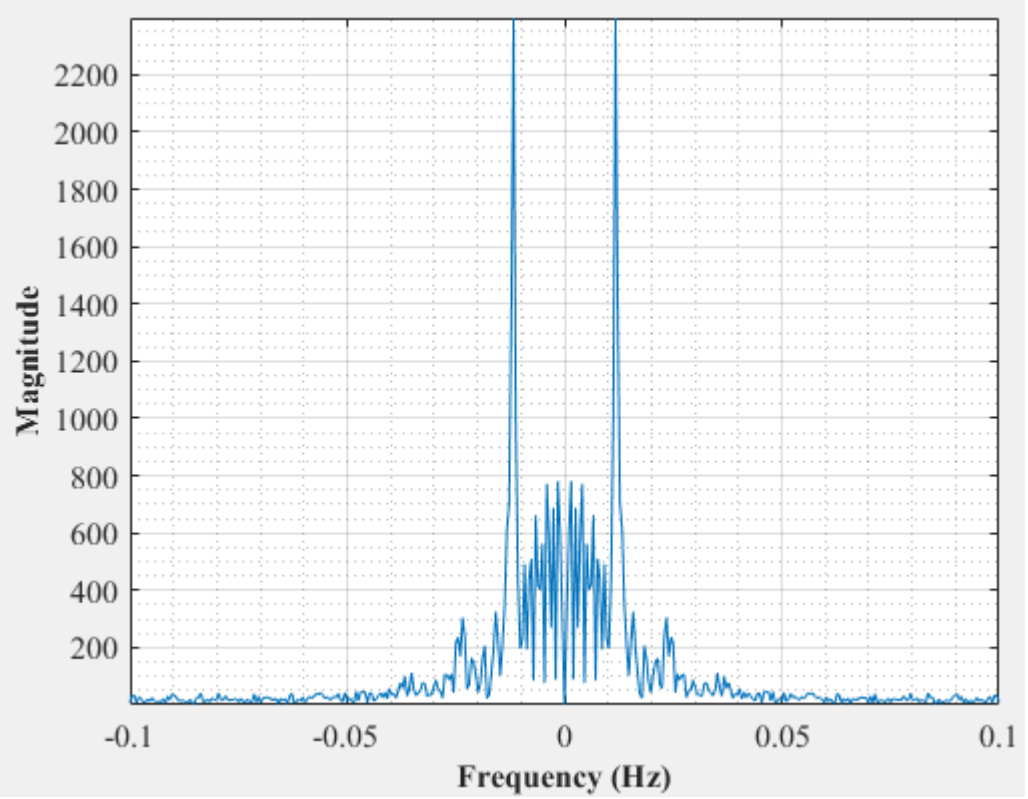


*Figure D-76: Dominant Frequency for a uniformly packed vessel at 2 dm$^3$/minute rotameter flow rate- Test 7*

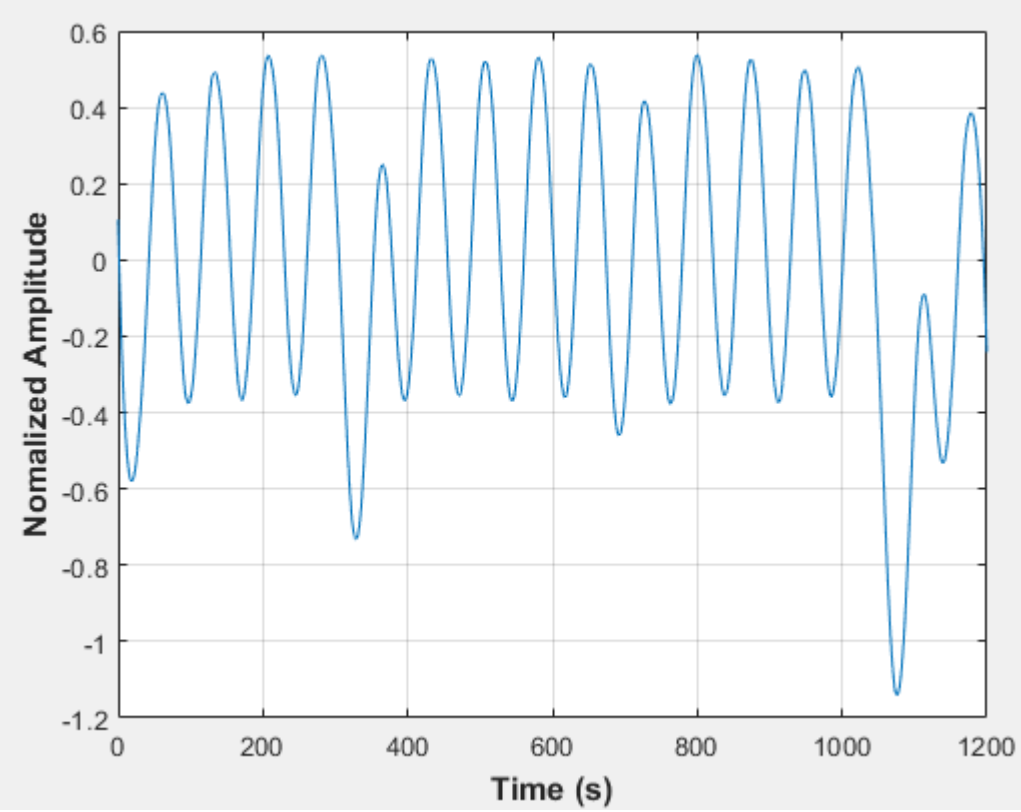


*Figure D-77: Pressure fluctuations in a uniformly packed vessel at 2.33 $dm^3$/minute rotameter flow rate- Test 1*

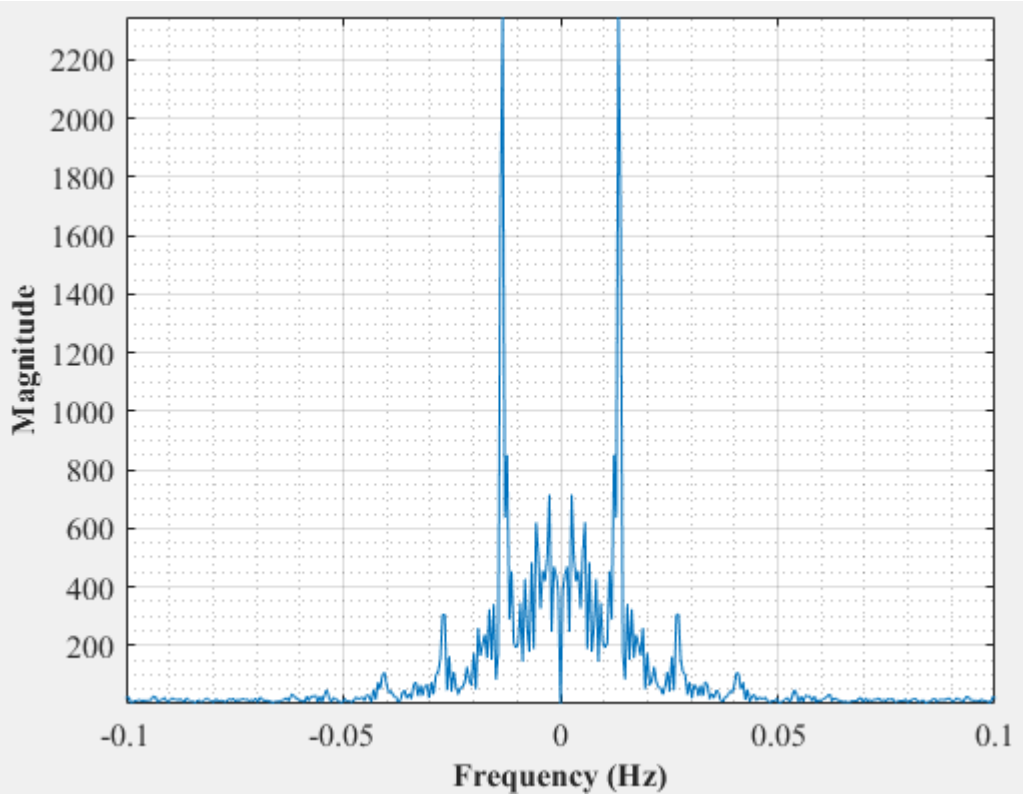


*Figure D-78: Dominant Frequency for a uniformly packed vessel at 2.33 $dm^3$/minute rotameter flow rate- Test 1*

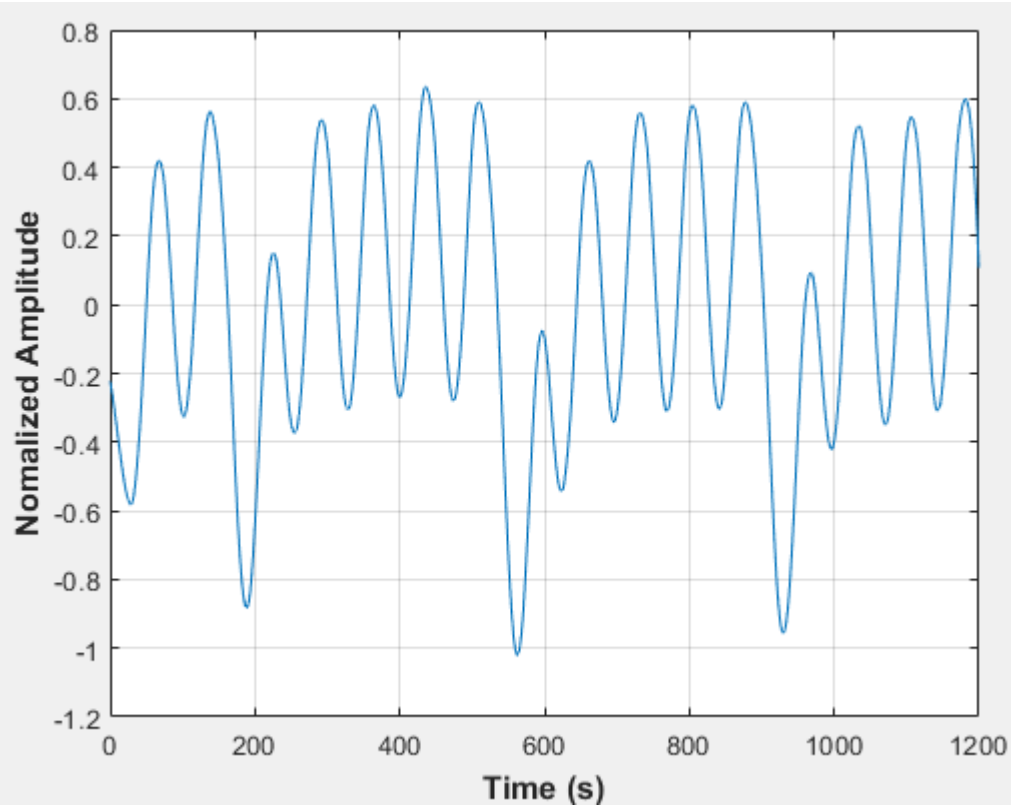


*Figure D-79: Pressure fluctuations in a uniformly packed vessel at 2.33 dm$^3$/minute rotameter flow rate- Test 2*

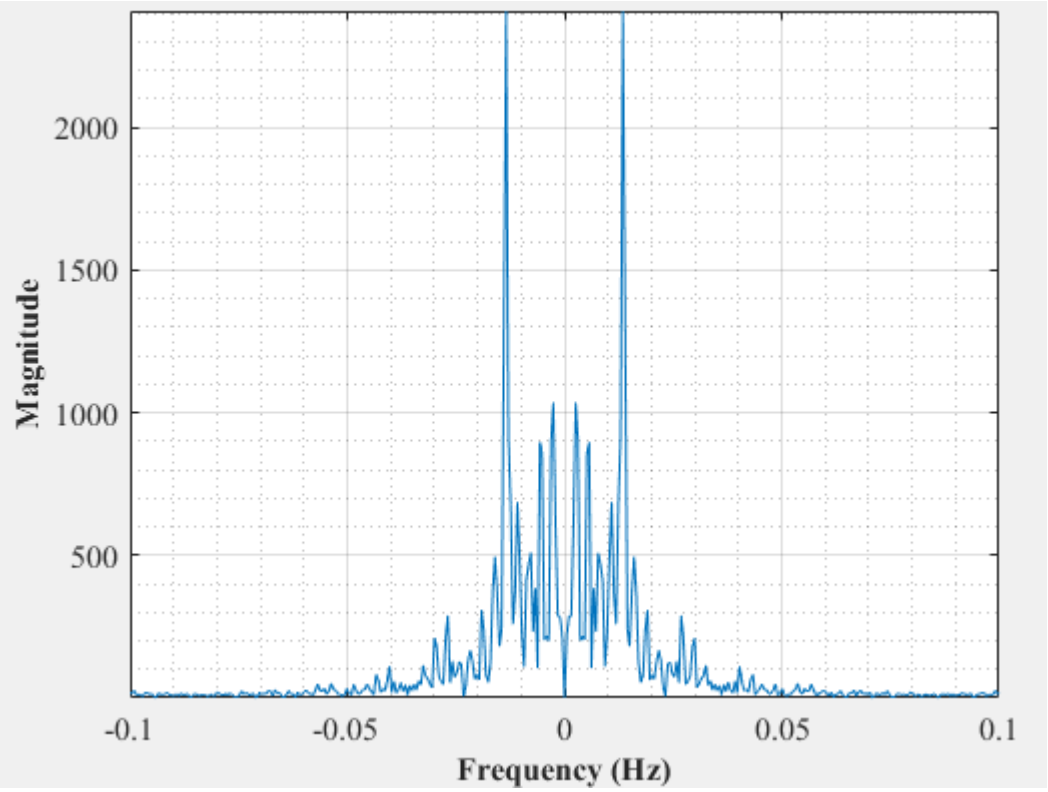


*Figure D-80: Dominant Frequency for a uniformly packed vessel at 2.33 dm$^3$/minute rotameter flow rate- Test 2*

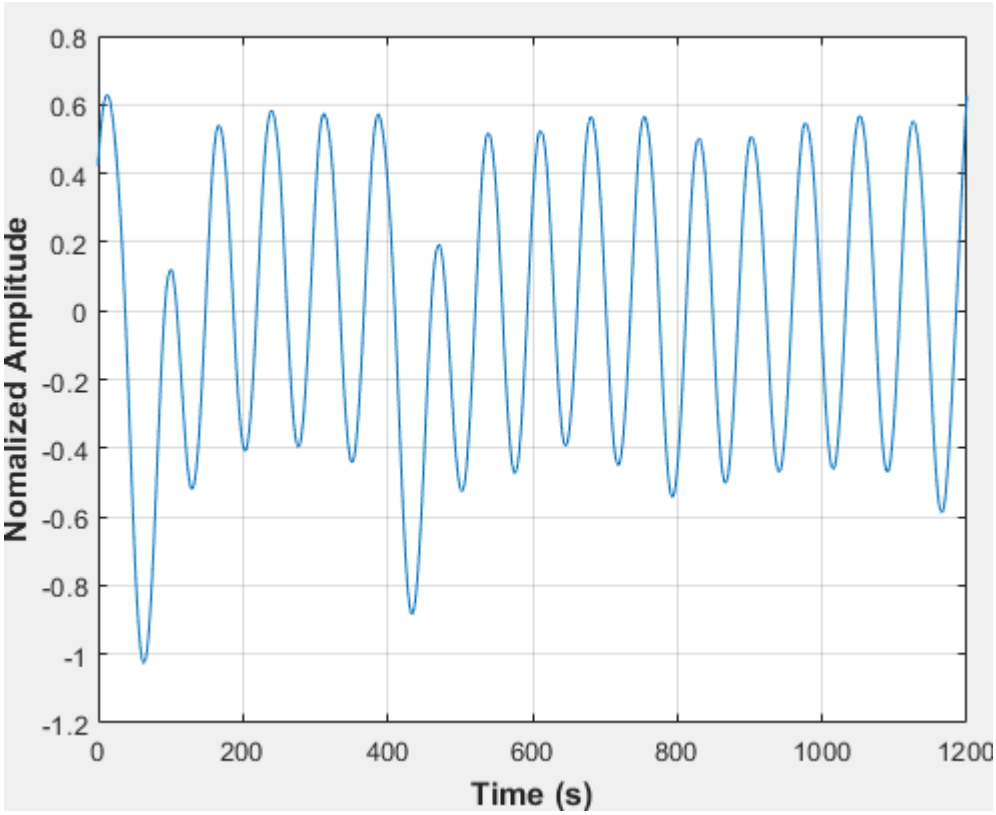


*Figure D-81: Pressure fluctuations in a uniformly packed vessel at 2.33 dm$^3$/minute rotameter flow rate- Test 3*

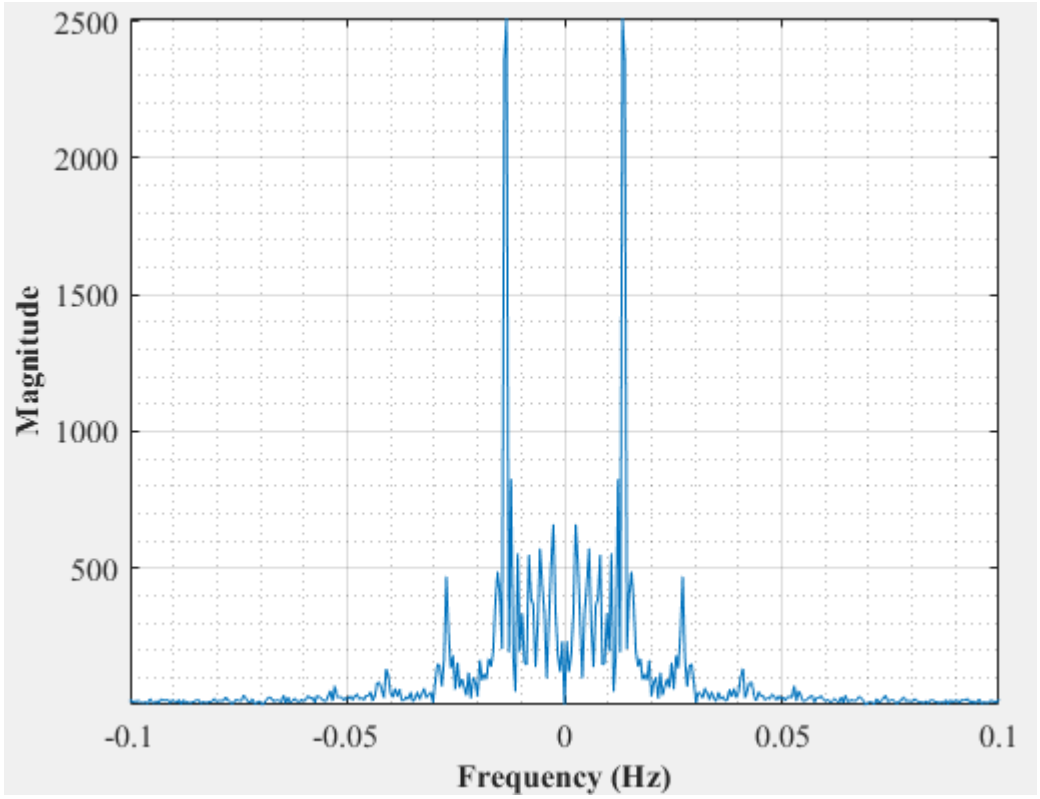


*Figure D-82: Dominant Frequency for a uniformly packed vessel at 2.33 dm$^3$/minute rotameter flow rate- Test 3*

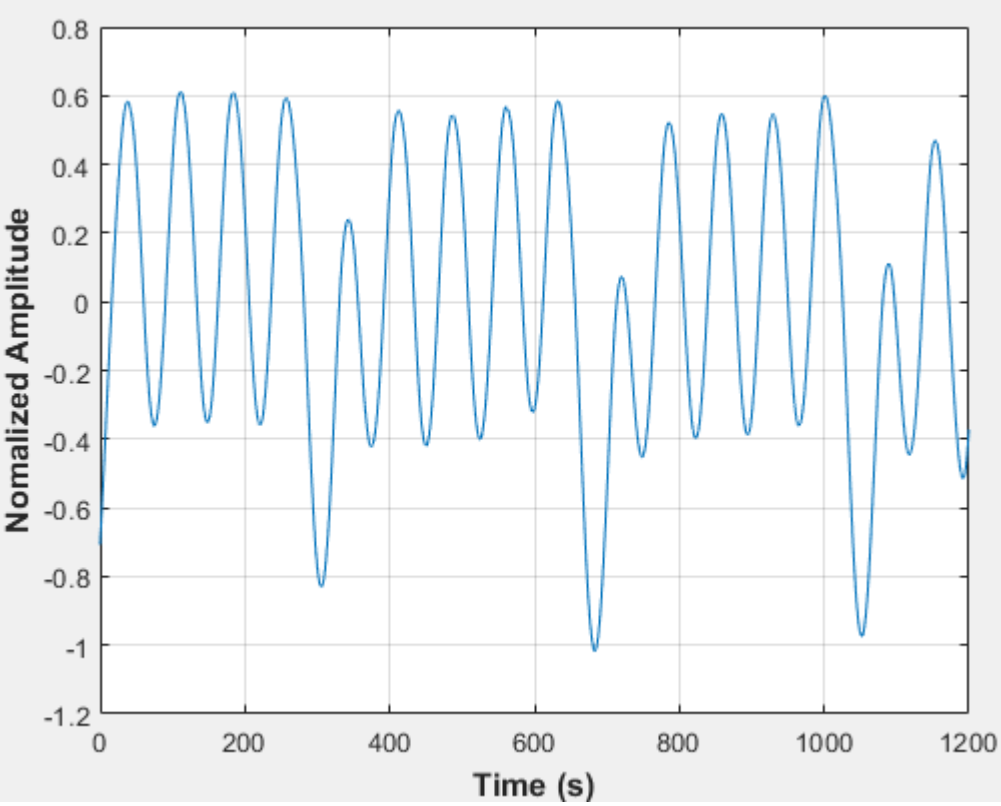


*Figure D-83: Pressure fluctuations in a uniformly packed vessel at 2.33 dm$^3$/minute rotameter flow rate- Test 4*

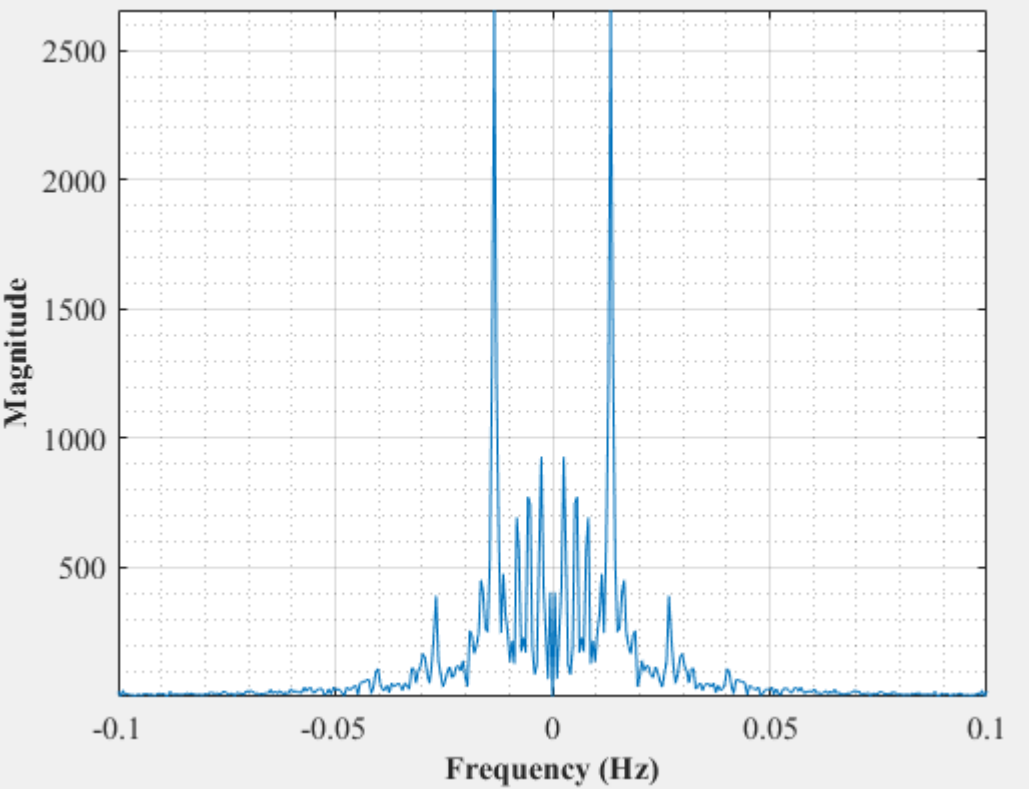


*Figure D-84: Dominant Frequency for a uniformly packed vessel at 2.33 dm$^3$/minute rotameter flow rate- Test 4*

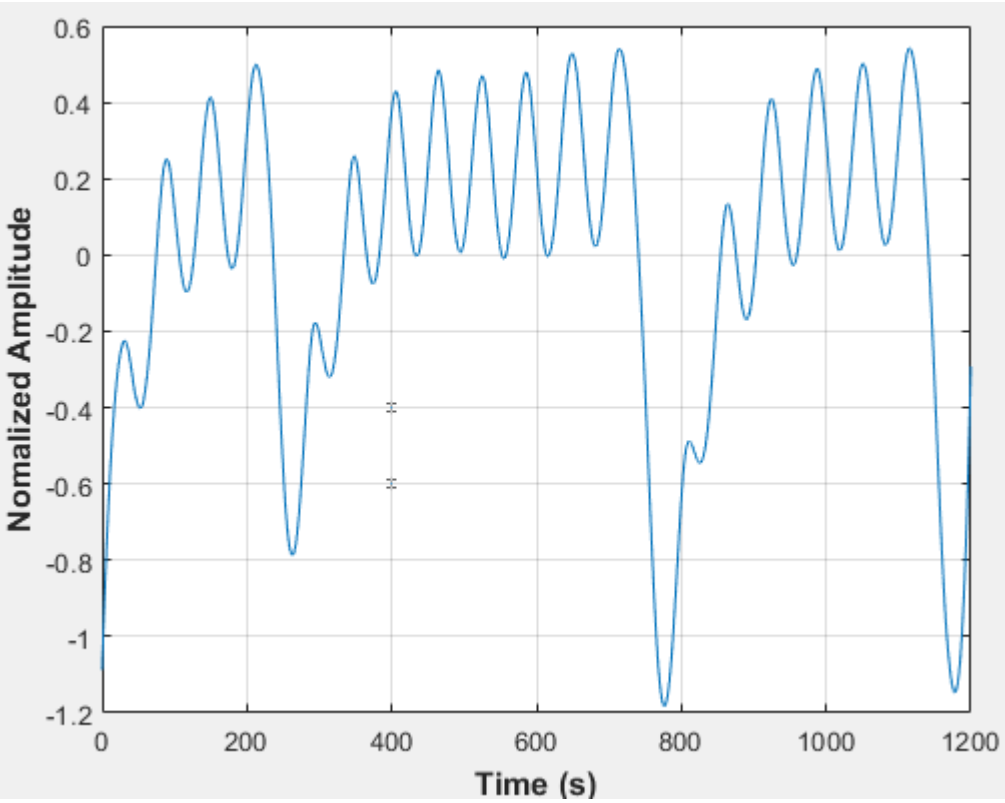


*Figure D-85: Pressure fluctuations in a uniformly packed vessel at 2.67 dm$^3$/minute rotameter flow rate- Test 1*

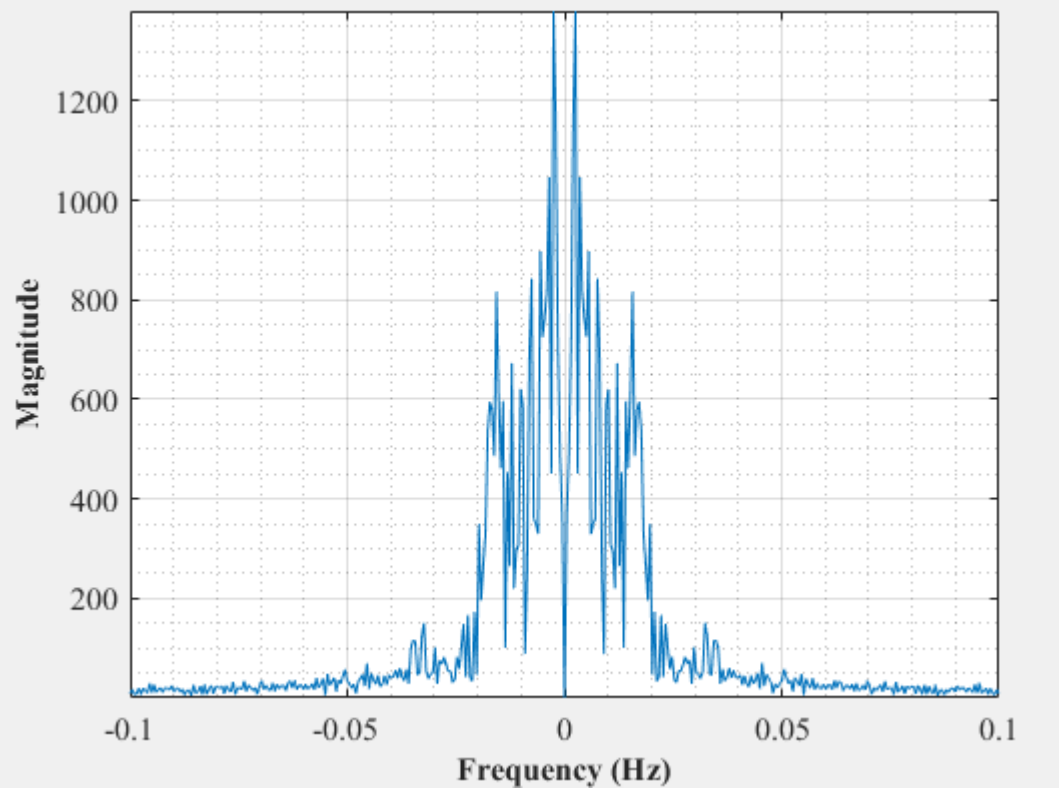


*Figure D-86: Dominant Frequency for a uniformly packed vessel at 2.67 dm$^3$/minute rotameter flow rate- Test 1*

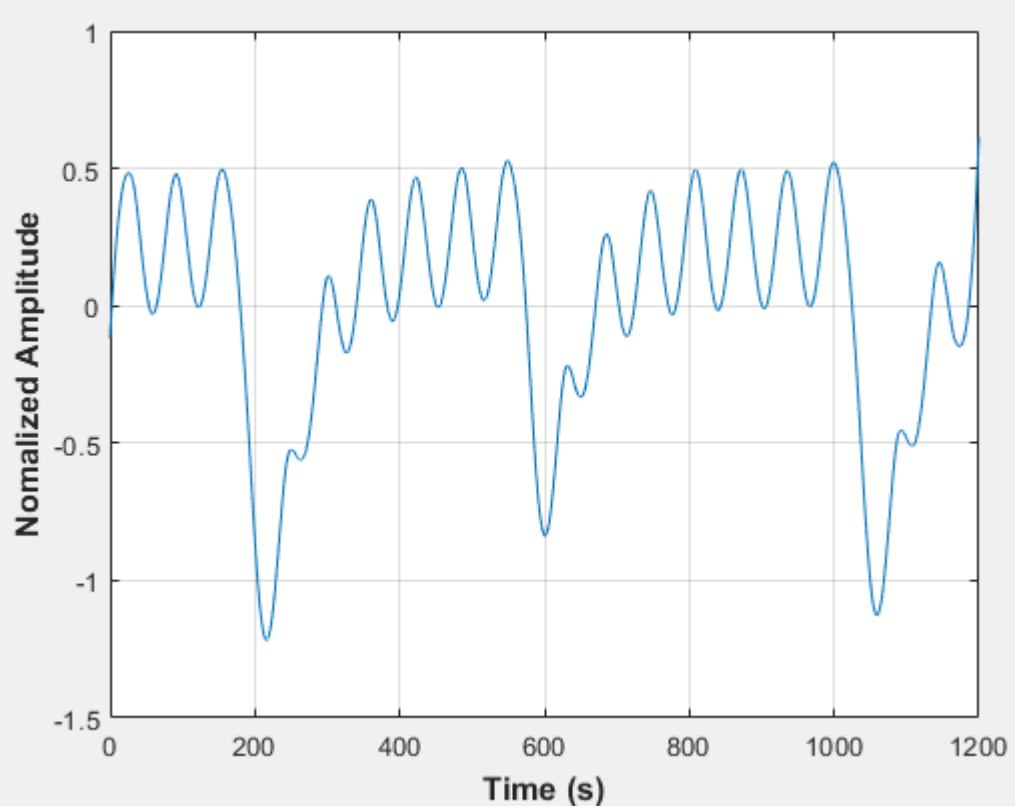


*Figure D-87: Pressure fluctuations in a uniformly packed vessel at 2.67 dm$^3$/minute rotameter flow rate- Test 2*

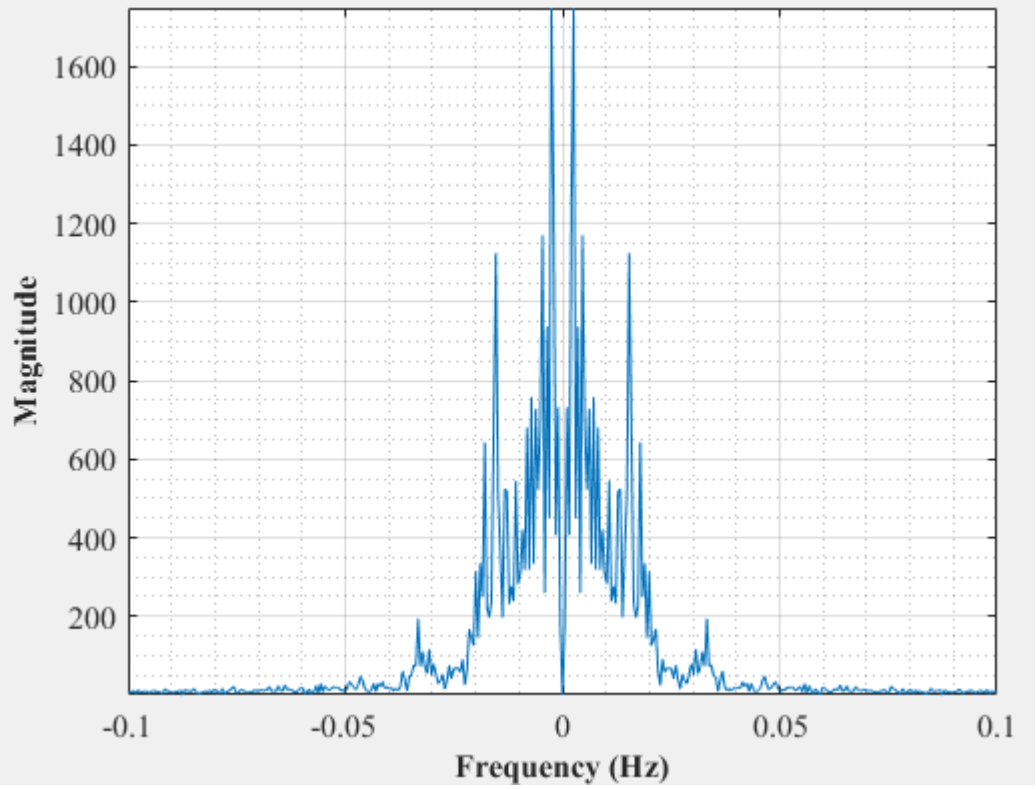


*Figure D-88: Dominant Frequency for a uniformly packed vessel at 2.67 dm$^3$/minute rotameter flow rate- Test 2*

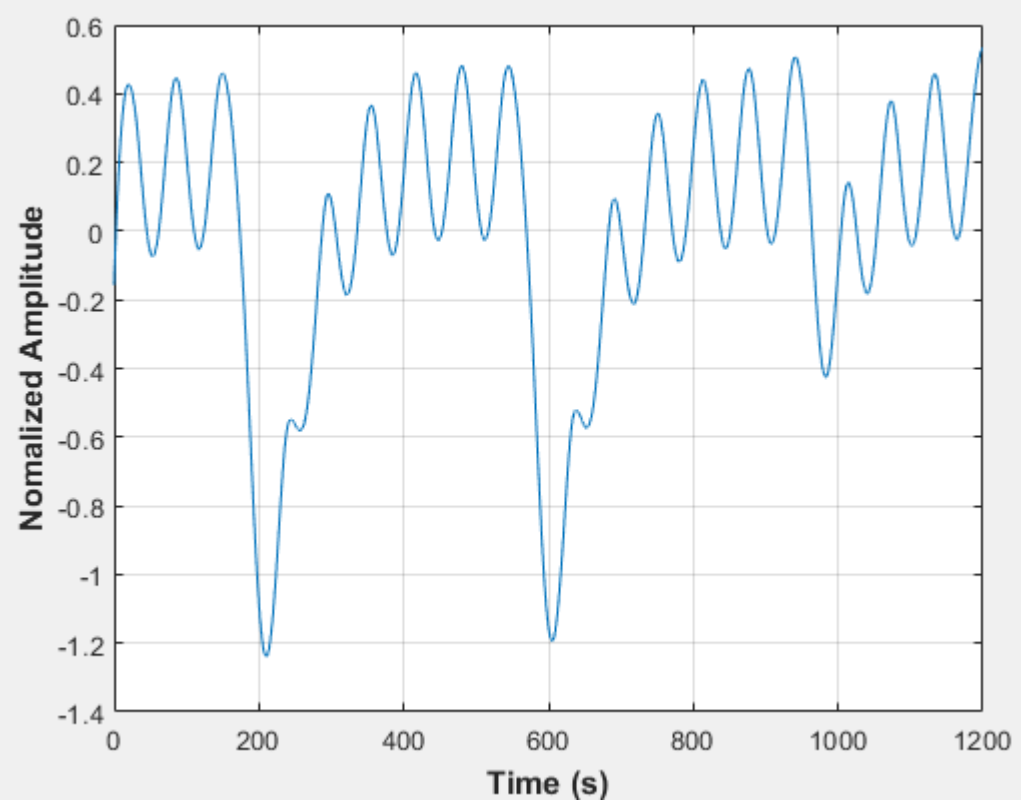


*Figure D-89: Pressure fluctuations in a uniformly packed vessel at 2.67 dm$^3$/minute rotameter flow rate- Test 3*

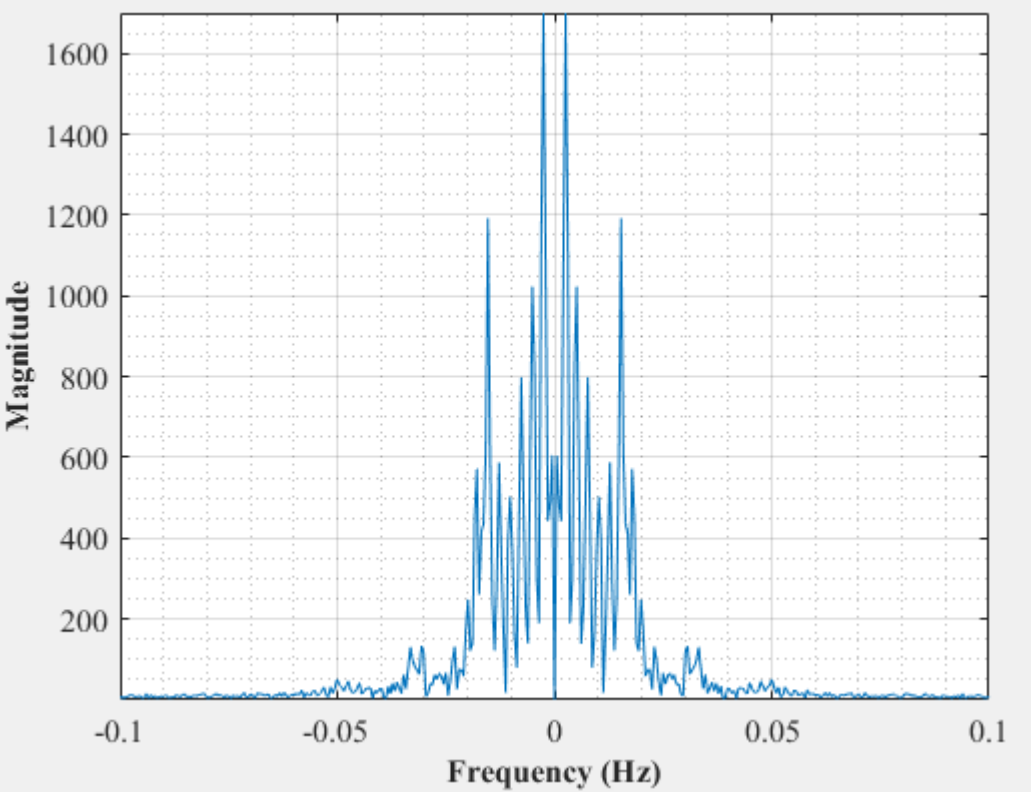


*Figure D-90: Dominant Frequency for a uniformly packed vessel at 2.67 dm$^3$/minute rotameter flow rate- Test 3*

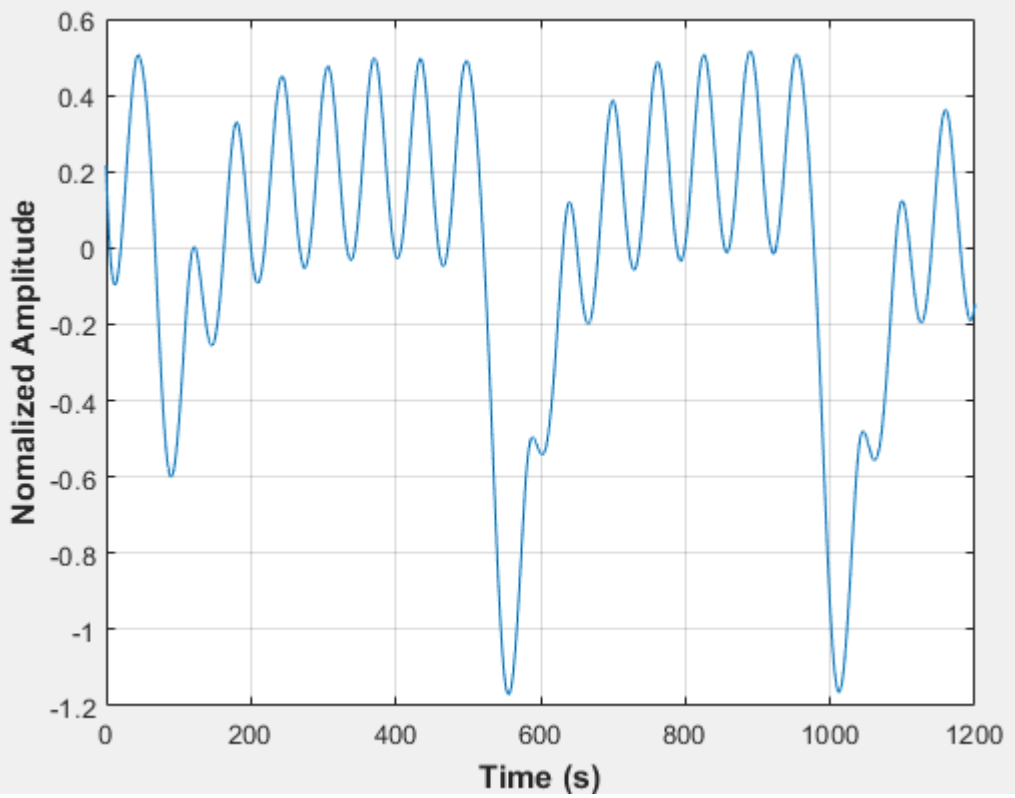


*Figure D-91: Pressure fluctuations in a uniformly packed vessel at 2.67 dm$^3$/minute rotameter flow rate- Test 4*

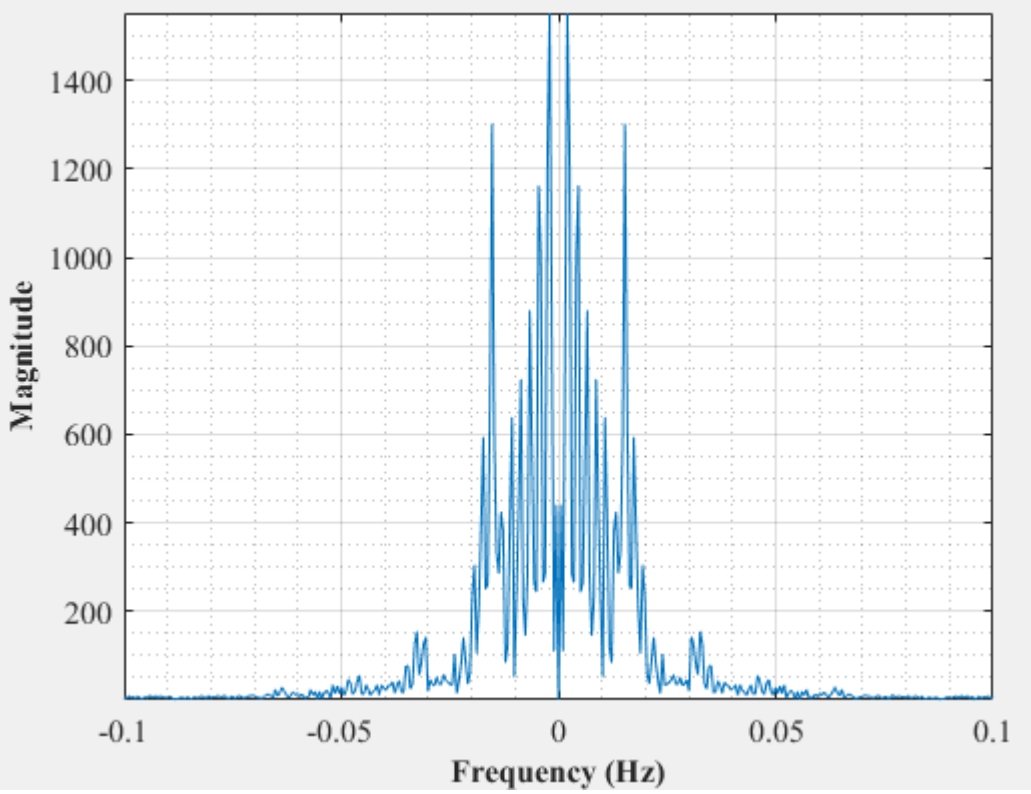


*Figure D-92: Dominant Frequency for a uniformly packed vessel at 2.67 dm$^3$/minute rotameter flow rate- Test 4*

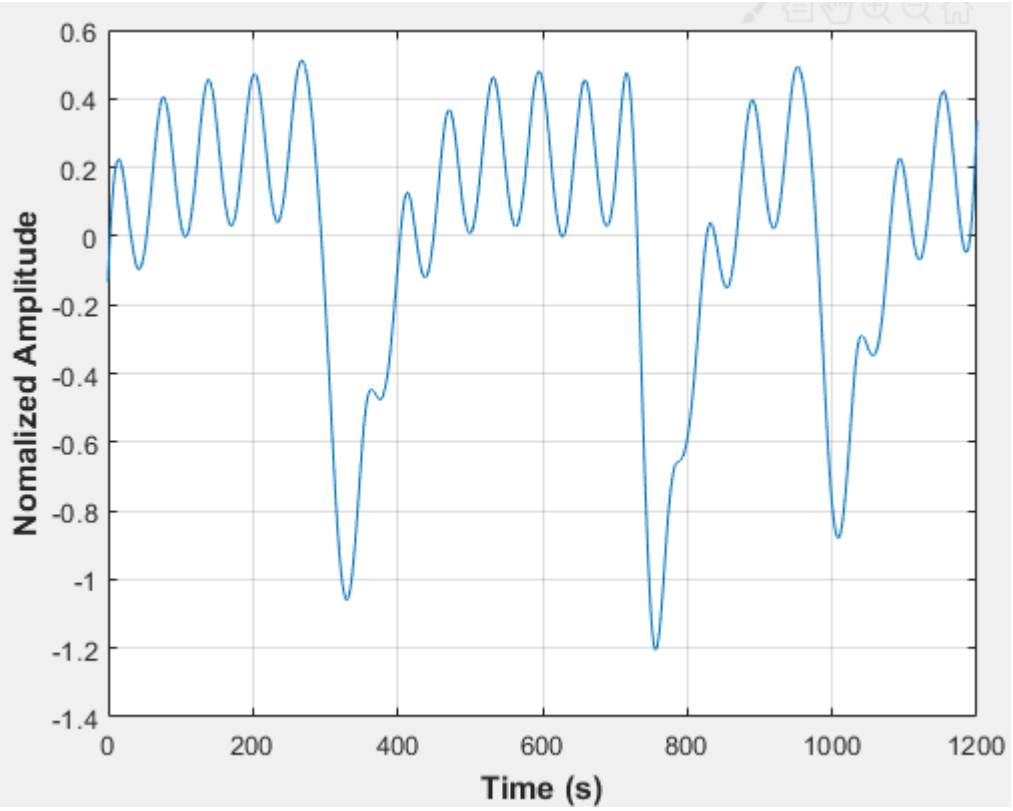


*Figure D-93: Pressure fluctuations in a uniformly packed vessel at 2.67 dm$^3$/minute rotameter flow rate- Test 5*

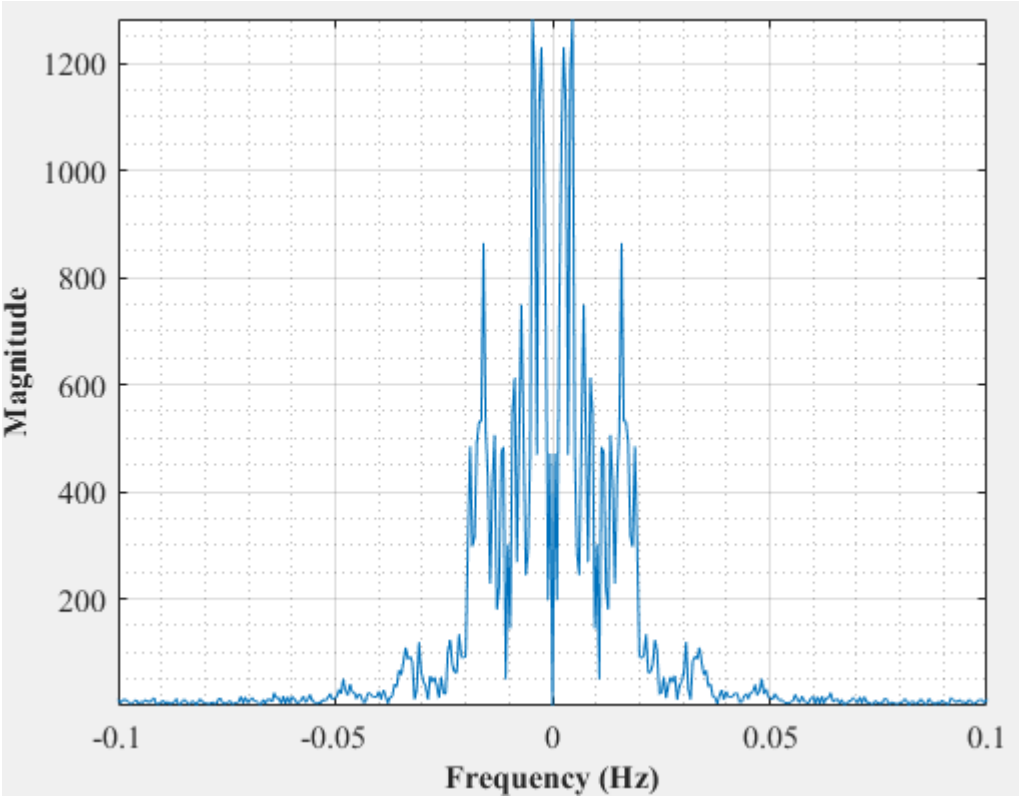


*Figure D-94: Dominant Frequency for a uniformly packed vessel at 2.67 dm$^3$/minute rotameter flow rate- Test 5*

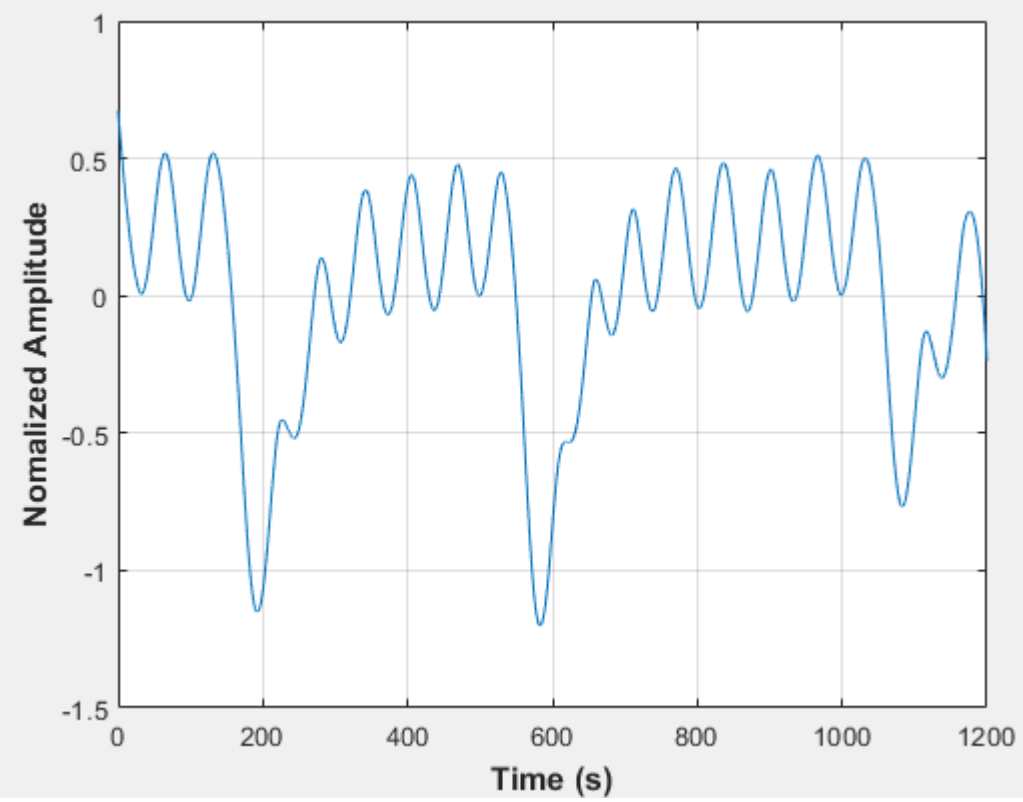


*Figure D-95: Pressure fluctuations in a uniformly packed vessel at 2.67 dm$^3$/minute rotameter flow rate- Test 6*

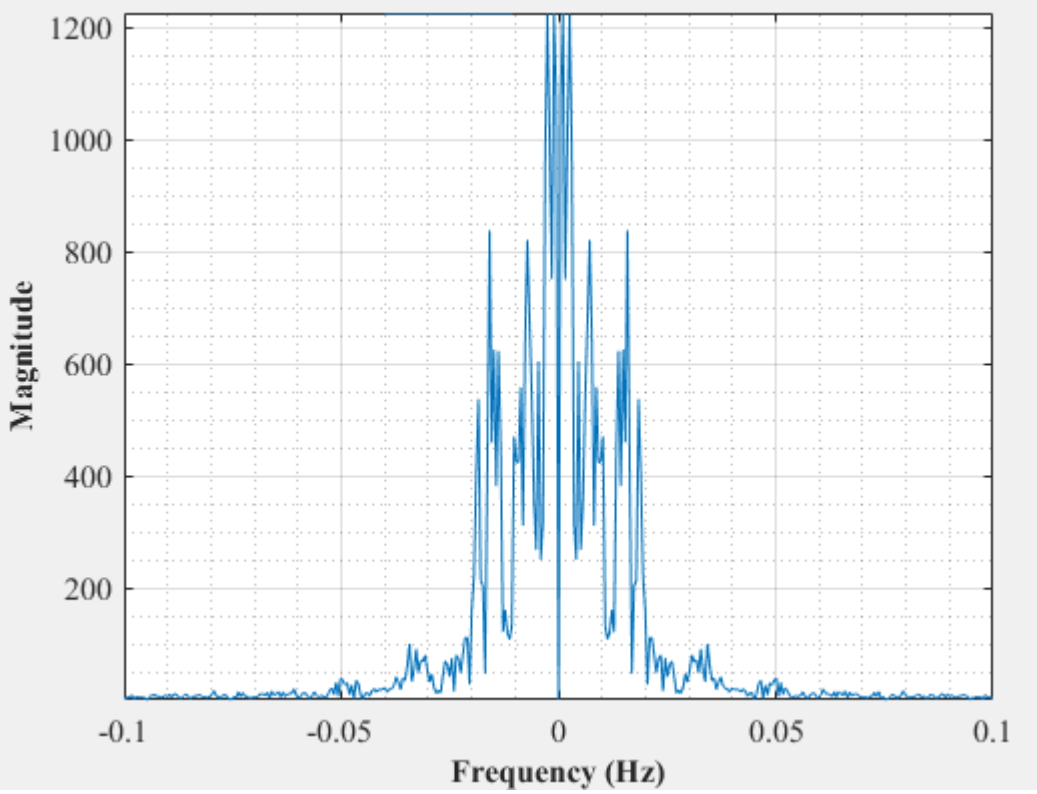


*Figure D-96: Dominant Frequency for a uniformly packed vessel at 2.67 dm$^3$/minute rotameter flow rate- Test 6*

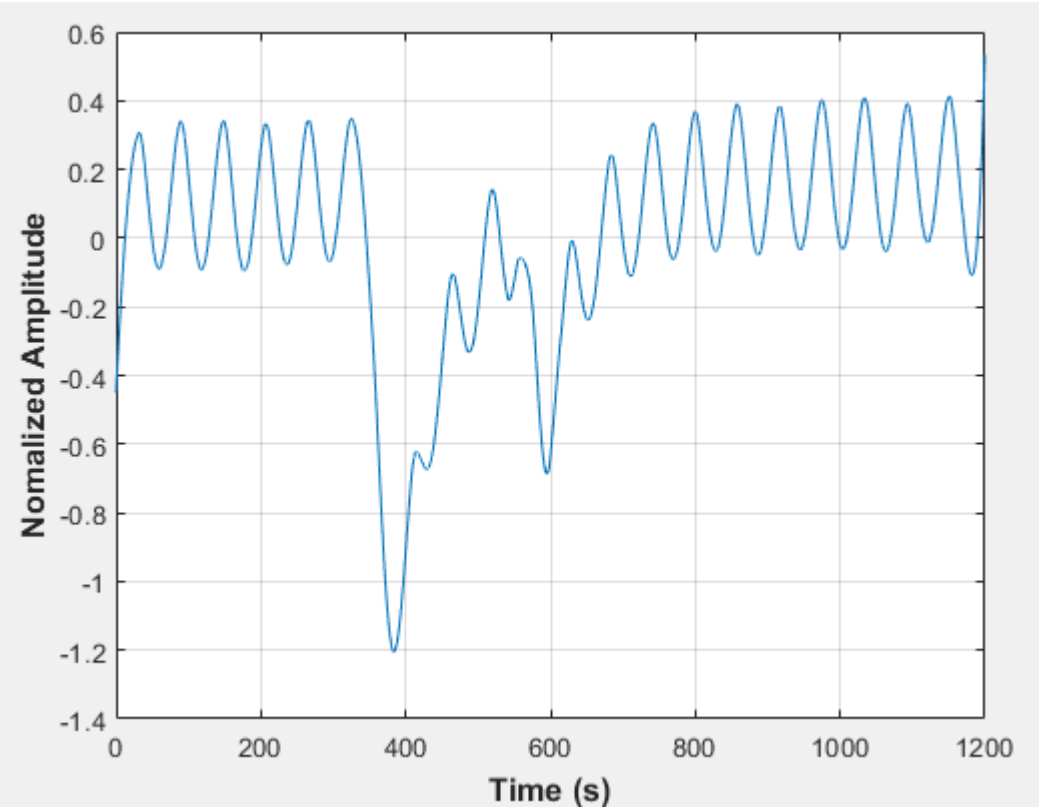


*Figure D-97: Pressure fluctuations in a uniformly packed vessel at 2.83 dm$^3$/minute rotameter flow rate- Test 1*

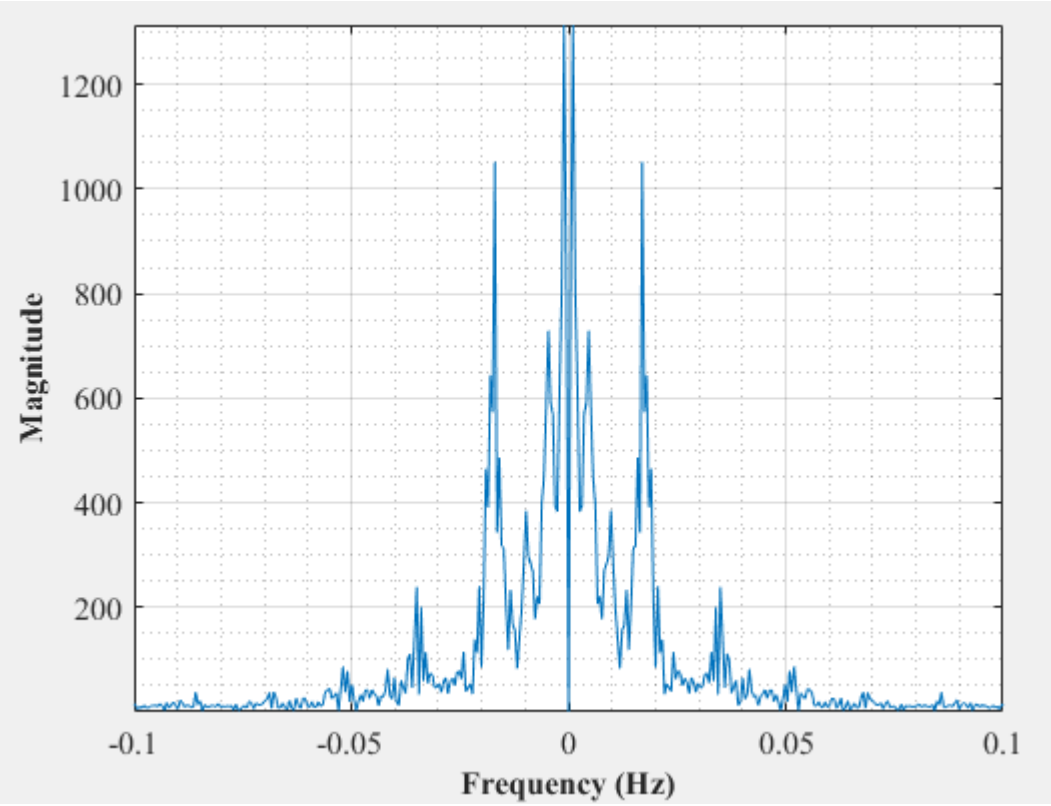


*Figure D-98: Dominant Frequency for a uniformly packed vessel at 2.83 dm$^3$/minute rotameter flow rate- Test 1*

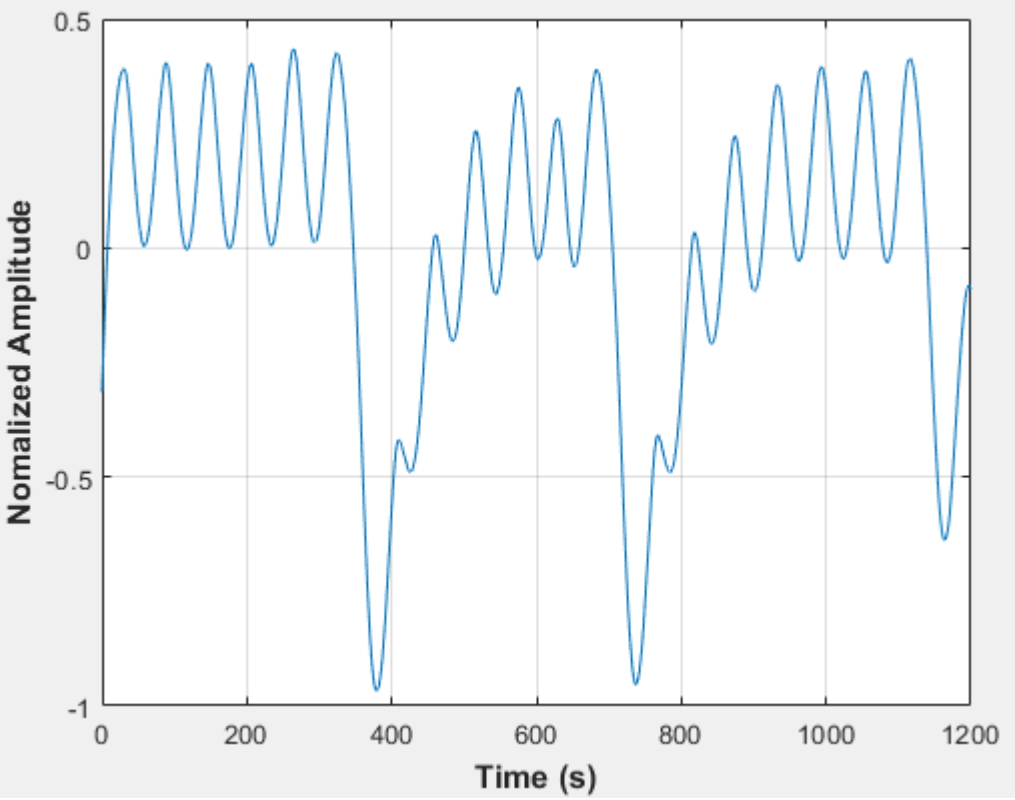


*Figure D-99: Pressure fluctuations in a uniformly packed vessel at 2.83 dm$^3$/minute rotameter flow rate- Test 2*

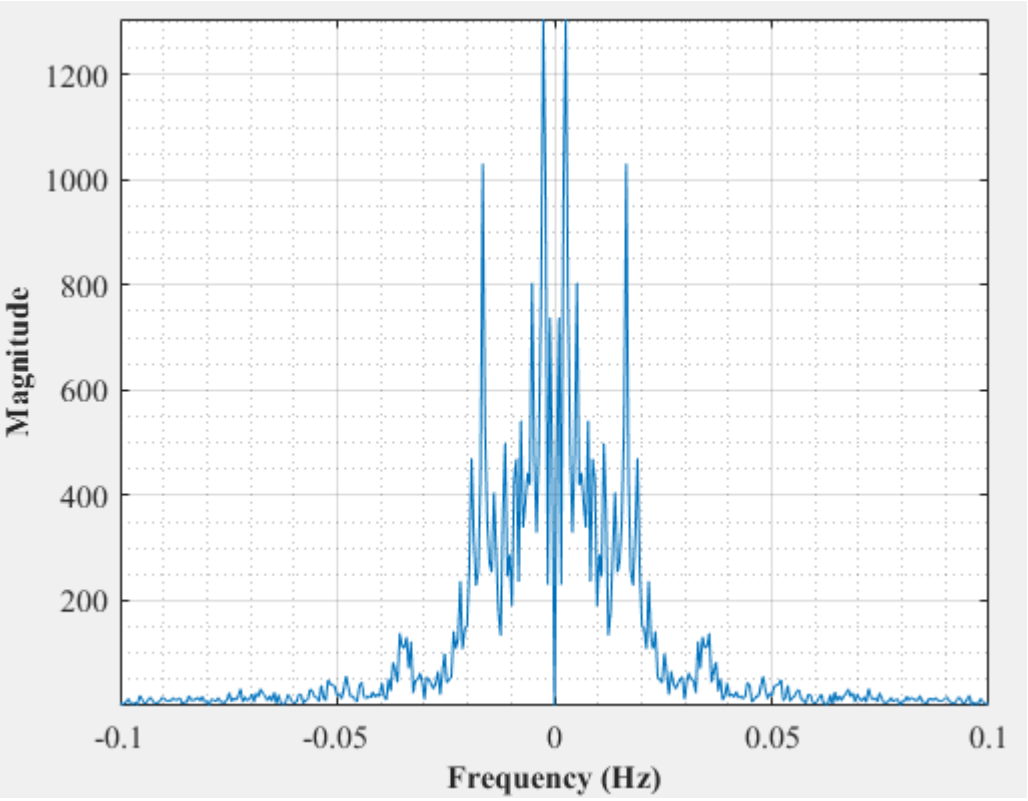


*Figure D-100: Dominant Frequency for a uniformly packed vessel at 2.83 dm$^3$/minute rotameter flow rate- Test 2*

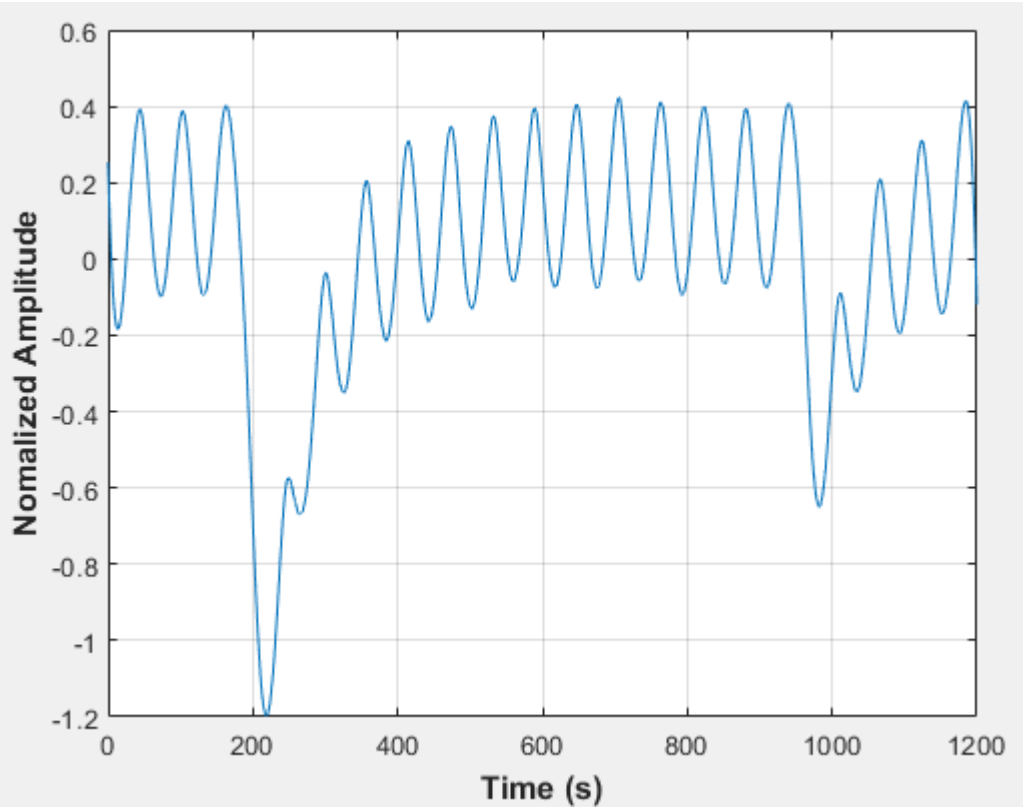


*Figure D-101: Pressure fluctuations in a uniformly packed vessel at 2.83 dm$^3$/minute rotameter flow rate- Test 3*

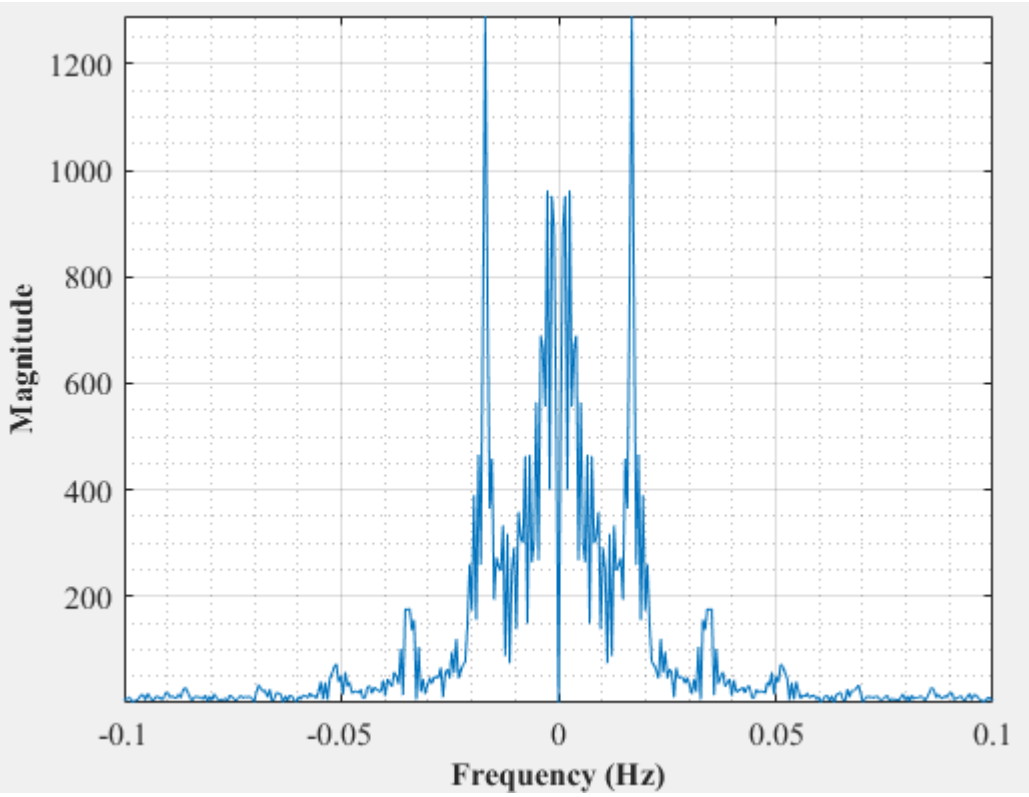


*Figure D-102: Dominant Frequency for a uniformly packed vessel at 2.83 dm$^3$/minute rotameter flow rate- Test 3*

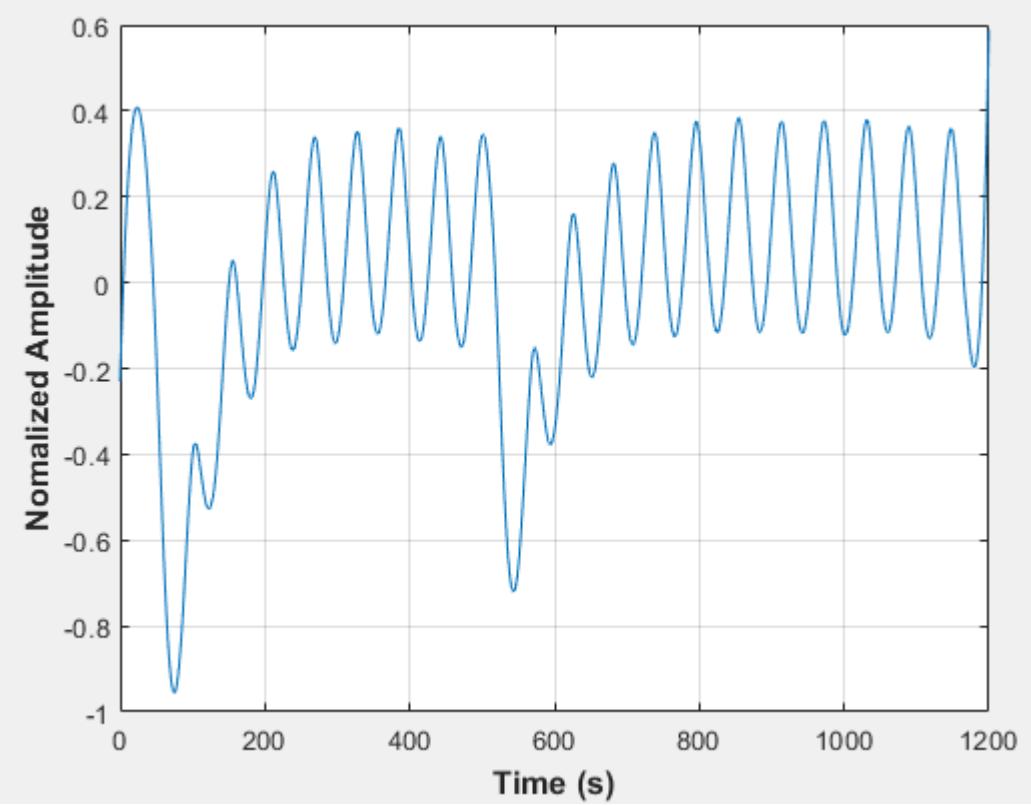


*Figure D-103: Pressure fluctuations in a uniformly packed vessel at 2.83 dm$^3$/minute rotameter flow rate- Test 4*

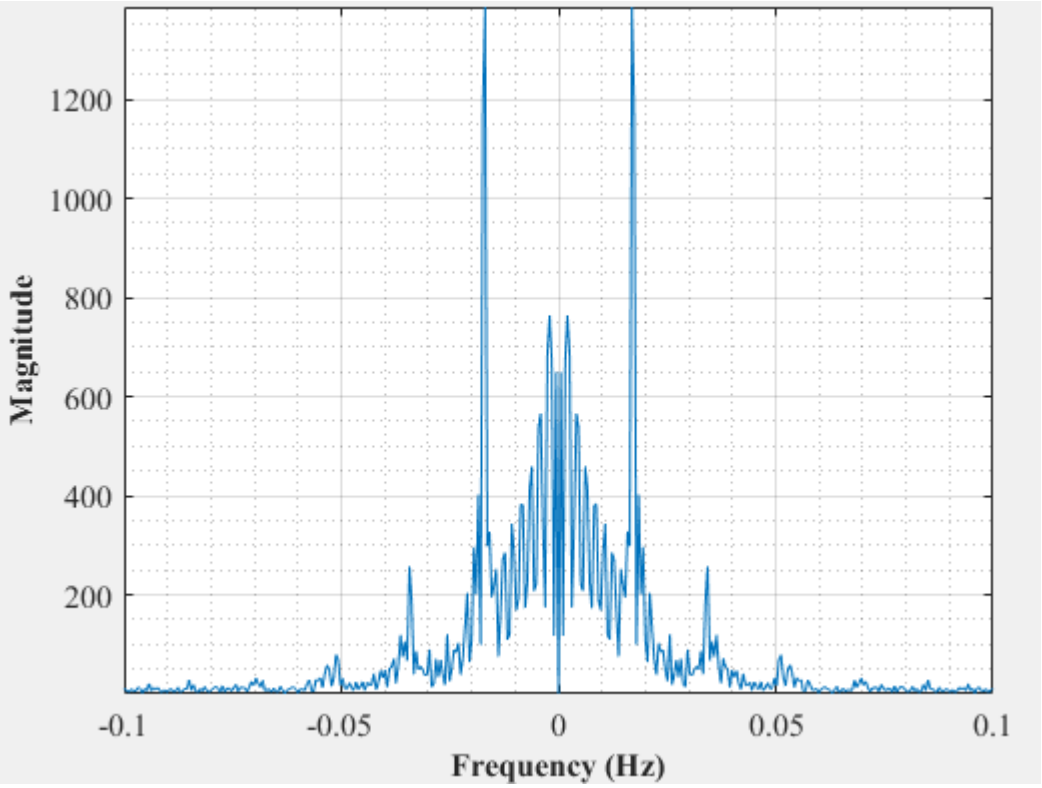


*Figure D-104: Dominant Frequency for a uniformly packed vessel at 2.83 dm$^3$/minute rotameter flow rate- Test 4*

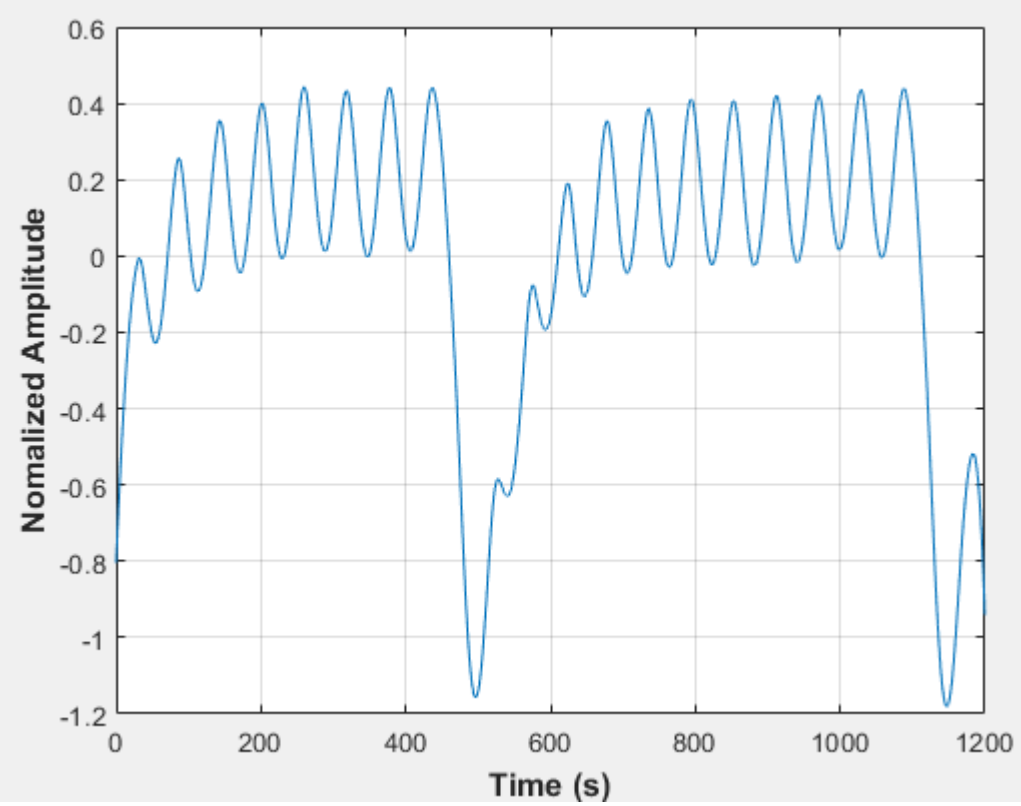


*Figure D-105: Pressure fluctuations in a uniformly packed vessel at 2.83 dm$^3$/minute rotameter flow rate- Test 5*

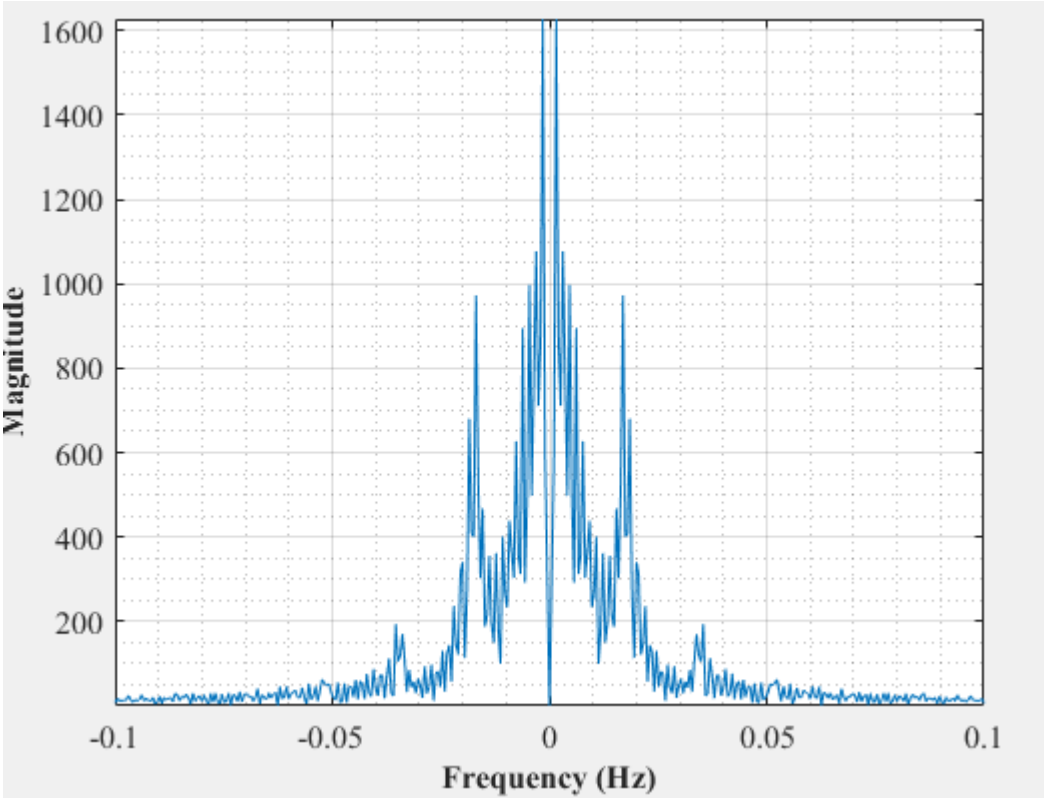


*Figure D-106: Dominant Frequency for a uniformly packed vessel at 2.83 dm$^3$/minute rotameter flow rate- Test 5*

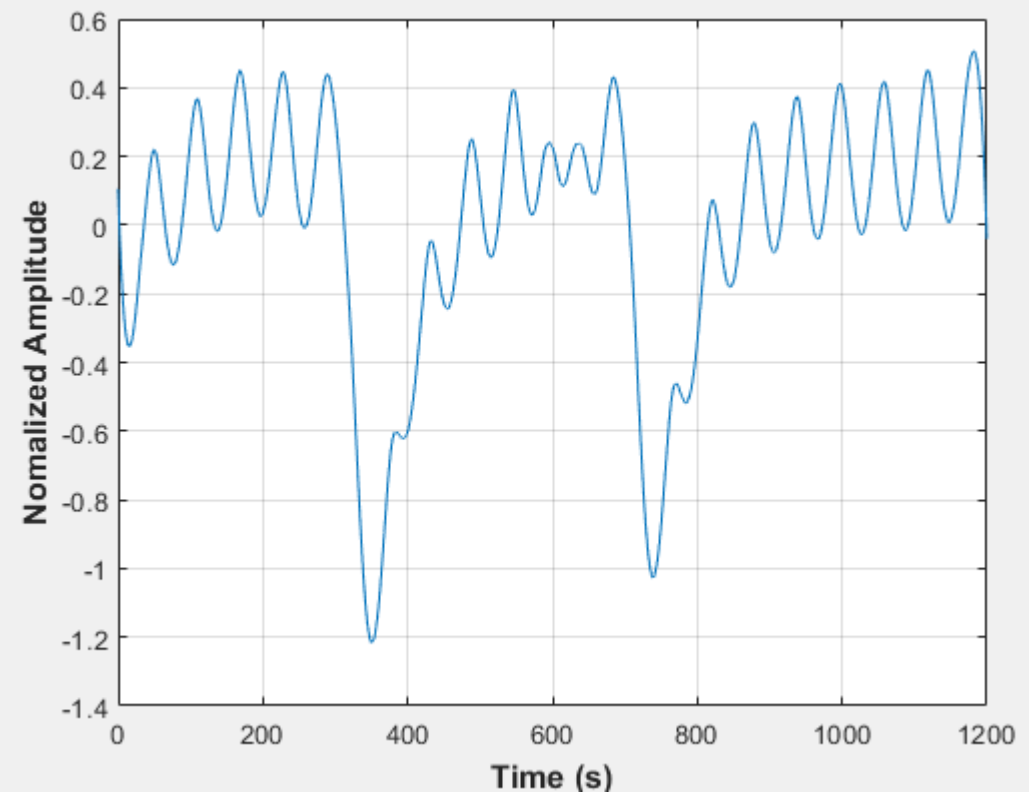


*Figure D-107: Pressure fluctuations in a uniformly packed vessel at 2.83 dm$^3$/minute rotameter flow rate- Test 6*

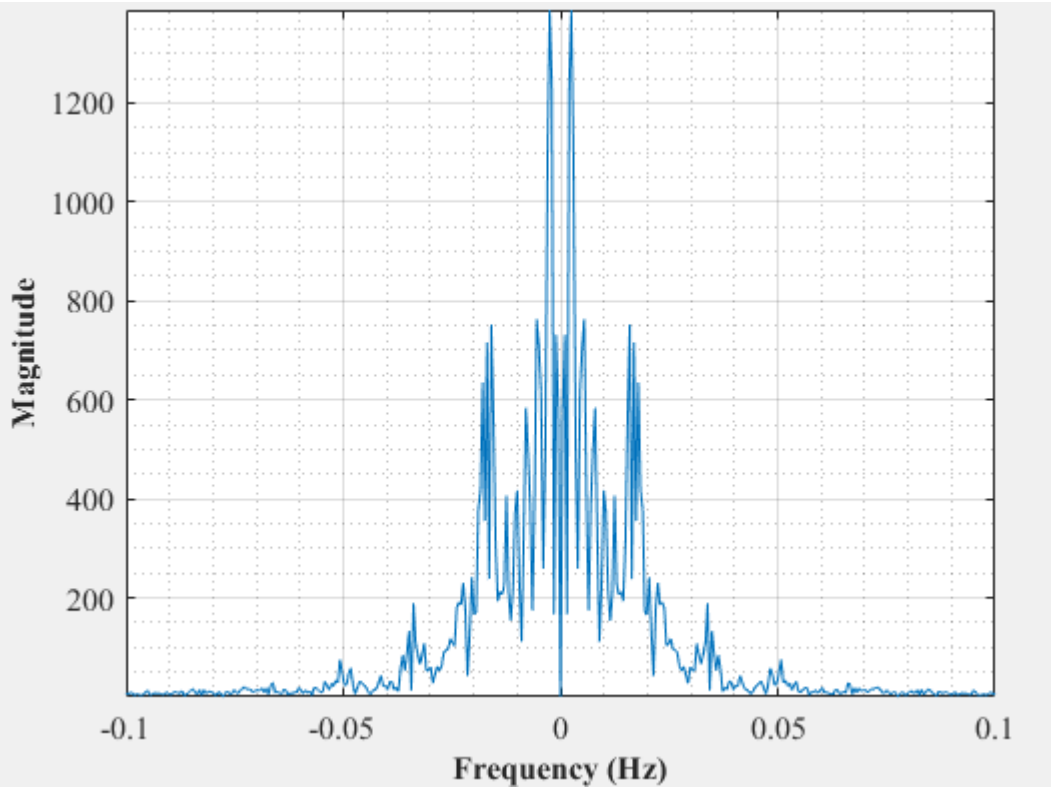


*Figure D-108: Dominant Frequency for a uniformly packed vessel at 2.83 dm$^3$/minute rotameter flow rate- Test 6*

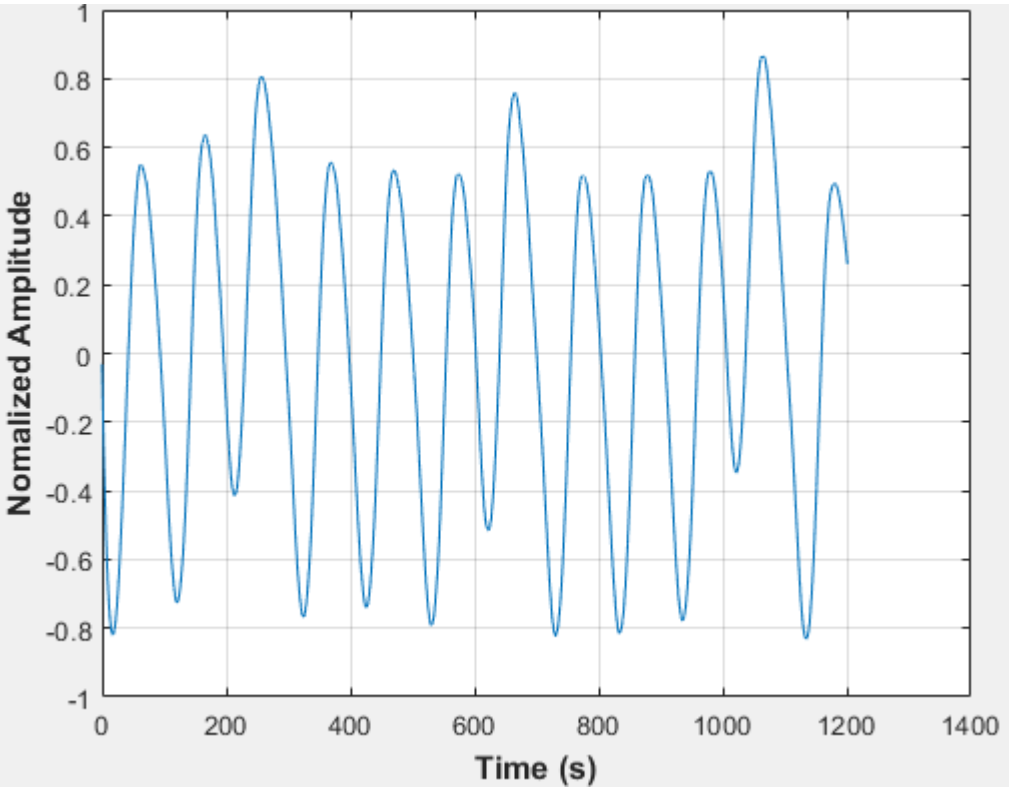


*Figure D-109: Pressure fluctuations in a non-uniformly packed vessel (large and small at the center) at 1.67 dm$^3$/minute rotameter flow rate- Test 1*

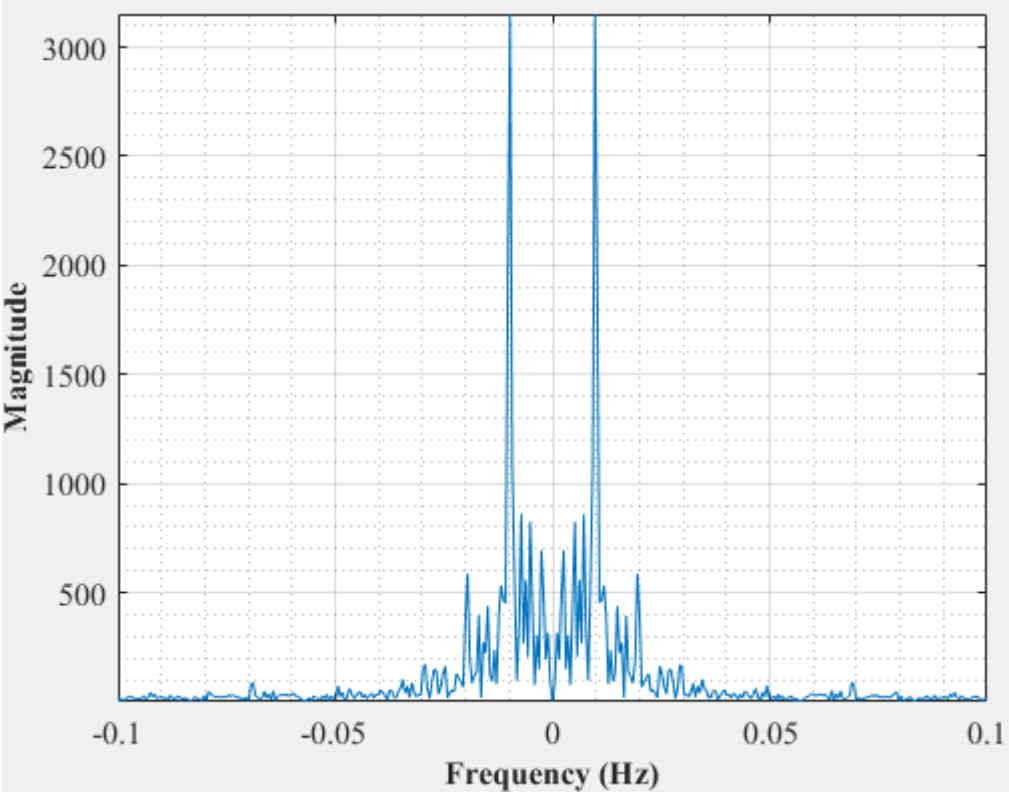


*Figure D-110: Dominant Frequency for a non-uniformly packed vessel (large and small at the center) at 1.67 dm$^3$/minute rotameter flow rate- Test 1*

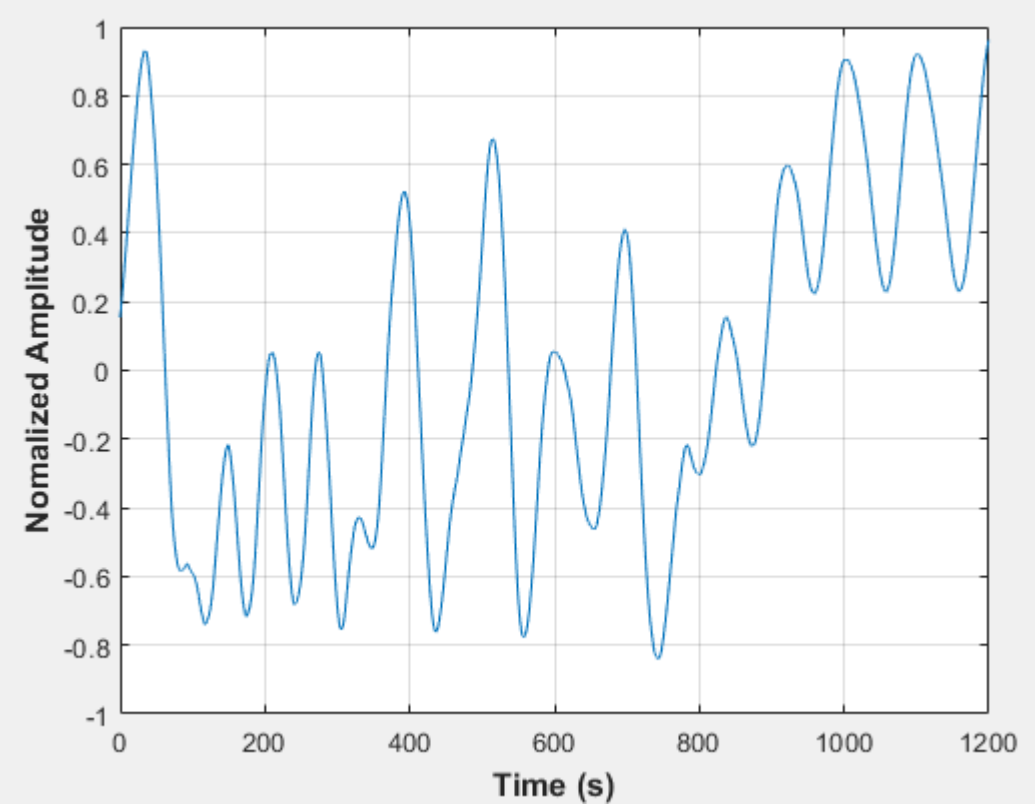


*Figure D-111: Pressure fluctuations in a non-uniformly packed vessel (large and small at the center) at 1.67 dm$^3$/minute rotameter flow rate- Test 2*

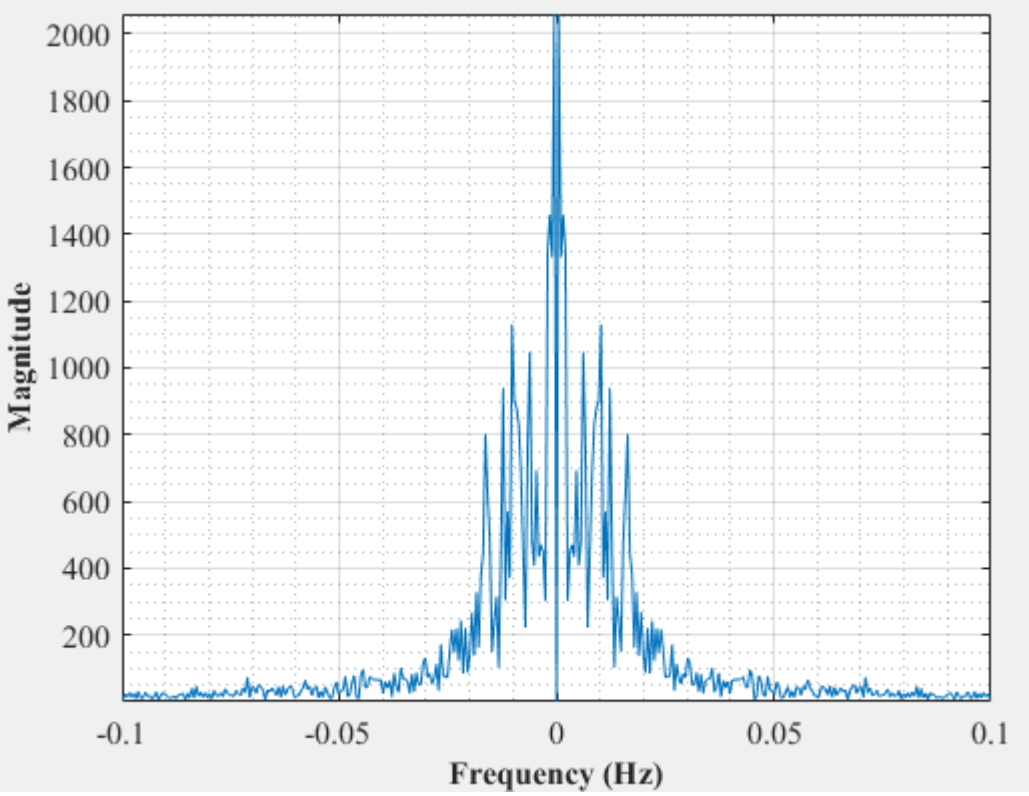


*Figure D-112: Dominant Frequency for a non-uniformly packed vessel (large and small at the center) at 1.67 dm$^3$/minute rotameter flow rate- Test 2*

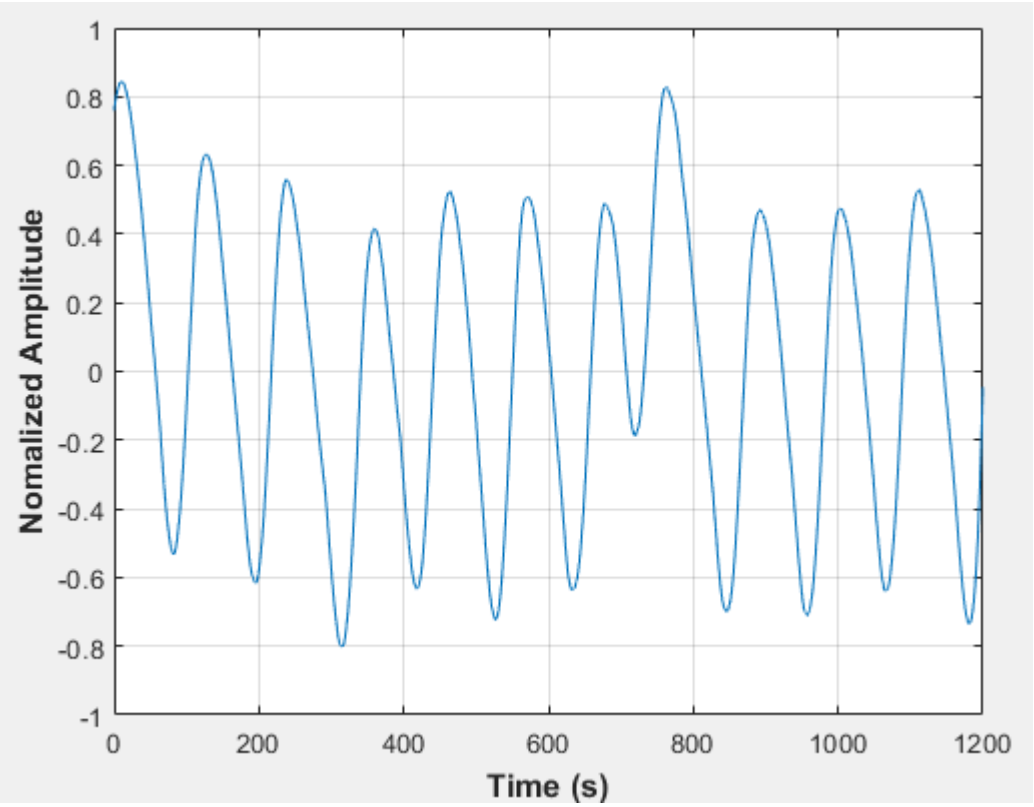


*Figure D-113: Pressure fluctuations in a non-uniformly packed vessel (large and small at the center) at 1.67 $dm^3$/minute rotameter flow rate- Test 3*

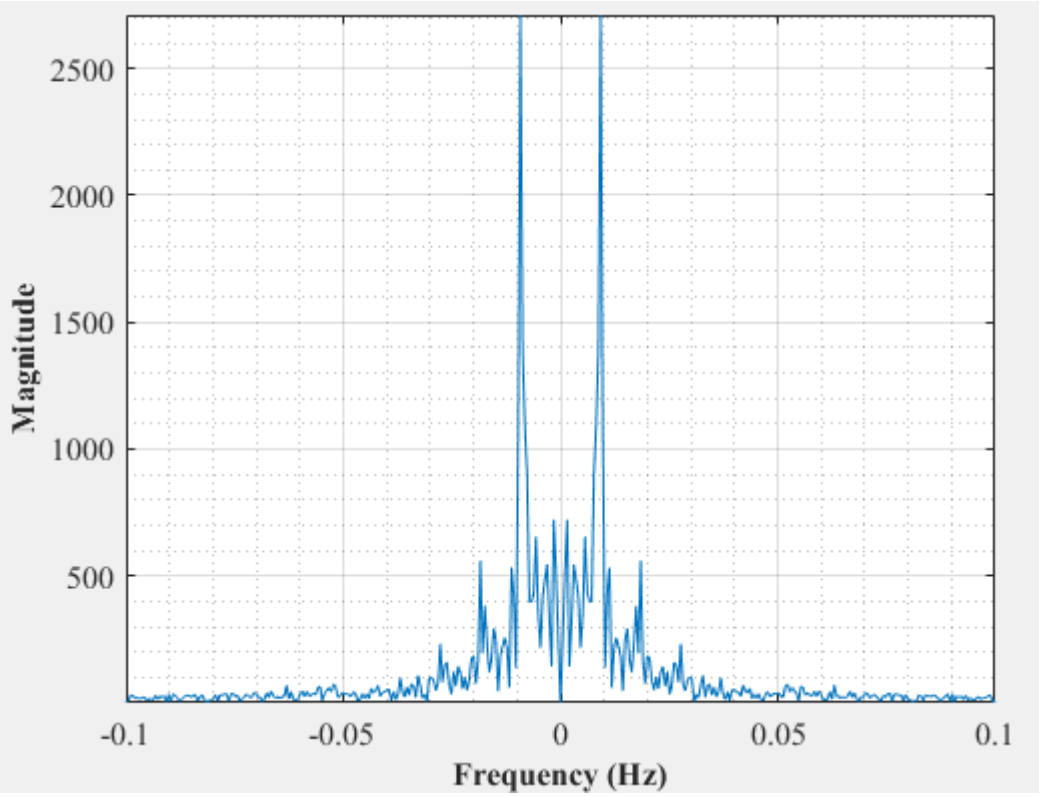


*Figure D-114: Dominant Frequency for a non-uniformly packed vessel (large and small at the center) at 1.67 $dm^3$/minute rotameter flow rate- Test3*

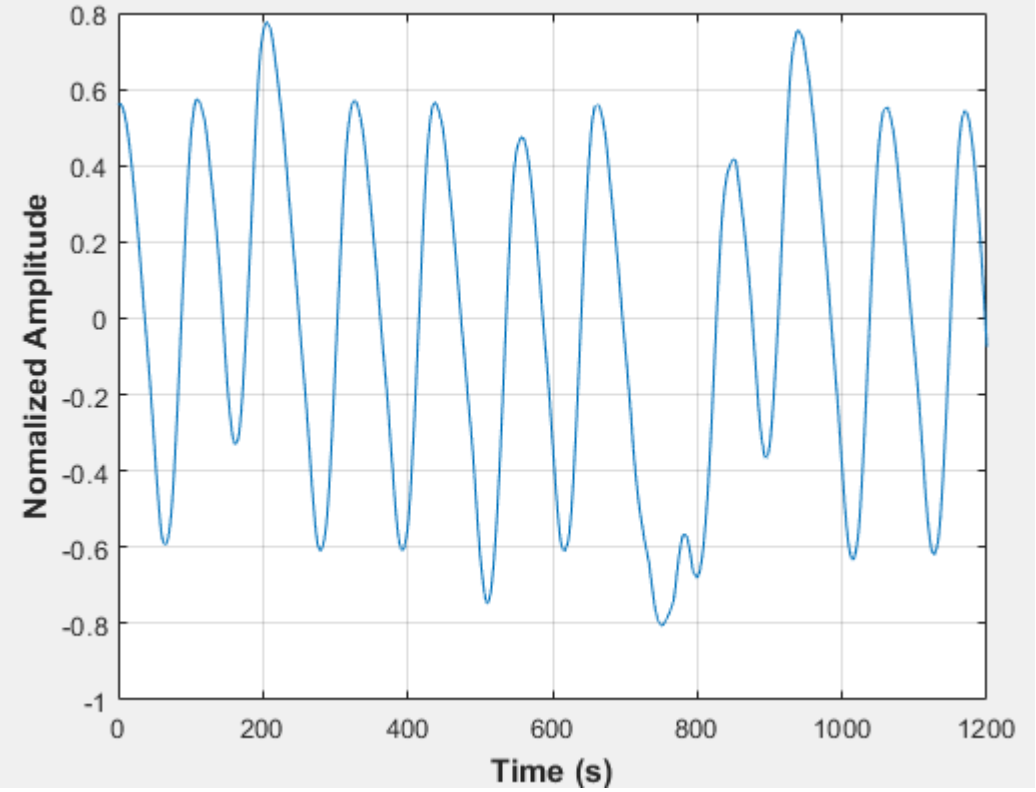


*Figure D-115: Pressure fluctuations in a non-uniformly packed vessel (large and small at the center) at 1.67 dm$^3$/minute rotameter flow rate- Test 4*

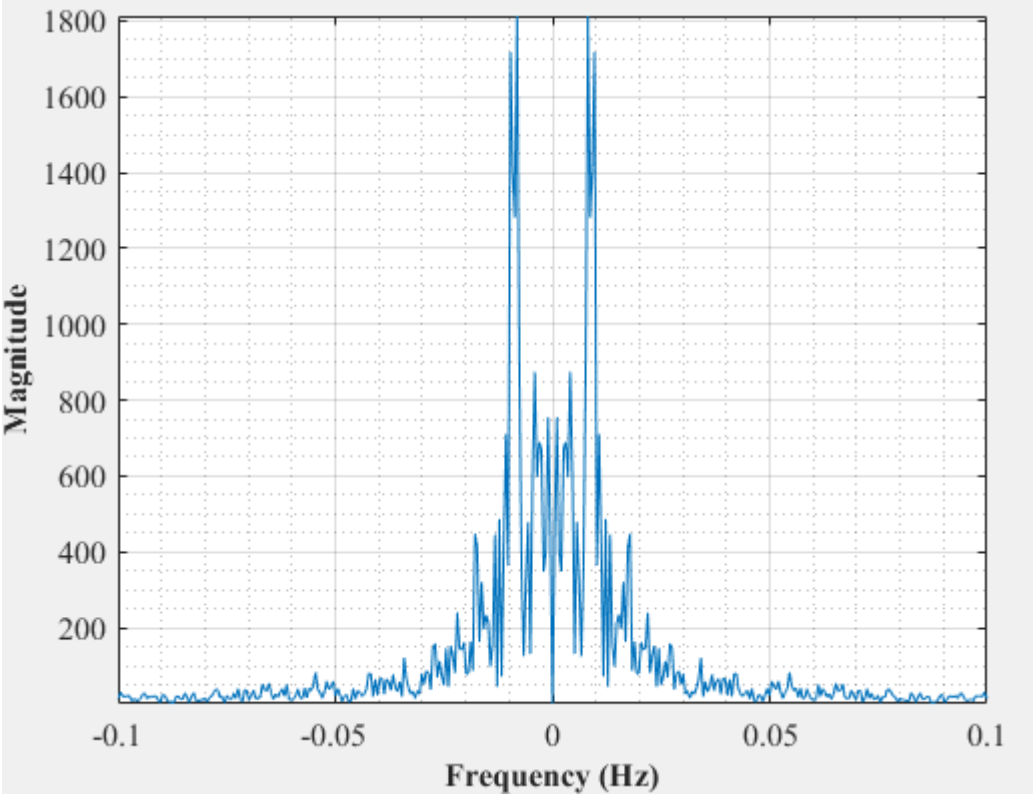


*Figure D-116: Dominant Frequency for a non-uniformly packed vessel (large and small at the center) at 1.67 dm$^3$/minute rotameter flow rate- Test 4*

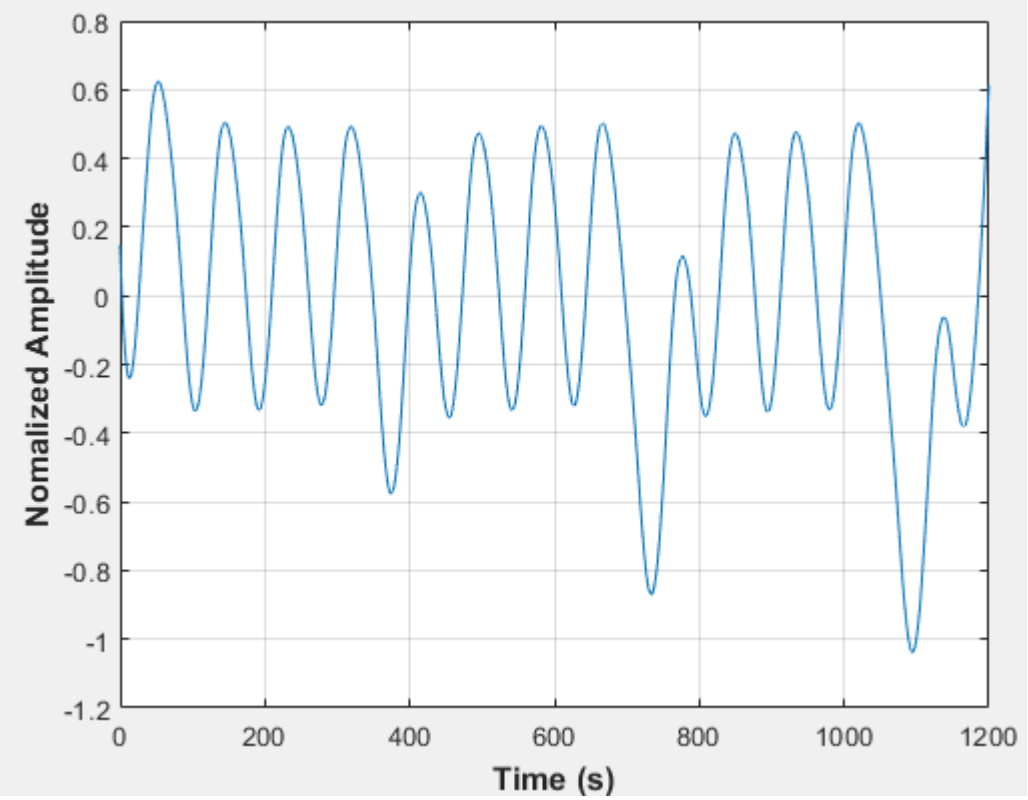


*Figure D-117: Pressure fluctuations in a non-uniformly packed vessel (large and small at the center) at 2 dm$^3$/minute rotameter flow rate- Test 1*

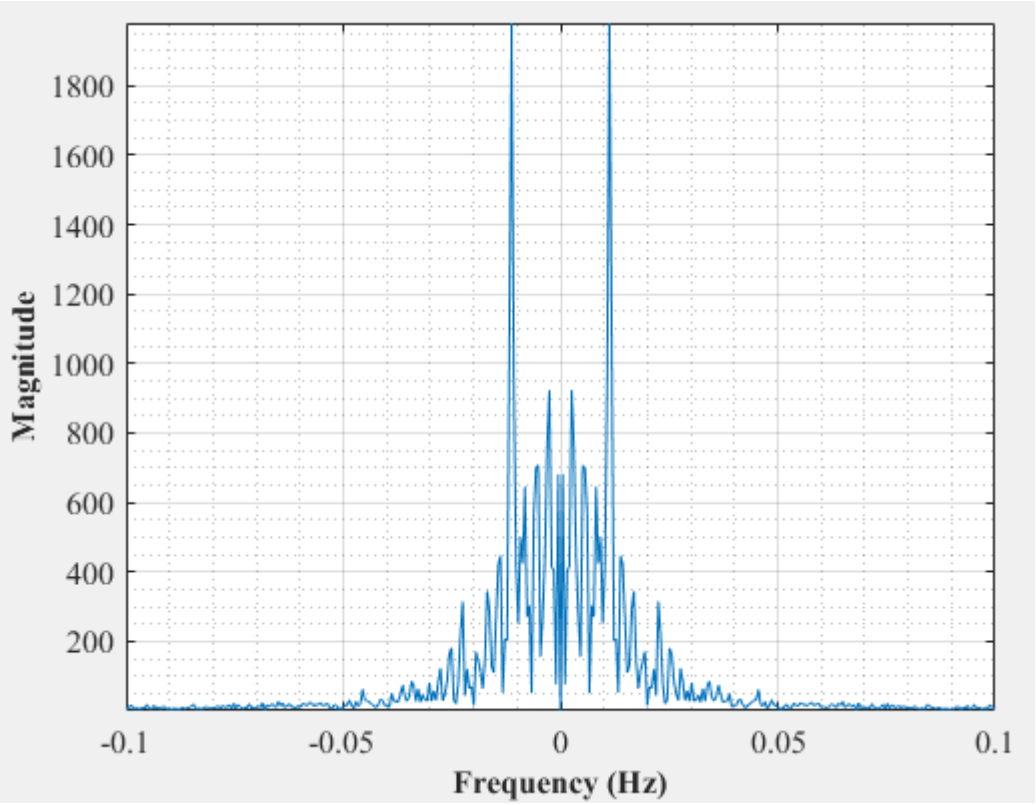


*Figure D-118: Dominant Frequency for a non-uniformly packed vessel (large and small at the center) at 2 dm$^3$/minute rotameter flow rate- Test 1*

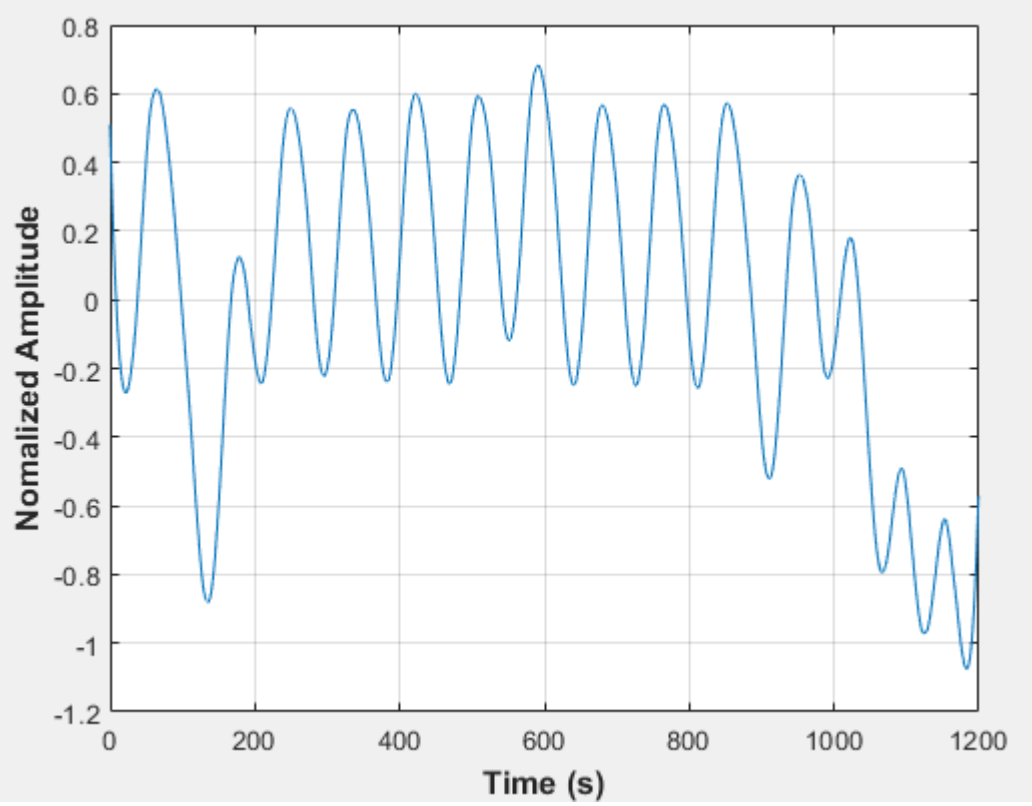


*Figure D-119: Pressure fluctuations in a non-uniformly packed vessel (large and small at the center) at 2 dm$^3$/minute rotameter flow rate- Test 2*

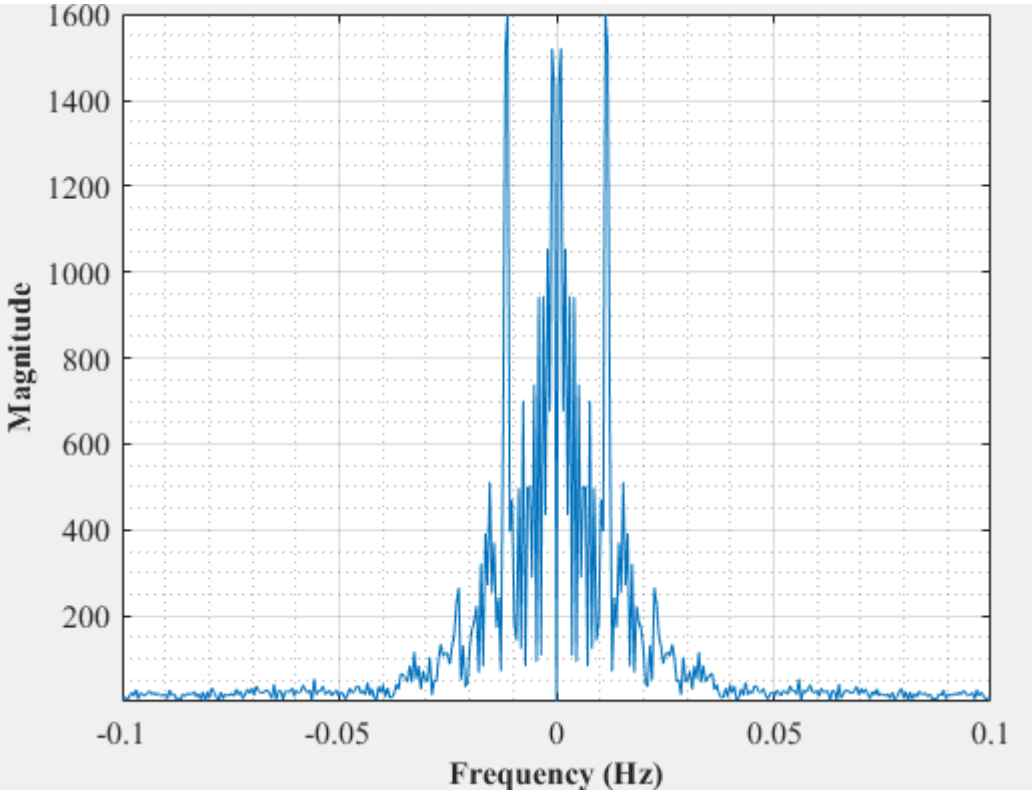


*Figure D-120: Dominant Frequency for a non-uniformly packed vessel (large and small at the center) at 2 dm$^3$/minute rotameter flow rate- Test 2*

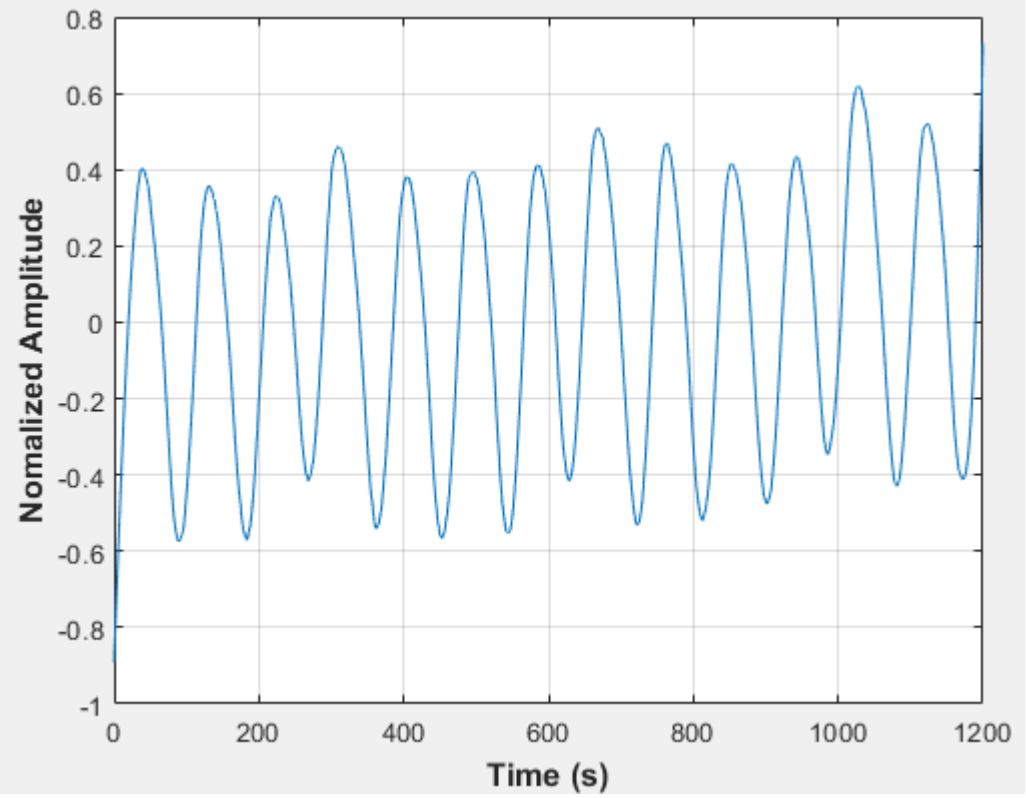


*Figure D-121: Pressure fluctuations in a non-uniformly packed vessel (large and small at the center) at 2 dm$^3$/minute rotameter flow rate- Test 3*

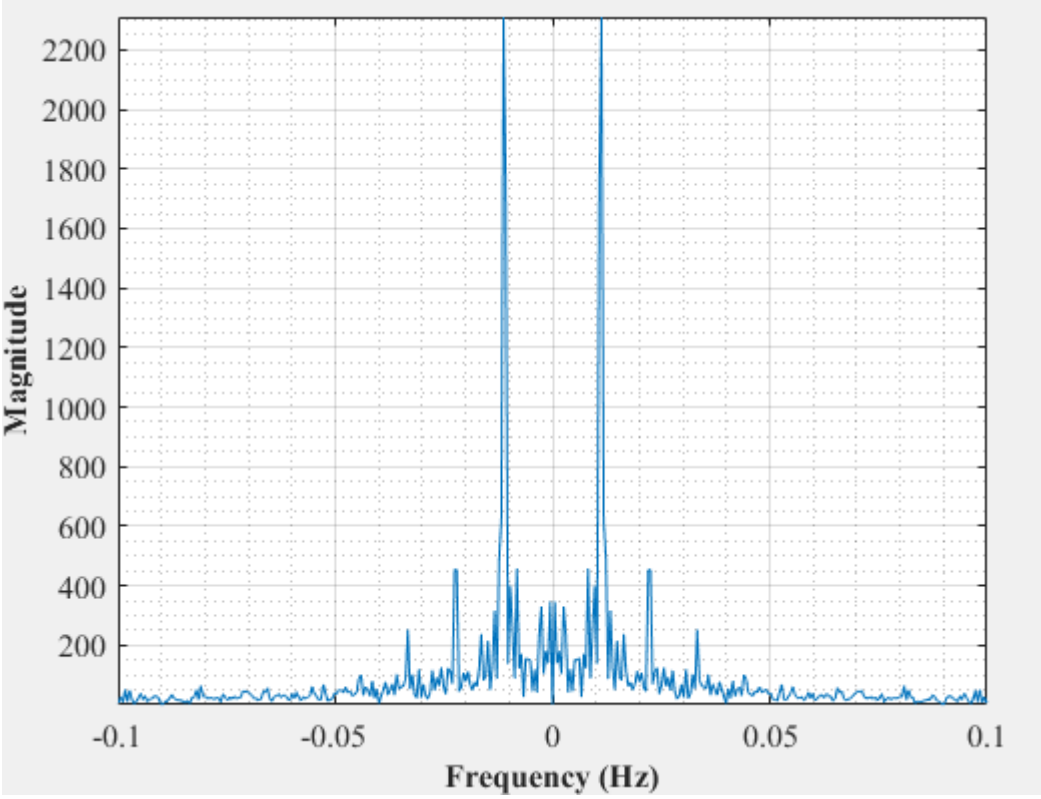


*Figure D-122: Dominant Frequency for a non-uniformly packed vessel (large and small at the center) at 2 dm$^3$/minute rotameter flow rate- Test 3*

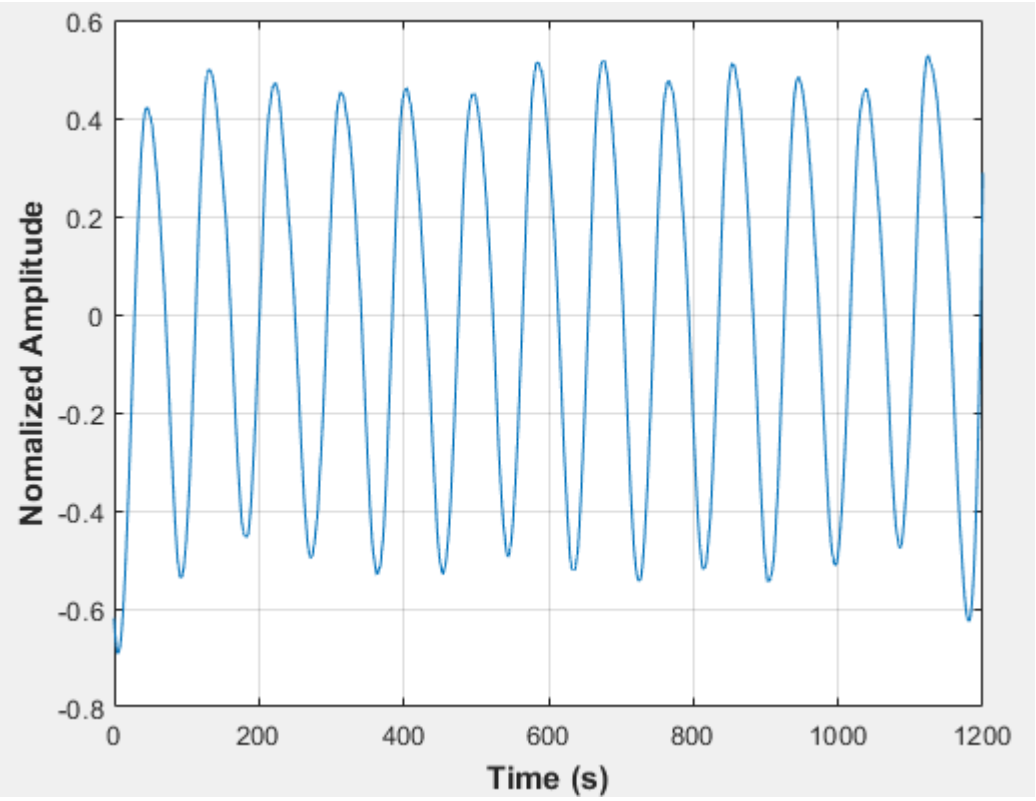


*Figure D-123: Pressure fluctuations in a non-uniformly packed vessel (large and small at the center) at 2 dm$^3$/minute rotameter flow rate- Test 4*

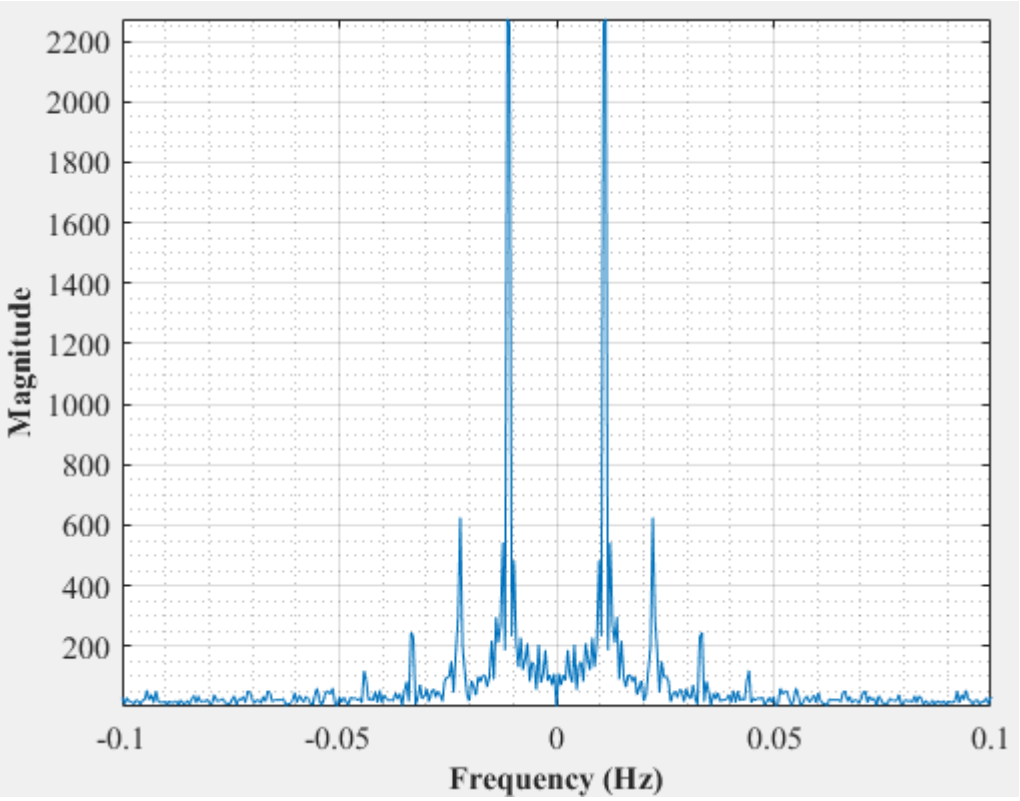


*Figure D-124: Dominant Frequency for a non-uniformly packed vessel (large and small at the center) at 2 dm$^3$/minute rotameter flow rate- Test 4*

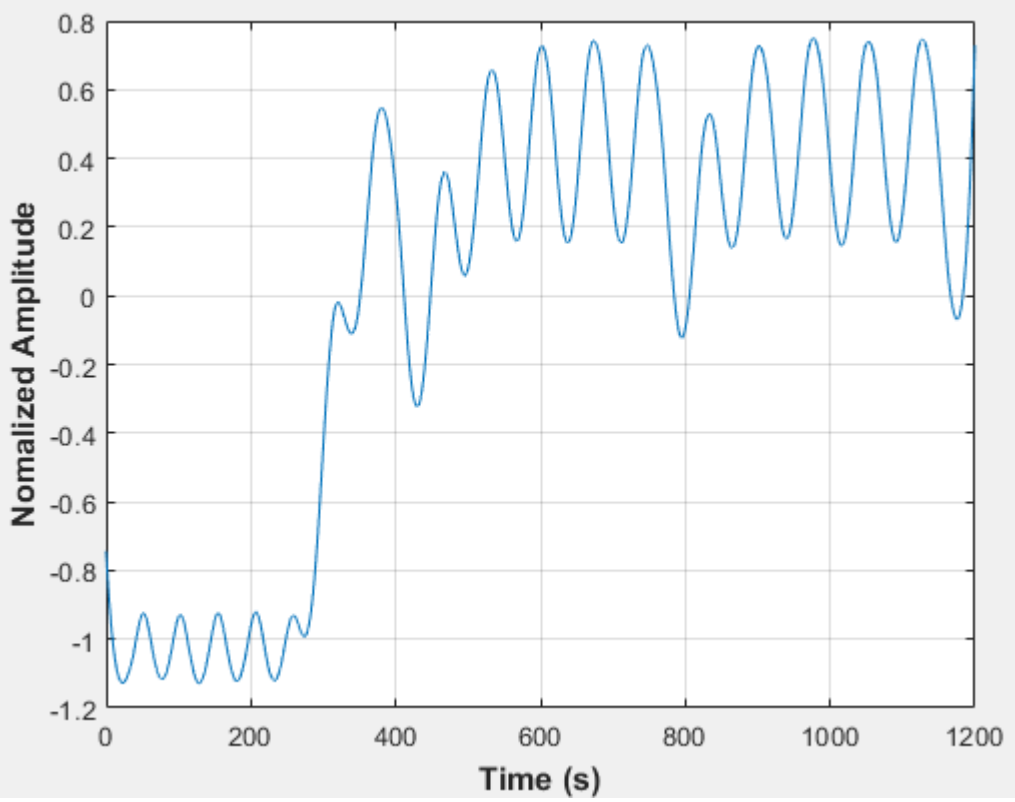


*Figure D-125: Pressure fluctuations in a non-uniformly packed vessel (large and small at the center) at 2.33 dm$^3$/minute rotameter flow rate- Test 1*

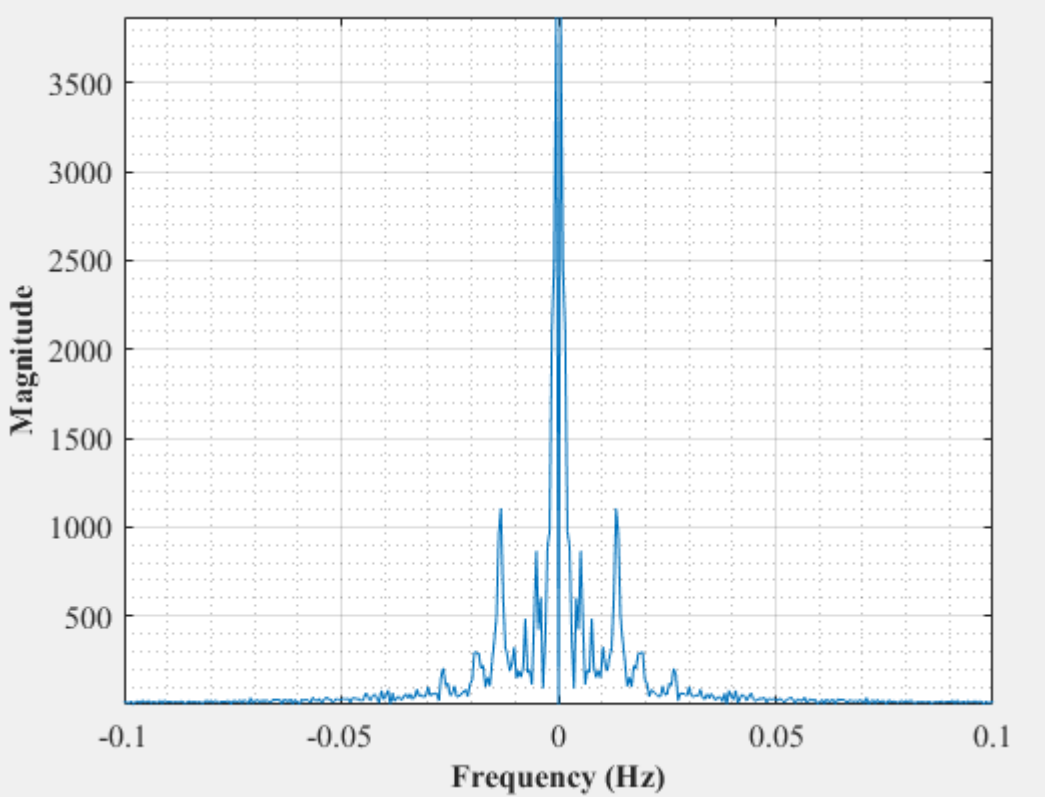


*Figure D-126: Dominant Frequency for a non-uniformly packed vessel (large and small at the center) at 2.33 dm$^3$/minute rotameter flow rate- Test 1*

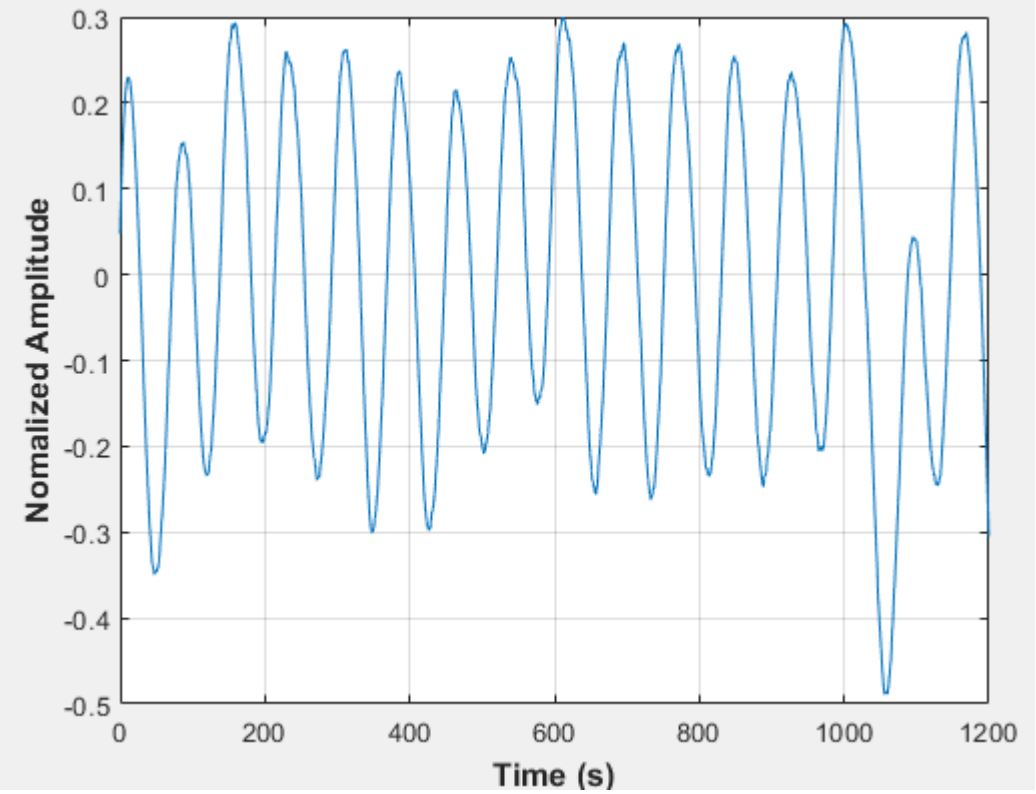


*Figure D-127: Pressure fluctuations in a non-uniformly packed vessel (large and small at the center) at 2.33 dm$^3$/minute rotameter flow rate- Test 2*

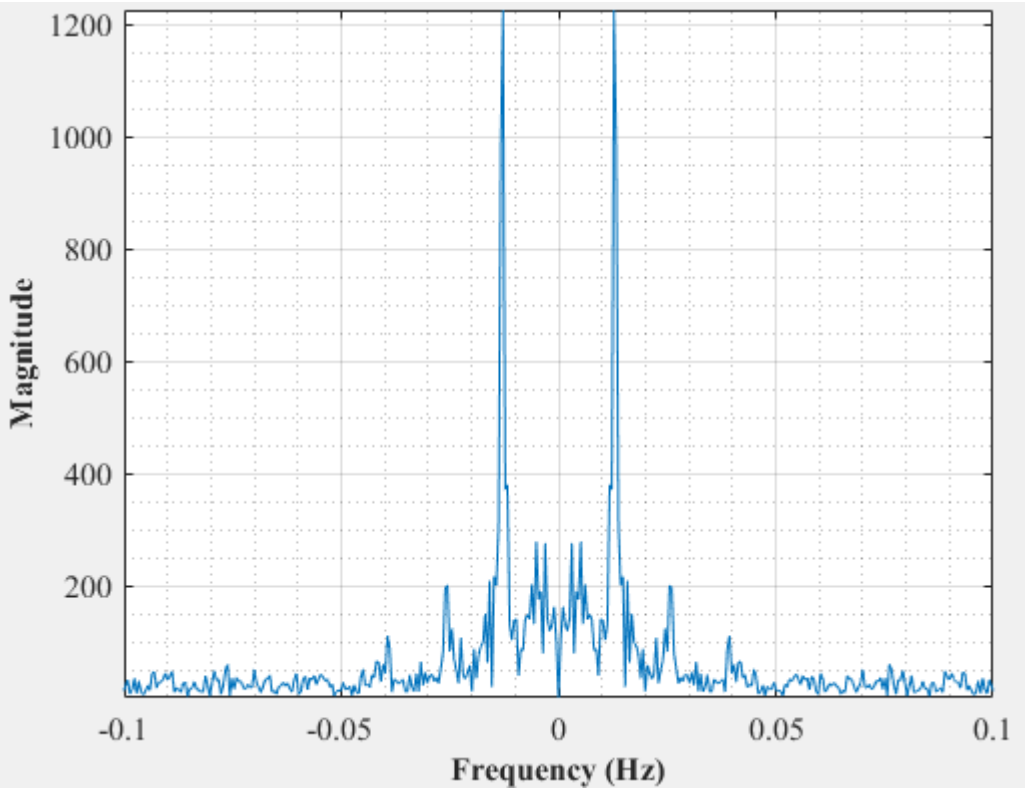


*Figure D-128: Dominant Frequency for a non-uniformly packed vessel (large and small at the center) at 2.33 dm$^3$/minute rotameter flow rate- Test 2*

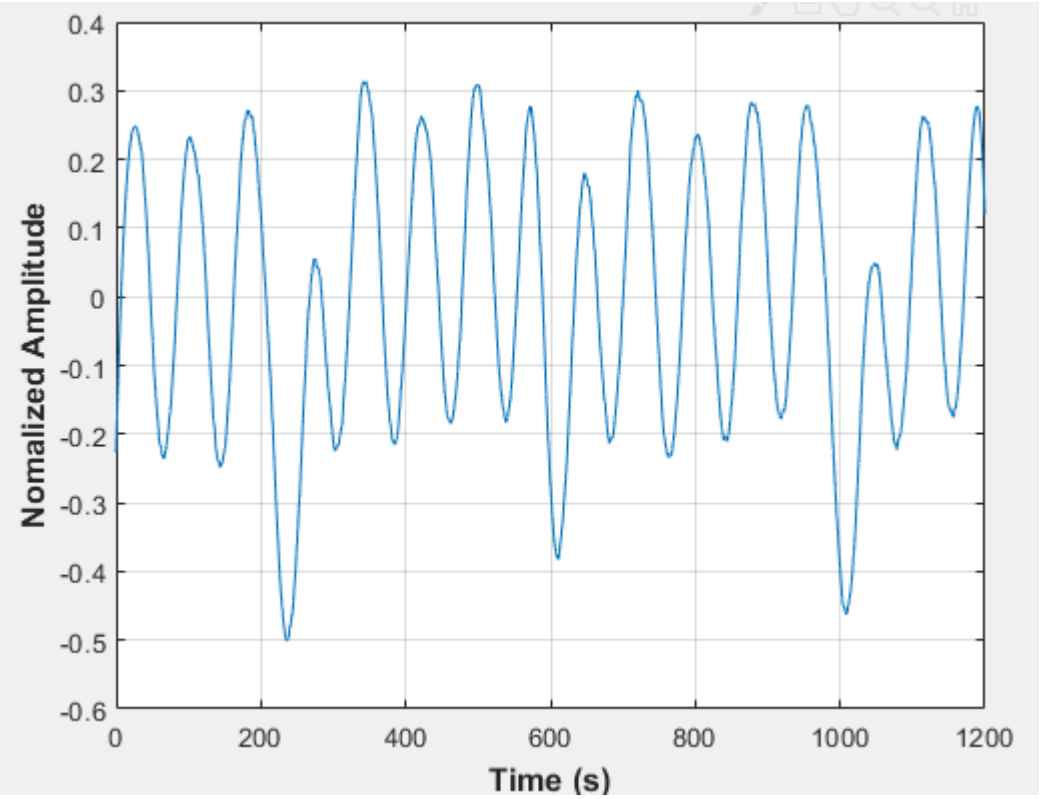


*Figure D-129: Pressure fluctuations in a non-uniformly packed vessel (large and small at the center) at 2.33 dm$^3$/minute rotameter flow rate- Test 3*

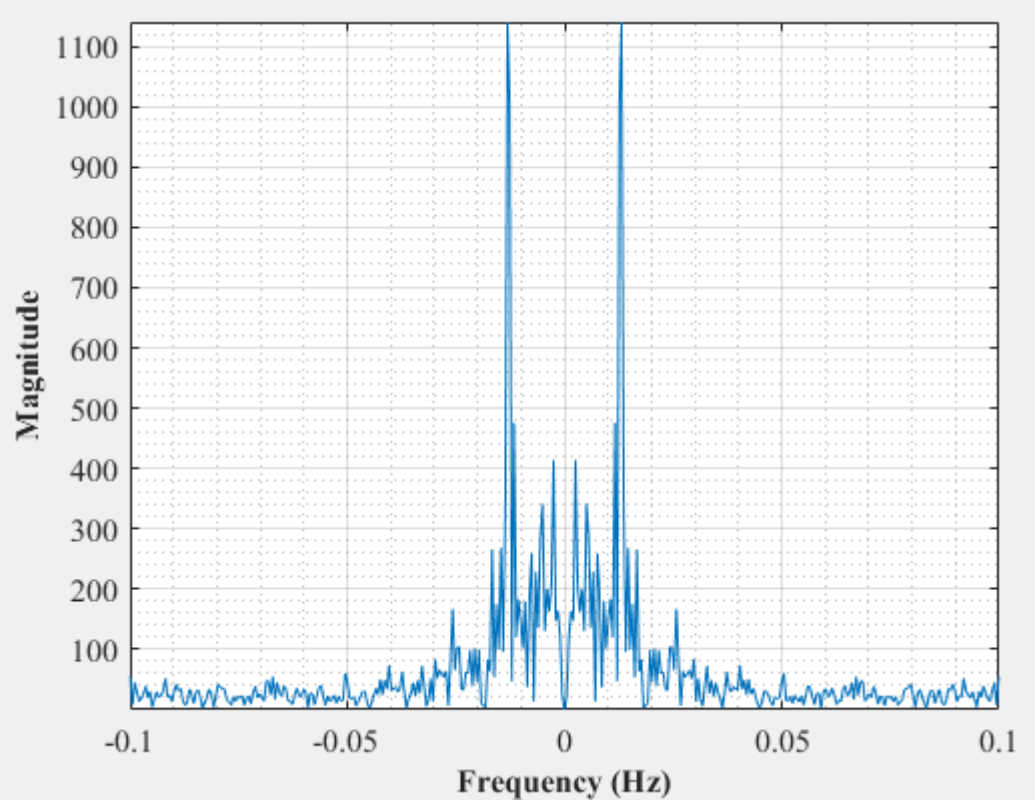


*Figure D-130: Dominant Frequency for a non-uniformly packed vessel (large and small at the center) at 2.33 dm$^3$/minute rotameter flow rate- Test 3*

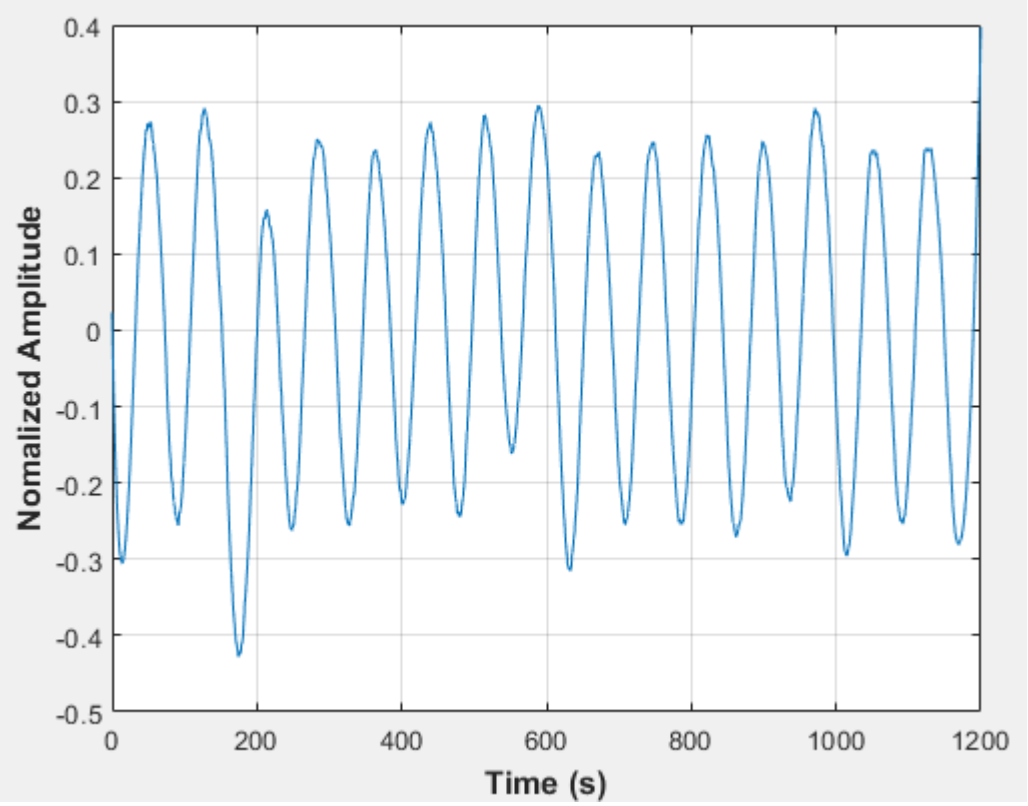


*Figure D-131: Pressure fluctuations in a non-uniformly packed vessel (large and small at the center) at 2.33 dm$^3$/minute rotameter flow rate- Test 4*

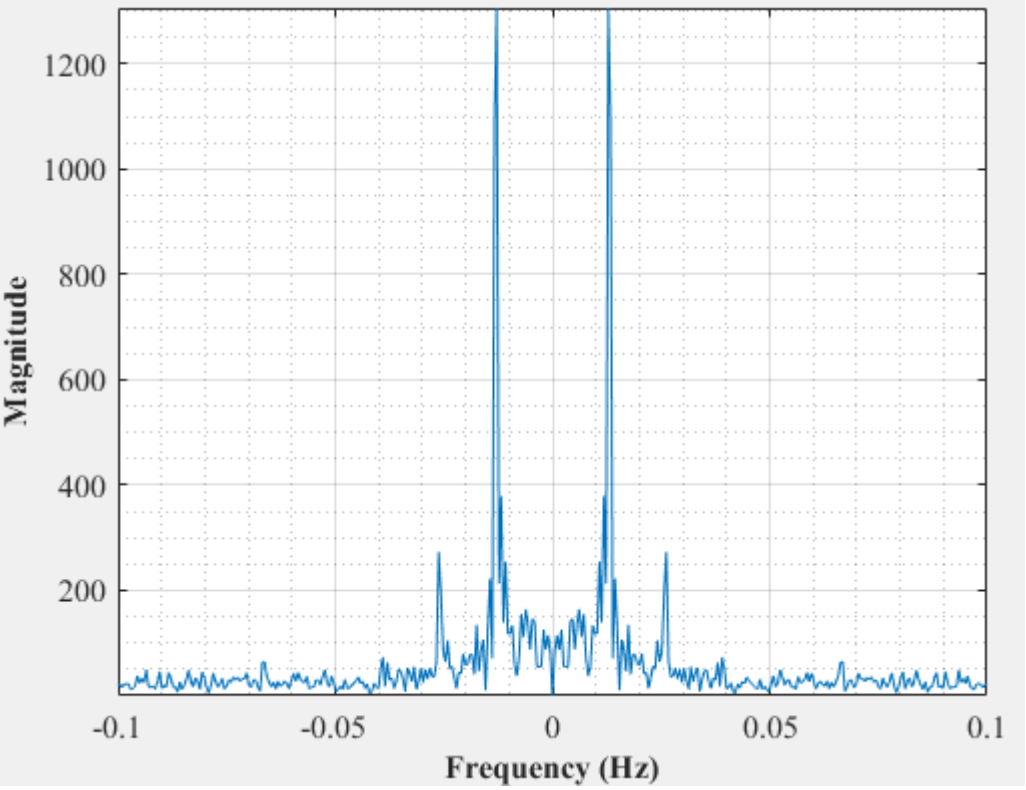


*Figure D-132: Dominant Frequency for a non-uniformly packed vessel (large and small at the center) at 2.33 dm$^3$/minute rotameter flow rate- Test 4*

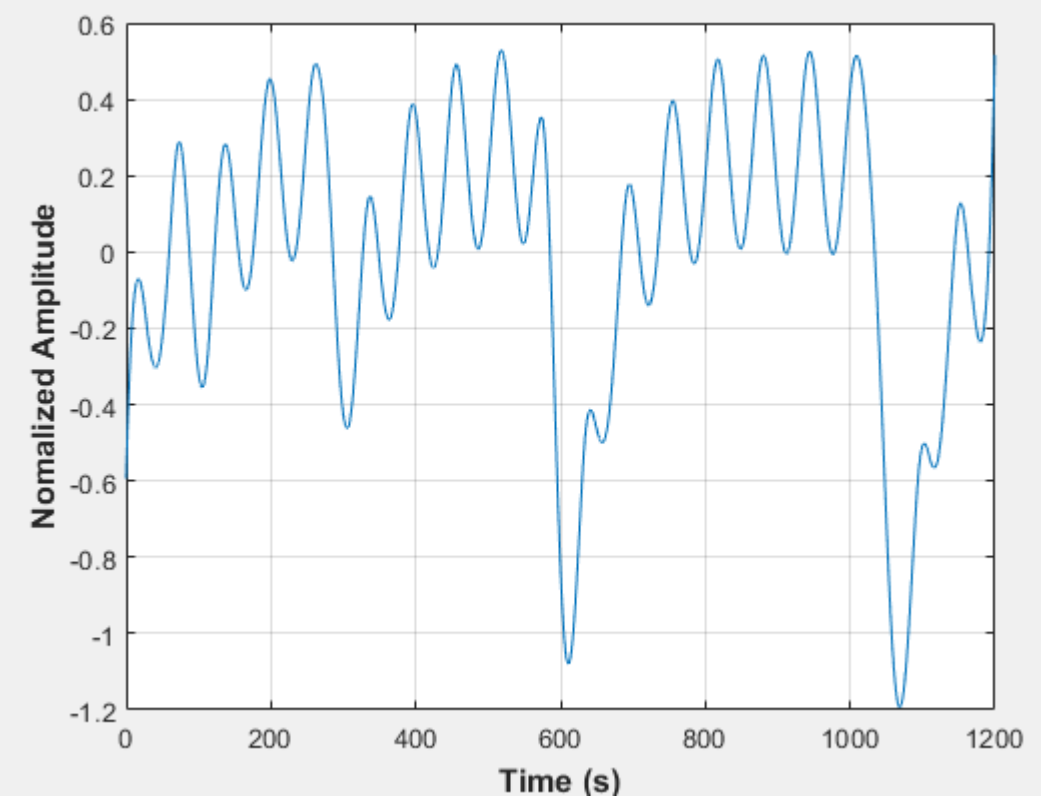


*Figure D-133: Pressure fluctuations in a non-uniformly packed vessel (large and small at the center) at 2.67 dm$^3$/minute rotameter flow rate- Test 1*

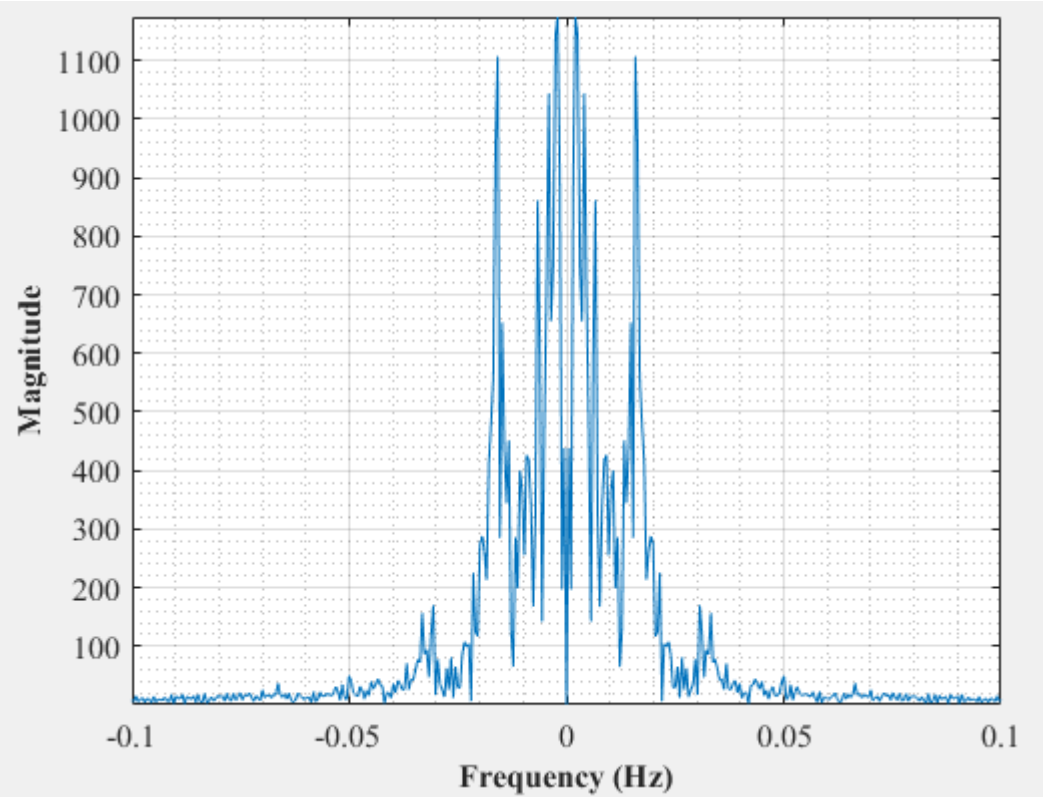


*Figure D-134: Dominant Frequency for a non-uniformly packed vessel (large and small at the center) at 2.67 dm$^3$/minute rotameter flow rate- Test 1*

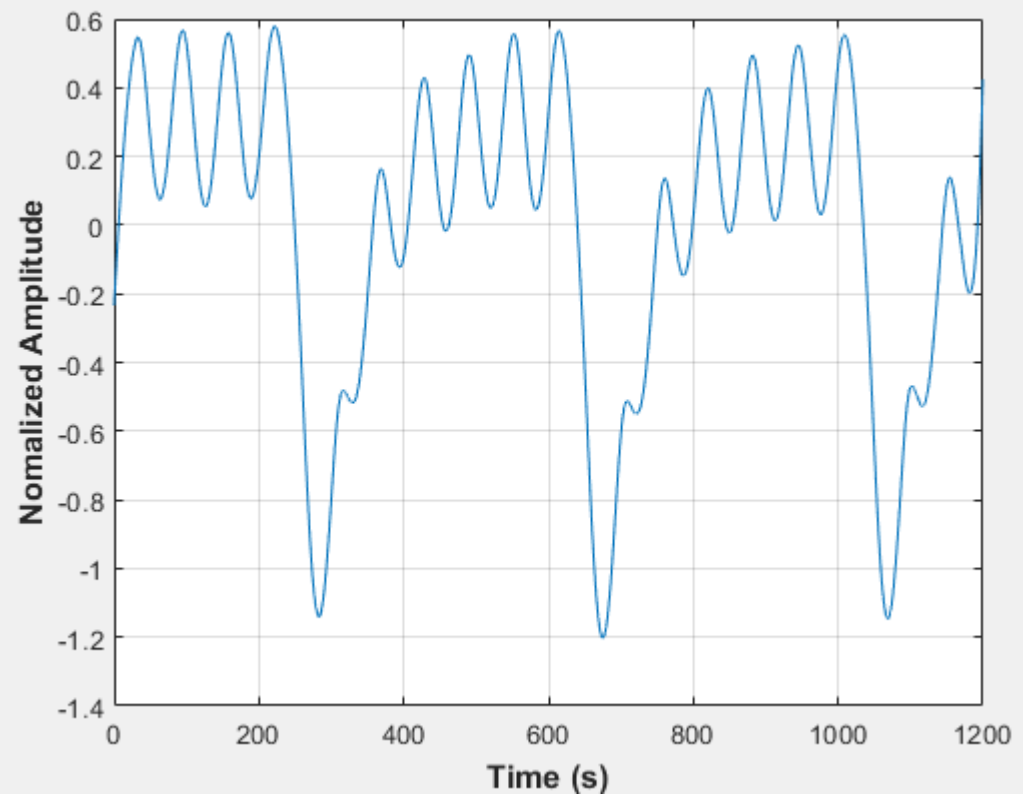


*Figure D-135: Pressure fluctuations in a non-uniformly packed vessel (large and small at the center) at 2.67 $dm^3$/minute rotameter flow rate- Test 2*

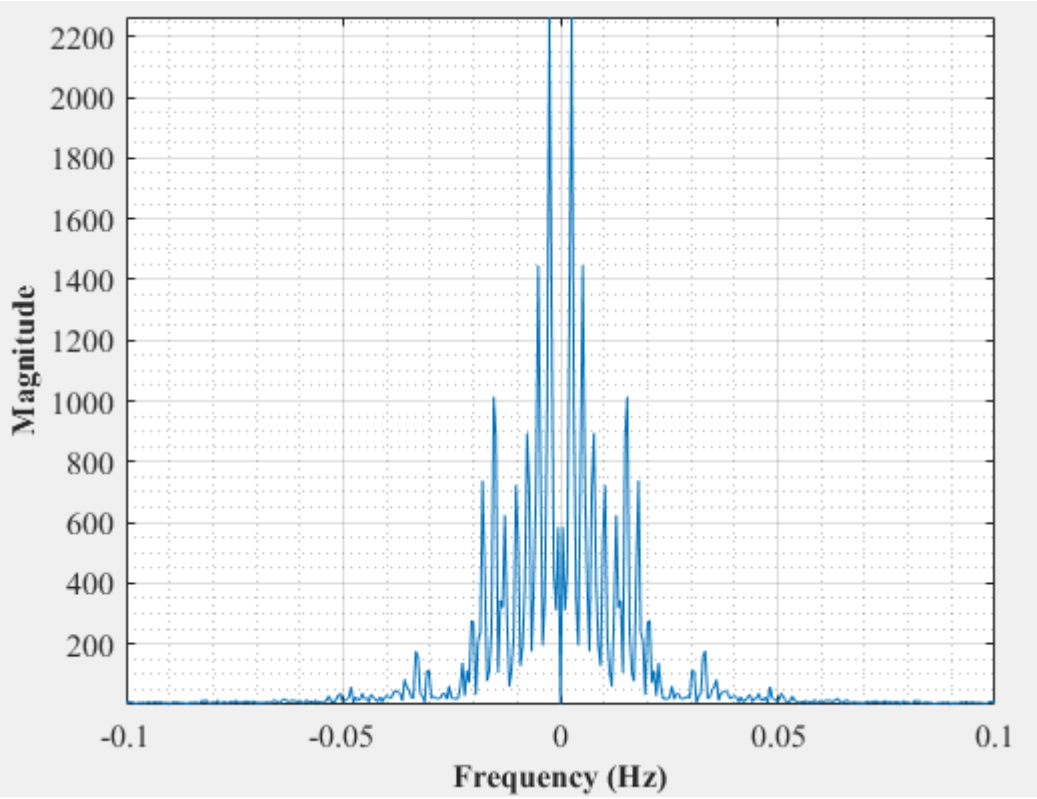


*Figure D-136: Dominant Frequency for a non-uniformly packed vessel (large and small at the center) at 2.67 $dm^3$/minute rotameter flow rate- Test 2*

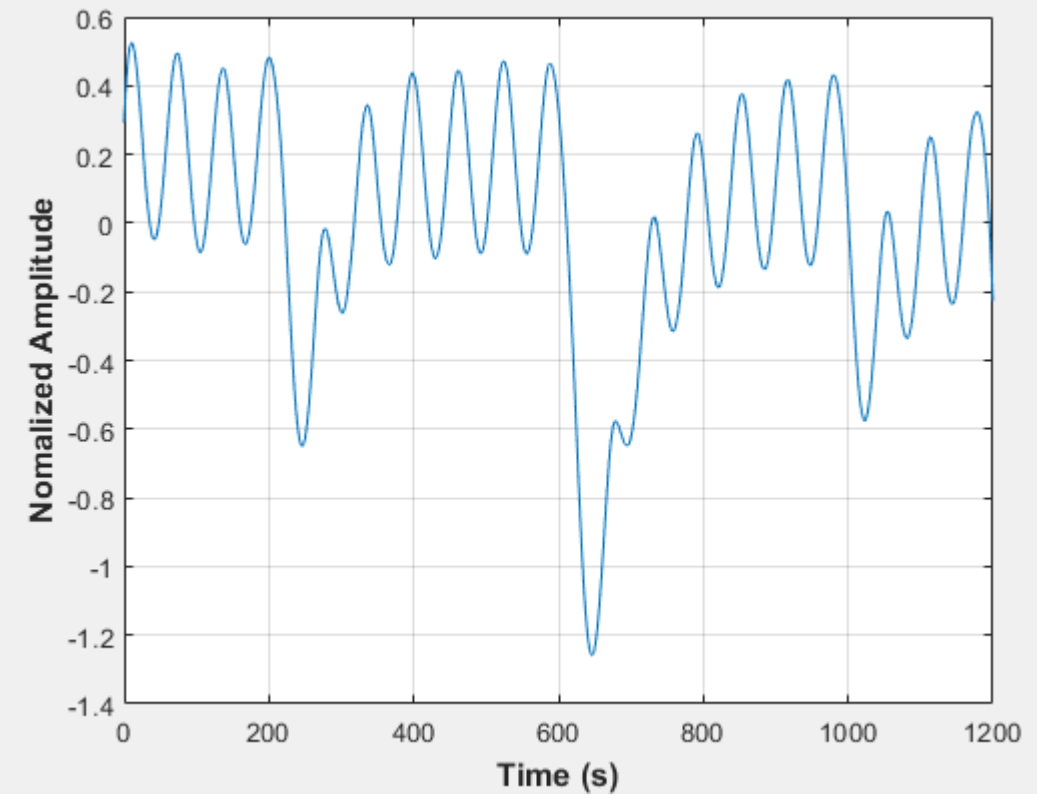


*Figure D-137: Pressure fluctuations in a non-uniformly packed vessel (large and small at the center) at 2.67 dm$^3$/minute rotameter flow rate- Test 3*

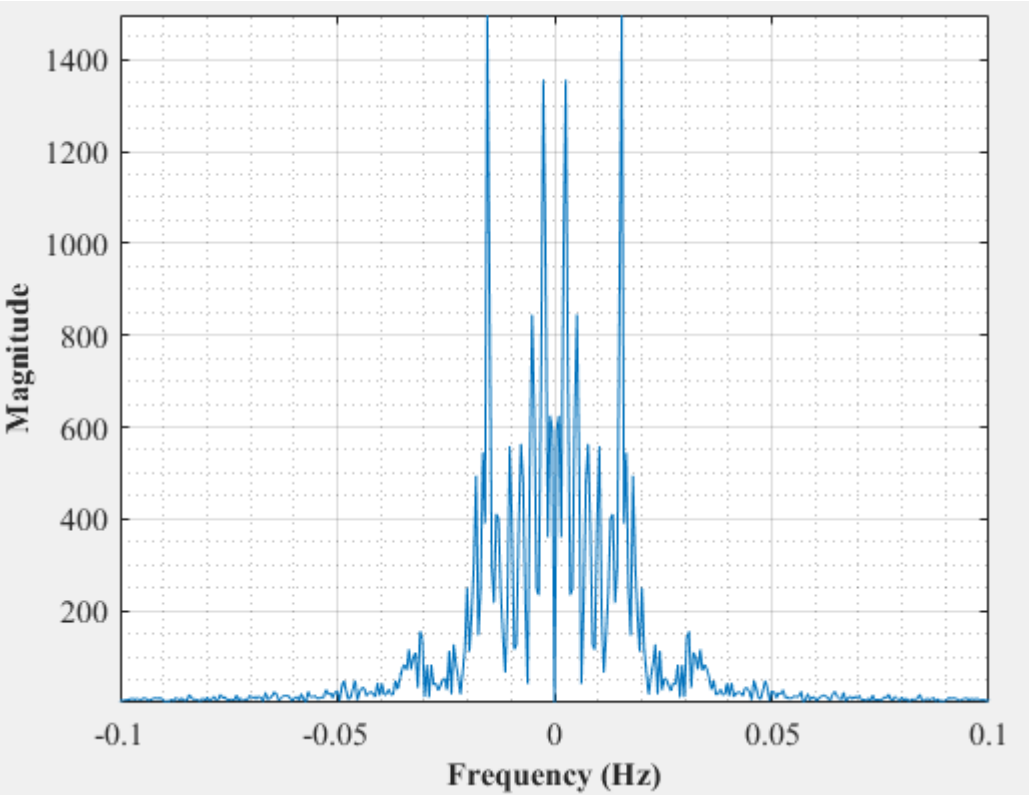


*Figure D-138: Dominant Frequency for a non-uniformly packed vessel (large and small at the center) at 2.67 dm$^3$/minute rotameter flow rate- Test 3*

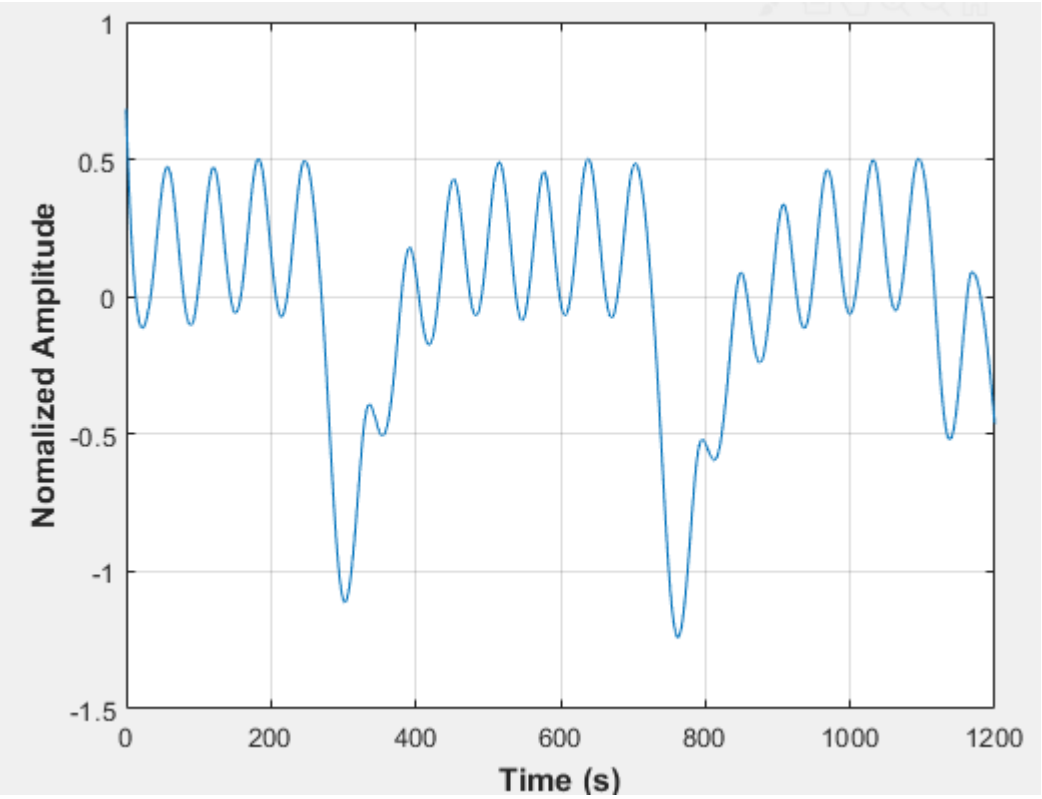


*Figure D-139: Pressure fluctuations in a non-uniformly packed vessel (large and small at the center) at 2.67 dm$^3$/minute rotameter flow rate- Test 4*

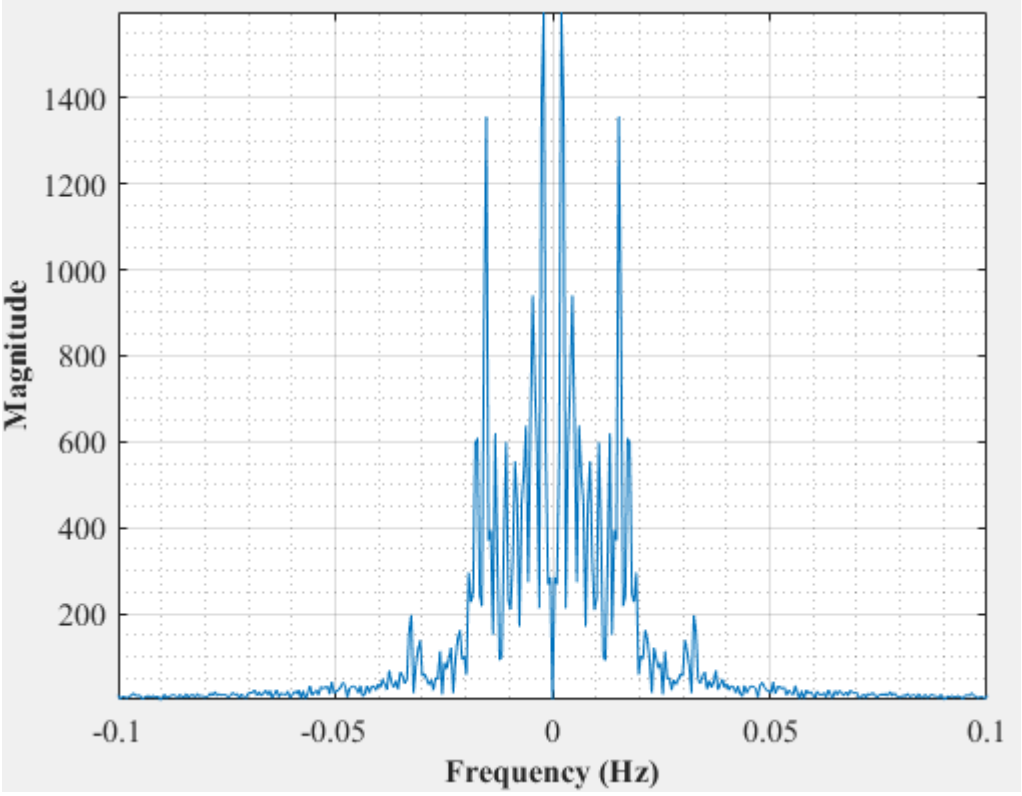


*Figure D-140: Dominant Frequency for a non-uniformly packed vessel (large and small at the center) at 2.67 dm$^3$/minute rotameter flow rate- Test 4*

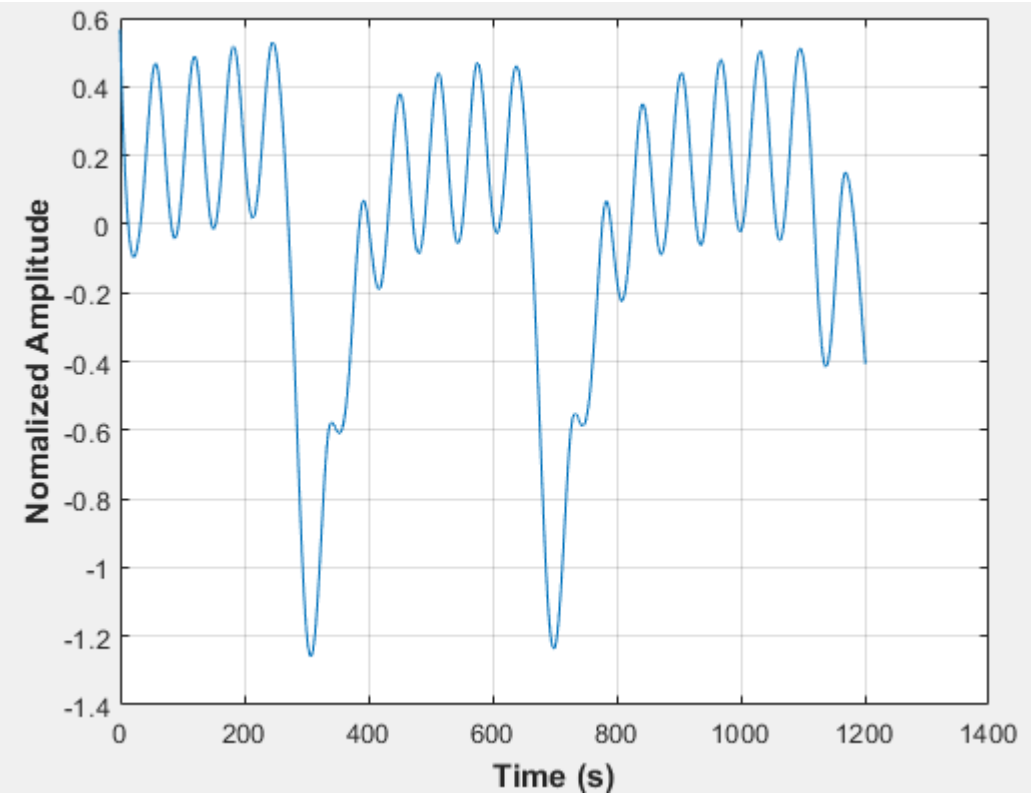


*Figure D-141: Pressure fluctuations in a non-uniformly packed vessel (large and small at the center) at 2.67 dm$^3$/minute rotameter flow rate- Test 5*

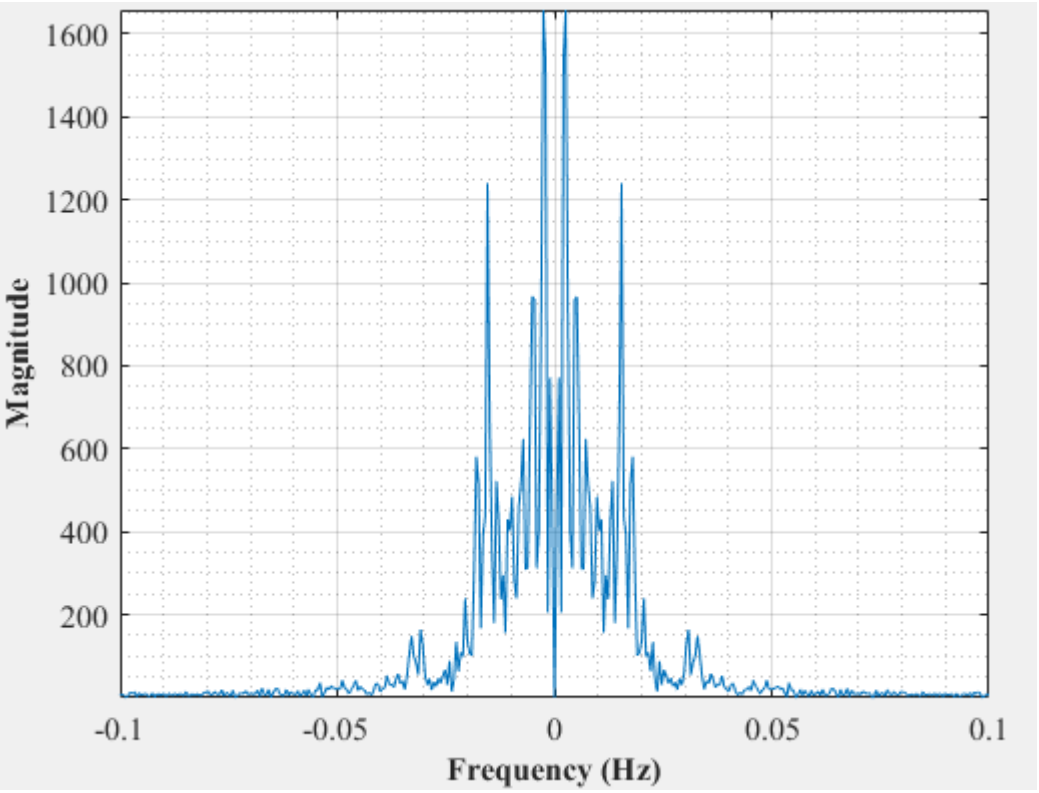


*Figure D-142: Dominant Frequency for a non-uniformly packed vessel (large and small at the center) at 2.67 dm$^3$/minute rotameter flow rate- Test 5*

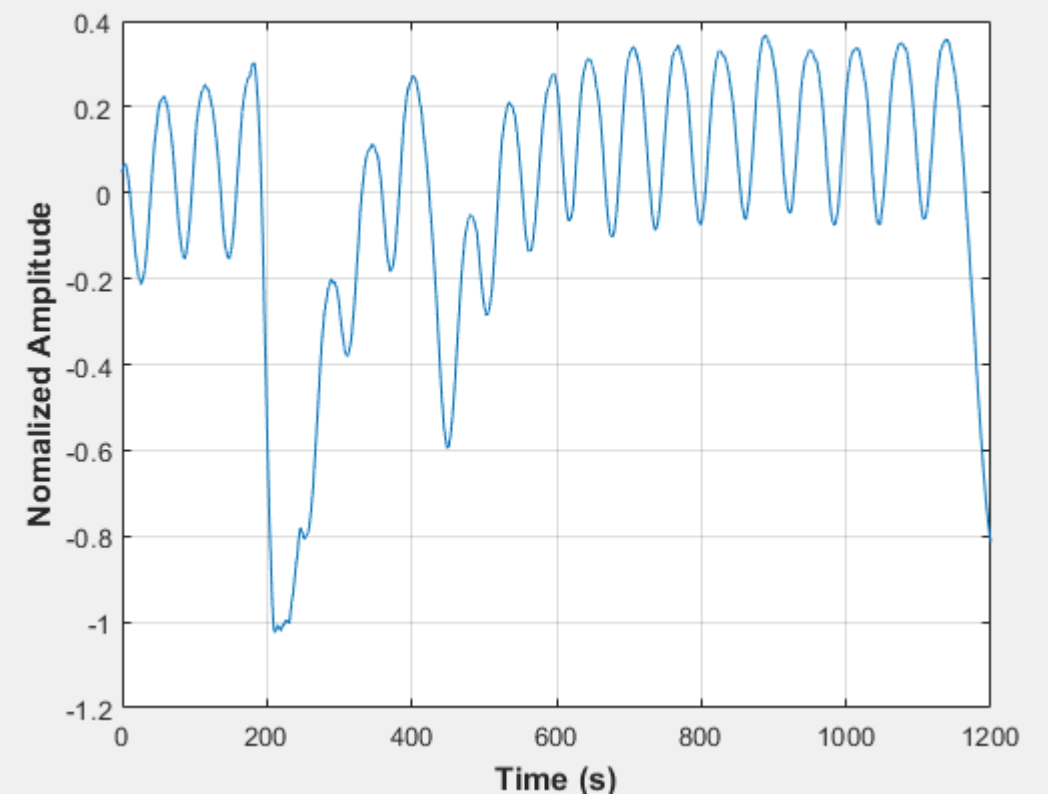


*Figure D-143: Pressure fluctuations in a non-uniformly packed vessel (large and small at the center) at 2.83 dm$^3$/minute rotameter flow rate- Test 1*

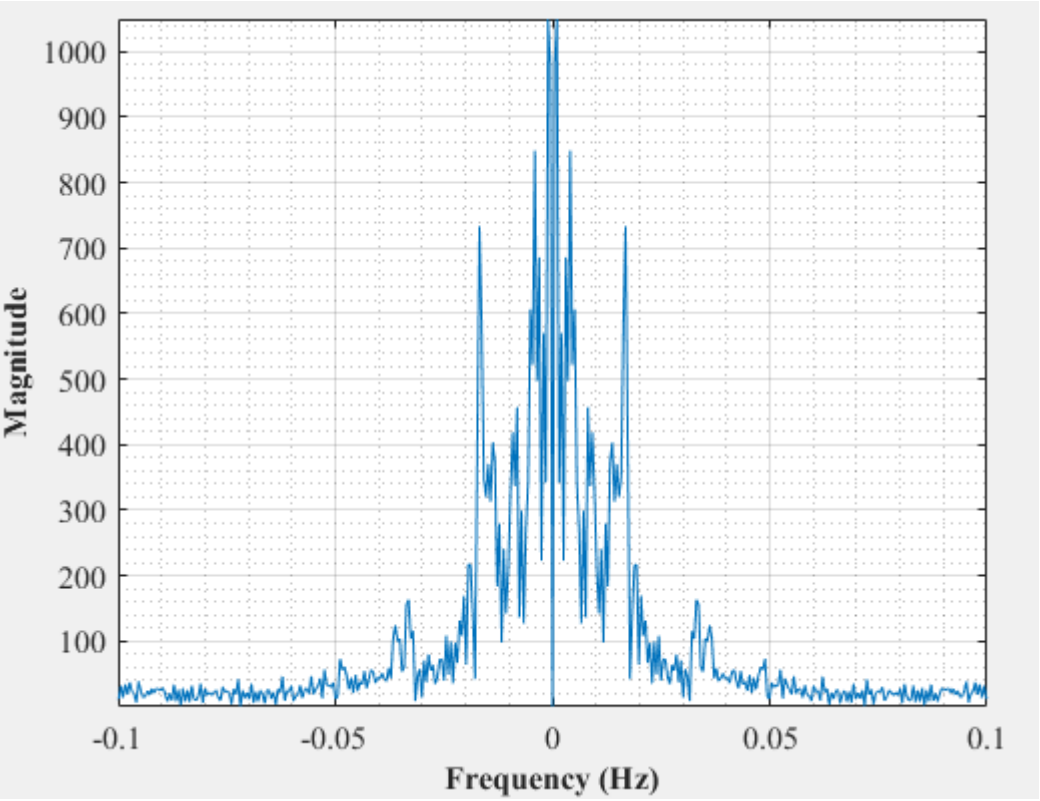


*Figure D-144: Dominant Frequency for a non-uniformly packed vessel (large and small at the center) at 2.83 dm$^3$/minute rotameter flow rate- Test 1*

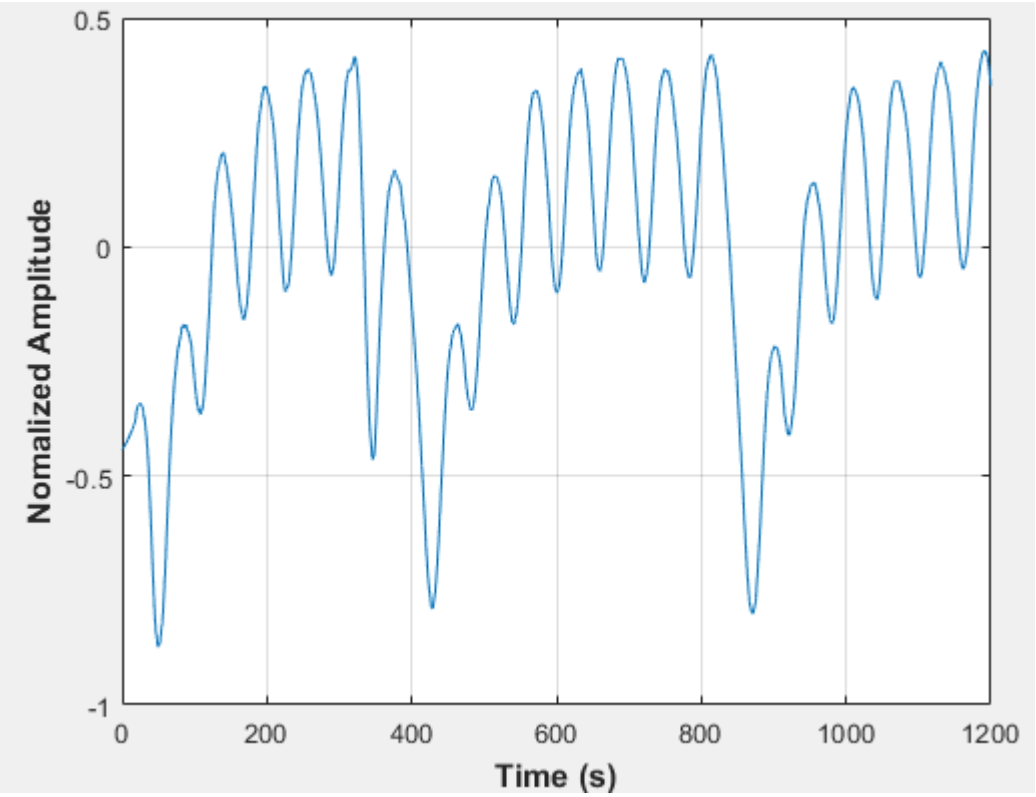


*Figure D-145: Pressure fluctuations in a non-uniformly packed vessel (large and small at the center) at 2.83 dm$^3$/minute rotameter flow rate- Test 2*

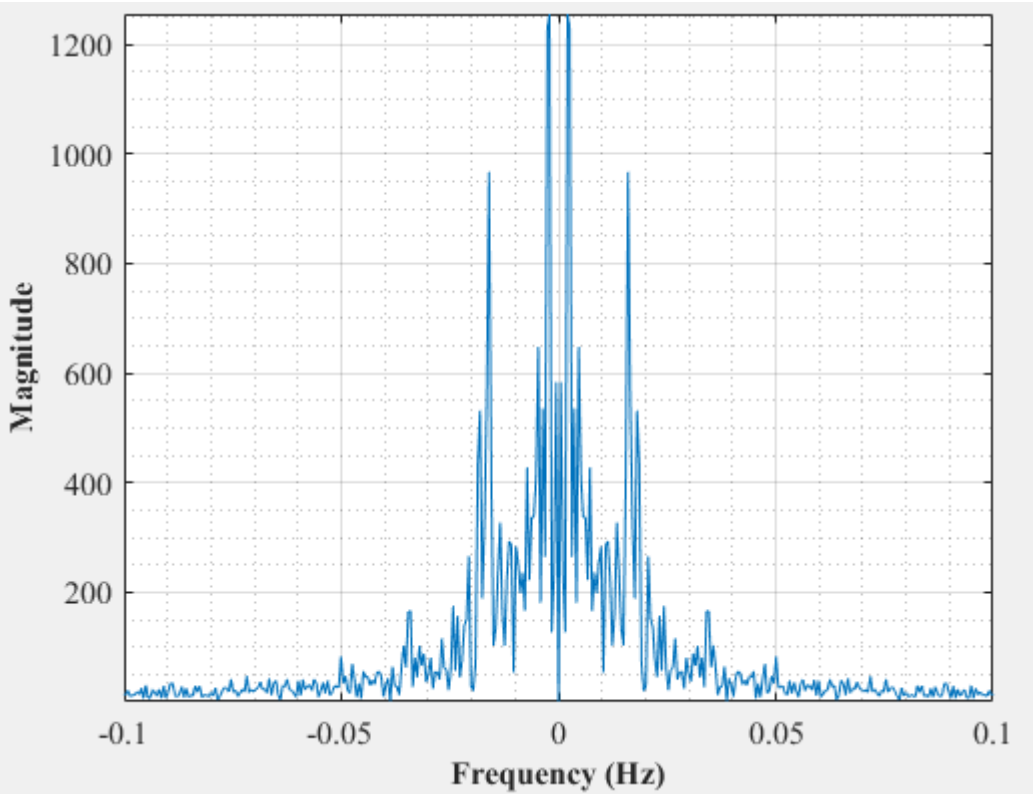


*Figure D-146: Dominant Frequency for a non-uniformly packed vessel (large and small at the center) at 2.83 dm$^3$/minute rotameter flow rate- Test 2*

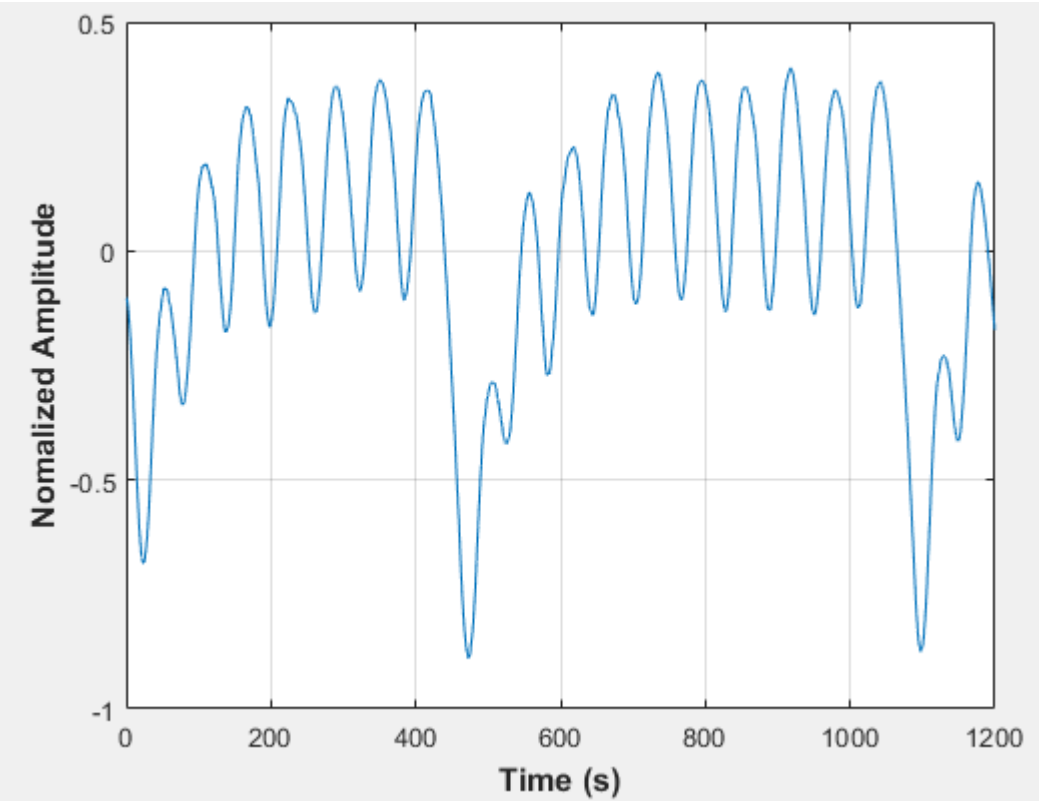


*Figure D-147: Pressure fluctuations in a non-uniformly packed vessel (large and small at the center) at 2.83 $dm^3$/minute rotameter flow rate- Test 3*

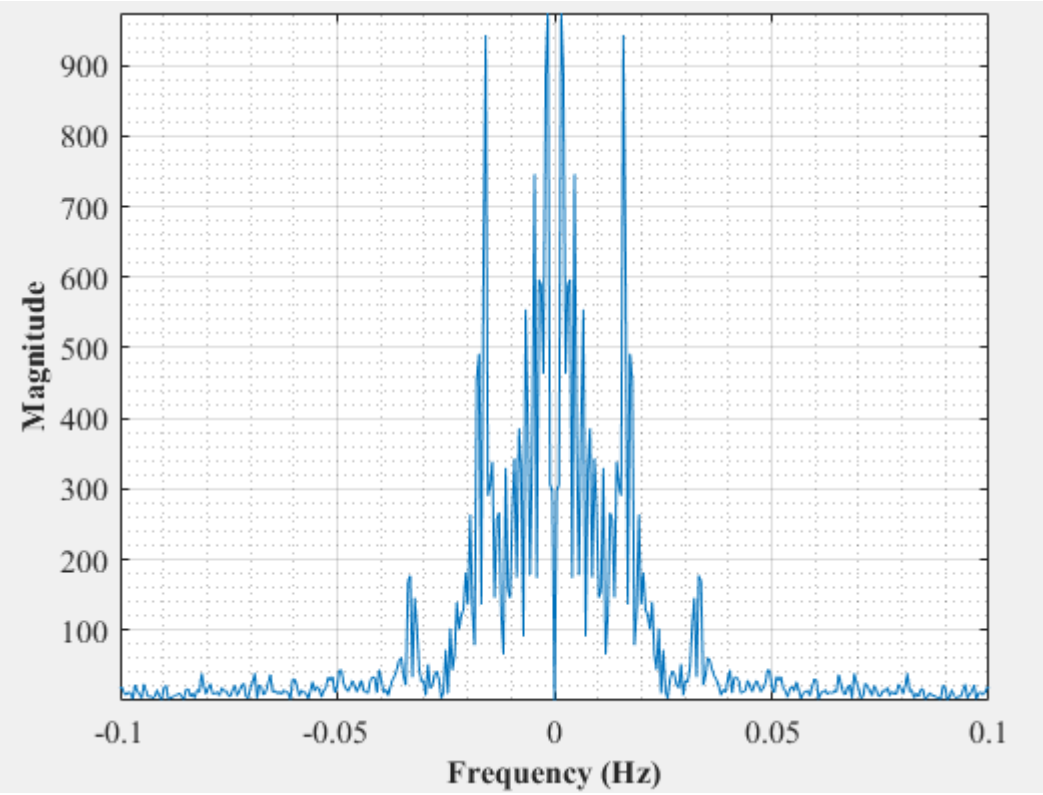


*Figure D-148: Dominant Frequency for a non-uniformly packed vessel (large and small at the center) at 2.83 $dm^3$/minute rotameter flow rate- Test 3*

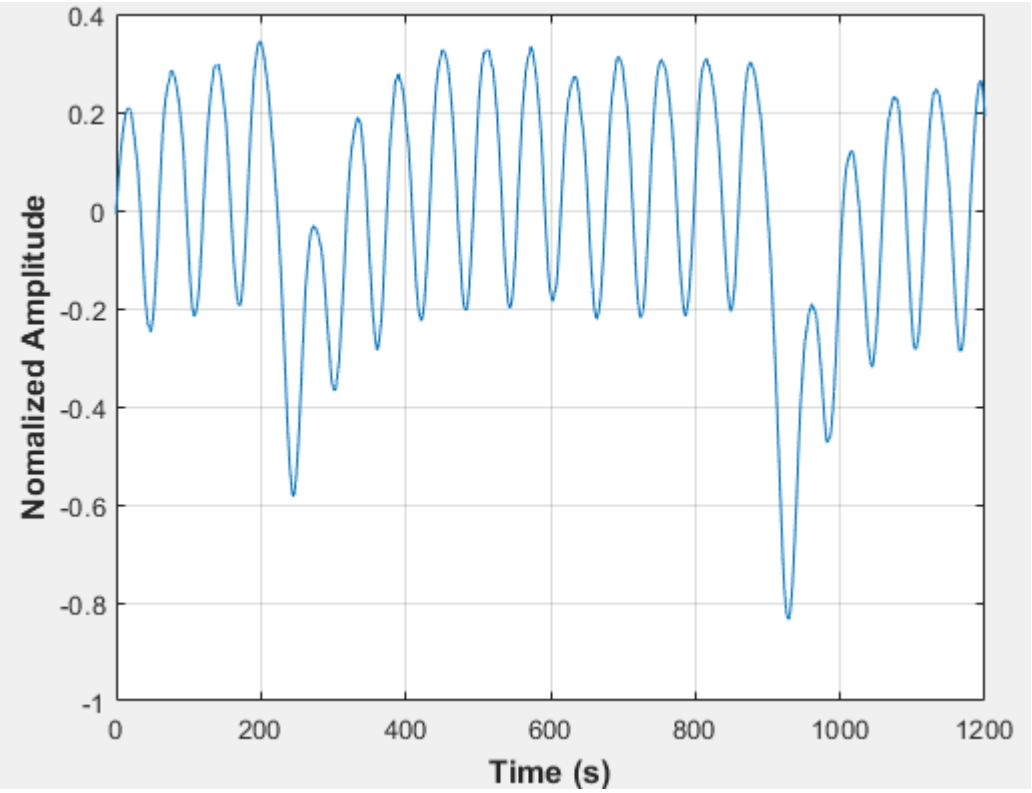


*Figure D-149: Pressure fluctuations in a non-uniformly packed vessel (large and small at the center) at 2.83 dm$^3$/minute rotameter flow rate- Test 4*

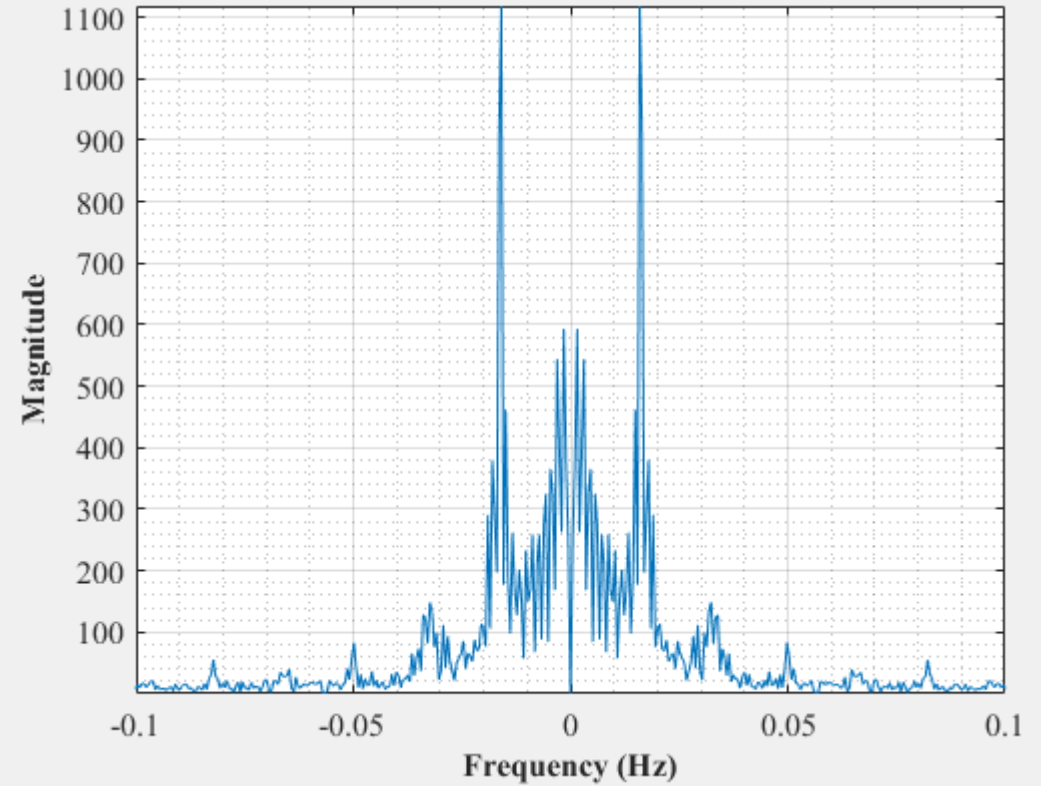


*Figure D-150: Dominant Frequency for a non-uniformly packed vessel (large and small at the center) at 2.83 dm$^3$/minute rotameter flow rate- Test 4*

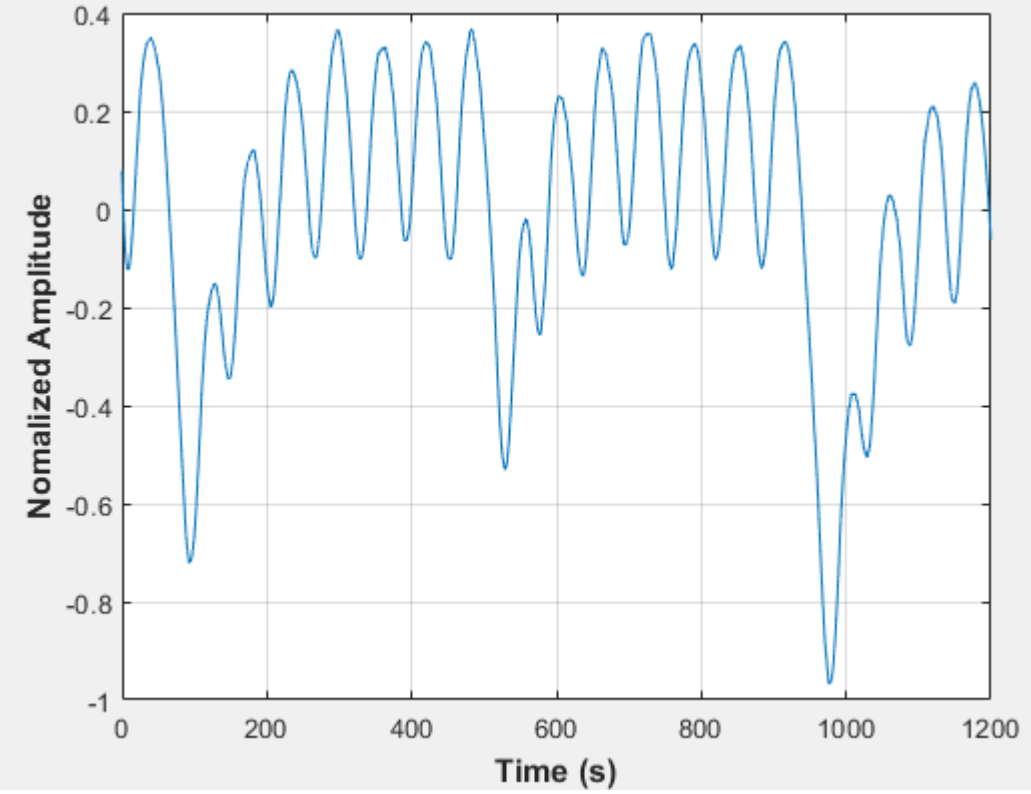


*Figure D-151: Pressure fluctuations in a non-uniformly packed vessel (large and small at the center) at 2.83 dm$^3$/minute rotameter flow rate- Test 5*

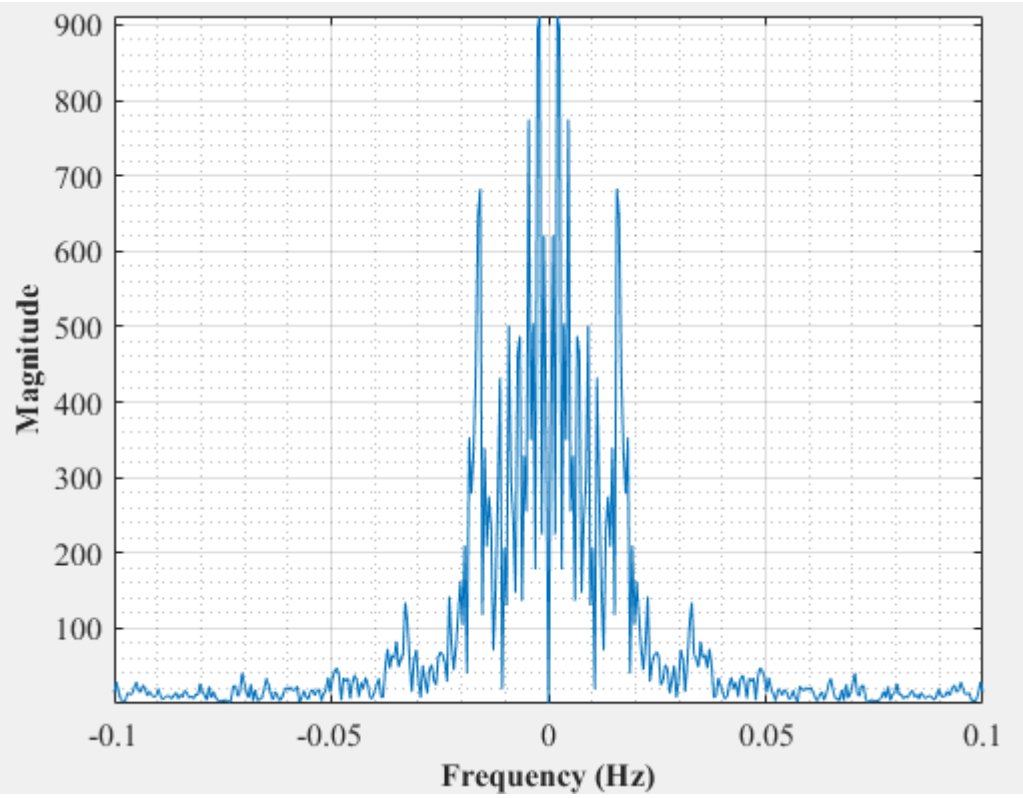


*Figure D-152: Dominant Frequency for a non-uniformly packed vessel (large and small at the center) at 2.83 dm$^3$/minute rotameter flow rate- Test 5*

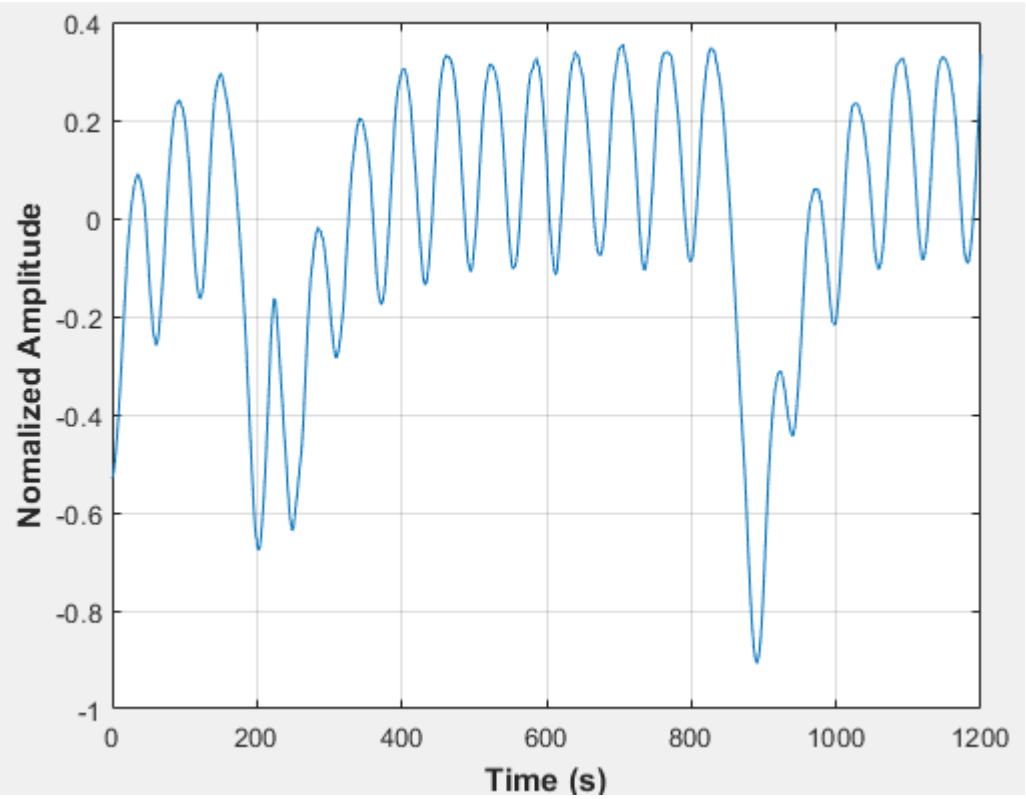


*Figure D-153: Pressure fluctuations in a non-uniformly packed vessel (large and small at the center) at 2.83 dm$^3$/minute rotameter flow rate- Test 6*

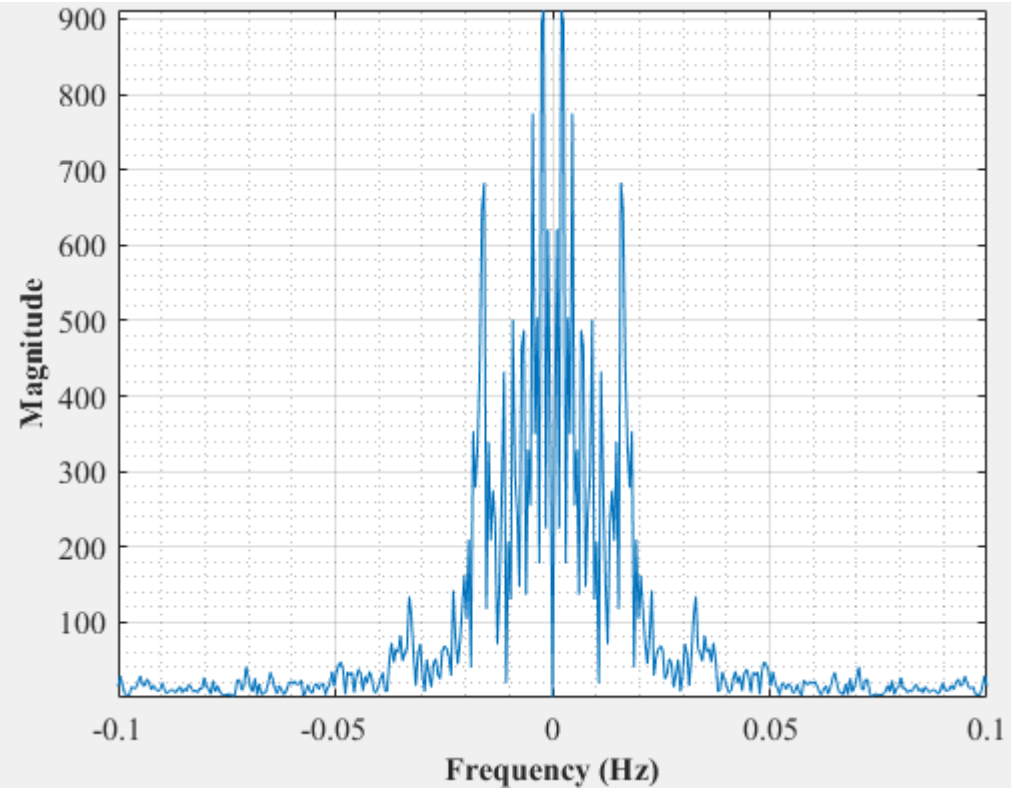


*Figure D-154: Dominant Frequency for a non-uniformly packed vessel (large and small at the center) at 2.83 dm$^3$/minute rotameter flow rate- Test 6*

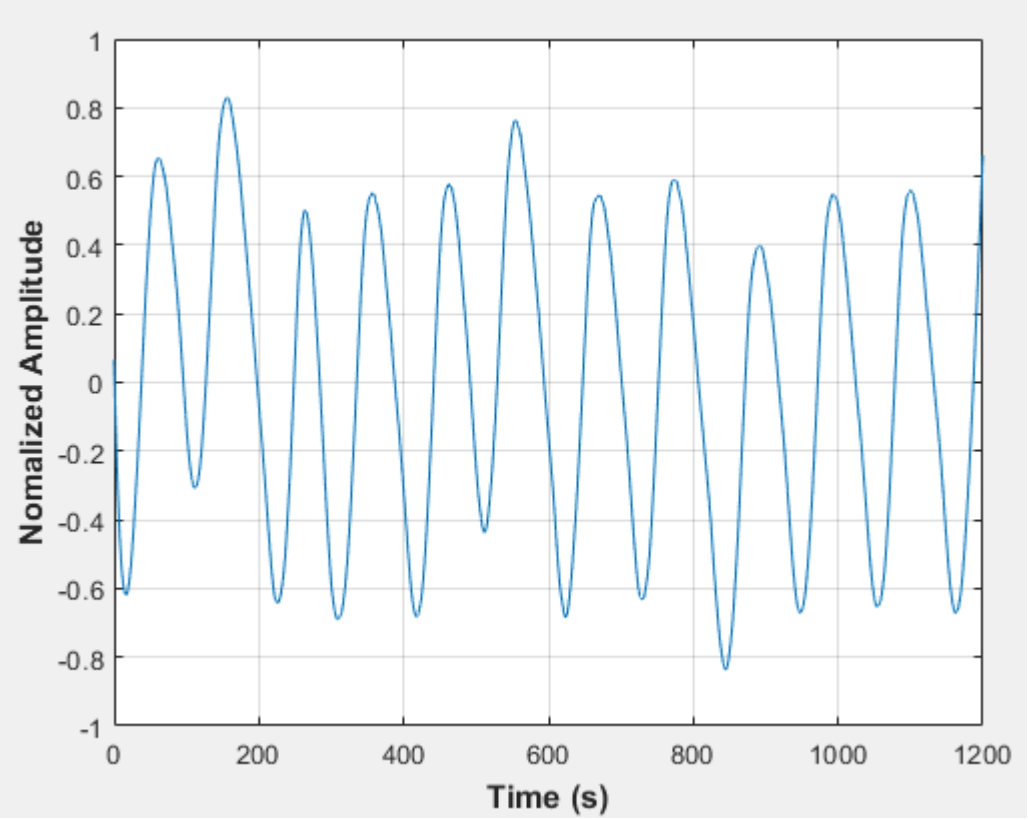


*Figure D-155: Pressure fluctuations in a non-uniformly packed vessel (large and small at the side) at 1.67 dm$^3$/minute rotameter flow rate- Test 1*

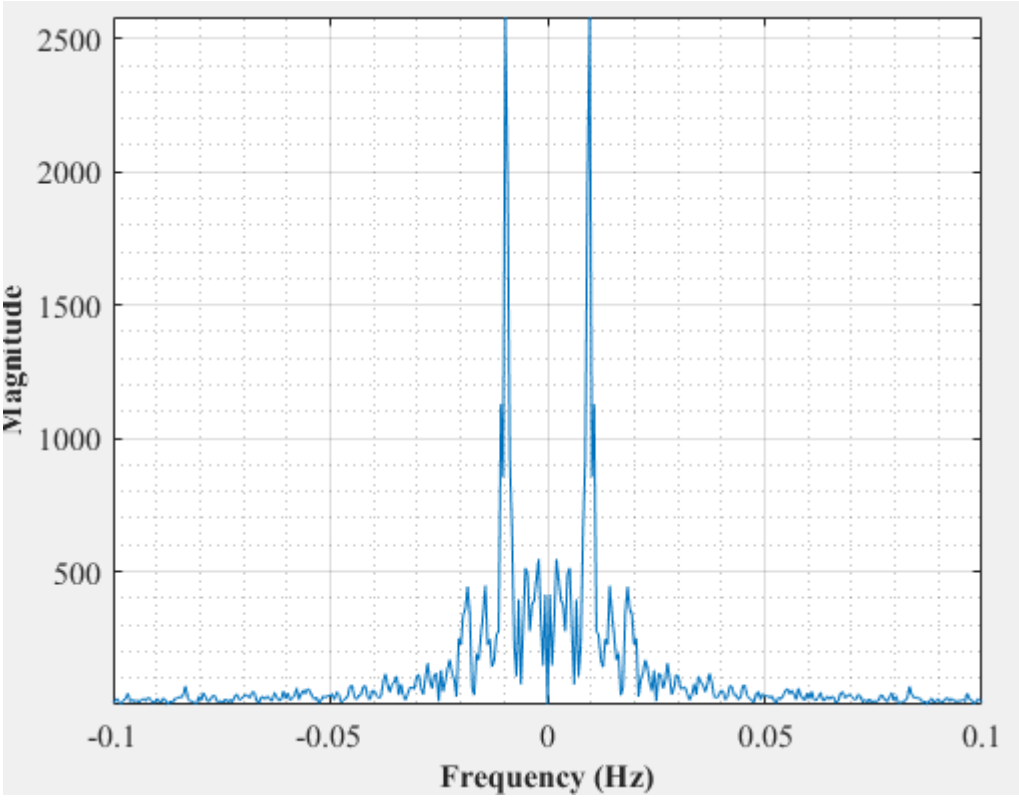


*Figure D-156: Dominant Frequency for a non-uniformly packed vessel (large and small at the side) at 1.67 dm$^3$/minute rotameter flow rate- Test 1*

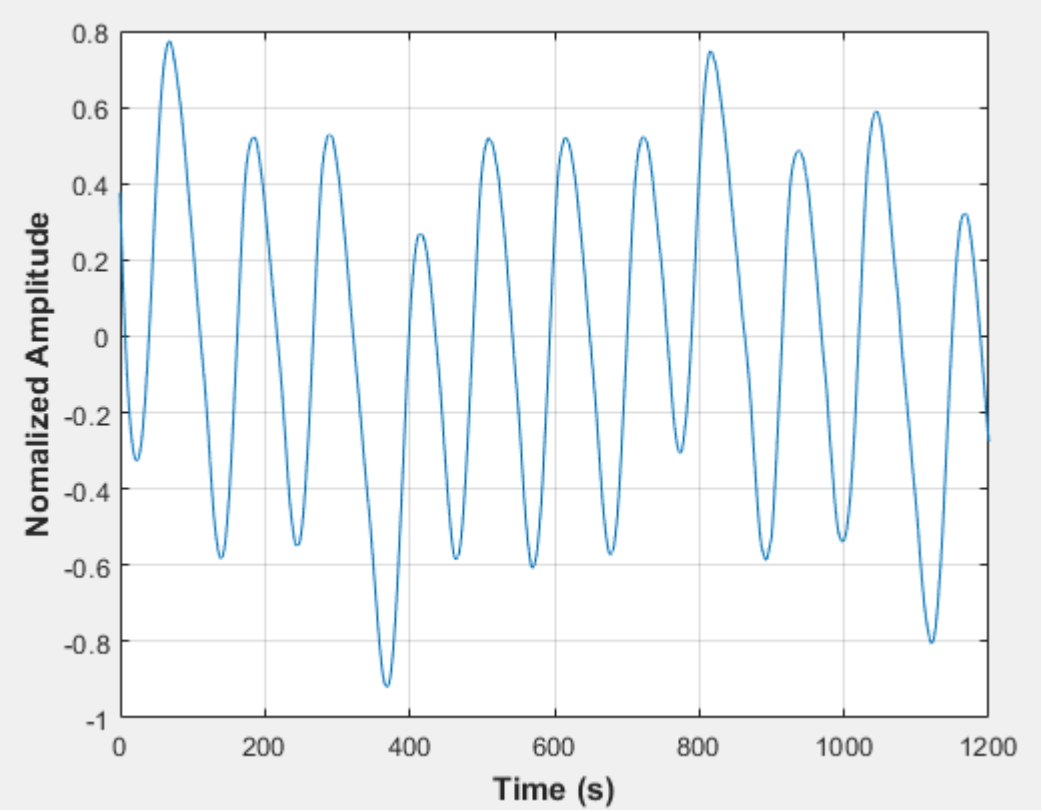


*Figure D-157: Pressure fluctuations in a non-uniformly packed vessel (large and small at the side) at 1.67 dm$^3$/minute rotameter flow rate- Test 2*

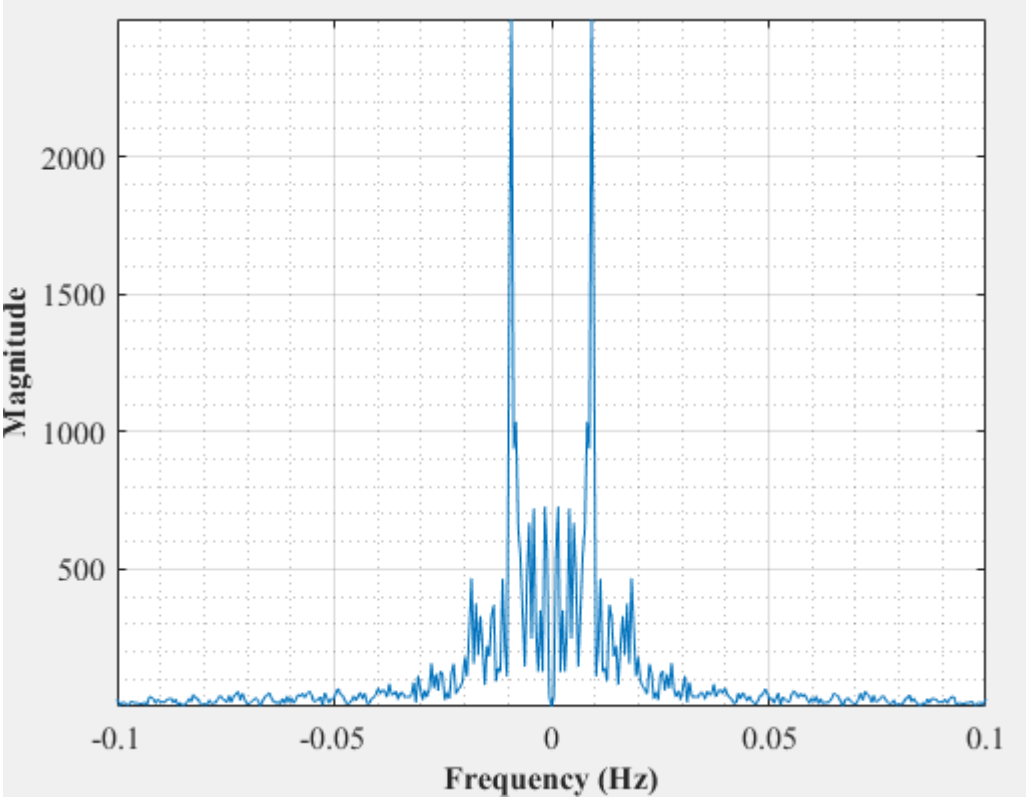


*Figure D-158: Dominant Frequency for a non-uniformly packed vessel (large and small at the side) at 1.67 dm$^3$/minute rotameter flow rate- Test 2*

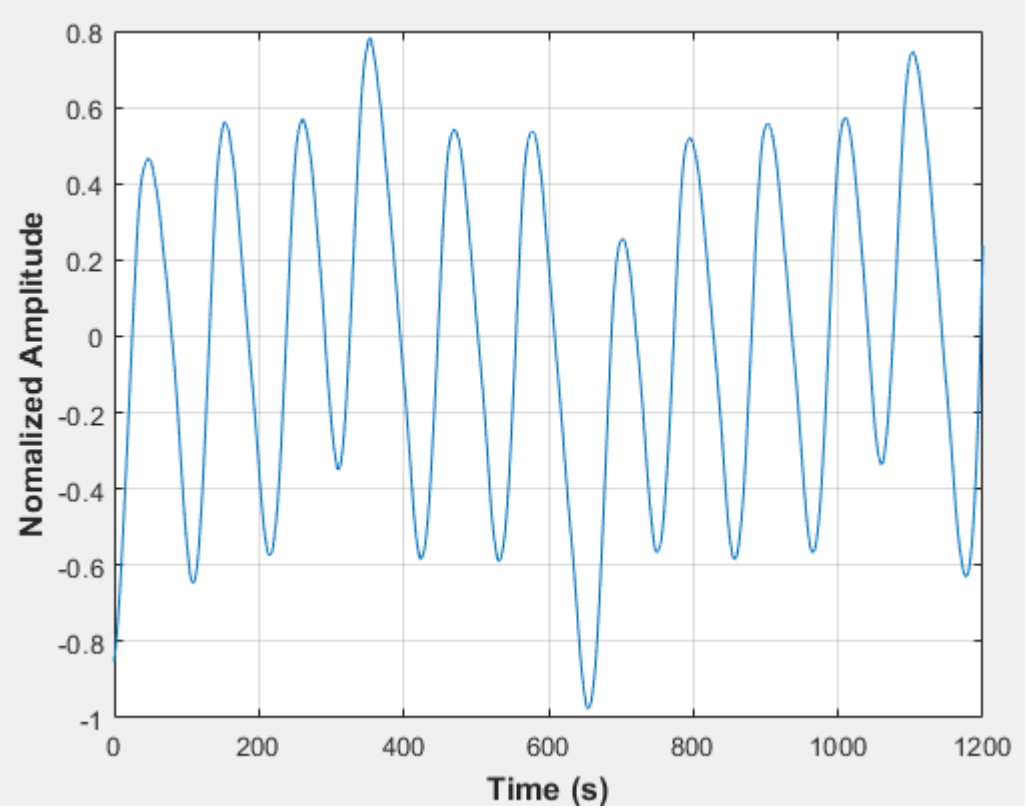


*Figure D-159: Pressure fluctuations in a non-uniformly packed vessel (large and small at the side) at 1.67 dm$^3$/minute rotameter flow rate- Test 3*

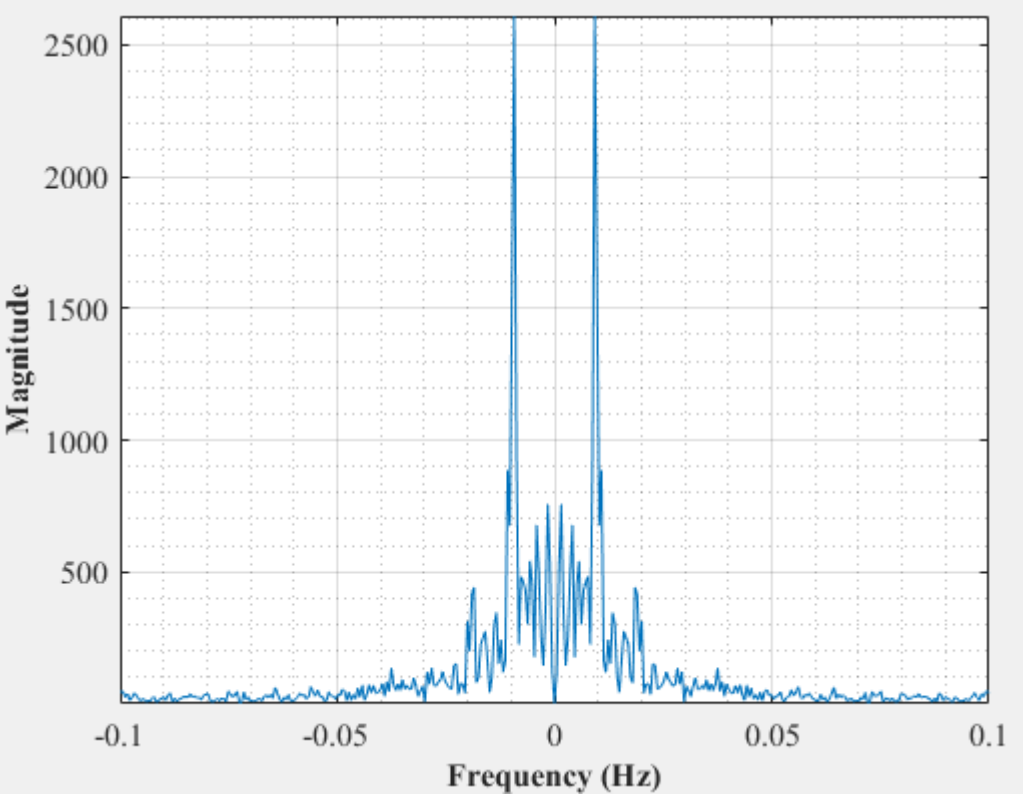


*Figure D-160: Dominant Frequency for a non-uniformly packed vessel (large and small at the side) at 1.67 dm$^3$/minute rotameter flow rate- Test 3*

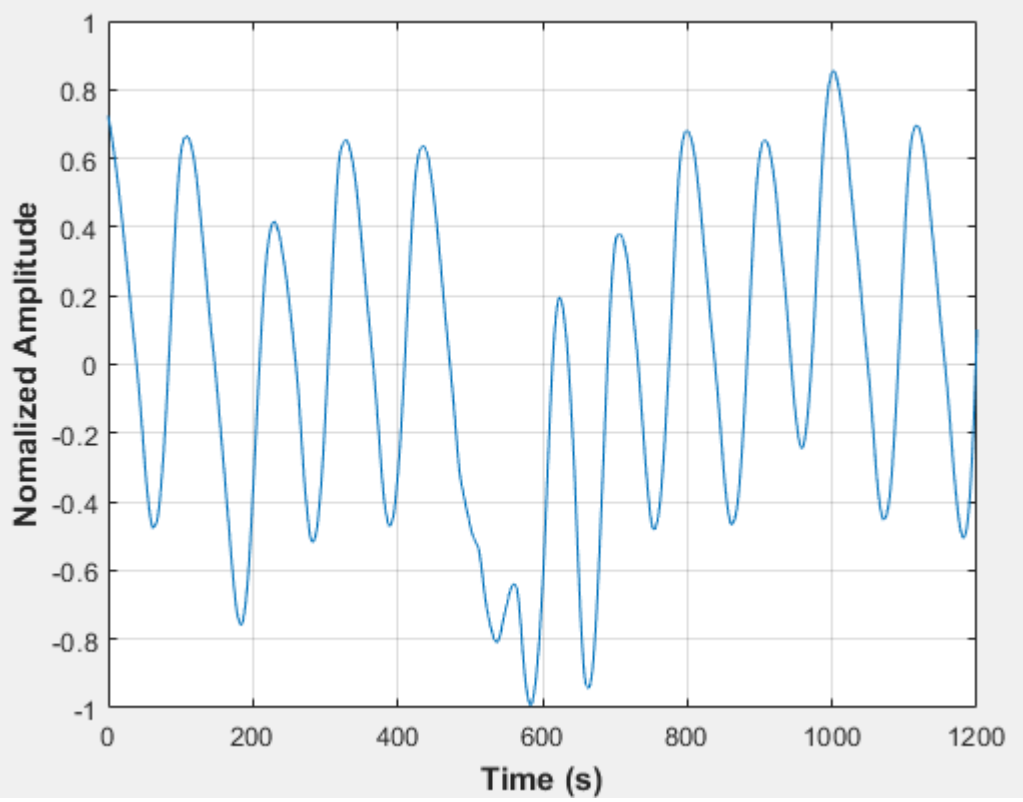


*Figure D-161: Pressure fluctuations in a non-uniformly packed vessel (large and small at the side) at 1.67 dm$^3$/minute r rotameter flow rate- Test 4*

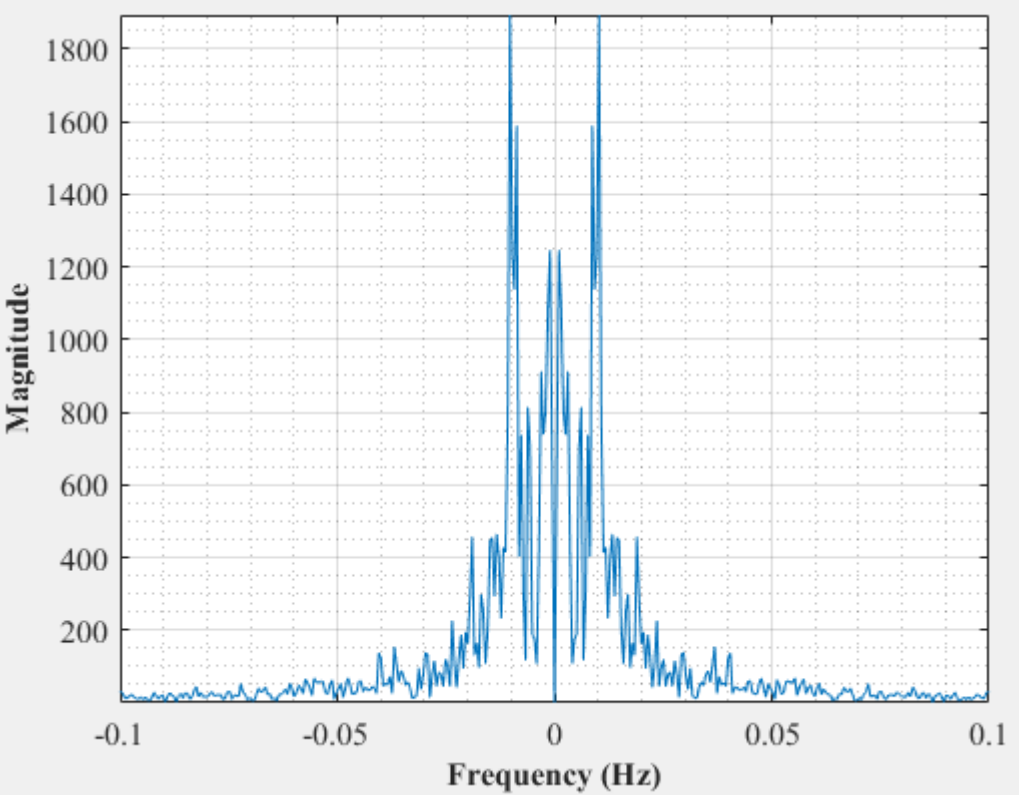


*Figure D-162: Dominant Frequency for a non-uniformly packed vessel (large and small at the side) at 1.67 dm$^3$/minute rotameter flow rate- Test 4*

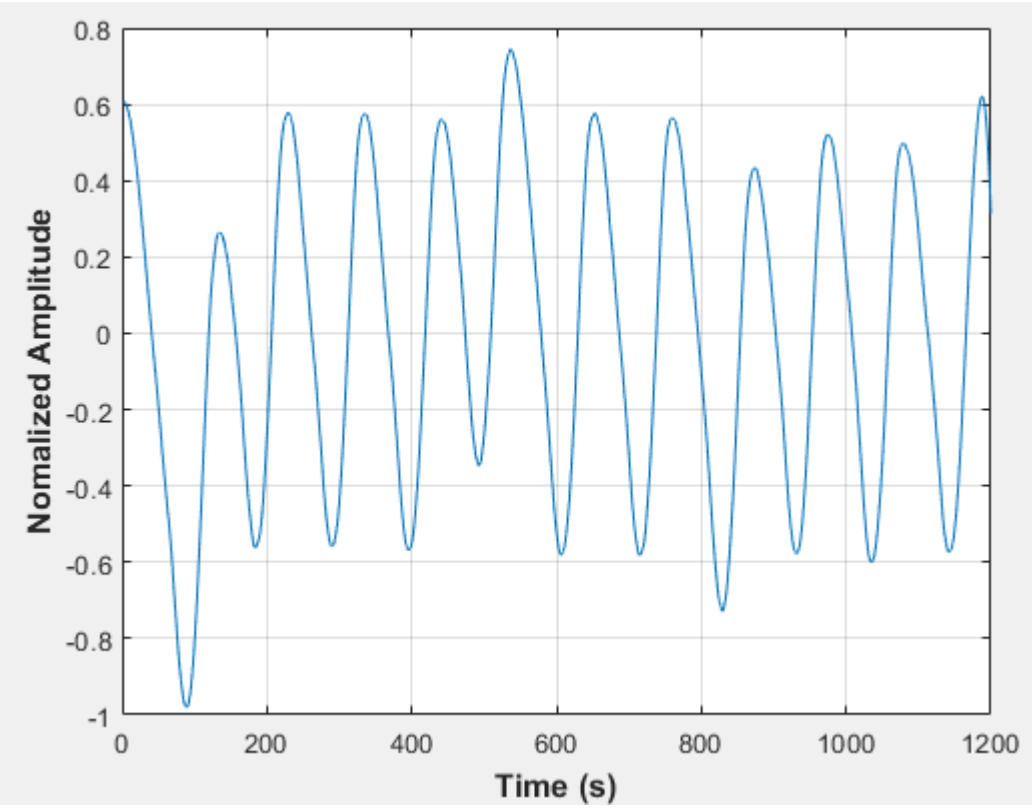


*Figure D-163: Pressure fluctuations in a non-uniformly packed vessel (large and small at the side) at 1.67 dm$^3$/minute rotameter flow rate- Test 5*

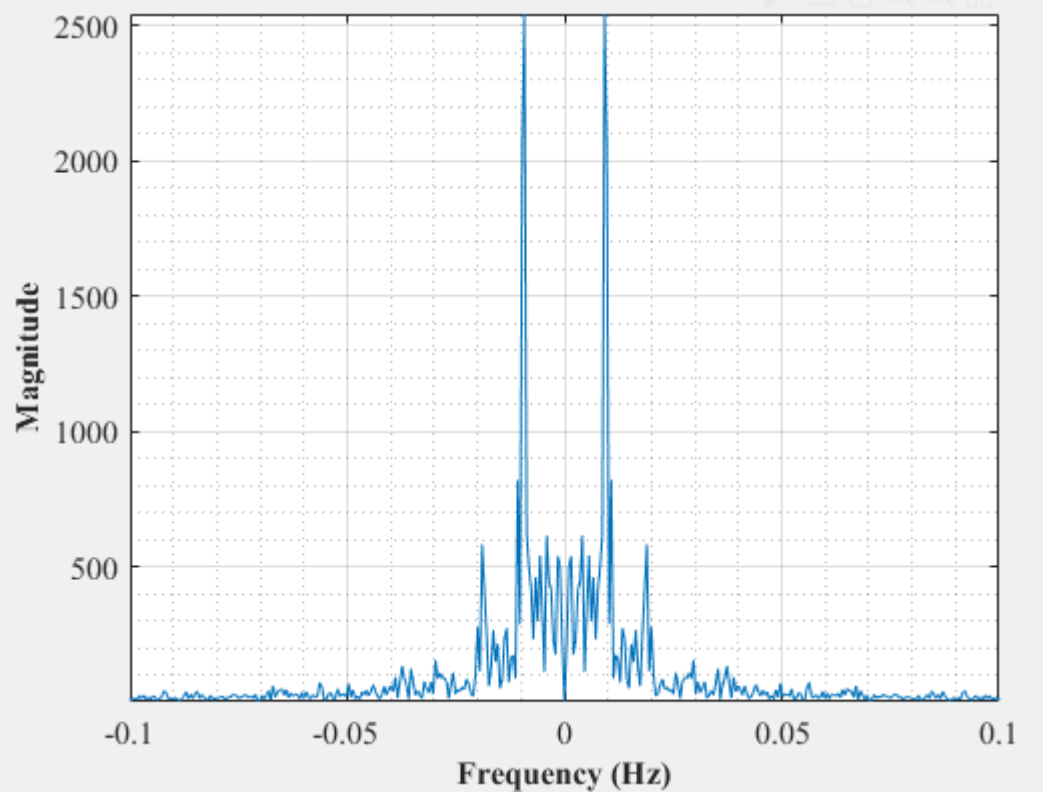


*Figure D-164: Dominant Frequency for a non-uniformly packed vessel (large and small at the side) at 1.67 dm$^3$/minute rotameter flow rate- Test 5*

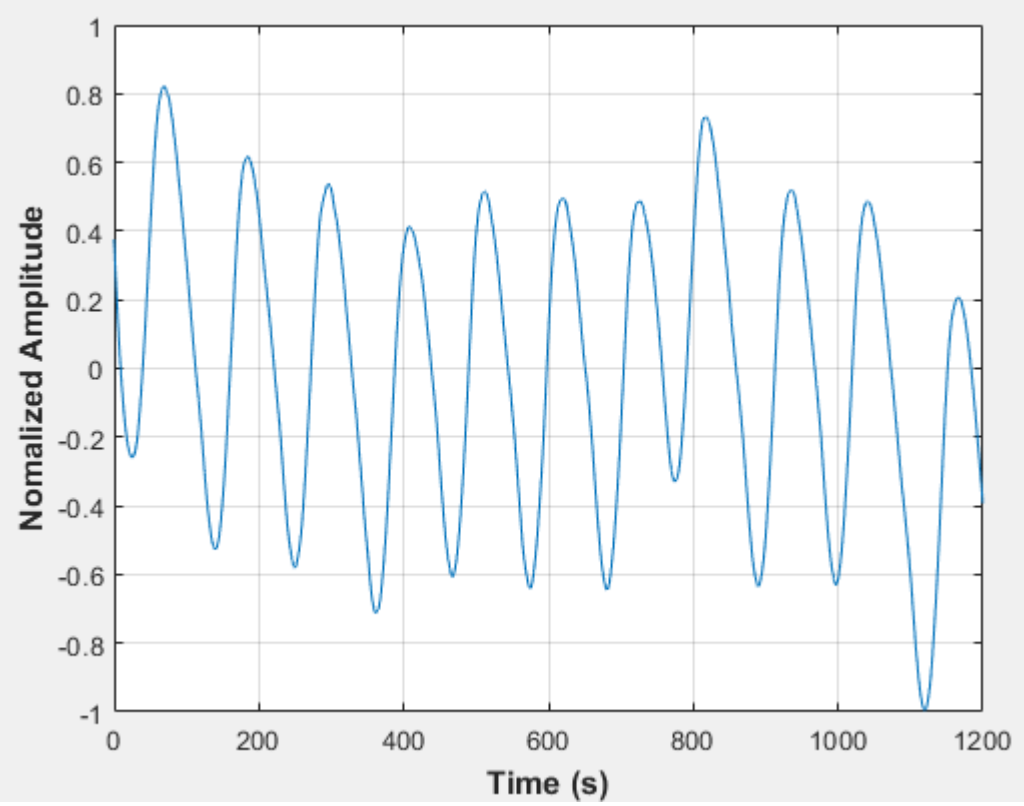


*Figure D-165: Pressure fluctuations in a non-uniformly packed vessel (large and small at the side) at 1.67 dm$^3$/minute rotameter flow rate- Test 6*

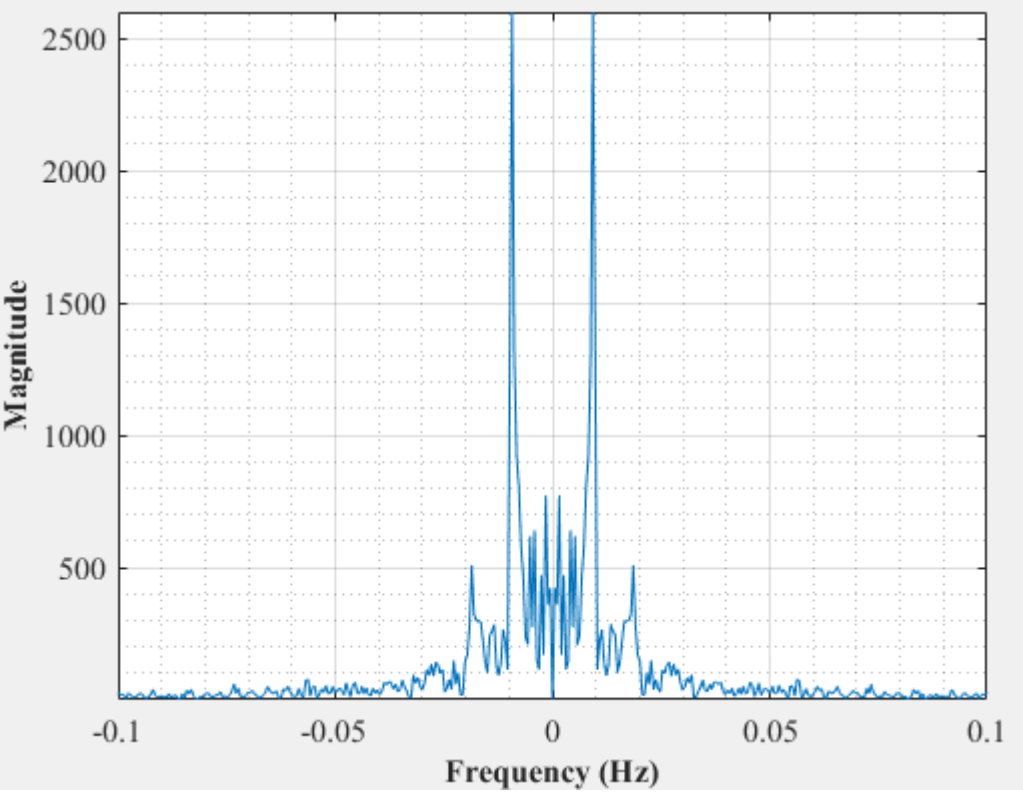


*Figure D-166: Dominant Frequency for a non-uniformly packed vessel (large and small at the side) at 1.67 dm$^3$/minute rotameter flow rate- Test 6*

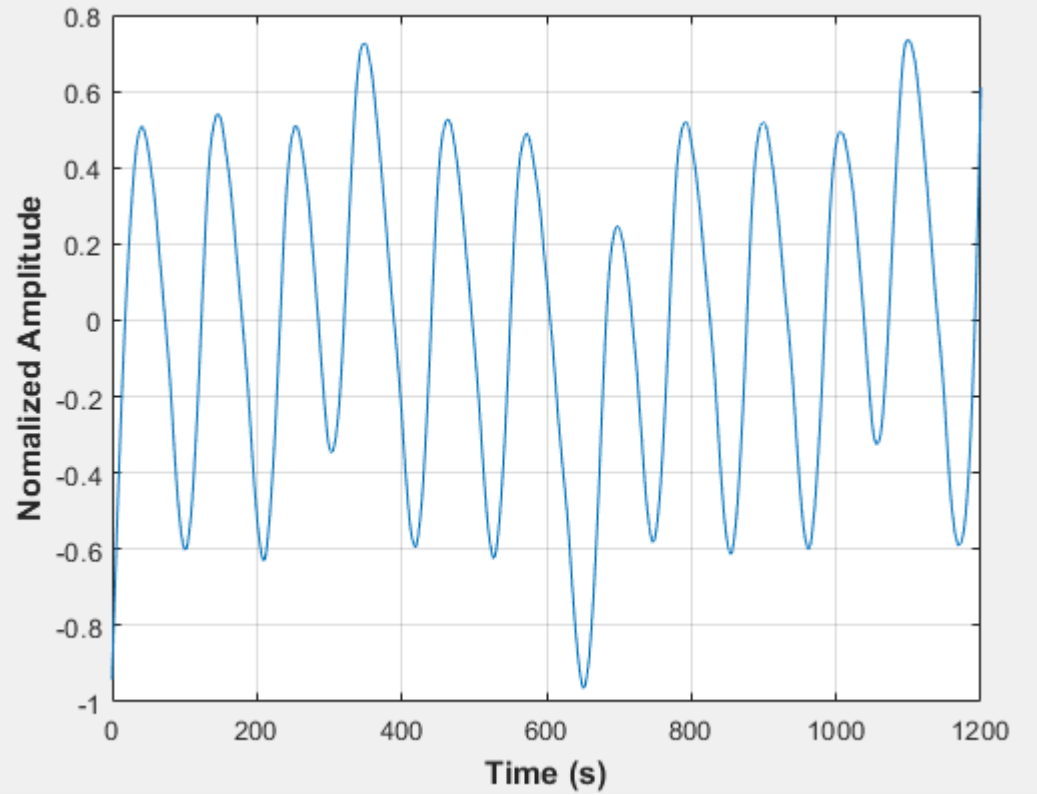


*Figure D-167: Pressure fluctuations in a non-uniformly packed vessel (large and small at the side) at 1.67 dm$^3$/minute rotameter flow rate- Test 7*

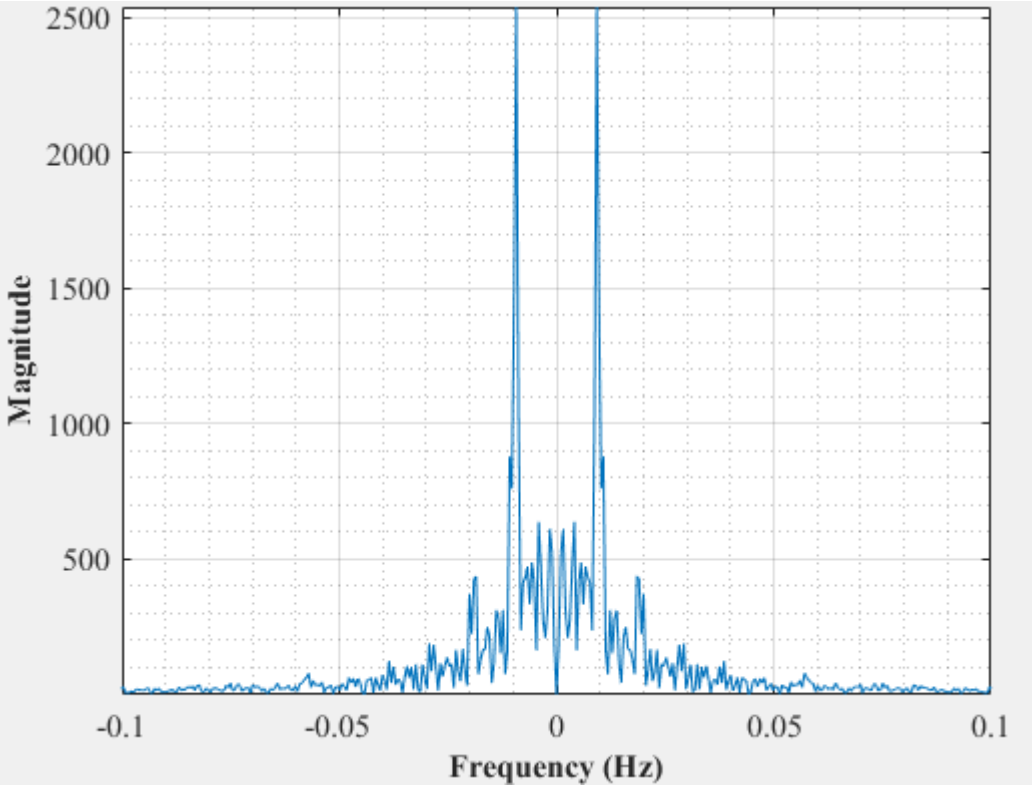


*Figure D-168: Dominant Frequency for a non-uniformly packed vessel (large and small at the side) at 1.67 dm$^3$/minute rotameter flow rate- Test 7*

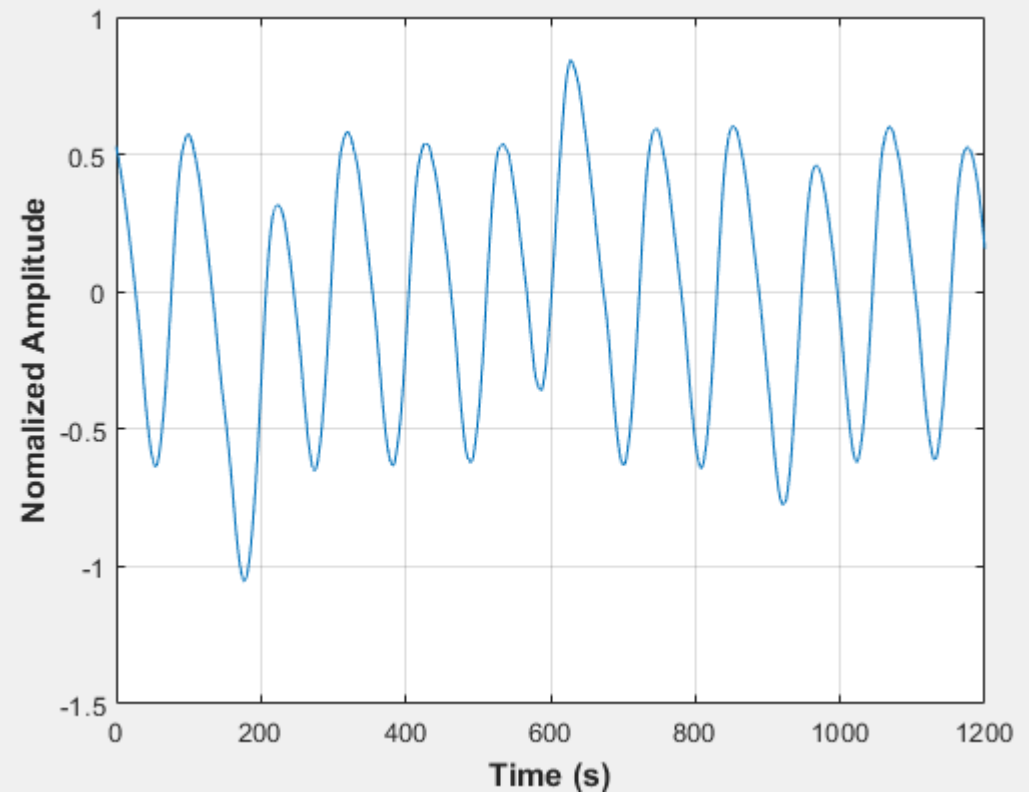


*Figure D-169: Pressure fluctuations in a non-uniformly packed vessel (large and small at the side) at 1.67 dm$^3$/minute rotameter flow rate- Test 8*

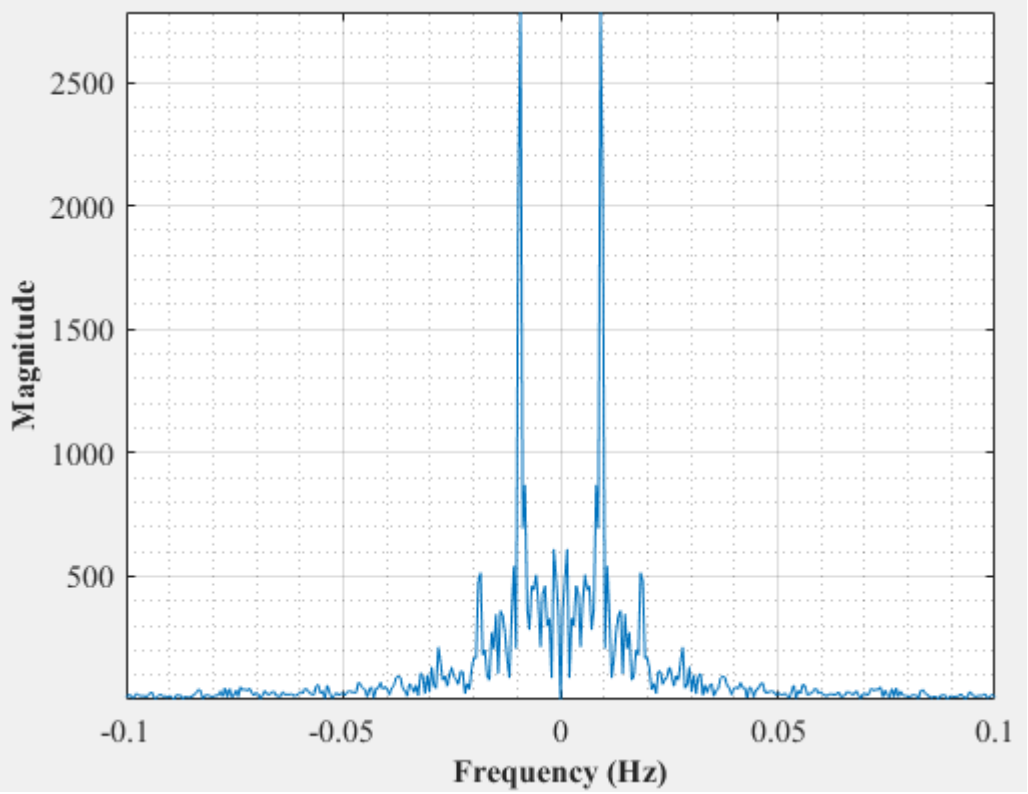


*Figure D-170: Dominant Frequency for a non-uniformly packed vessel (large and small at the side) at 1.67 dm$^3$/minute rotameter flow rate- Test 8*

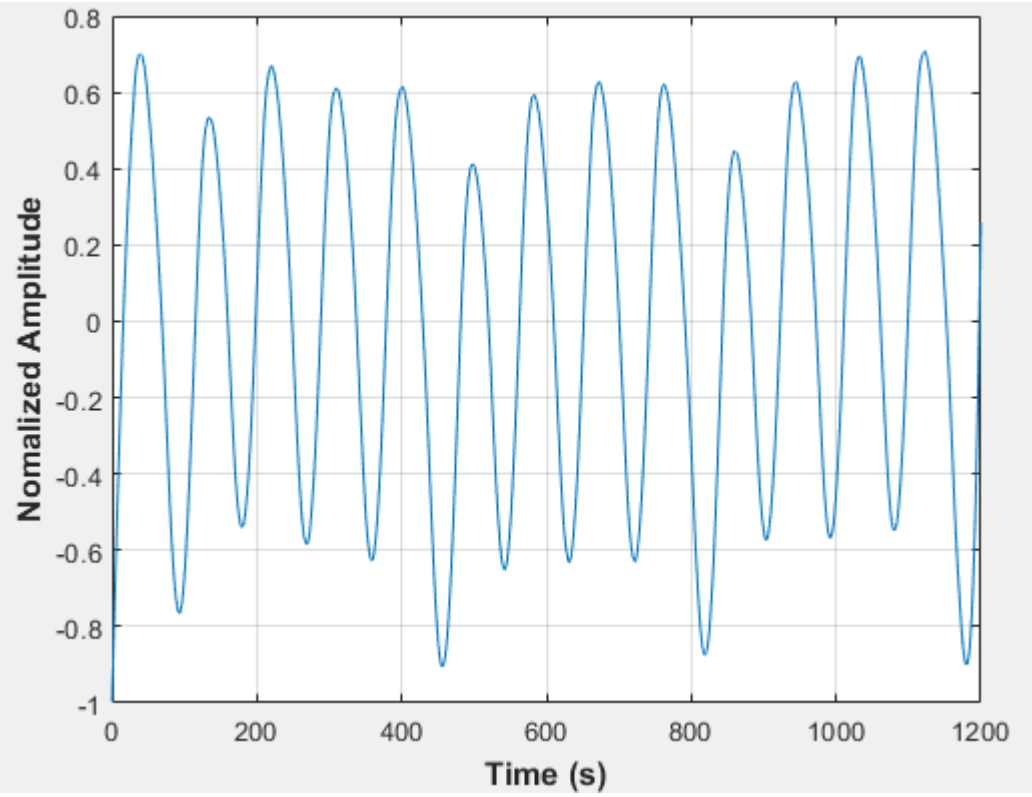


*Figure D-171: Pressure fluctuations in a non-uniformly packed vessel (large and small at the side) at 2 dm$^3$/minute rotameter flow rate- Test 1*

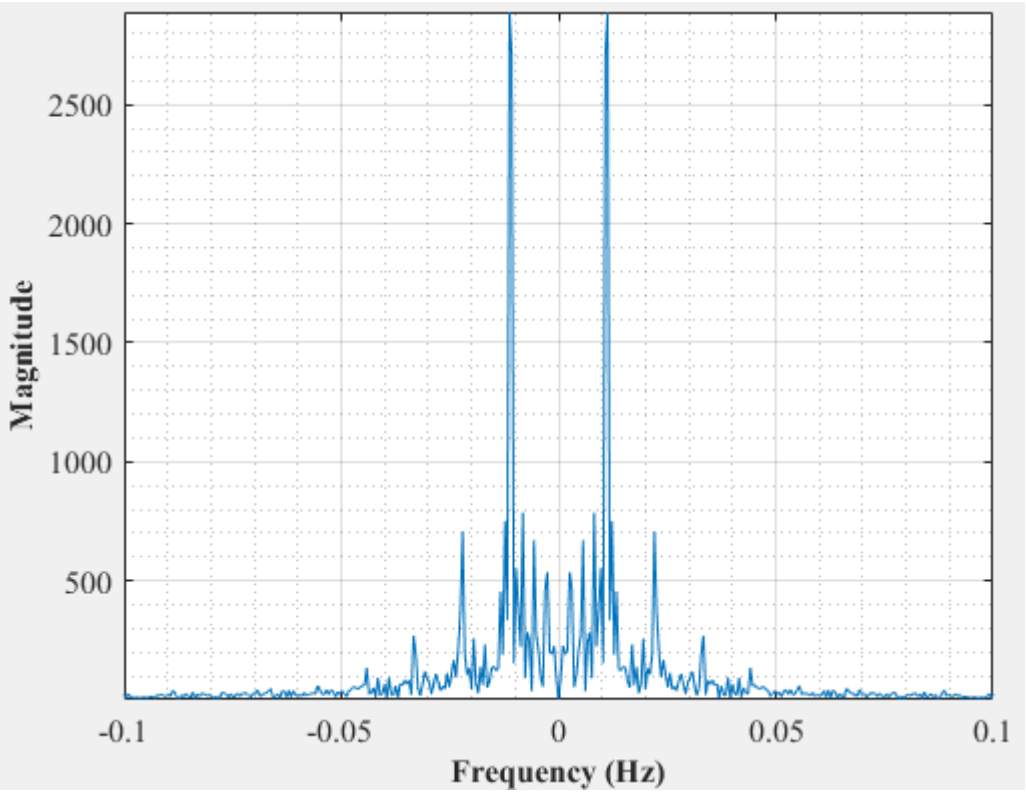


*Figure D-172: Dominant Frequency for a non-uniformly packed vessel (large and small at the side) at 2 dm$^3$/minute rotameter flow rate- Test 1*

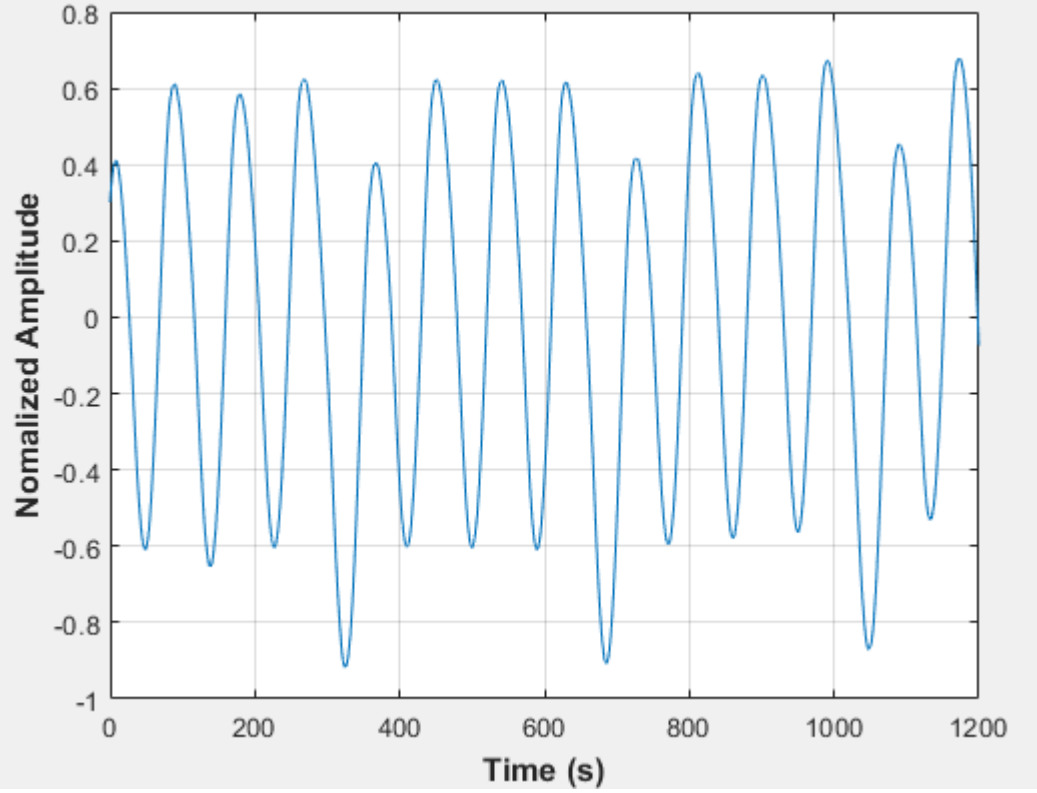


*Figure D-173: Pressure fluctuations in a non-uniformly packed vessel (large and small at the side) at 2 dm$^3$/minute rotameter flow rate- Test 2*

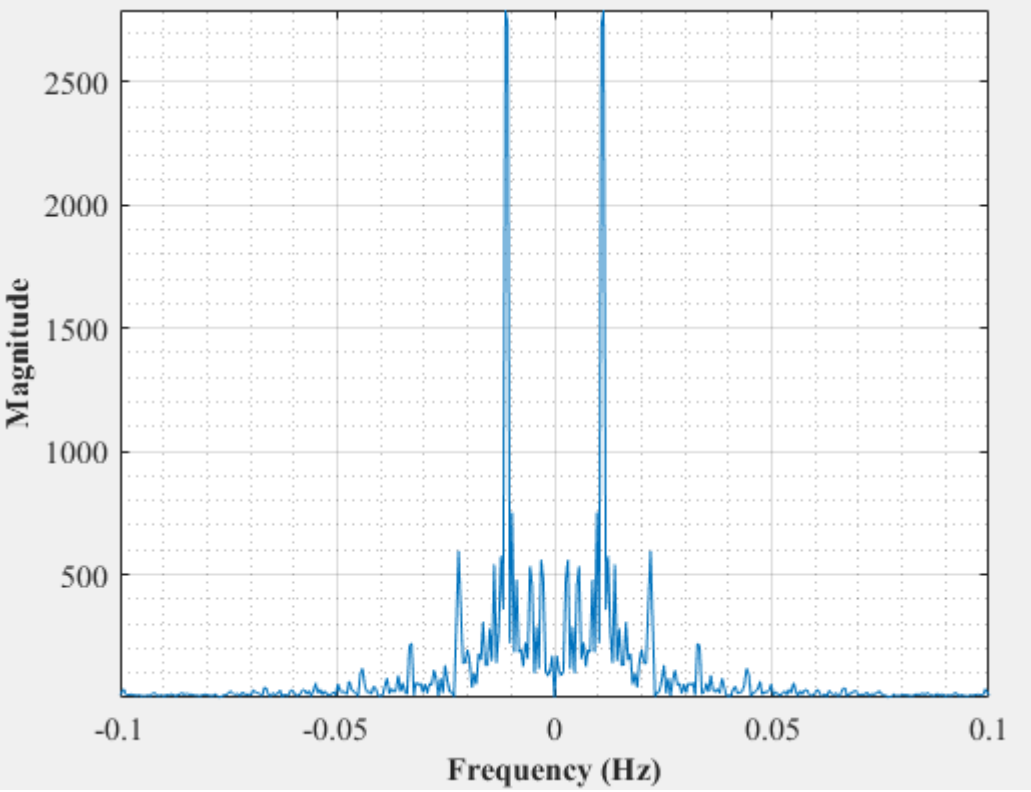


*Figure D-174: Dominant Frequency for a non-uniformly packed vessel (large and small at the side) at 2 dm$^3$/minute rotameter flow rate- Test 2*

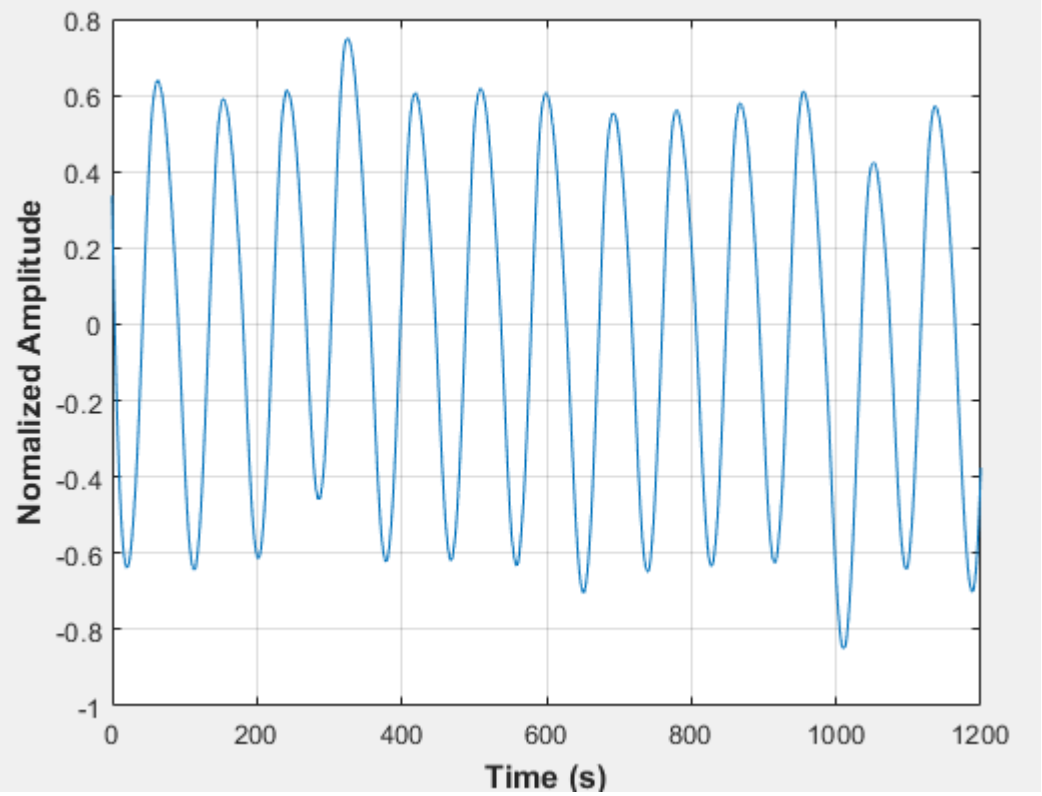


*Figure D-175: Pressure fluctuations in a non-uniformly packed vessel (large and small at the side) at 2 dm$^3$/minute rotameter flow rate- Test 3*

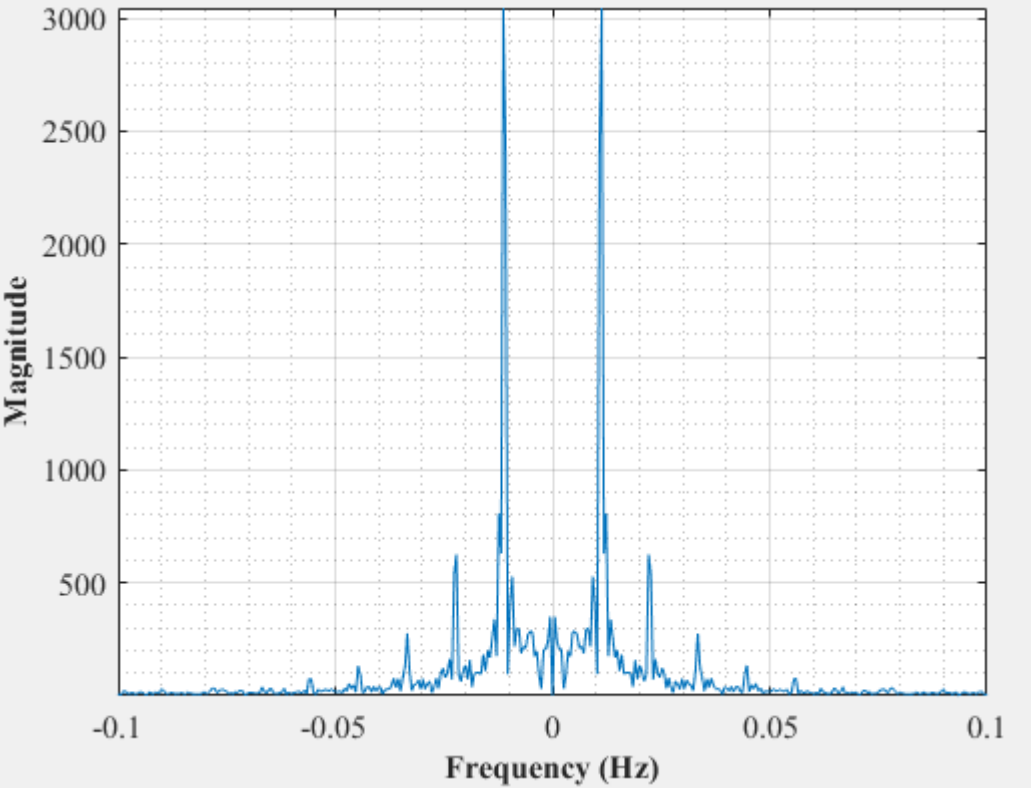


*Figure D-176: Dominant Frequency for a non-uniformly packed vessel (large and small at the side) at 2 dm$^3$/minute rotameter flow rate- Test 3*

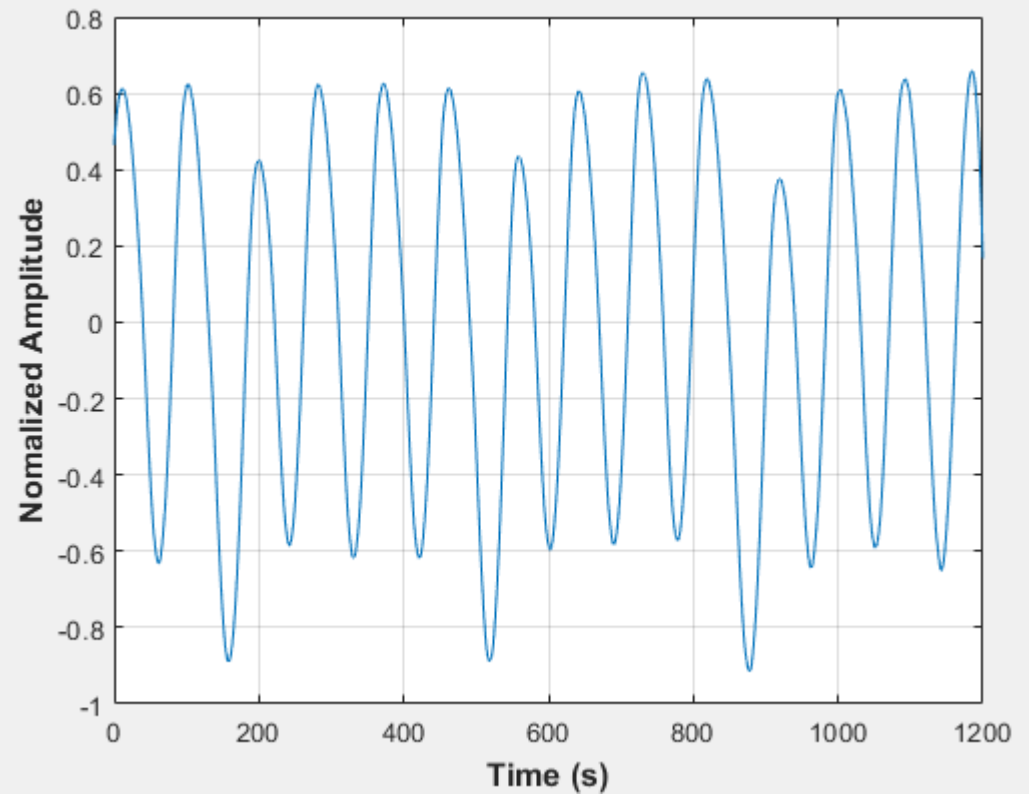


*Figure D-177: Pressure fluctuations in a non-uniformly packed vessel (large and small at the side) at 2 dm$^3$/minute rotameter flow rate- Test 4*

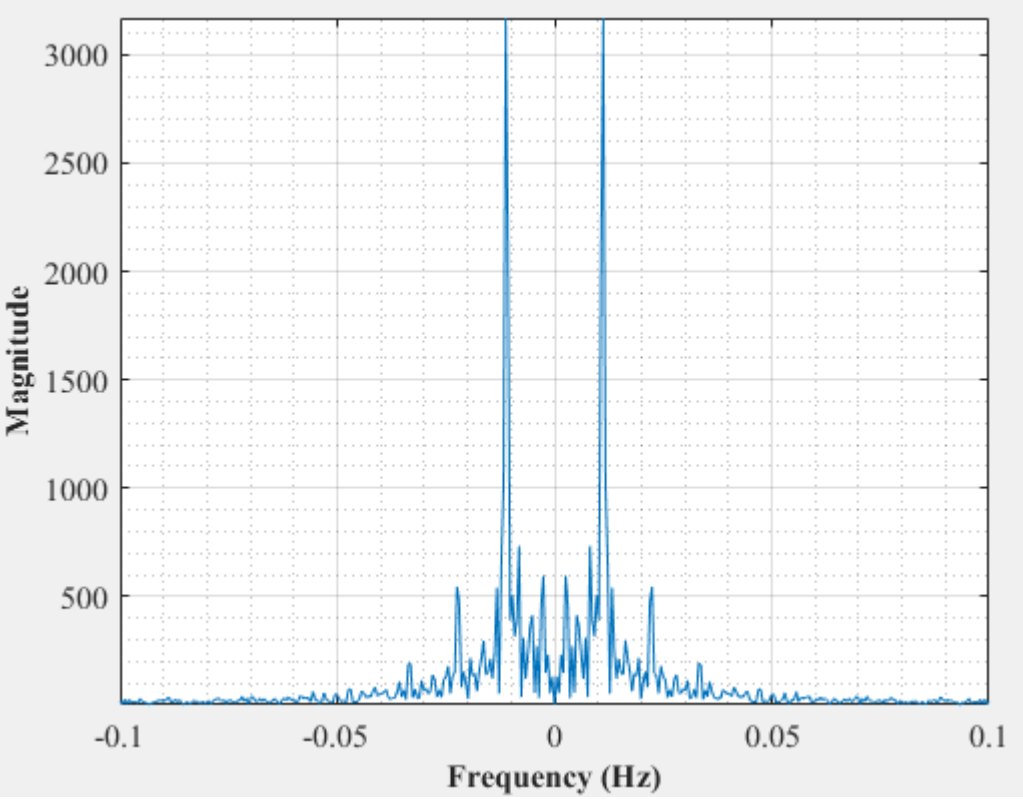


*Figure D-178: Dominant Frequency for a non-uniformly packed vessel (large and small at the side) at 2 dm$^3$/minute rotameter flow rate- Test 4*

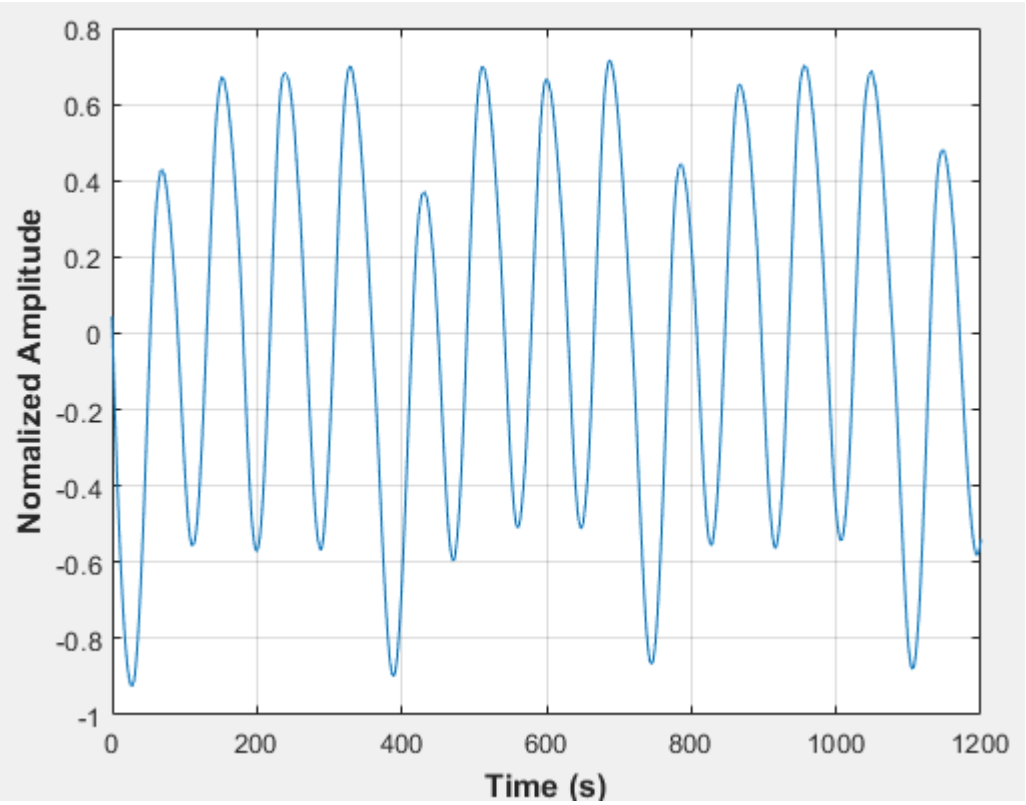


*Figure D-179: Pressure fluctuations in a non-uniformly packed vessel (large and small at the side) at 2 dm³/minute rotameter flow rate- Test 5*

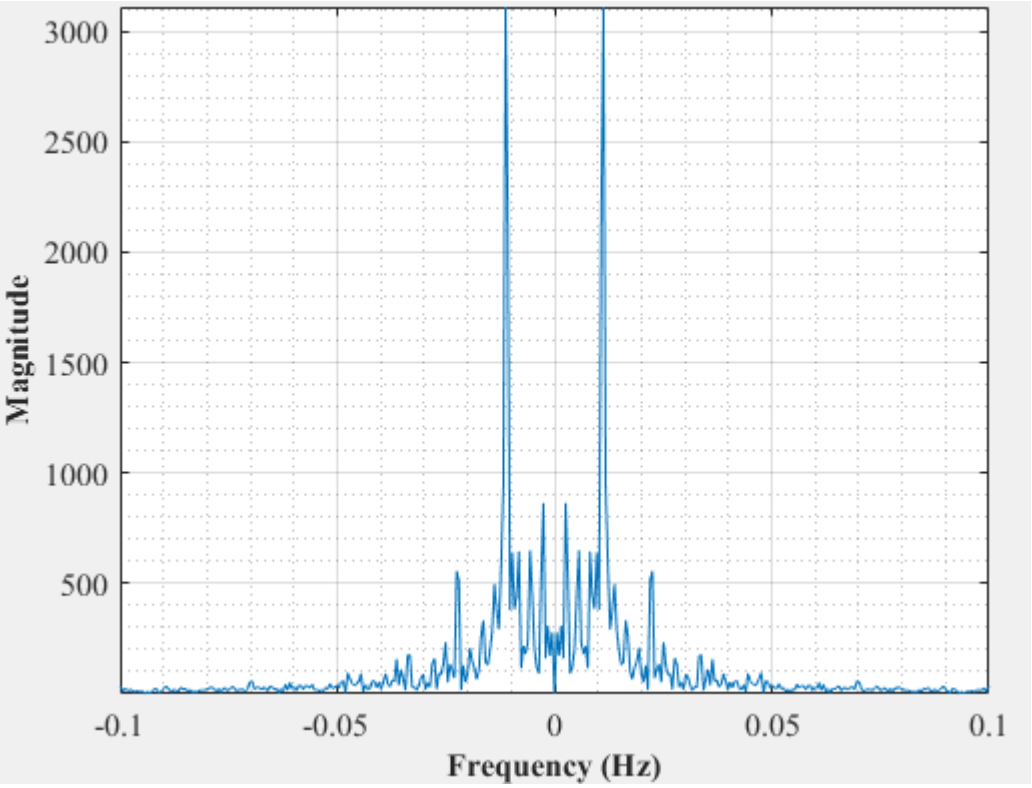


*Figure D-180: Dominant Frequency for a non-uniformly packed vessel (large and small at the side) at 2 dm³/minute rotameter flow rate- Test 5*

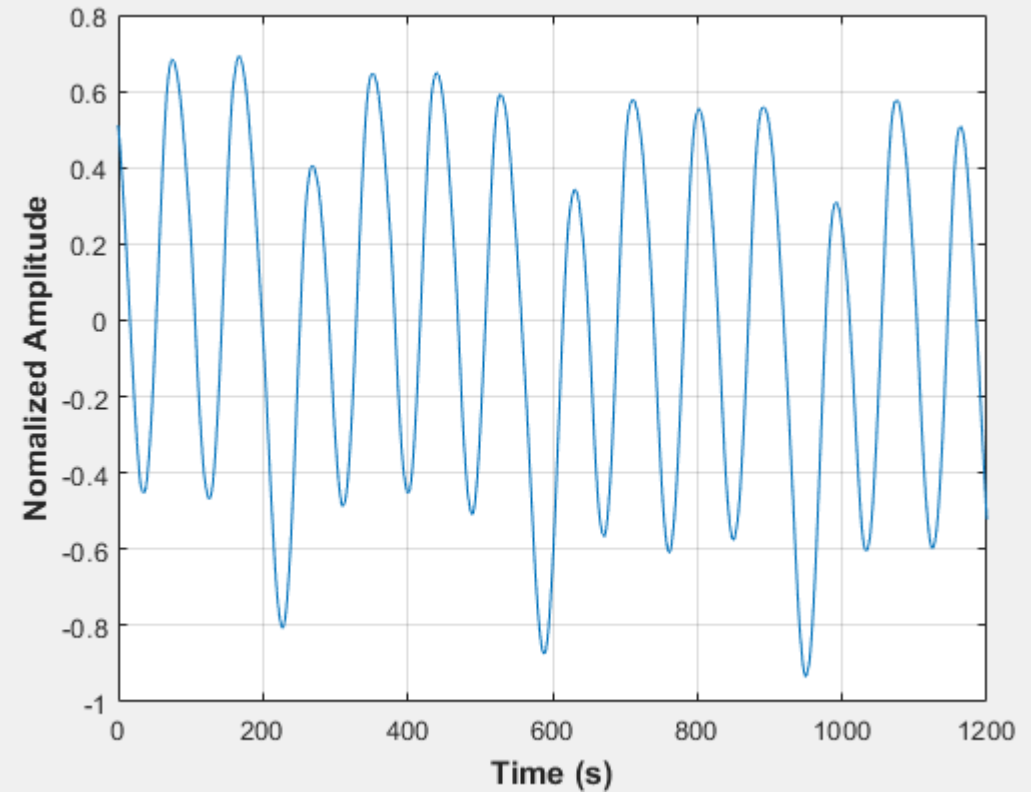


*Figure D-181: Pressure fluctuations in a non-uniformly packed vessel (large and small at the side) at 2 dm$^3$/minute rotameter flow rate- Test 6*

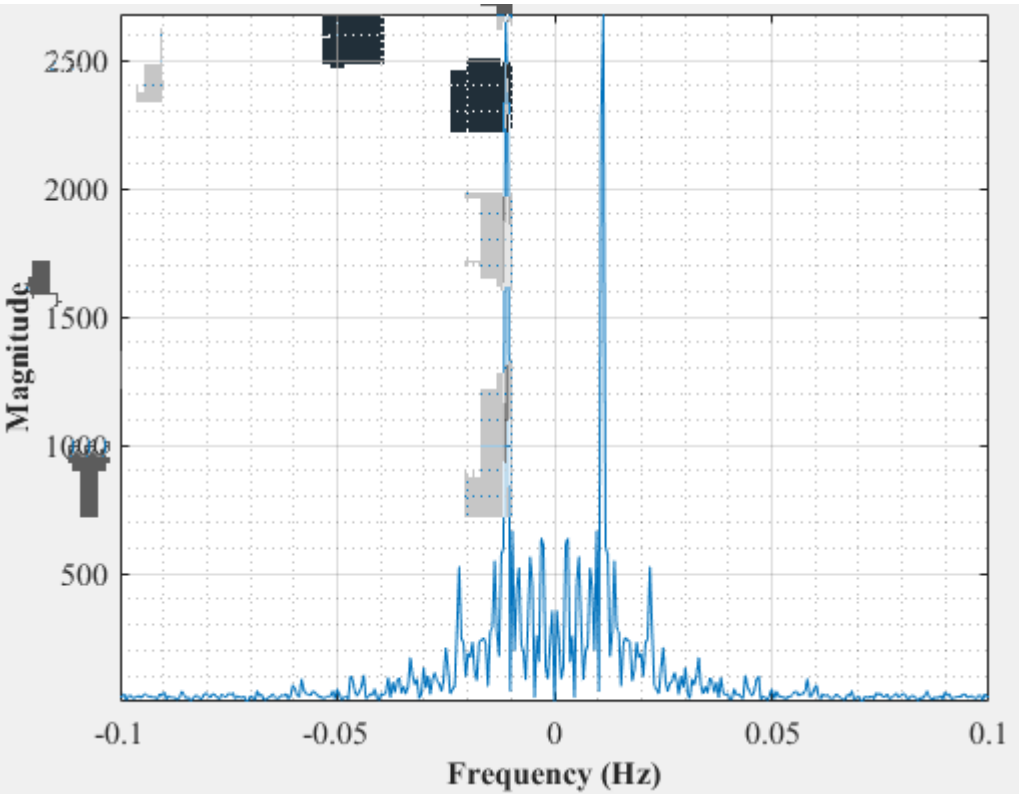


*Figure D-182: Dominant Frequency for a non-uniformly packed vessel (large and small at the side) at 2 dm$^3$/minute rotameter flow rate- Test 6*

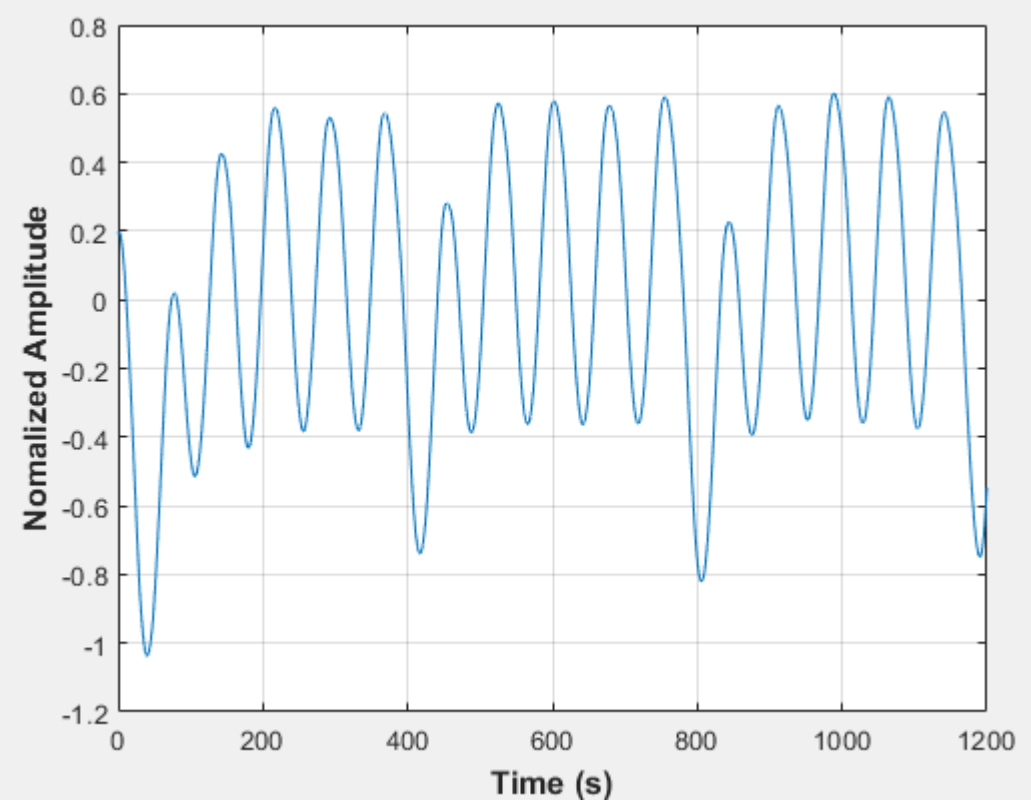


*Figure D-183: Pressure fluctuations in a non-uniformly packed vessel (large and small at the side) at 2.33 dm$^3$/minute rotameter flow rate- Test 1*

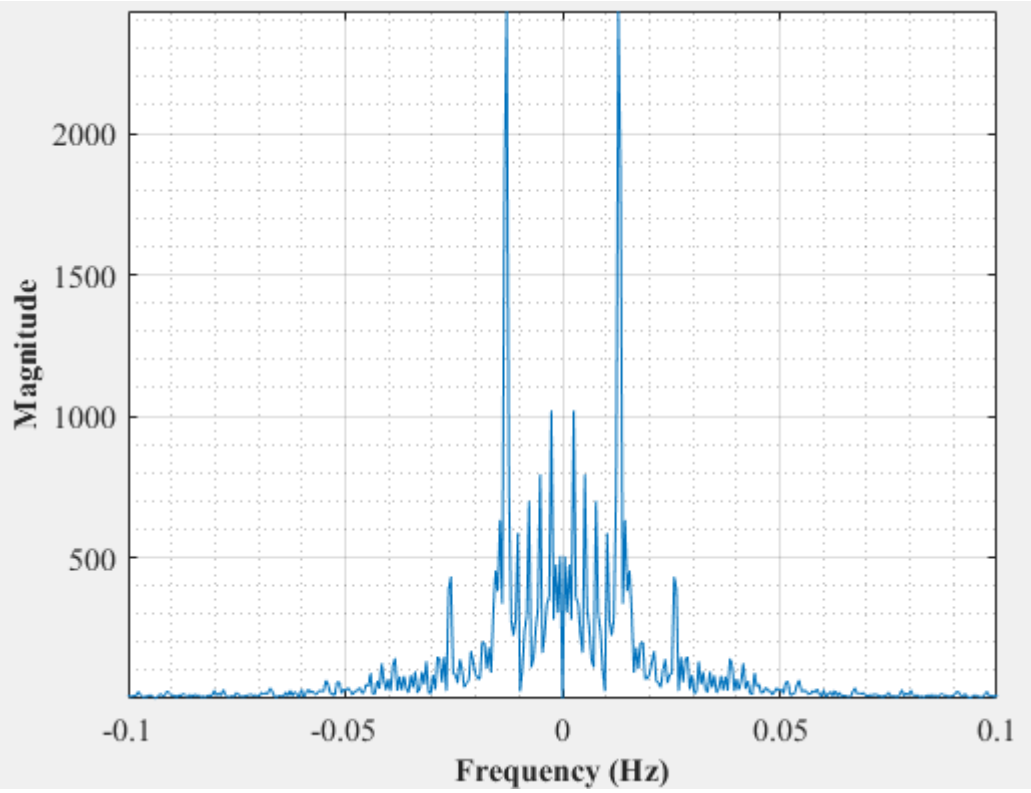


*Figure D-184: Dominant Frequency for a non-uniformly packed vessel (large and small at the side) at 2.33 dm$^3$/minute rotameter flow rate- Test 1*

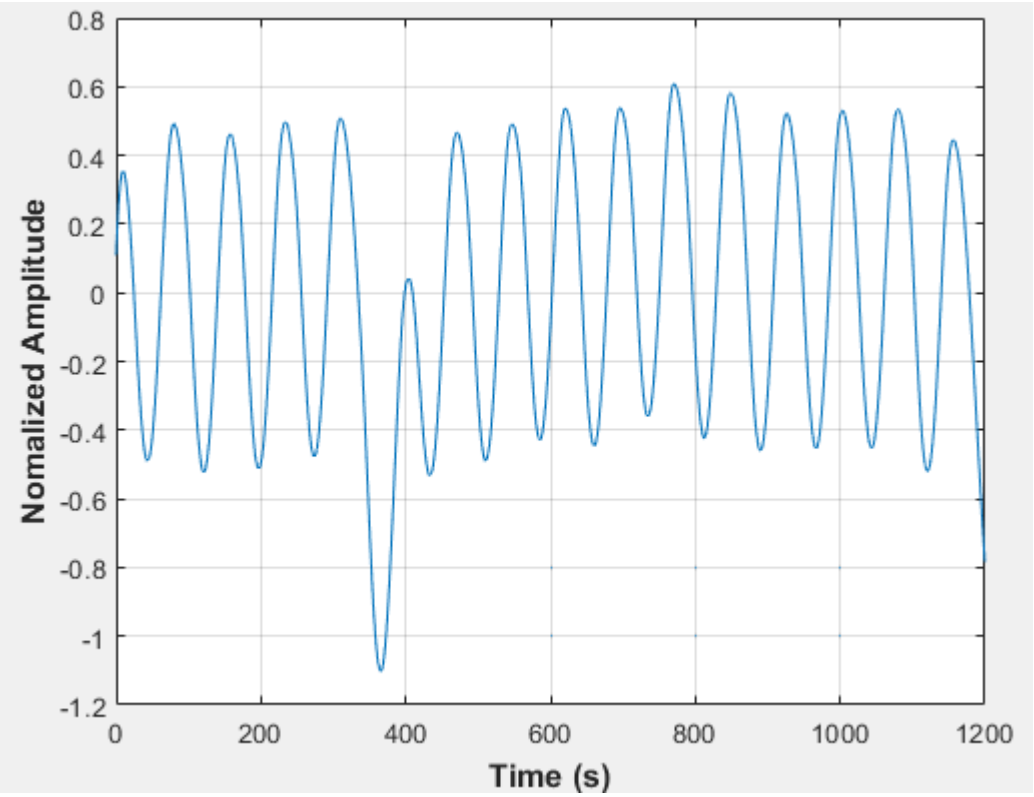


*Figure D-185: Pressure fluctuations in a non-uniformly packed vessel (large and small at the side) at 2.33 dm$^3$/minute rotameter flow rate- Test 2*

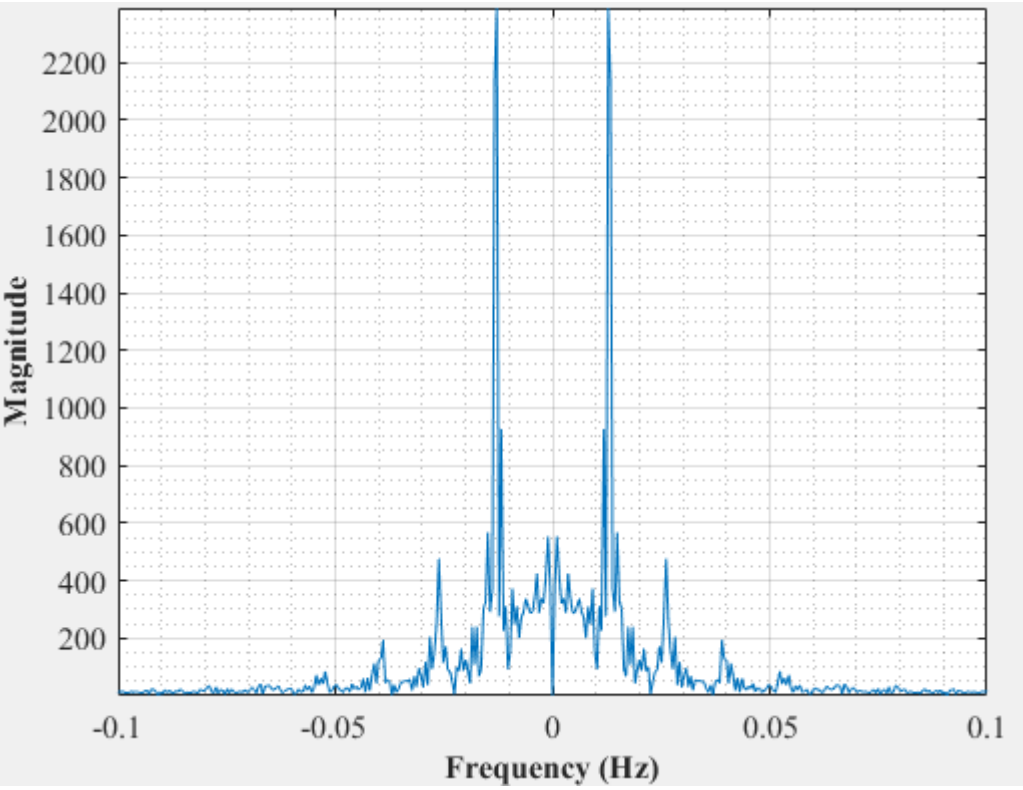


*Figure D-186: Dominant Frequency for a non-uniformly packed vessel (large and small at the side) at 2.33 dm$^3$/minute rotameter flow rate- Test 2*

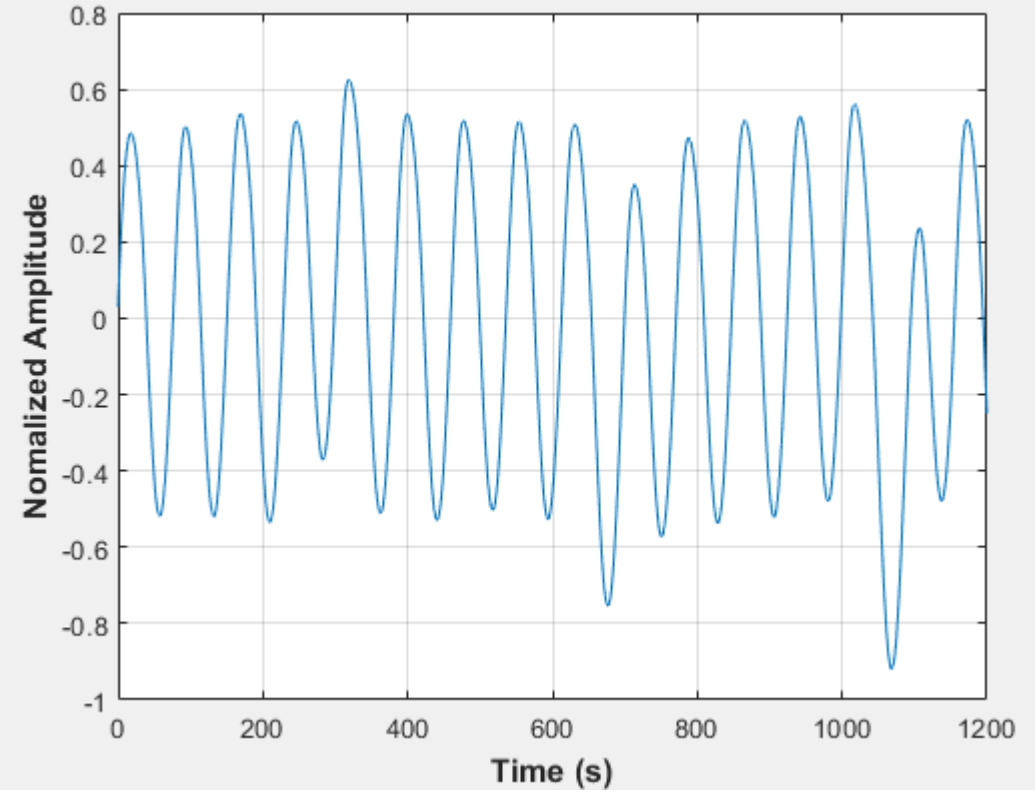


*Figure D-187: Pressure fluctuations in a non-uniformly packed vessel (large and small at the side) at 2.33 dm$^3$/minute rotameter flow rate- Test 3*

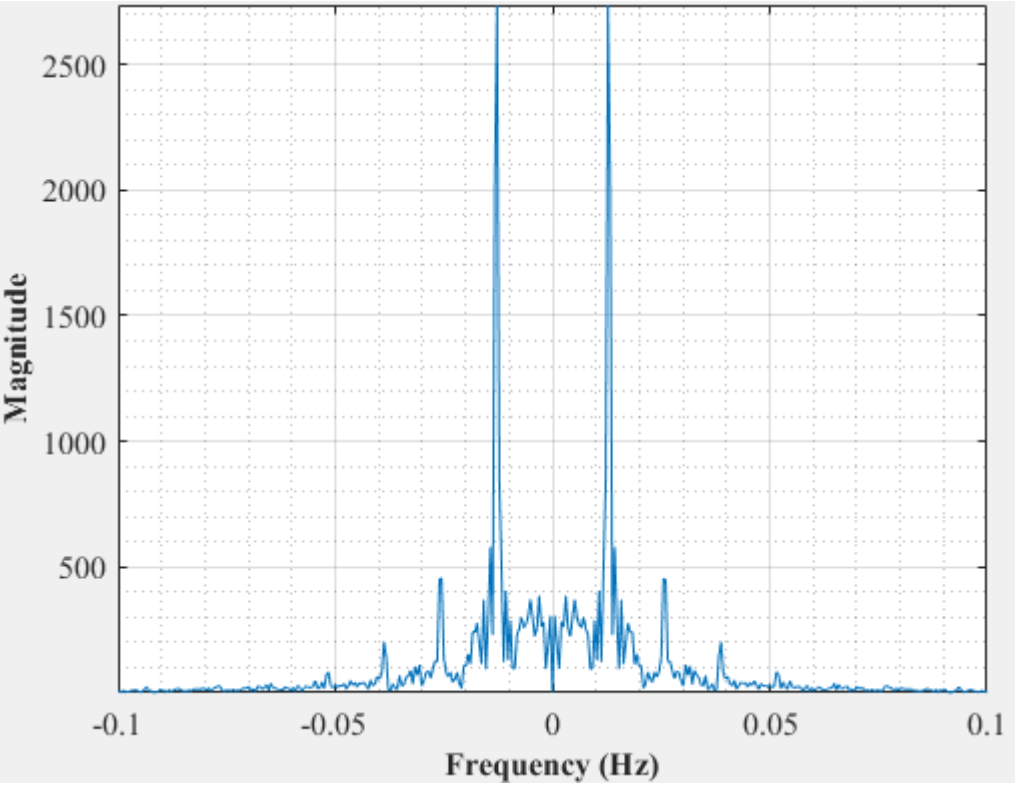


*Figure D-188: Dominant Frequency for a non-uniformly packed vessel (large and small at the side) at 2.33 dm$^3$/minute rotameter flow rate- Test 3*

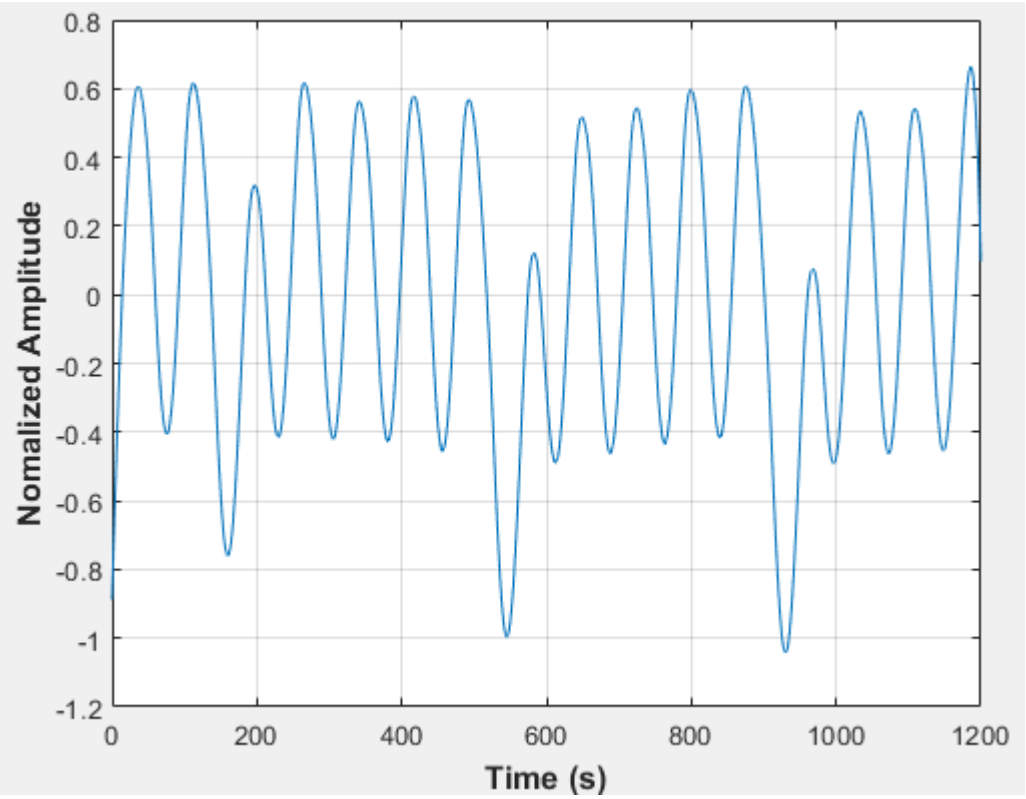


*Figure D-189: Pressure fluctuations in a non-uniformly packed vessel (large and small at the side) at 2.33 dm$^3$/minute rotameter flow rate- Test 4*

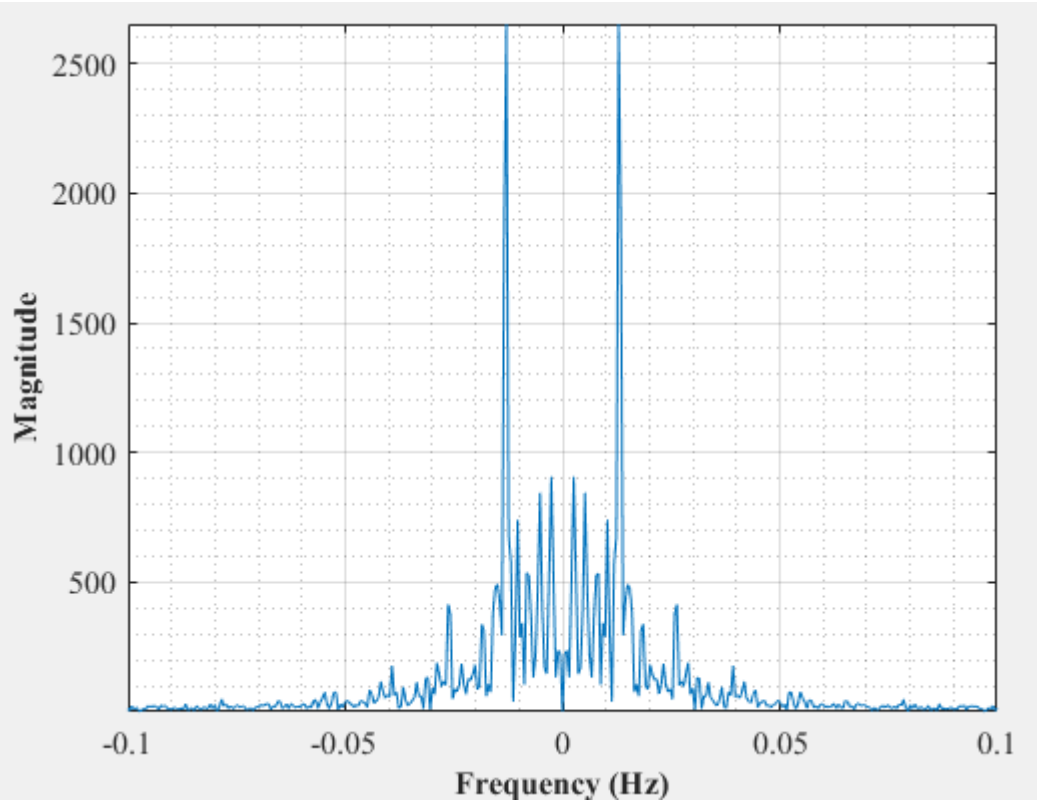


*Figure D-190: Dominant Frequency for a non-uniformly packed vessel (large and small at the side) at 2.33 dm$^3$/minute rotameter flow rate- Test 4*

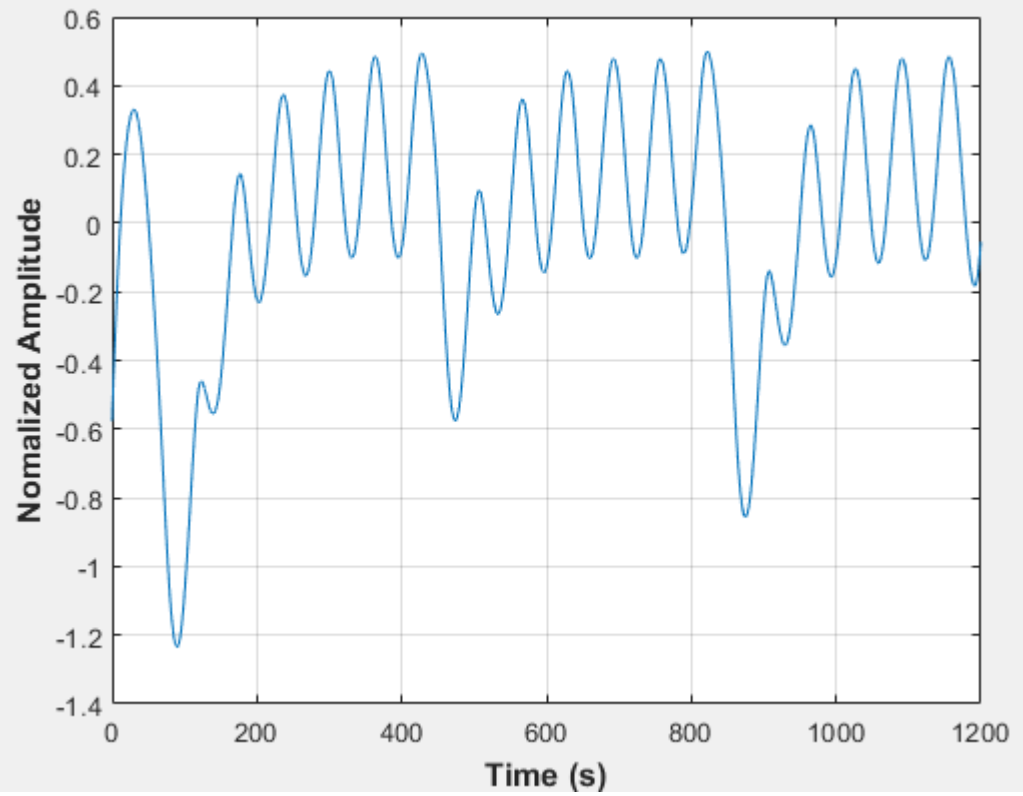


*Figure D-191: Pressure fluctuations in a non-uniformly packed vessel (large and small at the side) at 2.67 dm$^3$/minute rotameter flow rate- Test 1*

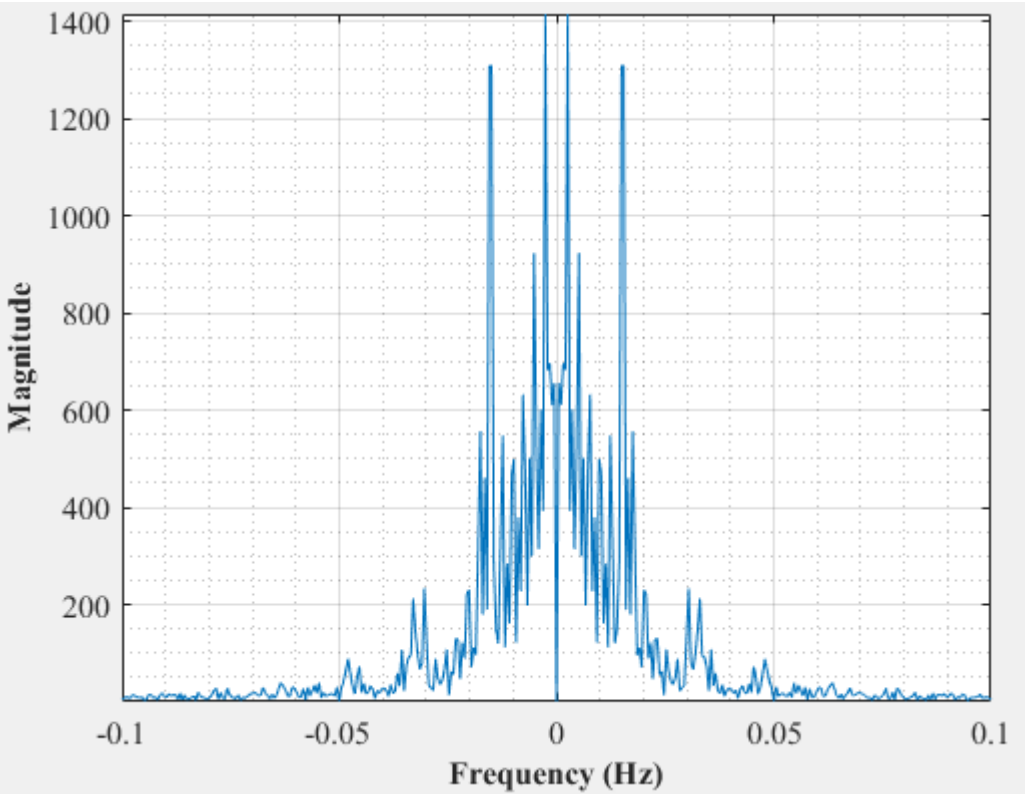


*Figure D-192: Dominant Frequency for a non-uniformly packed vessel (large and small at the side) at 2.67 dm$^3$/minute rotameter flow rate- Test 1*

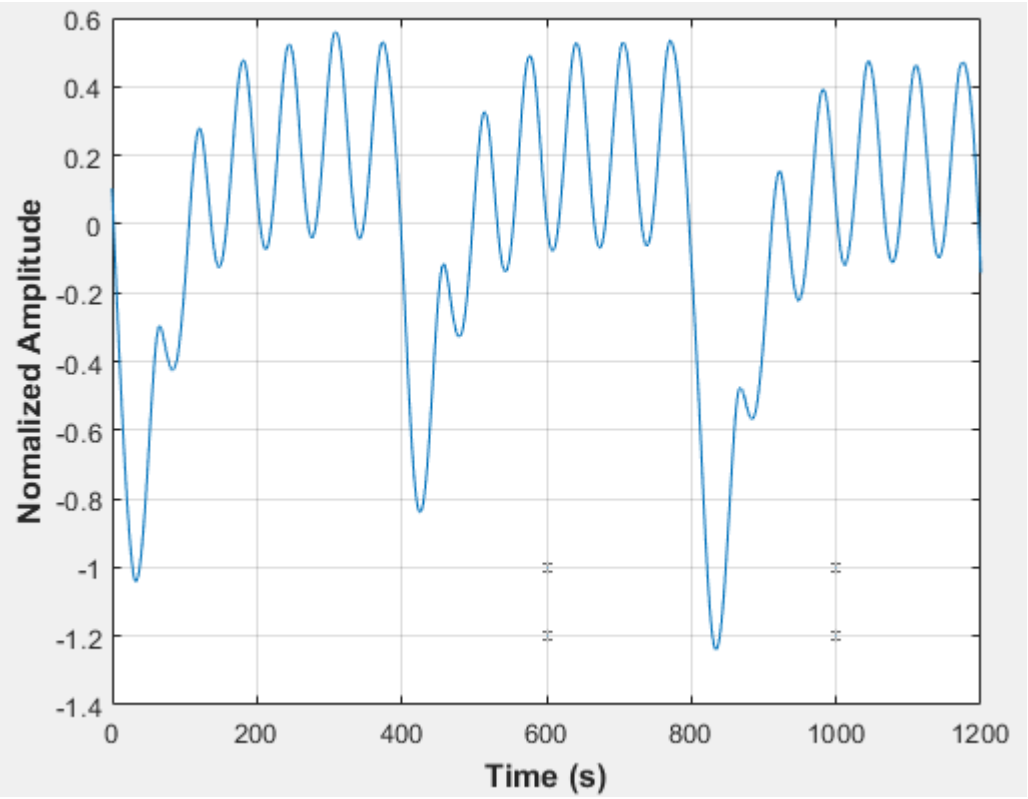


*Figure D-193: Pressure fluctuations in a non-uniformly packed vessel (large and small at the side) at 2.67 dm$^3$/minute rotameter flow rate- Test 2*

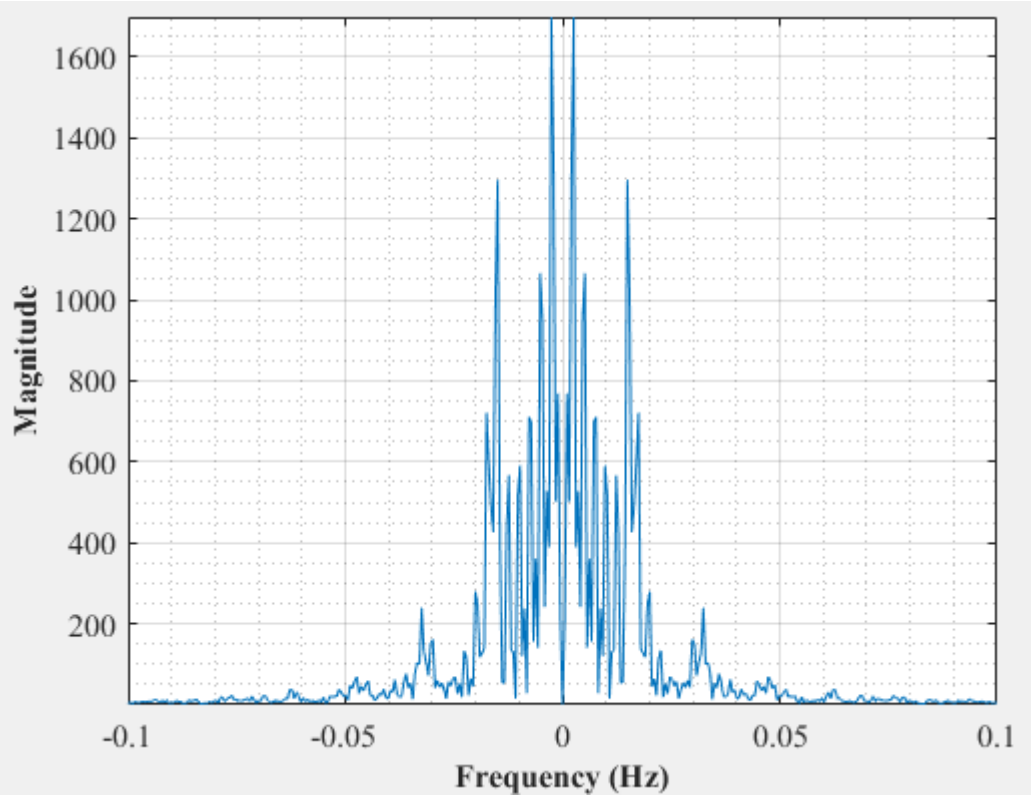


*Figure D-194: Dominant Frequency for a non-uniformly packed vessel (large and small at the side) at 2.67 dm$^3$/minute rotameter flow rate- Test 2*

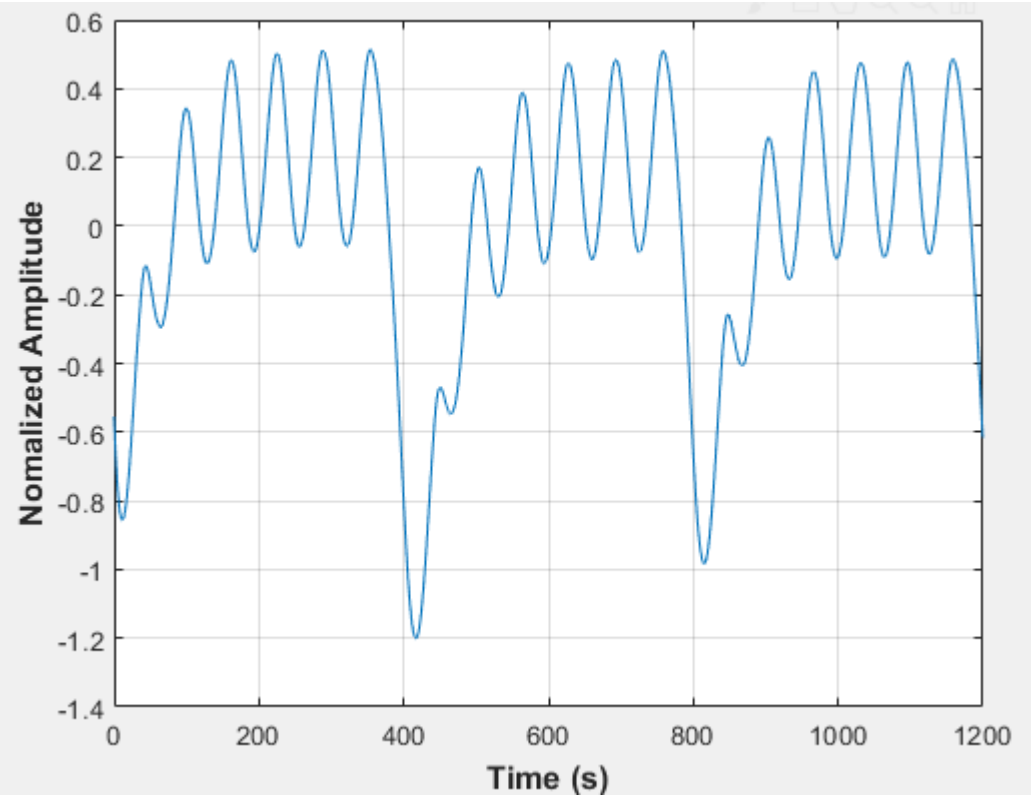


*Figure D-195: Pressure fluctuations in a non-uniformly packed vessel (large and small at the side) at 2.67 dm$^3$/minute rotameter flow rate- Test 3*

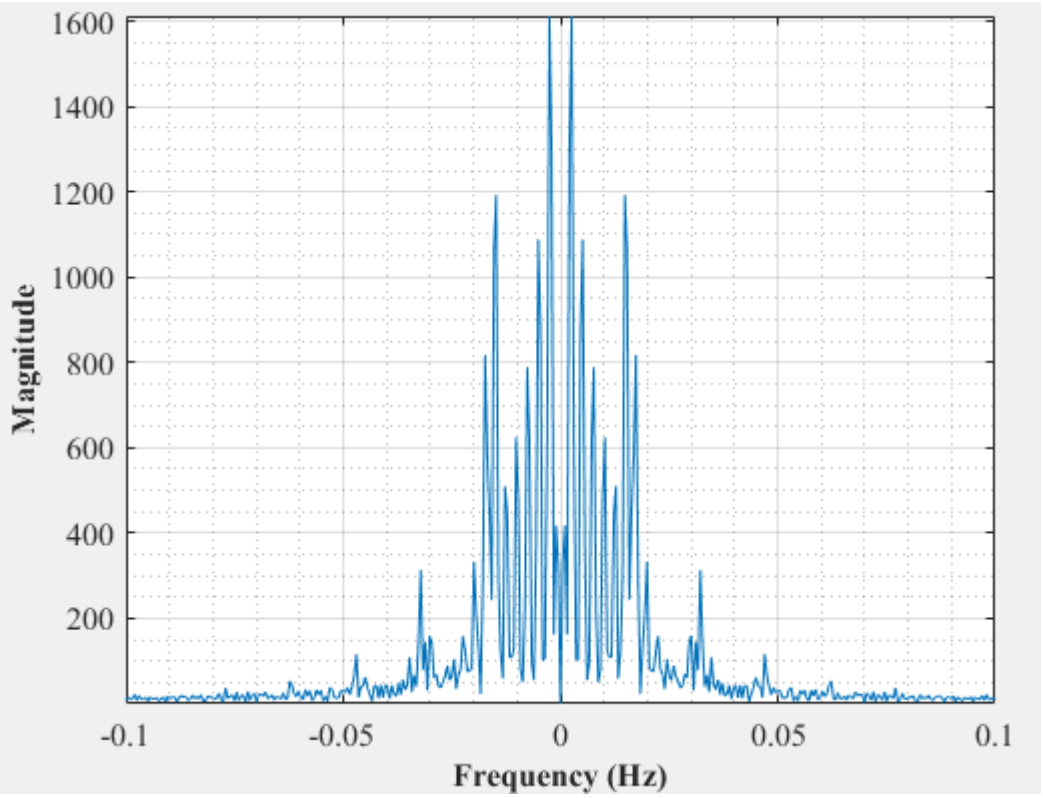


*Figure D-196: Dominant Frequency for a non-uniformly packed vessel (large and small at the side) at 2.67 dm$^3$/minute rotameter flow rate- Test 3*

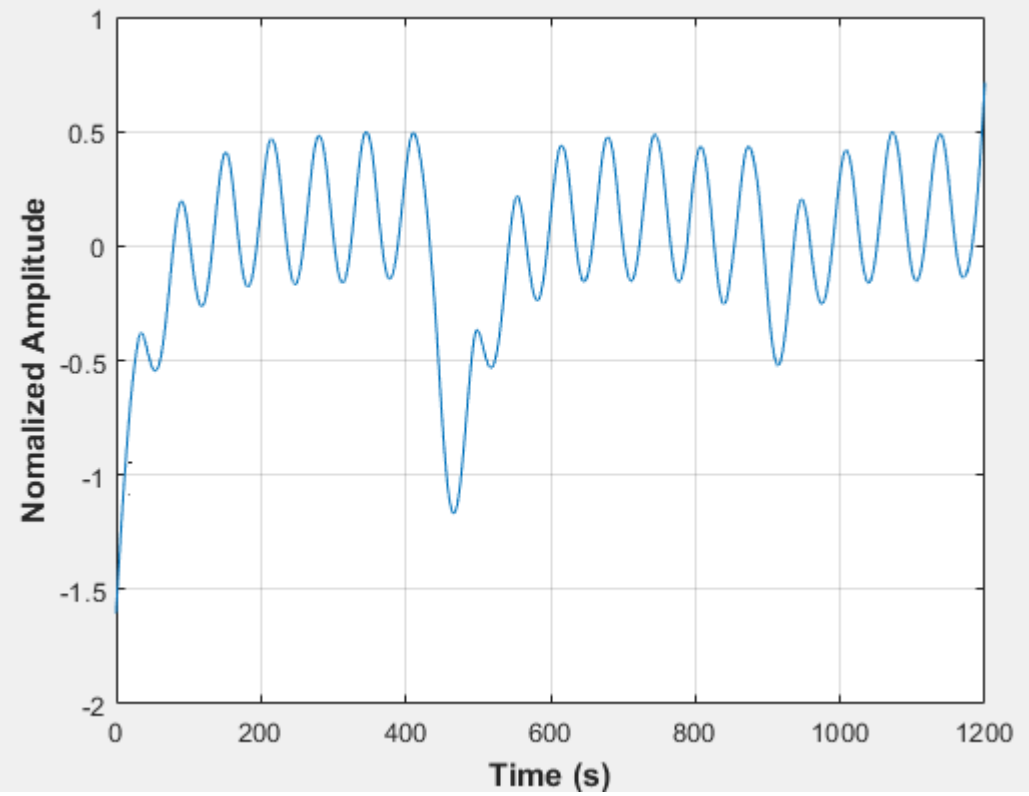


*Figure D-197: Pressure fluctuations in a non-uniformly packed vessel (large and small at the side) at 2.67 dm$^3$/minute rotameter flow rate- Test 4*

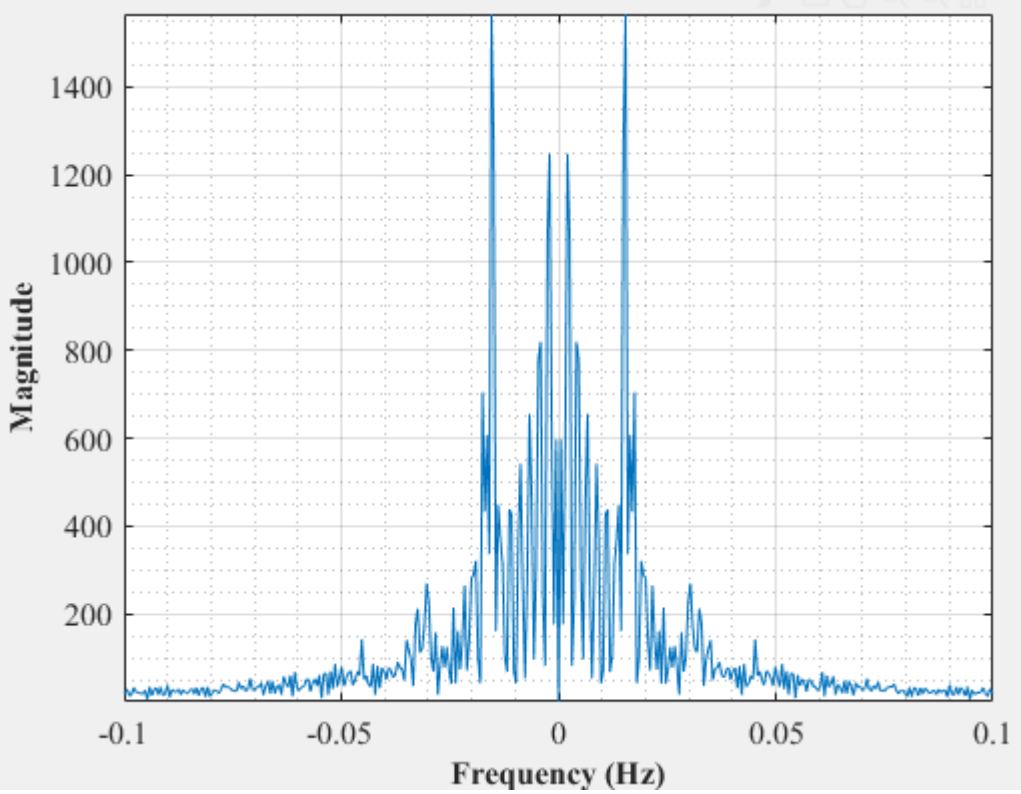


*Figure D-198: Dominant Frequency for a non-uniformly packed vessel (large and small at the side) at 2.67 dm$^3$/minute rotameter flow rate- Test 4*

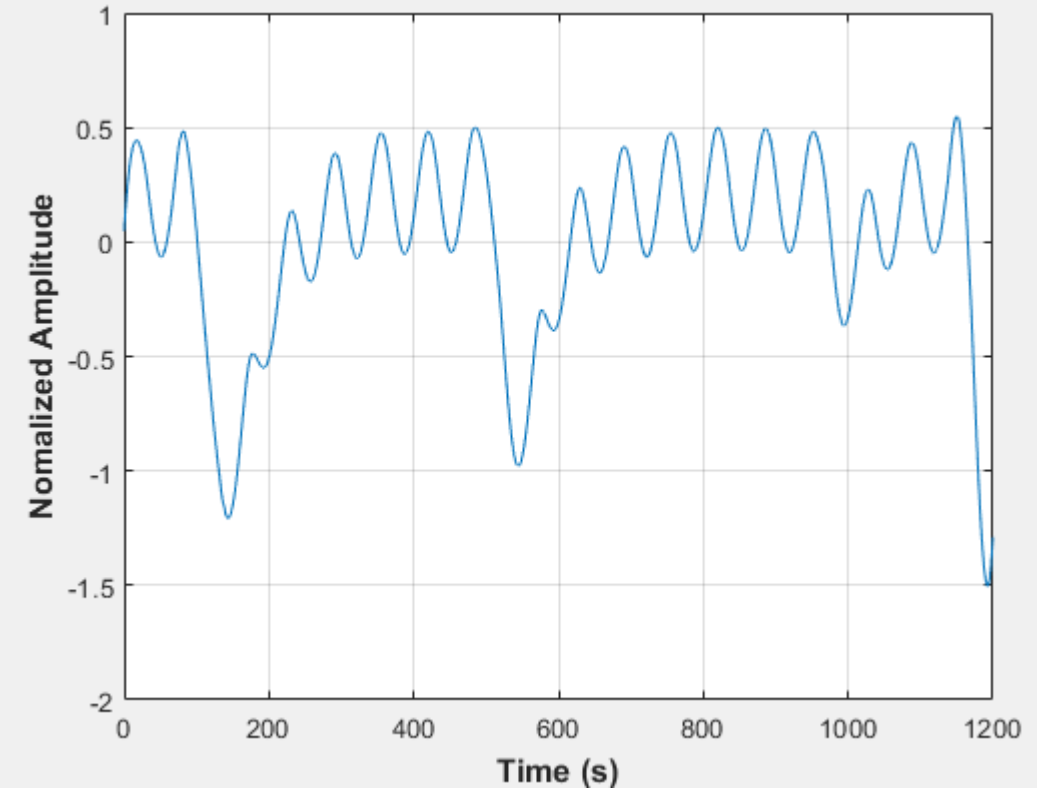


*Figure D-199: Pressure fluctuations in a non-uniformly packed vessel (large and small at the side) at 2.67 dm$^3$/minute rotameter flow rate- Test 5*

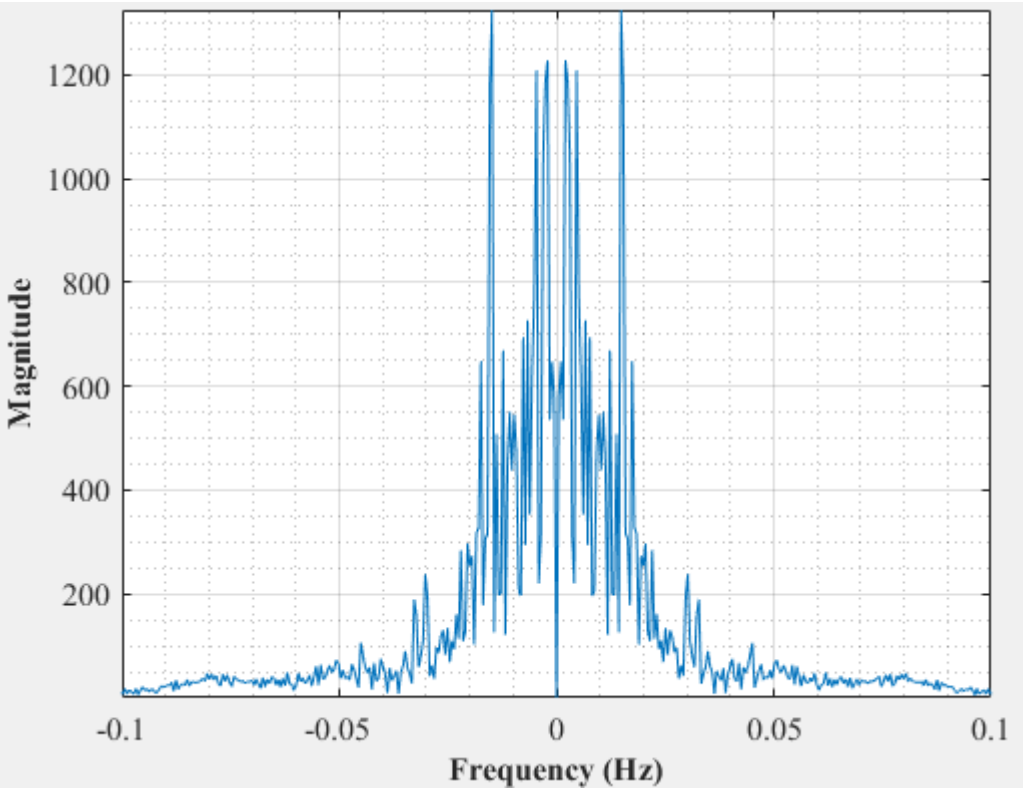


*Figure D-200: Dominant Frequency for a non-uniformly packed vessel (large and small at the side) at 2.67 dm$^3$/minute rotameter flow rate- Test 5*

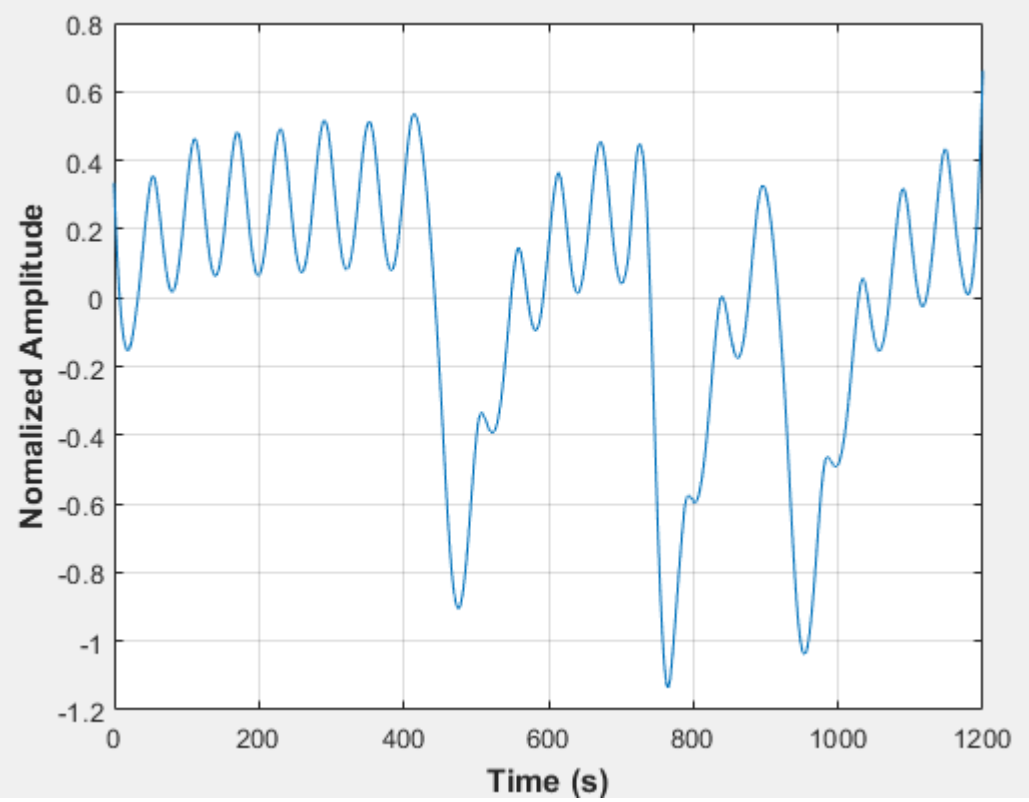


*Figure D-201: Pressure fluctuations in a non-uniformly packed vessel (large and small at the side) at 2.83 dm$^3$/minute rotameter flow rate- Test 1*

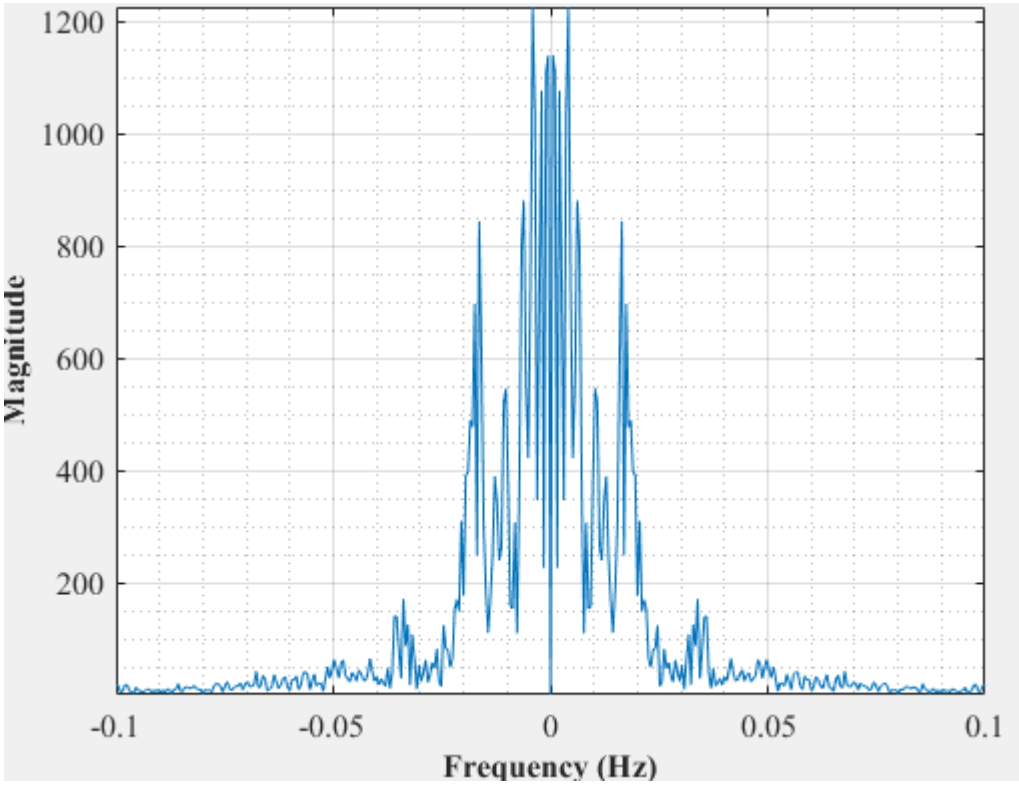


*Figure D-202: Dominant Frequency for a non-uniformly packed vessel (large and small at the side) at 2.83 dm$^3$/minute rotameter flow rate- Test 1*

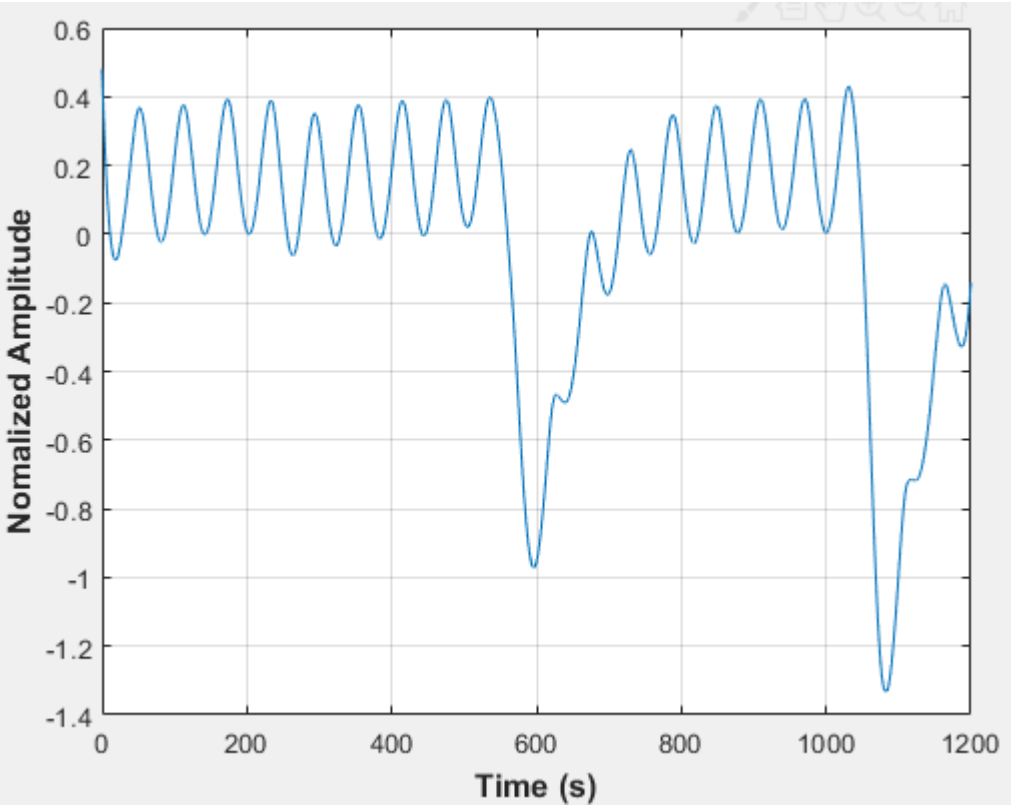


*Figure D-203: Pressure fluctuations in a non-uniformly packed vessel (large and small at the side) at 2.83 dm$^3$/minute rotameter flow rate- Test 2*

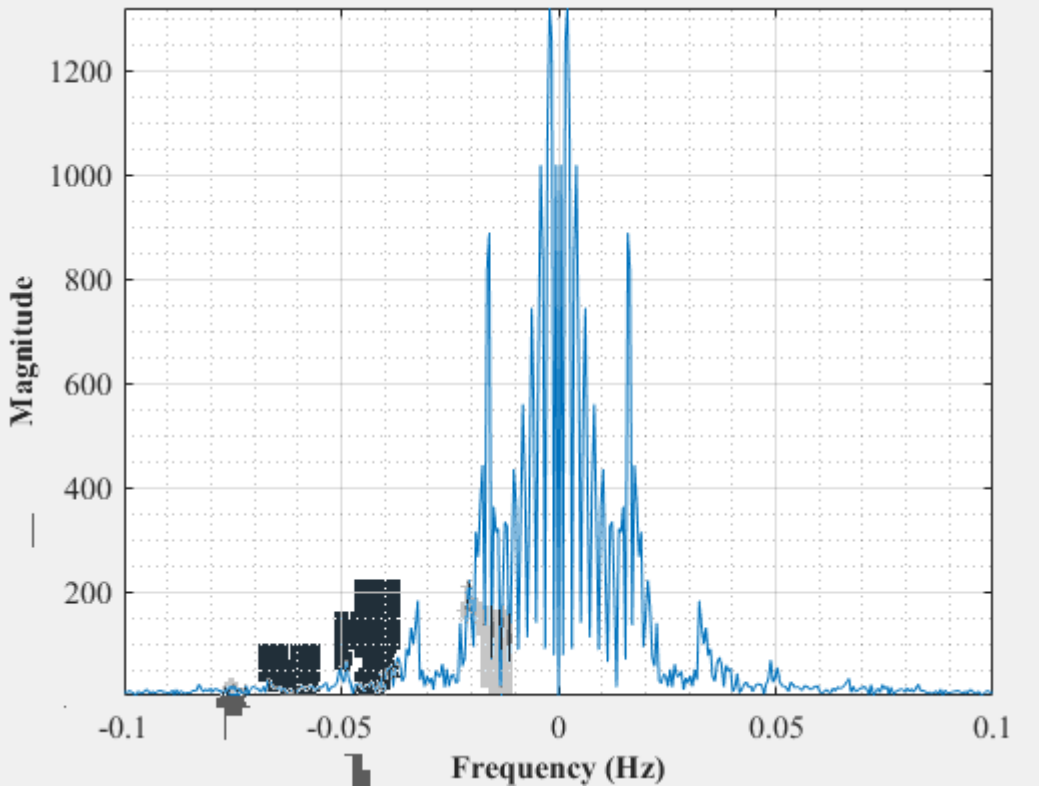


*Figure D-204: Dominant Frequency for a non-uniformly packed vessel (large and small at the side) at 2.83 dm$^3$/minute rotameter flow rate- Test 2*

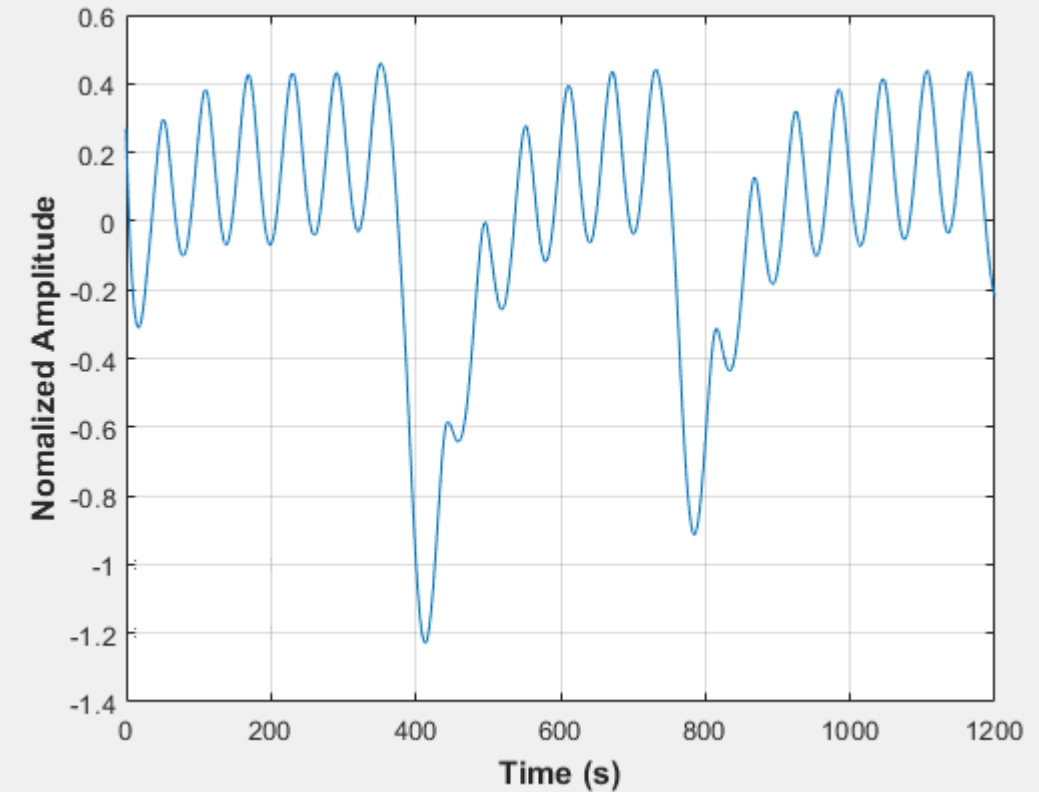


*Figure D-205: Pressure fluctuations in a non-uniformly packed vessel (large and small at the side) at 2.83 dm$^3$/minute rotameter flow rate- Test 3*

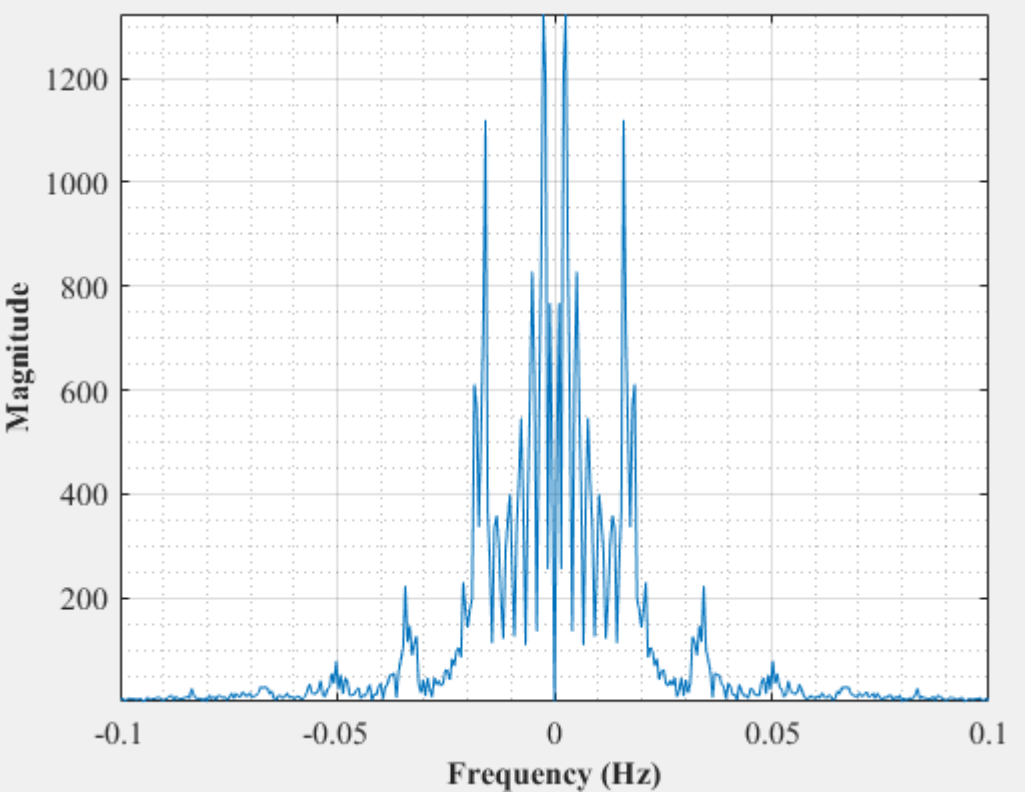


*Figure D-206: Dominant Frequency for a non-uniformly packed vessel (large and small at the side) at 2.83 dm$^3$/minute rotameter flow rate- Test 3*

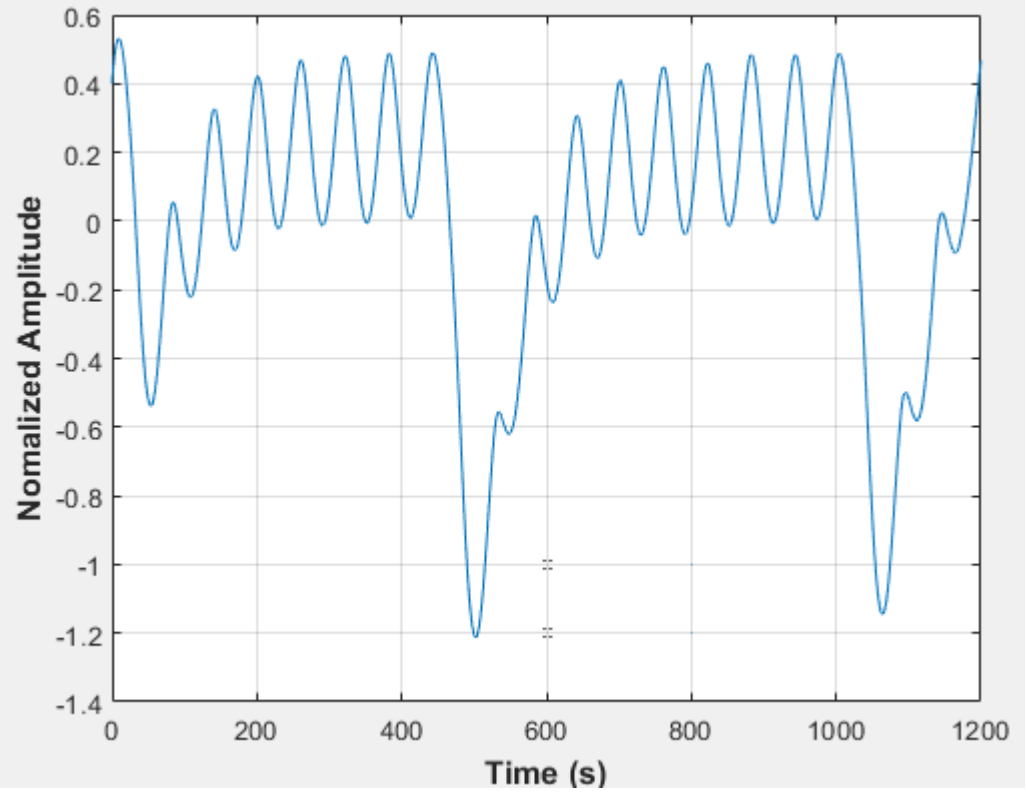


*Figure D-207: Pressure fluctuations in a non-uniformly packed vessel (large and small at the side) at 2.83 dm$^3$/minute rotameter flow rate- Test 4*

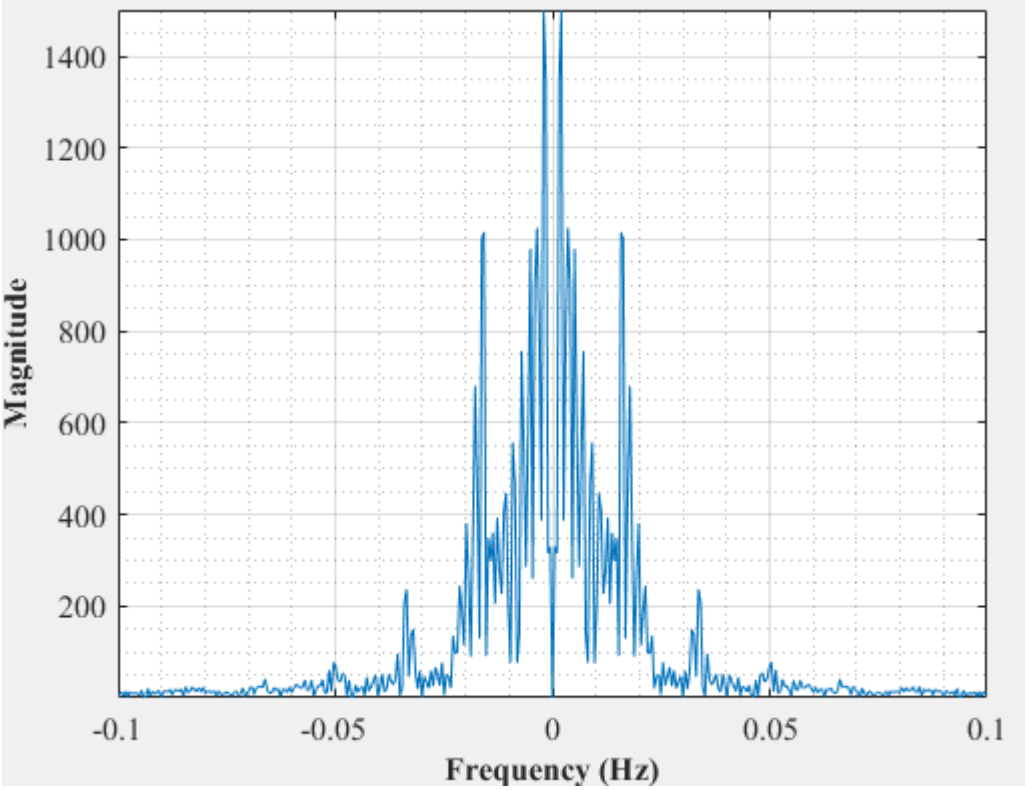


*Figure D-208: Dominant Frequency for a non-uniformly packed vessel (large and small at the side) at 2.83 dm$^3$/minute rotameter flow rate- Test 4*

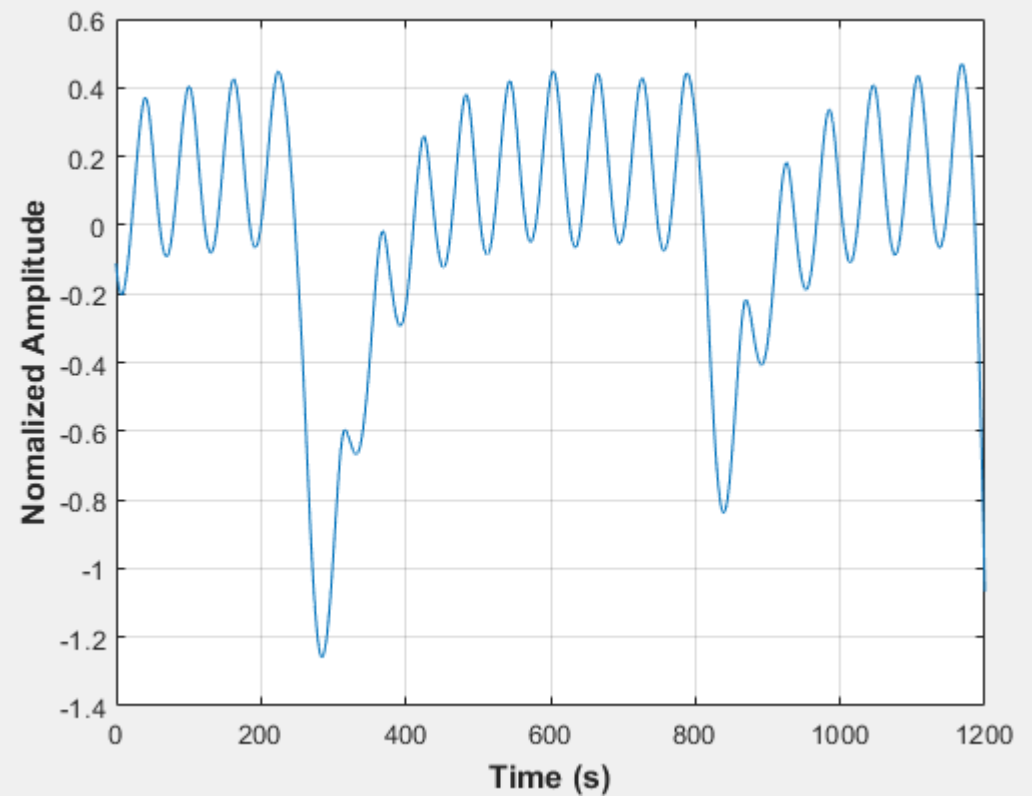


*Figure D-209: Pressure fluctuations in a non-uniformly packed vessel (large and small at the side) at 2.83 $dm^3$/minute rotameter flow rate- Test 5*

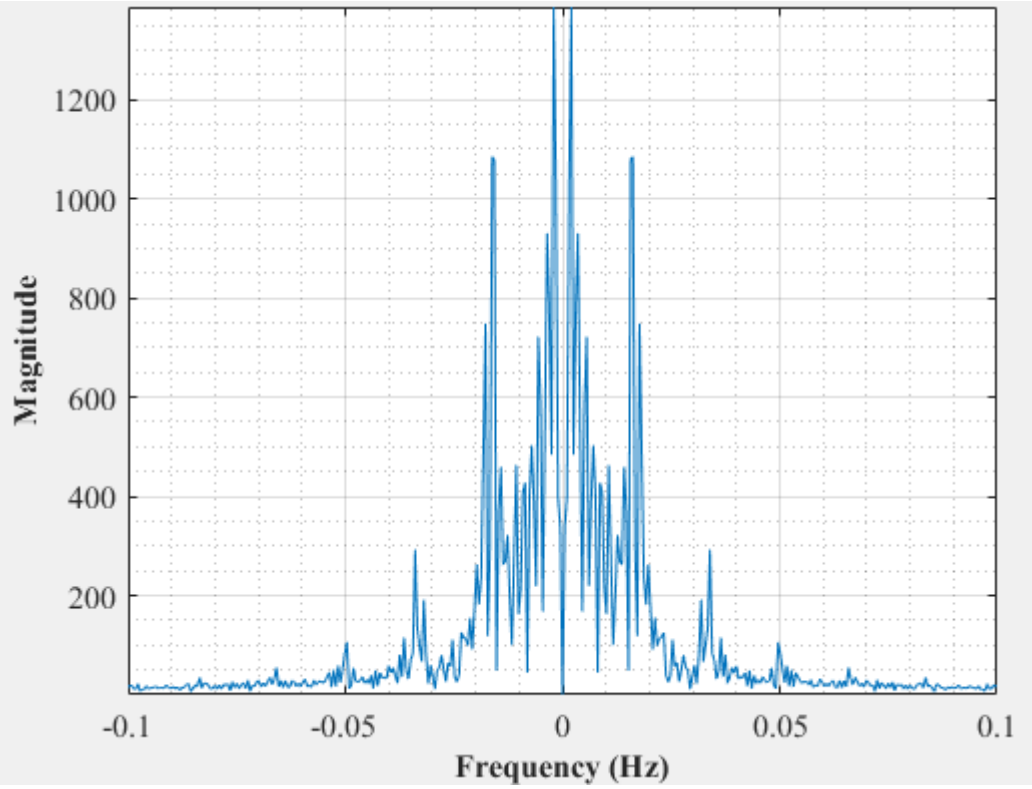


*Figure D-210: Dominant Frequency for a non-uniformly packed vessel (large and small at the side) at 2.83 $dm^3$/minute rotameter flow rate- Test 5*

*Table D-1: Frequency (mHz) Data at Various Flowrates- 75% full Vessel*

**1.67 $dm^3$ per minute**

| | T1 | T2 | T3 | T4 | T5 | T6 | T7 | T8 | Average |
|---|---|---|---|---|---|---|---|---|---|
| **Empty Tube** | 10,44 | 9,17 | 9,17 | 9,09 | | | | | 9,47 |
| **Large** | 9,57 | 10,26 | 10,35 | 10,00 | 9,09 | | | | 9,85 |
| **Large small centre** | 9,82 | 10,00 | 9,09 | 9,43 | | | | | 9,59 |
| **Large small side** | 9,82 | 9,17 | 9,24 | 9,82 | 9,26 | 9,17 | 9,24 | 9,09 | 9,35 |

**2 $dm^3$ per minute**

| | T1 | T2 | T3 | T4 | T5 | T6 | T7 | T8 | Average |
|---|---|---|---|---|---|---|---|---|---|
| **Empty Tube** | 10,91 | 10,92 | 10,71 | 12,82 | | | | | 11,34 |
| **Large** | 11,30 | 11,50 | 11,50 | 11,30 | 11,02 | 11,86 | 11,82 | | 11,47 |
| **Large small centre** | 11,61 | 12,17 | 10,91 | 10,83 | | | | | 11,38 |
| **Large small side** | 10,92 | 11,21 | 11,21 | 11,01 | 11,02 | 11,02 | | | 11,06 |

**2.33 $dm^3$ per minute**

| | T1 | T2 | T3 | T4 | T5 | T6 | T7 | T8 | Average |
|---|---|---|---|---|---|---|---|---|---|
| **Empty Tube** | 15,00 | 12,73 | 14,78 | 14,17 | 14,17 | | | | 14,17 |
| **Large** | 13,39 | 13,64 | 13,64 | 13,64 | | | | | 13,58 |
| **Large small centre** | 12,77 | 12,82 | 13,04 | 13,39 | | | | | 13,01 |
| **Large small side** | 13,04 | 12,82 | 12,93 | 13,04 | | | | | 12,96 |

**2.67 $dm^3$ per minute**

| | T1 | T2 | T3 | T4 | T5 | T6 | T7 | T8 | Average |
|---|---|---|---|---|---|---|---|---|---|
| **Empty Tube** | 15,83 | 15,46 | 14,91 | 15,18 | 15,04 | | | | 15,28 |
| **Large** | 14,29 | 13,33 | 13,56 | 13,33 | 13,56 | 13,33 | | | 13,57 |
| **Large small centre** | 15,83 | 15,13 | 15,39 | 15,00 | 15,00 | | | | 15,27 |
| **Large small side** | 15,04 | 15,04 | 15,00 | 15,32 | 15,18 | | | | 15,12 |

**2.83 $dm^3$ per minute**

| | T1 | T2 | T3 | T4 | T5 | T6 | T7 | T8 | Average |
|---|---|---|---|---|---|---|---|---|---|
| **Empty Tube** | 15,93 | 15,79 | 15,52 | 15,83 | 15,83 | 15,79 | 15,93 | | 15,80 |
| **Large** | 16,67 | 15,25 | 16,67 | 16,67 | 16,38 | 15,83 | | | 16,24 |
| **Large small centre** | 15,65 | 15,97 | 16,24 | 15,83 | 15,97 | 15,93 | | | 15,93 |
| **Large small side** | 14,66 | 15,25 | 15,97 | 16,22 | 16,07 | | | | 15,63 |

*Table D-2: Amplitude Data at Various Flowrates- 75% full Vessel*

**1.67 $dm^3$ per minute**

| | T1 | T2 | T3 | T4 | T5 | T6 | T7 | T8 | **Average** |
|---|---|---|---|---|---|---|---|---|---|
| **Empty Tube** | 0,63 | 0,51 | 0,54 | 0,56 | | | | | 0,56 |
| **Large** | 0,60 | 0,48 | 0,56 | 0,40 | | | | | 0,51 |
| **Large small centre** | 0,65 | 0,68 | 0,55 | 0,53 | | | | | 0,60 |
| **Large small side** | 0,60 | 0,53 | 0,57 | 0,52 | 0,58 | 0,55 | 0,54 | 0,57 | 0,56 |

**2 $dm^3$ per minute**

| | T1 | T2 | T3 | T4 | T5 | T6 | T7 | T8 | **Average** |
|---|---|---|---|---|---|---|---|---|---|
| **Empty Tube** | 0,65 | 0,65 | 0,59 | 0,73 | | | | | 0,66 |
| **Large** | 0,51 | 0,45 | 0,48 | 0,51 | 0,46 | 0,45 | 0,48 | | 0,47 |
| **Large small centre** | 0,41 | 0,42 | 0,46 | 0,36 | | | | | 0,41 |
| **Large small side** | 0,57 | 0,63 | 0,62 | 0,61 | 0,62 | 0,62 | | | 0,61 |

**2.33 $dm^3$ per minute**

| | T1 | T2 | T3 | T4 | T5 | T6 | T7 | T8 | **Average** |
|---|---|---|---|---|---|---|---|---|---|
| **Empty Tube** | 0,28 | 0,28 | 0,29 | 0,23 | 0,28 | | | | 0,27 |
| **Large** | 0,46 | 0,46 | 0,51 | 0,50 | | | | | 0,48 |
| **Large small centre** | 0,26 | 0,28 | 0,25 | 0,25 | | | | | 0,26 |
| **Large small side** | 0,48 | 0,48 | 0,51 | 0,51 | | | | | 0,49 |

**2.67 $dm^3$ per minute**

| | T1 | T2 | T3 | T4 | T5 | T6 | T7 | T8 | **Average** |
|---|---|---|---|---|---|---|---|---|---|
| **Empty Tube** | 0,26 | 0,27 | 0,29 | 0,27 | 0,29 | | | | 0,28 |
| **Large** | 0,29 | 0,32 | 0,30 | 0,29 | 0,31 | 0,29 | | | 0,30 |
| **Large small centre** | 0,26 | 0,28 | 0,28 | 0,28 | 0,27 | | | | 0,28 |
| **Large small side** | 0,30 | 0,28 | 0,31 | 0,30 | 0,30 | | | | 0,30 |

**2.83 $dm^3$ per minute**

| | T1 | T2 | T3 | T4 | T5 | T6 | T7 | T8 | **Average** |
|---|---|---|---|---|---|---|---|---|---|
| **Empty Tube** | 0,26 | 0,28 | 0,26 | 0,30 | 0,28 | 0,28 | 0,26 | | 0,27 |
| **Large** | 0,21 | 0,23 | 0,25 | 0,24 | 0,23 | 0,23 | | | 0,23 |
| **Large small centre** | 0,22 | 0,23 | 0,23 | 0,25 | 0,26 | 0,23 | | | 0,24 |
| **Large small side** | 0,24 | 0,22 | 0,24 | 0,25 | 0,25 | | | | 0,24 |

## APPENDIX E: Large vessel experiments- Fully packed

### Introduction

This section shows the graphs for the experiments done on the large vessel while it was full of packing material. Figures E-1 to E-158 show amplitudes and frequency curves for the first batch of experiments. Tables E-1 and E-2 show the summary from the amplitude and frequency data obtained from the experiments.

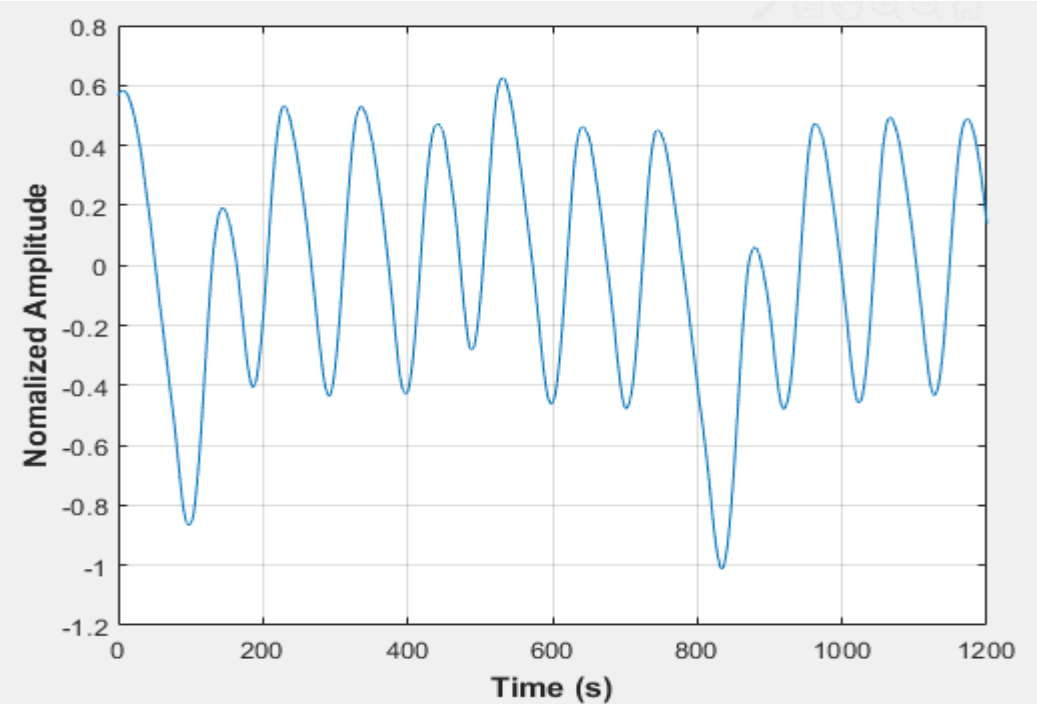


*Figure E-1: Pressure fluctuations in a uniformly packed vessel at 1.67 dm$^3$/minute rotameter flow rate- Test 1*

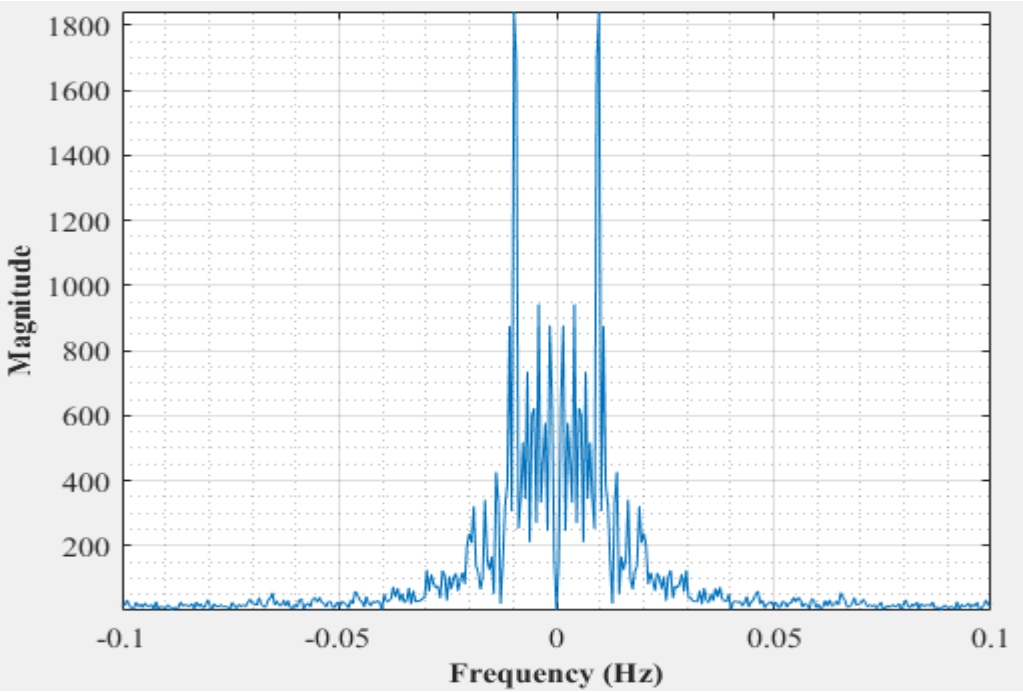


*Figure E-2: Dominant Frequency for a uniformly packed vessel at 1.67 dm$^3$/minute rotameter flow rate- test 1*

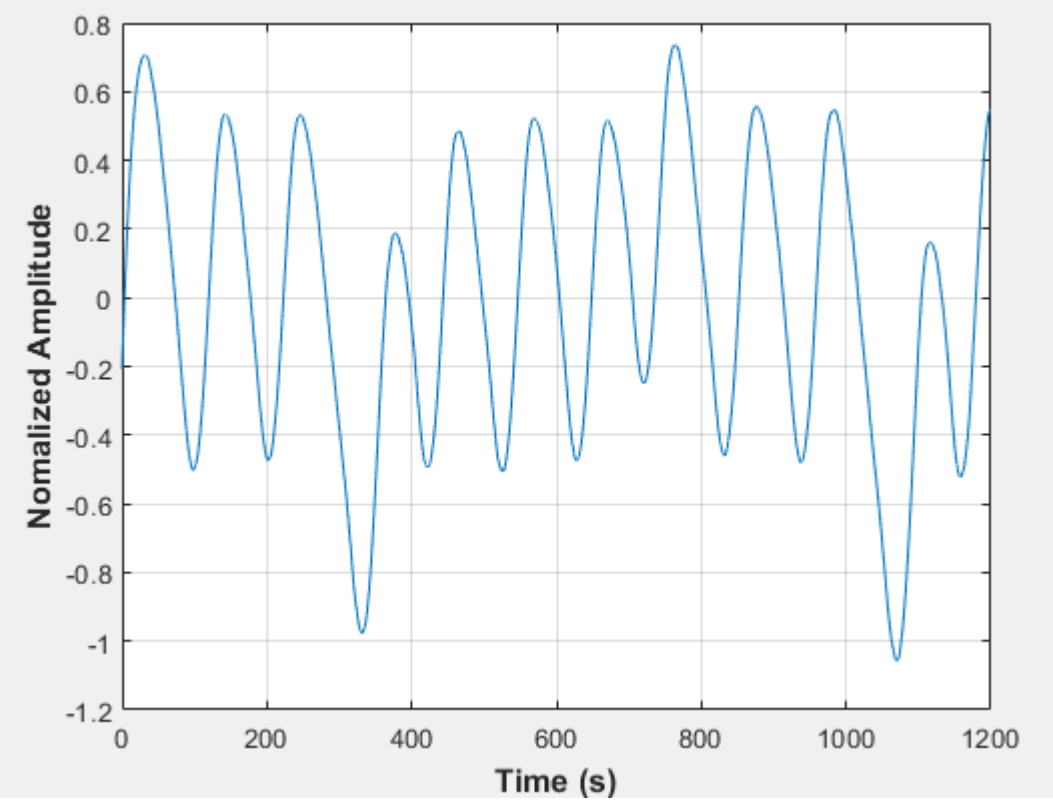


*Figure E-3: Pressure fluctuations in a uniformly packed vessel at 1.67 dm$^3$/minute rotameter flow rate- Test 2*

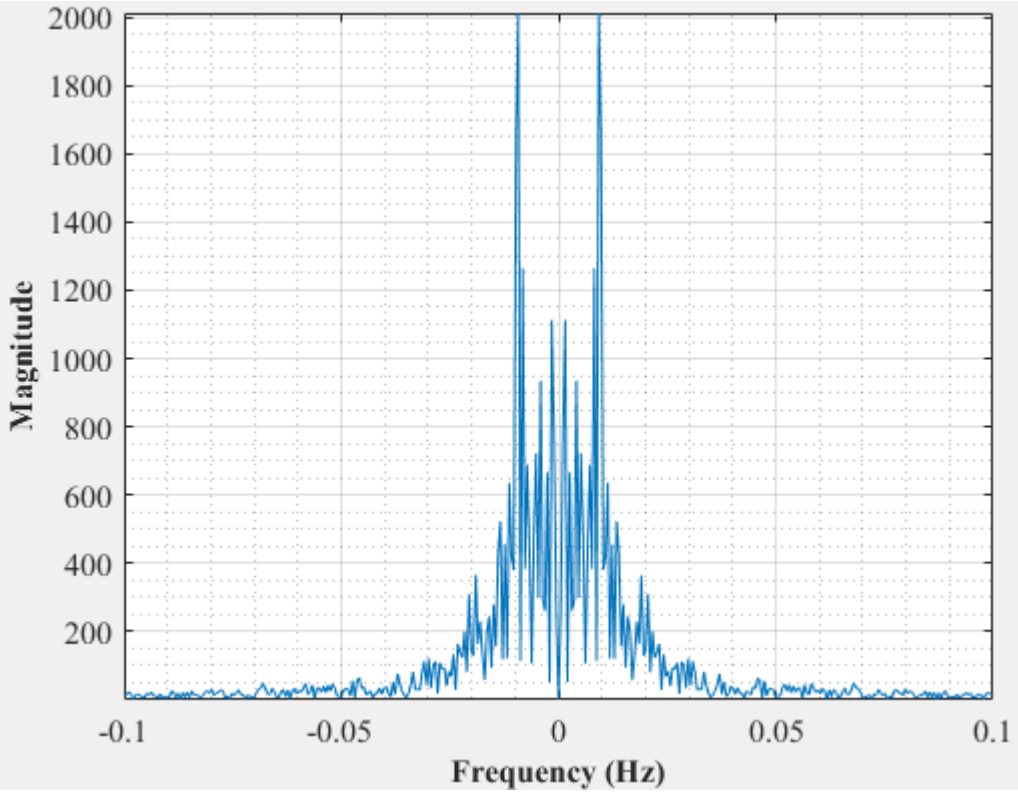


*Figure E-4: Dominant Frequency for a uniformly packed vessel at 1.67 dm$^3$/minute rotameter flow rate- test 2*

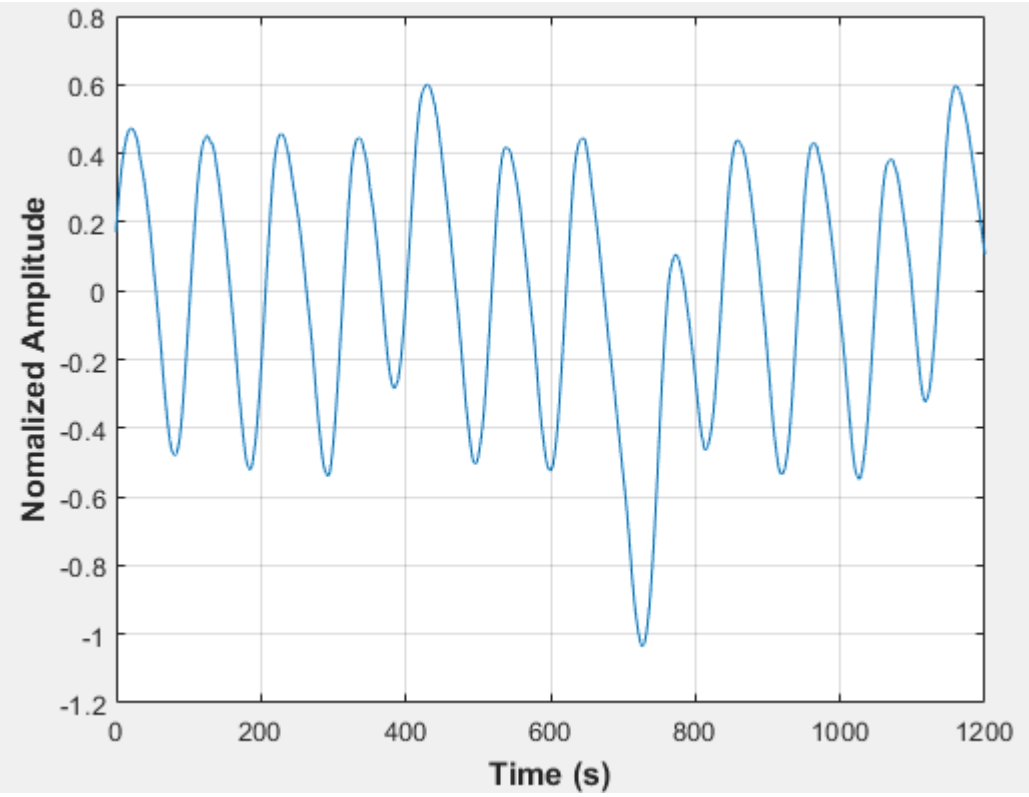


*Figure E-5: Pressure fluctuations in a uniformly packed vessel at 1.67 $dm^3$/minute rotameter flow rate- Test 3*

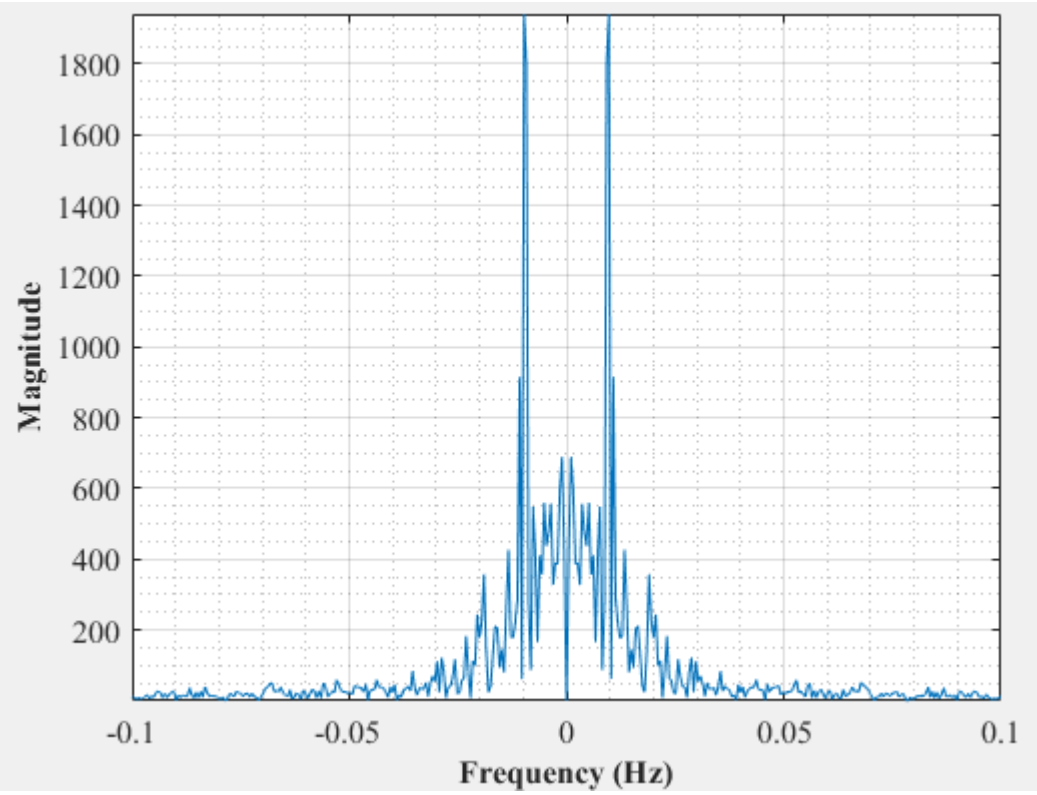


*Figure E-6: Dominant Frequency for a uniformly packed vessel at 1.67 $dm^3$/minute rotameter flow rate- test 3*

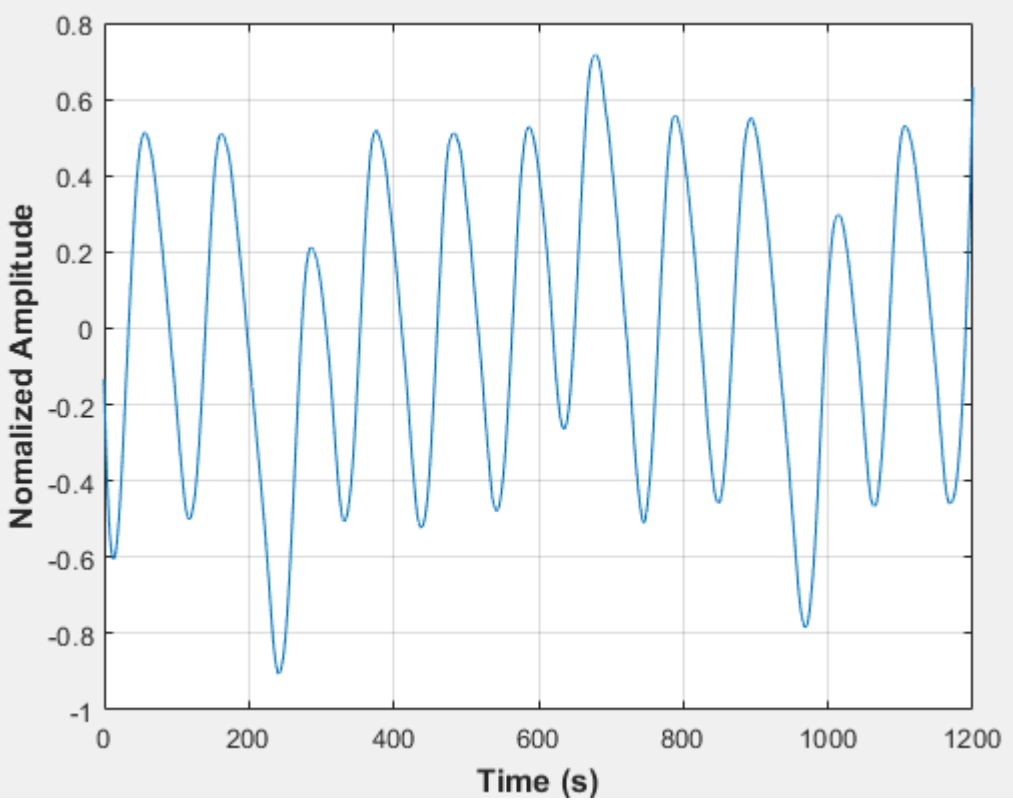


*Figure E-7: Pressure fluctuations in a uniformly packed vessel at 1.67 dm$^3$/minute rotameter flow rate- Test 4*

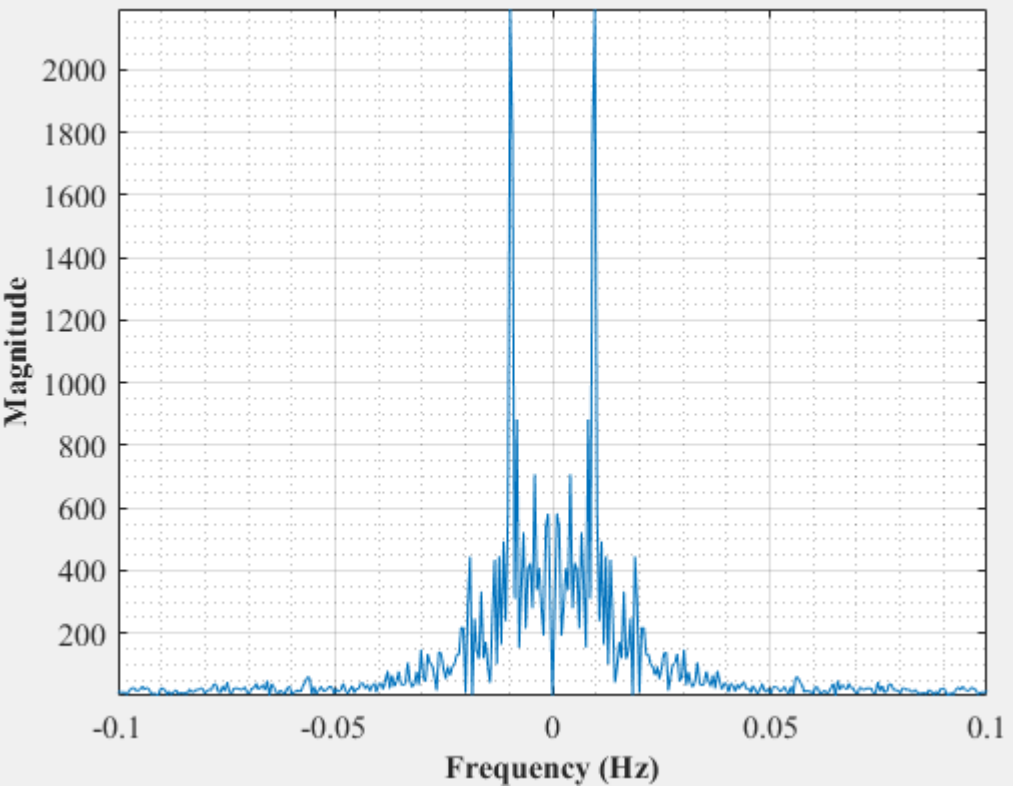


*Figure E-8: Dominant Frequency for a uniformly packed vessel at 1.67 dm$^3$/minute rotameter flow rate- test 4*

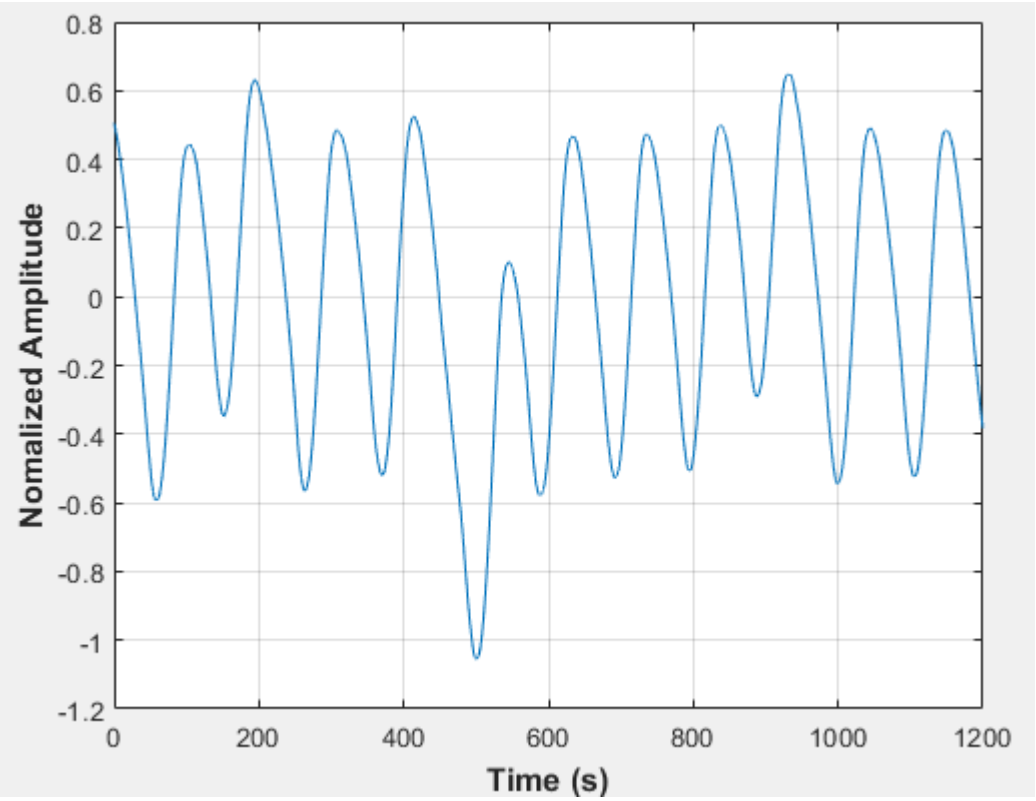


*Figure E-9: Pressure fluctuations in a uniformly packed vessel at 1.67 $dm^3$/minute rotameter flow rate- Test 5*

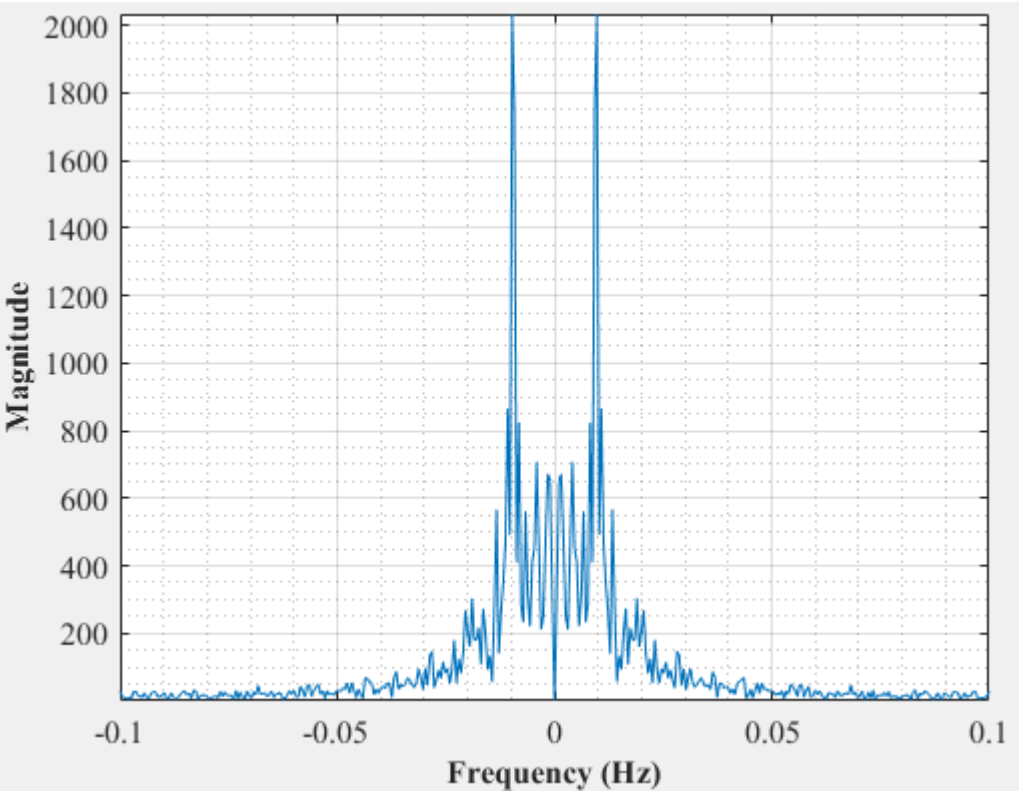


*Figure E-10: Dominant Frequency for a uniformly packed vessel at 1.67 $dm^3$/minute rotameter flow rate- Test 5*

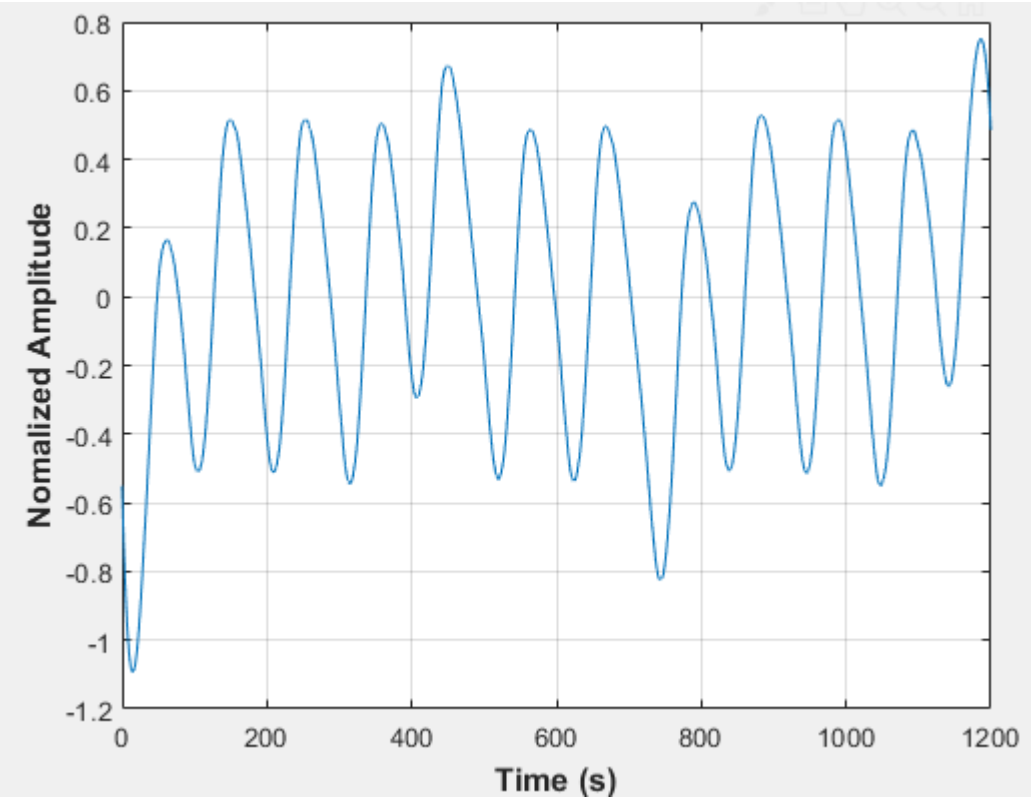


*Figure E-11: Pressure fluctuations in a uniformly packed vessel at 1.67 dm$^3$/minute rotameter flow rate- Test 6*

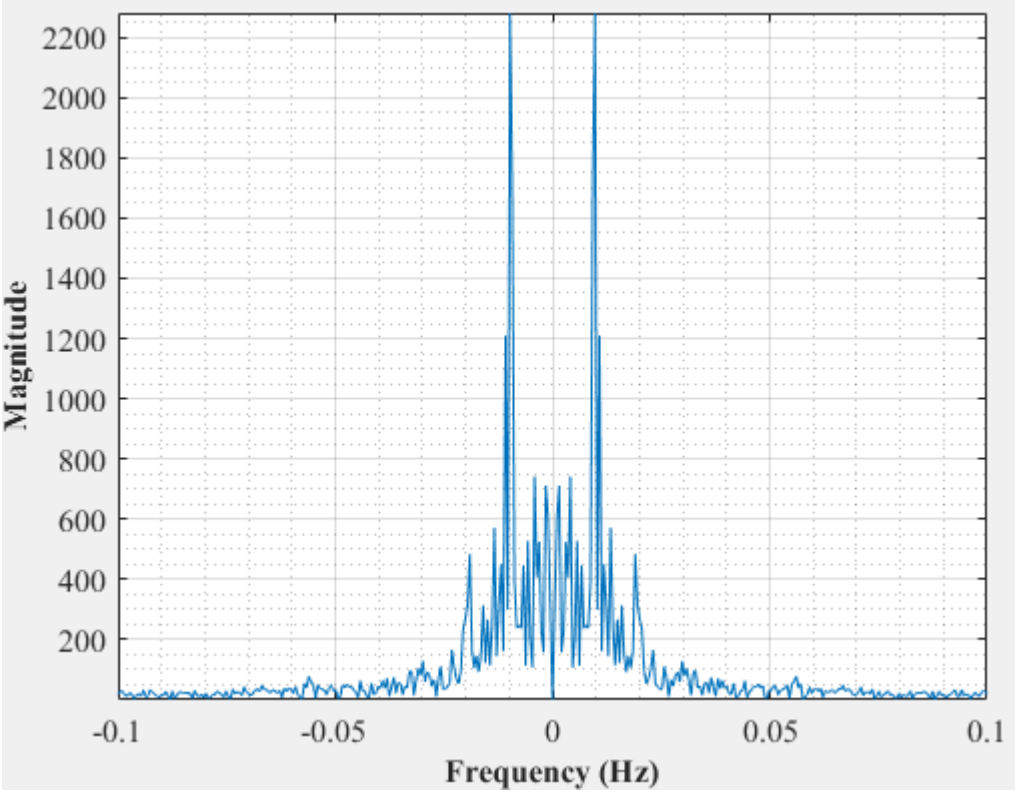


*Figure E-12: Dominant Frequency for a uniformly packed vessel at 1.67 dm$^3$/minute rotameter flow rate- Test 6*

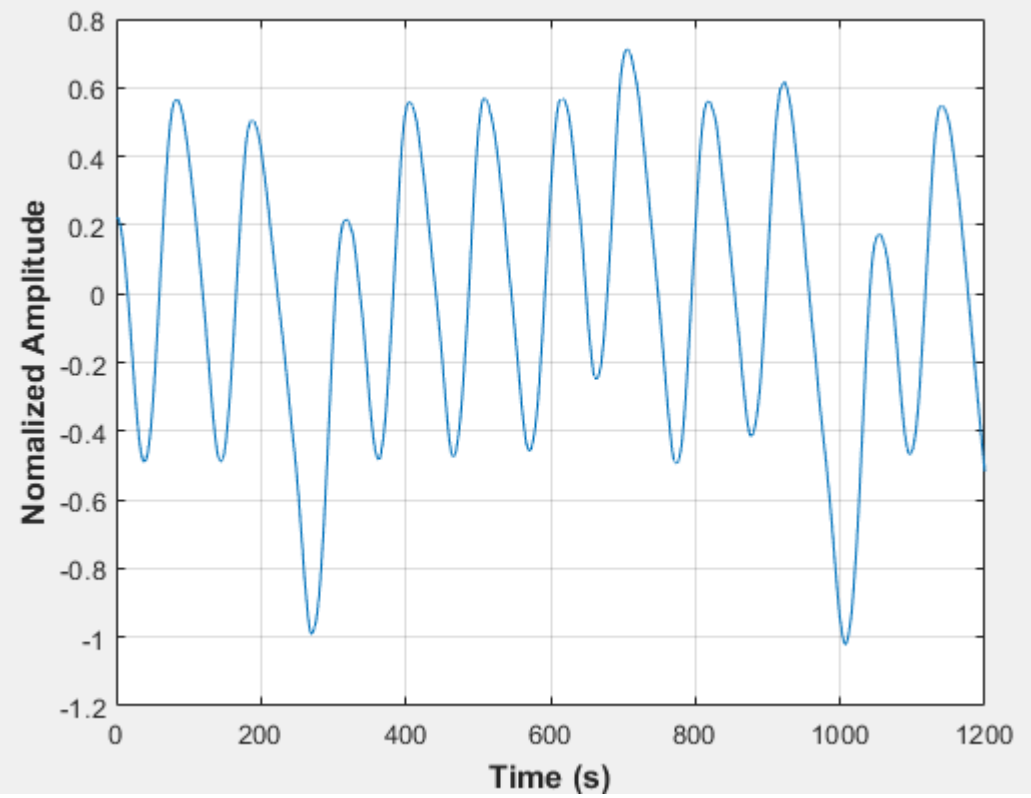


*Figure E-13: Pressure fluctuations in a uniformly packed vessel at 1.67 $dm^3$/minute rotameter flow rate- Test 7*

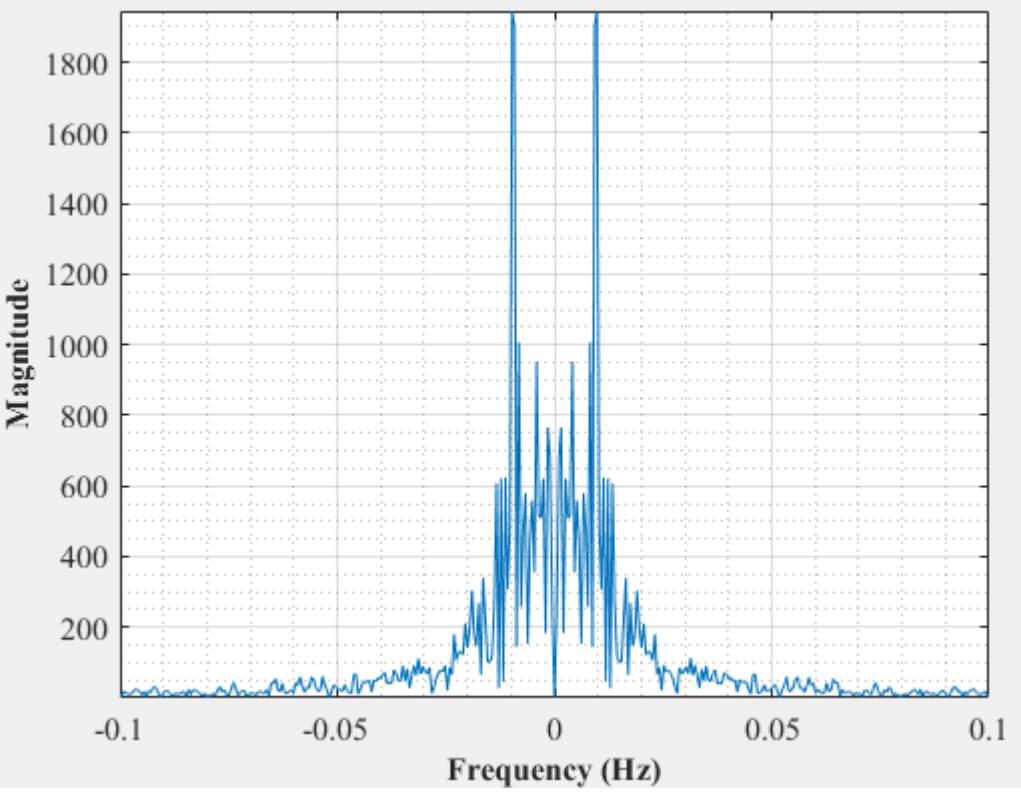


*Figure E-14: Dominant Frequency for a uniformly packed vessel at 1.67 $dm^3$/minute rotameter flow rate- Test 7*

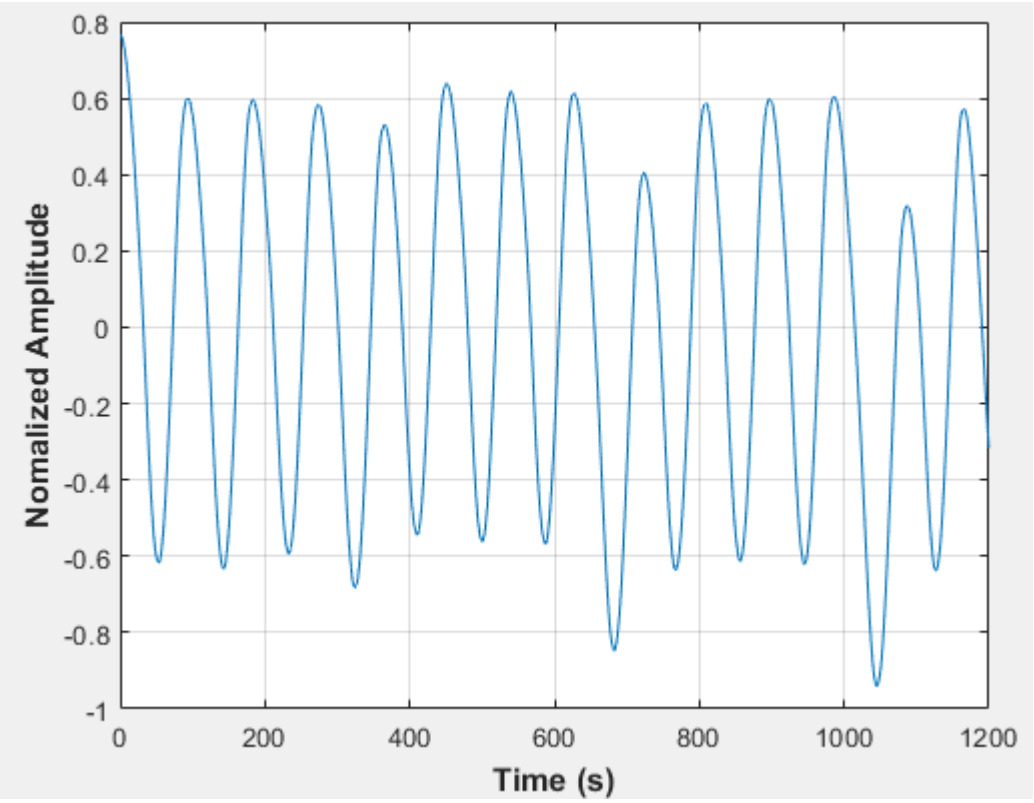


*Figure E-15: Pressure fluctuations in a uniformly packed vessel at 2 dm$^3$/minute rotameter flow rate- Test 1*

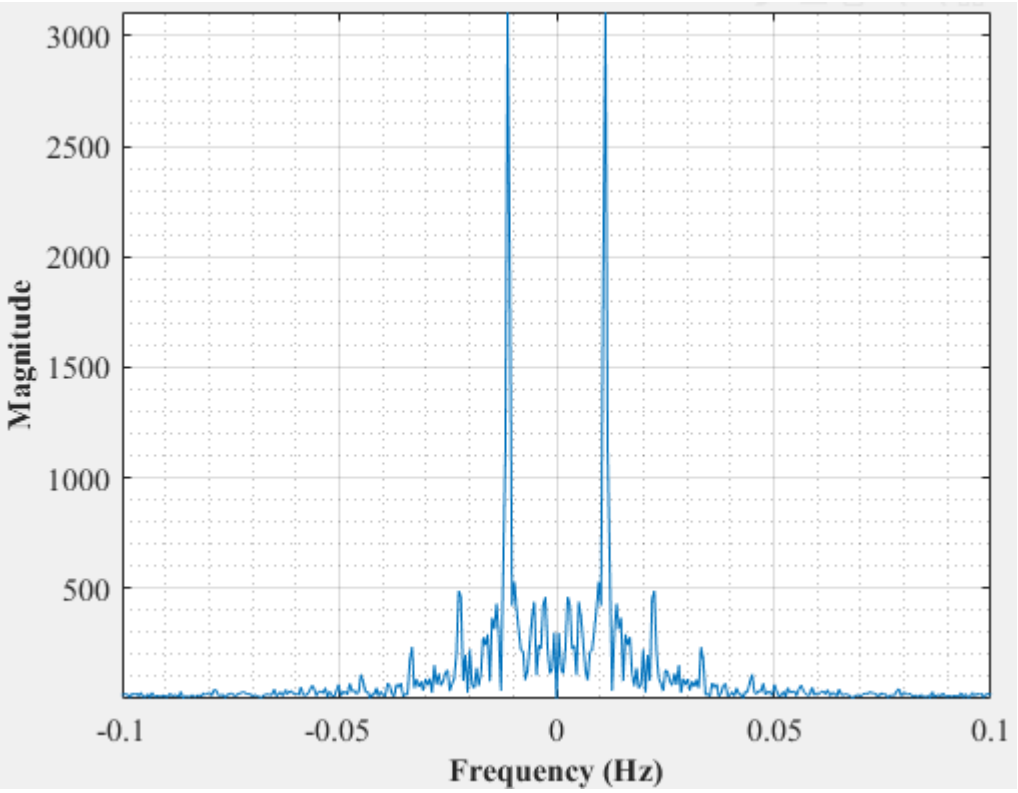


*Figure E-16: Dominant Frequency for a uniformly packed vessel at 2 dm$^3$/minute rotameter flow rate- Test 1*

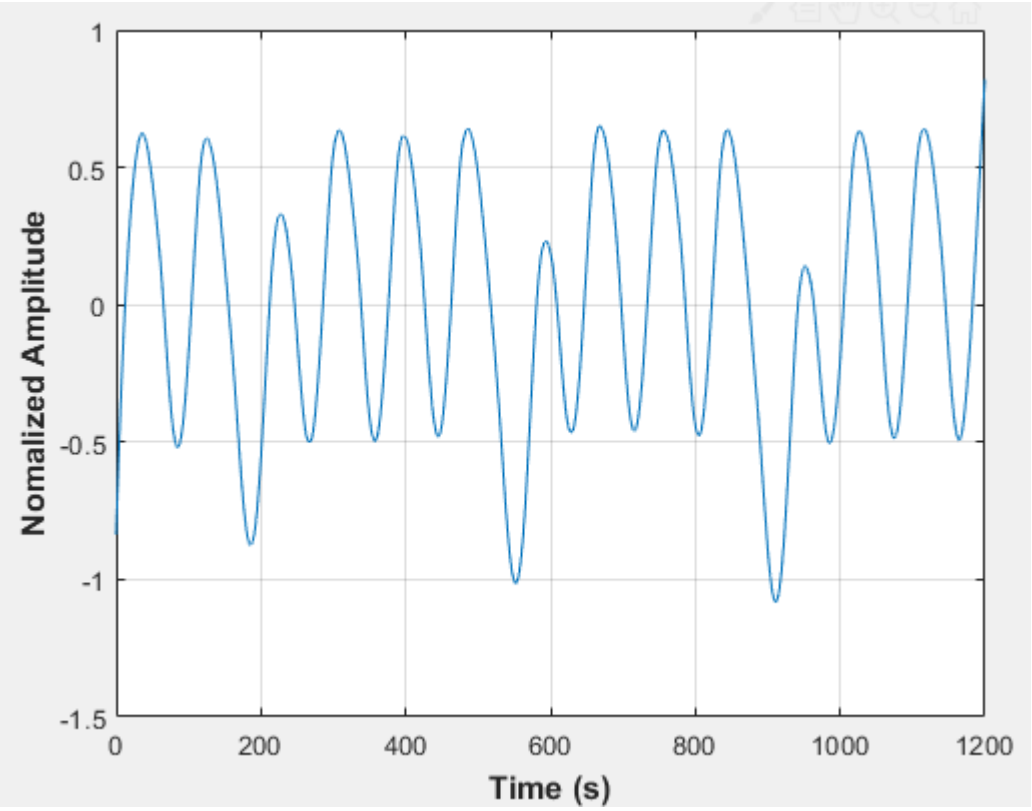


*Figure E-17: Pressure fluctuations in a uniformly packed vessel at 2 dm$^3$/minute rotameter flow rate- Test 2*

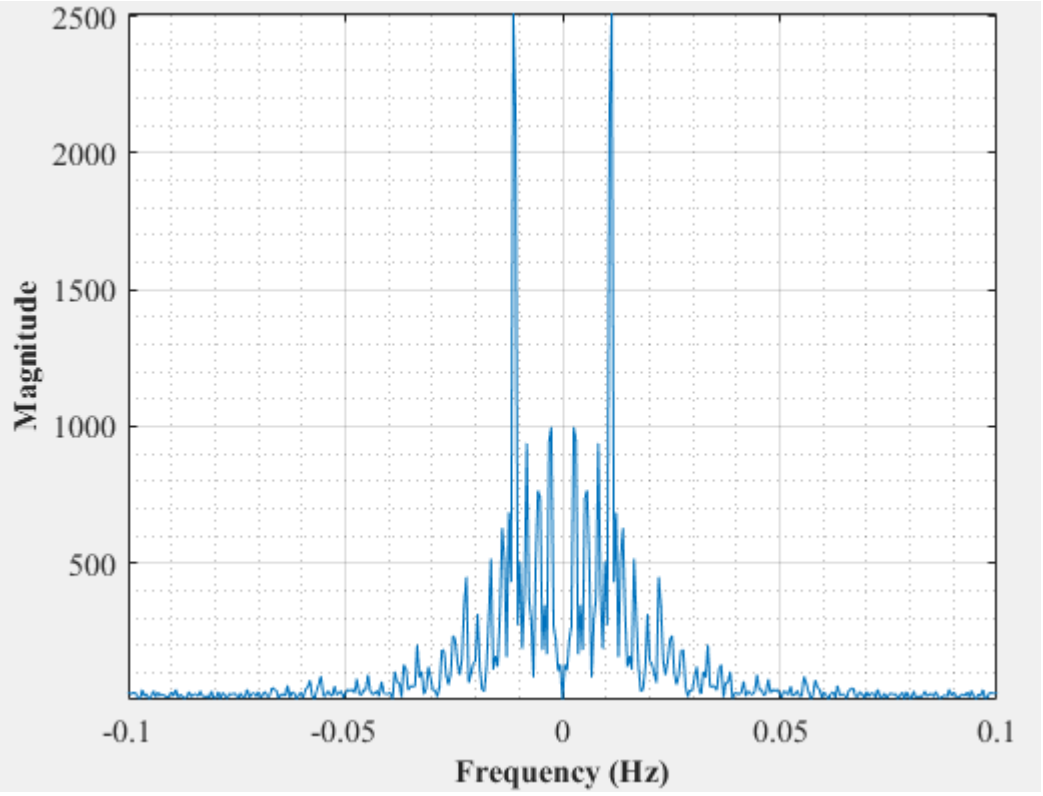


*Figure E-18: Dominant Frequency for a uniformly packed vessel at 2 dm$^3$/minute rotameter flow rate- Test 2*

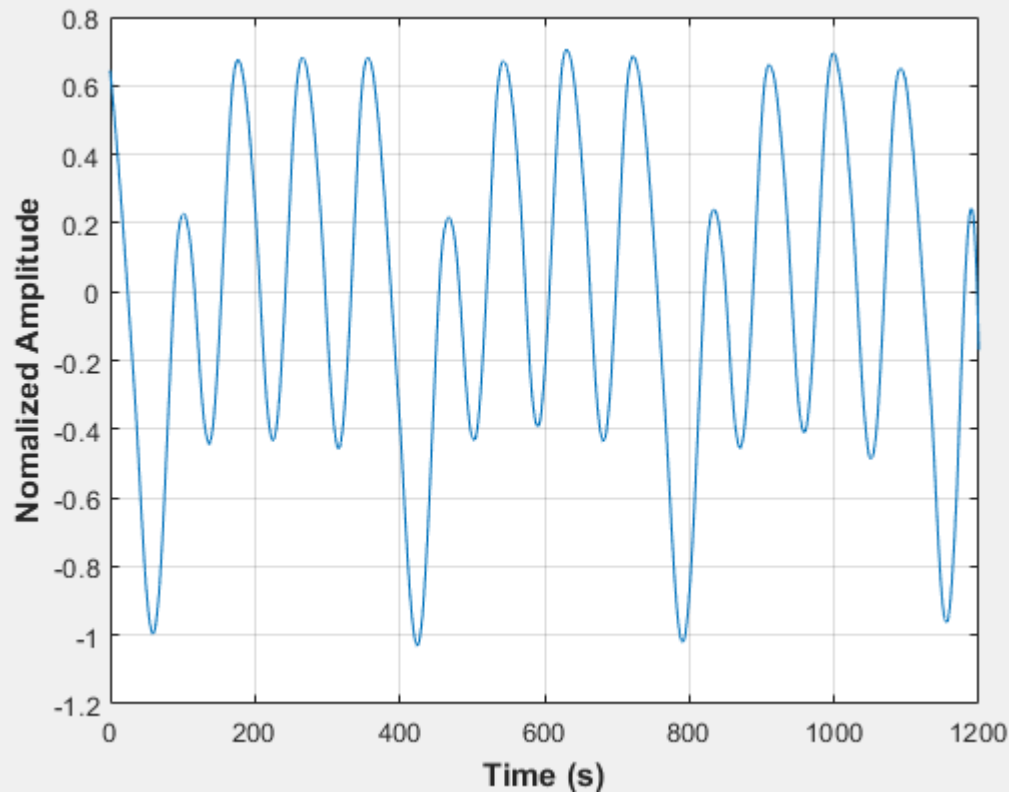


*Figure E-19: Pressure fluctuations in a uniformly packed vessel at 2 dm$^3$/minute rotameter flow rate- Test 3*

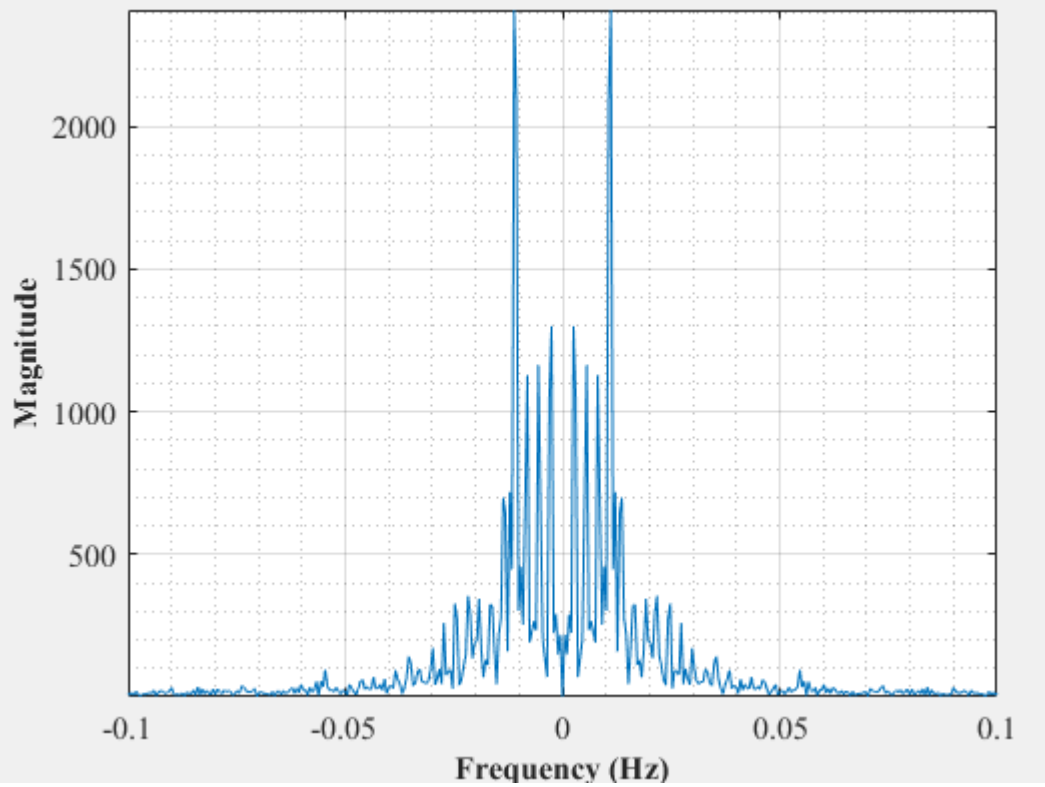


*Figure E-20: Dominant Frequency for a uniformly packed vessel at 2 dm$^3$/minute rotameter flow rate- Test 3*

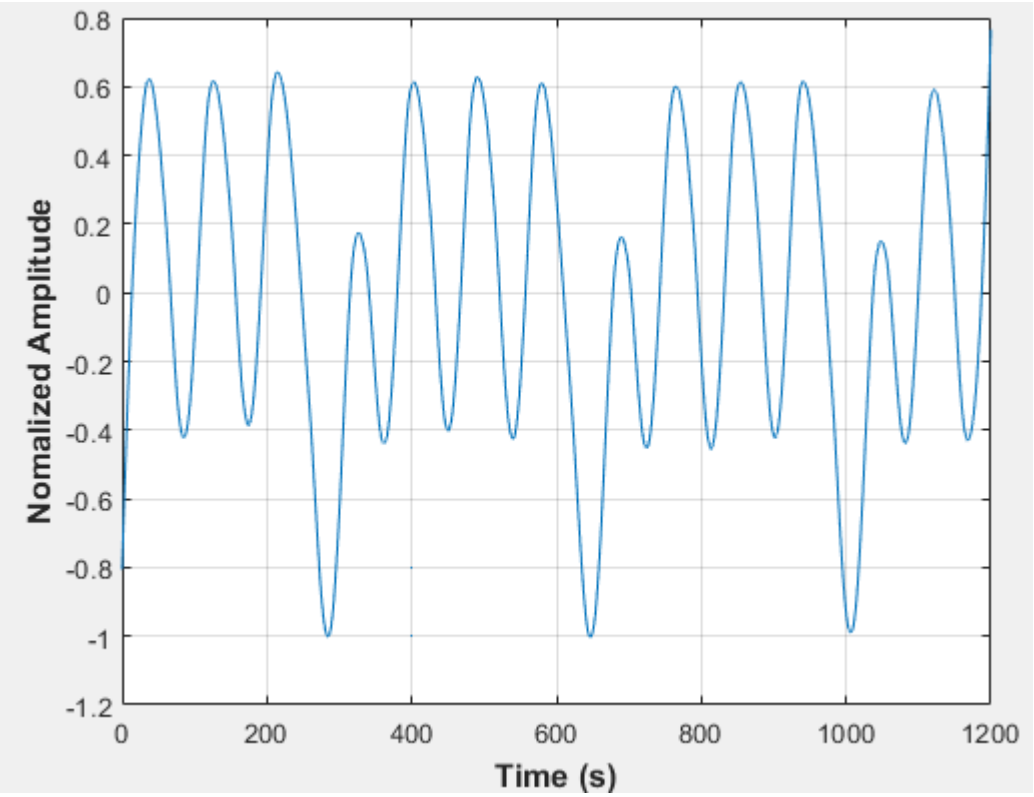


*Figure E-21: Pressure fluctuations in a uniformly packed vessel at 2 dm$^3$/minute rotameter flow rate- Test 4*

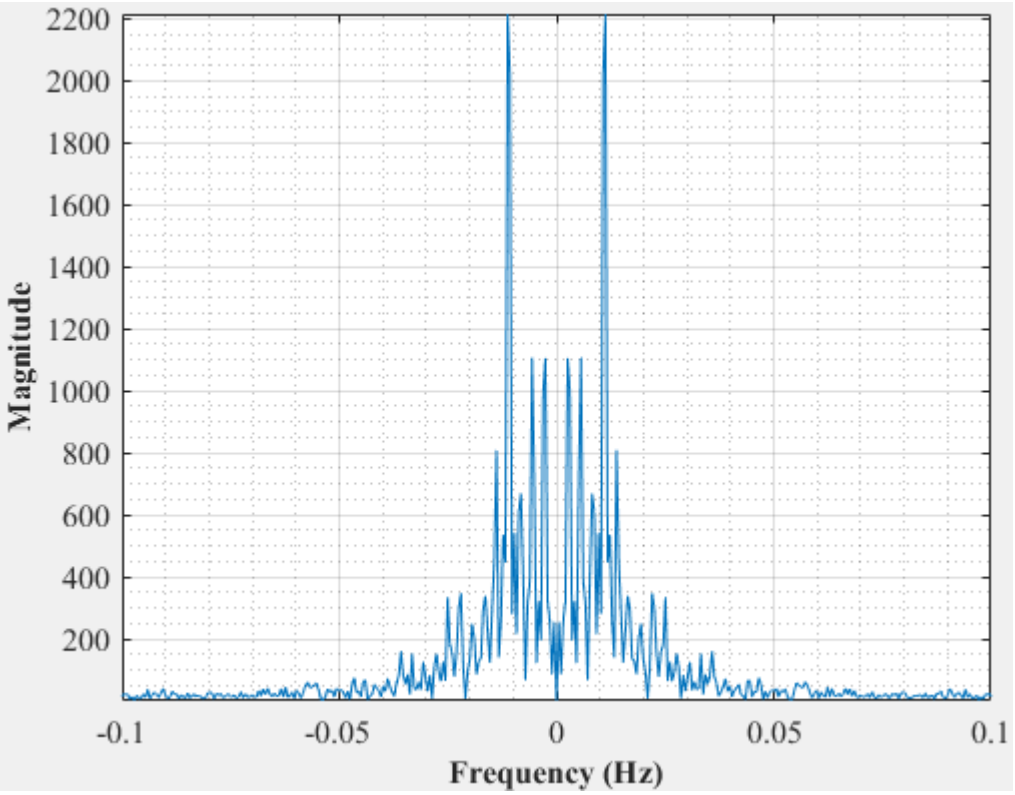


*Figure E-22: Dominant Frequency for a uniformly packed vessel at 2 dm$^3$/minute rotameter flow rate- Test 4*

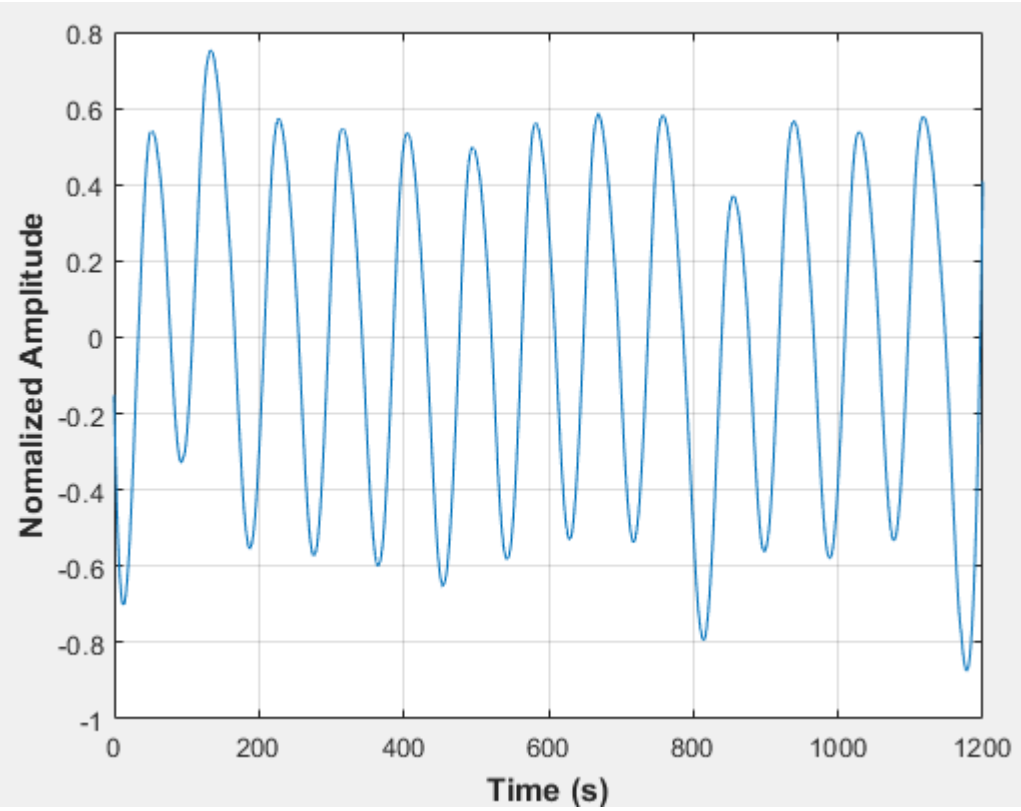


*Figure E-23: Pressure fluctuations in a uniformly packed vessel at 2 dm$^3$/minute rotameter flow rate- Test 5*

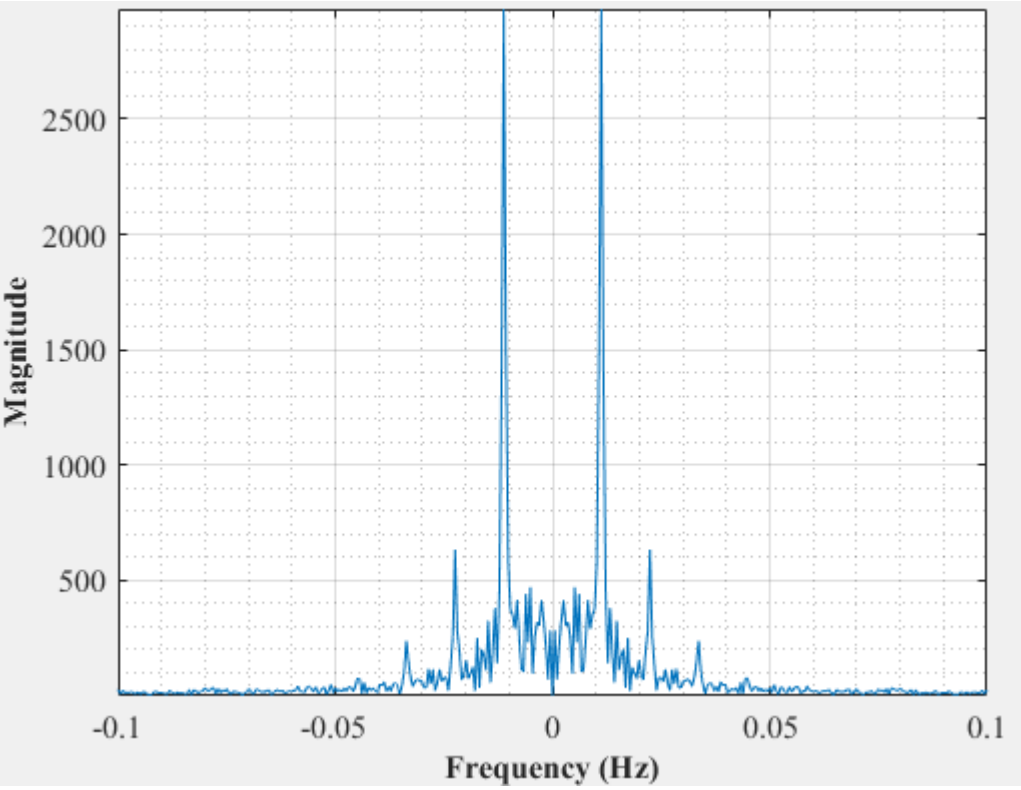


*Figure E-24: Dominant Frequency for a uniformly packed vessel at 2 dm$^3$/minute rotameter flow rate- Test 5*

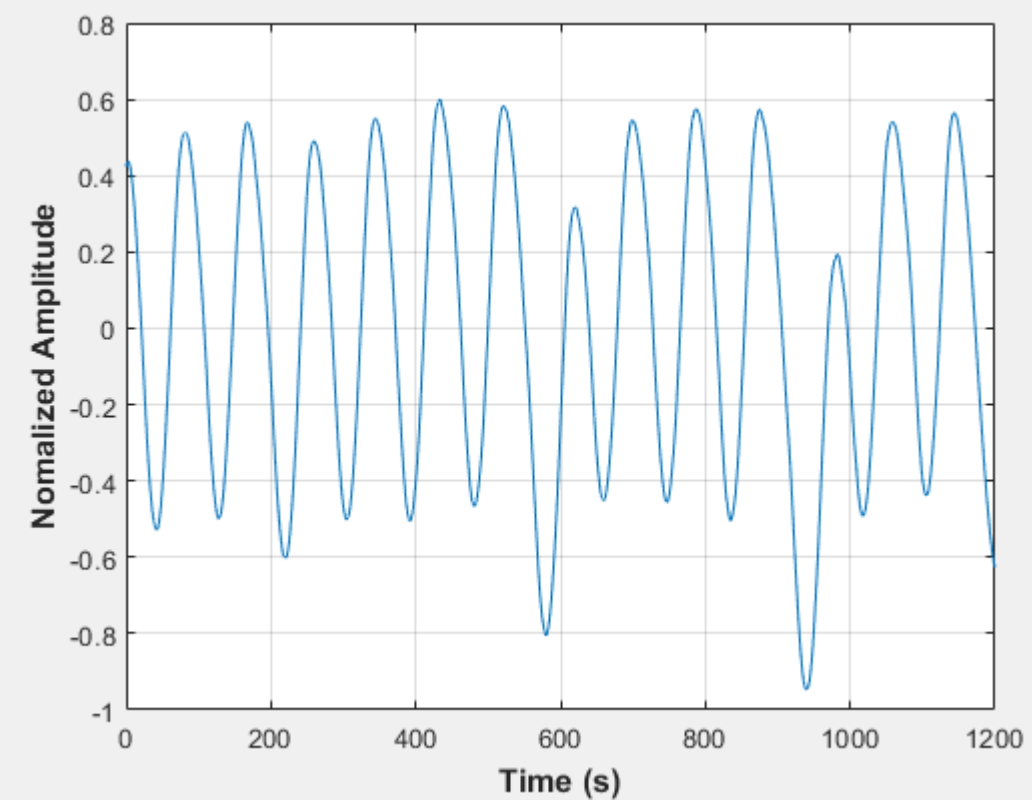


*Figure E-25: Pressure fluctuations in a uniformly packed vessel at 2 dm$^3$/minute rotameter flow rate- Test 6*

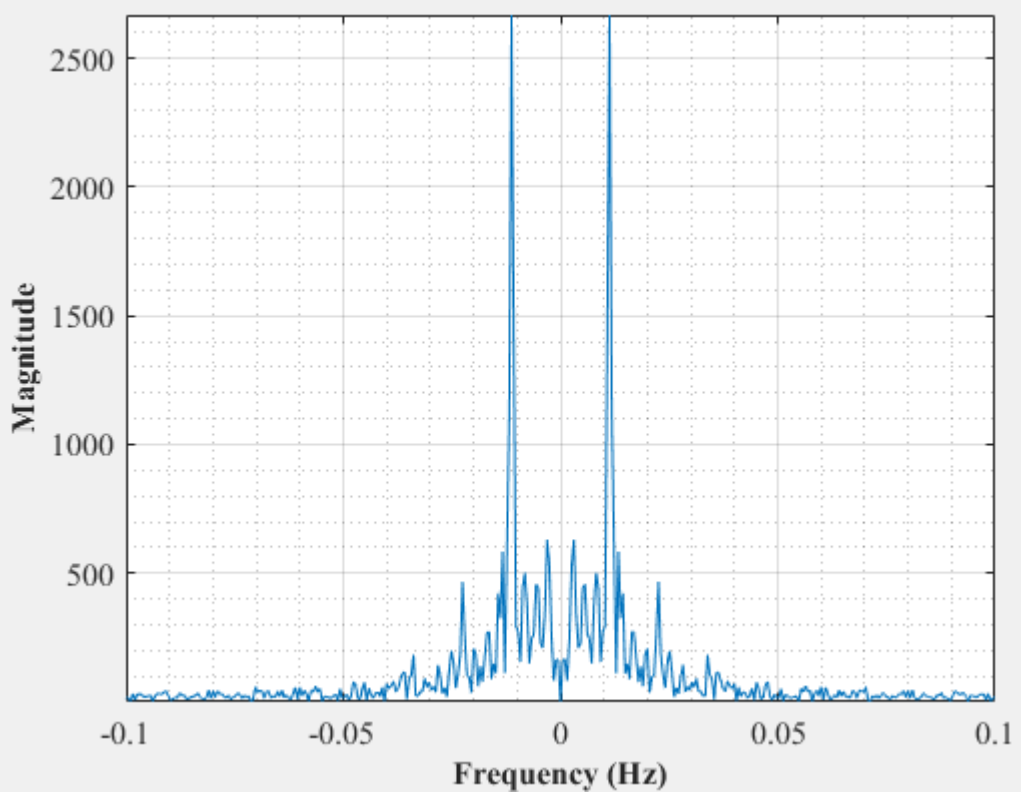


*Figure E-26: Dominant Frequency for a uniformly packed vessel at 2 dm$^3$/minute rotameter flow rate- Test 6*

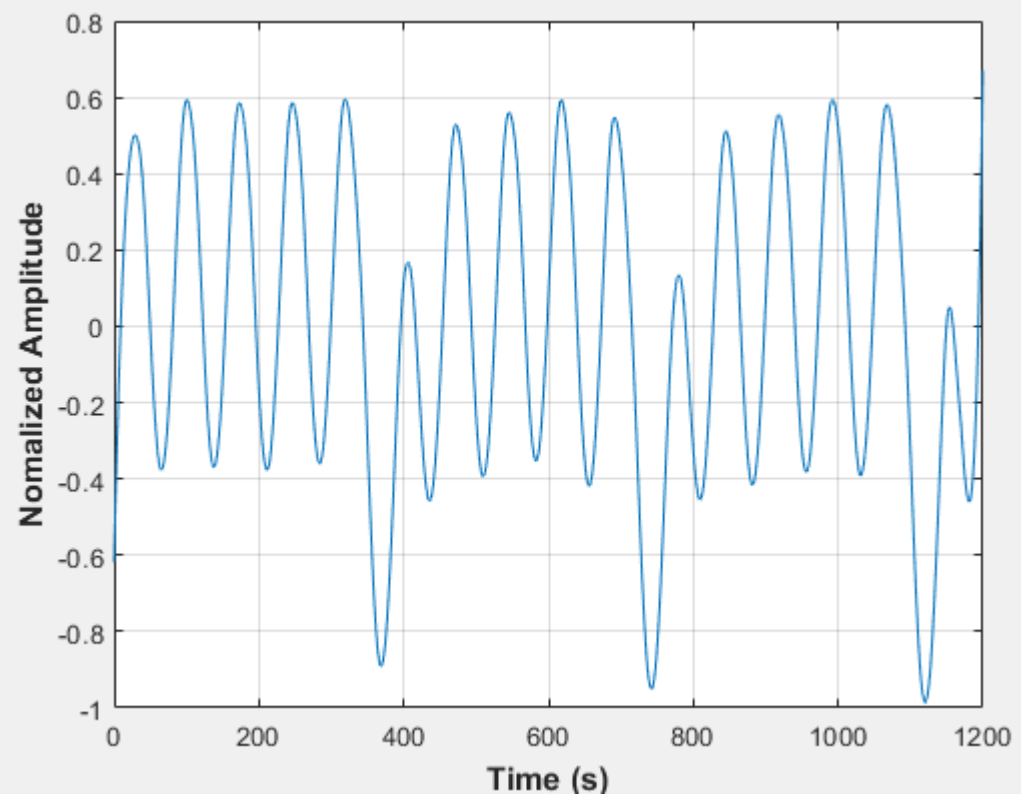


*Figure E-27: Pressure fluctuations in a uniformly packed vessel at 2.33 dm$^3$/minute rotameter flow rate- Test 1*

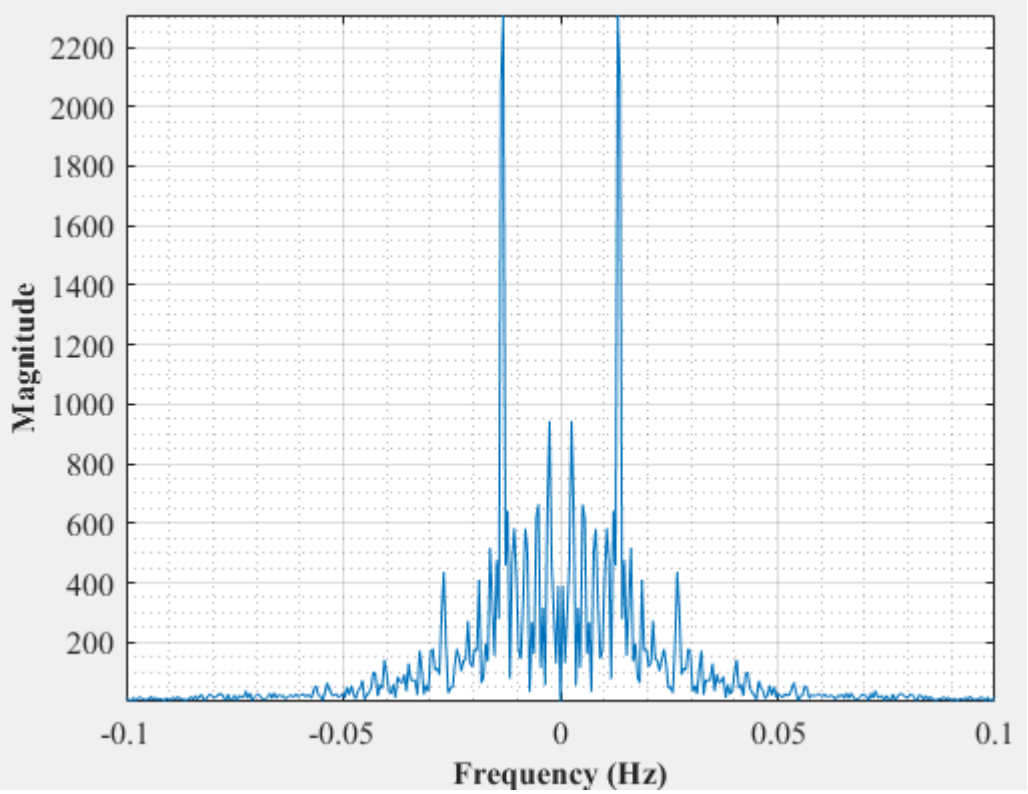


*Figure E-28: Dominant Frequency for a uniformly packed vessel at 2.33 dm$^3$/minute rotameter flow rate- Test 1*

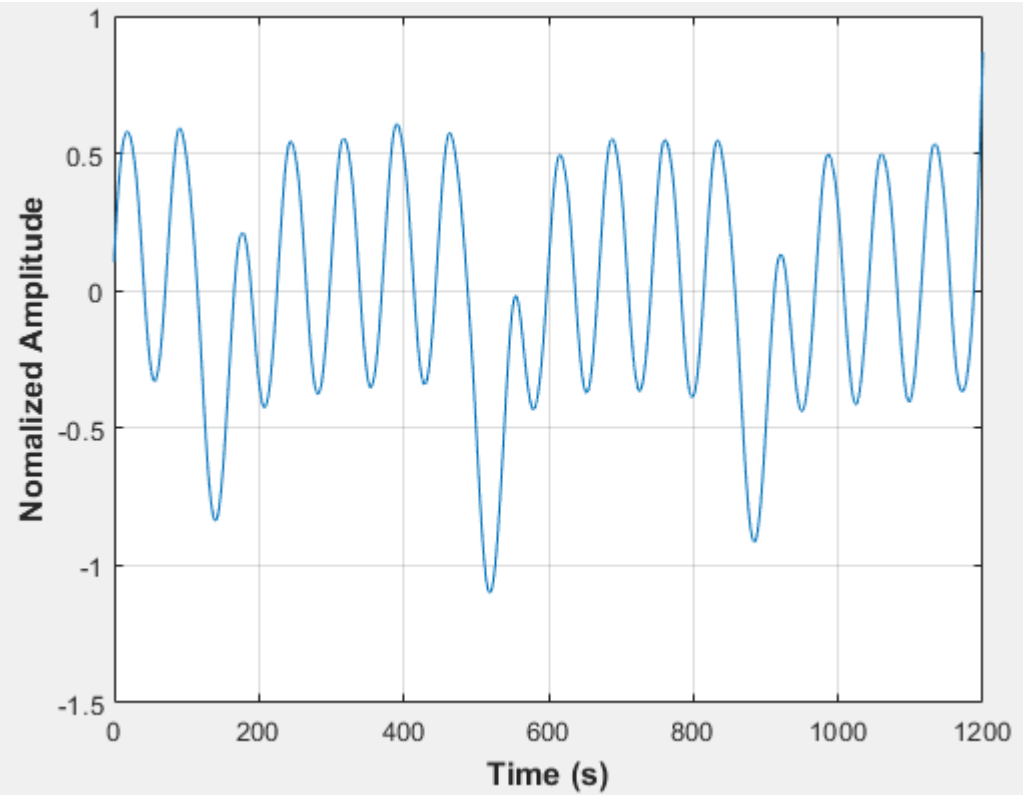


*Figure E-29: Pressure fluctuations in a uniformly packed vessel at 2.33 dm$^3$/minute rotameter flow rate- Test 2*

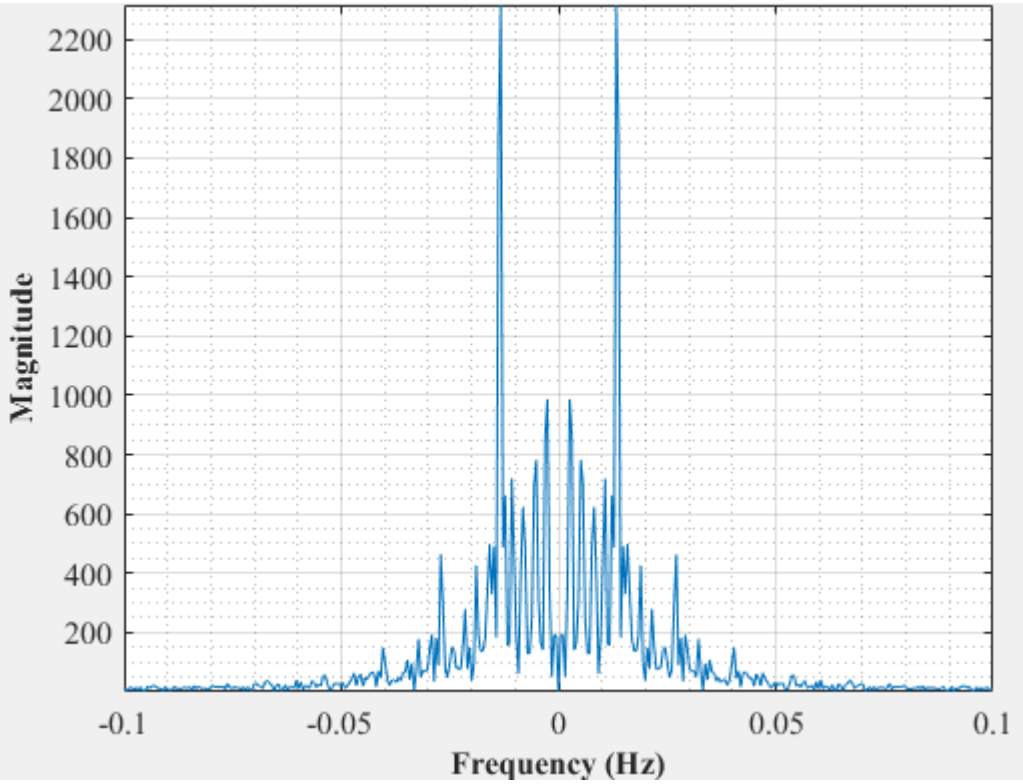


*Figure E-30: Dominant Frequency for a uniformly packed vessel at 2.33 dm$^3$/minute rotameter flow rate- Test 2*

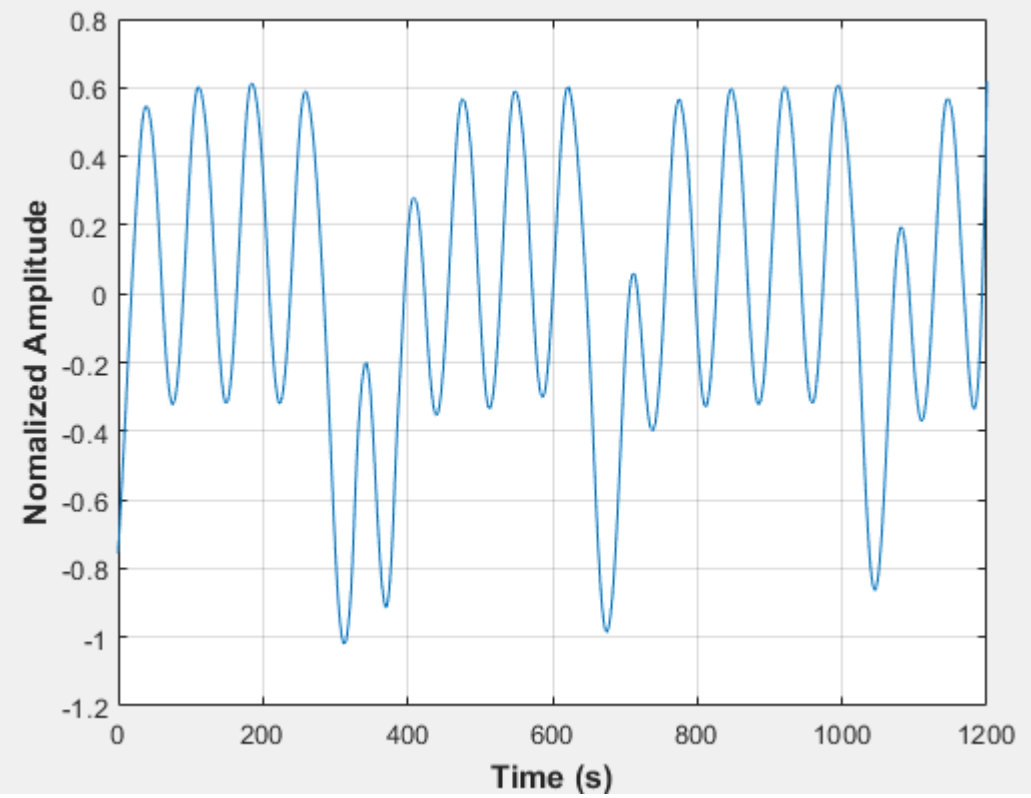


*Figure E-31: Pressure fluctuations in a uniformly packed vessel at 2.33 $dm^3$/minute rotameter flow rate- Test 3*

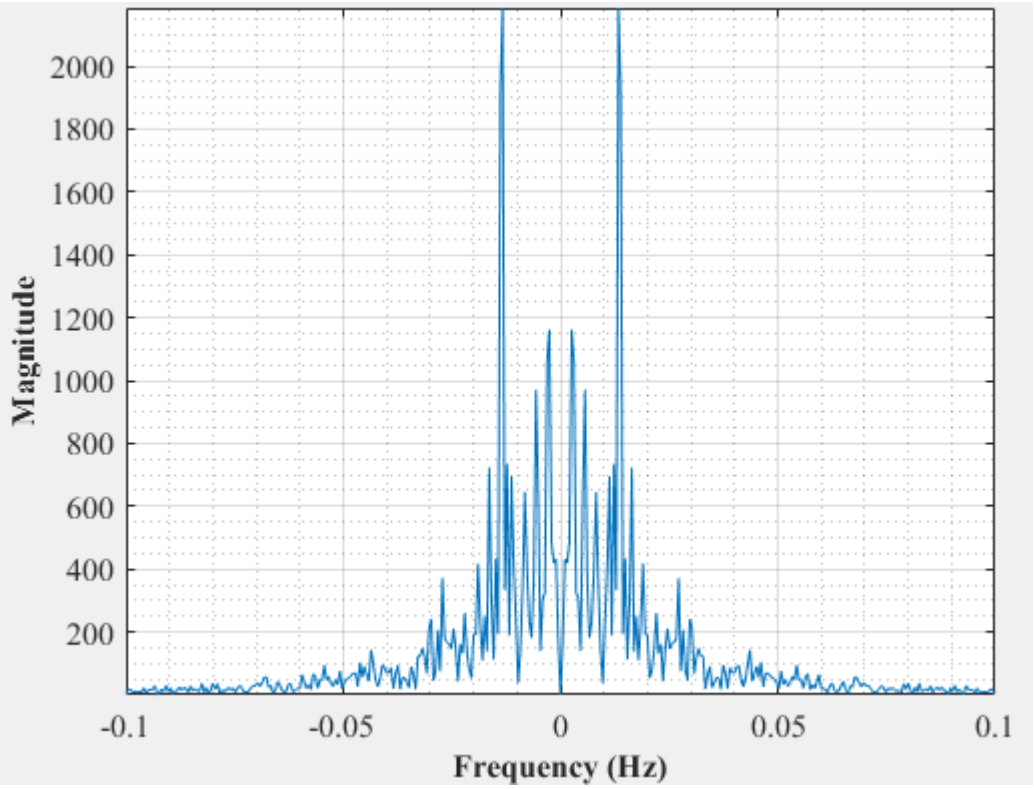


*Figure E-32: Dominant Frequency for a uniformly packed vessel at 2.33 $dm^3$/minute rotameter flow rate- Test 3*

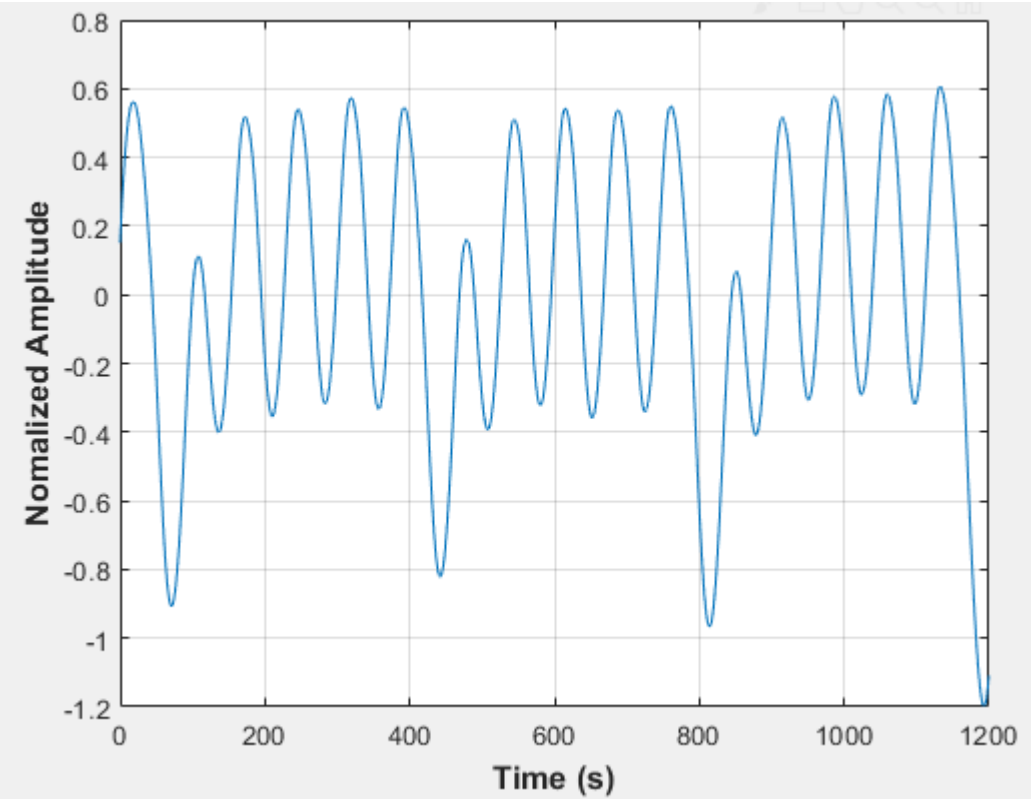


*Figure E-33: Pressure fluctuations in a uniformly packed vessel at 2.33 dm$^3$/minute rotameter flow rate- Test 4*

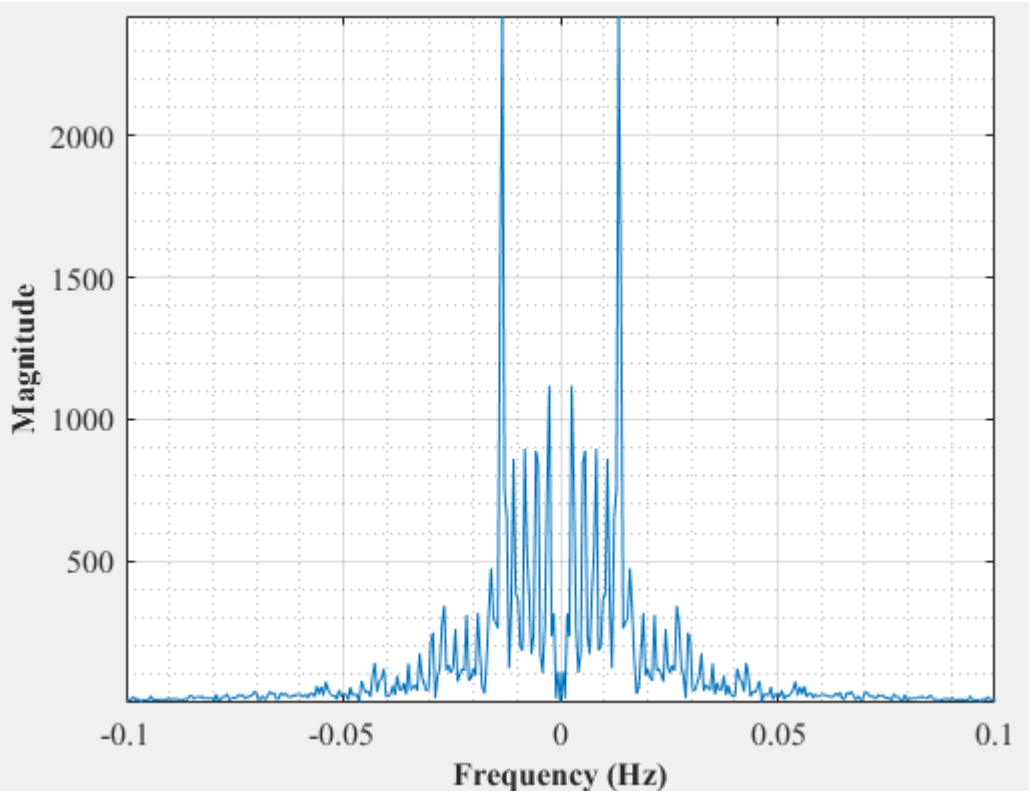


*Figure E-34: Dominant Frequency for a uniformly packed vessel at 2.33 dm$^3$/minute rotameter flow rate- Test 4*

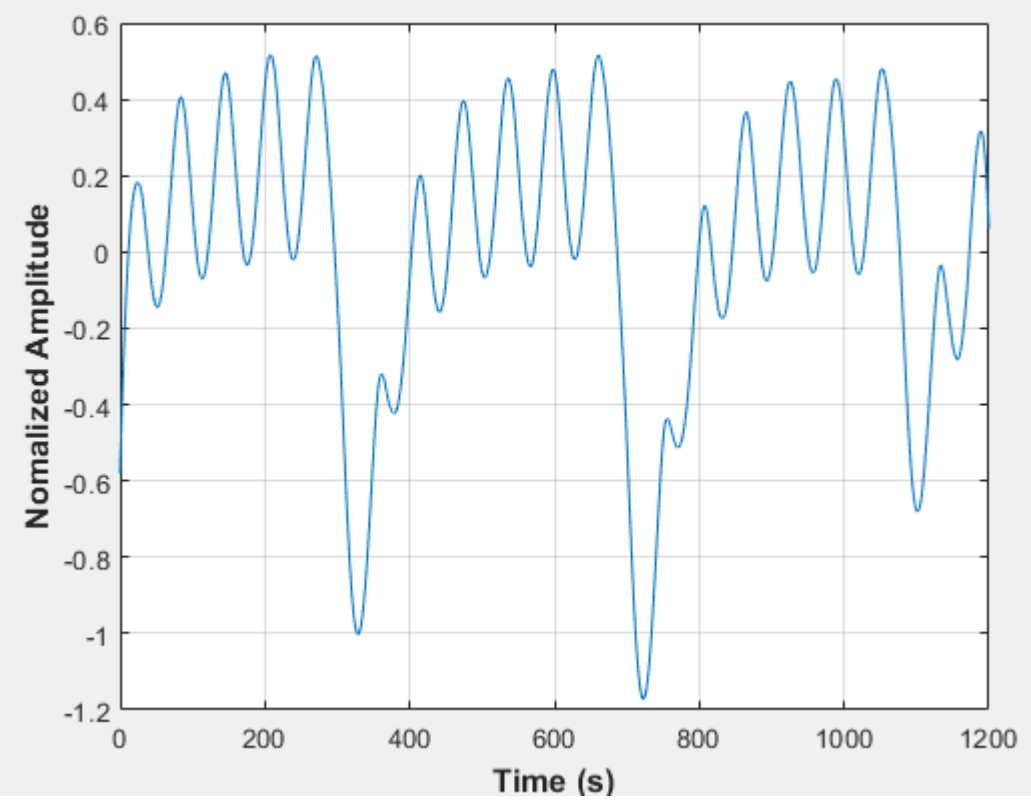


*Figure E-35: Pressure fluctuations in a uniformly packed vessel at 2.67 dm$^3$/minute rotameter flow rate- Test 1*

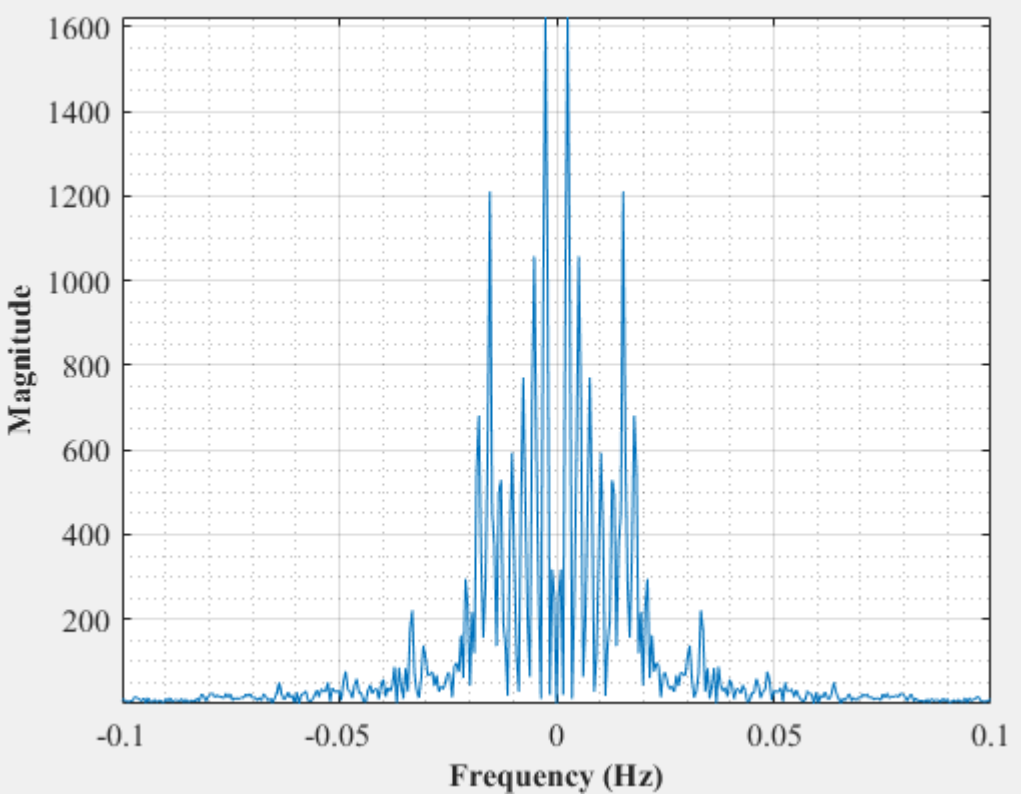


*Figure E-36: Dominant Frequency for a uniformly packed vessel at 2.67 dm3/minute rotameter flow rate- Test 1*

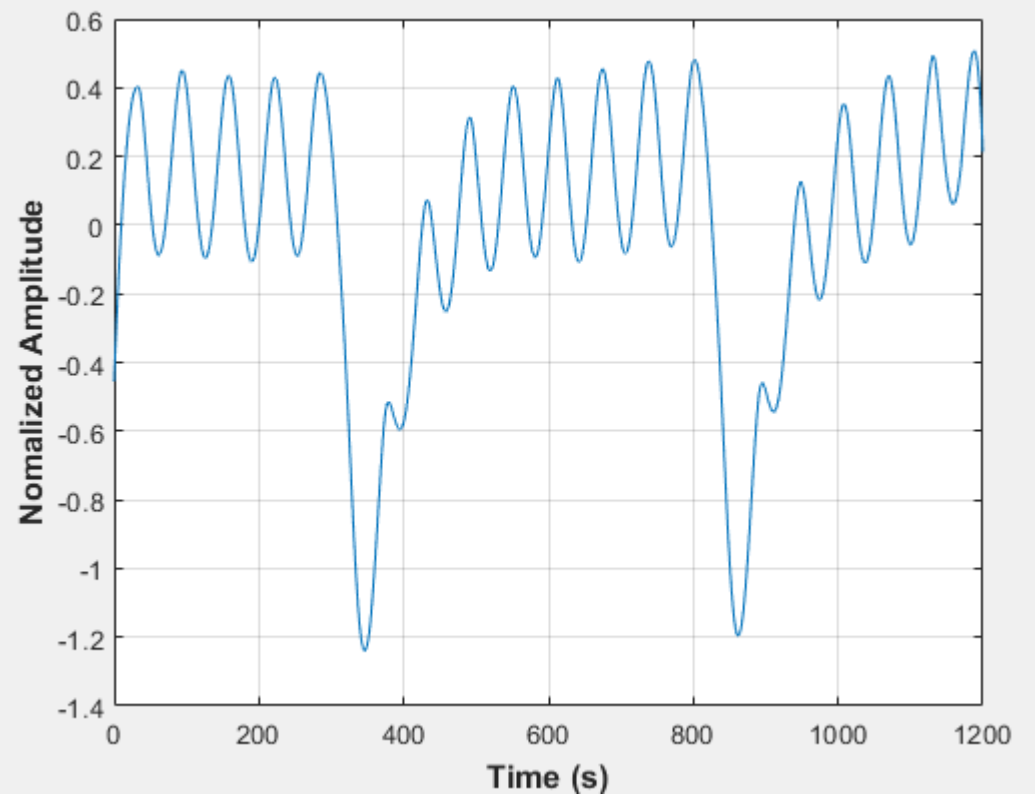


*Figure E-37: Pressure fluctuations in a uniformly packed vessel at 2.67 dm3/minute rotameter flow rate- Test 2*

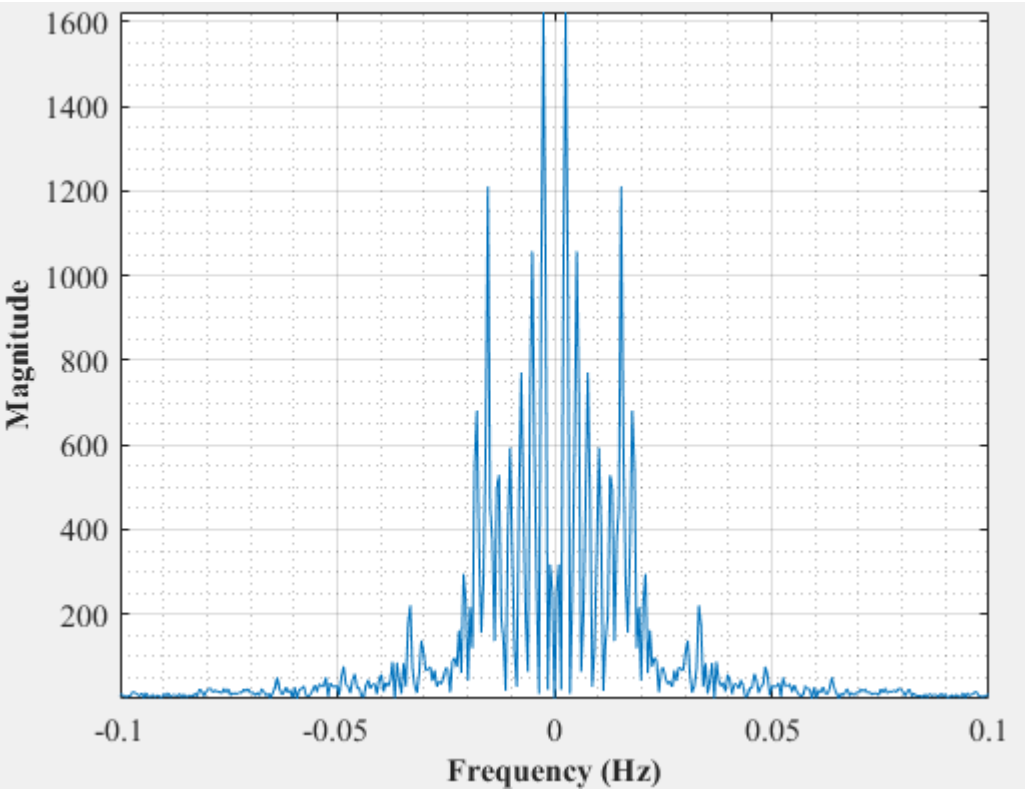


*Figure E-38: Dominant Frequency for a uniformly packed vessel at 2.67 dm3/minute rotameter flow rate- Test 2*

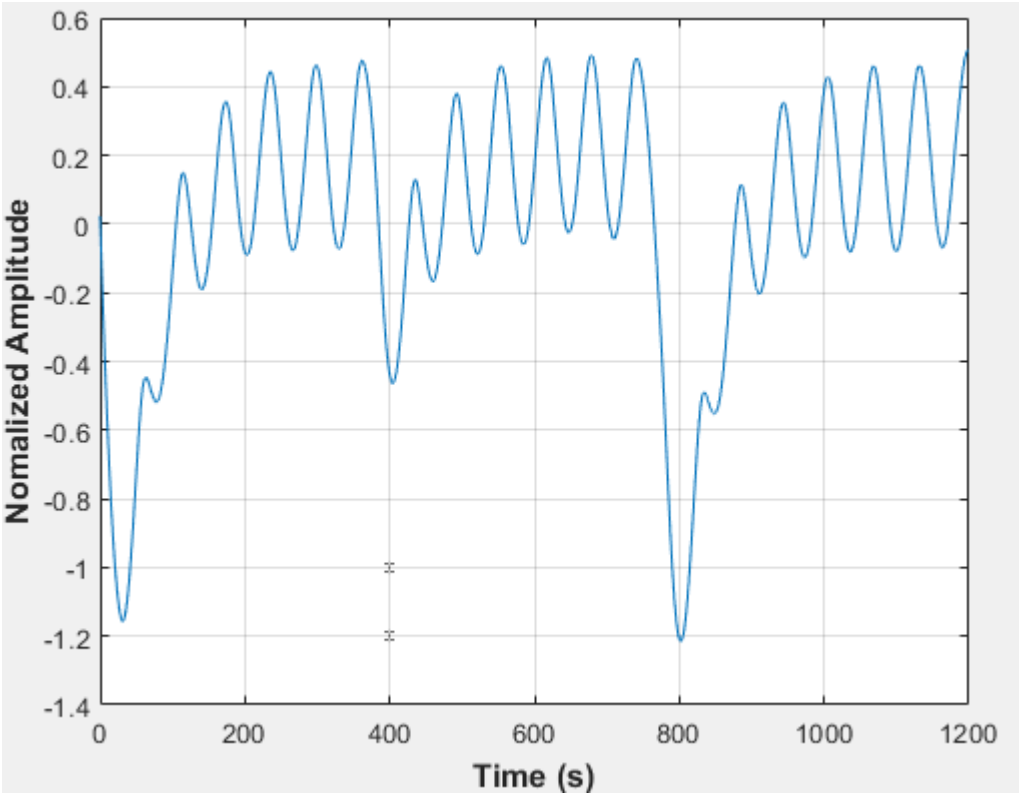


*Figure E-39: Pressure fluctuations in a uniformly packed vessel at 2.67 dm3/minute rotameter flow rate- Test 3*

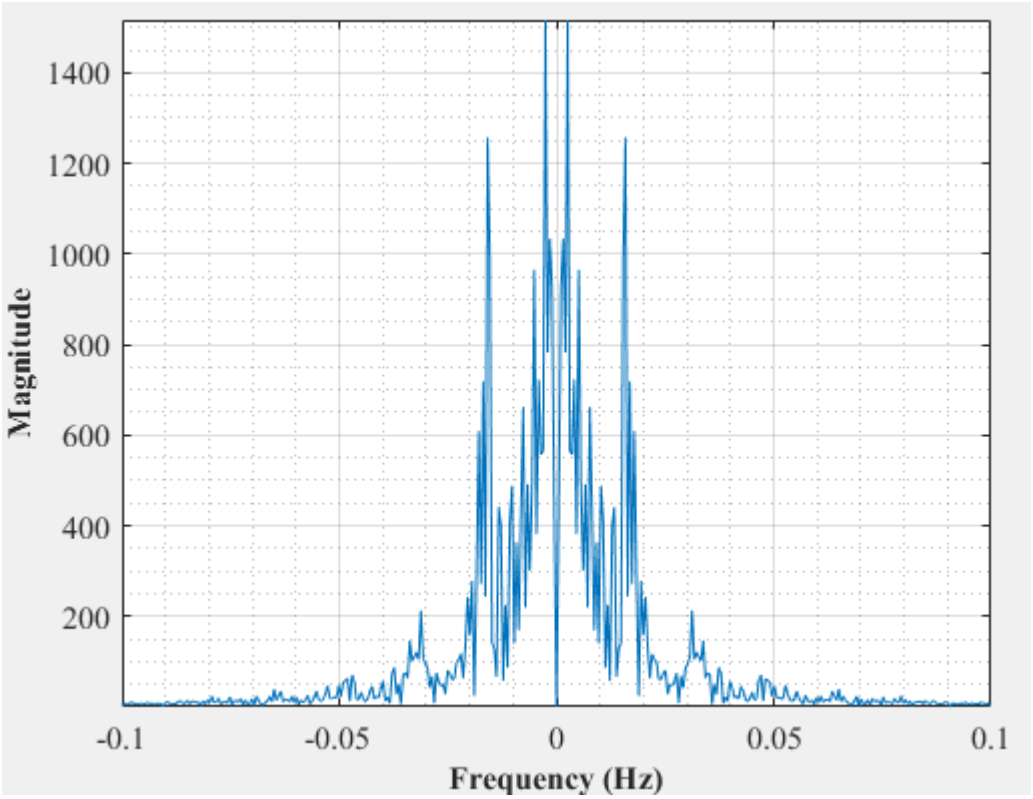


*Figure E-40: Dominant Frequency for a uniformly packed vessel at 2.67 dm3/minute rotameter flow rate- Test 3*

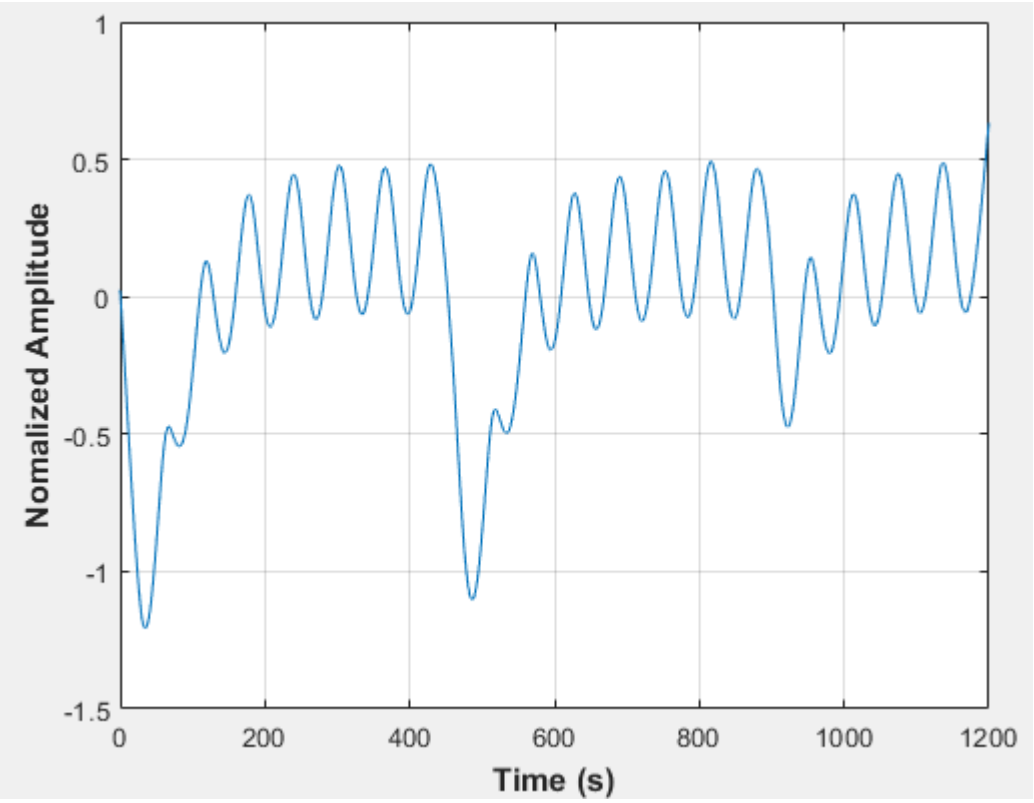


*Figure E-41: Pressure fluctuations in a uniformly packed vessel at 2.67 dm3/minute rotameter flow rate- Test 4*

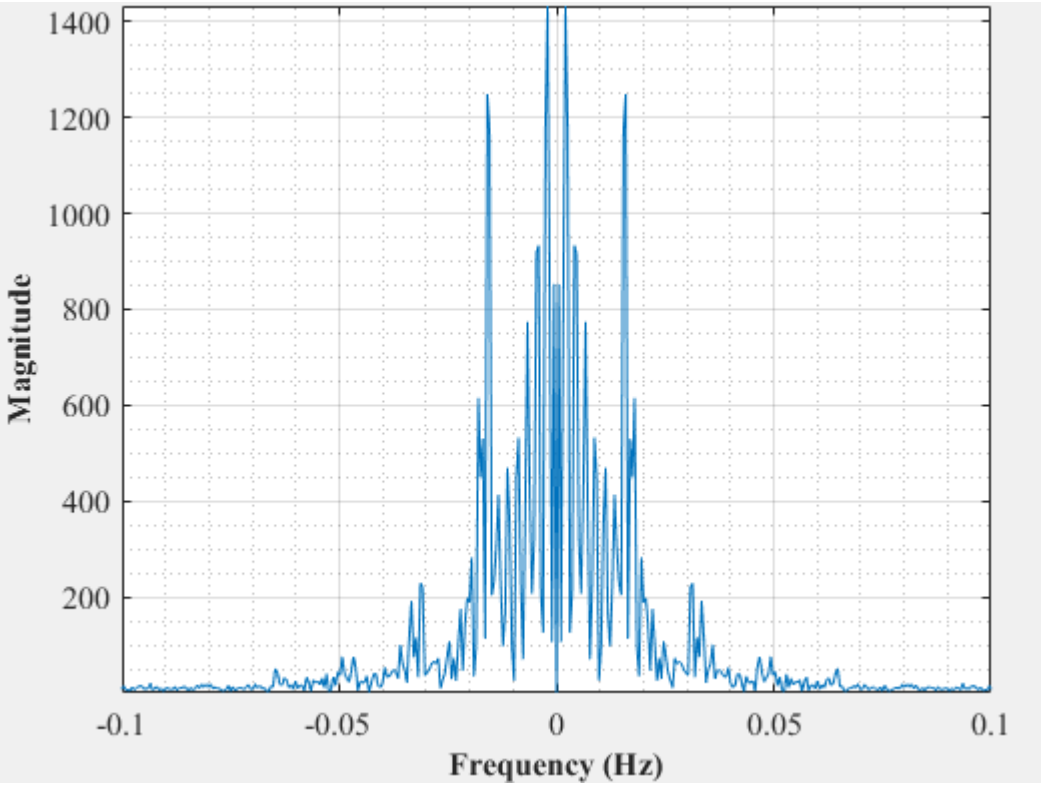


*Figure E-42: Dominant Frequency for a uniformly packed vessel at 2.67 dm3/minute rotameter flow rate- Test 4*

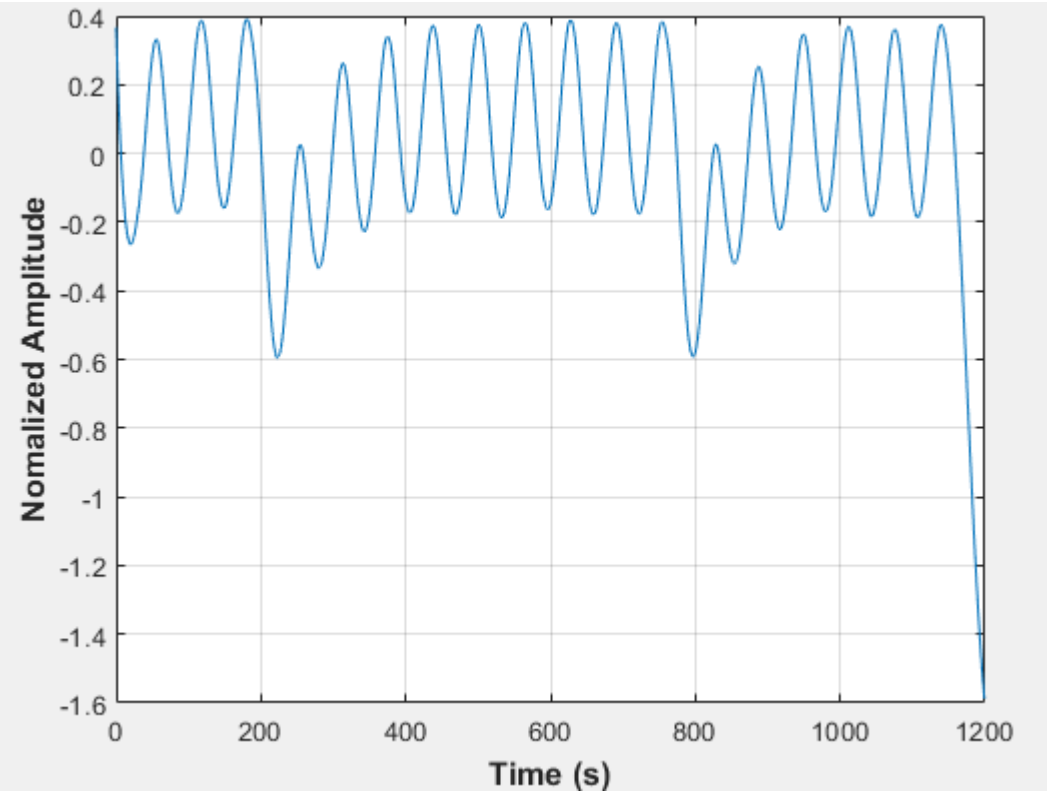


*Figure E-43: Pressure fluctuations in a uniformly packed vessel at 2.67 dm3/minute rotameter flow rate- Test 5*

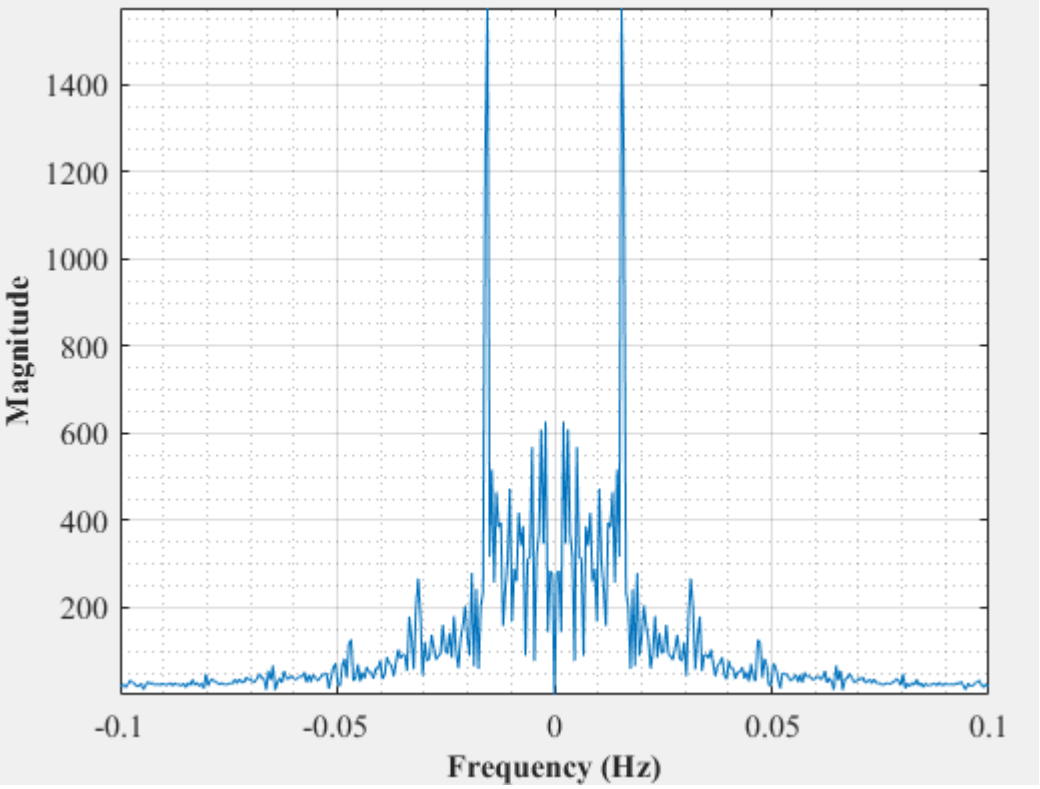


*Figure E-44: Dominant Frequency for a uniformly packed vessel at 2.67 dm3/minute rotameter flow rate- Test 5*

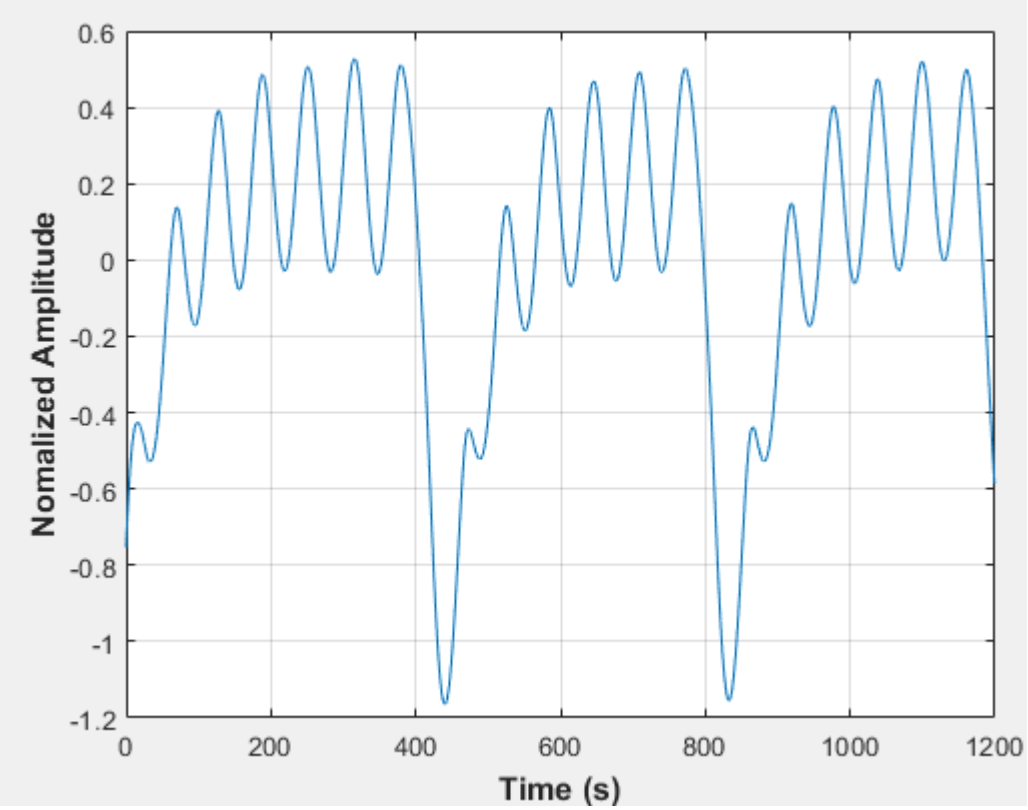


*Figure E-45: Pressure fluctuations in a uniformly packed vessel at 2.67 dm3/minute rotameter flow rate- Test 6*

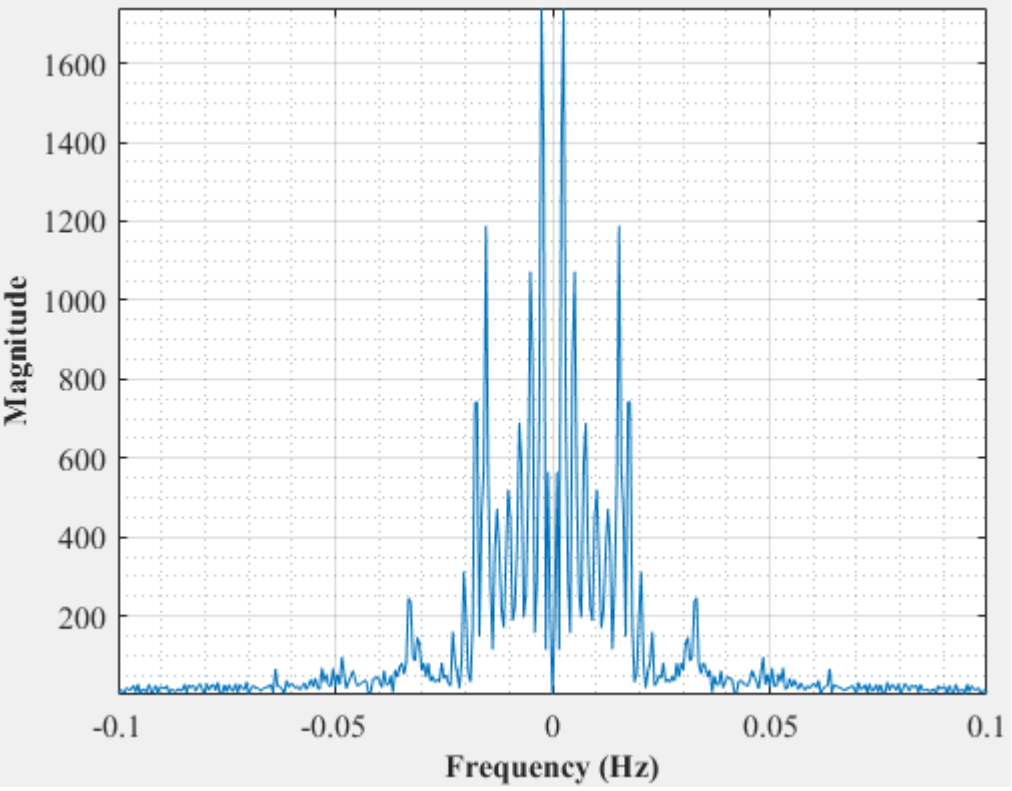


*Figure E-46: Dominant Frequency for a uniformly packed vessel at 2.67 dm3/minute rotameter flow rate- Test 6*

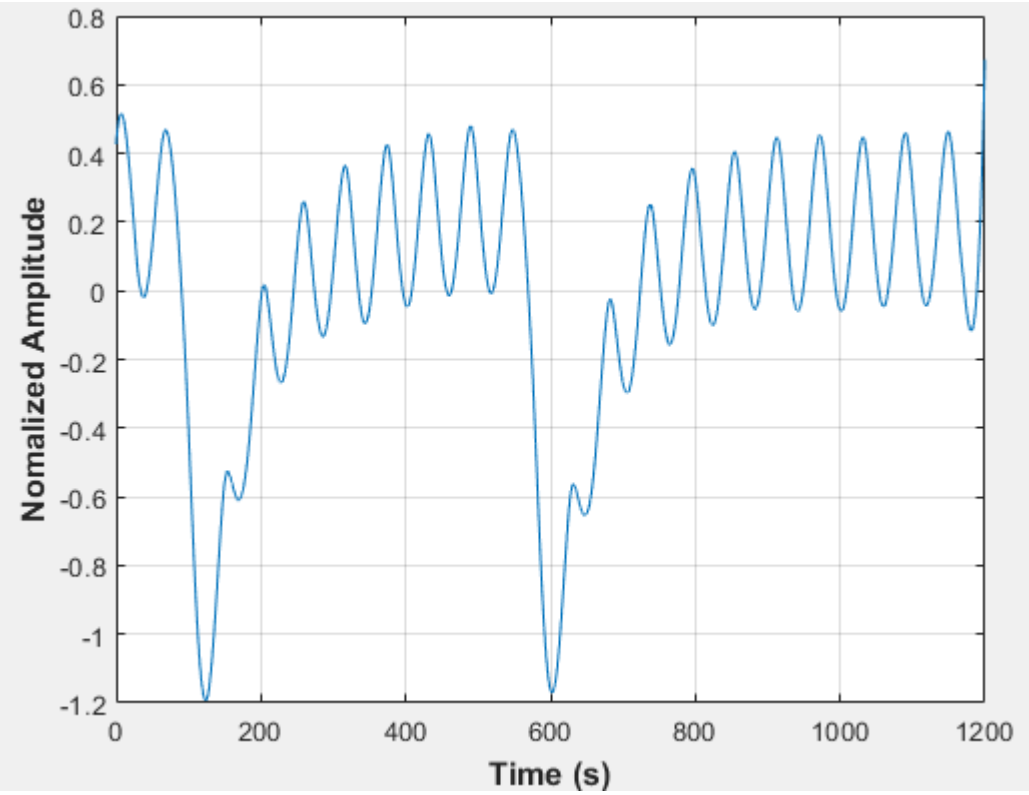


*Figure E-47: Pressure fluctuations in a uniformly packed vessel at 2.83 dm3/minute rotameter flow rate- Test 1*

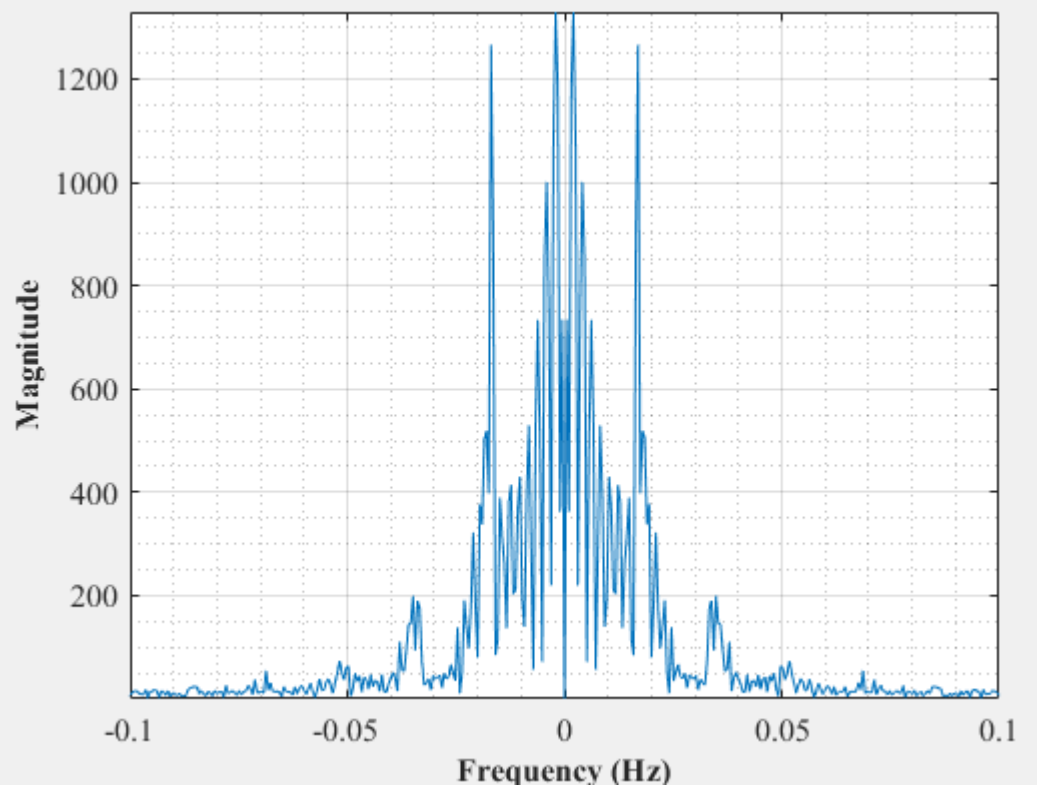


*Figure E-48: Dominant Frequency for a uniformly packed vessel at 2.83 dm3/minute rotameter flow rate- Test 1*

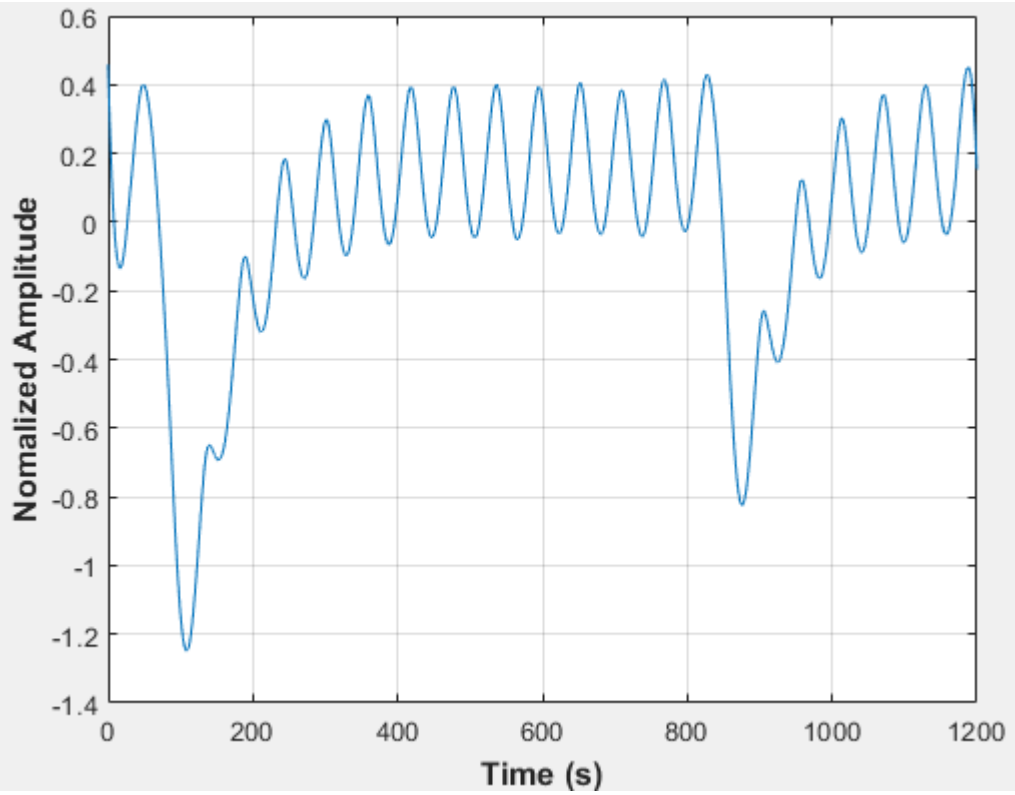


*Figure E-49: Pressure fluctuations in a uniformly packed vessel at 2.83 dm3/minute rotameter flow rate- Test 2*

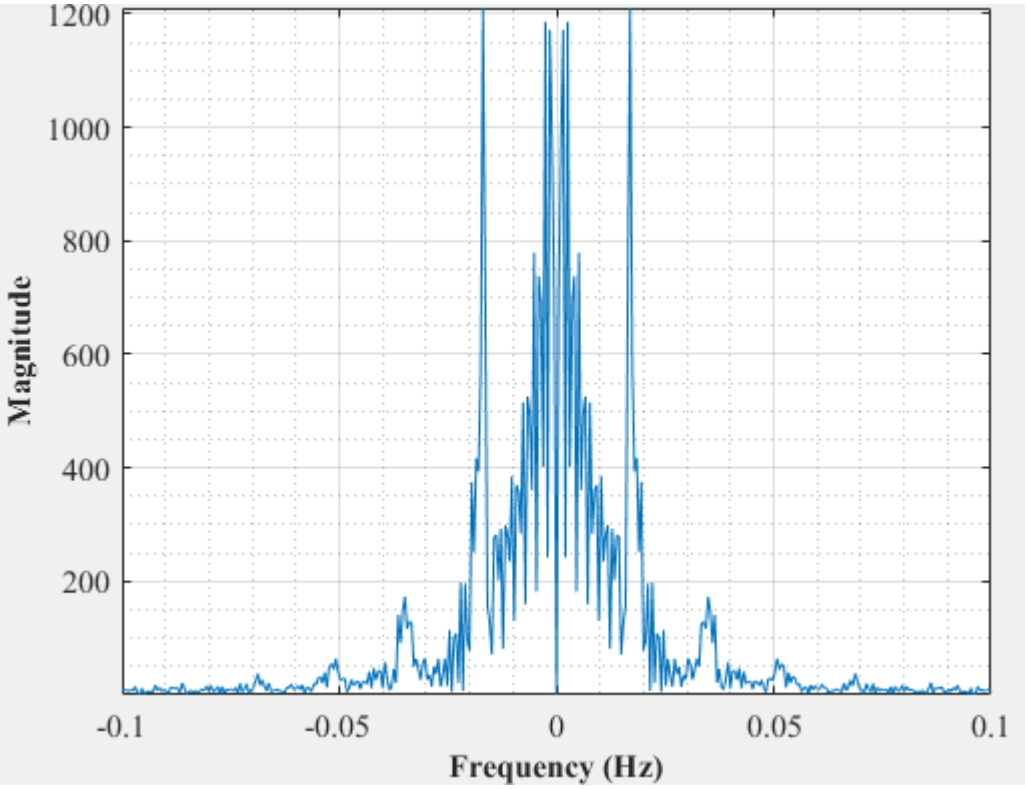


*Figure E-50: Dominant Frequency for a uniformly packed vessel at 2.83 dm3/minute rotameter flow rate- Test 2*

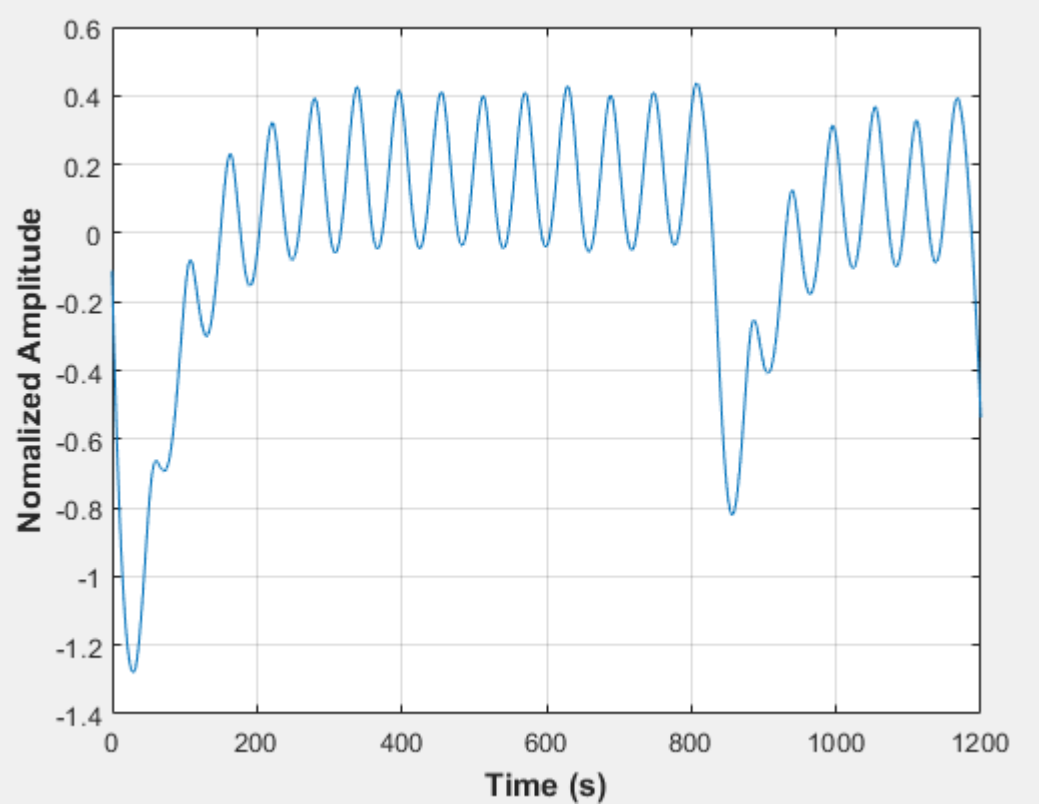


*Figure E-51: Pressure fluctuations in a uniformly packed vessel at 2.83 dm3/minute rotameter flow rate- Test 3*

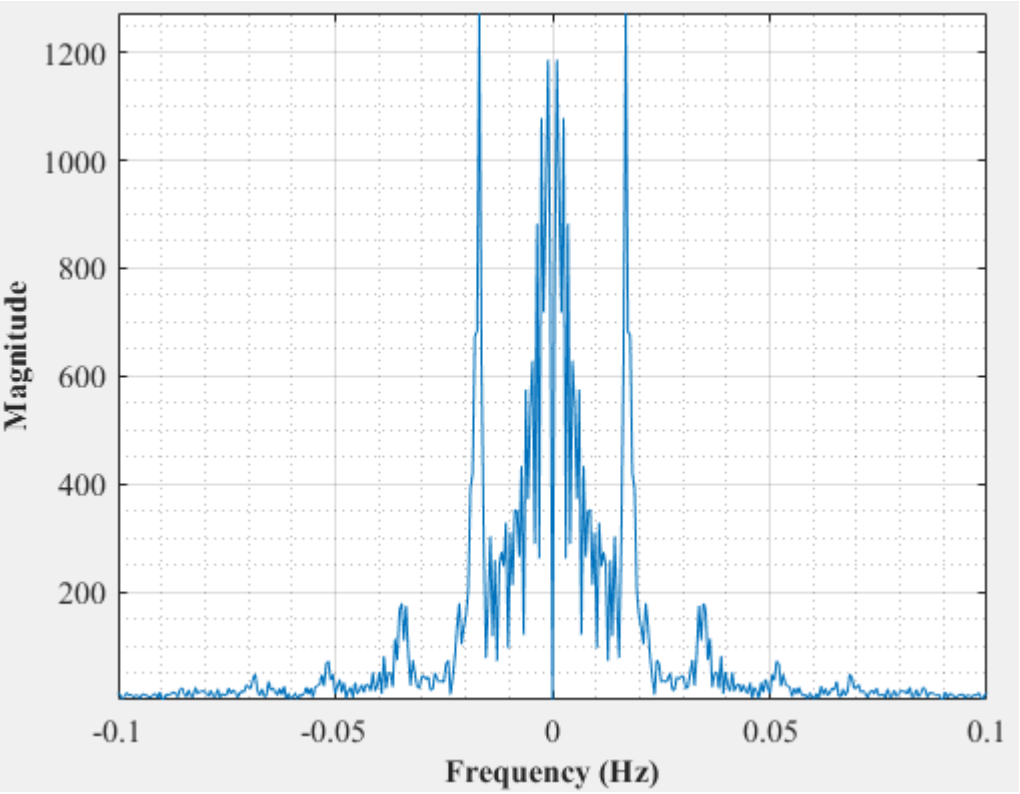


*Figure E-52: Dominant Frequency for a uniformly packed vessel at 2.83 dm3/minute rotameter flow rate- Test 3*

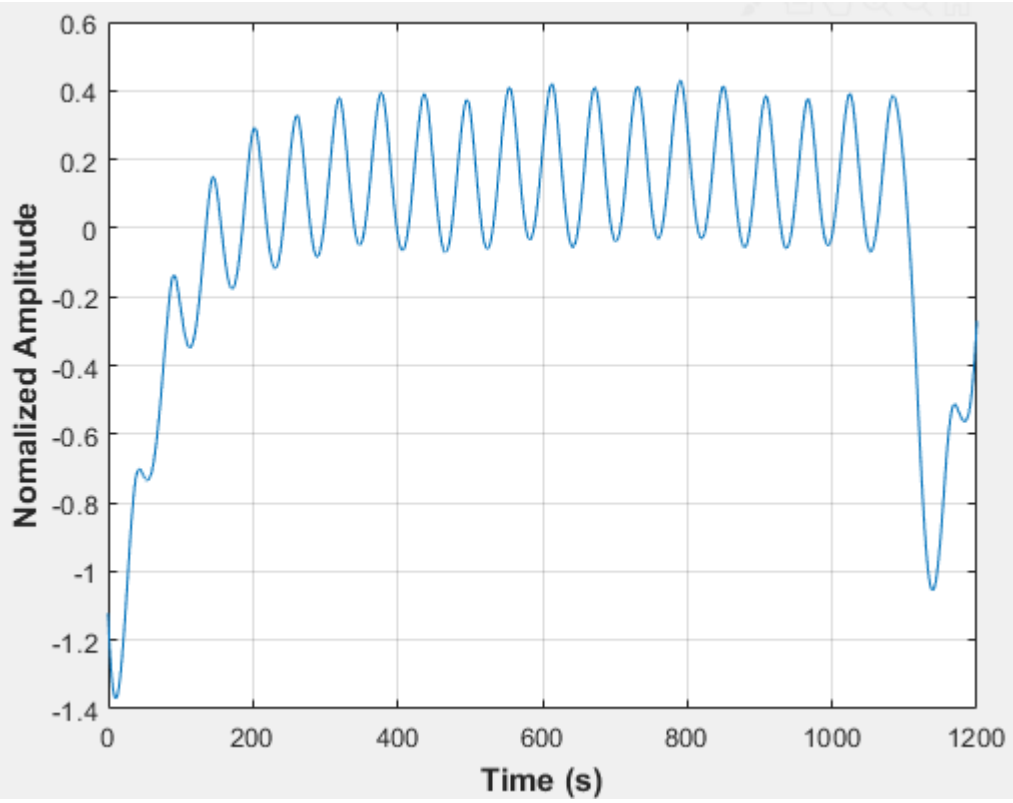


*Figure E-53: Pressure fluctuations in a uniformly packed vessel at 2.83 dm3/minute rotameter flow rate- Test 4*

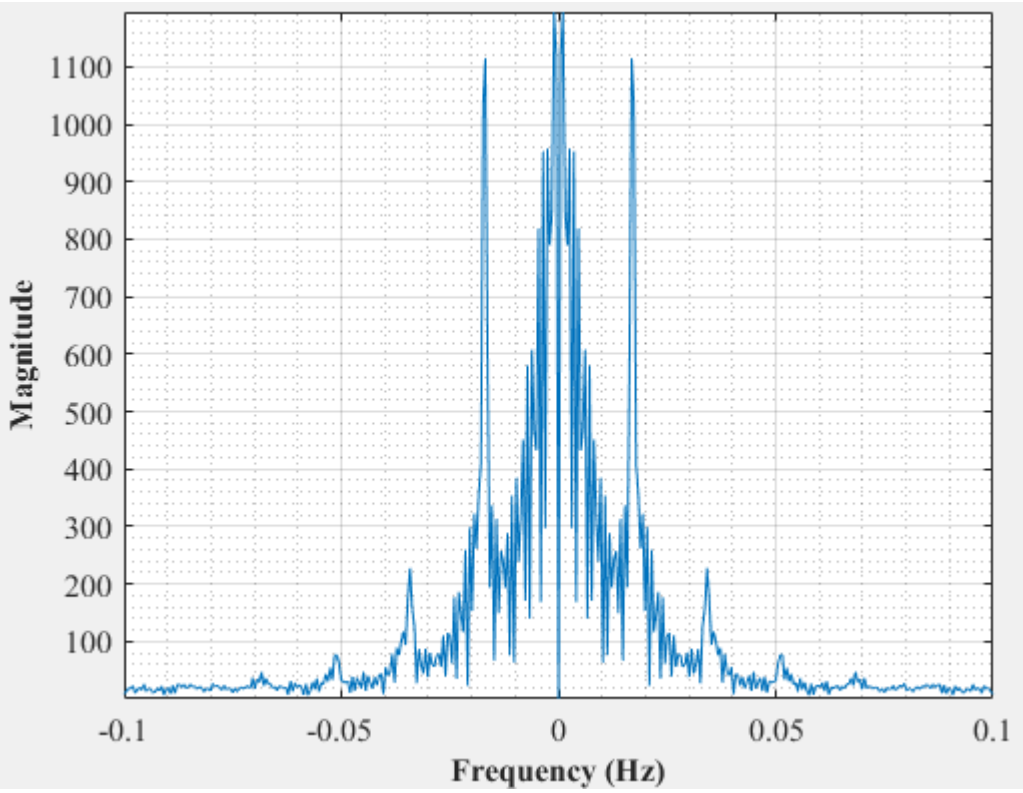


*Figure E-54: Dominant Frequency for a uniformly packed vessel at 2.83 dm3/minute rotameter flow rate- Test 4*

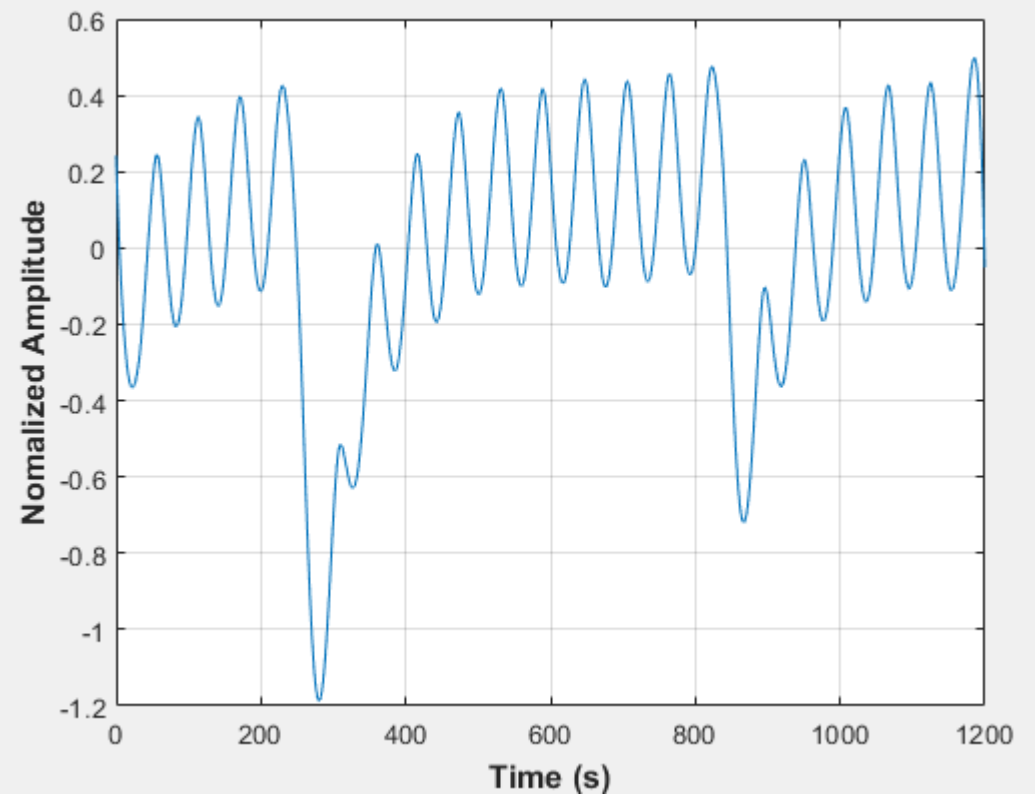


*Figure E-55: Pressure fluctuations in a uniformly packed vessel at 2.83 dm3/minute rotameter flow rate- Test 5*

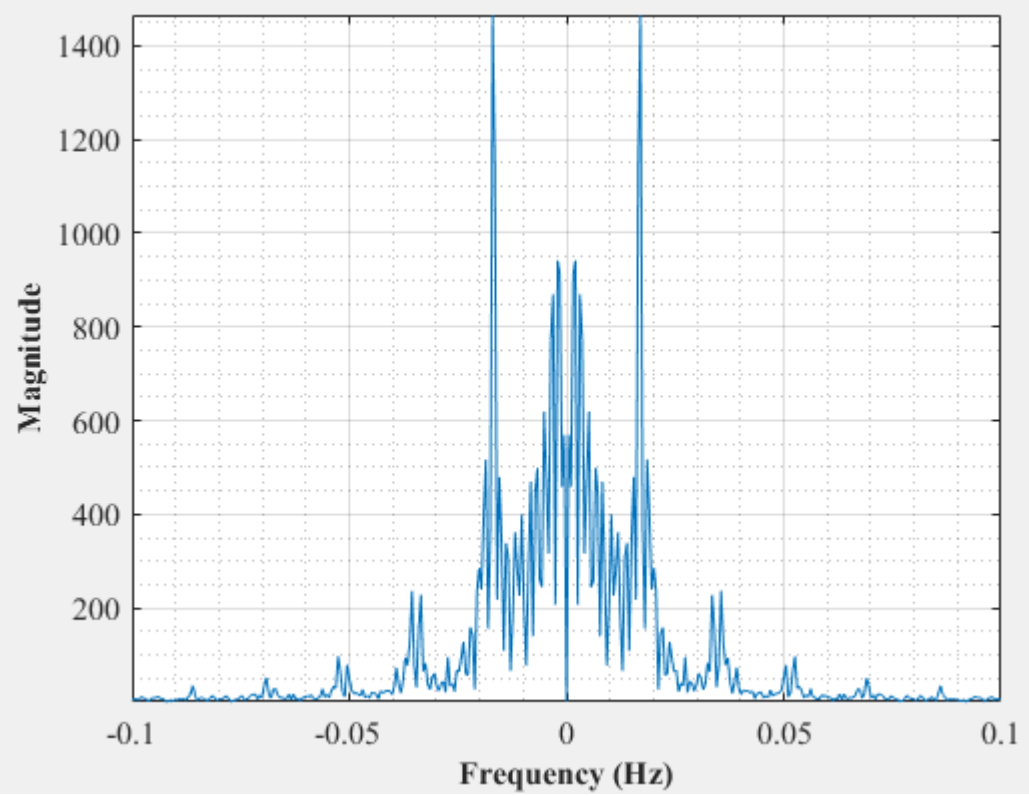


*Figure E-56: Dominant Frequency for a uniformly packed vessel at 2.83 dm3/minute rotameter flow rate- Test 5*

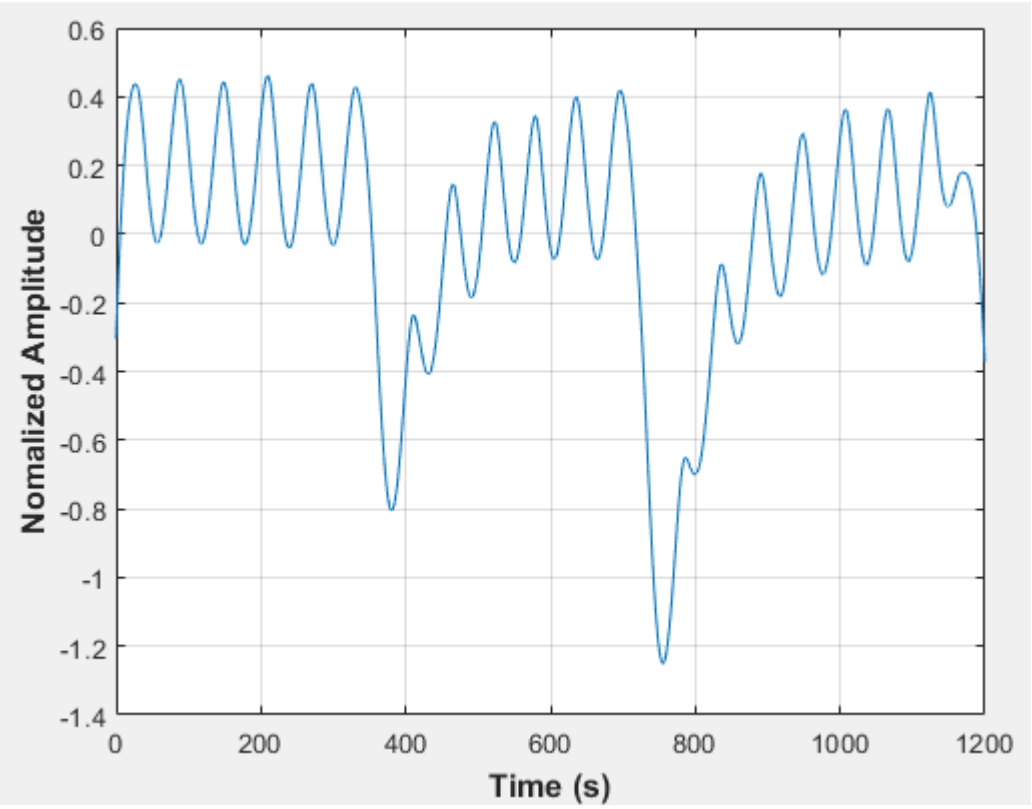


*Figure E-57: Pressure fluctuations in a uniformly packed vessel at 2.83 dm3/minute rotameter flow rate- Test 6*

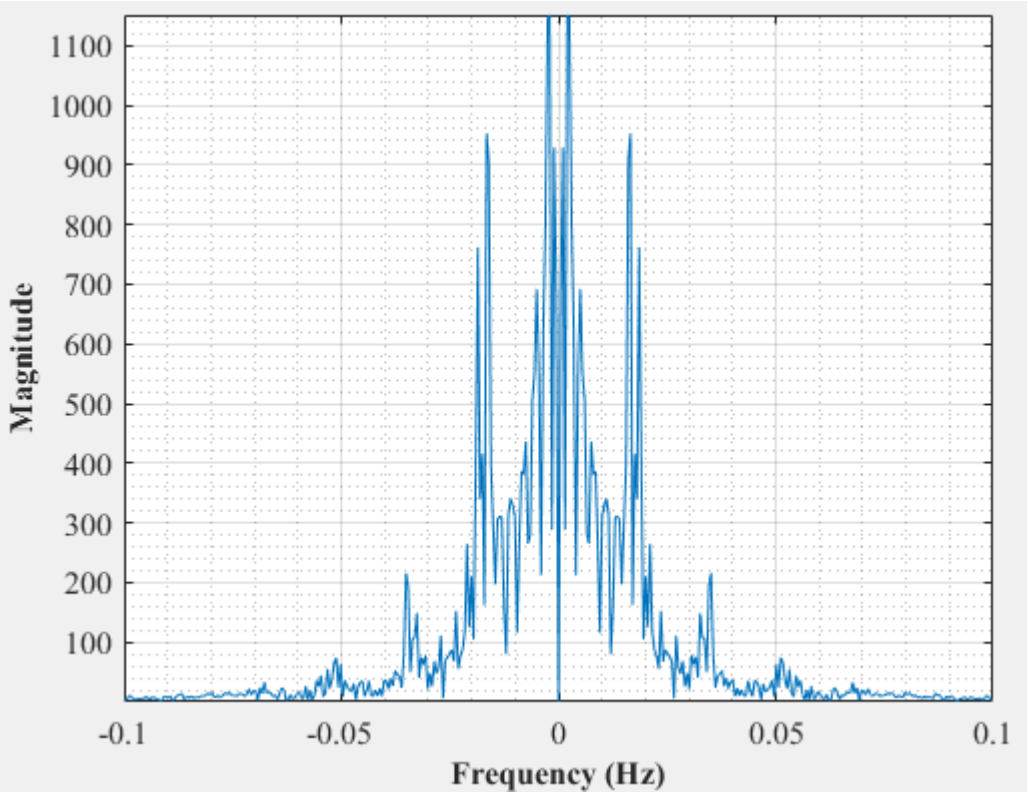


*Figure E-58: Dominant Frequency for a uniformly packed vessel at 2.83 dm3/minute rotameter flow rate- Test 6*

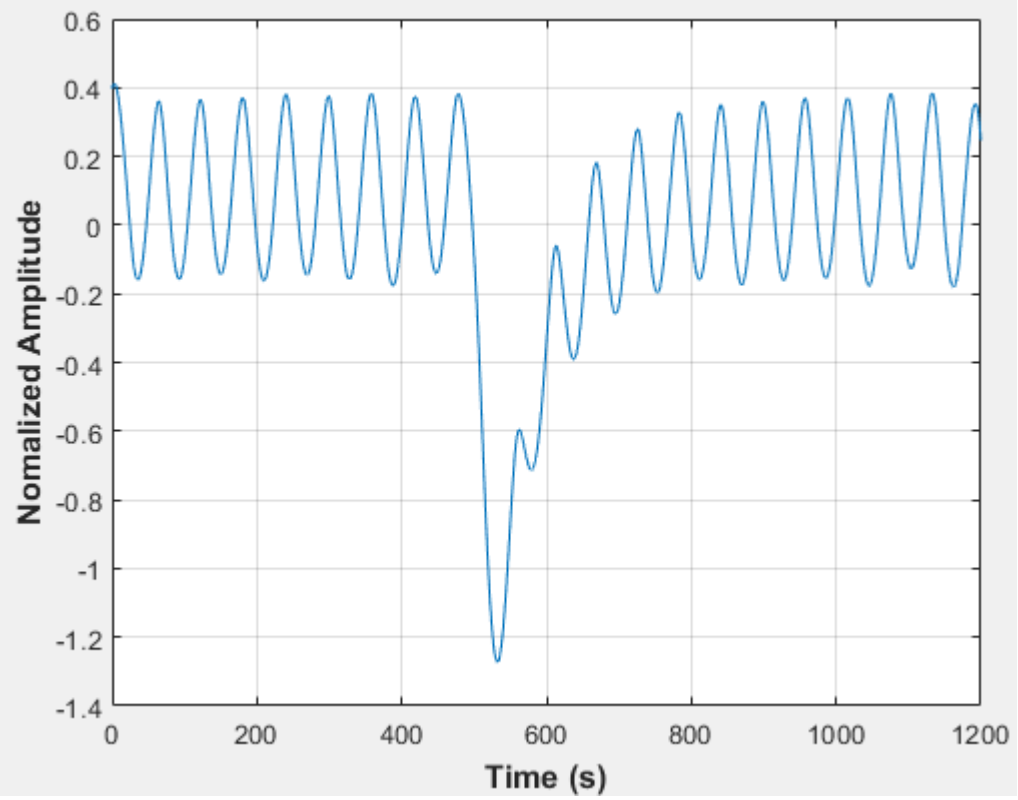


*Figure E-59: Pressure fluctuations in a uniformly packed vessel at 2.83 dm3/minute rotameter flow rate- Test 7*

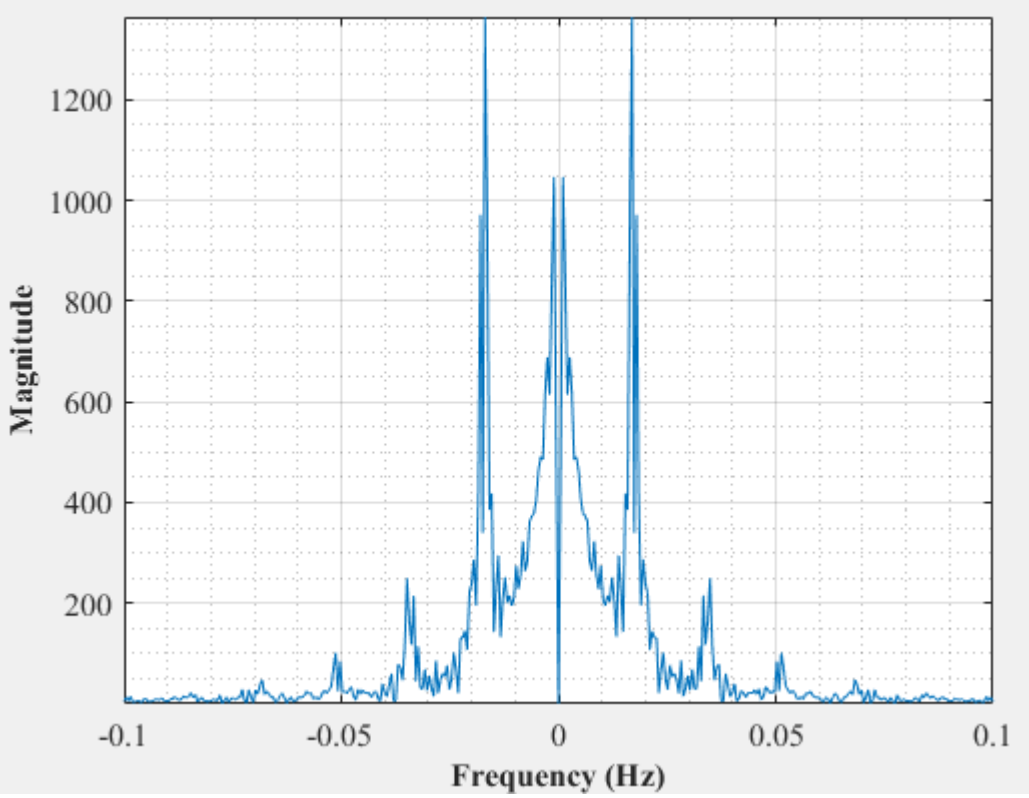


*Figure E-60: Dominant Frequency for a uniformly packed vessel at 2.83 dm3/minute rotameter flow rate- Test 7*

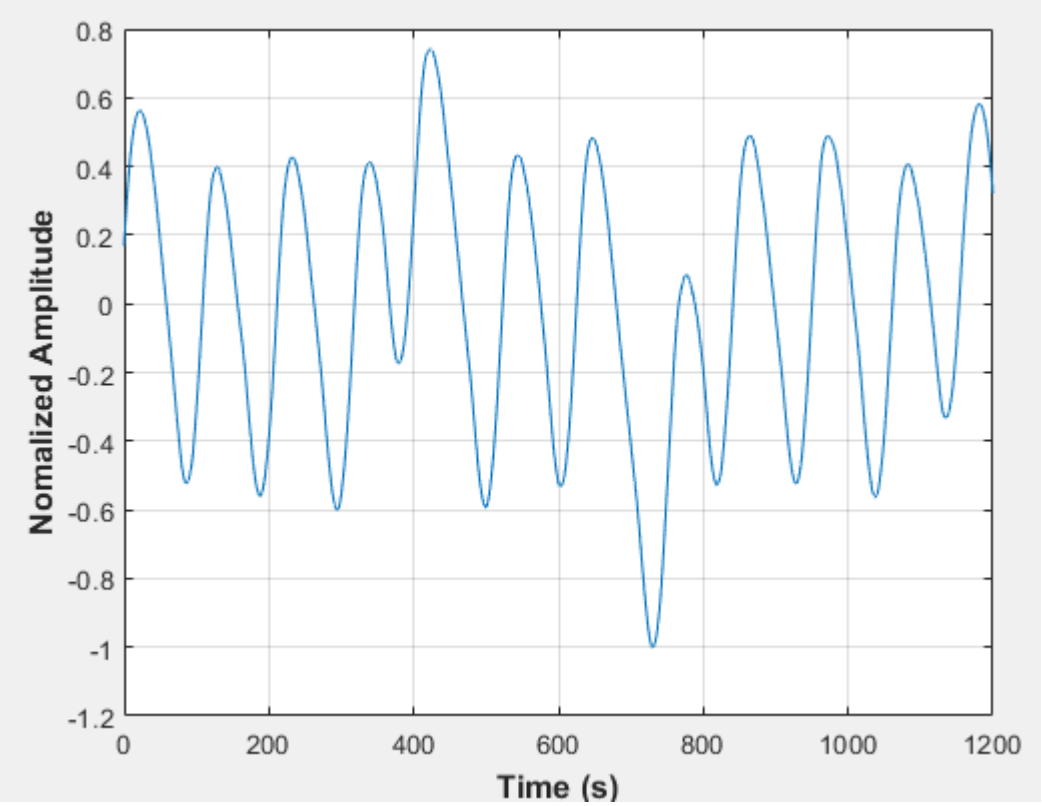


*Figure E-61: Pressure fluctuations in a non-uniformly packed vessel (large and small at the center) at 1.67 dm3/minute rotameter flow rate- Test 1*

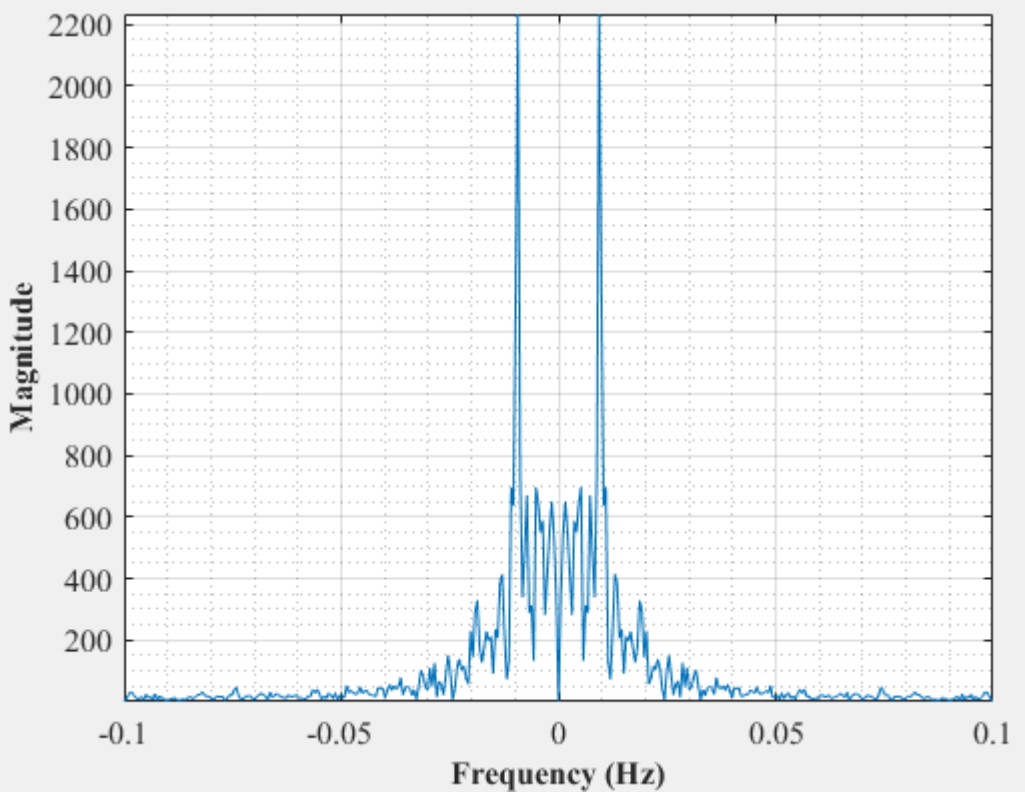


*Figure E-62: Dominant Frequency for a non-uniformly packed vessel (large and small at the center) at 1.67 $dm^3$/minute rotameter flow rate- Test 1*

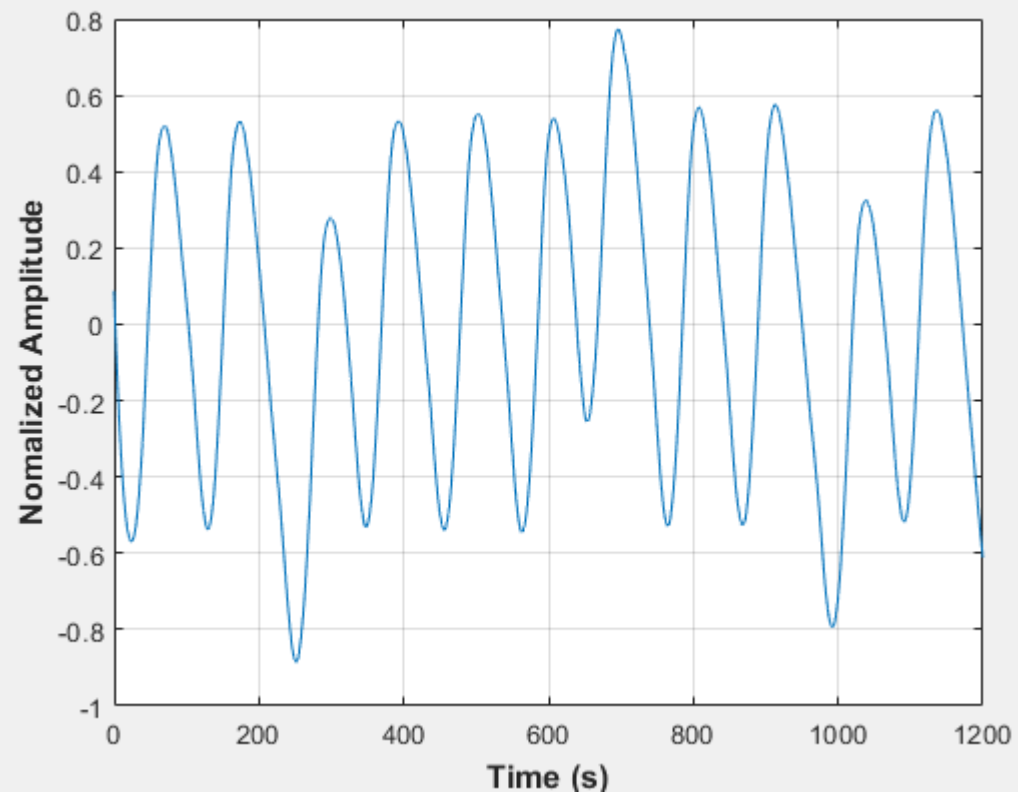


*Figure E-63: Pressure fluctuations in a non-uniformly packed vessel (large and small at the center) at 1.67 dm$^3$/minute rotameter flow rate- Test 2*

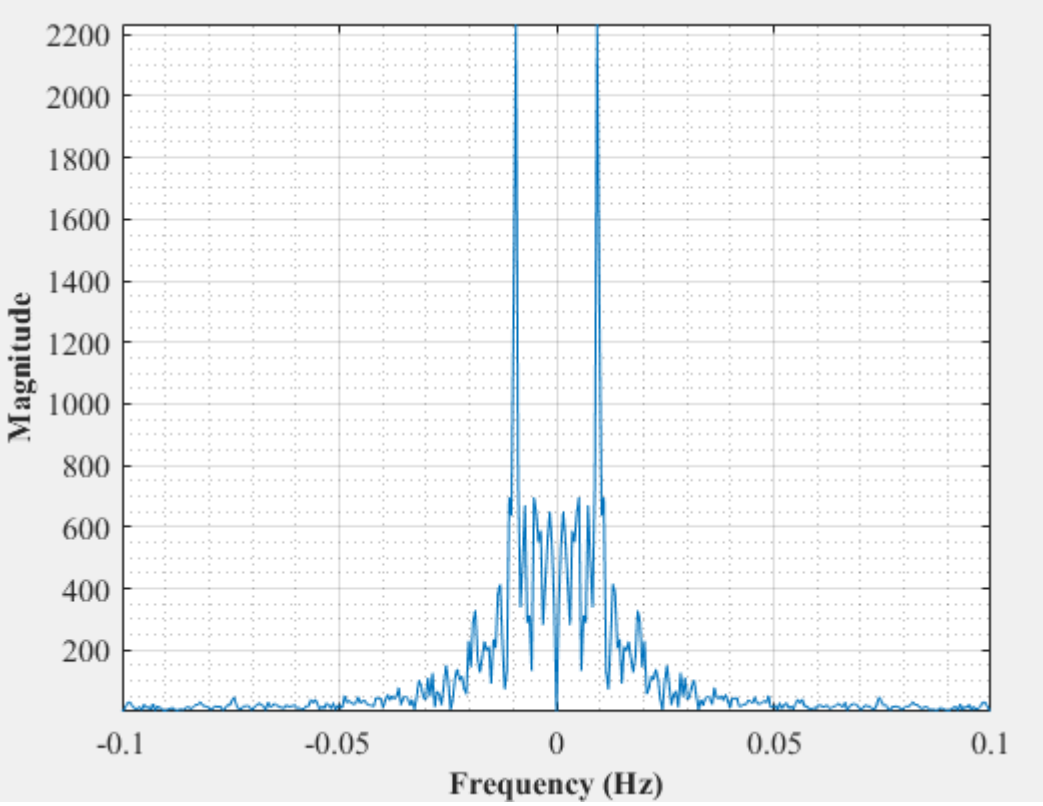


*Figure E-64: Dominant Frequency for a non-uniformly packed vessel (large and small at the center) at 1.67 dm$^3$/minute rotameter flow rate- Test 2*

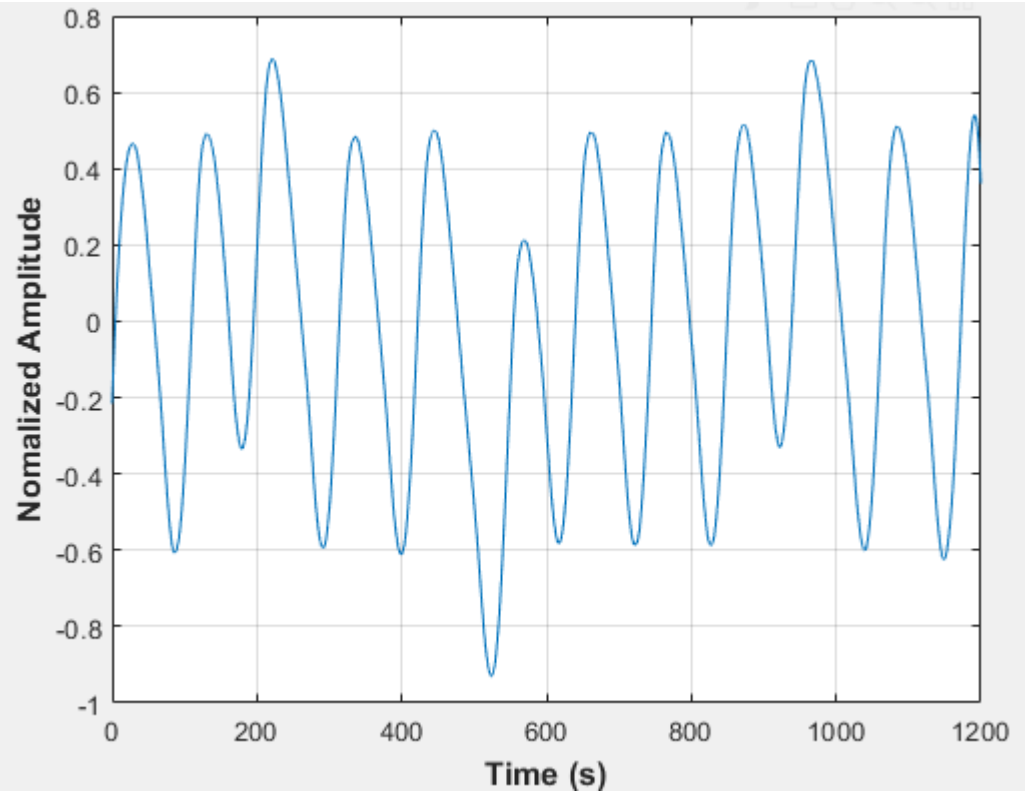


*Figure E-65: Pressure fluctuations in a non-uniformly packed vessel (large and small at the center) at 1.67 dm$^3$/minute rotameter flow rate- Test 3*

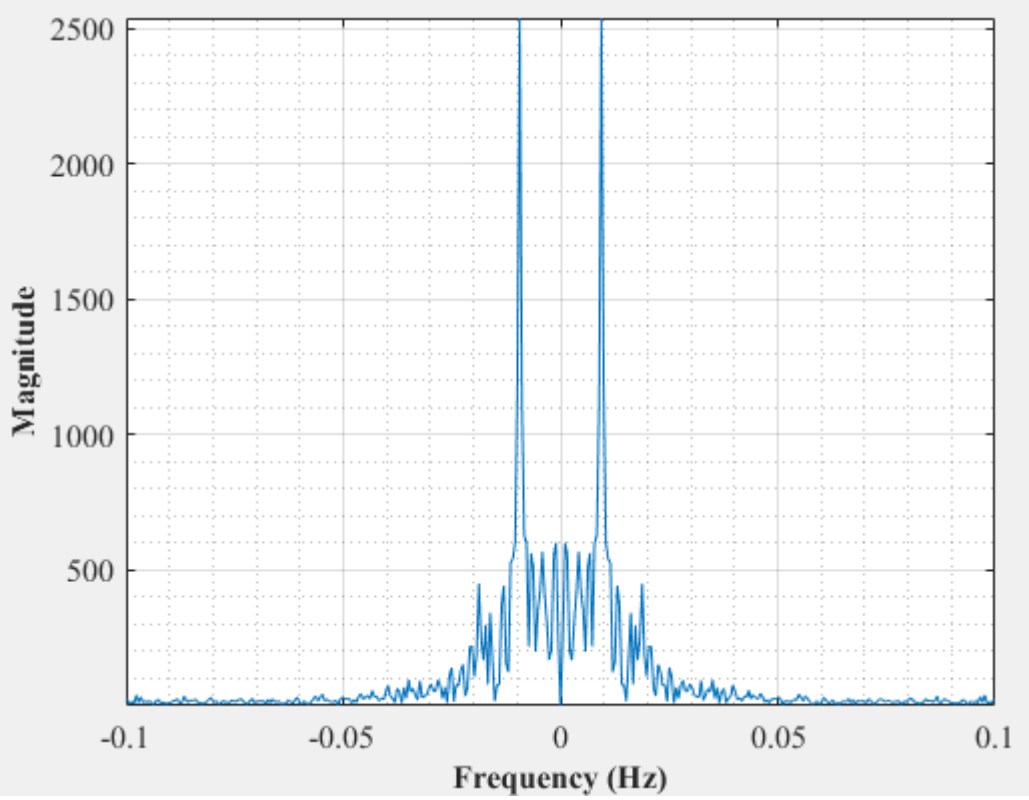


*Figure E-66: Dominant Frequency for a non-uniformly packed vessel (large and small at the center) at 1.67 dm$^3$/minute rotameter flow rate- Test 3*

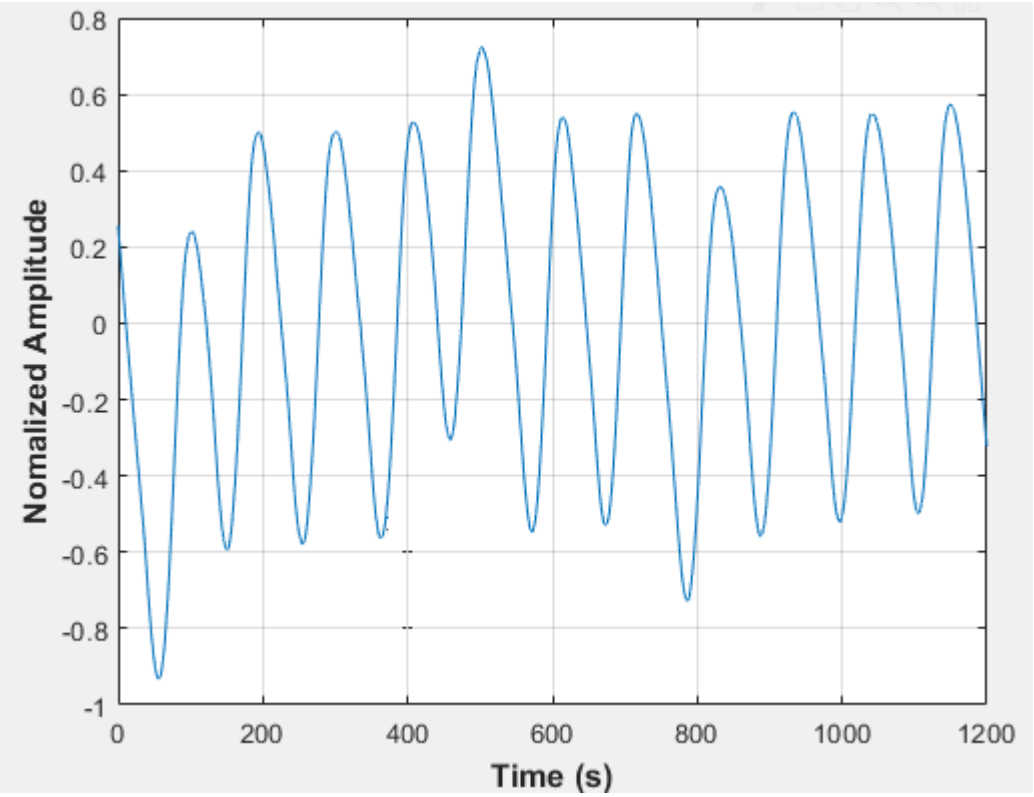


*Figure E-67: Pressure fluctuations in a non-uniformly packed vessel (large and small at the center) at 1.67 dm$^3$/minute rotameter flow rate- Test 4*

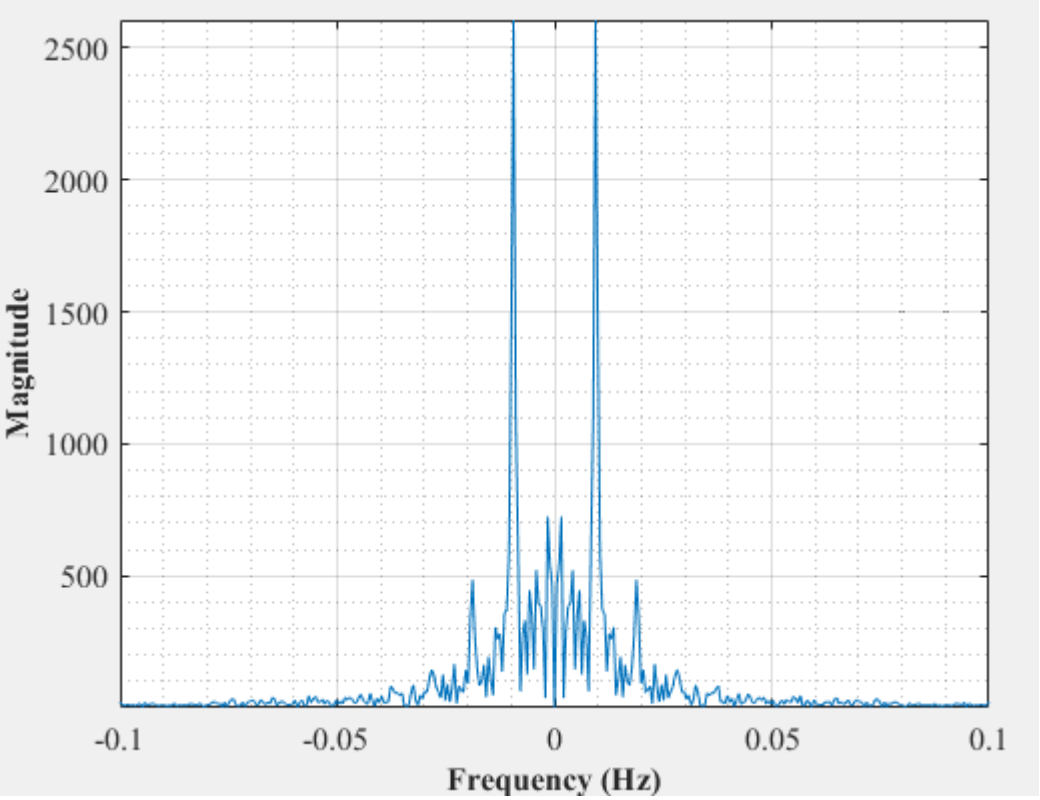


*Figure E-68: Dominant Frequency for a non-uniformly packed vessel (large and small at the center) at 1.67 dm$^3$/minute rotameter flow rate- Test 4*

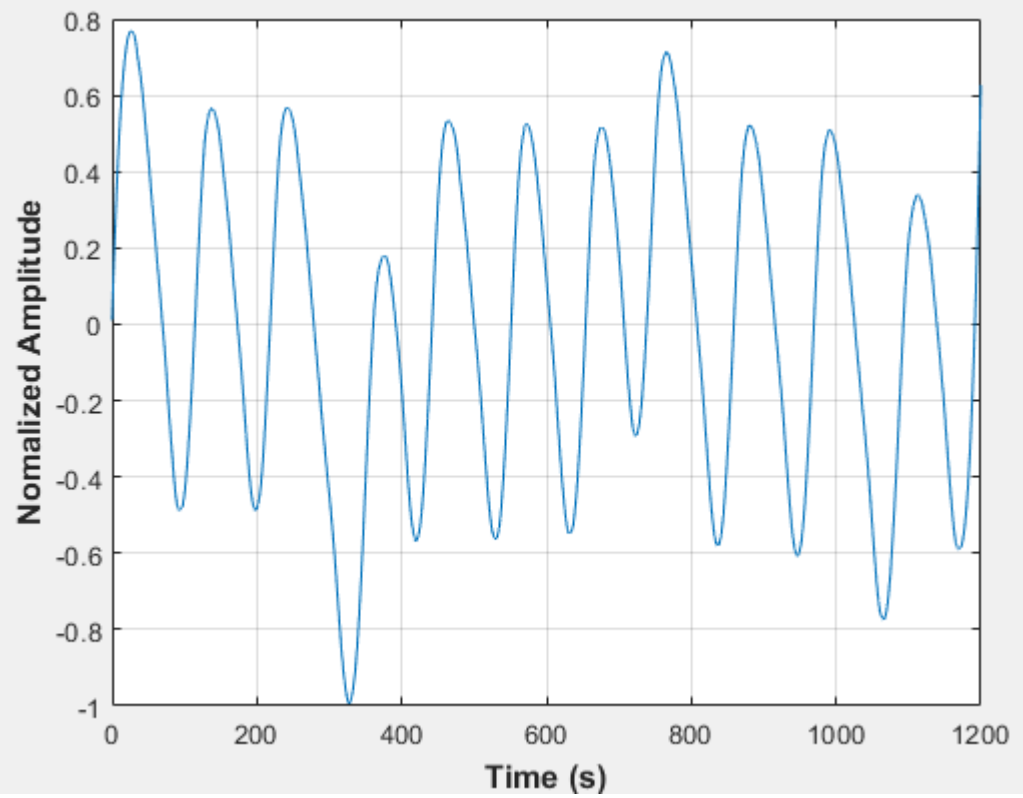


*Figure E-69: Pressure fluctuations in a non-uniformly packed vessel (large and small at the center) at 1.67 dm$^3$/minute rotameter flow rate- Test 5*

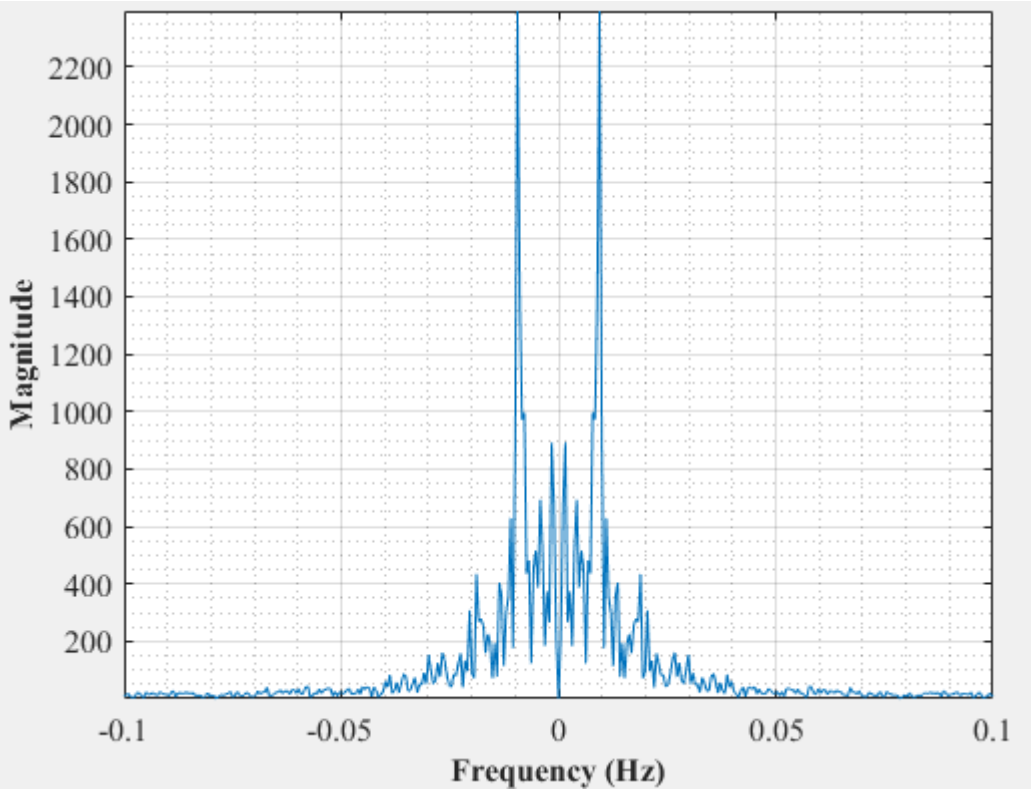


*Figure E-70: Dominant Frequency for a non-uniformly packed vessel (large and small at the center) at 1.67 dm$^3$/minute rotameter flow rate- Test 5*

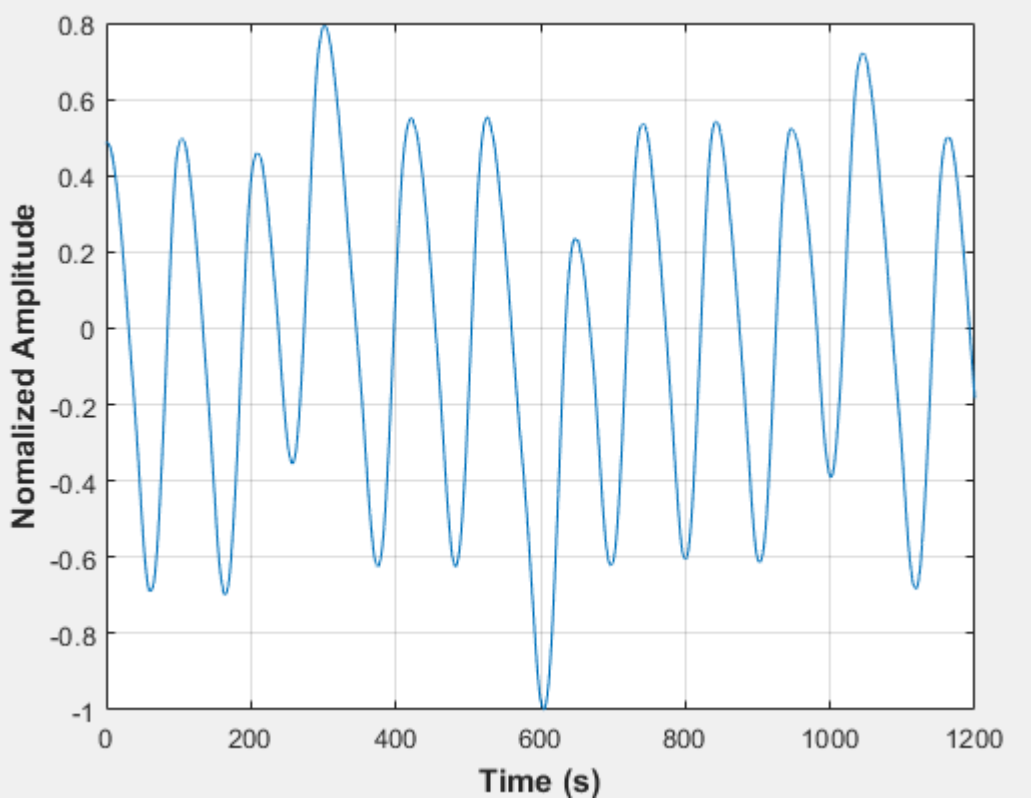


*Figure E-71: Pressure fluctuations in a non-uniformly packed vessel (large and small at the center) at 1.67 $dm^3$/minute rotameter flow rate- Test 6*

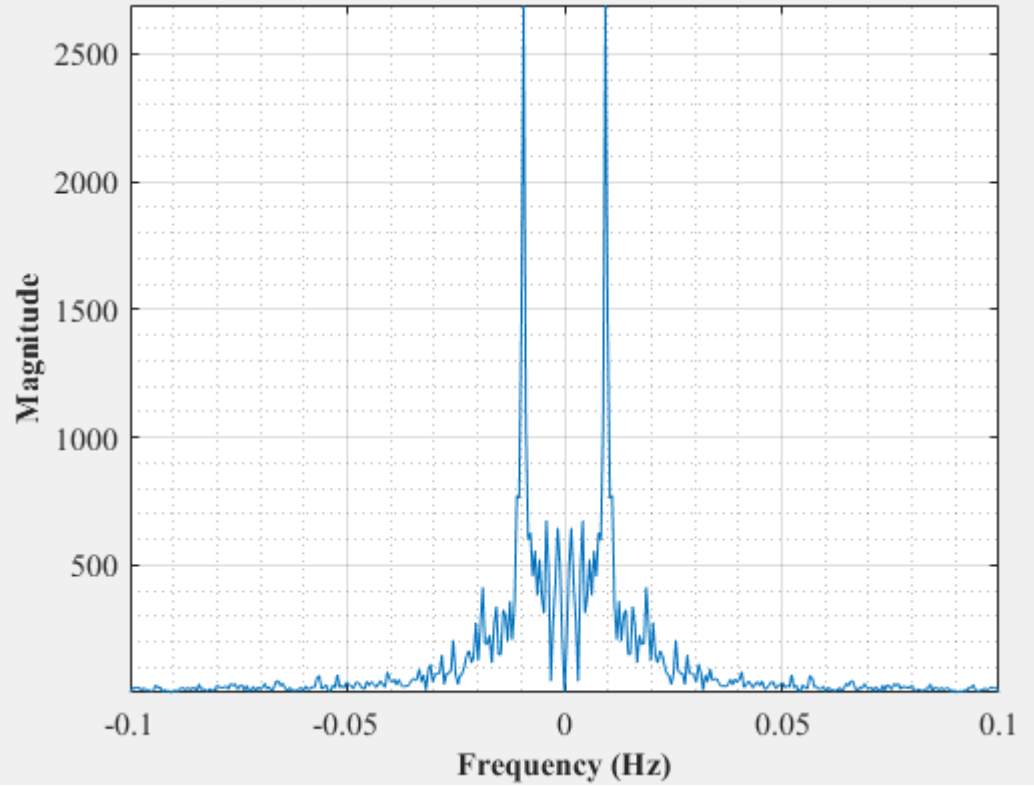


*Figure E-72: Dominant Frequency for a non-uniformly packed vessel (large and small at the center) at 1.67 $dm^3$/minute rotameter flow rate- Test 6*

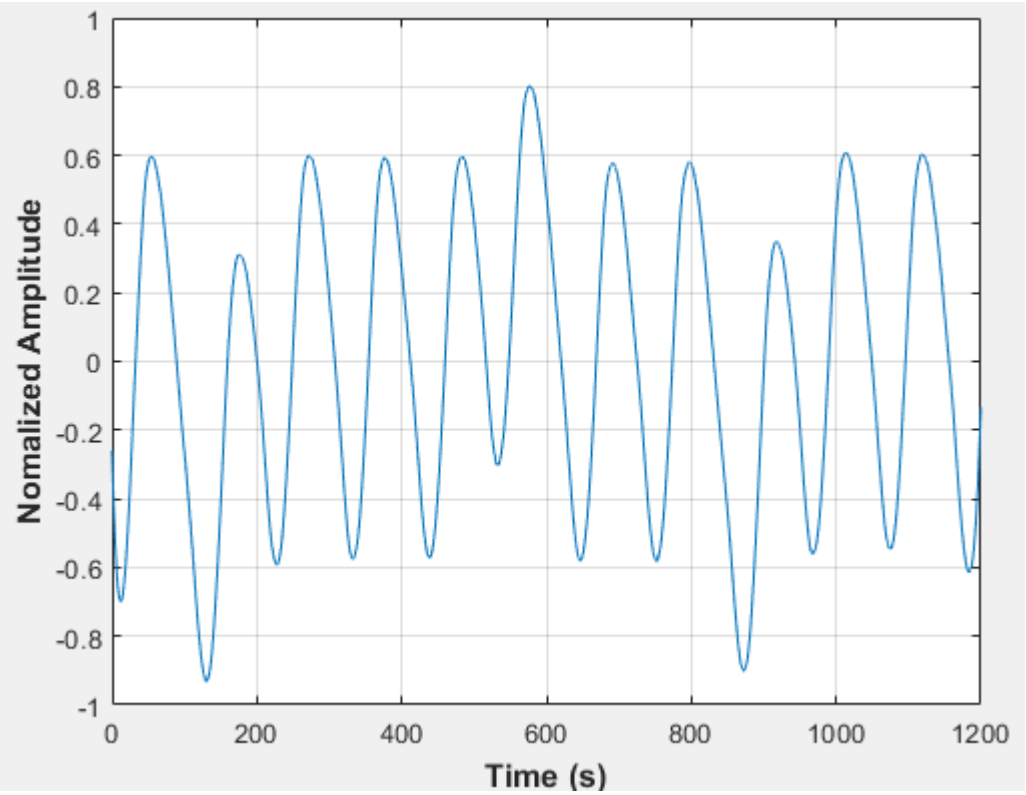


*Figure E-73: Pressure fluctuations in a non-uniformly packed vessel (large and small at the center) at 1.67 dm$^3$/minute rotameter flow rate- Test 7*

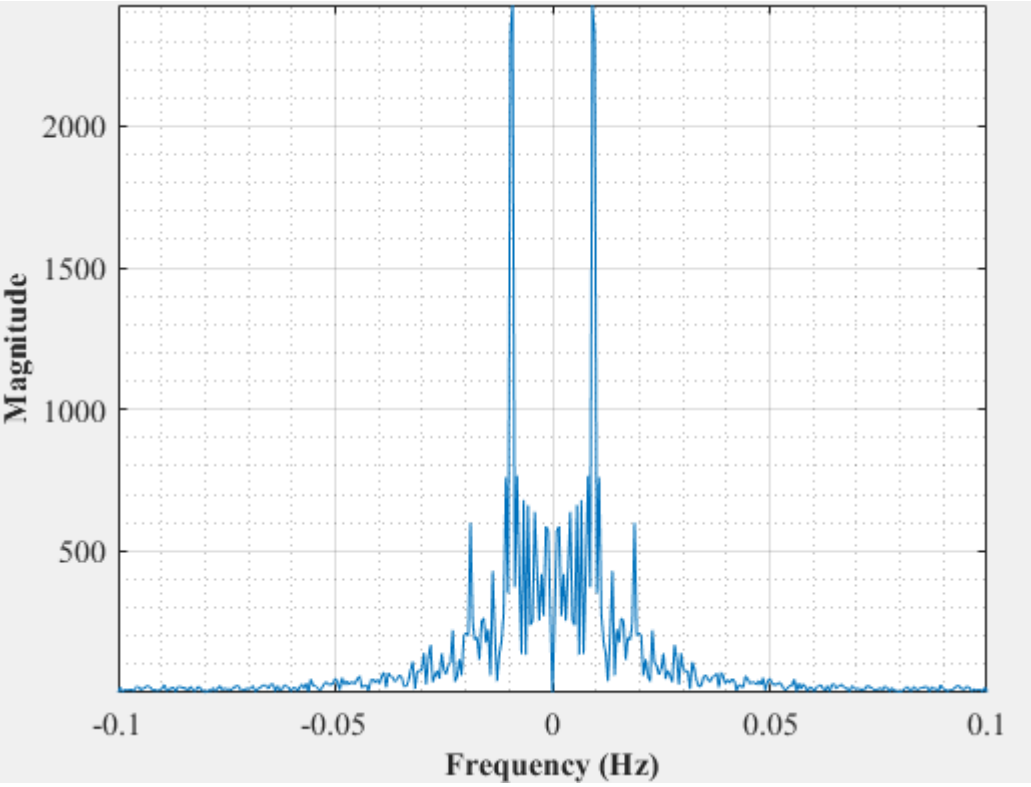


*Figure E-74: Dominant Frequency for a non-uniformly packed vessel (large and small at the center) at 1.67 dm$^3$/minute rotameter flow rate- Test 7*

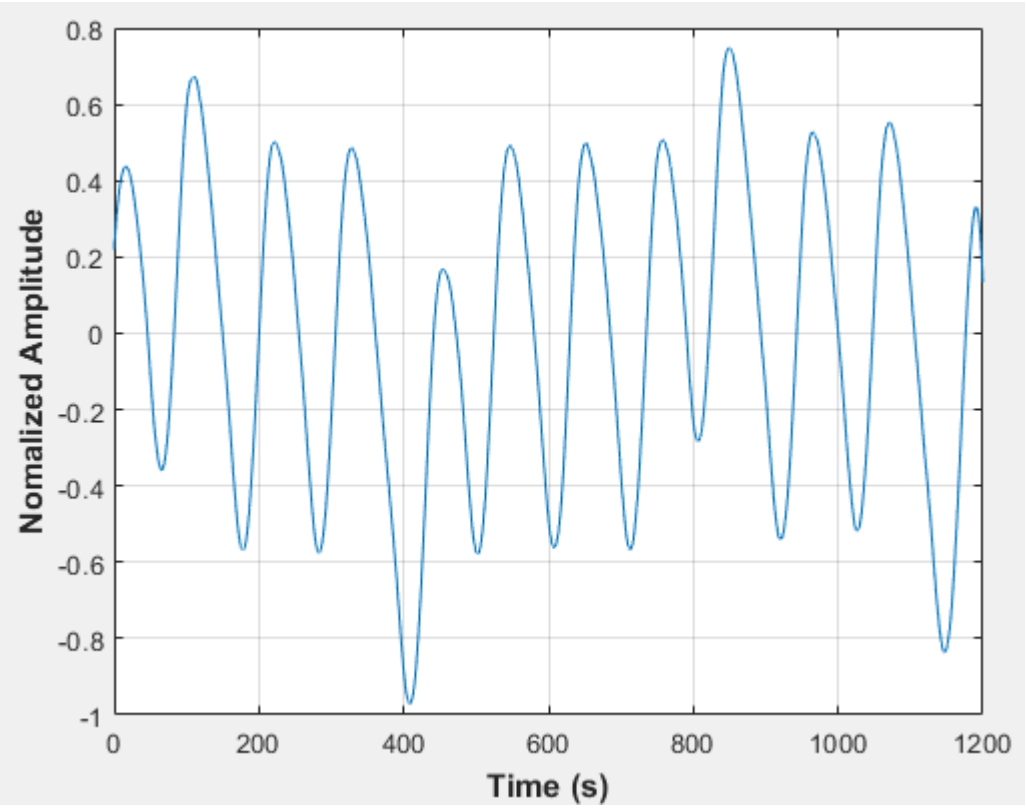


*Figure E-75: Pressure fluctuations in a non-uniformly packed vessel (large and small at the center) at 1.67 dm$^3$/minute rotameter flow rate- Test 8*

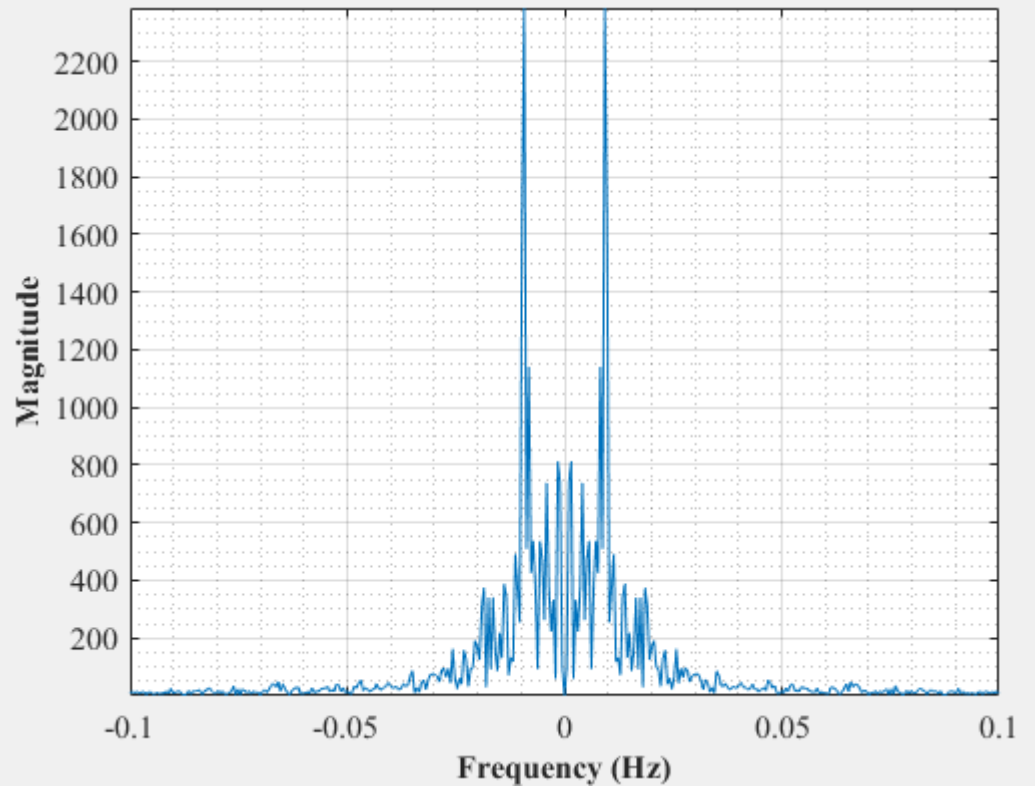


*Figure E-76: Dominant Frequency for a non-uniformly packed vessel (large and small at the center) at 1.67 dm$^3$/minute rotameter flow rate- Test 8*

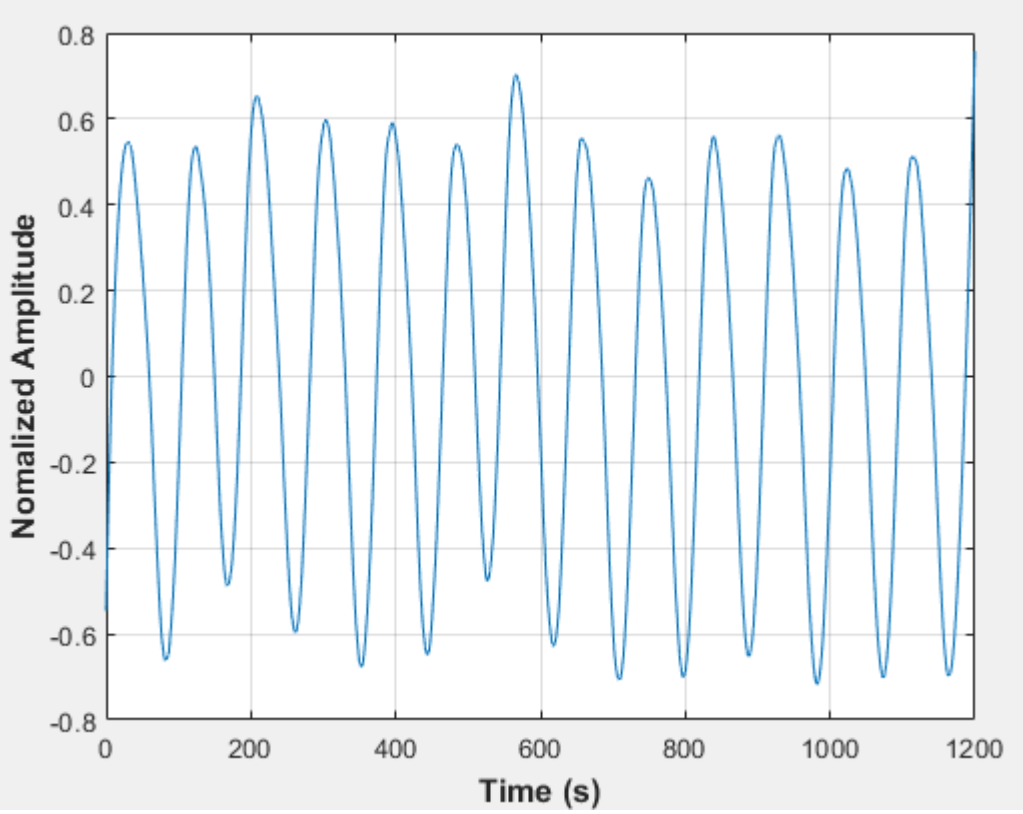


*Figure E-77: Pressure fluctuations in a non-uniformly packed vessel (large and small at the center) at 2 $dm^3$/minute rotameter flow rate- Test 1*

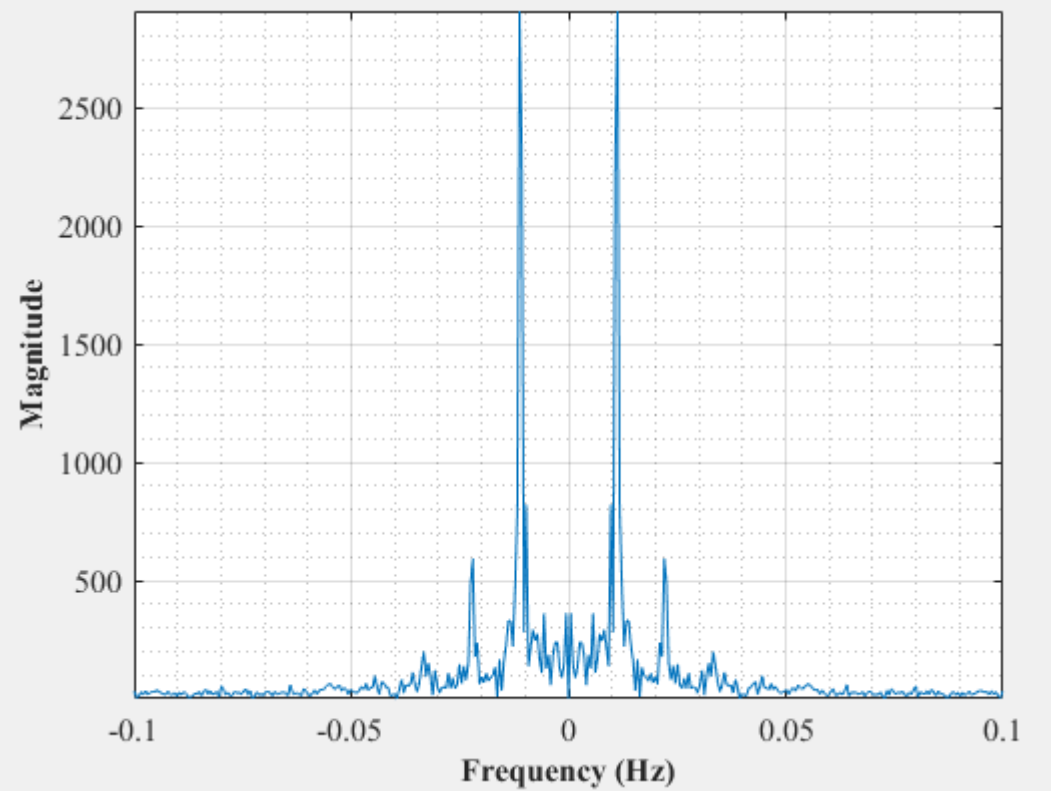


*Figure E-78: Dominant Frequency for a non-uniformly packed vessel (large and small at the center) at 2 $dm^3$/minute rotameter flow rate- Test 1*

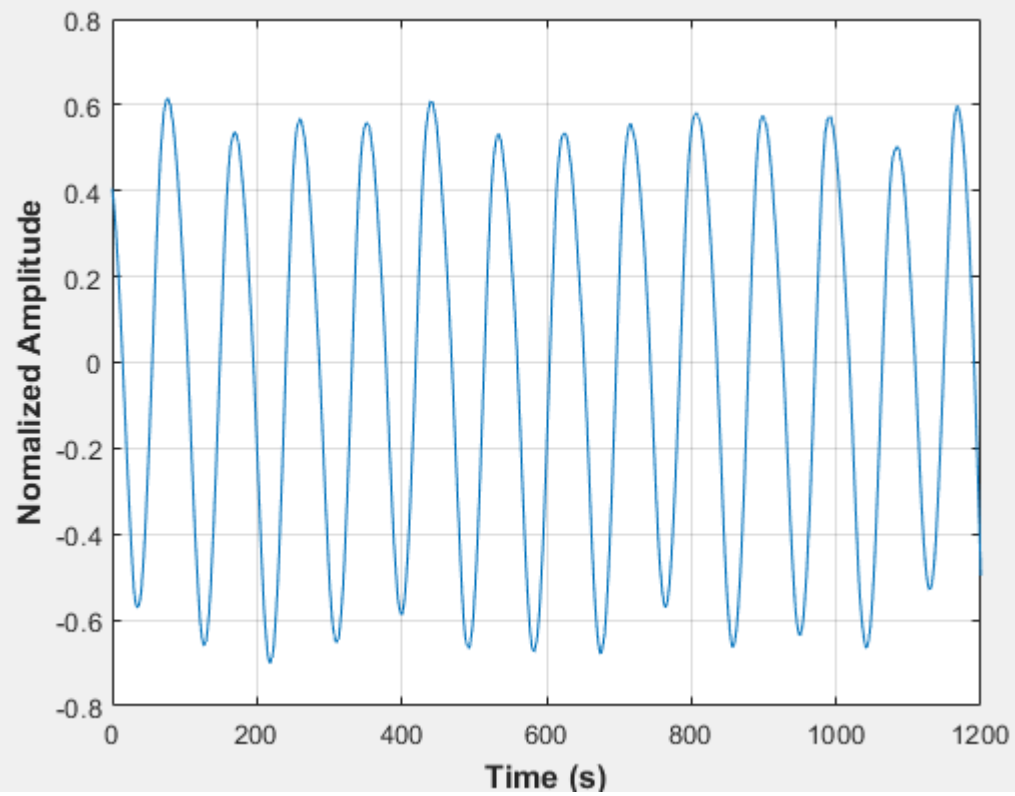


*Figure E-79: Pressure fluctuations in a non-uniformly packed vessel (large and small at the center) at 2 dm$^3$/minute rotameter flow rate- Test 2*

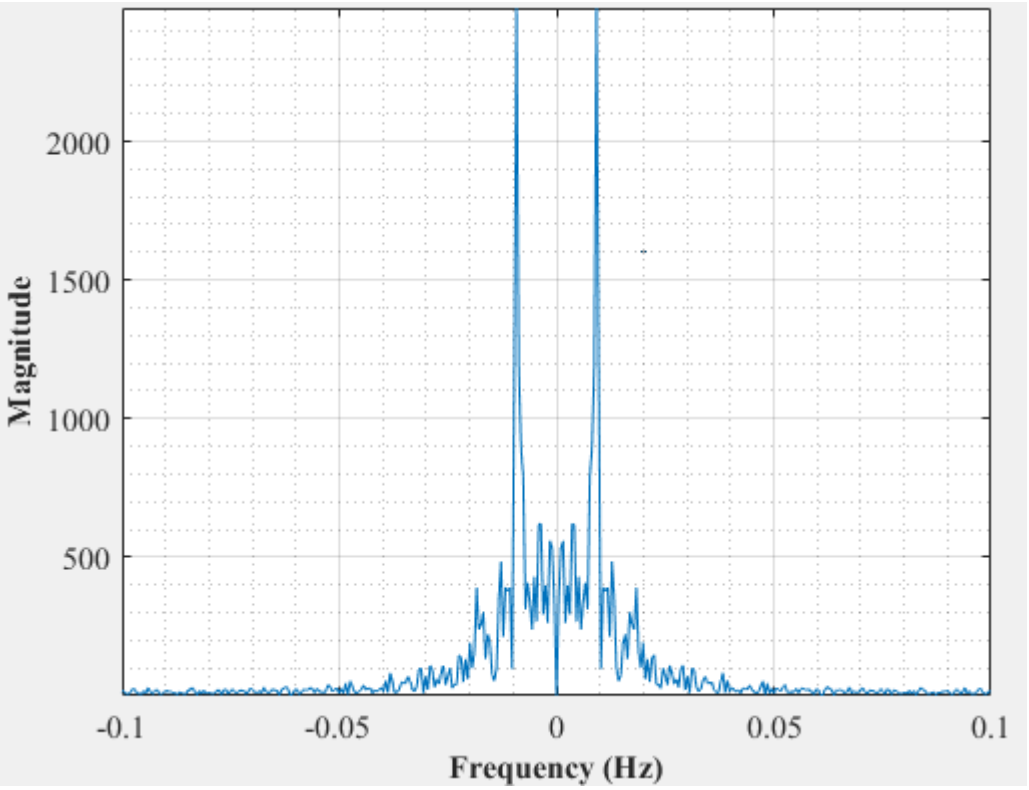


*Figure E-80: Dominant Frequency for a non-uniformly packed vessel (large and small at the center) at 2 dm$^3$/minute rotameter flow rate- Test 2*

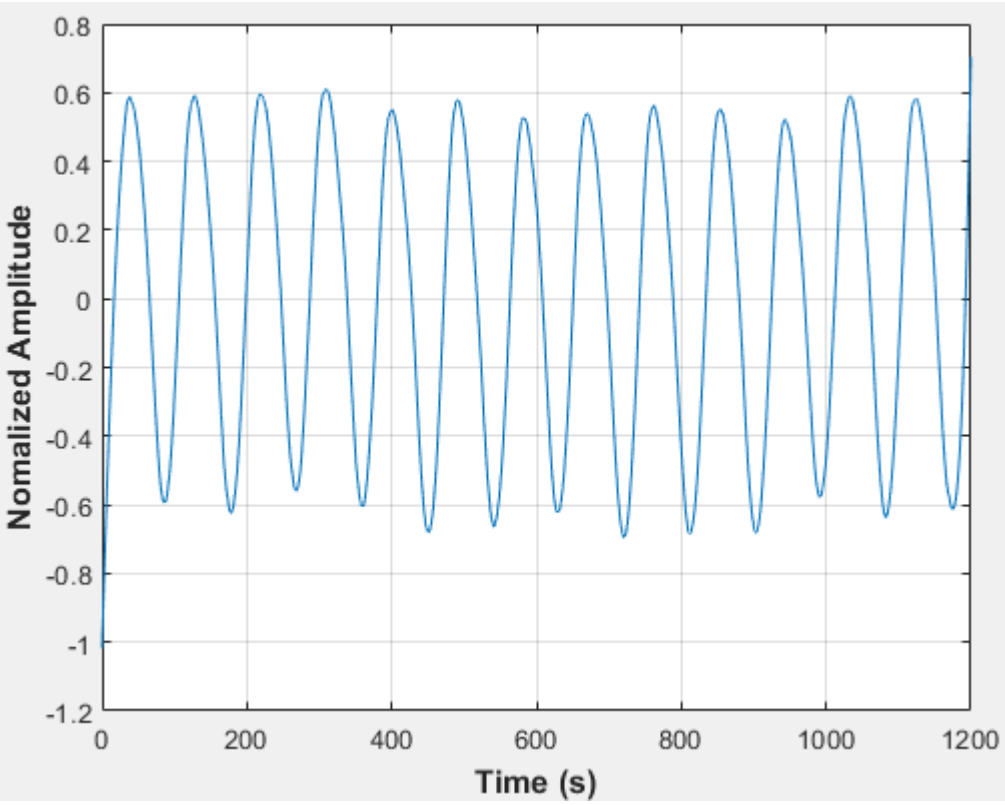


*Figure E-81: Pressure fluctuations in a non-uniformly packed vessel (large and small at the center) at 2 dm$^3$/minute rotameter flow rate- Test 3*

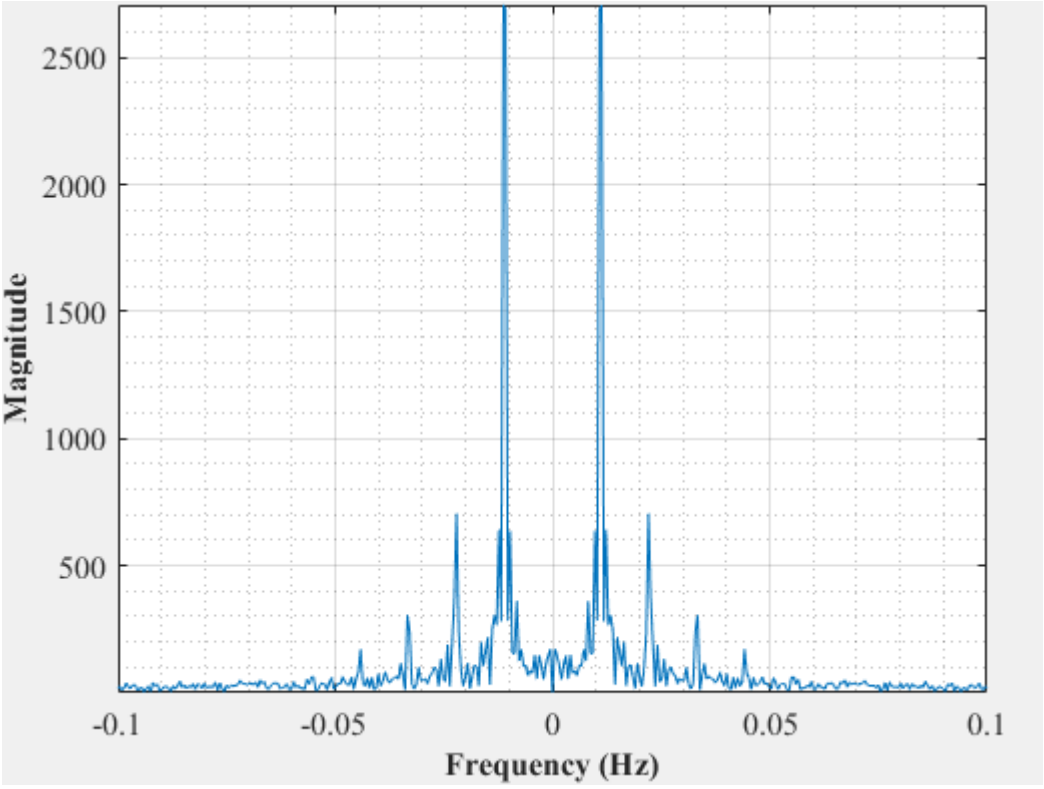


*Figure E-82: Dominant Frequency for a non-uniformly packed vessel (large and small at the center) at 2 dm$^3$/minute rotameter flow rate- Test 3*

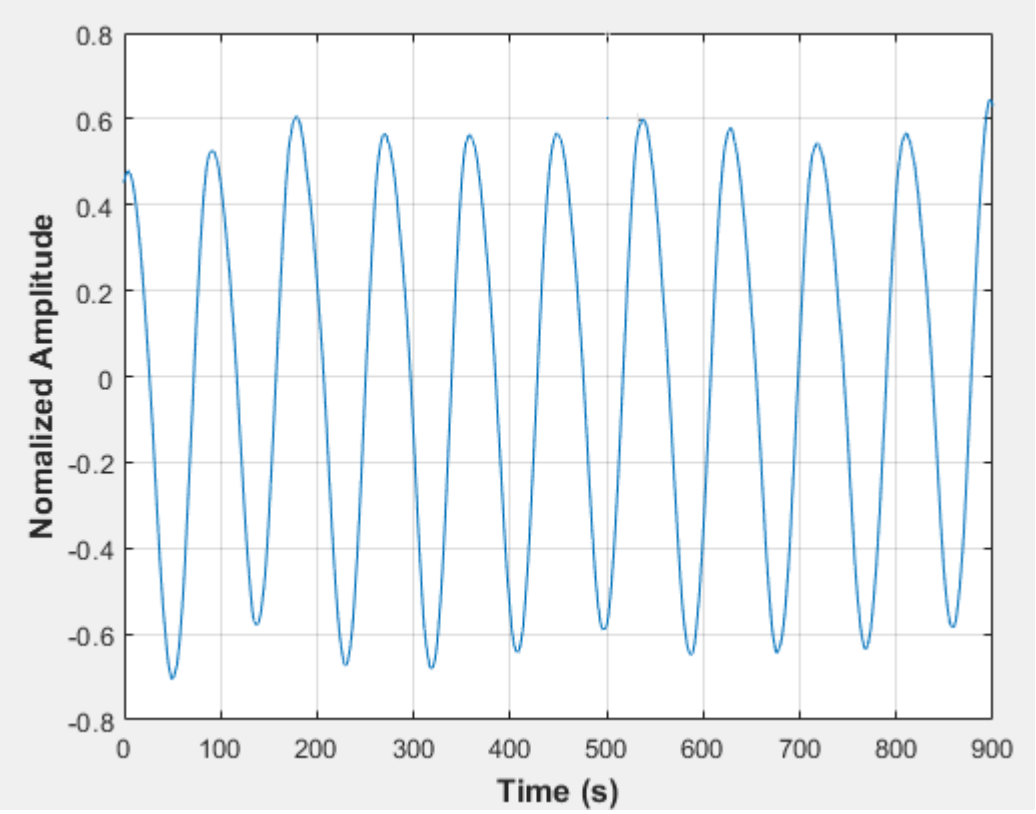


*Figure E-83: Pressure fluctuations in a non-uniformly packed vessel (large and small at the center) at 2 dm$^3$/minute rotameter flow rate- Test 4*

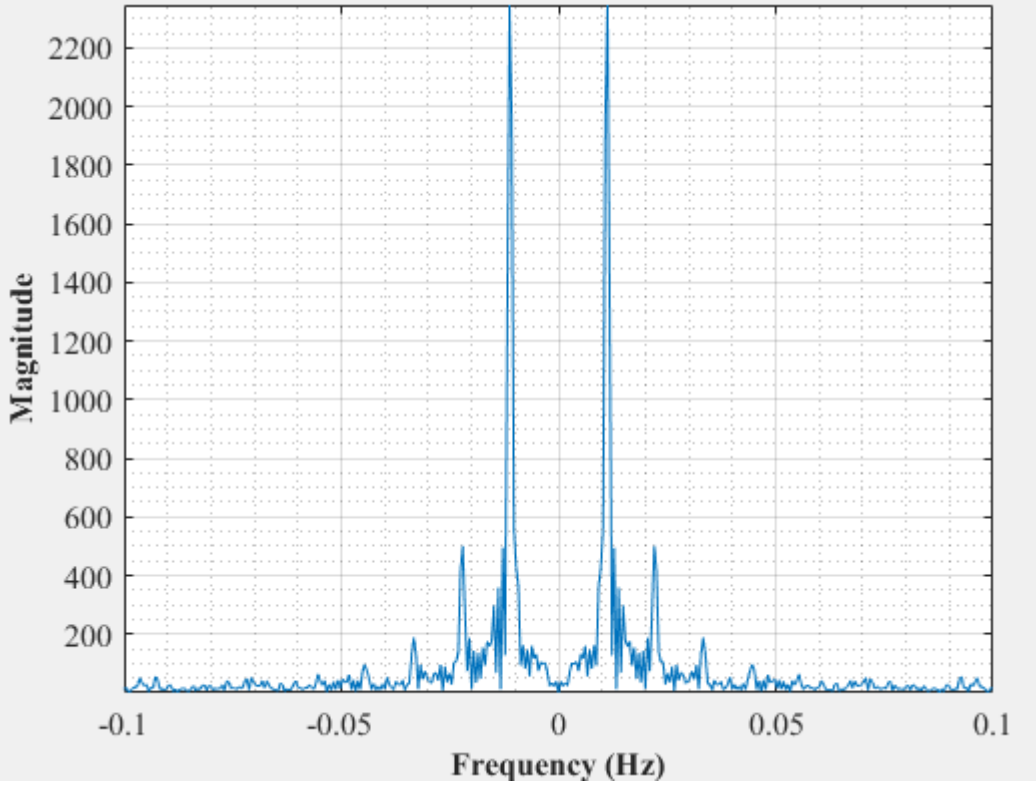


*Figure E-84: Dominant Frequency for a non-uniformly packed vessel (large and small at the center) at 2 dm$^3$/minute rotameter flow rate- Test 4*

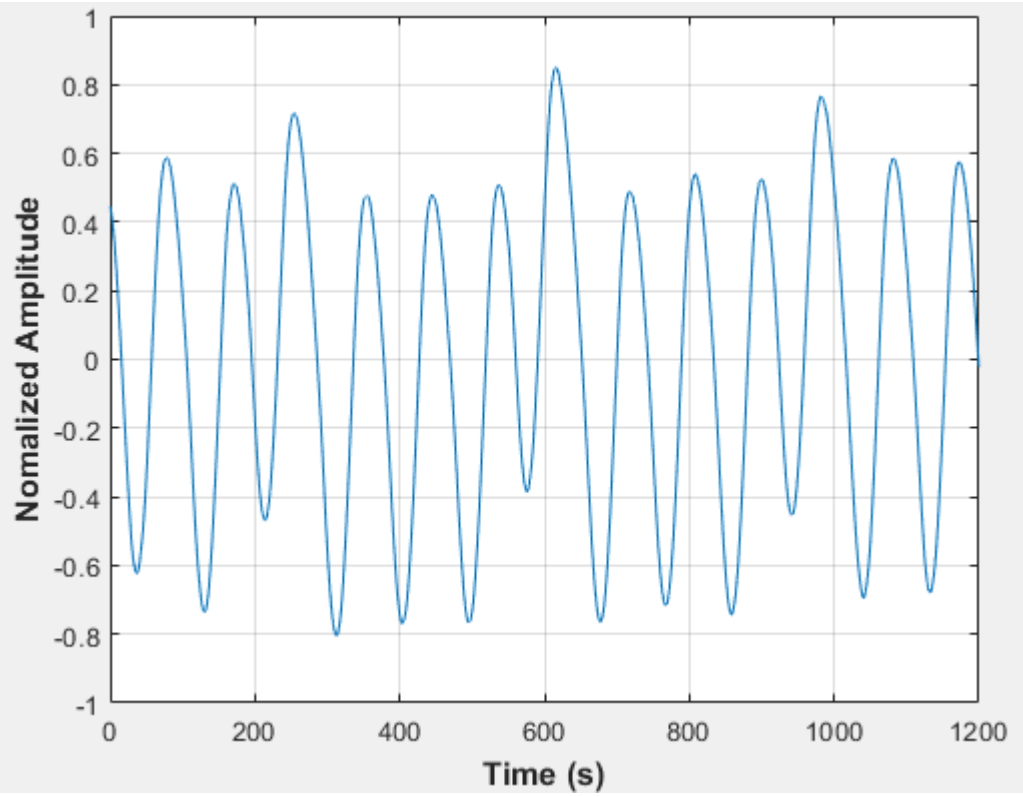


*Figure E-85: Pressure fluctuations in a non-uniformly packed vessel (large and small at the center) at 2 $dm^3$/minute rotameter flow rate- Test 5*

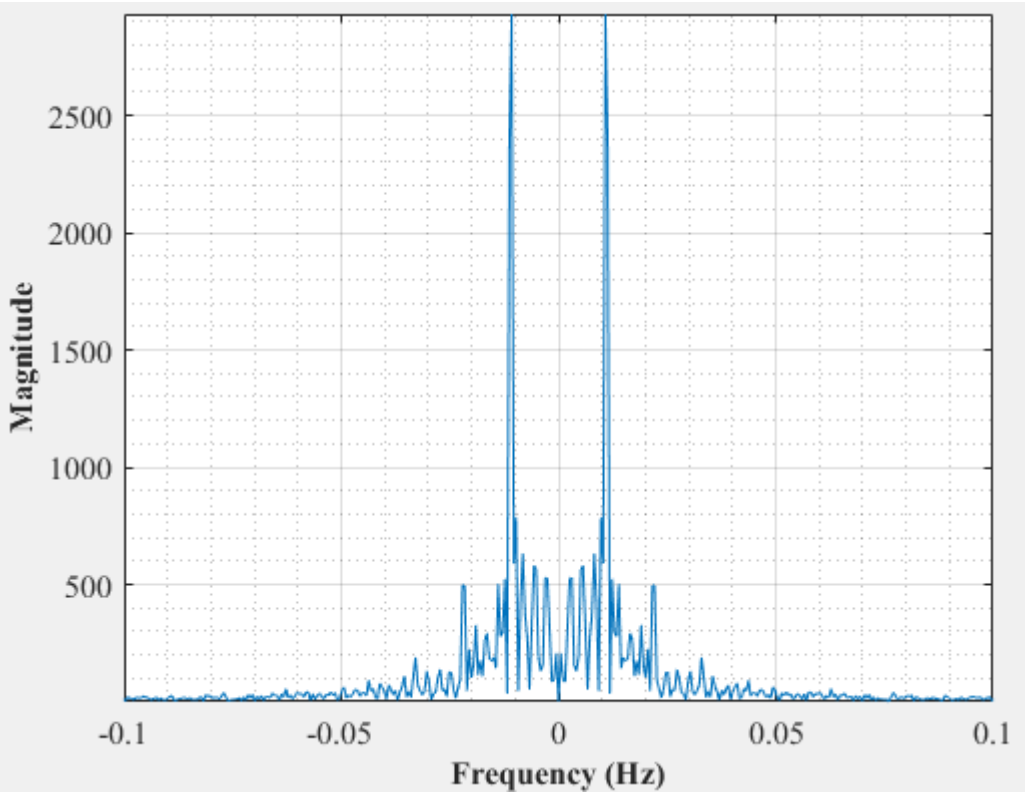


*Figure E-86: Dominant Frequency for a non-uniformly packed vessel (large and small at the center) at 2 $dm^3$/minute rotameter flow rate- Test 5*

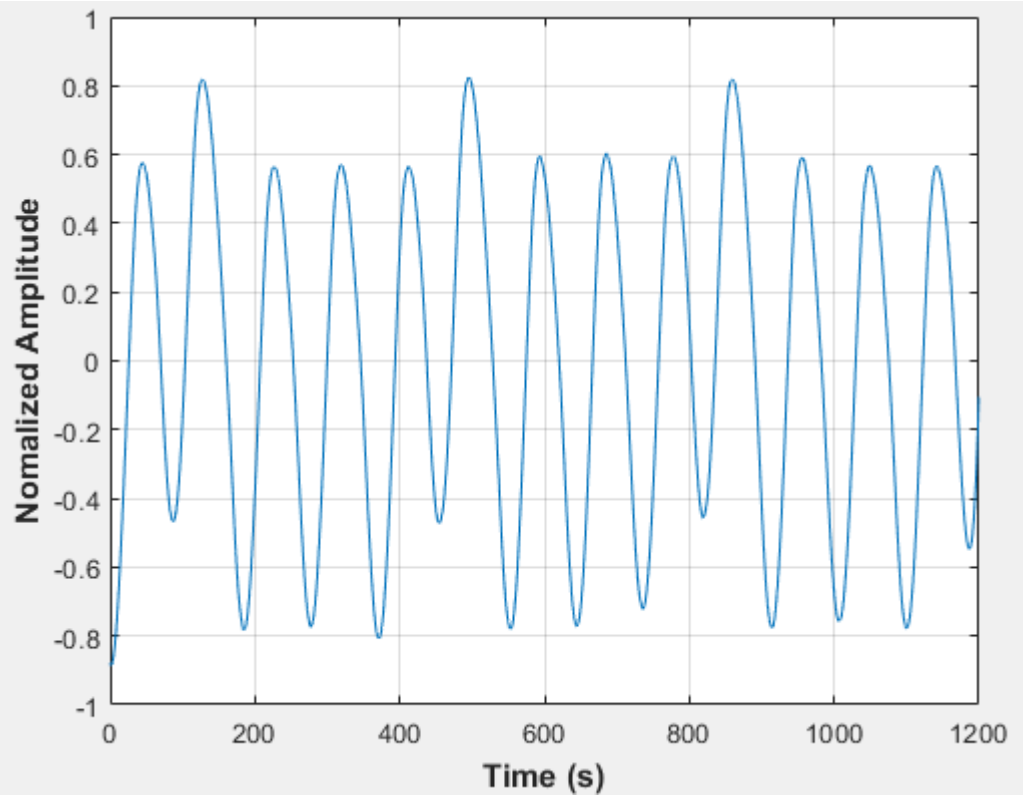


*Figure E-87: Pressure fluctuations in a non-uniformly packed vessel (large and small at the center) at 2 $dm^3$/minute rotameter flow rate- Test 6*

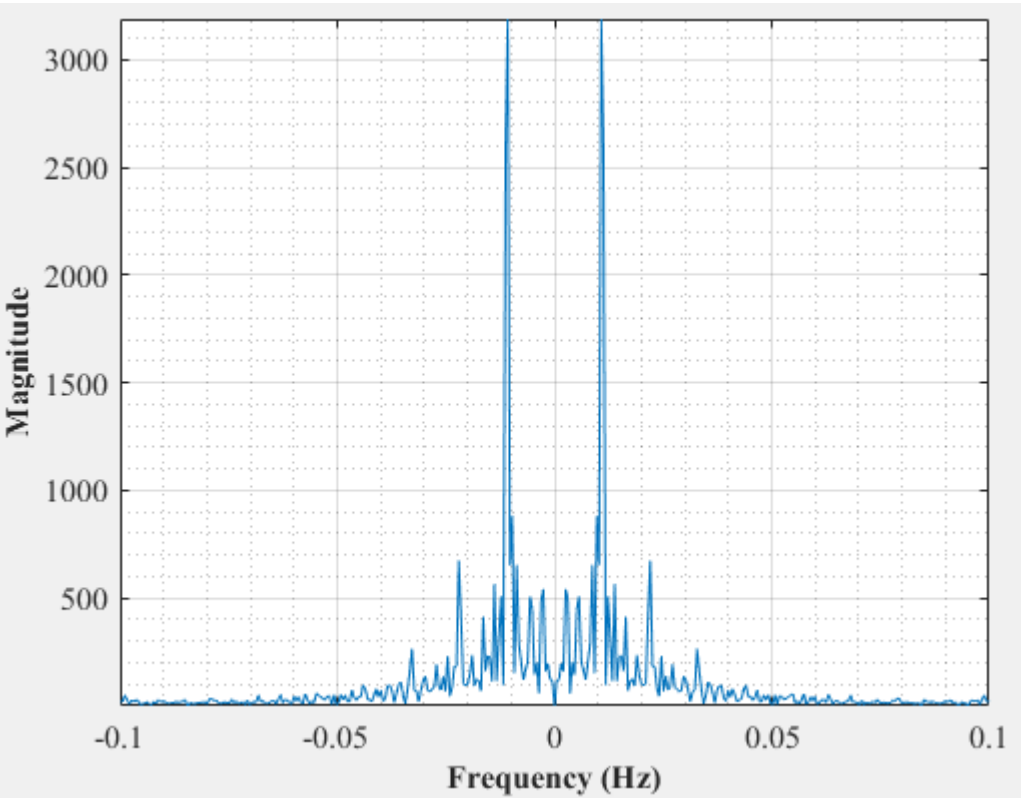


*Figure E-88: Dominant Frequency for a non-uniformly packed vessel (large and small at the center) at 2 $dm^3$/minute rotameter flow rate- Test 6*

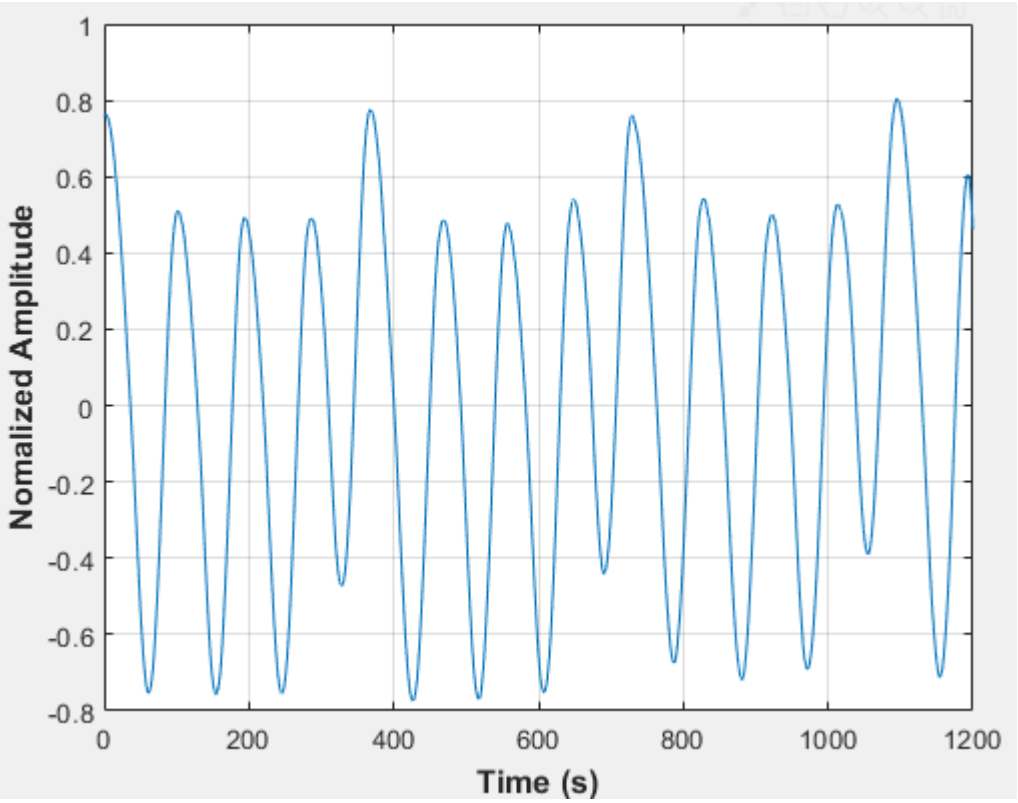


*Figure E-89: Pressure fluctuations in a non-uniformly packed vessel (large and small at the center) at 2 dm$^3$/minute rotameter flow rate- Test 7*

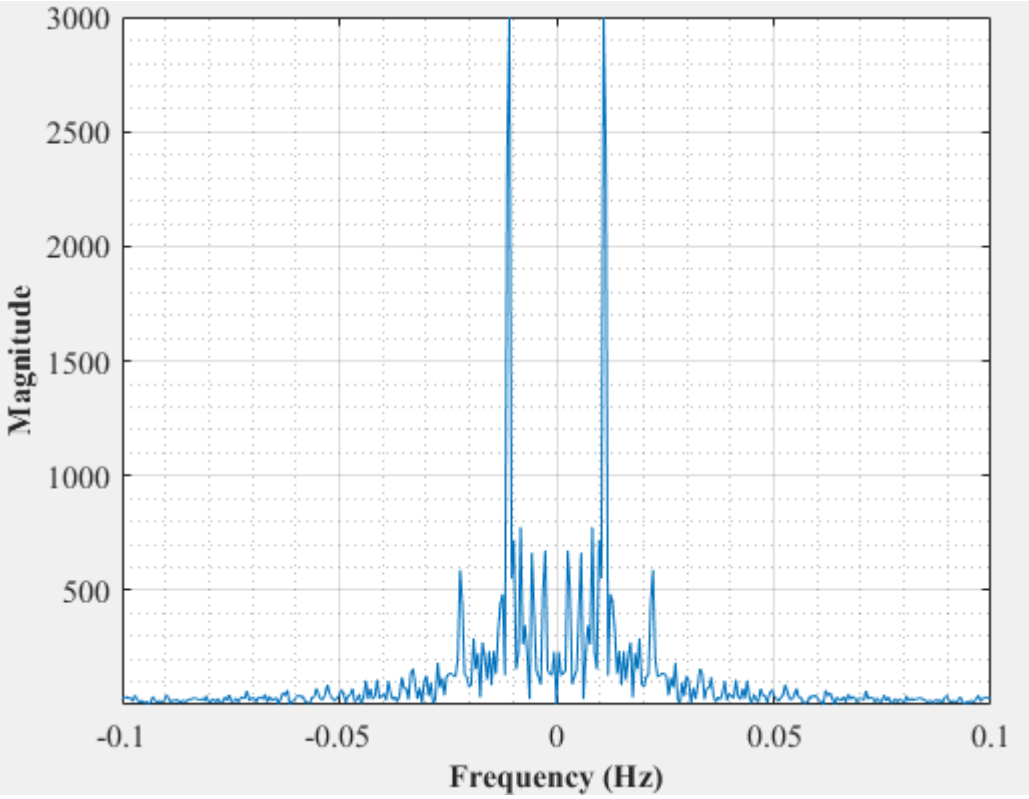


*Figure E-90: Dominant Frequency for a non-uniformly packed vessel (large and small at the center) at 2 dm$^3$/minute rotameter flow rate- Test 7*

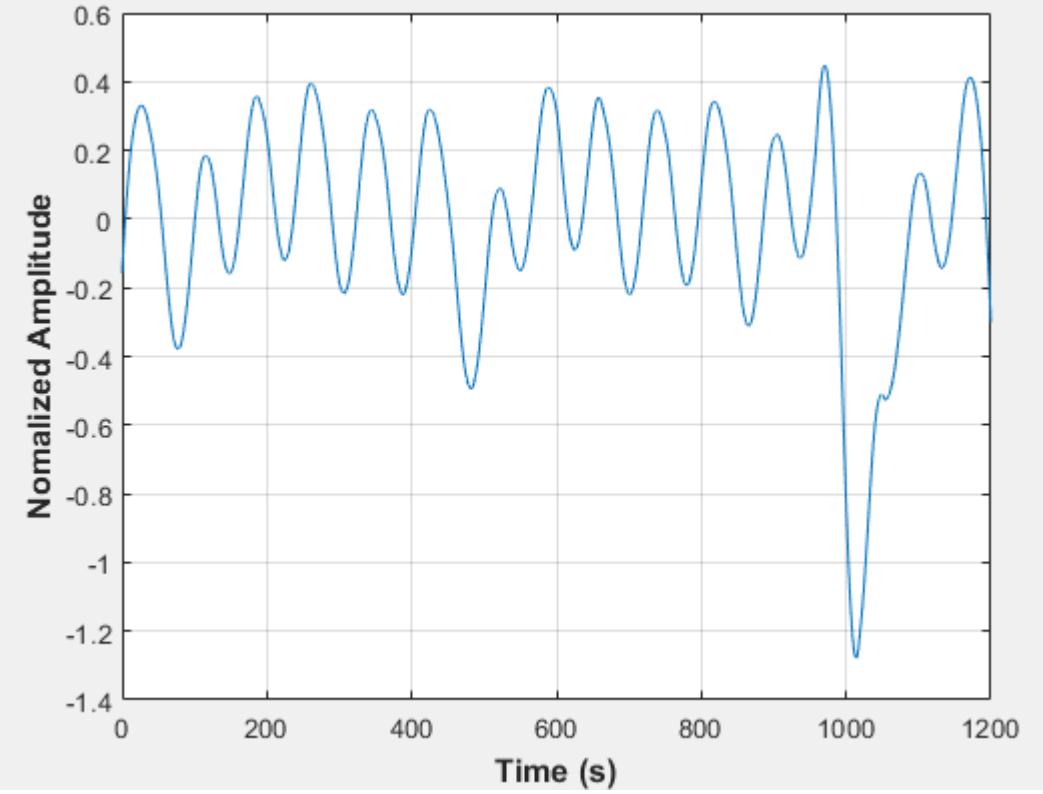


*Figure E-91: Pressure fluctuations in a non-uniformly packed vessel (large and small at the center) at 2.33 dm$^3$/minute rotameter flow rate- Test 1*

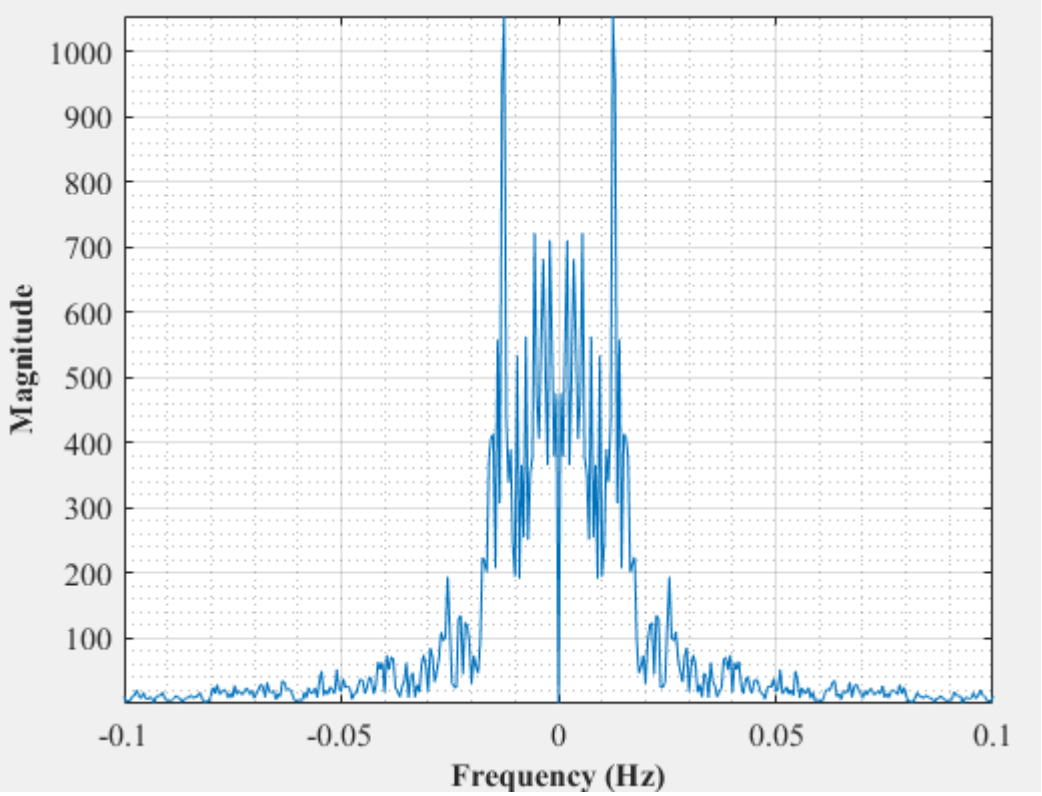


*Figure E-92: Dominant Frequency for a non-uniformly packed vessel (large and small at the center) at 2.33 dm$^3$/minute rotameter flow rate- Test 1*

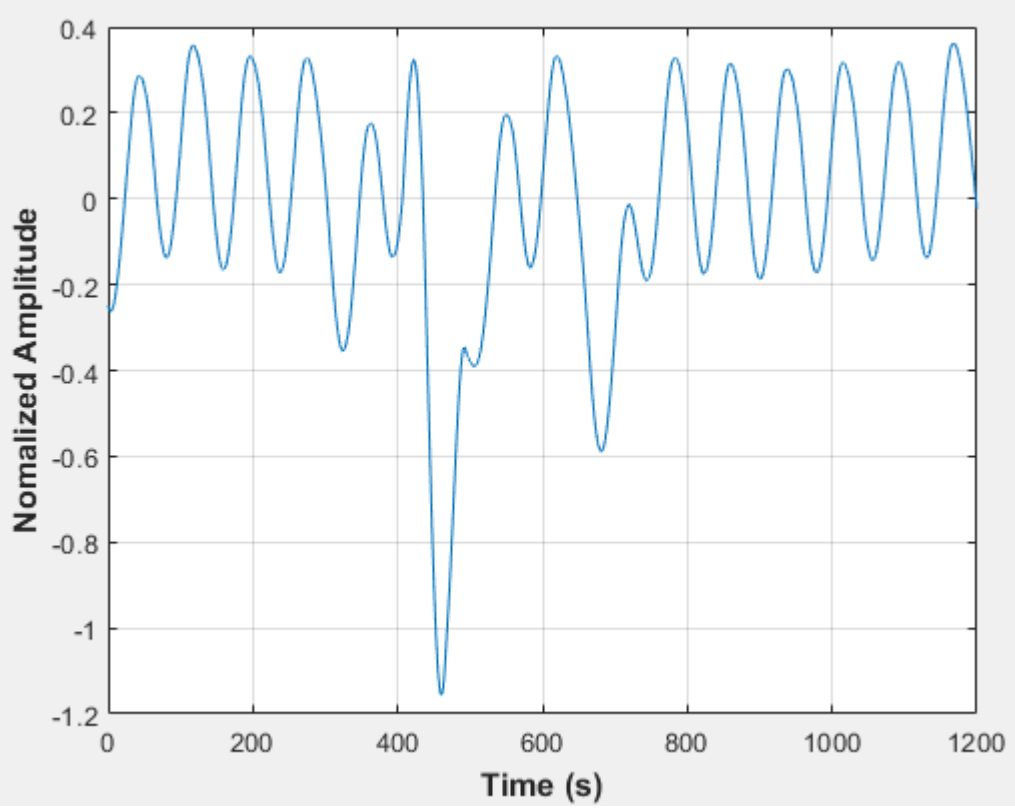


*Figure E-93: Pressure fluctuations in a non-uniformly packed vessel (large and small at the center) at 2.33 $dm^3$/minute rotameter flow rate- Test 2*

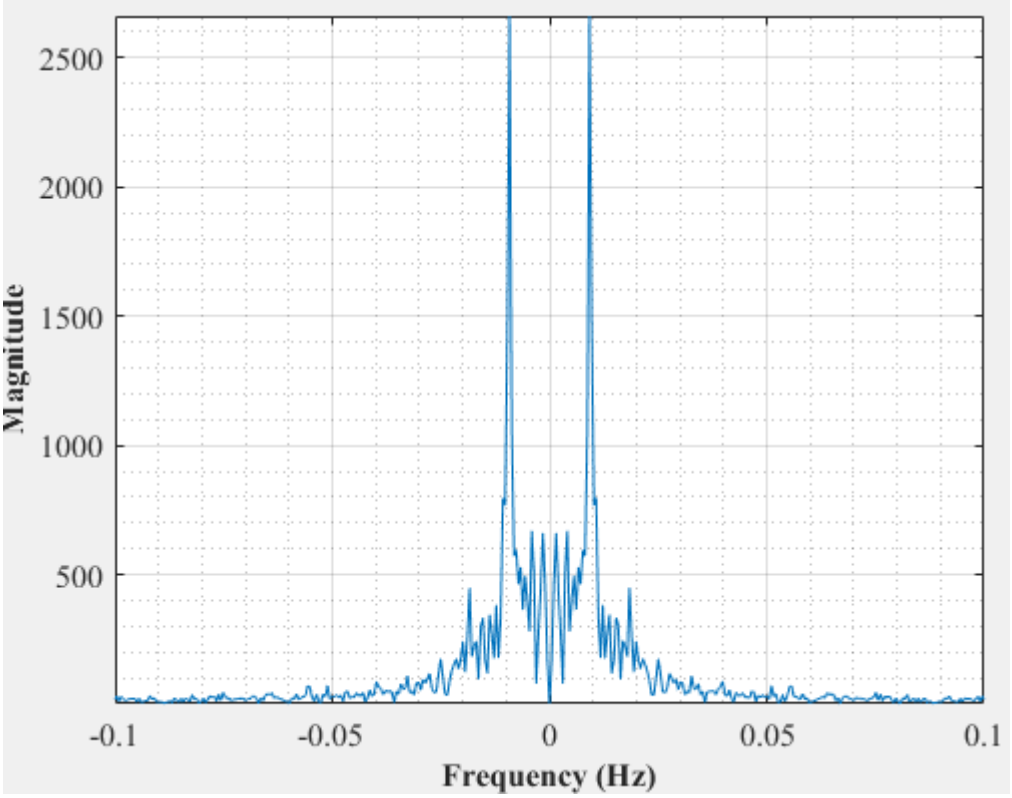


*Figure E-94: Dominant Frequency for a non-uniformly packed vessel (large and small at the center) at 2.33 $dm^3$/minute rotameter flow rate- Test 2*

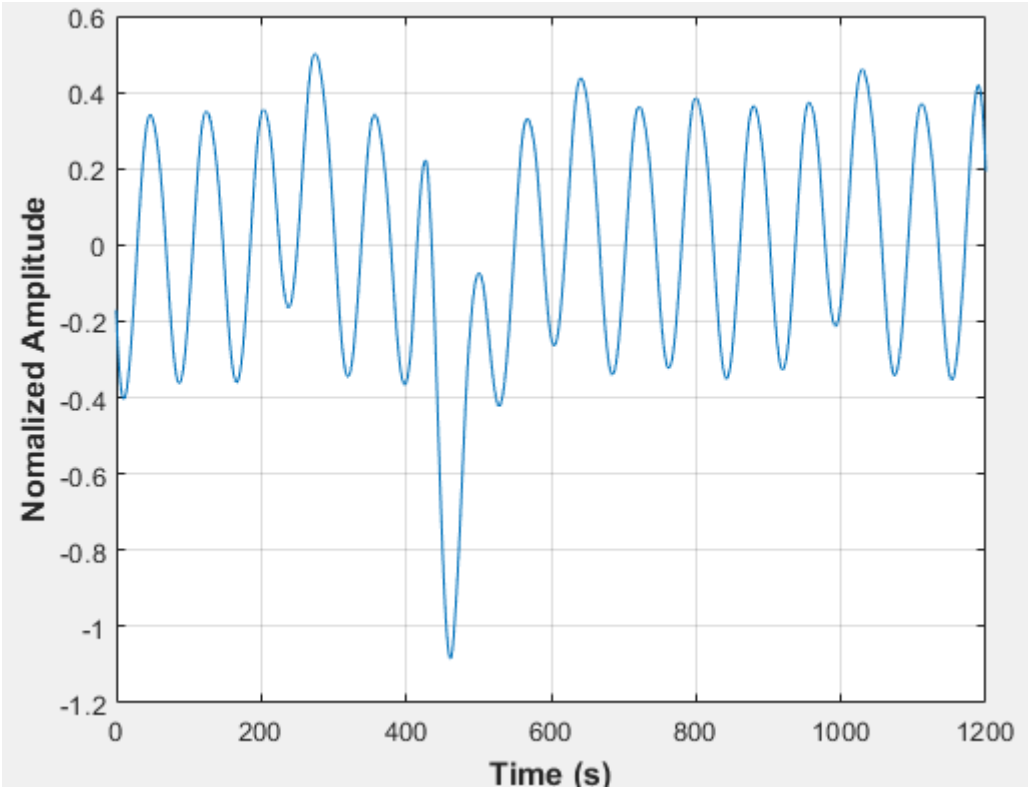


*Figure E-95: Pressure fluctuations in a non-uniformly packed vessel (large and small at the center) at 2.33 dm$^3$/minute rotameter flow rate- Test 3*

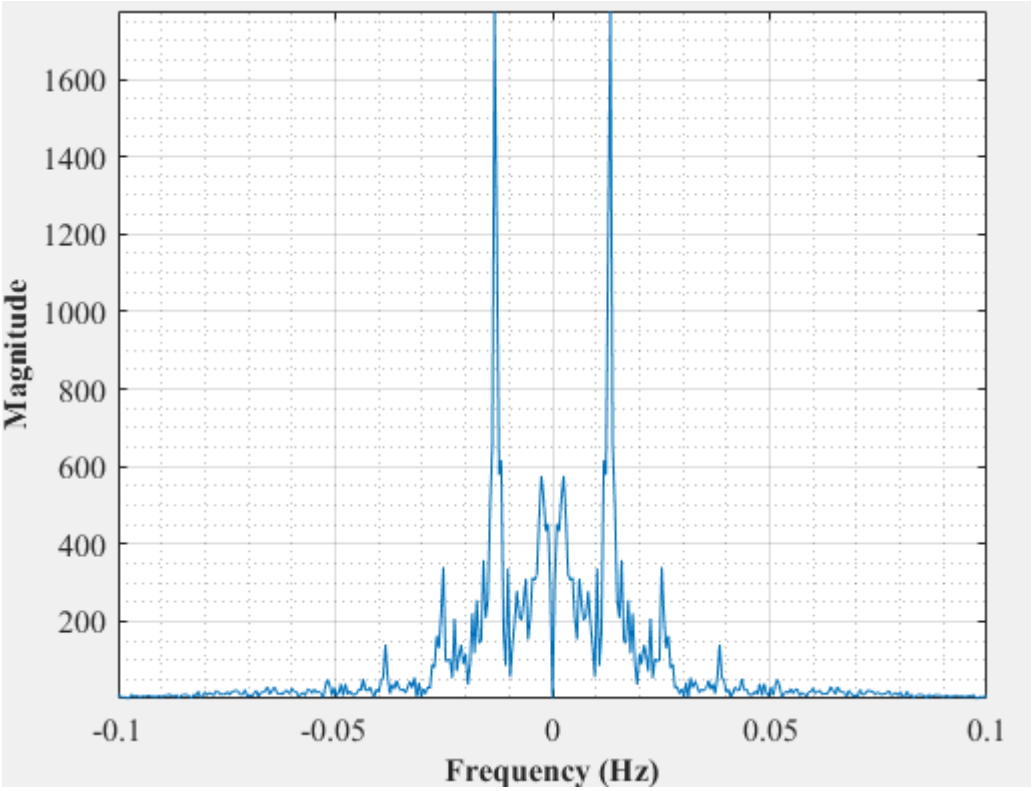


*Figure E-96: Dominant Frequency for a non-uniformly packed vessel (large and small at the center) at 2.33 dm$^3$/minute rotameter flow rate- Test 3*

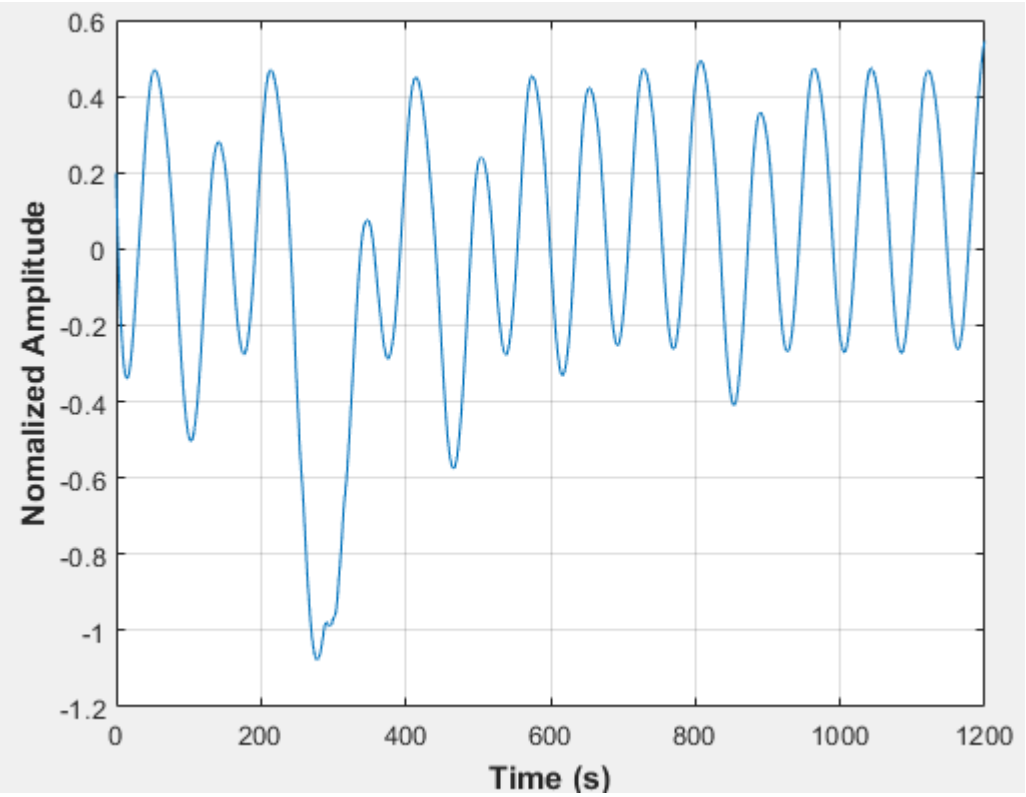


*Figure E-97: Pressure fluctuations in a non-uniformly packed vessel (large and small at the center) at 2.33 dm$^3$/minute rotameter flow rate- Test 4*

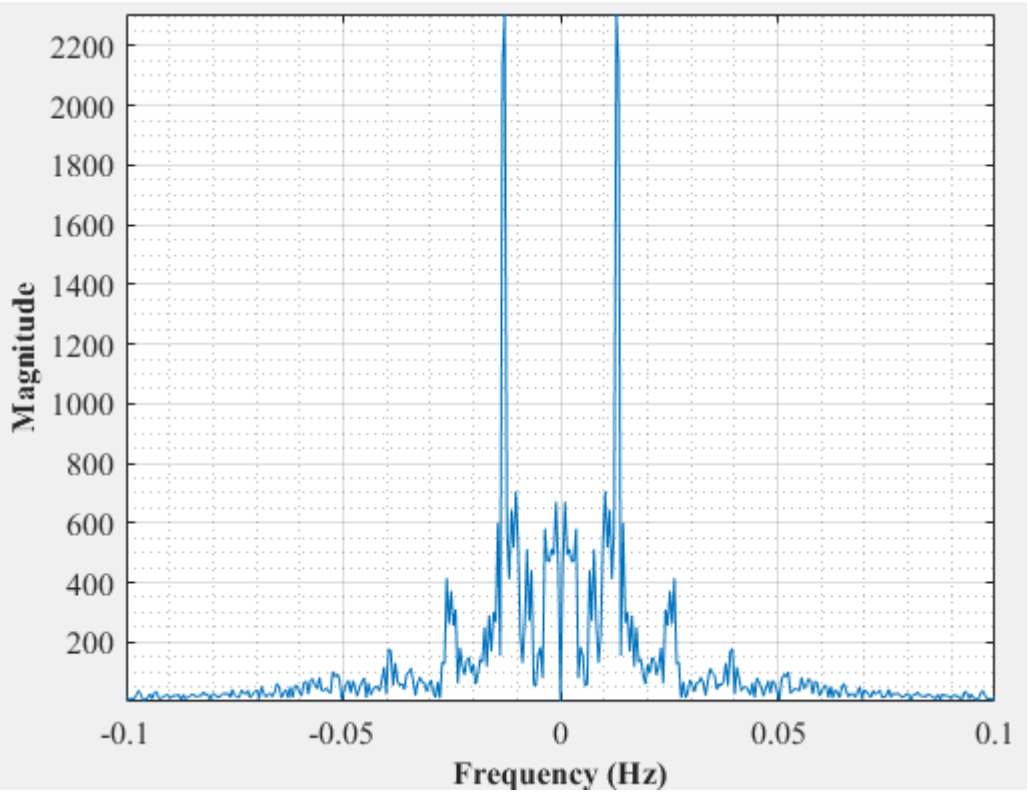


*Figure E-98: Dominant Frequency for a non-uniformly packed vessel (large and small at the center) at 2.33 dm$^3$/minute rotameter flow rate- Test 4*

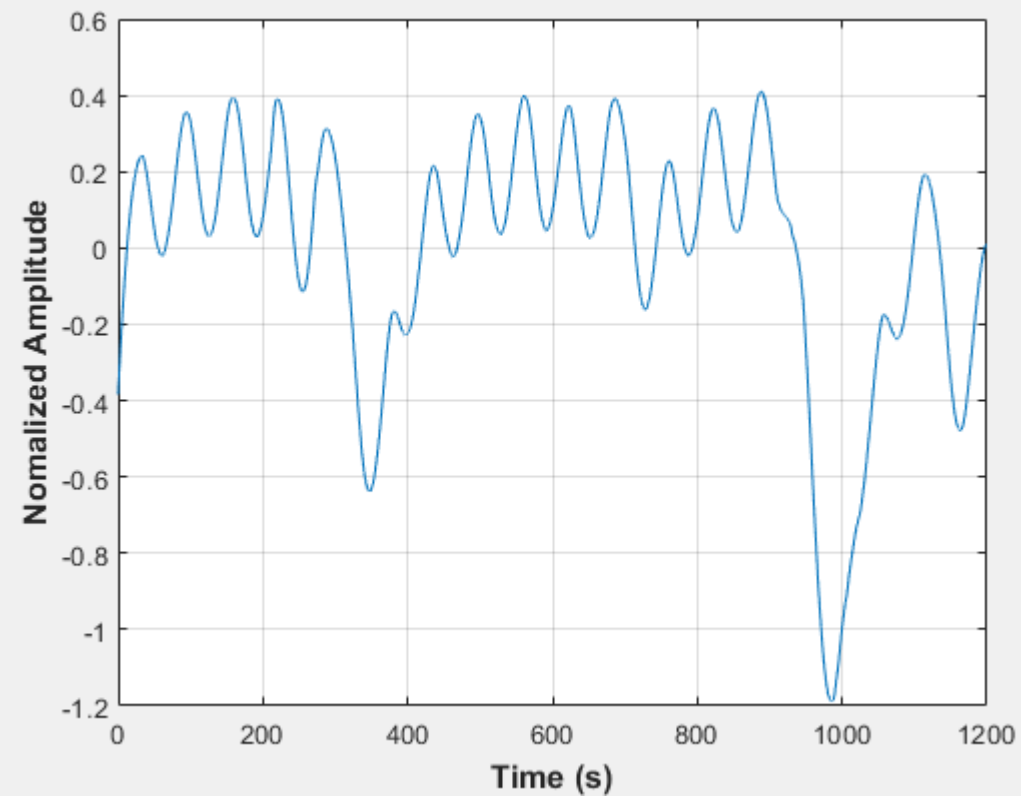


*Figure E-99: Pressure fluctuations in a non-uniformly packed vessel (large and small at the center) at 2.67 $dm^3$/minute rotameter flow rate- Test 1*

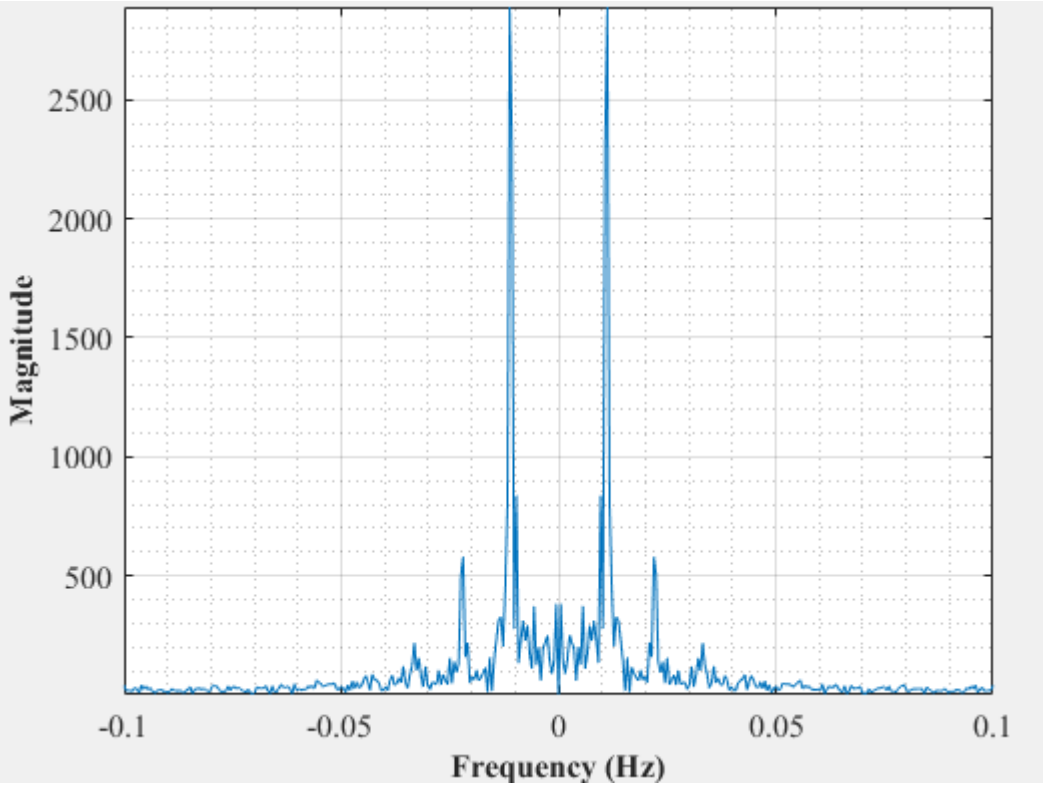


*Figure E-100: Dominant Frequency for a non-uniformly packed vessel (large and small at the center) at 2.67 $dm^3$/minute rotameter flow rate- Test 1*

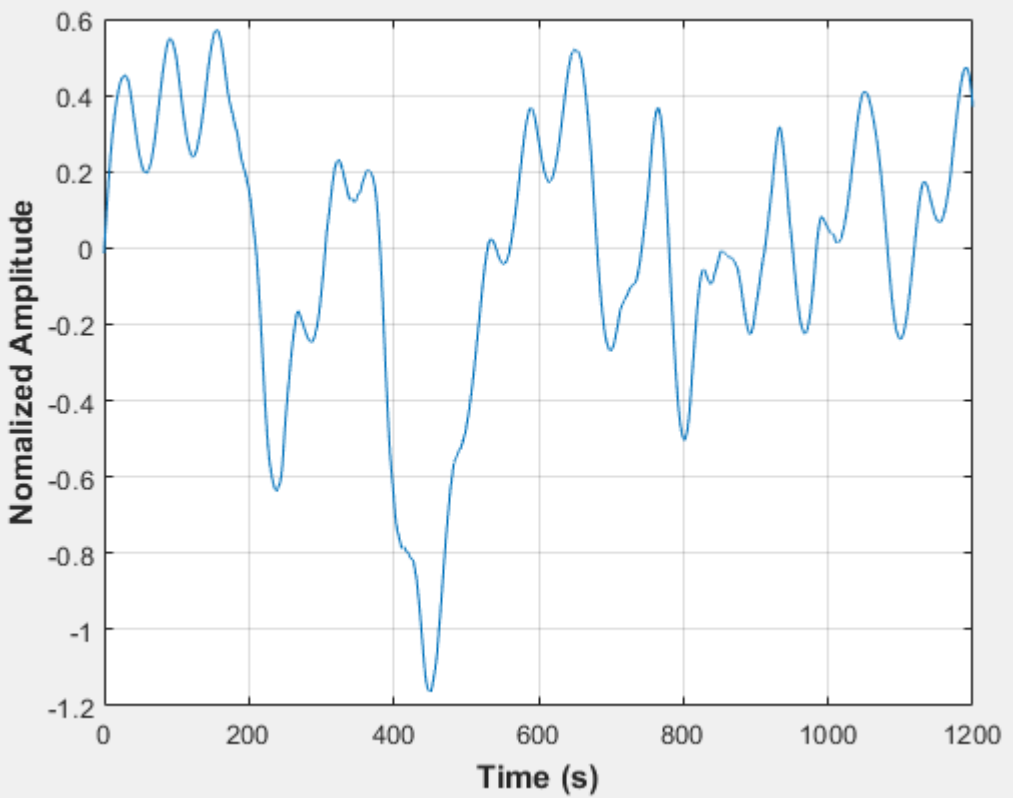


*Figure E-101: Pressure fluctuations in a non-uniformly packed vessel (large and small at the center) at 2.67 $dm^3$/minute rotameter flow rate- Test 2*

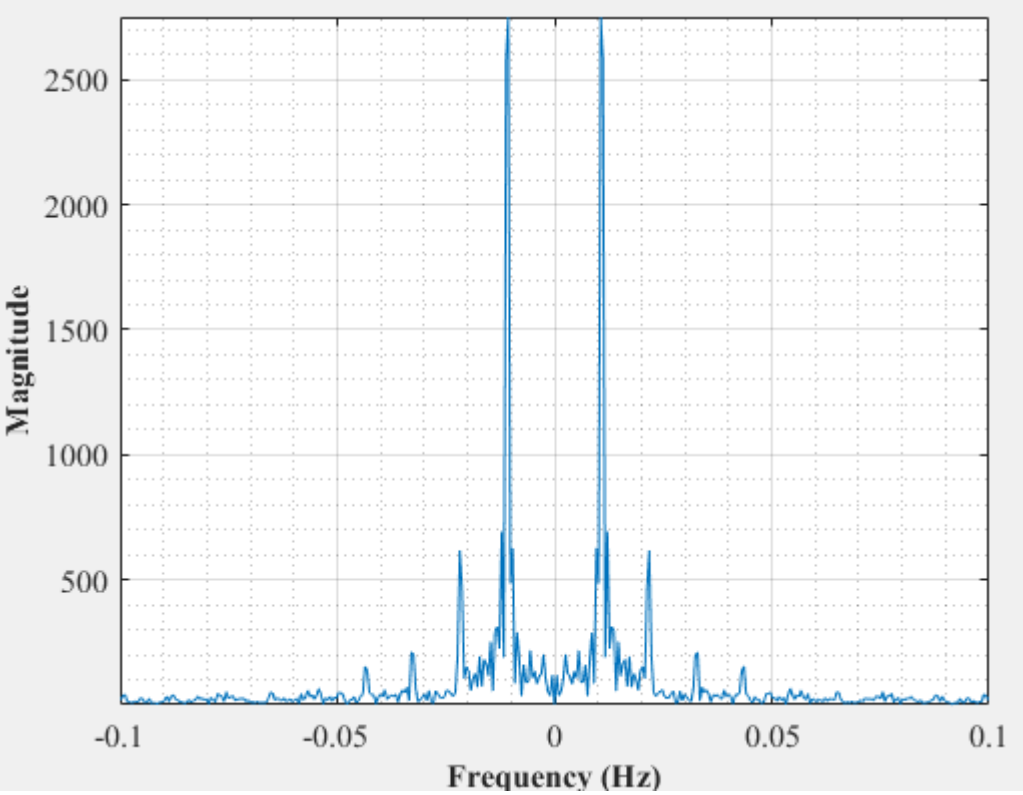


*Figure E-102: Dominant Frequency for a non-uniformly packed vessel (large and small at the center) at 2.67 $dm^3$/minute rotameter flow rate- Test 2*

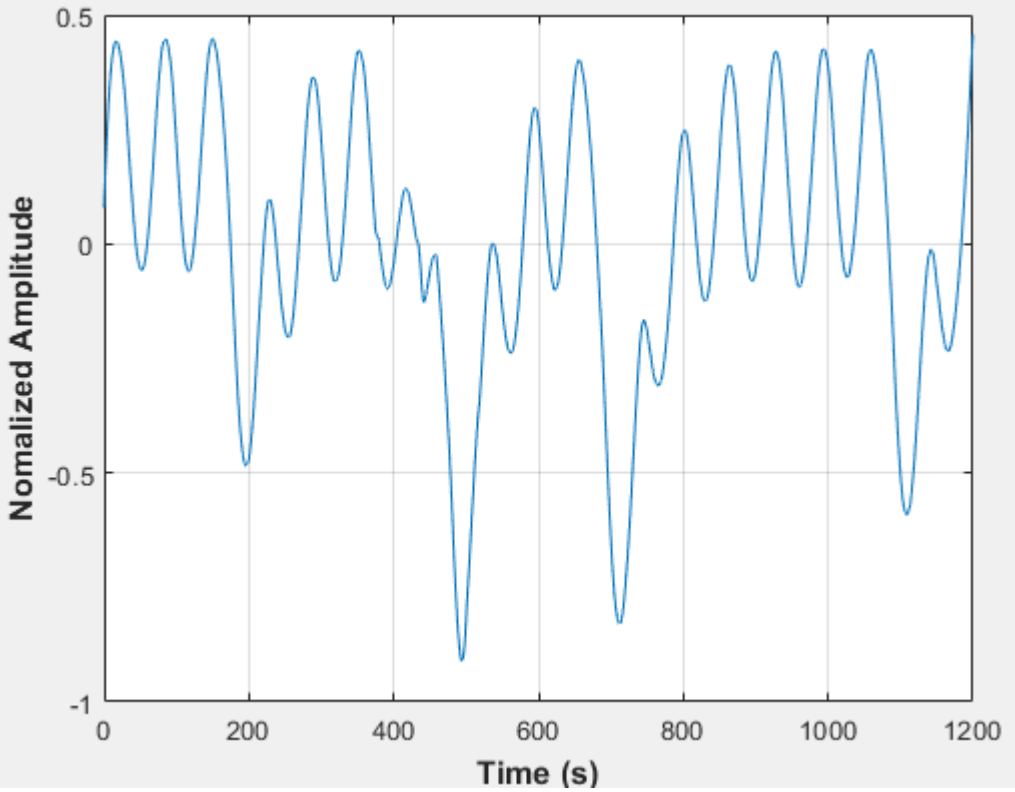


*Figure E-103: Pressure fluctuations in a non-uniformly packed vessel (large and small at the center) at 2.67 $dm^3$/minute rotameter flow rate- Test 3*

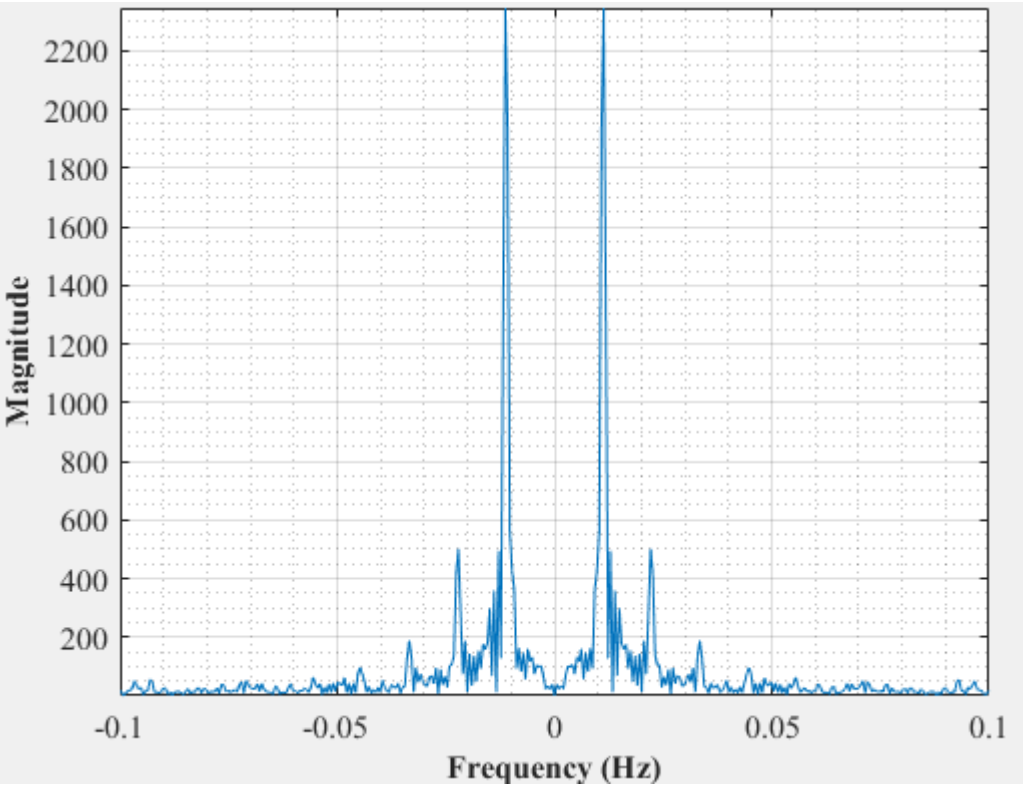


*Figure E-104: Dominant Frequency for a non-uniformly packed vessel (large and small at the center) at 2.67 $dm^3$/minute rotameter flow rate- Test 3*

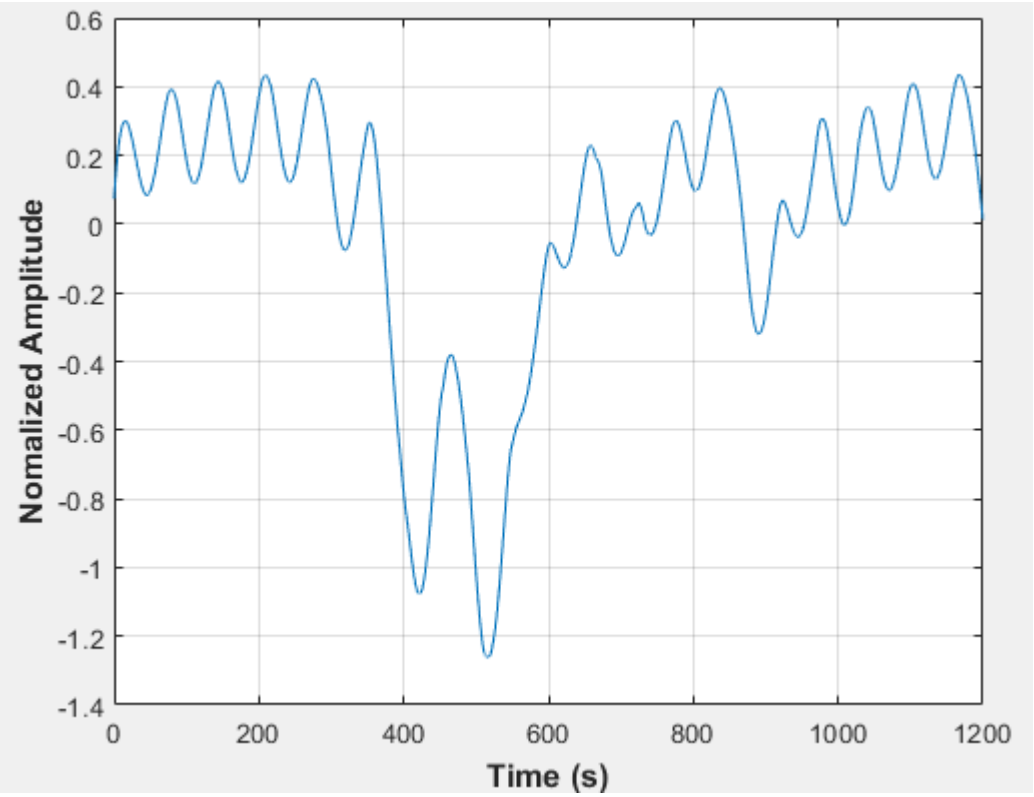


*Figure E-105: Pressure fluctuations in a non-uniformly packed vessel (large and small at the center) at 2.67 dm$^3$/minute rotameter flow rate- Test 4*

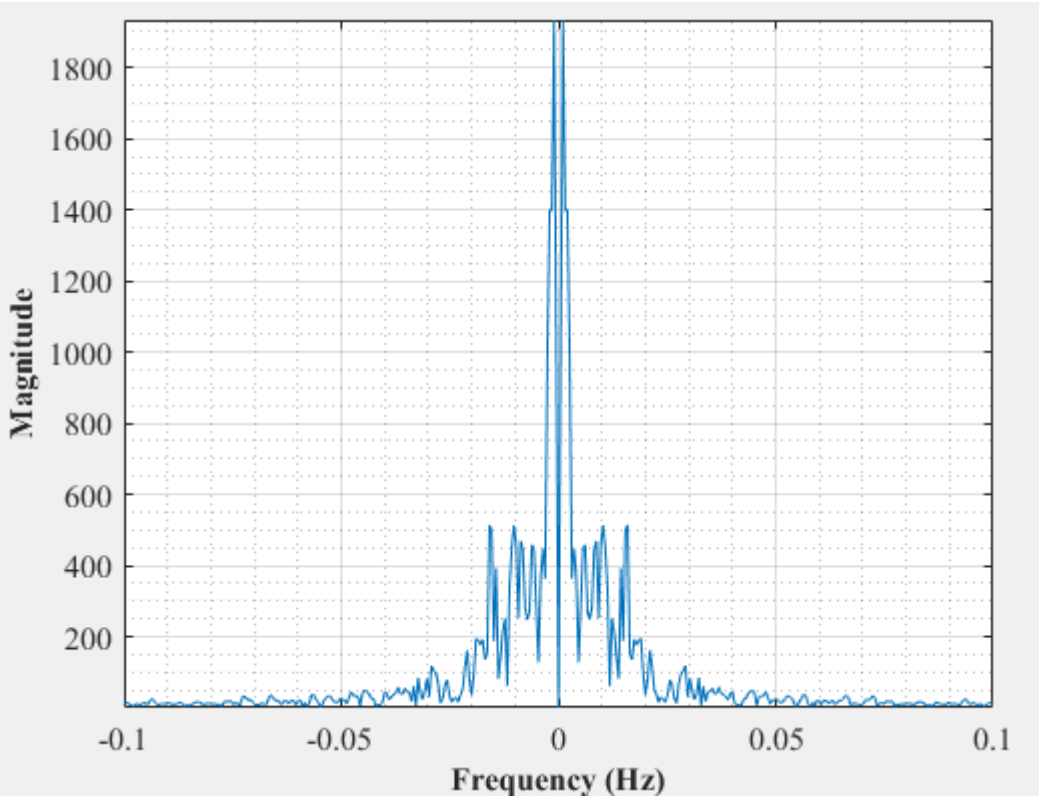


*Figure E-106: Dominant Frequency for a non-uniformly packed vessel (large and small at the center) at 2.67 dm$^3$/minute rotameter flow rate- Test 4*

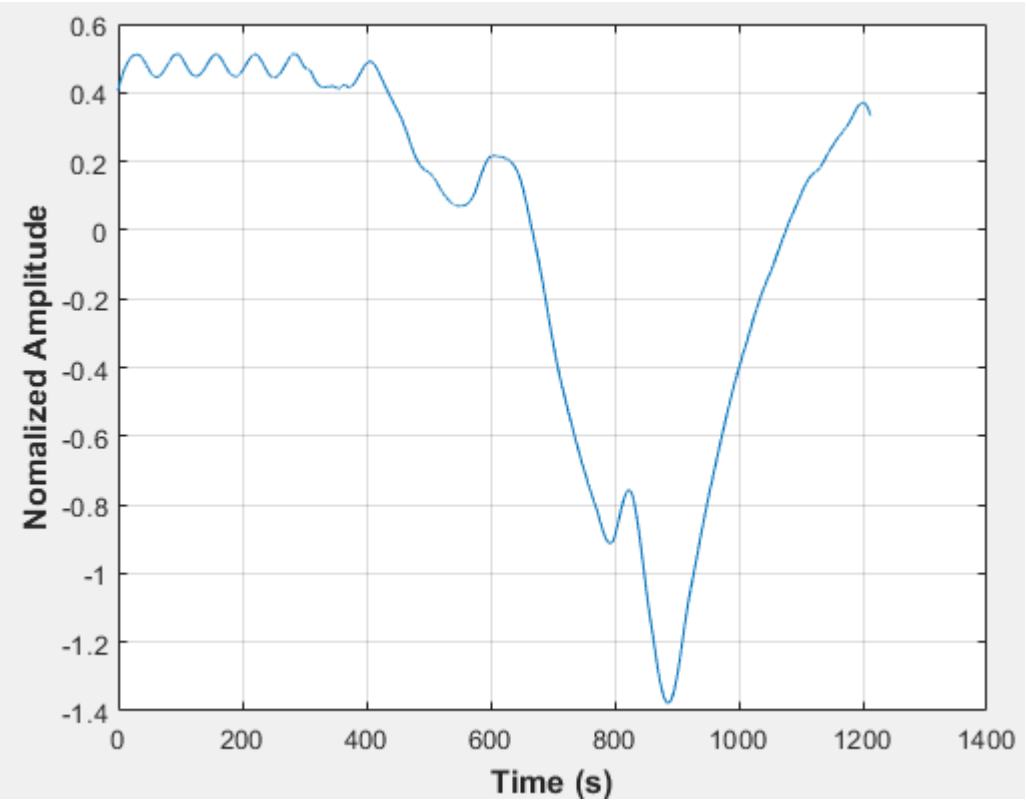


*Figure E-107: Pressure fluctuations in a non-uniformly packed vessel (large and small at the center) at 2.83 dm$^3$/minute rotameter flow rate- Test 1*

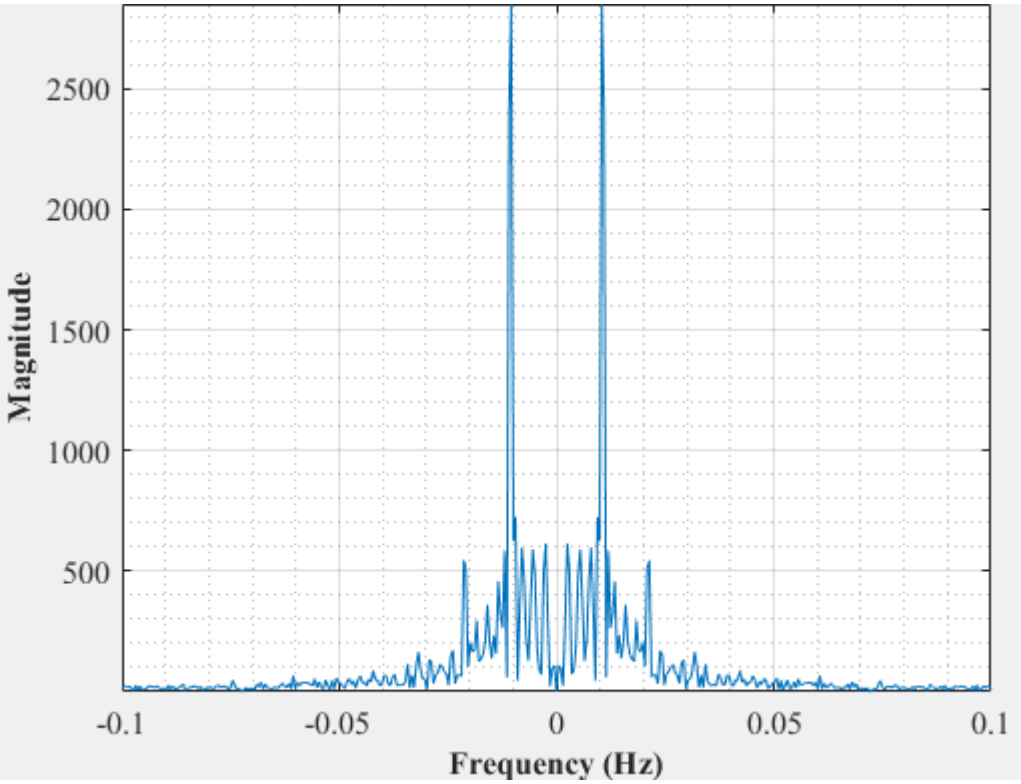


*Figure E-108: Dominant Frequency for a non-uniformly packed vessel (large and small at the center) at 2.83 dm$^3$/minute rotameter flow rate- Test 1*

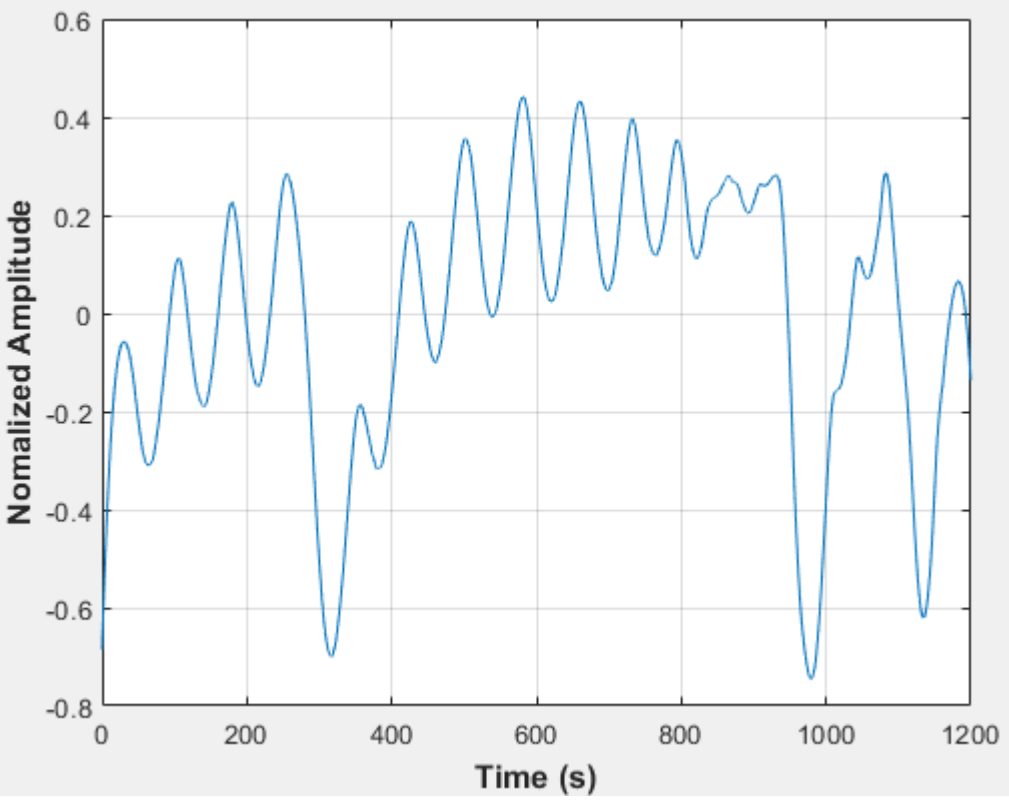


*Figure E-109: Pressure fluctuations in a non-uniformly packed vessel (large and small at the center) at 2.83 dm$^3$/minute rotameter flow rate- Test 2*

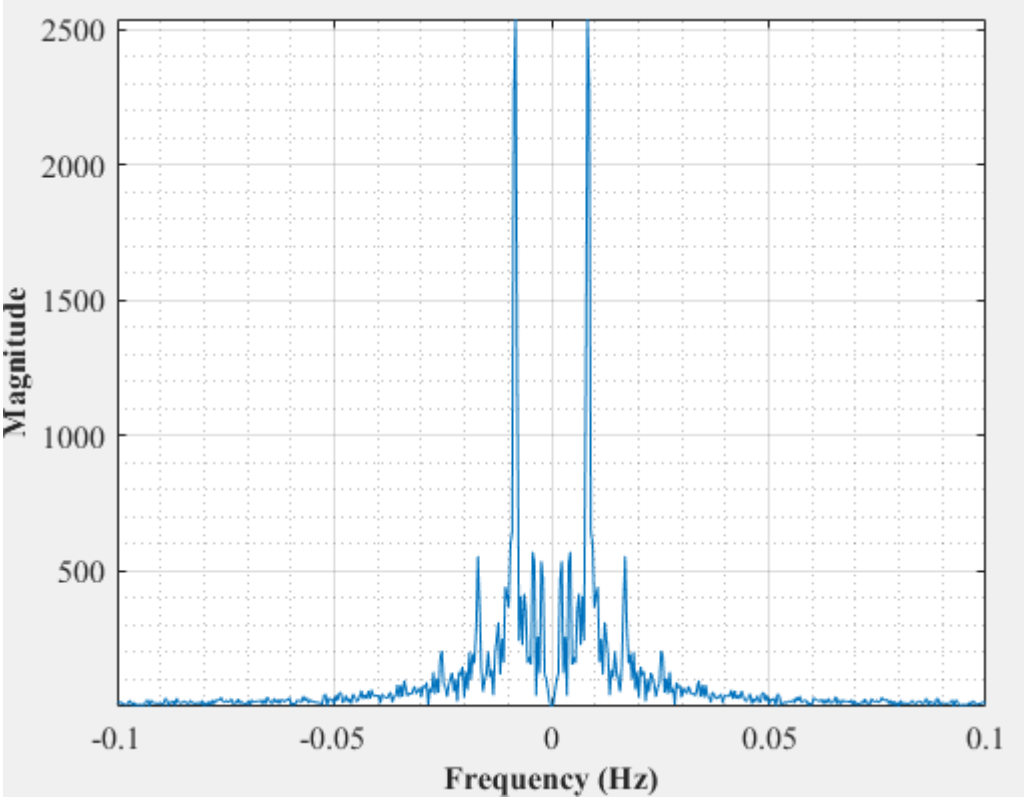


*Figure E-110: Dominant Frequency for a non-uniformly packed vessel (large and small at the center) at 2.83 dm$^3$/minute rotameter flow rate- Test 2*

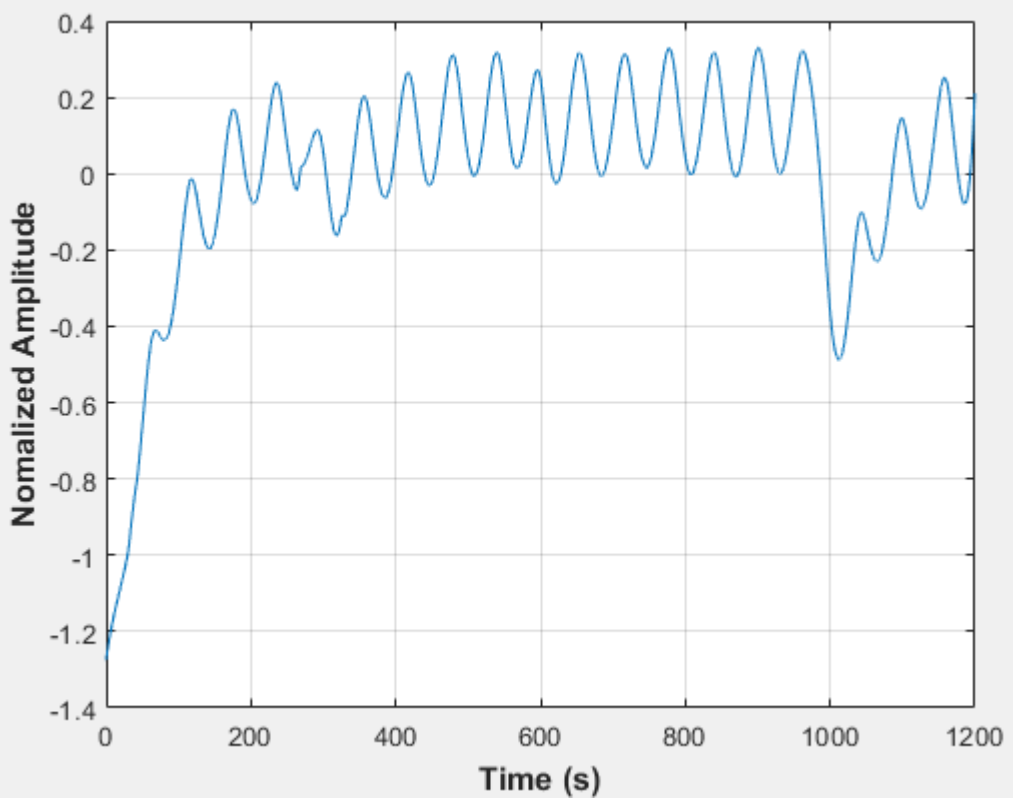


*Figure E-111: Pressure fluctuations in a non-uniformly packed vessel (large and small at the center) at 2.83 $dm^3$/minute rotameter flow rate- Test 3*

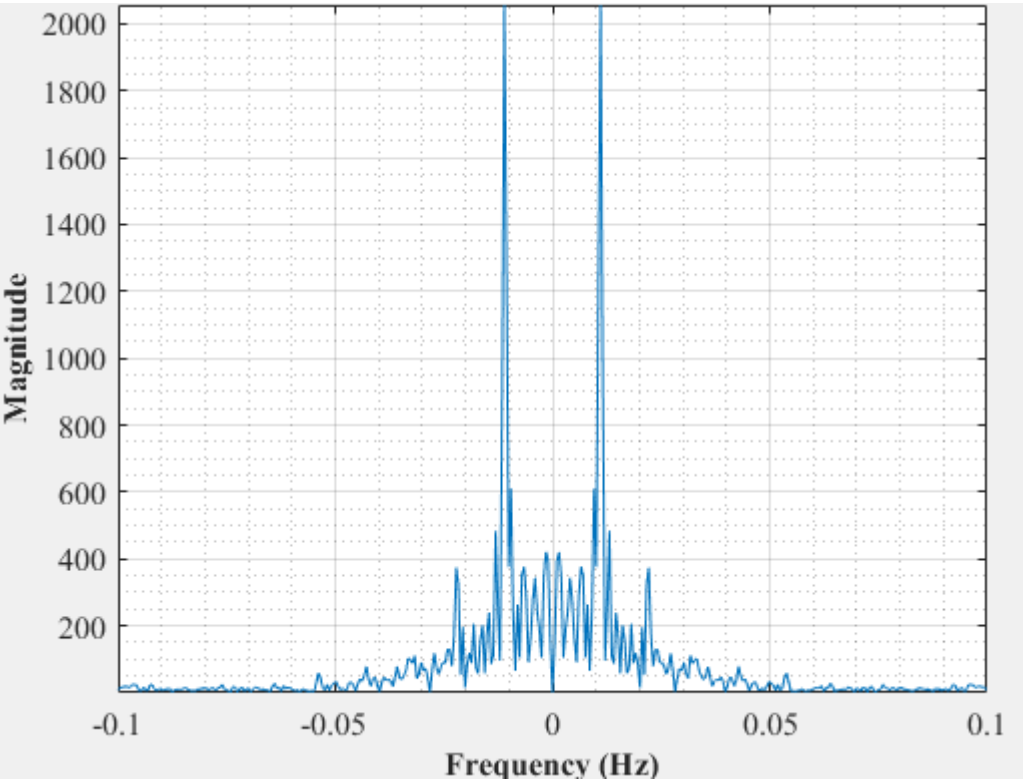


*Figure E-112: Dominant Frequency for a non-uniformly packed vessel (large and small at the center) at 2.83 $dm^3$/minute rotameter flow rate- Test 3*

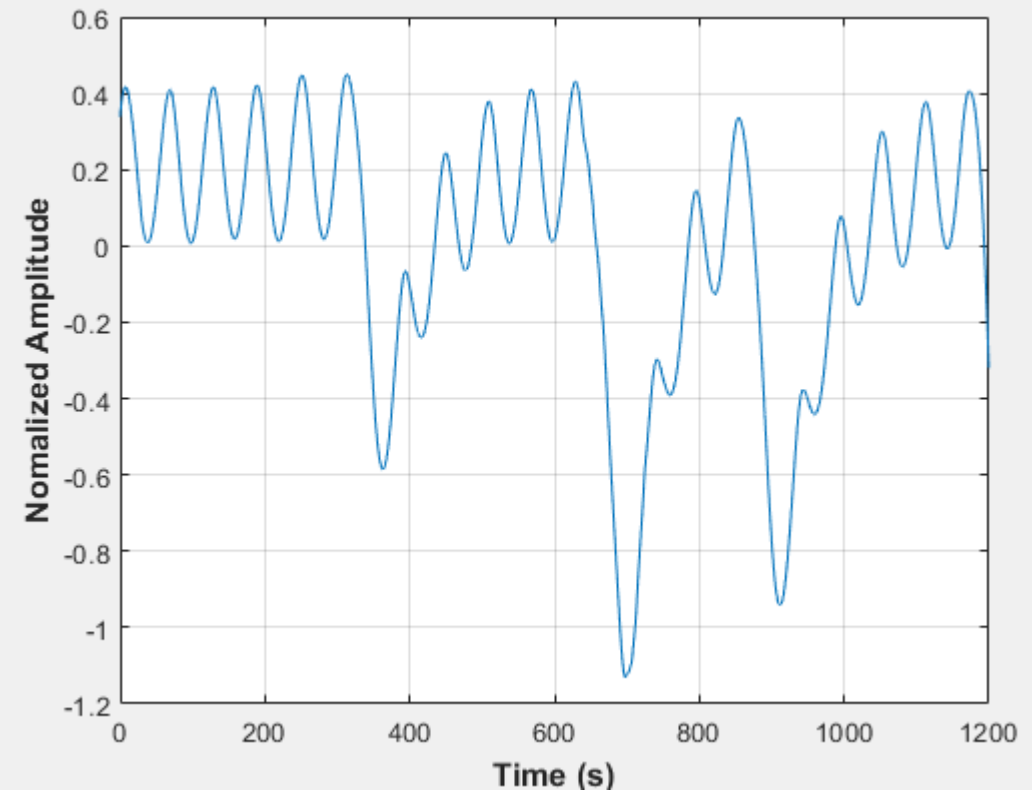


*Figure E-113: Pressure fluctuations in a non-uniformly packed vessel (large and small at the center) at 2.83 dm$^3$/minute rotameter flow rate- Test 4*

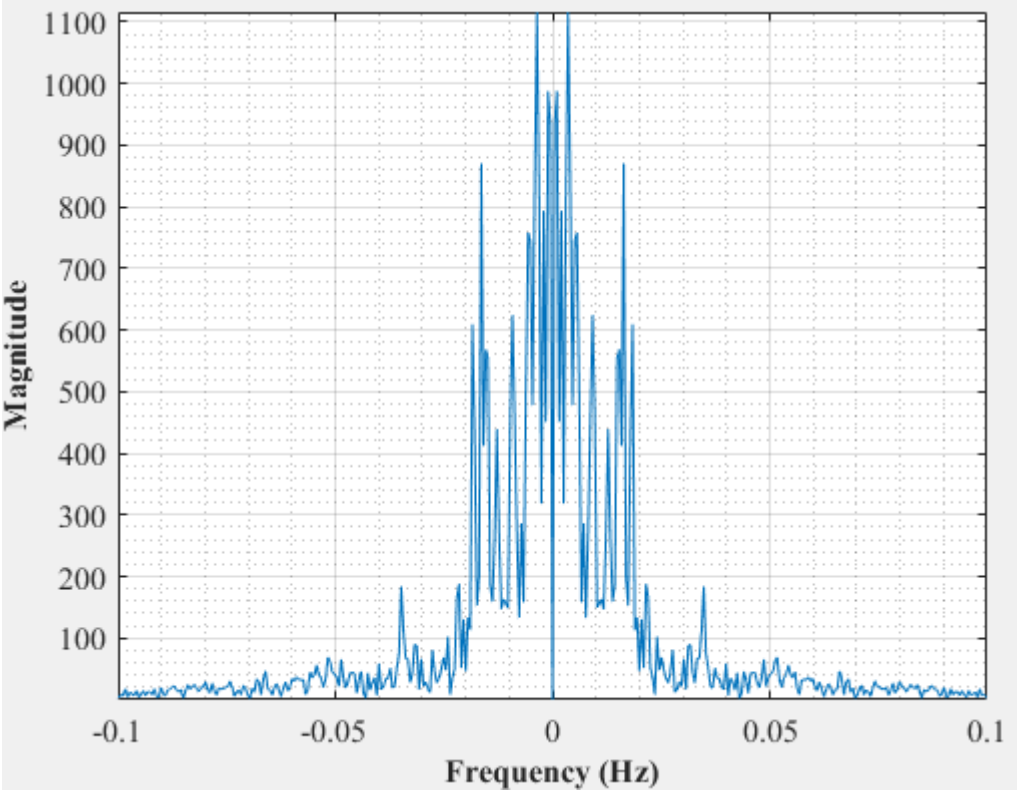


*Figure E-114: Dominant Frequency for a non-uniformly packed vessel (large and small at the center) at 2.83 dm$^3$/minute rotameter flow rate- Test 4*

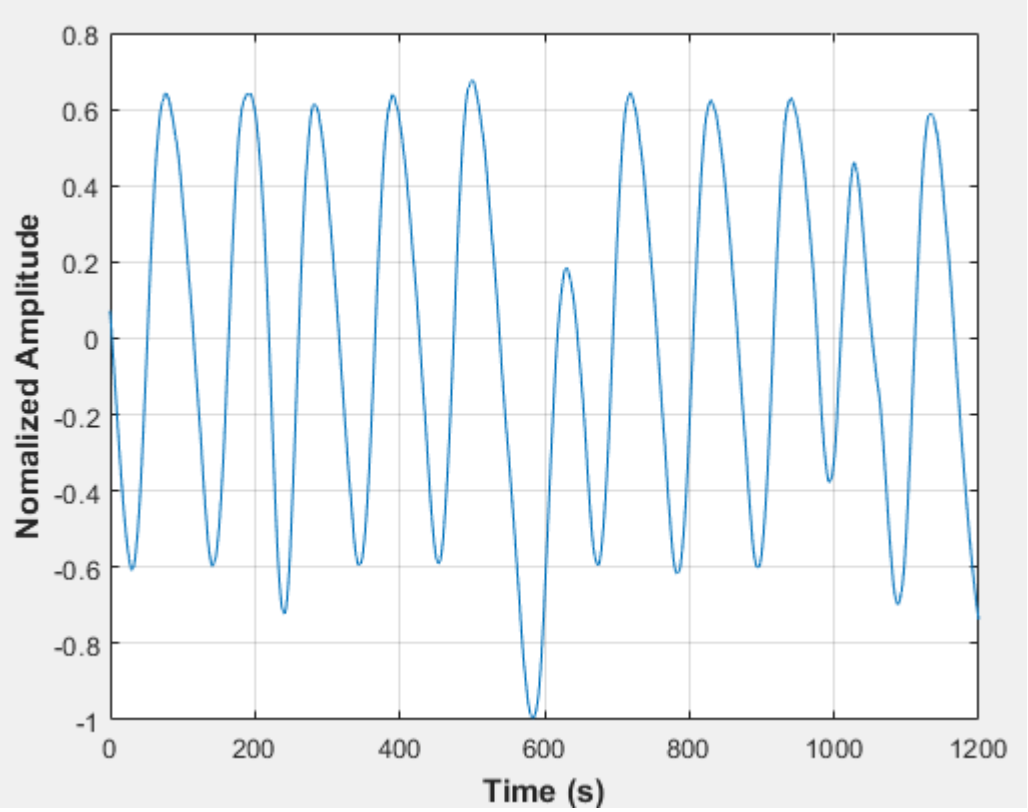


*Figure E-115: Pressure fluctuations in a non-uniformly packed vessel (large and small at the side) at 1.67 dm$^3$/minute rotameter flow rate- Test 1*

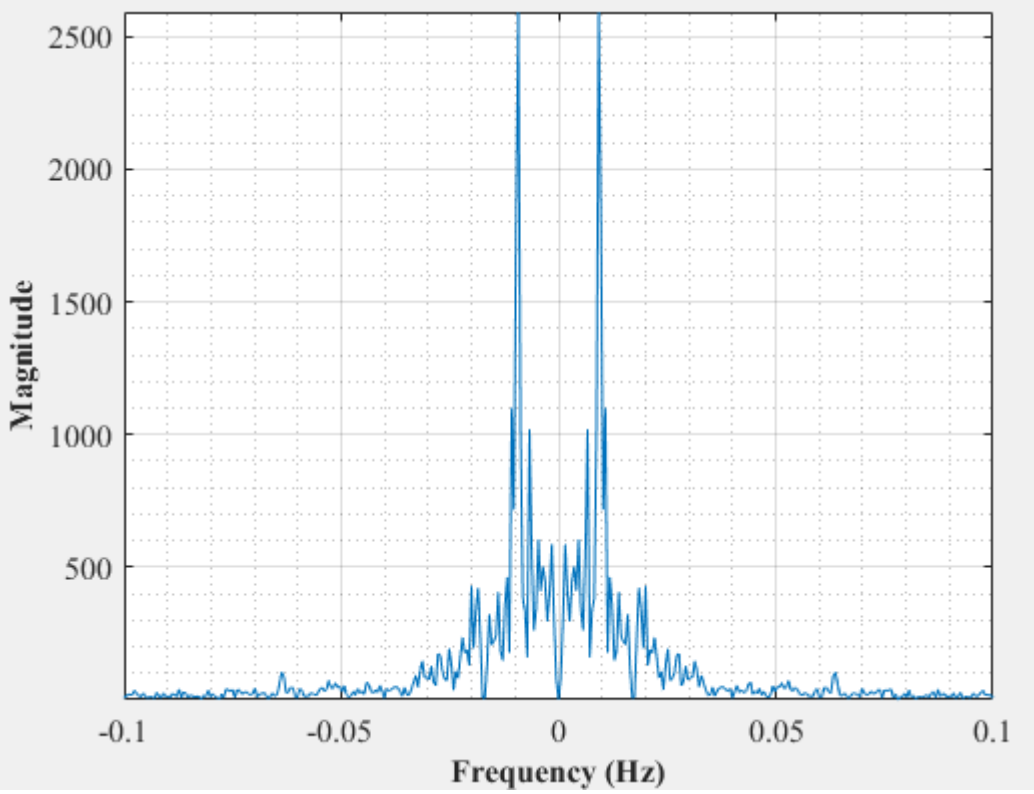


*Figure E-116: Dominant Frequency for a non-uniformly packed vessel (large and small at the side) at 1.67 dm$^3$/minute rotameter flow rate- Test 1*

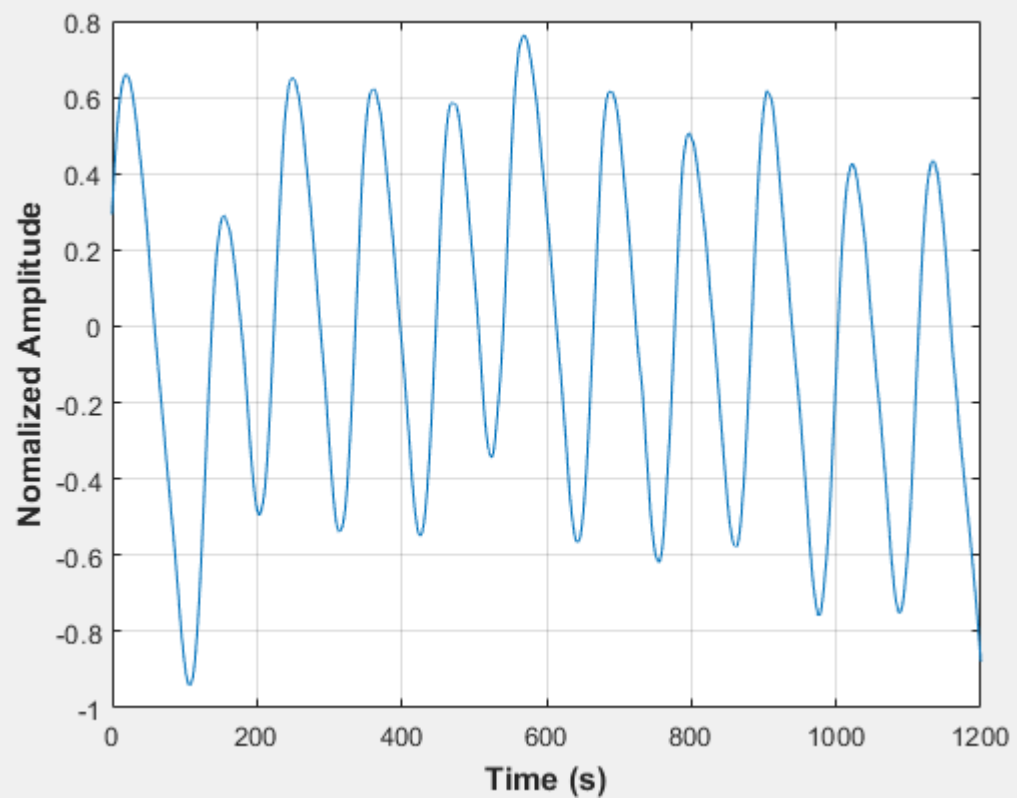


*Figure E-117: Pressure fluctuations in a non-uniformly packed vessel (large and small at the side) at 1.67 dm$^3$/minute rotameter flow rate- Test 2*

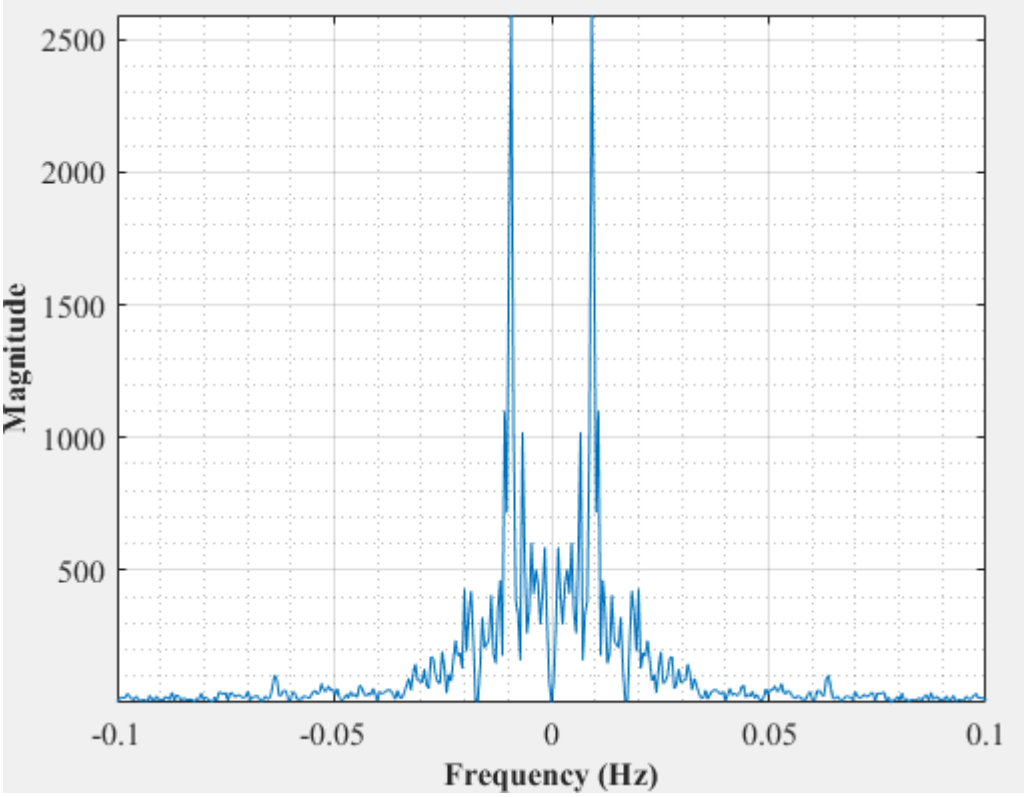


*Figure E-118: Dominant Frequency for a non-uniformly packed vessel (large and small at the side) at 1.67 dm$^3$/minute rotameter flow rate- Test 2*

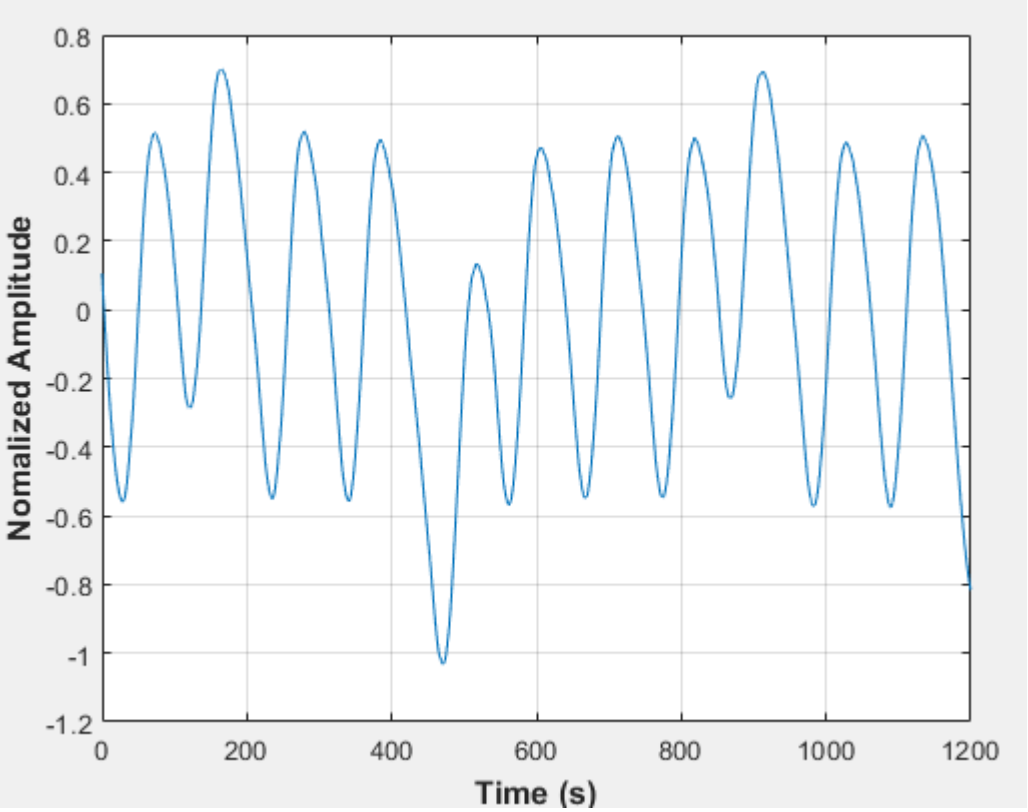


*Figure E-119: Pressure fluctuations in a non-uniformly packed vessel (large and small at the side) at 1.67 dm$^3$/minute rotameter flow rate- Test 3*

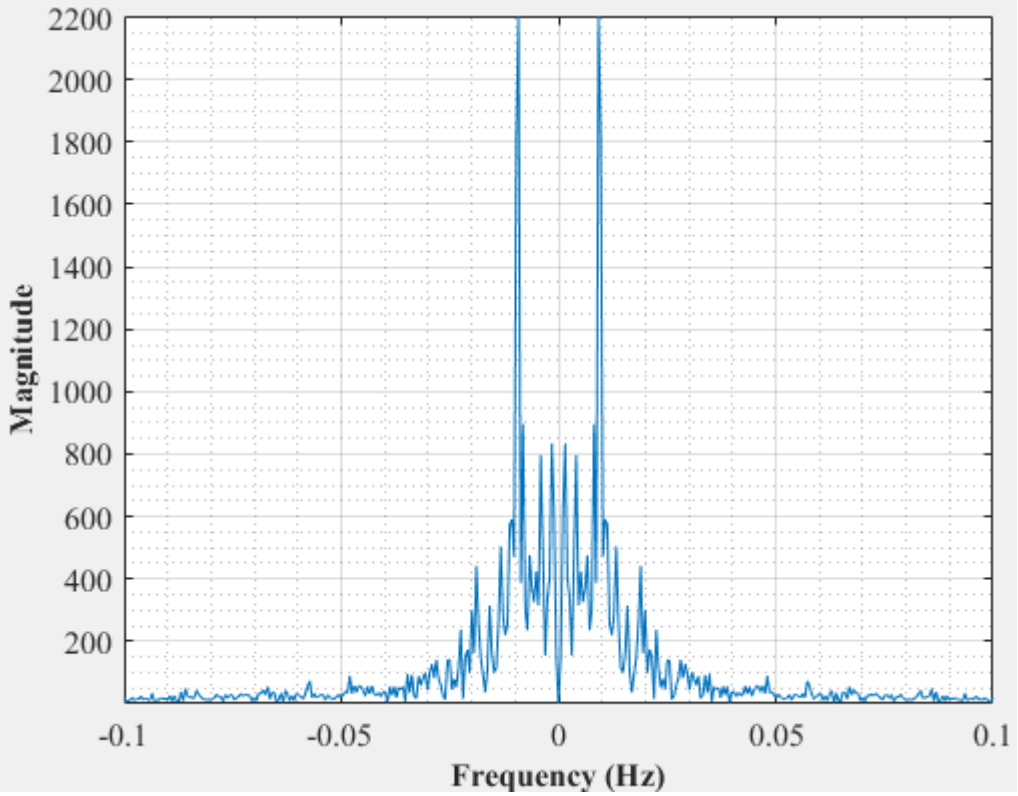


*Figure E-120: Dominant Frequency for a non-uniformly packed vessel (large and small at the side) at 1.67 dm$^3$/minute rotameter flow rate- Test 3*

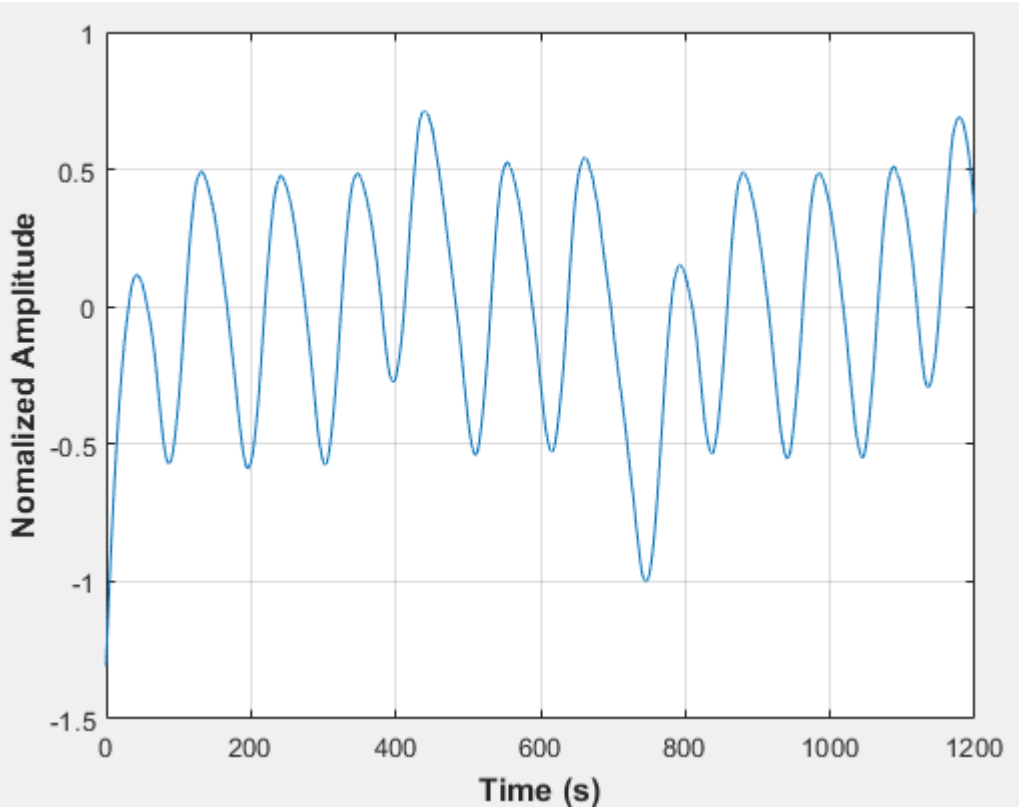


*Figure E-121: Pressure fluctuations in a non-uniformly packed vessel (large and small at the side) at 1.67 dm$^3$/minute rotameter flow rate- Test 4*

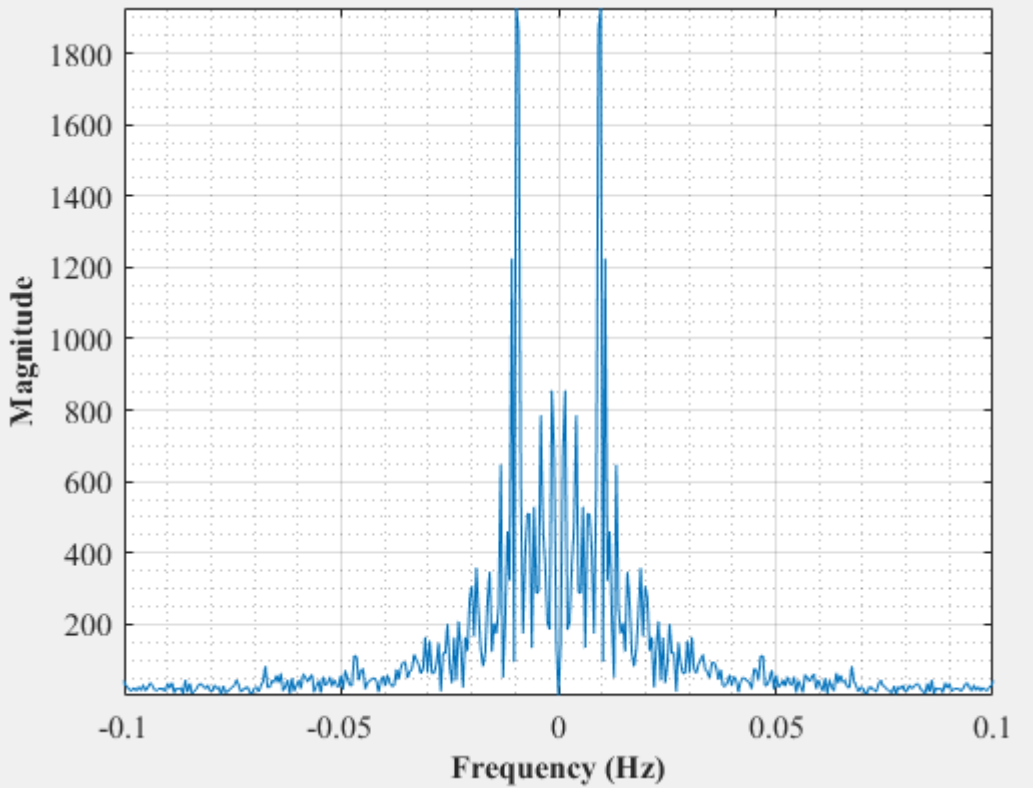


*Figure E-122: Dominant Frequency for a non-uniformly packed vessel (large and small at the side) at 1.67 dm$^3$/minute rotameter flow rate- Test 4*

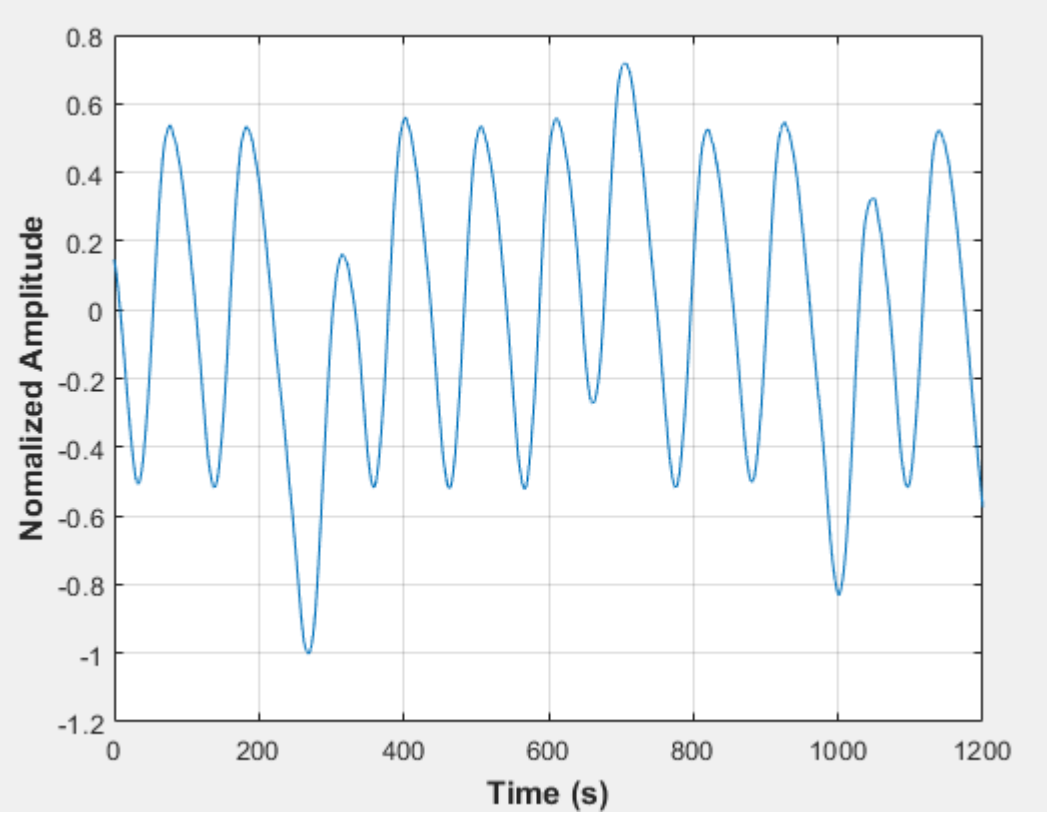


*Figure E-123: Pressure fluctuations in a non-uniformly packed vessel (large and small at the side) at 1.67 dm$^3$/minute rotameter flow rate- Test 5*

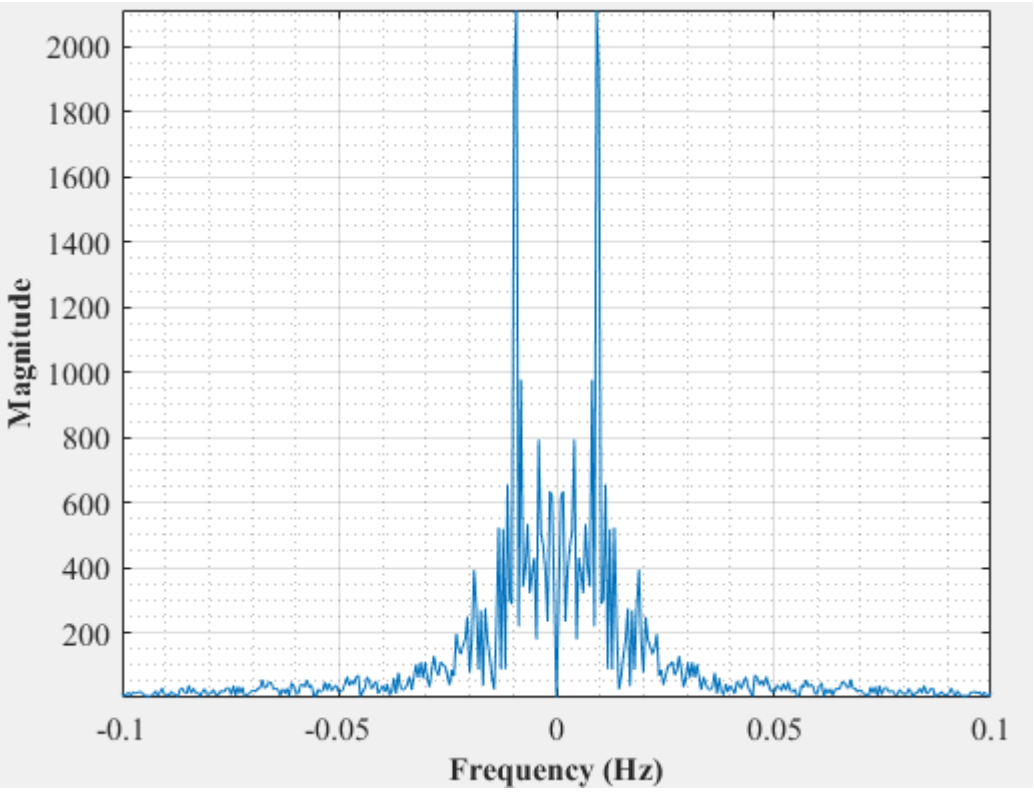


*Figure E-124: Dominant Frequency for a non-uniformly packed vessel (large and small at the side) at 1.67 dm$^3$/minute rotameter flow rate- Test 5*

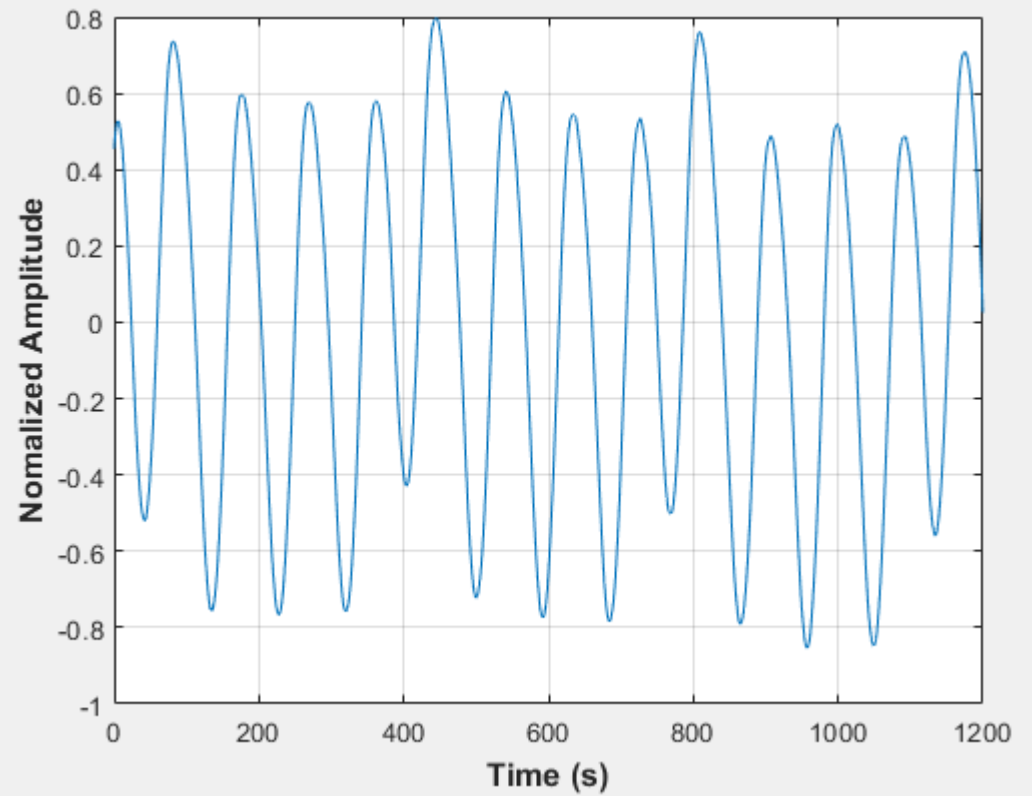


*Figure E-125: Pressure fluctuations in a non-uniformly packed vessel (large and small at the side) at 2 dm$^3$/minute rotameter flow rate- Test 1*

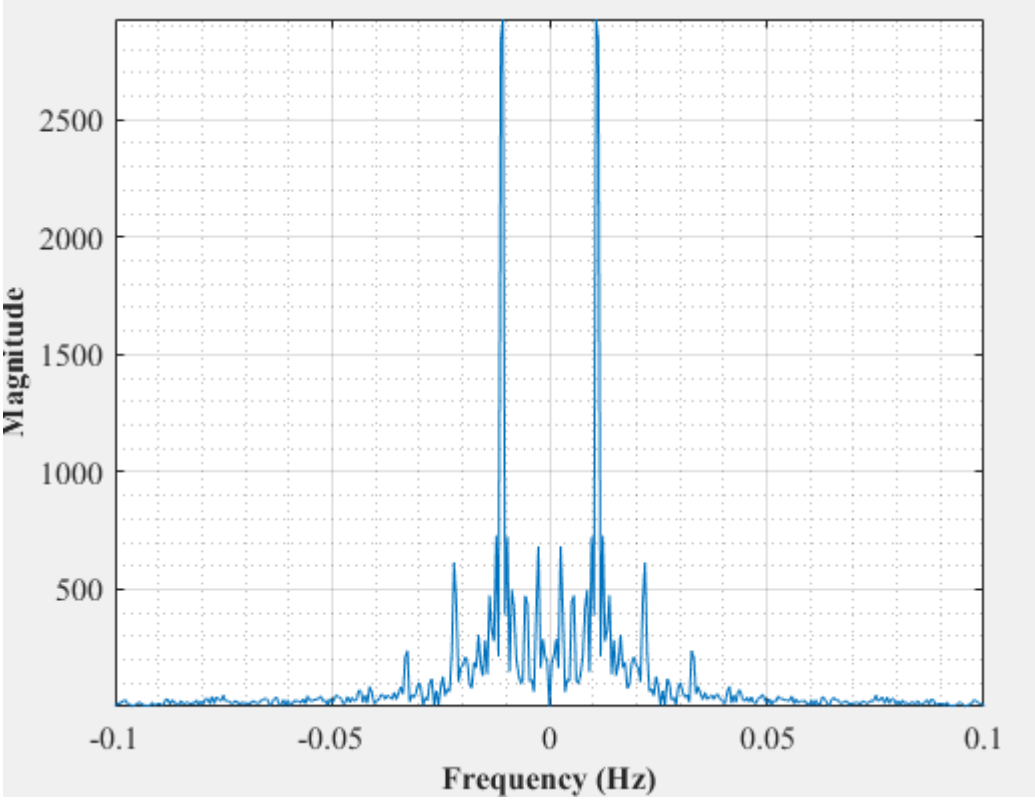


*Figure E-126: Dominant Frequency for a non-uniformly packed vessel (large and small at the side) at 2 dm$^3$/minute rotameter flow rate- Test 1*

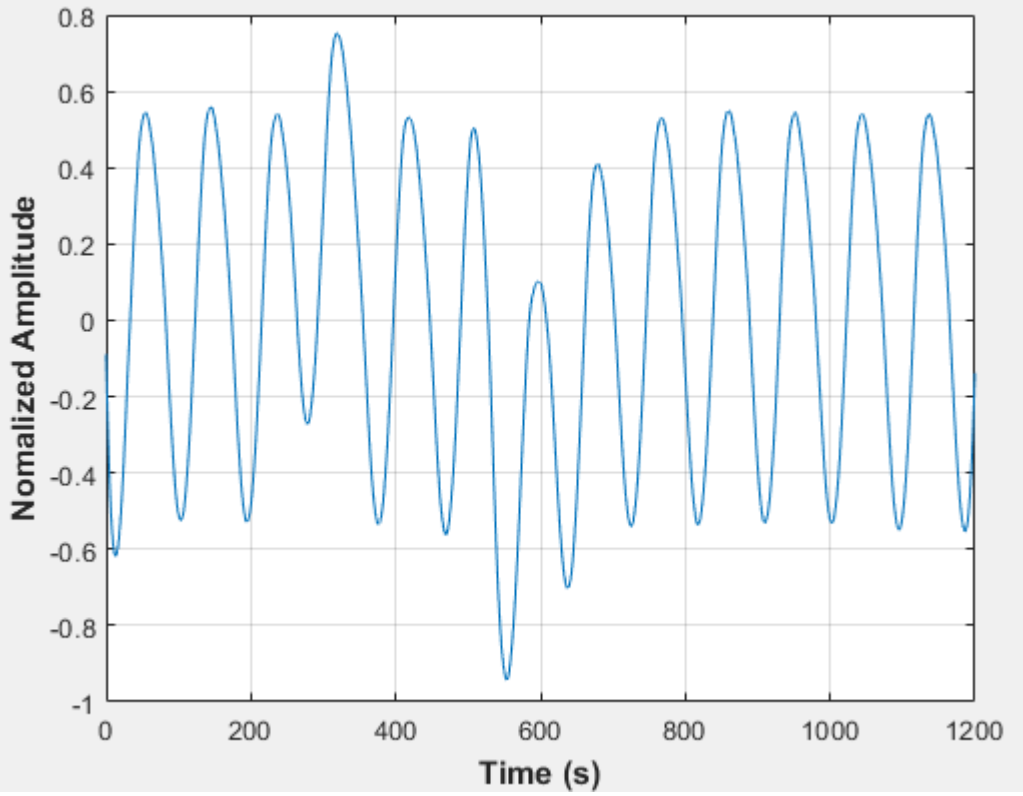


*Figure E-127: Pressure fluctuations in a non-uniformly packed vessel (large and small at the side) at 2 dm$^3$/minute rotameter flow rate- Test 2*

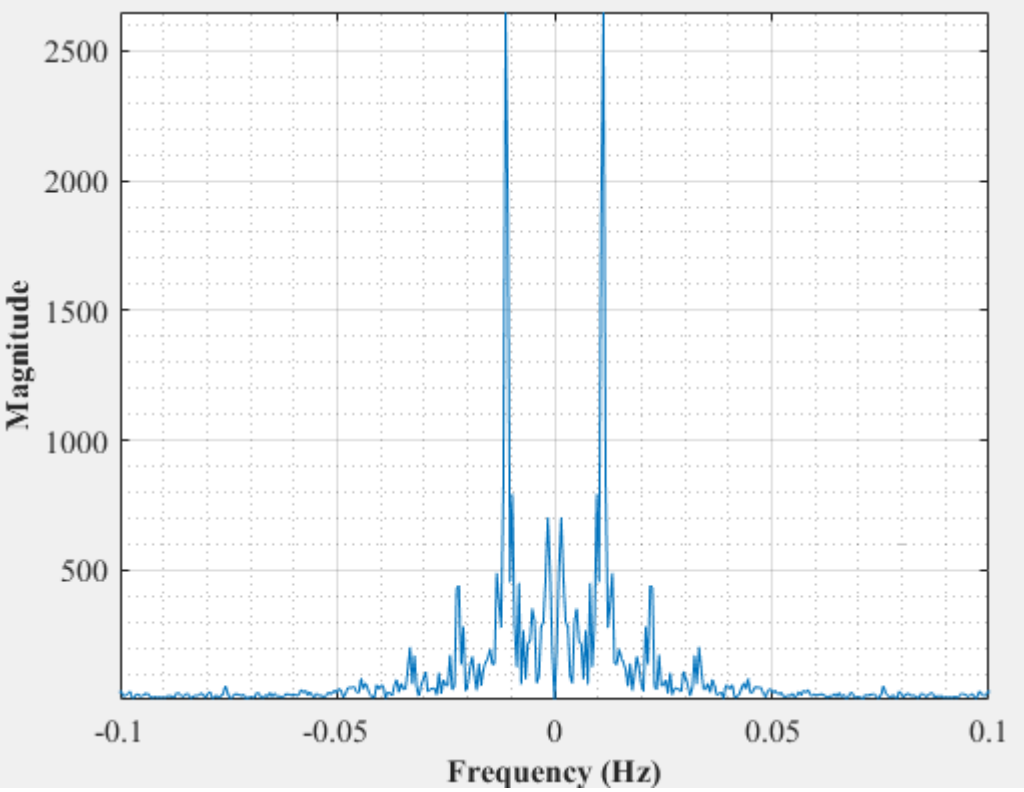


*Figure E-128: Dominant Frequency for a non-uniformly packed vessel (large and small at the side) at 2 dm$^3$/minute rotameter flow rate- Test 2*

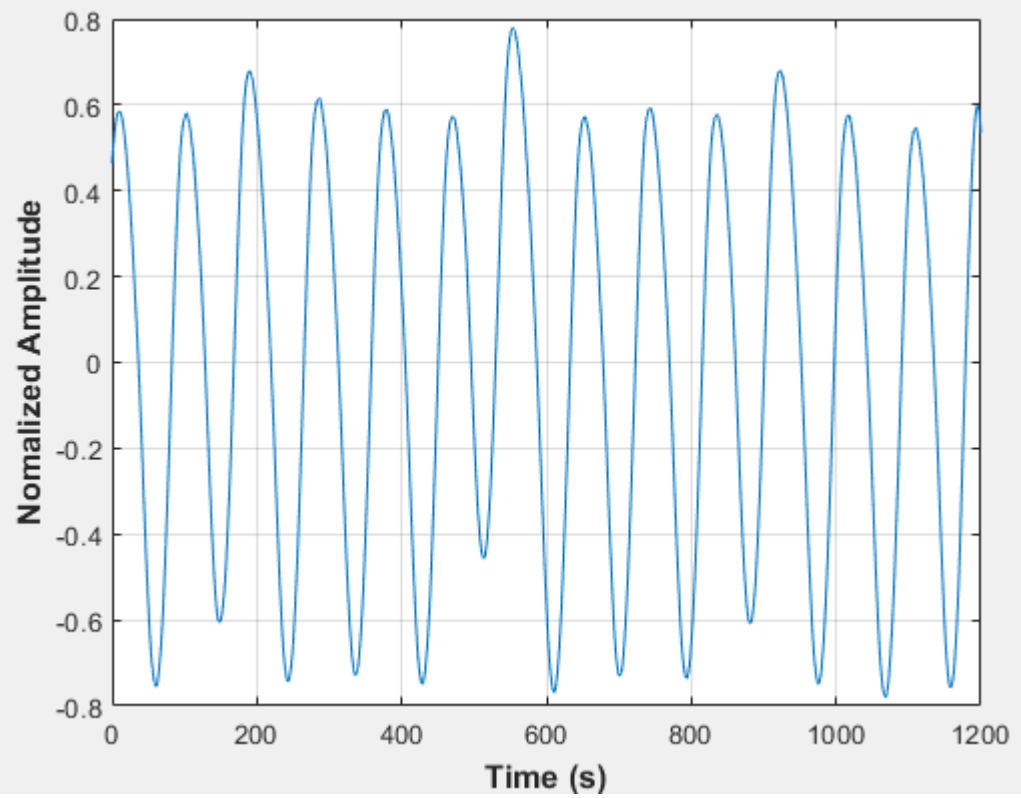


*Figure E-129: Pressure fluctuations in a non-uniformly packed vessel (large and small at the side) at 2 dm$^3$/minute rotameter flow rate- Test 3*

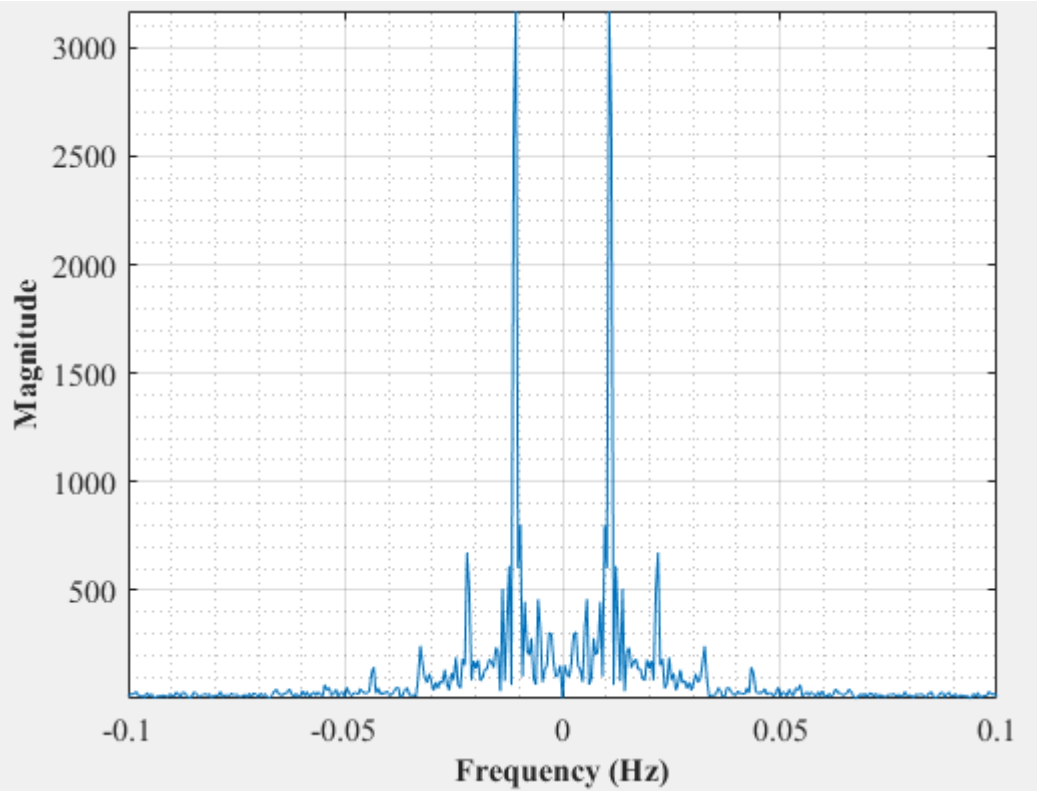


*Figure E-130: Dominant Frequency for a non-uniformly packed vessel (large and small at the side) at 2 dm$^3$/minute rotameter flow rate- Test 3*

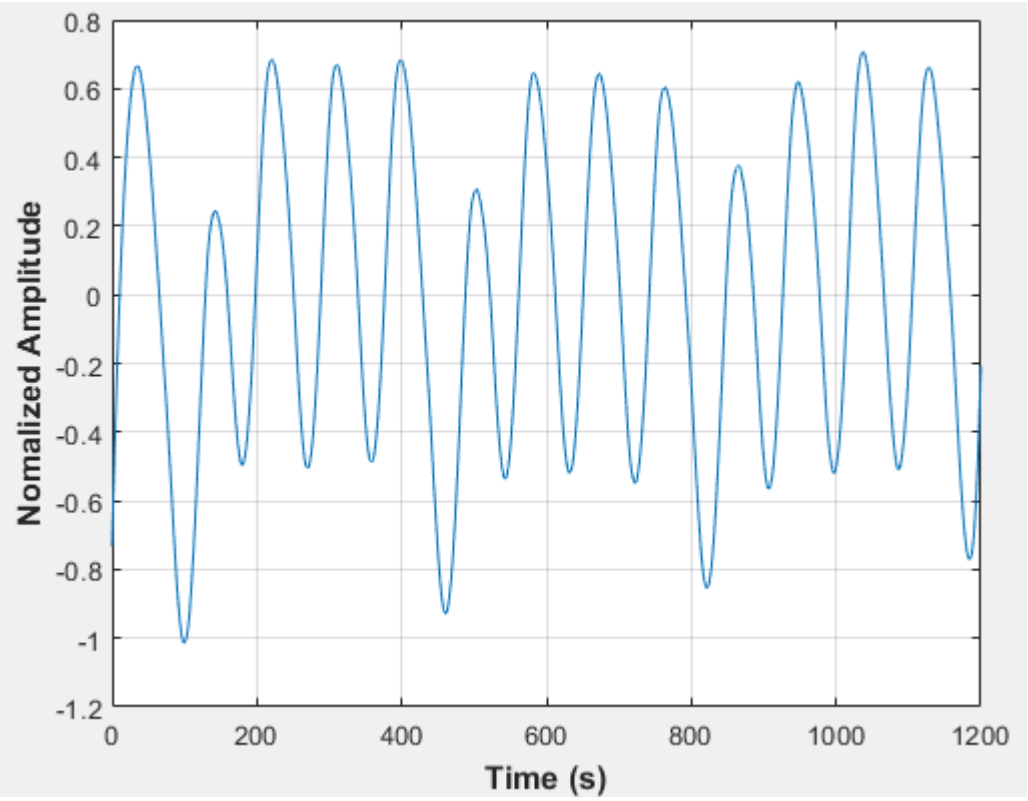


*Figure E-131: Pressure fluctuations in a non-uniformly packed vessel (large and small at the side) at 2 dm$^3$/minute rotameter flow rate- Test 4*

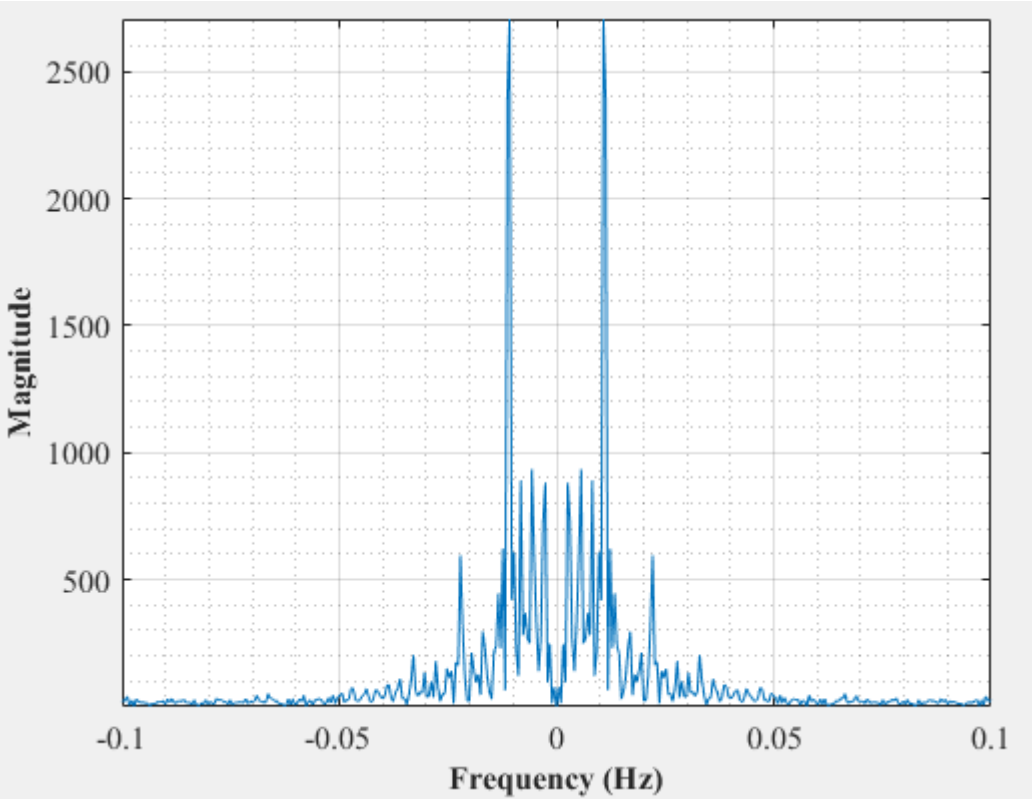


*Figure E-132: Dominant Frequency for a non-uniformly packed vessel (large and small at the side) at 2 dm$^3$/minute rotameter flow rate- Test 4*

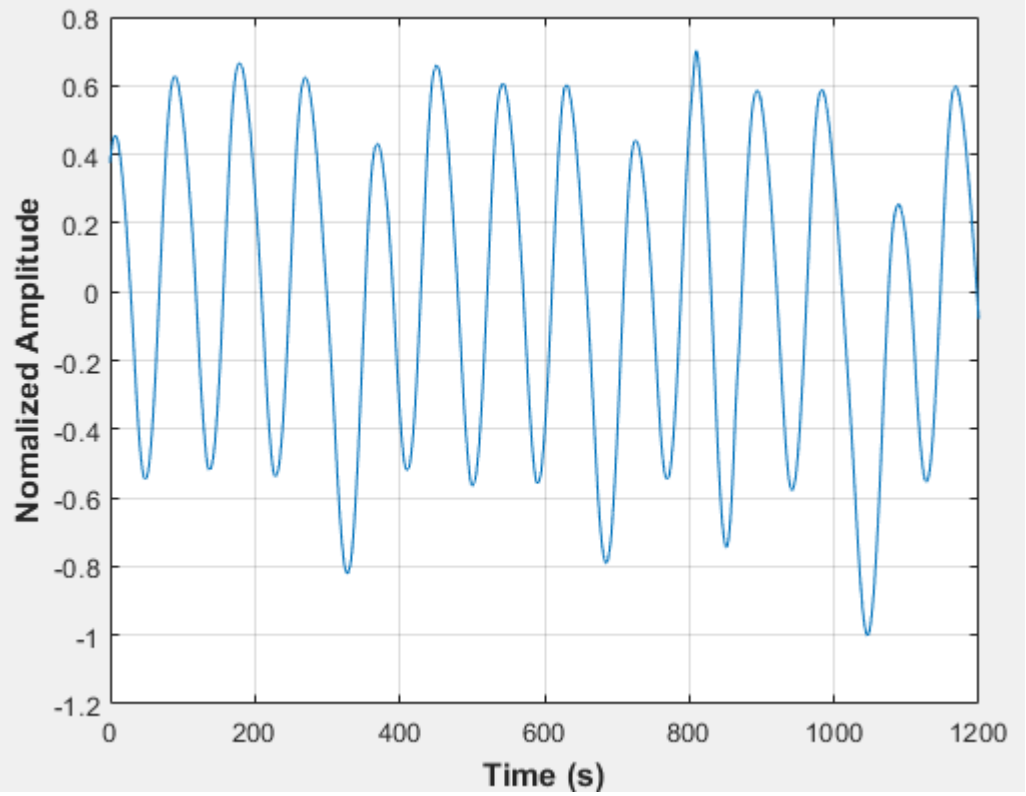


*Figure E-133: Pressure fluctuations in a non-uniformly packed vessel (large and small at the side) at 2 dm$^3$/minute rotameter flow rate- Test 5*

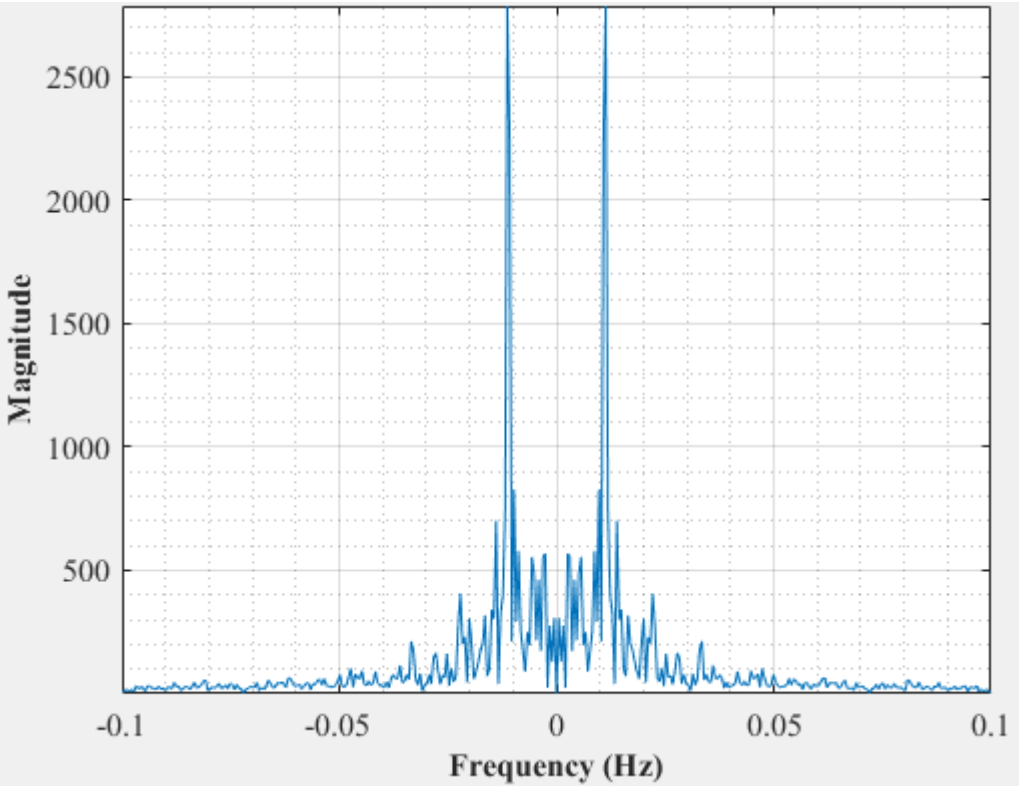


*Figure E-135: Dominant Frequency for a non-uniformly packed vessel (large and small at the side) at 2 dm$^3$/minute rotameter flow rate- Test 5*

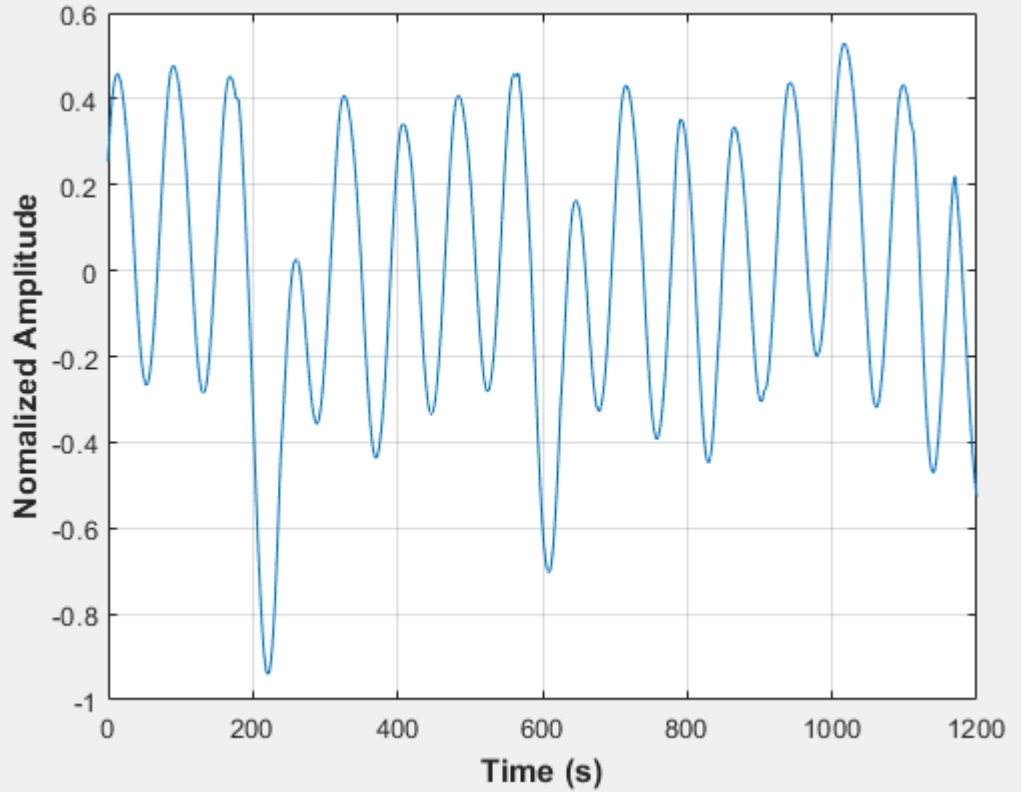


*Figure E-135: Pressure fluctuations in a non-uniformly packed vessel (large and small at the side) at 2.33 $dm^3$/minute rotameter flow rate- Test 1*

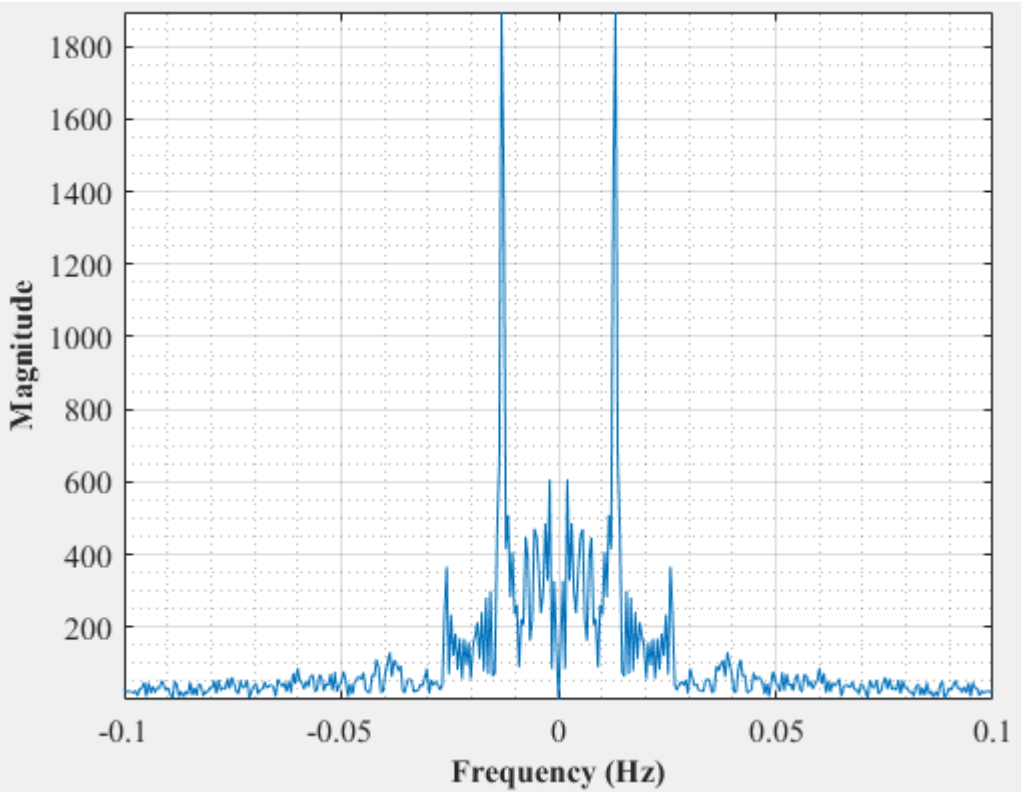


*Figure E-137: Dominant Frequency for a non-uniformly packed vessel (large and small at the side) at 2.33 $dm^3$/minute rotameter flow rate- Test 1*

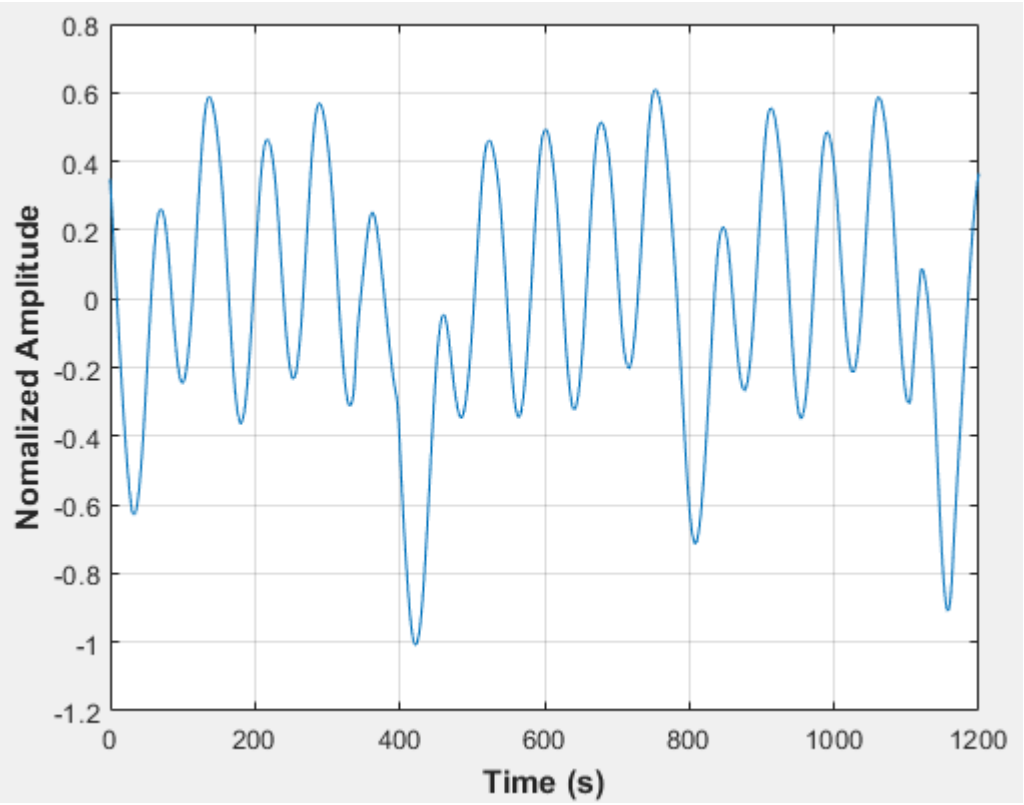


*Figure E-137: Pressure fluctuations in a non-uniformly packed vessel (large and small at the side) at 2.33 dm$^3$/minute rotameter flow rate- Test 2*

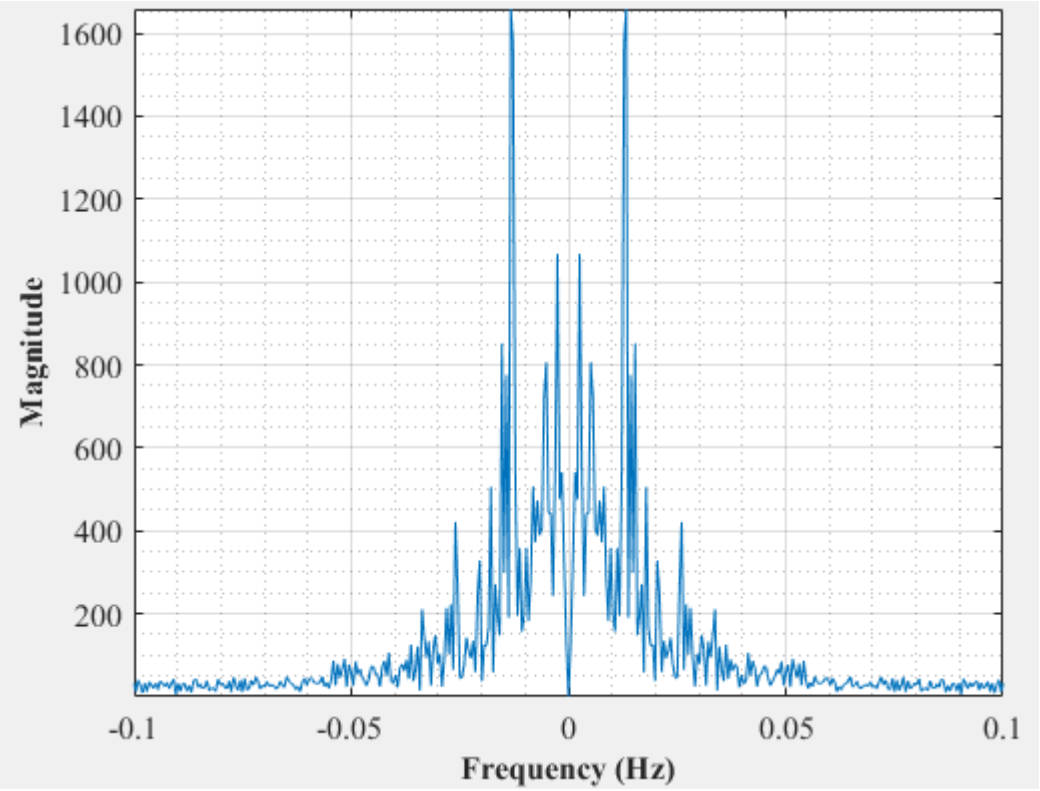


*Figure E-138: Dominant Frequency for a non-uniformly packed vessel (large and small at the side) at 2.33 dm$^3$/minute rotameter flow rate- Test 2*

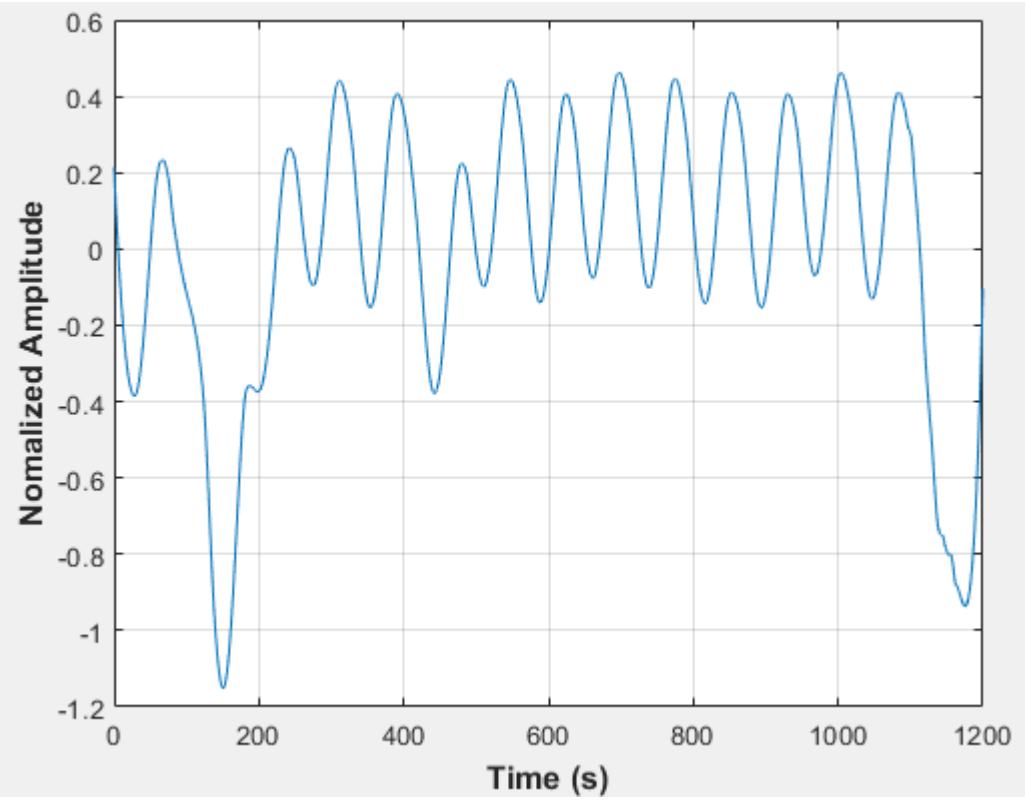


*Figure E-139: Pressure fluctuations in a non-uniformly packed vessel (large and small at the side) at 2.33 $dm^3$/minute rotameter flow rate- Test 3*

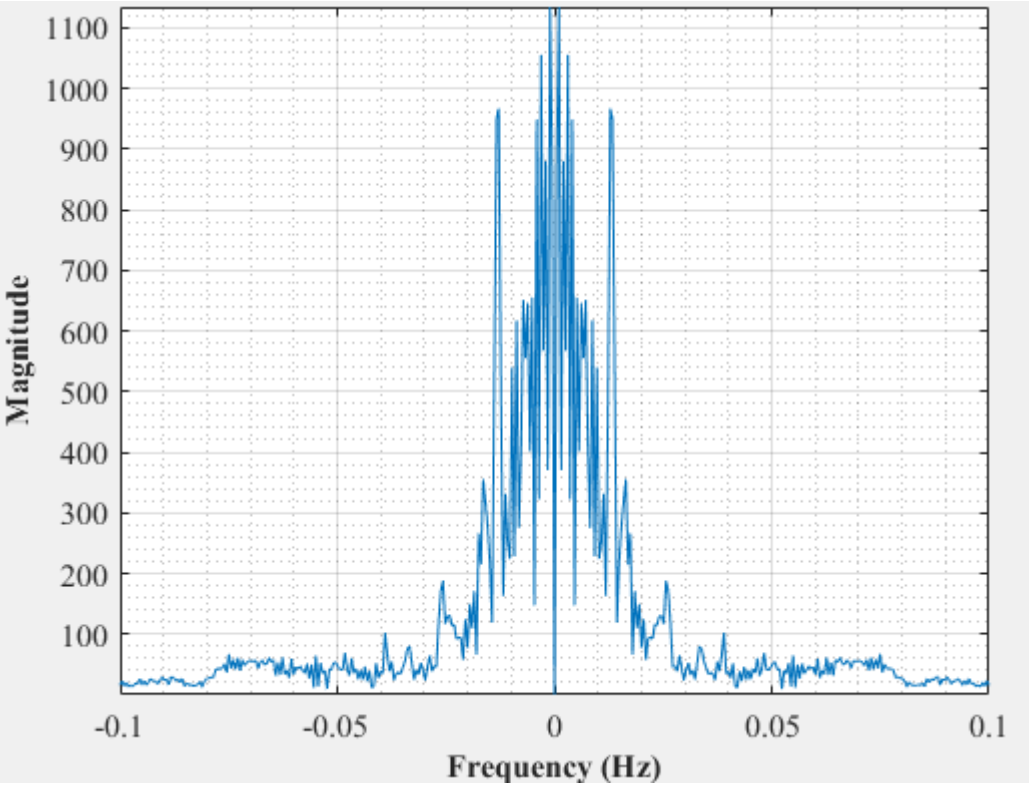


*Figure E-140: Dominant Frequency for a non-uniformly packed vessel (large and small at the side) at 2.33 $dm^3$/minute rotameter flow rate- Test 3*

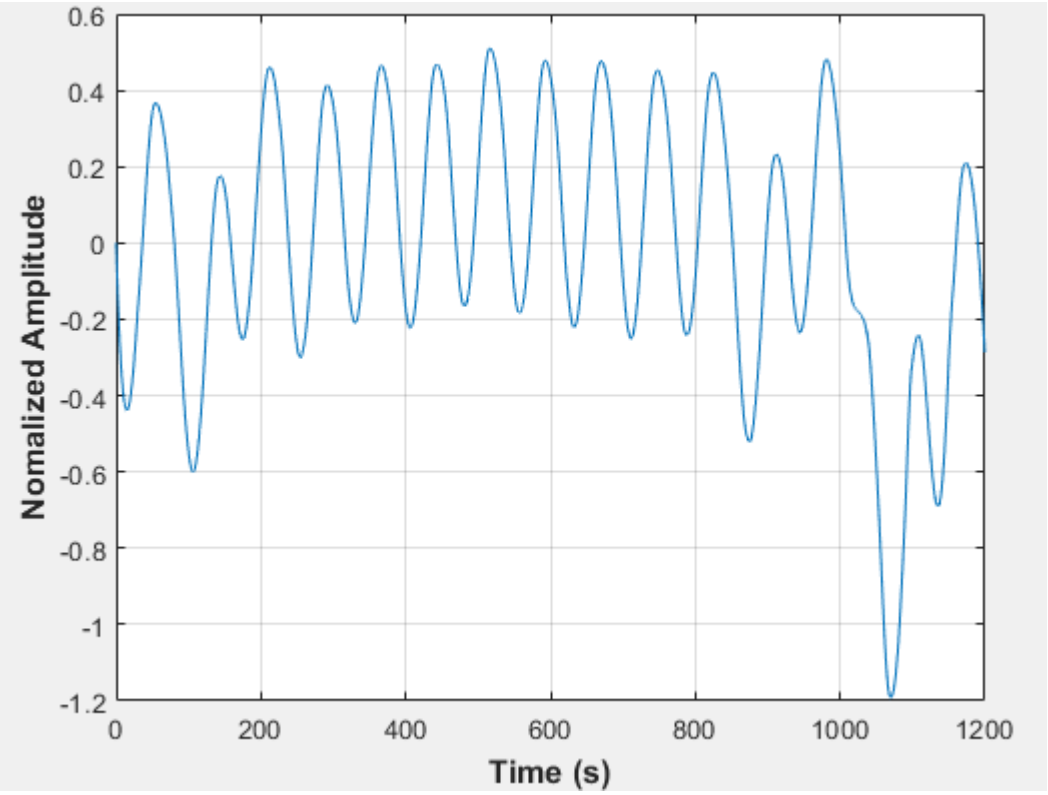


*Figure E-141: Pressure fluctuations in a non-uniformly packed vessel (large and small at the side) at 2.33 dm$^3$/minute rotameter flow rate- Test 4*

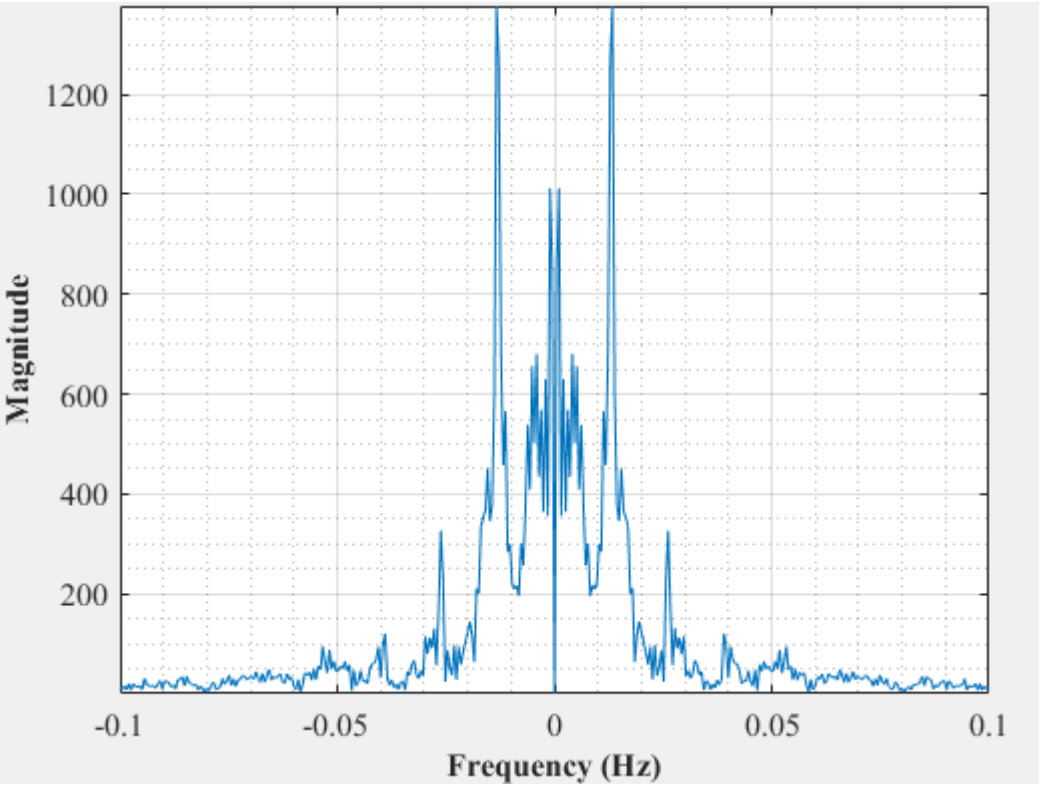


*Figure E-142: Dominant Frequency for a non-uniformly packed vessel (large and small at the side) at 2.33 dm$^3$/minute rotameter flow rate- Test 4*

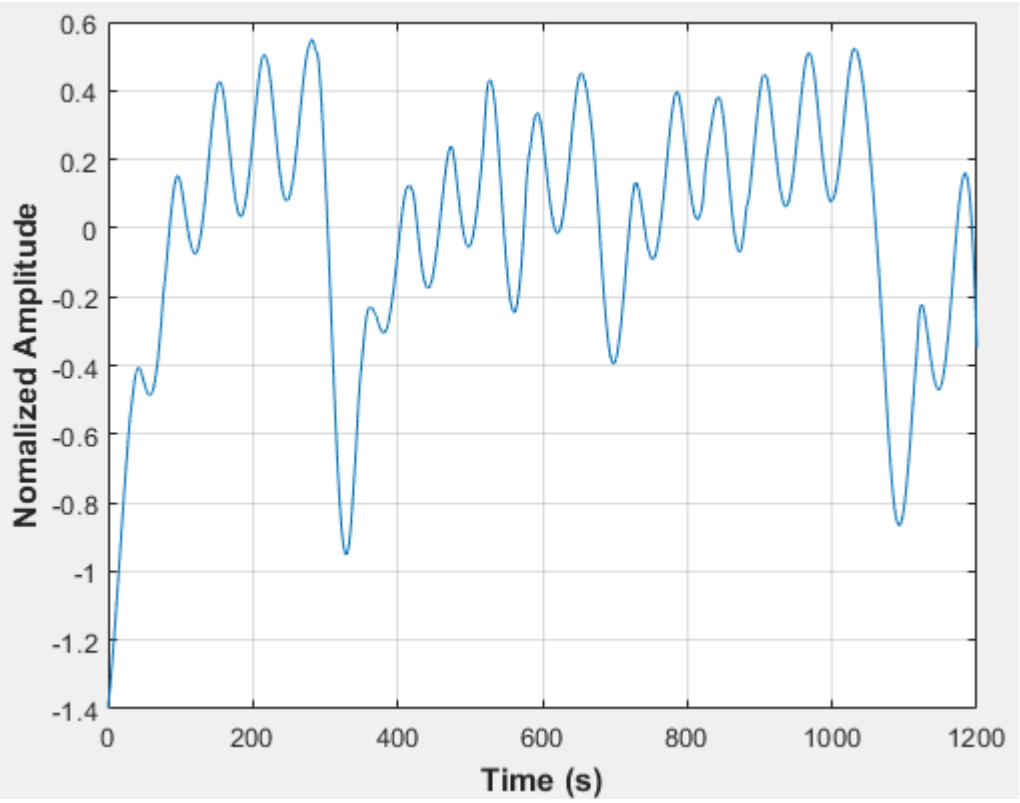


*Figure E-143: Pressure fluctuations in a non-uniformly packed vessel (large and small at the side) at 2.67 dm$^3$/minute rotameter flow rate- Test 1*

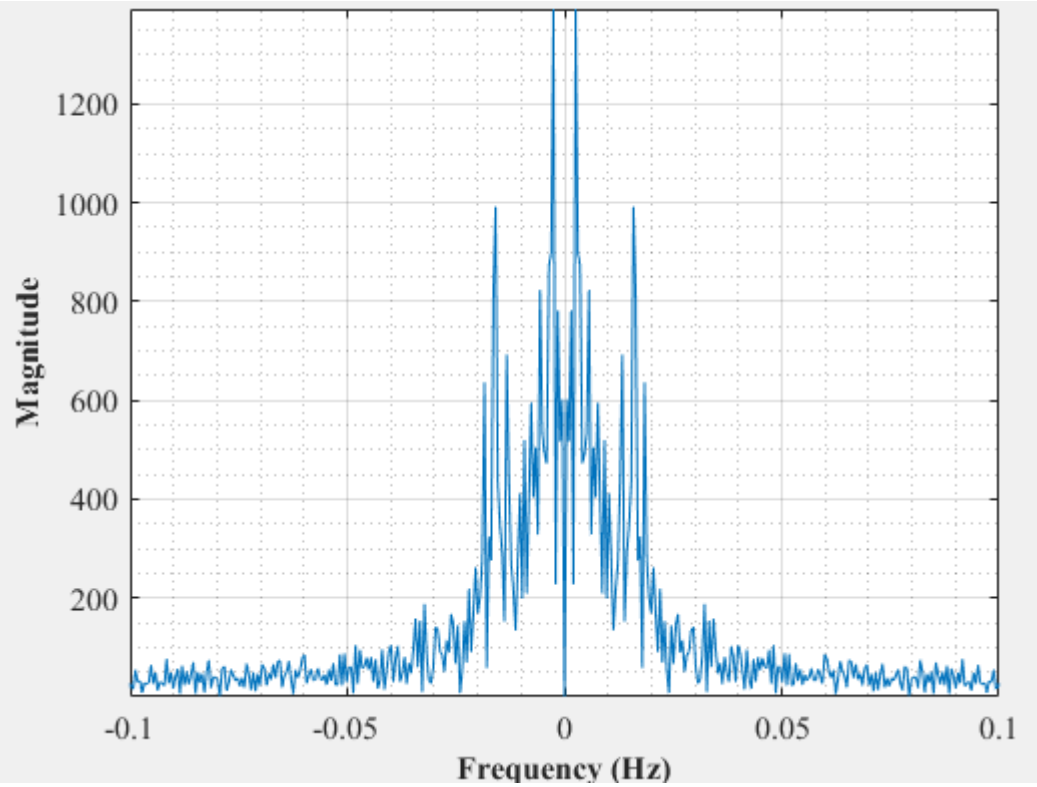


*Figure E-144: Dominant Frequency for a non-uniformly packed vessel (large and small at the side) at 2.67 dm$^3$/minute rotameter flow rate- Test 1*

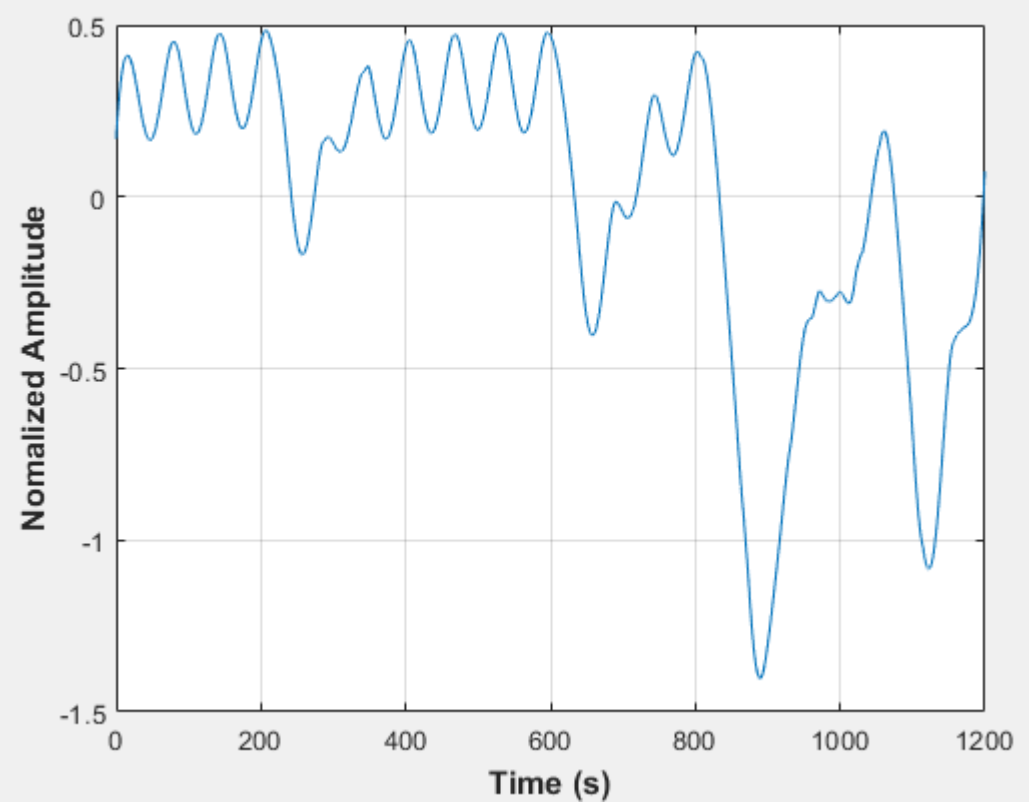


*Figure E-145: Pressure fluctuations in a non-uniformly packed vessel (large and small at the side) at 2.67 dm$^3$/minute rotameter flow rate- Test 2*

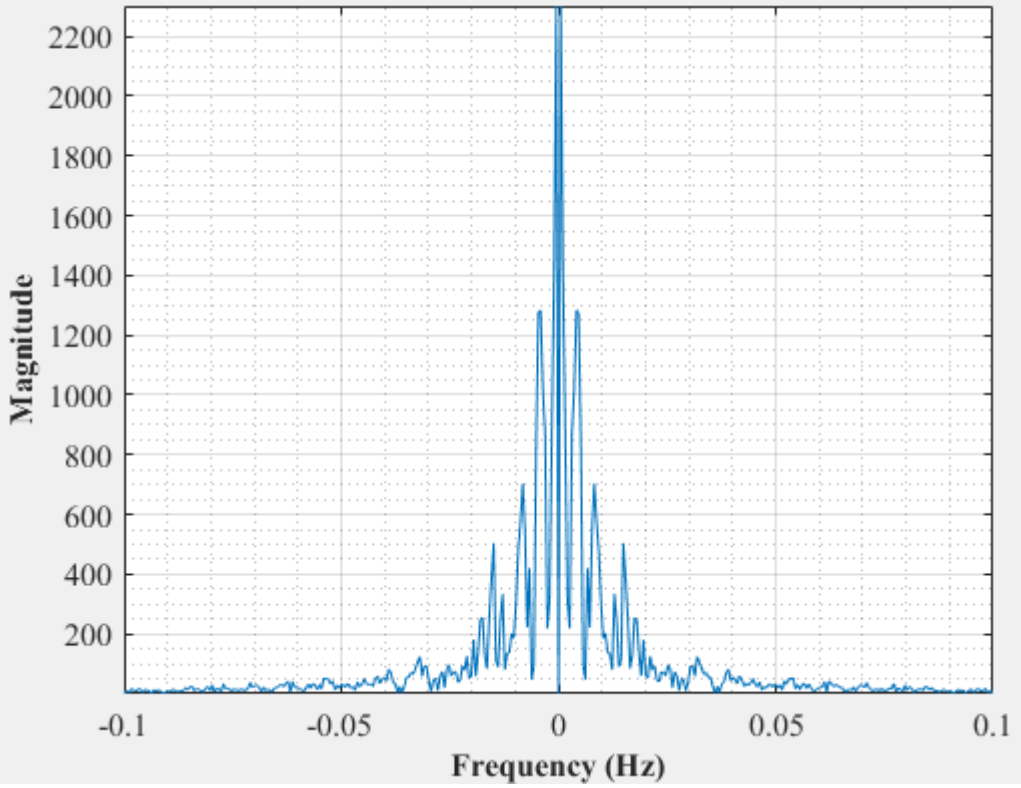


*Figure E-146: Dominant Frequency for a non-uniformly packed vessel (large and small at the side) at 2.67 dm$^3$/minute rotameter flow rate- Test 2*

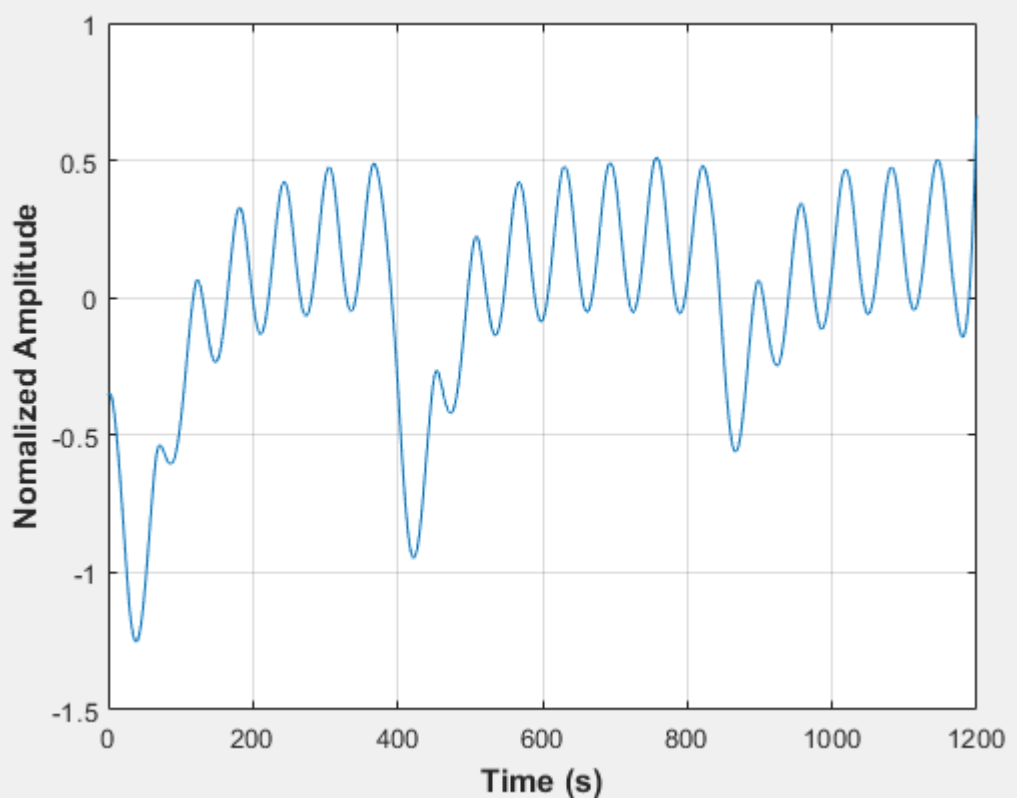


*Figure E-147: Pressure fluctuations in a non-uniformly packed vessel (large and small at the side) at 2.67 dm$^3$/minute rotameter flow rate- Test 3*

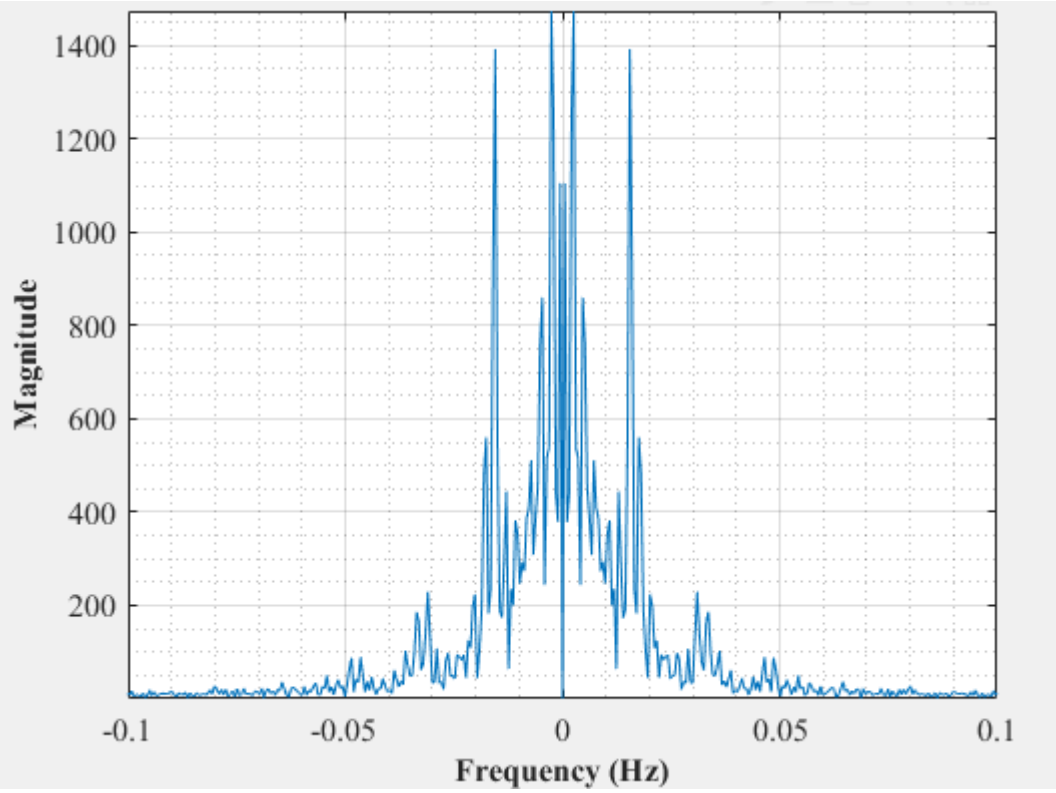


*Figure E-148: Dominant Frequency for a non-uniformly packed vessel (large and small at the side) at 2.67 dm$^3$/minute rotameter flow rate- Test 3*

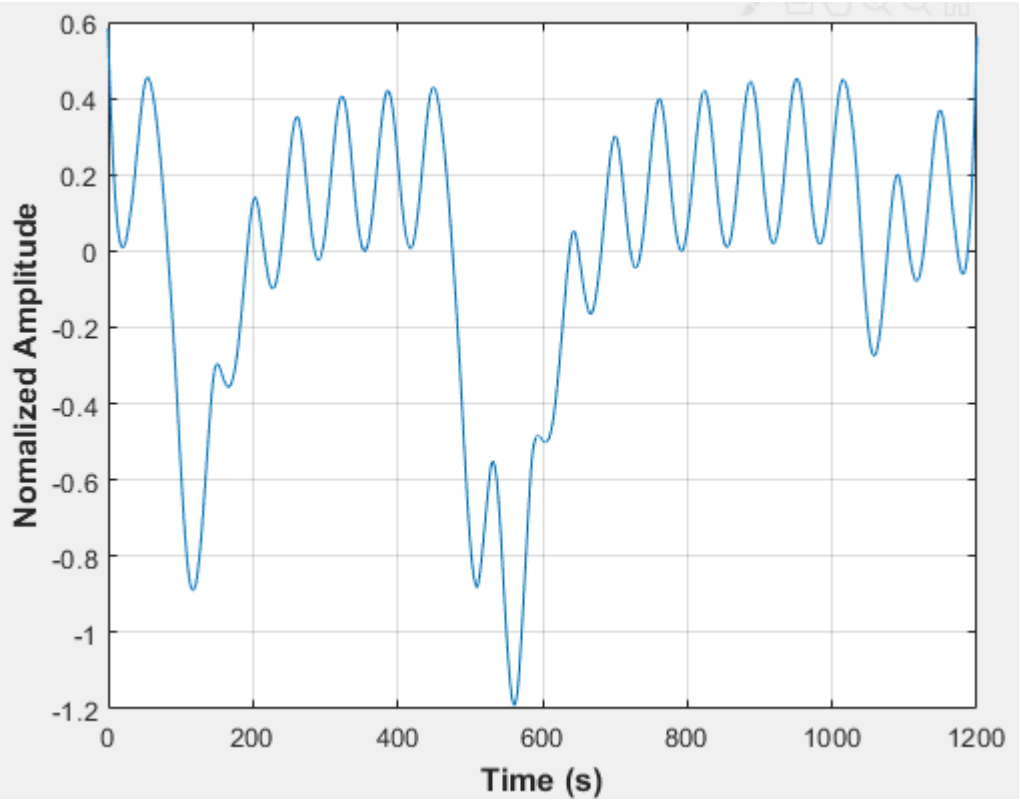


*Figure E-149: Pressure fluctuations in a non-uniformly packed vessel (large and small at the side) at 2.67 dm$^3$/minute rotameter flow rate- Test 4*

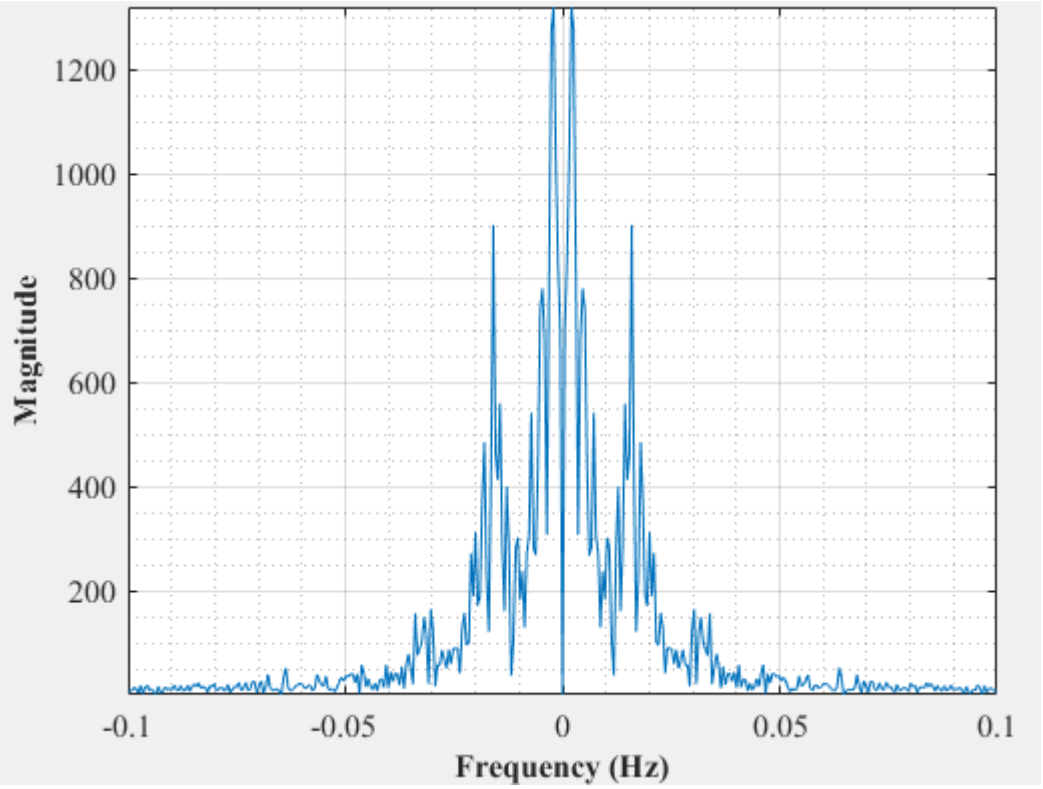


*Figure E-150: Dominant Frequency for a non-uniformly packed vessel (large and small at the side) at 2.67 dm$^3$/minute rotameter flow rate- Test 4*

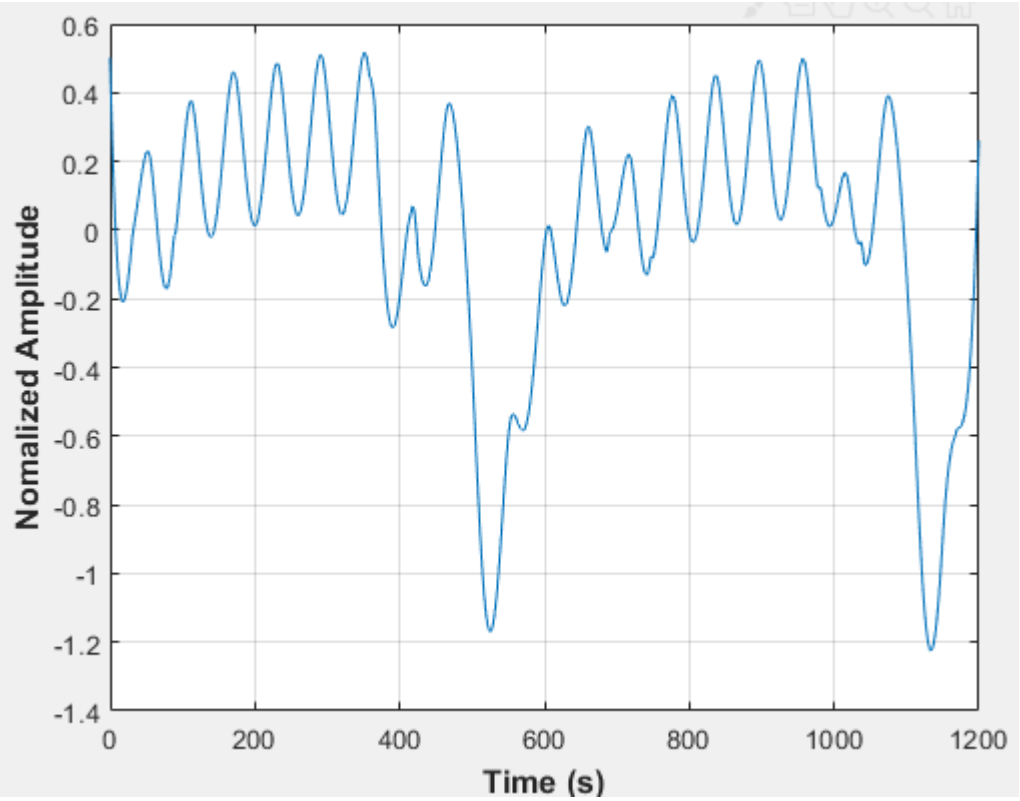


*Figure E-151: Pressure fluctuations in a non-uniformly packed vessel (large and small at the side) at 2.83 $dm^3$/minute rotameter flow rate- Test 1*

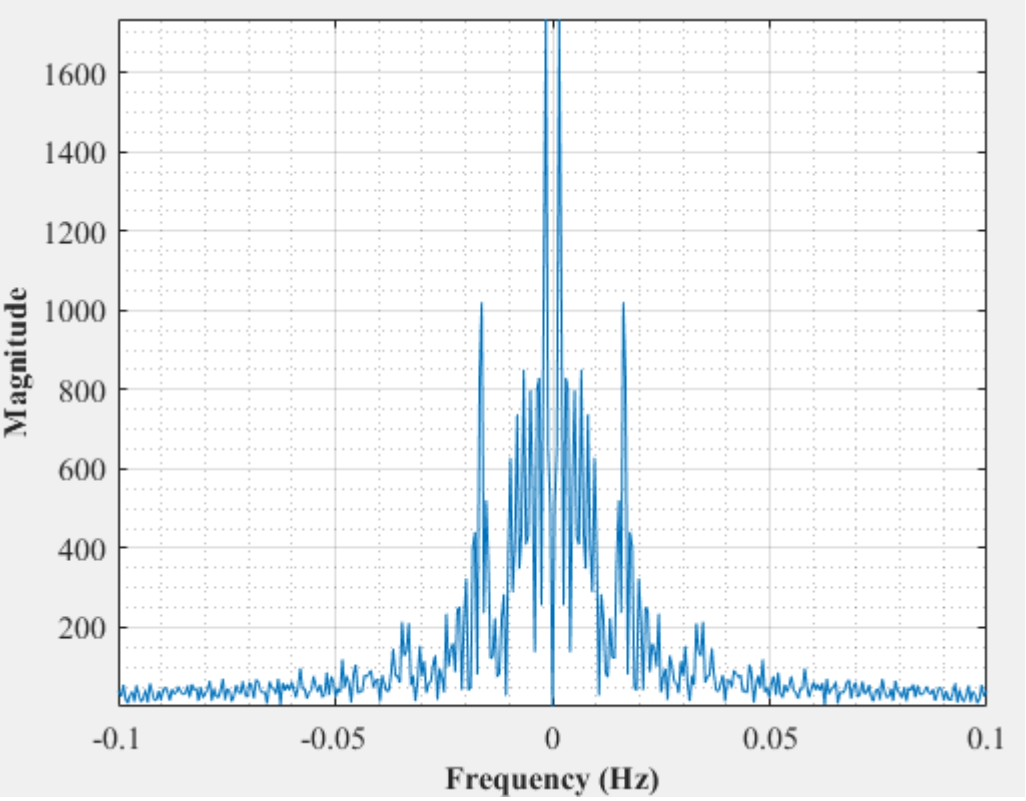


*Figure E-152: Dominant Frequency for a non-uniformly packed vessel (large and small at the side) at 2.83 $dm^3$/minute rotameter flow rate- Test 1*

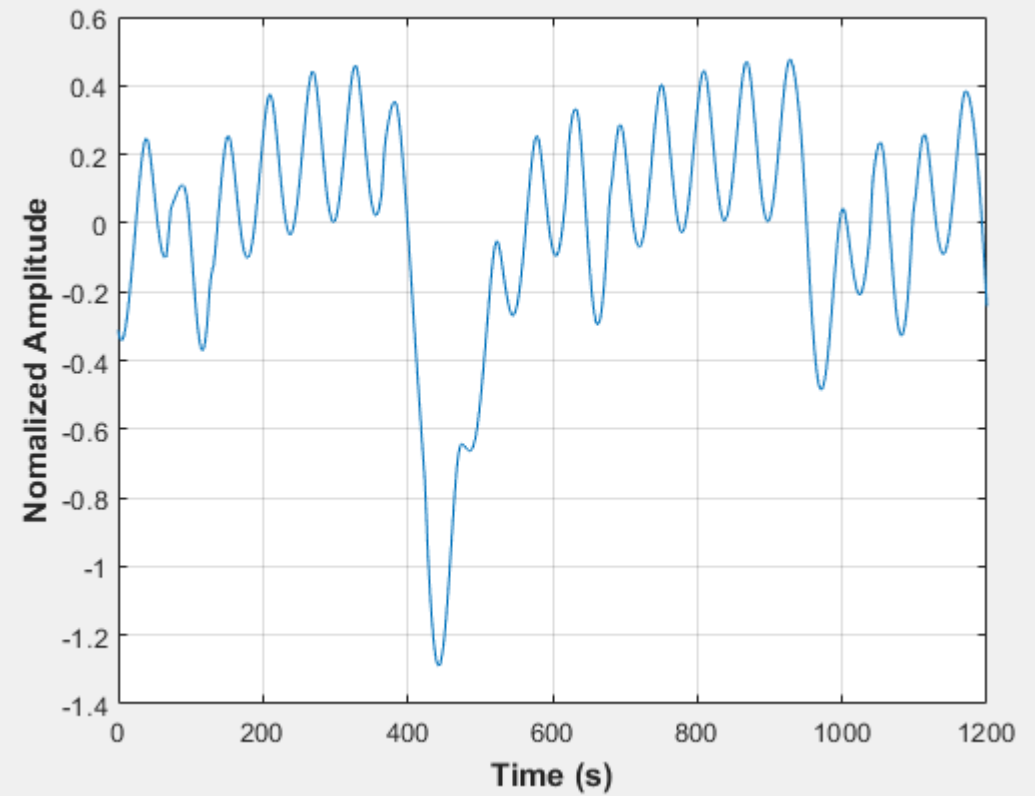


*Figure E-153: Pressure fluctuations in a non-uniformly packed vessel (large and small at the side) at 2.83 dm$^3$/minute rotameter flow rate- Test 2*

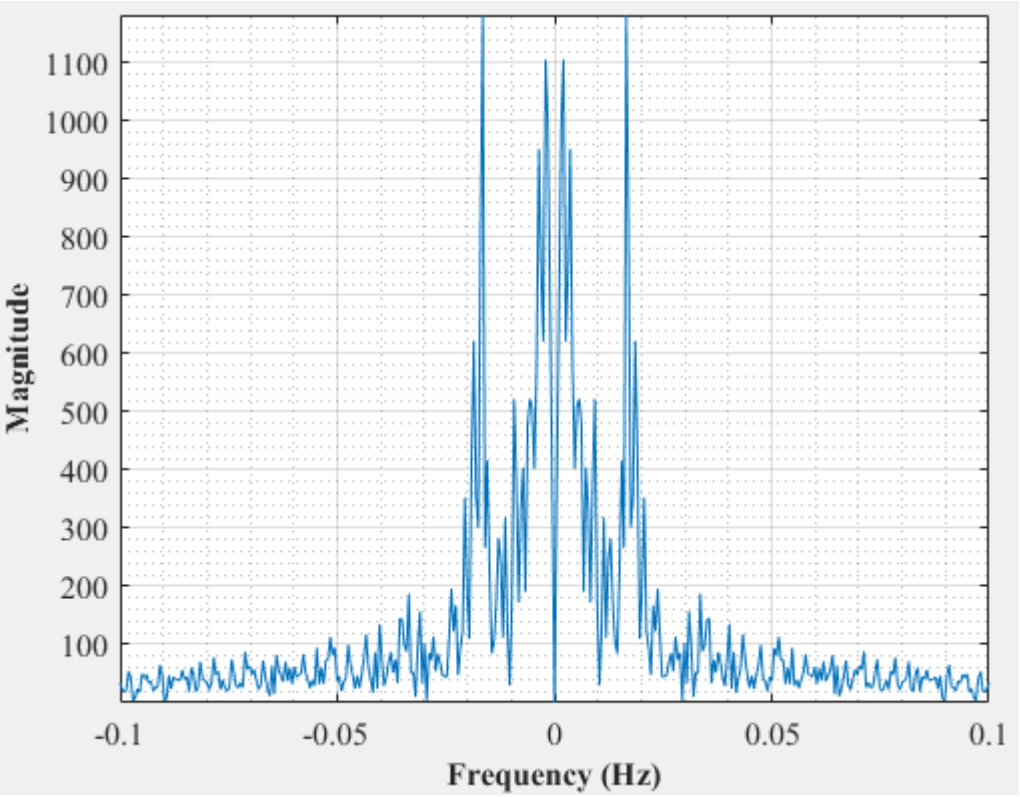


*Figure E-154: Dominant Frequency for a non-uniformly packed vessel (large and small at the side) at 2.83 dm$^3$/minute rotameter flow rate- Test 2*

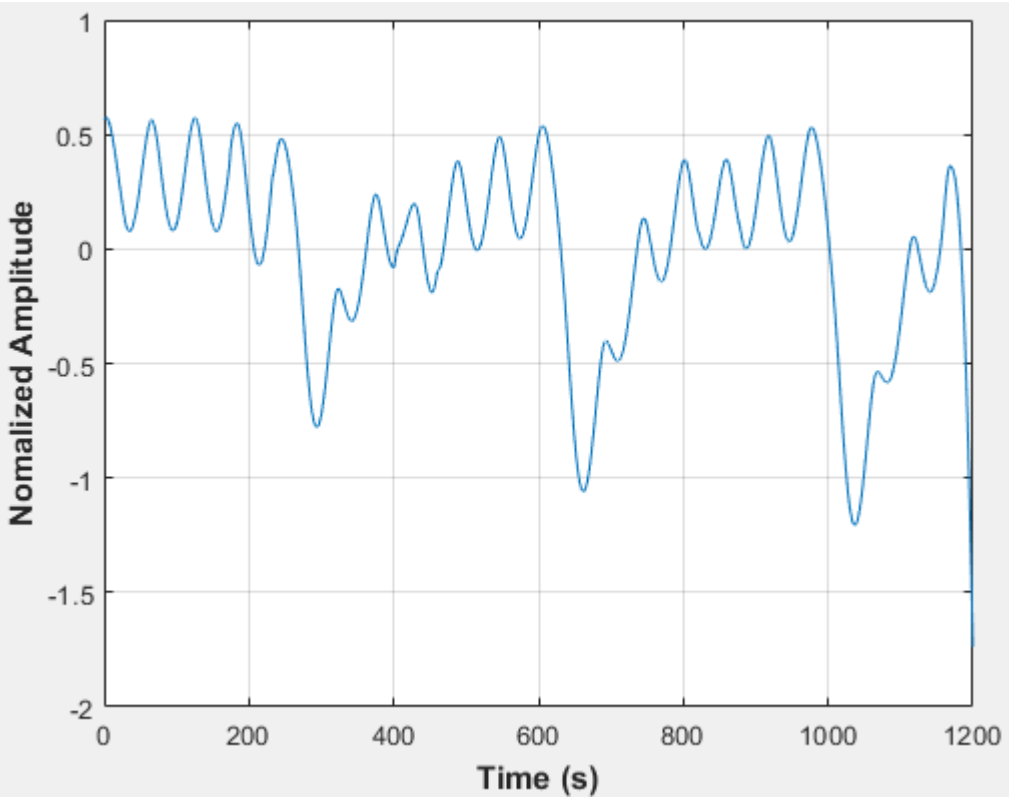


*Figure E-155: Pressure fluctuations in a non-uniformly packed vessel (large and small at the side) at 2.83 dm$^3$/minute rotameter flow rate- Test 3*

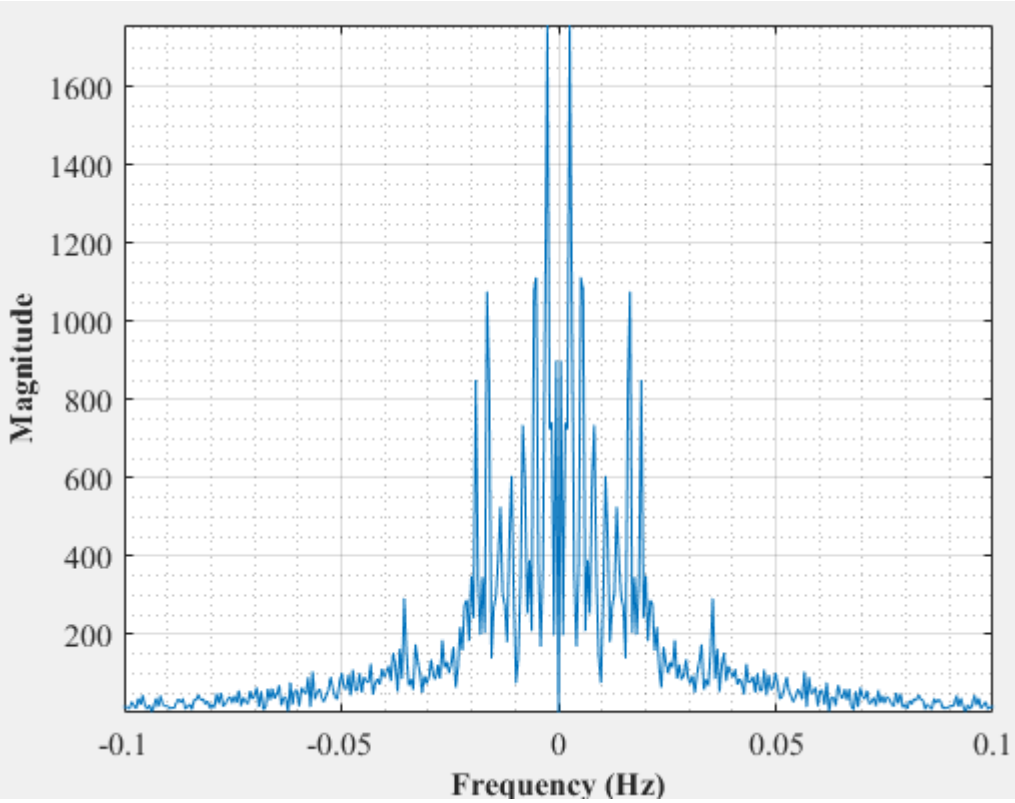


*Figure E-156: Dominant Frequency for a non-uniformly packed vessel (large and small at the side) at 2.83 dm$^3$/minute rotameter flow rate- Test 3*

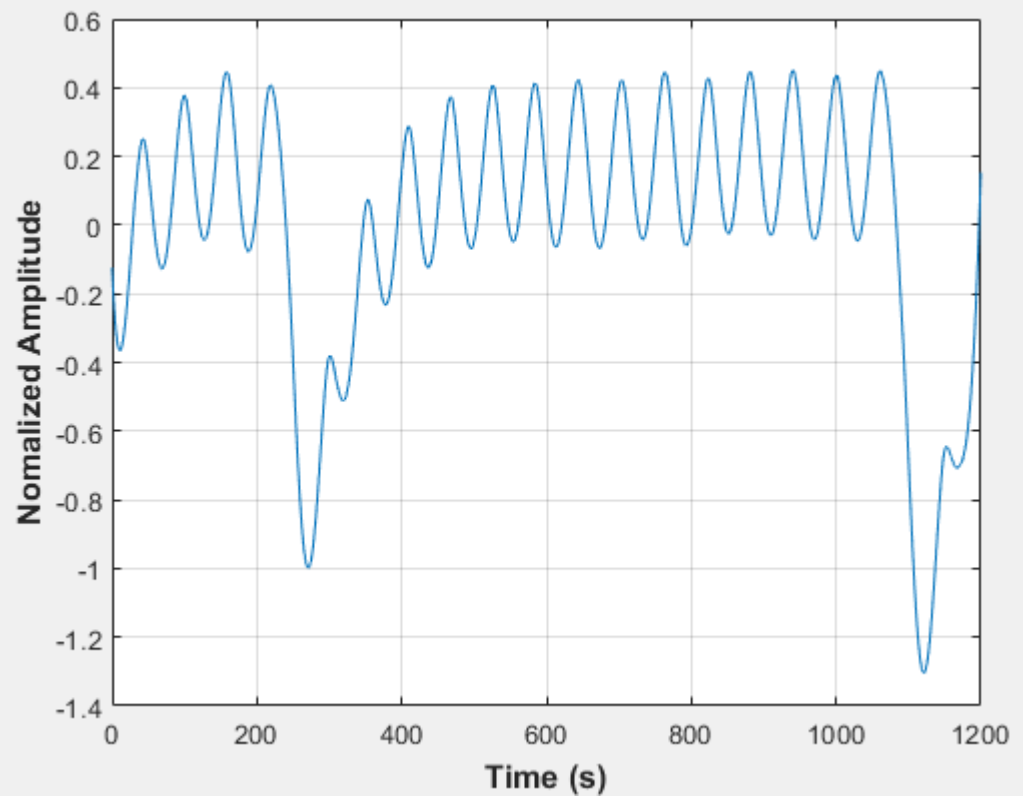


*Figure E-157: Pressure fluctuations in a non-uniformly packed vessel (large and small at the side) at 2.83 dm$^3$/minute rotameter flow rate- Test 4*

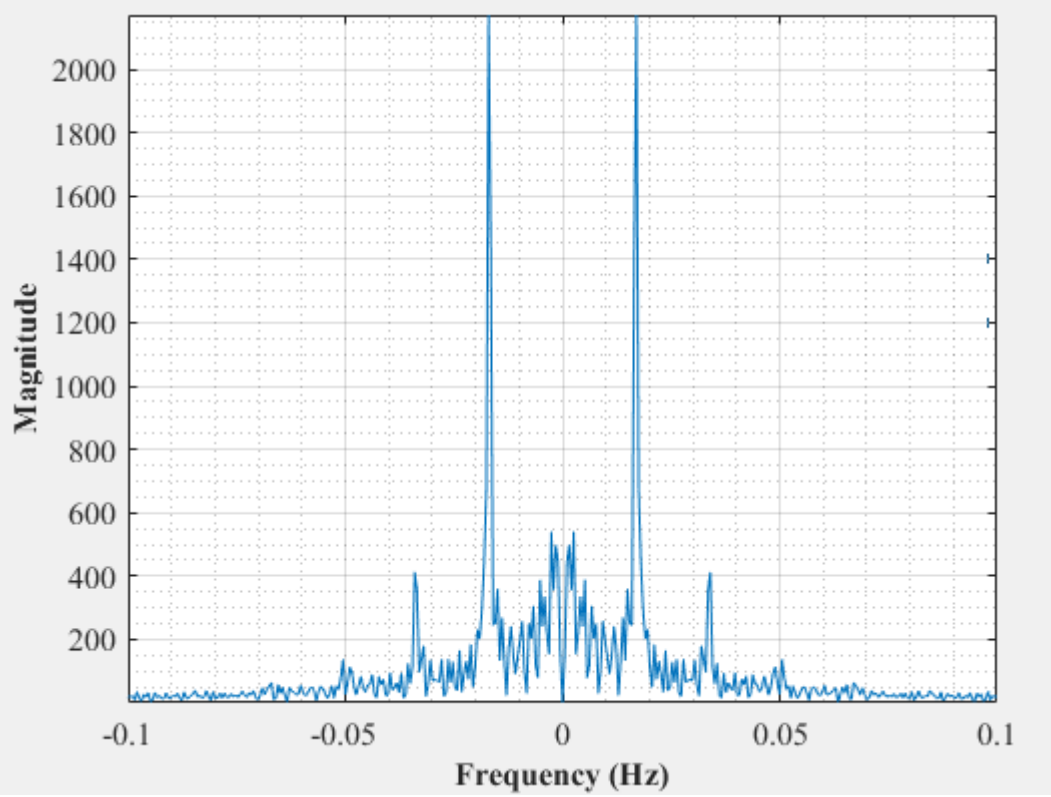


*Figure E-158: Dominant Frequency for a non-uniformly packed vessel (large and small at the side) at 2.83 dm$^3$/minute rotameter flow rate- Test 4*

*Table E-1: Frequency (mHz) Data at Various Flowrates- Full Vessel*

**1.67 $dm^3$ per minute**

| | T1 | T2 | T3 | T4 | T5 | T6 | T7 | T8 | Average |
|---|---|---|---|---|---|---|---|---|---|
| **Empty Tube** | 10,44 | 9,17 | 9,17 | 9,09 | | | | | 9,47 |
| **Large** | 9,52 | 9,32 | 9,32 | 9,52 | 9,48 | 9,57 | 10,00 | | 9,53 |
| **Large small centre** | 9,79 | 9,27 | 9,24 | 9,76 | 9,75 | 9,75 | 9,78 | 9,76 | 9,64 |
| **Large small side** | 9,40 | 9,09 | 9,48 | 9,82 | 9,32 | | | | 9,42 |

**2 $dm^3$ per minute**

| | T1 | T2 | T3 | T4 | T5 | T6 | T7 | T8 | Average |
|---|---|---|---|---|---|---|---|---|---|
| **Empty Tube** | 10,91 | 10,92 | 10,71 | 12,82 | | | | | 11,34 |
| **Large** | 11,21 | 11,02 | 10,91 | 11,02 | 11,40 | 11,40 | | | 11,16 |
| **Large small centre** | 10,83 | 10,83 | 10,83 | 10,98 | 10,91 | 10,91 | 10,91 | | 10,89 |
| **Large small side** | 10,81 | 11,02 | 10,91 | 11,11 | 10,91 | | | | 10,95 |

**2.33 $dm^3$ per minute**

| | T1 | T2 | T3 | T4 | T5 | T6 | T7 | T8 | Average |
|---|---|---|---|---|---|---|---|---|---|
| **Empty Tube** | 15,00 | 12,73 | 14,78 | 14,17 | 14,17 | | | | 14,17 |
| **Large** | 13,45 | 13,33 | 13,39 | 13,39 | | | | | 13,39 |
| **Large small centre** | 12,50 | 12,73 | 12,17 | 13,04 | | | | | 12,61 |
| **Large small side** | 13,39 | 11,71 | 12,73 | 13,16 | | | | | 12,75 |

**2.67 $dm^3$ per minute**

| | T1 | T2 | T3 | T4 | T5 | T6 | T7 | T8 | Average |
|---|---|---|---|---|---|---|---|---|---|
| **Empty Tube** | 15,83 | 15,46 | 14,91 | 15,18 | 15,04 | | | | 15,28 |
| **Large** | 15,39 | 15,52 | 15,52 | 15,79 | 15,65 | 15,79 | | | 15,61 |
| **Large small centre** | 11,67 | 13,79 | 13,91 | 15,00 | | | | | 13,59 |
| **Large small side** | 16,07 | 11,67 | 16,07 | 15,18 | | | | | 14,75 |

**2.83 $dm^3$ per minute**

| | T1 | T2 | T3 | T4 | T5 | T6 | T7 | T8 | Average |
|---|---|---|---|---|---|---|---|---|---|
| **Empty Tube** | 15,93 | 15,79 | 15,52 | 15,83 | 15,83 | 15,79 | 15,93 | | 15,80 |
| **Large** | 17,12 | 16,67 | 16,96 | 16,81 | 16,96 | 16,96 | 16,52 | | 16,86 |
| **Large small centre** | 16,36 | 16,17 | 15,65 | 15,32 | 16,07 | | | | 15,92 |
| **Large small side** | 16,36 | 16,22 | 16,38 | 16,36 | | | | | 16,33 |

*Table E-2: Amplitude Data at Various Flowrates- Full Vessel*

**1.67 $dm^3$ per minute**

| | T1 | T2 | T3 | T4 | T5 | T6 | T7 | T8 | **Average** |
|---|---|---|---|---|---|---|---|---|---|
| **Empty Tube** | 0,63 | 0,51 | 0,54 | 0,56 | | | | | 0,56 |
| **Large** | 0,46 | 0,51 | 0,52 | 0,46 | 0,51 | 0,51 | 0,47 | | 0,49 |
| **Large small centre** | 0,49 | 0,53 | 0,54 | 0,54 | 0,55 | 0,56 | 0,59 | 0,54 | 0,54 |
| **Large small side** | 0,60 | 0,61 | 0,52 | 0,49 | 0,53 | | | | 0,55 |

**2 $dm^3$ per minute**

| | T1 | T2 | T3 | T4 | T5 | T6 | T7 | T8 | **Average** |
|---|---|---|---|---|---|---|---|---|---|
| **Empty Tube** | 0,73 | 0,65 | 0,65 | 0,59 | | | | | 0,66 |
| **Large** | 0,60 | 0,56 | 0,56 | 0,52 | 0,57 | 0,52 | | | 0,56 |
| **Large small centre** | 0,59 | 0,60 | 0,60 | 0,60 | 0,61 | 0,66 | 0,62 | | 0,61 |
| **Large small side** | 0,59 | 0,59 | 0,65 | 0,53 | 0,64 | | | | 0,60 |

**2.33 $dm^3$ per minute**

| | T1 | T2 | T3 | T4 | T5 | T6 | T7 | T8 | **Average** |
|---|---|---|---|---|---|---|---|---|---|
| **Empty Tube** | 0,28 | 0,28 | 0,29 | 0,23 | 0,28 | | | | 0,27 |
| **Large** | 0,47 | 0,49 | 0,44 | 0,47 | | | | | 0,47 |
| **Large small centre** | 0,27 | 0,27 | 0,37 | 0,36 | | | | | 0,32 |
| **Large small side** | 0,39 | 0,40 | 0,31 | 0,36 | | | | | 0,36 |

**2.67 $dm^3$ per minute**

| | T1 | T2 | T3 | T4 | T5 | T6 | T7 | T8 | **Average** |
|---|---|---|---|---|---|---|---|---|---|
| **Empty Tube** | 0,26 | 0,27 | 0,29 | 0,27 | 0,29 | | | | 0,28 |
| **Large** | 0,29 | 0,27 | 0,26 | 0,27 | 0,27 | 0,26 | | | 0,27 |
| **Large small centre** | 0,25 | 0,20 | 0,19 | 0,24 | | | | | 0,22 |
| **Large small side** | 0,23 | 0,24 | 0,27 | 0,25 | | | | | 0,25 |

**2.83 $dm^3$ per minute**

| | T1 | T2 | T3 | T4 | T5 | T6 | T7 | T8 | **Average** |
|---|---|---|---|---|---|---|---|---|---|
| **Empty Tube** | 0,26 | 0,28 | 0,26 | 0,30 | 0,28 | 0,28 | 0,26 | | 0,27 |
| **Large** | 0,28 | 0,25 | 0,23 | 0,24 | 0,23 | 0,27 | 0,24 | | 0,25 |
| **Large small centre** | 0,17 | 0,21 | 0,23 | 0,15 | | | | | 0,19 |
| **Large small side** | 0,23 | 0,23 | 0,25 | 0,24 | | | | | 0,24 |

## APPENDIX F- Simulation results

### Introduction

This section shows the results of the simulations done using the small vessel as well as the large vessel configurations at different packing configurations as discussed in Chapter 4 of the thesis (Model Development).

### Uniform Packing-pressure drop a constant fraction of input pressure

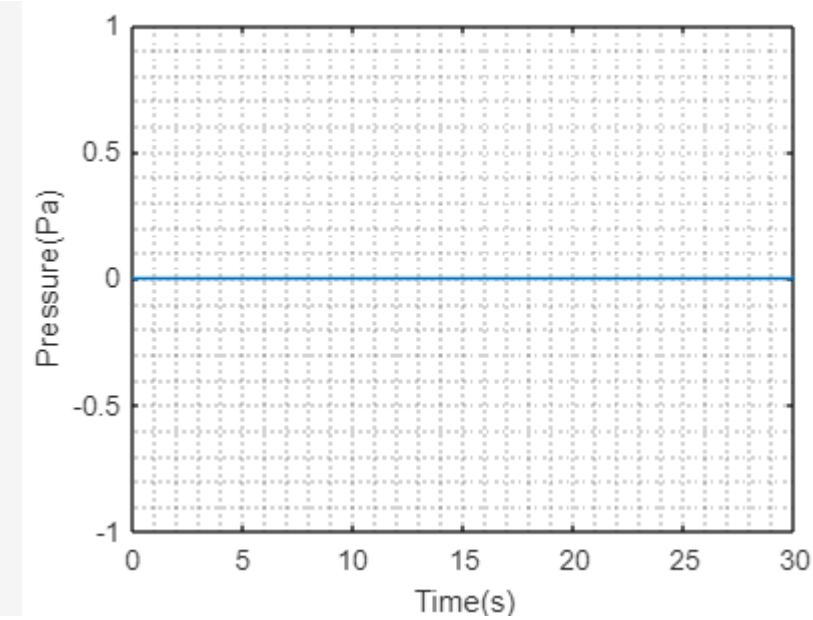


*Figure F-0-7: Pressure fluctuations in a uniformly packed vessel when the Pressure drop is 100 % of incoming Pressure*

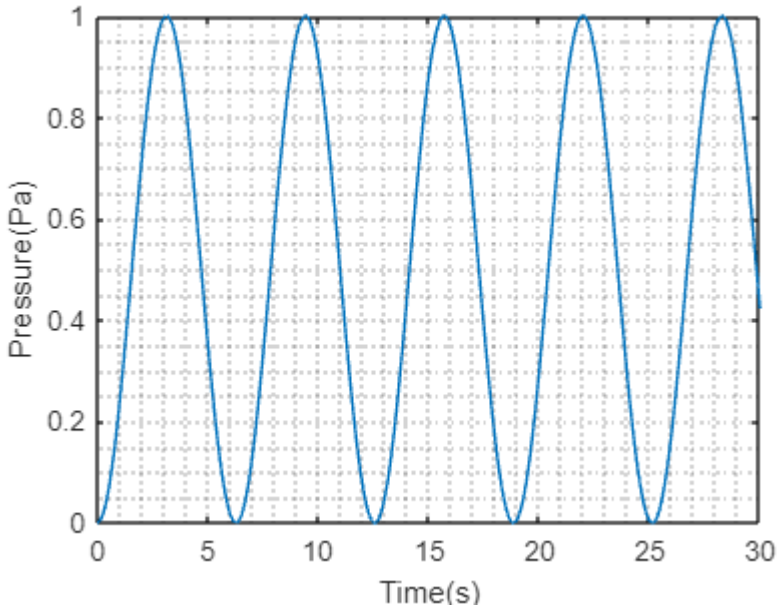


*Figure F-2: Pressure fluctuations in a uniformly packed vessel when the Pressure drop is 50 % of incoming Pressure*

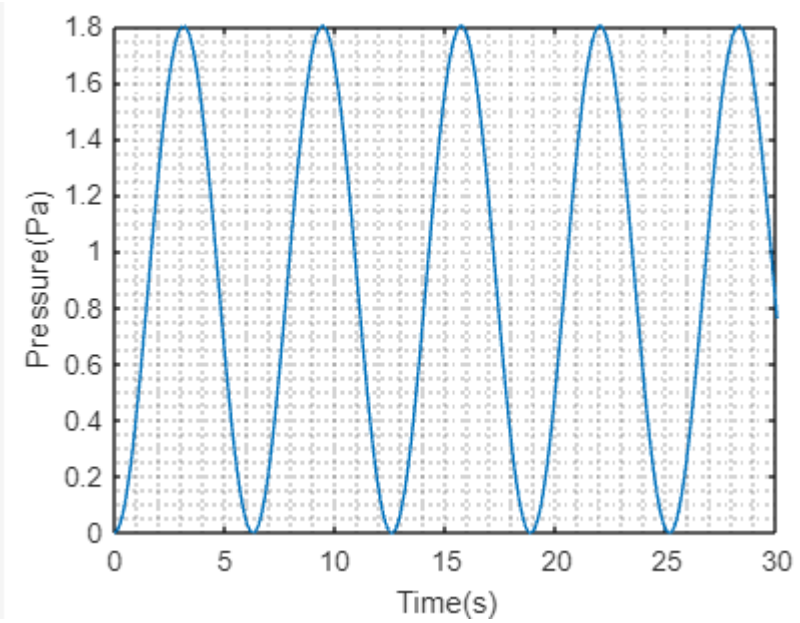


*Figure F-3: Pressure fluctuations in a uniformly packed vessel when the Pressure drop is 10 % of incoming Pressure*

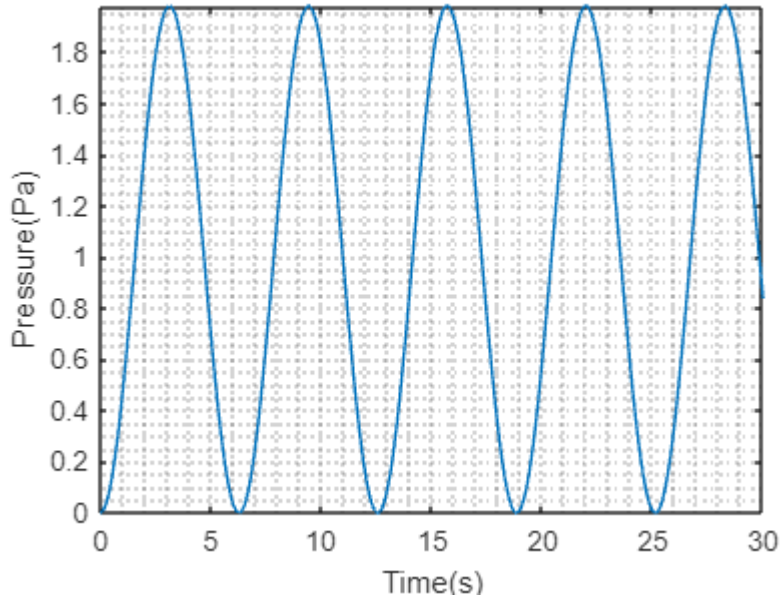


*Figure F-4: Pressure fluctuations in a uniformly packed vessel when the Pressure drop is 1 % of incoming Pressure*

## Uniform packing, constant velocity

## Large vessel

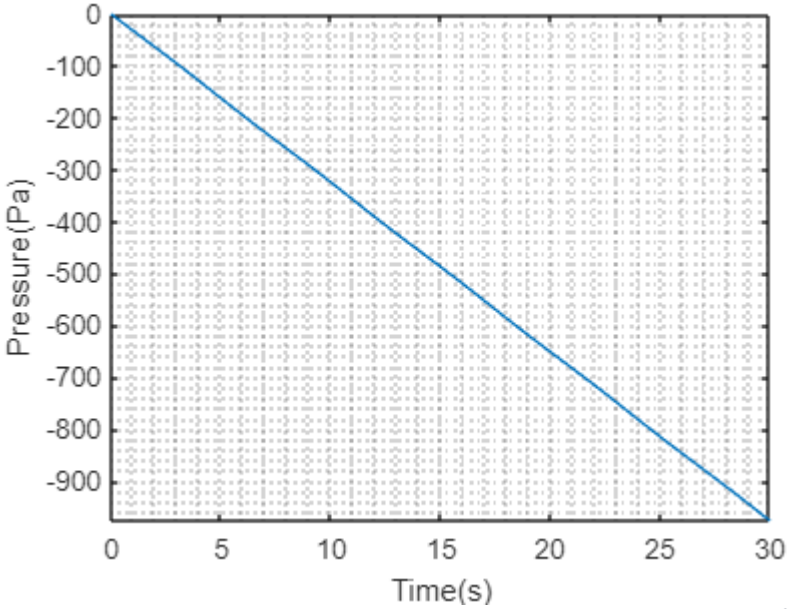


*Figure F-5: Pressure fluctuations in a uniformly packed vessel at a flowrate of 1m$^3$/s*

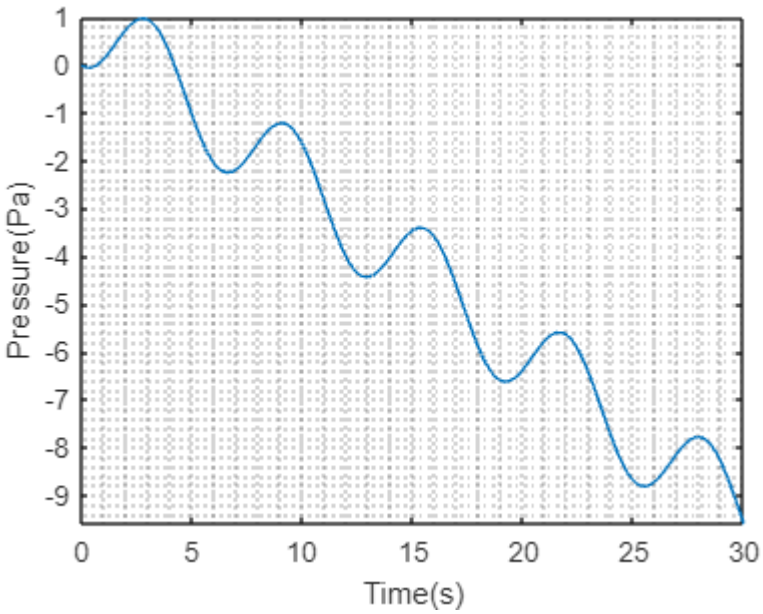


*Figure F-6: Pressure fluctuations in a uniformly packed vessel at a flowrate of 0.1m$^3$/s*

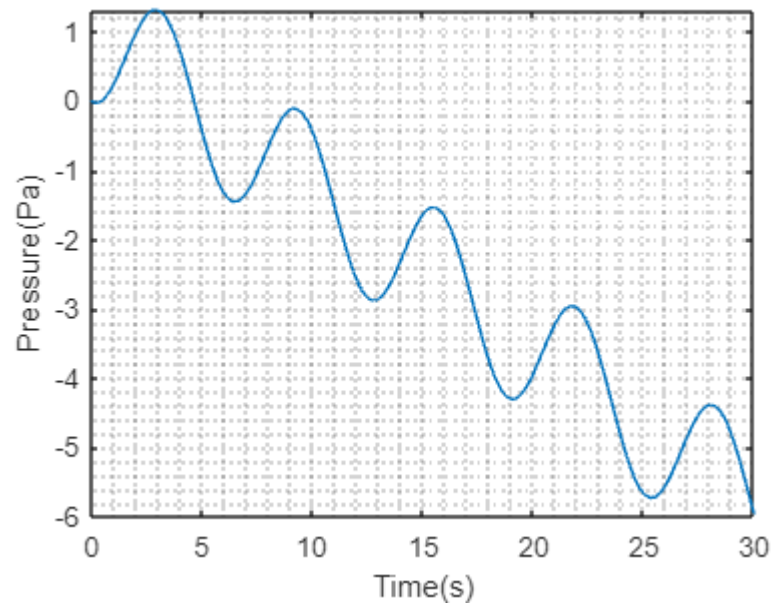


*Figure F-7: Pressure fluctuations in a uniformly packed vessel at a flowrate of 0.08m$^3$/s*

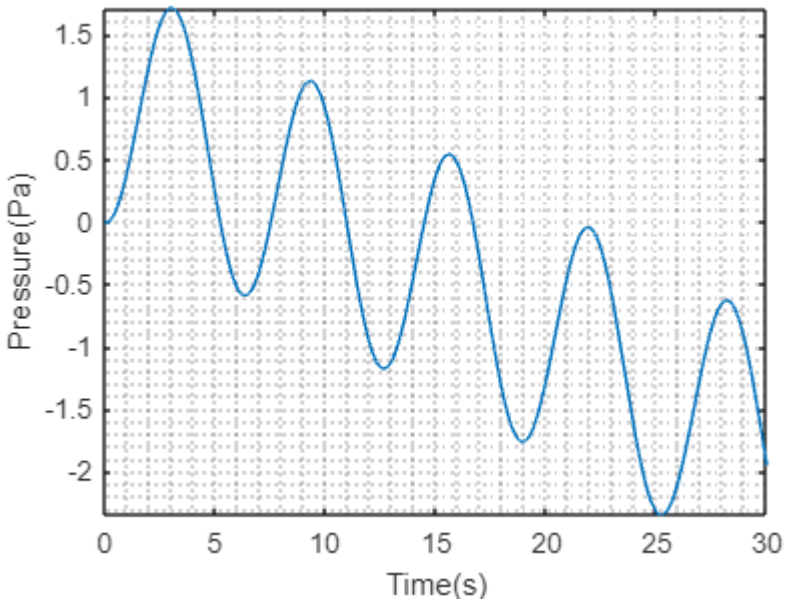


*Figure F-8: Pressure fluctuations in a uniformly packed vessel at a flowrate of 0.05m$^3$/s*

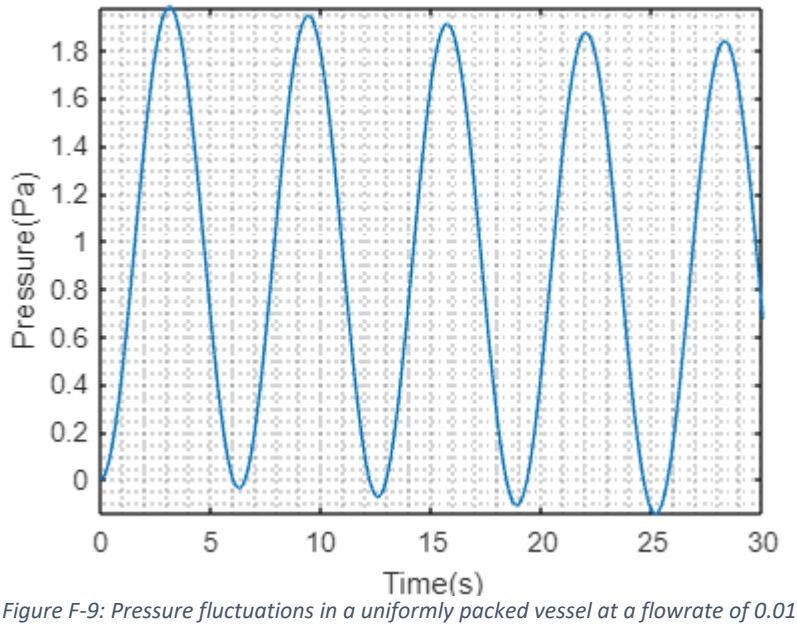


*Figure F-9: Pressure fluctuations in a uniformly packed vessel at a flowrate of 0.01m$^3$/s*

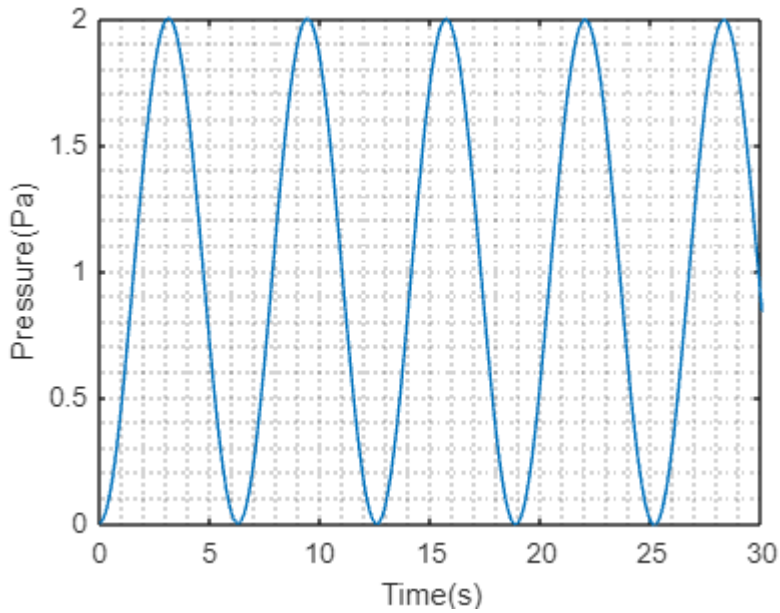


*Figure F-10: Pressure fluctuations in a uniformly packed vessel at a flowrate of 0.001m$^3$/s*

**Small vessel**

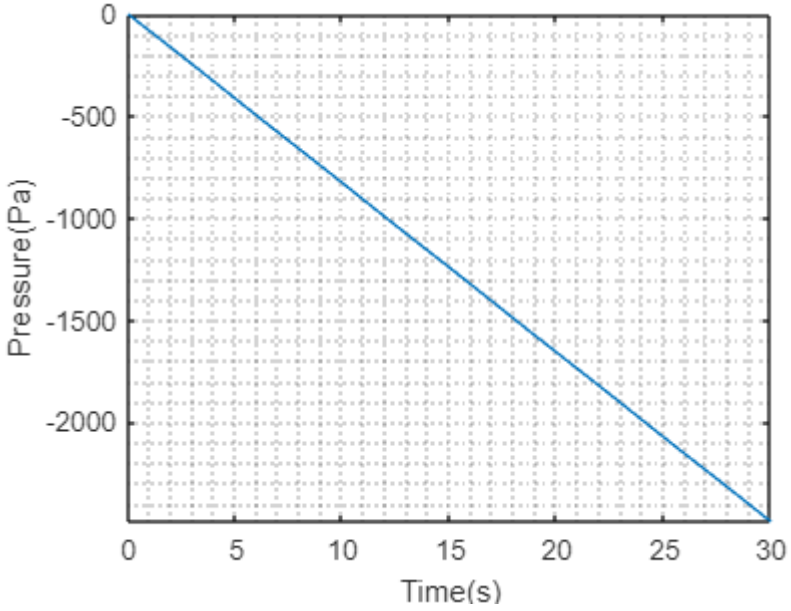


*Figure F-11: Pressure fluctuations in a uniformly packed vessel at a flowrate of 1m$^3$/s*

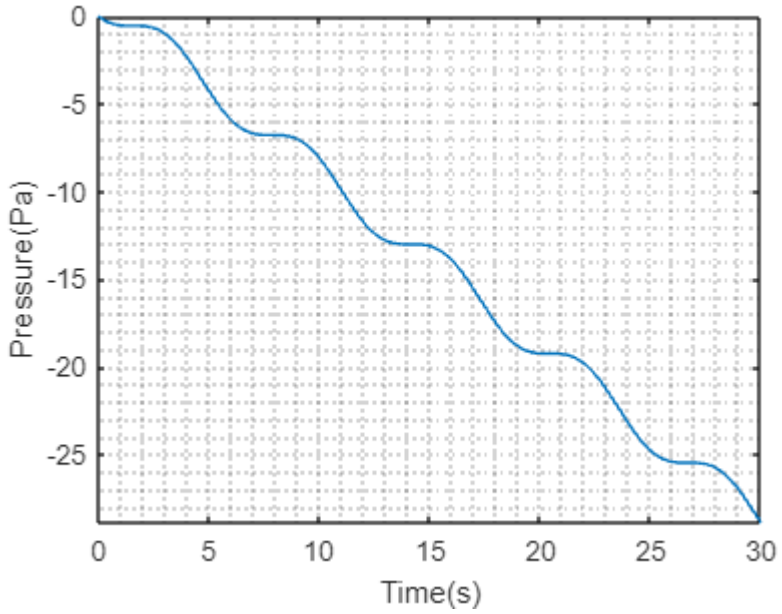


*Figure F-12: Pressure fluctuations in a uniformly packed vessel at a flowrate of 0.1m$^3$/s*

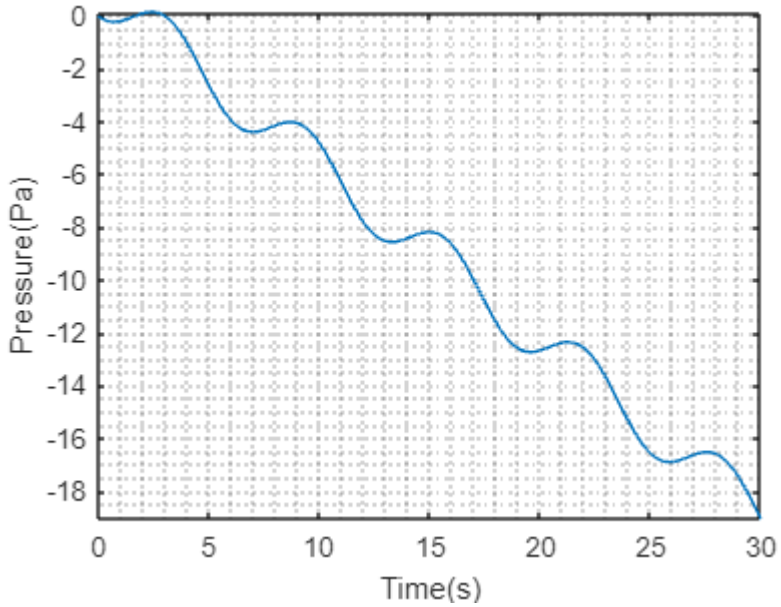


*Figure F-13: Pressure fluctuations in a uniformly packed vessel at a flowrate of 0.08m$^3$/s*

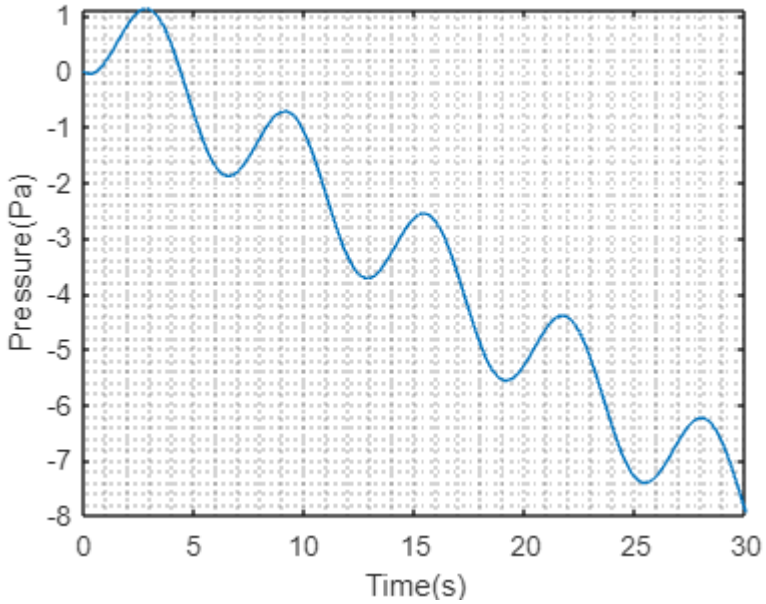


*Figure F-14: Pressure fluctuations in a uniformly packed vessel at a flowrate of 0.05m$^3$/s*

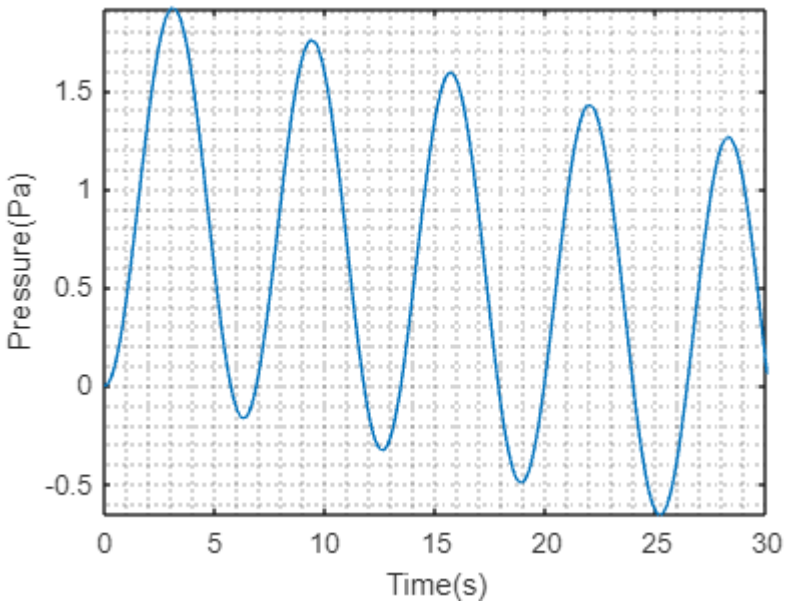


*Figure F-15: Pressure fluctuations in a uniformly packed vessel at a flowrate of 0.01m$^3$/s*

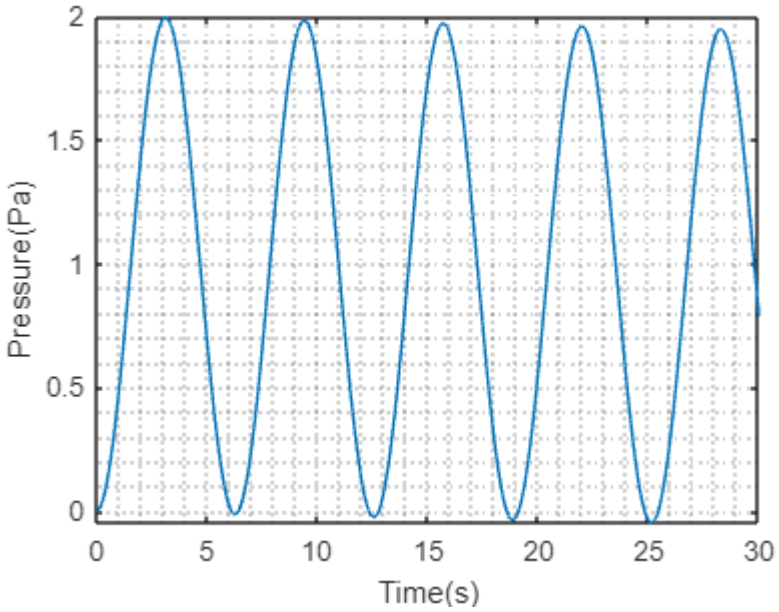


*Figure F-16: Pressure fluctuations in a uniformly packed vessel at a flowrate of 0.001m$^3$/s*

**Largesmallside**
**Big Vessel**

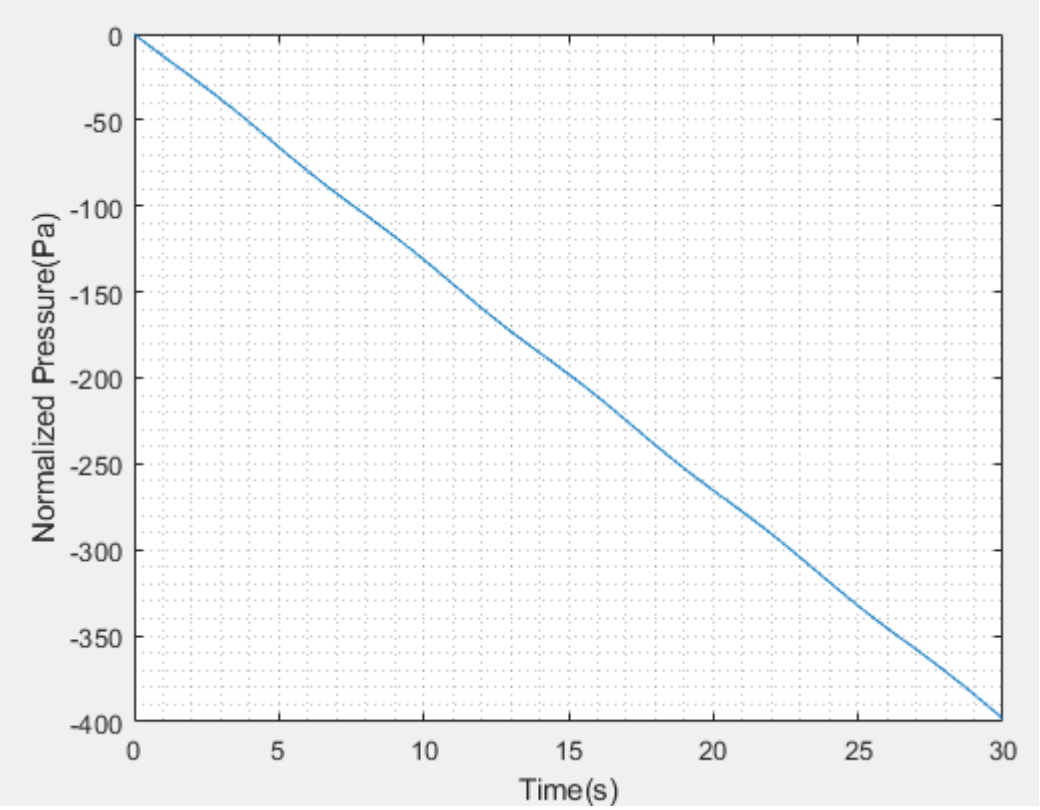


*Figure F-17: Pressure fluctuations in a non-uniformly packed vessel (large and small at the side) at a flowrate of 1m$^3$/s*

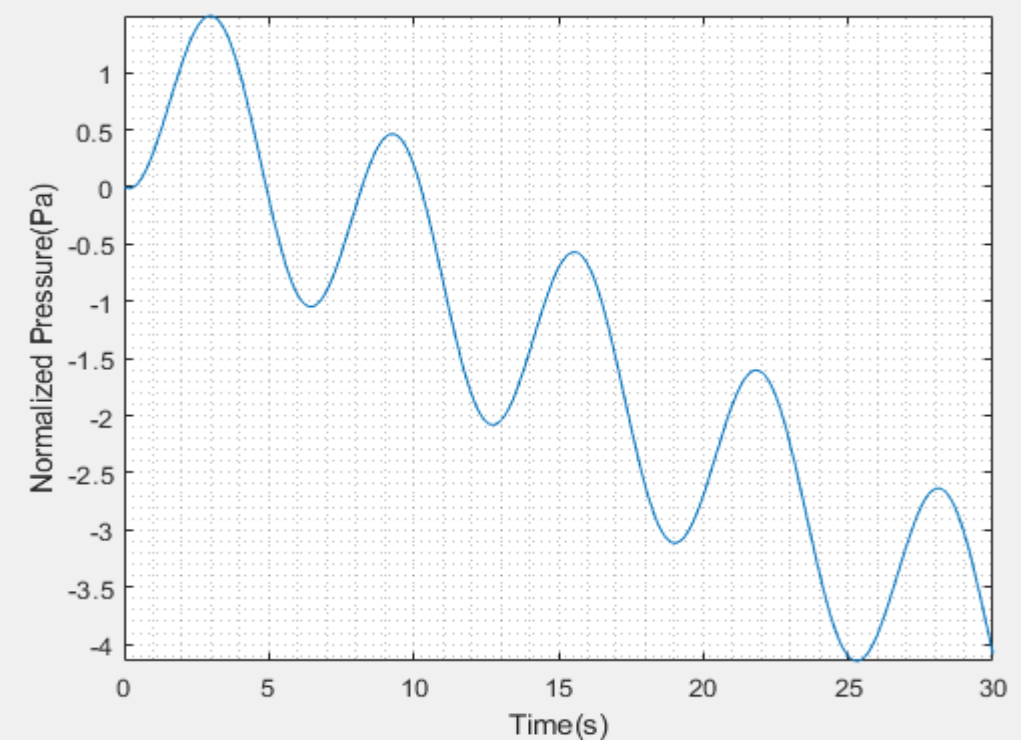


*Figure F-18: Pressure fluctuations in a non-uniformly packed vessel (large and small at the side) at a flowrate of 0.1m$^3$/s*

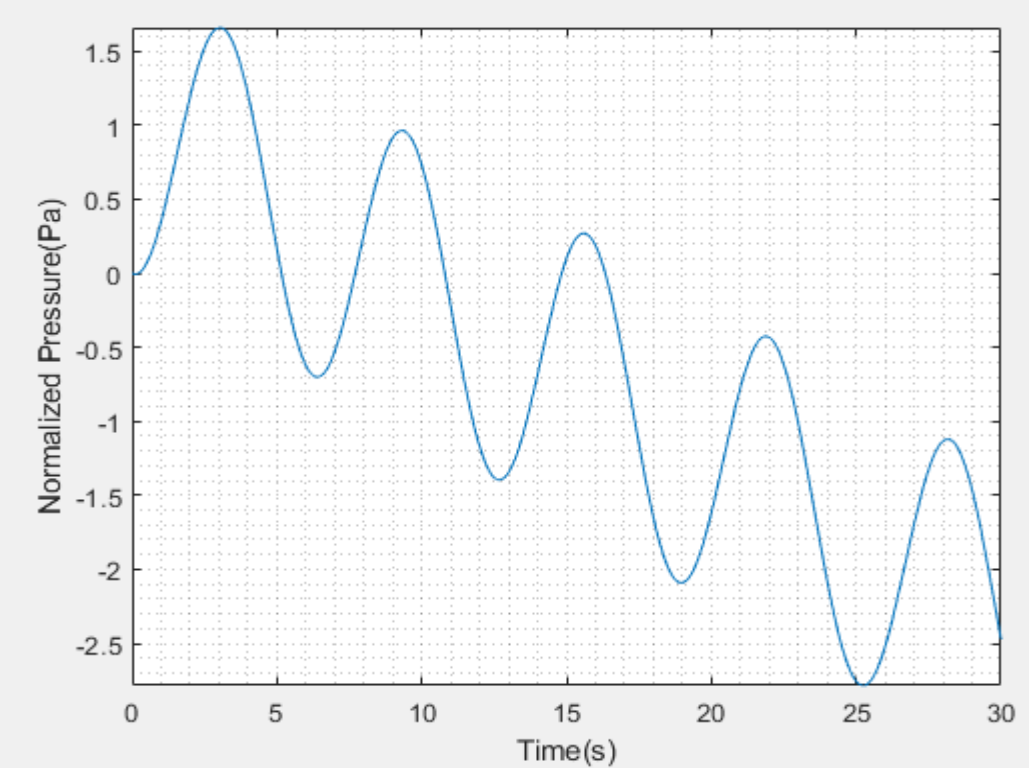


*Figure F-19: Pressure fluctuations in a non-uniformly packed vessel (large and small at the side) at a flowrate of 0.08m³/s*

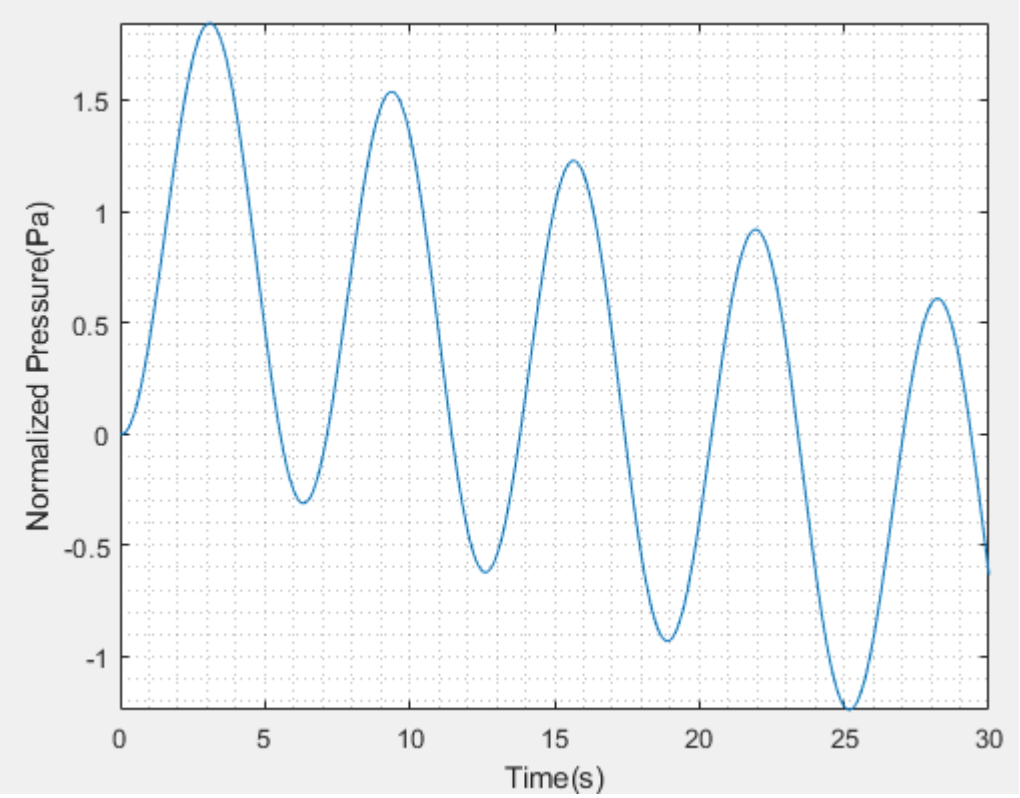


*Figure F-20: Pressure fluctuations in a non-uniformly packed vessel (large and small at the side) at a flowrate of 0.05m³/s*

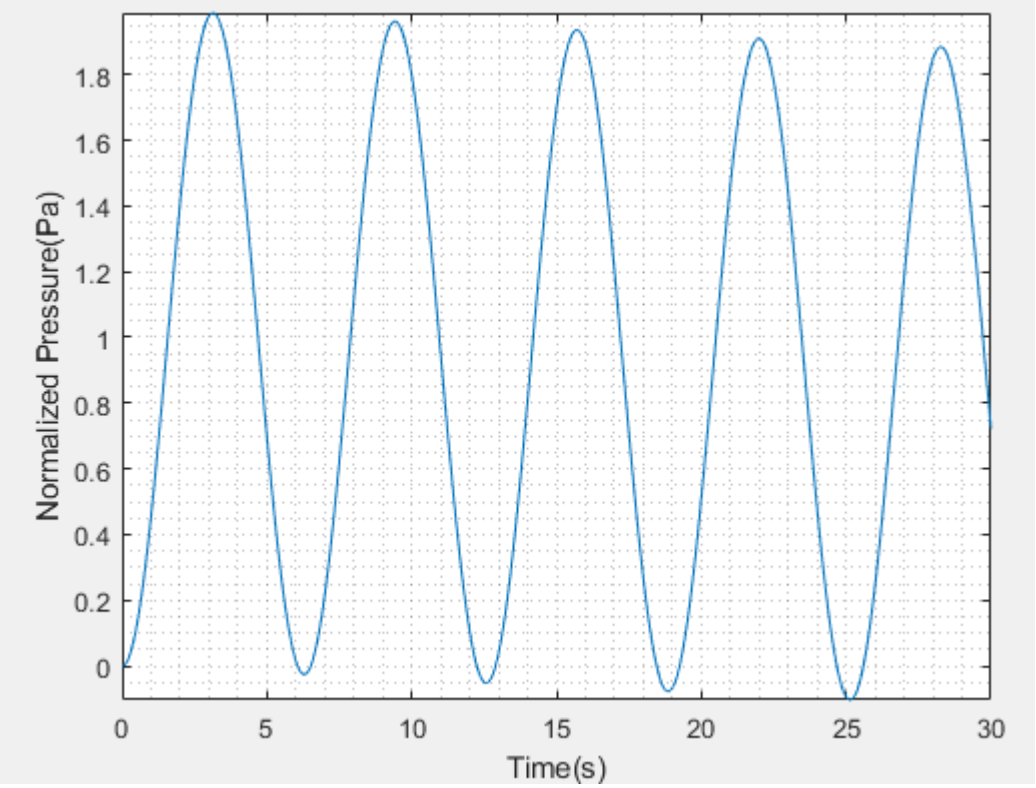


*Figure F-21: Pressure fluctuations in a non-uniformly packed vessel (large and small at the side) at a flowrate of 0.01m$^3$/s*

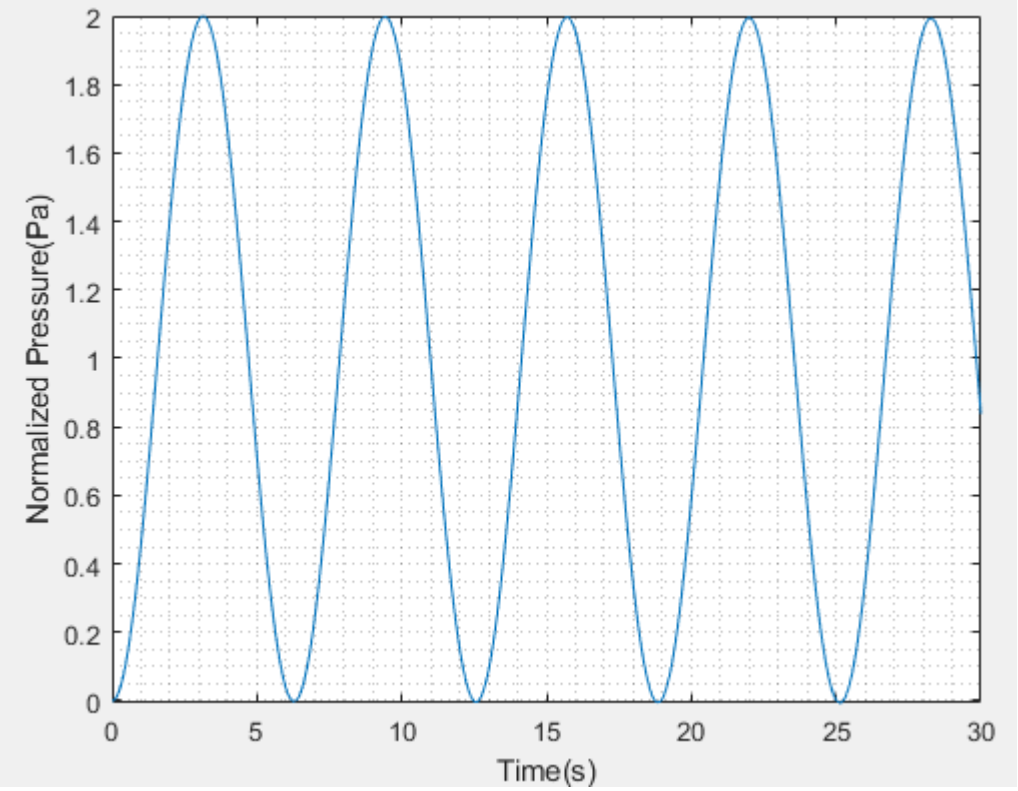


*Figure F-22: Pressure fluctuations in a non-uniformly packed vessel (large and small at the side) at a flowrate of 0.001m$^3$/s*

## Small vessel

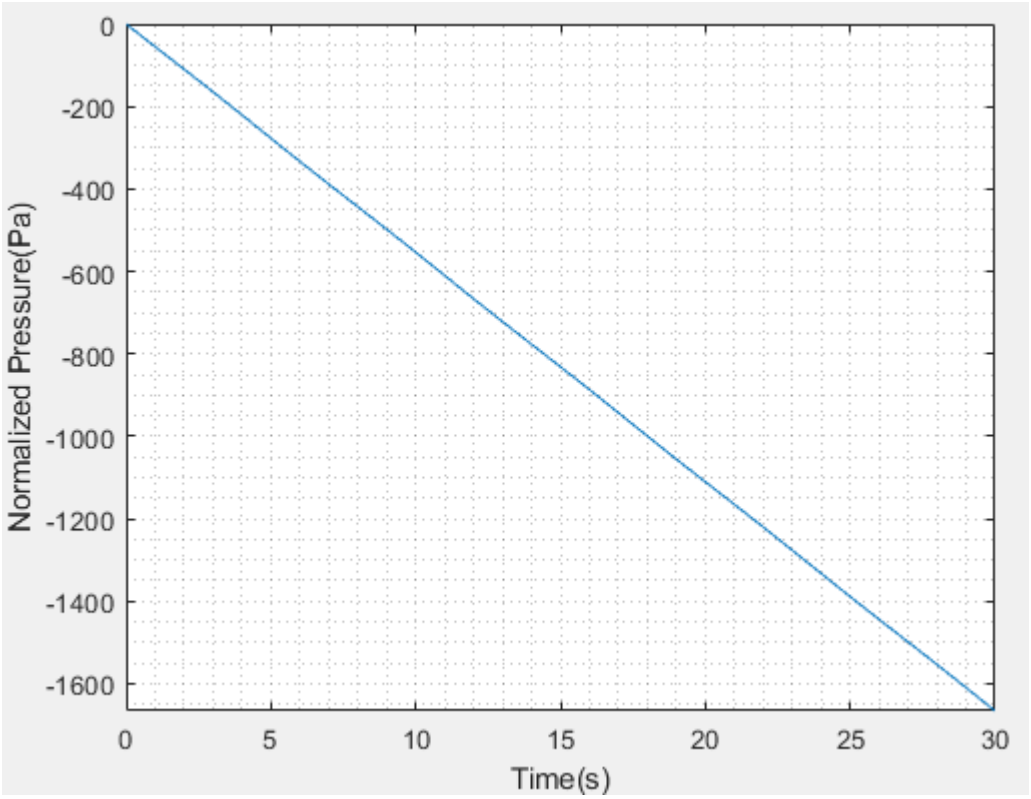


*Figure F-23: Pressure fluctuations in a non-uniformly packed vessel (large and small at the side) at a flowrate of 1m$^3$/s*

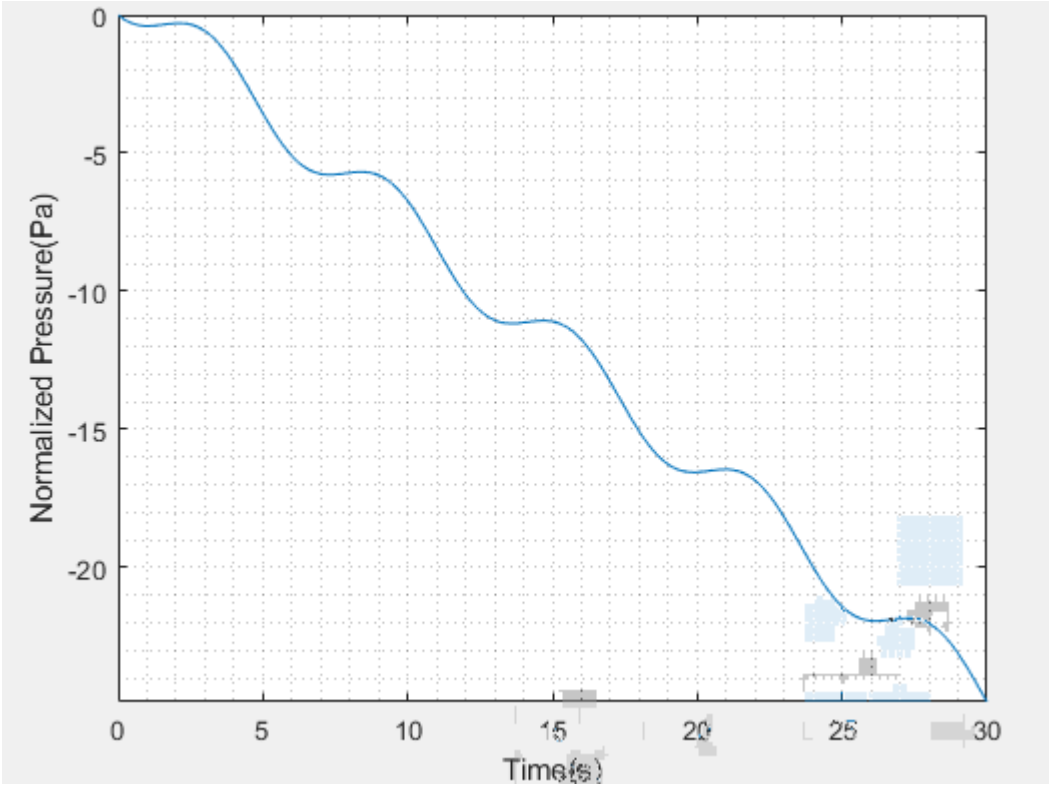


*Figure F-24: Pressure fluctuations in a non-uniformly packed vessel (large and small at the side) at a flowrate of 0.1m$^3$/s*

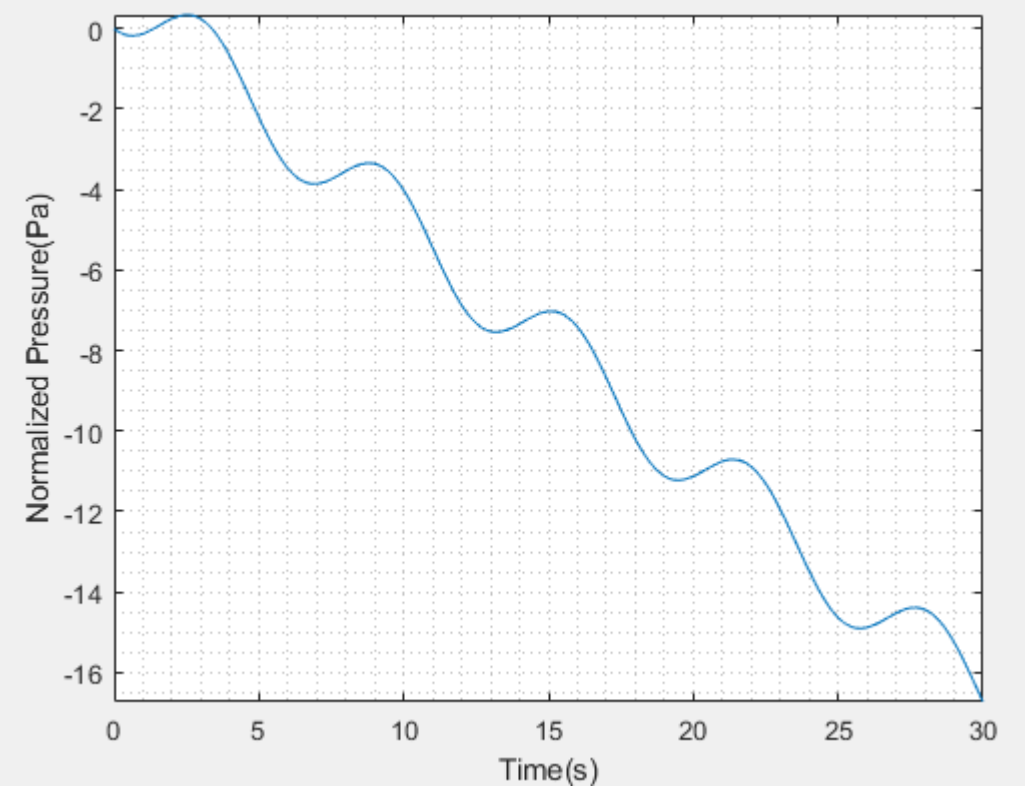


*Figure F-25: Pressure fluctuations in a non-uniformly packed vessel (large and small at the side) at a flowrate of 0.08m$^3$/s*

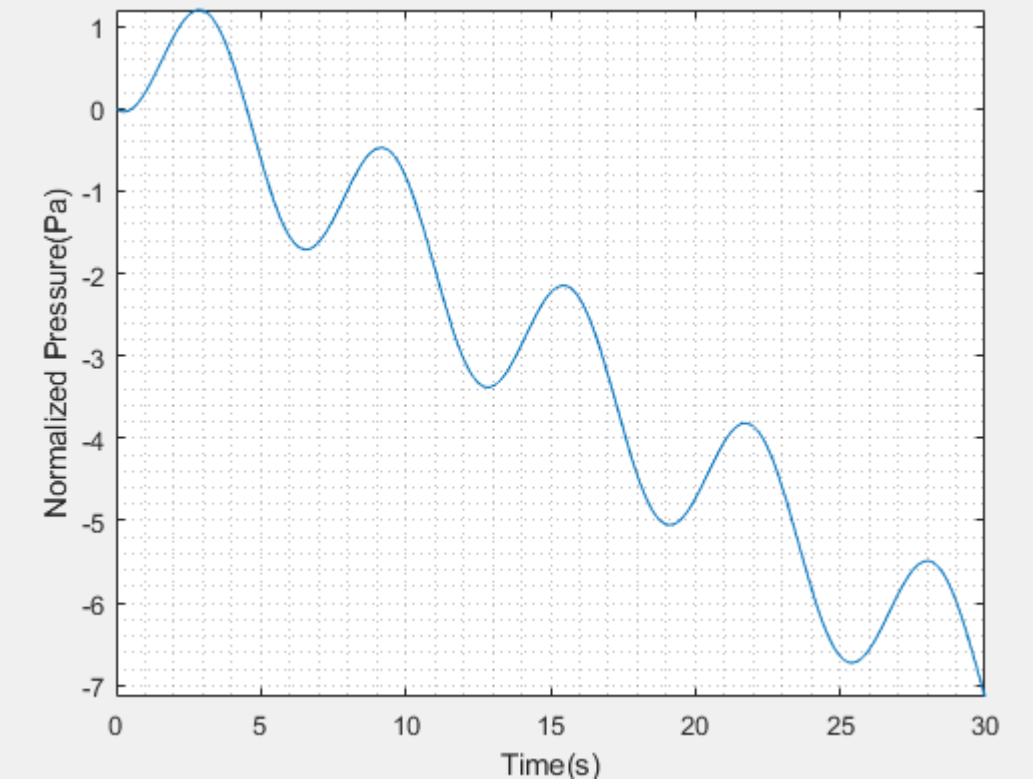


*Figure F-26: Pressure fluctuations in a non-uniformly packed vessel (large and small at the side) at a flowrate of 0.05m$^3$/s*

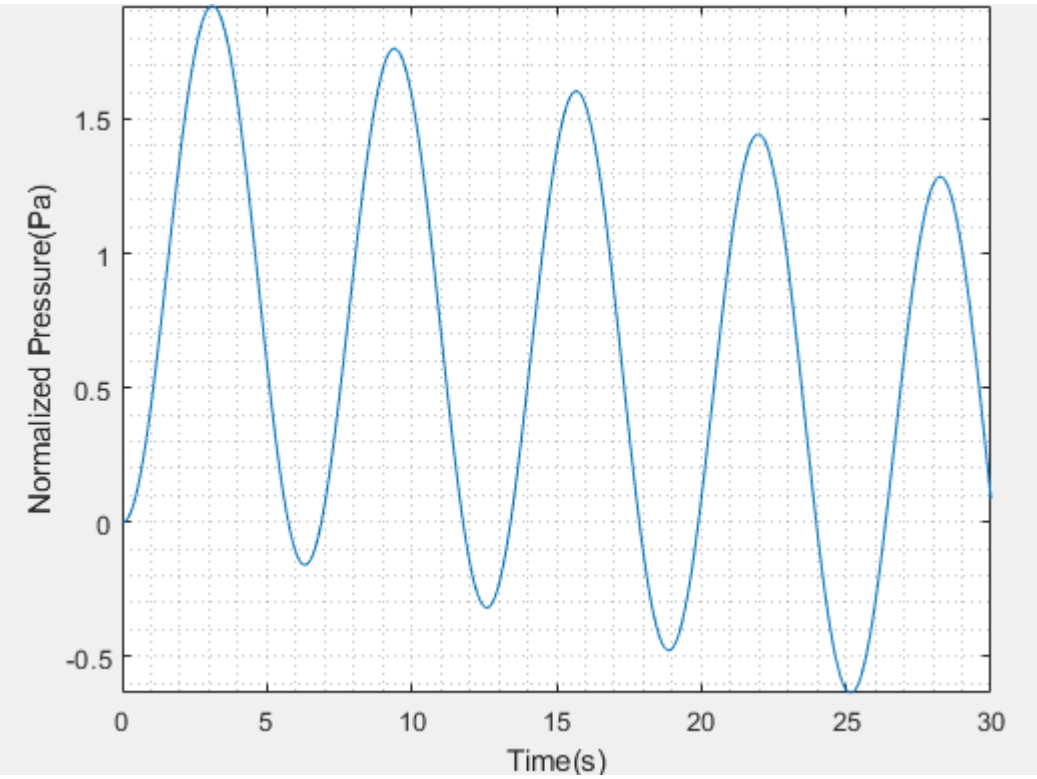


*Figure F-27: Pressure fluctuations in a non-uniformly packed vessel (large and small at the side) at a flowrate of 0.01m³/s*

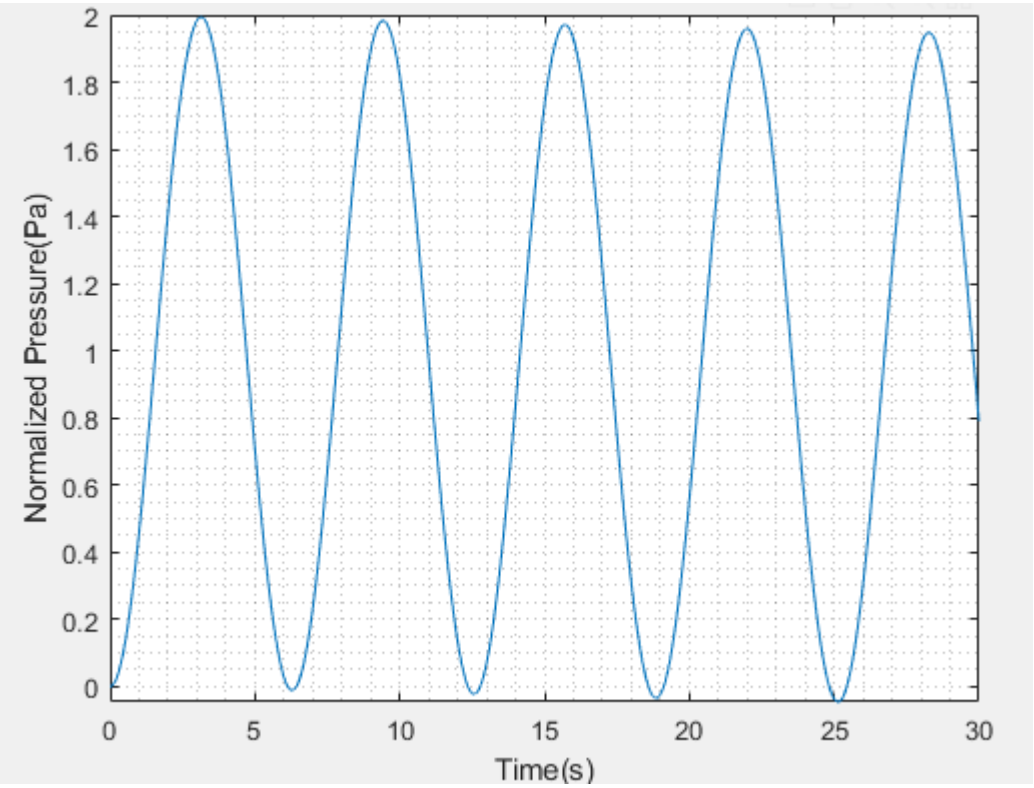


*Figure F-28: Pressure fluctuations in a non-uniformly packed vessel (large and small at the side) at a flowrate of 0.001m³/s*

**Large small centre**
**Large vessel**

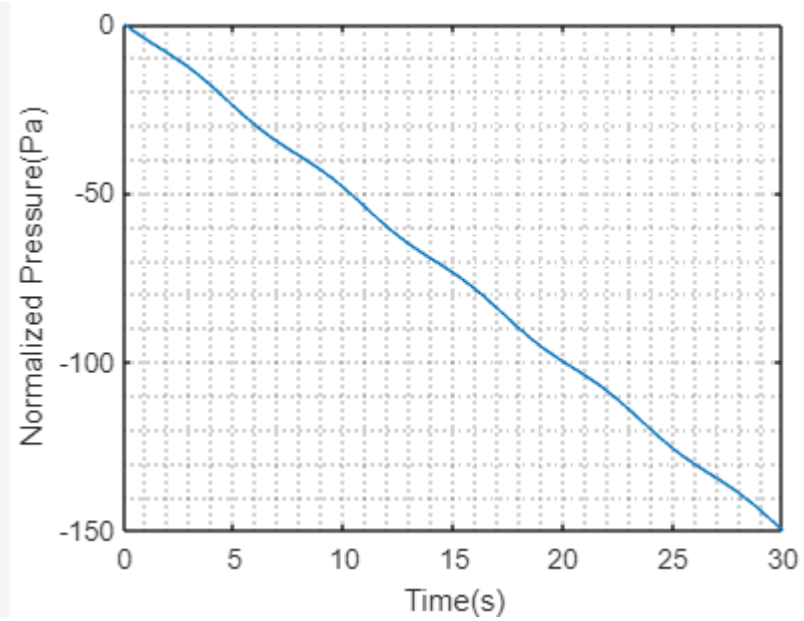


*Figure F-29: Pressure fluctuations in a non-uniformly packed vessel (large and small at the center) at a flowrate of 1m$^3$/s*

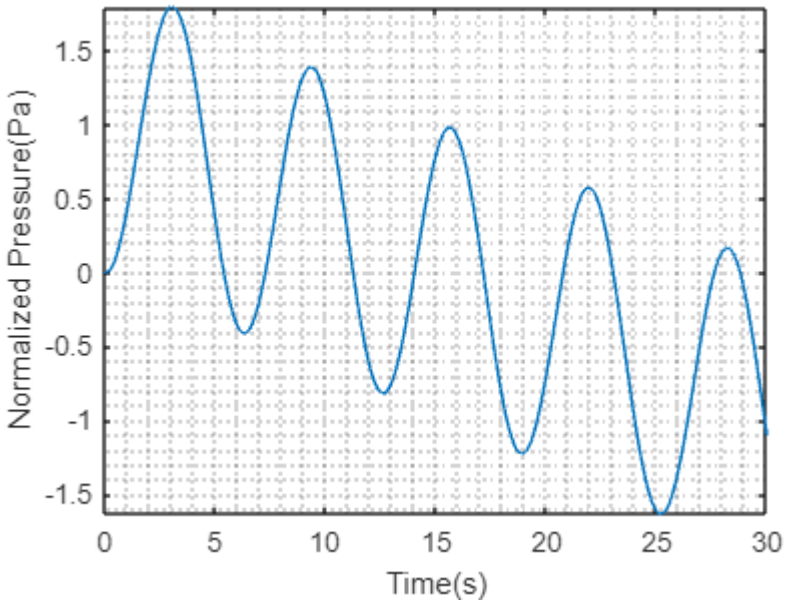


*Figure F-30: Pressure fluctuations in a non-uniformly packed vessel (large and small at the center) at a flowrate of 0.1m$^3$/s*

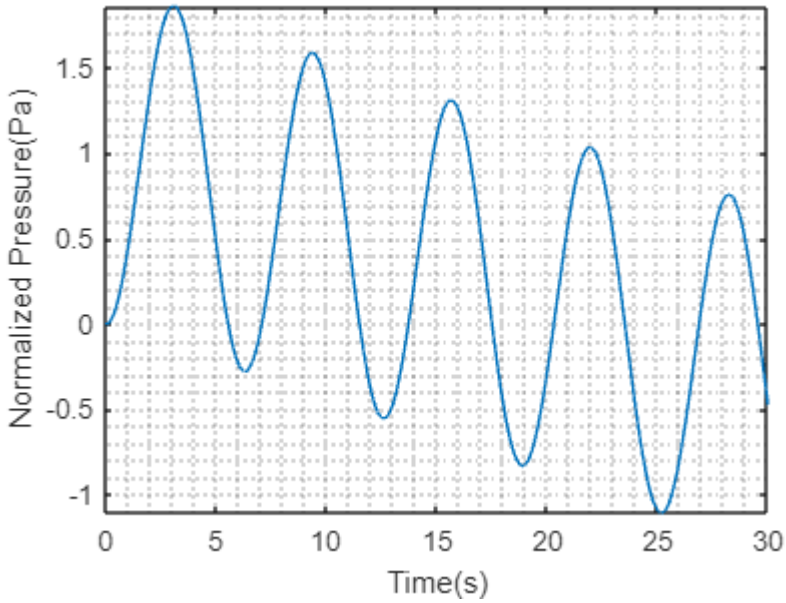


*Figure F-31: Pressure fluctuations in a non-uniformly packed vessel (large and small at the center) at a flowrate of 0.08m$^3$/s*

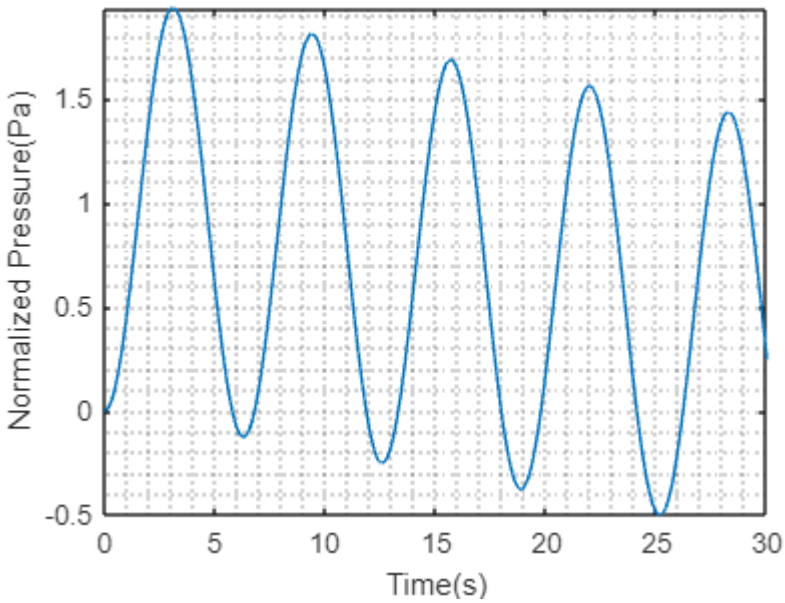


*Figure F-32: Pressure fluctuations in a non-uniformly packed vessel (large and small at the center) at a flowrate of 0.05m$^3$/s*

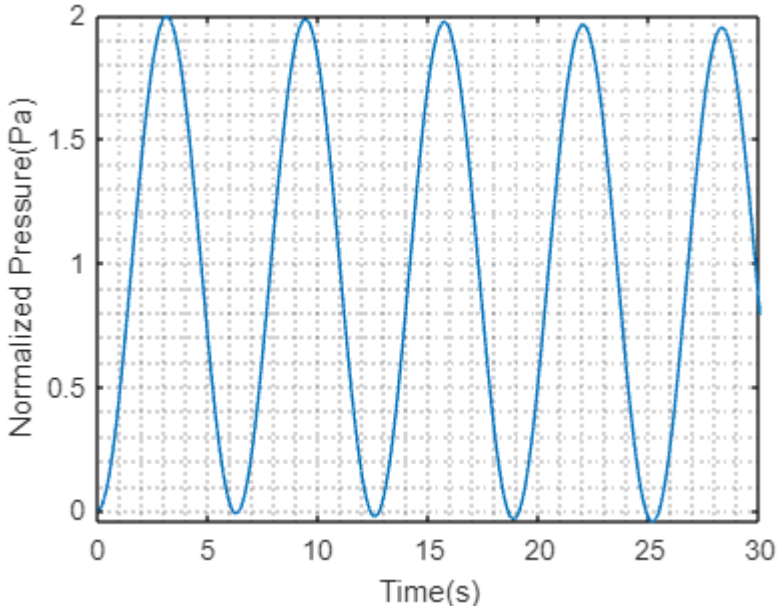


*Figure F-33: Pressure fluctuations in a non-uniformly packed vessel (large and small at the center) at a flowrate of 0.01$m^3/s$*

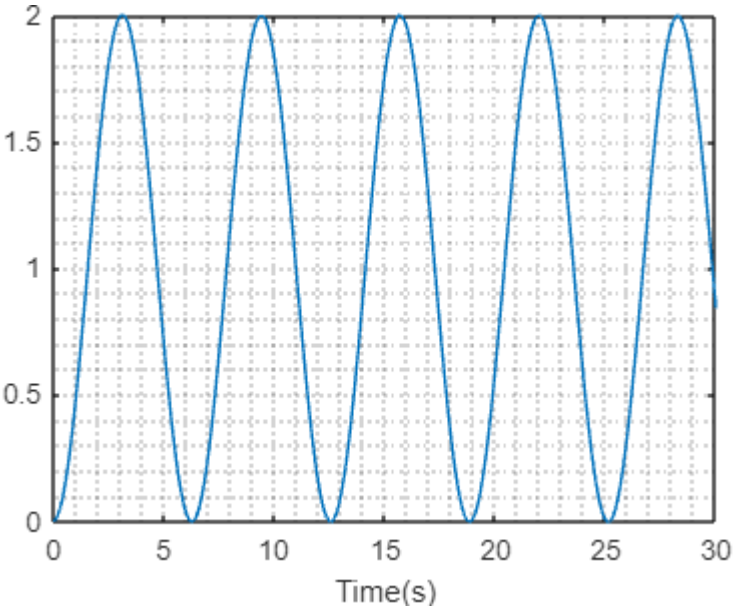


*Figure F-34: Pressure fluctuations in a non-uniformly packed vessel (large and small at the center) at a flowrate of 0.001$m^3/s$*

Small vessel

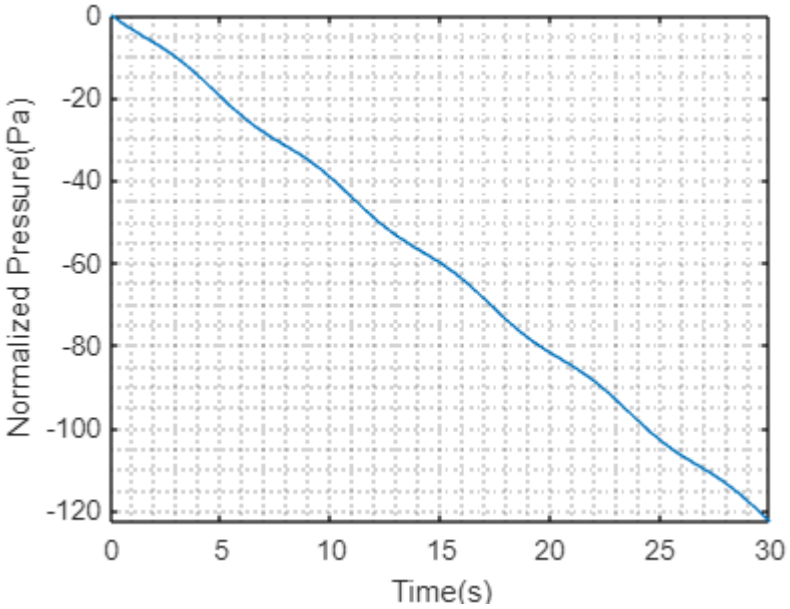


*Figure F-35: Pressure fluctuations in a non-uniformly packed vessel (large and small at the center) at a flowrate of $1m^3/s$*

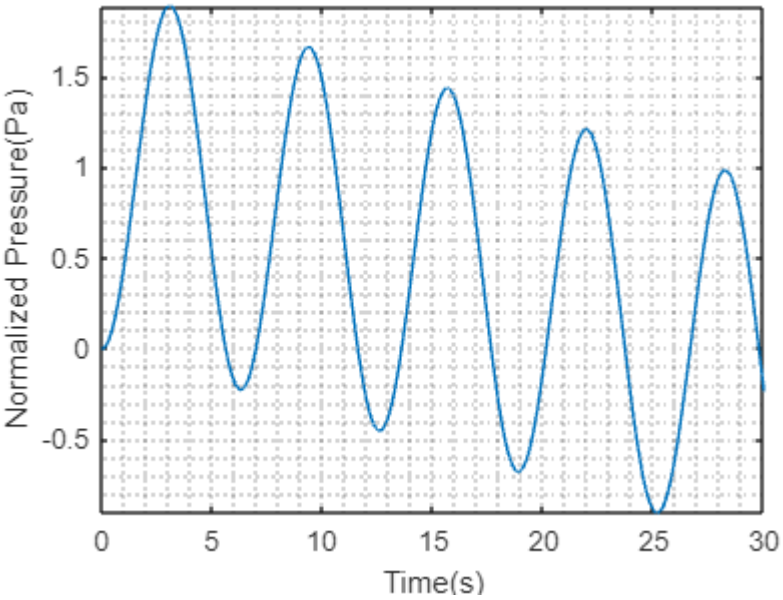


*Figure F-36: Pressure fluctuations in a non-uniformly packed vessel (large and small at the center) at a flowrate of $0.1m^3/s$*

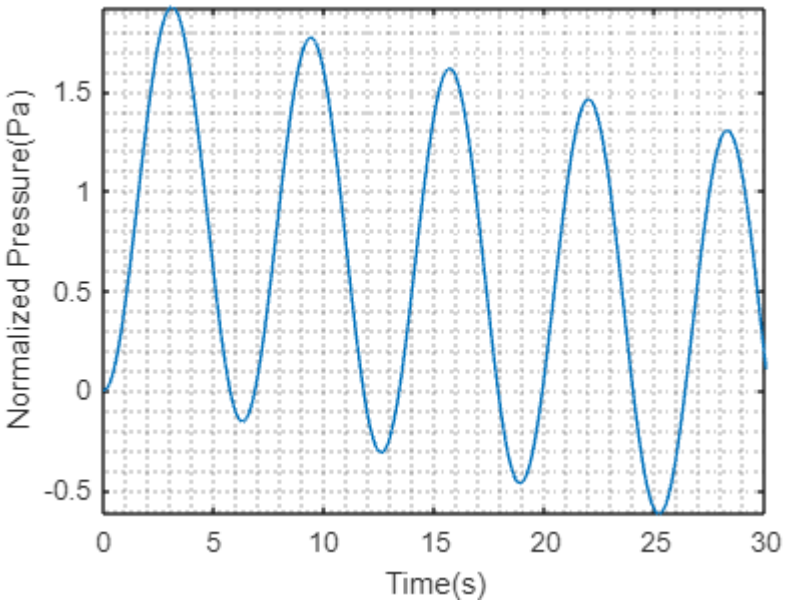


*Figure F-37: Pressure fluctuations in a non-uniformly packed vessel (large and small at the center) at a flowrate of 0.08m$^3$/s*

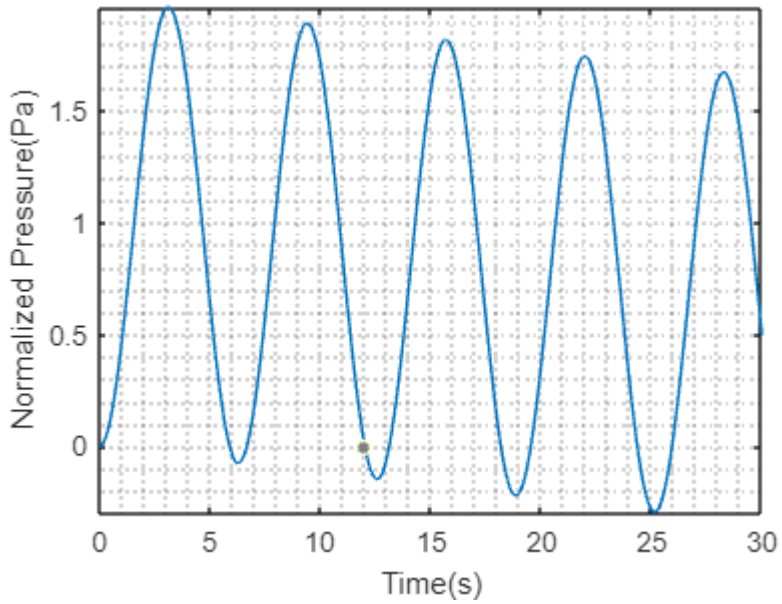


*Figure F-38: Pressure fluctuations in a non-uniformly packed vessel (large and small at the center) at a flowrate of 0.05m$^3$/s*

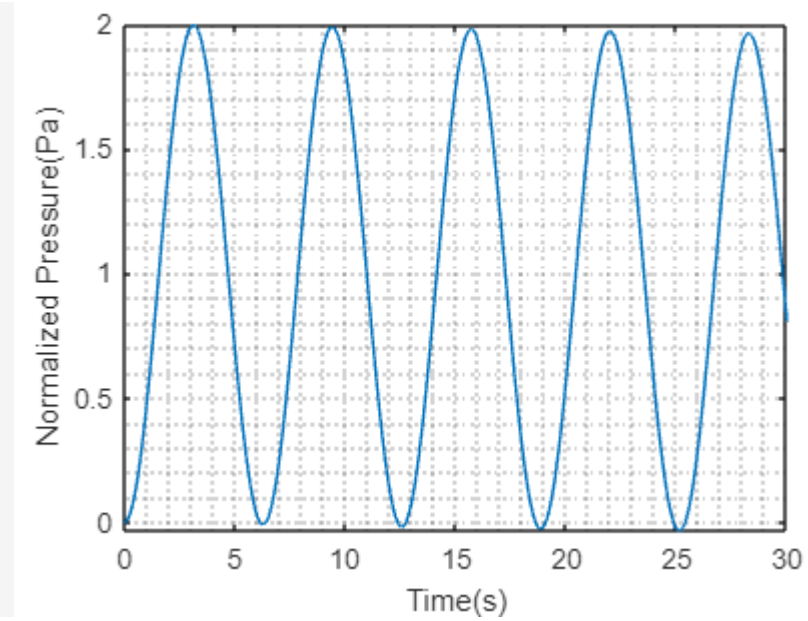


*Figure F-39: Pressure fluctuations in a non-uniformly packed vessel (large and small at the center) at a flowrate of 0.01m$^3$/s*

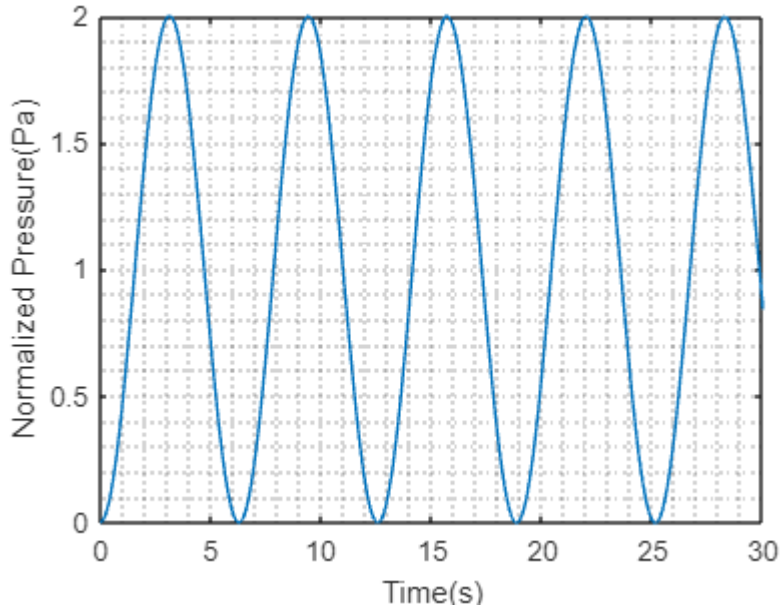


*Figure F-40: Pressure fluctuations in a non-uniformly packed vessel (large and small at the center) at a flowrate of 0.001m$^3$/s*

## APPENDIX G- Calculations and MATLAB codes

### Correction of Flowrates

The readings on the rotameter are given as percentage of the maximum allowable flowrate of 272 $dm^3$/minute, due to this, the actual flowrates had to calculated from the pressure-time data obtained. Due to the large quantity of results, a single point shall be used for this sample calculation. The following procedure was applied using a Microsoft excel spreadsheet to every data point obtained from the experiment.

The rotameter was calibrated at 85 kPa and 20 ˚C, to account for the change in pressure and temperature occurring during the experiment an equation which incorporated the corrections had to be used to obtain the actual final flowrate. The following equation was used from Dwyer Instruments (Dwyer Instruments, 2020):

$$q'_G = q''_G \times \sqrt{\frac{P}{P_s} \times \frac{T_s}{T}} \qquad \text{(Eqn G-1)}$$

Where: $q'_G$ is the gas flow with volume corrected to measurement at standard conditions.

$q''_G$ is the standard gas flowrate.

$P_s$ is the standard (calibrated) pressure in mmHg.

$T_s$ is the standard(calibrated) temperature in ˚R.

P is the absolute pressure of the gas in mmHg.

T is the absolute temperature in ˚R.

For 19 % of the total rotameter flow, at a temperature of 26.5˚C, a pressure of 258 440 Pa at the top of the vessel was recorded.

$$q''_G = 0.19 \times 272 \text{ d}m^3/\text{minute} = 51.68 \text{ d}m^3/\text{minute}$$

Converting Pa to mmHg: $\frac{258\,440 \text{ Pa}}{101325 \text{ Pa}} \times 760 \text{ mmHg} = 1938.45 \text{ mmHg}$

Converting ˚C to ˚R: $\left[26.5 \times \frac{9}{5}\right] + 32 = 79.7 \text{ °F}$

$$79.7\text{°F} + 460 = 539.7 \text{ ˚R}$$

Using this data to calculate the corrected flowrate at this point:

$$q'_G = q''_G \times \sqrt{\frac{P}{P_s} \times \frac{T_s}{T}} = 51.68 \times \sqrt{\frac{1938.45}{637.55} \times \frac{528}{539.7}} = 89.12 \text{ min l/min}$$

**MODEL DEVELOPMENT**

**4.1.1 Gas Pressure drop as a constant fraction of inlet pressure**

**Case 1: Constant Gas Velocity**

Equation 4-5 in main Thesis (Re-written as Eqn G-2), gives the relation when pressure drop is a constant fraction of the inlet pressure,

$$P_{out}(t) = P_{in}(t) - b(P_{in}(t)) \quad \text{(Eqn G-2)}$$

Upon rearranging,

$$P_{out}(t) = P_{in}(t)\lfloor(1 - b)\rfloor$$

Gas inlet pressure is a sine function as it originates of compression.

$$P_{in}(t) = ASin(wt) \quad \text{(Eqn G-3)}$$

$$P_{out}(t) = \big(ASin(wt)\big)\lfloor(1 - b)\rfloor = ASin(wt) - AbSin(wt) \quad \text{(Eqn G-4)}$$

From the laws of Laplace transforms,

$$L\left(\frac{d^n f(x)}{dx^n}\right) = s^n F(s) - \sum_{k=1}^{n} s^{k-1} \frac{d^{n-k}}{dx^{n-k}} f \quad \text{(Eqn G-5)}$$

$$L(1) = \frac{1}{s} \quad \text{(Eqn G-6)}$$

$$L^{-1}(L\big(f(x)\big) = f(x) \quad \text{(Eqn G-7)}$$

$$L\big(Sin\ (wt)\big) = \frac{w}{s^2+w^2} \quad \text{(Eqn G-8)}$$

Taking Laplace on equation G-4

$$L(\frac{dP_{out}}{dt}) = L(ASin(wt)\lfloor(1 - b)\rfloor) \quad \text{(Eqn G-9)}$$

$$sP(s) = A\left(\frac{w}{s^2+w^2}\right) - \frac{b}{s} - Ab(\frac{w}{s^2+w^2}) \quad \text{(Eqn G-10)}$$

Upon rearranging equation G-10 becomes,

$$P(s) = \frac{A}{s}\left(\frac{w}{s^2 + w^2}\right) - \frac{Ab}{s}(\frac{w}{s^2 + w^2})$$

Taking inverse Laplace transform on both sides of equation,

$$L^{-1}\big(P(s)\big) = L^{-1}\left(\frac{A}{s}\left(\frac{w}{s^2+w^2}\right)\right) - L^{-1}\left(\frac{b}{s^2}\right) - L^{-1}\left(\frac{Ab}{s}\left(\frac{w}{s^2+w^2}\right)\right)$$

$$P(t) = \frac{(b-1)\big(ACos(wt)\big)}{w} - \frac{A(b-1)}{w} \quad \text{(Eqn G-11)}$$

### 4.1.2 Gas pressure drop as a non-constant fraction of inlet pressure

When the pressure drop is not a constant fraction of the inlet pressure, change in pressure is affected by diameter and porosity of the catalyst in the packed bed reactor.

Where, the relation between the gas leaving the vessel with respect to time is expressed in Equation 4-8 (main Thesis) as,

$$P_{out}(t) = ASin(wt) - \Delta P \quad \text{(Eqn G-12)}$$

Whereas the pressure drop in a packed bed is given by the Ergun equation (Ergun, 1952);

$$\frac{\Delta P}{L} = 150\frac{(1-\varepsilon)^2}{\varepsilon^3}\frac{\mu.u}{d_p^2} + 1.75\frac{(1-\varepsilon)}{\varepsilon^3}\frac{\rho u^2}{d_p} \quad \text{(Eqn G-13)}$$

where, $L$ is the length of the packed bed (m), $\varepsilon$ is the porosity of the catalyst, $\mu$ is the dynamic viscosity of the fluid (Pa. s), $u$ is superficial fluid velocity measured at average pressure (m/s), $d_p$ is the diameter of the catalyst (m) and $\rho$ is the density of the fluid (kg/m$^3$).

Taking Laplace transform on equation G-12

$$sP(s) = A\left(\frac{w}{s^2+w^2}\right) - \frac{\Delta P}{s} \quad \text{(Eqn G-14)}$$

Diving equation G-14 by s

$$P(s) = \frac{A}{s}\left(\frac{w}{s^2+w^2}\right) - \frac{\Delta P}{s^2} \quad \text{(Eqn G-15)}$$

Taking inverse Laplace on both sides of equation G-15

$$L^{-1}(P(s)) = L^{-1}\left(\frac{A}{s}\left(\frac{w}{s^2+w^2}\right)\right) - L^{-1}\left(\frac{\Delta P}{s^2}\right) \quad \text{(Eqn G-16)}$$

Leading to,

$$P(t) = \frac{A}{w} - \frac{Acos(wt)}{w} - \Delta Pt \quad \text{(Eqn G-17)}$$

**MODEL ARRANGEMENT 2- NON-UNIFORM PACKING (with small packing at the side of the vessel)**

**Case 1: Constant gas velocity**

$$P_{out1}(t) = x(ASin(wt))\lfloor(1 - b)\rfloor \quad \text{(Eqn G-18)}$$

Taking Laplace on Equation G-18 (Equation 4-24 in main Thesis) and applying the Ergun equation for pressure drop across a packed bed reactor (Workings shown in Appendix G, Equations G-18—G-26) gives,

$$P_{out1}(t) = L(AxSin(wt)\lfloor(1 - b)\rfloor) \quad \text{(Eqn G-19)}$$

$$sP(s) = Ax\left(\frac{w}{s^2+w^2}\right) - Abx(\frac{w}{s^2+w^2}) \quad \text{(Eqn G-20)}$$

Upon rearranging equation G-20 becomes,

$$P(s) = Ax\left(\frac{w}{s^2+w^2}\right) - \frac{Abx}{s^2}(\frac{w}{s^2+w^2}) \quad \text{(Eqn G-21)}$$

Taking inverse Laplace transform on both sides on equation G21,

$$L^{-1}\big(P(s)\big) = L^{-1}\left(Ax\left(\frac{w}{s^2+w^2}\right)\right) - L^{-1}\left(\frac{a_o bx}{s^2}\right) - L^{-1}\left(\frac{Abx}{s^2}\left(\frac{w}{s^2+w^2}\right)\right)$$

which gives,

$$P(t) = \frac{Axcos(wt)(b-1)}{w} - \frac{Ax(b-1)}{w} \quad \text{(Eqn G-22)}$$

For stream 2,

$$P_{out2}(t) = (1-x)(ASin(wt))\lfloor(1 - b)\rfloor$$

$$P(t) = \frac{Ax(b-1)(x-1)}{w} - \frac{Axcos(wt)(b-1)(x-1)}{w} \quad \text{(Eqn G-23)}$$

The overall pressure drop from the 2 streams,

$$P_{out}(t) = P_{in}(t) - \Delta P$$

$$\frac{\Delta P}{L} = 150\frac{(1-\varepsilon)^2}{\varepsilon^3}\frac{\mu.u}{d_p^2} + 1.75\frac{(1-\varepsilon)}{\varepsilon^3}\frac{\rho u^2}{d_p}$$

$$\Delta P = L\left[150\frac{(1-\varepsilon)^2}{\varepsilon^3}\frac{\mu.u}{d_p^2} + 1.75\frac{(1-\varepsilon)}{\varepsilon^3}\frac{\rho u^2}{d_p}\right]$$

$$P_{in}(t) = ASin(wt)$$

$$P_{out}(t) = \big(ASin(wt)\big) - L\left[150\frac{(1-\varepsilon)^2}{\varepsilon^3}\frac{\mu.u}{d_p^2} + 1.75\frac{(1-\varepsilon)}{\varepsilon^3}\frac{\rho u^2}{d_p}\right] \quad \text{(Eqn G-24)}$$

Since we have different packings,

Pressure drop in stream 1

$$\Delta P1 = L\left[150\frac{(1-\varepsilon_1)^2}{\varepsilon_1^3}\frac{\mu.u_1}{d_{p1}^2} + 1.75\frac{(1-\varepsilon_1)}{\varepsilon_1^3}\frac{\rho {u_1}^2}{d_{p1}}\right]$$

Pressure drop in stream 2

$$\Delta P2 = L\left[150\frac{(1-\varepsilon_2)^2}{\varepsilon_2^3}\frac{\mu.u_2}{d_{p2}^2} + 1.75\frac{(1-\varepsilon_2)}{\varepsilon_2^3}\frac{\rho {u_2}^2}{d_{p2}}\right]$$

where, $\varepsilon_1$ is the porosity of small catalyst, $u_1$ is the superficial velocity in stream 1, $d_{p1}$ is the diameter of small catalyst, $\varepsilon_2$ is the porosity of large catalyst, $u_2$ is the superficial velocity in stream 2 and $d_{p2}$ is the diameter of large catalyst

For conservation of momentum, the pressure drop across the two different routes is the same.

$$\Delta P1 = \Delta P2 = \Delta P$$

$$L\left[150\frac{(1-\varepsilon_1)^2}{\varepsilon_1^3}\frac{\mu.u_1}{d_{p1}^2} + 1.75\frac{(1-\varepsilon_1)}{\varepsilon_1^3}\frac{\rho {u_1}^2}{d_{p1}}\right] = L\left[150\frac{(1-\varepsilon_2)^2}{\varepsilon_2^3}\frac{\mu.u_2}{d_{p2}^2} + 1.75\frac{(1-\varepsilon_2)}{\varepsilon_2^3}\frac{\rho {u_2}^2}{d_{p2}}\right] \qquad \text{(Eqn G-25)}$$

Therefore

$$P_{out}(t) = \big(ASin(wt)\big) - \Delta P$$

$$P(t) = \frac{A}{w} - \frac{Acos(wt)}{w} - \Delta Pt \qquad \text{(Eqn G-26)}$$

Where

$$\Delta P = L\left[150\frac{(1-\varepsilon_1)^2}{\varepsilon_1^3}\frac{\mu.u_1}{d_{p1}^2} + 1.75\frac{(1-\varepsilon_1)}{\varepsilon_1^3}\frac{\rho {u_1}^2}{d_{p1}}\right] = L\left[150\frac{(1-\varepsilon_2)^2}{\varepsilon_2^3}\frac{\mu.u_2}{d_{p2}^2} + 1.75\frac{(1-\varepsilon_2)}{\varepsilon_2^3}\frac{\rho {u_2}^2}{d_{p2}}\right]$$

Two different reactors with 2 different sets of packing materials were used when modelling.

**For Large vessel**

| **Property** | **Value** |
|---|---|
| $\rho$ | 1.18 kg.m$^{-3}$ |
| $\mu$ | 1.85X10$^{-5}$ |
| $\varepsilon_1$ | 0.693 |

| | |
|---|---|
| $\varepsilon_2$ | 0.715 |
| $d_{p1}$ | 0.02 |
| $d_{p2}$ | 0.05 |

Dividing both sides of equation G-25 by $L$ and substituting particle diameters and porosities

$1.97u_1 + 95.8{u_1}^2 = 0.247u_2 + 32.3{u_2}^2$ (Eqn G-27)

**When $\boldsymbol{u = 1}$**, $u_2 = 1 - u_1$

Substituting for $u_2$

$1.97u_1 + 95.8{u_1}^2 = 0.247(1 - u_1) + 32.3(1 - u_1)^2$

$$66.9u_1 + 63.5{u_1}^2 - 32.6 = 0$$

$$u_1 = 0.362$$

$$u_2 = 0.638$$

Likewise, when $\boldsymbol{u = 0.1}$

$$u_1 = 0.324$$

$$u_2 = 0.676$$

When $\boldsymbol{u = 0.08}$

$$u_1 = 0.315$$

$$u_2 = 0.685$$

When $\boldsymbol{u = 0.05}$

$$u_1 = 0.292$$

$$u_2 = 0.708$$

When $\boldsymbol{u = 0.01}$

$$u_1 = 0.191$$

$$u_2 = 0.809$$

When $\boldsymbol{u = 0.001}$

$$u_1 = 0.122$$

$$u_2 = 0.878$$

**For Small vessel**

$$\varepsilon_1 = 0.510$$

$$\varepsilon_2 = 0.751$$

$$d_{p1} = 0.007$$

$$d_{p2} = 0.015$$

Dividing both sides of equation G-25 by *L* and substituting particle diameters and porosities

$$102u_1 + 1092{u_1}^2 = 1.80u_2 + 81.1{u_2}^2 \qquad \text{(Eqn G-28)}$$

When $u = 1$, $u_2 = 1 - u_1$

Substituting for $u_2$

$$102u_1 + 1092{u_1}^2 = 1.80(1 - u_1) + 81.1(1 - u_1)^2$$

$$266u_1 + 1011{u_1}^2 - 82.9 = 0$$

$$u_1 = 0.184$$

$$u_2 = 0.816$$

Likewise, when $\boldsymbol{u = 0.1}$

$$u_1 = 0.077$$

$$u_2 = 0.923$$

When $\boldsymbol{u = 0.08}$

$$u_1 = 0.068$$

$$u_2 = 0.932$$

When $\boldsymbol{u = 0.05}$

$$u_1 = 0.055$$

$$u_2 = 0.945$$

When $\boldsymbol{u = 0.01}$

$$u_1 = 0.025$$

$$u_2 = 0.975$$

When $\boldsymbol{u = 0.001}$

$$u_1 = 0.018$$

$$u_2 = 0.982$$

**MODEL ARRANGEMENT 3- MIXED PACKING (small catalyst at the centre of vessel)**

Equation 4-27 in main Thesis shows that,

$$\Delta P = L\left[150\frac{(1-\varepsilon_1)^2}{\varepsilon_1^3}\frac{\mu.u_1}{d_{p1}^2} + 1.75\frac{(1-\varepsilon_1)}{\varepsilon_1^3}\frac{\rho {u_1}^2}{d_{p1}}\right] = L\left[150\frac{(1-\varepsilon_2)^2}{\varepsilon_2^3}\frac{\mu.u_2}{d_{p2}^2} + 1.75\frac{(1-\varepsilon_2)}{\varepsilon_2^3}\frac{\rho {u_2}^2}{d_{p2}}\right] =$$

$$L\left[150\frac{(1-\varepsilon_3)^2}{\varepsilon_3^3}\frac{\mu.u_1}{d_{p3}^2} + 1.75\frac{(1-\varepsilon_3)}{\varepsilon_3^3}\frac{\rho {u_2}^2}{d_{p3}}\right] \quad \text{(Eqn G-28)}$$

**For Large Vessel**

| **Property** | **Value** |
|---|---|
| $\rho$ | 1.18 kg.m$^{-3}$ |
| $\mu$ | 1.85X10$^{-5}$ |
| $\varepsilon_1 = \varepsilon_3$ | 0.715 |
| $\varepsilon_2$ | 0.693 |
| $d_{p1} = d_{p3}$ | 0.05 |
| $d_{p2}$ | 0.02 |

$$u = u_1 + u_2 + u_3$$

$$u_1 = u_3$$

Therefore $u = 2u_1 + u_2$

For same length of packed bed and dividing both sides of the equation by *L* and substituting particle diameters and porosities in Equation G-28,

$$0.247u_1 + 32.3{u_1}^2 = 1.97u_2 + 95.8{u_2}^2 = 0.247u_3 + 32.3{u_3}^2 \quad \text{(Eqn 4-29)}$$

$$u = u_1 + u_2 + u_3$$

$$u_1 = u_3$$

When $u = 1$, $u_2 = 1 - 2u_1$

Substituting for $u_2$

$$0.247u_1 + 32.3{u_1}^2 = 1.97(1 - 2u_1) + 95.8(1 - 2u_1)^2$$

$$387u_1 - 351{u_1}^2 - 97.8 = 0$$

$$u_1 = u_3 = 0.390$$

$$u_2 = 0.219$$

Likewise, when $\boldsymbol{u = 0.1}$

$$u_1 = u_3 = 0.411$$

$$u_2 = 0.177$$

When $\boldsymbol{u = 0.08}$

$$u_1 = u_3 = 0.416$$

$$u_2 = 0.169$$

When $\boldsymbol{u = 0.05}$

$$u_1 = u_3 = 0.426$$

$$u_2 = 0.149$$

When $\boldsymbol{u = 0.01}$

$$u_1 = u_3 = 0.456$$

$$u_2 = 0.088$$

When $\boldsymbol{u = 0.001}$

$$u_1 = u_3 = 0.469$$

$$u_2 = 0.062$$

**For Small Vessel**

$$\varepsilon_1 = \varepsilon_3 = 0.751$$

$$\varepsilon_2 = 0.510$$

$$d_{p1} = d_{p3} = 0.007$$

$$d_{p2} = 0.015$$

$$u = u_1 + u_2 + u_3$$

$$u_1 = u_3$$

Therefore $u = 2u_1 + u_2$

$1.80u_1 + 81.1{u_1}^2 = 102u_2 + 1092{u_2}^2 = 1.80u_3 + 81.1{u_3}^2$ (Eqn 4-46)

$u_1 = u_3$

When $u = 1$, $u_2 = 1 - 2u_1$

Substituting for $u_2$

$$1.80u_1 + 81.1{u_1}^2 = 102(1 - 2u_1) + 1092(1 - 2u_1)^2$$

$$4573u_1 - 4286{u_1}^2 - 1194 = 0$$

$$u_1 = u_3 = 0.456$$

$$u_2 = 0.089$$

Likewise, when $\boldsymbol{u = 0.1}$

$$u_1 = u_3 = 0.487$$

$$u_2 = 0.027$$

When $\boldsymbol{u = 0.08}$

$$u_1 = u_3 = 0.488$$

$$u_2 = 0.023$$

When $\boldsymbol{u = 0.05}$

$$u_1 = u_3 = 0.491$$

$$u_2 = 0.018$$

When $\boldsymbol{u = 0.01}$

$$u_1 = u_3 = 0.495$$

$$u_2 = 0.011$$

When $\boldsymbol{u = 0.001}$

$$u_1 = u_3 = 0.496$$

$$u_2 = 0.009$$

# MATLAB Codes

1. **MATLAB code for smoothing the sinusoidal curves and finding the dominant frequency**

```
Sheet2=2;
sheet=Sheet2;
excelFileName='Big Vessel Large Small Centre Packing Results.xlsx';
uiimport('Big Vessel Large Small Centre Packing Results.xlsx')
[numbers]=xlsread(excelFileName,Sheet2,'N5:N10065')
Fs = 10061/1199.88;            % Sampling frequency
Fn = Fs/2;                   % Nyquist Frequency
T = 1/Fs;              % Sampling period
x=[numbers];
L = length(x)              % Length of signal
t = (0:L-1)*T;         % Time vector
figure (1)
plot(t,x)
out=fft(x,L)/L;
xlabel('Time (s)','FontSize',12,'FontWeight','bold');
ylabel('Nomalized Amplitude','FontSize',12,'FontWeight','bold');
figure (2)
plot(out)
Fv = linspace(0,1,fix(L/2)+1)*Fn;
Iv = 1:length(Fv);           % Index Vector
figure(3)                    % Plot FFT
plot(Fv, abs(out(Iv)))
grid
xlabel('Frequency (Hz)')
ylabel('Amplitude')
figure (4)
plot (t,x)
hold on
y=sgolayfilt(x,3,501);
plot(t,y)
hold off
legend('signal','sgolay')
xlabel('Time (s)','FontSize',12,'FontWeight','bold');
ylabel('Nomalized Amplitude','FontSize',12,'FontWeight','bold');
figure (5)
y=sgolayfilt(x,3,501);
plot(t,y), grid ('on')
```

```
xlabel('Time (s)','FontSize',12,'FontWeight','bold');
ylabel('Nomalized Amplitude','FontSize',12,'FontWeight','bold');
figure (6)
z = x - mean(x);                                                    % <= ADDED LINE
nfft = 16384; % next larger power of 2
y = fft(z,nfft); % Fast Fourier Transform
y = abs(fftshift(y)); % raw power spectrum density
[v,k] = max(y) % find maximum
f_scale = (-nfft/2:nfft/2-1)* Fs/nfft; % frequency scale
plot(f_scale, y),axis('tight'),grid('on')
grid minor
xlim([-0.1 0.1])
fest = f_scale(k); % dominant frequency estimate
set(get(gcf,'CurrentAxes'),'FontName','Times New Roman','FontSize',12)
xlabel('Frequency (Hz)','FontSize',12,'FontWeight','bold');
ylabel('Magnitude','FontSize',12,'FontWeight','bold');
fprintf('Dominant freq.: true %f Hz, estimated %f Hznn\n', fest, fest)
fprintf('Frequency step (resolution) = %f Hznn\n', f_scale(2))
```

## 2. MATLAB Codes for the Model

**Pressure drop a constant fraction of input pressure**

```
syms  A b P(t) w t Fs T
b=0.001;
eqn=diff(P,t)==sin(t)-b*sin(t);
cond=P(0)==0;
P=dsolve(eqn,cond)
fplot(P,[0 30])
xlabel('Time(s)')
ylabel('Pressure(Pa)')
grid minor
```

**Uniform packing, constant velocity**

```
syms A w P(t) dP a
Fs=10000/1199.98;
T=1/Fs;
L = 10000;
q=1.184;
e=0.69268;
v=1.849*10.^-5;
u=8.333*10.^-4;
d=0.02;
w=0.939;
A=(150*u*v*(1-e).^2)/((e.^3)*(d.^2))
B=(1.75*(u.^2)*q*(1-e))/((e.^3)*(d))
dP=(A+B)*4
eqn=diff(P,t)==sin(w*t)-dP
cond=P(0)==0;
P=dsolve(eqn,cond)
fplot(P,[0 60])
grid minor
```

## Large and Small packing at the side

```
syms A w P(t) dP a P1(t) P2(t) P3(t) P4(t) P5(t)
q=1.184;
e1=0.69268;
e2=0.71487;
v=1.849*(10.^-5);
U1=1;
u1=0.362493*U1;
u2=0.637507*U1;
d1=0.02;
d2=0.05;
A1=(150*u1*v*((1-e1).^2))/((e1.^3)*(d1.^2))
B1=(1.75*(u1.^2)*q*(1-e1))/((e1.^3)*(d1))
dP1=(A1+B1)
A2=(150*u2*v*((1-e2).^2))/((e2.^3)*(d2.^2))
B2=(1.75*(u2.^2)*q*(1-e2))/((e2.^3)*(d2))
dP2=(A2+B2)
dP=dP2;
eqn1=diff(P,t)==sin(t)-dP1;
eqn2=diff(P,t)==sin(t)-dP2;
eqn=diff(P,t)==sin(t)-dP
cond=P(0)==0;
P=dsolve(eqn,cond)
figure(1)
fplot(P,[0 30])
xlabel('Time(s)')
ylabel('Normalized Pressure(Pa)')
grid minor
figure(2)
U2=0.1;
u3=0.32407*U2;
u4=0.67593*U2;
d1=0.02;
d2=0.05;
A3=(150*u3*v*((1-e1).^2))/((e1.^3)*(d1.^2))
B3=(1.75*(u3.^2)*q*(1-e1))/((e1.^3)*(d1))
dP3=(A3+B3)
A4=(150*u4*v*((1-e2).^2))/((e2.^3)*(d2.^2))
B4=(1.75*(u4.^2)*q*(1-e2))/((e2.^3)*(d2))
dP4=(A4+B4)
eqn3=diff(P1,t)==sin(t)-dP3;
eqn4=diff(P1,t)==sin(t)-dP4;
eqn5=diff(P1,t)==sin(t)-dP4
cond1=P1(0)==0;
P1=dsolve(eqn5,cond1)
figure(2)
fplot(P1,[0 30])
xlabel('Time(s)')
ylabel('Normalized Pressure(Pa)')
grid minor
figure(3)
U3=0.08;
u5=0.3152*U3;
u6=0.6848*U3;
d1=0.02;
d2=0.05;
A5=(150*u5*v*((1-e1).^2))/((e1.^3)*(d1.^2))
B5=(1.75*(u5.^2)*q*(1-e1))/((e1.^3)*(d1))
dP5=(A5+B5)
A6=(150*u6*v*((1-e2).^2))/((e2.^3)*(d2.^2))
B6=(1.75*(u6.^2)*q*(1-e2))/((e2.^3)*(d2))
dP6=(A6+B6)
```

```
eqn5=diff(P2,t)==sin(t)-dP5;
eqn6=diff(P2,t)==sin(t)-dP6;
eqn=diff(P2,t)==sin(t)-dP6
cond2=P2(0)==0;
P2=dsolve(eqn,cond2)
figure(3)
fplot(P2,[0 30])
xlabel('Time(s)')
ylabel('Normalized Pressure(Pa)')
grid minor
figure(4)
U4=0.05;
u7=0.29222*U4;
u8=0.70778*U4;
d1=0.02;
d2=0.05;
A7=(150*u7*v*((1-e1).^2))/((e1.^3)*(d1.^2))
B7=(1.75*(u7.^2)*q*(1-e1))/((e1.^3)*(d1))
dP7=(A7+B7)
A8=(150*u8*v*((1-e2).^2))/((e2.^3)*(d2.^2))
B8=(1.75*(u8.^2)*q*(1-e2))/((e2.^3)*(d2))
dP8=(A8+B8)
eqn7=diff(P3,t)==sin(t)-dP7;
eqn8=diff(P3,t)==sin(t)-dP8;
eqn=diff(P3,t)==sin(t)-dP8
cond3=P3(0)==0;
P3=dsolve(eqn,cond3)
figure(4)
fplot(P3,[0 30])
xlabel('Time(s)')
ylabel('Normalized Pressure(Pa)')
grid minor
figure(5)
U5=0.01;
u9=0.19104*U5;
u10=0.80896*U5;
d1=0.02;
d2=0.05;
A9=(150*u9*v*((1-e1).^2))/((e1.^3)*(d1.^2))
B9=(1.75*(u9.^2)*q*(1-e1))/((e1.^3)*(d1))
dP9=(A9+B9)
A10=(150*u10*v*((1-e2).^2))/((e2.^3)*(d2.^2))
B10=(1.75*(u10.^2)*q*(1-e2))/((e2.^3)*(d2))
dP10=(A10+B10)
eqn9=diff(P4,t)==sin(t)-dP9;
eqn10=diff(P4,t)==sin(t)-dP10;
eqn=diff(P4,t)==sin(t)-dP10
cond4=P4(0)==0;
P4=dsolve(eqn,cond4)
figure(5)
fplot(P4,[0 30])
xlabel('Time(s)')
ylabel('Normalized Pressure(Pa)')
grid minor
figure(6)
U6=0.001;
u11=0.12195*U6;
u12=0.87805*U6;
d1=0.02;
d2=0.05;
A11=(150*u11*v*((1-e1).^2))/((e1.^3)*(d1.^2))
```

```
B11=(1.75*(u11.^2)*q*(1-e1))/((e1.^3)*(d1))
dP11=(A11+B11)
A12=(150*u12*v*((1-e2).^2))/((e2.^3)*(d2.^2))
B12=(1.75*(u12.^2)*q*(1-e2))/((e2.^3)*(d2))
dP12=(A12+B12)
eqn11=diff(P5,t)==sin(t)-dP11;
eqn12=diff(P5,t)==sin(t)-dP12;
eqn=diff(P5,t)==sin(t)-dP12
cond5=P5(0)==0;
P5=dsolve(eqn,cond5)
figure(6)
fplot(P5,[0 30])
xlabel('Time(s)')
ylabel('Normalized Pressure(Pa)')
grid minor
```

### Large and Small packing at the center

```
syms A w P(t) dP a P1(t) P2(t) P3(t) P4(t) P5(t)
q=1.184;
e1=0.71487;
e2=0.69268;
e3=e1;
v=1.849*10.^-5;
figure(1)
U1=1;
u1=0.39048*U1;
u3=u1;
u2=0.21904*U1;
d1=0.05;
d3=d1;
d2=0.02;
A1=(150*u1*v*(1-e1).^2)/((e1.^3)*(d1.^2))
A3=A1;
B1=(1.75*(u1.^2)*q*(1-e1))/((e1.^3)*(d1))
B3=B1;
dP1=(A1+B1)
dP3=dP1;
A2=(150*u2*v*(1-e2).^2)/((e2.^3)*(d2.^2))
B2=(1.75*(u2.^2)*q*(1-e2))/((e2.^3)*(d2))
dP2=(A2+B2)
dP=dP2;
eqn1=diff(P,t)==sin(t)-dP1;
eqn2=diff(P,t)==(sin(t))-dP2;
eqn=diff(P,t)==sin(t)-dP
cond=P(0)==0;
P=dsolve(eqn,cond)
figure(1)
fplot(P,[0 30])
xlabel('Time(s)')
ylabel('Normalized Pressure(Pa)')
grid minor
figure(2)
U2=0.1;
u4=0.41147*U2;
u6=u4;
u5=0.17706*U2;
d1=0.05;
```

```
d3=d1;
d2=0.02;
A4=(150*u4*v*(1-e1).^2)/((e1.^3)*(d1.^2))
A6=A4;
B4=(1.75*(u4.^2)*q*(1-e1))/((e1.^3)*(d1))
B6=B4;
dP4=(A4+B4)
dP6=dP4;
A5=(150*u5*v*(1-e2).^2)/((e2.^3)*(d2.^2))
B5=(1.75*(u5.^2)*q*(1-e2))/((e2.^3)*(d2))
dP5=(A5+B5)
dP=dP5;
eqn3=diff(P1,t)==sin(t)-dP4;
eqn4=diff(P1,t)==(sin(t))-dP5;
eqn=diff(P1,t)==sin(t)-dP
cond1=P1(0)==0;
P1=dsolve(eqn,cond1)
figure(2)
fplot(P1,[0 30])
xlabel('Time(s)')
ylabel('Normalized Pressure(Pa)')
grid minor
figure(3)
U3=0.08;
u7=0.41573*U3;
u9=u7;
u8=0.16854*U3;
d1=0.05;
d3=d1;
d2=0.02;
A7=(150*u7*v*(1-e1).^2)/((e1.^3)*(d1.^2))
A9=A7;
B7=(1.75*(u7.^2)*q*(1-e1))/((e1.^3)*(d1))
B9=B7;
dP7=(A7+B7)
dP9=dP7;
A8=(150*u8*v*(1-e2).^2)/((e2.^3)*(d2.^2))
B8=(1.75*(u8.^2)*q*(1-e2))/((e2.^3)*(d2))
dP8=(A8+B8)
dP=dP8;
eqn5=diff(P2,t)==sin(t)-dP7;
eqn6=diff(P2,t)==(sin(t))-dP8;
eqn=diff(P2,t)==sin(t)-dP
cond2=P2(0)==0;
P2=dsolve(eqn,cond2)
figure(3)
fplot(P2,[0 30])
xlabel('Time(s)')
ylabel('Normalized Pressure(Pa)')
grid minor
figure(4)
U4=0.05;
u10=0.42574*U4;
u9=u10;
u11=0.14852*U4;
d1=0.05;
d3=d1;
d2=0.02;
A10=(150*u10*v*(1-e1).^2)/((e1.^3)*(d1.^2))
```

```
A12=A10;
B10=(1.75*(u10.^2)*q*(1-e1))/((e1.^3)*(d1))
B12=B10;
dP10=(A10+B10)
dP12=dP10;
A11=(150*u11*v*(1-e2).^2)/((e2.^3)*(d2.^2))
B11=(1.75*(u11.^2)*q*(1-e2))/((e2.^3)*(d2))
dP11=(A11+B11)
dP=dP11;
eqn7=diff(P3,t)==sin(t)-dP10;
eqn8=diff(P3,t)==(sin(t))-dP11;
eqn=diff(P3,t)==sin(t)-dP
cond3=P3(0)==0;
P3=dsolve(eqn,cond3)
figure(4)
fplot(P3,[0 30])
xlabel('Time(s)')
ylabel('Normalized Pressure(Pa)')
grid minor
figure(5)
U5=0.01;
u13=0.4562*U5;
u15=u13;
u14=0.0876*U5;
d1=0.05;
d3=d1;
d2=0.02;
A13=(150*u13*v*(1-e1).^2)/((e1.^3)*(d1.^2))
A15=A13;
B13=(1.75*(u13.^2)*q*(1-e1))/((e1.^3)*(d1))
B15=B13;
dP13=(A13+B13)
dP15=dP13;
A14=(150*u14*v*(1-e2).^2)/((e2.^3)*(d2.^2))
B14=(1.75*(u14.^2)*q*(1-e2))/((e2.^3)*(d2))
dP14=(A14+B14)
dP=dP14;
eqn9=diff(P4,t)==sin(t)-dP13;
eqn10=diff(P4,t)==(sin(t))-dP14;
eqn=diff(P4,t)==sin(t)-dP
cond4=P4(0)==0;
P4=dsolve(eqn,cond4)
figure(5)
fplot(P4,[0 30])
xlabel('Time(s)')
ylabel('Normalized Pressure(Pa)')
grid minor
figure(6)
U6=0.001;
u16=0.46891*U6;
u15=u16;
u17=0.06218*U6;
d1=0.05;
d3=d1;
d2=0.02;
A16=(150*u16*v*(1-e1).^2)/((e1.^3)*(d1.^2))
A18=A16;
B16=(1.75*(u16.^2)*q*(1-e1))/((e1.^3)*(d1))
B18=B16;
```

```
dP16=(A16+B16)
dP8=dP16;
A17=(150*u17*v*(1-e2).^2)/((e2.^3)*(d2.^2))
B17=(1.75*(u17.^2)*q*(1-e2))/((e2.^3)*(d2))
dP17=(A17+B17)
dP=dP17;
eqn11=diff(P5,t)==sin(t)-dP16;
eqn12=diff(P5,t)==(sin(t))-dP17;
eqn=diff(P5,t)==sin(t)-dP
cond5=P5(0)==0;
P5=dsolve(eqn,cond5)
figure(6)
fplot(P5,[0 30])
xlabel('Time(s)')
ylabel('Normalized Pressure(Pa)')
grid minor
```